ROBUST CONTROL
The Parametric Approach

S. P. Bhattacharyya
Texas A&M University

H. Chapellat
Schlumberger Corporation

L. H. Keel
Tennessee State University

This book was published previously by Prentice Hall PTR (1995) with ISBN 0-13-781576-X.

THIS BOOK IS DEDICATED TO

Krishna Lee, Mohadev and Shona Lee

S.P. Bhattacharyya

My beloved family: Pierre, Jacqueline, Laetitia, Patrick, Véronique et Pascale

H. Chapellat

Sook, Allen and Jessica

L.H. Keel

Contents

FOREWORD

Control systems need to be designed so that certain essential properties remain unchanged under perturbations. The design problem of maintaining invariance of system properties under small perturbations of the system parameters were considered in the initial stages of the development of Control Theory. These properties included the stability and performance of systems. It was understood later that even more important was the requirement that a control system function satisfactorily under large perturbations. Thus the problems of stability and performance validation for a family of controlled systems with parameters or frequency responses lying within admissible sets, have attracted considerable attention. This field has come to be known as Robust Control.

The theory of Robust Control has been elegantly developed within the H_∞ framework. This framework can effectively deal with robust stability and performance problems under unstructured perturbations. It is however quite deficient in addressing the same issues when parameter uncertainty is considered.

The treatment of robust stability problems under parameter uncertainty has been pioneered by the Italian mathematician Faedo (1953) and the Russian scientist Kharitonov (1978). A rich array of useful results have been developed over the last ten years and at present there exists an extensive literature in this specific field.

The authors of the present book are well known as experts in the area of Robust Control under parameter uncertainty. They have actively participated in the development of the theory, and their personal contribution cannot be overestimated. It suffices to mention their developments of the Generalized Kharitonov Theorem, the theory of disk polynomials, the extremal properties of interval systems, the calculation of the real parametric stability margin and their contributions to design problems under simultaneous parametric and nonparametric uncertainty, among others.

The book contains a complete account of most of the fundamental results in this field. The proofs of the results are elegant, simple and insightful. At the same time careful attention is paid to basic aspects of control problems such as design, performance, and synthesis and their relationship to the theory developed. The organization and sequence of the material has many significant merits and the

entire book is written with great expertise, style, rigour and clarity.

The reader will find here a unified approach to robust stability theory. It includes both linear and nonlinear systems. A systematic use of frequency domain methods allowed the authors to combine different types of uncertainty and to link parametric robust stability with nonlinear perturbations and the results of H_∞ theory. Numerous examples of various origins, as well as exercises are included. It will be helpful to a broad audience of control theorists and students, and indispensable to the specialist in Robust Control.

The book should stand as an outstanding and fundamental contribution to the science of automatic control and I commend the authors for their effort. I felt a true pleasure when reading this book, and I believe the reader will share my feelings.

Ya. Z. Tsypkin
Institute of Control Science
Moscow, Russia
August 1994

PREFACE

The subject of robust control began to receive worldwide attention in the late 1970's when it was found that Linear Quadratic Optimal Control (H_2 optimal control), state feedback through observers, and other prevailing methods of control system synthesis such as Adaptive Control, lacked any guarantees of stability or performance under uncertainty. Thus, the issue of robustness, prominent in Classical Control, took rebirth in a modern setting.

H_∞ optimal control was proposed as a first approach to the solution of the robustness problem. This elegant approach, and its offshoots, such as μ theory, have been intensely developed over the past 12 years or so, and constitutes one of the triumphs of control theory. The theory provides a precise formulation and solution of the problem of synthesizing an output feedback compensator that minimizes the H_∞ norm of a prescribed system transfer function. Many robust stabilization and performance problems can be cast in this formulation and there now exists effective, and fairly complete theory for control system synthesis subjected to perturbations, in the H_∞ framework.

The H_2 or H_∞ theory delivers an "optimal" feedback compensator for the system. Before such a compensator can be deployed in a physical (real-world) system it is natural to test its capabilities with regard to additional design criteria, not covered by the optimality criterion used. In particular the performance of any controller under real parameter uncertainty, as well as mixed parametric-unstructured uncertainty, is an issue which is vital to most control systems. However, optimal H_2 or H_∞ theory is incapable of providing a direct and nonconservative answer to this important question.

The problem of robustness under parametric uncertainty received a shot in the arm in the form of Kharitonov's Theorem for interval polynomials, which appeared in the mid-1980's in the Western literature. It was originally published in 1978 in a Russian journal. With this surprising theorem the entire field of robust control under real parametric uncertainty came alive and it can be said that Kharitonov's Theorem is the most important occurrence in this area after the development of the Routh-Hurwitz criterion. A significant development following Kharitonov's Theorem was the calculation, in 1985, by Soh, Berger and Dabke of the radius of the

stability ball in the space of coefficients of a polynomial.

From the mid-1980's rapid and spectacular developments have taken place in this field. As a result we now have a rigorous, coherent, and comprehensive theory to deal directly and effectively with real parameter uncertainty in control systems. This theory nicely complements the optimal H_2 and H_∞ theories as well as Classical Control and considerably extends the range of possibilities available to the control specialist.

The main accomplishment of this theory is that it allows us to determine if a linear time invariant control system, containing several uncertain real parameters remains stable as the parameters vary over a set. This question can be answered in a precise manner, that is, nonconservatively, when the parameters appear linearly or multilinearly in the characteristic polynomial. In developing the solution to the above problem, several important control system design problems are answered. These are 1) the calculation of the real parametric stability margin, 2) the determination of stability and stability margins under mixed parametric and unstructured (norm-bounded or nonlinear) uncertainty 3) the evaluation of the worst case or robust performance measured in the H_∞ norm, over a prescribed parametric uncertainty set and 4) the extension of classical design techniques involving Nyquist, Nichols and Bode plots and root-loci to systems containing several uncertain real parameters.

These results are made possible because the theory developed provides *built-in* solutions to several extremal problems. It identifies apriori the critical subset of the uncertain parameter set over which stability or performance will be lost and thereby reduces to a very small set, usually points or lines, the parameters over which robustness must be verified. This built-in optimality of the parametric theory is its main strong point particularly from the point of view of applications. It allows us, for the first time, to devise methods to effectively carry out robust stability and performance analysis of control systems under parametric and mixed uncertainty. To balance this rather strong claim we point out that a significant deficiency of control theory at the present time is the lack of nonconservative synthesis methods to achieve robustness under parameter uncertainty. Nevertheless, even here the sharp analysis results obtained in the parametric framework can be exploited in conjunction with synthesis techniques developed in the H_∞ framework to develop design techniques to partially cover this drawback.

The objective of this book is to describe the parametric theory in a self-contained manner. The book is suitable for use as a graduate textbook and also for self-study. The entire subject matter of the book is developed from the single fundamental fact that the roots of a polynomial depend continuously on its coefficients. This fact is the basis of the Boundary Crossing Theorem developed in Chapter 1 and is repeatedly used throughout the book. Surprisingly enough this simple idea, used systematically is sufficient to derive even the most mathematically sophisticated results. This economy and transparency of concepts is another strength of the parametric theory. It makes the results accessible and appealing to a wide audience and allows for a unified and systematic development of the subject. The contents

of the book can therefore be covered in one semester despite the size of the book. In accordance with our focus we do not develop any results in H_∞ or H_2 theory although some results from H_∞ theory are used in the chapter on synthesis. In Chapter 0, which serves as an extension of this preface, we rapidly overview some basic aspects of control systems, uncertainty models and robustness issues. We also give a brief historical sketch of Control Theory, and then describe the contents of the rest of the chapters in some detail.

The theory developed in the book is presented in mathematical language. The results described in these theorems and lemmas however are completely oriented towards control systems applications and in fact lead to effective algorithms and graphical displays for design and analysis. We have throughout included examples to illustrate the theory and indeed the reader who wants to avoid reading the proofs can understand the significance and utility of the results by reading through the examples. A MATLAB based software package, the Robust Parametric Control ToolBox, has been developed by the authors in collaboration with Samir Ahmad, our graduate student. It implements most of the theory presented in the book. In fact, all the examples and figures in this book have been generated by this ToolBox. We gratefully acknowledge Samir's dedication and help in the preparation of the numerical examples given in the book. A demonstration diskette illustrating this package is included with this book.

S.P.B. would like to thank R. Kishan Baheti, Director of the Engineering Systems Program at the National Science Foundation, for supporting his research program. L.H.K. thanks Harry Frisch and Frank Bauer of NASA Goddard Space Flight Center and Jer-Nan Juang of NASA Langley Research Center for their support of his research, and Mike Busby, Director of the Center of Excellence in Information Systems at Tennessee State University for his encouragement.

It is a pleasure to express our gratitude to several colleagues and coworkers in this field. We thank Antonio Vicino, Alberto Tesi, Mario Milanese, Jo W. Howze, Aniruddha Datta, Mohammed Mansour, J. Boyd Pearson, Peter Dorato, Yakov Z. Tsypkin, Boris T. Polyak, Vladimir L. Kharitonov, Kris Hollot, Juergen Ackermann, Diedrich Hinrichsen, Tony Pritchard, Dragoslav D. Siljak, Charles A. Desoer, Soura Dasgupta, Suhada Jayasuriya, Rama K. Yedavalli, Bob R. Barmish, Mohammed Dahleh, and Biswa N. Datta for their, support, enthusiasm, ideas and friendship. In particular we thank Nirmal K. Bose, John A. Fleming and Bahram Shafai for thoroughly reviewing the manuscript and suggesting many improvements.

We are indeed honored that Academician Ya. Z. Tsypkin, one of the leading control theorists of the world, has written a Foreword to our book. Professor Tsypkin's pioneering contributions range from the stability analysis of time-delay systems in the 1940's, learning control systems in the 1960's to robust control under parameter uncertainty in the 1980's and 1990's. His observations on the contents of the book and this subject based on this wide perspective are of great value.

The first draft of this book was written in 1989. We have added new results of our own and others as we became aware of them. However, because of the rapid pace of developments of the subject and the sheer volume of literature that has been

published in the last few years, it is possible that we have inadvertently omitted some results and references worthy of inclusion. We apologize in advance to any authors or readers who feel that we have not given credit where it is due.

S. P. Bhattacharyya

H. Chapellat

L. H. Keel

December 5, 1994.

Chapter 0

BACKGROUND AND MOTIVATION

In this chapter we make some introductory and motivational remarks describing the problems of robust stability and control. The first section is written for the reader who is relatively unfamiliar with basic control concepts, terminology and techniques. Next, a brief historical sketch of control theory is included to serve as a background for the contents of the book. Finally these contents and their organization are described in some detail.

0.1 INTRODUCTION TO CONTROL

A **control system** is a mechanism which makes certain physical variables of a system, called a **plant**, behave in a prescribed manner, despite the presence of uncertainties and disturbances.

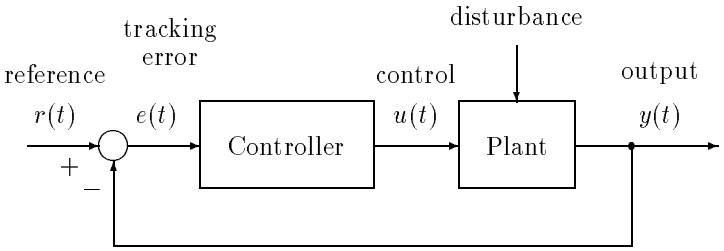

Figure 0.1. Unity feedback control system

The plant or system to be controlled is a dynamic system, such as an aircraft, chemical process, machine tool, electric motor or robot, and the control objective is to make the system output $y(t)$ follow a reference input $r(t)$ as closely as possible

despite the disturbances affecting the system. Automatic control is achieved by employing feedback. In a **unity feedback** or **closed loop system** (see Figure 0.1), control action is taken by applying the input $u(t)$ to the plant, and this is based on the difference, at each instant of time t, between the actual value of the plant output to be controlled $y(t)$ and the prescribed reference or desired output $r(t)$. The **controller** is designed to drive this difference, the **tracking error** $e(t)$ to zero. Such control systems are also called **regulators** or **servomechanisms**.

Stability and **performance** are two of the fundamental issues in the design, analysis and evaluation of control systems. Stability means that, in the absence of external excitation, all signals in the system decay to zero. Stability of the closed loop system is an absolute requirement since its absence causes signals to grow without bound, eventually destroying and breaking down the plant. This is what happens when an aircraft crashes, or a satellite spins out of control or a nuclear reactor core heats up uncontrollably and melts down. In many interesting applications the open loop plant is unstable and the job of feedback control is to **stabilize** the system. While feedback is necessary to make the system track the reference input, its presence in control systems causes the potential for instability to be everpresent and very real. We shall make this notion more precise below in the context of servomechanisms. In engineering systems it is of fundamental importance that control systems be designed so that stability is preserved in the face of various classes of **uncertainties**. This property is known as **robust stability**.

The **performance** of a system usually refers to its ability to track reference signals closely and reject disturbances. A well designed control system or servomechanism should be capable of tracking all reference signals belonging to a **class** of signals, without excessive error, despite various types of uncertainties. In other words the worst case performance over the uncertainty set should be acceptable. This is, roughly speaking, referred to as **robust performance**.

The uncertainties encountered in control systems are both in the environment and within the system. In the first place the reference signal to be tracked is usually not known beforehand. Then there are disturbance signals tending to offset the tracking. For example the load torque on the shaft of an electric motor, whose speed is to be maintained constant, can be regarded as a disturbance.

As far as the system is concerned the main source of uncertainty is the behaviour of the plant. These uncertainties can occur, for example, due to changes of operating points, as in an aircraft flying at various altitudes and loadings, or a power system delivering power at differing load levels. Large changes can also occur in an uncontrolled fashion for example, when sensor or actuator failures occur. The complexity of even the simplest plants is such that any mathematical representation of the system must include significant uncertainty.

In analysis and design it is customary to work with a **nominal** mathematical model. This is invariably assumed to be **linear** and **time invariant**, because this is the only class of systems for which there exists any reasonably general design theory. Nevertheless, such models are usually a gross oversimplification and it is therefore necessary to test the validity of any proposed design by testing its performance

when the model is significantly different from the nominal.

In summary the requirements of robust stability and performance are meant to ensure that the control system functions **reliably** despite the presence of significant uncertainty regarding the model of the system and the precise description of the external signals to be tracked or rejected. In the next few subsections we discuss these requirements and their impact on control system modelling, design, and evaluation, in greater detail.

0.1.1 Regulators and Servomechanisms

The block diagram of a typical feedback control system is shown in Figure 0.2.

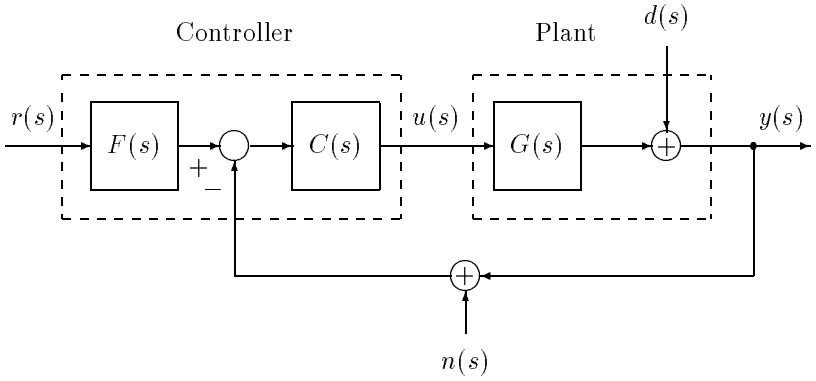

Figure 0.2. General feedback configuration

Here, as in the rest of the book, we will be considering linear time invariant systems which can be represented, after Laplace transformation, in terms of the complex variable s. In Figure 0.2 the vectors u and y represent (the Laplace transforms of) the plant inputs and outputs respectively, d represents disturbance signals reflected to the plant output, n represents measurement noise and r represents the reference signals to be tracked. The plant and the feedback controller are represented by the rational proper transfer matrices $G(s)$, and $C(s)$ respectively, while $F(s)$ represents a feedforward controller or prefilter. The usual problem considered in control theory assumes that $G(s)$ is given while $C(s)$ and $F(s)$ are to be designed. Although every control system has a unique structure and corresponding signal flow representation the standard system represented above is general enough that it captures the essential features of most feedback control systems.

0.1.2 Performance: Tracking and Disturbance Rejection

In the system of Figure 0.2 the plant output $y(t)$ is supposed to follow or track the command reference signal $r(t)$ as closely as possible despite the disturbances

$d(t)$ and the measurement noise $n(t)$. The exogenous signals r, d, n are of course not known exactly as time functions but are known qualitatively. Based on this knowledge the control designer uses certain classes of test signals to evaluate any proposed design. A typical design specification could state that the system is to have zero steady state error whenever the command reference r and disturbance d consist of steps and ramps of arbitrary and unknown magnitude and slope. Often the measurement noise n is known to have most of its energy lying in a frequency band $[\omega_1, \omega_2]$. In addition to steps and ramps the signals r and d would have significant energy in a low frequency band $[0, \omega_0]$. A reasonable requirement to impose is that y track r with "small" error for every signal in this uncertainty class without excessive use of control energy.

There are two approaches to achieving this objective. One approach is to require that the average error over the uncertainty class be small. The other approach is to require that the error response to the worst case exogenous signal from the given class be less than a prespecified value. These correspond to regarding the control system as an operator mapping the exogenous signals to the error and imposing bounds on the norms of these operators or transfer functions. We examine these ideas more precisely by deriving the equations of the closed loop system. These are:

$$\begin{aligned} y(s) &= G(s)u(s) + d(s) \\ u(s) &= C(s)\left[F(s)r(s) - n(s) - y(s)\right] \\ e(s) &:= r(s) - y(s) \qquad \text{(tracking error)}. \end{aligned}$$

Solving the above equations, (we drop the explicit dependence on s whenever it is obvious)

$$\begin{aligned} y &= \left[I + GC\right]^{-1} d + \left[I + GC\right]^{-1} GCFr - \left[I + GC\right]^{-1} GCn \\ e &= -\left[I + GC\right]^{-1} d + \left[I - (I + GC)^{-1}GCF\right] r + \left[I + GC\right]^{-1} GCn. \end{aligned}$$

Introducing the **sensitivity function** $S(s)$ and the **complementary sensitivity function** $T(s)$:

$$\begin{aligned} S &:= \left[I + GC\right]^{-1} \\ T &:= \left[I + GC\right]^{-1} GC \end{aligned}$$

we can rewrite the above equations more compactly as

$$\begin{aligned} y &= Sd + TFr - Tn \\ e &= -Sd + (I - TF)r + Tn. \end{aligned}$$

As we have mentioned, in many practical cases the control system is of **unity feedback type** which means that the feedback controller is driven only by the tracking error. In such cases the feedforward element $F(s)$ is the identity and the system equations simplify to

$$\begin{aligned} y &= Sd + Tr - Tn \\ e &= -Sd + Sr + Tn. \end{aligned}$$

Ideally the response of the tracking error e to each of the signals r, d and n should be zero. This translates to the requirement that the transfer functions $S(s)$ and $T(s)$ should both be "small" in a suitable sense. However we see that

$$S(s) + T(s) = I, \qquad \text{for all } s \in \mathbb{C}$$

and thus there is a **built-in trade off** since S and T cannot be small at the same values of s. This trade off can be resolved satisfactorily if the frequency bands in which r and d lie is disjoint from that in which n lies. In this case $S(j\omega)$ should be kept small over the frequency band $[0, \omega_0]$ to provide accurate tracking of low frequency signals and $T(j\omega)$ should be kept small over the frequency band $[\omega_1, \omega_2]$, to attenuate noise.

Suppose for the moment, that the plant is a single-input, single-output (SISO) system. Then G, C, F, S and T are scalar transfer functions. In this case, we have, for the unity feedback case,

$$u = \frac{T}{G}r - \frac{T}{G}n - \frac{T}{G}d.$$

From Parseval's Theorem we have

$$\int_0^\infty u^2(t)dt = \frac{1}{2\pi}\int_{-\infty}^{+\infty} |u(j\omega)|^2 d\omega$$

and so we see that the control signal energy can be kept small by keeping the magnitude of $T(j\omega)$ as small as possible over the frequency bands of r, d and n. This obviously conflicts with the requirement of making $S(j\omega)$ small over the band $[0, \omega_0]$. Thus for good tracking, $T(j\omega)$ must necessarily be large over $[0, \omega_0]$ but then should rapidly decrease with increasing frequency to "conserve" control energy.

The above arguments also extend to multiinput-multioutput (MIMO) systems. We know that the "gain" of a SISO linear system, with transfer function $M(s)$, for a sinusoidal input of radian frequency ω is given by $|M(j\omega)|$. When $M(s)$ is a proper transfer function with poles in the open left half plane we can define the maximum gain, which is also the H_∞ norm of M:

$$\sup_{0 \le \omega \le \infty} |M(j\omega)| := \|M\|_\infty.$$

For a MIMO system, $M(j\omega)$ is a *matrix* and the corresponding H_∞ norm of M is defined in terms of the maximum singular value $\bar{\sigma}_M(\omega)$ of $M(j\omega)$:

$$\sup_{0 \le \omega \le \infty} \bar{\sigma}_M(\omega) := \|M\|_\infty.$$

The above requirements on S and T can be stated in terms of norms. Let the stable transfer matrix $W(s)$ denote a low pass filter transfer function matrix with

$$W(j\omega) \simeq I, \quad \text{for } \omega \in [0, \omega_0]$$
$$W(j\omega) \simeq 0, \quad \text{for } \omega \ge \omega_0.$$

Similarly let the stable transfer function matrix $V(s)$ denote a bandpass filter with

$$\begin{aligned} V(j\omega) &\simeq I, \quad \text{for } \omega \in B := [\omega_1, \omega_2] \\ V(j\omega) &\simeq 0, \quad \text{for } \omega \notin B. \end{aligned}$$

Then the requirement that S be small over the band $[0, \omega_0]$ and that T be small over the band B can be stated in a **worst case** form:

$$\begin{aligned} \|WS\|_\infty &\leq \epsilon_1 \\ \|VT\|_\infty &\leq \epsilon_2. \end{aligned}$$

0.1.3 Quantitative feedback theory

In classical control theory, the objective is to find a feedback compensator to satisfy the above or similar types of design objectives for the nominal system. This type of approach was extended to the domain of uncertain systems by the **Quantitative Feedback Theory (QFT)** approach pioneered by Horowitz [120] in the early 1960's. In the QFT approach, which we briefly outline here, one considers the plant model $G(s, \mathbf{p})$ with the uncertain parameter $\mathbf{p}$ lying in a set Ω and a control system configuration including feedback *as well as* feedforward elements. The quality of tracking is measured by the closeness to unity of the transfer function relating y to r, the sensitivity of the feedback loop by the transfer function S, and the noise rejection properties of the loop by the transfer function T. Typically the tracking performance and sensitivity reduction specifications are to be robustly attained over a low frequency range $[0, \omega_0]$ and the noise rejection specifications are to be achieved over a high frequency range $[\omega_1, \infty)$. For SISO systems the specifications assume the forms

$$m_1(\omega) \leq \left| F(j\omega) \frac{C(j\omega)G(j\omega, \mathbf{p})}{1 + C(j\omega)G(j\omega, \mathbf{p})} \right| < m_2(\omega), \quad \text{for } \omega \in [0, \omega_0]$$

$$\begin{aligned} |S(j\omega, \mathbf{p})| &< l_1(\omega), \quad \text{for } \omega \in [0, \omega_0] \\ |T(j\omega, \mathbf{p})| &< l_2(\omega), \quad \text{for } \omega \in [\omega_1, \infty) \end{aligned}$$

for suitably chosen frequency dependent functions $m_1(\omega), m_2(\omega), l_1(\omega)$ and $l_2(\omega)$. Robust design means that the above performance specifications are met for all $\mathbf{p} \in \Omega$ by a suitable choice of feedback and feedforward compensators which stabilize the feedback system for all $\mathbf{p} \in \Omega$. An additional requirement in QFT design is that the bandwidth of the feedback controller $C(s)$ be as small as possible.

The advantage of the feedforward compensator is roughly, that it frees up the feedback controller $C(s)$ to carry out certain closely related tasks such as robust stabilization, sensitivity and noise reduction, while the feedforward controller can subsequently attempt to satisfy the tracking requirement. This freedom allows for a

better chance of finding a solution and also reducing the bandwidth of the feedback controller, often referred to in QFT theory as the "cost of feedback". QFT design is typically carried out by loopshaping the nominal loop gain $L_0 = G_0C$, on the Nichols chart, to satisfy a set of bounds at each frequency, with each bound reflecting a performance specification. Once such an L_0 is found, the controller $C(s)$ can be found by "dividing" out the plant and the feedforward filter $F(s)$ can be computed from the tracking specification. The QFT approach thus has the flavor of classical frequency domain based design, however with the added ingredient of robustness. QFT techniques have been extended to multivariable and even nonlinear systems.

0.1.4 Perfect Steady State Tracking

Control systems are often evaluated on the basis of their ability to track certain test signals such as steps and ramps accurately. To make the system track arbitrary steps with zero steady state error it is enough to use unity feedback ($F = I$) and to place one integrator or pole at the origin in each input channel of the error driven controller $C(s)$. This causes each element of $S(s)$ to have a zero at the origin, as required, to cancel the $s = 0$ poles of r and d, to ensure perfect steady state tracking. Likewise, if steps and ramps are to be tracked then *two* integrators, or poles at $s = 0$ must be included.

These types of controllers have been known from the early days of automatic control in the last century when it was known that steady state tracking and disturbance rejection of steps, ramps etc. could be achieved by incorporating enough **integral action** in a unity feedback control loop (see Figure 0.1). When the closed loop is stable such a controller *automatically converges to the correct control input* which is required to maintain zero error in the steady state. A precise model of the plant is not needed nor is it necessary to know the plant parameters; all that is required is that the closed loop be robustly stable. The generalization of this principle, known as the **Internal Model Principle**, states that in order to track with zero steady state error the control system should contain, internal to the feedback loop, a model signal generator of the unstable external reference and disturbances and the controller should be driven by the tracking error.

Although a controller incorporating integral action, or an unstable internal model, allows the system to achieve reliable tracking, it potentially makes the system **more prone to instability** because the forward path is **rendered unstable**. The designer therefore faces the task of setting the rest of the controller parameters, the part that stabilizes the closed loop system, so that closed loop stability is preserved under various contingencies. In practice this is usually done by using a fixed linear time invariant model of the plant, called the **nominal model**, stabilizing this model, and ensuring that adequate **stability margins** are attained about this nominal in order to preserve closed loop stability under all the possible system uncertainties.

0.1.5 The Characteristic Polynomial and Nyquist Criterion

For linear time invariant control systems, stability is characterized by the root locations of the characteristic polynomial. Consider the standard feedback control system shown in Figure 0.3. If the plant and controller are linear, time invariant

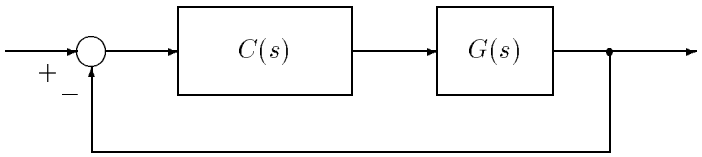

Figure 0.3. Standard feedback system

dynamic systems they can be described by their respective real rational transfer function matrices $G(s)$ and $C(s)$. Suppose that $\mathbf{p}$ is a vector of physical parameters contained in the plant and that $\mathbf{x}$ denotes a vector of adjustable design parameters contained in the controller. For continuous time systems we therefore write

$$C(s) = N_c(s,\mathbf{x})D_c^{-1}(s,\mathbf{x}) \quad \text{and} \quad G(s) = D_p^{-1}(s,\mathbf{p})N_p(s,\mathbf{p})$$

where N_c, D_c, N_p and D_p are polynomial matrices in the complex variable s. The **characteristic polynomial** of the closed loop control system is given by

$$\delta(s,\mathbf{x},\mathbf{p}) = \det\left[D_c(s,\mathbf{x})D_p(s,\mathbf{p}) + N_c(s,\mathbf{x})N_p(s,\mathbf{p})\right].$$

System stability is equivalent to the condition that the characteristic polynomial have all its roots in a certain region $\mathcal{S}$ of the complex plane. For continuous time systems the stability region $\mathcal{S}$ is the open left half, $\mathbb{C}^-$, of the complex plane and for discrete time systems it is the open unit disc, $\mathbb{D}^1$, centered at the origin.

As an example, suppose the controller is a PID controller and has transfer function

$$C(s) = K_P + \frac{K_I}{s} + K_D s$$

and the plant has transfer function $G(s)$ which we write in two alternate forms

$$G(s) = \frac{\mu(s-\alpha)}{(s-\beta)(s-\gamma)} = \frac{a_1 s + a_0}{b_2 s^2 + b_1 s + b_0}. \tag{0.1}$$

The characteristic polynomial is given by

$$\delta(s) = s(s-\beta)(s-\gamma) + \mu(s-\alpha)(K_P s + K_I + K_D s^2)$$

and also by

$$\delta(s) = s(b_2 s^2 + b_1 s + b_0) + (a_1 s + a_0)(K_P s + K_I + K_D s^2).$$

If a state space model of the strictly proper plant and proper controller are employed, we have, setting the external input to zero, the following set of differential equations describing the system in the time domain:

$$\begin{aligned}
&\text{Plant :} && \dot{x}_p = A_p x_p + B_p u \\
& && y = C_p x_p \\
&\text{Controller :} && \dot{x}_c = A_c x_c + B_c y \\
& && u = C_c x_c + D_c y \\
&\text{Closed loop :} && \begin{bmatrix} \dot{x}_p \\ \dot{x}_c \end{bmatrix} = \underbrace{\begin{bmatrix} A_p + B_p D_c C_p & B_p C_c \\ B_c C_p & A_c \end{bmatrix}}_{A_{cl}} \begin{bmatrix} x_p \\ x_c \end{bmatrix}
\end{aligned}$$

and the closed loop characteristic polynomial is given by

$$\delta(s) = \det\left[sI - A_{cl}\right].$$

Similar equations hold in the discrete time case.

If one fixes the parameters at the nominal values $\mathbf{p} = \mathbf{p}^0$ and $\mathbf{x} = \mathbf{x}^0$ the root locations of the characteristic polynomial indicate whether the system is stable or not. In control theory it is known that the nominal plant transfer function can always be stabilized by some fixed controller $\mathbf{x} = \mathbf{x}^0$ unless it contains unstable cancellations. For state space systems the corresponding requirement is that the unstable system modes of A be controllable from u and observable from y.

An alternative and sometimes more powerful method of stability verification is the **Nyquist criterion**. Here one seeks to determine conditions on the open loop system $G(s)C(s)$ that guarantee that the closed loop will be stable. The answer is provided by the Nyquist criterion. Consider the SISO case and introduce the Nyquist contour consisting of the imaginary axis along with a semicircle of infinite radius which together enclose the right half of the complex plane (RHP). The directed plot of $G(s)C(s)$, evaluated as s traverses this contour in the clockwise direction is called the **Nyquist plot**. The Nyquist criterion states that the closed loop is stable if and only if the Nyquist plot encircles the $-1 + j0$ point P times in the counterclockwise direction, where P is the number of RHP poles of $G(s)C(s)$. A similar condition can be stated for multivariable systems. The power of the Nyquist criterion is due to the fact that the Nyquist plot is just the frequency response of the open loop system and can often be measured experimentally, thus eliminating the need for having a detailed mathematical model of the system.

The design of a stabilizing controller for the nominal plant can be accomplished in a variety of ways such as classical control, Linear Quadratic Optimal state feedback implemented by observers, and pole placement controllers. The more difficult and unsolved problem is achieving stability in the presence of uncertainty, namely robust stability.

0.1.6 Uncertainty Models and Robustness

The linear time invariant models that are usually employed are **approximations** which are made to render the design and analysis of complex systems tractable. In reality most systems are nonlinear and a linear time invariant model is obtained by fixing the operating point and linearizing the system equations about it. As the operating point changes so do the parameters of the corresponding linear approximation. Thus there is **significant uncertainty** regarding the "true" plant model, and it is necessary that a controller that stabilizes the system do so for the entire range of expected variations in the plant parameters. In addition other reasonable, but less structured perturbations of the plant model must also be tolerated without disrupting closed loop stability. These unstructured perturbations arise typically from truncating a complex model by retaining only some of the dominant modes, which usually lie in the low frequency range. Therefore unstructured uncertainty is usually operational in a high frequency range. The tolerance of both these types of uncertainty is,qualitatively speaking, the problem of robust stability.

In classical control design the above problem is dealt with by means of the Bode or Nyquist plots and the notions of **gain or phase margin**. It is customary to fix the controller structure based on existing hardware and software constraints and to optimize the design over the numerical values of the fixed number of adjustable controller parameters and any adjustable plant parameters. Thus most often the controller to be designed is constrained to be of the proportional, integral, or PID (proportional, integral and derivative) lag, lead or lead-lag types. Robustness was interpreted to mean that the closed loop system remained stable, despite an adequate amount of uncertainty about the nominal Bode and Nyquist plots, because these represent the measured data from the physical system. This requirement in turn was quantified roughly as the gain and phase margin of the closed loop system.

Gain and Phase Margin

In the gain margin calculation one considers the loop breaking m (see Figure 0.4) and inserts a gain at that point. Thus the open loop plant transfer function $G(s)$ is replaced by its perturbed version $kG(s)$ and one determines the range of excursion of k about its nominal value of 1 for which stability is preserved (Figure 0.5). Likewise in the phase margin calculation one replaces $G(s)$ by $e^{-j\theta}G(s)$ (Figure 0.6) and determines the range of θ for which closed loop stability is preserved.

The importance of these concepts lie in the fact that they provide measures of the robustness of a given designed controller since they indicate the **distance from instability** or **stability margin** of the closed-loop system under gain and phase perturbations of the plant's frequency response. They can be readily determined from the Nyquist or Bode plots and are thus useful in design. However it is to be emphasized that this notion of distance to instability does not extend in an obvious way to the realistic case where *several independent parameters* are simultaneously subject to perturbation. We also remark here that simultaneous gain and phase perturbations constitute a mixed real-complex perturbation problem which has only

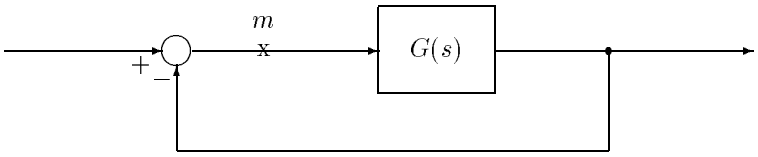

Figure 0.4. Unity feedback system

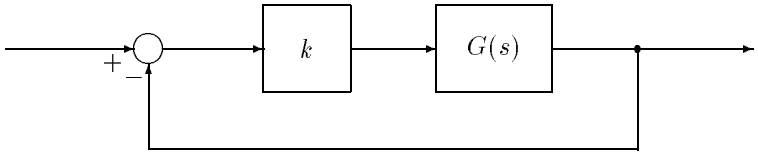

Figure 0.5. Gain margin calculation

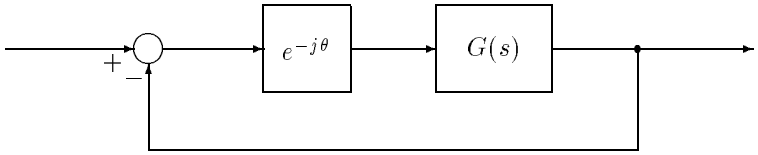

Figure 0.6. Phase margin calculation

recently been effectively analyzed by the techniques described in this book. Finally the analysis of robust performance can be reduced to robust stability problems involving frequency dependent perturbations which cannot be captured by gain and phase margin alone.

Parametric Uncertainty

Consider equation (0.1) in the example treated above. The parametric uncertainty in the plant model may be expressed in terms of the gain μ and the pole and zero locations α, β, γ. Alternatively it may be expressed in terms of the transfer function coefficients a_0, a_1, b_0, b_1, b_2. Each of these sets of plant parameters are subject to variation. The PID gains are, in this example, the adjustable controller parameters. Thus, in the first case, the uncertain plant parameter vector is

$$\mathbf{p}_1 = \begin{bmatrix} \mu & \alpha & \beta & \gamma \end{bmatrix},$$

the controller parameter vector is

$$\mathbf{x} = \begin{bmatrix} K_P & K_I & K_D \end{bmatrix}$$

and the characteristic polynomial is

$$\delta(s, \mathbf{p}_1, \mathbf{x}) = s(s-\beta)(s-\gamma) + \mu(s-\alpha)(K_P s + K_I + K_D s^2).$$

In the second case the uncertain plant parameter vector is

$$\mathbf{p}_2 = \begin{bmatrix} a_0 & a_1 & b_0 & b_1 & b_2 \end{bmatrix}$$

and the characteristic polynomial is

$$\delta(s, \mathbf{p}_2, \mathbf{x}) = s(b_2 s^2 + b_1 s + b_0) + (a_1 s + a_0)(K_P s + K_I + K_D s^2).$$

In most control systems the controller remains fixed during operation while the plant parameter varies over a wide range about a nominal value $\mathbf{p}^0$. The term **robust parametric stability** refers to the ability of a control system to maintain stability despite such large variations. Robustness with respect to parameter variations is necessary because of inherent uncertainties in the modelling process and also because of actual parameter variations that occur during the operation of the system. In the design process, the parameters $\mathbf{x}$ of a controller are regarded as adjustable variables and robust stability with respect to these parameters is also desirable in order to allow for adjustments to a nominal design to accommodate other design constraints. Additionally, it is observed that if *insensitivity* with respect to plant parameters is obtained, it is generally obtained at the expense of *heightened sensitivity* with respect to controller parameters. Thus, in many cases, it may be reasonable to lump the plant and controller parameters into a global parameter vector $\mathbf{p}$, with respect to which the system performance must be evaluated.

The **maximal** range of variation of the parameter $\mathbf{p}$, measured in a suitable norm, for which closed loop stability is preserved is the **parametric stability margin**, and is a measure of the performance of the controller $\mathbf{x}$. In other words

$$\rho_x := \sup \left\{ \alpha : \delta(s, \mathbf{x}, \mathbf{p}) \ \text{ stable}, \quad \|\mathbf{p} - \mathbf{p}^0\| < \alpha \right\}$$

is the parametric stability margin of the system with the controller $\mathbf{x}$. Since ρ represents the *maximal perturbation*, it is indeed a bona fide performance measure to compare the robustness of two proposed controller designs $\mathbf{x}_1$ and $\mathbf{x}_2$. This calculation is an important aid in analysis and design.

Consider a family of polynomials $\delta(s, \mathbf{p})$ of degree n, where the real parameter $\mathbf{p}$ ranges over a connected set Ω. If it is known that one member of the family is stable, a useful technique of verifying robust stability of the family is to ascertain that

$$\delta(j\omega, \mathbf{p}) \neq 0, \quad \text{for all } \mathbf{p} \in \Omega, \quad \omega \in \mathbb{R}.$$

This can also be written as the **zero exclusion condition**

$$0 \notin \delta(j\omega, \Omega), \quad \text{for all } \omega \in \mathbb{R}.$$

The zero exclusion condition is exploited in this text to derive various types of robust stability and performance margins.

We note that the closed loop characteristic polynomial coefficients in the above examples, are linear functions of the controller parameter $\mathbf{x}$. On the other hand, in the first case, the characteristic polynomial coefficients are multilinear functions of the uncertain parameter $\mathbf{p}_1$ whereas in the second representation they are linear functions of the uncertain parameter $\mathbf{p}_2$. In these cases the zero exclusion condition can be verified easily and so can stability margins. Motivated by such examples, the majority of robust parametric stability results developed in this book are directed towards the *linear* and *multilinear* dependency cases, which fortunately, fit many practical applications and also turn out to be mathematically tractable.

The problem of determining $\mathbf{x}$ to achieve stability and a prescribed level of parametric stability margin ρ is the *synthesis* problem, and in a mathematical sense is unsolved. However in an engineering sense, many effective techniques exist for robust parametric controller design. In particular the exact calculation of ρ_x can itself be used in an iterative loop to adjust $\mathbf{x}$ to robustify the system.

Nonparametric and Mixed Uncertainty

Nonparametric uncertainty refers to that aspect of system uncertainty associated with unmodelled dynamics, truncation of high frequency modes, nonlinearities and the effects of linearization and even time-variation and randomness in the system. It is often accounted for by, for instance, replacing the transfer function of the plant $G(s)$ by the perturbed version $G(s) + \Delta G(s)$ (additive unstructured uncertainty), and letting $\Delta G(s)$ range over a ball of H_∞ functions of prescribed radius. The problem then is to ensure that the closed loop remains stable under all such perturbations, and the worst case performance is acceptable in some precise sense.

If the plant transfer function $G(s)$ is not fixed but a function of the parameter $\mathbf{p}$ we have the **mixed uncertainty** problem where the plant transfer function is $G(s, \mathbf{p}) + \Delta G(s)$ and stabilization must be achieved while $\mathbf{p}$ ranges over a ball in parameter space and $\Delta G(s)$ ranges over an H_∞ ball.

Another model of nonparametric uncertainty that is in use in control theory is in the **Absolute Stability problem** where a fixed system is perturbed by a family of **nonlinear feedback gains** that are known to lie in a prescribed sector. By replacing the fixed system with a parameter dependent one we again obtain the more realistic mixed uncertainty problem.

There are now some powerful methods available for quantifying the different amounts of parametric and nonparametric uncertainty that can be tolerated in the above situations. These results in fact extend to the calculation of stability and performance margins for control systems containing several physically distinct interconnected subsystems subjected to mixed uncertainties. Problems of this type

are treated in Chapters 9 - 14 of this book. To complete this overview we briefly describe in the next two subsections the H_∞ and μ approaches to control design.

0.1.7 H_∞ Optimal Control

In this section we attempt to give a very brief sketch of H_∞ optimal control theory and its connection to robust control. A good starting point is the sensitivity minimization problem where a controller is sought so that the weighted sensitivity function or error transfer function, with the nominal plant, is small in the H_∞ norm. In other words we want to solve the problem

$$\inf_C \|W(s)(I + G_0(s)C(s))^{-1}\|_\infty$$

where the infimum is sought over all stabilizing controllers $C(s)$. A crucial step in the solution is the so-called YJBK parametrization of all rational, proper, stabilizing controllers. Write

$$G_0(s) = N(s)D^{-1}(s) = \tilde{D}^{-1}(s)\tilde{N}(s)$$

where $N(s), D(s), \tilde{D}(s), \tilde{N}(s)$ are real, rational, stable, proper (RRSP) matrices with $N(s), D(s)$ being right coprime and $\tilde{D}(s), \tilde{N}(s)$ being left coprime over the ring of RRSP matrices. Let $\tilde{A}(s), \tilde{B}(s)$ be any RRSP matrices satisfying

$$\tilde{N}(s)A(s) + \tilde{D}(s)B(s) = I.$$

The YJBK parametrization states that every stabilizing controller for $G_0(s)$ can be generated by the formula

$$C(s) = (A(s) + D(s)X(s))(B(s) - N(s)X(s))^{-1}$$

by letting $X(s)$ range over all RRSP matrices for which $\det[B(s) - N(s)X(s)] \neq 0$. The weighted sensitivity function minimization problem can now be rewritten as

$$\inf_C \|W(s)(I + G_0(s)C(s))^{-1}\|_\infty = \inf_X \|W(s)(B(s) - N(s)X(s))\tilde{D}(s)\|_\infty$$

where the optimization is now over the free parameter $X(s)$ which is only required to be RRSP.

The form of the optimization problem obtained in the above example is not unique to the sensitivity minimization problem. In fact all closed loop transfer functions of interest can be expressed as affine functions of the free parameter $X(s)$. Thus the generic H_∞ optimization problem that is solved in the literature, known as the model matching problem takes the form

$$\inf_X \|Y_1(s) - Y_2(s)X(s)Y_3(s)\|_\infty$$

where all matrices are RRSP. Various techniques have been developed for the solution of this optimization problem. The most important of these are based on

inner outer factorization of transfer matrices and matrix Nevanlinna-Pick interpolation theory, and its state space counterpart involving the solution of two Riccati equations.

Suppose that $C(s)$ is a compensator stabilizing the nominal plant $G_0(s)$. We ask whether it stabilizes a family of plants $G_0(s) + \Delta G(s)$ around $G_0(s)$. The family in question can be specified in terms of a frequency dependent bound on the admissible, **additive** perturbations of the frequency response $G_0(j\omega)$

$$\|\Delta G(j\omega)\| = \|G(j\omega) - G_0(j\omega)\| \leq |r(j\omega)|$$

where $r(s)$ is a RRSP transfer function. Under the assumption that every admissible $G(s)$ and $G_0(s)$ have the same number of unstable poles it can be easily shown, based on the Nyquist criterion that, $C(s)$ stabilizes the entire family of plants if and only if

$$\|C(j\omega)(I + G_0(j\omega)C(j\omega))^{-1}\| \cdot |r(j\omega)| < 1, \quad \text{for all } \omega \in \mathbb{R}. \tag{0.2}$$

The robust stability question posed above can also be formulated in terms of perturbations which are H_∞ functions and lie in a prescribed ball

$$\mathcal{B} := \{\Delta G(s) : \|\Delta G\|_\infty \leq \alpha\}$$

in which case the corresponding condition for robust stability is

$$\|C(s)(I + G_0(s)C(s))^{-1}\|_\infty < \frac{1}{\alpha}. \tag{0.3}$$

If the perturbation of $G_0(s)$ is specified in the **multiplicative** form $G(s) = G_0(s)(I + \Delta G(s))$ where $\Delta G(s)$ is constrained to lie in the H_∞ ball of radius α, and the number of unstable poles of $G(s)$ remains unchanged, we have the robust stability condition

$$\|(I + C(s)G_0(s))^{-1}C(s)G_0(s)\|_\infty < \frac{1}{\alpha}. \tag{0.4}$$

The conditions (0.2), (0.3), (0.4) can all be derived from the Nyquist criterion by imposing the requirement that the number of encirclements required for stability of the nominal system remain invariant under perturbations. This amounts to verifying that

$$|I + G(j\omega)C(j\omega)| \neq 0, \quad \text{for all } \omega \in \mathbb{R}$$

for deriving (0.2), (0.3), and

$$|I + C(j\omega)G(j\omega)| \neq 0, \quad \text{for all } \omega \in \mathbb{R}$$

for deriving (0.4). The conditions (0.3), (0.4) are examples of the so-called Small Gain Condition and can be derived from a general result called the **Small Gain Theorem**. This theorem states that a feedback connection of stable operators remains stable if and only if the product of the gains is strictly bounded by 1. Thus

a feedback loop consisting of a stable system $G_0(s)$ perturbed by stable feedback perturbations $\Delta \in H_\infty$ remains stable, if and only if

$$\bar{\sigma}(\Delta) = \|\Delta\|_\infty < \frac{1}{\|G_0\|_\infty}.$$

Now consider the question of existence of a robustly stabilizing compensator from the set of compensators stabilizing the nominal plant. From the relations derived above we see that we need to determine in each case if a compensator $C(s)$ satisfying (0.3) or (0.4) respectively exists. By using the YJBK parametrization we can rewrite (0.3) as

$$\inf_X \|(A(s) + D(s)X(s))\tilde{D}(s)\|_\infty < \frac{1}{\alpha}$$

and (0.4) as

$$\inf_X \|(A(s) + D(s)X(s))\tilde{N}(s)\|_\infty < \frac{1}{\alpha}.$$

However these problems are precisely of the form of the H_∞ model matching problem. Therefore the standard machinery can be used to determine whether a robustly stabilizing compensator exists within the family of compensators that stabilize $G_0(s)$. From the above discussion it is clear that in the norm-bounded formulation robust stability and robust performance problems are closely related.

0.1.8 μ Theory

The objective of μ theory is to refine the small gain condition derived in H_∞ optimal control, by imposing constraints on the perturbation structure allowed and thus derive robustness results for a more realistic problem. By introducing fictitious signals and perturbation blocks if necessary it is always possible to formulate robust stability and performance problems in a unified framework as robust stability problems with structured feedback perturbations.

The starting point in this approach is the construction of an artificial stable system $M(s)$, which is scaled and defined so that the uncertain elements, which can be real or complex can be pulled out and arranged as a block diagonal feedback perturbation

$$\Delta = diag[\Delta_1, \Delta_2, \cdots, \Delta_m]$$

with each Δ_i being of size $k_i \times k_i$ repeated m_i times and with $\bar{\sigma}(\Delta_i) \leq 1$. Both performance and robust stability requirements can be reduced in this setting to the condition

$$\det[I + M(j\omega)\Delta(j\omega)] \neq 0, \quad \text{for all } \omega \in \mathbb{R}. \tag{0.5}$$

In the above problem formulation the matrices representing the perturbations Δ_i can be of arbitrary size and can be real or complex and can have repeated parameters. The condition (0.5) is similar to the small gain condition derived earlier with the important difference that the allowed perturbation matrices Δ must respect

the block diagonal structure imposed. In this general setting the verification of the inequality (0.5) is a N-P complete problem and is therefore hard for problems of significant dimension. In the special case where the Δ_i consist only of complex blocks a sufficient condition (necessary and sufficient condition when $n \leq 3$) for the the inequality (0.5) to hold is

$$\inf_D \bar{\sigma}(DM(j\omega)D^{-1}) < 1, \quad \text{for all } \omega \in \mathbb{R} \tag{0.6}$$

where the matrix D is a real block diagonal matrix which possesses the same structure as Δ. The attractive feature about the second problem is that it is convex in D. Techniques of verifying this inequality constitutes the μ analysis machinery.

To proceed to the question of synthesis one can now write out the stable system $M(s)$ in terms of the compensator $C(s)$ or its YJBK representation. This leads to the problem

$$\inf_X \inf_D \|(D[Y_1(s) - Y_2(s)X(s)Y_3(s)]D^{-1})\|_\infty < 1. \tag{0.7}$$

In μ synthesis one attempts to find a solution to the above problem by alternating between D and $X(s)$. This is known as D-K iteration. Whenever D is fixed we have a standard model matching problem which provides the optimum $X(s)$. However the structured matrix D must be chosen to guarantee that the condition (0.7) has a solution and this is difficult. In the case where real parameter uncertainty exists the Δ_i containing real numbers would have to be replaced, in this approach, by complex parameters, which inherently introduces conservatism.

In the next section we give a rapid sketch of the history of control theory tracing the important conceptual developments. This is done partly to make the reader appreciate more fully the significance of the present developments.

0.2 HISTORICAL BACKGROUND

Control theory had its beginnings in the middle of the last century when Maxwell published his paper "On Governors" [178] in 1868. Maxwell's paper was motivated by the need to understand and correct the observed unstable (oscillatory) behaviour of many locomotive steam engines in operation at the time. Maxwell showed that the behaviour of a dynamic system could be approximated in the vicinity of an equilibrium point by a *linear* differential equation. Consequently the stability or instability of such a system could be determined from the location of the roots of the *characteristic equation* of this linear differential equation. The speed of locomotives was controlled by centrifugal governors and so the problem was to determine the design parameters of the controller (flyball mass and inertia, spring tension etc.) to ensure stability of the closed loop system. Maxwell posed this in general terms: Determine the constraints on the coefficients of a polynomial that ensure that the roots are confined to the left half plane, the stability region for continuous time systems.

This problem had actually been already solved for the first time [109] by the French mathematician Hermite in 1856! In his proof, Hermite related the location of

the zeros of a polynomial with respect to the real line to the signature of a particular quadratic form. In 1877, the English physicist E.J. Routh, using the theory of Cauchy indices and of Sturm sequences, gave his now famous algorithm [198] to compute the number k of roots which lie in the right half of the complex plane $\mathrm{Re}(s) \geq 0$. This algorithm thus gave a necessary and sufficient condition for stability in the particular case when $k = 0$. In 1895, A. Hurwitz drawing his inspiration from Hermite's work, gave another criterion [121] for the stability of a polynomial. This new set of necessary and sufficient conditions took the form of n determinantal inequalities, where n is the degree of the polynomial to be tested. Equivalent results were discovered at the beginning of the century by I. Schur [202, 203] and A. Cohn [69] for the discrete-time case, where the stability region is the interior of the unit disc in the complex plane.

One of the main concerns of control engineers had always been the analysis and design of systems that are subjected to various type of uncertainties or perturbations. These may take the form of noise or of some particular external disturbance signals. Perturbations may also arise within the system, in its physical parameters. This latter type of perturbations, termed parametric perturbations, may be the result of actual variations in the physical parameters of the system, due to aging or changes in the operating conditions. For example in aircraft design, the coefficients of the models that are used depends heavily on the flight altitude. It may also be the consequence of uncertainties or errors in the model itself; for example the mass of an aircraft varies between an upper limit and a lower limit depending on the passenger and baggage loading. From a design standpoint, this type of parameter variation problem is also encountered when the *controller structure* is fixed but its parameters are adjustable. The choice of controller structure is usually dictated by physical, engineering, hardware and other constraints such as simplicity and economics. In this situation, the designer is left with a restricted number of controller or design parameters that have to be adjusted so as to obtain a satisfactory behavior for the closed-loop system; for example, PID controllers have only three parameters that can be adjusted.

The characteristic polynomial of a closed-loop control system containing a plant with uncertain parameters will depend on those parameters. In this context, it is necessary to analyse the stability of a *family* of characteristic polynomials. It turns out that the Routh-Hurwitz conditions which are so easy to check for a single polynomial, are almost useless for families of polynomials because they lead to conditions that are highly nonlinear in the unknown parameters. Thus, in spite of the fundamental need for dealing with systems affected by parametric perturbations, engineers were faced from the outset with a major stumbling block in the form of the nonlinear character of the Routh-Hurwitz conditions, which moreover was the only tool available to deal with this problem.

One of the most important and earliest contributions to stability analysis under parameter perturbations was made by Nyquist in his classic paper [184] of 1932 on feedback amplifier stability. This problem arose directly from his work on the problems of long-distance telephony. This was soon followed by the work of Bode [42]

which eventually led to the introduction of the notions of **gain** and **phase margins** for feedback systems. Nyquist's criterion and the concepts of gain and phase margin form the basis for much of the classical control system design methodology and are widely used by practicing control engineers.

The next major period in the evolution of control theory was the period between 1960 and 1975 when the state-variable approach and the ideas of optimal control in the time-domain were introduced. This phase in the theory of automatic control systems arose out of the important new technological problems that were encountered at that time: the launching, maneuvering, guidance and tracking of space vehicles. A lot of effort was expended and rapid developments in both theory and practice took place. Optimal control theory was developed under the influence of many great researchers such as Pontryagin [192], Bellman [25, 26], Kalman [125] and Kalman and Bucy [128]. Kalman [126] introduced a number of key state-variable concepts. Among these were controllability, observability, optimal linear-quadratic regulator (LQR), state-feedback and optimal state estimation (Kalman filtering).

In the LQR problem the dynamics of the system to be controlled are represented by the state space model which is a set of linear first order differential equations

$$\dot{x}(t) = Ax(t) + Bu(t)$$

where $x(t)$ represents the n dimensional state vector at time t. The objective of control is to keep x close to zero without excessive control effort. This objective is to be achieved by minimizing the quadratic cost function

$$I = \int_0^\infty (x'(t)Qx(t) + u'(t)Ru(t)dt.$$

The solution is provided by the **optimal state feedback** control

$$u(t) = Fx(t)$$

where the state feedback matrix F is calculated from the algebraic Riccati equation:

$$A'P + PA + Q - PBR^{-1}B'P = 0$$

$$F = -R^{-1}B'P.$$

The optimal state feedback control produced by the LQR problem was guaranteed to be stabilizing for any performance index of the above form, provided only that the pair (Q, A) is detectable and (A, B) is stabilizable. This means that the characteristic roots of the closed loop system which equal the eigenvalues $\sigma(A + BF)$ of $A + BF$ lie in the left half of the complex plane.

At this point it is important to emphasize that, essentially, the focus was on optimality of the nominal system and the problem of plant uncertainty was largely ignored during this period. One notable exception was to be found in a 1963 paper [244] by Zames introducing the concept of the "small gain" principle, which

plays such a key role in robust stability criteria today. Another was in a 1964 paper by Kalman [127] which demonstrated that for SISO (single input-single output) systems the optimal LQR state-feedback control laws had some very strong guaranteed robustness properties, namely an infinite gain margin and a 60 degree phase margin, which in addition were independent of the particular quadratic index chosen. This is illustrated in Figure 0.7 where the state feedback system designed via LQR optimal control has the above guaranteed stability margins at the loop breaking point m.

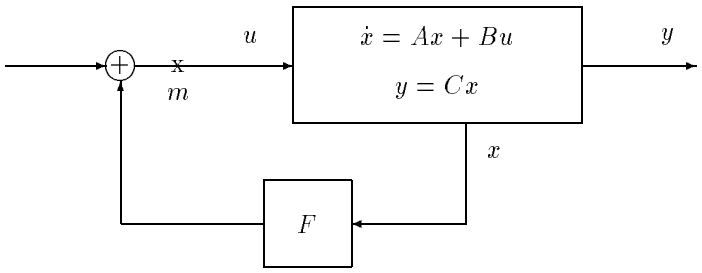

Figure 0.7. State feedback configuration

In implementations, the state variables, which are generally unavailable for direct measurement, would be substituted by their "estimates" generated by an observer or Kalman filter. This takes the form

$$\dot{\hat{x}}(t) = A\hat{x}(t) + Bu(t) + L(y(t) - C\hat{x}(t))$$

where $\hat{x}(t)$ is the estimate of the state $x(t)$ at time t. From the above equations it follows that

$$(\dot{x} - \dot{\hat{x}})(t) = (A - LC)(x - \hat{x})(t)$$

so that the estimation error converges to zero, regardless of initial conditions and the input $u(t)$, provided that L is chosen so that $A - LC$ has stable eigenvalues.

To close the feedback loop the optimal feedback control $u = Fx$ would be replaced by the **suboptimal** observed state feedback control $\hat{u} = F\hat{x}$. It is easily shown that the resulting closed loop system has characteristic roots which are precisely the eigenvalues $A + BF$ and those of $A - LC$. This means that the "optimal" eigenvalues were preserved in an output feedback implementation and suggested that the design of the state estimator could be decoupled from that of the optimal controller. This and some related facts came to be known as the **separation principle**.

Invoking this separation principle, control scientists were generally led to believe that the extraordinary robustness properties of the LQR state feedback design were preserved when the control was implemented as an output feedback. We depict

this in Figure 0.8 where the stability margin at the point m continues to equal that obtained in the state feedback system.

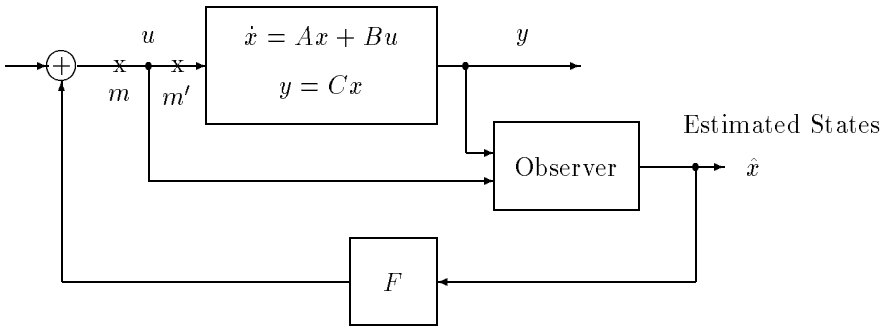

Figure 0.8. Observed state feedback configuration

In 1968 Pearson [187] proposed a scheme whereby an output feedback compensator could be designed to optimize the closed loop dynamics in the LQR sense, by including the requisite number of integrators in the optimal control problem formulation *from the outset*. The philosophy underlying this approach is that the system that is *implemented should also be optimal* and not suboptimal as in the previous observed state feedback case. In [52] Brasch and Pearson showed that arbitrary pole placement could be achieved in the closed loop system by a controller of order no higher than the controllability index or the observability index.

In the late 1960's and early 1970's the interest of control theorists turned to the servomechanism problem. Tracking and disturbance rejection problems with persistent signals such as steps, ramps and sinusoids could not be solved in an obvious way by the existing methods of optimal control. The reason is that unless the proper signals are included in the performance index the cost function usually turns out to be unbounded. In [35] and [36] Bhattacharyya and Pearson gave a solution to the multivariable servomechanism problem. The solution technique in [36] was based on an **output regulator problem** formulated and solved by Bhattacharyya, Pearson and Wonham [37] using the elegant geometric theory of linear systems [237] being developed at that time by Wonham. It clarified the conditions under which the servo problem could be solved by relating it to the stabilization of a suitably defined error system. The robust servomechanism problem, based on error feedback, was treated by Davison [79], and later Francis and Wonham [96] developed the **Internal Model Principle** which established the *necessity* of using error driven controllers, and consequently internal models with suitable redundancy, for reliable tracking and disturbance rejection.

In Ferreira [93] and Ferreira and Bhattacharyya [94] the multivariable servomechanism problem was interpreted as a problem wherein the exogenous signal poles are

to be assigned as the zeroes of the error transfer functions. The notion of **blocking zeros** was introduced in [94] and it was shown that robust servo performance, which is equivalent to robust assignment of blocking zeros to the error transfer function, could be achieved by employing error driven controllers containing as poles, in each error channel, the poles of the exogenous signal generators.

It was not realized until the late 1970's that the separation principle of state feedback and LQR control theory really applies to the *nominal system* and is *not* valid for the perturbed system. This fact was dramatically exposed in a paper by Doyle in 1978 [87] who showed by a counterexample that all the guaranteed robustness properties (gain and phase margins) of the LQR design vanished in an output feedback implementation. Referring to the Figure 0.8 we emphasize that the stability margins that are relevant are those that hold at the point m' and *not* those that hold at m. In other words injecting uncertainties at m implies that the observer is aware of the perturbations in the system, which is unrealistic. On the other hand stability margins at m' reflect the realistic situation, that uncertainty in the plant model is unknown to the observer. Doyle's observation really brought back to the attention of the research community the importance of designing feedback controllers which can be *assured* to have desirable robustness properties, and thus a renewed interest appeared in the problem of plant uncertainty. It was realized that the state space based approach via LQR optimal control was inadequate for robust stability. The geometric approach of Wonham [237], which had proved successful in solving many control synthesis problems, was also inadequate for handling robustness issues because it assumed exact knowledge of the plant.

At about this time, significant results were being reported on the analysis of multivariable systems in the frequency domain. In particular, the concept of coprime matrix fraction description of multivariable systems was introduced as a design tool by Youla, Jabr and Bongiorno [241, 242] and Desoer, Liu, Murray and Saeks [81]. In [242] and Kucera [156] a parameterization of all stabilizing controllers was given and this parameterization (which is commonly referred to as the *YJBK parameterization*) has come to play a fundamental role in the theory of robust stabilization of multivariable systems. Also, the Nyquist stability criterion was generalized to multivariable systems by Rosenbrock [197], and Mac Farlane and Postlethwaite [166].

This confluence of interests naturally led to a frequency domain formulation for the robust control problem. More precisely, uncertainty or perturbations in a system with transfer function $G(s)$ were modelled as,

i) $G(s) \longrightarrow G(s)\,(I + \Delta G(s))$, or

ii) $G(s) \longrightarrow G(s) + \Delta G(s)$ with $\|\Delta G(s)\| < \alpha$.

Here $\|\Delta G(s)\|$ denotes a suitable norm in the space of stable transfer function matrices, and case i) represents a *multiplicative* perturbation whereas case ii) represents an *additive* perturbation. From our present perspective, this type of perturbation in a plant model will be referred to as *unstructured* or *norm bounded perturbations*. One reason for this designation is that the norms which are commonly employed in

i) and ii) completely discard all the phase information regarding the perturbation. Also, there is no obvious connection between bounds on the coefficients or other parameters of $G(s)$ and the transfer function norm bounds.

The solution to the robust stabilization problem, namely the problem of determining a controller for a prescribed level of unstructured perturbations, was given in 1984 by Kimura [148] for the case of SISO systems. The multivariable robust stabilization problem was solved in 1986 by Vidyasagar and Kimura [234] and Glover [103].

These results were in fact a by-product of an important line of research initiated by Zames [245] concerning the optimal disturbance rejection problem which can be summarized as the problem of designing a feedback controller which minimizes the worst case effect over a class of disturbances on the system outputs. This problem is mathematically equivalent to the so-called sensitivity minimization problem or to the problem of minimizing the norm of the error transfer function. Note that the idea of designing a feedback control so as to reduce the sensitivity of the closed-loop is a very classical idea which goes back to the work of Bode [42].

In his seminal paper [245] of 1981, Zames proposed the idea of designing feedback controllers which do not merely reduce the sensitivity of the closed-loop system but actually optimize the sensitivity in an appropriate sense. The crucial idea was to consider the sensitivity function as a map between spaces of bounded energy signals and to minimize its induced operator norm. This translates to the physical assumption that the disturbance signal that hits each system is precisely the worst disturbance for *that* system.

The induced operator norm for a convolution operator between spaces of finite energy signals is the so-called H_∞ norm which derives its name from the theory of Hardy spaces in functional analysis. Zames' fundamental paper thus introduced for the first time the H_∞ approach to control system design. In this same paper the solution of the H_∞ sensitivity minimization problem was given for the special case of a system with a single right half plane zero. This paper led to a flurry of results concerning the solution of the H_∞ optimal sensitivity minimization problem or of the H_∞ optimal disturbance rejection problem. Francis and Zames [97] gave a solution for the SISO case, and the multivariable problem was solved by Doyle [89], Chang and Pearson [53] and Safonov and Verma [201]. In [90, 88] Doyle showed the equivalence between robust performance and sensitivity in H_∞ problems. A state space solution to the H_∞ disturbance rejection problem was given by Doyle, Glover, Khargonekar and Francis [91].

Following the same norm optimization design philosophy, Vidyasagar proposed in [233] the L_1 optimal disturbance rejection problem. In this problem, the disturbances that affect the system are no longer bounded energy (L_2) signals but bounded amplitude (L_∞) signals. The L_1 optimal disturbance rejection problem was solved by Dahleh and Pearson in 1987 [73].

0.3 THE PARAMETRIC THEORY

It is important to point out that during the 1960's and 70's the problem of stability under large parameter uncertainty was almost completely ignored by controls researchers. The notable exceptions are Horowitz [120] who in 1963 proposed a quantitative approach to feedback theory, and Šiljak [211] who advocated the use of parameter plane and optimization techniques for control system analysis and design under parameter uncertainty. This was mainly due to the perception that the real parametric robust stability problem was an impossibly difficult one, precluding neat results and effective computational techniques. Supposedly, the only way to deal with it would be to complexify real parameters and to overbound the uncertainty sets induced in the complex plane by real parameter uncertainty with complex plane discs.

The situation changed dramatically with the advent of a remarkable theorem [143] due to the Russian control theorist V.L. Kharitonov. Kharitonov's Theorem showed that the left half plane (Hurwitz) stability of a family of polynomials of fixed but arbitrary degree corresponding to an entire box in the coefficient space could be verified by checking the stability of four prescribed vertex polynomials. The result is extremely appealing because the apparently impossible task of verifying the stability of a continuum of polynomials could now be carried out by simply using the Routh-Hurwitz conditions on 4 fixed polynomials. The number 4 is also surprising in view of the fact that a) for polynomials of degree n the box of polynomials in question has 2^{n+1} vertices in general and b) the Hurwitz region is not convex or even connected. From a computational point of view the fixed number 4 of test polynomials independent of the dimension of the parameter space is very attractive and dramatically counterbalances the usual arguments regarding increase in complexity with dimension.

Kharitonov's work was published in 1978 in the Russian technical literature but his results remained largely unknown for several years partly due to the fact that Kharitonov's original proofs were written in a very condensed form.

The appearance of Kharitonov's Theorem led to a tremendous resurgence of interest in the study of robust stability under **real parametric uncertainty**. For the first time since Routh's and Hurwitz's results, researchers started to believe that the robust control problem for real parametric uncertainties could be approached without conservatism and overbounding, and with computational efficiency built right into the theory. Moreover, it has also revealed the *effectiveness* and *transparency* of methods which exploit the algebraic and geometric properties of the stability region in parameter space, as opposed to blind formulation of an optimization problem. This has led to an outpouring of results in this field over the last few years.

The first notable result following Kharitonov's Theorem is due to Soh, Berger and Dabke [214] in 1985 who, in a sense, adopted a point of view opposite to Kharitonov's. Starting with an already stable polynomial $\delta(s)$, they gave a way to compute the radius of the largest stability ball in the space of polynomial *coefficients* around δ. In their setting, the vector space of all polynomials of degree less than

or equal to n is identified with $\mathbb{R}^{n+1}$ equipped with its Euclidean norm, and the largest stability hypersphere is defined by the fact that every polynomial within the sphere is stable whereas at least one polynomial on the sphere itself is unstable.

The next significant development in this field was a paper by Bartlett, Hollot and Lin [21] which considered a family of polynomials whose coefficients vary in an arbitrary polytope of $\mathbb{R}^{n+1}$, with its edges not necessarily parallel to the coordinate axes as in Kharitonov's problem. They proved that the root space of the entire family is bounded by the root loci of the exposed edges. In particular the entire family is stable if and only if all the edges are proved to be stable. Moreover this result applies to general stability regions and is not restricted to Hurwitz stability.

In 1987 Biernacki, Hwang and Bhattacharyya [40] extended the results of [214] and calculated the largest stability ball in the space of *parameters* of the plant transfer function itself. This work was done for the case of a plant with a single input and multiple outputs, or the dual case of a plant with multiple inputs and a single output, and a numerical procedure was given to compute the stability radius. These and other results on parametric robust stability were reported in a monograph [29] by Bhattacharyya.

In 1989, Chapellat and Bhattacharyya [58] proved the Generalized Kharitonov Theorem (GKT) which gave necessary and sufficient conditions for robust stability of a closed loop system containing an interval plant in the forward path. An interval plant is a plant where each transfer function coefficient can vary in a prescribed interval. The solution provided by GKT reveals an extremal set of line segments from which all the important parameters of the behaviour of the entire set of uncertain systems can be extracted. The number of extremal line segments is also *independent* of the number of uncertain parameters.

The extremal set characterizes robust stability under parametric uncertainty, worst case parametric stability margin, frequency domain plots such as Bode and Nyquist envelopes, worst case H_∞ stability margins and mixed uncertainty stability and performance margins. The characterization enjoys the *built-in computational efficiency* of the theory and provides closed form or almost closed form solutions to entire classes of control design problems that could previously only be approached as optimization problems on a case by case basis. In a series of recent papers the Generalized Kharitonov Theorem has been established as a fundamental and unifying approach to control system design under uncertainty. In combination with the recently developed highly efficient computational techniques of determining stability margins, such as the Tsypkin-Polyak locus [225, 226] and those based on the Mapping Theorem of Zadeh and Desoer [243], the GKT provides the control engineer with a powerful set of techniques for analysis and design.

The above fundamental results have laid a solid foundation. The future development of the theory of robust stability and control under parametric and mixed perturbations rests on these. The objective of our book is to describe these results for the use of students of control theory, practicing engineers and researchers.

0.4 DISCUSSION OF CONTENTS

We begin Chapter 1 with a new look at classical stability criteria for a single polynomial. We consider a family of polynomials where the coefficients depend continuously on a set of parameters, and introduce the **Boundary Crossing Theorem** which establishes, roughly, that along any continuous path in parameter space connecting a stable polynomial to an unstable one, the first encounter with instability must be with a polynomial which has unstable roots only on the stability boundary. This is a straightforward consequence of the continuity of the roots of a polynomial with respect to its coefficients. Nevertheless, this simple theorem serves as the unifying idea for the entire subject of robust parametric stability as presented in this book. In Chapter 1 we give simple derivations of the **Routh** and **Jury** stability tests as well the **Hermite-Biehler Theorem** based on this result. The results developed in the rest of the chapters depend directly or indirectly on the Boundary Crossing Theorem.

In Chapter 2 we study the problem of determining the stability of a **line segment** joining a pair of polynomials. The pair is said to be **strongly stable** if the entire segment is stable. This is the simplest case of robust stability of a parametrized family of polynomials. A first characterization is obtained in terms of the **Bounded Phase Lemma** which is subsequently generalized to general polytopic families in Chapter 4. We then develop necessary and sufficient conditions for strong stability in the form of the **Segment Lemma** treating both the Hurwitz and Schur cases. We then establish the **Vertex Lemma** which gives some useful sufficient conditions for strong stability of a pair based on certain standard forms for the difference polynomial. We also discuss the related notion of **Convex Directions**. The Segment and Vertex Lemmas are used in proving the Generalized Kharitonov Theorem in Chapter 7.

In Chapter 3 we consider the problem of determining the robust stability of a parametrized family of polynomials where the parameter is just the set of polynomial coefficients. This is the problem treated by Soh, Berger and Dabke in 1985. Using orthogonal projection we derive quasi-closed form expressions for the **real stability radius in coefficient space** in the Euclidean norm. We then describe the **Tsypkin-Polyak locus** which determines the stability radius in the ℓ_p norm for arbitrary p in a convenient graphical form. Then we deal with a family of complex polynomials where each coefficient is allowed to vary in a **disc** in the complex plane and give a constructive solution to the problem of robust stability determination in terms of the H_∞ norms of two transfer functions. The proof relies on a lemma which gives a robust Hurwitz characterization of the H_∞ norm which is useful in its own right.

In Chapter 4 we extend these results to the parameter space concentrating on the case of linear parametrization, where the polynomial coefficients are affine linear functions of the real parameter vector $\mathbf{p}$. We develop the procedure for calculating the **real parametric stability margin** measured in the ℓ_1, ℓ_2 and ℓ_∞ norms. The main conceptual tool is once again the Boundary Crossing Theorem and its compu-

tational version the **Zero Exclusion Principle**. We consider the special case in which **p** varies in a box. For linearly parametrized systems this case gives rise to a **polytope of polynomials** in coefficient space. For such families we establish the important fact that stability is determined by the **exposed edges** and in special cases by the vertices. It turns out that this result on exposed edges also follows from a more powerful result, namely the Edge Theorem, which is established in Chapter 6. Here we show that this stability testing property of the exposed edges carries over to complex polynomials as well as to quasipolynomials which arise in control systems containing time-delay. A computationally efficient solution to testing the stability of general polytopic families is given by the **Bounded Phase Lemma**, which reduces the problem to checking the maximal phase difference over the vertex set, evaluated along the boundary of the stability region. The **Tsypkin-Polyak locus** for stability margin determination is also described for such polytopic systems. We close the chapter by giving an extension of the theory of disc polynomials developed in Chapter 3 to the case of **linear disc polynomials** where the characteristic polynomial is a linear combination with polynomial coefficients of complex coefficients which can vary in prescribed discs in the complex plane.

In Chapter 5 we turn our attention to the robust stability of **interval polynomial** families. We state and prove **Kharitonov's Theorem** which deals with the Hurwitz stability of such families, treating both the real and the complex cases. This theorem is interpreted as a generalization of the Hermite-Biehler Interlacing Theorem and a simple derivation is also given using the Vertex Lemma of Chapter 2. An important **extremal property** of the Kharitonov polynomials is established, namely that the worst case real stability margin in the coefficient space over an interval family occurs *precisely* on the Kharitonov vertices. This fact is used to give an application of Kharitonov polynomials to **robust state feedback stabilization**. Finally the problem of **Schur stability of interval polynomials** is studied. Here it is established that a subset of the exposed edges of the underlying interval box suffices to determine the stability of the entire family.

In Chapter 6 we state and prove the **Edge Theorem**. This important result shows that the **root space boundary** of a polytope of polynomials is exactly determined by the root loci of the exposed edges. Since each exposed edge is a one parameter family of polynomials, this result allows us to constructively determine the root space of a family of linearly parametrized systems. This is an effective tool in control system analysis and design.

In Chapter 7 we generalize Kharitonov's problem by considering the robust Hurwitz stability of a linear combination, with polynomial coefficients, of interval polynomials. This formulation is motivated by the problem of robust stability of a feedback control system containing a fixed compensator and an interval plant in its forward path and we refer to such systems as linear interval systems. The solution is provided by the **Generalized Kharitonov Theorem** which shows that for a compensator to robustly stabilize the system it is sufficient that it stabilizes a prescribed set of **line segments** in the plant parameter space. Under special conditions on the compensator it suffices to stabilize the **Kharitonov vertices**. These

line segments, labeled **extremal segments**, play a fundamental characterizing role in later chapters.

In Chapter 8 we develop some **extremal frequency domain properties** of linear interval control systems. The extremal segments are shown to possess boundary properties that are useful for generating the **frequency domain templates** and the **Nyquist, Bode and Nichols envelopes** of linear interval systems. The **extremal gain and phase margins** of these systems occur on these segments. We show how these concepts are useful in extending classical design techniques to linear interval systems by giving some examples of **robust parametric classical control design**.

In Chapter 9 we consider mixed uncertainty problems, namely the **robust stability and performance** of control systems subjected to parametric uncertainty as well as unstructured perturbations. The parameter uncertainty is modeled through a linear interval system whereas two types of unstructured uncertainty are considered, namely H^∞ norm bounded uncertainty and nonlinear sector bounded perturbations. The latter class of problems is known as the Absolute Stability problem. We present **robust versions** of the **Small Gain Theorem** and the **Absolute Stability Problem** which allow us to quantify the worst case parametric or unstructured stability margins that the closed loop system can tolerate. This results in the robust versions of the well-known Lur'e criterion, Popov criterion and the Circle criterion of nonlinear control theory.

Chapters 10 and 11 deal with the robust stability of polynomials containing uncertain interval parameters which appear affine multilinearly in the coefficients. The main tool to solve this problem is the **Mapping Theorem** described in the 1963 book of Zadeh and Desoer. We state and prove this theorem and apply it to the robust stability problem. In Chapter 11 we continue to develop results on **multilinear interval systems** extending the Generalized Kharitonov Theorem and the frequency domain properties of Chapters 7, 8 and 9 to the multilinear case.

In Chapter 12 we deal with parameter perturbations in **state space models**. The same mapping theorem is used to give an effective solution to the robust stability of state space systems under real parametric interval uncertainty. This is followed by some techniques for calculating **robust parametric stability regions using Lyapunov theory**. We also include results on the calculation of the **real and complex stability radius** defined in terms of the operator (induced) norm of a feedback matrix as well as some results on the Schur stability of nonnegative interval matrices.

In Chapter 13 we describe some **synthesis techniques**. To begin with we demonstrate a **direct synthesis** procedure whereby any minimum phase interval plant of order n, with m zeros can be robustly stabilized by a fixed stable minimum phase compensator of order $n - m - 1$. Then we show, by examples, how standard results from H^∞ theory such as the Small Gain Theorem, Nevanlinna-Pick interpolation and the two Riccati equation approach can be exploited to deal with parametric perturbations using the extremal properties developed earlier.

In Chapter 14 some examples of **interval identification and design** applied

to two experimental space structures are described as an application demonstrating the practical use of the theory described in the book.

The contents of the book have been used in a one-semester graduate course on Robust Control. The numerical exercises given at the end of the chapters should be worked out for a better understanding of the theory. They can be solved by using a MATLAB based Parametric Robust Control Toolbox available separately. A demonstration diskette based on this ToolBox is included in this book, and includes solutions to some of the examples.

0.5 NOTES AND REFERENCES

Most of the important papers on robust stability under norm bounded perturbations are contained in the survey volume [83] edited by Dorato in 1987. Dorato and Yedavalli [86] have also edited in 1990, a volume of papers collected from IEEE Conferences which contains a large collection of papers on parametric stability. Šiljak [212] gave a (1989) survey of parametric robust stability. Many of the results presented in this book were obtained in the M.S. (1987) and Ph.D. (1990) theses [54, 55] of H. Chapellat and the Ph.D (1986) thesis [131] of L. H. Keel. The 1987 book [29] of Bhattacharyya, and the recent books [2] and [14] by Ackermann and Barmish respectively concentrate on the parametric approach. The monograph [85] by Dorato, Fortuna and Muscato, and the 1985 book [232] of Vidyasagar all deal with H_∞ optimization and the book [84] by Dorato, Abdallah and Cerone deals with Linear Quadratic Optimal Control. The book [167] by Maciejowski is a design oriented textbook on control systems concentrating on robustness issues. In the book of Boyd and Barratt [51] several control design problems are treated as convex optimization problems. The proceedings [180, 32, 172] of several International Workshops on Robust Control held since 1988, and edited respectively by Milanese, Tempo and Vicino [180], Hinrichsen and Mårtensson [110], Bhattacharyya and Keel [32] and Mansour, Balemi and Truöl [172], are also useful references.

Chapter 1

STABILITY THEORY VIA THE BOUNDARY CROSSING THEOREM

In this chapter we introduce the Boundary Crossing Theorem for polynomials. Although intuitively obvious, this theorem, used systematically, can lead to many useful and nontrivial results in stability theory. In fact it plays a fundamental role in most of the results on robust stability. We illustrate its usefulness here by using it to give extremely simple derivations of the Hermite-Biehler Theorem and of the Routh and Jury tests.

1.1 INTRODUCTION

This chapter develops some results on stability theory for a given fixed polynomial. This theory has been extensively studied and has a vast body of literature. Instead of giving a complete account of all existing results we concentrate on a few fundamental results which will be used extensively in the remainder of this book to deal with stability problems related to families of polynomials. These results are presented in a unified and elementary fashion and the approach consists of a systematic use of the following fact: Given a parametrized family of polynomials and any continuous path in the parameter space leading from a stable to an unstable polynomial, then, the first unstable point that is encountered in traversing this path corresponds to a polynomial whose unstable roots lie on the boundary (and not in the interior) of the instability region in the complex plane.

The above result, called the Boundary Crossing Theorem, is established rigorously in the next section. The proof follows simply from the continuity of the roots of a polynomial with respect to its coefficients. The consequences of this result, however, are quite far reaching, and this is demonstrated in the subsequent sections by using it to give simple derivations of the classical Hermite-Biehler Theorem, the Routh test for left half plane stability and the Jury test for unit disc stability.

The purpose of this chapter is to give a simple exposition of these fundamental results which makes them particularly easy to learn and understand. Moreover the Boundary Crossing Theorem will play an important role in later chapters dealing with Kharitonov's Theorem and its generalization, the stability of families of polynomials, and in the calculation of stability margins for control systems.

Many results of stability theory extend far beyond the realm of polynomials. The Hermite-Biehler Theorem, in particular, extends to a vast class of entire functions. In the last section of this chapter some of these extensions are briefly overviewed, with an emphasis on those results which are more directly related to problems in control theory.

1.2 THE BOUNDARY CROSSING THEOREM

We begin with the well known Principle of the Argument of complex variable theory. Let $\mathcal{C}$ be a simple closed contour in the complex plane and $w = f(z)$ a function of the complex variable z, which is analytic on $\mathcal{C}$. Let Z and P denote the number of zeros and poles, respectively, of $f(z)$ contained in $\mathcal{C}$. Let $\Delta_C \arg[f(z)]$ denote the net change of argument (angle) of $f(z)$ as z transverses the contour $\mathcal{C}$.

Theorem 1.1 (Principle of the Argument)

$$\Delta_C \arg[f(z)] = 2\pi(Z - P) \tag{1.1}$$

An important consequence of this result is the well known theorem of Rouché.

Theorem 1.2 (Rouché's Theorem)
Let $f(z)$ and $g(z)$ be two functions which are analytic inside and on a simple closed contour $\mathcal{C}$ in the complex plane. If

$$|g(z)| < |f(z)| \tag{1.2}$$

for any z on $\mathcal{C}$, then $f(z)$ and $f(z) + g(z)$ have the same number (multiplicities included) of zeros inside $\mathcal{C}$.

Proof. Since $f(z)$ cannot vanish on $\mathcal{C}$, because of (1.2), we have

$$\begin{aligned}\Delta_C \arg[f(z) + g(z)] &= \Delta_C \arg\left\{ f(z)\left[1 + \frac{g(z)}{f(z)}\right]\right\} \\ &= \Delta_C \arg[f(z)] + \Delta_C \arg\left[1 + \frac{g(z)}{f(z)}\right].\end{aligned} \tag{1.3}$$

Moreover, since

$$\left|\frac{g(z)}{f(z)}\right| < 1$$

for all $z \in \mathcal{C}$, the variable point

$$w = 1 + \frac{g(z)}{f(z)}$$

stays in the disc $|w-1|<1$ as z describes the curve $\mathcal{C}$. Therefore w cannot wind around the origin, which means that

$$\Delta_C \arg\left[1+\frac{g(z)}{f(z)}\right]=0. \tag{1.4}$$

Combining (1.3) and (1.4), we find that

$$\Delta_C \arg\left[f(z)+g(z)\right]=\Delta_C \arg[f(z)].$$

Since $f(z)$ and $g(z)$ are analytic in and on $\mathcal{C}$ the theorem now follows as an immediate consequence of the argument principle. ♣

Note that the condition $|g(z)|<|f(z)|$ on $\mathcal{C}$ implies that neither $f(z)$ nor $f(z)+g(z)$ may have a zero on $\mathcal{C}$. Theorem 1.2 is just one formulation of Rouché's Theorem but it is sufficient for our purposes. The next theorem is a simple application of Rouché's Theorem. It is however most useful since it applies to polynomials.

Theorem 1.3 *Let*

$$P(s)=p_0+p_1s+\cdots+p_ns^n=\prod_{j=1}^{m}(s-s_j)^{t_j},\ p_n\neq 0, \tag{1.5}$$

$$Q(s)=(p_0+\epsilon_0)+(p_1+\epsilon_1)s+\cdots+(p_n+\epsilon_n)s^n, \tag{1.6}$$

and consider a circle $\mathcal{C}_k$, of radius r_k, centered at s_k which is a root of $P(s)$ of multiplicity t_k. Let r_k be fixed in such a way that,

$$0<r_k<\min|s_k-s_j|,\quad \text{for}\quad j=1,2,\cdots,k-1,k+1,\cdots,m. \tag{1.7}$$

Then, there exists a positive number ϵ, such that $|\epsilon_i|\leq\epsilon$, for $i=0,1,\cdots,n$, implies that $Q(s)$ has precisely t_k zeros inside the circle $\mathcal{C}_k$.

Proof. $P(s)$ is non-zero and continuous on the compact set $\mathcal{C}_k$ and therefore it is possible to find $\delta_k>0$ such that

$$|P(s)|\geq\delta_k>0,\quad \text{for all } s\in\mathcal{C}_k. \tag{1.8}$$

On the other hand, consider the polynomial $R(s)$, defined by

$$R(s)=\epsilon_0+\epsilon_1s+\cdots+\epsilon_ns^n. \tag{1.9}$$

If s belongs to the circle $\mathcal{C}_k$, then

$$\begin{aligned}|R(s)|&\leq\sum_{j=0}^{n}|\epsilon_j||s^j|\leq\sum_{j=0}^{n}|\epsilon_j|\big(|s-s_k|+|s_k|\big)^j\\&\leq\epsilon\underbrace{\sum_{j=0}^{n}\big(r_k+|s_k|\big)^j}_{M_k}.\end{aligned}$$

Thus if ϵ is chosen so that $\epsilon < \frac{\delta_k}{M_k}$, it is concluded that

$$|R(s)| < |P(s)| \quad \text{for all } s \text{ on } \mathcal{C}_k, \tag{1.10}$$

so that by Rouché's Theorem, $P(s)$ and $Q(s) = P(s) + R(s)$ have the same number of zeros inside $\mathcal{C}_k$. Since the choice of r_k ensures that $P(s)$ has just one zero of multiplicity t_k at s_k, we see that $Q(s)$ has precisely t_k zeros in $\mathcal{C}_k$. ♣

Corollary 1.1 *Fix m circles $\mathcal{C}_1, \cdots, \mathcal{C}_m$, that are pairwise disjoint and centered at $s_1, s_2, \cdots, s_m$ respectively. By repeatedly applying the previous theorem, it is always possible to find an $\epsilon > 0$ such that for any set of numbers $\{\epsilon_0, \cdots, \epsilon_n\}$ satisfying $|\epsilon_i| \leq \epsilon$, for $i = 0, 1, \cdots, n$, $Q(s)$ has precisely t_j zeros inside each of the circles $\mathcal{C}_j$.*

Note, that in this case, $Q(s)$ always has $t_1 + t_2 + \cdots + t_m = n$ zeros and must remain therefore of degree n, so that necessarily $\epsilon < |p_n|$. The above theorem and corollary lead to our main result, the Boundary Crossing Theorem.

Let us consider the complex plane C and let $\mathcal{S} \subset C$ be any given open set. We know that $\mathcal{S}$, its boundary $\partial\mathcal{S}$ together with the interior $\mathcal{U}^o$ of the closed set $\mathcal{U} = C - \mathcal{S}$ form a partition of the complex plane, that is

$$\mathcal{S} \cup \partial\mathcal{S} \cup \mathcal{U}^o = C, \qquad \mathcal{S} \cap \mathcal{U}^o = \mathcal{S} \cap \partial\mathcal{S} = \partial\mathcal{S} \cap \mathcal{U}^o = \emptyset. \tag{1.11}$$

Assume moreover that each one of these three sets is non-empty. These assumptions are very general. In stability theory one might choose for $\mathcal{S}$ the open left half plane $\mathcal{C}^-$ (for continuous-time systems) or the open unit disc $\mathcal{D}$ (for discrete-time systems) or suitable subsets of these, as illustrated in Figure 1.1.

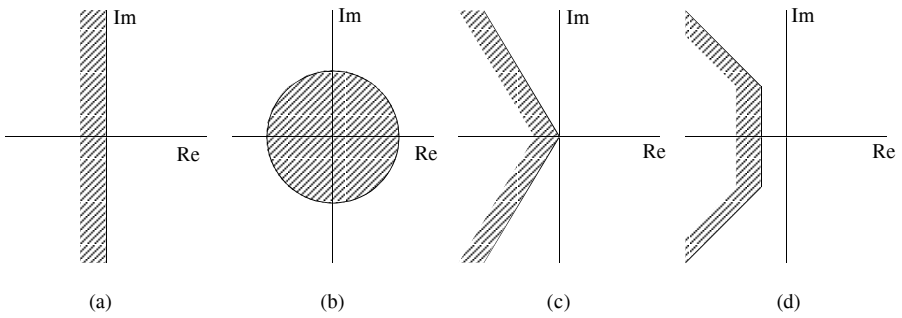

Figure 1.1. Some typical stability regions

Consider a family of polynomials $P(\lambda, s)$ satisfying the following assumptions.

Assumption 1.1. $P(\lambda, s)$ is a family of polynomials of

1) fixed degree n, (invariant degree),

2) continuous with respect to λ on a fixed interval $I = [a, b]$.

In other words, a typical element of $P(\lambda, s)$ can be written as

$$P(\lambda, s) = p_0(\lambda) + p_1(\lambda)s + \cdots + p_n(\lambda)s^n, \tag{1.12}$$

where $p_0(\lambda), p_1(\lambda), \cdots, p_n(\lambda)$ are continuous functions of λ on I and where $p_n(\lambda) \neq 0$ for all $\lambda \in I$. From the results of Theorem 1.3 and its corollary, it is immediate that in general, for any open set $\mathcal{O}$, the set of polynomials of degree n that have all their roots in $\mathcal{O}$ is itself open. In the case above, if for some $t \in I$, $P(t, s)$ has all its roots in $\mathcal{S}$, then it is always possible to find a positive real number α such that

$$\text{for all } t' \in (t - \alpha, t + \alpha) \cap I, P(t', s) \text{ also has all its roots in } \mathcal{S}. \tag{1.13}$$

This leads to the following fundamental result.

Theorem 1.4 (Boundary Crossing Theorem)
Under the Assumptions 1.1, suppose that $P(a, s)$ has all its roots in $\mathcal{S}$ whereas $P(b, s)$ has at least one root in $\mathcal{U}$. Then, there exists at least one ρ in $(a, b]$ such that:

a) $P(\rho, s)$ has all its roots in $\mathcal{S} \cup \partial\mathcal{S}$, and

b) $P(\rho, s)$ has at least one root in $\partial\mathcal{S}$.

Proof. To prove this result, let us introduce the set E of all real numbers t belonging to $(a, b]$ and satisfying the following property:

$$\mathcal{P}: \qquad \text{for all } t' \in (a, t), \quad P(t', s) \text{ has all its roots in } \mathcal{S}. \tag{1.14}$$

By assumption, we know that $P(a, s)$ itself has all its roots in $\mathcal{S}$, and therefore as mentioned above, it is possible to find $\alpha > 0$ such that

$$\text{for all } t' \in [a, a + \alpha) \cap I, \quad P(t', s) \text{ also has all its roots in } \mathcal{S}. \tag{1.15}$$

From this it is easy to conclude that E is not empty since, for example, $a + \frac{\alpha}{2}$ belongs to E.

Moreover, from the definition of E the following property is obvious:

$$t_2 \in E, \text{ and } a < t_1 < t_2, \text{ implies that } t_1 \text{ itself belongs to } E. \tag{1.16}$$

Given this, it is easy to see that E is an interval and if

$$\rho := \sup_{t \in E} t \tag{1.17}$$

then it is concluded that $E = (a, \rho]$.

A) On the one hand it is impossible that $P(\rho, s)$ has all its roots in $\mathcal{S}$. If this were the case then necessarily $\rho < b$, and it would be possible to find an $\alpha > 0$ such that $\rho + \alpha < b$ and

$$\text{for all } \; t' \in (\rho - \alpha, \rho + \alpha) \cap I, \quad P(t', s) \text{ also has all its roots in } \mathcal{S}. \tag{1.18}$$

As a result, $\rho + \frac{\alpha}{2}$ would belong to E and this would contradict the definition of ρ in (1.17).

B) On the other hand, it is also impossible that $P(\rho, s)$ has even one root in the interior of $\mathcal{U}$, because a straightforward application of Theorem 1.3 would grant the possibility of finding an $\alpha > 0$ such that

$$\text{for all } \; t' \in (\rho - \alpha, \rho + \alpha) \cap I, \quad P(t', s) \text{ has at least one root in } \mathcal{U}^0, \tag{1.19}$$

and this would contradict the fact that $\rho - \epsilon$ belongs to E for ϵ small enough.

From A) and B) it is thus concluded that $P(\rho, s)$ has all its roots in $\mathcal{S} \cup \partial\mathcal{S}$, and at least one root in $\partial\mathcal{S}$. ♣

The above result is in fact very intuitive and just states that in going from one open set to another open set disjoint from the first, the root set of a continuous family of polynomials $P(\lambda, s)$ of fixed degree must intersect at some intermediate stage the boundary of the first open set. If $P(\lambda, s)$ loses degree over the interval $[a, b]$, that is if $p_n(\lambda)$ in (1.12) vanishes for some values of λ, then the Boundary Crossing Theorem does not hold.

Example 1.1. Consider the Hurwitz stability of the polynomial

$$a_1 s + a_0 \qquad \text{where} \qquad \mathbf{p} := [a_0 \;\; a_1].$$

Referring to Figure 1.2, we see that the polynomial is Hurwitz stable for $\mathbf{p} = \mathbf{p}_0$. Now let the parameters travel along the path C_1 and reach the unstable point $\mathbf{p}_1$. Clearly no polynomial on this path has a $j\omega$ root for finite ω and thus boundary crossing *does not* occur. However, observe that the assumption of constant degree does not hold on this path because the point of intersection between the path C_1 and the a_0 axis corresponds to a polynomial where loss of degree occurs. On the other hand, if the parameters travel along the path C_2 and reach the unstable point $\mathbf{p}_2$, there is no loss of degree along the path C_2 and indeed a polynomial on this path has $s = 0$ as a root at $a_0 = 0$ and thus boundary crossing does occur. We illustrate this point in Figure 1.3(a). Along the path C_2, where no loss of degree occurs, the root passes through the stability boundary ($j\omega$ axis). However, on the path C_1 the polynomial passes from stable to unstable without its root passing through the stability boundary.

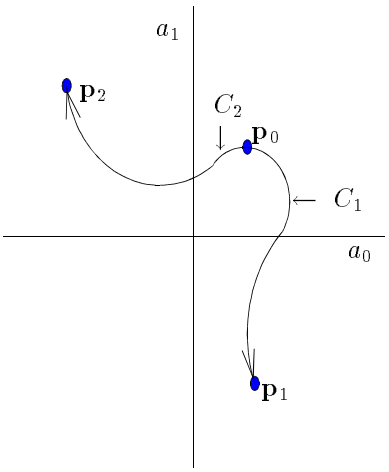

Figure 1.2. Degree loss on C_1, no loss on C_2 (Example 1.1)

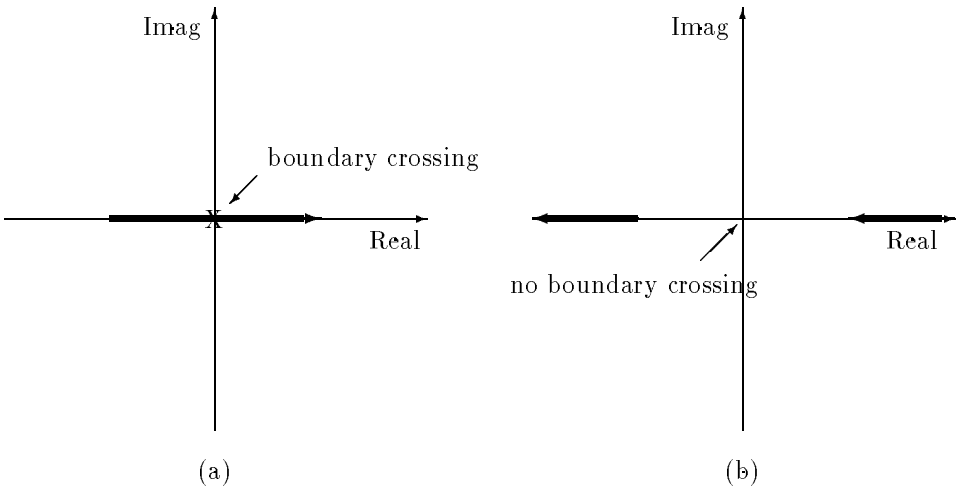

Figure 1.3. (a) Root locus corresponding to the path C_2 (b) Root locus corresponding to the path C_1 (Example 1.1)

The above example shows that the invariant degree assumption is important. Of course we can eliminate the assumption regarding invariant degree and modify the statement of the Boundary Crossing Theorem to require that any path connecting $P_a(s)$ and $P_b(s)$ contains a polynomial which has a root on the boundary or which drops in degree. If degree dropping does occur, it is always possible to apply the result on subintervals over which $p_n(\lambda)$ has a constant sign. In other words if the family of polynomials $P(\lambda, s)$ does not have a constant degree then of course Theorem 1.4 cannot be directly applied but that does not complicate the analysis terribly and similar results can be derived.

The following result gives an example of a situation where the assumption on the degree can be relaxed. As usual let $\mathcal{S}$ be the stability region of interest.

Theorem 1.5 *Let $\{P_n(s)\}$ be a sequence of stable polynomials of bounded degree and assume that this sequence converges to a polynomial $Q(s)$. Then the roots of $Q(s)$ are contained in $\mathcal{S} \cup \partial\mathcal{S}$.*

In words the above theorem says that the limit of a sequence of stable polynomials of bounded degree can only have unstable roots which are on the boundary of the stability region.

Proof. By assumption, there exists an integer N such that degree$[P_n] \leq N$ for all $n \geq 0$. Therefore we can write for all n,

$$P_n(s) = p_{0,n} + p_{1,n}s + \cdots + p_{N,n}s^N. \tag{1.20}$$

Since the sequence $\{P_n(s)\}$ converges to $Q(s)$ then $Q(s)$ itself has degree less than or equal to N so that we can also write,

$$Q(s) = q_0 + q_1 s + \cdots + q_N s^N. \tag{1.21}$$

Moreover

$$\lim_{n \longrightarrow +\infty} p_{k,n} = q_k, \quad \text{for } k = 0, 1, \cdots, N. \tag{1.22}$$

Now, suppose that $Q(s)$ has a root s^* which belongs to $\mathcal{U}^o$. We show that this leads to a contradiction. Since $\mathcal{U}^o$ is open, one can find a positive number r such that the disc $\mathcal{C}$ centered at s^* and of radius r is included in $\mathcal{U}^o$. By Theorem 1.3, there exists a positive number ϵ, such that for $|\epsilon_i| \leq \epsilon$, for $i = 0, 1, \cdots, N$, the polynomial

$$(q_0 + \epsilon_0) + (q_1 + \epsilon_1)s + \cdots + (q_N + \epsilon_N)s^N \tag{1.23}$$

has at least one root in $\mathcal{C} \subset \mathcal{U}^o$. Now, according to (1.22) it is possible to find an integer n_0 such that

$$n \geq n_0 \implies |p_{k,n} - q_k| < \epsilon, \quad \text{for } k = 0, 1, \cdots, N. \tag{1.24}$$

But then (1.24) implies that for $n \geq n_0$,

$$(q_0 + p_{0,n} - q_0) + (q_1 + p_{1,n} - q_1)s + \cdots + (q_N + p_{N,n} - q_N)s^N = P_n(s) \tag{1.25}$$

has at least one root in $\mathcal{C} \subset \mathcal{U}^o$, and this contradicts the fact that $P_n(s)$ is stable for all n. ♣

1.2.1 Zero Exclusion Principle

The Boundary Crossing Theorem can be applied to a family of polynomials to detect the presence of unstable polynomials in the family. Suppose that $\delta(s, \mathbf{p})$ denotes a polynomial whose coefficients depend continuously on the parameter vector $\mathbf{p} \in \mathbb{R}^l$ which varies in a set $\Omega \in \mathbb{R}^l$ and thus generates the family of polynomials

$$\mathbf{\Delta}(s) := \{\delta(s, \mathbf{p}) : \mathbf{p} \in \Omega\}. \tag{1.26}$$

We are given a stability region $\mathcal{S}$ and would like to determine if the family $\mathbf{\Delta}(s)$ contains unstable polynomials. Let us assume that there is at least one stable polynomial $\delta(s, \mathbf{p}_a)$ in the family and every polynomial in the family has the same degree. Then if $\delta(s, \mathbf{p}_b)$ is an unstable polynomial, it follows from the Boundary Crossing Theorem that on any continuous path connecting $\mathbf{p}_a$ to $\mathbf{p}_b$ there must exist a point $\mathbf{p}_c$ such that the polynomial $\delta(s, \mathbf{p}_c)$ contains roots on the stability boundary $\partial\mathcal{S}$. If such a path can be constructed entirely inside Ω, that is, if Ω is pathwise connected, then the point $\mathbf{p}_c$ lies in Ω. In this case the presence of unstable polynomials in the family is equivalent to the presence of polynomials in the family with boundary roots. If s^* is a root of a polynomial in the family it follows that $\delta(s^*, \mathbf{p}) = 0$ for some $\mathbf{p} \in \Omega$ and this implies that $0 \in \mathbf{\Delta}(s^*)$. Therefore the presence of unstable elements in $\mathbf{\Delta}(s)$ can be detected by generating the complex plane image set $\mathbf{\Delta}(s^*)$ of the family at $s^* \in \partial\mathcal{S}$, sweeping s^* along the stability boundary $\partial\mathcal{S}$, and checking if the zero exclusion condition $0 \notin \mathbf{\Delta}(s^*)$ is violated for some $s^* \in \partial\mathcal{S}$. This is stated formally as an alternative version of the Boundary Crossing Theorem.

Theorem 1.6 (Zero Exclusion Principle)
Assume that the family of polynomials (1.26) is of constant degree, contains at least one stable polynomial, and Ω is pathwise connected. Then the entire family is stable if and only if

$$0 \notin \mathbf{\Delta}(s^*), \quad \text{for all } s^* \in \partial\mathcal{S}.$$

The Zero Exclusion Principle can be used to derive both theoretical and computational solutions to many robust stability problems. It is systematically exploited in Chapters 2-12 to derive various results on robust parametric stability.

In the rest of this chapter however we restrict attention to the problem of stability determination of a *fixed* polynomial and demonstrate the power of the Boundary Crossing Theorem in tackling some classical stability problems.

1.3 THE HERMITE-BIEHLER THEOREM

We first present the Hermite-Biehler Theorem, sometimes referred to as the Interlacing Theorem. For the sake of simplicity we restrict ourselves to the case of polynomials with real coefficients. The corresponding result for complex polynomials will be stated separately. We deal with the Hurwitz case first and then the Schur case.

1.3.1 Hurwitz Stability

Consider a polynomial of degree n,

$$P(s) = p_0 + p_1 s + p_2 s^2 + \cdots + p_n s^n. \tag{1.27}$$

$P(s)$ is said to be a *Hurwitz* polynomial if and only if all its roots lie in the open left half of the complex plane. We have the two following properties.

Property 1.1. If $P(s)$ is a real Hurwitz polynomial then all its coefficients are non zero and have the same sign, either all positive or all negative.

Proof. Follows from the fact that $P(s)$ can be factored into a product of first and second degree real Hurwitz polynomials for which the property obviously holds. ♣

Property 1.2. If $P(s)$ is a Hurwitz polynomial of degree n, then $\arg[P(j\omega)]$, also called the phase of $P(j\omega)$, is a continuous and strictly increasing function of ω on $(-\infty, +\infty)$. Moreover the net increase in phase from $-\infty$ to $+\infty$ is

$$\arg[P(+j\infty)] - \arg[P(-j\infty)] = n\pi. \tag{1.28}$$

Proof. If $P(s)$ is Hurwitz then we can write

$$P(s) = p_n \prod_{i=1}^{n} (s - s_i), \text{ with } s_i = a_i + jb_i, \text{ and } a_i < 0. \tag{1.29}$$

Then we have,

$$\begin{aligned} \arg[P(j\omega)] &= \arg[p_n] + \sum_{i=1}^{n} \arg[j\omega - a_i - jb_i] \\ &= \arg[p_n] + \sum_{i=1}^{n} \arctan\left[\frac{\omega - b_i}{-a_i}\right] \end{aligned} \tag{1.30}$$

and thus $\arg[P(j\omega)]$ is a sum of a constant plus n continuous, strictly increasing functions. Moreover each of these n functions has a net increase of π in going from $\omega = -\infty$ to $\omega = +\infty$, as shown in Figure 1.4. ♣

The even and odd parts of a real polynomial $P(s)$ are defined as:

$$\begin{aligned} P^{\text{even}}(s) &:= p_0 + p_2 s^2 + p_4 s^4 + \cdots \\ P^{\text{odd}}(s) &:= p_1 s + p_3 s^3 + p_5 s^5 + \cdots \quad . \end{aligned} \tag{1.31}$$

Define

$$\begin{aligned} P^e(\omega) &:= P^{\text{even}}(j\omega) = p_0 - p_2\omega^2 + p_4\omega^4 - \cdots \\ P^o(\omega) &:= \frac{P^{\text{odd}}(j\omega)}{j\omega} = p_1 - p_3\omega^2 + p_5\omega^4 - \cdots \quad . \end{aligned} \tag{1.32}$$

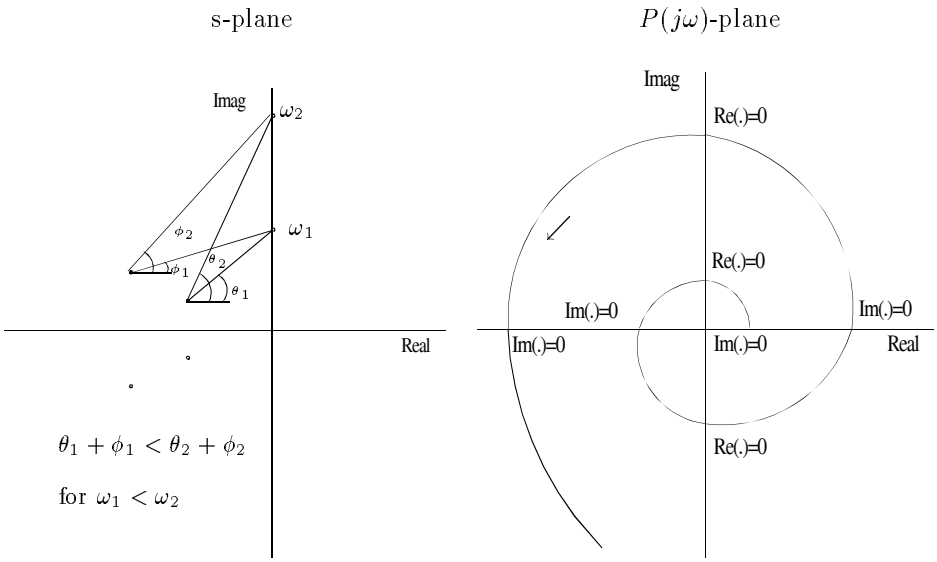

Figure 1.4. Monotonic phase increase property for Hurwitz polynomials

$P^e(\omega)$ and $P^o(\omega)$ are both polynomials in ω^2 and as an immediate consequence their root sets will always be symmetric with respect to the origin of the complex plane.

Suppose now that the degree of the polynomial $P(s)$ is even, that is $n = 2m$, $m > 0$. In that case we have

$$\begin{aligned} P^e(\omega) &= p_0 - p_2\omega^2 + p_4\omega^4 - \cdots + (-1)^m p_{2m}\omega^{2m} \\ P^o(\omega) &= p_1 - p_3\omega^2 + p_5\omega^4 - \cdots + (-1)^{m-1} p_{2m-1}\omega^{2m-2}. \end{aligned} \tag{1.33}$$

Definition 1.1. A real polynomial $P(s)$ satisfies the interlacing property if

a) p_{2m} and p_{2m-1} have the same sign.

b) All the roots of $P^e(\omega)$ and $P^o(\omega)$ are real and distinct and the m positive roots of $P^e(\omega)$ together with the $m-1$ positive roots of $P^o(\omega)$ interlace in the following manner:

$$0 < \omega_{e,1} < \omega_{o,1} < \omega_{e,2} < \cdots < \omega_{e,m-1} < \omega_{o,m-1} < \omega_{e,m}. \tag{1.34}$$

If, on the contrary, the degree of $P(s)$ is odd, then $n = 2m+1, m \geq 0$, and

$$\begin{aligned} P^e(\omega) &= p_0 - p_2\omega^2 + p_4\omega^4 - \cdots + (-1)p_{2m}^m\omega^{2m} \\ P^o(\omega) &= p_1 - p_3\omega^2 + p_5\omega^4 - \cdots + (-1)^m p_{2m+1}\omega^{2m} \end{aligned} \tag{1.35}$$

and the definition of the interlacing property, for this case, is then naturally modified to

a) p_{2m+1} and p_{2m} have the same sign.

b) All the roots of $P^e(\omega)$ and $P^o(\omega)$ are real and the m positive roots of $P^e(\omega)$ together with the m positive roots of $P^o(\omega)$ interlace in the following manner:

$$0 < \omega_{e,1} < \omega_{o,1} < \cdots < \omega_{e,m-1} < \omega_{o,m-1} < \omega_{e,m} < \omega_{o,m}. \tag{1.36}$$

An alternative description of the interlacing property is as follows: $P(s) = P^{\text{even}}(s) + P^{\text{odd}}(s)$ satisfies the interlacing property if and only if

a) the leading coefficients of $P^{\text{even}}(s)$ and $P^{\text{odd}}(s)$ are of the same sign, and

b) all the zeroes of $P^{\text{even}}(s) = 0$ and of $P^{\text{odd}}(s) = 0$ are distinct, lie on the imaginary axis and alternate along it.

We can now enunciate and prove the following theorem.

Theorem 1.7 (Interlacing or Hermite-Biehler Theorem)
A real polynomial $P(s)$ is Hurwitz if and only if it satisfies the interlacing property.

Proof. To prove the necessity of the interlacing property consider a real Hurwitz polynomial of degree n,

$$P(s) = p_0 + p_1 s + p_2 s^2 + \cdots + p_n s^n.$$

Since $P(s)$ is Hurwitz it follows from Property 1.1 that all the coefficients p_i have the same sign, thus part a) of the interlacing property is already proven and one can assume without loss of generality that all the coefficients are positive. To prove part b) it is assumed arbitrarily that $P(s)$ is of even degree so that $n = 2m$. Now, we also know from Property 1.2 that the phase of $P(j\omega)$ strictly increases from $-n\pi/2$ to $n\pi/2$ as ω runs from $-\infty$ to $+\infty$. Due to the fact that the roots of $P(s)$ are symmetric with respect to the real axis it is also true that $\arg(P(j\omega))$ increases from 0 to $+n\pi/2 = m\pi$ as ω goes from 0 to $+\infty$. Hence as ω goes from 0 to $+\infty$, $P(j\omega)$ starts on the positive real axis ($P(0) = p_0 > 0$), circles strictly counterclockwise around the origin $m\pi$ radians before going to infinity, and never passes through the origin since $P(j\omega) \neq 0$ for all ω. As a result it is very easy to see that the plot of $P(j\omega)$ has to cut the imaginary axis m times so that the *real* part of $P(j\omega)$ becomes zero m times as ω increases, at the positive values

$$\omega_{\mathcal{R},1}, \quad \omega_{\mathcal{R},2}, \quad \cdots, \quad \omega_{\mathcal{R},m}. \tag{1.37}$$

Similarly the plot of $P(j\omega)$ starts on the positive real axis and cuts the real axis another $m-1$ times as ω increases so that the imaginary part of $P(j\omega)$ also becomes zero m times (including $\omega = 0$) at

$$0, \quad \omega_{\mathcal{I},1}, \quad \omega_{\mathcal{I},2}, \quad \cdots, \quad \omega_{\mathcal{I},m-1} \tag{1.38}$$

before growing to infinity as ω goes to infinity. Moreover since $P(j\omega)$ *circles* around the origin we obviously have

$$0 < \omega_{\mathcal{R},1} < \omega_{\mathcal{I},1} < \omega_{\mathcal{R},2} < \omega_{\mathcal{I},2} < \cdots < \omega_{\mathcal{R},m-1} < \omega_{\mathcal{I},m-1} < \omega_{\mathcal{R},m}. \tag{1.39}$$

Now the proof of necessity is completed by simply noticing that the real part of $P(j\omega)$ is nothing but $P^e(\omega)$, and the imaginary part of $P(j\omega)$ is $\omega P^o(j\omega)$.

For the converse assume that $P(s)$ satisfies the interlacing property and suppose for example that $P(s)$ is of degree $n = 2m$ and that p_{2m}, p_{2m-1} are both positive. Consider the roots of $P^e(\omega)$ and $P^o(\omega)$,

$$0 < \omega^p_{e,1} < \omega^p_{o,1} < \cdots < \omega^p_{e,m-1} < \omega^p_{o,m-1} < \omega^p_{e,m}. \tag{1.40}$$

From this, $P^e(\omega)$ and $P^o(\omega)$ can be written as

$$P^e(\omega) = p_{2m} \prod_{i=1}^{m} (\omega^2 - {\omega^p_{e,i}}^2)$$

$$P^o(\omega) = p_{2m-1} \prod_{i=1}^{m-1} (\omega^2 - {\omega^p_{o,i}}^2).$$

Now, consider a polynomial $Q(s)$ that is known to be stable, of the same degree $2m$ and with all its coefficients positive. For example, take $Q(s) = (s+1)^{2m}$. In any event, write

$$Q(s) = q_0 + q_1 s + q_2 s^2 + \cdots + q_{2m} s^{2m}.$$

Since $Q(s)$ is stable, it follows from the first part of the theorem that $Q(s)$ satisfies the interlacing property, so that $Q^e(\omega)$ has m positive roots $\omega^q_{e,1}$, $\cdots$, $\omega^q_{e,m}$ and $Q^o(\omega)$ has $m-1$ positive roots $\omega^q_{o,1}$, $\cdots$, $\omega^q_{o,m-1}$, and,

$$0 < \omega^q_{e,1} < \omega^q_{o,1} < \cdots < \omega^q_{e,m-1} < \omega^q_{o,m-1} < \omega^q_{e,m}. \tag{1.41}$$

Therefore we can also write:

$$Q^e(\omega) = q_{2m} \prod_{i=1}^{m} (\omega^2 - {\omega^q_{e,i}}^2)$$

$$Q^o(\omega) = q_{2m-1} \prod_{i=1}^{m-1} (\omega^2 - {\omega^q_{o,i}}^2).$$

Consider now the polynomial $P_\lambda(s) := P^{ev\,en}_\lambda(s) + sP^{o\,dd}_\lambda(s)$ defined by

$$P^e_\lambda(\omega) := \big((1-\lambda)q_{2m} + \lambda p_{2m}\big) \prod_{i=1}^{m} \Big(\omega^2 - \big[(1-\lambda)(\omega^q_{e,i})^2 + \lambda(\omega^p_{e,i})^2\big]\Big)$$

$$P^o_\lambda(\omega) := \big((1-\lambda)q_{2m-1} + \lambda p_{2m-1}\big) \prod_{i=1}^{m-1} \Big(\omega^2 - \big[(1-\lambda)(\omega^q_{o,i})^2 + \lambda(\omega^p_{o,i})^2\big]\Big).$$

Obviously, the coefficients of $P_\lambda(s)$ are polynomial functions in λ which are therefore continuous on $[0,1]$. Moreover, the coefficient of the highest degree term in $P_\lambda(s)$ is $(1-\lambda)q_{2m} + \lambda p_{2m}$ and always remains positive as λ varies from 0 to 1. For $\lambda = 0$ we have $P_0(s) = Q(s)$ and for $\lambda = 1$, $P_1(s) = P(s)$. Suppose now that $P(s)$ is not Hurwitz. From the Boundary Crossing Theorem it is then clear that there necessarily exists some λ in $(0,1]$ such that $P_\lambda(s)$ has a root on the imaginary axis. However, $P_\lambda(s)$ has a root on the imaginary axis if and only if $P^e_\lambda(\omega)$ and $P^o_\lambda(\omega)$ have a common real root. But, obviously, the roots of $P^e_\lambda(\omega)$ satisfy

$$\omega^{\lambda}_{e,i}{}^2 = (1-\lambda)\omega^{q}_{e,i}{}^2 + \lambda\omega^{p}_{e,i}{}^2, \tag{1.42}$$

and those of $P^o_\lambda(\omega)$,

$$\omega^{\lambda}_{o,i}{}^2 = (1-\lambda)\omega^{q}_{o,i}{}^2 + \lambda\omega^{p}_{o,i}{}^2. \tag{1.43}$$

Now, take any two roots of $P^e_\lambda(\omega)$ in (1.42). If $i < j$, from (1.40) $\omega^{p}_{e,i}{}^2 < \omega^{p}_{e,j}{}^2$, and similarly from (1.41), $\omega^{q}_{e,i}{}^2 < \omega^{q}_{e,j}{}^2$, so that

$$\omega^{\lambda}_{e,i}{}^2 < \omega^{\lambda}_{e,j}{}^2.$$

In the same way, it can be seen that the same ordering as in (1.40) and (1.41) is preserved between the roots of $P^o_\lambda(\omega)$, and also between any root of $P^e_\lambda(\omega)$ and any root of $P^o_\lambda(\omega)$. In other words, part b) of the interlacing property is invariant under such convex combinations so that we also have for every λ in $[0,1]$:

$$0 < \omega^{\lambda}_{e,1}{}^2 < \omega^{\lambda}_{o,1}{}^2 < \cdots < \omega^{\lambda}_{e,m-1}{}^2 < \omega^{\lambda}_{o,m-1}{}^2 < \omega^{\lambda}_{e,m}{}^2.$$

But this shows that, whatever the value of λ in $[0,1]$, $P^e_\lambda(\omega)$ and $P^o_\lambda(\omega)$ can never have a common root, and this therefore leads to a contradiction which completes the proof. ♣

It is clear that the interlacing property is equivalent to the monotonic phase increase property. If the stability region $\mathcal{S}$ is such that a stable polynomial does not have the monotonic phase increase property, the interlacing of the real and imaginary parts will in general fail to hold. However, even in the case of such a region $\mathcal{S}$ the boundary crossing property must hold. This means that the transition from stability to instability can only occur if the real and imaginary parts simultaneously become zero at some boundary point.

A Frequency Domain Plot for Hurwitz Stability

The interlacing property of a polynomial can be verified by plotting either the graphs of $P^e(\omega)$ and $P^o(\omega)$ or the polar plot of $P(j\omega)$ as shown below.

Example 1.2.

$$P(s) = s^9 + 11s^8 + 52s^7 + 145s^6 + 266s^5 + 331s^4 + 280s^3 + 155s^2 + 49s + 6.$$

Then

$$P(j\omega) := P^e(\omega) + j\omega P^o(\omega)$$

with

$$P^e(\omega) = 11\omega^8 - 145\omega^6 + 331\omega^4 - 155\omega^2 + 6$$
$$P^o(\omega) = \omega^8 - 52\omega^6 + 266\omega^4 - 280\omega^2 + 49.$$

The plots of $P^e(\omega)$ and $P^o(\omega)$ are shown in Figure 1.5. They show that the polynomial $P(s)$ is Hurwitz because it satisfies the interlacing property.

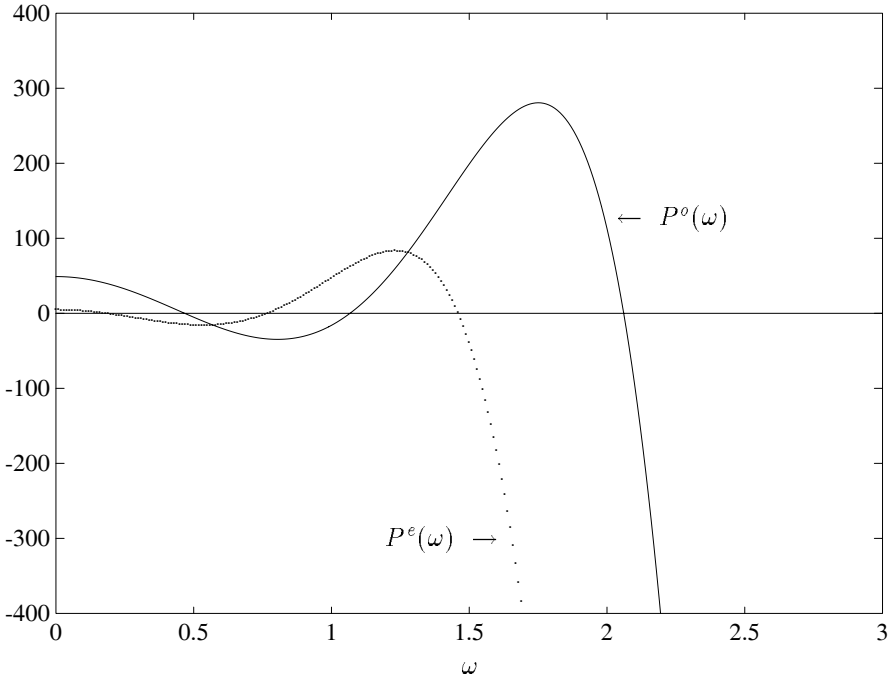

Figure 1.5. Interlacing property for Hurwitz polynomials (Example 1.2)

Example 1.3.

$$P(s) = s^9 + 21s^8 + 52s^7 + 145s^6 + 266s^5 + 331s^4 + 280s^3 + 155s^2 + 49s + 6.$$

Then

$$P(j\omega) := P^e(\omega) + j\omega P^o(\omega)$$

where

$$P^e(\omega) = 21\omega^8 - 145\omega^6 + 331\omega^4 - 155\omega^2 + 6$$
$$P^o(\omega) = \omega^8 - 52\omega^6 + 266\omega^4 - 280\omega^2 + 49.$$

The plots of $P^e(\omega)$ and $P^o(\omega)$ are shown in Figure 1.6. They show that the polynomial $P(s)$ is not Hurwitz because it fails to satisfy the interlacing property.

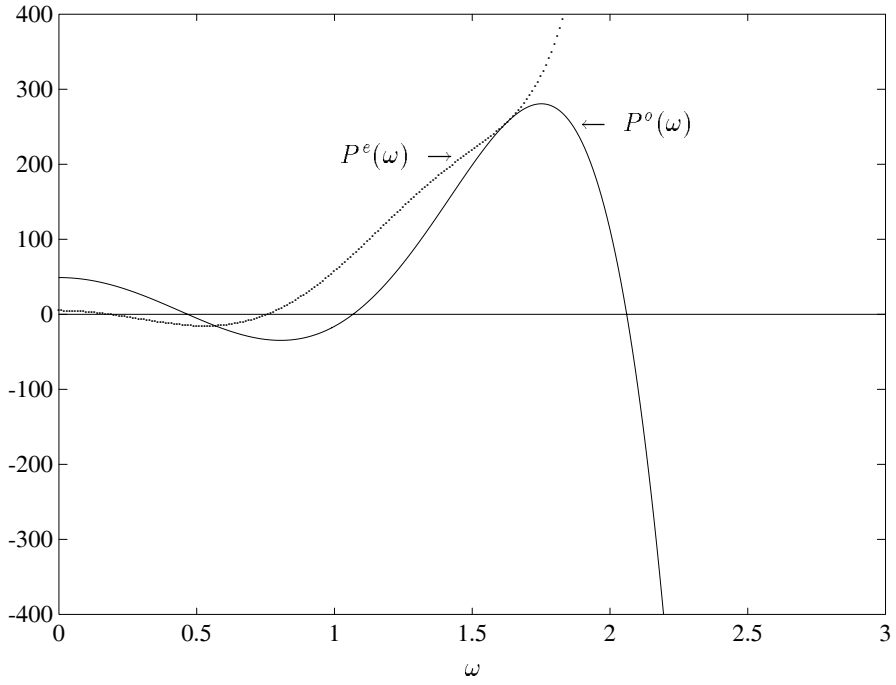

Figure 1.6. Interlacing fails for nonHurwitz polynomials (Example 1.3)

Both the plots in the above examples are unbounded as ω tends to ∞. A bounded plot containing the same information can be constructed as follows. For a polynomial

$$P(s) = p_0 + p_1 s + \cdots + p_n s^n, \quad p_n > 0$$

write as usual

$$P(j\omega) = P^e(\omega) + j\omega P^o(\omega)$$

and let $S(\omega)$ and $T(\omega)$ denote arbitrary continuous positive functions on $0 \leq \omega < \infty$. Let

$$x(\omega) := \frac{P^e(\omega)}{S(\omega)}, \quad y(\omega) := \frac{P^o(\omega)}{T(\omega)}.$$

Lemma 1.1 *A real polynomial $P(s)$ is Hurwitz if and only if the frequency plot $z(\omega) := x(\omega) + jy(\omega)$ moves strictly counterclockwise and goes through n quadrants in turn.*

Proof. The Hermite-Biehler Theorem and the monotonic phase property of Hurwitz polynomials shows that the plot of $P(j\omega)$ must go through n quadrants if and only if $P(s)$ is Hurwitz. Since the signs of $P^e(\omega)$ and $x(\omega)$, $\omega P^o(\omega)$ and $y(\omega)$ coincide for $\omega > 0$, the lemma is true. ♣

Although the $P(j\omega)$ plot is unbounded, the plot of $z(\omega)$ can always be bounded by choosing the functions $T(\omega)$ and $S(\omega)$ appropriately. For example $T(\omega)$ and $S(\omega)$ can be chosen to be polynomials with degrees equal to that of $P^e(\omega)$ and $P^o(\omega)$ respectively. A similar result can be derived for the complex case. Lemma 1.1 is illustrated with the following example.

Example 1.4. Taking the same polynomial as in Example 1.2:

$$P(s) = s^9 + 11s^8 + 52s^7 + 145s^6 + 266s^5 + 331s^4 + 280s^3 + 155s^2 + 49s + 6$$

and writing

$$P(j\omega) := P^e(\omega) + j\omega P^o(\omega)$$

we have

$$P^e(\omega) = 11\omega^8 - 145\omega^6 + 331\omega^4 - 155\omega^2 + 6$$
$$P^o(\omega) = \omega^8 - 52\omega^6 + 266\omega^4 - 280\omega^2 + 49.$$

We choose

$$S(\omega) = \omega^8 + \omega^6 + \omega^4 + \omega^2 + 1$$
$$T(\omega) = \omega^8 + \omega^6 + \omega^4 + \omega^2 + 1.$$

The function $z(\omega)$ in Figure 1.7 turns strictly counterclockwise and goes through nine quadrants and this shows that the polynomial $P(s)$ is Hurwitz according to Lemma 1.1.

It will be shown in Chapter 3 that the weighting functions $S(\omega)$ and $T(\omega)$ can be suitably chosen to extend this frequency domain criterion to verify robust Hurwitz stability of an l_p ball in coefficient space.

1.3.2 Hurwitz Stability for Complex Polynomials

The Hermite-Biehler Theorem for complex polynomials is given below. Its proof is a straightforward extension of that of the real case and will not be given. Let $P(s)$ be a complex polynomial

$$P(s) = (a_0 + jb_0) + (a_1 + jb_1)s + \cdots + (a_{n-1} + jb_{n-1})s^{n-1} + (a_n + jb_n)s^n. \quad (1.44)$$

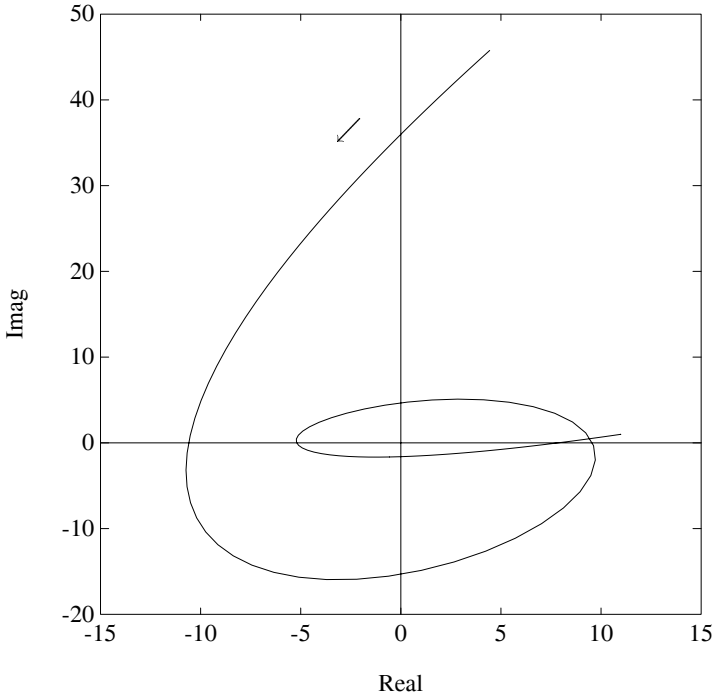

Figure 1.7. Frequency plot of $z(\omega)$ (Example 1.4)

Define

$$\begin{aligned} P_R(s) &= a_0 + jb_1 s + a_2 s^2 + jb_3 s^3 + \cdots \\ P_I(s) &= jb_0 + a_1 s + jb_2 s^2 + a_3 s^3 + \cdots \end{aligned} \tag{1.45}$$

and write

$$P(j\omega) = P^r(\omega) + jP^i(\omega),$$

where

$$\begin{aligned} P^r(\omega) &:= P_R(j\omega) = a_0 - b_1\omega - a_2\omega^2 + b_3\omega^3 + \cdots , \\ P^i(\omega) &:= \frac{1}{j} P_I(j\omega) = b_0 + a_1\omega - b_2\omega^2 - a_3\omega^3 + \cdots . \end{aligned} \tag{1.46}$$

The Hermite-Biehler Theorem for complex polynomials can then be stated as follows.

Theorem 1.8 *The complex polynomial $P(s)$ in (1.44) is a Hurwitz polynomial if and only if,*

1) $a_{n-1}a_n + b_{n-1}b_n > 0$,

2) The zeros of $P^r(\omega)$ *and* $P^i(\omega)$ *are all simple and real and interlace, as* ω *runs from* $-\infty$ *to* $+\infty$.

Note that condition 1) follows directly from the fact that the sum of the roots of the polynomial $P(s)$ in (1.44) is equal to

$$-\frac{a_{n-1}+jb_{n-1}}{a_n+jb_n} = -\frac{a_{n-1}a_n + b_{n-1}b_n + j(b_{n-1}a_n - a_{n-1}b_n)}{a_n^2+b_n^2},$$

so that if $P(s)$ is Hurwitz, then the real part of the above complex number must be negative.

1.3.3 The Hermite-Biehler Theorem: Schur Case

In fact it is always possible to derive results similar to the interlacing theorem with respect to any stability region $\mathcal{S}$ which has the property that the phase of a stable polynomial evaluated along the boundary of $\mathcal{S}$ increases monotonically. In this case the stability of the polynomial with respect to $\mathcal{S}$ is equivalent to the interlacing of its real and imaginary parts evaluated along the boundary of $\mathcal{S}$. Here we concentrate on the case where $\mathcal{S}$ is the open unit disc. This is the stability region for discrete time systems.

Definition 1.2. A polynomial,

$$P(z) = p_n z^n + p_{n-1}z^{n-1} + \cdots + p_1 z + p_0,$$

is said to be a Schur polynomial if all its roots lie in the open unit disc of the complex plane. A necessary condition for Schur stability is $|p_n| > |p_0|$ (see Property 1.3).

A frequency plot for Schur stability

$P(z)$ can be written as

$$P(z) = p_n(z-z_1)(z-z_2)\cdots(z-z_n) \tag{1.47}$$

where the z_i's are the n roots of $P(z)$. If $P(z)$ is Schur, all these roots are located inside the unit disc $|z|<1$, so that when z varies along the unit circle, $z = e^{j\theta}$, the argument of $P(e^{j\theta})$ increases monotonically. For a Schur polynomial of degree n, $P(e^{j\theta})$ has a net increase of argument of $2n\pi$, and thus the plot of $P(e^{j\theta})$ encircles the origin n times. This can be used as a frequency domain test for Schur stability.

Example 1.5. Consider the stable polynomial

$$\begin{aligned} P(z) &= 2z^4 - 3.2z^3 + 1.24z^2 + 0.192z - 0.1566 \\ &= 2(z+0.3)(z-0.5+0.2j)(z-0.5-0.2j)(z-0.9) \end{aligned}$$

Let us evaluate $P(z)$ when z varies along the unit circle. The plot obtained in Figure 1.8 encircles the origin four times, which shows that this fourth order polynomial is Schur stable.

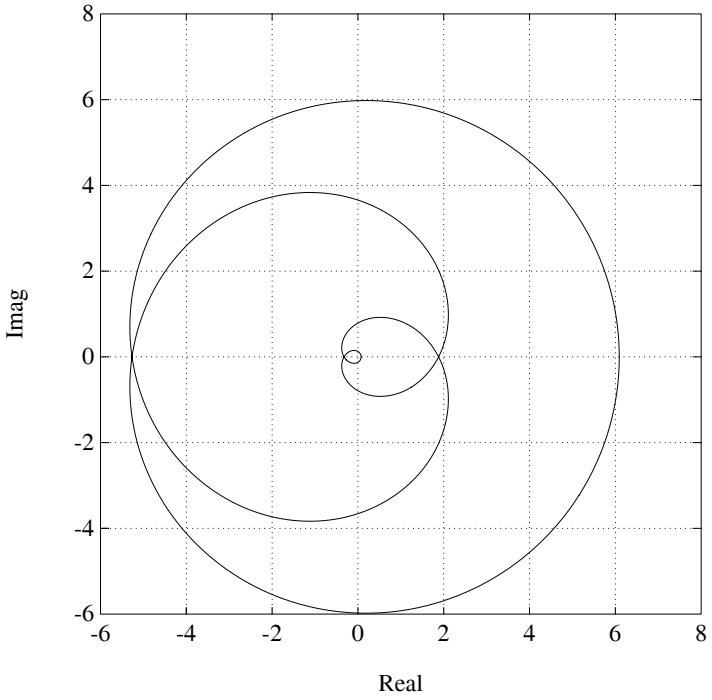

Figure 1.8. Plot of $P(e^{j\theta})$ (Example 1.5)

A simplification can be made by considering the *reversed polynomial* $z^n P(z^{-1})$.

$$\begin{aligned} z^n P(z^{-1}) &= p_0 z^n + p_1 z^{n-1} + \cdots + p_n \\ &= p_n(1 - z_1 z)(1 - z_2 z) \cdots (1 - z_n z) \end{aligned} \tag{1.48}$$

$z^n P(z^{-1})$ becomes zero at $z = z_i^{-1}$, $i = 1, \cdots, n$. If $P(z)$ is Schur the z_i's have modulus less than one, so that the z_i^{-1} are located outside the unit disc. If we let $z = e^{j\theta}$ vary along the unit circle the net increase of argument of $e^{jn\theta}P(e^{-j\theta})$ must therefore be *zero*. This means that for Schur stability of $P(z)$ it is necessary and sufficient that the frequency plot, $e^{jn\theta}P(e^{-j\theta})$ of the reverse polynomial *not encircle the origin.*

Example 1.6. Consider the polynomial in the previous example. The plot of $z^n P(z^{-1})$ when z describes the unit circle is shown in Figure 1.9. As seen, the plot does not encircle the origin and thus we conclude that $P(z)$ is stable.

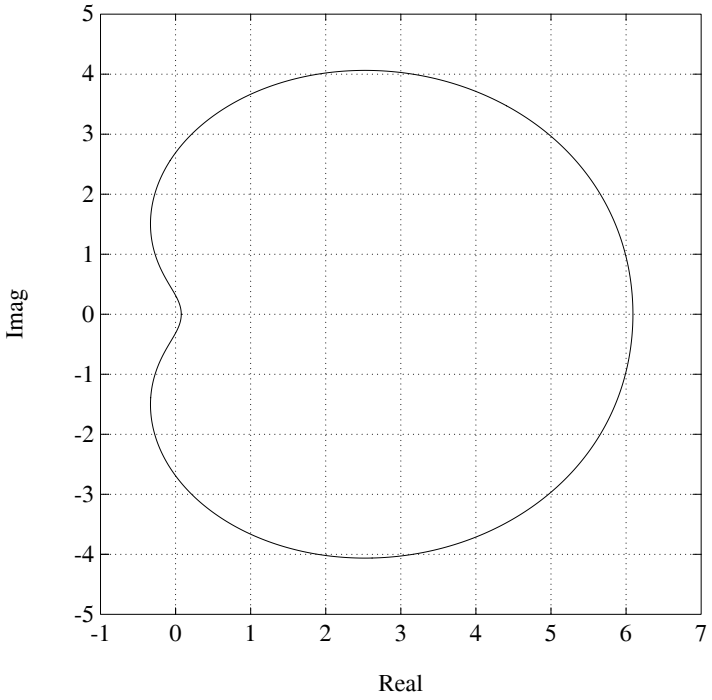

Figure 1.9. Plot of $e^{j4\theta}P(e^{-j\theta})$ (Example 1.6)

We see that when using the plot of $P(z)$ we must verify that the plot of $P(e^{j\theta})$ encircles the origin the correct number of times n, whereas using the reverse polynomial $R(z) = z^n P(z^{-1})$ we need only check that the plot of $R(e^{j\theta})$ excludes the origin. This result holds for real as well as complex polynomials.

For a real polynomial, it is easy to see from the above that the stability of $P(z)$ is equivalent to the interlacing of the real and imaginary parts of $P(z)$ evaluated along the upper-half of the unit-circle. Writing $P(e^{j\theta}) = R(\theta) + jI(\theta)$ we have:

$$R(\theta) = p_n \cos(n\theta) + \cdots + p_1 \cos(\theta) + p_0$$

and,

$$I(\theta) = p_n \sin(n\theta) + \cdots + p_1 \sin(\theta).$$

Lemma 1.2 *A real polynomial P(z) is Schur with $|p_n| > |p_0|$ if and only if*

a) $R(\theta)$ has exactly n zeros in $[0, \pi]$,

b) $I(\theta)$ has exactly $n+1$ zeros in $[0, \pi]$, and

c) the zeros of $R(\theta)$ and $I(\theta)$ interlace.

Example 1.7. Consider the polynomial

$$P(z) = z^5 + 0.2z^4 + 0.3z^3 + 0.4z^2 + 0.03z + 0.02.$$

As seen in Figure 1.10 the polynomial $P(z)$ is Schur since $\mathrm{Re}[P(e^{j\theta})]$ and $\mathrm{Im}[P(e^{j\theta})]$ have respectively 5 and 6 distinct zeros for $\theta \in [0, \pi]$, and the zeros of $\mathrm{Re}[P(e^{j\theta})]$ interlace with the zeros of $\mathrm{Im}[P(e^{j\theta})]$.

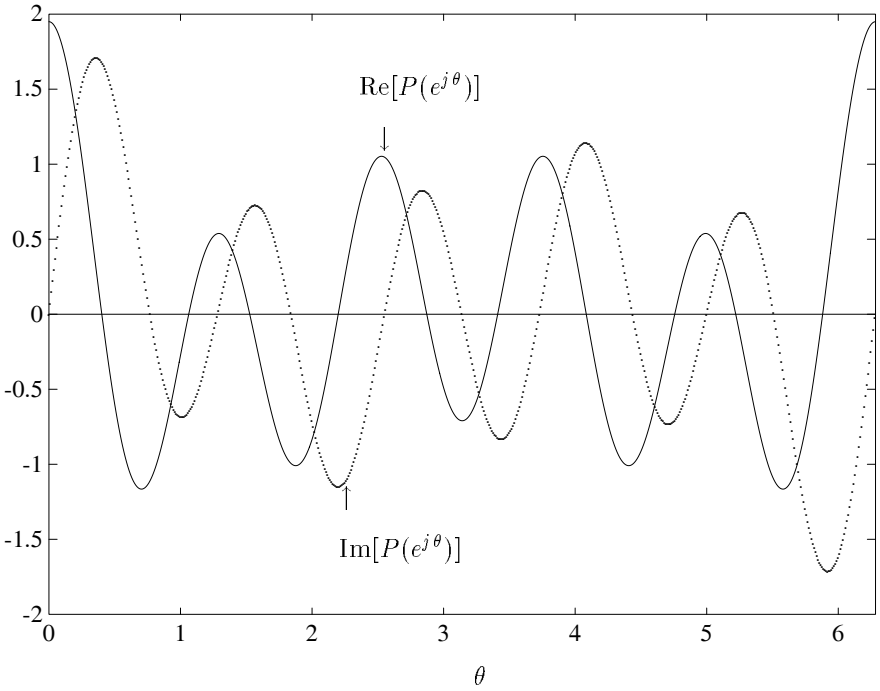

Figure 1.10. $\mathrm{Re}[P(e^{j\theta})]$ and $\mathrm{Im}[P(e^{j\theta})]$(Schur case)(Example 1.7)

Example 1.8. Consider the polynomial

$$P(z) = z^5 + 2z^4 + 0.3z^3 + 0.4z^2 + 0.03z + 0.02.$$

Since $\mathrm{Re}[P(e^{j\theta})]$ and $\mathrm{Im}[P(e^{j\theta})]$ each do not have $2n = 10$ distinct zeros for $0 \leq \theta < 2\pi$, as shown in Figure 1.11, the polynomial $P(z)$ is not Schur.

These conditions, can in fact be further refined to the interlacing on the unit circle of the two polynomials $P_s(z)$ and $P_a(z)$ which represent the *symmetric* and

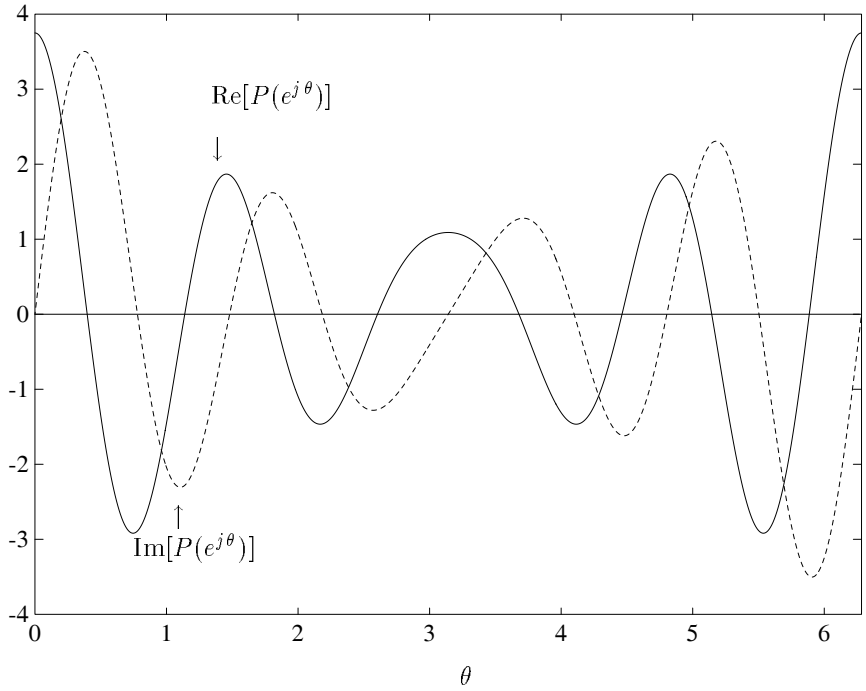

Figure 1.11. Re$[P(e^{j\theta})]$ and Im$[P(e^{j\theta})]$ (nonSchur case) (Example 1.8)

asymmetric parts of the real polynomial $P(z) = P_s(z) + P_a(z)$:

$$P_s(z) = \frac{1}{2}\left[P(z) + z^n P\left(\frac{1}{z}\right)\right], \quad \text{and} \quad P_a(z) = \frac{1}{2}\left[P(z) - z^n P\left(\frac{1}{z}\right)\right].$$

Theorem 1.9 *A real polynomial P(z) is Schur if and only if $P_s(z)$ and $P_a(z)$ satisfy the following:*

a) $P_s(z)$ and $P_a(z)$ are polynomials of degree n with leading coefficients of the same sign.

b) $P_s(z)$ and $P_a(z)$ have only simple zeros which belong to the unit circle.

c) The zeros of $P_s(z)$ and $P_a(z)$ interlace on the unit circle.

Proof. Let $P(z) = p_0 + p_1 z + p_2 z^2 \cdots + p_n z^n$. The condition a) is equivalent to $p_n^2 - p_0^2 > 0$ which is clearly necessary for Schur stability (see Property 1.3). Now we apply the bilinear transformation of the unit circle into the left half plane and use

the Hermite Biehler Theorem for Hurwitz stability. It is known that the bilinear mapping,

$$z = \frac{s+1}{s-1}$$

maps the open unit disc into the open left half plane. It can be used to transform a polynomial $P(z)$ into $\hat{P}(s)$ as follows:

$$(s-1)^n P\left(\frac{s+1}{s-1}\right) = \hat{P}(s).$$

Write

$$\hat{P}(s) = \hat{p}_0 + \hat{p}_1 s + \cdots + \hat{p}_{n-1} s^{n-1} + \hat{p}_n s^n$$

where each $\hat{p}_i$ is a function which depends on the coefficients of $P(z)$. It follows that if the transformation is degree preserving then $P(z)$ is Schur stable if and only if $\hat{P}(s)$ is Hurwitz stable. It is easy to verify that the transformation described above is degree preserving if and only if

$$\hat{p}_n = \sum_{i=0}^{i=n} p_i = P(1) \neq 0$$

and that this holds is implied by condition c).

The transformation of $P(z)$ into $\hat{P}(s)$ is a linear transformation T. That is, $\hat{P}(s)$ is the image of $P(z)$ under the mapping T. Then $TP(z) = \hat{P}(s)$ may be written explicitly as

$$(s-1)^n P\left(\frac{s+1}{s-1}\right) = TP(z) = \hat{P}(s).$$

For example, for $n = 4$, expressing $P(z)$ and $\hat{P}(s)$ in terms of their coefficient vectors

$$\begin{bmatrix} 1 & 1 & 1 & 1 & 1 \\ -4 & -2 & 0 & 2 & 4 \\ 6 & 0 & -2 & 0 & 6 \\ -4 & 2 & 0 & -2 & 4 \\ 1 & -1 & 1 & -1 & 1 \end{bmatrix} \begin{bmatrix} p_0 \\ p_1 \\ p_2 \\ p_3 \\ p_4 \end{bmatrix} = \begin{bmatrix} \hat{p}_0 \\ \hat{p}_1 \\ \hat{p}_2 \\ \hat{p}_3 \\ \hat{p}_4 \end{bmatrix}.$$

Consider the symmetric and anti-symmetric parts of $P(z)$, and their transformed images, given by $TP_s(z)$ and $TP_a(z)$ respectively. A straightforward computation shows that

$$TP_s(z) = \hat{P}^{\text{even}}(s), \quad TP_a(z) = \hat{P}^{\text{odd}}(s), \qquad n \text{ even}$$

and

$$TP_s(z) = \hat{P}^{\text{odd}}(s), \quad TP_a(z) = \hat{P}^{\text{even}}(s), \qquad n \text{ odd}.$$

The conditions b) and c) now follow immediately from the interlacing property for Hurwitz polynomials applied to $\hat{P}(s)$. ♣

The functions $P_s(z)$ and $P_a(z)$ are easily evaluated as z traverses the unit circle. Interlacing may be verified from a plot of the zeros of these functions as in Figure 1.12.

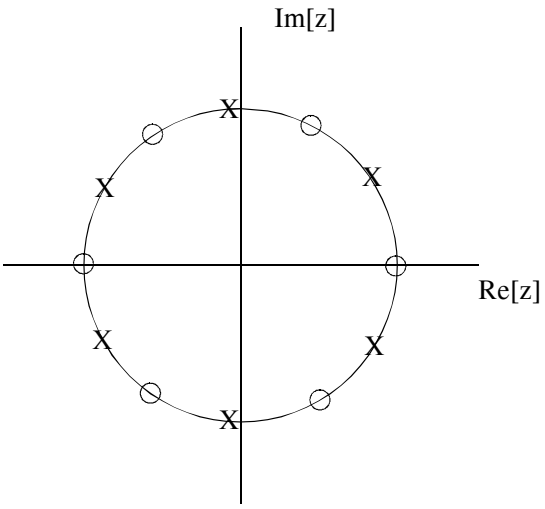

Figure 1.12. Interlacing of the symmetric and anti-symmetric parts of a polynomial on the unit circle

General Stability Regions

The Hermite-Biehler interlacing theorem holds for any stability region $\mathcal{S}$ which has the property that the phase of any polynomial which is stable with respect to $\mathcal{S}$ varies monotonically along the boundary $\partial\mathcal{S}$. The left half plane and the unit circle satisfy this criterion. Obviously there are many other regions of practical interest for which this property holds. For example, the regions shown in Figure 1.1.(c) and (d) also satisfy this condition.

In the next two sections we display another application of the Boundary Crossing Theorem by using it to derive the Jury and Routh tables for Schur and Hurwitz stability respectively.

1.4 SCHUR STABILITY TEST

The problem of checking the stability of a discrete time system reduces to the determination of whether or not the roots of the characteristic polynomial of the system lie strictly within the unit disc, that is whether or not the characteristic polynomial is a Schur polynomial. In this section we develop a simple test procedure for this problem based on the Boundary Crossing Theorem. The procedure turns out to be equivalent to Jury's test for Schur stability.

The development here is given generally for complex polynomials and of course it applies to real polynomials as well. Now, let

$$P(z) = p_0 + p_1 z + \cdots + p_n z^n,$$

be a polynomial of degree n. The following is a simple necessary condition.

Property 1.3. A necessary condition for $P(z)$ to be a Schur polynomial is that

$$|p_n| > |p_0|.$$

Indeed, if $P(z)$ has all its roots $z_1, \cdots, z_n$ inside the unit-circle then the product of these roots is given by

$$(-1)^n \prod_{i=1}^{n} z_i = \frac{p_0}{p_n},$$

$$\text{hence} \quad \left|\frac{p_0}{p_n}\right| = \prod_{i=1}^{n} |z_i| < 1.$$

Now, consider a polynomial $P(z)$ of degree n,

$$P(z) = p_0 + p_1 z + \cdots + p_n z^n.$$

Let $\overline{z}$ denote the conjugate of z and define

$$Q(z) = z^n \overline{P\left(\frac{1}{\overline{z}}\right)} = \overline{p}_0 z^n + \overline{p}_1 z^{n-1} + \cdots + \overline{p}_{n-1} z + \overline{p}_n,$$

$$R(z) = \frac{1}{z}\left[P(z) - \frac{p_0}{\overline{p}_n} Q(z)\right]. \tag{1.49}$$

It is easy to see that $R(z)$ is always of degree less than or equal to $n-1$. The following key lemma allows the degree of the test polynomial to be reduced without losing stability information.

Lemma 1.3 *If $P(z)$ satisfies $|p_n| > |p_0|$, we have the following equivalence*

$$P(z) \textit{ is a Schur polynomial} \Longleftrightarrow R(z) \textit{ is a Schur polynomial.}$$

Proof. First notice that obviously,

$$R(z) \text{ is a Schur polynomial} \Longleftrightarrow zR(z) \text{ is a Schur polynomial.}$$

Now consider the family of polynomials

$$P_\lambda(z) = P(z) - \lambda \frac{p_0}{\overline{p}_n} Q(z), \text{ where } \lambda \in [0, 1].$$

It can be seen that $P_0(z) = P(z)$, and $P_1(z) = zR(z)$. Moreover the coefficient of degree n of $P_\lambda(z)$ is

$$p_n - \lambda \frac{|p_0|^2}{\overline{p}_n},$$

and satisfies

$$\left| p_n - \lambda \frac{|p_0|^2}{\overline{p}_n} \right| > |p_n| - \lambda \left| \frac{p_0}{p_n} \right| |p_0| > |p_n| - |p_0| > 0,$$

so that $P_\lambda(z)$ remains of fixed degree n.

Assume now by way of contradiction that one of these two polynomials $P_0(z)$ or $P_1(z)$ is stable whereas the other one is not. Then, from the Boundary Crossing Theorem it can be concluded that there must exist a λ in $[0,1]$ such that $P_\lambda(z)$ has a root on the unit-circle at the point $z_0 = e^{j\theta}$, $\theta \in [0, 2\pi)$, that is

$$P_\lambda(z_0) = P(z_0) - \lambda \frac{p_0}{\overline{p}_n} \; z_0^n \; \overline{P\left[\frac{1}{\overline{z}_0}\right]} = 0. \tag{1.50}$$

But for any complex number z on the unit circle, $\overline{z} = \frac{1}{z}$, and therefore (1.50) implies that,

$$P_\lambda(z_0) = P(z_0) - \lambda \frac{p_0}{\overline{p}_n} \; z_0^n \; \overline{P(z_0)} = 0. \tag{1.51}$$

Taking the complex conjugate of this last expression it is deduced that

$$\overline{P(z_0)} - \lambda \frac{\overline{p}_0}{p_n} \; \overline{z}_0^n \; P(z_0) = 0. \tag{1.52}$$

Therefore, from (1.51) and (1.52) after using the fact that $|z_0| = 1$,

$$P(z_0) \left(1 - \lambda^2 \frac{|p_0|^2}{|p_n|^2} \right) = 0. \tag{1.53}$$

By assumption $\lambda^2 \dfrac{|p_0|^2}{|p_n|^2} < 1$, and therefore (1.53) implies that,

$$P(z_0) = 0. \tag{1.54}$$

But then this implies that

$$\overline{P(z_0)} = \overline{P\left(\frac{1}{\overline{z}_0}\right)} = 0,$$

and therefore (see (1.49))

$$R(z_0) = 0. \tag{1.55}$$

But (1.54) and (1.55) contradict the assumption that one of the two polynomials $P(z)$ and $zR(z)$ is stable, and this concludes the proof of the lemma. ♣

The above lemma leads to the following procedure for successively reducing the degree and testing for stability.

Algorithm 1.1. (Schur stability for real or complex polynomials)

1) Set $P^{(0)}(z) = P(z)$,

2) Verify $|p_n^{(i)}| > |p_0^{(i)}|$,

3) Construct $P^{(i+1)}(z) = \frac{1}{z}\left[P^{(i)}(z) - \frac{p_0^{(i)}}{\overline{p_n^{(i)}}} z^n \overline{P(\frac{1}{\overline{z}})}\right]$,

4) Go back to 2) until you either find that 2) is violated ($P(z)$ is not Schur) or until you reach $P^{(n-1)}(z)$ (which is of degree 1) in which case condition 2) is also sufficient and $P(z)$ is a Schur polynomial.

It can be verified by the reader that this procedure leads precisely to the Jury stability test.

Example 1.9. Consider a real polynomial of degree 3 in the variable z,

$$P(z) = z^3 + az^2 + bz + c.$$

According to the algorithm, we form the following polynomial

$$\begin{aligned} P^{(1)}(z) &= \frac{1}{z}\left[P(z) - cz^3\overline{P\left(\frac{1}{\overline{z}}\right)}\right] \\ &= (1-c^2)z^2 + (a-bc)z + b - ac, \end{aligned}$$

and then,

$$\begin{aligned} P^{(2)}(z) &= \frac{1}{z}\left[P^{(1)}(z) - \left(\frac{b-ac}{1-c^2}\right) z^2 \overline{P^{(1)}\left(\frac{1}{\overline{z}}\right)}\right] \\ &= \frac{\left(1-c^2\right)^2 - (b-ac)^2}{1-c^2} z + (a-bc)\left(1 - \frac{b-ac}{1-c^2}\right). \end{aligned}$$

On the other hand, the Jury table is given by,

$$\begin{bmatrix} c & b & a & 1 \\ 1 & a & b & c \\ c^2-1 & cb-a & ca-b & \\ ca-b & cb-a & c^2-1 & \\ \left(c^2-1\right)^2 - (ca-b)^2 & (cb-a)[(c^2-1)-(ca-b)] & & \end{bmatrix}$$

Here, the first two lines of this table correspond to the coefficients of $P(z)$, the third and fourth lines to those of $P^{(1)}(z)$ and the last one to a constant times $P^{(2)}(z)$, and the tests to be carried out are exactly similar.

1.5 HURWITZ STABILITY TEST

We now turn to the problem of left half plane or Hurwitz stability for real polynomials and develop an elementary test procedure for it based on the Interlacing Theorem and therefore on the Boundary Crossing Theorem. This procedure turns out to be equivalent to Routh's well known test.

Let $P(s)$ be a real polynomial of degree n, and assume that all the coefficients of $P(s)$ are positive,

$$P(s) = p_0 + p_1 s + \cdots + p_n s^n, \qquad p_i > 0, \quad \text{for} \quad i = 0, \cdots, n \ .$$

Remember that $P(s)$ can be decomposed into its odd and even parts as

$$P(s) = P^{\text{even}}(s) + P^{\text{odd}}(s).$$

Now, define the polynomial $Q(s)$ of degree $n-1$ by:

$$\begin{aligned} \text{If } n = 2m: \quad Q(s) &= \left[P^{\text{even}}(s) - \frac{p_{2m}}{p_{2m-1}} s P^{\text{odd}}(s) \right] + P^{\text{odd}}(s), \\ \text{If } n = 2m+1: \quad Q(s) &= \left[P^{\text{odd}}(s) - \frac{p_{2m+1}}{p_{2m}} s P^{\text{even}}(s) \right] + P^{\text{even}}(s) \end{aligned} \tag{1.56}$$

that is in general, with $\mu = \frac{p_n}{p_{n-1}}$,

$$Q(s) = p_{n-1} s^{n-1} + (p_{n-2} - \mu p_{n-3}) s^{n-2} + p_{n-3} s^{n-3} + (p_{n-4} - \mu p_{n-5}) s^{n-4} + \cdots. \tag{1.57}$$

Then the following key result on degree reduction is obtained.

Lemma 1.4 *If $P(s)$ has all its coefficients positive,*

$$P(s) \text{ is stable} \iff Q(s) \text{ is stable.}$$

Proof. Assume, for example that, $n = 2m$, and use the interlacing theorem.

(a) Assume that $P(s) = p_0 + \cdots + p_{2m} s^{2m}$ is stable and therefore satisfies the interlacing theorem. Let

$$0 < \omega_{e,1} < \omega_{o,1} < \omega_{e,2} < \omega_{o,2} < \cdots < \omega_{e,m-1} < \omega_{o,m-1} < \omega_{e,m},$$

be the interlacing roots of $P^e(\omega)$ and $P^o(\omega)$. One can easily check that (1.56) implies that $Q^e(\omega)$ and $Q^o(\omega)$ are given by

$$\begin{aligned} Q^e(\omega) &= P^e(\omega) + \mu \omega^2 P^o(\omega), \quad \mu = \frac{p_{2m}}{p_{2m-1}}, \\ Q^o(\omega) &= P^o(\omega). \end{aligned}$$

From this it is already concluded that $Q^o(\omega)$ has the required number of positive roots, namely the $m-1$ roots of $P^o(\omega)$:

$$\omega_{o,1}, \quad \omega_{o,2}, \quad \cdots, \quad \omega_{o,m-1}.$$

Moreover, due to the form of $Q^e(\omega)$, it can be deduced that,

$$\begin{aligned} Q^e(0) &= P^e(0) > 0, \\ Q^e(\omega_{o,1}) &= P^e(\omega_{o,1}) < 0, \\ &\vdots \\ Q^e(\omega_{o,m-2}) &= P^e(\omega_{o,m-2}), \text{ has the sign of } (-1)^{m-2}, \\ Q^e(\omega_{o,m-1}) &= P^e(\omega_{o,m-1}), \text{ has the sign of } (-1)^{m-1}. \end{aligned}$$

Hence, it is already established that $Q^e(\omega)$ has $m-1$ positive roots $\omega'_{e,1}$, $\omega'_{e,2}$, $\cdots$, $\omega'_{e,m-1}$, that do interlace with the roots of $Q^o(\omega)$. Since moreover $Q^e(\omega)$ is of degree $m-1$ in ω^2, these are the only positive roots it can have. Finally, it has been seen that the sign of $Q^e(\omega)$ at the last root $\omega_{o,m-1}$ of $Q^o(\omega)$ is that of $(-1)^{m-1}$. But the highest coefficient of $Q^e(\omega)$ is nothing but

$$q_{2m-2}(-1)^{m-1}.$$

From this q_{2m-2} must be strictly positive, as $q_{2m-1} = p_{2m-1}$ is, otherwise $Q^e(\omega)$ would again have a change of sign between $\omega_{o,m-1}$ and $+\infty$, which would result in the contradiction of $Q^e(\omega)$ having m positive roots (whereas it is a polynomial of degree only $m-1$ in ω^2). Therefore $Q(s)$ satisfies the interlacing property and is stable if $P(s)$ is.

(b) Conversely assume that $Q(s)$ is stable. Write

$$P(s) = [Q^{\text{even}}(s) + \mu s Q^{\text{odd}}(s)] + Q^{\text{odd}}(s) \quad \mu = \frac{p_{2m}}{p_{2m-1}}.$$

By the same reasoning as in a) it can be seen that $P^o(\omega)$ already has the required number $m-1$ of positive roots, and that $P^e(\omega)$ already has $m-1$ roots in the interval $(0, \omega_{o,m-1})$ that interlace with the roots of $P^o(\omega)$. Moreover the sign of $P^e(\omega)$ at $\omega_{o,m-1}$ is the same as $(-1)^{m-1}$ whereas the term $p_{2m}s^{2m}$ in $P(s)$, makes the sign of $P^e(\omega)$ at $+\infty$ that of $(-1)^m$. Thus $P^e(\omega)$ has an m^{th} positive root,

$$\omega_{e,m} > \omega_{o,m-1},$$

so that $P(s)$ satisfies the interlacing property and is therefore stable.

♣

The above lemma shows how the stability of a polynomial $P(s)$ can be checked by successively reducing its degree as follows.

Algorithm 1.2. (Hurwitz stability for real polynomials)

1) Set $P^{(0)}(s) = P(s)$,

2) Verify that all the coefficients of $P^{(i)}(s)$ are positive,

3) Construct $P^{(i+1)}(s) = Q(s)$ according to (1.57),

4) Go back to 2) until you either find that any 2) is violated ($P(s)$ is not Hurwitz) or until you reach $P^{(n-2)}(s)$ (which is of degree 2) in which case condition 2) is also sufficient ($P(s)$ is Hurwitz).

The reader may verify that this procedure is identical to Routh's test since it generates the Routh table. The proof also shows the known property that for a stable polynomial not only the first column but the entire Routh table must consist only of positive numbers. However the procedure described here does not allow to count the stable and unstable zeroes of the polynomial as can be done with Routh's Theorem.

Example 1.10. Consider a real polynomial of degree 4,

$$P(s) = s^4 + as^3 + bs^2 + cs + d.$$

Following the algorithm above we form the polynomials,

$$\mu = \frac{1}{a}, \text{ and } P^{(1)}(s) = as^3 + \left(b - \frac{c}{a}\right) s^2 + cs + d,$$

and then,

$$\mu = \frac{a^2}{ab - c}, \text{ and } P^{(2)} = \left(b - \frac{c}{a}\right) s^2 + \left(c - \frac{a^2 d}{ab - c}\right) s + d.$$

Considering that at each step only the even or the odd part of the polynomial is modified, it is needed to verify the positiveness of the following set of coefficients,

$$\begin{bmatrix} 1 & b & d \\ a & c & \\ b - \frac{c}{a} & d & \\ c - \frac{a^2 d}{ab - c} & & \end{bmatrix}$$

But this is just the Routh table for this polynomial.

Note that a lemma similar to Lemma 1.4 could be derived where the assumption that all the coefficients of $P(s)$ are positive is replaced by the assumption that only the two highest degree coefficients p_{n-1} and p_n are positive. The corresponding algorithm would then exactly lead to checking that the first column of the Routh table is positive. However since the algorithm requires that the entire table be constructed, it is more efficient to check that every new coefficient is positive.

Complex polynomials

A similar algorithm can be derived for checking the Hurwitz stability of complex polynomials. The proof which is very similar to the real case is omitted and a precise description of the algorithm is given below.

Let $P(s)$ be a complex polynomial of degree n,

$$P(s) = (a_0+jb_0)+(a_1+jb_1)s+\cdots+(a_{n-1}+jb_{n-1})s^{n-1}+(a_n+jb_n)s^n, \;\; a_n+jb_n \neq 0.$$

Let,

$$T(s) = \frac{1}{a_n + jb_n} P(s).$$

Thus $T(s)$ can be written as,

$$T(s) = (c_0 + jd_0) + (c_1 + jd_1)s + \cdots + (c_{n-1} + jd_{n-1})s^{n-1} + s^n,$$

and notice that,

$$c_{n-1} = \frac{a_{n-1}a_n + b_{n-1}b_n}{a_n^2 + b_n^2}.$$

Assume that $c_{n-1} > 0$, which is a necessary condition for $P(s)$ to be Hurwitz (see Theorem 1.8). As usual write, $T(s) = T_R(s) + T_I(s)$, where

$$\begin{aligned} T_R(s) &= c_0 + jd_1 s + c_2 s^2 + jd_3 s^3 + \cdots \;, \\ T_I(s) &= jd_0 + c_1 s + jd_2 s^2 + c_3 s^3 + \cdots \;. \end{aligned}$$

Now define the polynomial $Q(s)$ of degree $n-1$ by:

$$\begin{aligned} \text{If } n = 2m: \qquad Q(s) &= \left[T_R(s) - \frac{1}{c_{2m-1}} s T_I(s)\right] + T_I(s), \\ \text{If } n = 2m+1: \qquad Q(s) &= \left[T_I(s) - \frac{1}{c_{2m}} s T_R(s)\right] + T_R(s), \end{aligned}$$

that is in general, with $\mu = \frac{1}{c_{n-1}}$,

$$\begin{aligned} Q(s) = {} & [c_{n-1} + j(d_{n-1} - \mu d_{n-2})]s^{n-1} + [(c_{n-2} - \mu c_{n-3}) + jd_{n-2}]s^{n-2} \\ & + [c_{n-3} + j(d_{n-3} - \mu d_{n-4})]s^{n-3} + \cdots. \end{aligned}$$

Now, exactly as in the real case, the following lemma can be proved.

Lemma 1.5 *If $P(s)$ satisfies $a_{n-1}a_n + b_{n-1}b_n > 0$, then*

$$P(s) \text{ is Hurwitz stable} \iff Q(s) \text{ is Hurwitz stable.}$$

The corresponding algorithm is as follows.

Algorithm 1.3. (Hurwitz stability for complex polynomials)

1) Set $P^{(0)}(s) = P(s)$,

2) Verify that the last two coefficients of $P^{(i)}(s)$ satisfy $a_{n-1}^{(i)} a_n^{(i)} + b_{n-1}^{(i)} b_n^{(i)} > 0$,

3) Construct $T^{(i)}(s) = \dfrac{1}{a_n^{(i)} + j b_n^{(i)}} P^{(i)}(s)$,

4) Construct $P^{(i+1)}(s) = Q(s)$ as above,

5) Go back to 2) until you either find that any 2) is violated ($P(s)$ is not Hurwitz) or until you reach $P^{(n-1)}(s)$ (which is of degree 1) in which case condition 2) is also sufficient ($P(s)$ is Hurwitz).

1.6 A FEW COMPLEMENTS

Polynomial functions are analytic in the entire complex plane and thus belong to the so-called class of *entire functions*. It is not straightforward however, to obtain a general version of the Boundary Crossing Theorem that would apply to any family of entire functions. The main reason for this is the fact that a general entire function may have a finite or infinite number of zeros, and the concept of a *degree* is not defined except for polynomials. Similar to Theorem 1.3 for the polynomial case, the following theorem can be considered as a basic result for the analysis of continuous families of entire functions.

Theorem 1.10 *Let A be an open subset of the complex plane C, F a metric space, and f be a complex-valued function continuous in $A \times F$ such that for each α in F, $z \longrightarrow f(z, \alpha)$ is analytic in A. Let also B be an open subset of A whose closure $\overline{B}$ in C is compact and included in A, and let $\alpha_0 \in F$ be such that no zeros of $f(z, \alpha_0)$ belong to the boundary ∂B of B. Then, there exists a neighborhood W of α_0 in F such that,*

1) For all $\alpha \in W$, $f(z, \alpha)$ has no zeros on ∂B.

2) For all $\alpha \in W$, the number (multiplicities included) of zeros of $f(z, \alpha)$ which belong to B is independent of α.

The proof of this theorem is not difficult and is very similar to that of Theorem 1.3. It uses Rouché's Theorem together with the compactness assumption on B. Loosely speaking, the above result states the continuity of the zeros of a parametrized family of analytic functions with respect to the parameter values. However, it only applies to the zeros which are contained in a given compact subset of the complex plane and therefore, in terms of stability, a more detailed analysis is required. In the polynomial case, Theorem 1.3 is used together with a knowledge of the degree of the family to arrive at the Boundary Crossing Theorem. The degree of a polynomial indicates not only the number of its zeros in the complex plane, but also

its rate of growth at infinity. For more general families of entire functions it is precisely by using this additional notion of growth at infinity that results which are similar to the Boundary Crossing Theorem may sometimes be derived. Clearly, each particular case requires its own analysis. Much deeper results however may be achieved and some of these are presented in the remainder of this section. These results demonstrate the possibility of extending the Hermite-Biehler Theorem to more general classes of entire functions, and some extensions that seem to be of particular interest for Control Theory are selected here.

Let $P(s)$ be a real or complex polynomial. Write,

$$P(j\omega) = P^r(\omega) + jP^i(\omega) \tag{1.58}$$

where $P^r(\omega)$ and $P^i(\omega)$ are real polynomials in ω which represent respectively the real and imaginary part of $P(j\omega)$. The Hermite-Biehler Theorem for real or complex polynomials can be stated in the following way.

Theorem 1.11 (Hermite-Biehler)
$P(s)$ has all its roots in the open left-half of the complex plane if and only if,

a) $P^r(\omega)$ and $P^i(\omega)$ have only simple roots and these roots interlace.

b) For all ω in $\mathbb{R}$, $\quad P^{i\prime}(\omega)P^r(\omega) - P^i(\omega)P^{r\prime}(\omega) > 0.$

In condition b) the symbol $'$ indicates derivation with respect to ω. Moreover it can be shown that condition b) can be replaced by the following condition,

b') $P^{i\prime}(\omega_o)P^r(\omega_o) - P^i(\omega_o)P^{r\prime}(\omega_o) > 0, \quad$ for some ω_o in $\mathbb{R}$.

In other words it is enough that condition b) be satisfied at only one point on the real line.

It is quite easy to see that the Hermite-Biehler Theorem does not carry over to arbitrary entire functions $f(s)$ of the complex variable s. In fact counterexamples can be found which show that conditions a) and b) above are neither necessary nor sufficient for an entire function to have all its zeros in the open left-half plane. The theorem however holds for a large class of entire functions and two such theorems are given below without proofs.

One of the earliest attempt at generalizing the Hermite-Biehler Theorem was made by L. S. Pontryagin. In his paper he studied entire functions of the form $P(s, e^s)$, where $P(s,t)$ is a polynomial in two variables. Before stating his result, some preliminary definitions are needed. Let $P(s,t)$ be a polynomial in two variables with real or complex coefficients,

$$P(s,t) = \sum_k \sum_i a_{ik} s^i t^k. \tag{1.59}$$

Let r be the highest degree in s and p be the highest degree in t. $P(s,t)$ is said to have a principal term if and only if $a_{rp} \neq 0$. For example

$$P(s,t) = s + t,$$

does not have a principal term but the following polynomial does

$$P(s,t) = s + t + st.$$

The first result of Pontryagin can be stated as follows.

Theorem 1.12 *If the polynomial $P(s,t)$ does not have a principal term then the function,*

$$f(s) = P(s, e^s),$$

has an unbounded number of zeros with arbitrarily large positive real parts.

In the case where $P(s,t)$ does have a principal term, the main result of Pontryagin's paper is then to show that the Hermite-Biehler Theorem extends to this class of entire functions. More precisely we have the following theorem.

Theorem 1.13 *Let $f(s) = P(s, e^s)$, where $P(s,t)$ is a polynomial with a principal term, and write*

$$f(j\omega) = f^r(\omega) + jf^i(\omega),$$

where $f^r(\omega)$ and $f^i(\omega)$ represent respectively the real and imaginary parts of $f(j\omega)$. Then in order that $f(s)$ have all its zeros in the open left-half plane it is necessary and sufficient that the following two conditions hold,

a) $f^r(\omega)$ and $f^i(\omega)$ have only simple roots and these roots interlace,

b) For all ω in $\mathbb{R}$, $f^{i\prime}(\omega)f^r(\omega) - f^i(\omega)f^{r\prime}(\omega) > 0$.

Another interesting extension of the Hermite-Biehler Theorem is now given. Let $f(s)$ be an entire function of the form,

$$f(s) = \sum_{k=1}^{n} e^{\lambda_k s} P_k(s), \tag{1.60}$$

where $P_k(s)$ for $k = 1, \cdots, n$ is an arbitrary polynomial with real or complex coefficients, and the λ_k's are real number which satisfy,

$$\lambda_1 < \lambda_2 < \cdots < \lambda_n, \quad |\lambda_1| < \lambda_n \ . \tag{1.61}$$

The Hermite-Biehler Theorem also holds for this class of entire functions. Write as usual $f(j\omega) = f^r(\omega) + jf^i(\omega)$.

Theorem 1.14 *Under the above assumptions, the entire function $f(s)$ in (1.60) has all its zeros in the open left-half plane if and only if*

a) $f^r(\omega)$ and $f^i(\omega)$ have only simple roots and these roots interlace.

b) For all ω in $\mathbb{R}$, $f^{i\prime}(\omega)f^r(\omega) - f^i(\omega)f^{r\prime}(\omega) > 0$.

Moreover in both Theorems 1.13 and 1.14, condition b) may be replaced by the weaker condition,

b′) $f^{i\prime}(\omega_0)f^r(\omega_0) - f^i(\omega_0)f^{r\prime}(\omega_0) > 0$, for some ω_0 in $\mathbb{R}$.

Time-delay systems

In control problems involving time delays, we often deal with characteristic equations of the form

$$\delta(s) = d(s) + e^{-sT_1}n_1(s) + e^{-sT_2}n_2(s) + \cdots + e^{-sT_m}n_m(s). \tag{1.62}$$

which are also known as quasipolynomials. Under the assumption that $\deg[d(s)] = n$ and $\deg[n_i(s)] < n$ and

$$0 < T_1 < T_2 < \cdots < T_m,$$

it is easy to show using Theorems 1.13 and 1.14 that the stability of $\delta(s)$ can be checked using the interlacing condition. More precisely, we have

Theorem 1.15 *Under the above assumptions, $\delta(s)$ in (1.62) is Hurwitz stable if and only if*

a) $\delta^r(\omega)$ and $\delta^i(\omega)$ have only simple roots and these roots interlace.

b) $\delta^{i\prime}(\omega_0)\delta^r(\omega_0) - \delta^i(\omega_0)\delta^{r\prime}(\omega_0) > 0$, for some ω_0 in $\mathbb{R}$.

We note that the interlacing condition a) needs to be checked only up to a finite frequency. This follows from the fact that the phasors of $n_i(j\omega)/d(j\omega)$ tend to zero as ω tend to ∞. This ensures that the quasipolynomial $\delta(s)$ has the monotonic phase property for a sufficiently large ω. Therefore, the interlacing condition needs to be verified only for low frequency range.

An immediate consequence of the above result is the following Boundary Crossing Theorem for quasipolynomials. Consider the quasipolynomial family

$$Q(s,\lambda) = d(s,\lambda) + e^{-sT_1}n_1(s,\lambda) + e^{-sT_2}n_2(s,\lambda) + \cdots + e^{-sT_m}n_m(s,\lambda). \tag{1.63}$$

where $\lambda \in [a,b]$ and we assume that 1) $Q(s,a)$ is Hurwitz, 2) $Q(s,b)$ is not Hurwitz, 3) $\deg[d(s,\lambda)] = n,\ \forall\ \lambda \in [a,b]$ and 4) $\deg[n_i(s,\lambda)] < n,\ \forall\ \lambda \in [a,b]$.

Theorem 1.16 (Boundary Crossing Theorem for Quasipolynomials) *Under the above assumptions there exists at least one ρ in $(a,b]$ such that $Q(0,\rho) = 0$ or $Q(j\omega,\rho) = 0$ for some $\omega \in [-\infty,+\infty]$.*

These results are particularly useful for the stability analysis of control systems which contain time-delays. We illustrate this in the example below.

Example 1.11. Consider the quasipolynomial:

$$\delta(s) = d(s) + e^{-sT_1}n_1(s) + e^{-sT_2}n_2(s)$$

where

$$\begin{aligned} d(s) &= s^9 + 5s^8 + 20s^7 + 100s^6 + 200s^5 + 100s^4 + 100s^3 + 50s^2 + 15s + 1 \\ n_1(s) &= 3s^8 + 10s^7 + 10s^6 + 15s^5 + 100s^4 + 50s^3 + 50s^2 + 10s + 2 \\ n_2(s) &= 2s^8 + 22s^7 + 35s^6 + 51s^5 + 131s^4 + 130s^3 + 55s^2 + 24s + 3 \end{aligned}$$

with $T_1 = 0.1$ sec and $T_2 = 0.3$ sec. We write

$$\begin{aligned} d(j\omega) &= d^{\mathrm{e}}(\omega) + j\omega d^{\mathrm{o}}(\omega) \\ n_1(j\omega) &= n_1^{\mathrm{e}}(\omega) + j\omega n_1^{\mathrm{o}}(\omega) \\ n_2(j\omega) &= n_2^{\mathrm{e}}(\omega) + j\omega n_2^{\mathrm{o}}(\omega) \end{aligned}$$

and $\delta(j\omega) = \delta_r(\omega) + j\delta_i(\omega)$. We have

$$\begin{aligned} \delta_r(\omega) &= d^{\mathrm{e}}(\omega) + \cos(\omega T_1) n_1^{\mathrm{e}}(\omega) - \omega \sin(\omega T_1) n_1^{\mathrm{o}}(\omega) \\ &\quad + \cos(\omega T_2) n_2^{\mathrm{e}}(\omega) - \omega \sin(\omega T_2) n_2^{\mathrm{o}}(\omega) \\ \delta_i(\omega) &= \omega d^{\mathrm{o}}(\omega) + \omega \cos(\omega T_1) n_1^{\mathrm{o}}(\omega) - \sin(\omega T_1) n_1^{\mathrm{e}}(\omega) \\ &\quad + \omega \cos(\omega T_2) n_2^{\mathrm{o}}(\omega) - \sin(\omega T_2) n_2^{\mathrm{e}}(\omega). \end{aligned}$$

Figure 1.13 shows that $\delta_r(\omega)$ and $\delta_i(\omega)$ are interlacing. Thus, we conclude that the quasipolynomial $\delta(s)$ is Hurwitz.

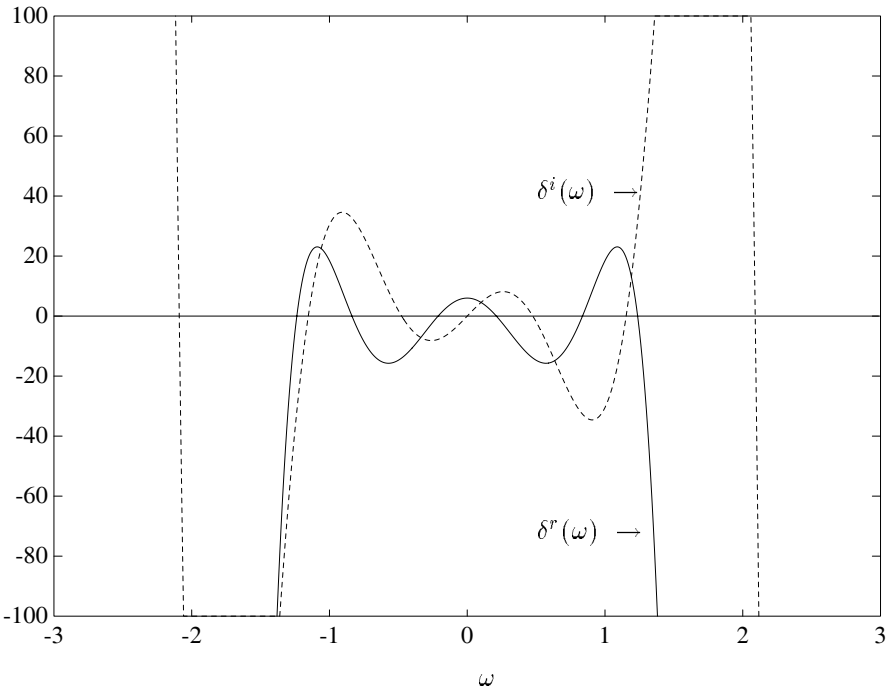

Figure 1.13. Interlacing property for a quasipolynomial (Example 1.11)

1.7 EXERCISES

The purpose of Problems 1-5 is to illustrate some possible uses of the Boundary Crossing Theorem and of the Interlacing (Hermite-Biehler) Theorem. In all the problems the word stable means *Hurwitz-stable*, and all stable polynomials are assumed to have *positive* coefficients. The following standard notation is also used: Let $P(s)$ be any polynomial. Denote by $P^{\rm even}(s)$ the even part of $P(s)$, and by $P^{\rm odd}(s)$ its odd part, that is

$$P(s) = \underbrace{(p_0 + p_2 s^2 + p_4 s^4 + \cdots)}_{P^{\rm even}(s)} + \underbrace{(p_1 s + p_3 s^3 + p_5 s^5 + \cdots)}_{P^{\rm odd}(s)}.$$

Also denote,

$$P^e(\omega) := P^{\rm even}(j\omega) = p_0 - p_2\omega^2 + p_4\omega^4 + \cdots$$
$$P^o(\omega) := \frac{P^{\rm odd}(j\omega)}{j\omega} = p_1 - p_3\omega^2 + p_5\omega^4 + \cdots.$$

Also for any polynomial $Q(t)$ of the variable t, the notation $\left[Q\right]'(t)$ designates the derivative of $Q(t)$ with respect to t.

1.1 Suppose that the polynomial $P(s) = P^{\rm even}(s) + P^{\rm odd}(s)$ is stable. Prove that the following two polynomials are also stable:

$$Q(s) = P^{\rm even}(s) + [P^{\rm even}]'(s) = p_0 + 2p_2 s + p_2 s^2 + 4p_4 s^3 + \cdots,$$

$$R(s) = \left[P^{\rm odd}\right]'(s) + P^{\rm odd}(s) = p_1 + p_1 s + 3p_3 s^2 + p_3 s^3 + \cdots.$$

Hint: In both cases use the Hermite-Biehler (i.e. Interlacing) Theorem. First, check that part a) of the theorem is trivially satisfied. To prove part b) of the theorem for $Q(s)$, show that $-\omega Q^o(\omega) = \left[P^e\right]'(\omega)$. To conclude use the fact that for any continuous function $f(t)$, if $f(a) = f(b) = 0$ for some real numbers $a < b$, and if f is differentiable on the interval $[a, b]$, then there exists a real number c such that:

$$a < c < b \quad \text{and} \quad f'(c) = 0. \quad \text{(Rolle's Theorem)}.$$

Proceed similarly to prove part b) of the theorem for $R(s)$.

1.2 Suppose that:

$$P_1(s) = P^{\rm even}(s) + P_1^{\rm odd}(s)$$
$$P_2(s) = P^{\rm even}(s) + P_2^{\rm odd}(s)$$

are two stable polynomials with the same 'even' part. Show that the polynomial $Q_{\lambda,\mu}(s)$ defined by:

$$Q_{\lambda,\mu}(s) = P^{\rm even}(s) + \lambda P_1^{\rm odd}(s) + \mu P_2^{\rm odd}(s),$$

is stable for all $\lambda > 0$ and $\mu > 0$.
Hint: You can use directly the Boundary Crossing Theorem. In doing so, check that

$$Q^o_{\lambda,\mu}(\omega) = \lambda P^o_1(\omega) + \mu P^o_2(\omega),$$

and use the fact that the sign of $P^o_i(\omega)$ alternates at the positive roots of $P^e(\omega)$, and does not depend on i.

1.3 Suppose that $P(s)$ is a stable polynomial:

$$P(s) = p_0 + p_1 s + p_2 s^2 + \cdots + p_n s^n, \ n \geq 1.$$

Write as usual: $P(j\omega) = P^e(\omega) + j\omega P^o(\omega)$.

a) Show that the polynomial $Q_\lambda(s)$ associated with:

$$Q^e_\lambda(\omega) = P^e(\omega) - \lambda P^o(\omega),$$

and,

$$Q^o_\lambda(\omega) = P^o(\omega),$$

is stable for all λ satisfying $0 \leq \lambda < \frac{p_0}{p_1}$.

b) Deduce from a) that

$$\frac{p_{2k}}{p_{2k+1}} \geq \frac{p_0}{p_1}, \quad \text{for all} \quad k \geq 1.$$

Hint: In part a) use the Boundary Crossing Theorem. In doing so, check carefully that the highest coefficient of $Q_\lambda(s)$ equals p_n for all values of λ and therefore the degree of $Q_\lambda(s)$ is n no matter what λ is.

To prove b) use the fact that since $Q_\lambda(s)$ is stable for all λ in the range $[0, \frac{p_0}{p_1})$, then in particular the coefficients of $Q_\lambda(s)$ must remain positive for all values of λ.

1.4 Prove that if $P(s)$ is a stable polynomial then:

$$\frac{p_0}{2p_2} \leq \frac{p_{2k}}{(2k+2)p_{2k+2}}, \quad \text{for all } k \geq 1.$$

Hint: Use Exercise 1.1 and apply part (b) of Exercise 1.3.

1.5 Let $P(s)$ be an arbitrary polynomial of degree $n > 0$. Prove that if $P(s)$ satisfies part b) of the interlacing condition, but violates part a) in the sense that $p_n p_{n-1} < 0$, then $P(s)$ is completely unstable, that is $P(s)$ has all its roots in the *open right half plane*. Give the Schur counterpart of this result.
Hint: Consider the polynomial $Q(s) = P(-s)$.

1.6 Show, by using the Boundary Crossing Theorem that the set ${\mathcal{H}_n}^+$ consisting of n^{th} degree Hurwitz polynomials with positive coefficients is connected. A similar result holds for Schur stable polynomials and in fact for any stability region $\mathcal{S}$.

1.7 Write $s = \sigma + j\omega$ and let the stability region be defined by

$$\mathcal{S} := \{s : \sigma < \omega^2 - 1\}.$$

Consider the parametrized family of polynomials

$$p(s,\lambda) = s^3 + (10 - 14\lambda)s^2 + (65\lambda^2 - 94\lambda + 34)s \\ +(224\lambda^2 - 102\lambda^3 - 164\lambda + 40), \quad \lambda \in [0,1].$$

Verify that $p(s,0)$ is stable and $p(s,1)$ is unstable with respect to $\mathcal{S}$. Use the Boundary Crossing Theorem to determine the range of values of λ for which the family is stable and the points on the stability boundary through which the roots cross over from stability to instability.
Hint: Consider a point (σ,ω) on the stability boundary and impose the condition for this point to be a root of $p(s,\lambda)$ in the form of two polynomial equations in ω with coefficients which are polynomial functions of λ. Now use the eliminant to obtain a polynomial equation in λ the roots of which determine the possible values of λ for which boundary crossing may occur.

1.8 Use Algorithm 1.1 to check that the following complex polynomial is a Schur polynomial,

$$P(z) = 32z^4 + (8 + 32j)z^3 + (-16 + 4j)z^2 - (2 + 8j)z + 2 - j.$$

Use Algorithm 1.3 to check that the following complex polynomial is a Hurwitz polynomial,

$$P(s) = s^4 + 6s^3 + (14 + j)s^2 + (15 + 3j)s + 2j + 6.$$

1.9 Show using the Hermite Biehler Theorem that the polynomial $P(s) + jQ(s)$ with $P(s)$ and $Q(s)$ being real polynomials has no zeroes in the lower half plane $Im\ s \leq 0$ if and only if

i) $P(s)$ and $Q(s)$ have only simple real zeroes which interlace and

ii) $Q'(s_0)P(s_0) - P'(s_0)Q(s_0) > 0$ for some point s_0 on the real axis.

Hint: Use the monotonic phase property.

1.10 Rework Example 1.11 with $d(s)$, $n_1(s)$, $n_2(s)$ and T_1 as before. Determine the maximal value of T_2 for which the system is stable by using the interlacing property.

1.8 NOTES AND REFERENCES

The material of section 1.2 is mainly based on Marden [175] and Dieudonné [82]. In particular the statement of Theorem 1.2 (Rouché's Theorem) follows Marden's book

very closely. The Boundary Crossing Theorem and the unified proof of the Hermite-Biehler Theorem, Routh and Jury tests based on the Boundary Crossing Theorem were developed by Chapellat, Mansour and Bhattacharyya [68] and the treatment given here closely follows this reference. The stability theory for a single polynomial bears countless references, going back to the last century. For a modern exposition of stability theory, the best reference remains Gantmacher [101] and to a lesser extent Marden [175]. The Hermite-Biehler Theorem for Hurwitz polynomials can be found in the book of Guillemin [105]. The corresponding theorem for the discrete time case is stated in Bose [43] where earlier references are also given. The complex case was treated in Bose and Shi [49]. Jury's test is described in [124]. Vaidyanathan and Mitra [228] have given a unified network interpretation of classical stability results. It is to be noted that the type of proof given here of Jury's criterion for Schur stability can also be found in the Signal Processing literature in conjunction with lattice filters (see, for example, the book by Haykin [108]). A considerable amount of research has been done on the distribution of the zeros of entire functions and numerous papers can be found in the literature. For a particularly enlightening summary of this research the reader can consult the book of B. Ja. Levin [160]. Theorems 1.13 and 1.14 are due to Pontryagin [192]. The stability theory of time-delay systems is treated in the book [106] by Hale. A unified approach to the proofs of various stability criteria based on the monotonicity of the argument and the Boundary Crossing Theorem has been described by Mansour [169].

Chapter 2

STABILITY OF A LINE SEGMENT

In this chapter we develop some results on the stability of a line segment of polynomials. A complete analysis of this problem for both the Hurwitz and Schur cases is given and the results are summarized as the Segment Lemma. We also prove the Vertex Lemma and the Real and Complex Convex Direction Lemmas which give certain useful conditions under which the stability of a line segment of polynomials can be ascertained from the stability of its endpoints. These results are based on some fundamental properties of the phase of Hurwitz polynomials and segments which are also proved.

2.1 INTRODUCTION

In the previous chapter, we discussed the stability of a fixed polynomial by using the Boundary Crossing Theorem. In this chapter we focus on the problem of determining the stability of a line segment joining two fixed polynomials which we refer to as the endpoints. This line segment of polynomials is a convex combination of the two endpoints. This kind of problem arises in robust control problems containing a single uncertain parameter, such as a gain or a time constant, when stability of the system must be ascertained for the entire interval of uncertainty. We give some simple solutions to this problem for both the Hurwitz and Schur cases and collectively call these results the Segment Lemma.

In general, the stability of the endpoints does not guarantee that of the entire segment of polynomials. For example consider the segment joining the two polynomials

$$P_1(s) = 3s^4 + 3s^3 + 5s^2 + 2s + 1 \quad \text{and} \quad P_2(s) = s^4 + s^3 + 5s^2 + 2s + 5.$$

It can be checked that both $P_1(s)$ and $P_2(s)$ are Hurwitz stable and yet the polynomial at the midpoint

$$\frac{P_1(s) + P_2(s)}{2} \quad \text{has a root at} \quad s = j.$$

However, if the polynomial representing the difference of the endpoints assumes certain special forms, the stability of the endpoints does indeed guarantee stability of the entire segment. These forms which are frequency independent are described in the Vertex Lemma and again both Hurwitz and Schur versions of this lemma are given. The conditions specified by the Vertex Lemma are useful for reducing robust stability determinations over a continuum of polynomials to that of a discrete set of points. A related notion, that of *convex directions*, requires that segment stability hold for all stable endpoints and asks for conditions on the difference polynomial that guarantee this. Conditions are established here for convex directions in the real and complex cases. The proofs of the Vertex Lemma and the Convex Direction Lemmas depend on certain phase relations for Hurwitz polynomials and segments which are established here. These are also of independent interest.

2.2 BOUNDED PHASE CONDITIONS

Let $\mathcal{S}$ be an open set in the complex plane representing the stability region and let $\partial\mathcal{S}$ denote its boundary. Suppose $\delta_1(s)$ and $\delta_2(s)$ are polynomials (real or complex) of degree n. Let

$$\delta_\lambda(s) := \lambda\delta_1(s) + (1-\lambda)\delta_2(s)$$

and consider the following *one parameter family* of polynomials:

$$[\delta_1(s), \delta_2(s)] := \{\delta_\lambda(s) : \lambda \in [0,1]\}\,.$$

This family will be referred to as a *segment* of polynomials. We shall say that the segment is stable if and only if every polynomial on the segment is stable. This property is also referred to as *strong stability* of the pair $(\delta_1(s), \delta_2(s))$.

We begin with a lemma which follows directly from the Boundary Crossing Theorem (Chapter 1). Let $\phi_{\delta_i}(s_0)$ denote the argument of the complex number $\delta_i(s_0)$.

Lemma 2.1 (Bounded Phase Lemma)
Let $\delta_1(s)$ and $\delta_2(s)$ be stable with respect to $\mathcal{S}$ and assume that the degree of $\delta_\lambda(s) = n$ for all $\lambda \in [0,1]$. Then the following are equivalent:

a) the segment $[\delta_1(s), \delta_2(s)]$ is stable with respect to $\mathcal{S}$

b) $\delta_\lambda(s^*) \neq 0$, for all $s^* \in \partial\mathcal{S}$; $\lambda \in [0,1]$

c) $|\phi_{\delta_1}(s^*) - \phi_{\delta_2}(s^*)| \neq \pi$ radians for all $s^* \in \partial\mathcal{S}$,

d) The complex plane plot of $\dfrac{\delta_1(s^*)}{\delta_2(s^*)}$, for $s^* \in \partial\mathcal{S}$ does not cut the negative real axis.

Proof. The equivalence of a) and b) follows from the Boundary Crossing Theorem. The equivalence of b) and c) is best illustrated geometrically in Figure 2.1. In words

this simply states that whenever $\delta_\lambda(s^*) = 0$ for some $\lambda \in [0,1]$ the phasors $\delta_1(s^*)$ and $\delta_2(s^*)$ must line up with the origin with their endpoints on opposite sides of it. This is expressed by the condition $|\phi_{\delta_1}(s^*) - \phi_{\delta_2}(s^*)| = \pi$ radians.

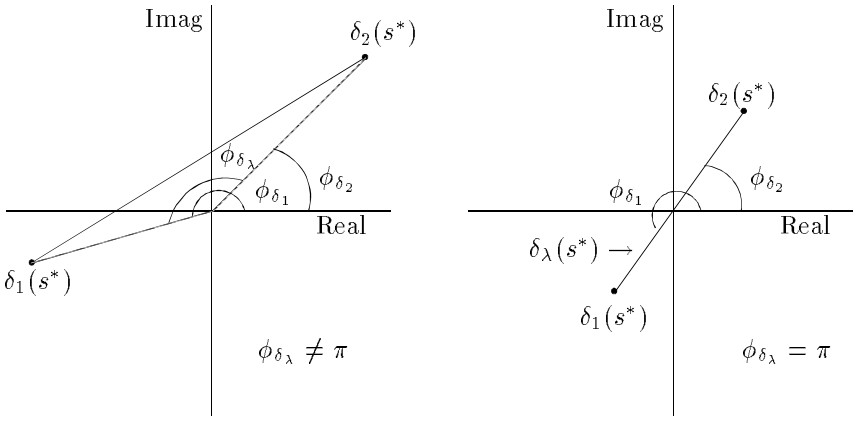

Figure 2.1. Image set of $\delta_\lambda(s^*)$ and ϕ_{δ_λ}

The equivalence of b) and d) follows from the fact that if

$$\lambda\delta_1(s^*) + (1-\lambda)\delta_2(s^*) = 0$$

then

$$\frac{\delta_1(s^*)}{\delta_2(s^*)} = -\left(\frac{1-\lambda}{\lambda}\right).$$

As λ varies from 0 to 1, the right hand side of the above equation generates the negative real axis. Hence $\delta_\lambda(s^*) = 0$ for some $\lambda \in [0,1]$ if and only if $\dfrac{\delta_1(s^*)}{\delta_2(s^*)}$ is negative and real. ♣

This Lemma essentially states that the entire segment is stable provided the end points are, the degree remains invariant and the phase difference between the endpoints evaluated along the stability boundary is bounded by π. This condition will be referred to as the *Bounded Phase Condition*. We illustrate this result with some examples.

Example 2.1. (Real Polynomials) Consider the following feedback system shown in Figure 2.2. Suppose that we want to check the robust Hurwitz stability of the closed loop system for $\alpha \in [2,3]$. We first examine the stability of the two endpoints of the characteristic polynomial

$$\delta(s,\alpha) = s^3 + 2\alpha s^2 + (\alpha+1)s + (\alpha-1).$$

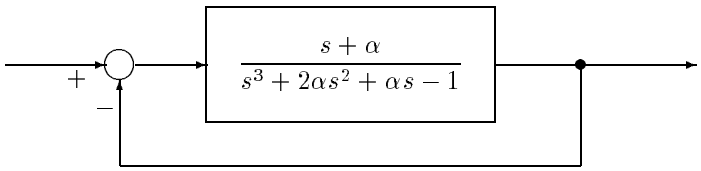

Figure 2.2. Feedback system (Example 2.1)

We let

$$\delta_1(s) := \delta(s,\alpha)|_{\alpha=2} = s^3 + 4s^2 + 3s + 1$$
$$\delta_2(s) := \delta(s,\alpha)|_{\alpha=3} = s^3 + 6s^2 + 4s + 2$$

Then $\delta_\lambda(s) = \lambda\delta_1(s) + (1-\lambda)\delta_2(s)$. We check that the endpoints $\delta_1(s)$ and $\delta_2(s)$ are stable. Then we verify the bounded phase condition, namely that the phase difference $|\phi_{\delta_1}(j\omega) - \phi_{\delta_2}(j\omega)|$ between these endpoints never reaches 180° as ω runs from 0 to ∞. Thus, the segment is robustly Hurwitz stable. This is shown in Figure 2.3.

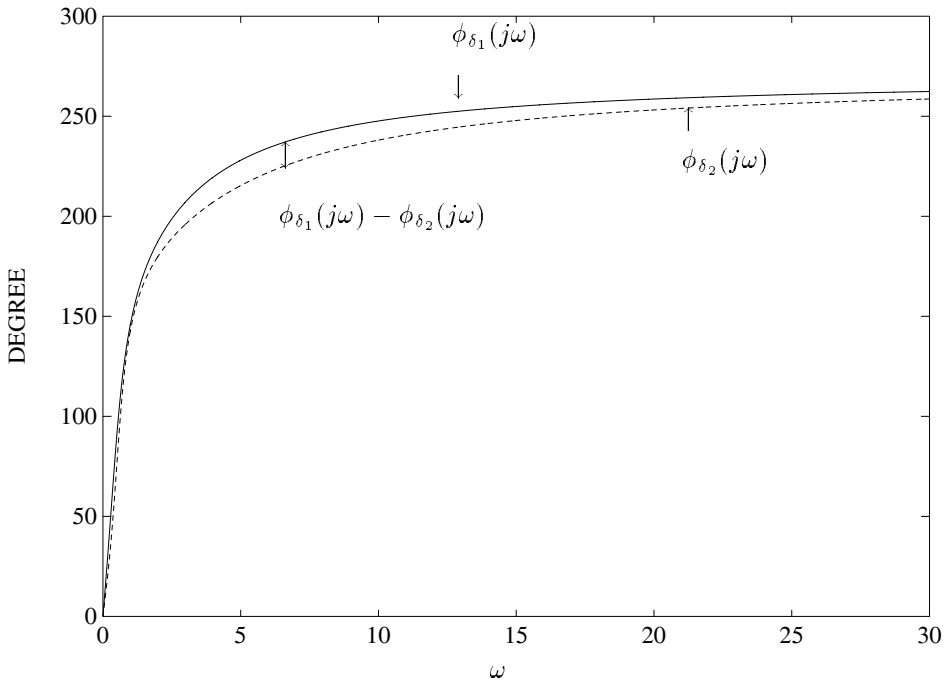

Figure 2.3. Phase difference of the endpoints of a stable segment (Example 2.1)

The condition d) of Lemma 2.1 can also be easily verified by drawing the polar plot of $\delta_1(j\omega)/\delta_2(j\omega)$.

Example 2.2. (Complex Polynomials) Consider the Hurwitz stability of the line segment joining the two complex polynomials:

$$\delta_1(s) = s^4 + (8-j)s^3 + (28-j5)s^2 + (50-j3)s + (33+j9)$$
$$\delta_2(s) = s^4 + (7+j4)s^3 + (46+j15)s^2 + (165+j168)s + (-19+j373).$$

We first verify that the two endpoints $\delta_1(s)$ and $\delta_2(s)$ are stable. Then we plot $\phi_{\delta_1}(j\omega)$ and $\phi_{\delta_2}(j\omega)$ with respect to ω (Figure 2.4). As we can see, the Bounded Phase Condition is satisfied, that is the phase difference $|\phi_{\delta_1}(j\omega) - \phi_{\delta_2}(j\omega)|$ never reaches $180°$, so we conclude that the given segment $[\delta_1(s), \delta_2(s)]$ is stable.

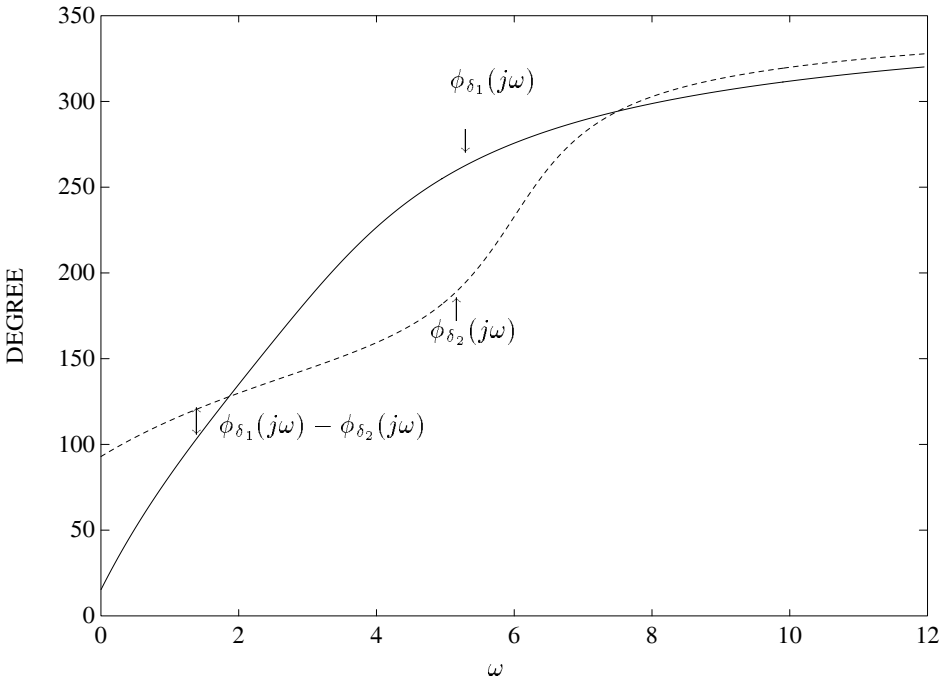

Figure 2.4. Phase difference vs ω for a complex segment (Example 2.2)

We can also use the condition d) of Lemma 2.1. As shown in Figure 2.5, the plot of $\delta_1(j\omega)/\delta_2(j\omega)$ does not cut the negative real axis of the complex plane. Therefore, the segment is stable.

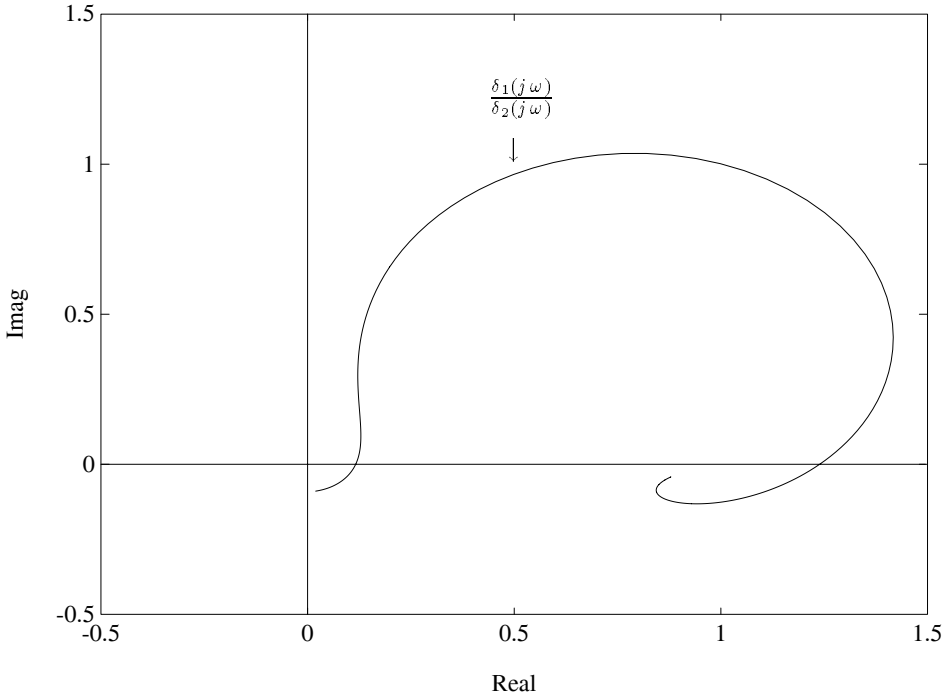

Figure 2.5. A Stable segment: $\frac{\delta_1(j\omega)}{\delta_2(j\omega)} \cap \mathbb{R}^- = \emptyset$ (Example 2.2)

Example 2.3. (Schur Stability) Let us consider the Schur stability of the segment joining the two polynomials

$$\delta_1(z) = z^5 + 0.4z^4 - 0.33z^3 + 0.058z^2 + 0.1266z + 0.059$$
$$\delta_2(z) = z^5 - 2.59z^4 + 2.8565z^3 - 1.4733z^2 + 0.2236z - 0.0121.$$

First we verify that the roots of both $\delta_1(z)$ and $\delta_2(z)$ lie inside the unit circle. In order to check the stability of the given segment, we simply evaluate the phases of $\delta_1(z)$ and $\delta_2(z)$ along the stability boundary, namely the unit circle. Figure 2.6 shows that the phase difference $\phi_{\delta_1}(e^{j\theta}) - \phi_{\delta_2}(e^{j\theta})$ reaches 180° at around $\theta = 0.81$ radians. Therefore, we conclude that there exists an unstable polynomial along the segment.

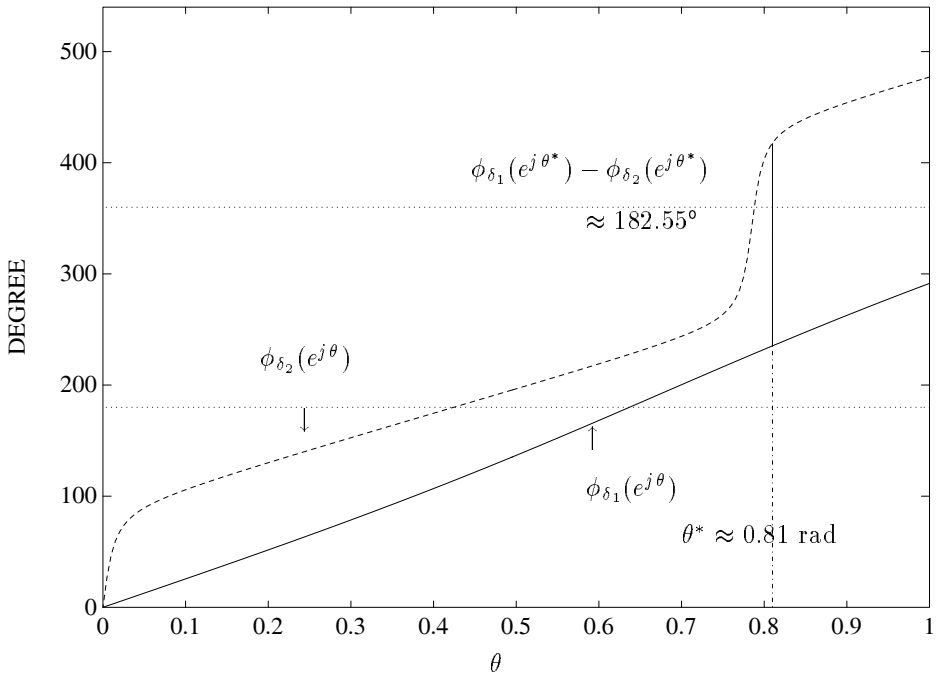

Figure 2.6. An unstable segment (Example 2.3)

Lemma 2.1 can be extended to a more general class of segments. In particular, let $\delta_1(s)$, $\delta_2(s)$ be quasipolynomials of the form

$$\begin{aligned} \delta_1(s) &= as^n + \sum e^{-sT_i} a_i(s) \\ \delta_2(s) &= bs^n + \sum e^{-sH_i} b_i(s) \end{aligned} \tag{2.1}$$

where $T_i, H_i \geq 0$, $a_i(s)$, $b_i(s)$ have degrees less than n and a and b are arbitrary but nonzero and of the same sign. The Hurwitz stability of $\delta_1(s)$, $\delta_2(s)$ is then equivalent to their roots being in the left half plane.

Lemma 2.2 *Lemma 2.1 holds for Hurwitz stability of the quasipolynomials of the form specified in (2.1).*

The proof of this lemma follows from the fact that Lemma 2.1 is equivalent to the Boundary Crossing Theorem which applies to Hurwitz stability of quasipolynomials $\delta_i(s)$ of the form given (see Theorem 1.14, Chapter 1).

Example 2.4. (Quasi-polynomials) Let us consider the Hurwitz stability of the line segment joining the following pair of quasi-polynomials:

$$\delta_1(s) = (s^2 + 3s + 2) + e^{-sT_1}(s + 1) + e^{-sT_2}(2s + 1)$$
$$\delta_2(s) = (s^2 + 5s + 3) + e^{-sT_1}(s + 2) + e^{-sT_2}(2s + 1)$$

where $T_1 = 1$ and $T_2 = 2$. We first check the stability of the endpoints by examining the frequency plots of

$$\frac{\delta_1(j\omega)}{(j\omega + 1)^2} \quad \text{and} \quad \frac{\delta_2(j\omega)}{(j\omega + 1)^2}.$$

Using the Principle of the Argument (equivalently, the Nyquist stability criterion) the condition for $\delta_1(s)$ (or $\delta_2(s)$) having all its roots in the left half plane is simply that the plot should not encircle the origin since the denominator term $(s + 1)^2$ does not have right half plane roots. Figure 2.7 shows that both endpoints $\delta_1(s)$ and $\delta_2(s)$ are stable.

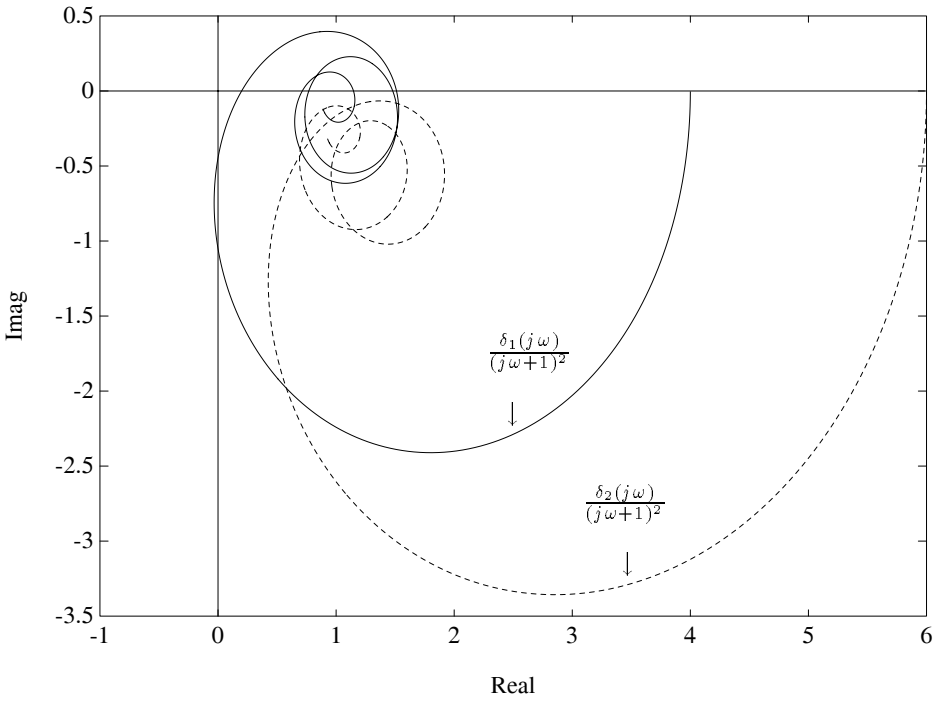

Figure 2.7. Stable quasi-polynomials (Example 2.4)

We generate the polar plot of $\delta_1(j\omega)/\delta_2(\omega)$ (Figure 2.8). As this plot does not cut the negative real axis the stability of the segment $[\delta_1(s), \delta_2(s)]$ is guaranteed by

condition d) of Lemma 2.1.

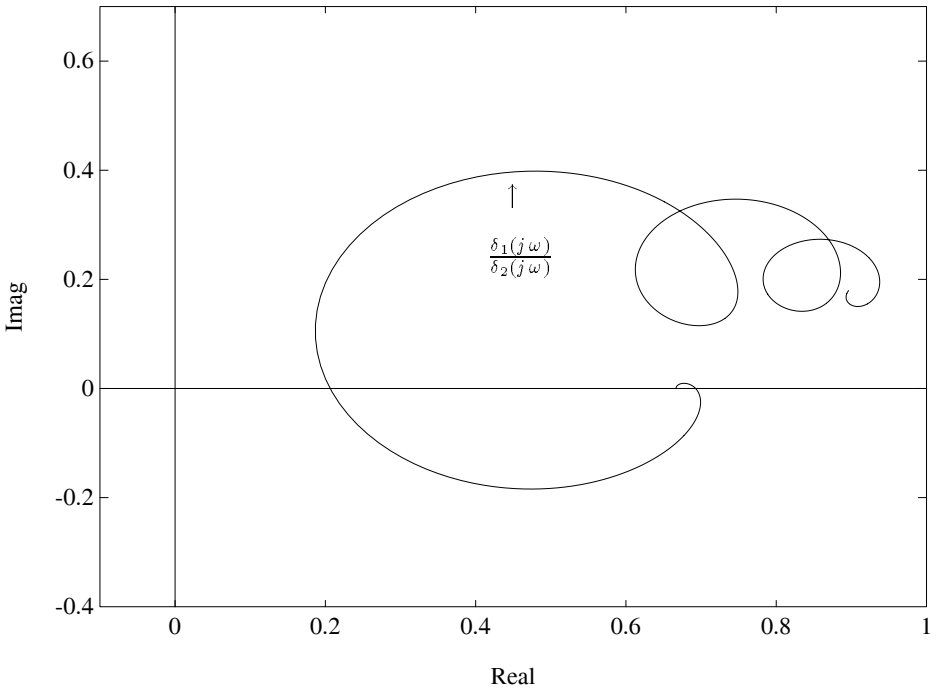

Figure 2.8. Stable segment of quasipolynomials (Example 2.4)

In the next section we focus specifically on the Hurwitz and Schur cases. We show how the frequency sweeping involved in using these results can always be *avoided* by isolating and checking only those frequencies where the phase difference can potentially reach 180°.

2.3 SEGMENT LEMMA

2.3.1 Hurwitz Case

In this subsection we are interested in strong stability of a line segment of polynomials joining two Hurwitz polynomials. We start by introducing a simple lemma which deals with convex combinations of two real polynomials, and finds the conditions under which one of these convex combinations can have a pure imaginary

root. Recall the even-odd decomposition of a real polynomial $\delta(s)$ and the notation $\delta(j\omega) = \delta^e(\omega) + j\omega\delta^o(\omega)$ where $\delta^e(\omega)$ and $\delta^o(\omega)$ are real polynomials in ω^2.

Lemma 2.3 *Let $\delta_1(\cdot)$ and $\delta_2(\cdot)$ be two arbitrary real polynomials (not necessarily stable). Then there exists $\lambda \in [0,1]$ such that $(1-\lambda)\delta_1(\cdot) + \lambda\delta_2(\cdot)$ has a pure imaginary root $j\omega$, with $\omega > 0$ if and only if*

$$\begin{cases} \delta_1^e(\omega)\delta_2^o(\omega) - \delta_2^e(\omega)\delta_1^o(\omega) = 0 \\ \delta_1^e(\omega)\delta_2^e(\omega) \leq 0 \\ \delta_1^o(\omega)\delta_2^o(\omega) \leq 0 \end{cases}$$

Proof. Suppose first that there exists some $\lambda \in [0,1]$ and $\omega > 0$ such that

$$(1-\lambda)\delta_1(j\omega) + \lambda\delta_2(j\omega) = 0. \tag{2.2}$$

We can write,

$$\begin{aligned} \delta_i(j\omega) &= \delta_i^{\text{even}}(j\omega) + \delta_i^{\text{odd}}(j\omega) \\ &= \delta_i^e(\omega) + j\omega\delta_i^o(\omega), \qquad \text{for} \quad i = 1, 2. \end{aligned} \tag{2.3}$$

Thus, taking (2.3) and the fact that $\omega > 0$ into account, (2.2) is equivalent to

$$\begin{cases} (1-\lambda)\delta_1^e(\omega) + \lambda\delta_2^e(\omega) = 0 \\ (1-\lambda)\delta_1^o(\omega) + \lambda\delta_2^o(\omega) = 0. \end{cases} \tag{2.4}$$

But if (2.4) holds then necessarily

$$\delta_1^e(\omega)\delta_2^o(\omega) - \delta_2^e(\omega)\delta_1^o(\omega) = 0, \tag{2.5}$$

and since λ and $1-\lambda$ are both nonnegative, (2.4) also implies that

$$\delta_1^e(\omega)\delta_2^e(\omega) \leq 0 \quad \text{and} \quad \delta_1^o(\omega)\delta_2^o(\omega) \leq 0, \tag{2.6}$$

and therefore this proves that the condition is necessary.
For the converse there are two cases:

c1) Suppose that

$$\delta_1^e(\omega)\delta_2^o(\omega) - \delta_2^e(\omega)\delta_1^o(\omega) = 0, \quad \delta_1^e(\omega)\delta_2^e(\omega) \leq 0, \quad \delta_1^o(\omega)\delta_2^o(\omega) \leq 0,$$

for some $\omega \geq 0$, but that we do not have $\delta_1^e(\omega) = \delta_2^e(\omega) = 0$, then

$$\lambda = \frac{\delta_1^e(\omega)}{\delta_1^e(\omega) - \delta_2^e(\omega)}$$

satisfies (2.4), and one can check easily that λ is in $[0,1]$.

c2) Suppose now that

$$\delta_1^e(\omega)\delta_2^o(\omega) - \delta_2^e(\omega)\delta_1^o(\omega) = 0, \text{ and } \delta_1^e(\omega) = \delta_2^e(\omega) = 0. \tag{2.7}$$

Then we are left with,

$$\delta_1^o(\omega)\delta_2^o(\omega) \leq 0.$$

Here again, if we do not have $\delta_1^o(\omega) = \delta_2^o(\omega) = 0$, then the following value of λ satisfies (2.4)

$$\lambda = \frac{\delta_1^o(\omega)}{\delta_1^o(\omega) - \delta_2^o(\omega)}.$$

If $\delta_1^o(\omega) = \delta_2^o(\omega) = 0$, then from (2.7) we conclude that both $\lambda = 0$ and $\lambda = 1$ satisfy (2.4) and this completes the proof. ♣

Based on this we may now state the Segment Lemma for the Hurwitz case.

Lemma 2.4 (Segment Lemma: Hurwitz Case)
Let $\delta_1(s)$, $\delta_2(s)$ be real Hurwitz polynomials of degree n with leading coefficients of the same sign. Then the line segment of polynomials $[\delta_1(s), \delta_2(s)]$ is Hurwitz stable if and only there exists no real $\omega > 0$ such that

$$\begin{array}{ll} 1) & \delta_1^e(\omega)\delta_2^o(\omega) - \delta_2^e(\omega)\delta_1^o(\omega) = 0 \\ 2) & \delta_1^e(\omega)\delta_2^e(\omega) \leq 0 \\ 3) & \delta_1^o(\omega)\delta_2^o(\omega) \leq 0. \end{array} \tag{2.8}$$

Proof. The proof of this result again follows from the Boundary Crossing Theorem of Chapter 1. We note that since the two polynomials $\delta_1(s)$ and $\delta_2(s)$ are of degree n with leading coefficients of the same sign, every polynomial on the segment is of degree n. Moreover, no polynomial on the segment has a real root at $s = 0$ because in such a case $\delta_1(0)\delta_2(0) \leq 0$, and this along with the assumption on the sign of the leading coefficients, contradicts the assumption that $\delta_1(s)$ and $\delta_2(s)$ are both Hurwitz. Therefore an unstable polynomial can occur on the segment if and only if a segment polynomial has a root at $s = j\omega$ with $\omega > 0$. By the previous lemma this can occur if and only if the conditions (2.8) hold. ♣

If we consider the image of the segment $[\delta_1(s), \delta_2(s)]$ evaluated at $s = j\omega$, we see that the conditions (2.8) of the Segment Lemma are the necessary and sufficient condition for the line segment $[\delta_1(j\omega), \delta_2(j\omega)]$ to pass through the origin of the complex plane. This in turn is equivalent to the phase difference condition $|\phi_{\delta_1}(j\omega) - \phi_{\delta_2}(j\omega)| = 180°$. We illustrate this in Figure 2.9.

Example 2.5. Consider the robust Hurwitz stability problem of the feedback system treated in Example 2.1. The characteristic polynomial is:

$$\delta(s, \alpha) = s^3 + 2\alpha s^2 + (\alpha + 1)s + (\alpha - 1).$$

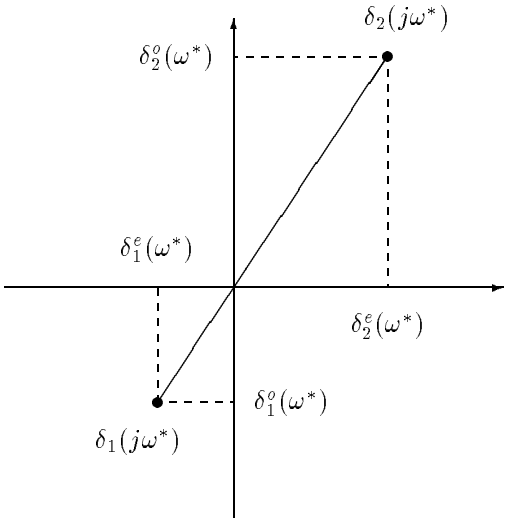

$$\delta_1^e(\omega^*)\delta_2^e(\omega^*) < 0$$

$$\delta_1^o(\omega^*)\delta_2^o(\omega^*) < 0$$

$$\frac{\delta_1^o(\omega^*)}{\delta_1^e(\omega^*)} = \frac{\delta_2^o(\omega^*)}{\delta_2^e(\omega^*)}$$

$$\Updownarrow$$

$$\delta_1^e(\omega^*)\delta_2^o(\omega^*) - \delta_2^e(\omega^*)\delta_1^o(\omega^*) = 0$$

$$\Leftrightarrow \quad |\phi_{\delta_1}(j\omega^*) - \phi_{\delta_2}(j\omega^*)| = 180^\circ$$

Figure 2.9. Segment Lemma: geometric interpretation

We have already verified the stability of the endpoints

$$\delta_1(s) := \delta(s,\alpha)|_{\alpha=2} = s^3 + 4s^2 + 3s + 1$$
$$\delta_2(s) := \delta(s,\alpha)|_{\alpha=3} = s^3 + 6s^2 + 4s + 2.$$

Robust stability of the system is equivalent to that of the segment

$$\delta_\lambda(s) = \lambda\delta_1(s) + (1-\lambda)\delta_2(s),$$

To apply the Segment Lemma we compute the real positive roots of the polynomial

$$\delta_1^e(\omega)\delta_2^o(\omega) - \delta_2^e(\omega)\delta_1^o(\omega) =$$
$$(-4\omega^2 + 1)(-\omega^2 + 4) - (-6\omega^2 + 2)(-\omega^2 + 3) = 0.$$

This equation has no real root in ω and thus there is no $j\omega$ root on the line segment. Thus, from the Segment Lemma, the segment $[\delta_1(s), \delta_2(s)]$ is stable and the closed loop system is robustly stable. Although frequency sweeping is unnecessary we have plotted in Figure 2.10 the image set of the line segment. As expected this plot avoids the origin of the complex plane for all ω.

2.3.2 Schur Case

Let us now consider the problem of checking the Schur stability of the line joining two real polynomials $P_1(z)$ and $P_2(z)$. We wish to know whether every polynomial of the form

$$\lambda P_1(z) + (1-\lambda)P_2(z), \quad \lambda \in [0,1]$$

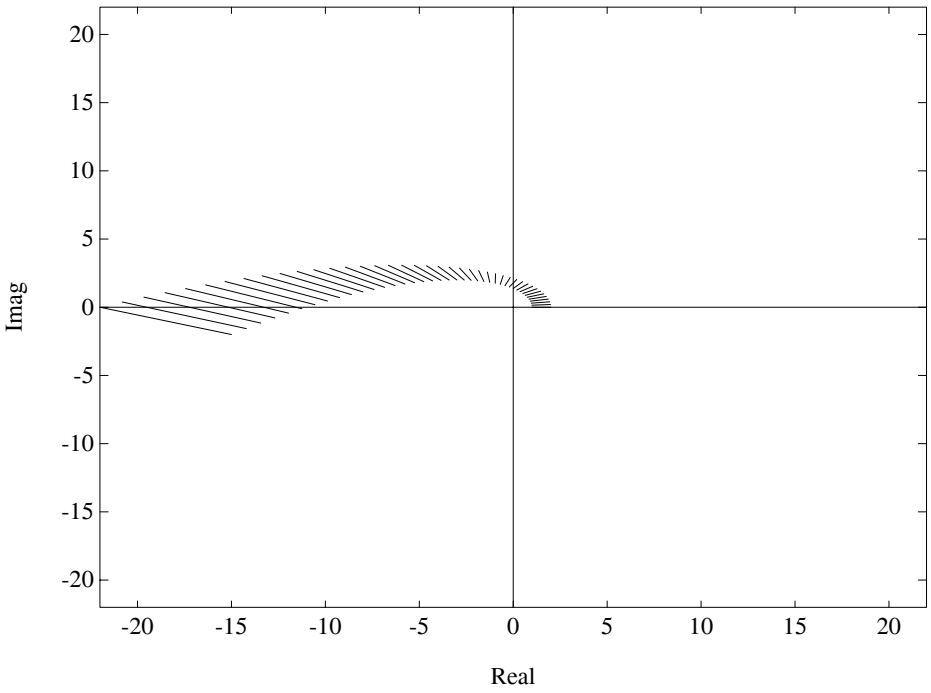

Figure 2.10. Image set of a stable segment (Example 2.5)

is Schur stable. Assume that there is at least one stable polynomial along the segment and that the degree remains constant along the segment. It follows then from the Boundary Crossing Theorem that if there exists a polynomial on the segment with an unstable root outside the unit circle, by continuity there must exist a polynomial on the segment with a root located on the boundary of the stability region, namely on the unit circle. In the following we give some simple and systematic tests for checking this. We will assume that the leading coefficients of the two extreme polynomials are of same sign. This is a necessary and sufficient condition for every polynomial on the segment to be of the same degree.

We begin with the following result.

Lemma 2.5 (Schur Segment Lemma 1)
Let $P_1(z)$ and $P_2(z)$ be two real Schur polynomials of degree n, with the leading coefficients of the same sign. A polynomial on the line segment $[P_1(z), P_2(z)]$ has a root on the unit circle if and only if there exists z_0 with $|z_0| = 1$ such that

$$P_1(z_0)P_2(z_0^{-1}) - P_2(z_0)P_1(z_0^{-1}) = 0 \tag{2.9}$$

$$\text{Im}\left[\frac{P_1(z_0)}{P_2(z_0)}\right] = 0 \tag{2.10}$$

and

$$\text{Re}\left[\frac{P_1(z_0)}{P_2(z_0)}\right] \leq 0 \tag{2.11}$$

Proof.
Necessity Suppose that there exists z_0 with $|z_0| = 1$ and $\lambda \in [0,1]$ such that

$$\lambda P_1(z_0) + (1-\lambda)P_2(z_0) = 0 \tag{2.12}$$

Since $|z_0| = 1$ and (2.12) is real, we have

$$\lambda P_1(z_0^{-1}) + (1-\lambda)P_2(z_0^{-1}) = 0. \tag{2.13}$$

From (2.12) and (2.13) it follows that

$$P_1(z_0)P_2(z_0^{-1}) - P_1(z_0^{-1})P_2(z_0) = 0. \tag{2.14}$$

Separating (2.12) into real and imaginary parts and using the fact that $\lambda \in [0,1]$, it follows that

$$\text{Re}[P_1(z_0)]\text{Im}[P_2(z_0)] - \text{Im}[P_1(z_0)]\text{Re}[P_2(z_0)] = 0 \tag{2.15}$$

and

$$\text{Re}[P_1(z_0)]\text{Re}[P_2(z_0)] \leq 0 \quad \text{and} \quad \text{Im}[P_1(z_0)]\text{Im}[P_2(z_0)] \leq 0. \tag{2.16}$$

This is equivalent to

$$\text{Im}\left[\frac{P_1(z_0)}{P_2(z_0)}\right] = 0 \tag{2.17}$$

and

$$\text{Re}\left[\frac{P_1(z_0)}{P_2(z_0)}\right] \leq 0 \tag{2.18}$$

proving the necessity of the conditions.

Sufficiency Suppose that

$$P_1(z_0)P_2(z_0^{-1}) - P_2(z_0)P_1(z_0^{-1}) = 0 \tag{2.19}$$

$$\text{Im}\left[\frac{P_1(z_0)}{P_2(z_0)}\right] = 0 \tag{2.20}$$

and

$$\text{Re}\left[\frac{P_1(z_0)}{P_2(z_0)}\right] \leq 0. \tag{2.21}$$

We note that $P_1(z_0) \neq P_2(z_0)$, otherwise (2.19)-(2.21) would imply that $P_1(z_0) = P_2(z_0) = 0$ which contradicts the assumption that $P_1(z)$ and $P_2(z)$ are both Schur. Then

$$\lambda = \frac{P_2(z_0)}{P_2(z_0) - P_1(z_0)} \tag{2.22}$$

satisfies (2.12) and one can easily check that $\lambda \in [0, 1]$. ♣

In the above lemma, we need to compute the zeros of (2.9) which is not a polynomial. Instead we can form the polynomial

$$P_1(z_0) z_0^n P_2(z_0^{-1}) - P_2(z_0) z_0^n P_1(z_0^{-1}) = 0$$

whose unit circle roots coincide with those of (2.9). Note that $z^n P_i(z^{-1})$ is simply the "reverse" polynomial of $P_i(z)$.

Symmetric-antisymmetric Decomposition

Recall the symmetric-antisymmetric decomposition introduced in Chapter 1. A given real polynomial can be decomposed into a symmetric part $h(z)$ and an antisymmetric part $g(z)$ defined as follows:

$$P(z) = a_n z^n + a_{n-1} z^{n-1} + \cdots + a_1 z + a_0 = h(z) + g(z) \tag{2.23}$$

and

$$h(z) = \frac{1}{2}\left(P(z) + z^n P(z^{-1})\right), \qquad g(z) = \frac{1}{2}\left(P(z) - z^n P(z^{-1})\right).$$

We also have

$$h(z) = \alpha_n z^n + \cdots + \alpha_0 \quad \text{and} \quad g(z) = \beta_n z^n + \cdots + \beta_0$$

where

$$\alpha_i = \frac{a_i + a_{n-i}}{2}, \qquad \beta_i = \frac{a_i - a_{n-i}}{2}, \qquad i = 0, \cdots, n. \tag{2.24}$$

This decomposition plays a role similar to the even-odd decomposition in the Hurwitz case. We can enunciate the following lemma.

Lemma 2.6 (Schur Segment Lemma 2)
Let $P_1(z)$ and $P_2(z)$ be two real polynomials of degree n with the following symmetric-antisymmetric decomposition:

$$P_1(z) = h_1(z) + g_1(z) \quad \text{and} \quad P_2(z) = h_2(z) + g_2(z)$$

There exists $\lambda \in [0, 1]$ and z_0 with $|z_0| = 1$ such that

$$\lambda P_1(z_0) + (1 - \lambda) P_2(z_0) = 0$$

if and only if

$$h_1(z_0) g_2(z_0) - g_1(z_0) h_2(z_0) = 0, \quad z_0^{-n} h_1(z_0) h_2(z_0) \leq 0, \quad z_0^{-n} g_1(z_0) g_2(z_0) \geq 0.$$

Proof.
Necessity Assume $z_0 = e^{j\theta}$ is a root of $\lambda P_1(z) + (1-\lambda)P_2(z) = 0$. Then

$$\lambda\left(h_1(z_0) + g_1(z_0)\right) + (1-\lambda)(h_2(z_0) + g_2(z_0)) = 0. \tag{2.25}$$

Since $|z_0| = 1$ this is equivalent to

$$\lambda\left(z_0^{-\frac{n}{2}}h_1(z_0) + z_0^{-\frac{n}{2}}g_1(z_0)\right) + (1-\lambda)\left(z_0^{-\frac{n}{2}}h_2(z_0) + z_0^{-\frac{n}{2}}g_2(z_0)\right) = 0. \tag{2.26}$$

Now observe that

$$\begin{aligned} z_0^{-\frac{n}{2}}h(z_0) &= \frac{1}{2}\left[(a_n + a_0)z_0^{\frac{n}{2}} + (a_{n-1} + a_1)z_0^{\frac{n}{2}-1} + \cdots + (a_0 + a_n)z_0^{-\frac{n}{2}}\right] \\ &= \frac{1}{2}\left[(a_n + a_0)\left(\cos\frac{n}{2}\theta + j\sin\frac{n}{2}\theta\right) + \cdots + (a_0 + a_n)\left(\cos\frac{n}{2}\theta - j\sin\frac{n}{2}\theta\right)\right] \\ &= (a_n + a_0)\cos\frac{n}{2}\theta + (a_{n-1} + a_1)\cos\left(\frac{n}{2} - 1\right)\theta + \cdots \end{aligned}$$

is real and

$$\begin{aligned} z_0^{-\frac{n}{2}}g(z_0) &= \frac{1}{2}\left[(a_n - a_0)z_0^{\frac{n}{2}} + (a_{n-1} - a_1)z_0^{\frac{n}{2}-1} + \cdots + (a_0 - a_n)z_0^{-\frac{n}{2}}\right] \\ &= \frac{1}{2}\left[(a_n - a_0)\left(\cos\frac{n}{2}\theta + j\sin\frac{n}{2}\theta\right) + \cdots + (a_0 - a_n)\left(\cos\frac{n}{2}\theta - j\sin\frac{n}{2}\theta\right)\right] \\ &= j\left[(a_n - a_0)\sin\frac{n}{2}\theta + (a_{n-1} + a_1)\sin\left(\frac{n}{2} - 1\right)\theta + \cdots\right] \end{aligned}$$

is imaginary. Thus, we rewrite (2.26) as follows:

$$\lambda\left(z_0^{-\frac{n}{2}}h_1(z_0) + jz_0^{-\frac{n}{2}}\frac{g_1(z_0)}{j}\right) + (1-\lambda)\left(z_0^{-\frac{n}{2}}h_2(z_0) + z_0^{-\frac{n}{2}}\frac{g_2(z_0)}{j}\right) = 0. \tag{2.27}$$

Note that $z_0^{-\frac{n}{2}}h_1(z_0)$ and $z_0^{-\frac{n}{2}}h_2(z_0)$ are real parts, and $z_0^{-\frac{n}{2}}\frac{g_1(z_0)}{j}$ and $z_0^{-\frac{n}{2}}\frac{g_1(z_0)}{j}$ are imaginary parts. Therefore, (2.27) is equivalent to:

$$\lambda z_0^{-\frac{n}{2}}h_1(z_0) + (1-\lambda)z_0^{-\frac{n}{2}}h_2(z_0) = 0 \tag{2.28}$$

and

$$\lambda z_0^{-\frac{n}{2}}\frac{g_1(z_0)}{j} + (1-\lambda)z_0^{-\frac{n}{2}}\frac{g_2(z_0)}{j} = 0. \tag{2.29}$$

As $z_0 \neq 0$ and both λ and $(1-\lambda)$ are nonnegative we get

$$h_1(z_0)g_2(z_0) - g_1(z_0)h_2(z_0) = 0, \quad z_0^{-n}h_1(z_0)h_2(z_0) \leq 0, \quad z_0^{-n}g_1(z_0)g_2(z_0) \geq 0$$

which proves the necessity of these conditions.

Sufficiency For the converse we have two cases:

a) Suppose

$$h_1(z_0)g_2(z_0)-g_1(z_0)h_2(z_0)=0, \quad z_0^{-n}h_1(z_0)h_2(z_0)\le 0, \quad z_0^{-n}g_1(z_0)g_2(z_0)\ge 0$$

but we do not have $h_1(z_0)=h_2(z_0)=0$. Then

$$\lambda=\frac{h_2(z_0)}{h_2(z_0)-h_1(z_0)} \tag{2.30}$$

satisfies (2.25) and one can verify that $\lambda\in[0,1]$.

b) Now assume that

$$z_0^{-n}(h_1(z_0)g_2(z_0)-g_1(z_0)h_2(z_0))=0,$$

$$h_1(z_0)=h_2(z_0)=0, \quad z_0^{-n}g_1(z_0)g_2(z_0)\ge 0$$

but we do not have $g_1(z_0)=g_2(z_0)=0$. In this case

$$\lambda=\frac{g_2(z_0)}{g_2(z_0)-g_1(z_0)} \ \in[0,1] \tag{2.31}$$

satisfies (2.25).

If $g_1(z_0)=g_2(z_0)=0$, then $\lambda=0$ or $\lambda=1$ satisfies (2.25), which concludes the proof of the lemma. ♣

Example 2.6. Consider the segment joining the two polynomials

$$P_1(z)=z^3+1.5z^2+1.2z+0.5 \quad \text{and} \quad P_2(z)=z^3-1.2z^2+1.1z-0.4.$$

The symmetric-antisymmetric decomposition

$$P_1(z)=h_1(z)+g_1(z) \quad \text{and} \quad P_2(z)=h_2(z)+g_2(z)$$

where

$$\begin{aligned} h_1(z)&=0.75z^3+1.35z^2+1.35z+0.75\\ g_1(z)&=0.25z^3+0.15z^2-0.15z-0.25\\ h_2(z)&=0.3z^3-0.05z^2-0.05z+0.3\\ g_1(z)&=0.7z^3-1.15z^2+1.15z-0.7 \end{aligned}$$

The polynomial

$$h_1(z)g_2(z)-g_1(z)h_2(z)$$

has four roots z_0 on the unit circle such that

$$z_0^{-n}h_1(z_0)h_2(z_0)\le 0 \quad \text{and} \quad z_0^{-n}g_1(z_0)g_2(z_0)\ge 0$$

z_0	$z_0^{-n}h_1(z_0)h_2(z_0)$	$z_0^{-n}g_1(z_0)g_2(z_0)$
$z_{01} = -0.298 - 0.9546j$	-0.1136	0.5651
$z_{02} = -0.298 + 0.9546j$	-0.1136	0.5651
$z_{03} = 0.2424 - 0.9702j$	-0.4898	0.0874
$z_{04} = 0.2424 + 0.9702j$	-0.4898	0.0874

For both $z_0 = z_{01}$ and $z_0 = z_{02}$ we find

$$\lambda_1 = \frac{h_2(z_0)}{h_2(z_0) - h_1(z_0)} = 0.7755$$

yielding

$$\lambda_1 P_1(z) + (1 - \lambda_1)P_2(z) = z^3 + 0.8939z^2 + 1.1775z + 0.2979$$

and one can check that the above polynomial has a pair of complex conjugate roots at z_{01} and z_{02}.

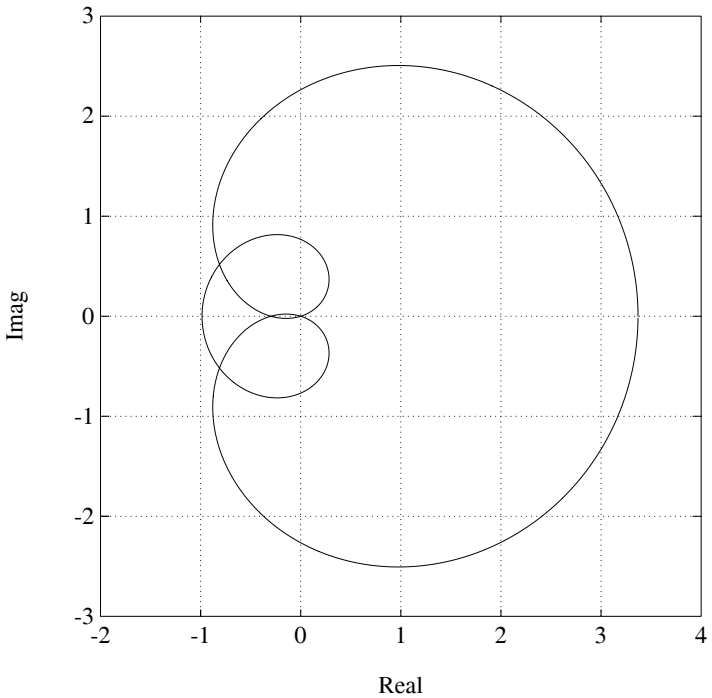

Figure 2.11. Unit circle image of the polynomial corresponding to $\lambda_1 = 0.7755$ (Example 2.6)

In Figure 2.11 we can check that the complex plane plot of $\lambda_1 P_1(e^{j\theta}) + (1 - \lambda_1)P_2(e^{j\theta})$ contains the origin, which implies that the convex combination of $P_1(z)$ and $P_2(z)$ has roots on the unit circle for $\lambda = \lambda_1$.

Similarly for $z_0 = z_{03}$ and $z_0 = z_{04}$

$$\lambda_2 = \frac{h_2(z_0)}{h_2(z_0) - h_1(z_0)} = 0.1751$$

yielding

$$\lambda_2 P_1(z) + (1 - \lambda_2)P_2(z) = z^3 - 0.7272z^2 + 1.1175z - 0.2424$$

which has roots at z_{03} and z_{04}. The image set of $\lambda P_1(e^{j\theta}) + (1 - \lambda)P_2(e^{j\theta})$ for $\lambda = \lambda_2$ in Figure 2.12 contains the origin, which means that $\lambda_2 P_1(z) + (1 - \lambda_2)P_2(z)$ has a root on the unit circle for $\lambda = \lambda_2$.

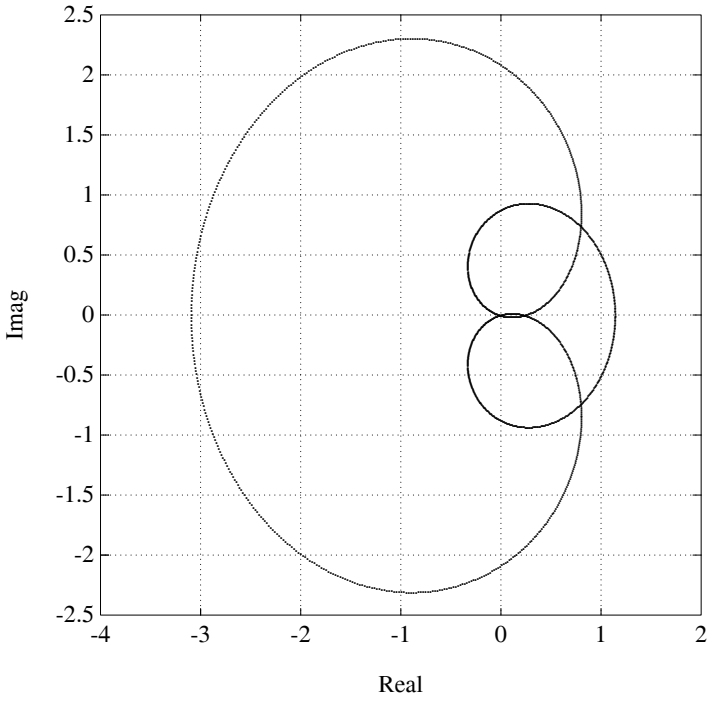

Figure 2.12. Unit circle image set of the polynomial corresponding to $\lambda_2 = 0.1751$ (Example 2.6)

In order to find the stable-unstable regions on the line $[P_1(z), P_2(z)]$, let us take some test polynomials corresponding to different values of λ.

$$\begin{array}{lll} \lambda = 0.1: & \lambda P_1(z) + (1-\lambda)P_2(z) = z^3 - 0.93z^2 + 1.11z - 0.31 & \text{stable.} \\ \lambda = 0.5: & \lambda P_1(z) + (1-\lambda)P_2(z) = z^3 + 0.15z^2 + 1.15z + 0.05 & \text{unstable.} \\ \lambda = 0.8: & \lambda P_1(z) + (1-\lambda)P_2(z) = z^3 + 0.96z^2 + 1.18z + 0.32 & \text{stable.} \end{array}$$

The partitioning of the segment into stable and unstable pieces is shown in Figure 2.13.

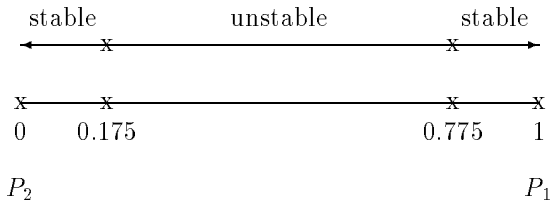

Figure 2.13. Stability regions along the segment (Example 2.6)

Trigonometric Version

Let us again consider a real polynomial $P(z)$ of degree n, and write

$$P(z) = h(z) + g(z) \tag{2.32}$$

$$P(z) = 2z^{\frac{n}{2}} \left(\frac{z^{-\frac{n}{2}} h(z)}{2} + \frac{z^{-\frac{n}{2}} g(z)}{2} \right). \tag{2.33}$$

Note that

$$\frac{1}{2} z^{-\frac{n}{2}} h(z) = \frac{\alpha_n}{2} z^{\frac{n}{2}} + \cdots + \frac{\alpha_1}{2} z^{-\left(\frac{n}{2}-1\right)} + \frac{\alpha_0}{2} z^{-\frac{n}{2}} \tag{2.34}$$

$$\frac{1}{2} z^{-\frac{n}{2}} g(z) = \frac{\beta_n}{2} z^{\frac{n}{2}} + \cdots + \frac{\beta_1}{2} z^{-\left(\frac{n}{2}-1\right)} + \frac{\beta_0}{2} z^{-\frac{n}{2}} \tag{2.35}$$

where α_i, β_j are real with $\alpha_i = \alpha_{n-i}$ and $\beta_i = -\beta_{n-i}$ for $i = 0, \cdots, n$. When $z = e^{j\theta}$ we get

$$\frac{e^{-j\frac{n\theta}{2}} h(e^{j\theta})}{2} = h^*(\theta)$$

$$\frac{e^{-j\frac{n\theta}{2}} g(e^{j\theta})}{2} = j g^*(\theta)$$

where

$$h^*(\theta) = \begin{cases} \alpha_n \cos\frac{n}{2}\theta + \alpha_{n-1} \cos\left(\frac{n}{2}-1\right)\theta + \cdots + \alpha_{\frac{n}{2}} & \text{if } n \text{ even} \\ \alpha_n \cos\frac{n}{2}\theta + \alpha_{n-1} \cos\left(\frac{n}{2}-1\right)\theta + \cdots + \alpha_{\frac{n+1}{2}} \cos\frac{\theta}{2} & \text{if } n \text{ odd} \end{cases} \tag{2.36}$$

and

$$g^*(\theta) = \begin{cases} \left(\beta_n \sin\frac{n}{2}\theta + \beta_{n-1}\sin\left(\frac{n}{2}-1\right)\theta + \cdots + \beta_{\frac{n}{2}+1}\sin\theta\right) & \text{if } n \text{ even} \\ \left(\beta_n \sin\frac{n}{2}\theta + \beta_{n-1}\sin\left(\frac{n}{2}-1\right)\theta + \cdots + \beta_{\frac{n}{2}+1}\sin\frac{\theta}{2}\right) & \text{if } n \text{ odd} \end{cases} \tag{2.37}$$

We write

$$P(e^{j\theta}) = 2e^{jn\frac{\theta}{2}}\left(h^*(\theta) + jg^*(\theta)\right) \tag{2.38}$$

$$P(e^{j\theta}) = 2e^{jn\frac{\theta}{2}}\delta(\theta). \tag{2.39}$$

We can then enunciate another version of the Segment Lemma.

Lemma 2.7 (Schur Segment Lemma 3)
Let $P_1(z)$ and $P_2(z)$ be two polynomials of degree n, with

$$P_1(e^{j\theta}) = 2e^{jn\frac{\theta}{2}}\left(h_1^*(\theta) + jg_1^*(\theta)\right)$$
$$P_2(e^{j\theta}) = 2e^{jn\frac{\theta}{2}}\left(h_2^*(\theta) + jg_2^*(\theta)\right)$$

On the segment joining $P_1(z)$ and $P_2(z)$ there exists a polynomial with a root on the unit circle if and only if there exists $\theta \in [0, 2\pi)$ such that

$$h_1^*(\theta)g_2^*(\theta) - g_1^*(\theta)h_2^*(\theta) = 0$$
$$h_1^*(\theta)h_2^*(\theta) \le 0$$
$$g_1^*(\theta)g_2^*(\theta) \le 0.$$

The proof is omitted as it is similar to the previous cases.

2.4 SOME FUNDAMENTAL PHASE RELATIONS

In this section, we develop some auxiliary results that will aid us in establishing the Convex Direction Lemma and the Vertex Lemma, which deal with conditions under which vertex stability implies segment stability. The above results depend heavily on some fundamental formulas for the rate of change of phase with respect to frequency for fixed Hurwitz polynomials and for a segment of polynomials. These are derived in this section.

2.4.1 Phase Properties of Hurwitz Polynomials

Let $\delta(s)$ be a real or complex polynomial and write

$$\delta(j\omega) = p(\omega) + jq(\omega) \tag{2.40}$$

where $p(\omega)$ and $q(\omega)$ are real functions. Also let

$$X(\omega) := \frac{q(\omega)}{p(\omega)} \tag{2.41}$$

and

$$\varphi_\delta(\omega) := \tan^{-1}\frac{q(\omega)}{p(\omega)} = \tan^{-1} X(\omega). \tag{2.42}$$

Let $\mathrm{Im}[x]$ and $\mathrm{Re}[x]$ denote the imaginary and real parts of the complex number x.

Lemma 2.8 *If $\delta(s)$ is a real or complex Hurwitz polynomial*

$$\frac{dX(\omega)}{d\omega} > 0, \quad \text{for all } \omega \in [-\infty, +\infty]. \tag{2.43}$$

Equivalently

$$\mathrm{Im}\left[\frac{1}{\delta(j\omega)}\frac{d\delta(j\omega)}{d\omega}\right] > 0 \quad \text{for all } \omega \in [-\infty, +\infty]. \tag{2.44}$$

Proof. A Hurwitz polynomial satisfies the monotonic phase increase property

$$\frac{d\varphi_\delta(\omega)}{d\omega} = \frac{1}{1+X^2(\omega)}\frac{dX(\omega)}{d\omega} > 0 \quad \text{for all } \omega \in [-\infty, +\infty]$$

and this implies

$$\frac{dX(\omega)}{d\omega} > 0 \quad \text{for all } \omega \in [-\infty, +\infty].$$

The formula

$$\frac{d\varphi_\delta(\omega)}{d\omega} = \mathrm{Im}\left[\frac{1}{\delta(j\omega)}\frac{d\delta(j\omega)}{d\omega}\right] \tag{2.45}$$

follows from the relations

$$\begin{aligned}\frac{1}{\delta(j\omega)}\frac{d\delta(j\omega)}{d\omega} &= \frac{1}{p(\omega)+jq(\omega)}\left(\frac{dp(\omega)}{d\omega} + j\frac{dq(\omega)}{d\omega}\right) \\ &= \frac{\left[p(\omega)\frac{dp(\omega)}{d\omega} + q(\omega)\frac{dq(\omega)}{d\omega}\right] + j\left[p(\omega)\frac{dq(\omega)}{d\omega} - q(\omega)\frac{dp(\omega)}{d\omega}\right]}{p^2(\omega)+q^2(\omega)}\end{aligned} \tag{2.46}$$

and

$$\frac{d\varphi_\delta(\omega)}{d\omega} = \frac{\left[p(\omega)\frac{dq(\omega)}{d\omega} - q(\omega)\frac{dp(\omega)}{d\omega}\right]}{p^2(\omega)+q^2(\omega)}. \tag{2.47}$$

♣

We shall see later that inequality (2.43) can be strengthened when $\delta(s)$ is a *real* Hurwitz polynomial.

Now let $\delta(s)$ be a *real* polynomial of degree n. We write:

$$\delta(s) = \delta^{\mathrm{even}}(s) + \delta^{\mathrm{odd}}(s) = h(s^2) + sg(s^2) \tag{2.48}$$

where h and g are real polynomials in s^2. Then

$$\begin{aligned}\delta(j\omega) &= h(-\omega^2) + j\omega g(-\omega^2) \\ &= \rho_\delta(\omega)e^{j\varphi_\delta(\omega)}.\end{aligned} \tag{2.49}$$

We associate with the real polynomial $\delta(s)$ the two auxiliary even degree complex polynomials

$$\underline{\delta}(s) := h(s^2) + jg(s^2) \tag{2.50}$$

and

$$\bar{\delta}(s) := h(s^2) - js^2 g(s^2) \tag{2.51}$$

and write formulas analogous to (2.49) for $\underline{\delta}(j\omega)$ and $\bar{\delta}(j\omega)$. $\delta(s)$ is *antiHurwitz* if and only if all its zeros lie in the open right half plane ($\mathrm{Re}[s] > 0$). Let $t = s^2$ be a new complex variable.

Lemma 2.9 *Consider*

$$h(t) + jg(t) = 0 \tag{2.52}$$

and

$$h(t) - jtg(t) = 0 \tag{2.53}$$

as equations in the complex variable t. If $\delta(s) = h(s^2) + sg(s^2)$ is Hurwitz and degree $\delta(s) \geq 2$ each of these equations has all its roots in the lower-half of the complex plane ($\mathrm{Im}[t] \leq 0$). When degree $[\delta(s)] = 1$ (2.53) has all its roots in $\mathrm{Im}[t] \leq 0$.

Proof. The statement regarding the case when degree$[\delta(s)] = 1$ can be directly checked. We therefore proceed with the assumption that degree$[\delta(s)] > 1$. Let

$$\delta(s) = a_0 + a_1 s + \cdots + a_n s^n. \tag{2.54}$$

Since $\delta(s)$ is Hurwitz we can assume without loss of generality that $a_i > 0$, $i = 0, \cdots, n$. We have

$$\begin{aligned} h(-\omega^2) &= a_0 + a_2(-\omega^2) + a_4(-\omega^2)^2 + \cdots \\ \omega g(-\omega^2) &= \omega \left[a_1 + a_3(-\omega^2) + a_5(-\omega^2)^2 + \cdots \right]. \end{aligned} \tag{2.55}$$

As s runs from 0 to $+j\infty$, $-\omega^2$ runs from 0 to $-\infty$. We first recall the Hermite-Biehler Theorem of Chapter 1. According to this Theorem if $\delta(s)$ is Hurwitz stable, all the roots of the two equations

$$h(t) = 0 \quad \text{and} \quad g(t) = 0 \tag{2.56}$$

are distinct, real and negative. Furthermore the interlacing property holds and the maximum of the roots is one of $h(t) = 0$. For the rest of the proof we will assume that $\delta(s)$ is of odd degree. A similar proof will hold for the case that $\delta(s)$ is of even degree. Let degree$[\delta(s)] = 2m + 1$ with $m \geq 1$. Note that the solutions of

$$h(t) + jg(t) = 0 \tag{2.57}$$

are identical with the solutions of

$$\frac{g(t)}{h(t)} = j. \tag{2.58}$$

Let us denote the roots of $h(t) = 0$ by $\lambda_1, \lambda_2, \cdots, \lambda_m$ where $\lambda_1 < \lambda_2 < \cdots < \lambda_m$. The sign of $h(t)$ changes alternately in each interval $]\lambda_i, \lambda_{i+1}[$, $(i = 1, \cdots, m-1)$.

If $\frac{g(t)}{h(t)}$ is expressed by partial fractions as

$$\frac{g(t)}{h(t)} = \frac{c_1}{t-\lambda_1} + \frac{c_2}{t-\lambda_2} + \cdots + \frac{c_m}{t-\lambda_m}, \tag{2.59}$$

then each $c_i, i = 1, \cdots, m$ should be positive. This is because when $t = -\omega^2$ passes increasingly (from left to right) through λ_i, the sign of $\frac{g(t)}{h(t)}$ changes from $-$ to $+$. This follows from the fact that $g(t)$ has just one root in each interval and $a_0 > 0$, $a_1 > 0$.

If we suppose

$$\mathrm{Im}[t] \geq 0, \tag{2.60}$$

then

$$\mathrm{Im}\left[\frac{c_i}{t-\lambda_i}\right] \leq 0 \quad i = 1, \cdots, m \tag{2.61}$$

and consequently we obtain

$$\mathrm{Im}\left[\frac{g(t)}{h(t)}\right] = \sum_{1 \leq i \leq m} \mathrm{Im}\left[\frac{c_i}{t-\lambda_i}\right] \leq 0. \tag{2.62}$$

Such a t cannot satisfy the relation in (2.58). This implies that the equation

$$h(t) + jg(t) = 0 \tag{2.63}$$

in t has all its roots in the lower-half of the complex plane $\mathrm{Im}[t] \leq 0$. We can treat $[h(t) - jtg(t)]$ similarly. ♣

This lemma leads to a key monotonic phase property.

Lemma 2.10 *If $\delta(s)$ is Hurwitz and of degree ≥ 2 then*

$$\frac{d\varphi_\delta}{d\omega} > 0 \tag{2.64}$$

and

$$\frac{d\varphi_{\bar{\delta}}}{d\omega} > 0. \tag{2.65}$$

Proof. From the previous lemma we have by factorizing $h(-\omega^2) + jg(-\omega^2)$

$$h(-\omega^2) + jg(-\omega^2) = a_n(-\omega^2 - \alpha_1) \cdots (-\omega^2 - \alpha_m) \tag{2.66}$$

with some $\alpha_1, \alpha_2, \cdots, \alpha_m$ whose imaginary parts are negative. Now

$$\arg\left[h(-\omega^2) + jg(-\omega^2)\right] = \sum_{i=1}^{m} \arg(-\omega^2 - \alpha_i). \tag{2.67}$$

When $(-\omega^2)$ runs from 0 to $(-\infty)$, each component of the form $\arg(-\omega^2 - \alpha_i)$ is monotonically increasing. Consequently $\arg\left[h(-\omega^2) + jg(-\omega^2)\right]$ is monotonically increasing as $(-\omega^2)$ runs from 0 to $(-\infty)$. In other words, $\arg\left[h(s^2) + jg(s^2)\right]$ is monotonically increasing as $s(= j\omega)$ runs from 0 to $j\infty$. This proves (2.64); (2.65) is proved in like manner. ♣

The dual result is given without proof.

Lemma 2.11 *If $\delta(s)$ is antiHurwitz*

$$\frac{d\varphi_{\underline{\delta}}}{d\omega} < 0 \tag{2.68}$$

and

$$\frac{d\varphi_{\bar{\delta}}}{d\omega} < 0 \tag{2.69}$$

We remark that in Lemma 2.10 $\underline{\delta}(s)$ and $\bar{\delta}(s)$ are *not* Hurwitz even though they enjoy the respective monotonic phase properties in (2.64) and (2.65). Similarly in Lemma 2.11 $\underline{\delta}(s)$ and $\bar{\delta}(s)$ are not antiHurwitz even though they enjoy the monotonic phase properties in (2.68) and (2.69), respectively.

The above results allow us to tighten the bound given in Lemma 2.8 on the rate of change of phase of a real Hurwitz polynomial.

Theorem 2.1 *For a real Hurwitz polynomial*

$$\delta(s) = h(s^2) + sg(s^2),$$

the rate of change of the argument of $\delta(j\omega)$ is bounded below by:

$$\frac{d\varphi_\delta(\omega)}{d\omega} \geq \left|\frac{\sin\left(2\varphi_\delta(\omega)\right)}{2\omega}\right|, \quad \text{for all } \omega > 0. \tag{2.70}$$

Equivalently with

$$X(\omega) = \frac{\omega g\left(-\omega^2\right)}{h\left(-\omega^2\right)}$$

we have

$$\frac{dX(\omega)}{d\omega} \geq \left|\frac{X(\omega)}{\omega}\right|, \quad \text{for all } \omega > 0. \tag{2.71}$$

In (2.70) and (2.71) equality holds only when degree $[\delta(s)] = 1$.

Proof. The equivalence of the two conditions (2.70) and (2.71) follows from

$$\frac{d\varphi_\delta(\omega)}{d\omega} = \frac{1}{1 + X^2(\omega)}\frac{dX(\omega)}{d\omega}$$

and

$$\begin{aligned}\frac{1}{1+X^2(\omega)}\left|\frac{X(\omega)}{\omega}\right| &= \left|\frac{1}{1+X^2(\omega)}\frac{X(\omega)}{\omega}\right| \\ &= \left|\frac{h^2\left(-\omega^2\right)}{h^2\left(-\omega^2\right)+\omega^2 g^2\left(-\omega^2\right)}\frac{g\left(-\omega^2\right)}{h\left(-\omega^2\right)}\right| \\ &= \left|\cos^2\left(\varphi_\delta(\omega)\right)\frac{1}{\omega}\tan\left(\varphi_\delta(\omega)\right)\right| \\ &= \left|\frac{1}{\omega}\cos\left(\varphi_\delta(\omega)\right)\sin\left(\varphi_\delta(\omega)\right)\right| \\ &= \left|\frac{\sin\left(2\varphi_\delta(\omega)\right)}{2\omega}\right|.\end{aligned}$$

We now prove (2.71). The fact that equality holds in (2.71) in the case where $\delta(s)$ has degree equal to 1 can be easily verified directly. We therefore proceed with the assumption that degree$[\delta(s)] \geq 2$. From Lemma 2.8, we know that

$$\frac{dX(\omega)}{d\omega} > 0$$

so that

$$\begin{aligned}\frac{dX(\omega)}{d\omega} &= \frac{\frac{d\left(\omega g\left(-\omega^2\right)\right)}{d\omega}h\left(-\omega^2\right)-\frac{d\left(h\left(-\omega^2\right)\right)}{d\omega}\left(\omega g\left(-\omega^2\right)\right)}{h^2\left(-\omega^2\right)} \\ &= \frac{g\left(-\omega^2\right)h\left(-\omega^2\right)+\omega\dot{g}\left(-\omega^2\right)h\left(-\omega^2\right)-\omega\dot{h}\left(-\omega^2\right)g\left(-\omega^2\right)}{h^2\left(-\omega^2\right)} \\ &= \underbrace{\frac{g\left(-\omega^2\right)}{h\left(-\omega^2\right)}}_{\frac{X(\omega)}{\omega}}+\omega\underbrace{\frac{\dot{g}\left(-\omega^2\right)h\left(-\omega^2\right)-\dot{h}\left(-\omega^2\right)g\left(-\omega^2\right)}{h^2\left(-\omega^2\right)}}_{\frac{d}{d\omega}\left(\frac{g(-\omega^2)}{h(-\omega^2)}\right)} > 0.\end{aligned}$$

From Lemma 2.10 we have

$$\frac{d\varphi_{\underline{\delta}}}{d\omega} > 0 \quad \text{and} \quad \frac{d\varphi_{\bar{\delta}}}{d\omega} > 0$$

where

$$\underline{\delta}(s) = h\left(s^2\right)+jg\left(s^2\right) \quad \text{and} \quad \bar{\delta}(s) = h\left(s^2\right)-js^2 g\left(s^2\right).$$

First consider

$$\frac{d\varphi_{\underline{\delta}}}{d\omega} = \frac{1}{1+\left(\frac{g(-\omega^2)}{h(-\omega^2)}\right)^2}\frac{d}{d\omega}\left(\frac{g(-\omega^2)}{h(-\omega^2)}\right) > 0.$$

Since

$$\frac{1}{1+\left(\frac{g(-\omega^2)}{h(-\omega^2)}\right)^2} > 0$$

we have

$$\frac{d}{d\omega}\left(\frac{g(-\omega^2)}{h(-\omega^2)}\right) > 0.$$

Thus, for $\omega > 0$ we have

$$\frac{dX(\omega)}{d\omega} = \frac{X(\omega)}{\omega} + \omega\frac{d}{d\omega}\left(\frac{g\left(-\omega^2\right)}{h\left(-\omega^2\right)}\right) > \frac{X(\omega)}{\omega}. \tag{2.72}$$

Now consider

$$\frac{d\varphi_{\bar{\delta}}}{d\omega} = \frac{1}{1+\left(\frac{\omega^2 g(-\omega^2)}{h(-\omega^2)}\right)^2}\frac{d}{d\omega}\left(\frac{\omega^2 g\left(-\omega^2\right)}{h\left(-\omega^2\right)}\right) > 0.$$

Here, we have

$$\begin{aligned}\frac{d}{d\omega}\left(\frac{\omega^2 g\left(-\omega^2\right)}{h\left(-\omega^2\right)}\right) &= \omega\left[2\frac{g\left(-\omega^2\right)}{h\left(-\omega^2\right)} + \frac{\omega\left[h\left(-\omega^2\right)\dot{g}\left(-\omega^2\right) - g\left(-\omega^2\right)\dot{h}\left(-\omega^2\right)\right]}{h^2\left(-\omega^2\right)}\right] \\ &= \omega\left[2\frac{X(\omega)}{\omega} + \omega\frac{d}{d\omega}\left(\frac{g\left(-\omega^2\right)}{h\left(-\omega^2\right)}\right)\right] > 0.\end{aligned}$$

With $\omega > 0$, it follows that

$$2\frac{X(\omega)}{\omega} + \omega\frac{d}{d\omega}\left(\frac{g\left(-\omega^2\right)}{h\left(-\omega^2\right)}\right) > 0$$

and therefore

$$\underbrace{\frac{X(\omega)}{\omega} + \omega\frac{d}{d\omega}\left(\frac{g\left(-\omega^2\right)}{h\left(-\omega^2\right)}\right)}_{\frac{dX(\omega)}{d\omega}} > -\frac{X(\omega)}{\omega}. \tag{2.73}$$

Combining (2.72) and (2.73), we have, when degree$[\delta(s)] \geq 2$,

$$\frac{dX(\omega)}{d\omega} > \left|\frac{X(\omega)}{\omega}\right|, \quad \text{for all } \omega > 0.$$

♣

A useful technical result can be derived from the above Theorem.

Lemma 2.12 *Let $\omega_0 > 0$ and the constraint*

$$\varphi_\delta(\omega_0) = \theta \tag{2.74}$$

be given. The infimum value of

$$\left.\frac{d\varphi_\delta(\omega)}{d\omega}\right|_{\omega=\omega_0} \tag{2.75}$$

taken over all real Hurwitz polynomials $\delta(s)$ of a prescribed degree satisfying (2.74) is given by

$$\left|\frac{\sin(2\theta)}{2\omega_0}\right|. \tag{2.76}$$

The infimum is actually attained only when $0 < \theta < \frac{\pi}{2}$ and $\delta(s)$ is of degree one, by polynomials of the form

$$\delta(s) = K(s\tan\theta + \omega_0). \tag{2.77}$$

For polynomials of degree (> 1) the infimum can be approximated to arbitrary accuracy.

Proof. The lower bound on the infimum given in (2.76) is an immediate consequence of (2.70) in Theorem 2.1. The fact that (2.77) attains the bound (2.76) can be checked directly. To prove that the infimum can be approximated to arbitrary accuracy it suffices to construct a sequence of Hurwitz polynomials $\delta_k(s)$ of prescribed degree n each satisfying (2.74) and such that

$$\lim_{k\to\infty} \left.\frac{d\varphi_{\delta_k}(\omega)}{d\omega}\right|_{\omega=\omega_0} = \left|\frac{\sin(2\theta)}{2\omega_0}\right|. \tag{2.78}$$

For example when $0 < \theta < \frac{\pi}{2}$ we can take

$$\delta_k(s) = K\left(s\tan\theta + \omega_0 + \frac{1}{k}\right)(\epsilon_k s + 1)^{n-1}, \qquad k = 1, 2, \ldots. \tag{2.79}$$

where $\epsilon_k > 0$ is adjusted to satisfy the constraint (2.74) for each k:

$$\varphi_{\delta_k}(\omega_0) = \theta. \tag{2.80}$$

It is easy to see that $\epsilon_k \to 0$ and (2.78) holds. A similar construction can be carried out for other values of θ provided that the degree n is large enough that the the constraint (2.80) can be satisfied; in particular $n \geq 4$ is always sufficient for arbitrary θ. ♣

Remark 2.1. In the case of complex Hurwitz polynomials the lower bound on the rate of change of phase with respect to ω is zero and the corresponding statement is that

$$\left.\frac{d\varphi_{\delta_k}(\omega)}{d\omega}\right|_{\omega=\omega_0} \tag{2.81}$$

can be made as small as desired by choosing complex Hurwitz polynomials $\delta_k(s)$ satisfying the constraint (2.80).

These technical results are useful in certain constructions related to convex directions.

2.4.2 Phase Relations for a Segment

Consider now a line segment $\lambda\delta_1(s) + (1-\lambda)\delta_2(s)$, $\lambda \in [0,1]$ generated by the two real polynomials $\delta_1(s)$ and $\delta_2(s)$ of degree n with leading coefficients and constant coefficients of the same sign. The necessary and sufficient condition for a polynomial in the interior of this segment to acquire a root at $s = j\omega_0$ is that

$$\begin{aligned} \lambda_0\delta_1^e(\omega_0) + (1-\lambda_0)\delta_2^e(\omega_0) &= 0 \\ \lambda_0\delta_1^o(\omega_0) + (1-\lambda_0)\delta_2^o(\omega_0) &= 0 \end{aligned} \tag{2.82}$$

for some $\lambda_0 \in (0,1)$. Since the segment is real and the constant coefficients are of the same sign it is sufficient to verify the above relations for $\omega_0 > 0$. Therefore the above equations are equivalent to

$$\lambda_0\delta_1^e(\omega_0) + (1-\lambda_0)\delta_2^e(\omega_0) = 0 \tag{2.83}$$

$$\lambda_0\omega_0\delta_1^o(\omega_0) + (1-\lambda_0)\omega_0\delta_2^o(\omega_0) = 0. \tag{2.84}$$

and also to

$$\begin{aligned} \lambda_0\delta_1^e(\omega_0) + (1-\lambda_0)\delta_2^e(\omega_0) &= 0 \\ \lambda_0\omega_0^2\delta_1^o(\omega_0) + (1-\lambda_0)\omega_0^2\delta_2^o(\omega_0) &= 0 \end{aligned} \tag{2.85}$$

since $\omega_0 > 0$. Noting that

$$\begin{aligned} \underline{\delta}_1(j\omega) &= \delta_1^e(\omega) + j\delta_1^o(\omega) = \rho_{\underline{\delta}_1}(\omega)e^{j\varphi_{\underline{\delta}_1}(\omega)} \\ \underline{\delta}_2(j\omega) &= \delta_2^e(\omega) + j\delta_2^o(\omega) = \rho_{\underline{\delta}_2}(\omega)e^{j\varphi_{\underline{\delta}_2}(\omega)} \\ \bar{\delta}_1(j\omega) &= \delta_1^e(\omega) + j\omega^2\delta_1^o(\omega) = \varphi_{\bar{\delta}_1}(\omega)e^{j\varphi_{\bar{\delta}_1}(\omega)} \\ \bar{\delta}_2(j\omega) &= \delta_2^e(\omega) + j\omega^2\delta_2^o(\omega) = \rho_{\bar{\delta}_2}(\omega)e^{j\varphi_{\bar{\delta}_2}(\omega)} \end{aligned} \tag{2.86}$$

we can write (2.82), (2.84), and (2.85), respectively in the equivalent forms

$$\lambda_0\delta_1(j\omega_0) + (1-\lambda_0)\delta_2(j\omega_0) = 0 \tag{2.87}$$

$$\lambda_0\underline{\delta}_1(j\omega_0) + (1-\lambda_0)\underline{\delta}_2(j\omega_0) = 0 \tag{2.88}$$

and

$$\lambda_0\bar{\delta}_1(j\omega_0) + (1-\lambda_0)\bar{\delta}_2(j\omega_0) = 0. \tag{2.89}$$

Now let

$$\begin{aligned} \delta_1(j\omega) &= \delta_1^e(\omega) + j\omega\delta_1^o(\omega) = \rho_{\delta_1}(\omega)e^{j\varphi_{\delta_1}(\omega)} \\ \delta_2(j\omega) &= \delta_2^e(\omega) + j\omega\delta_2^o(\omega) = \rho_{\delta_2}(\omega)e^{j\varphi_{\delta_2}(\omega)} \end{aligned} \tag{2.90}$$

$$\delta_0(s) := \delta_1(s) - \delta_2(s) \tag{2.91}$$

$$\begin{aligned} \underline{\delta}_0(j\omega) &:= \underline{\delta}_1(j\omega) - \underline{\delta}_2(j\omega) \\ \bar{\delta}_0(j\omega) &:= \bar{\delta}_1(j\omega) - \bar{\delta}_2(j\omega). \end{aligned} \tag{2.92}$$

We now state a key technical lemma.

Lemma 2.13 *Let $\delta_1(s), \delta_2(s)$ be real polynomials of degree n with leading coefficients of the same sign and assume that $\lambda_0 \in (0,1)$ and $\omega_0 > 0$ satisfy (2.85)-(2.89). Then*

$$\left.\frac{d\varphi_{\delta_0}}{d\omega}\right|_{\omega=\omega_0} = \lambda_0 \left.\frac{d\varphi_{\delta_2}}{d\omega}\right|_{\omega=\omega_0} + (1-\lambda_0)\left.\frac{d\varphi_{\delta_1}}{d\omega}\right|_{\omega=\omega_0} \tag{2.93}$$

$$\left.\frac{d\varphi_{\underline{\delta}_0}}{d\omega}\right|_{\omega=\omega_0} = \lambda_0 \left.\frac{d\varphi_{\underline{\delta}_2}}{d\omega}\right|_{\omega=\omega_0} + (1-\lambda_0)\left.\frac{d\varphi_{\underline{\delta}_1}}{d\omega}\right|_{\omega=\omega_0} \tag{2.94}$$

and

$$\left.\frac{d\varphi_{\bar{\delta}_0}}{d\omega}\right|_{\omega=\omega_0} = \lambda_0 \left.\frac{d\varphi_{\bar{\delta}_2}}{d\omega}\right|_{\omega=\omega_0} + (1-\lambda_0)\left.\frac{d\varphi_{\bar{\delta}_1}}{d\omega}\right|_{\omega=\omega_0}. \tag{2.95}$$

Proof. We prove only (2.93) in detail. If

$$\delta(j\omega) = p(\omega) + jq(\omega) \tag{2.96}$$

then

$$\tan\varphi_\delta(\omega) = \frac{q(\omega)}{p(\omega)}. \tag{2.97}$$

Let $\dot{q}(\omega) := \frac{dq(\omega)}{d\omega}$ and differentiate (2.97) with respect to ω to get

$$(1+\tan^2\varphi_\delta(\omega))\frac{d\varphi_\delta}{d\omega} = \frac{p(\omega)\dot{q}(\omega) - q(\omega)\dot{p}(\omega)}{p^2(\omega)} \tag{2.98}$$

and

$$\frac{d\varphi_\delta}{d\omega} = \frac{p(\omega)\dot{q}(\omega) - q(\omega)\dot{p}(\omega)}{p^2(\omega)+q^2(\omega)}. \tag{2.99}$$

We apply the formula in (2.99) to

$$\delta_0(j\omega) = (p_1(\omega) - p_2(\omega)) + j(q_1(\omega) - q_2(\omega)) \tag{2.100}$$

to get

$$\frac{d\varphi_{\delta_0}}{d\omega} = \frac{(p_1-p_2)(\dot{q}_1-\dot{q}_2) - (q_1-q_2)(\dot{p}_1-\dot{p}_2)}{(p_1-p_2)^2+(q_1-q_2)^2}. \tag{2.101}$$

Using (2.87)

$$\lambda_0 p_1(\omega_0) + (1-\lambda_0)p_2(\omega_0) = 0 \tag{2.102}$$

and

$$\lambda_0 q_1(\omega_0) + (1-\lambda_0) q_2(\omega_0) = 0. \tag{2.103}$$

Since $\delta_1(s)$ and $\delta_2(s)$ are Hurwitz $\lambda_0 \neq 0$, and $\lambda_0 \neq 1$, so that

$$p_1(\omega_0) - p_2(\omega_0) = -\frac{p_2(\omega_0)}{\lambda_0} = \frac{p_1(\omega_0)}{1-\lambda_0} \tag{2.104}$$

and

$$q_1(\omega_0) - q_2(\omega_0) = -\frac{q_2(\omega_0)}{\lambda_0} = \frac{q_1(\omega_0)}{1-\lambda_0}. \tag{2.105}$$

Substituting these relations in (2.101) we have

$$\begin{aligned}
\left.\frac{d\varphi_{\delta_0}}{d\omega}\right|_{\omega=\omega_0} &= \left.\frac{\frac{1}{1-\lambda_0} p_1\dot{q}_1 + \frac{1}{\lambda_0} p_2\dot{q}_2 - \frac{1}{1-\lambda_0} q_1\dot{p}_1 - \frac{1}{\lambda_0} q_2\dot{p}_2}{(p_1-p_2)^2 + (q_1-q_2)^2}\right|_{\omega=\omega_0} \\
&= \left.\frac{\frac{1}{1-\lambda_0}(p_1\dot{q}_1 - q_1\dot{p}_1)}{\frac{p_1^2+q_1^2}{(1-\lambda_0)^2}}\right|_{\omega=\omega_0} + \left.\frac{\frac{1}{\lambda_0}(p_2\dot{q}_2 - q_2\dot{p}_2)}{\frac{p_2^2+q_2^2}{\lambda_0^2}}\right|_{\omega=\omega_0} \\
&= (1-\lambda_0)\left.\frac{p_1\dot{q}_1 - q_1\dot{p}_1}{p_1^2+q_1^2}\right|_{\omega=\omega_0} + \lambda_0 \left.\frac{p_2\dot{q}_2 - q_2\dot{p}_2}{p_2^2+q_2^2}\right|_{\omega=\omega_0} \\
&= (1-\lambda_0)\left.\frac{d\varphi_{\delta_1}}{d\omega}\right|_{\omega=\omega_0} + \lambda_0 \left.\frac{d\varphi_{\delta_2}}{d\omega}\right|_{\omega=\omega_0}.
\end{aligned} \tag{2.106}$$

This proves (2.93). The proofs of (2.94) and (2.95) are identical starting from (2.88) and (2.89), respectively. ♣

The relation (2.93) holds for complex segments also. Suppose that $\delta_i(s), i = 1, 2$ are complex Hurwitz polynomials of degree n and consider the complex segment $\delta_2(s) + \lambda\delta_0(s), \lambda \in [0,1]$ with $\delta_0(s) = \delta_1(s) - \delta_2(s)$. The condition for a polynomial in the interior of this segment to have a root at $s = j\omega_0$ is

$$\delta_2(j\omega_0) + \lambda_0\delta_0(j\omega_0) = 0, \quad \lambda_0 \in (0,1). \tag{2.107}$$

It is straightforward to derive from the above, just as in the real case that

$$\left.\frac{d\varphi_{\delta_0}}{d\omega}\right|_{\omega=\omega_0} = \lambda_0 \left.\frac{d\varphi_{\delta_2}}{d\omega}\right|_{\omega=\omega_0} + (1-\lambda_0)\left.\frac{d\varphi_{\delta_1}}{d\omega}\right|_{\omega=\omega_0}. \tag{2.108}$$

The relationship (2.108) can be stated in terms of

$$X_i(\omega) := \tan\ \varphi_{\delta_i}(\omega), \quad i = 0, 1, 2. \tag{2.109}$$

Using the fact that

$$\frac{d\varphi_{\delta_i}(\omega)}{d\omega} = \frac{1}{(1+X_i^2(\omega))}\frac{dX_i(\omega)}{d\omega}, \quad i = 0, 1, 2 \tag{2.110}$$

(2.108) can be written in the equivalent form

$$\frac{1}{(1+X_0^2(\omega))}\frac{dX_0(\omega)}{d\omega}\bigg|_{\omega=\omega_0} =$$

$$\lambda_0\frac{1}{(1+X_2^2(\omega))}\frac{dX_2(\omega)}{d\omega}\bigg|_{\omega=\omega_0} + (1-\lambda_0)\frac{1}{(1+X_1^2(\omega))}\frac{dX_1(\omega)}{d\omega}\bigg|_{\omega=\omega_0}. \tag{2.111}$$

Geometric reasoning (the image set of the segment at $s = j\omega_0$ passes through the origin) shows that

$$|X_0(\omega)|_{\omega=\omega_0} = |X_1(\omega)|_{\omega=\omega_0} = |X_2(\omega)|_{\omega=\omega_0}. \tag{2.112}$$

Using (2.112) in (2.111) we obtain the following result.

Lemma 2.14 *Let $[\lambda\delta_1(s) + (1-\lambda)\delta_2(s)]$, $\lambda \in [0,1]$ be a real or complex segment of polynomials. If a polynomial in the interior of this segment, corresponding to $\lambda = \lambda_0$ has a root at $s = j\omega_0$ then*

$$\frac{dX_0(\omega)}{d\omega}\bigg|_{\omega=\omega_0} = \lambda_0\,\frac{dX_2(\omega)}{d\omega}\bigg|_{\omega=\omega_0} + (1-\lambda_0)\,\frac{dX_1(\omega)}{d\omega}\bigg|_{\omega=\omega_0}. \tag{2.113}$$

These auxiliary results will help us to establish the Convex Direction and Vertex Lemmas in the following sections.

2.5 CONVEX DIRECTIONS

It turns out that it is possible to give necessary and sufficient conditions on $\delta_0(s)$ under which strong stability of the pair $(\delta_2(s), \delta_0(s)+\delta_2(s))$ will hold for *every* $\delta_2(s)$ and $\delta_0(s)+\delta_2(s)$ that are Hurwitz. This is accomplished using the notion of *convex directions.*

As before let $\delta_1(s)$ and $\delta_2(s)$ be polynomials of degree n. Write

$$\delta_0(s) := \delta_1(s) - \delta_2(s)$$

and let

$$\delta_\lambda(s) = \lambda\delta_1(s) + (1-\lambda)\delta_2(s) = \delta_2(s) + \lambda\delta_0(s) \tag{2.114}$$

and let us assume that the degree of every polynomial on the segment $\{\delta_\lambda(s) : \lambda \in [0,1]\}$ is n. Now, the problem of interest is: Give necessary and sufficient conditions on $\delta_0(s)$ under which stability of the segment in (2.114) is guaranteed whenever the endpoints are Hurwitz stable? A polynomial $\delta_0(s)$ satisfying the above property is called *a convex direction.* There are two distinct results on convex directions corresponding to the real and complex cases. We begin with the complex case.

Complex Convex Directions

In the complex case we have the following result.

Lemma 2.15 (Complex Convex Direction Lemma)
Let $\delta_\lambda(s) : \lambda \in [0,1]$ be a complex segment of polynomials of degree n defined as in (2.114). The complex polynomial $\delta_0(s)$ is a convex direction if and only if

$$\frac{d\varphi_{\delta_0}(\omega)}{d\omega} \leq 0 \tag{2.115}$$

for every frequency $\omega \in \mathbb{R}$ such that $\delta_0(j\omega) \neq 0$. Equivalently

$$\frac{dX_0(\omega)}{d\omega} \leq 0 \tag{2.116}$$

for every frequency $\omega \in \mathbb{R}$ such that $\delta_0(j\omega) \neq 0$.

Proof. The equivalence of the two conditions (2.115) and (2.116) is obvious. Suppose now that (2.116) is true. In the first place if ω_0 is such that $\delta_0(j\omega_0) = 0$, it follows that $\delta_2(j\omega_0) + \lambda_0\delta_0(j\omega_0) \neq 0$ for any real $\lambda_0 \in [0,1]$ as this would contradict the fact that $\delta_2(s)$ is Hurwitz. Now from Lemma (2.14) we see that the segment has a polynomial with a root at $s = j\omega_0$ only if

$$\left.\frac{dX_0(\omega)}{d\omega}\right|_{\omega=\omega_0} = \lambda_0 \left.\frac{dX_2(\omega)}{d\omega}\right|_{\omega=\omega_0} + (1-\lambda_0)\left.\frac{dX_1(\omega)}{d\omega}\right|_{\omega=\omega_0}. \tag{2.117}$$

Since $\delta_1(s)$ and $\delta_2(s)$ are Hurwitz it follows from Lemma 2.8 that

$$\frac{dX_i(\omega)}{d\omega} > 0, \quad \omega \in \mathbb{R}; \quad i = 1,2. \tag{2.118}$$

and $\lambda_0 \in (0,1)$. Therefore the right hand side of (2.117) is strictly positive whereas the left hand side is nonpositive by hypothesis. This proves that there cannot exist any $\omega_0 \in \mathbb{R}$ for which (2.117) holds. The stability of the segment follows from the Boundary Crossing Theorem (Chapter 1).

The proof of necessity is based on showing that if the condition (2.115) fails to hold it is possible to construct a Hurwitz polynomial $p_2(s)$ such that the end point $p_1(s) = p_2(s) + \delta_0(s)$ is Hurwitz stable and the segment joining them is of constant degree but contains unstable polynomials. The proof is omitted as it is similar to the real case which is proved in detail in the next lemma. It suffices to mention that when $\omega = \omega^*$ is such that

$$\left.\frac{d\varphi_{\delta_0}(\omega)}{d\omega}\right|_{\omega=\omega^*} > 0 \tag{2.119}$$

we can take

$$p_1(s) = (s - j\omega^*)t(s) + \mu\delta_0(s) \tag{2.120}$$

$$p_2(s) = (s - j\omega^*)t(s) - \mu\delta_0(s) \tag{2.121}$$

where $t(s)$ is chosen to be a complex Hurwitz polynomial of degree greater than the degree of $\delta_0(s)$, and satisfying the conditions:

$$\begin{aligned} &|X_0(\omega^*)| = |X_t(\omega^*)| \\ &\left.\frac{d\varphi_{\delta_0}(\omega)}{d\omega}\right|_{\omega=\omega^*} > \left.\frac{d\varphi_t(\omega)}{d\omega}\right|_{\omega=\omega^*} > 0. \end{aligned} \tag{2.122}$$

The existence of such $t(s)$ is clear from Remark 2.1 following Lemma 2.12. The proof is completed by noting that $p_i(s)$ are Hurwitz, the segment joining $p_1(s)$ and $p_2(s)$ is of constant degree (for small enough $|\mu|$), but the segment polynomial $\frac{1}{2}(p_1(s) + p_2(s))$ has $s = j\omega^*$ as a root. ♣

Real Convex Directions

The following Lemma gives the necessary and sufficient condition for $\delta_0(s)$ to be a convex direction in the real case.

Lemma 2.16 (Real Convex Direction Lemma)
Consider the real segment $\{\delta_\lambda(s) : \lambda \in [0,1]\}$ of degree n. The real polynomial $\delta_0(s)$ is a convex direction if and only if

$$\frac{d\varphi_{\delta_0}(\omega)}{d\omega} \leq \left|\frac{\sin\left(2\varphi_{\delta_0}(\omega)\right)}{2\omega}\right| \tag{2.123}$$

is satisfied for every frequency $\omega > 0$ such that $\delta_0(j\omega) \neq 0$. Equivalently

$$\frac{dX_0(\omega)}{d\omega} \leq \left|\frac{X_0(\omega)}{\omega}\right| \tag{2.124}$$

for every frequency $\omega > 0$ such that $\delta_0(j\omega) \neq 0$.

Proof. The equivalence of the conditions (2.124) and (2.123) has already been shown (see the proof of Theorem 2.1) and so it suffices to prove (2.124). If degree $\delta_i(s) = 1$ for $i = 1, 2$, degree $\delta_0(s) \leq 1$ and (2.124) holds. In this case it is straightforward to verify from the requirements that the degree along the segment is 1 and $\delta_i(s)$, $i = 1, 2$ are Hurwitz, that no polynomial on the segment has a root at $s = 0$. Hence such a segment is stable by the Boundary Crossing Theorem. We assume henceforth that degree$[\delta_i(s)] \geq 2$ for $i = 1, 2$. In general the assumption of invariant degree along the segment (the leading coefficients of $\delta_i(s)$ are of the same sign) along with the requirement that $\delta_i(s), i = 1, 2$ are Hurwitz imply that the constant coefficients of $\delta_i(s), i = 1, 2$ are also of the same sign. This rules out the possibility of any polynomial in the segment having a root at $s = 0$.

Now if $\omega_0 > 0$ is such that $\delta_0(j\omega_0) = 0$, and $\delta_2(j\omega_0) + \lambda_0\delta_0(j\omega_0) = 0$ for some real $\lambda_0 \in (0, 1)$ it follows that $\delta_2(j\omega_0) = 0$. However this would contradict the fact that $\delta_2(s)$ is Hurwitz. Thus such a $j\omega_0$ also cannot be a root of any polynomial on

the segment. To proceed let us first consider the case where $\delta_0(s) = as + b$ with $b \neq 0$. Here (2.124) is again seen to hold. From Lemma 2.13 it follows that $s = j\omega_0$ is a root of a polynomial on the segment only if for some $\lambda_0 \in (0,1)$

$$\left.\frac{d\varphi_{\underline{\delta}_0}}{d\omega}\right|_{\omega=\omega_0} = \lambda_0 \left.\frac{d\varphi_{\underline{\delta}_2}}{d\omega}\right|_{\omega=\omega_0} + (1-\lambda_0)\left.\frac{d\varphi_{\underline{\delta}_1}}{d\omega}\right|_{\omega=\omega_0}. \tag{2.125}$$

In the present case we have

$$\tan \varphi_{\underline{\delta}_0}(\omega) = \frac{a}{b} \tag{2.126}$$

and therefore the left hand side of (2.125)

$$\left.\frac{d\varphi_{\underline{\delta}_0}}{d\omega}\right|_{\omega=\omega_0} = 0. \tag{2.127}$$

Since $\delta_i(s), i = 1, 2$ are Hurwitz and of degree ≥ 2 we have from Lemma 2.10 that

$$\left.\frac{d\varphi_{\underline{\delta}_i}}{d\omega}\right|_{\omega=\omega_0} > 0 \tag{2.128}$$

so that the right hand side of (2.125)

$$\lambda_0 \left.\frac{d\varphi_{\underline{\delta}_2}}{d\omega}\right|_{\omega=\omega_0} + (1-\lambda_0)\left.\frac{d\varphi_{\underline{\delta}_1}}{d\omega}\right|_{\omega=\omega_0} > 0. \tag{2.129}$$

This contradiction shows that such a $j\omega_0$ cannot be a root of any polynomial on the segment, which must therefore be stable.

We now consider the general case where degree$[\delta_0(s)] \geq 2$ or $\delta_0(s) = as$. From Lemma 2.14 we see that the segment has a polynomial with a root at $s = j\omega_0$ only if

$$\left.\frac{dX_0(\omega)}{d\omega}\right|_{\omega=\omega_0} = \lambda_0 \left.\frac{dX_2(\omega)}{d\omega}\right|_{\omega=\omega_0} + (1-\lambda_0)\left.\frac{dX_1(\omega)}{d\omega}\right|_{\omega=\omega_0}. \tag{2.130}$$

Since $\delta_1(s)$ and $\delta_2(s)$ are Hurwitz it follows from Theorem 2.1 that we have

$$\frac{dX_i(\omega)}{d\omega} > \left|\frac{X_i(\omega)}{\omega}\right|, \quad \omega > 0; \quad i = 1, 2 \tag{2.131}$$

and $\lambda_0 \in (0,1)$. Furthermore we have

$$|X_0(\omega)|_{\omega=\omega_0} = |X_1(\omega)|_{\omega=\omega_0} = |X_2(\omega)|_{\omega=\omega_0} \tag{2.132}$$

so that the right hand side of (2.130) satisfies

$$\lambda_0 \left.\frac{dX_2(\omega)}{d\omega}\right|_{\omega=\omega_0} + (1-\lambda_0)\left.\frac{dX_1(\omega)}{d\omega}\right|_{\omega=\omega_0} \tag{2.133}$$

$$> \lambda_0 \left| \frac{X_2(\omega)}{\omega} \right|_{\omega=\omega_0} + (1-\lambda_0) \left| \frac{X_1(\omega)}{\omega} \right|_{\omega=\omega_0} = \left| \frac{X_0(\omega_0)}{\omega_0} \right|. \tag{2.134}$$

On the other hand the left hand side of (2.130) satisfies

$$\left| \frac{dX_0(\omega)}{d\omega} \right|_{\omega=\omega_0} \leq \left| \frac{X_0(\omega_0)}{\omega_0} \right|. \tag{2.135}$$

This contradiction proves that there cannot exist any $\omega_0 \in \mathbb{R}$ for which (2.130) holds. Thus no polynomial on the segment has a root at $s = j\omega_0$, $\omega_0 > 0$ and the stability of the entire segment follows from the Boundary Crossing Theorem of Chapter 1. This completes the proof of sufficiency.

The proof of necessity requires us to show that if the condition (2.123) fails there exists a Hurwitz polynomial $r_2(s)$ such that $r_1(s) = r_2(s) + \delta_0(s)$ is also Hurwitz stable but the segment joining them is not. Suppose then that $\delta_0(s)$ is a given polynomial of degree n and $\omega^* > 0$ is such that $\delta_0(j\omega^*) \neq 0$ but

$$\frac{d\varphi_{\delta_0}(\omega)}{d\omega} > \left| \frac{\sin\left(2\varphi_{\delta_0}(\omega)\right)}{2\omega} \right| \tag{2.136}$$

for some $\omega^* > 0$. It is then possible to construct a real Hurwitz polynomial $t(s)$ of degree $\geq n-2$ such that

$$r_1(s) := (s^2 + {\omega^*}^2)t(s) + \mu\delta_0(s) \tag{2.137}$$

and

$$r_2(s) := (s^2 + {\omega^*}^2)t(s) - \mu\delta_0(s) \tag{2.138}$$

are Hurwitz and have leading coefficients of the same sign for sufficiently small $|\mu|$. It suffices to choose $t(s)$ so that

$$\left. \frac{d\varphi_{\delta_0}}{d\omega} \right|_{\omega=\omega^*} > \left. \frac{d\varphi_t}{d\omega} \right|_{\omega=\omega^*} > \left| \frac{\sin 2\varphi_{\delta_0}(\omega^*)}{2\omega^*} \right| = \left| \frac{\sin 2\varphi_t(\omega^*)}{2\omega^*} \right|. \tag{2.139}$$

The fact that such $t(s)$ exists is guaranteed by Lemma 2.12. It remains to prove that $r_i(s)$, $i = 1, 2$ can be made Hurwitz stable by choice of μ.

For sufficiently small $|\mu|$, $n-2$ of the zeros of $r_i(s), i = 1, 2$ are close to those of $t(s)$, and hence in the open left half plane while the remaining two zeros are close to $\pm j\omega^*$. To prove that that the roots lying close to $\pm j\omega^*$ are in the open left half plane we let $s(\mu)$ denote the root close to $j\omega^*$ and analyse the behaviour of the real part of $s(\mu)$ for small values of μ. We already know that

$$\mathrm{Re}[s(\mu)]|_{\mu=0} = 0. \tag{2.140}$$

We will establish the fact that $\mathrm{Re}[s(\mu)]$ has a local maximum at $\mu = 0$ and this together with (2.140) will show that $\mathrm{Re}[s(\mu)]$ is negative in a neighbourhood of

$\mu = 0$, proving that $r_i(s)$, $i = 1, 2$ are stable. To prove that $\mathrm{Re}[s(\mu)]$ has a local maximum at $\mu = 0$ it suffices to establish that

$$\frac{d}{d\mu}\mathrm{Re}\left[s(\mu)\right]\Big|_{\mu=0} = 0 \tag{2.141}$$

and

$$\frac{d^2}{d\mu^2}\mathrm{Re}\left[s(\mu)\right]\Big|_{\mu=0} < 0. \tag{2.142}$$

Now since $s(\mu)$ is a root of $r_1(s)$ we have

$$r_1\left(s(\mu)\right) = \left(s(\mu) - j\omega^*\right) u\left(s(\mu)\right) + \mu\delta_0\left(s(\mu)\right) = 0 \tag{2.143}$$

where

$$u(s) := (s + j\omega^*)t(s). \tag{2.144}$$

By differentiating (2.143) with respect to μ we get

$$\frac{ds(\mu)}{d\mu} = -\frac{\delta_0\left(s(\mu)\right)}{u\left(s(\mu)\right) + \left(s(\mu) - j\omega^*\right)\frac{du(s(\mu))}{ds(\mu)} + \mu\frac{d\delta_0(s(\mu))}{ds(\mu)}} \tag{2.145}$$

and hence

$$\frac{ds(\mu)}{d\mu}\Big|_{\mu=0} = -\frac{\delta_0(j\omega^*)}{u(j\omega^*)} = -\frac{\delta_0(j\omega^*)}{2j\omega^* t(j\omega^*)}. \tag{2.146}$$

From the fact that

$$\left|\frac{\sin 2\varphi_{\delta_0}(\omega^*)}{2\omega^*}\right| = \left|\frac{\sin 2\varphi_t(\omega^*)}{2\omega^*}\right| \tag{2.147}$$

(see (2.139)) it follows that $\delta_0(j\omega^*)$ and $t(j\omega^*)$ have arguments that are equal or differ by π radians so that

$$\frac{\delta_0(j\omega^*)}{t(j\omega^*)} \tag{2.148}$$

is purely real. Therefore we have

$$\frac{d}{d\mu}\mathrm{Re}\left[s(\mu)\right]\Big|_{\mu=0} = 0.$$

To complete the proof we need to establish that

$$\frac{d^2}{d\mu^2}\mathrm{Re}\left[s(\mu)\right]\Big|_{\mu=0} < 0.$$

By differentiating (2.145) once again with respect to μ we can obtain the second derivative. After some calculation we get:

$$\frac{d^2 s(\mu)}{d\mu^2}\Big|_{\mu=0} = -\frac{j}{2(\omega^*)^2}\frac{\delta_0^2(j\omega^*)}{t^2(j\omega^*)}\left(\frac{1}{u(j\omega^*)}\left.\frac{du(j\omega)}{d\omega}\right|_{\omega=\omega^*} - \frac{1}{\delta_0(j\omega^*)}\left.\frac{d\delta_0(j\omega)}{d\omega}\right|_{\omega=\omega^*}\right).$$

Using the fact that $\frac{\delta_0(j\omega^*)}{t(j\omega^*)}$ is purely real and the formulas (see (2.45))

$$\mathrm{Im}\left[\frac{1}{u(j\omega^*)}\,\frac{du(j\omega)}{d\omega}\right]\Big|_{\omega=\omega^*} = \left.\frac{d\varphi_u}{d\omega}\right|_{\omega=\omega^*} \tag{2.149}$$

$$\mathrm{Im}\left[\frac{1}{\delta_0(j\omega^*)}\,\frac{d\delta_0(j\omega)}{d\omega}\right]\Big|_{\omega=\omega^*} = \left.\frac{d\varphi_{\delta_0}}{d\omega}\right|_{\omega=\omega^*} \tag{2.150}$$

we get

$$\left.\frac{d^2}{d\mu^2}\mathrm{Re}\,[s(\mu)]\right|_{\mu=0} = -\frac{1}{2(\omega^*)^2}\frac{\delta_0^2(j\omega^*)}{t^2(j\omega^*)}\left(\left.\frac{d\varphi_{\delta_0}}{d\omega}\right|_{\omega=\omega^*} - \left.\frac{d\varphi_u}{d\omega}\right|_{\omega=\omega^*}\right). \tag{2.151}$$

Now

$$\left.\frac{d\varphi_u}{d\omega}\right|_{\omega=\omega^*} = \left.\frac{d\varphi_t}{d\omega}\right|_{\omega=\omega^*} \tag{2.152}$$

and by construction

$$\left.\frac{d\varphi_{\delta_0}}{d\omega}\right|_{\omega=\omega^*} > \left.\frac{d\varphi_t}{d\omega}\right|_{\omega=\omega^*}.$$

Once again using the fact that $\frac{\delta_0(j\omega^*)}{t(j\omega^*)}$ is real we finally have from (2.151):

$$\left.\frac{d^2}{d\mu^2}\mathrm{Re}\,[s(\mu)]\right|_{\mu=0} < 0. \tag{2.153}$$

This proves that the real part of $s(\mu)$ is negative for μ in the neighbourhood of $\mu = 0$ and therefore $r_1(s)$ must be stable as claimed. An identical argument shows that $r_2(s)$ is stable. The proof is now completed by the fact that $r_i(s)$, $i = 1, 2$ are Hurwitz and the segment joining them is of constant degree but the segment polynomial $\frac{1}{2}(r_1(s) + r_2(s))$ has $s = j\omega^*$ as a root. Thus $\delta_0(s)$ is not a convex direction. ♣

We illustrate the usefulness of convex directions by some examples.

Example 2.7. Consider the line segment joining the following two endpoints which are Hurwitz:

$$\delta_1(s) := s^4 + 12.1s^3 + 8.46s^2 + 11.744s + 2.688$$
$$\delta_2(s) := 2s^4 + 9s^3 + 12s^2 + 10s + 3.$$

We first verify the stability of the segment by using the Segment Lemma. The positive real roots of the polynomial

$$\delta_1^e(\omega)\delta_2^o(\omega) - \delta_2^e(\omega)\delta_1^o(\omega) = 0$$

that is

$$(\omega^4 - 8.46\omega^2 + 2.688)(-9\omega^2 + 10) - (2\omega^4 - 12\omega^2 + 3)(-12.1\omega^2 + 11.744) = 0$$

are

$$2.1085, \qquad 0.9150, \qquad 0.3842.$$

However, none of these ωs satisfy the conditions 2) and 3) of the Segment Lemma (Lemma 2.4). Thus, we conclude that the entire line segment is Hurwitz.

Next we apply the Real Convex Direction Lemma to the difference polynomial

$$\begin{aligned}\delta_0(s) &:= \delta_2(s) - \delta_1(s) \\ &= s^4 - 3.1s^3 + 3.54s^2 - 1.744s + 0.312\end{aligned}$$

so that

$$\delta_0(j\omega) = \underbrace{(\omega^4 - 3.54\omega^2 + 0.312)}_{\delta_0^r(\omega)} + j\underbrace{(3.1\omega^3 - 1.744\omega)}_{\delta_0^i(\omega)}$$

and the two functions that need to be evaluated are

$$\begin{aligned}\frac{d}{d\omega}\varphi_{\delta_0}(\omega) &= \frac{\delta_0^r(\omega)\left(\frac{d\delta_0^i(\omega)}{d\omega}\right) - \left(\frac{d\delta_0^r(\omega)}{d\omega}\right)\delta_0^i(\omega)}{\left(\delta_0^r(\omega)\right)^2 + \left(\delta_0^i(\omega)\right)^2} \\ &= \frac{(\omega^4 - 3.54\omega^2 + 0.312)(9.3\omega^2 - 1.744) - (4\omega^3 - 7.08\omega)(3.1\omega^3 - 1.744\omega)}{(\omega^4 - 3.54\omega^2 + 0.312)^2 + (3.1\omega^3 - 1.744\omega)^2}\end{aligned}$$

and

$$\begin{aligned}\left|\frac{\sin\left(2\varphi_{\delta_0}(\omega)\right)}{2\omega}\right| &= \left|\frac{\delta_0^r(\omega)\delta_0^i(\omega)}{\omega\left[(\delta_0^r(\omega))^2 + (\delta_0^i(\omega))^2\right]}\right| \\ &= \left|\frac{(\omega^4 - 3.54\omega^2 + 0.312)(3.1\omega^2 - 1.744)}{(\omega^4 - 3.54\omega^2 + 0.312)^2 + (3.1\omega^3 - 1.744\omega)^2}\right|.\end{aligned}$$

These two functions are depicted in Figure 2.14. Since the second function dominates the first for each ω the plots show that $\delta_0(s)$ is a convex direction. Consequently, the line segment joining the given $\delta_1(s)$ and $\delta_2(s)$ is Hurwitz. Furthermore since $\delta_0(s)$ is a convex direction, we know, in addition, that every line segment of the form $\delta(s) + \lambda\delta_0(s)$ for $\lambda \in [0, 1]$ is Hurwitz for *an arbitrary* Hurwitz polynomial $\delta(s)$ of degree 4 with positive leading coefficient, provided $\delta(s) + \delta_0(s)$ is stable. This additional information is not furnished by the Segment Lemma.

Example 2.8. Consider the Hurwitz stability of the segment joining the following two polynomials:

$$\begin{aligned}\delta_1(s) &= 1.4s^4 + 6s^3 + 2.2s^2 + 1.6s + 0.2 \\ \delta_2(s) &= 0.4s^4 + 1.6s^3 + 2s^2 + 1.6s + 0.4.\end{aligned}$$

Since $\delta_1(s)$ and $\delta_2(s)$ are stable, we can apply the Segment Lemma to check the stability of the line segment $[\delta_1(s), \delta_2(s)]$. First we compute the roots of the polynomial equation:

$$\delta_1^e(\omega)\delta_2^o(\omega) - \delta_2^e(\omega)\delta_1^o(\omega) =$$

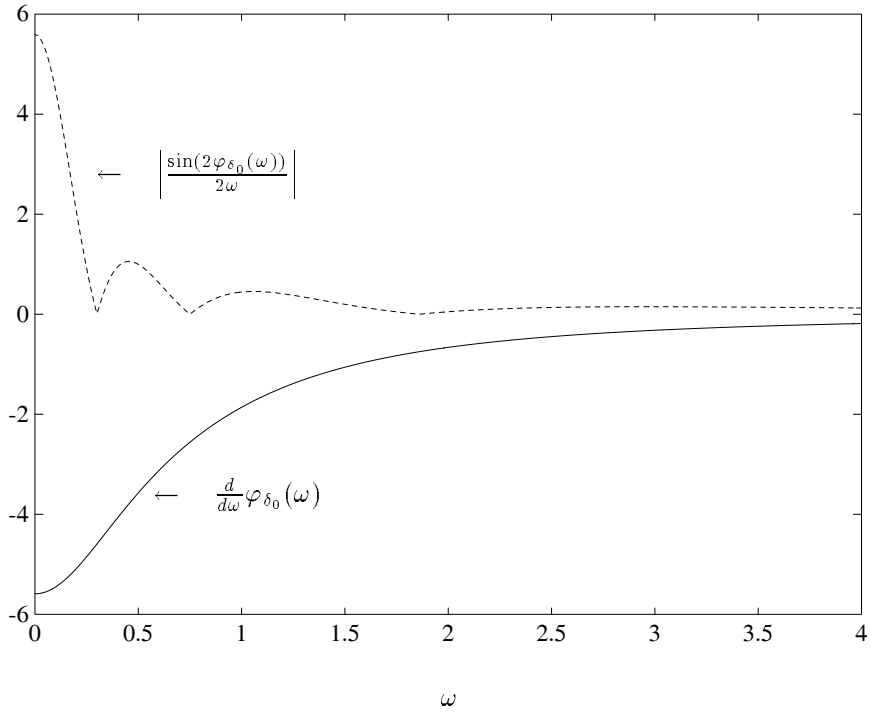

Figure 2.14. $\delta_0(s)$ is a convex direction (Example 2.8)

$$(1.4\omega^4 - 2.2\omega^2 + 0.2)(-1.6\omega^2 + 1.6) - (0.4\omega^4 - 2\omega^2 + 0.4)(-6\omega^2 + 1.6) = 0.$$

There is one positive real root $\omega \approx 6.53787$. We proceed to check the conditions 2) and 3) of the Segment Lemma (Lemma 2.4):

$$\begin{aligned}(1.4\omega^4 - 2.2\omega^2 + 0.2)(0.4\omega^4 - 2\omega^2 + 0.4)|_{\omega \approx 6.53787} > 0 \\ (-6\omega^2 + 1.6)(-1.6\omega^2 + 1.6)|_{\omega \approx 6.53787} > 0.\end{aligned}$$

Thus, we conclude that the segment $[\delta_1(s), \delta_2(s)]$ is stable.

Now let us apply the Real Convex Direction Lemma to the difference polynomial

$$\begin{aligned}\delta_0(s) &= \delta_1(s) - \delta_2(s) \\ &= s^4 + 4.4s^3 + 0.2s^2 - 0.2.\end{aligned}$$

We have

$$\delta_0(j\omega) = \underbrace{(\omega^4 - 0.2\omega^2 - 0.2)}_{\delta_0^r(\omega)} + j\,\underbrace{(-4.4\omega^3)}_{\delta_0^i(\omega)}.$$

The two functions that need to be evaluated are

$$\frac{d\varphi_{\delta_0}(\omega)}{d\omega} = \frac{(\omega^4 - 0.2\omega^2 - 0.2)(-13.2\omega^2) - (4\omega^3 - 0.4\omega)(-4.4\omega^3)}{(\omega^4 - 0.2\omega^2 - 0.2)^2 + (-4.4\omega^3)^2}$$

and

$$\left|\frac{\sin(2\varphi_{\delta_0}(\omega))}{2\omega}\right| = \left|\frac{(\omega^4 - 0.2\omega^2 - 0.2)(-4.4\omega^2)}{(\omega^4 - 0.2\omega^2 - 0.2)^2 + (-4.4\omega^3)^2}\right|.$$

These two functions are depicted in Figure 2.15. Since the second function does not dominate the first at each ω we conclude that $\delta_0(s)$ is not a convex direction.

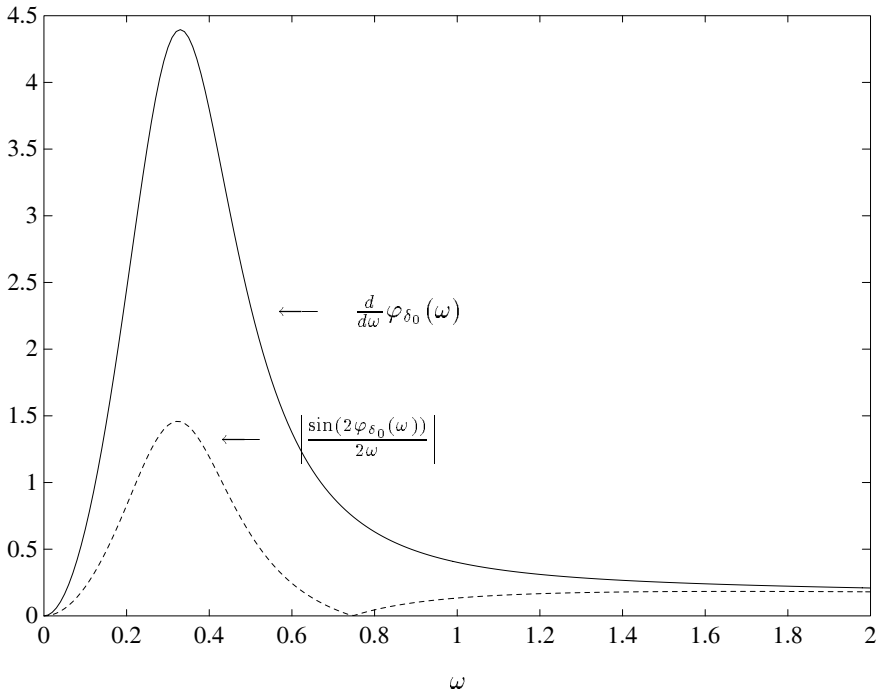

Figure 2.15. $\delta_0(s)$ is a nonconvex direction (Example 2.9)

Remark 2.2. This example reinforces the fact that the segment joining $\delta_1(s)$ and $\delta_2(s)$ can be stable even though $\delta_0(s) = \delta_1(s) - \delta_2(s)$ is not a convex direction. On the other hand, even though this particular segment is stable, there exists at least one Hurwitz polynomial $\delta_2(s)$ of degree 4 such that the segment $[\delta_2(s), \delta_2(s)+\delta_0(s)]$ is not Hurwitz even though $\delta_2(s)$ and $\delta_2(s) + \delta_0(s)$ are.

2.6 THE VERTEX LEMMA

The conditions given by the Convex Direction Lemmas are frequency dependent. It is possible to give frequency-independent conditions on $\delta_0(s)$ under which Hurwitz stability of the vertices implies stability of every polynomial on the segment $[\delta_1(s), \delta_2(s)]$. In this section we first consider various special forms of the difference polynomial $\delta_0(s)$ for which this is possible. In each case we use Lemma 2.13 and Hurwitz stability of the vertices to contradict the hypothesis that the segment has unstable polynomials. We then combine the special cases to obtain the general result. This main result is presented as the Vertex Lemma.

We shall assume throughout this subsection that each polynomial on the segment $[\delta_1(s), \delta_2(s)]$ is of degree n. This will be true if and only if $\delta_1(s)$ and $\delta_2(s)$ are of degree n and their leading coefficients are of the same sign. We shall assume this without loss of generality.

We first consider real polynomials of the form

$$\delta_0(s) = s^t(as + b)P(s)$$

where t is a nonnegative integer and $P(s)$ is odd or even. Suppose arbitrarily, that t is even and $P(s) = E(s)$ an even polynomial. Then

$$\delta_0(s) = \underbrace{s^t E(s) b}_{\delta_0^{\mathrm{even}}(s)} + \underbrace{s^{t+1} E(s) a}_{\delta_0^{\mathrm{odd}}(s)}. \tag{2.154}$$

Defining $\underline{\delta}_0(j\omega)$ as before we see that

$$\tan \underline{\delta}_0(\omega) = \frac{a}{b} \tag{2.155}$$

so that

$$\frac{d\varphi_{\underline{\delta}_0}}{d\omega} = 0. \tag{2.156}$$

From Lemma 2.13 (i.e., (2.94)), we see that

$$\lambda_0 \frac{d\varphi_{\underline{\delta}_2}}{d\omega}\bigg|_{\omega=\omega_0} + (1-\lambda_0)\frac{d\varphi_{\underline{\delta}_1}}{d\omega}\bigg|_{\omega=\omega_0} = 0 \tag{2.157}$$

and from Lemma 2.10 we see that if $\delta_1(s)$ and $\delta_2(s)$ are Hurwitz, then

$$\frac{d\varphi_{\underline{\delta}_2}}{d\omega} > 0 \tag{2.158}$$

and

$$\frac{d\varphi_{\underline{\delta}_1}}{d\omega} > 0 \tag{2.159}$$

so that (2.157) cannot be satisfied for $\lambda_0 \in [0, 1]$. An identical argument works when t is odd. The case when $P(s) = O(s)$ is an odd polynomial can be handled similarly by using (2.95) in Lemma 2.13. The details are left to the reader. Thus we are led to the following result.

Lemma 2.17 *If $\delta_0(s) = s^t(as+b)P(s)$ where $t \geq 0$ is an integer, a and b are arbitrary real numbers and $P(s)$ is an even or odd polynomial, then stability of the segment $[\delta_1(s),\delta_2(s)]$ is implied by those of the endpoints $\delta_1(s)$, $\delta_2(s)$.*

We can now prove the following general result.

Lemma 2.18 (Vertex Lemma: Hurwitz Case)

a) Let $\delta_1(s)$ and $\delta_2(s)$ be real polynomials of degree n with leading coefficients of the same sign and let

$$\begin{aligned}\delta_0(s) &= \delta_1(s) - \delta_2(s) \\ &= A(s)s^t(as+b)P(s)\end{aligned} \tag{2.160}$$

where $A(s)$ is antiHurwitz, $t \geq 0$ is an integer, a, b are arbitrary real numbers, and $P(s)$ is even or odd. Then stability of the segment $[\delta_1(s),\ \delta_2(s)]$ is implied by that of the endpoints $\delta_1(s)$, $\delta_2(s)$.

b) When $\delta_0(s)$ is not of the form specified in a), stability of the endpoints is not sufficient to guarantee that of the segment.

Proof.

a) Write

$$A(s) = A^{\text{even}}(s) + A^{\text{odd}}(s) \tag{2.161}$$

and let

$$\bar{A}(s) := A^{\text{even}}(s) - A^{\text{odd}}(s). \tag{2.162}$$

Since $A(s)$ is antiHurwitz, $\bar{A}(s)$ is Hurwitz. Now consider the segment $[\bar{A}(s)\delta_1(s),\ \bar{A}(s)\delta_2(s)]$ which is Hurwitz if and only if $[\delta_1(s),\ \delta_2(s)]$ is Hurwitz. But

$$\begin{aligned}\bar{A}(s)\delta_0(s) &= \bar{A}(s)\delta_1(s) - \bar{A}(s)\delta_2(s) \\ &= \underbrace{[(A^{\text{even}}(s))^2 - (A^{\text{odd}}(s))^2]}_{T(s)} s^t(as+b)P(s).\end{aligned} \tag{2.163}$$

Since $T(s)$ is an even polynomial we may use Lemma 2.17 to conclude that the segment $[\bar{A}(s)\delta_1(s),\ \bar{A}(s)\delta_2(s)]$ is Hurwitz if and only if $\bar{A}(s)\delta_1(s)$ and $\bar{A}(s)\delta_2(s)$ are. Since $\bar{A}(s)$ is Hurwitz it follows that the segment $[\delta_1(s),\ \delta_2(s)]$ is Hurwitz if and only if the endpoints $\delta_1(s)$ and $\delta_2(s)$ are.

b) We prove this part by means of the following example. Consider the segment

$$\delta_\lambda(s) = (2+14\lambda)s^4 + (5+14\lambda)s^3 + (6+14\lambda)s^2 + 4s + 3.5. \tag{2.164}$$

Now set $\lambda = 0$ and $\lambda = 1$, then we have

$$\begin{aligned}\delta_\lambda|_{\lambda=0} &= \delta_1(s) = 2s^4 + 5s^3 + 6s^2 + 4s + 3.5 \\ \delta_\lambda|_{\lambda=1} &= \delta_2(s) = 16s^4 + 19s^3 + 20s^2 + 4s + 3.5\end{aligned}$$

and consequently,

$$\begin{aligned}\delta_0(s) &= \delta_2(s) - \delta_1(s) \\ &= 14s^4 + 14s^3 + 14s^2 \\ &= 14s^2(s^2 + s + 1).\end{aligned}$$

It can be verified that two endpoints $\delta_1(s)$ and $\delta_2(s)$ are Hurwitz. Notice that since $(s^2 + s + 1)$ is Hurwitz with a pair of complex conjugate roots, $\delta_0(s)$ cannot be partitioned into the form of (2.160). Therefore, we conclude that when $\delta_0(s)$ is not of the form specified in (2.160), stability of the endpoints is not sufficient to guarantee that of the segment.

♣

Remark 2.3. We remark that the form of $\delta_0(s)$ given in (2.160) is a real convex direction.

Example 2.9. Suppose that the transfer function of a plant containing an uncertain parameter is written in the form:

$$P(s) = \frac{P_2}{P_1(s) + \lambda P_0(s)}$$

where the uncertain parameter λ varies in $[0, 1]$, and the degree of $P_1(s)$ is greater than those of $P_0(s)$ or $P_2(s)$. Suppose that a unity feedback controller is to be designed so that the plant output follows step and ramp inputs and rejects sinusoidal disturbances of radian frequency ω_0. Let us denote the controller by

$$C(s) = \frac{Q_2(s)}{Q_1(s)}.$$

A possible choice of $Q_1(s)$ which will meet the tracking and disturbance rejection requirements is

$$Q_1(s) = s^2(s^2 + \omega_0^2)(as + b)$$

with $Q_2(s)$ being of degree 5 or less. The stability of the closed loop requires that the segment

$$\delta_\lambda(s) = Q_2(s)P_2(s) + Q_1(s)(P_1(s) + \lambda P_0(s),$$

be Hurwitz stable. The corresponding difference polynomial $\delta_0(s)$ is

$$\delta_0(s) = Q_1(s)P_0(s).$$

With $Q_1(s)$ of the form shown above, it follows that $\delta_0(s)$ is of the form specified in the Vertex Lemma if $P_0(s)$ is anti-Hurwitz or even or odd or product thereof. Thus, in such a case robust stability of the closed loop would be equivalent to the stability of the two vertex polynomials

$$\begin{aligned}\delta_1(s) &= Q_2(s)P_2(s) + Q_1(s)P_1(s) \\ \delta_2(s) &= Q_2(s)P_2(s) + Q_1(s)P_1(s) + Q_1(s)P_0(s).\end{aligned}$$

Let $\omega_0 = 1$, $a = 1$, and $b = 1$ and

$$P_1(s) = s^2 + s + 1, \quad P_0(s) = s(s-1), \quad P_2(s) = s^2 + 2s + 1$$

$$Q_2(s) = s^5 + 5s^4 + 10s^3 + 10s^2 + 5s + 1.$$

Since $P_0(s) = s(s-1)$ is the product of an odd and an antiHurwitz polynomial, the conditions of the Vertex Lemma are satisfied and robust stability is equivalent to that of the two vertex polynomials

$$\delta_1(s) = 2s^7 + 9s^6 + 24s^5 + 38s^4 + 37s^3 + 22s^2 + 7s + 1$$
$$\delta_2(s) = 3s^7 + 9s^6 + 24s^5 + 38s^4 + 36s^3 + 22s^2 + 7s + 1.$$

Since $\delta_1(s)$ and $\delta_2(s)$ are Hurwitz, the controller

$$C(s) = \frac{Q_2(s)}{Q_1(s)} = \frac{s^5 + 5s^4 + 10s^3 + 10s^2 + 5s + 1}{s^2(s^2+1)(s+1)}$$

robustly stabilizes the closed loop system and provides robust asymptotic tracking and disturbance rejection.

The Vertex Lemma can easily be extended to the case of Schur stability.

Lemma 2.19 (Vertex Lemma: Schur Case)

a) Let $\delta_1(z)$ and $\delta_2(z)$ be polynomials of degree n with $\delta_1(1)$ and $\delta_2(1)$ nonzero and of the same sign, and with leading coefficients of the same sign. Let

$$\begin{aligned}\delta_0(z) &= \delta_1(z) - \delta_2(z) \\ &= A(z)(z-1)^{t_1}(z+1)^{t_2}(az+b)P(z) \qquad (2.165)\end{aligned}$$

where $A(z)$ is antiSchur, t_1, $t_2 \geq 0$ are integers, a, b are arbitrary real numbers, and $P(z)$ is symmetric or antisymmetric. Then Schur stability of the segment $[\delta_1(z), \delta_2(z)]$ is implied by that of the endpoints $\delta_1(z)$, $\delta_2(z)$.

b) When $\delta_0(z)$ is not of the form specified in a), Schur stability of the endpoints is not sufficient to guarantee that of the segment.

Proof. The proof is based on applying the bilinear transformation and using the corresponding results for the Hurwitz case. Let $P(z)$ be any polynomial and let

$$\hat{P}(s) := (s-1)^n P\left(\frac{s+1}{s-1}\right).$$

If $P(z)$ is of degree n, so is $\hat{P}(s)$ provided $P(1) \neq 0$. Now apply the bilinear transformation to the polynomials $\delta_0(z)$, $\delta_1(z)$ and $\delta_2(z)$ to get $\hat{\delta}_0(s)$, $\hat{\delta}_1(s)$ and $\hat{\delta}_2(s)$, where $\hat{\delta}_0(s) = \hat{\delta}_1(s) - \hat{\delta}_2(s)$. The proof consists of showing that under the

assumption that $\delta_0(z)$ is of the form given in (2.165), $\hat{\delta}_0(s)$, $\hat{\delta}_1(s)$, and $\hat{\delta}_2(s)$ satisfy the conditions of the Vertex Lemma for the Hurwitz case. Since $\delta_1(1)$ and $\delta_2(1)$ are of the same sign, $\delta_\lambda(1) = \lambda\delta_1(1) + (1-\lambda)\delta_2(1) \neq 0$ for $\lambda \in [0,1]$. This in turn implies that $\hat{\delta}_\lambda(s)$ is of degree n for all $\lambda \in [0,1]$. A straightforward calculation shows that

$$\hat{\delta}_0(s) = \hat{A}(s)2^{t_1}(2s)^{t_2}(cs+d)\hat{P}(s)$$

which is precisely the form required in the Vertex Lemma for the Hurwitz case. Thus, the segment $\hat{\delta}_\lambda(s)$ cannot have a $j\omega$ root and the segment $\delta_\lambda(z)$ cannot have a root on the unit circle. Therefore, Schur stability of $\delta_1(z)$ and $\delta_2(z)$ guarantees that of the segment. ♣

2.7 EXERCISES

2.1 Consider the standard unity feedback control system given in Figure 2.16

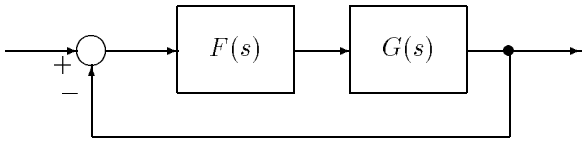

Figure 2.16. A unity feedback system

where

$$G(s) := \frac{s+1}{s^2(s+p)}, \qquad F(s) = \frac{(s-1)}{s(s+3)(s^2-2s+1.25)}$$

and the parameter p varies in the interval $[1,5]$.

a) Verify the robust stability of the closed loop system. Is the Vertex Lemma applicable to this problem?

b) Verify your answer by the s-plane root locus (or Routh-Hurwitz criteria).

2.2 Rework the problem in Exercise 2.1 by transforming via the bilinear transformation to the z plane, and using the Schur version of the Segment or Vertex Lemma. Verify your answer by the z-plane root locus (or Jury's test).

2.3 The closed loop characteristic polynomial of a missile of mass M flying at constant speed is:

$$\delta(s) = \left(-83,200 + 108,110K - 9,909.6K\frac{1}{M}\right.$$

$$+\left(-3,328+10,208.2K+167.6\frac{1}{M}\right)s$$
$$+\left(-1,547.79K\frac{1}{M}+1,548-877.179K+6.704\frac{1}{M}-2.52497K\frac{1}{M}\right)s^2$$
$$+\left(64-24.1048K+0.10475\frac{1}{M}\right)s^3+s^4.$$

where the nominal value of M, $M^0=1$. Find the range of K for robust stability if $\frac{1}{M}\in[1,4]$.
Answer: $K=[-0.8,1.2]$.

2.4 For the feedback system shown in Figure 2.17

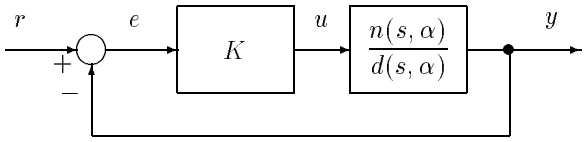

Figure 2.17. Feedback control system

where

$$n(s,\alpha)=s^2+(3-\alpha)s+1$$
$$d(s,\alpha)=s^3+(4+\alpha)s^2+6s+4+\alpha.$$

Partition the (K,α) plane into stable and unstable regions. Show that the stable region is bounded by

$$5+K(3-\alpha)>0$$

and

$$K+\alpha+4>0.$$

2.5 Consider the feedback system shown in Figure 2.18.

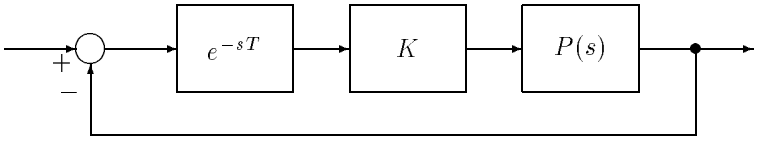

Figure 2.18. Feedback control system

Let

$$P(s) = \frac{n(s)}{d(s)} = \frac{6s^3 + 18s^2 + 30s + 25}{s^4 + 6s^3 + 18s^2 + 30s + 25}.$$

Determine the robust stability of the system for $T = 0.1$sec with $0 < K < 1$.
Hint: Check that

$$P_0(s) = d(s) \quad \text{and} \quad P_1(s) = d(s) + e^{-sT} n(s)$$

are stable and the plot $\dfrac{P_0(j\omega)}{P_1(j\omega)}$ does not cut the negative real axis.

2.6 Consider the system given in Figure 2.19

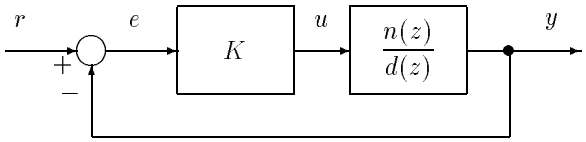

Figure 2.19. Feedback control system

and let

$$n(z) = \left(z - \frac{1+j}{4}\right)\left(z - \frac{1-j}{4}\right)\left(z + \frac{1}{2}\right)$$
$$d(z) = \left(z + \frac{3}{4}\right)\left(z - \frac{1}{2}\right)\left(z - \frac{-j-1}{2}\right)\left(z - \frac{j-1}{2}\right).$$

Find the range of stabilizing K using the Schur Segment Lemma.
Answer: $K < -1.53$ and $K > -0.59$

2.7 Show that $\delta_0(s)$ given in (2.160) is a convex direction.

2.8 Show that the following polynomials are convex directions.

a) $\delta_0(s) = (s - r_1)(s + r_2)(s - r_3)(s + r_4)\cdots(s + (-1)^m r_m)$

where $0 < r_1 < r_2 < r_3 < \cdots < r_m$.

b) $\delta_0(s) = (s + r_1)(s - r_2)(s + r_3)(s - r_4)\cdots(s - (-1)^m r_m)$

where $0 \le r_1 \le r_2 \le r_3 \le \cdots \le r_m$.

2.9 Is the following polynomial a convex direction?

$$\delta_0(s) = s^4 - 2s^3 - 13s^2 + 14s + 24$$

2.10 Consider the two Schur polynomials:

$$P_1(z) = z^4 + 2.5z^3 + 2.56z^2 + 1.31z + 0.28$$
$$P_2(z) = z^4 + 0.2z^3 + 0.17z^2 + 0.052z + 0.0136$$

Check the Schur stability of the segment joining these two polynomials by using:

a) Schur Segment Lemma 1

b) Schur Segment Lemma 2

c) Schur Segment Lemma 3

d) Bounded Phase Lemma

2.11 Consider the feedback control system shown in Figure 2.20

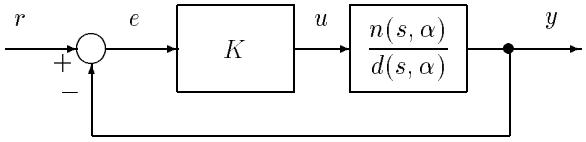

Figure 2.20. Feedback control system

where

$$n(s,\alpha) = s + \alpha$$
$$d(s,\alpha) = s^2 + (2\alpha)s^2 + \alpha s - 1$$

and $\alpha \in [2, 3]$. Partition the K axis into robustly stabilizing and nonstabilizing regions.
Answer: Stabilizing for $K \in (-4.5, 0.33)$ only.

2.12 Repeat Exercise 2.11 when there is a time delay of 1sec. in the feedback loop.

2.13 Consider a feedback system with plant transfer function $G(s)$ and controller transfer function $C(s)$:

$$G(s) = \frac{N(s)}{D(s)} \quad C(s) = K. \tag{2.166}$$

Show that if $N(s)$ is a convex direction there exists at most one segment of stabilizing gains K.

2.14 Prove that $\delta_0(s)$ given in the Vertex Lemma (2.160) is a real convex direction.

2.15 Carry out the construction of the polynomial $\delta_k(s)$ required in the proof of Lemma 2.12 for the angle θ lying in the second, third and fourth quadrants.

2.8 NOTES AND REFERENCES

The Segment Lemma for the Hurwitz case was derived by Chapellat and Bhattacharyya [57]. An alternative result on segment stability involving the Hurwitz matrix has been given by Bialas [39]. Bose [46] has given analytical tests for the Hurwitz and Schur stability of convex combinations of polynomials. The Convex Direction Lemmas for the real and complex cases and Lemma 2.12 are due to Rantzer [195]. The Schur Segment Lemma 1 (Lemma 2.5) is due to Zeheb [246] and Schur Segment Lemma 2 (Lemma 2.6) and Schur Segment Lemma 3 (Lemma 2.7) are due to Tin [224]. The results leading up to the Vertex Lemma were developed by various researchers: the monotonic phase properties given in Lemmas 2.10 and 2.11 are due to Mansour and Kraus [173]. An alternative proof of Lemma 2.9 is given in Mansour [169]. In Bose [47] monotonicity results for Hurwitz polynomials are derived from the point of view of reactance functions and it is stated that Theorem 2.1 follows from Tellegen's Theorem in network theory. The direct proof of Theorem 2.1 given here as well as the proofs of the auxiliary Lemmas in Section 4 are due to Keel and Bhattacharyya [136]. Lemma 2.17 is due to Hollot and Yang [119] who first proved the vertex property of first order compensators. Mansour and Kraus gave an independent proof of the same lemma [173], and Peterson [189] dealt with the antiHurwitz case. The unified proof of the Vertex Lemma given here, based on Lemma 2.13 was first reported in Bhattacharyya [31] and Bhattacharyya and Keel [32]. The vertex result given in Exercise 2.8 was proved by Kang [129] using the alternating Hurwitz minor conditions. The polynomial used in Exercise 2.9 is taken from Barmish [12]. Vertex results for quasipolynomials have been developed by Kharitonov and Zhabko [147].

Chapter 3

THE STABILITY BALL IN COEFFICIENT SPACE

In this chapter we develop procedures to determine maximal stability regions in the space of coefficients of a polynomial. The central idea used is the Boundary Crossing Theorem and its alternative version the Zero Exclusion Theorem of Chapter 1. We begin by calculating the largest ℓ_2 stability ball centered at a given point in the space of coefficients of a polynomial. Explicit formulas are developed for the Schur and Hurwitz cases by applying the Orthogonal Projection Theorem. Following this, we present the graphical approach of Tsypkin and Polyak to calculate the largest ℓ_p stability ball, in coefficient space, for arbitrary p. Then we deal with the robust Hurwitz and Schur stability of a family of disc polynomials, namely complex polynomials whose coefficients lie in prescribed discs in the complex plane.

3.1 INTRODUCTION

In considering robust stability with respect to parametric uncertainty, one is naturally led to formulate the following problem: Given a stability region in the complex plane and a nominal stable polynomial, find the largest region of a prescribed shape in the coefficient space around the nominal polynomial where the stability property is maintained. In this chapter we present some neat solutions for the left half plane (Hurwitz stability) and the unit circle (Schur stability) considering both real and complex coefficients. Our development, however, will clearly show that a general answer can be formulated by invoking the Boundary Crossing Theorem of Chapter 1, at least when the region of interest can be associated with a norm. This will always be assumed in this chapter. We remark that Kharitonov's Theorem (Chapter 5) deals essentially with a special case of this problem when the stability region is the left-half plane and the coefficient uncertainty is interval. We start by calculating the largest ℓ_2 stability ball in the space of coefficients of a real polynomial, treating both Hurwitz and Schur stability.

3.2 THE BALL OF STABLE POLYNOMIALS

Recall the Boundary Crossing Theorem of Chapter 1. Let the stability region $\mathcal{S}$ be any given open set of the complex plane C, $\partial\mathcal{S}$ its boundary, and $\mathcal{U}^o$ the interior of the closed set $\mathcal{U} = C - \mathcal{S}$. Assume that these three sets $\mathcal{S}$, $\partial\mathcal{S}$, and $\mathcal{U}^o$ are nonempty. For any given n, the set $\mathcal{P}_n$ of real polynomials of degree less than or equal to n is a vector space of dimension $n+1$ and as usual we identify this with $\mathbb{R}^{n+1}$ to which it is isomorphic. Let $\|\cdot\|$ be an arbitrary norm defined on $\mathcal{P}_n$. The *open balls* induced by this norm are of the form,

$$B(P_o(s), r) = \{P(s) \in \mathcal{P}_n \ : \ \|P(s) - P_o(s)\| < r\}. \tag{3.1}$$

With such an open ball is associated the *hypersphere*,

$$S(P_o(s), r) = \{P(s) \in \mathcal{P}_n \ : \ \|P(s) - P_o(s)\| = r\}, \tag{3.2}$$

which is just the boundary of $B(P_o(s), r)$. Now, as mentioned in Chapter 1, the subset of $\mathcal{P}_n$ consisting of all polynomials $\delta(s)$ which are of degree n and which have all their roots in $\mathcal{S}$ is an open set. As a direct consequence, given a polynomial $\delta(s)$ of degree n with all its roots contained in $\mathcal{S}$, there exists a positive real number ϵ such that every polynomial contained in $B(\delta(s), \epsilon)$ is of degree n and has all its roots in $\mathcal{S}$. In other words, letting $d^o(\cdot)$ denote the degree of a polynomial, we have that ϵ satisfies the following property:

Property 3.1.

$$\|\beta(s) - \delta(s)\| < \epsilon \implies \begin{cases} d^o(\beta(s)) = n \\ \beta(s) \quad \text{has all its roots in } \mathcal{S}. \end{cases}$$

As in the proof of the Boundary Crossing Theorem, it is then possible to consider, for the given stable polynomial $\delta(s)$, the subset of all positive real numbers having the Property 3.1:

$$R_\delta := \{t \ : \ t > 0, \ t \text{ satisfies Property 3.1}\}.$$

We have just seen that R_δ is not empty. But obviously the elements of R_δ satisfy

$$t_2 \in R_\delta \ \text{ and } \ 0 < t_1 < t_2 \Longrightarrow t_1 \in R_\delta.$$

Therefore R_δ is in fact an interval

$$(0, \rho(\delta)] \qquad \text{where: } \rho(\delta) = \sup_{t \in R_\delta} t.$$

Clearly, $\rho(\delta)$ has to be finite and $\rho(\delta)$ also satisfies Property 3.1 (that is why we closed the interval on the right). We have just proved the existence and uniqueness of a real number $\rho(\delta)$ characterized by :

1. $\rho(\delta)$ satisfies Property 3.1.

2. No real r greater than $\rho(\delta)$ satisfies Property 3.1.

We now give a precise characterization of $\rho(\delta)$.

Theorem 3.1 *Given a polynomial $\delta(s)$, of degree n, having all its roots in $\mathcal{S}$, there exists a positive real number $\rho(\delta)$ such that:*

a) Every polynomial contained in $B(\delta(s), \rho(\delta))$ has all its roots in $\mathcal{S}$ and is of degree n.

b) At least one polynomial on the hypersphere $S(\delta(s), \rho(\delta))$ has one of its roots in $\partial\mathcal{S}$ or is of degree less than n.

c) However, no polynomial lying on the hypersphere (even those of degree $< n$) can ever have a root in $\mathcal{U}^o$.

Proof. Clearly a) is true since $\rho(\delta)$ satisfies Property 3.1. We now prove b) and c). Since no real r greater than $\rho(\delta)$ satisfies Property 3.1, then for every $n \geq 1$ there exists a polynomial of degree less than n or with a root in $\mathcal{U} = C - \mathcal{S}$, say $\gamma_n(s)$, contained in the ball $\mathcal{B}(\delta(s), \rho(\delta) + \frac{1}{n})$. Being contained in the closure of $B(\delta(s), \rho(\delta) + 1)$ which is a compact set, this sequence must then contain a convergent subsequence $\gamma_{\phi(n)}(s)$. Let $\gamma(s)$ be its limit. Then $\gamma(s)$ is necessarily lying on the hypersphere $S(\delta(s), \rho(\delta))$, and it is also necessarily of degree less than n or with a root in $\mathcal{U}$; otherwise the existence of $\rho(\gamma)$ would contradict the fact that $\gamma(s)$ is the limit of a sequence of polynomials of degree less than n or with a root in $\mathcal{U}$.

To proceed, we need to invoke Rouché's Theorem (Theorem 1.2, Chapter 1). Suppose that there is a polynomial lying on $S(\delta(s), \rho(\delta))$ say $\gamma(s)$, which is of degree n but has at least one root s_k in $\mathcal{U}^o$. A consequence is that the set of polynomials of degree n with at least one root in the open set $\mathcal{U}^o$ is itself open. Thus it would be possible to find a ball of radius $\epsilon > 0$ around $\gamma(s)$ containing only polynomials of degree n and with at least one root in $\mathcal{U}^o$. This would then result in a contradiction because since $\gamma(s)$ lies on the hypersphere $\mathcal{S}(\delta(s), \rho(\delta))$, the intersection

$$B(\gamma(s), \epsilon) \cap B(\delta(s), \rho(\delta))$$

is certainly nonempty.

On the other hand suppose that this polynomial $\gamma(s)$ with at least one root in $\mathcal{U}^o$ is of degree less than n. For $\epsilon > 0$ consider the polynomial,

$$\gamma_\epsilon(s) = \epsilon\delta(s) + (1 - \epsilon)\gamma(s).$$

It is clear that $\gamma_\epsilon(s)$ is always of degree n and is inside $B(\delta(s), \rho(\delta))$ since

$$\|\delta(s) - \gamma_\epsilon(s)\| = (1 - \epsilon)\|\delta(s) - \gamma(s)\| < \rho(\delta).$$

This means that $\gamma_\epsilon(s)$ has all its roots in $\mathcal{S}$.Now, a straightforward application of Rouché's theorem shows that for ϵ small enough $\gamma_\epsilon(s)$ also has at least one root in $\mathcal{U}^o$, and this is again a contradiction. ♣

Of course, this result can be applied to a number of situations depending on the region $\mathcal{S}$ of interest and on the norm $\|\cdot\|$ chosen on $\mathcal{P}_n$. Below we consider the two cases of Hurwitz and Schur stability with the Euclidean norm. In both these cases a neat expression can be given for the corresponding $\rho(\delta)$.

3.3 THE REAL ℓ_2 STABILITY BALL

On $\mathcal{P}_n$, the usual inner product and the associated Euclidean norm are defined as follows. If

$$P(s) = p_0 + p_1 s + \cdots + p_n s^n,$$

and

$$R(s) = r_0 + r_1 s + \cdots + r_n s^n,$$

then the inner product of $P(s)$ and $R(s)$ is given by

$$< P(s), R(s) >= p_0 r_0 + p_1 r_1 + \cdots + p_n r_n = \sum_{i=0}^{n} p_i r_i.$$

The Euclidean norm of a polynomial $P(s)$ is then:

$$\|P(s)\|_2^2 =< P(s), P(s) >= p_0^2 + p_1^2 + \cdots + p_n^2.$$

We can now look at the left-half plane case.

3.3.1 Hurwitz Stability

For this case we first have to introduce some subspaces of $\mathcal{P}_n$. Let Δ_0 be the subset of all elements $P(s)$ of $\mathcal{P}_n$ such that

$$P(0) = 0.$$

Δ_0 is a subspace of dimension n generated by the basis vectors

$$s, s^2, s^3, \cdots, s^{n-1}, s^n.$$

Dually, let Δ_n be the subset of all elements $P(s)$ of $\mathcal{P}_n$ that are of degree less than n, that is such that $p_n = 0$. Δ_n is also a subspace of dimension n, generated by the basis vectors

$$1, s, s^2, \cdots, s^{n-2}, s^{n-1}.$$

Finally, for each real $\omega \geq 0$, we can consider the subset Δ_ω of all elements of $\mathcal{P}_n$ which are divisible by $s^2 + \omega^2$. Equivalently, Δ_ω is the set of all elements of $\mathcal{P}_n$ that have $+j\omega$ and $-j\omega$ among their roots. Δ_ω is also a subspace. It is of dimension $n-1$ and is generated by the basis vectors

$$s^2 + \omega^2, s^3 + \omega^2 s, \cdots, s^{n-1} + \omega^2 s^{n-3}, s^n + \omega^2 s^{n-2}.$$

It is to be noted however that the Δ_ω's are only defined when $n \geq 2$; we will assume this in what follows, but will explain what happens when $n < 2$.

Now, since $(\mathcal{P}_n, \|\cdot\|_2)$ is a Euclidean vector space, it is possible to apply the Projection Theorem. For any element $P(s)$ of $\mathcal{P}_n$, and for any subspace $\mathcal{V}$, there is a unique vector $\pi_P(s)$ in $\mathcal{V}$ at which the distance between $P(s)$ and all elements of $\mathcal{V}$ is minimized; $\pi_P(s)$ is nothing but the orthogonal projection of $P(s)$ on $\mathcal{V}$, and $\|P(s) - \pi_P(s)\|$ is called the *distance* from $P(s)$ to the subspace $\mathcal{V}$. Given then a Hurwitz stable polynomial

$$\delta(s) = \delta_0 + \delta_1 s + \delta_2 s^2 + \cdots + \delta_n s^n,$$

we let d_0, d_n, and d_ω denote the distances from $\delta(s)$ to the subspaces Δ_0, Δ_n, and Δ_ω respectively. Finally let us define

$$d_{\min} := \inf_{\omega \geq 0} d_\omega.$$

Applying Theorem 3.1 here tells us that the radius $\rho(\delta)$ of the largest stability hypersphere around $\delta(s)$ is characterized by the fact that every polynomial in $B(\delta(s),\rho(\delta))$ is stable and of degree n whereas at least one polynomial on the hypersphere $S(\delta(s),\rho(\delta))$ is of degree less than n or has a root on the imaginary axis. In fact we have the following result.

Theorem 3.2 *The radius of the largest stability hypersphere around a stable polynomial $\delta(s)$ is given by*

$$\rho(\delta) = \min(d_0, d_n, d_{\min}) \tag{3.3}$$

Proof. Let

$$r = \min(d_o, d_n, d_{\min}).$$

Clearly the open ball $B(\delta(s), r)$ centered at $\delta(s)$ and of radius r cannot contain any polynomial having a root which is 0 or purely imaginary or any polynomial of degree less than n. From our characterization of the stability hypersphere given in Theorem 3.1 above we deduce that $\rho(\delta) \geq r$ necessarily. On the other hand from the definition of r we can see that any ball centered at $\delta(s)$ and of radius greater than r must contain at least one unstable polynomial or a polynomial of degree less than n. Thus, necessarily again, $\rho(\delta) \leq r$. As a consequence we get that

$$\rho(\delta) = r = \min(d_o, d_n, d_{\min}).$$

♣

In (3.3) it is very easy to prove that

$$d_0 = |\delta_0|, \quad \text{and} \quad d_n = |\delta_n|.$$

The main problem then is to compute $d_{\min}$. In the following we will show how d_ω can be obtained in closed-form for any degree n. We will then show how

$d_{\min} = \inf_{\omega \geq 0} d_\omega$ can also be computed very easily by carrying out two similar minimizations over the finite range $[0, 1]$. Therefore let $\delta(s)$ be an arbitrary stable polynomial of degree n. As usual separate $\delta(s)$ into odd and even parts:

$$\delta(s) = \delta_0 + \delta_1 s + \cdots + \delta_n s^n = \underbrace{\delta^{\text{even}}(s)}_{\text{even degree terms}} + \underbrace{\delta^{\text{odd}}(s)}_{\text{odd degree terms}} .$$

Theorem 3.3 *The distance d_ω between $\delta(s)$ and Δ_ω is given by:*

i) $n = 2p$:

$$d_\omega^2 = \frac{[\delta^e(\omega)]^2}{1 + \omega^4 + \cdots + \omega^{4p}} + \frac{[\delta^o(\omega)]^2}{1 + \omega^4 + \cdots + \omega^{4(p-1)}}. \tag{3.4}$$

ii) $n = 2p + 1$:

$$d_\omega^2 = \frac{[\delta^e(\omega)]^2 + [\delta^o(\omega)]^2}{1 + \omega^4 + \cdots + \omega^{4p}}. \tag{3.5}$$

Proof. We know that $\mathcal{P}_n$ is a vector space of dimension $n + 1$. Δ_ω on the other hand is of dimension $n - 1$ and is generated by the following elements:

$$s^2 + \omega^2, s^3 + \omega^2 s, s^4 + \omega^2 s^2, \cdots, s^n + \omega^2 s^{n-2}. \tag{3.6}$$

Therefore $\Delta_\omega^\perp$ is of dimension 2. Let $p_1(s)$ and $p_2(s)$ be an orthogonal basis for $\Delta_\omega^\perp$. Let $v_\delta^\omega(s)$ denote the orthogonal projection of $\delta(s)$ on Δ_ω. By definition of the orthogonal projection, $\delta - v_\delta^\omega$ is an element of $\Delta_\omega^\perp$ and we can write

$$\delta - v_\delta^\omega = \alpha_1 p_1 + \alpha_2 p_2. \tag{3.7}$$

Taking the inner product of both members of (3.7) with $p_1(s)$ and $p_2(s)$ successively and remembering that $p_1(s)$ and $p_2(s)$ are orthogonal to each other as well as to any element of Δ_ω, we get

$$\alpha_1 = \frac{< \delta, p_1 >}{\|p_1\|^2} \qquad \text{and} \qquad \alpha_2 = \frac{< \delta, p_2 >}{\|p_2\|^2}. \tag{3.8}$$

But the definition of the orthogonal projection also implies that

$$d_\omega^2 = \|\delta - v_\delta^\omega\|^2. \tag{3.9}$$

Thus,combining (3.7), (3.8), (3.9) and again taking into account the fact that $p_1(s)$ and $p_2(s)$ are chosen to be orthogonal, we get

$$d_\omega^2 = \frac{< \delta, p_1 >^2}{\|p_1\|^2} + \frac{< \delta, p_2 >^2}{\|p_2\|^2}. \tag{3.10}$$

It just remains for us to find $p_1(s)$ and $p_2(s)$.

i) $n = 2p$: In this case we can choose

$$p_1(s) = 1 - \omega^2 s^2 + \omega^4 s^4 + \cdots + (-1)^p \omega^{2p} s^{2p},$$
$$p_2(s) = s - \omega^2 s^3 + \omega^4 s^5 + \cdots + (-1)^{(p-1)} \omega^{2(p-1)} s^{2p-1}.$$

One can check very easily that $p_1(s)$ and $p_2(s)$ are orthogonal to each element of (3.6) and also orthogonal to each other. Moreover they satisfy

$$< p_1, \delta > = \delta^e(\omega)$$
$$< p_2, \delta > = \delta^o(\omega)$$

and

$$\|p_1\|^2 = 1 + \omega^4 + \omega^8 + \cdots + \omega^{4p}$$
$$\|p_2\|^2 = 1 + \omega^4 + \omega^8 + \cdots + \omega^{4(p-1)}.$$

The expression in (3.4) for d_ω^2 then follows from (3.10) and the properties above.

ii) $n = 2p + 1$: In this case $p_1(s)$ remains unchanged but $p_2(s)$ becomes

$$p_2(s) = s - \omega^2 s^3 + \omega^4 s^5 + \cdots + (-1)^{(p-1)} \omega^{2(p-1)} s^{2p-1} + (-1)^p \omega^{2p} s^{2p+1}.$$

$p_1(s)$ and $p_2(s)$ have then the same properties as when n is even except that

$$\|p_1\|^2 = \|p_2\|^2 = 1 + \omega^4 + \omega^8 + \cdots + \omega^{4p}$$

and therefore we have the expression in (3.5) for d_ω^2 when n is odd. Moreover, the formula in (3.7) tells us exactly what the projection $v_\delta^\omega(s)$ is:

$$v_\delta^\omega(s) = \delta(s) - \alpha_1 p_1(s) - \alpha_2 p_2(s).$$

♣

Having this expression for d_ω, the next step is to find:

$$d_{\min} = \inf_{\omega \geq 0} d_\omega.$$

A simple manipulation will show that there is no need to carry out a minimization over the infinite range $[0, \infty)$. We will consider the case when $n = 2p$, but a similar derivation holds if n is odd.

First it is clear that

$$d_{\min}^2 = \min\left(\inf_{\omega \in [0,1]} d_\omega^2, \inf_{\omega \in [0,1]} d_{\frac{1}{\omega}}^2 \right).$$

We have

$$|\delta^e(\omega)|^2 = \left(\delta_0 - \delta_2 \omega^2 + \delta_4 \omega^4 + \cdots + (-1)^p \delta_{2p} \omega^{2p}\right)^2$$
$$|\delta^o(\omega)|^2 = \left(\delta_1 - \delta_3 \omega^2 + \delta_5 \omega^4 + \cdots + (-1)^{p-1} \delta_{2p-1} \omega^{2p-2}\right)^2$$

which yields:

$$\left|\delta^e\left(\frac{1}{\omega}\right)\right|^2 = \frac{1}{\omega^{4p}}\left[\delta_{2p} - \delta_{2p-2}\omega^2 + \delta_{2p-4}\omega^4 + \cdots + (-1)^p\delta_0\omega^{2p}\right]^2$$
$$\left|\delta^o\left(\frac{1}{\omega}\right)\right|^2 = \frac{1}{\omega^{4(p-1)}}\left[\delta_{2p-1} - \delta_{2p-3}\omega^2 + \delta_{2p-5}\omega^4 + \cdots + (-1)^{p-1}\delta_1\omega^{2p-2}\right]^2.$$

Now

$$d^2_{\frac{1}{\omega}} = \frac{\frac{1}{\omega^{4p}}\left[\delta_{2p} - \delta_{2p-2}\omega^2 + \delta_{2p-4}\omega^4 + \cdots + (-1)^p\delta_0\omega^{2p}\right]^2}{1 + \frac{1}{\omega^4} + \frac{1}{\omega^8} + \cdots + \frac{1}{\omega^{4p}}} + \frac{\frac{1}{\omega^{4(p-1)}}\left[\delta_{2p-1} - \delta_{2p-3}\omega^2 + \delta_{2p-5}\omega^4 + \cdots + (-1)^{p-1}\delta_1\omega^{2p-2}\right]^2}{1 + \frac{1}{\omega^4} + \frac{1}{\omega^8} + \cdots + \frac{1}{\omega^{4(p-1)}}}.$$

This last expression however is nothing but:

$$d^2_{\frac{1}{\omega}} = \frac{\left[\delta_{2p} - \delta_{2p-2}\omega^2 + \delta_{2p-4}\omega^4 + \cdots + (-1)^p\delta_0\omega^{2p}\right]^2}{1 + \omega^4 + \omega^8 + \cdots + \omega^{4p}} + \frac{\left[\delta_{2p-1} - \delta_{2p-3}\omega^2 + \delta_{2p-5}\omega^4 + \cdots + (-1)^{p-1}\delta_1\omega^{2p-2}\right]^2}{1 + \omega^4 + \omega^8 + \cdots + \omega^{4(p-1)}}$$

and we can see that $d^2_{\frac{1}{\omega}}$ has exactly the same structure as d^2_ω.

Can $d^2_{\frac{1}{\omega}}$ be considered as the "d^2_ω" of some other polynomial? The answer is yes. Consider $\delta'(s) = s^n\delta\left(\frac{1}{s}\right)$, the "reverse" polynomial which in our case is

$$\delta'(s) = s^{2p}\delta\left(\frac{1}{s}\right) = \delta_{2p} + \delta_{2p-1}s + \delta_{2p-2}s^2 + \cdots + \delta_2 s^{2p-2} + \delta_1 s^{2p-1} + \delta_0 s^{2p}.$$

Then

$$\delta'^e(\omega) = \delta'_{\text{even}}(j\omega) = \delta_{2p} - \delta_{2p-2}\omega^2 + \delta_{2p-4}\omega^4 + \cdots + (-1)^p\delta_0\omega^{2p}$$
$$\delta'^o(\omega) = \frac{\delta'_{\text{odd}}(j\omega)}{j\omega} = \delta_{2p-1} - \delta_{2p-3}\omega^2 + \delta_{2p-5}\omega^4 + \cdots + (-1)^{p-1}\delta_1\omega^{2p-2}.$$

Thus we see that in fact $d^2_{\frac{1}{\omega}}$ corresponds to d^2_ω computed for $\delta'(s)$. Suppose now that you have a subroutine DMIN ($\underline{\delta}$) that takes the vector of coefficients $\underline{\delta}$ as input and returns the minimum of d^2_ω over [0, 1]. Then the following algorithm will compute $d_{\min}$ by simply calling DMIN two times:

1. Set $\underline{\delta} = (\delta_0, \delta_1, \cdots, \delta_n)$.
2. First call: $d_1 = \text{DMIN}(\underline{\delta})$.

3. Switch: set $\underline{\delta} = (\delta_n, \delta_{n-1}, \cdots, \delta_0)$.

4. Second call: $d_2 = \mathrm{DMIN}(\underline{\delta})$.

5. $d_{\min} = \min(d_1, d_2)$.

Moreover, d_ω^2 as given in (3.4) or (3.5) is a rational function of relative degree 0 with no real poles and therefore is extremely well behaved in $[0, 1]$. As a consequence the subroutine $DMIN$ is not particularly hard to implement.

Incidentally, we already knew that the two polynomials $\delta(s)$ and $\delta'(s) = s^n \delta\left(\frac{1}{s}\right)$ are stable together (i.e. one is stable if and only if the other one is stable). The development above tells us that moreover $\rho(\delta) = \rho(\delta')$.

In the case when $n = 1$, then the subspaces Δ_ω are not defined. However, if we apply the formula in (3.5) anyway, we find that

$$d_\omega^2 = \delta_0^2 + \delta_1^2, \quad \forall\ \omega \geq 0. \tag{3.11}$$

Therefore, $d_{\min}$ itself is given by the same expression, and when we compute $\rho(\delta)$, we find

$$[\rho(\delta)]^2 = \min(\delta_0^2, \delta_1^2, \delta_0^2 + \delta_1^2) = \min(\delta_0^2, \delta_1^2).$$

Thus even if we apply our formula for $n = 1$ we get the correct answer for $\rho(\delta)$. The same argument holds in the trivial case $n = 0$.

The Monic Case

In some applications it can happen that the leading coefficient is fixed and not subject to perturbation. Consider the situation where we are given a stable *monic* polynomial

$$\beta(s) = \beta_0 + \beta_1 s + \cdots + \beta_{n-1} s^{n-1} + s^n$$

and we want to find the closest *monic* polynomial with a root at $j\omega$. For convenience, the general distance d_ω that we computed in Theorem 3.2 will now be denoted $d_\omega^n[\delta(s)]$, to stress the fact that it applies to the polynomial $\delta(s)$ which is of degree n. Along the same lines, the distance for a monic polynomial of degree n will be denoted by $\bar{d}_\omega^n[\beta(s)]$. We then have the following result.

Theorem 3.4 *The distance $\bar{d}_\omega^n[\beta(s)]$ from the monic polynomial of degree n to the affine subspace of all monic polynomials with a root at $j\omega$ is given by*

$$\bar{d}_\omega^n[\beta(s)] = d_\omega^{n-1}[\beta(s) - s^n - \omega^2 s^{n-2}].$$

Proof. We know that Δ_ω is a vector space of dimension $n-1$ generated by the basis

$$s^2 + \omega^2, s^3 + \omega^2 s, \cdots, s^n + \omega^2 s^{n-2}.$$

The generic element of Δ_ω can be written as the linear combination

$$\lambda_1(s^2 + \omega^2) + \lambda_2(s^3 + \omega^2 s) + \cdots + \lambda_{n-1}(s^n + \omega^2 s^{n-2}).$$

Now, the generic monic polynomial of Δ_ω must satisfy $\lambda_{n-1} = 1$ and therefore can be written as,

$$\lambda_1(s^2+\omega^2) + \lambda_2(s^3+\omega^2 s) + \cdots + (s^n + \omega^2 s^{n-2}).$$

As a consequence, the distance that we are looking for can be expressed as

$$\bar{d}_\omega^n[\beta(s)] =$$

$$\inf_{\lambda_1,\lambda_2,\cdots,\lambda_{n-2}} \|\beta(s) - \lambda_1(s^2+\omega^2) - \lambda_2(s^3+\omega^2 s) - \cdots - (s^n + \omega^2 s^{n-2})\|.$$

But this can be rewritten as

$$d_\omega^{n\,\prime}[\beta(s)] =$$

$$\inf_{\lambda_1,\lambda_2,\cdots,\lambda_{n-2}} \|(\beta(s) - s^n - \omega^2 s^{n-2}) - \lambda_1(s^2+\omega^2) - \cdots - \lambda_{n-2}(s^{n-1} + \omega^2 s^{n-3})\|.$$

But since $\beta(s) - s^n - \omega^2 s^{n-2}$ is a polynomial of degree less than or equal to $n-1$, this last infimum is nothing but

$$d_\omega^{n-1}[\beta(s) - s^n - \omega^2 s^{n-2}].$$

♣

An example of the above calculation follows.

Example 3.1. Consider the Hurwitz polynomial

$$\delta(s) := 6 + 49s + 155s^2 + 280s^3 + 331s^4 + 266s^5 + 145s^6 + 52s^7 + 11s^8 + s^9.$$

and the problem of calculating $\rho(\delta)$ for it.

All coefficients are subject to perturbation If we assume that all coefficients of $\delta(s)$ including the leading coefficient are subject to perturbation, we need to apply Theorem 3.2 which deals with the stability margin for nonmonic polynomials. Consequently, we have

$$d_\omega^2 = \frac{[\delta^e(\omega)]^2 + [\delta^o(\omega)]^2}{1 + \omega^4 + \cdots + \omega^{4p}}$$

where $p = 4$ and

$$\delta^e(\omega) = 6 - 155\omega^2 + 331\omega^4 - 145\omega^6 + 11\omega^8$$
$$\delta^o(\omega) = 49 - 280\omega^2 + 266\omega^4 - 52\omega^6 + \omega^8.$$

In order to compute $d_{\min}$ analytically we first compute real positive ω's satisfying

$$\frac{d(d_\omega)}{d\omega} = 0.$$

With these real positive ωs we evaluate d_ω. Then we have

ω	d_ω
3.2655	1.7662
1.8793	6.8778
1.6185	6.5478
0.7492	27.7509
0.4514	13.0165

From this, we have

$$d_{\min} = \inf_{\omega \geq 0} d_\omega = 1.7662 \text{ at } \omega = 3.2655$$

$$d_0 = 6 \quad \text{and} \quad d_n = 1.$$

Therefore, $\rho(\delta) = \min(d_0, d_n, d_{\min}) = 1$. Figure 3.1 shows the plot of d_ω with respect to ω. The graphical solution agrees with the analytical solution given earlier. This means that as we blow up the stability ball, the family first loses degree, then acquires a $j\omega$ root at $\omega = 3.2655$, and subsequently a root at the origin.

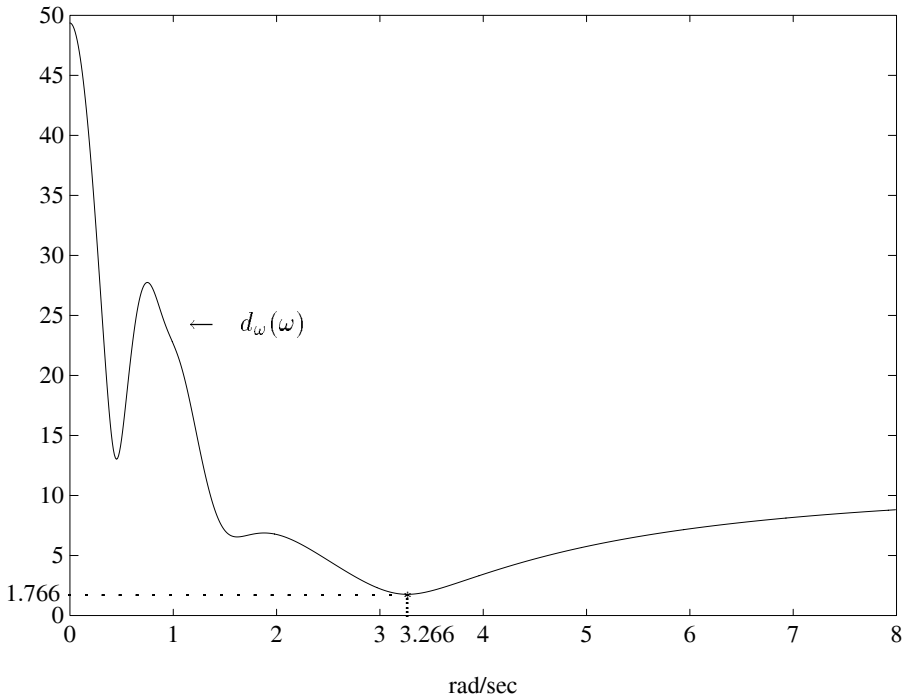

Figure 3.1. $d_\omega(\omega)$ vs. ω (all coefficients perturbing) (Example 3.1)

The leading coefficient is fixed Now let us assume that the leading coefficient of the polynomial family remains fixed at the value 1:

$$\beta(s) := 6 + 49s + 155s^2 + 280s^3 + 331s^4 + 266s^5 + 145s^6 + 52s^7 + 11s^8 + s^9.$$

Then we need to apply Theorem 3.4. We have

$$\bar{d}^n_\omega[\beta(s)]_{n=9} = d^8_\omega[\beta(s) - s^9 - \omega^2 s^7] := d^8_\omega[\alpha(s)]$$

and

$$d^2_\omega = \frac{[\alpha^e(\omega)]^2}{1 + \omega^4 + \cdots + \omega^{16}} + \frac{[\alpha^o(\omega)]^2}{1 + \omega^4 + \cdots + \omega^{12}}$$

where

$$\begin{aligned}\alpha^e(\omega) &= 6 - 155\omega^2 + 331\omega^4 - 145\omega^6 + 11\omega^8 \\ \alpha^o(\omega) &= 49 - 280\omega^2 + 266\omega^4 + (-52 + \omega^2)\omega^6 \\ &= 49 - 280\omega^2 + 266\omega^4 - 52\omega^6 + \omega^8.\end{aligned}$$

As before, we first compute real positive ω's satisfying

$$\frac{d(d_\omega)}{d\omega} = 0.$$

With these real positive ω's we evaluate d_ω. Then we have

ω	d_ω
6.7639	8.0055
3.9692	20.6671
2.0908	6.5621
0.7537	27.8492
0.4514	13.0165

From this, we have

$$d_{\min} = \inf_{\omega \geq 0} d_\omega = 6.5621 \text{ at } \omega = 2.0908.$$

Therefore, $\rho(\delta) = \min(d_0, d_{\min}) = 6$. Figure 3.2 show the plot of d_ω with respect to ω. The graphical solution agrees with the analytical solution given earlier. This means that as the family is enlarged it first acquires a root at the origin and subsequently a $j\omega$ root at $\omega = 2.0908$.

3.3.2 Schur Stability

In this section we calculate the ℓ_2 stability ball in coefficient space for Schur stability. Let $P(z)$ denote a generic real polynomial of degree n and $\mathcal{P}_n$ denote the vector space over the reals of polynomials of degree n or less. We start by introducing the

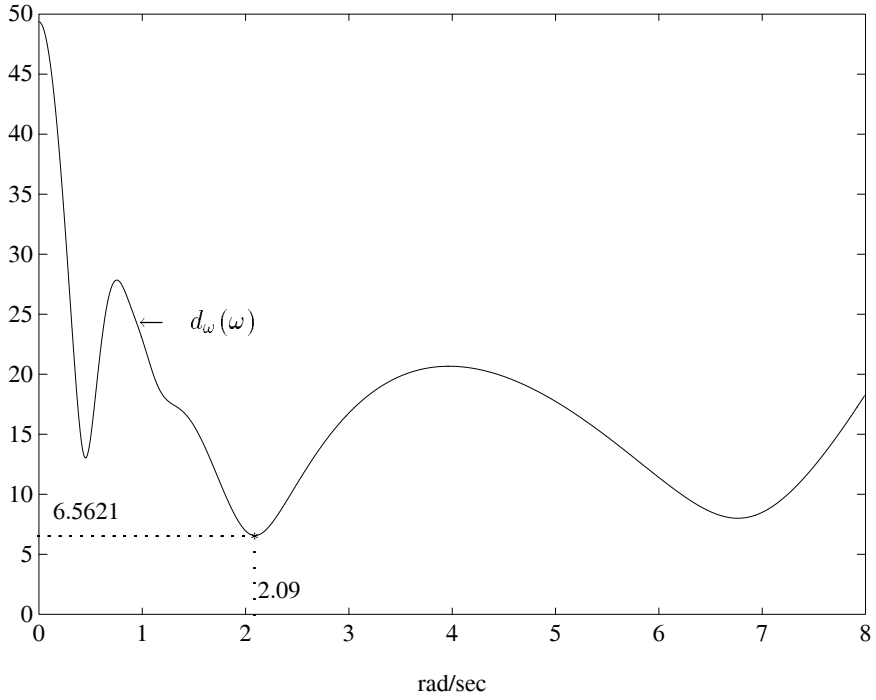

Figure 3.2. $d_\omega(\omega)$ vs. ω (leading coefficient fixed) (Example 3.1)

relevant subspaces of $\mathcal{P}_n$. Let Δ_{+1} be the subset of all elements $P(z)$ of $\mathcal{P}_n$ with a root at $z = +1$. Δ_{+1} is a subspace of dimension n and a basis for Δ_{+1} is the set

$$z-1, z(z-1), z^2(z-1), \cdots z^{n-1}(z-1).$$

It is easy to see that $\Delta_{+1}^{\perp}$ is generated by the polynomial,

$$P_{+1}(z) = 1 + z + z^2 + \cdots + z^n. \tag{3.12}$$

Let Δ_{-1} be the subset of all elements $P(z)$ of $\mathcal{P}_n$ with a root at $z = -1$. Δ_{-1} is also a subspace of dimension n and a basis is the set

$$z+1, z(z+1), z^2(z+1), \cdots z^{n-1}(z+1).$$

$\Delta_{-1}^{\perp}$ is generated by the polynomial,

$$P_{-1}(z) = 1 - z + z^2 - \cdots + (-1)^n z^n. \tag{3.13}$$

For each $0 < \theta < \pi$, we can introduce the set Δ_θ of all polynomials in $\mathcal{P}_n$ with a pair of roots at $e^{j\theta}$ and $e^{-j\theta}$. Δ_θ is also a subspace of dimension $n-1$, and a basis

for Δ_θ is given by

$$z^2 - z2\cos\theta + 1, z(z^2 - z2\cos\theta + 1), z^2(z^2 - z2\cos\theta + 1), \cdots z^{n-2}(z^2 - z2\cos\theta + 1). \tag{3.14}$$

It is easy to verify that a basis for $\Delta_\theta^\perp$ is given by:

$$q_\theta^1(z) = 1 + (\cos\theta)z + (\cos 2\theta)z^2 + \cdots + (\cos(n-1)\theta)z^{n-1} + (\cos n\theta)z^n$$
$$q_\theta^2(z) = (\sin\theta)z + (\sin 2\theta)z^2 + \cdots + (\sin(n-1)\theta)z^{n-1} + (\sin n\theta)z^n.$$

Now let

$$P(z) = p_0 + p_1 z + p_2 z^2 + \cdots + p_n z^n$$

be a real Schur polynomial of degree n. Let d_{+1}, d_{-1} and d_θ designate the distances from $P(z)$ to the subspaces Δ_{+1}, Δ_{-1}, Δ_θ, respectively, and let us define

$$d_{\min} = \inf_{0<\theta<\pi} d_\theta.$$

Just as in the continuous case we have the following theorem.

Theorem 3.5 *The radius of the largest stability hypersphere around a Schur polynomial $P(z)$ of degree n is given by:*

$$\rho(P) = \min(d_{+1}, d_{-1}, d_{\min}).$$

The distances from $P(z)$ to the subspaces Δ_{+1}, and Δ_{-1}, are respectively:

$$d_{+1} = \frac{|< P(z), P_{+1}(z) >|}{\|P_{+1}(z)\|} = \frac{|P(1)|}{\sqrt{n+1}}$$

and

$$d_{-1} = \frac{|< P(z), P_{-1}(z) >|}{\|P_{-1}(z)\|} = \frac{|P(-1)|}{\sqrt{n+1}}.$$

The distance d_θ between P(z) and the subspace Δ_θ is given by:

$$d_\theta^2 = \frac{\lambda_2^2\|q_\theta^1(z)\|^2 - 2\lambda_1\lambda_2 < q_\theta^1(z), q_\theta^2(z) > +\lambda_1^2\|q_\theta^2(z)\|^2}{\|q_\theta^1(z)\|^2\|q_\theta^2(z)\|^2 - < q_\theta^1(z), q_\theta^2(z) >^2}.$$

where

$$\lambda_1 = < q_\theta^1(z), P(z) >= \mathrm{Re}[P(e^{j\theta})]$$
$$\lambda_2 = < q_\theta^2(z), P(z) >= \mathrm{Im}[P(e^{j\theta})]$$

and,

$$\|q_\theta^1(z)\|^2 = \sum_{k=0}^{n} \cos^2 k\theta = \frac{1}{2}\left[\sum_{k=0}^{n}(1 + \cos 2k\theta)\right]$$

$$= \frac{n+1}{2} + \frac{1}{2}(\cos n\theta)\left(\frac{\sin(n+1)\theta}{\sin\theta}\right)$$

$$\|q_\theta^2(z)\|^2 = \sum_{k=0}^{n}(\sin k\theta)^2 = \frac{1}{2}\left[\sum_{k=0}^{n}(1-\cos 2k\theta)\right]$$

$$= \frac{n+1}{2} - \frac{1}{2}(\cos n\theta)\left(\frac{\sin(n+1)\theta}{\sin\theta}\right)$$

$$< q_\theta^1(z), q_\theta^2(z) > = \sum_{k=0}^{n}(\cos k\theta)(\sin k\theta) = \frac{1}{2}\left[\sum_{k=0}^{n}\sin 2k\theta\right]$$

$$= \frac{1}{2}(\sin n\theta)\left(\frac{\sin(n+1)\theta}{\sin\theta}\right).$$

Proof. The proof is exactly similar to the Hurwitz case and uses the Orthogonal Projection Theorem. We know that $\Delta_\theta^\perp$ is generated by $q_\theta^1(z)$ and $q_\theta^2(z)$. The formula that results is slightly more complicated due to the fact that $q_\theta^1(z)$ and $q_\theta^2(z)$ are not orthogonal to each other. However one can easily compute that the denominator of d_θ^2 is

$$\frac{\left[(n+1)^2 - \dfrac{\sin^2(n+1)\theta}{\sin^2\theta}\right]}{4}.$$

♣

For the discrete time case also it is of interest to consider the case of monic polynomials, and to compute the distance $\bar{d}_{+1}$, $\bar{d}_{-1}$ and $\bar{d}_\theta$ from a given monic polynomial

$$Q(z) = q_0 + q_1 z + \cdots + q_{n-1}z^{n-1} + z^n$$

to the set of all monic polynomials with a root at $z = 1$, or $z = -1$, or a pair of roots at $e^{j\theta}$, $e^{-j\theta}$ respectively. We have the following theorem.

Theorem 3.6 *The distances $\bar{d}_{+1}$, $\bar{d}_{-1}$ and $\bar{d}_\theta^n[Q(z)]$ are given by,*

$$\bar{d}_{+1} = \frac{|Q(1)|}{\sqrt{n}}$$

$$\bar{d}_{-1} = \frac{|Q(-1)|}{\sqrt{n}}$$

$$\bar{d}_\theta^n[Q(z)] = d_\theta^{n-1}\left[Q(z) - z^n + 2\cos\theta z^{n-1} - z^{n-2}\right].$$

The proof of this result is left to the reader, but it basically uses the same ideas as for the Hurwitz case. We illustrate the use of the above formulas with an example.

Example 3.2. Consider the Schur stable polynomial

$$\delta(z) := 0.1 + 0.2z + 0.4z^2 + 0.3z^3 + z^4$$

and the problem of computing $\rho(\delta)$ for it.

All coefficients are subject to perturbation Let us assume that all coefficients of $\delta(z)$ including the leading coefficient are subject to perturbation. Then we need to apply Theorem 3.5. Consequently, we have

$$d_\theta^2 = \frac{\lambda_2^2\|q_\theta^1(z)\|^2 - 2\lambda_1\lambda_2 < q_\theta^1(z), q_\theta^2(z) > +\lambda_1^2\|q_\theta^2(z)\|^2}{\|q_\theta^1(z)\|^2\|q_\theta^2(z)\|^2 - < q_\theta^1(z), q_\theta^2(z) >^2}.$$

where

$$\begin{aligned}
\lambda_1 &= \mathrm{Re}[\delta(e^{j\theta})] \\
&= 0.1 + 0.2\cos\theta + 0.4\cos 2\theta + 0.3\cos 3\theta + \cos 4\theta \\
\lambda_2 &= \mathrm{Im}[\delta(e^{j\theta})] \\
&= 0.2\sin\theta + 0.4\sin 2\theta + 0.3\sin 3\theta + \sin 4\theta \\
\|q_\theta^1(z)\|^2 &= \frac{5}{2} + \frac{1}{2}(\cos 4\theta)\left(\frac{\sin 5\theta}{\sin\theta}\right) \\
\|q_\theta^2(z)\|^2 &= \frac{5}{2} - \frac{1}{2}(\cos 4\theta)\left(\frac{\sin(5\theta)}{\sin\theta}\right) \\
< q_\theta^1(z), q_\theta^2(z) > &= \frac{1}{2}(\sin 4\theta)\left(\frac{\sin(5\theta)}{\sin\theta}\right).
\end{aligned}$$

The graph of d_θ is depicted in Figure 3.3. We find that

$$d_{\min} = \inf_{0\le\theta\le\pi} d_\theta = 0.4094.$$

Since

$$\begin{aligned}
d_{+1} &= \frac{|\delta(1)|}{\sqrt{5}} = 0.8944 \\
d_{-1} &= \frac{|\delta(-1)|}{\sqrt{5}} = 0.4472,
\end{aligned}$$

we have the first encounter with instability at $z = e^{j\theta}$, $\theta = 1.54$, and

$$\rho(\delta) = \min(d_{+1}, d_{-1}, d_{\min}) = 0.4094.$$

The leading coefficient is fixed Write

$$\beta(z) := 0.1 + 0.2z + 0.4z^2 + 0.3z^3 + z^4.$$

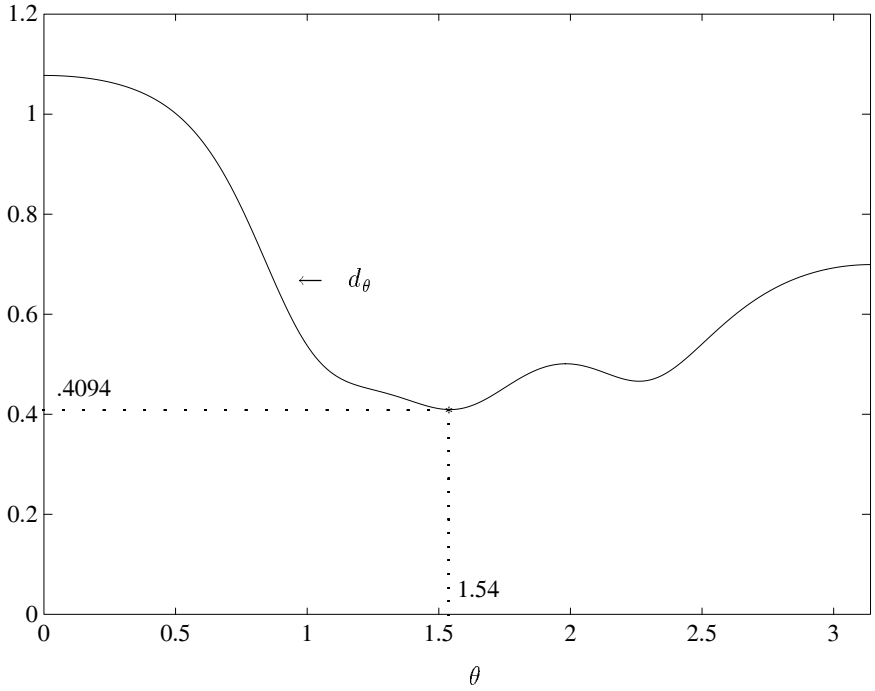

Figure 3.3. d_θ vs. θ (non-monic discrete polynomial: Example 3.2)

Applying Theorem 3.6 which deals with the stability margin for monic polynomials, we have

$$\begin{aligned}\bar{d}_\theta^n[\beta(z)]_{n=4} &= d_\theta^n[\beta(z) - z^4 + 2\cos\theta z^3 - z^2]_{n=3} \\ &= d_\theta^n[(.3 + 2\cos\theta)z^3 - .6z^2 + .2z + .1]_{n=3}.\end{aligned}$$

Now

$$[d_\theta]^2 = \frac{\lambda_2^2\|q_\theta^1(z)\|^2 - 2\lambda_1\lambda_2 < q_\theta^1(z), q_\theta^2(z) > +\lambda_1^2\|q_\theta^2(z)\|^2}{\|q_\theta^1(z)\|^2\|q_\theta^2(z)\|^2 - < q_\theta^1(z), q_\theta^2(z) >^2}.$$

where

$$\begin{aligned}\lambda_1 &= .1 + .2\cos\theta - .6\cos 2\theta + (.3 + 2\cos\theta)\cos 3\theta \\ \lambda_2 &= .2\sin\theta - 0.6\sin 2\theta + (0.3 + 2\cos\theta)\sin 3\theta \\ \|q_\theta^1(z)\|^2 &= 2 + \frac{1}{2}(\cos 3\theta)\left(\frac{\sin 4\theta}{\sin\theta}\right) \\ \|q_\theta^2(z)\|^2 &= 2 - .5(\cos 3\theta)\left(\frac{\sin 4\theta}{\sin\theta}\right)\end{aligned}$$

$$< q^1\theta(z), q^2_\theta(z) > = .5(\sin 3\theta)\left(\frac{\sin 4\theta}{\sin \theta}\right).$$

The graph of d_θ is shown in Figure 3.4.

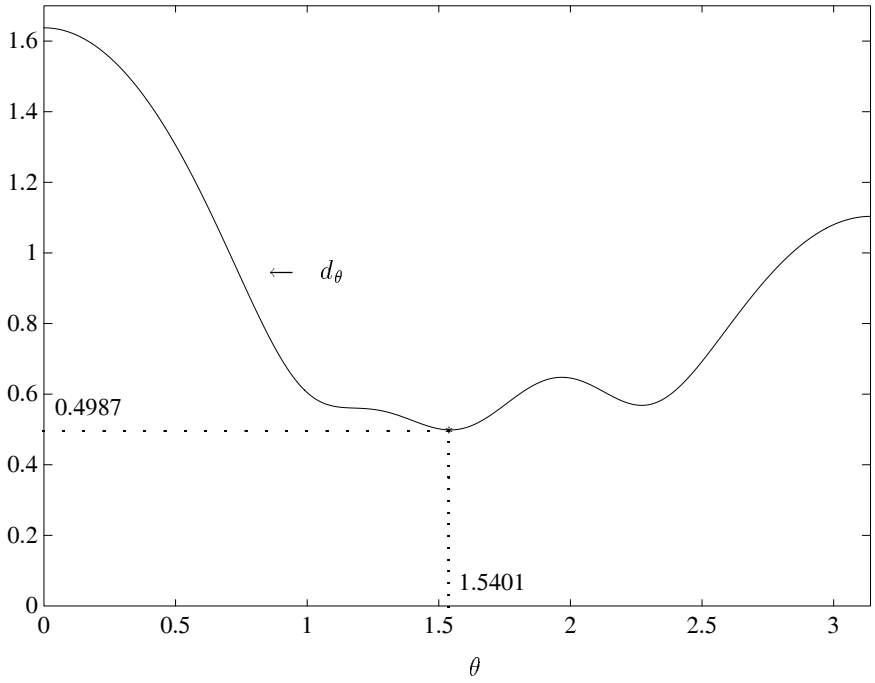

Figure 3.4. d_θ vs. θ (monic discrete polynomial: Example 3.2)

We find that

$$d_{\min} = \inf_{0 \le \theta \le \pi} d_\theta = 0.4987.$$

Also

$$\bar{d}_{+1} = \frac{|\beta(1)|}{\sqrt{4}} = 1$$
$$\bar{d}_{-1} = \frac{|\beta(-1)|}{\sqrt{4}} = 0.5.$$

Therefore,

$$\rho(\delta) = \min(\bar{d}_{+1}, \bar{d}_{-1}, d_{\min}) = 0.4987.$$

3.4 THE TSYPKIN-POLYAK LOCUS: ℓ_p STABILITY BALL

In this section we consider the problem of determining the Hurwitz stability of a ball of polynomials specified by a weighted ℓ_p norm in the coefficient space for an arbitrary positive integer p. The solution given here was developed by Tsypkin and Polyak and is graphical in nature. It is based on a complex plane frequency domain plot and is therefore particularly suitable for computer implementation. Three cases are considered in some detail : $p = \infty$ (interval uncertainty), $p = 2$ (ellipsoidal uncertainty) and $p = 1$ (octahedral uncertainty). As we shall see the fundamental idea underlying the solution is, once again, a systematic use of the Boundary Crossing Theorem.

Let us parametrize the real polynomial

$$A(s) = a_0 + a_1 s + \cdots + a_n s^n \tag{3.15}$$

by its coefficient vector $\mathbf{a} = [a_0, a_1, \cdots, a_n]$. We consider a family of polynomials $A(s)$ centered at a nominal point $\mathbf{a}^0 = [a_0^0, a_1^0, \cdots, a_n^0]$ with the coefficients lying in the weighted ℓ_p ball of radius ρ,

$$\mathcal{B}_p(\mathbf{a}^0, \rho) := \left\{ \mathbf{a} \ : \ \left[\sum_{k=0}^{n} \left| \frac{a_k - a_k^0}{\alpha_k} \right|^p \right]^{\frac{1}{p}} \leq \rho \right\}. \tag{3.16}$$

In (3.16) $\alpha_k > 0$ are given weights, $1 \leq p \leq \infty$ is a fixed integer, $\rho \geq 0$ is a prescribed common margin for the perturbations. The case $p = \infty$ corresponds to the *box*

$$\mathcal{B}_\infty(\mathbf{a}^0, \rho) := \left\{ \mathbf{a} \ : \ \left[\max_k \left| \frac{a_k - a_k^0}{\alpha_k} \right| \right] \leq \rho \right\}. \tag{3.17}$$

We assume that $a_n^0 > 0$. For $\alpha_k = \alpha$ the set $\mathcal{B}_p(\mathbf{a}^0, \rho)$ is a ball with radius ρ in ℓ_p-space. For $p = 1$ the set $\mathcal{B}_1(\mathbf{a}^0, \rho)$ is a *weighted diamond*. Since there is a one to one correspondence between the point $\mathbf{a}$ and the corresponding polynomial $A(s)$, we loosely refer to the set $\mathcal{B}_p(\mathbf{a}^0, \rho)$ as an ℓ_p ball of polynomials. *Robust stability* will mean here that a ball of prescribed radius in a certain norm contains only Hurwitz polynomials of degree n. Our objective in this section is to derive a procedure for checking whether or not all polynomials in the ball $\mathcal{B}_p(\mathbf{a}^0, \rho)$ are Hurwitz for a prescribed value of ρ and also to determine the maximal ρ which guarantees robust stability.

Write $A_0(j\omega) = U_0(\omega) + j\omega V_0(\omega)$ where

$$U_0(\omega) = a_0^0 - a_2^0\omega^2 + a_4^0\omega^4 - \cdots, \tag{3.18}$$

$$V_0(\omega) = a_1^0 - a_3^0\omega^2 + a_5^0\omega^4 - \cdots \tag{3.19}$$

Let q be the index conjugate to p:

$$\frac{1}{p} + \frac{1}{q} = 1. \tag{3.20}$$

For $1 < p < \infty$ introduce

$$S_p(\omega) := \left[\alpha_0^q + (\alpha_2\omega^2)^q + (\alpha_4\omega^4)^q + \cdots\right]^{\frac{1}{q}} \tag{3.21}$$

$$T_p(\omega) := \left[\alpha_1^q + (\alpha_3\omega^2)^q + (\alpha_5\omega^4)^q + \cdots\right]^{\frac{1}{q}}. \tag{3.22}$$

For $p = 1$ define

$$S_1(\omega) := \max_{k \text{ even}} \alpha_k\omega^k,$$
$$T_1(\omega) := \max_{k \text{ odd}} \alpha_k\omega^{k-1}$$

and for $p = \infty$ define

$$S_\infty(\omega) := \alpha_0 + \alpha_2\omega^2 + \cdots, \qquad T_\infty(\omega) := \alpha_1 + \alpha_3\omega^2 + \cdots. \tag{3.23}$$

Now, for each p let

$$x(\omega) := \frac{U_0(\omega)}{S_p(\omega)}, \qquad y(\omega) := \frac{V_0(\omega)}{T_p(\omega)} \tag{3.24}$$

and

$$z(\omega) := x(\omega) + jy(\omega). \tag{3.25}$$

In the procedure developed below we require the frequency plot of $z(\omega) = x(\omega) + jy(\omega)$ as ω runs from 0 to ∞. This plot is bounded and its endpoints $z(0)$, $z(\infty)$ are given by

$$x(0) = \frac{a_0^0}{\alpha_0}$$

$$x(\infty) = \begin{cases} (-1)^{\frac{n}{2}}\dfrac{a_n^0}{\alpha_n}, & \text{n even} \\ (-1)^{\frac{n-1}{2}}\dfrac{a_{n-1}^0}{\alpha_{n-1}}, & \text{n odd} \end{cases}$$

$$y(0) = \frac{a_1^0}{\alpha_1} \tag{3.26}$$

$$y(\infty) = \begin{cases} (-1)^{\frac{n}{2}-1}\dfrac{a_{n-1}^0}{\alpha_{n-1}}, & \text{n even} \\ (-1)^{\frac{n-1}{2}}\dfrac{a_n^0}{\alpha_n}, & \text{n odd} \end{cases}$$

Now, in the complex plane we introduce the ℓ_p disc with radius ρ:

$$\mathcal{D}_p(\rho) := \left\{z = x + jy \ : \ [|x|^p + |y|^p]^{\frac{1}{p}} \le \rho\right\}. \tag{3.27}$$

Theorem 3.7 *Each polynomial in the ball $\mathcal{B}_p(\mathbf{a}^0, \rho)$ is Hurwitz stable if and only if the plot of $z(\omega)$:*

A) goes through n quadrants in the counterclockwise direction,

B) does not intersect the ℓ_p disc with radius ρ, $\mathcal{D}_p(\rho)$, and

C) its boundary points $z(0)$, $z(\infty)$ have coordinates with absolute values greater than ρ.

Conditions B and C are respectively equivalent to the requirements

$$[|x(\omega)|^p + |y(\omega)|^p]^{\frac{1}{p}} > \rho, \qquad \text{for all } 0 \leq \omega < \infty \tag{3.28}$$

and

$$|x(0)| > \rho, \quad |y(0)| > \rho, \quad |x(\infty)| > \rho, \quad |y(\infty)| > \rho. \tag{3.29}$$

We also remark that condition C may be replaced by the equivalent:

$$a_0^0 > \rho\alpha_0, \quad a_n^0 > \rho\alpha_n, \quad a_1^0 > \rho\alpha_1, \quad a_{n-1}^0 > \rho\alpha_{n-1}. \tag{3.30}$$

From this theorem it is clear that the maximal ρ preserving robust Hurwitz stability of the ball $\mathcal{B}_p(\mathbf{a}^0, \rho)$ can be found by finding the radius of the maximal ℓ_p disc that can be inscribed in the frequency plot $z(\omega)$ without violating the boundary conditions in (3.29).

Proof.
Necessity. Assume that all polynomials in $\mathcal{B}_p(\mathbf{a}^0, \rho)$ are Hurwitz. Then $A_0(s)$ is also Hurwitz, and it follows from the monotonic phase property of Hurwitz polynomials discussed in Chapter 1 with $S(\omega) = S_p(\omega)$, $T(\omega) = T_p(\omega)$ that condition A must hold. To show that condition C must also hold we observe that a necessary condition for a polynomial $A(s) = \sum_{k=0}^n a_k s^k$ with $a_0 > 0$ to be Hurwitz is that $a_k > 0$, $k = 0, 1, \cdots$. If we choose $a_k = a_k^0 - \rho\alpha_k$ for some k and $a_i = a_i^0$, for $i \neq k$ it follows that the corresponding polynomial $A(s)$ lies in $\mathcal{B}_p(\mathbf{a}^0, \rho)$, is therefore Hurwitz and hence $a_k > 0$ or $a_k^0/\alpha_k > \rho$. With $k = 0, 1, n-1$ and n we get (3.29) and (3.30).

Suppose now that condition B fails. Then there exists $0 \leq \omega_0 < \infty$ such that

$$z(\omega_0) = x(\omega_0) + jy(\omega_0) \in \mathcal{D}_p(\rho) \tag{3.31}$$

We complete the proof of necessity of Condition B by showing that under these conditions $\mathcal{B}_p(\mathbf{a}^0, \rho)$ contains an unstable polynomial. We treat the three cases $1 < p < \infty$, $p = 1$ and $p = \infty$ separately. In each case a contradiction is developed by displaying a polynomial $A_1(s) \in \mathcal{B}_p(\mathbf{a}^0, \rho)$ which has a root at $s = j\omega_0$ and is therefore not Hurwitz. Write $x(\omega_0) = x_0$, $y(\omega_0) = y_0$.

Case 1: $1 < p < \infty$.

In this case the condition $z(\omega_0) = x(\omega_0) + jy(\omega_0) \in \mathcal{D}_p(\rho)$ is equivalent to

$$|x_0|^p + |y_0|^p \leq \rho^p. \tag{3.32}$$

Now write $S_0 := S_p(\omega_0)$, $T_0 := T_p(\omega_0)$ and consider the polynomial $A_1(s)$ with coefficients a_k^1 defined as follows:

$$a_{2i}^1 = a_{2i}^0 - (-1)^i x_0 S_0^{-\frac{q}{p}} \alpha_{2i}^q \omega_0^{\frac{2iq}{p}}, \qquad i = 0, 1, \cdots$$

$$a_{2i+1}^1 = a_{2i+1}^0 - (-1)^i y_0 T_0^{-\frac{q}{p}} \alpha_{2i+1}^q \omega_0^{\frac{2iq}{p}}, \qquad i = 0, 1, \cdots.$$

Then

$$\sum_{k \text{ even}} \left| \frac{a_k^1 - a_k^0}{\alpha_k} \right|^p = |x_0|^p S_0^{-q} \sum_{k \text{ even}} (\alpha_k \omega_0^k)^q = |x_0|^p$$

$$\sum_{k \text{ odd}} \left| \frac{a_k^1 - a_k^0}{\alpha_k} \right|^p = |y_0|^p T_0^{-q} \sum_{k \text{ odd}} (\alpha_k \omega_0^{k-1})^q = |y_0|^p$$

so that

$$\sum_{k=0}^{n} \left| \frac{a_k^1 - a_k^0}{\alpha_k} \right|^p = |x_0|^p + |y_0|^p \leq \rho^p. \tag{3.33}$$

Thus $A_1(s) \in \mathcal{B}_p(\mathbf{a}^0, \rho)$. But

$$\begin{aligned} A_1(j\omega_0) &= U_0(\omega_0) - x_0 S_0^{-\frac{q}{p}} \sum_{k \text{ even}} \alpha_k^q \omega_0^{\frac{kq}{p}} \omega_0^k \\ &\quad + j\omega_0 \left[V_0(\omega_0) - y_0 T_0^{-\frac{q}{p}} \sum_{k \text{ odd}} \alpha_k^q \omega_0^{\frac{(k-1)q}{p}} \omega_0^{k-1} \right] \\ &= [U_0(\omega_0) - x_0 S_p(\omega_0)] + j\omega_0 [V_0(\omega_0) - y_0 T_p(\omega_0)] \\ &= 0. \end{aligned}$$

Hence $A_1(s)$ has the imaginary root $j\omega_0$ and is not Hurwitz.

Case 2: $p = 1$.

Here

$$\mathcal{B}_1(\mathbf{a}^0, \rho) = \left\{ \mathbf{a} : \sum_{k=0}^{n} \left| \frac{a_k^1 - a_k^0}{\alpha_k} \right| \leq \rho \right\} \tag{3.34}$$

$$\begin{aligned} S_1(\omega_0) &= \max_{k \text{ even}} \alpha_k \omega_0^k \;:=\; \alpha_m \omega_0^m \\ T_1(\omega_0) &= \max_{k \text{ odd}} \alpha_k \omega_0^{k-1} \;:=\; \alpha_t \omega_0^{t-1}. \end{aligned}$$

and the condition $z(\omega_0) \in \mathcal{D}_1(\rho)$ is equivalent to

$$|x_0| + |y_0| \leq \rho. \tag{3.35}$$

Now construct the polynomial $A_1(s) = \sum_{k=0}^{n} a_k^1 s^k$ with

$$a_k^1 = a_k^0, \quad k \neq m, \quad k \neq t \tag{3.36}$$
$$a_m^1 = a_m^0 - (-1)^{\frac{m}{2}} x_0 \alpha_m \tag{3.37}$$
$$a_t^1 = a_t^0 - (-1)^{\frac{(t-1)}{2}} y_0 \alpha_t. \tag{3.38}$$

Then

$$\sum_{k=0}^{n} \left| \frac{(a_k^1 - a_k^0)}{\alpha_k} \right| = |x_0| + |y_0| \leq \rho \tag{3.39}$$

so that $A_1(s) \in \mathcal{B}_1(\mathbf{a}^0, \rho)$. However

$$A_1(j\omega_0) = \left[U^0(\omega_0) - x_0 S_1(\omega_0)\right] + j\omega_0 \left[V^0(\omega_0) - y_0 T_1(\omega_0)\right] = 0. \tag{3.40}$$

Hence $A_1(s)$ has the imaginary root $j\omega_0$, i.e. A_1 is not Hurwitz.

Case 3: $p = \infty$.

In this case we have

$$\mathcal{B}_\infty(\mathbf{a}^0, \rho) = \left\{ \mathbf{a} : \frac{|a_k^1 - a_k^0|}{\alpha_k} \leq \rho, \quad k = 0, 1, 2 \cdots \right\} \tag{3.41}$$

and

$$S_\infty(\omega) = \alpha_0 + \alpha_2 \omega^2 + \cdots, \qquad T_\infty(\omega) = \alpha_1 + \alpha_3 \omega^2 + \cdots \tag{3.42}$$

The ℓ_∞ disc is given by

$$\mathcal{D}_\infty(\rho) = \{z = x + jy : |x| \leq \rho, \quad |y| \leq \rho\} \tag{3.43}$$

and Condition B is violated if and only if

$$|x_0| \leq \rho, \qquad |y_0| \leq \rho. \tag{3.44}$$

Now consider the polynomial $A_1(s) = \sum_{k=0}^{n} a_k^1 s^k$ with the coefficients chosen as

$$a_k^1 = a_k^0 - (-1)^{\frac{k}{2}} x_0 \alpha_k, \qquad k \text{ even} \tag{3.45}$$
$$a_k^1 = a_k^0 - (-1)^{\frac{(k-1)}{2}} y_0 \alpha_k, \qquad k \text{ odd}. \tag{3.46}$$

Then

$$\frac{|a_k^1 - a_k^0|}{\alpha_k} = |x_0| \leq \rho, \quad k \text{ even}, \qquad \frac{|a_k^1 - a_k^0|}{\alpha_k} = |y_0| \leq \rho, \quad k \text{ odd} \tag{3.47}$$

so that $A_1(s) \in \mathcal{B}_\infty(\mathbf{a}^0, \rho)$. But

$$A_1(j\omega_0) = [U^0(\omega_0) - x_0 S_\infty(\omega_0)] + j\omega_0 \left[V^0(\omega_0) - y_0 T_\infty(\omega_0)\right] = 0. \tag{3.48}$$

showing that $A_1(s)$ has an imaginary axis root and is therefore not Hurwitz.

Thus we have shown for all $1 \leq p \leq \infty$ that the assumption that B does not hold leads to a contradiction. This completes the proof of necessity of the conditions A, B and C.

Sufficiency. Suppose now that conditions A, B and C hold but there exists a polynomial $\tilde{A}(s) = \sum_{k=0}^{n} \tilde{a}_k s^k \in \mathcal{B}_p(\mathbf{a}^0, \rho)$ which is not Hurwitz. Consider the convex combination $A_\lambda(s) = \lambda A_0(s) + (1-\lambda)\tilde{A}(s), \quad 0 \leq \lambda \leq 1$. The leading coefficient a_n^λ of $A_\lambda(s)$ is positive since $a_n^0 > 0$, $\tilde{a}_n \geq a_n^0 - \rho\alpha_n > 0$ while $a_n^\lambda = \lambda a_n^0 + (1-\lambda)\tilde{a}_n, \quad 0 \leq \lambda \leq 1$. The roots of $A_\lambda(s)$ are then continuous functions of λ. Since $A_0(s)$ is Hurwitz and $\tilde{A}(s)$ is not, by the Boundary Crossing Theorem of Chapter 1 there exists some $\bar{\lambda}, \quad 0 \leq \bar{\lambda} < 1$ such that $A_{\bar{\lambda}}(s)$ has a root on the imaginary axis. Moreover since $A_0(s)$ and $\tilde{A}(s)$ are in the convex set $\mathcal{B}_p(\mathbf{a}^0, \rho)$ it follows that $A_{\bar{\lambda}}(s)$ is also in $\mathcal{B}_p(\mathbf{a}^0, \rho)$.

Denote the coefficients of $A_{\bar{\lambda}}(s)$ as $\bar{a}_k$ and its imaginary root as $j\omega_0$. We can write

$$\bar{a}_k := a_k^0 + \mu_k \alpha_k,$$

where

$$\left[\sum_{k=0}^{n} |\mu_k|^p\right]^{\frac{1}{p}} \leq \rho.$$

Writing

$$\bar{A}(j\omega_0) \triangleq \bar{U}(\omega_0) + j\omega_0 \bar{V}(\omega_0) = 0$$

it follows that

$$\bar{U}(\omega_0) = U_0(\omega_0) + \sum_{k \text{ even}} (-1)^{\frac{k}{2}} \mu_k \alpha_k \omega_0^k,$$
$$\bar{V}(\omega_0) = V_0(\omega_0) + \sum_{k \text{ odd}} (-1)^{\frac{(k-1)}{2}} \mu_k \alpha_k \omega_0^{k-1}.$$

If $\omega_0 = 0$ then $\bar{U}(0) = 0, \quad 0 = U_0(0) + \mu_0\alpha_0, \quad a_0^0 = |U_0(0)| = |\mu_0|\alpha_0 \leq \rho\alpha_0$, and this contradicts condition C. If $\omega_0 \neq 0$, then $\bar{A}(j\omega_0) = 0$ implies that

$$\bar{U}(\omega_0) = 0, \qquad \bar{V}(\omega_0) = 0. \tag{3.49}$$

From $\bar{U}(\omega_0) = 0$, we have

$$|U_0(\omega_0)| = \left| \sum_{k \text{ even}} (-1)^{1+\frac{k}{2}} \mu_k \alpha_k \omega_0^k \right|$$

$$\leq \left[\sum_{k \text{ even}} |\mu_k|^p\right]^{\frac{1}{p}} \left[\sum_{k \text{ even}} (\alpha_k \omega_0^k)^q\right]^{\frac{1}{q}} \quad \text{(Hölder's inequality)}$$

$$= \left[\sum_{k \text{ even}} |\mu_k|^p\right]^{\frac{1}{p}} S_p(\omega_0).$$

Similarly, from $\bar{V}(\omega_0) = 0$, we have

$$|V_0(\omega_0)| = \left|\sum_{k \text{ odd}} (-1)^{1+\frac{k-1}{2}} \mu_k \alpha_k \omega_0^{k-1}\right|$$

$$\leq \left[\sum_{k \text{ odd}} |\mu_k|^p\right]^{\frac{1}{p}} T_p(\omega_0).$$

Hence

$$[|x(\omega_0)|^p + |y(\omega_0)|^p]^{\frac{1}{p}} = \left[\frac{|U_0(\omega_0)|^p}{|S_p(\omega_0)|^p} + \frac{|V_0(\omega_0)|^p}{|T_p(\omega_0)|^p}\right]^{\frac{1}{p}}$$

$$\leq \left[\sum_{k \text{ even}} |\mu_k|^p + \sum_{k \text{ odd}} |\mu_k|^p\right]^{\frac{1}{p}}$$

$$= \left[\sum_{k=0}^{n} |\mu_k|^p\right]^{\frac{1}{p}}$$

$$\leq \rho.$$

which shows that condition B is violated. Thus the assumption that $\tilde{A}(s)$ is non-Hurwitz leads to a contradiction. This completes the proof of sufficiency and of the theorem. ♣

Discussion

(1) It is useful to interpret the above theorem in terms of the complex plane image of the ball of polynomials $A(s) \in \mathcal{B}_p(\mathbf{a}^0, \rho)$. For all $A(s) \in \mathcal{B}_p(\mathbf{a}^0, \rho)$ the set $A(j\omega) = U(\omega) + j\omega V(\omega)$ is described by the inequality

$$\left[\left|\frac{U(\omega) - U_0(\omega)}{S_p(\omega)}\right|^p + \left|\frac{V(\omega) - V_0(\omega)}{T_p(\omega)}\right|^p\right]^{\frac{1}{p}} \leq \rho,$$

and the conditions of the Theorem specify that this set should not contain the origin for all $\omega > 0$. This coincides with the Zero Exclusion Theorem of Chapter 1.

(2) The assumption $\alpha_k > 0$, $k = 0, 1, \cdots, n$ may be dropped although in this case the frequency plot $z(\omega)$ will be unbounded for $\alpha_0 = 0$ or $\alpha_n = 0$.

(3) If conditions B and C hold but A fails then the nominal polynomial $A^0(s)$ is not Hurwitz. In this case all polynomials in $\mathcal{B}_p(\mathbf{a}^0, \rho)$ have the same number of roots in the open left half-plane as the nominal polynomial $A_0(s)$.

(4) If $\rho_{\max}$ is the radius of the largest ℓ_p disc inscribed in the plot $z(\omega)$ with $z(\omega_0)$ being a point of contact and conditions A, B and C hold, then the polynomial $A_1(s)$ constructed in the proof is the critical polynomial that destroys stability.

(5) The theorem requires us to generate the plot of $z(\omega)$ for $0 < \omega < \infty$, verify that it goes through n quadrants in the counterclockwise direction, avoids the ℓ_p disc $\mathcal{D}_p(\rho)$ and ensure that the endpoints $z(0)$ and $z(\infty)$ lie outside the square of side 2ρ centered at the origin in the complex plane. Obviously this is ideally suited for visual representation, with the complex plane represented by a computer screen.

Summary of Computations

We summarize the results of the theorem for the special cases $p = 1$, $p = 2$ and $p = \infty$ in terms of what needs to be computed.

In the case $p = 1$, $z(\omega)$ is given by

$$x(\omega) = \frac{a_0^0 - a_2^0\omega^2 + a_4\omega^4 - \cdots}{\max_{k \text{ even}} \alpha_k \omega^k},$$

$$y(\omega) = \frac{a_1^0 - a_3^0\omega^2 + a^5\omega^4 - \cdots}{\max_{k \text{ odd}} \alpha_k \omega^{k-1}}$$

and the plot should not intersect the rhombus $|x| + |y| \leq \rho$.

When $p = 2$, $z(\omega)$ is given by

$$x(\omega) = \frac{a_0^0 - a_2^0\omega^2 + a_4^0\omega^4 - \cdots}{(\alpha_0^2 + \alpha_2^2\omega^4 + \alpha_4^2\omega^8 + \cdots)^{\frac{1}{2}}},$$

$$y(\omega) = \frac{a_1^0 - a_3^0\omega^2 + a_5^0\omega^4 - \cdots}{(\alpha_1^2 + \alpha_3^2\omega^4 + \alpha_5^2\omega^8 + \cdots)^{\frac{1}{2}}}$$

and this plot must not intersect the circle $|x|^2 + |y|^2 \leq \rho^2$.

When $p = \infty$, the frequency plot $z(\omega) = x(\omega) + jy(\omega)$ is given by

$$x(\omega) = \frac{a_0^0 - a_2^0\omega^2 + a_4^0\omega^4 - \cdots}{\alpha_0 + \alpha_2\omega^2 + \alpha_4\omega^4 + \cdots},$$

$$y(\omega) = \frac{a_1^0 - a_3^0\omega^2 + a_5^0\omega^4 - \cdots}{\alpha_1 + \alpha_3\omega^2 + \alpha_5\omega^4 + \cdots}$$

and must not intersect the square $|x| \leq \rho$, $|y| \leq \rho$.

We illustrate the above Theorem with an example.

Example 3.3. Consider the polynomial

$$A(s) = s^6 + 14s^5 + 80.25s^4 + 251.25s^3 + 502.25s^2 + 667.25s + 433.5.$$

With the choice of

$$\alpha = [0.1,\ 1.4,\ 5.6175,\ 15.075,\ 25.137,\ 33.36,\ 43.35]$$

we have the following stability margins:

$$\begin{aligned} p = 1, &\qquad \rho = 3.6252 \\ p = 2, &\qquad \rho = 2.8313 \\ p = \infty, &\qquad \rho = 1.2336. \end{aligned}$$

The required plot of $z(\omega)$ and the discs $\mathcal{D}_1(\rho), \mathcal{D}_2(\rho)$ and $\mathcal{D}_\infty(\rho)$ are shown in Figures 3.5, 3.6, and 3.7.

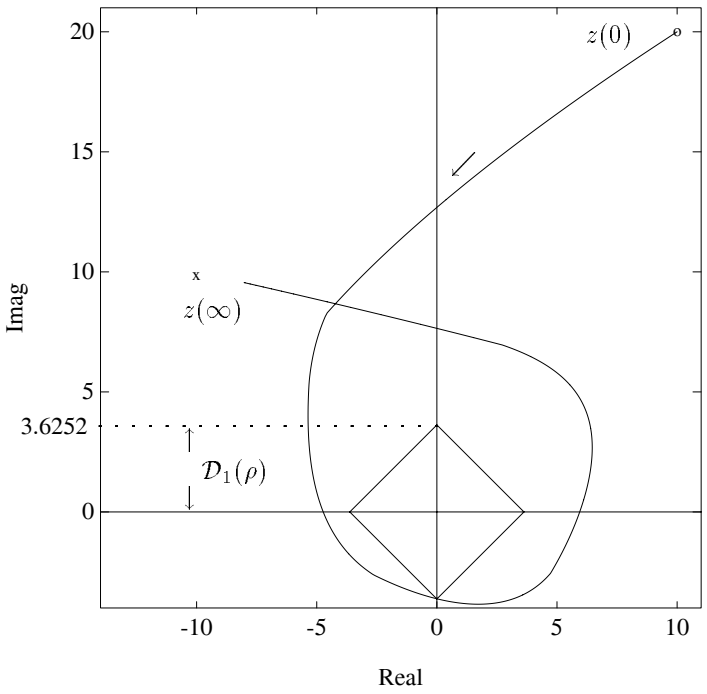

Figure 3.5. Tsypkin - Polyak locus: ℓ_1 stability margin (Example 3.3)

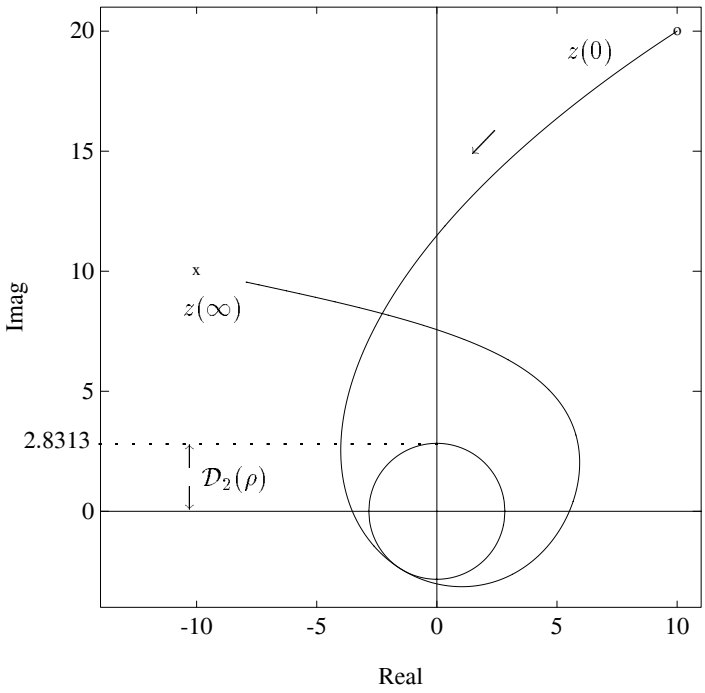

Figure 3.6. Tsypkin - Polyak locus: ℓ_2 stability margin (Example 3.3)

3.5 ROBUST STABILITY OF DISC POLYNOMIALS

In this section we consider an alternative model of uncertainty. We deal with the robust stability of a set $\mathcal{F}_D$ of *disc* polynomials, which are characterized by the fact that each coefficient of a typical element $P(s)$ in $\mathcal{F}_D$ can be any complex number in an arbitrary but fixed disc of the complex plane. The motivation for considering robust stability of disc polynomials is the same as the one for considering robust stability of the ℓ_p ball of polynomials: namely it is a device for taking into account variation of parameters in prescribed ranges. We let $\mathcal{S}$ be the stability region of interest and consider $n+1$ arbitrary discs D_i, $i = 0, \cdots, n$ in the complex plane. Each disc D_i is centered at the point β_i and has radius $r_i \geq 0$. Now, let $\mathcal{F}_D$ be the family of all complex polynomials,

$$\delta(z) = \delta_0 + \delta_1 z + \cdots + \delta_n z^n,$$

such that

$$\delta_j \in D_j, \quad \text{for } j = 0, \cdots, n \ . \tag{3.50}$$

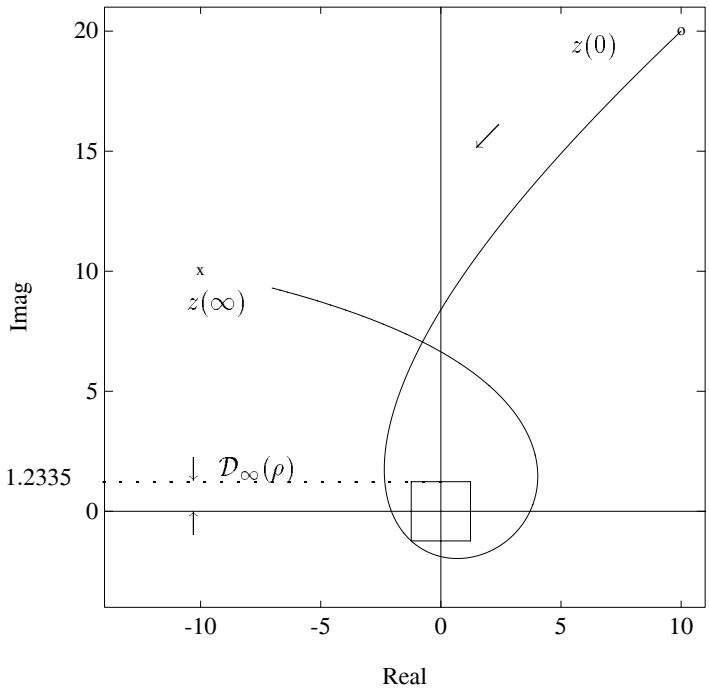

Figure 3.7. Tsypkin - Polyak locus: ℓ_∞ stability margin (Example 3.3)

In other words every coefficient δ_j of the polynomial $\delta(z)$ in $\mathcal{F}_D$ satisfies

$$|\delta_j - \beta_j| \leq r_j. \tag{3.51}$$

We assume that every polynomial in $\mathcal{F}_D$ is of degree n:

$$0 \notin D_n. \tag{3.52}$$

Figure 3.8 illustrates an example of such a family of complex polynomials. Each disc D_i describes the possible range of values for the coefficient δ_i. The problem here is to give necessary and sufficient conditions under which it can be established that all polynomials in $\mathcal{F}_D$ have their roots in $\mathcal{S}$. This problem is solved for both Hurwitz and Schur stability . For example, we prove that the Hurwitz stability of $\mathcal{F}_D$ is equivalent to the stability of the *center* polynomial together with the fact that two specific stable proper rational functions must have an H_∞-norm less than 1.

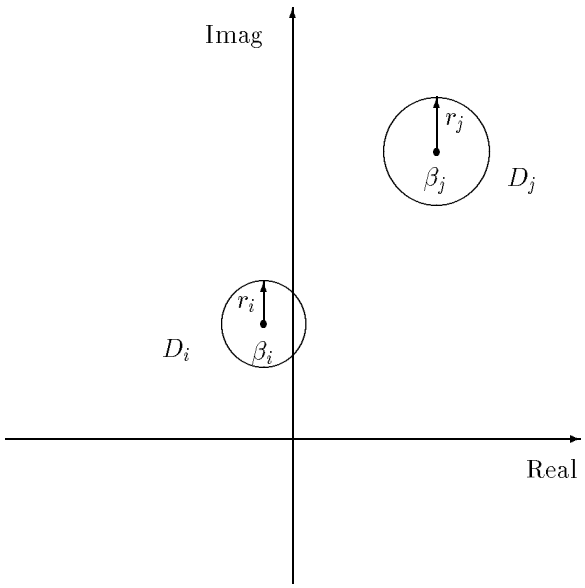

Figure 3.8. Disks around the coefficients (β_i, β_j)

3.5.1 Hurwitz Case

Let $g(s) = \frac{n(s)}{d(s)}$ where $n(s)$ and $d(s)$ are complex polynomials such that the degree of $n(s)$ is less than or equal to the degree of $d(s)$ and such that $d(s)$ is Hurwitz. In other words $g(s)$ is a proper, stable, complex, rational function. The H_∞-norm of $g(s)$ is then defined as

$$\|g\|_\infty := \sup_{\omega \in \mathbf{R}} \left| \frac{n(j\omega)}{d(j\omega)} \right|. \tag{3.53}$$

Now, let $\beta(s)$ be the *center* polynomial, that is the polynomial whose coefficients are the centers of the discs D_j:

$$\beta(s) = \beta_0 + \beta_1 s + \cdots + \beta_n s^n. \tag{3.54}$$

Construct polynomials $\gamma_1(s)$ and $\gamma_2(s)$ as follows:

$$\begin{aligned} \gamma_1(s) &:= r_0 - jr_1 s - r_2 s^2 + jr_3 s^3 + r_4 s^4 - jr_5 s^5 - \cdots, \\ \gamma_2(s) &:= r_0 + jr_1 s - r_2 s^2 - jr_3 s^3 + r_4 s^4 + jr_5 s^5 - \cdots \end{aligned}$$

and let $g_1(s)$ and $g_2(s)$ be the two proper rational functions

$$g_1(s) = \frac{\gamma_1(s)}{\beta(s)}, \qquad g_2(s) = \frac{\gamma_2(s)}{\beta(s)}. \tag{3.55}$$

The main result on Hurwitz stability of disc polynomials is the following.

Theorem 3.8 *Each member of the family of polynomials $\mathcal{F}_D$ is Hurwitz if and only if*

1) $\beta(s)$ is Hurwitz, and,

2) $\|g_1\|_\infty < 1$ and $\|g_2\|_\infty < 1$.

For the proof we first need to establish two simple lemmas. The first lemma characterizes proper, stable, complex rational functions with H_∞-norm less than 1 and is useful in its own right.

Lemma 3.1 *If $g(s) = \frac{n(s)}{d(s)}$ is a proper stable complex rational function with $\deg(d(s)) = q$, then $\|g\|_\infty < 1$ if and only if the following hold:*

a1) $|n_q| < |d_q|$,

b1) $d(s) + e^{j\theta} n(s)$ *is Hurwitz for all θ in $[0, 2\pi)$.*

Proof. Condition a1) is obviously necessary because when ω goes to infinity, the ratio in (3.53) tends to the limit $\left|\frac{n_q}{d_q}\right|$. The necessity of condition b1) on the other hand follows from the Boundary Crossing Theorem and Rouché's theorem on analytic functions (Chapter 1) since $|d(j\omega)| > |e^{j\theta} n(j\omega)| = |n(j\omega)|$.

For sufficiency suppose that conditions a1) and b1) are true, and let us assume by contradiction that $\|g\|_\infty \geq 1$. Since $|g(j\omega)|$ is a continuous function of ω and since its limit, as ω goes to infinity, is $\left|\frac{n_q}{d_q}\right| < 1$, then there must exist at least one ω_o in $\mathbb{R}$ for which

$$|g(j\omega_o)| = \left|\frac{n(j\omega_o)}{d(j\omega_o)}\right| = 1.$$

But this implies that $n(j\omega_o)$ and $d(j\omega_o)$ differ only by a complex number of modulus 1 and therefore it is possible to find θ_o in $[0, 2\pi)$ such that:

$$n(j\omega_o) + e^{j\theta_o} d(j\omega_o) = 0$$

and this obviously contradicts condition b1). ♣

Now, using the definition of $\beta(s)$ given in (3.54), it is easy to see that a typical polynomial $\delta(s)$ in $\mathcal{F}_D$ can be written as:

$$\delta(s) = \beta(s) + \sum_{k=0}^{n} z_k r_k s^k \tag{3.56}$$

where the z_k, $k = 0, \cdots, n$, are arbitrary complex numbers of modulus less than or equal to 1.

The next lemma gives a first set of necessary and sufficient conditions under which stability of $\mathcal{F}_D$ can be ascertained.

Lemma 3.2 *The family of complex polynomials $\mathcal{F}_D$ contains only Hurwitz polynomials if and only if the following conditions hold:*

a2) $\beta(s)$ is Hurwitz,

b2) For all complex numbers $z_0, \cdots, z_n$ of modulus less than or equal to one we have:

$$\left\| \frac{\sum_{k=0}^{n} z_k r_k s^k}{\beta(s)} \right\|_\infty < 1.$$

Proof. We start by proving that conditions a2) and b2) are sufficient. Here again, if $\beta(s)$ is known to be stable, and if condition b2) holds then a straightforward application of Rouché's theorem yields that any polynomial $\delta(s)$ in (3.56) is also Hurwitz.

Conversely, it is clear again from Rouché's Theorem, that condition a2) is necessary, since $\beta(s)$ is in $\mathcal{F}_D$. Thus, let us assume that $\beta(s)$ is stable and let us prove that condition b2) is also satisfied.

To do so we use the characterization derived in Lemma 3.1. First of all, remember that one of our assumptions on the family $\mathcal{F}_D$ is that the n^{th} disc D_n does not contain the origin of the complex plane (see (3.52)). This implies in particular that for any complex number z_n of modulus less than or equal to 1:

$$\left| \frac{z_n r_n}{\beta_n} \right| \leq \frac{r_n}{|\beta_n|} < 1. \tag{3.57}$$

Now let us assume by contradiction that condition b2) is not satisfied. In this case there would exist at least one set $\{z_0, \cdots, z_n\}$, of $n+1$ complex numbers of modulus less than or equal to one, for which:

$$\left\| \frac{\sum_{k=0}^{n} z_k r_k s^k}{\beta(s)} \right\|_\infty \geq 1. \tag{3.58}$$

Condition (3.57) shows that condition a1) of Lemma 3.1 is always satisfied with

$$\beta(s) = d(s) \quad \text{and} \quad \sum_{k=0}^{n} z_k r_k s^k = n(s).$$

Now (3.58) implies by Lemma 3.1 that for this particular set $\{z_0, \cdots, z_n\}$ it is possible to find at least one real θ_o in $[0, 2\pi)$ such that:

$$\beta(s) + e^{j\theta_o} \sum_{k=0}^{n} z_k r_k s^k \quad \text{is unstable.} \tag{3.59}$$

However if we let $z'_k = e^{j\theta_o} z_k$ for $k = 0$ to $k = n$, then all the complex numbers z'_k also have modulus less than or equal to one, which implies that the polynomial in (3.59) is an element of $\mathcal{F}_D$ and this contradicts the fact that $\mathcal{F}_D$ contains only Hurwitz polynomials. ♣

We can now complete the proof of Theorem 3.8.

Proof of Theorem 3.8 Let us start with Lemma 3.2 and let us consider condition b2). Let $z_0, \cdots, z_n$ be $n+1$ arbitrary complex numbers of modulus less than or equal to 1, and let,

$$n(s) := z_0 r_0 + z_1 r_1 s + \cdots + z_n r_n s^n.$$

We can write

$$n(j\omega) = \sum_{k=0}^{n} z_k r_k (j\omega)^k = \sum_{k=0}^{n} z_k r_k e^{j\,k\frac{\pi}{2}} \omega^k. \tag{3.60}$$

For all k in $\{0, \cdots, n\}$ it is possible to write

$$z_k = t_k e^{j\,\theta_k}, \quad \text{where} \quad t_k \in [0,1], \quad \text{and} \quad \theta_k \in [0, 2\pi). \tag{3.61}$$

Using (3.60) and (3.61), we see that

$$n(j\omega) = \sum_{k=0}^{n} t_k r_k e^{j\left(\theta_k + k\frac{\pi}{2}\right)} \omega^k. \tag{3.62}$$

Therefore we always have the following inequalities:

$$\text{If } \omega \geq 0 \text{ then } \quad |n(j\omega)| \leq \sum_{k=0}^{n} r_k \omega^k \tag{3.63}$$

and,

$$\text{If } \quad \omega \leq 0 \quad \text{then} \quad |n(j\omega)| \leq \sum_{k=0}^{k=n} (-1)^k r_k \omega^k. \tag{3.64}$$

However, it is clear that the upper bound in (3.63) is achieved for the particular choice of z_k determined by $t_k = 1, \theta_k = -k\frac{\pi}{2}$, for which $n(s) = \gamma_1(s)$.

On the other hand the upper bound in (3.64) is also achieved for the particular choice $t_k = 1, \theta_k = k\frac{\pi}{2}$, leading this time to $n(s) = \gamma_2(s)$.

As a direct consequence, condition b2) is then satisfied if and only if condition 2) in Theorem 3.8 is true, and this completes the proof of the theorem. ♣

3.5.2 Schur Case

We again consider the family of disc polynomials $\mathcal{F}_D$ defined in (3.51) and (3.52). This time the problem is to derive necessary and sufficient conditions for Schur stability of the entire family. In this case we call $g(z) = \frac{n(z)}{d(z)}$ a proper, stable, complex rational function if $n(z)$ and $d(z)$ are complex polynomials such that the degree of $n(z)$ is less than or equal to the degree of $d(z)$ and if $d(z)$ is Schur (i.e.

$d(z)$ has all its roots in the open unit disc). The H_∞-norm of $g(z)$ is then defined as:

$$\|g\|_\infty := \sup_{\theta \in [0,2\pi)} \left| \frac{n(e^{j\theta})}{d(e^{j\theta})} \right|. \tag{3.65}$$

Again, let the center polynomial be:

$$\beta(z) = \beta_0 + \beta_1 z + \cdots + \beta_n z^n. \tag{3.66}$$

Then we have the following main result on Schur stability of disc polynomials.

Theorem 3.9 *The family of complex disc polynomials $\mathcal{F}_D$ contains only Schur polynomials if and only if the following conditions hold:*

1) $\beta(z)$ is Schur, and

2) The following inequality holds,

$$\sum_{k=0}^{k=n} r_k < \inf_{\theta \in [0,2\pi)} |\beta(e^{j\theta})|.$$

To prove this result, we need the following lemma which is completely analogous to Lemma 3.2.

Lemma 3.3 *The family of complex polynomials $\mathcal{F}_D$ contains only Schur polynomials if and only if the following conditions hold:*

a3) $\beta(z)$ is Schur,

b3) For any complex numbers $z_0, \cdots, z_n$ of modulus less than or equal to one we have:

$$\left\| \frac{\sum_{k=0}^n z_k r_k z^k}{\beta(z)} \right\|_\infty < 1.$$

Proof. The sufficiency of conditions a3) and b3) is quite straightforward and follows again from Rouché's Theorem. The necessity of condition a3) is also clear. Thus assume that $\beta(z)$ is stable and suppose by contradiction that for some set $\{z_0, \cdots, z_n\}$ of complex numbers of modulus less than or equal to 1, we have,

$$\left\| \frac{\sum_{k=0}^n z_k r_k z^k}{\beta(z)} \right\|_\infty \geq 1. \tag{3.67}$$

Let

$$n(z) = \sum_{k=0}^{n} z_k r_k z^k. \tag{3.68}$$

It is clear that as $\lambda \longrightarrow 0$:

$$\left\| \frac{\lambda n(z)}{\beta(z)} \right\|_\infty \longrightarrow 0.$$

Therefore, by continuity of the norm, it is possible to find λ_o in $(0,1)$ such that

$$\left\| \frac{\lambda_o n(z)}{\beta(z)} \right\|_\infty = 1. \tag{3.69}$$

Since the unit circle is a compact set, we deduce from (3.69) and the definition of the H_∞ norm in (3.53), that there exists θ_o in $[0, 2\pi)$ for which:

$$|\lambda_o n(e^{j\theta_o})| = |\beta(e^{j\theta_o})|.$$

Thus it is possible to find a complex number of modulus one, say $e^{j\phi}$, such that:

$$\beta(e^{j\theta_o}) + e^{j\phi}\lambda_o n(e^{j\theta_o}) = 0. \tag{3.70}$$

Therefore, the polynomial

$$\beta(z) + e^{j\phi}\lambda_o n(z),$$

is not Schur, and yet as is easy to see, it belongs to $\mathcal{F}_D$. Thus we have reached a contradiction. ♣

Proof of Theorem 3.9 To prove Theorem 3.9, we just need to look at condition b3) of Lemma 3.3.

For any complex numbers z_i of modulus less than or equal to one, we have the following inequality:

$$\left| \frac{\sum_{k=0}^n z_k r_k e^{jk\theta}}{\beta(e^{j\theta})} \right| \leq \frac{\sum_{k=0}^n r_k}{|\beta(e^{j\theta})|}. \tag{3.71}$$

If we consider the continuous function of θ which appears on the right hand side of this inequality, then we know that it reaches its maximum for some value θ_o in $[0, 2\pi)$. At this maximum, it suffices to choose $z_k = e^{-jk\theta_o}$ to transform (3.71) into an equality. It follows that condition b3) is satisfied if and only if this maximum is strictly less than one, and this is equivalent to condition 2) of Theorem 3.9. ♣

3.5.3 Some Extensions

We focus on the Hurwitz stability case below, but similar results obviously hold for the Schur case.

1) **Case of real centers:** In the case where the discs D_j are centered on the real axis, that is when $\beta(s)$ is a polynomial with real coefficients, then $g_1(s)$ and $g_2(s)$ have the same H_∞-norm, and therefore one has to check the norm of only one rational function.

2) **Maximal Hurwitz disc families:** Consider a stable nominal polynomial

$$\beta^o(s) = \beta_0^o + \beta_1^o s + \cdots + \beta_n^o s^n,$$

and let $r_0, \cdots, r_n$ be $n+1$ fixed real numbers which are greater than or equal to 0. Using our result, it is very easy to find the largest positive number

$\epsilon_{\max}$ of all positive numbers ϵ such that the family of disc polynomials whose coefficients are contained in the open discs with centers β_j^o and of radii ϵr_j, is entirely stable. To do so let:

$$\gamma_1(s) = r_0 - jr_1 s - r_2 s^2 + jr_3 s^3 + r_4 s^4 - jr_5 s^5 - \cdots,$$
$$\gamma_2(s) = r_0 + jr_1 s - r_2 s^2 - jr_3 s^3 + r_4 s^4 + jr_5 s^5 - \cdots,$$

and form

$$g_1(s) = \frac{\gamma_1(s)}{\beta^o(s)}, \qquad g_2(s) = \frac{\gamma_2(s)}{\beta^o(s)}.$$

Now, if $\|g_1\|_\infty = \eta_1$ and $\|g_2\|_\infty = \eta_2$, then

$$\epsilon_{\max} = \min\left(\frac{1}{\eta_1}, \frac{1}{\eta_2}\right).$$

The quantities η_1 and η_2 can of course be found from the polar plots of $g_1(j\omega)$ and $g_2(j\omega)$ respectively.

We illustrate the above results with an example.

Example 3.4. Consider the nominal polynomial

$$\beta^o(s) = (2 - j3.5) + (1.5 - j6)s + (9 - j27)s^2 + (3.5 - j18)s^3 + (-1 - j11)s^4$$

Suppose that each coefficient δ_i perturbs inside a corresponding disc with radius r_i and

$$r_0 = 2, \quad r_1 = 1, \quad r_2 = 8, \quad r_3 = 3, \quad r_4 = 1.$$

We want to check the robust Hurwitz stability of this family of disc polynomials. We first verify the stability of the nominal polynomial. It is found that $\beta^o(s)$ has roots at

$$-0.4789 - j1.5034, \quad -0.9792 + j1.0068, \quad -0.1011 + j0.4163, \quad -0.0351 - j0.3828\ .$$

and is therefore Hurwitz. Now form

$$\begin{aligned}\gamma_1(s) &= r_0 - jr_1 s - r_2 s^2 + jr_3 s^3 + r_4 s^4 \\ &= 2 - js - 8s^2 + j3s^3 + s^4 \\ \gamma_2(s) &= r_0 + jr_1 s - r_2 s^2 - jr_3 s^3 + r_4 s^4 \\ &= 2 + js - 8s^2 - j3s^3 + s^4,\end{aligned}$$

and

$$g_1(s) = \frac{\gamma_1(s)}{\beta^o(s)} \quad \text{and} \quad g_2(s) = \frac{\gamma_2(s)}{\beta^o(s)}.$$

From the frequency plot of $g_i(j\omega)$ (Figure 3.9) we can see that $\|g_1\|, \|g_2\| > 1$. Thus the condition of Theorem 3.8 is violated. Therefore, the given disc polynomial family contains unstable elements.

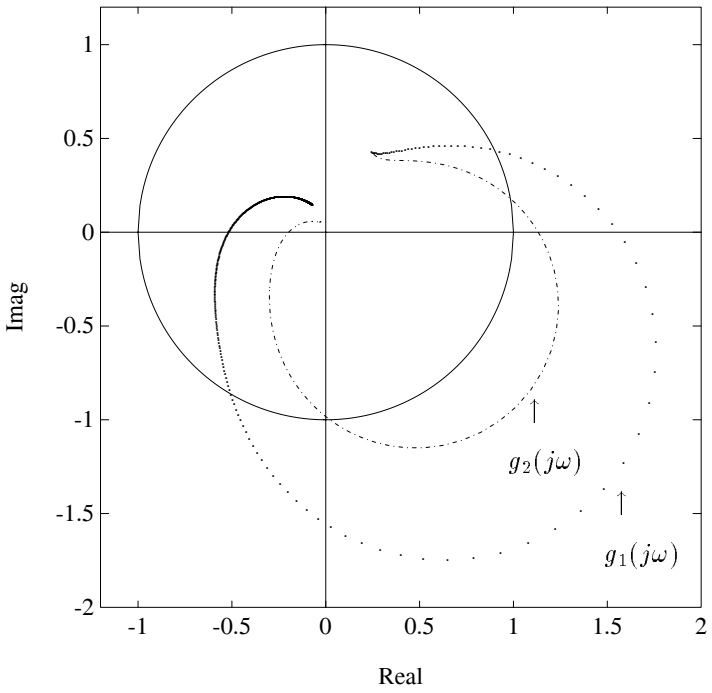

Figure 3.9. $g_1(j\omega)$ and $g_2(j\omega)$ (unstable family: Example 3.4)

Now suppose we want to proportionally reduce the size of the discs so that the resulting smaller family becomes robustly stable. We compute

$$\|g_1\|_\infty = 2.0159 := \eta_1 \quad \text{and} \quad \|g_2\|_\infty = 1.3787 := \eta_2$$

and we have

$$\epsilon_{\max} = \min\left(\frac{1}{\eta_1}, \frac{1}{\eta_2}\right) = 0.4960 \ .$$

We now modify the radii of discs to $\hat{r}_i = \epsilon_{\max} r_i$ for $i = 0, 1, 2, 3, 4$. Consequently,

$$\hat{\gamma}_1(s) = 0.9921 - j0.4961s - 3.9684s^2 + j1.4882s^3 + 0.4961s^4$$
$$\hat{\gamma}_2(s) = 0.9921 + j0.4961s - 3.9684s^2 - j1.4882s^3 + 0.4961s^4,$$

and

$$\hat{g}_1(s) = \frac{\hat{\gamma}_1(s)}{\beta^o(s)} \quad \text{and} \quad \hat{g}_2(s) = \frac{\hat{\gamma}_2(s)}{\beta^o(s)}.$$

Figure 3.10 shows that $\|g_1\|_\infty < 1$ and $\|g_2\|_\infty < 1$ which verifies the robust stability of the disc polynomial family with the adjusted disc radii.

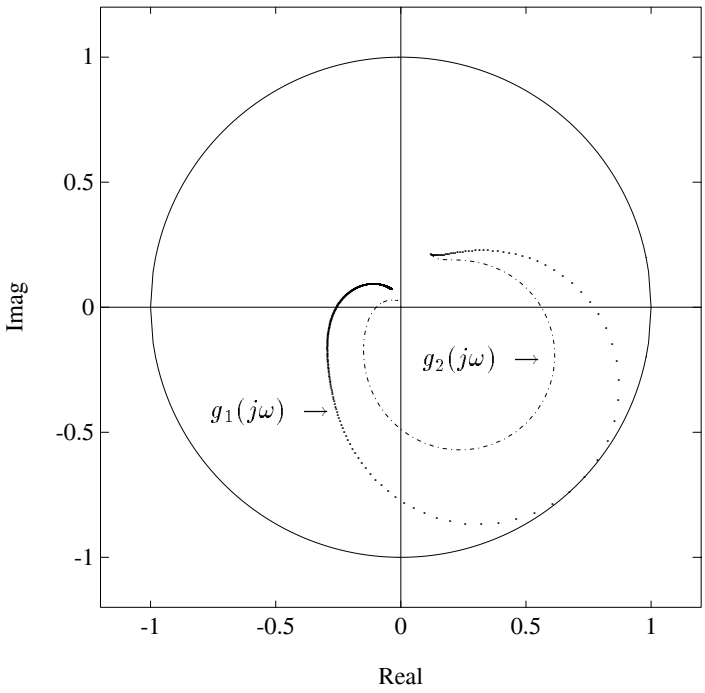

Figure 3.10. $\hat{g}_1(j\omega)$ and $\hat{g}_2(j\omega)$ (stable family: Example 3.4)

3.6 EXERCISES

3.1 Calculate the radius of the Hurwitz stability ball in the coefficient space for each of the polynomials

a) $(s+1)^3$

b) $(s+2)^3$

c) $(s+3)^3$

d) $(s+1)(s^2+s+1)$

e) $(s+2)(s^2+s+1)$

f) $(s+1)(s^2+2s+2)$

g) $(s+2)(s^2+2s+2)$

considering both the cases where the leading coefficient is fixed and subject to perturbation.

3.2 Derive a closed form expression for the radius of the Hurwitz stability ball for the polynomial $a_2 s^2 + a_1 s + a_0$.

3.3 Calculate the radius of the Schur stability ball in the coefficient space for the polynomials

a) $z^3(z + 0.5)^3$

b) $(z - 0.5)^3$

c) $z(z^2 + z + 0.5)$

d) $z(z + 0.5)(z - 0.5)$

e) $z(z^2 - z + 0.5)$

f) $z^2(z + 0.5)$

considering both the cases where the leading coefficient is fixed and where it is subject to perturbation.

3.4 Consider the feedback system shown in Figure 3.11. The characteristic poly-

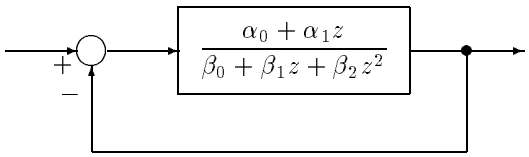

Figure 3.11. Feedback control system

nomial of the closed loop system is

$$\begin{aligned}\delta(z) &= (\alpha_0 + \beta_0) + (\alpha_1 + \beta_1)z + \beta_2 z^2 \\ &= \delta_0 + \delta_1 z + \delta_2 z^2\end{aligned}$$

with nominal value

$$\delta^0(z) = \frac{1}{2} - z + z^2.$$

Find $\epsilon_{\max}$ so that with $\delta_i \in [\delta_i^0 - \epsilon, \delta_i^0 + \epsilon]$ the closed loop system is robustly Schur stable.
Answer: $\epsilon_{\max} = 0.17$.

3.5 Consider the feedback system shown in Figure 3.12.

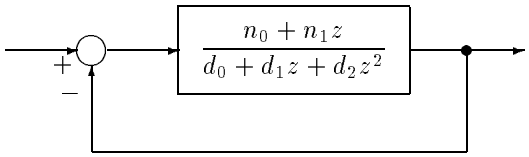

Figure 3.12. Feedback control system

Assume that the nominal values of the coefficients of the transfer function are

$$\left[n_0^0, n_1^0\right] = [-1, 2] \quad \text{and} \quad [d_0, d_1, d_2] = [-1, -2, 8].$$

Now let

$$n_i \in [n_i^0 - \epsilon, n_i^0 + \epsilon] \quad \text{and} \quad d_j \in [d_j^0 - \epsilon, d_j^0 + \epsilon]$$

and find $\epsilon_{\max}$ for robust Schur stability.
Answer: $\epsilon_{\max} = 1.2$.

3.6 Consider the third degree polynomial $P_r(s)$ given by

$$P_r(s) = \left(s - re^{j\frac{3\pi}{4}}\right)(s + r)\left(s - re^{j\frac{5\pi}{4}}\right).$$

In other words, the roots of $P_r(s)$ are equally distributed on the left-half of the circle of radius r in the complex plane. Now, let $m(r)$ be the sum of the squares of the coefficients of $P_r(s)$. One can easily compute that

$$m(r) = 2\left(1 + \sqrt{2}r + 2r^2 + \sqrt{2}r^3 + r^4\right).$$

We consider the normalized polynomial,

$$\delta_r(s) = \frac{1}{\sqrt{m(r)}} P_r(s).$$

Compute

$$\rho(r) = \inf_{\omega > 0} d_\omega(\delta_r),$$

for increasing values of r and plot $\rho(r)$ as a function of r.

3.7 In the Schur case consider the third degree polynomial $P_r(z)$ given by

$$P_r(z) = \left(z - re^{j\frac{2\pi}{3}}\right)\left(z - re^{j\frac{4\pi}{3}}\right)(z - r).$$

In other words, the roots of $P_r(s)$ are equally distributed on the circle of radius r in the complex plane. Again, let $m(r)$ be the sum of the squares of the coefficients of $P_r(z)$, and consider the normalized polynomial,

$$\delta_r(z) = \frac{1}{\sqrt{m(r)}} P_r(z).$$

Compute

$$\rho(r) = \inf_{\theta > 0} d_\theta(\delta_r),$$

for increasing values of r $(0 \leq r < 1)$ and plot $\rho(r)$ as a function of r.

3.8 The purpose of this problem is to calculate the distance $d_\omega(P)$ for different choices of norms on $\mathcal{P}_n$, the vector space of all real polynomials of degree less than or equal to n.

As usual we identify $\mathcal{P}_n$ with $\mathbb{R}^{n+1}$. Let $\|\cdot\|$ be a given norm on $\mathcal{P}_n$. For a fixed $\omega > 0$, we denote by Δ_ω the subspace of $\mathcal{P}_n$ which consists of all polynomials $\delta(s)$ which satisfy: $\delta(j\omega) = 0$. Let $P(s)$ be an arbitrary but fixed element of $\mathcal{P}_n$. We then define,

$$d_\omega(P) = \inf_{\delta \in \Delta_\omega} \|P - \delta\|.$$

1) Compute $d_\omega(P)$ when $\|\cdot\|$ is the ℓ_∞ norm $\|\cdot\|_\infty$, that is,

$$\|\delta_0 + \delta_1 s + \cdots + \delta_n s^n\|_\infty = \max_{0 \leq k \leq n} |\delta_k| \ .$$

2) Compute $d_\omega(P)$ when $\|\cdot\|$ is the ℓ_1 norm $\|\cdot\|_1$, that is,

$$\|\delta_0 + \delta_1 s + \cdots + \delta_n s^n\|_1 = \sum_{k=0}^{n} |\delta_k|.$$

3) More generally, compute $d_\omega(P)$ when $\|\cdot\|$ is the ℓ_p norm $\|\cdot\|_p$ $(1 < p < +\infty)$, that is,

$$\|\delta_0 + \delta_1 s + \cdots + \delta_n s^n\|_p = \left(\sum_{k=0}^{n} |\delta_k|^p \right)^{\frac{1}{p}} .$$

Hint: In all cases use the following result of Banach space theory, which plays an essential role in the study of extremal problems. Let X be an arbitrary Banach space and let $\|\cdot\|$ denote the norm on X. Let also M be a closed subspace of X. Then for any fixed x in X we have,

$$\inf_{m \in M} \|x - m\| = \max_{x^* \in M^\perp} | < x^*, x > |$$

where "max" indicates that the supremum is attained and where $M^\perp$ is the *annihilator* of M, that is the subspace of X^* which consists of all linear functionals x^* which satisfy,

$$\forall \quad m \in M, \quad < x^*, m >= 0.$$

Note that in general for $1 \leq p \leq +\infty$,

$$(\mathbb{R}^n, \|\cdot\|_p)^* = (\mathbb{R}^n, \|\cdot\|_q)$$

where q is the *conjugate* of p which is defined by

$$\frac{1}{p} + \frac{1}{q} = 1.$$

3.9 Repeat Exercise 3.8, but this time to calculate $d_\theta(P)$ where $\theta \in (0, \pi)$ and

$$d_\theta(P) = \inf_{\delta \in \Delta_\theta} \|P - \delta\|.$$

Here Δ_θ designates the subspace of $\mathcal{P}_n$ consisting of all polynomials $\delta(s)$ which are such that $\delta(e^{j\theta}) = 0$.

3.10 Prove the distance formulas in Theorems 3.6.

3.11 Consider the standard unity feedback control system with transfer functions $G(s)$ and $C(s)$ in the forward path. Let

$$G(s) = \frac{p_0 + p_1 s}{s^2(s + q_0)} \quad \text{and} \quad C(s) = 1.$$

Determine the stability margin in the space of parameters (p_0, p_1, q_0) assuming the nominal value $(p_0^0, p_1^0, q_0^0) = (1, 1, 2)$.

3.12 Using the Tsypkin-Polyak locus calculate the weighted ℓ_1, ℓ_2 and ℓ_∞ stability margins in the coefficient space for the polynomial

$$\delta(s) = s^4 + 6s^3 + 13s^2 + 12s + 4$$

choosing the weights proportional to the magnitude of each nominal value.

3.13 For the nominal polynomial

$$\delta(s) = s^3 + 5s^2 + (3 - j)s + 6 - 2j$$

find the largest number $\epsilon_{\max}$ such that all polynomials with coefficients centered at the nominal value and of radius $\epsilon_{\max}$ are Hurwitz stable.

3.14 Consider a feedback control system with the plant transfer function

$$G(s) = \frac{n_0 + n_1 s + \cdots + n_{n-1} s^{n-1} + n_n s^n}{d_0 + d_1 s + \cdots + d_{n-1} s^{n-1} + d_n s^n}$$

and the controller transfer function

$$C(s) = \frac{b_0 + b_1 s + \cdots + b_{m-1} s^{m-1} + b_m s^m}{a_0 + a_1 s + \cdots + a_{m-1} s^{m-1} + a_m s^m}.$$

Let $\delta(s)$ be the closed loop characteristic polynomial with coefficients

$$\underline{\delta} := \begin{bmatrix} \delta_0 & \delta_1 & \cdots & \delta_{n+m-1} & \delta_{n+m} \end{bmatrix}^T$$

and let $x := [b_0 \;\; b_1 \;\; \cdots \;\; b_m \;\; a_0 \;\; a_1 \;\; \cdots \;\; a_m]^T$. Then we can write $\delta = M_p x$ where

$$M_p := \underbrace{\begin{bmatrix} d_0 & & & n_0 & & \\ d_1 & d_0 & & n_1 & n_0 & \\ d_2 & d_1 & \ddots & n_2 & n_1 & \ddots \\ \vdots & d_2 & & \vdots & n_2 & \\ \vdots & \vdots & & \vdots & \vdots & \\ d_n & \vdots & & n_n & \vdots & \\ & d_n & & & n_n & \\ & & \ddots & & & \ddots \end{bmatrix}}_{M_p \in \mathbf{R}^{(n+m+1) \times 2(m+1)}}.$$

Prove that x stabilizes the plant if there exists δ such that

$$d(\delta, M_p) < \rho(\delta)$$

where $\rho(\delta)$ is the Euclidean radius of the largest stability hypersphere centered at δ and $d(\delta, M_p)$ is the Euclidean distance between δ and the subspace spanned by the columns of M_p.

3.7 NOTES AND REFERENCES

The ℓ_2 stability hypersphere in coefficient space was first calculated by Soh, Berger and Dabke [214]. Here we have endeavored to present this result for both the Hurwitz and Schur cases in its greatest generality. The calculation of the ℓ_p stability ball is due to Tsypkin and Polyak [225]. These calculations have been extended to the case of complex polynomials by Kogan [149] and bivariate polynomials by Polyak and Shmulyian [191]. A simplified proof of the Tsypkin-Polyak locus has been given by Mansour [170]. The problem of ascertaining the robust stability of disc polynomials was formulated and solved in Chapellat, Dahleh and Bhattacharyya [61]. Exercise 3.14 is taken from Bhattacharyya, Keel and Howze [34].

Chapter 4

THE PARAMETRIC STABILITY MARGIN

In this chapter we extend the stability ball calculation developed in Chapter 3 to accommodate *interdependent* perturbations among the polynomial coefficients. This is the usual situation that one encounters in control systems containing uncertain parameters. We calculate the radius of the largest stability ball in the space of real parameters under the assumption that these uncertain parameters enter the characteristic polynomial coefficients *linearly or affinely*. This radius serves as a quantitative measure of the real parametric stability margin for control systems. Both *ellipsoidal* and *polytopic* uncertainty regions are considered. Examples are included to illustrate the calculation of the parametric stability margin for continuous time and discrete time control systems and also those containing time delay. In the polytopic case we establish the stability testing property of the *exposed edges* and some *extremal properties* of edges and vertices. These are useful for calculating the *worst case stability margin* over an given uncertainty set which in turn is a measure of the *robust performance* of the system. The graphical Tsypkin-Polyak plot for stability margin calculation (parameter space version) and the theory of linear disc polynomials are described.

4.1 INTRODUCTION

In Chapter 3 we calculated the radius of the stability ball for a family of real polynomials in the space of the polynomial coefficients. The underlying assumption was that these coefficients could perturb *independently*. This assumption is rather restrictive. In control problems, the characteristic polynomial coefficients do not in general perturb independently. At the first level of detail every feedback system is composed of at least two subsystems, namely controller and plant connected in a feedback loop. The characteristic polynomial coefficients of such a system is a function of plant parameters and controller parameters. Although both parameters influence the coefficients, the nature of the two sets of parameters are quite different. The plant contains parameters that are subject to uncontrolled variations

depending on the physical operating conditions, disturbances, modeling errors, etc. The controller parameters on the other hand, are often fixed during the operation of the system. However, at the design stage, they are also uncertain parameters to be chosen.

Consider the standard feedback system shown in Figure 4.1.

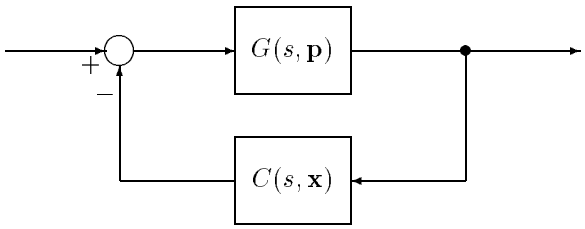

Figure 4.1. Standard feedback system with parameters

Suppose that the plant transfer function contains the real parameter vector $\mathbf{p}$ and the controller is characterized by the real vector $\mathbf{x}$. Let these transfer functions be respectively

$$G(s) = G(s, \mathbf{p}), \qquad C(s) = C(s, \mathbf{x}).$$

The parameter vector $\mathbf{p}$ specifies the plant completely and the choice of the vector $\mathbf{x}$ likewise uniquely determines the controller $C(s)$.

The Parametric Stability Margin

Suppose that $\mathbf{p}^0$ denotes the nominal value of the plant parameter vector $\mathbf{p}$. Consider a *fixed* controller $C^0(s)$, with parameter $\mathbf{x}^0$, which stabilizes the nominal plant $G(s, \mathbf{p}^0)$. Now let $\Delta\mathbf{p} = \mathbf{p} - \mathbf{p}^0$ denote a perturbation of the plant parameter vector from the nominal $\mathbf{p}^0$. A natural question that occurs now is: How large can the perturbation $\mathbf{\Delta p}$ be, without destroying closed loop stability? A bound on the size of $\mathbf{\Delta p}$ for which closed loop stability is guaranteed is useful as it provides us with a ball in parameter space within which the parameters can freely vary without destroying closed loop stability. An even more useful quantity to know is the *maximal* size of such a stability ball. Besides providing us with a nonconservative evaluation of the size of the stability region, this would also also serve as a bona fide measure of the performance of the controller $C^0(s)$. Accordingly the *parametric stability margin* is defined as the length of the smallest perturbation $\Delta\mathbf{p}$ which destabilizes the closed loop. This margin serves as a quantitative measure of the robustness of the closed system with respect to parametric uncertainty evaluated at the nominal point $\mathbf{p}^0$. It is useful in controller *design* as a means of comparing the performance of proposed controllers.

The determination of the parametric stability margin is the problem that one faces in robustness analysis. This problem can be solved with $\mathbf{p}$ fixed at the nominal point $\mathbf{p}^0$ or with $\mathbf{p}$ lying in a prescribed uncertainty set Ω. In the latter case it is desirable to find the *worst case stability margin* over the uncertainty set. This worst case margin is a measure of the worst case *performance* of the controller $\mathbf{x}^0$ over Ω. This is regarded also as a measure of the *robust performance* of the controller and can also be the basis of comparison of two proposed controllers.

In synthesis or design problems one is faced with the task of choosing the controller parameter $\mathbf{x}$ to *increase* or *maximize* these margins. In addition control design involves several other issues such as tolerance of unstructured uncertainty and nonlinearities, quality of transient response, integrity against loop failures, and boundedness of various signal levels in the closed loop system. Because of the complexity and interrelatedness of these issues it is probably tempting to treat the entire design exercise as an optimization problem with various mathematical constraints reflecting the physical requirements. In the control literature this approach has been developed in recent years, to a high level of sophistication, with the aid of the Youla parametrization of all stabilizing controllers. The latter parametrization allowed for the systematic search over the set of all stabilizing controllers to achieve performance objectives such as H_∞ norm or ℓ_1 norm optimization. However relatively little progress has been made with this approach in the sphere of control problems involving real parametric stability margins and also in problems where the controller has a fixed number of adjustable parameters.

In this chapter we deal only with the real parametric stability margin. Even in this apparently simple case the analysis and synthesis problems mentioned above are unsolved problems in general. In the special case where the parameters enter the characteristic polynomial coefficients in an affine *linear* or *multilinear* fashion the problem of calculating the real parametric stability margin now has neat solutions. Fortunately, both these cases fit nicely into the framework of control system problems. In the present chapter, we deal with the linear (including affine) case where an exact calculation of the parametric stability margin can be given. The multilinear case will be dealt with in Chapters 10 and 11. The calculation of stability margins for systems subject to both parametric and unstructured perturbations will be treated in Chapter 9.

The Linear Case

The characteristic polynomial of the standard closed loop system in Figure 4.1 can be expressed as

$$\delta(s, \mathbf{x}, \mathbf{p}) = \sum_{i=0}^{n} \delta_i(\mathbf{x}, \mathbf{p}) s^i.$$

As an example suppose that the plant and controller transfer functions, denoted respectively by $G(s, \mathbf{p})$ and $C(s, \mathbf{x})$ are:

$$G(s, \mathbf{p}) := \frac{p_3}{s^2 + p_1 s + p_2}, \qquad C(s, \mathbf{x}) := \frac{x_3}{x_1 s + x_2}.$$

Then the characteristic polynomial of the closed loop system is

$$\delta(s,\mathbf{x},\mathbf{p}) = \underbrace{x_1}_{\delta_3(\mathbf{x},\mathbf{p})} s^3 + \underbrace{(p_1x_1 + x_2)}_{\delta_2(\mathbf{x},\mathbf{p})} s^2 + \underbrace{(p_2x_1 + p_1x_2)}_{\delta_1(\mathbf{x},\mathbf{p})} s + \underbrace{(p_2x_2 + p_3x_3)}_{\delta_0(\mathbf{x},\mathbf{p})}.$$

For fixed values of the plant parameter $\mathbf{p}$, we see that the coefficients of the characteristic polynomial are linear functions of the controller parameter $\mathbf{x}$:

$$\begin{bmatrix} 1 & 0 & 0 \\ p_1 & 1 & 0 \\ p_2 & p_1 & 0 \\ 0 & p_2 & p_3 \end{bmatrix} \begin{bmatrix} x_1 \\ x_2 \\ x_3 \end{bmatrix} = \begin{bmatrix} \delta_3(\mathbf{x}) \\ \delta_2(\mathbf{x}) \\ \delta_1(\mathbf{x}) \\ \delta_0(\mathbf{x}) \end{bmatrix}.$$

Similarly, for fixed values of the controller parameter $\mathbf{x}$, the coefficients of the characteristic polynomial are linear functions of the plant parameter $\mathbf{p}$ as follows:

$$\begin{bmatrix} 0 & 0 & 0 \\ x_1 & 0 & 0 \\ x_2 & x_1 & 0 \\ 0 & x_2 & x_3 \end{bmatrix} \begin{bmatrix} p_1 \\ p_2 \\ p_3 \end{bmatrix} + \begin{bmatrix} x_1 \\ x_2 \\ 0 \\ 0 \end{bmatrix} = \begin{bmatrix} \delta_3(\mathbf{p}) \\ \delta_2(\mathbf{p}) \\ \delta_1(\mathbf{p}) \\ \delta_0(\mathbf{p}) \end{bmatrix}.$$

The characteristic polynomial can also be written in the following forms:

$$\begin{aligned} \delta(s,\mathbf{p}) &= \underbrace{(x_1s^2 + x_2s)}_{a_1(s)}p_1 + \underbrace{(x_1s + x_2)}_{a_2(s)}p_2 + \underbrace{x_3}_{a_3(s)}p_3 + \underbrace{(x_1s^3 + x_2s^2)}_{b(s)} \\ &= \underbrace{(x_1s + x_2)}_{F_1(s)}\underbrace{(s^2 + p_1s + p_2)}_{P_1(s)} + \underbrace{x_3}_{F_2(s)}\underbrace{p_3}_{P_2(s)}. \end{aligned}$$

Motivated by this we will consider in this chapter the case where the controller $\mathbf{x}$ is fixed and therefore $\delta_i(\mathbf{x},\mathbf{p})$ are linear functions of the parameters $\mathbf{p}$. We will sometimes refer to this simply as the linear case. Therefore, we will consider the characteristic polynomial of the form

$$\delta(s,\mathbf{p}) = a_1(s)p_1 + a_2(s)p_2 + \cdots + a_l(s)p_l + b(s) \tag{4.1}$$

where $a_i(s)$, $i = 1, 2, \cdots, l$ and $b(s)$ are fixed polynomials and p_1, p_2, $\cdots$, p_l are the uncertain parameters. We will also develop results for the following form of the characteristic polynomial:

$$\delta(s,\mathbf{p}) = F_1(s)P_1(s) + F_2(s)P_2(s) + \cdots + F_m(s)P_m(s) \tag{4.2}$$

wherein the $F_i(s)$ are fixed and the coefficients of $P_i(s)$ are the uncertain parameters. The uncertain parameters will be allowed to lie in a set Ω which could be ellipsoidal or box-like.

The problems of interest will be: Are all characteristic polynomials corresponding to the parameter set Ω, stable? How large can the set Ω be without losing

stability? What is the smallest value (worst case) of the stability margin over a given uncertainty set Ω? How do we determine the stability margin if time delays are also present in the system of Figure 4.1? We shall provide constructive solutions to these questions in this chapter. We start in the next section with a characterization of the stability ball in parameter space based on the Boundary Crossing Theorem.

4.2 THE STABILITY BALL IN PARAMETER SPACE

In this section we give a useful characterization of the parametric stability margin in the general case. This can be done by finding the largest stability ball in parameter space, centered at a "stable" nominal parameter value $\mathbf{p}^0$. Let $\mathcal{S} \subset \mathcal{C}$ denote as usual an open set which is symmetric with respect to the real axis. $\mathcal{S}$ denotes the stability region of interest. In continuous-time systems $\mathcal{S}$ may be the open left half plane or subsets thereof. For discrete-time systems $\mathcal{S}$ is the open unit circle or a subset of it. Now let $\mathbf{p}$ be a vector of real parameters,

$$\mathbf{p} = [p_1, p_2, \cdots, p_l]^T.$$

The characteristic polynomial of the system is denoted by

$$\delta(s, \mathbf{p}) = \delta_n(\mathbf{p})s^n + \delta_{n-1}(\mathbf{p})s^{n-1} + \cdots + \delta_0(\mathbf{p}).$$

The polynomial $\delta(s, \mathbf{p})$ is a real polynomial with coefficients that depend continuously on the real parameter vector $\mathbf{p}$. We suppose that for the *nominal parameter* $\mathbf{p} = \mathbf{p}^0$, $\delta(s, \mathbf{p}^0) := \delta^0(s)$ is stable with respect to $\mathcal{S}$ (has its roots in $\mathcal{S}$). Write

$$\triangle\mathbf{p} := \mathbf{p} - \mathbf{p}^0 = [p_1 - p_1^0, p_2 - p_2^0, \cdots, p_l - p_l^0]$$

to denote the perturbation in the parameter $\mathbf{p}$ from its nominal value $\mathbf{p}^0$. Now let us introduce a norm $\|\cdot\|$ in the space of the parameters $\mathbf{p}$ and introduce the open ball of radius ρ

$$\mathcal{B}(\rho, \mathbf{p}^0) = \{\mathbf{p} : \|\mathbf{p} - \mathbf{p}^0\| < \rho\}. \tag{4.3}$$

The hypersphere of radius ρ is defined by

$$\mathcal{S}(\rho, \mathbf{p}^0) = \{\mathbf{p} : \|\mathbf{p} - \mathbf{p}^0\| = \rho\}. \tag{4.4}$$

With the ball $\mathcal{B}(\rho, \mathbf{p}^0)$ we associate the family of uncertain polynomials:

$$\mathbf{\Delta}_\rho(s) := \{\delta(s, \mathbf{p}^0 + \Delta\mathbf{p}) : \|\Delta\mathbf{p}\| < \rho\}. \tag{4.5}$$

Definition 4.1. The *real parametric stability margin* in parameter space is defined as the radius, denoted $\rho^*(\mathbf{p}^0)$, of the *largest* ball centered at $\mathbf{p}^0$ for which $\delta(s, \mathbf{p})$ remains stable whenever $\mathbf{p} \in \mathcal{B}(\rho^*(\mathbf{p}^0), \mathbf{p}^0)$.

This stability margin then tells us how much we can perturb the original parameter $\mathbf{p}^0$ and yet remain stable. Our first result is a characterization of this maximal stability ball. To simplify notation we write ρ^* instead of $\rho^*(\mathbf{p}^0)$.

Theorem 4.1 *With the assumptions as above the parametric stability margin ρ^* is characterized by:*

a) There exists a largest stability ball $\mathcal{B}(\rho^*, \mathbf{p}^0)$ centered at $\mathbf{p}^0$, with the property that:

a1) For every $\mathbf{p}'$ within the ball, the characteristic polynomial $\delta(s, \mathbf{p}')$ is stable and of degree n.

a2) At least one point $\mathbf{p}''$ on the hypersphere $\mathcal{S}(\rho^*, \mathbf{p}^0)$ itself is such that $\delta(s, \mathbf{p}'')$ is unstable or of degree less than n.

b) Moreover if $\mathbf{p}''$ is any point on the hypersphere $\mathcal{S}(\rho^*, \mathbf{p}^0)$ such that $\delta(s, \mathbf{p}'')$ is unstable, then the unstable roots of $\delta(s, \mathbf{p}'')$ can only be on the stability boundary.

The proof of this theorem is identical to that of Theorem 3.1 of Chapter 3 and is omitted. It is based on continuity of the roots on the parameter $\mathbf{p}$. This theorem gives the first simplification for the calculation of the parametric stability margin ρ^*. It states that to determine ρ^* it suffices to calculate the minimum "distance" of $\mathbf{p}^0$ from the set of those points $\mathbf{p}$ which endow the characteristic polynomial with a root on the stability boundary, or which cause loss of degree. This last calculation can be carried out using the complex plane image of the family of polynomials $\mathbf{\Delta}_\rho(s)$ evaluated along the stability boundary. We will describe this in the next section.

The parametric stability margin or distance to instability is measured in the norm $\|\cdot\|$, and therefore the numerical value of ρ^* will depend on the specific norm chosen. We will consider, in particular, the weighted ℓ_p norms. These are defined as follows: Let $w = [w_1, w_2, \cdots, w_l]$ with $w_i > 0$ be a set of positive *weights*.

$$\begin{aligned}
\ell_1 \text{ norm} &: \quad \|\Delta\mathbf{p}\|_1^w := \sum_{i=1}^{l} w_i |\Delta p_i| \\
\ell_2 \text{ norm} &: \quad \|\Delta\mathbf{p}\|_2^w := \sqrt{\sum_{i=1}^{l} w_i^2 \Delta p_i^2} \\
\ell_p \text{ norm} &: \quad \|\Delta\mathbf{p}\|_p^w := \left[\sum_{i=1}^{l} |w_i \Delta p_i|^p\right]^{\frac{1}{p}} \\
\ell_\infty \text{ norm} &: \quad \|\Delta\mathbf{p}\|_\infty^w := \max_i w_i |\Delta p_i|.
\end{aligned}$$

We will write $\|\Delta\mathbf{p}\|$ to refer to a generic weighted norm when the weight and type of norm are unimportant.

4.3 THE IMAGE SET APPROACH

The parametric stability margin may be calculated by using the complex plane image of the polynomial family $\mathbf{\Delta}_\rho(s)$ evaluated at each point on the stability boundary $\partial\mathcal{S}$. This is based on the following idea. Suppose that the family has constant degree n and $\delta(s,\mathbf{p}^0)$ is stable but $\mathbf{\Delta}_\rho(s)$ contains an unstable polynomial. Then the continuous dependence of the roots on $\mathbf{p}$ and the Boundary Crossing Theorem imply that there must also exist a polynomial in $\mathbf{\Delta}_\rho(s)$ such that it has a root, at a point, s^*, on the stability boundary $\partial\mathcal{S}$. In this case *the complex plane image set* $\mathbf{\Delta}_\rho(s^*)$ *must contain the origin of the complex plane.* This suggests that to detect the presence of instability in a family of polynomials of constant degree, we generate the image set of the family at each point of the stability boundary and determine if the origin is included in or excluded from this set. This fact was stated in Chapter 1 as the Zero Exclusion Principle, and we repeat it here for convenience.

Theorem 4.2 (Zero Exclusion Principle)
For given $\rho \geq 0$ and $\mathbf{p}^0$, suppose that the family of polynomials $\mathbf{\Delta}_\rho(s)$ is of constant degree and $\delta(s,\mathbf{p}^0)$ is stable. Then every polynomial in the family $\mathbf{\Delta}_\rho(s)$ is stable with respect to $\mathcal{S}$ if and only if the complex plane image set $\mathbf{\Delta}_\rho(s^*)$ excludes the origin for every $s^* \in \partial\mathcal{S}$.

Proof. As stated earlier this is simply a consequence of the continuity of the roots of $\delta(s,\mathbf{p})$ on $\mathbf{p}$ and the Boundary Crossing Theorem (Chapter 1). ♣

In fact, the above can be used as a computational tool to determine the maximum value ρ^* of ρ for which the family is stable. If $\delta(s,\mathbf{p}^0)$ is stable, it follows that there always exists an open stability ball around $\mathbf{p}^0$ since the stability region $\mathcal{S}$ is itself open. Therefore, for small values of ρ the image set $\mathbf{\Delta}_\rho(s^*)$ will exclude the origin for every point $s^* \in \partial\mathcal{S}$. As ρ is increased from zero, a *limiting* value ρ_0 may be reached where some polynomial in the corresponding family $\mathbf{\Delta}_{\rho_0}(s)$ loses degree or a polynomial in the family acquires a root s^* on the stability boundary. From Theorem 4.1 it is clear that this value ρ_0 is equal to ρ^*, the stability margin. In case the limiting value ρ_0 is never achieved, the stability margin ρ^* is infinity.

An alternative way to determine ρ^* is as follows: Fixing s^* at a point in the boundary of $\mathcal{S}$, let $\rho_0(s^*)$ denote the limiting value of ρ such that $0 \in \mathbf{\Delta}_\rho(s^*)$:

$$\rho_0(s^*) := \inf\{\rho : 0 \in \mathbf{\Delta}_\rho(s^*)\}.$$

Then, we define

$$\rho_b = \inf_{s^* \in \partial\mathcal{S}} \rho_0(s^*).$$

In other words, ρ_b is the limiting value of ρ for which some polynomial in the family $\mathbf{\Delta}_\rho(s)$ *acquires a root on the stability boundary* $\partial\mathcal{S}$. Also let the limiting value of ρ for which some polynomial in $\mathbf{\Delta}_\rho(s)$ *loses degree* be denoted by ρ_d:

$$\rho_d := \inf\left\{\rho : \delta_n(\mathbf{p}^0 + \Delta\mathbf{p}) = 0, \quad \|\Delta\mathbf{p}\| < \rho\right\}.$$

We have established the following theorem.

Theorem 4.3 *The parametric stability margin*

$$\rho^* = \min\{\rho_b, \rho_d\}.$$

Remark 4.1. We note that this theorem remains valid even when the stability region $\mathcal{S}$ is not connected. For instance, one may construct the stability region as a union of disconnected regions $\mathcal{S}_i$ surrounding each root of the nominal polynomial. In this case the stability boundary must also consist of the union of the individual boundary components $\partial\mathcal{S}_i$. The functional dependence of the coefficients δ_i on the parameters $\mathbf{p}$ is also not restricted in any way except for the assumption of continuity.

The above theorem shows that the problem of determining ρ^* can be reduced to the following steps:

A) determine the "local" stability margin $\rho(s^*)$ at each point s^* on the boundary of the stability region,

B) minimize the function $\rho(s^*)$ over the entire stability boundary and thus determine ρ_b

C) calculate ρ_d, and set

D) $\rho^* = \min\{\rho_b, \rho_d\}$.

In general the determination of ρ^* is a *difficult nonlinear optimization* problem. However, the breakdown of the problem into the steps described above, exploits the structure of the problem and has the advantage that the local stability margin calculation $\rho(s^*)$ with s^* frozen, can be simple. In particular, when the parameters enter linearly into the characteristic polynomial coefficients, this calculation can be done in closed form. It reduces to a least square problem for the ℓ_2 case, and equally simple linear programming or vertex problems for the ℓ_∞ or ℓ_1 cases. The dependence of ρ_b on s^* is in general highly nonlinear but this part of the minimization can be easily performed computationally because sweeping the boundary $\partial\mathcal{S}$ is a *one-dimensional search*. In the next section, we describe and develop this calculation in greater detail.

4.4 STABILITY MARGIN COMPUTATION IN THE LINEAR CASE

We develop explicit formulas for the parametric stability margin in the case in which the characteristic polynomial coefficients depend linearly on the uncertain parameters. In such cases we may write without loss of generality that

$$\delta(s, \mathbf{p}) = a_1(s)p_1 + \cdots + a_l(s)p_l + b(s) \tag{4.6}$$

where $a_i(s)$ and $b(s)$ are real polynomials and the parameters p_i are real. As before, we write $\mathbf{p}$ for the vector of uncertain parameters, $\mathbf{p}^0$ denotes the nominal parameter vector and $\triangle\mathbf{p}$ the perturbation vector. In other words

$$\begin{aligned}\mathbf{p} &= [p_1, p_2, \cdots, p_l] \qquad \mathbf{p}^0 = [p_1^0, p_2^0, \cdots, p_l^0] \\ \triangle\mathbf{p} &= [p_1 - p_1^0, p_2 - p_2^0, \cdots, p_l - p_l^0] \\ &= [\triangle p_1, \triangle p_2, \cdots, \triangle p_l].\end{aligned}$$

Then the characteristic polynomial can be written as

$$\delta(s, \mathbf{p}^0 + \Delta\mathbf{p}) = \underbrace{\delta(s, \mathbf{p}^0)}_{\delta^0(s)} + \underbrace{a_1(s)\triangle p_1 + \cdots + a_l(s)\triangle p_l}_{\triangle\delta(s,\triangle\mathbf{p})}. \tag{4.7}$$

Now let s^* denote a point on the stability boundary $\partial\mathcal{S}$. For $s^* \in \partial\mathcal{S}$ to be a root of $\delta(s, \mathbf{p}^0 + \triangle\mathbf{p})$ we must have

$$\delta(s^*, \mathbf{p}^0) + a_1(s^*)\triangle p_1 + \cdots + a_l(s^*)\triangle p_l = 0. \tag{4.8}$$

We rewrite this equation introducing the weights $w_i > 0$.

$$\delta(s^*, \mathbf{p}^0) + \frac{a_1(s^*)}{w_1} w_1\triangle p_1 + \cdots + \frac{a_l(s^*)}{w_l} w_l\triangle p_l = 0. \tag{4.9}$$

Obviously, the minimum $\|\triangle\mathbf{p}\|^w$ norm solution of this equation gives us $\rho(s^*)$, the calculation involved in step A in the last section.

$$\rho(s^*) = \inf\left\{\|\triangle\mathbf{p}\|^w \;:\; \delta(s^*, \mathbf{p}^0) + \frac{a_1(s^*)}{w_1} w_1\triangle p_1 + \cdots + \frac{a_l(s^*)}{w_l} w_l\triangle p_l = 0\right\}.$$

Similarly, corresponding to loss of degree we have the equation

$$\delta_n(\mathbf{p}^0 + \Delta\mathbf{p}) = 0. \tag{4.10}$$

Letting a_{in} denote the coefficient of the n^{th} degree term in the polynomial $a_i(s)$, $i = 1, 2, \cdots, l$ the above equation becomes

$$\underbrace{a_{1n}p_1^0 + a_{2n}p_2^0 + \cdots + a_{ln}p_l^0}_{\delta_n(\mathbf{p}^0)} + a_{1n}\triangle p_1 + a_{2n}\triangle p_2 + \cdots a_{ln}\triangle p_l = 0. \tag{4.11}$$

We can rewrite this after introducing the weight $w_i > 0$

$$\underbrace{a_{1n}p_1^0 + a_{2n}p_2^0 + \cdots + a_{ln}p_l^0}_{\delta_n(\mathbf{p}^0)} + \frac{a_{1n}}{w_1} w_1\triangle p_1 + \frac{a_{2n}}{w_2} w_2\triangle p_2 + \cdots + \frac{a_{ln}}{w_l} w_l\triangle p_l = 0. \tag{4.12}$$

The minimum norm $\|\triangle\mathbf{p}\|^w$ solution of this equation gives us ρ_d.

We consider the above equations in some more detail. Recall that the polynomials are assumed to be real. The equation (4.12) is real and can be rewritten in the form

$$\underbrace{\begin{bmatrix} \frac{a_{1n}}{w_1} & \cdots & \frac{a_{ln}}{w_l} \end{bmatrix}}_{A_n} \underbrace{\begin{bmatrix} w_1\triangle p_1 \\ \vdots \\ w_l\triangle p_l \end{bmatrix}}_{t_n} = \underbrace{-\delta_n^0}_{b_n}. \tag{4.13}$$

In (4.9), two cases may occur depending on whether s^* is real or complex. If $s^* = s_r$ where s_r is real, we have the single equation

$$\underbrace{\begin{bmatrix} \frac{a_1(s_r)}{w_1} & \cdots & \frac{a_l(s_r)}{w_l} \end{bmatrix}}_{A(s_r)} \underbrace{\begin{bmatrix} w_1\triangle p_1 \\ \vdots \\ w_l\triangle p_l \end{bmatrix}}_{t(s_r)} = \underbrace{-\delta^0(s_r)}_{b(s_r)}. \tag{4.14}$$

Let x_r and x_i denote the real and imaginary parts of a complex number x, i.e.

$$x = x_r + jx_i \qquad \text{with } x_r, x_i \text{ real.}$$

Using this notation, we will write

$$a_k(s^*) = a_{kr}(s^*) + ja_{ki}(s^*)$$

and

$$\delta^0(s^*) = \delta_r^0(s^*) + j\delta_i^0(s^*).$$

If $s^* = s_c$ where s_c is complex, (4.9) is equivalent to two equations which can be written as follows:

$$\underbrace{\begin{bmatrix} \frac{a_{1r}(s_c)}{w_1} & \cdots & \frac{a_{lr}(s_c)}{w_l} \\ \frac{a_{1i}(s_c)}{w_1} & \cdots & \frac{a_{li}(s_c)}{w_l} \end{bmatrix}}_{A(s_c)} \underbrace{\begin{bmatrix} w_1\triangle p_1 \\ \vdots \\ w_l\triangle p_l \end{bmatrix}}_{t(s_c)} = \underbrace{\begin{bmatrix} -\delta_r^0(s_c) \\ -\delta_i^0(s_c) \end{bmatrix}}_{b(s_c)}. \tag{4.15}$$

These equations completely determine the parametric stability margin in any norm. Let $t^*(s_c)$, $t^*(s_r)$, and t_n^* denote the minimum norm solutions of (4.15), (4.14), and (4.13), respectively. Thus,

$$\|t^*(s_c)\| = \rho(s_c) \tag{4.16}$$

$$\|t^*(s_r)\| = \rho(s_r) \tag{4.17}$$

$$\|t_n^*\| = \rho_d. \tag{4.18}$$

If any of the above equations (4.13)-(4.15) do not have a solution, the corresponding value of $\rho(\cdot)$ is set equal to infinity.

Let $\partial\mathcal{S}_r$ and $\partial\mathcal{S}_c$ denote the real and complex subsets of $\partial\mathcal{S}$:

$$\partial\mathcal{S} = \partial\mathcal{S}_r \cup \partial\mathcal{S}_c.$$

$$\rho_r := \inf_{s_r \in \partial\mathcal{S}_r} \rho(s_r)$$
$$\rho_c := \inf_{s_c \in \partial\mathcal{S}_c} \rho(s_c),$$

Therefore,

$$\rho_b = \inf\{\rho_r\,, \rho_c\}. \tag{4.19}$$

We now consider the specific case of the ℓ_2 norm.

4.5 ℓ_2 STABILITY MARGIN

In this section we suppose that the length of the perturbation vector $\triangle\mathbf{p}$ is measured by a weighted ℓ_2 norm. That is, the minimum ℓ_2 norm solution of the equations (4.13), (4.14) and (4.15) are desired. Consider first (4.15). Assuming that $A(s_c)$ has full row rank=2, the minimum norm solution vector $t^*(s_c)$ can be calculated as follows:

$$t^*(s_c) = A^T(s_c)\left[A(s_c)A^T(s_c)\right]^{-1} b(s_c). \tag{4.20}$$

Similarly if (4.14) and (4.13) are consistent (i.e., $A(s_r)$ and A_n are nonzero vectors), we can calculate the solution as

$$t^*(s_r) = A^T(s_r)\left[A(s_r)A^T(s_r)\right]^{-1} b(s_r) \tag{4.21}$$

$$t_n^* = A_n^T\left[A_n A_n^T\right]^{-1} b_n. \tag{4.22}$$

If $A(s_c)$ has less than full rank the following two cases can occur.

Case 1: Rank $A(s_c) = 0$ In this case the equation is inconsistent since $b(s_c) \neq 0$ (otherwise $\delta^0(s_c) = 0$ and $\delta^0(s)$ would not be stable with respect to $\mathcal{S}$ since s_c lies on $\partial\mathcal{S}$). In this case (4.15) has no solution and we set

$$\rho(s_c) = \infty.$$

Case 2: Rank $A(s_c) = 1$ In this case the equation is consistent if and only if

$$\text{rank}\,[A(s_c), b(s_c)] = 1.$$

If the above rank condition for consistency is satisfied, we replace the two equations (4.15) by a single equation and determine the minimum norm solution of this latter equation. If the rank condition for consistency does not hold, equation (4.15) cannot be satisfied and we again set $\rho(s_c) = \infty$.

Example 4.1. (ℓ_2 **Schur stability margin**) Consider the discrete time control system with the controller and plant specified respectively by their transfer functions:

$$C(z) = \frac{z+1}{z^2}, \quad G(z,\mathbf{p}) = \frac{(-0.5-2p_0)z + (0.1+p_0)}{z^2 - (1+0.4p_2)z + (0.6+10p_1+2p_0)}.$$

The characteristic polynomial of the closed loop system is:

$$\delta(z,\mathbf{p}) = z^4 - (1+0.4p_2)z^3 + (0.1+10p_1)z^2 - (0.4+p_0)z + (0.1+p_0).$$

The nominal value of $\mathbf{p}^0 = [p_0^0\ p_1^0\ p_2^0] = [0,\ 0.1,\ 1]$. The perturbation is denoted as usual by the vector

$$\Delta\mathbf{p} = \begin{bmatrix} \Delta p_0 & \Delta p_1 & \Delta p_2 \end{bmatrix}.$$

The polynomial is Schur stable for the nominal parameter $\mathbf{p}^0$. We compute the ℓ_2 stability margin of the polynomial with weights $w_1 = w_2 = w_3 = 1$. Rewrite

$$\delta(z,\mathbf{p}^0+\Delta\mathbf{p}) = (-z+1)\Delta p_0 + 10z^2\Delta p_1 - 0.4z^3\Delta p_2 + (z^4 - 1.4z^3 + 1.1z^2 - 0.4z + 0.1)$$

and note that the degree remains invariant (=4) for all perturbations so that $\rho_d = \infty$. The stability region is the unit circle. For $z = 1$ to be a root of $\delta(z,\mathbf{p}^0+\Delta\mathbf{p})$ (see (4.14)), we have

$$\underbrace{\begin{bmatrix} 0 & 10 & -0.4 \end{bmatrix}}_{A(1)} \underbrace{\begin{bmatrix} \Delta p_0 \\ \Delta p_1 \\ \Delta p_2 \end{bmatrix}}_{t(1)} = \underbrace{-0.4}_{b(1)}.$$

Thus,

$$\rho(1) = \|t^*(1)\|_2 = \left\| A^T(1)\left[A(1)A^T(1)\right]^{-1} b(1) \right\|_2 = 0.04\ .$$

Similarly, for the case of $z = -1$ (see (4.14)), we have

$$\underbrace{\begin{bmatrix} 2 & 10 & 0.4 \end{bmatrix}}_{A(-1)} \underbrace{\begin{bmatrix} \Delta p_0 \\ \Delta p_1 \\ \Delta p_2 \end{bmatrix}}_{t(-1)} = \underbrace{-4}_{b(-1)}.$$

and $\rho(-1) = \|t^*(-1)\|_2 = 0.3919$. Thus $\rho_r = 0.04$.

For the case in which $\delta(z,\mathbf{p}^0+\Delta\mathbf{p})$ has a root at $z = e^{j\theta}$, $\theta \neq \pi$, $\theta \neq 0$, using (4.15), we have

$$\underbrace{\begin{bmatrix} -\cos\theta + 1 & 10\cos 2\theta & -0.4\cos 3\theta \\ -\sin\theta & 10\sin 2\theta & -0.4\sin 3\theta \end{bmatrix}}_{A(\theta)} \underbrace{\begin{bmatrix} \Delta p_0 \\ \Delta p_1 \\ \Delta p_2 \end{bmatrix}}_{t(\theta)}$$

$$= \underbrace{-\begin{bmatrix} \cos 4\theta - 1.4\cos 3\theta + 1.1\cos 2\theta - 0.4\cos\theta + 0.1 \\ \sin 4\theta - 1.4\sin 3\theta + 1.1\sin 2\theta - 0.4\sin\theta \end{bmatrix}}_{b(\theta)}.$$

Thus,

$$\rho(e^{j\theta}) = \|t^*(\theta)\|_2 = \left\| A^T(\theta)\left[A(\theta)A^T(\theta)\right]^{-1} b(\theta) \right\|.$$

Figure 4.2 shows the plot of $\rho(e^{j\theta})$.

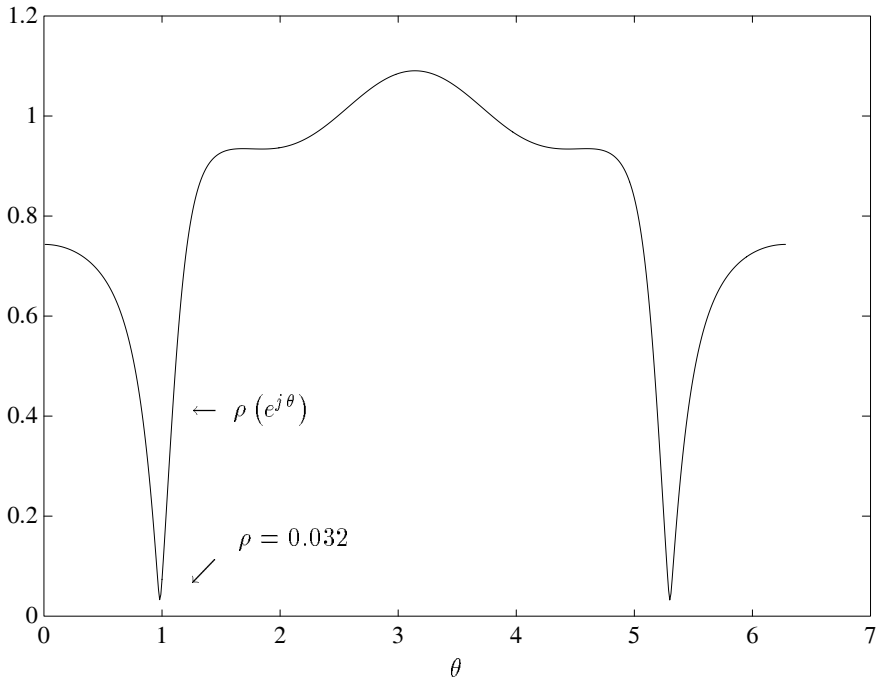

Figure 4.2. $\rho(\theta)$ (Example 4.1)

Therefore, the ℓ_2 parametric stability margin is

$$\rho_c = 0.032 = \rho_b = \rho^*.$$

Example 4.2. Consider the continuous time control system with the plant

$$G(s,\mathbf{p}) = \frac{2s + 3 - \frac{1}{3}p_1 - \frac{5}{3}p_2}{s^3 + (4 - p_2)s^2 + (-2 - 2p_1)s + (-9 + \frac{5}{3}p_1 + \frac{16}{3}p_2)}$$

and the proportional integral (PI) controller

$$C(s) = 5 + \frac{3}{s}.$$

The characteristic polynomial of the closed loop system is

$$\delta(s, \mathbf{p}) = s^4 + (4 - p_2)s^3 + (8 - 2p_1)s^2 + (12 - 3p_2)s + (9 - p_1 - 5p_2).$$

We see that the degree remains invariant under the given set of parameter variations and therefore $\rho_d = \infty$. The nominal values of the parameters are

$$\mathbf{p}^0 = [p_1^0 \ , \ p_2^0] = [0 \ , \ 0].$$

Then

$$\Delta\mathbf{p} = \begin{bmatrix} \Delta p_1 & \Delta p_2 \end{bmatrix} = \begin{bmatrix} p_1 & p_2 \end{bmatrix}.$$

The polynomial is stable for the nominal parameter $\mathbf{p}^0$. Now we want to compute the ℓ_2 stability margin of this polynomial with weights $w_1 = w_2 = 1$. We first evaluate $\delta(s, \mathbf{p})$ at $s = j\omega$:

$$\delta(j\omega, \mathbf{p}^0 + \Delta\mathbf{p}) = (2\omega^2 - 1)\Delta p_1 + (j\omega^3 - 3j\omega - 5)\Delta p_2 + \omega^4 - 4j\omega^3 - 8\omega^2 + 12j\omega + 9.$$

For the case of a root at $s = 0$ (see (4.14)), we have

$$\underbrace{\begin{bmatrix} -1 & -5 \end{bmatrix}}_{A(0)} \underbrace{\begin{bmatrix} \Delta p_1 \\ \Delta p_2 \end{bmatrix}}_{t(0)} = \underbrace{-9.}_{b(0)}$$

Thus,

$$\rho(0) = \|t^*(0)\|_2 = \left\| A^T(0) \begin{bmatrix} A(0)A^T(0) \end{bmatrix}^{-1} b(0) \right\|_2 = \frac{9\sqrt{26}}{26}.$$

For a root at $s = j\omega$, $\omega > 0$, using the formula given in (4.15), we have with $w_1 = w_2 = 1$

$$\underbrace{\begin{bmatrix} (2\omega^2 - 1) & -5 \\ 0 & (\omega^2 - 3) \end{bmatrix}}_{A(j\omega)} \underbrace{\begin{bmatrix} \Delta p_1 \\ \Delta p_2 \end{bmatrix}}_{t(j\omega)} = \underbrace{\begin{bmatrix} -\omega^4 + 8\omega^2 - 9 \\ 4\omega^2 - 12 \end{bmatrix}}_{b(j\omega)}. \tag{4.23}$$

Here, we need to determine if there exists any ω for which the rank of the matrix $A(j\omega)$ drops. It is easy to see from the matrix $A(j\omega)$, that the rank drops when $\omega = \frac{1}{\sqrt{2}}$ and $\omega = \sqrt{3}$.

rank $A(j\omega) = 1$: For $\omega = \frac{1}{\sqrt{2}}$, we have rank $A(j\omega) = 1$ and rank $[A(j\omega), b(j\omega)] = 2$, and so there is no solution to (4.23). Thus

$$\rho\left(j\frac{1}{\sqrt{2}}\right) = \infty.$$

For $\omega = \sqrt{3}$, rank $A(j\omega) = \text{rank}\,[A(j\omega), b(j\omega)]$, and we do have a solution to (4.23). Therefore

$$\underbrace{\begin{bmatrix} 5 & -5 \end{bmatrix}}_{A(j\sqrt{3})} \underbrace{\begin{bmatrix} \Delta p_1 \\ \Delta p_2 \end{bmatrix}}_{t(j\sqrt{3})} = \underbrace{6}_{b(j\sqrt{3})} .$$

Consequently,

$$\rho(j\sqrt{3}) = \left\| t^*(j\sqrt{3}) \right\|_2 = \left\| A^T(j\sqrt{3}) \left[\; A(j\sqrt{3})A^T(j\sqrt{3}) \; \right]^{-1} b(j\sqrt{3}) \right\|_2 = \frac{3\sqrt{2}}{5}.$$

rank $A(j\omega) = 2$: In this case (4.23) has a solution (which happens to be unique) and the length of the least square solution is found by

$$\begin{aligned} \rho(j\omega) = \|t^*(j\omega)\|_2 &= \left\| A^T(j\omega) \left[A(j\omega)A^T(j\omega) \right]^{-1} b(j\omega) \right\|_2 \\ &= \sqrt{\left(\frac{\omega^4 - 8\omega^2 - 11}{2\omega^2 - 1} \right)^2 + 16}. \end{aligned}$$

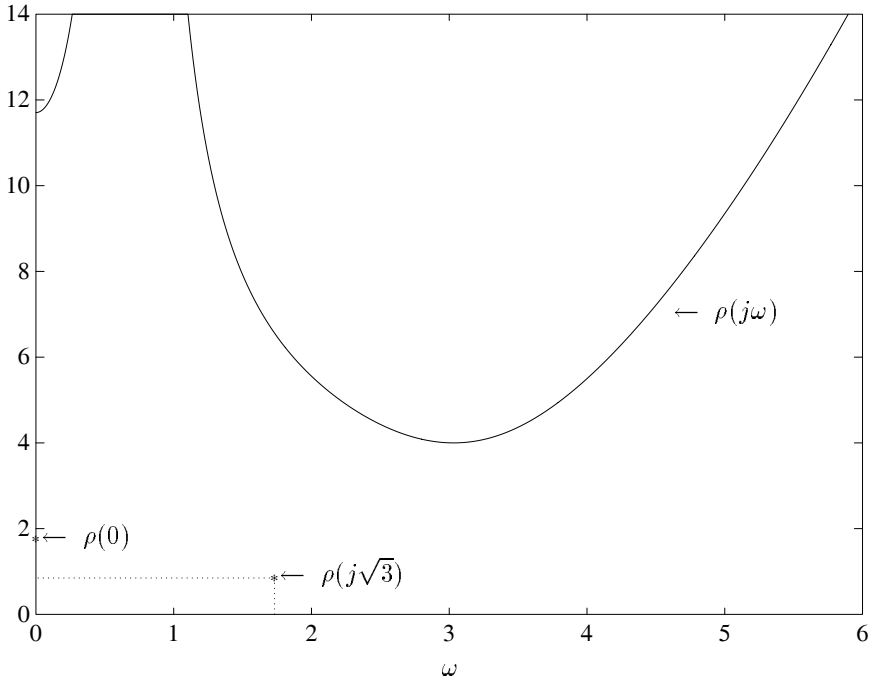

Figure 4.3. $\rho(j\omega)$, (Example 4.2)

Figure 4.3 shows the plot of $\rho(j\omega)$ for $\omega > 0$. The values of $\rho(0)$ and $\rho(j\sqrt{3})$ are also shown in Figure 4.3. Therefore,

$$\rho(j\sqrt{3}) = \rho_b = \frac{3\sqrt{2}}{5} = \rho^*$$

is the stability margin.

4.5.1 Discontinuity of the Stability Margin

In the last example we notice that the function $\rho(j\omega)$ has a discontinuity at $\omega = \omega^* = \sqrt{3}$. The reason for this discontinuity is that in the neighborhood of ω^*, the minimum norm solution of (4.15) is given by the formula for the rank 2 case. On the other hand, at $\omega = \omega^*$, the minimum norm solution is given by the formula for the rank 1 case. Thus the discontinuity of the function $\rho(j\omega)$ is due to the drop of rank from 2 to 1 of the coefficient matrix $A(j\omega)$ at ω^*. Furthermore, we have seen that if the rank of $A(j\omega^*)$ drops from 2 to 1 but the rank of $[A(j\omega^*), b(j\omega^*)]$ does not also drop, then the equation is inconsistent at ω^* and $\rho(j\omega^*)$ is infinity. In this case, this discontinuity in $\rho(j\omega)$ does not cause any problem in finding the global minimum of $\rho(j\omega)$. Therefore, the only values of ω^* that can cause a problem are those for which the rank of $[A(j\omega^*), b(j\omega^*)]$ drops to 1. Given the problem data, the occurrence of such a situation can be *predicted* by setting all 2×2 minors of the matrix $[A(j\omega), b(j\omega)]$ equal to zero and solving for the common real roots if any. These frequencies can then be treated separately in the calculation. Therefore, such discontinuities do not pose any problem from the computational point of view. Since the parameters for which rank dropping occurs lie on a proper algebraic variety, any slight and arbitrary perturbation of the parameters will dislodge them from this variety and restore the rank of the matrix. If the parameters correspond to physical quantities such arbitrary perturbations are natural and hence such discontinuities should not cause any problem from a physical point of view either.

4.5.2 ℓ_2 Stability Margin for Time-delay Systems

The results given above for determining the largest stability ellipsoid in parameter space for polynomials can be extended to quasipolynomials. This extension is useful when parameter uncertainty is present in systems containing time delays. As before, we deal with the case where the uncertain parameters appear linearly in the coefficients of the quasipolynomial.

Let us consider real quasipolynomials

$$\delta(s, \mathbf{p}) = p_1 Q_1(s) + p_2 Q_2(s) + \cdots + p_l Q_l(s) + Q_0(s) \tag{4.24}$$

where

$$Q_i(s) = s^{n_i} + \sum_{k=1}^{n_i} \sum_{j=1}^{m} a_{kj}^i s^{n_i - k} e^{-\tau_j^i s}, \qquad i = 0, 1, \cdots, l \tag{4.25}$$

and we assume that $n_0 > n_i,\ \ i = 1, 2, \cdots, l$ and that all parameters occurring in the equations (4.24) and (4.25) are real. Control systems containing time delays often have characteristic equations of this form (see Example 4.3).

The uncertain parameter vector is denoted $\mathbf{p} = [p_1, p_2, \cdots, p_l]$. The nominal value of the parameter vector is $\mathbf{p} = \mathbf{p}^0$, the nominal quasipolynomial $\delta(s, \mathbf{p}^0) = \delta^0(s)$ and $\mathbf{p} - \mathbf{p}^0 = \Delta\mathbf{p}$ denotes the deviation or perturbation from the nominal. The parameter vector is assumed to lie in the ball of radius ρ centered at $\mathbf{p}^0$:

$$\mathcal{B}(\rho, \mathbf{p}^0) = \{\mathbf{p} \ : \ \|\mathbf{p} - \mathbf{p}^0\|_2 < \rho\}. \tag{4.26}$$

The corresponding set of quasipolynomials is:

$$\mathbf{\Delta}_\rho(s) := \{\delta(s, \mathbf{p}^0 + \Delta\mathbf{p}) \ : \ \|\Delta\mathbf{p}\|_2 < \rho\}. \tag{4.27}$$

Recall the discussion in Chapter 1 regarding the Boundary Crossing Theorem applied to this class of quasipolynomials. From this discussion and the fact that in the family (4.24) the e^{-st} terms are associated only with the lower degree terms it follows that it is legitimate to say that each quasipolynomial defined above is Hurwitz stable if all its roots lie inside the left half of the complex plane. As before we shall say that the family is Hurwitz stable if each quasipolynomial in the family is Hurwitz. We observe that the "degree" of each quasipolynomial in $\mathbf{\Delta}_\rho(s)$ is the same since $n_0 > n_i$, and therefore by the Theorem 1.14 (Boundary Crossing Theorem applied to quasipolynomials), stability can be lost only by a root crossing the $j\omega$ axis. Accordingly, for every $-\infty < \omega < \infty$ we can introduce a set in the parameter space

$$\mathbf{\Pi}(\omega) = \{\mathbf{p} \ : \ \delta(j\omega, \mathbf{p}) = 0\}$$

This set corresponds to quasipolynomials that have $j\omega$ as a root. Of course for some particular ω this set may be empty. If $\mathbf{\Pi}(\omega)$ is nonempty we can define the distance between $\mathbf{\Pi}(\omega)$ and the nominal point $\mathbf{p}^0$:

$$\rho(\omega) = \inf_{\mathbf{p} \in \mathbf{\Pi}(\omega)} \{\|\mathbf{p} - \mathbf{p}^0\|\}.$$

If $\mathbf{\Pi}(\omega)$ is empty for some ω we set the corresponding $\rho(\omega) := \infty$. We also note that since all coefficients in (4.24) and (4.25) are assumed to be real, $\mathbf{\Pi}(\omega) = \mathbf{\Pi}(-\omega)$ and accordingly $\rho(\omega) = \rho(-\omega)$

Theorem 4.4 *The family of quasipolynomials $\mathbf{\Delta}_\rho(s)$ is Hurwitz stable if and only if the quasipolynomial $\delta^0(s)$ is stable and*

$$\rho < \rho^* = \inf_{0 \le \omega < \infty} \rho(\omega).$$

The proof of this theorem follows from the fact that the Boundary Crossing Theorem of Chapter 1 applies to the special class of degree invariant quasipolynomials $\mathbf{\Delta}_\rho(s)$. The problem of calculating $\rho(\omega)$, the ℓ_2 norm of the smallest length perturbation vector $\Delta\mathbf{p}$ for which $\delta(s, \mathbf{p}^0 + \Delta\mathbf{p})$ has a root at $j\omega$, can be solved exactly as in Section 4.5 where we dealt explicitly with the polynomial case. We illustrate this with an example.

Example 4.3. **(ℓ_2 stability margin for time delay system)** The model of a satellite attitude control system, Figure 4.4, containing a time delay in the loop, is shown.

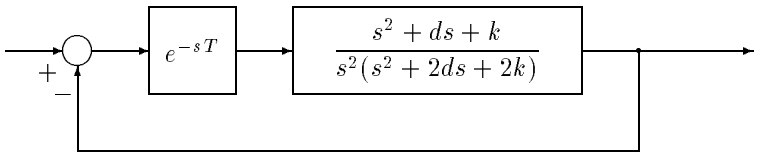

Figure 4.4. A satellite attitude control system with time-delay (Example 4.3)

The characteristic equation of the system is the quasipolynomial

$$\delta(s,\mathbf{p}) = s^4 + 2ds^3 + (e^{-sT} + 2k)s^2 + e^{-sT}ds + e^{-sT}k.$$

The nominal parameters are

$$\mathbf{p}^0 = [k^0 \quad d^0] = [0.245 \quad 0.0218973] \quad \text{and} \quad T = 0.1.$$

The Hurwitz stability of the nominal system may be easily verified by applying the interlacing property. To compute the ℓ_2 real parametric stability margin around the nominal values of parameters, let

$$\Delta\mathbf{p} = [\Delta k \quad \Delta d].$$

We have

$$\begin{aligned}\delta(j\omega, \mathbf{p}^0 + \Delta\mathbf{p}) = {} & \omega^4 - \omega^2\cos\omega T - 2k^0\omega^2 - 2\Delta k\omega^2 + d^0\omega\sin\omega T \\ & + \Delta d\omega\sin\omega T + k^0\cos\omega T + \Delta k\cos\omega T \\ & + j(-2d^0\omega^3 - 2\Delta d\omega^3 + \omega^2\sin\omega T + d^0\omega\cos\omega T \\ & + \Delta d\omega\cos\omega T - k^0\sin\omega T - \Delta k\sin\omega T)\end{aligned}$$

or

$$\underbrace{\begin{bmatrix} -2\omega^2 + \cos\omega T & \omega\sin\omega T \\ -\sin\omega T & -2\omega^3 + \omega\cos\omega T \end{bmatrix}}_{A(j\omega)} \underbrace{\begin{bmatrix} \Delta k \\ \Delta d \end{bmatrix}}_{t(j\omega)} =$$

$$\underbrace{\begin{bmatrix} -\omega^4 + \omega^2\cos\omega T + 2k^0\omega^2 - d^0\omega\sin\omega T - k^0\cos\omega T \\ 2d^0\omega^3 - \omega^2\sin\omega T - d^0\omega\cos\omega T + k^0\sin\omega T \end{bmatrix}}_{b(j\omega)}.$$

Therefore

$$\begin{aligned}\rho(j\omega) &= \|t^*(j\omega)\|_2 \\ &= \left\| A^T(j\omega)\left[A(j\omega)A^T(j\omega)\right]^{-1} b(j\omega)\right\|_2 .\end{aligned}$$

From Figure 4.5, the minimum value of $\rho_b = 0.0146$.

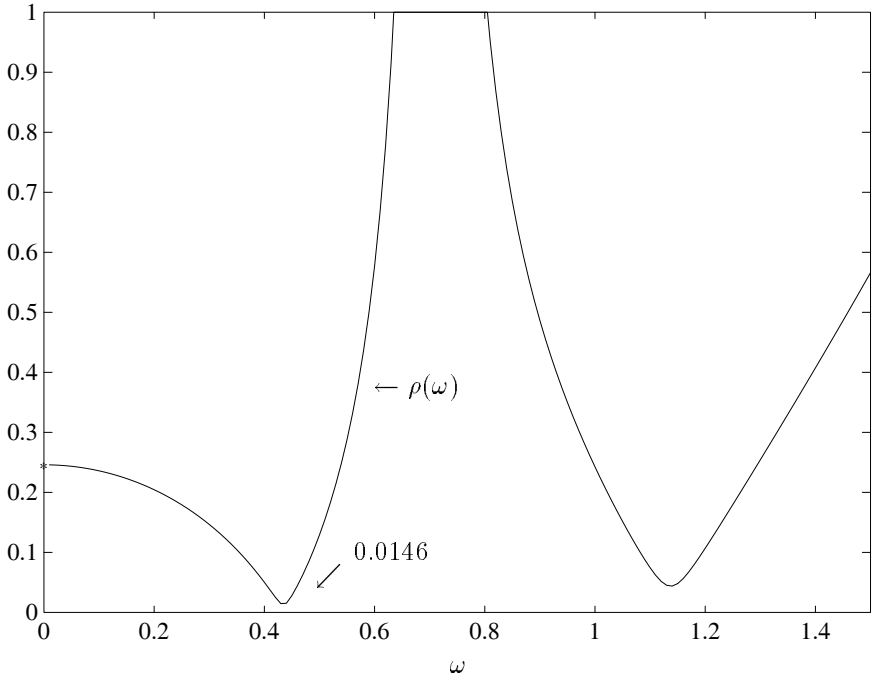

Figure 4.5. ℓ_2 stability margin for a quasipolynomial (Example 4.3)

The additional condition from the constant coefficient, corresponding to a root at $s = 0$ is

$$|\Delta k| < k^0 = 0.245.$$

Therefore, the ℓ_2 stability margin is 0.0146 .

Remark 4.2. In any specific example, the minimum of $\rho(\omega)$ needs to be searched only over a finite range of ω rather than over $[0, \infty)$. This is because the function $\rho(\omega)$ will be increasing for higher frequencies ω. This fact follows from the assumption regarding degrees ($n_0 > n_i$) and Theorem 1.14 (Chapter 1).

4.6 ℓ_∞ AND ℓ_1 STABILITY MARGINS

If $\Delta\mathbf{p}$ is measured in the ℓ_∞ or ℓ_1 norm, we face the problem of determining the corresponding minimum norm solution of a linear equation of the type $At = b$ at each point on the stability boundary. Problems of this type can always be converted to a suitable linear programming problem. For instance, in the ℓ_∞ case, this problem is equivalent to the following optimization problem:

$$\text{Minimize } \beta$$

subject to the constraints:

$$At = b$$

$$-\beta \leq t_i \leq \beta, \qquad i = 1, 2, \cdots, l. \tag{4.28}$$

This is a standard linear programming (LP) problem and can therefore be solved by existing, efficient algorithms.

For the ℓ_1 case, we can similarly formulate a linear programming problem by introducing the variables,

$$|t_i| := y_i^+ - y_i^-, \qquad i = 1, 2, \cdots, l$$

Then we have the LP problem:

$$\text{Minimize} \sum_{i=1}^{l} \{y_i^+ - y_i^-\} \tag{4.29}$$

subject to

$$At = b$$

$$y_i^- - y_i^+ \leq t_i \leq y_i^+ - y_i^- \qquad i = 1, 2, \cdots, l.$$

We do not elaborate further on this approach. The reason is that ℓ_∞ and ℓ_1 cases are special cases of polytopic families of perturbations. We deal with this general class next.

4.7 POLYTOPIC FAMILIES

In this section we deal with the case where each component p_i of the real parameter vector $\mathbf{p} := [p_1, p_2, \cdots, p_l]^T$ can vary independently of the other components. In other words, we assume that $\mathbf{p}$ lies in an uncertainty set which is box-like:

$$\mathbf{\Pi} := \{\mathbf{p} : p_i^- \leq p_i \leq p_i^+, \quad i = 1, 2, \cdots, l\}. \tag{4.30}$$

Represent the system characteristic polynomial

$$\delta(s) := \delta_0 + \delta_1 s + \delta_2 s^2 + \cdots + \delta_n s^n \tag{4.31}$$

by the vector $\underline{\delta} := [\delta_0, \delta_1, \cdots, \delta_n]^T$. We assume that each component δ_i of $\underline{\delta}$, is a *linear* function of $\mathbf{p}$. To be explicit,

$$\begin{aligned}\delta(s, \mathbf{p}) &:= \delta_0(\mathbf{p}) + \delta_1(\mathbf{p})s + \delta_2(\mathbf{p})s^2 + \cdots + \delta_n(\mathbf{p})s^n \\ &:= p_1 Q_1(s) + p_2 Q_2(s) + \cdots + p_l Q_l(s) + Q_0(s).\end{aligned}$$

By equating coefficients of like powers of s we can write this as

$$\underline{\delta} = T\mathbf{p} + b,$$

where $\underline{\delta}, \mathbf{p}$ and b are column vectors, and

$$T : \mathbb{R}^l \longrightarrow \mathbb{R}^{n+1}$$

is a linear map. In other words, $\underline{\delta}$ is a linear (or affine) transformation of $\mathbf{p}$. Now introduce the coefficient set

$$\mathbf{\Delta} := \{\underline{\delta} : \underline{\delta} = T\mathbf{p} + b, \quad \mathbf{p} \in \mathbf{\Pi}\} \tag{4.32}$$

of the set of polynomials

$$\mathbf{\Delta}(s) := \{\delta(s, \mathbf{p}) : \mathbf{p} \in \mathbf{\Pi}\}. \tag{4.33}$$

4.7.1 Exposed Edges and Vertices

To describe the geometry of the set $\mathbf{\Delta}$ (equivalently $\mathbf{\Delta}(s)$) we introduce some basic facts regarding polytopes. Note that the set $\mathbf{\Pi}$ is in fact an example of a special kind of *polytope*. In general, a polytope in n-dimensional space is the convex hull of a set of points called *generators* in this space. A set of generators is *minimal* if removal of any point from the set alters the convex hull. A minimal set of generators is unique and constitutes the *vertex set* of the polytope. Consider the special polytope $\mathbf{\Pi}$, which we call a *box*. The vertices $\mathbf{V}$ of $\mathbf{\Pi}$ are obtained by setting each p_i to p_i^+ or p_i^-:

$$\mathbf{V} := \{\mathbf{p} : p_i = p_i^- \text{ or } p_i = p_i^+, \quad i = 1, 2, \cdots, l\}. \tag{4.34}$$

The *exposed edges* $\mathbf{E}$ of the box $\mathbf{\Pi}$ are defined as follows. For fixed i,

$$\mathbf{E}_i := \{\mathbf{p} : p_i^- \leq p_i \leq p_i^+, \quad p_j = p_j^- \text{ or } p_j^+, \quad \text{for all } j \neq i\} \tag{4.35}$$

then

$$\mathbf{E} := \cup_{i=1}^{l} \mathbf{E}_i. \tag{4.36}$$

We use the notational convention

$$\mathbf{\Delta} = T\mathbf{\Pi} + b \tag{4.37}$$

as an alternative to (4.32).

Lemma 4.1 *Let $\mathbf{\Pi}$ be a box and T a linear map, then $\mathbf{\Delta}$ is a polytope. If $\mathbf{\Delta}_{\mathrm{V}}$ and $\mathbf{\Delta}_{\mathrm{E}}$ denote the vertices and exposed edges of $\mathbf{\Delta}$ and $\mathbf{E}$ and $\mathbf{V}$ denote the exposed edges and vertices of $\mathbf{\Pi}$, we have*

$$\mathbf{\Delta}_{\mathrm{V}} \subset T\mathbf{V} + b$$
$$\mathbf{\Delta}_{\mathrm{E}} \subset T\mathbf{E} + b.$$

This lemma shows us that the polynomial set $\mathbf{\Delta}(s)$ is a *polytopic family* and that the vertices and exposed edges of $\mathbf{\Delta}$ can be obtained by mapping the vertices and exposed edges of $\mathbf{\Pi}$. Since $\mathbf{\Pi}$ is an axis parallel box its vertices and exposed edges are easy to identify. For an arbitrary polytope in n dimensions, it is difficult to distinguish the "exposed edges" computationally. This lemma is therefore useful even though the mapped edges and vertices of $\mathbf{\Pi}$ contain more elements than only the vertices and exposed edges of $\mathbf{\Delta}$. These facts are now used to characterize the image set of the family $\mathbf{\Delta}(s)$. Fixing $s = s^*$, we let $\mathbf{\Delta}(s^*)$ denote the *image set* of the points $\delta(s^*, \mathbf{p})$ in the complex plane obtained by letting $\mathbf{p}$ range over $\mathbf{\Pi}$:

$$\mathbf{\Delta}(s^*) := \{\delta(s^*, \mathbf{p}) : \mathbf{p} \in \mathbf{\Pi}\}. \tag{4.38}$$

Introduce the *vertex polynomials*:

$$\mathbf{\Delta}_{\mathrm{V}}(s) := \{\delta(s, \mathbf{p}) : \mathbf{p} \in \mathbf{V}\}$$

and the *edge polynomials*:

$$\mathbf{\Delta}_{\mathrm{E}}(s) := \{\delta(s, \mathbf{p}) : \mathbf{p} \in \mathbf{E}\}$$

Their respective images at $s = s^*$ are

$$\mathbf{\Delta}_{\mathrm{V}}(s^*) := \{\delta(s^*, \mathbf{p}) : \mathbf{p} \in \mathbf{V}\} \tag{4.39}$$

and

$$\mathbf{\Delta}_{\mathrm{E}}(s^*) := \{\delta(s^*, \mathbf{p}) : \mathbf{p} \in \mathbf{E}\}. \tag{4.40}$$

The set $\mathbf{\Delta}(s^*)$ is a convex polygon in the complex plane whose vertices and exposed edges originate from the vertices and edges of $\mathbf{\Pi}$. More precisely, we have the following lemma which describes the geometry of the image set in this polytopic case. Let *co* $(\cdot)$ denote the convex hull of the set $(\cdot)$.

Lemma 4.2

1) $\mathbf{\Delta}(s^*) = co\ (\mathbf{\Delta}_{\mathrm{V}}(s^*))$,

2) The vertices of $\mathbf{\Delta}(s^*)$ are contained in $\mathbf{\Delta}_{\mathrm{V}}(s^*)$,

3) The exposed edges of $\mathbf{\Delta}(s^*)$ are contained in $\mathbf{\Delta}_{\mathrm{E}}(s^*)$.

This lemma states that the vertices and exposed edges of the complex plane polygon $\mathbf{\Delta}(s^*)$ are contained in the images at s^* of the mapped vertices and edges of the box $\mathbf{\Pi}$. We illustrate this in the Figure 4.6.

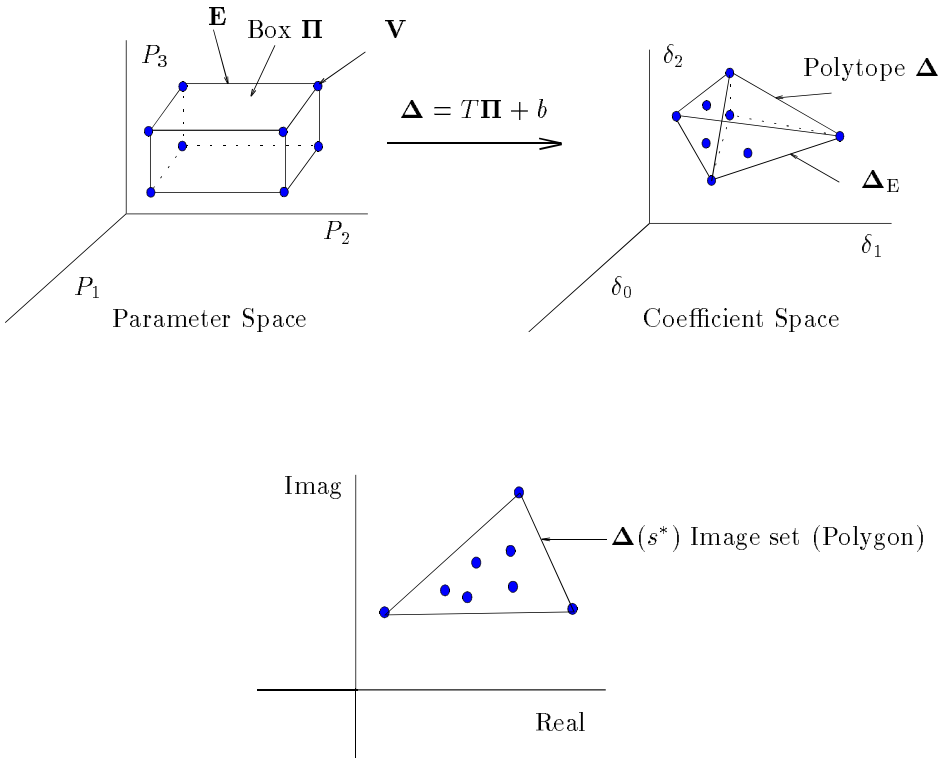

Figure 4.6. Vertices and edges of $\mathbf{\Pi}$, $\mathbf{\Delta}$ and $\mathbf{\Delta}(s^*)$

The above results will be useful in determining the robust stability of the family $\mathbf{\Delta}(s)$ with respect to an open stability region $\mathcal{S}$. In fact they are the key to establishing the important result that the stability of a polytopic family can be determined from its edges.

Assumption 4.1. Assume the family of polynomials $\mathbf{\Delta}(s)$ is of

1) constant degree, and

2) there exists at least one point $s^0 \in \partial\mathcal{S}$ such that $0 \notin \mathbf{\Delta}(s^0)$.

Theorem 4.5 *Under the above assumptions $\mathbf{\Delta}(s)$ is stable with respect to $\mathcal{S}$ if and only if $\mathbf{\Delta}_{\mathrm{E}}(s)$ is stable with respect to $\mathcal{S}$.*

Proof. Following the image set approach described in Section 4.3, it is clear that under the assumption of constant degree and the existence of at least one stable polynomial in the family, the stability of $\mathbf{\Delta}(s)$ is guaranteed if the image set $\mathbf{\Delta}(s^*)$ excludes the origin for every $s^* \in \partial\mathcal{S}$. Since $\mathbf{\Delta}(s^0)$ excludes the origin it follows that $\mathbf{\Delta}(s^*)$ excludes the origin for every $s^* \in \partial\mathcal{S}$ if and only if the edges of $\mathbf{\Delta}(s^*)$ exclude the origin. Here we have implicitly used the assumption that the image set moves continuously with respect to s^*. From Lemma 4.2, this is equivalent to the condition that $\mathbf{\Delta}_{\mathrm{E}}(s^*)$ excludes the origin for every $s^* \in \partial\mathcal{S}$. This condition is finally equivalent to the stability of the set $\mathbf{\Delta}_{\mathrm{E}}(s)$. ♣

Theorem 4.5 has established that to determine the stability of $\mathbf{\Delta}(s)$, it suffices to check the stability of the exposed edges. The stability verification of a multiparameter family is therefore reduced to that of a set of one parameter families. In fact this is precisely the kind of problem that was solved in Chapter 2 by the Segment Lemma and the Bounded Phase Lemma. In the next subsection we elaborate on the latter approach.

4.7.2 Bounded Phase Conditions for Checking Robust Stability of Polytopes

From a computational point of view it is desirable to introduce some further simplification into the problem of verifying the stability of a polytope of polynomials. Note that from Theorem 4.2 (Zero Exclusion Principle), to verify robust stability we need to determine whether or not the image set $\mathbf{\Delta}(s^*)$ *excludes* the origin for every point $s^* \in \partial\mathcal{S}$. This computation is particularly easy since $\mathbf{\Delta}(s^*)$ is a *convex polygon*. In fact, a convex polygon in the complex plane excludes the origin if and only if the angle subtended at the origin by its vertices is less than π radians (180°).

Consider the convex polygon $\mathcal{P}$ in the complex plane with vertices $[v_1, v_2, \cdots] := \mathbf{V}$. Let p_0 be an arbitrary point in $\mathcal{P}$ and define

$$\phi_{v_i} := \arg\left(\frac{v_i}{p_0}\right). \tag{4.41}$$

We adopt the convention that every angle lies between $-\pi$ and $+\pi$. Now define

$$\begin{aligned} \phi^+ &:= \sup_{v_i \in \mathbf{V}} \phi_{v_i}, \qquad && 0 \le \phi^+ \le \pi \\ \phi^- &:= \inf_{v_i \in \mathbf{V}} \phi_{v_i}, \qquad && -\pi < \phi^- \le 0. \end{aligned}$$

The *angle subtended* at the origin by $\mathcal{P}$ is given by

$$\Phi_{\mathcal{P}} := \phi^+ - \phi^- . \tag{4.42}$$

$\mathcal{P}$ excludes the origin if and only if $\Phi_{\mathcal{P}} < \pi$. Applying this fact to the convex polygon $\mathbf{\Delta}(s^*)$, we can easily conclude the following.

Theorem 4.6 (Bounded Phase Theorem)
Under the assumptions

a) every polynomial in $\mathbf{\Delta}(s)$ is of the same degree ($\delta_n(\mathbf{p}) \neq 0, \mathbf{p} \in \mathbf{\Pi}$),

b) at least one polynomial in $\mathbf{\Delta}(s)$ is stable with respect to $\mathcal{S}$,

the set of polynomials $\mathbf{\Delta}(s)$ is stable with respect to the open stability region $\mathcal{S}$ if and only if

$$\Phi_{\mathbf{\Delta}_V}(s^*) < \pi, \qquad \textit{for all } s^* \in \partial\mathcal{S}. \tag{4.43}$$

The computational burden imposed by this theorem is that we need to evaluate the maximal phase difference across the vertex of $\mathbf{\Pi}$. The condition (4.43) will be referred to conveniently as the Bounded Phase Condition. We illustrate Theorems 4.5 and 4.6 in the example below.

Example 4.4. Consider the standard feedback control system with the plant

$$G(s) = \frac{s+a}{s^2+bs+c}$$

where the parameters vary within the ranges:

$$\begin{aligned} a &\in [1,2] = [a^-, a^+], \\ b &\in [9,11] = [b^-, b^+], \\ c &\in [15,18] = [c^-, c^+] \end{aligned}$$

The controller is

$$C(s) = \frac{3s+2}{s+5}.$$

We want to examine whether this controller robustly stabilizes the plant. The closed loop characteristic polynomial is:

$$\delta(s) = a(3s+2) + b(s^2+5s) + c(s+5) + (s^3+8s^2+2s).$$

The polytope of polynomials whose stability is to be checked is:

$$\mathbf{\Delta}(s) = \left\{ \delta(s) \ : \ a \in [a^-, a^+], \quad b \in [b^-, b^+], \quad c \in [c^-, c^+] \right\}$$

We see that the degree is invariant over the uncertainty set. From Theorem 4.5 this polytope is stable if and only if the exposed edges are. Here, we write the 12 edge polynomials $\mathbf{\Delta}_{\mathrm{E}}(s)$:

$$\begin{aligned}
\delta_{E_1}(s) &= \left(\lambda a^- + (1-\lambda)a^+\right)(3s+2) + b^-(s^2+5s) + c^-(s+5) + (s^3+8s^2+2s)\\
\delta_{E_2}(s) &= \left(\lambda a^- + (1-\lambda)a^+\right)(3s+2) + b^-(s^2+5s) + c^+(s+5) + (s^3+8s^2+2s)\\
\delta_{E_3}(s) &= \left(\lambda a^- + (1-\lambda)a^+\right)(3s+2) + b^+(s^2+5s) + c^-(s+5) + (s^3+8s^2+2s)\\
\delta_{E_4}(s) &= \left(\lambda a^- + (1-\lambda)a^+\right)(3s+2) + b^+(s^2+5s) + c^+(s+5) + (s^3+8s^2+2s)\\
\delta_{E_5}(s) &= a^-(3s+2) + \left(\lambda b^- + (1-\lambda)b^+\right)(s^2+5s) + c^-(s+5) + (s^3+8s^2+2s)\\
\delta_{E_6}(s) &= a^-(3s+2) + \left(\lambda b^- + (1-\lambda)b^+\right)(s^2+5s) + c^+(s+5) + (s^3+8s^2+2s)\\
\delta_{E_7}(s) &= a^+(3s+2) + \left(\lambda b^- + (1-\lambda)b^+\right)(s^2+5s) + c^-(s+5) + (s^3+8s^2+2s)\\
\delta_{E_8}(s) &= a^+(3s+2) + \left(\lambda b^- + (1-\lambda)b^+\right)(s^2+5s) + c^+(s+5) + (s^3+8s^2+2s)\\
\delta_{E_9}(s) &= a^-(3s+2) + b^-(s^2+5s) + \left(\lambda c^- + (1-\lambda)c^+\right)(s+5) + (s^3+8s^2+2s)\\
\delta_{E_{10}}(s) &= a^-(3s+2) + b^+(s^2+5s) + \left(\lambda c^- + (1-\lambda)c^+\right)(s+5) + (s^3+8s^2+2s)\\
\delta_{E_{11}}(s) &= a^+(3s+2) + b^-(s^2+5s) + \left(\lambda c^- + (1-\lambda)c^+\right)(s+5) + (s^3+8s^2+2s)\\
\delta_{E_{12}}(s) &= a^+(3s+2) + b^+(s^2+5s)\left(\lambda c^- + (1-\lambda)c^+\right)(s+5) + (s^3+8s^2+2s).
\end{aligned}$$

The robust stability of $\mathbf{\Delta}(s)$ is equivalent to the stability of the above 12 edges. From Theorem 4.6, it is also equivalent to the condition that $\mathbf{\Delta}(s)$ has at least one stable polynomial, that $0 \notin \mathbf{\Delta}(j\omega)$ for at least one ω and that the *maximum phase difference* over the vertex set is less than 180° for any frequency ω (bounded phase condition). At $\omega = 0$ we have

$$0 \notin \mathbf{\Delta}(j0) = 2a + 5c = 2[1,2] + 5[15,18].$$

Also it may be verified that the center point of the box is stable. Thus we examine the maximum phase difference,evaluated at each frequency, over the following eight vertex polynomials:

$$\begin{aligned}
\delta_{v_1}(s) &= a^-(3s+2) + b^-(s^2+5s) + c^-(s+5) + (s^3+8s^2+2s)\\
\delta_{v_2}(s) &= a^-(3s+2) + b^-(s^2+5s) + c^+(s+5) + (s^3+8s^2+2s)\\
\delta_{v_3}(s) &= a^-(3s+2) + b^+(s^2+5s) + c^-(s+5) + (s^3+8s^2+2s)\\
\delta_{v_4}(s) &= a^-(3s+2) + b^+(s^2+5s) + c^+(s+5) + (s^3+8s^2+2s)\\
\delta_{v_5}(s) &= a^+(3s+2) + b^-(s^2+5s) + c^-(s+5) + (s^3+8s^2+2s)\\
\delta_{v_6}(s) &= a^+(3s+2) + b^-(s^2+5s) + c^+(s+5) + (s^3+8s^2+2s)\\
\delta_{v_7}(s) &= a^+(3s+2) + b^+(s^2+5s) + c^-(s+5) + (s^3+8s^2+2s)\\
\delta_{v_8}(s) &= a^+(3s+2) + b^+(s^2+5s) + c^+(s+5) + (s^3+8s^2+2s).
\end{aligned}$$

Figure 4.7 shows that the maximum phase difference over all vertices does not reach 180° at any ω. Therefore, we conclude that the controller $C(s)$ robustly stabilizes the plant $G(s)$.

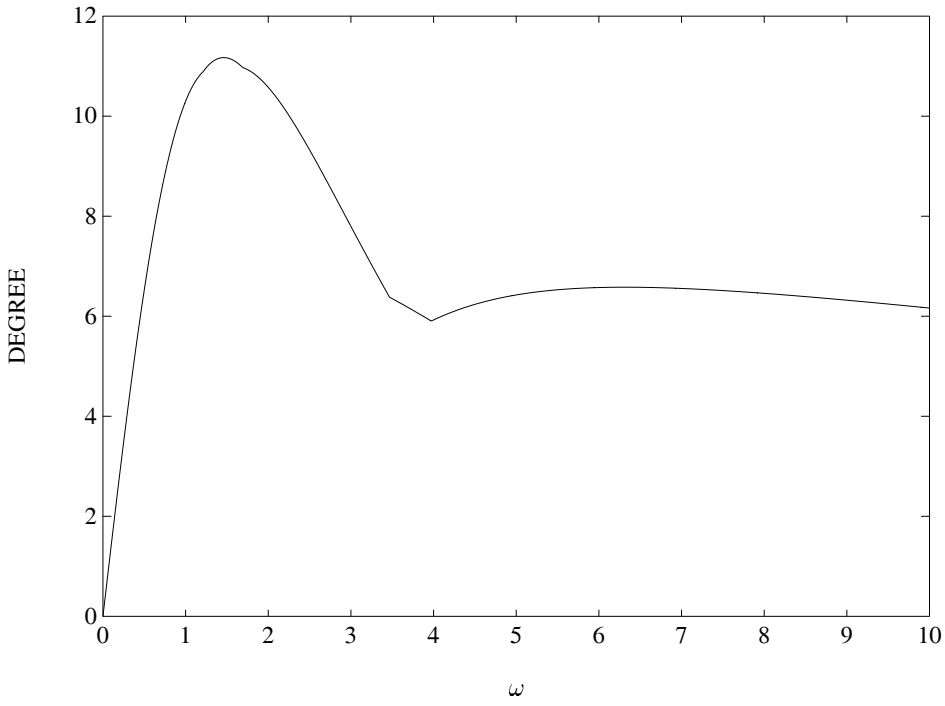

Figure 4.7. Maximum phase differences of vertices (Example 4.4)

In the next example we show how the maximal stability box can be found using the Bounded Phase Condition.

Example 4.5. Continuing with the previous example (Example 4.4), suppose that we now want to expand the range of parameter perturbations and determine the largest size box of parameters stabilized by the controller given. We define a variable sized parameter box as follows:

$$a \in [a^- - \epsilon, a^+ + \epsilon], \quad b \in [b^- - \epsilon, b^+ + \epsilon], \quad c \in [c^- - \epsilon, c^+ + \epsilon].$$

We can easily determine the maximum value of ϵ for which robust stability is preserved by simply applying the Bounded Phase Condition while increasing the value of ϵ. Figure 4.8 shows that the maximum phase difference over the vertex set (attained at some frequency) plotted as a function of ϵ. We find that at $\epsilon = 6.5121$, the phase difference over the vertex set reaches 180° at $\omega = 1.3537$. Therefore, we conclude that the maximum value of ϵ is 6.5120. This means that the controller $C(s)$ can robustly stabilize the family of plants $G(s, \mathbf{p})$ where the ranges of the

parameters are

$$a \in [-5.512, 8.512], \quad b \in [2.488, 17.512], \quad c \in [8.488, 24.512].$$

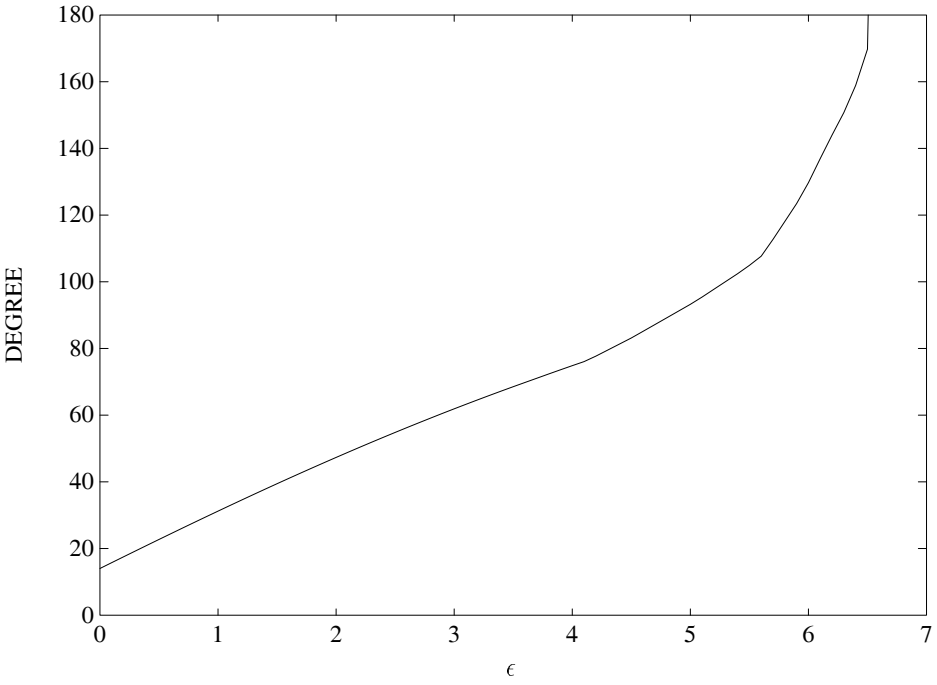

Figure 4.8. Maximum phase differences of vertices vs. ϵ (Example 4.5)

The purpose of the next example is to draw the reader's attention to the importance of the Assumptions 4.1 under which Theorem 4.5 is valid. The example illustrates that a polytopic family can have exposed edges that are stable even though the family is unstable, when the second item in Assumptions 4.1 fails to hold. In particular it cautions the reader that it is important to verify that the image set excludes the origin at least at one point on the stability boundary.

Example 4.6. Consider the family of polynomials

$$\mathbf{\Delta}(s, \mathbf{p}) := s + p_1 - jp_2$$

where $p_1 \in [1,2]$ and $p_2 \in [0,1]$. Suppose that the stability region is the *outside* of the shaded circle in Figure 4.9:

$$\mathcal{S} := \{s \in \mathbb{C} \ : \ |s + (-1.5 + j0.25)| > 0.2\}$$

The vertex polynomials are

$$\mathbf{\Delta}_{\mathrm{V}}(s) := \{s+1, s+1-j, s+2, s+2-j\}.$$

The root loci of the elements of $\mathbf{\Delta}_{\mathrm{E}}(s)$ is shown in Figure 4.9 along with the instability region (shaded region). Figure 4.9 shows that all elements of $\mathbf{\Delta}_{\mathrm{E}}(s)$ are stable with respect to the stability region $\mathcal{S}$. One might conclude from this, in view of the theorem, that the set $\mathbf{\Delta}(s)$ is stable.

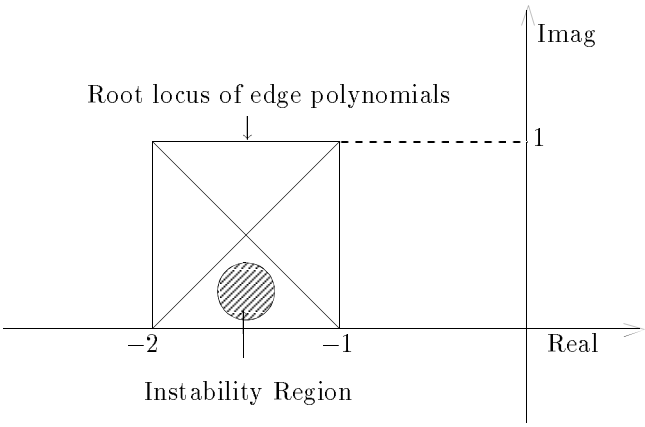

Figure 4.9. Instability region and edges (Example 4.6)

However, this is not true as $\delta(s, \mathbf{p})$ is unstable at $p_1 = 1.5$, $p_2 = 0.25$. The apparent contradiction with the conclusion of the theorem is because the theorem attempts to ascertain the presence of unstable elements in the family by detecting Boundary Crossing. In this particular example, no Boundary Crossing occurs as we can see from the plots of the image sets of the exposed edges evaluated along the boundary of $\mathcal{S}$ (see Figure 4.10). However, we can easily see that item 2) of Assumptions 4.1 is violated since there is *no frequency* at which the origin is excluded from the image set. Therefore, there is no contradiction with the theorem.

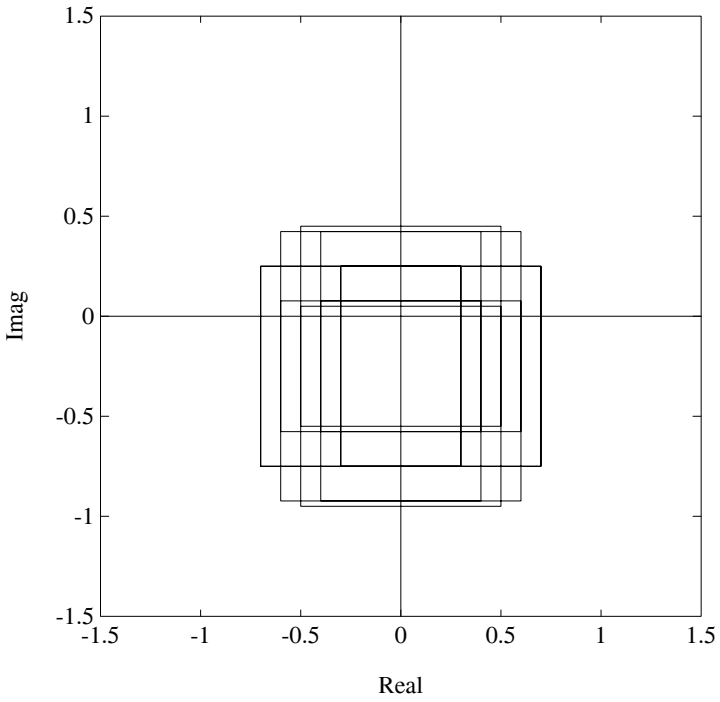

Figure 4.10. Image sets of edges evaluated along $\partial\mathcal{S}$ include the origin (Example 4.6)

The next example deals with the determination of robust Schur stability.

Example 4.7. Consider the discrete time control system, in the standard feedback configuration with controller and plant transfer functions given as

$$C(z) = \frac{1}{z^2} \text{ and } G(z, \mathbf{p}) = \frac{p_2 - p_1 z}{z^2 - (p_1 + 0.23)z - 0.37}.$$

The characteristic polynomial of the closed loop system is

$$\delta(z, \mathbf{p}) = z^4 - (p_1 + 0.23)z^3 - 0.37z^2 - p_1 z + p_2.$$

The nominal values of parameters are $p_1^0 = 0.17$ and $p_2^0 = 0.265$. It is verified that the polynomial $\delta(z, p_1^0, p_2^0)$ is Schur stable. We want now to determine the maximum perturbation that the parameters can undergo without losing stability. One way to estimate this is to determine the maximum value of ϵ (stability margin) such that $\delta(z, \mathbf{p})$ remains stable for all

$$p_1 \in [p_1^0 - \epsilon, p_1^0 + \epsilon], \qquad p_2 \in [p_2^0 - \epsilon, p_2^0 + \epsilon].$$

This can be accomplished by checking the Schur stability of the exposed edges for each fixed value of ϵ. It can also be done by computing the maximum phase difference over the 4 vertices at each point on the stability boundary, namely the unit circle. The smallest value of ϵ that makes an edge unstable is the stability margin. Figure 4.11 shows that at $\epsilon = 0.1084$ the Bounded Phase Condition is violated and the maximum phase difference of the vertices reaches 180°. This implies that an edge becomes unstable for $\epsilon = 0.1084$. Therefore, the stability margin is < 0.1084.

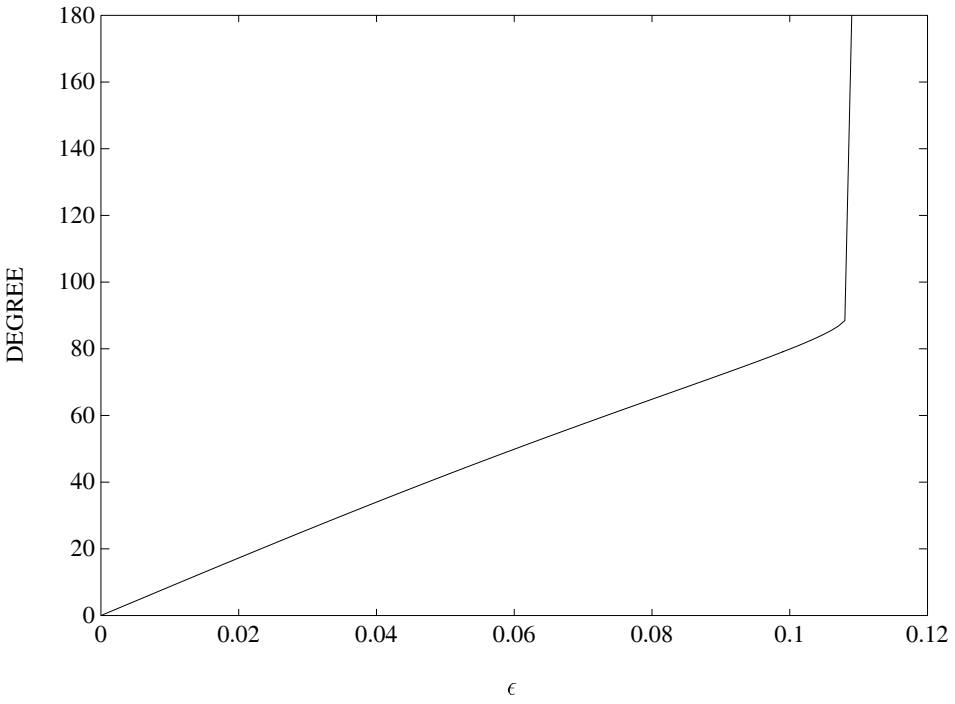

Figure 4.11. Maximum phase difference vs. ϵ (Example 4.7)

The next example deals with a control system where each root is required to remain confined in a stability region. It also shows how the controller can be chosen to maximize the stability margin.

Example 4.8. In a digital tape transport system, the open loop transfer function between tape position and driving motor supply voltage is

$$G(s) = \frac{n_0 + n_1 s}{d_0 + d_1 s + d_2 s^2 + d_3 s^3 + d_4 s^4 + d_5 s^5}.$$

The coefficients n_i and d_i depend linearly on two uncertain physical parameters, K (elastic constant of the tape) and D (friction coefficient). The parameter vector is

$$\mathbf{p} = [D, K]^T$$

with the nominal parameter values

$$\mathbf{p}^0 = [D^0, K^0]^t = [20, 4 \times 10^4]^T.$$

Considering a proportional controller

$$C(s) = K_p$$

the closed loop characteristic polynomial is written as

$$\delta(s) = \delta_0 + \delta_1 s + \cdots + \delta_5 s^5.$$

The equation connecting $\underline{\delta} = [\delta_5, \cdots, \delta_0]^T$ and $\mathbf{p}$ is

$$\underbrace{\begin{bmatrix} \delta_5 \\ \delta_4 \\ \delta_3 \\ \delta_2 \\ \delta_1 \\ \delta_0 \end{bmatrix}}_{\underline{\delta}} = \underbrace{\begin{bmatrix} 0 & 0 \\ 0.025 & 0 \\ 0.035 & 0.25 \times 10^{-4} \\ 0.01045 & 0.35 \times 10^{-4} \\ 0.03 K_p & 0.1045 \times 10^{-4} \\ 0 & 0.3 \times 10^{-4} K_p \end{bmatrix}}_{A} \underbrace{\begin{bmatrix} D \\ K \end{bmatrix}}_{t} + \underbrace{\begin{bmatrix} 1 \\ 2.25 \\ 1.5225 \\ 0.2725 \\ 0 \\ 0 \end{bmatrix}}_{b}.$$

In the following, we choose as the "stability" region $\mathcal{S}$ the union of two regions in the complex plane ($s = \sigma + j\omega$):

1) a disc $\mathcal{D}$ centered on the negative real axis at $\sigma = -0.20$ and with radius $R = 0.15$ (containing closed loop dominant poles);

2) a half plane $\mathcal{H}$: $\sigma < -0.50$.

The boundary ∂S of the "stability region" is the union of two curves which are described (in the upper half plane) by the following maps $B_{\mathcal{D}}$ and $B_{\mathcal{H}}$:

$$\partial\mathcal{D} : s = B_{\mathcal{D}}(\gamma) = (-0.20 + 0.15\cos\gamma) + j(0.15\sin\gamma), \qquad 0 \le \gamma \le \pi$$
$$\partial\mathcal{H} : s = B_{\mathcal{H}}(\omega) = -0.50 + j\omega, \qquad 0 \le \omega < \infty$$

Our objective is to obtain the parameter K_p of the maximally robust controller, in the sense that it guarantees "stability" with respect to the above region while maximizing the size of a perturbation box centered at $\mathbf{p}^0$. In other words we seek to maximize the perturbation range tolerated by the system subject to the requirement that the closed loop poles remain in the prescribed region $\mathcal{S}$.

To do this we first determine the range of controller parameter values which ensure that the nominal system has roots in $\mathcal{S}$. This can be found by a root locus plot of the system with respect to the controller parameter K_p with the plant parameters held at their nominal values. This root locus plot is given in Figure 4.12. The range is found to be

$$K_p \in [0.0177, 0.0397].$$

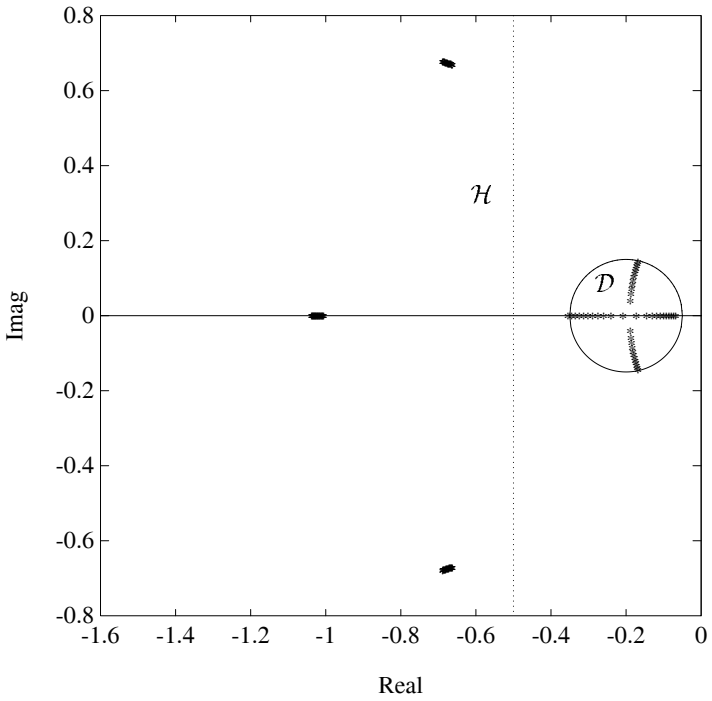

Figure 4.12. Root locus of the nominal closed system with respect to K_p (Example 4.8)

Then for each setting of the controller parameter in this range we determine the ℓ_∞ margin by determining the maximal phase difference over the vertex set evaluated over the stability boundary defined above. In this manner we sweep over the controller parameter range. The maximally robust controller is found to be

$$C(s) = K_p^* \approx 0.0397.$$

The maximal ℓ_∞ stability margin obtained is

$$\rho^* \approx 14.76.$$

Figure 4.13 shows that the optimal parameter K_p^* which produces the largest ρ ($\rho^* \approx 14.76$) locates the closed loop poles, evaluated at the nominal point, *on the stability boundary.* As the plant parameters perturb away from the nominal the roots move inward into the stability region. However this is true only under the assumption that the controller parameter K_p is *not subject to perturbation.* In fact a slight perturbation of the controller parameter set at $K_p = K_p^*$ sends the roots out of the "stability" region as the root locus plot has shown. This highlights the fact that *robustification with respect to the plant parameters* has been obtained at the expense of *enhanced sensitivity* with respect to the controller parameters. This could have been avoided by including the controller parameter K_p as an additional uncertain parameter and searching for a nominal point in the augmented parameter space where the stability margin is large enough.

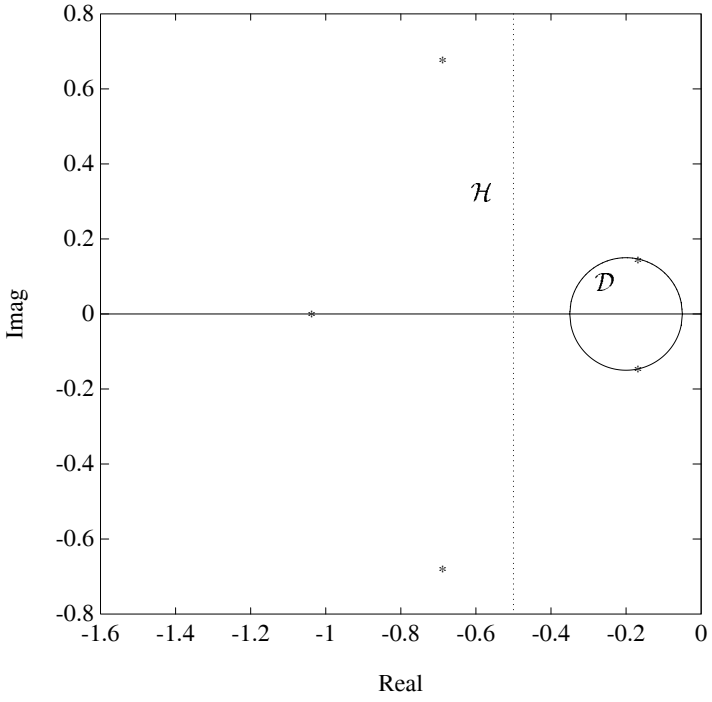

Figure 4.13. Root locations of the closed loop system at K_p^* (Example 4.8)

In the next example we again consider the problem of adjusting a controller gain to enhance the robustness with respect to plant parameters.

Example 4.9. Consider the plant and feedback controller

$$G(s) = \frac{1}{s^2 + p_1 s + p_2}, \qquad C(s) = \frac{K}{s}$$

where the nominal parameters are

$$\mathbf{p}^0 = [p_1^0 \quad p_2^0] = [5 \quad 1].$$

We find that $0 < K < 5$ stabilizes the nominal plant $G(s)$. In this example we want to find the optimum value of K such that the ℓ_2 stability margin ρ^* with respect to the parameters p_1, p_2 is the largest possible We first evaluate the ℓ_2 stability margin in terms of K. The characteristic polynomial is

$$\delta(s, \mathbf{p}, K) = s^3 + p_1 s^2 + p_2 s + K.$$

Thus we have

$$\delta(j\omega, \mathbf{p}, K) = -j\omega^3 - p_1\omega^2 + jp_2\omega + K = 0$$

and

$$\underbrace{\begin{bmatrix} -\omega^2 & 0 \\ 0 & \omega \end{bmatrix}}_{A(\omega)} \underbrace{\begin{bmatrix} \Delta p_1 \\ \Delta p_2 \end{bmatrix}}_{t} = \underbrace{\begin{bmatrix} -K + p_1^0\omega^2 \\ \omega^3 - \omega p_2^0 \end{bmatrix}}_{b(\omega, \mathbf{p}^0, K)}.$$

Therefore,

$$\rho(K) = \min_{\omega} \left\| A(\omega)^T \left(A(\omega) A(\omega)^T \right)^{-1} b(\omega, \mathbf{p}^0, K) \right\|_2$$

and the optimum value K^* corresponds to

$$\rho^* = \max_K \rho(K).$$

Figure 4.14 shows that the maximum value of the stability margin ρ^* is achieved as K tends to 0.

Again, it is interesting to observe that as K tends to 0 the system has a real root that tends to the imaginary axis. Therefore, at the same time that the real parametric stability margin is *increasing to its maximal value*, the robustness with respect to the parameter K is *decreasing drastically*. In fact as K tends to 0 the "optimum" value with respect to perturbations in $\mathbf{p} = [p_1, p_2]$, it will also be true that the slightest perturbation of the parameter K itself will destabilize the system. This is similar to what was observed in the previous example. It suggests the general precautionary guideline, that robustness with respect to plant parameters is often obtained at the expense of enhanced sensitivity with respect to the controller parameters.

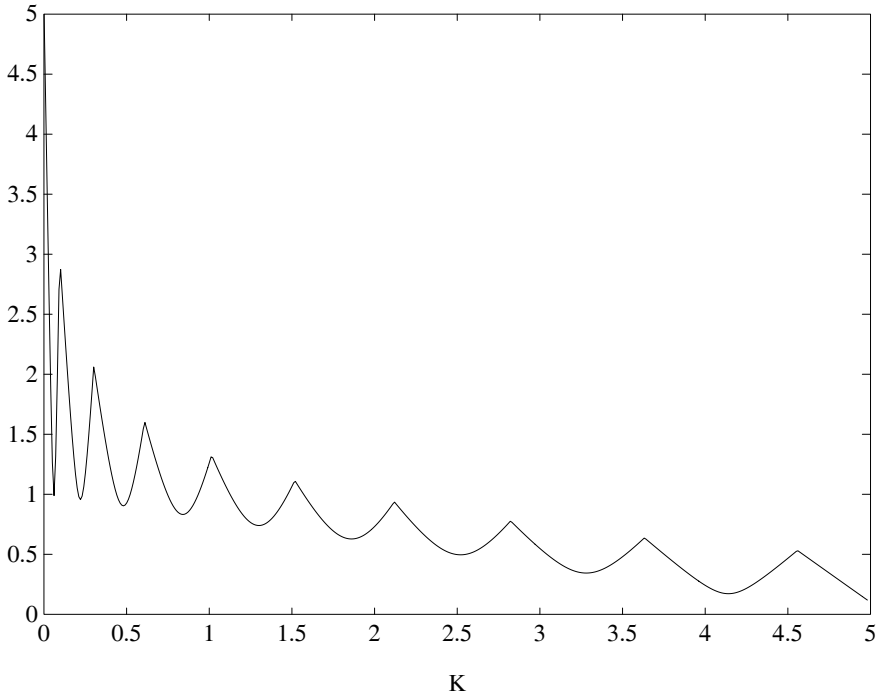

Figure 4.14. $\rho(K)$ vs. K (Example 4.9)

4.7.3 Polytopes of Complex Polynomials

The edge and vertex results developed above for a *real* polytope $\mathbf{\Delta}(s)$ carry over to a polytope of complex polynomials. This is because in either case the image set $\mathbf{\Delta}(s^*)$ is a polygon in the complex plane whose edges are contained in the set of images of the exposed edges of $\mathbf{\Delta}(s)$. Therefore when the degree remains invariant, stability of the exposed edges implies that of the entire polytope. Thus the stability of a complex polytopic family

$$a_1 Q_1(s) + a_2 Q_2(s) + \cdots + a_m Q_m(s)$$

with $a_i = \alpha_i + j\beta_i$ for $\alpha_i^- \leq \alpha_i \leq \alpha_i^+$, $\beta_i^- \leq \beta_i \leq \beta_i^+$, $i = 1, \cdots, m$ and $Q_i(s)$ being complex polynomials can be tested by considering the parameter vector $\mathbf{p} := [\alpha_1, \beta_1, \cdots, \alpha_m, \beta_m]$ and testing the exposed edges of the complex polynomials corresponding to the exposed edges of this box.

Example 4.10. Consider the parametrized polynomial

$$\delta(s, \mathbf{p}) = s^3 + (4 - j\alpha)s^2 + (\beta - j3)s + (\gamma - j(2 + \alpha))$$

where the parameters vary as:

$$\alpha \in [-0.7, 0.7],\ \beta \in [6.3, 7.7],\ \gamma \in [5.3, 6.7].$$

We verify that polynomial is Hurwitz stable for $(\alpha^0, \beta^0, \gamma^0) = (0, 7, 6)$. In order to check the robust stability of this polynomial we need to verify the stability of the set of edges connecting the following eight vertex polynomials:

$$\begin{aligned}
\delta_{V_1}(s) &= s^3 + (4 + j0.7)s^2 + (6.3 - j3)s + (5.3 - j1.3)\\
\delta_{V_2}(s) &= s^3 + (4 + j0.7)s^2 + (6.3 - j3)s + (6.7 - j1.3)\\
\delta_{V_3}(s) &= s^3 + (4 + j0.7)s^2 + (7.7 - j3)s + (5.3 - j1.3)\\
\delta_{V_4}(s) &= s^3 + (4 + j0.7)s^2 + (7.7 - j3)s + (6.7 - j1.3)\\
\delta_{V_5}(s) &= s^3 + (4 - j0.7)s^2 + (6.3 - j3)s + (5.3 - j2.7)\\
\delta_{V_6}(s) &= s^3 + (4 - j0.7)s^2 + (6.3 - j3)s + (6.7 - j2.7)\\
\delta_{V_7}(s) &= s^3 + (4 - j0.7)s^2 + (7.7 - j3)s + (5.3 - j2.7)\\
\delta_{V_8}(s) &= s^3 + (4 - j0.7)s^2 + (7.7 - j3)s + (6.7 - j2.7)
\end{aligned}$$

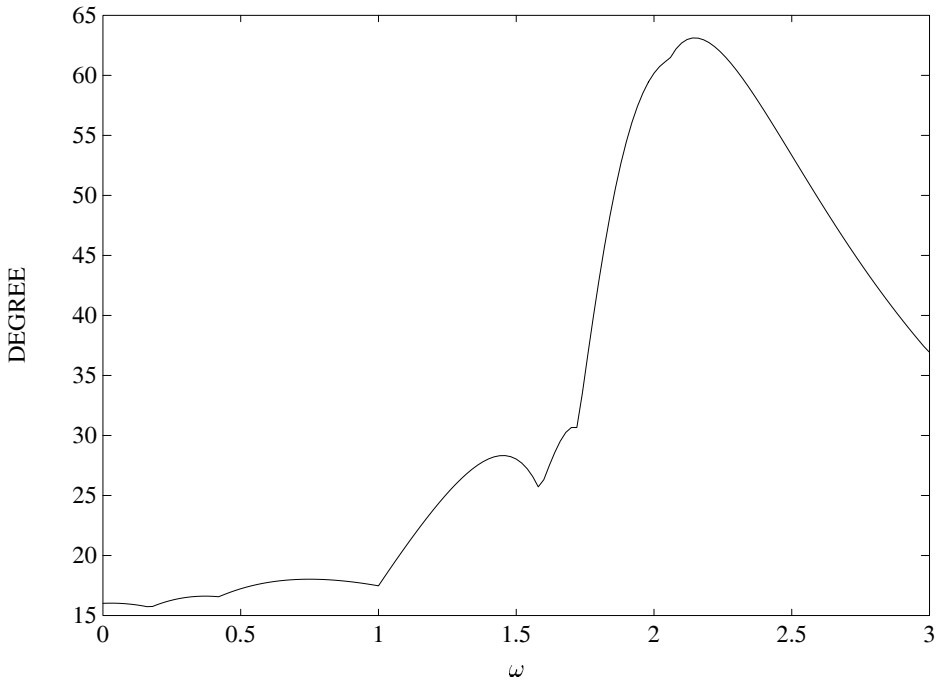

Figure 4.15. Maximum phase differences of vertices (checking the stability of edges) (Example 4.10)

The stability of these edges may be checked by verifying the Bounded Phase Condition. We examine whether at any frequency ω the maximum phase difference of the vertices reaches 180°. Figure 4.15 shows that the maximum phase difference over this vertex set never reaches 180° for any ω. Thus, we conclude that all edges are Hurwitz stable, and so is the given polynomial family.

4.7.4 Polytopes of Quasipolynomials

In fact the above idea can also be extended to determining the robust stability of time-delay systems containing parameter uncertainty. Consider the quasipolynomial family

$$P(s) = a_n s^n + a_{n-1} e^{-sT_{n-1}} P_{n-1}(s) + a_{n-2} e^{-sT_{n-2}} P_{n-2}(s) + \cdots + a_0 e^{-sT_0} P_0(s)$$

where each polynomial $P_i(s)$ is of degree less than n, may be real or complex,

$$0 < T_0 < T_1 < \cdots < T_{n-1}$$

are real and $a_i \in [a_i^-, a_i^+]$ are real parameters varying in the box

$$\mathbf{A} = \left\{ \mathbf{a} \ : \ a_i^- \leq a_i \leq a_i^+, \quad i = 0, 1, \cdots, n \right\}.$$

This corresponds to a polytope of quasipolynomials. The image of this polytope at $s = s^*$, is a polygon whose exposed edges originate from the exposed edges of $\mathbf{A}$. Under the assumption that the "degree" of the family remains invariant (a_n does not pass through zero) the Boundary Crossing Theorem applies to this family and we conclude from image set arguments that the stability of the exposed edges implies stability of the entire polytope. This is illustrated in the example below.

Example 4.11. Consider the feedback system with time delay as shown in Figure 4.16.

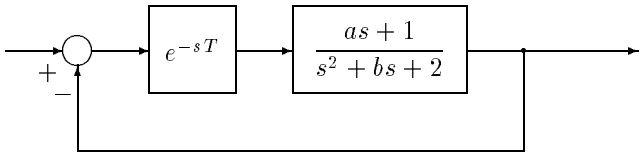

Figure 4.16. A time-delay system (Example 4.11)

The characteristic equation of the closed loop system is

$$\begin{aligned} \delta(s) &= (s^2 + bs + 2) + e^{-sT}(as + 1) \\ &= s^2 + bs + 2 + ae^{-sT}s + e^{-sT}. \end{aligned}$$

Suppose that the parameters a and b are bounded by $a \in [a^-, a^+]$ and $b \in [b^-, b^+]$. We have the following four vertex quasipolynomials

$$\begin{aligned} p_0(s) &= s^2 + b^- s + 2 + a^- e^{-sT} s + e^{-sT} \\ p_1(s) &= s^2 + b^- s + 2 + a^+ e^{-sT} s + e^{-sT} \\ p_2(s) &= s^2 + b^+ s + 2 + a^- e^{-sT} s + e^{-sT} \\ p_3(s) &= s^2 + b^+ s + 2 + a^+ e^{-sT} s + e^{-sT}. \end{aligned}$$

and four edges as follows:

$$[p_0(s), p_1(s)], \quad [p_0(s), p_2(s)], \quad [p_1(s), p_3(s)], \quad [p_2(s), p_3(s)].$$

Let us first take the edge joining $p_0(s)$ and $p_1(s)$. The stability of $p_0(s)$ can be easily checked by examining the frequency plot of

$$\frac{p_0(j\omega)}{(j\omega + 1)^n}$$

where n is the degree of $p_0(s)$. Using the Principle of the Argument (Chapter 1), the condition for $p_0(s)$ to have all left half plane roots is simply that the plot should not encircle the origin since the denominator term $(s+1)^n$ does not have right half plane roots. Once we verify the stability of the vertex polynomials $p_0(s)$, we need to check the stability of the edge $\lambda p_1(s) + (1-\lambda)p_0(s)$. For the stability of this edge, it is necessary that

$$\lambda p_1(j\omega) + (1-\lambda)p_0(j\omega) \neq 0, \quad \text{for} \quad 0 < \lambda \leq 1 \quad \text{and for all} \quad \omega \in \mathbb{R}.$$

This is also equivalent to

$$\frac{1-\lambda}{\lambda} + \frac{p_1(j\omega)}{p_0(j\omega)} \neq 0.$$

Since $(1-\lambda)/\lambda$ takes values in $[0, \infty)$ when λ varies in $(0, 1]$, it is necessary that $p_1(j\omega)/p_0(j\omega)$ should not take values in $[0, -\infty)$. Equivalently, the plot of $p_1(j\omega)/p_0(j\omega)$ should not cross the negative real axis of the complex plane.

For the choice of $a \in [0.5, 1.5]$, $b \in [1.5, 2.5]$, and $T = 0.5$, Figure 4.17 shows the frequency plots required to determine the stability of the remaining segments and thus the robust stability of the entire family of systems. From these figures we see that each of the frequency plots $\dfrac{p_i(j\omega)}{p_k(j\omega)}$ does not cut the negative real axis. Thus we conclude that the system is robustly stable.

The Bounded Phase Condition described earlier can also be applied to polytopes of complex polynomials and quasipolynomials. Essentially, we need to check that one member of the family is stable, the "degree" does not drop, and that the image set evaluated along the stability boundary excludes the origin. Since the image set is a convex polygon, the bounded phase condition

$$\Phi_{\mathbf{\Delta}_V} < \pi$$

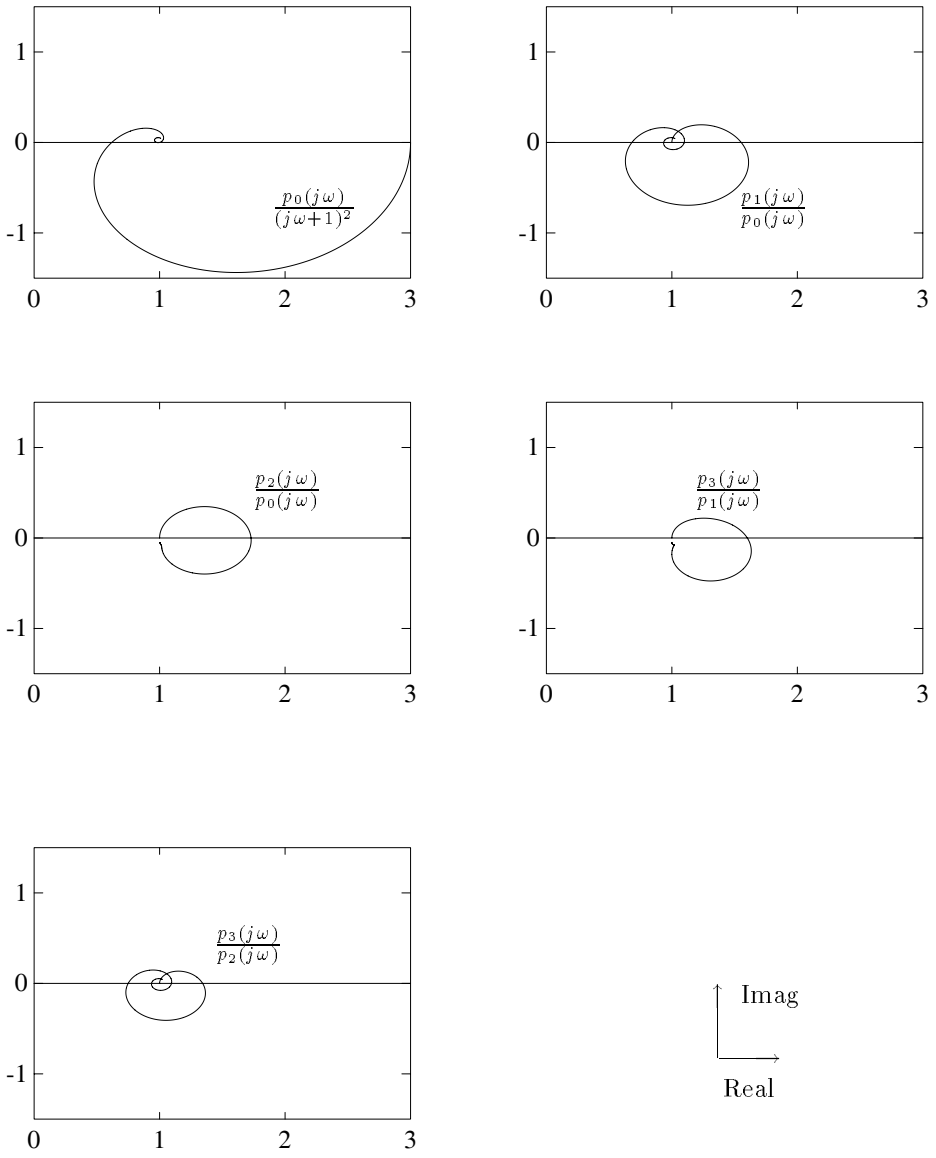

Figure 4.17. All frequency plots do not cut negative real axis (Example 4.11)

can be used to check robust stability. To illustrate this we now repeat Example 4.11 by using the Bounded Phase Condition.

Example 4.12. Consider the previous example. After verifying the stability of one member of the family and the degree invariance, we need to compute the maximum phase difference over the vertices at each frequency ω as follows. Let

$$\phi(\omega) = \phi_{\max}(\omega) - \phi_{\min}(\omega)$$

where

$$\phi_{\max}(\omega) = \max\left\{0, \arg\left(\frac{p_1(j\omega)}{p_0(j\omega)}\right), \arg\left(\frac{p_2(j\omega)}{p_0(j\omega)}\right), \arg\left(\frac{p_3(j\omega)}{p_0(j\omega)}\right)\right\}$$

$$\phi_{\min}(\omega) = \min\left\{0, \arg\left(\frac{p_1(j\omega)}{p_0(j\omega)}\right), \arg\left(\frac{p_2(j\omega)}{p_0(j\omega)}\right), \arg\left(\frac{p_3(j\omega)}{p_0(j\omega)}\right)\right\}$$

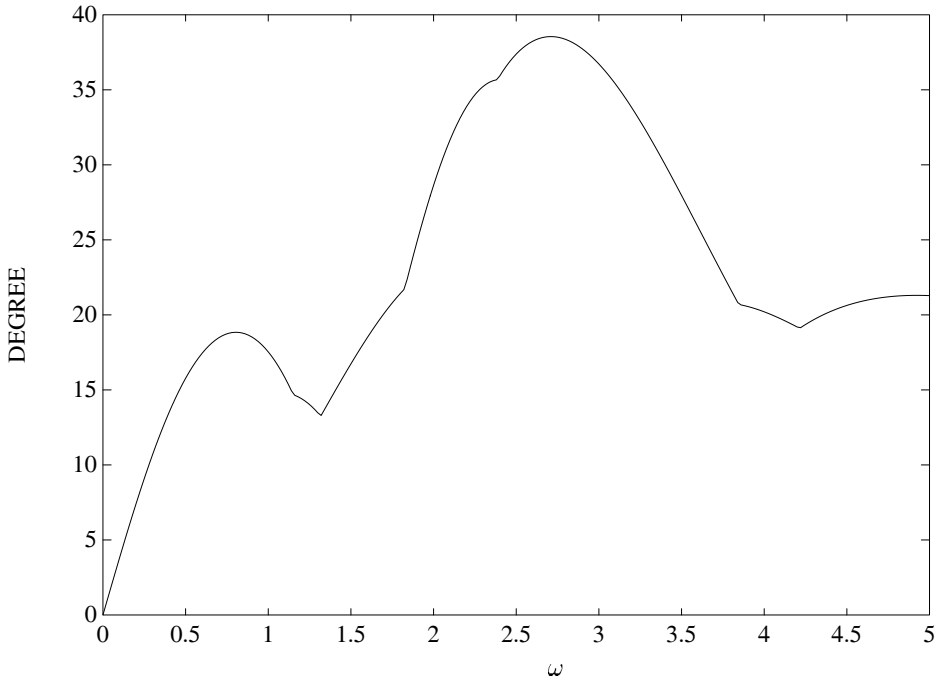

Figure 4.18. Maximum phase differences of vertices (Example 4.12)

Figure 4.18 shows the maximum phase difference $\phi(\omega)$ for $\omega \geq 0$. Since $\phi(\omega)$ never reaches 180°, at least one polynomial in the family is Hurwitz stable and the image set excludes the origin at some frequency, we conclude that the family is robustly stable.

4.8 EXTREMAL PROPERTIES OF EDGES AND VERTICES

In this section we deal with the problem of finding the *worst case stability margin* over a polytope of stable polynomials. This value of the worst case stability margin is a measure of the *robust performance* of the system or associated controller. As mentioned earlier this is a formidably difficult problem in the general case. In the linear case that is being treated in this chapter, it is feasible to determine robust performance by exploiting the image set boundary generating property of the exposed edges. Indeed for such families it is shown below that the worst case stability margins occur in general over the exposed edges. In special cases it can occur over certain vertices.

Consider the polytopic family of polynomials

$$\delta(s, \mathbf{p}) = p_1 Q_1(s) + p_2 Q_2(s) + \cdots + p_l Q_l(s) + Q_0(s) \tag{4.44}$$

with associated uncertainty set $\mathbf{\Pi}$ as defined in (4.30) and the exposed edges $\mathbf{E}$. Specifically, let

$$\mathbf{E}_i := \left\{ \mathbf{p} : p_i^- \leq p_i \leq p_i^+, \quad p_j = p_j^- \text{ or } p_j^+, \quad \text{for all } i \neq j \right\} \tag{4.45}$$

then

$$\mathbf{E} := \cup_{i=1}^{l} \mathbf{E}_i. \tag{4.46}$$

As before, we assume that the degree of the polynomial family remains invariant as $\mathbf{p}$ varies over $\mathbf{\Pi}$. Suppose that the stability of the family with respect to a stability region $\mathcal{S}$ has been proved. Then, with each point $\mathbf{p} \in \mathbf{\Pi}$ we can associate a stability ball of radius $\rho(\mathbf{p})$ in some norm $\|\mathbf{p}\|$. A natural question to ask at this point is: What is the minimum value of $\rho(\mathbf{p})$ as $\mathbf{p}$ ranges over $\mathbf{\Pi}$? It turns out that the minimum value of $\rho(\mathbf{p})$ is attained over the exposed edge set $\mathbf{E}$.

Theorem 4.7

$$\inf_{\mathbf{p} \in \mathbf{\Pi}} \rho(\mathbf{p}) = \inf_{\mathbf{p} \in \mathbf{E}} \rho(\mathbf{p}). \tag{4.47}$$

Proof. From the property that the edge set generates the boundary of the image set $\mathbf{\Delta}(s^*)$, we have

$$\begin{aligned}
\inf_{\mathbf{p} \in \mathbf{\Pi}} \rho(\mathbf{p}) &= \inf \{ \|\Delta \mathbf{p}\| : \delta(s, \mathbf{p} + \Delta \mathbf{p}) \text{ unstable for } \mathbf{p} \in \mathbf{\Pi} \} \\
&= \inf \{ \|\Delta \mathbf{p}\| : \delta(s^*, \mathbf{p} + \Delta \mathbf{p}) = 0, \quad s^* \in \partial \mathcal{S}, \quad \mathbf{p} \in \mathbf{\Pi} \} \\
&= \inf \{ \|\Delta \mathbf{p}\| : \delta(s^*, \mathbf{p} + \Delta \mathbf{p}) = 0, \quad s^* \in \partial \mathcal{S}, \quad \mathbf{p} \in \mathbf{E} \} \\
&= \inf_{\mathbf{p} \in \mathbf{E}} \rho(\mathbf{p}).
\end{aligned}$$

♣

This theorem is useful for determining the worst case parametric stability margin over an uncertainty box. Essentially it again reduces a multiparameter optimization problem to a set of one parameter optimization problems.

Further simplification can be obtained when the stability of the polytope can be guaranteed from the vertices. In this case we can find the worst case stability margin by evaluating $\rho(\mathbf{p})$ over the vertex set. For example, for the case of Hurwitz stability we have the following result which depends on the Vertex Lemma of Chapter 2.

Theorem 4.8 *Let $\delta(s)$ be a polytope of real Hurwitz stable polynomials of degree n of the form (4.44) with $Q_i(s)$ of the form*

$$Q_i(s) = s_i^t(a_i s + b_i)A_i(s)P_i(s) \tag{4.48}$$

where $t_i \geq 0$ are integers, a_i and b_i are arbitrary real numbers, $A_i(s)$ are antiHurwitz, and $P_i(s)$ are even or odd polynomials. Then

$$\inf_{\mathbf{p}\in\mathbf{\Pi}} \rho(\mathbf{p}) = \inf_{\mathbf{p}\in\mathbf{V}} \rho(\mathbf{p}). \tag{4.49}$$

The proof utilizes the Vertex Lemma of Chapter 2 but is otherwise identical to the argument used in the previous case and is therefore omitted. A similar result holds for the Schur case and can be derived using the corresponding Vertex Lemma from Chapter 2. We illustrate the usefulness of this result in determining the worst case performance evaluation and optimization of controllers in the examples below.

Example 4.13. Consider the plant

$$G(s) = \frac{p_2 s + 1}{p_1 s + p_0}$$

where the parameters $\mathbf{p} = [p_0 \quad p_1 \quad p_2]$ vary in

$$\mathbf{\Pi} := \{p_0 \in [2,4], \quad p_1 \in [4,6], \quad p_2 \in [10,15]\}.$$

This plant is robustly stabilized by the controller

$$C(s) = K\frac{s+5}{s(s-1)}$$

when $0.5 \leq K \leq 2$. The characteristic polynomial is

$$\delta(s, \mathbf{p}, K) = s^2(s-1)p_1 + s(s-1)p_0 + Ks(s+5)p_2 + K(s+5)$$

and

$$\delta(j\omega, \mathbf{p}, K) = -j\omega^3 p_1 - \omega^2(p_0 - p_1 - p_2 K) + j\omega(5Kp_2 - p_0 + K) + 5K.$$

This leads to

$$\underbrace{\begin{bmatrix} -\omega^2 & \omega^2 & -\omega^2 K \\ -\omega & -\omega^3 & 5\omega K \end{bmatrix}}_{A(\omega,K)} \underbrace{\begin{bmatrix} \Delta p_0 \\ \Delta p_1 \\ \Delta p_2 \end{bmatrix}}_{t} = \underbrace{\begin{bmatrix} \omega^2 p_0 - \omega^2 p_1 + \omega^2 K p_2 - 5K \\ \omega p_0 + \omega^3 p_1 - 5\omega K p_2 - \omega K \end{bmatrix}}_{b(\omega,\mathbf{p}^0,K)}$$

and the ℓ_2 stability margin around $\mathbf{p}^0$ is

$$\begin{aligned}\rho^*(\mathbf{p}^0, K) &= \min_{\omega} \rho(\omega, \mathbf{p}^0, K) \\ &= \min_{\omega} \left\| A^T(\omega, K) \left(A(\omega, K) A^T(\omega, K) \right)^{-1} b(\omega, \mathbf{p}^0, K) \right\|_2 .\end{aligned}$$

To determine the worst case ℓ_2 stability margin over $\mathbf{\Pi}$ for fixed $K = K_0$ we apply Theorem 4.7. This tells us that the worst case stability margin occurs on one of the edges $\mathbf{\Pi}_{\mathrm{E}}$ of $\mathbf{\Pi}$. The characteristic polynomial of the closed loop system is

$$\delta(s, \mathbf{p}) = \underbrace{s^2(s-1)}_{Q_1(s)} p_1 + \underbrace{s(s-1)}_{Q_2(s)} p_0 + \underbrace{K_0 s(s+5)}_{Q_3(s)} p_2 + K_0(s+5)$$

which shows that the vertex condition of Theorem 4.8 is satisfied so that the worst case stability margin occurs on one of the vertices of $\mathbf{\Pi}$. Therefore, the worst case ℓ_2 stability margin for $K = K_0$ is

$$\rho^*(K_0) = \min_{\mathbf{p} \in \mathbf{\Pi}_{\mathrm{v}}} \rho^*(\mathbf{p}, K_0).$$

Suppose that we wish to determine the value of $K \in [0.5, 2]$ that possesses the *maximum* value of the worst case ℓ_2 stability margin. This problem can be solved by repeating the procedure of determining $\rho^*(K)$ for each K in $[0.5, 2]$ and selecting the value of K whose corresponding $\rho^*(K)$ is maximum:

$$\rho^* = \max_K \rho^*(K)$$

From Figure 4.19, we find that the maximum worst case ℓ_2 stability margin is 5.8878 when $K = 2$.

4.9 THE TSYPKIN-POLYAK PLOT

In this section we deal with stability margin calculations for characteristic polynomials of the form:

$$\delta(s, \mathbf{p}) = F_1(s)P_1(s) + F_2(s)P_2(s) + \cdots + F_m(s)P_m(s)$$

where $F_i(s)$ are fixed real or complex polynomials and the coefficients of the real polynomials $P_i(s)$, are the uncertain parameters. The uncertain real parameter vector $\mathbf{p} = [p_1, p_2 \cdots]$ represents these coefficients. An elegant graphical solution to this problem has been given by Tsypkin and Polyak based on evaluation of the image set. This method is described below.

We begin by considering the polynomial family

$$\mathbf{Q}(s) = \left\{ A(s) + \rho \sum_{i=1}^{l} r_i B_i(s) \ : \quad |r_i| \le 1, \quad i = 1, \cdots, l \right\} \tag{4.50}$$

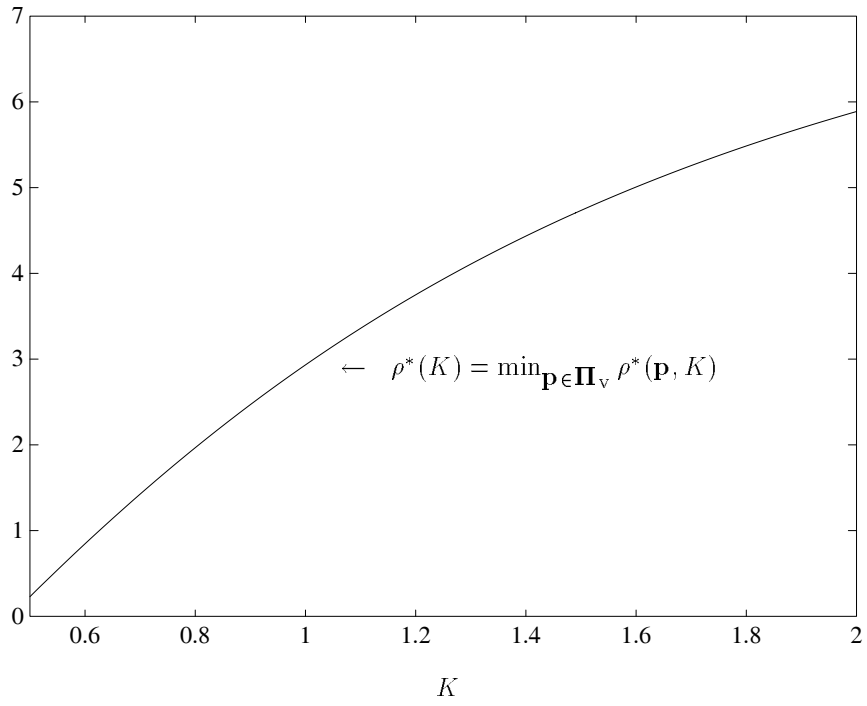

Figure 4.19. K vs. $\rho^*(K)$ (Example 4.13)

where $A(s)$ is a given real or complex polynomial of degree n and $B_1(s), \cdots, B_l(s)$ are given real or complex polynomials of degree $\leq n$, r_i are uncertain real parameters and the real parameter ρ is a common margin of perturbations or a dilation parameter. If we evaluate the above polynomial family at a point $s = s^*$ in the complex plane we obtain the image set of the family at that point. Because of the interval nature of the uncertain parameters, r_i, this set is a polygon. This polygon is determined by the complex numbers $A(s^*), B_1(s^*), \cdots, B_l(s^*)$. As discussed in the previous section, robust stability of a control system of which the polynomial above is the characteristic polynomial, requires that the family $\mathbf{Q}(s)$ be of constant degree. Under this assumption, the family $\mathbf{Q}(s)$ is stable if it contains at least one stable polynomial and the image set evaluated at each point of the stability boundary excludes the origin. The lemma given below gives an explicit geometric characterization of this condition.

Let us consider fixed nonzero complex numbers A, B_1, $\cdots$, B_l, and let

$$B_k = |B_k| e^{j\phi_k}, k = 1, 2, \cdots, l$$

and $A = |A|e^{j\theta}$. Introduce the set

$$\mathcal{B} = \left\{ \sum_{i=1}^{l} r_i B_i : |r_i| \leq 1 \right\},$$

which is a polygon in the complex plane with $2l$ or fewer vertices and opposite edges parallel to $B_i, i = 1, \cdots, l$. Consider the complex plane set $A + \rho\mathcal{B}$. This set is depicted in Figures 4.20 and 4.21.

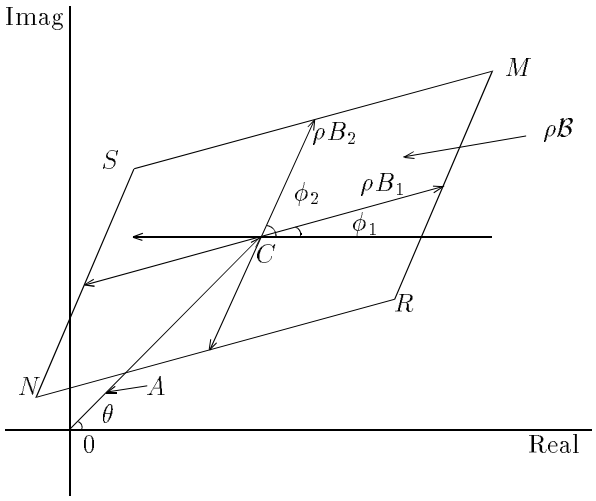

Figure 4.20. The set $A + \rho\mathcal{B}$

Lemma 4.3 *The zero exclusion condition*

$$0 \notin A + \rho\mathcal{B}, \qquad \rho > 0$$

is equivalent to

$$\max_{1 \leq k \leq l} \frac{|A||\sin(\theta - \phi_k)|}{\sum_{i=1}^{l} |B_i||\sin(\phi_i - \phi_k)|} > \rho, \quad \text{if } \sin(\phi_i - \phi_k) \neq 0 \text{ for some } i, k \tag{4.51}$$

$$\max_{1 \leq k \leq l} \frac{|A|}{\sum_{i=1}^{l} |B_i|} > \rho, \quad \text{if } \sin(\phi_i - \phi_k) \equiv 0 \text{ and } \sin(\theta - \phi_k) \equiv 0, \quad \forall\, i, k. \tag{4.52}$$

Proof. The origin is excluded from the convex set $A + \rho\mathcal{B}$ if and only if there exists a line L' which separates the set from the origin. Consider the projection of the set $A + \rho\mathcal{B}$ onto the orthogonal complement L' of the line L in the complex

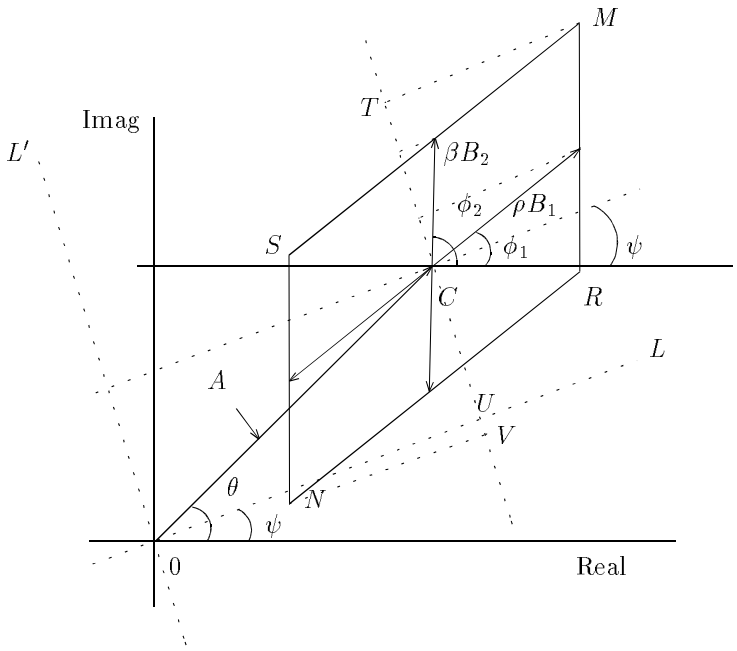

Figure 4.21. Projection of $A + \rho\mathcal{B}$ onto L'

plane passing through the origin at an angle ψ with the real axis (see Figure 4.21). This projection is of length

$$2\rho(|B_1||\sin(\phi_1 - \psi)| + \cdots + |B_l||\sin(\phi_l - \psi)|)$$

and is shown in the Figure 4.21 as TV. On the other hand the projection of the vector A on to L' is of length $|A||\sin(\theta - \psi)|$ and is shown as the line CU in Figure 4.21. A line separating the origin from the set exists if and only if there exists some $\psi \in [0, 2\pi)$ for which

$$|A||\sin(\theta - \psi)| > \rho(|B_1||\sin(\phi_1 - \psi)| + \cdots + |B_l||\sin(\phi_l - \psi)|).$$

Since the set $\mathcal{B}$ is a polygon it suffices to choose L to be parallel to one of its sides. This can be visualized as sliding the set along lines parallel to its sides and checking if the origin enters the set at any position. Thus it is enough to test that the above inequality holds at one of the values $\psi = \phi_i$, $i = 1, 2, \cdots, l$. This is precisely what is expressed by the formula (4.51) above. The formula (4.52) deals with the degenerate case when the set collapses to a line even though $l \neq 1$. ♣

The expressions (4.51) and (4.52) can also be written in the alternative form:

$$\max_{1\le k\le l} \frac{\left|\mathrm{Im}\left(\frac{A}{B_k}\right)\right|}{\sum_{i=1}^{l}\left|\mathrm{Im}\left(\frac{B_i}{B_k}\right)\right|} > \rho, \quad \text{if } \mathrm{Im}\left(\frac{B_i}{B_k}\right) \neq 0 \text{ for some } i,k \tag{4.53}$$

$$\max_{1\le k\le l} \frac{|A|}{\sum_{i=1}^{l}|B_i|} > \rho, \quad \text{if } \mathrm{Im}\left(\frac{B_i}{B_k}\right) \equiv 0 \text{ and } \left(\frac{A}{B_k}\right) \equiv 0, \quad \forall\ i,k. \tag{4.54}$$

We now apply this result to the special form of the characteristic polynomial (4.2).

Linear Interval Family

We consider the Hurwitz stability of the family of constant degree polynomials

$$\begin{aligned} \delta(s,\mathbf{p}) &= F_1(s)P_1(s) + \cdots + F_m(s)P_m(s), \\ P_i(s) &= p_{i0} + p_{i1}s + \cdots, \qquad\qquad |p_{ik} - p_{ik}^0| \le \rho\alpha_{ik}, \\ F_i(s) &= f_{i0} + f_{i1}s + \cdots. \end{aligned} \tag{4.55}$$

Here p_{ik}^0 are the coefficients of the nominal polynomials

$$P_i^0(s) = p_{i0}^0 + p_{i1}^0 s + \cdots$$

$\alpha_{ik} \ge 0$ are given and $\rho \ge 0$ is a common margin of perturbations. Everywhere below stable means Hurwitz stable. Denote

$$\begin{aligned} A(s) &= F_1(s)P_1^0(s) + \cdots + F_m(s)P_m^0(s), \\ S_i(\omega) &= \alpha_{i0} + \alpha_{i2}\omega^2 + \cdots \\ T_i(\omega) &= \omega(\alpha_{i1} + \alpha_{i3}\omega^2 + \cdots), \\ \theta(\omega) &= \arg\ A(j\omega), \\ \psi_i(\omega) &= \arg\ F_i(j\omega), \qquad i = 1,\cdots,m, \end{aligned} \tag{4.56}$$

where $0 \le \omega \le \infty$. The image set of the family has the form

$$A(j\omega) + \rho\mathcal{Q}(\omega)$$

where

$$\mathcal{Q}(\omega) = \left\{ \sum_{i=1}^{m} [s_i(\omega) + jt_i(\omega)]\, F_i(j\omega) : \quad |s_i(\omega)| \le S_i(\omega), \quad |t_i(\omega)| \le T_i(\omega) \right\}$$

This set may be rewritten as

$$\mathcal{Q}(\omega) = \tag{4.57}$$

$$\left\{ \sum_{i=1}^{m} [r_i S_i(\omega)F_i(j\omega) + r_{m+i}T_i(\omega)jF_i(j\omega)], \quad |r_i| \le 1, \quad |r_{m+i}| \le 1, \quad i = 1,\cdots,m. \right\}.$$

We apply Lemma 4.3 (see (4.51)) to the above set by setting $l = 2m$, $B_i = S_i(\omega)F_i(j\omega)$, $i = 1, 2, \cdots, m$ and $B_i = T_i(\omega)jF_i(j\omega)$, $i = m+1, \cdots, 2m$. Since

$$\begin{aligned} \arg F_i(j\omega) &= \psi_i(\omega), \\ \arg jF_i(j\omega) &= \psi_{m+i}(\omega) = \psi_i(\omega) + \frac{\pi}{2}, \end{aligned}$$

for $i = 1, 2, \cdots, m$, we can rewrite (4.51) as the maximum of two terms:

$$\begin{aligned} \max_{1\le k\le m} \frac{|A(j\omega)||\sin(\theta(\omega)-\psi_k(\omega))|}{\sum_{i=1}^{2m}|B_i||\sin(\psi_i(\omega)-\psi_k(\omega))|} &= \max_{1\le k\le m} \frac{|A(j\omega)||\sin(\theta(\omega)-\psi_k(\omega))|}{v_k(\omega)} \\ \max_{m+1\le k\le 2m} \frac{|A(j\omega)||\sin(\theta(\omega)-\psi_k(\omega))|}{\sum_{i=1}^{2m}|B_i||\sin(\psi_i(\omega)-\psi_k(\omega))|} &= \max_{1\le k\le m} \frac{|A(j\omega)||\cos(\theta(\omega)-\psi_k(\omega))|}{u_k(\omega)} \end{aligned}$$

where $u_k(\omega)$ and $v_k(\omega)$ are defined as

$$\begin{aligned} u_k(\omega) := \sum_{i=1}^{m} &[S_i(\omega)|F_i(j\omega)||\cos(\psi_i(\omega)-\psi_k(\omega))| \\ &+T_i(\omega)|F_i(j\omega)||\sin(\psi_i(\omega)-\psi_k(\omega))|], \qquad k = 1, 2, \cdots, m \\ v_k(\omega) := \sum_{i=1}^{m} &[S_i(\omega)|F_i(j\omega)||\sin(\psi_i(\omega)-\psi_k(\omega))| \\ &+T_i(\omega)|F_i(j\omega)||\cos(\psi_i(\omega)-\psi_k(\omega))|], \qquad k = 1, 2, \cdots, m. \end{aligned}$$

Let Γ be defined as:

$$\begin{aligned} \Gamma := \{\omega : &\cos(\psi_i(\omega)-\psi_k(\omega)) = \sin(\psi_i(\omega)-\psi_k(\omega)) = 0, \\ &\omega \in [0,\infty), \quad i,k = 1, \cdots, m\}. \end{aligned}$$

We note that $u_k(\omega) = 0$ if and only if $\omega \in \Gamma$. Likewise $v_k(\omega) = 0$ if and only if $\omega \in \Gamma$. Now define

$$\begin{aligned} x_k(\omega) &:= \frac{|A(j\omega)||\cos(\theta(\omega)-\psi_k(\omega))|}{u_k(\omega)}, && \omega \notin \Gamma \\ x_k(\omega) &:= \frac{|A(j\omega)|}{\sum_{i=1}^{m}[S_i(\omega)|F_i(j\omega)| + T_i(\omega)|F_i(j\omega)|]}, && \omega \in \Gamma \end{aligned} \tag{4.58}$$

for $k = 1, 2, \cdots, m$ and

$$\begin{aligned} y_k(\omega) &:= \frac{|A(j\omega)||\sin(\theta(\omega)-\psi_k(\omega))|}{v_k(\omega)}, && \omega \notin \Gamma \\ y_k(\omega) &:= \frac{|A(j\omega)|}{\sum_{i=1}^{m}[S_i(\omega)|F_i(j\omega)| + T_i(\omega)|F_i(j\omega)|]}, && \omega \in \Gamma \end{aligned} \tag{4.59}$$

for $k = 1, 2, \cdots, m$. Finally let

$$\mu(\omega) := \max_{1 \le k \le m} \max \{x_k(\omega), y_k(\omega)\}, \qquad 0 \le \omega \le \infty. \tag{4.60}$$

Notice that $\mu(\omega)$ is well defined for all $\omega \in [0, \infty]$. However the frequencies 0, ∞ and the points $\omega \in \Gamma$ may be points of discontinuity of the function $\mu(\omega)$. For $\omega = 0$, it is easy to see that

$$\mu(0) = \max_{1 \le k \le m} \{x_k(0)\} = \frac{|\sum_{i=1}^m p_{i0}^0 f_{i0}|}{\sum_{i=1}^m \alpha_{i0} |f_{i0}|} := \mu_0. \tag{4.61}$$

We also have

$$\mu_n = \frac{|\sum_{i=1}^m \sum_{k+l=n} p_{ik}^0 f_{il}|}{\sum_{i=1}^m \sum_{k+l=n} \alpha_{ik} |f_{il}|}. \tag{4.62}$$

To state the equivalent nontrignometric expressions for x_k and y_k let

$$\frac{F_i(j\omega)}{F_k(j\omega)} = U_{ik}(\omega) + jV_{ik}(\omega)$$
$$\frac{A(j\omega)}{F_k(j\omega)} = U_{0k}(\omega) + jV_{0k}(\omega).$$

As before let $\omega \in \Gamma$ denote the set of common roots of the equations

$$U_{ik}(\omega) = V_{ik}(\omega) = 0, \quad i = 1, \cdots, m. \tag{4.63}$$

We have

$$x_k(\omega) = \frac{|U_{0k}(\omega)|}{\sum_{i=1}^m [S_i(\omega)|U_{ik}(\omega)| + T_i(\omega)|V_{ik}(\omega)|]}, \qquad \omega \notin \Gamma \tag{4.64}$$

$$y_k(\omega) = \frac{|V_{0k}(\omega)|}{\sum_{i=1}^m [S_i(\omega)|V_{ik}(\omega)| + T_i(\omega)|U_{ik}(\omega)|]}, \qquad \omega \notin \Gamma \tag{4.65}$$

and for $\omega \in \Gamma$, $x_k(\omega)$, $y_k(\omega)$ are defined as before in (4.58) and (4.59). Now let

$$\mu_{\min} := \inf_{0 < \omega < \infty} \mu(\omega) \tag{4.66}$$

and

$$\rho^* = \min\{\mu_0, \mu_n, \mu_{\min}\}. \tag{4.67}$$

Theorem 4.9 *The family (4.55) is stable if and only if $A(s)$ is Hurwitz and*

$$\rho^* > \rho. \tag{4.68}$$

Proof. The theorem can be proved by evaluating the image set $\{\delta(j\omega, \mathbf{p})\}$ for the family (4.55) and applying Lemma 4.3 to it. Recall the image set of the family has the form

$$A(j\omega) + \rho\mathcal{Q}(\omega)$$

where $\mathcal{Q}(\omega)$ is of the form in (4.57). We again apply Lemma 4.3 to the above set by setting $l = 2m$, $B_i = S_i(\omega)F_i(j\omega)$, $i = 1, 2, \cdots, m$ and $B_i = T_i(\omega)jF_i(j\omega)$, $i = m+1, \cdots, 2m$. Then the condition that the polygon $A(j\omega)+\rho\mathcal{Q}(\omega)$ exclude the origin for $0 \leq \omega < \infty$ corresponds to the condition $\mu_{\min} > \rho$. The condition that $A(0) + \rho\mathcal{Q}(0)$ excludes the origin corresponds to $\mu_0 > \rho$ and the condition that all polynomials in the family be of degree n corresponds to $\mu_n > \rho$. ♣

The requirement that $A(s)$ be Hurwitz can be combined with the robustness condition, namely verification of the inequality (4.68). This leads us to the following criterion.

Theorem 4.10 *The family (4.55) is stable if and only if* $A(j\omega) \neq 0$, $\rho < \mu_0$, $\rho < \mu_n$ *and the complex plane plot*

$$z(\omega) = \frac{A(j\omega)}{|A(j\omega)|}\mu(\omega) \tag{4.69}$$

goes through n quadrants as ω *runs from* 0 *to* ∞ *and does not intersect the circle of radius* ρ*, centered at the origin.*

The plot of $z(\omega)$ is known as the *Tsypkin-Polyak* plot. The maximal value of ρ in (4.55) which preserves robust stability is equal to the radius ρ^* of the largest circle, enclosed in the $z(\omega)$ plot, subject of course to the conditions $\rho < \mu_0$, $\rho < \mu_n$.

We illustrate these results with an example.

Example 4.14. Consider the family of polynomials

$$\delta(s, \mathbf{p}) = \underbrace{(s^2 + 2s + 2)}_{F_1(s)}\underbrace{(p_{11}s + p_{10})}_{P_1(s)} + \underbrace{(s^4 + 2s^3 + 2s^2 + s)}_{F_2(s)}\underbrace{(p_{22}s^2 + p_{21}s + p_{20})}_{P_2(s)}$$

where the nominal values of parameters $\mathbf{p}$ in $P_1(s)$ and $P_2(s)$ are

$$\mathbf{p}^0 = [p_{11}^0 \;\; p_{10}^0 \;\; p_{22}^0 \;\; p_{21}^0 \;\; p_{20}^0] = [0.287 \;\; 0.265 \;\; 0.215 \;\; 2.06 \;\; 2.735].$$

We first verify that the nominal polynomial

$$\begin{aligned} A(s) &= F_1(s)P_1^0(s) + F_2(s)P_2^0(s) \\ &= 0.215s^6 + 2.49s^5 + 7.285s^4 + 10.092s^3 + 8.369s^2 + 3.839s + 0.53 \end{aligned}$$

is Hurwitz. We want to find the stability margin ρ such that the family remains Hurwitz for all parameter excursions satisfying

$$|p_{ik} - p_{ik}^0| \leq \rho\alpha_{ik}$$

with $\alpha_{ik} = 1$ for $ik = 10, 11, 20, 21, 22$. Here we use the nontrignometric expressions given in (4.64) and (4.65). We first compute

$$\begin{aligned}
\frac{F_1(j\omega)}{F_1(j\omega)} &= 1 + j0 = U_{11}(\omega) + jV_{11}(\omega) \\
\frac{F_2(j\omega)}{F_1(j\omega)} &= \frac{-\omega^6 - 2\omega^2}{\omega^2 + 4} + j\frac{-\omega^3 + 2\omega}{\omega^2 + 4} = U_{21}(\omega) + jV_{21}(\omega) \\
\frac{F_1(j\omega)}{F_2(j\omega)} &= \frac{-\omega^4 - 2}{\omega^6 + 1} + j\frac{\omega^2 - 2}{\omega^7 + \omega} = U_{12}(\omega) + jV_{12}(\omega) \\
\frac{F_2(j\omega)}{F_2(j\omega)} &= 1 + j0 = U_{22}(\omega) + jV_{22}(\omega)
\end{aligned}$$

and

$$\begin{aligned}
\frac{A(j\omega)}{F_1(j\omega)} &= \frac{0.215\omega^8 - 2.735\omega^6 + 2.755\omega^4 - 9.59\omega^2 + 1.06}{\omega^2 + 4} \\
&\qquad + j\frac{-2.06\omega^7 + 0.502\omega^5 - 7.285\omega^3 + 6.618\omega}{\omega^2 + 4} \\
&= U_{01}(\omega) + jV_{01}(\omega) \\
\frac{A(j\omega)}{F_2(j\omega)} &= \frac{-0.215\omega^8 + 2.735\omega^6 - 0.265\omega^4 - 0.502\omega^2 + 2.779}{\omega^6 + 1} \\
&\qquad + j\frac{2.06\omega^8 - 0.287\omega^6 + 1.751\omega^3 - 0.53}{\omega^7 + \omega} \\
&= U_{02}(\omega) + jV_{02}(\omega).
\end{aligned}$$

With the given choice of α_{ik}, we also have

$$S_1(\omega) = 1, \qquad S_2(\omega) = 1 + \omega^2, \qquad T_1(\omega) = \omega, \qquad T_2(\omega) = \omega.$$

From these we construct the function

$$z(\omega) = \frac{A(j\omega)}{|A(j\omega)|}\mu(\omega) = \frac{A(j\omega)}{|A(j\omega)|}\left[\max_{k=1,2} \max\{x_k(\omega), y_k(\omega)\}\right]$$

where $x_k(\omega)$ and $y_k(\omega)$ are given as follows:

$$x_1(\omega) = \frac{\left|\dfrac{0.215\omega^8 - 2.735\omega^6 + 2.755\omega^4 - 9.59\omega^2 + 1.06}{\omega^2 + 4}\right|}{1 + (1 + \omega^2)\left|\dfrac{-\omega^6 - 2\omega^2}{\omega^2 + 4}\right| + \omega\left|\dfrac{-\omega^3 + 2\omega}{\omega^2 + 4}\right|}$$

$$x_2(\omega) = \frac{\left|\dfrac{-0.215\omega^8 + 2.735\omega^6 - 0.265\omega^4 - 0.502\omega^2 + 2.779}{\omega^6 + 1}\right|}{\left|\dfrac{-\omega^4 - 2}{\omega^6 + 1}\right| + \omega\left|\dfrac{\omega^2 - 2}{\omega^7 + \omega}\right| + (1 - \omega^2)}$$

$$y_1(\omega) = \frac{\left| \dfrac{-2.06\omega^7 + 0.502\omega^5 - 7.285\omega^3 + 6.618\omega}{\omega^2 + 4} \right|}{\omega + (1+\omega^2)\left| \dfrac{-\omega^3 + 2\omega}{\omega^2 + 4} \right| + \omega \left| \dfrac{-\omega^6 - 2\omega^2}{\omega^2 + 4} \right|}$$

$$y_2(\omega) = \frac{\left| \dfrac{2.06\omega^8 - 0.287\omega^6 + 1.751\omega^3 - 0.53}{\omega^7 + \omega} \right|}{\left| \dfrac{\omega^2 - 2}{\omega^7 + \omega} \right| + \omega \left| \dfrac{-\omega^4 - 2}{\omega^6 + 1} \right| + \omega}.$$

μ_0 and μ_n are given by

$$\mu_0 = \frac{\left| \sum_{i=1}^{2} p_{i0}^0 f_{i0} \right|}{\sum_{i=1}^{2} \alpha_{i0} |f_{i0}|} = \frac{|(0.265)(2)|}{(1)|(2)|} = 0.265$$

$$\mu_n = \frac{\left| \sum_{i=1}^{2} \sum_{k+l=n} p_{ik}^0 f_{il} \right|}{\sum_{i=1}^{2} \sum_{k+l=n} \alpha_{ik} |f_{il}|} = \frac{|(0.215)(1)|}{(1)|(1)|} = 0.215$$

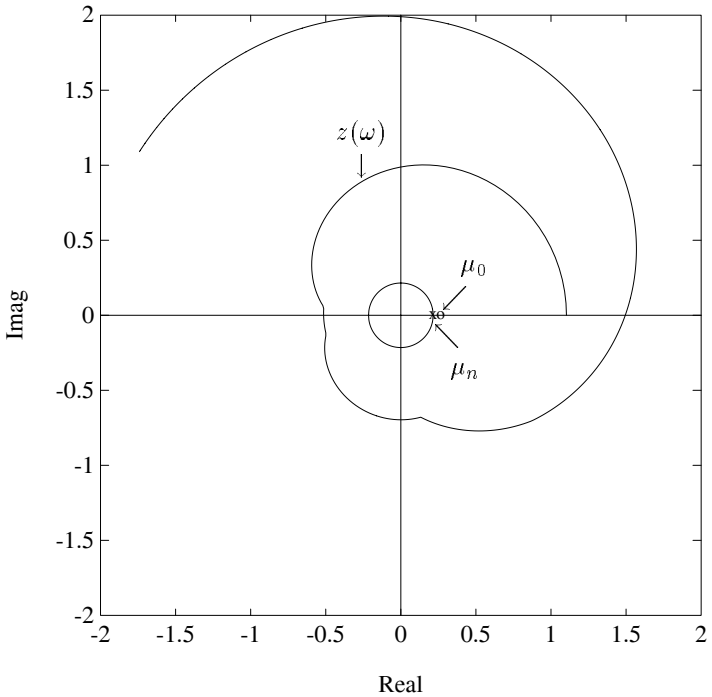

Figure 4.22. Tsypkin-Polyak locus for a polytopic family (Example 4.14)

Figure 4.22 displays the Tsypkin-Polyak plot $z(\omega)$ along with μ_0 and μ_n. The radius of the smallest circle which touches this plot is ρ^*. From the figure we find

$$\rho^* = 0.215.$$

4.10 ROBUST STABILITY OF LINEAR DISC POLYNOMIALS

In the last chapter we considered the robust stability of a family of *disc* polynomials. The main result derived there considered the coefficients themselves to be subject to *independent* perturbations. Here we consider interdependent perturbations by letting the coefficients depend linearly on a primary set of parameters δ_i.

Consider $n+1$ complex polynomials $P_0(s)$, $\cdots$, $P_n(s)$, such that

$$\deg(P_0(s)) > \max_{i \in \{1,2,\cdots,n\}} \deg(P_i(s)). \tag{4.70}$$

Let also $D_1,\cdots,D_n$ be n arbitrary discs in the complex plane, where D_i is centered at the complex number d_i and has radius r_i.

Now consider the set $\mathcal{P}$ of all polynomials of the form:

$$\delta(s) = P_0(s) + \sum_{i=1}^{n} \delta_i P_i(s), \quad \text{where } \delta_i \in D_i, \quad i = 1, 2, \cdots, n. \tag{4.71}$$

We refer to such a family as a *linear disc polynomial*. If we define $\beta(s)$ by

$$\beta(s) = P_0(s) + \sum_{i=1}^{n} d_i P_i(s) \tag{4.72}$$

then it is clear that Lemma 3.2 (Chapter 3) can be readily extended to the following result.

Lemma 4.4 *The family of complex polynomial $\mathcal{P}$ contains only Hurwitz polynomials if and only if the following conditions hold:*

a) $\beta(s)$ is Hurwitz

b) for any complex numbers $z_0,\cdots,z_n$ of modulus less than or equal to one we have:

$$\left\| \frac{\sum_{k=1}^{n} z_k r_k P_k(s)}{\beta(s)} \right\|_\infty < 1.$$

The proof of this Lemma follows from Rouché's Theorem in a manner identical to that of Lemma 3.2 in Chapter 3. Observe now, that for any complex numbers z_i of modulus less than or equal to one, we have the following inequality:

$$\left| \frac{\sum_{k=1}^{n} z_k r_k P_k(j\omega)}{\beta(j\omega)} \right| \leq f(\omega) \tag{4.73}$$

where

$$f(\omega) = \frac{\sum_{k=1}^{n} r_k |P_k(j\omega)|}{|\beta(j\omega)|}. \tag{4.74}$$

On the other hand, since $f(\omega)$ is a continuous function of ω which goes to 0 as ω goes to infinity, then $f(\omega)$ reaches its maximum for some finite value ω_0. At this point ω_0 it is always possible to write

$$P_k(j\omega_0) = e^{j\theta_k} |P_k(j\omega_0)|, \quad \text{with} \quad \theta_k \in [0, 2\pi) \quad \text{for} \quad k = 1, 2, \cdots, n$$

so we see that it is always possible to find a set of complex numbers $z_0, \cdots, z_n$ such that (4.73) becomes an equality at the point where $f(\omega)$ reaches its maximum. As a result we have the following generalization of the result on disc polynomials given in Chapter 3.

Theorem 4.11 *The family of complex polynomials $\mathcal{P}$ contains only Hurwitz polynomials if and only if the following conditions hold:*

a) $\beta(s)$ is Hurwitz

b) for all $\omega \in \mathbb{R}$,

$$\frac{\sum_{k=1}^{n} r_k |P_k(j\omega)|}{|\beta(j\omega)|} < 1.$$

A similar result holds also for the Schur case.

4.11 EXERCISES

4.1 In a standard unity feedback control system, the plant is

$$G(s) = \frac{a_1 s - 1}{s^2 + b_1 s + b_0}.$$

The parameters a_1, b_0 and b_1 have nominal values $a_1^0 = 1$, $b_1^0 = -1$, $b_0^0 = 2$ and are subject to perturbation. Consider the constant controller $C(s) = K$. Determine the range of values S_k of K for which the nominal system remains Hurwitz stable. For each value of $K \in S_k$ find the ℓ_2 stability margin $\rho(K)$ in the space of the three parameters subject to perturbation. Determine the optimally robust compensator value $K \in S_k$.

4.2 Repeat Exercise 4.1 using the ℓ_∞ stability margin.

4.3 Consider the polynomial

$$s^4 + s^3(12 + p_1 + p_3) + s^2(47 + 10.75p_1 + 0.75p_2 + 7p_3 + 0.25p_4)$$
$$+ s(32.5p_1 + 7.5p_2 + 12p_3 + 0.5p_4) + 18.75p_1 + 18.75p_2 + 10p_3 + 0.5p_4.$$

Determine the ℓ_2 Hurwitz stability margin in the parameter space $[p_1, p_2, p_3, p_4]$.

4.4 The nominal polynomial (i.e. with $\Delta p_i = 0$) in Exercise 4.3 has roots -5, -5, $-1-j$, $-1+j$. Let the stability boundary consist of two circles of radii 0.25 centered at $-1+j$ and $-1-j$ respectively and a circle of radius 1 centered at -5. Determine the maximal ℓ_2 stability ball for this case.

4.5 Repeat Exercise 4.4 with the ℓ_∞ stability margin.

4.6 The transfer function of a plant in a unity feedback control system is given by

$$G(s) = \frac{1}{s^3 + d_2(\mathbf{p})s^2 + d_1(\mathbf{p})s + d_0(\mathbf{p})}$$

where

$$\mathbf{p} = [p_1, p_2, p_3]$$

and

$$d_2(\mathbf{p}) = p_1 + p_2, \quad d_1(\mathbf{p}) = 2p_1 - p_3, \quad d_0(\mathbf{p}) = 1 - p_2 + 2p_3.$$

The nominal parameter vector is $\mathbf{p}^0 = [3, 3, 1]$ and the controller proposed is

$$C(s) = K_c \frac{1 + 0.667s}{1 + 0.0667s}$$

with the nominal value of the gain being $K_c = 15$. Compute the weighted ℓ_∞ Hurwitz stability margin with weights $[w_1, w_2, w_3] = [1, 1, 0.1]$.

4.7 In Exercise 4.6 assume that K_c is the only adjustable design parameter and let $\rho(K_c)$ denote the weighted ℓ_∞ Hurwitz stability margin with weights as in Problem 4.6. Determine the range of values of K_c for which all perturbations within the unit weighted ℓ_∞ ball are stabilized, i.e. for which $\rho(K_c) > 1$.

4.8 Repeat Exercises 4.6 and 4.7 with the weighted ℓ_2 stability margin.

4.9 In Exercises 4.7 and 4.8 determine the optimally robust controllers in the weighted ℓ_2 or weighted ℓ_∞ stability margins, over the range of values of K_c which stabilizes the nominal plant.

4.10 Consider a complex plane polygon $\mathcal{P}$ with consecutive vertices $z_1, z_2, \cdots z_N$ with $N > 2$. Show that a point z is excluded from (does not belong to) $\mathcal{P}$ if and only if

$$\min_{1 \le n \le N} \left\{ \mathrm{Im} \frac{z - z_i}{z_{i+1} - z_1} \right\} < 0.$$

Use this result to develop a test for stability of a polytopic family.

4.11 In a discrete time control system the transfer function of the plant is:

$$G(z) = \frac{z-2}{(z+1)(z+2)}.$$

Determine the transfer function of a first order controller

$$C(z) = \frac{\alpha_0 + \alpha_1 z}{z + \beta_0}$$

which results in a closed loop system that is deadbeat, i.e. the characteristic roots are all at the origin. Determine the largest ℓ_2 and ℓ_∞ stability balls centered at this controller in the space of controller parameters α_0, α_1, β_0 for which closed loop Schur stability is preserved.

4.12 Consider the Hurwitz stability of the family

$$\begin{aligned} \mathbf{P}(s) &= \left\{ P_0(s) + \rho \sum_{i=1}^{m} r_i P_i(s) : |r_i| \le 1 \right\} \\ P_i(s) &= a_{i0} + a_{i1} s + \cdots + a_{in} s^n, \quad a_{0n} \neq 0 \end{aligned} \tag{4.75}$$

Let ω_l denote a real root of the equations

$$\mathrm{Im}\left[\frac{P_i(j\omega)}{P_0(j\omega)}\right] = 0$$

and define

$$\begin{aligned} u_i(\omega) &= |P_i(j\omega)|, \\ \psi_i(\omega) &= \arg P_i(j\omega) \\ \rho(\omega) &= \max_{1 \le k \le m} \frac{u_0(\omega)|\sin(\psi_0(\omega) - \psi_k(\omega))|}{\sum_{i=1}^{m} u_i(\omega)|\sin(\psi_i(\omega) - \psi_k(\omega))|}, \quad \omega \neq \omega_l, \end{aligned}$$

and

$$\begin{aligned} \rho(\omega_l) &= \frac{|P_0(j\omega_l)|}{\sum_{i=1}^{\infty} |P_i(j\omega_l)|} \\ \rho(\infty) &= \frac{|a_{0n}|}{\sum_{i=1}^{m} |a_{in}|} \end{aligned}$$

Show that the family (4.75) is stable if and only if $P_0(s)$ is stable and $\rho(\omega) > \rho,\ 0 \le \omega \le \infty$.

4.13 Consider now the ℓ_p-analog of the above family:

$$P(s) = P_0(s) + \gamma \sum_{i=1}^{m} r_i P_i(s), \qquad \left[\sum_{i=1}^{m} |r_i|^p\right]^{\frac{1}{p}} \le 1 \tag{4.76}$$

where $1 \le p \le \infty$. This set of polynomials is not a polytope when $p \neq 1$ or $p \neq \infty$. Write

$$\frac{1}{p} + \frac{1}{q} = 1, \qquad P_i(j\omega) = u_i(\omega) e^{j\psi_i(\omega)}, \qquad i = 0, \cdots, m$$

$$\rho(\omega) = \max_{0 \le \phi \le 2\pi} \frac{u_0(\omega)\sin(\psi_0(\omega) - \phi)}{[\sum_{k=1}^{m} |u_k(\omega)\sin(\psi_k(\omega) - \phi)|^q]^{\frac{1}{q}}}$$

For $p = 2$ (ellipsoidal constraints) show that the condition for robust stability can be written in the form $\rho(\omega) > \rho$ by introducing:

$$P_i(j\omega) := U_i(\omega) + jV_i(\omega), \quad i = 0, \cdots, m$$

$$\Delta := \sum_{i=1}^{m} U_k^2 \sum_{i=1}^{m} V_k^2 - \left[\sum_{i=1}^{m} U_k V_k\right]^2$$

$$\alpha := \Delta^{-1}\left[V_0 \sum_{i=1}^{m} U_k V_k - U_0 \sum_{i=1}^{m} V_k^2\right]$$

$$\beta := \Delta^{-1}\left[U_0 \sum_{i=1}^{m} U_k V_k - V_0 \sum_{i=1}^{m} U_k^2\right]$$

$$\rho^2(\omega) = \alpha^2 \sum_{i=1}^{m} U_k^2 + 2\alpha\beta \sum_{i=1}^{m} U_k V_k + \beta^2 \sum_{i=1}^{m} V_k^2.$$

4.14 Consider the family of polynomials

$$a_0 + a_1 z + a_2 z^2 + \cdots + a_n z^n, \quad |a_k - a_k^0| < \rho\alpha_k$$

and denote the nominal polynomial as $A_0(z)$. Show that all polynomials in this family have their roots inside the unit circle if and only if the plot

$$z(\theta) = \frac{A_0(e^{j\theta})}{|A_0(e^{j\theta})|}\mu(\theta)$$

$$\mu(\theta) = \max_{0 \le i \le n} \frac{|\sum_{k=1}^{m} a_k^0 \sin(k-i)\theta|}{\sum_{k=1}^{m} \alpha_k |\sin(k-i)\theta|}, \qquad 0 < \theta < \pi$$

$$\mu(0) = \frac{|\sum_{k=1}^{m} a_k^0|}{\sum_{k=1}^{m} \alpha_k}$$

$$\mu(\pi) = \frac{|\sum_{k=1}^{m} (-1)^k a_k^0|}{\sum_{k=1}^{m} \alpha_k}$$

makes n turns around the origin as θ runs from 0 to 2π and does not intersect the circle of radius ρ.

4.15 Consider the Hurwitz stability of the family of polynomials

$$\delta(s, \mathbf{p}) = p_1 s(s + 9.5)(s - 1) - p_2(6.5s + 0.5)(s - 2)$$

where $p_1 \in [1, 1.1]$ and $p_2 \in [1.2, 1.25]$. Show that the family is robustly stable. Determine the worst case stability margins over the given uncertainty set using the ℓ_2 and then the ℓ_∞ norm.

4.12 NOTES AND REFERENCES

The problem of calculating the ℓ_2 stability margin in parameter space for Hurwitz stability in the linear case was solved in Biernacki, Hwang and Bhattacharyya [40], Chapellat, Bhattacharyya and Keel [62], Chapellat and Bhattachar-yya [59]. The problem of computing the real stability margin has been dealt with by Hinrichsen and Pritchard [114, 112, 111], Tesi and Vicino [220, 218], Vicino, Tesi and Milanese [230], DeGaston and Safonov [80], and Sideris and Sánches Peña [210]. Real parametric stability margins for discrete time control systems were calculated in Aguirre, Chapellat, and Bhattacharyya [4]. The calculation of the ℓ_2 stability margin in time delay systems (Theorem 4.4) is due to Kharitonov [145]. The type of pitfall pointed out in Example 4.6 is due to Soh and Foo [216]. The stability detecting property of exposed edges was generalized by Soh and Foo [215] to arbitrary analytic functions. The reduction of the ℓ_∞ problem to a linear programming problem was pointed out by Tesi and Vicino in [220]. The Tsypkin-Polyak plot, Theorems 4.9 and 4.10, and the results described in Exercises 4.12-4.14 were developed in [225, 226]. The problem of discontinuity of the parametric stability margin was highlighted by Barmish, Khargonekar, Shi, and Tempo [16], and Example 4.2 is adapted from [16]. A thorough analysis of the problem of discontinuity of the parametric stability margin has been carried out by Vicino and Tesi in [229]. The role of exposed edges in determining the stability of polytopes originates from and follows from the Edge Theorem due to Bartlett, Hollot, and Lin [21] which we develop in Chapter 6. This idea was explored in Fu and Barmish [99] for polytopes of polynomials and by Fu, Olbrot, and Polis [100] for polytopic systems with time-delay. Exercise 4.10 is taken from Kogan [149]. Example 4.8 is due to Vicino and Tesi [220] and is taken from [220]. The *image set* referred to here is also called the *value set* in the literature in this field.

Chapter 5

INTERVAL POLYNOMIALS: KHARITONOV'S THEOREM

In this chapter we present Kharitonov's Theorem on robust Hurwitz stability of interval polynomials, dealing with both the real and complex cases. This elegant result forms the basis for many of the results, to be developed later in the book, on robustness under parametric uncertainty. We develop an important extremal property of the associated Kharitonov polynomials and give an application of this theorem to state feedback stabilization. An extension of Kharitonov's Theorem to nested families of interval polynomials is described. Robust Schur stability of interval polynomials is also discussed and it is shown that robust stability can be ascertained from that of the upper edges.

5.1 INTRODUCTION

We devote this chapter mainly to a result proved in 1978 by V. L. Kharitonov, regarding the Hurwitz stability of a family of *interval polynomials*. This result was so surprising and elegant that it has been the starting point of a renewed interest in robust control theory with an emphasis on *deterministic bounded parameter perturbations*. It is important therefore that control engineers thoroughly understand both result and proof, and this is why we considerably extend our discussion of this subject.

In the next section we first state and prove Kharitonov's Theorem for real polynomials. We emphasize how this theorem generalizes the Hermite-Biehler Interlacing Theorem which is valid for a single polynomial. This has an appealing frequency domain interpretation in terms of *interlacing of frequency bands*. We then give an interpretation of Kharitonov's Theorem based on the evolution of the complex plane image set of the interval polynomial family. Here again the Boundary Crossing Theorem and the monotonic phase increase property of Hurwitz polynomials (Chapter 1) are the key concepts that are needed to establish the Theorem. This proof gives useful geometric insight into the working of the theorem and shows how the result is related to the Vertex Lemma (Chapter 2). We then state the theorem for the

case of an interval family of polynomials with complex coefficients. This proof follows quite naturally from the above interlacing point of view. Next, we develop an important *extremal property* of the Kharitonov polynomials. This property establishes that one of the four points represented by the Kharitonov polynomials is the closest to instability over the entire set of uncertain parameters. The latter result is independent of the norm used to measure the distance between polynomials in the coefficient space. We next give an application of the Kharitonov polynomials to robust state feedback stabilization. Following this we establish that Kharitonov's Theorem can be extended to nested families of interval polynomials which are neither interval or polytopic and in fact includes nonlinear dependence on uncertain parameters. In the last section we consider the robust Schur stability of an interval polynomial family. A stability test for this family is derived based on the upper edges which form a subset of all the exposed edges. We illustrate the application of these fundamental results to control systems with examples.

5.2 KHARITONOV'S THEOREM FOR REAL POLYNOMIALS

In this chapter stable will mean Hurwitz stable unless otherwise stated. Of course, we will say that a set of polynomials is stable if and only if each and every element of the set is a Hurwitz polynomial.

Consider now the set $\mathcal{I}(s)$ of real polynomials of degree n of the form

$$\delta(s) = \delta_o + \delta_1 s + \delta_2 s^2 + \delta_3 s^3 + \delta_4 s^4 + \cdots + \delta_n s^n$$

where the coefficients lie within given ranges,

$$\delta_0 \in [x_0, y_0],\ \delta_1 \in [x_1, y_1],\ \cdots,\ \delta_n \in [x_n, y_n].$$

Write

$$\underline{\delta} := [\delta_0,\ \delta_1,\ \cdots,\ \delta_n]$$

and identify a polynomial $\delta(s)$ with its coefficient vector $\underline{\delta}$. Introduce the hyperrectangle or box of coefficients

$$\mathbf{\Delta} := \left\{ \underline{\delta} : \underline{\delta} \in \mathbb{R}^{n+1},\quad x_i \le \delta_i \le y_i,\quad i = 0, 1, \cdots, n \right\}. \tag{5.1}$$

We assume that the degree remains invariant over the family, so that $0 \notin [x_n, y_n]$. Such a set of polynomials is called a real *interval* family and we loosely refer to $\mathcal{I}(s)$ as an interval polynomial. Kharitonov's Theorem provides a surprisingly simple necessary and sufficient condition for the Hurwitz stability of the entire family.

Theorem 5.1 (Kharitonov's Theorem)
Every polynomial in the family $\mathcal{I}(s)$ is Hurwitz if and only if the following four extreme polynomials are Hurwitz:

$$K^1(s) = x_o + x_1 s + y_2 s^2 + y_3 s^3 + x_4 s^4 + x_5 s^5 + y_6 s^6 + \cdots,$$

$$
\begin{aligned}
K^2(s) &= x_o + y_1 s + y_2 s^2 + x_3 s^3 + x_4 s^4 + y_5 s^5 + y_6 s^6 + \cdots, \\
K^3(s) &= y_o + x_1 s + x_2 s^2 + y_3 s^3 + y_4 s^4 + x_5 s^5 + x_6 s^6 + \cdots, \\
K^4(s) &= y_o + y_1 s + x_2 s^2 + x_3 s^3 + y_4 s^4 + y_5 s^5 + x_6 s^6 + \cdots.
\end{aligned} \tag{5.2}
$$

The box $\mathbf{\Delta}$ and the vertices corresponding to the Kharitonov polynomials are shown in Figure 5.1. The proof that follows allows for the interpretation of Kharitonov's

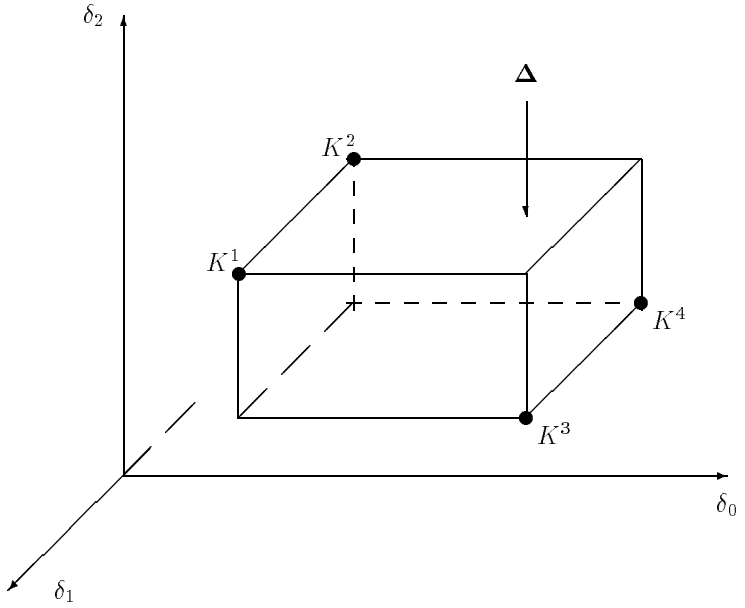

Figure 5.1. The box $\mathbf{\Delta}$ and the four Kharitonov vertices

Theorem as a generalization of the Hermite-Biehler Theorem for Hurwitz polynomials, proved in Theorem 1.7 of Chapter 1. We start by introducing two symmetric lemmas that will lead us naturally to the proof of the theorem.

Lemma 5.1 *Let*

$$
\begin{aligned}
P_1(s) &= P^{\text{even}}(s) + P_1^{\text{odd}}(s) \\
P_2(s) &= P^{\text{even}}(s) + P_2^{\text{odd}}(s)
\end{aligned}
$$

denote two stable polynomials of the same degree with the same even part $P^{\text{even}}(s)$ *and differing odd parts* $P_1^{\text{odd}}(s)$ *and* $P_2^{\text{odd}}(s)$ *satisfying*

$$
P_1^o(\omega) \leq P_2^o(\omega), \qquad \text{for all } \omega \in [0, \infty]. \tag{5.3}
$$

Then,

$$P(s) = P^{\text{even}}(s) + P^{\text{odd}}(s)$$

is stable for every polynomial $P(s)$ with odd part $P^{\text{odd}}(s)$ satisfying

$$P_1^o(\omega) \leq P^o(\omega) \leq P_2^o(\omega), \qquad \text{for all } \omega \in [0, \infty]. \tag{5.4}$$

Proof. Since $P_1(s)$ and $P_2(s)$ are stable, $P_1^o(\omega)$ and $P_2^o(\omega)$ both satisfy the interlacing property with $P^e(\omega)$. In particular, $P_1^o(\omega)$ and $P_2^o(\omega)$ are not only of the same degree, but the sign of their highest coefficient is also the same since it is in fact the same as that of the highest coefficient of $P^e(\omega)$. Given this it is easy to see that $P^o(\omega)$ cannot satisfy (5.4) unless it also has this same degree and the same sign for its highest coefficient. Then, the condition in (5.4) forces the roots of $P^o(\omega)$ to interlace with those of $P^e(\omega)$. Therefore, according to the Hermite-Biehler Theorem (Theorem 1.7, Chapter 1), $P^{\text{even}}(s) + P^{\text{odd}}(s)$ is stable. ♣

We remark that Lemma 5.1 as well as its dual, Lemma 5.2 given below, are special cases of the Vertex Lemma, developed in Chapter 2 and follow immediately from it. We illustrate Lemma 5.1 in the example below (see Figure 5.2).

Example 5.1. Let

$$P_1(s) = s^7 + 9s^6 + 31s^5 + 71s^4 + 111s^3 + 109s^2 + 76s + 12$$
$$P_2(s) = s^7 + 9s^6 + 34s^5 + 71s^4 + 111s^3 + 109s^2 + 83s + 12.$$

Then

$$P^{\text{even}}(s) = 9s^6 + 71s^4 + 109s^2 + 12$$
$$P_1^{\text{odd}}(s) = s^7 + 31s^5 + 111s^3 + 76s$$
$$P_2^{\text{odd}}(s) = s^7 + 34s^5 + 111s^3 + 83s.$$

Figure 5.2 shows that $P^e(\omega)$ and the tube bounded by $P_1^o(\omega)$ and $P_2^o(\omega)$ satisfy the interlacing property.

Thus, we conclude that every polynomial $P(s)$ with odd part $P^{\text{odd}}(s)$ satisfying

$$P_1^o(\omega) \leq P^o(\omega) \leq P_2^o(\omega), \qquad \text{for all } \omega \in [0, \infty]$$

is stable. For example, the dotted line shown inside the tube represents

$$P^{\text{odd}}(s) = s^7 + 32s^5 + 111s^3 + 79s.$$

The dual of Lemma 5.1 is:

Lemma 5.2 *Let*

$$P_1(s) = P_1^{\text{even}}(s) + P^{\text{odd}}(s)$$
$$P_2(s) = P_2^{\text{even}}(s) + P^{\text{odd}}(s)$$

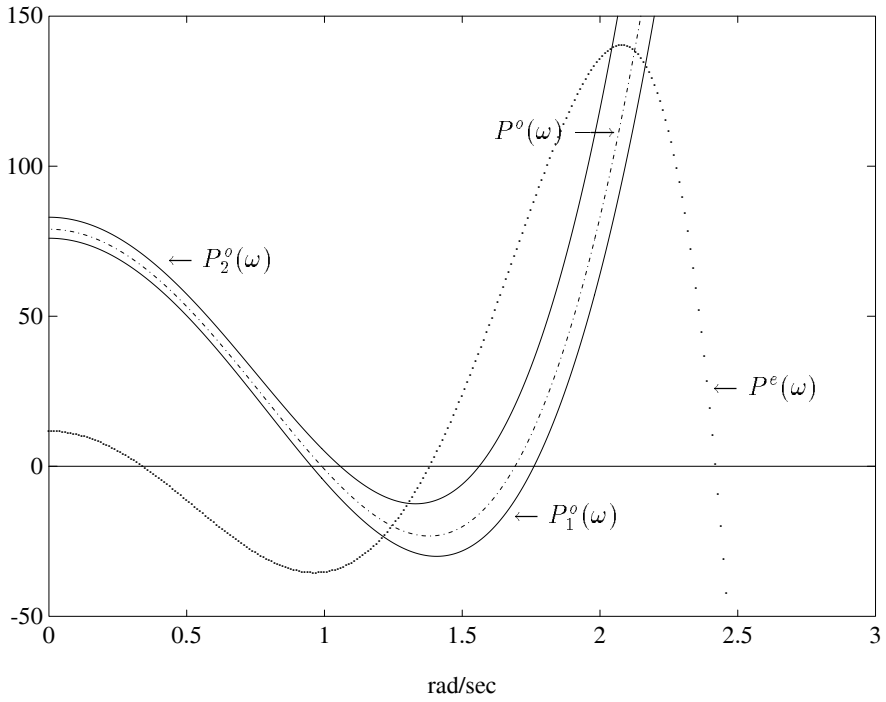

Figure 5.2. $P^e(\omega)$ and $(P_1^o(\omega), P_2^o(\omega))$ (Example 5.1)

denote two stable polynomials of the same degree with the same odd part $P^{\rm odd}(s)$ *and differing even parts* $P_1^{\rm even}(s)$ *and* $P_2^{\rm even}(s)$ *satisfying*

$$P_1^e(\omega) \leq P_2^e(\omega), \qquad \text{for all } \omega \in [0, \infty]. \tag{5.5}$$

Then,

$$P(s) = P^{\rm even}(s) + P^{\rm odd}(s)$$

is stable for every polynomial $P(s)$ *with even part* $P^{\rm even}(s)$ *satisfying*

$$P_1^e(\omega) \leq P^e(\omega) \leq P_2^e(\omega), \qquad \text{for all } \omega \in [0, \infty]. \tag{5.6}$$

We are now ready to prove Kharitonov's Theorem.

Proof of Kharitonov's Theorem The Kharitonov polynomials repeated below, for convenience are four specific vertices of the box $\mathbf{\Delta}$:

$$K^1(s) = x_o + x_1 s + y_2 s^2 + y_3 s^3 + x_4 s^4 + x_5 s^5 + y_6 s^6 + \cdots,$$
$$K^2(s) = x_o + y_1 s + y_2 s^2 + x_3 s^3 + x_4 s^4 + y_5 s^5 + y_6 s^6 + \cdots,$$

$$K^3(s) = y_o + x_1 s + x_2 s^2 + y_3 s^3 + y_4 s^4 + x_5 s^5 + x_6 s^6 + \cdots, \qquad (5.7)$$
$$K^4(s) = y_o + y_1 s + x_2 s^2 + x_3 s^3 + y_4 s^4 + y_5 s^5 + x_6 s^6 + \cdots.$$

These polynomials are built from two different even parts $K^{\text{even}}_{\max}(s)$ and $K^{\text{even}}_{\min}(s)$ and two different odd parts $K^{\text{odd}}_{\max}(s)$ and $K^{\text{odd}}_{\min}(s)$ defined below:

$$K^{\text{even}}_{\max}(s) := y_o + x_2 s^2 + y_4 s^4 + x_6 s^6 + y_8 s^8 + \cdots,$$
$$K^{\text{even}}_{\min}(s) := x_o + y_2 s^2 + x_4 s^4 + y_6 s^6 + x_8 s^8 + \cdots,$$

and

$$K^{\text{odd}}_{\max}(s) := y_1 s + x_3 s^3 + y_5 s^5 + x_7 s^7 + y_9 s^9 + \cdots,$$
$$K^{\text{odd}}_{\min}(s) := x_1 s + y_3 s^3 + x_5 s^5 + y_7 s^7 + x_9 s^9 + \cdots.$$

The Kharitonov polynomials in (5.2) or (5.7) can be rewritten as:

$$\begin{aligned} K^1(s) &= K^{\text{even}}_{\min}(s) + K^{\text{odd}}_{\min}(s), \\ K^2(s) &= K^{\text{even}}_{\min}(s) + K^{\text{odd}}_{\max}(s), \\ K^3(s) &= K^{\text{even}}_{\max}(s) + K^{\text{odd}}_{\min}(s), \\ K^4(s) &= K^{\text{even}}_{\max}(s) + K^{\text{odd}}_{\max}(s). \end{aligned} \qquad (5.8)$$

The motivation for the subscripts "max" and "min" is as follows. Let $\delta(s)$ be an arbitrary polynomial with its coefficients lying in the box $\mathbf{\Delta}$ and let $\delta^{\text{even}}(s)$ be its even part. Then

$$K^e_{\max}(\omega) = y_0 - x_2\omega^2 + y_4\omega^4 - x_6\omega^6 + y_8\omega^8 + \cdots,$$
$$\delta^e(\omega) = \delta_0 - \delta_2\omega^2 + \delta_4\omega^4 - \delta_6\omega^6 + \delta_8\omega^8 + \cdots,$$
$$K^e_{\min}(\omega) = x_0 - y_2\omega^2 + x_4\omega^4 - y_6\omega^6 + x_8\omega^8 + \cdots,$$

so that

$$K^e_{\max}(\omega) - \delta^e(\omega) = (y_0 - \delta_0) + (\delta_2 - x_2)\omega^2 + (y_4 - \delta_4)w^4 + (\delta_6 - x_6)\omega^6 + \cdots,$$

and

$$\delta^e(\omega) - K^e_{\min}(\omega) = (\delta_0 - x_0) + (y_2 - \delta_2)\omega^2 + (\delta_4 - x_4)\omega^4 + (y_6 - \delta_6)\omega^6 + \cdots.$$

Therefore,

$$K^e_{\min}(\omega) \le \delta^e(\omega) \le K^e_{\max}(\omega), \qquad \text{for all } \omega \in [0, \infty]. \qquad (5.9)$$

Similarly, if $\delta^{\text{odd}}(s)$ denotes the odd part of $\delta(s)$, and $\delta^{\text{odd}}(j\omega) = j\omega\delta^o(\omega)$ it can be verified that

$$K^o_{\min}(\omega) \le \delta^o(\omega) \le K^o_{max}(\omega), \qquad \text{for all } \omega \in [0, \infty]. \qquad (5.10)$$

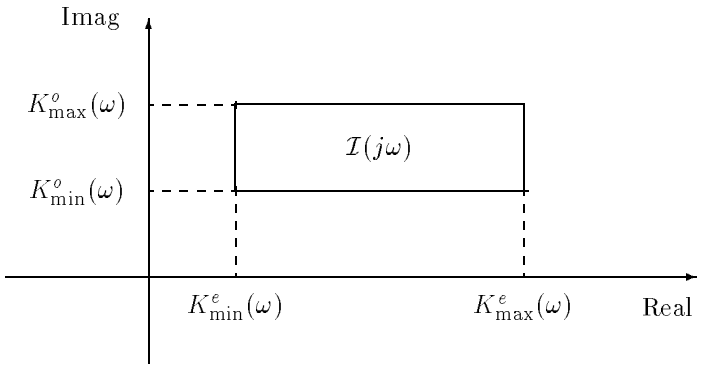

Figure 5.3. Axis parallel rectangle $\mathcal{I}(j\omega)$

Thus $\delta(j\omega)$ lies in an axis parallel rectangle $\mathcal{I}(j\omega)$ as shown in Figure 5.3.

To proceed with the proof of Kharitonov's Theorem we note that necessity of the condition is trivial since if all the polynomials with coefficients in the box $\mathbf{\Delta}$ are stable, it is clear that the Kharitonov polynomials must also be stable since their coefficients lie in $\mathbf{\Delta}$. For the converse, assume that the Kharitonov polynomials are stable, and let $\delta(s) = \delta^{\text{even}}(s) + \delta^{\text{odd}}(s)$ be an *arbitrary* polynomial belonging to the family $\mathcal{I}(s)$, with even part $\delta^{\text{even}}(s)$ and odd part $\delta^{\text{odd}}(s)$.

We conclude, from Lemma 5.1 applied to the stable polynomials $K^3(s)$ and $K^4(s)$ in (5.8), that

$$K^{\text{even}}_{\max}(s) + \delta^{\text{odd}}(s) \quad \text{is stable.} \tag{5.11}$$

Similarly, from Lemma 5.1 applied to the stable polynomials $K^1(s)$ and $K^2(s)$ in (5.8) we conclude that

$$K^{\text{even}}_{\min}(s) + \delta^{\text{odd}}(s) \quad \text{is stable.} \tag{5.12}$$

Now, since (5.9) holds, we can apply Lemma 5.2 to the two stable polynomials

$$K^{\text{even}}_{\max}(s) + \delta^{\text{odd}}(s) \quad \text{and} \quad K^{\text{even}}_{\min}(s) + \delta^{\text{odd}}(s)$$

to conclude that

$$\delta^{\text{even}}(s) + \delta^{\text{odd}}(s) = \delta(s) \quad \text{is stable.}$$

Since $\delta(s)$ was an arbitrary polynomial of $\mathcal{I}(s)$ we conclude that the entire family of polynomials $\mathcal{I}(s)$ is stable and this concludes the proof of the theorem. ♣

Remark 5.1. The Kharitonov polynomials can also be written with the highest order coefficient as the first term:

$$\hat{K^1}(s) = x_n s^n + y_{n-1}s^{n-1} + y_{n-2}s^{n-2} + x_{n-3}s^{n-3} + x_{n-4}s^{n-4} + \cdots,$$

$$\begin{aligned}
\hat{K}^2(s) &= x_n s^n + x_{n-1}s^{n-1} + y_{n-2}s^{n-2} + y_{n-3}s^{n-3} + x_{n-4}s^{n-4} + \cdots, \\
\hat{K}^3(s) &= y_n s^n + x_{n-1}s^{n-1} + x_{n-2}s^{n-2} + y_{n-3}s^{n-3} + y_{n-4}s^{n-4} + \cdots, \\
\hat{K}^4(s) &= y_n s^n + y_{n-1}s^{n-1} + x_{n-2}s^{n-2} + x_{n-3}s^{n-3} + y_{n-4}s^{n-4} + \cdots.
\end{aligned} \tag{5.13}$$

Remark 5.2. The assumption regarding invariant degree of the interval family can be relaxed. In this case some additional polynomials need to be tested for stability. This is dealt with in Exercise 5.13.

Remark 5.3. The assumption inherent in Kharitonov's Theorem that the coefficients perturb independently is crucial to the working of the theorem. In the examples below we have constructed some control problems where this assumption is satisfied. Obviously in many real world problems this assumption would fail to hold, since the characteristic polynomial coefficients would perturb interdependently through other primary parameters. However even in these cases Kharitonov's Theorem can give useful and computationally simple answers by overbounding the actual perturbations by an axis parallel box $\mathbf{\Delta}$ in coefficient space.

Remark 5.4. As remarked above Kharitonov's Theorem would give conservative results when the characteristic polynomial coefficients perturb interdependently. The Edge Theorem and the Generalized Kharitonov Theorem described in Chapters 6 and 7 respectively were developed precisely to deal nonconservatively with such dependencies.

Example 5.2. Consider the problem of checking the robust stability of the feedback system shown in Figure 5.4.

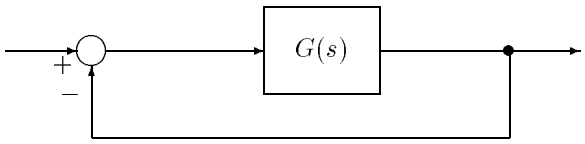

Figure 5.4. Feedback system (Example 5.2)

The plant transfer function is

$$G(s) = \frac{\delta_1 s + \delta_0}{s^2(\delta_4 s^2 + \delta_3 s^3 + \delta_2)}$$

with coefficients being bounded as

$$\delta_4 \in [x_4, y_4], \quad \delta_3 \in [x_3, y_3], \quad \delta_2 \in [x_2, y_2], \quad \delta_1 \in [x_1, y_1], \quad \delta_0 \in [x_0, y_0].$$

The characteristic polynomial of the family is written as

$$\delta(s) = \delta_4 s^4 + \delta_3 s^3 + \delta_2 s^2 + \delta_1 s + \delta_0.$$

The associated even and odd polynomials for Kharitonov's test are as follows:

$$K_{\min}^{\text{even}}(s) = x_0 + y_2 s^2 + x_4 s^4, \qquad K_{\max}^{\text{even}}(s) = y_0 + x_2 s^2 + y_4 s^4,$$
$$K_{\min}^{\text{odd}}(s) = x_1 s + y_3 s^3, \qquad K_{\max}^{\text{odd}}(s) = y_1 s + x_3 s^3.$$

The Kharitonov polynomials are:

$$K^1(s) = x_0 + x_1 s + y_2 s^2 + y_3 s^3 + x_4 s^4, \qquad K^2(s) = x_0 + y_1 s + y_2 s^2 + x_3 s^3 + x_4 s^4,$$
$$K^3(s) = y_0 + x_1 s + x_2 s^2 + y_3 s^3 + y_4 s^4, \qquad K^4(s) = y_0 + y_1 s + x_2 s^2 + x_3 s^3 + y_4 s^4.$$

The problem of checking the Hurwitz stability of the family therefore is reduced to that of checking the Hurwitz stability of these four polynomials. This in turn reduces to checking that the coefficients have the same sign (positive, say; otherwise multiply $\delta(s)$ by -1) and that the following inequalities hold:

$$\begin{aligned}
K^1(s) \quad &\text{Hurwitz} : y_2 y_3 > x_1 x_4, \qquad x_1 y_2 y_3 > x_1^2 x_4 + y_3^2 x_0, \\
K^2(s) \quad &\text{Hurwitz} : y_2 x_3 > y_1 x_4, \qquad y_1 y_2 x_3 > y_1^2 x_4 + x_3^2 x_0, \\
K^3(s) \quad &\text{Hurwitz} : x_2 y_3 > x_1 y_4, \qquad x_1 x_2 y_3 > x_1^2 y_4 + y_3^2 y_0, \\
K^4(s) \quad &\text{Hurwitz} : x_2 x_3 > y_1 y_4, \qquad y_1 x_2 x_3 > y_1^2 y_4 + x_3^2 y_0.
\end{aligned}$$

Example 5.3. Consider the control system shown in Figure 5.5.

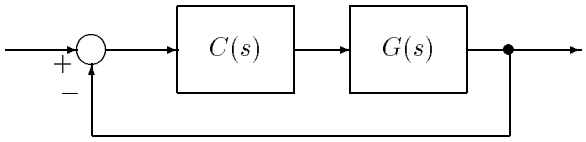

Figure 5.5. Feedback system with controller (Example 5.3)

The plant is described by the rational transfer function $G(s)$ with numerator and denominator coefficients varying independently in prescribed intervals. We refer to such a family of transfer functions $\mathbf{G}(s)$ as an *interval plant*. In the present example we take

$$\mathbf{G}(s) := \left\{ G(s) = \frac{n_2 s^2 + n_1 s + n_0}{s^3 + d_2 s^2 + d_1 s + d_0} : \begin{array}{l} n_0 \in [1, 2.5],\ n_1 \in [1, 6], \qquad n_2 \in [1, 7], \\ d_2 \in [-1, 1],\ d_1 \in [-0.5, 1.5],\ d_0 \in [1, 1.5] \end{array} \right\}.$$

The controller is a constant gain, $C(s) = k$ that is to be adjusted, if possible, to robustly stabilize the closed loop system. More precisely we are interested in determining the range of values of the gain $k \in [-\infty, +\infty]$ for which the closed loop system is robustly stable, i.e. stable for all $G(s) \in \mathbf{G}(s)$.

The characteristic polynomial of the closed loop system is:

$$\delta(k,s) = s^3 + \underbrace{(d_2 + kn_2)}_{\delta_2(k)} s^2 + \underbrace{(d_1 + kn_1)}_{\delta_1(k)} s + \underbrace{(d_0 + kn_0)}_{\delta_0(k)}.$$

Since the parameters d_i, n_j, $i = 0,1,2$, $j = 0,1,2$ vary independently it follows that for each fixed k, $\delta(k,s)$ is an interval polynomial. Using the bounds given to describe the family $\mathbf{G}(s)$ we get the following coefficient bounds for positive k:

$$\begin{aligned}
\delta_2(k) &\in [-1 + k, 1 + 7k], \\
\delta_1(k) &\in [-0.5 + k, 1.5 + 6k], \\
\delta_0(k) &\in [-1 + k, 1.5 + 2.5k].
\end{aligned}$$

Since the leading coefficient is $+1$ the remaining coefficients must be all positive for the polynomial to be Hurwitz. This leads to the constraints:

$$\text{(a)} \quad -1 + k > 0, \quad -0.5 + k > 0, \quad 1 + k > 0.$$

From Kharitonov's Theorem applied to third order interval polynomials it can be easily shown that to ascertain the Hurwitz stability of the entire family it suffices to check in addition to positivity of the coefficients, the Hurwitz stability of only the third Kharitonov polynomial $K_3(s)$. In this example we therefore have that the entire system is Hurwitz if and only if in addition to the above constraints (a) we have:

$$(-0.5 + k)(-1 + k) > 1.5 + 2.5k.$$

From this it follows that the closed loop system is robustly stabilized if and only if

$$k \in (2 + \sqrt{5}, +\infty].$$

To complete our treatment of this important result we give Kharitonov's Theorem for polynomials with complex coefficients in the next section.

5.3 KHARITONOV'S THEOREM FOR COMPLEX POLYNOMIALS

Consider the set $\mathcal{I}^*(s)$ of all complex polynomials of the form,

$$\delta(s) = (\alpha_0 + j\beta_0) + (\alpha_1 + j\beta_1)s + \cdots + (\alpha_n + j\beta_n)s^n \tag{5.14}$$

with

$$\alpha_0 \in [x_0, y_0], \quad \alpha_1 \in [x_1, y_1], \quad \cdots, \quad \alpha_n \in [x_n, y_n] \tag{5.15}$$

and

$$\beta_0 \in [u_0, v_0], \quad \beta_1 \in [u_1, v_1], \quad \cdots, \quad \beta_n \in [u_n, v_n]. \tag{5.16}$$

This is a complex interval family of polynomials of degree n which includes the real interval family studied earlier as a special case. It is natural to consider the generalization of Kharitonov's Theorem for the real case to this family. The Hurwitz stability of complex interval families will also arise naturally in studying the extremal H_∞ norms of interval systems in Chapter 9. Complex polynomials also arise in the study of phase margins of control systems and in time-delay systems. Kharitonov extended his result for the real case to the above case of complex interval families. We assume as before that the degree remains invariant over the family. Introduce two sets of complex polynomials as follows:

$$\begin{aligned}
K_1^+(s) &:= (x_0 + ju_0) + (x_1 + jv_1)s + (y_2 + jv_2)s^2 + (y_3 + ju_3)s^3 \\
&\quad +(x_4 + ju_4)s^4 + (x_5 + jv_5)s^5 + \cdots, \\
K_2^+(s) &:= (x_0 + jv_0) + (y_1 + jv_1)s + (y_2 + ju_2)s^2 + (x_3 + ju_3)s^3 \\
&\quad +(x_4 + jv_4)s^4 + (y_5 + jv_5)s^5 + \cdots, \\
K_3^+(s) &:= (y_0 + ju_0) + (x_1 + ju_1)s + (x_2 + jv_2)s^2 + (y_3 + jv_3)s^3 \\
&\quad +(y_4 + ju_4)s^4 + (x_5 + u_5)s^5 + \cdots, \\
K_4^+(s) &:= (y_0 + jv_0) + (y_1 + ju_1)s + (x_2 + ju_2)s^2 + (x_3 + jv_3)s^3 \\
&\quad +(y_4 + jv_4)s^4 + (y_5 + ju_5)s^5 + \cdots,
\end{aligned} \tag{5.17}$$

and

$$\begin{aligned}
K_1^-(s) &:= (x_0 + ju_0) + (y_1 + ju_1)s + (y_2 + jv_2)s^2 + (x_3 + jv_3)s^3 \\
&\quad +(x_4 + ju_4)s^4 + (y_5 + ju_5)s^5 + \cdots, \\
K_2^-(s) &:= (x_0 + jv_0) + (x_1 + ju_1)s + (y_2 + ju_2)s^2 + (y_3 + jv_3)s^3 \\
&\quad +(x_4 + jv_4)s^4 + (x_5 + ju_5)s^5 + \cdots, \\
K_3^-(s) &:= (y_0 + ju_0) + (y_1 + jv_1)s + (x_2 + jv_2)s^2 + (x_3 + ju_3)s^3 \\
&\quad +(y_4 + ju_4)s^4 + (y_5 + jv_5)s^5 + \cdots, \\
K_4^-(s) &:= (y_0 + jv_0) + (x_1 + jv_1)s + (x_2 + ju_2)s^2 + (y_3 + ju_3)s^3 \\
&\quad +(y_4 + jv_4)s^4 + (x_5 + jv_5)s^5 + \cdots.
\end{aligned} \tag{5.18}$$

Theorem 5.2 *The family of polynomials $\mathcal{I}^*(s)$ is Hurwitz if and only if the eight Kharitonov polynomials $K_1^+(s)$, $K_2^+(s)$, $K_3^+(s)$, $K_4^+(s)$, $K_1^-(s)$, $K_2^-(s)$, $K_3^-(s)$, $K_4^-(s)$ are all Hurwitz.*

Proof. The necessity of the condition is obvious because the eight Kharitonov polynomials are in $\mathcal{I}^*(s)$. The proof of sufficiency follows again from the Hermite-Biehler Theorem for complex polynomials (Theorem 1.8, Chapter 1).

Observe that the Kharitonov polynomials in (5.17) and (5.18) are composed of the following extremal polynomials:
For the "positive" Kharitonov polynomials define:

$$\begin{aligned}
R^+_{\max}(s) &:= y_0 + ju_1 s + x_2 s^2 + jv_3 s^3 + y_4 s^4 + \cdots \\
R^+_{\min}(s) &:= x_0 + jv_1 s + y_2 s^2 + ju_3 s^3 + x_4 s^4 + \cdots \\
I^+_{\max}(s) &:= jv_0 + y_1 s + ju_2 s^2 + x_3 s^3 + jv_4 s^4 + \cdots \\
I^+_{\min}(s) &:= ju_0 + x_1 s + jv_2 s_2 + y_3 s^3 + ju_4 s^4 + \cdots
\end{aligned}$$

so that

$$\begin{aligned}
K^+_1(s) &= R^+_{\min}(s) + I^+_{\min}(s) \\
K^+_2(s) &= R^+_{\min}(s) + I^+_{\max}(s) \\
K^+_3(s) &= R^+_{\max}(s) + I^+_{\min}(s) \\
K^+_4(s) &= R^+_{\max}(s) + I^+_{\max}(s).
\end{aligned}$$

For the "negative" Kharitonov polynomials we have

$$\begin{aligned}
R^-_{\max}(s) &= y_0 + jv_1 s + x_2 s^2 + ju_3 s^3 + y_4 s^4 + \cdots \\
R^-_{\min}(s) &= x_0 + ju_1 s + y_2 s^2 + jv_3 s^3 + x_4 s^4 + \cdots \\
I^-_{\max}(s) &= jv_0 + x_1 s + ju_2 s^2 + y_3 s^3 + jv_4 s^4 + \cdots \\
I^-_{\min}(s) &= ju_0 + y_1 s + jv_2 s^2 + x_3 s^3 + ju_4 s^4 + \cdots
\end{aligned}$$

and

$$\begin{aligned}
K^-_1(s) &= R^-_{\min}(s) + I^-_{\min}(s) \\
K^-_2(s) &= R^-_{\min}(s) + I^-_{\max}(s) \\
K^-_3(s) &= R^-_{\max}(s) + I^-_{\min}(s) \\
K^-_4(s) &= R^-_{\max}(s) + I^-_{\max}(s).
\end{aligned}$$

$R^{\pm}_{\max}(j\omega)$ and $R^{\pm}_{\min}(j\omega)$ are real and $I^{\pm}_{\max}(j\omega)$ and $I^{\pm}_{\min}(j\omega)$ are imaginary. Let $\mathrm{Re}[\delta(j\omega)] := \delta^r(\omega)$ and $\mathrm{Im}[\delta(j\omega)] := \delta^i(\omega)$ denote the real and imaginary parts of $\delta(s)$ evaluated at $s = j\omega$. Then we have:

$$\begin{aligned}
\delta^r(\omega) &= \alpha_0 - \beta_1\omega - \alpha_2\omega^2 + \beta_3\omega^3 + \cdots , \\
\delta^i(\omega) &= \beta_0 + \alpha_1\omega - \beta_2\omega^2 - \alpha_3\omega^3 + \cdots .
\end{aligned}$$

It is easy to verify that

$$\begin{cases}
R^+_{\min}(j\omega) \le \delta^r(\omega) \le R^+_{\max}(j\omega), & \text{for all } \omega \in [0, \infty] \\
\dfrac{I^+_{\min}(j\omega)}{j} \le \delta^i(\omega) \le \dfrac{I^+_{\max}(j\omega)}{j}, & \text{for all } \omega \in [0, \infty]
\end{cases} \tag{5.19}$$

$$\begin{cases}
R^-_{\min}(j\omega) \le \delta^r(\omega) \le R^-_{\max}(j\omega), & \text{for all } \omega \in [0, -\infty] \\
\dfrac{I^-_{\min}(j\omega)}{j} \le \delta^i(\omega) \le \dfrac{I^-_{\max}(j\omega)}{j}, & \text{for all } \omega \in [0, -\infty]
\end{cases} \tag{5.20}$$

The proof of the theorem is now completed as follows. The stability of the 4 positive Kharitonov polynomials guarantees interlacing of the "real tube" (bounded by $R^+_{\max}(j\omega)$ and $R^+_{\min}(j\omega)$) with the "imaginary tube" (bounded by $I^+_{\max}(j\omega)$ and $I^+_{\min}(j\omega)$) for $\omega \geq 0$. The relation in (5.19) then guarantees that the real and imaginary parts of an arbitrary polynomial in $\mathcal{I}^*(s)$ are forced to interlace for $\omega \geq 0$. Analogous arguments, using the bounds in (5.20) and the "negative" Kharitonov polynomials forces interlacing for $\omega \leq 0$. Thus by the Hermite-Biehler Theorem for complex polynomials δ(s) is Hurwitz. Since δ(s) was arbitrary, it follows that each and every polynomial in $\mathcal{I}^*(s)$ is Hurwitz. ♣

Remark 5.5. In the complex case the real and imaginary parts of $\delta(j\omega)$ are polynomials in ω and not ω^2, and therefore it is necessary to verify the interlacing of the roots on the entire imaginary axis and not only on its positive part. This is the reason why there are twice as many polynomials to check in the complex case.

5.4 INTERLACING AND IMAGE SET INTERPRETATION

In this section we interpret Kharitonov's Theorem in terms of the interlacing property or Hermite-Biehler Theorem and also in terms of the complex plane image of the set of polynomials $\mathcal{I}(s)$, evaluated at $s = j\omega$ for each $\omega \in [0, \infty]$. In Chapter 1 we have seen that the Hurwitz stability of a single polynomial $\delta(s) = \delta^{\text{even}}(s) + \delta^{\text{odd}}(s)$ is equivalent to the interlacing property of $\delta^e(\omega) = \delta^{\text{even}}(j\omega)$ and $\delta^o(\omega) = \dfrac{\delta^{\text{odd}}(j\omega)}{j\omega}$. In considering the Hurwitz stability of the interval family $\mathcal{I}(s)$ we see that the family is stable if and only if every element satisfies the interlacing property. In view of Kharitonov's Theorem it must therefore be true that verification of the interlacing property for the four Kharitonov polynomials guarantees the interlacing property of every member of the family. This point of view is expressed in the following version of Kharitonov's Theorem. Let $\omega^{\max}_{e_i}(\omega^{\min}_{e_i})$ denote the positive roots of $K^e_{\max}(\omega)(K^e_{\min}(\omega))$ and let $\omega^{\max}_{o_i}(\omega^{\min}_{o_i})$ denote the positive roots of $K^o_{\max}(\omega)(K^o_{\min}(\omega))$.

Theorem 5.3 (Interlacing Statement of Kharitonov's Theorem)
The family $\mathcal{I}(s)$ contains only stable polynomials if and only if

1) The polynomials $K^e_{\max}(\omega)$, $K^e_{\min}(\omega)$, $K^o_{\max}(\omega)$, $K^o_{\min}(\omega)$ have only real roots and the set of positive roots interlace as follows:

$$0 < \omega^{\min}_{e_1} < \omega^{\max}_{e_1} < \omega^{\min}_{o_1} < \omega^{\max}_{o_1} < \omega^{\min}_{e_2} < \omega^{\max}_{e_2} < \omega^{\min}_{o_2} < \omega^{\max}_{o_2} < \cdots,$$

2) $K^e_{\max}(0)$, $K^e_{\min}(0)$, $K^o_{\max}(0)$, $K^o_{\min}(0)$ are non zero and of the same sign.

This theorem is illustrated in Figure 5.6 which shows how the interlacing of the odd and even tubes implies the interlacing of the odd and even parts of each polynomial in the interval family. We illustrate this interlacing property of interval polynomials with an example.

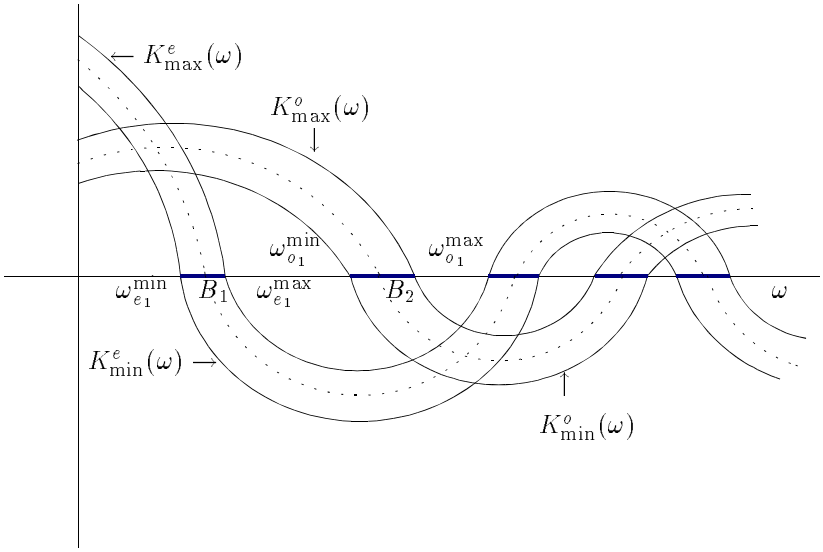

Figure 5.6. Interlacing odd and even tubes

Example 5.4. Consider the interval family

$$\delta(s) = s^7 + \delta_6 s^6 + \delta_5 s^5 + \delta_4 s^4 + \delta_3 s^3 + \delta_2 s^2 + \delta_1 s + \delta_0$$

where

$$\begin{array}{lll} \delta_6 \in [9, 9.5], & \delta_5 \in [31, 31.5], & \delta_4 \in [71, 71.5], \\ \delta_3 \in [111, 111.5], & \delta_2 \in [109, 109.5], & \delta_1 \in [76, 76.5], \\ \delta_0 \in [12, 12.5] & & \end{array}$$

Then

$$\begin{aligned} K^e_{\max}(\omega) &= -9\omega^6 + 71.5\omega^4 - 109\omega^2 + 12.5 \\ K^e_{\min}(\omega) &= -9.5\omega^6 + 71\omega^4 - 109.5\omega^2 + 12 \\ K^o_{\max}(\omega) &= -\omega^6 + 31.5\omega^4 - 111\omega^2 + 76.5 \\ K^o_{\min}(\omega) &= -\omega^6 + 31\omega^4 - 111.5\omega^2 + 76. \end{aligned}$$

We can verify the interlacing property of these polynomials (see Figure 5.7).

The illustration in Figure 5.7 shows how all polynomials with even parts bounded by $K^e_{\max}(\omega)$ and $K^e_{\min}(\omega)$ and odd parts bounded by $K^o_{\max}(\omega)$ and $K^o_{\min}(\omega)$ on the imaginary axis satisfy the interlacing property when the Kharitonov polynomials

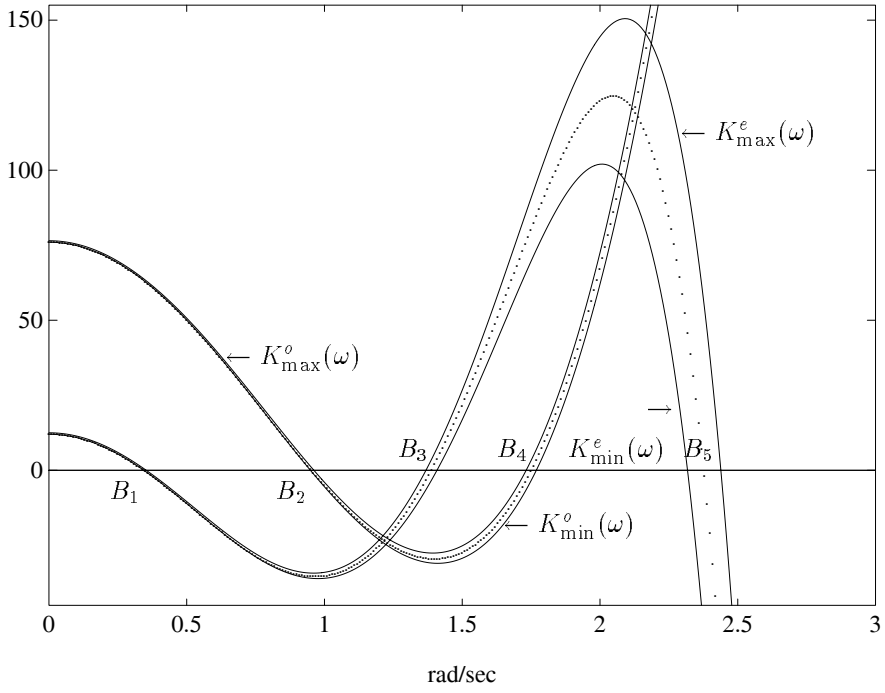

Figure 5.7. Interlacing property of an interval polynomial (Example 5.4)

are stable. Figure 5.7 also shows that the interlacing property for a *single* stable polynomial corresponding to a *point* δ in coefficient space generalizes to the *box* $\mathbf{\Delta}$ of stable polynomials as the requirement of "interlacing" of the odd and even "*tubes*." This interpretation is useful; for instance it can be used to show that for polynomials of order less than six, fewer than four Kharitonov polynomials need to be tested for robust stability (see Exercise 5.4).

Image Set Interpretation

It is instructive to interpret Kharitonov's Theorem in terms of the evolution of the complex plane image of $\mathcal{I}(s)$ evaluated along the imaginary axis. Let $\mathcal{I}(j\omega)$ denote the set of complex numbers $\delta(j\omega)$ obtained by letting the coefficients of $\delta(s)$ range over $\mathbf{\Delta}$:

$$\mathcal{I}(j\omega) := \{\delta(j\omega) : \underline{\delta} \in \mathbf{\Delta}\}\,.$$

Now it follows from the relations in (5.9) and (5.10) that $\mathcal{I}(j\omega)$ is a rectangle in the complex plane with the corners $K_1(j\omega)$, $K_2(j\omega)$, $K_3(j\omega)$, $K_4(j\omega)$ corresponding to

the Kharitonov polynomials evaluated at $s = j\omega$. This is shown in Figure 5.8. As ω runs from 0 to ∞ the rectangle $\mathcal{I}(j\omega)$ varies in shape size and location but its sides always remain parallel to the real and imaginary axes of the complex plane. We illustrate this by using a numerical example.

Example 5.5. Consider the interval polynomial of Example 5.4. The image set of this family is calculated for various frequencies. These frequency dependent rectangles are shown in Figure 5.8.

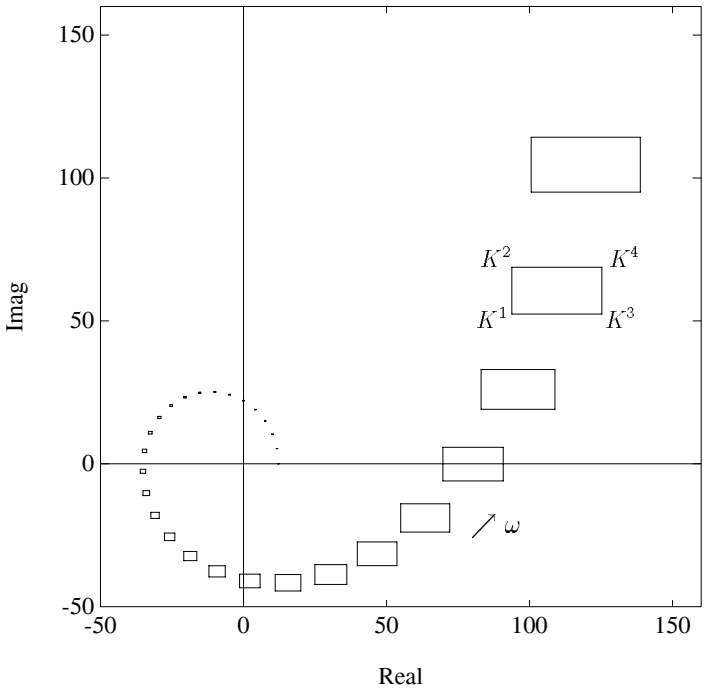

Figure 5.8. Image sets of interval polynomial (Kharitonov boxes) (Example 5.5)

5.4.1 Two Parameter Representation of Interval Polynomials

The observation that $\mathcal{I}(j\omega)$ is an axis parallel rectangle with the $K_i(j\omega)$, $i = 1, 2, 3, 4$ as corners motivates us to introduce a reduced family $\mathcal{I}_R(s) \subset \mathcal{I}(s)$ which generates the image set $\mathcal{I}(j\omega)$ at every ω. Let $\beta_0(s)$ denote the center polynomial of the family $\mathcal{I}(s)$:

$$\beta_0(s) := \frac{x_0 + y_0}{2} + \frac{x_1 + y_1}{2}s + \cdots + \frac{x_n + y_n}{2}s^n$$

and introduce the even and odd polynomials:

$$\beta_e(s) := K_{\max}^{\text{even}}(s) - K_{\min}^{\text{even}}(s) \tag{5.21}$$
$$\beta_o(s) := K_{\max}^{\text{odd}}(s) - K_{\min}^{\text{odd}}(s). \tag{5.22}$$

We define

$$\mathcal{I}_R(s) := \{\beta(s) = \beta_0(s) + \lambda_1\beta_e(s) + \lambda_2\beta_o(s) : |\lambda_i| \leq 1, i = 1, 2\}$$

It is easy to see that $\mathcal{I}_R(s) \subset \mathcal{I}(s)$ but

$$\mathcal{I}(j\omega) = \mathcal{I}_R(j\omega), \qquad \text{for all } \omega \geq 0.$$

This shows that the $n+1$-parameter interval polynomial family $\mathcal{I}(s)$ can *always* be replaced by the two-parameter testing family $\mathcal{I}_R(s)$ as far as any frequency evaluations are concerned since they both generate the same image at each frequency. We emphasize that this kind of parameter reduction based on properties of the image set holds in more general cases, i.e. even when the family under consideration is not interval and the stability region is not the left half plane. Of course in the interval Hurwitz case, Kharitonov's Theorem shows us a further reduction of the testing family to the four vertices $K_i(s)$. We show next how this can be deduced from the behaviour of the image set.

5.4.2 Image Set Based Proof of Kharitonov's Theorem

We give an alternative proof of Kharitonov's Theorem based on analysis of the image set. Suppose that the family $\mathcal{I}(s)$ is of degree n and contains at least one stable polynomial.Then stability of the family $\mathcal{I}(s)$ can be ascertained by verifying that no polynomial in the family has a root on the imaginary axis. This follows immediately from the Boundary Crossing Theorem of Chapter 1. Indeed if some element of $\mathcal{I}(s)$ has an unstable root then there must also exist a frequency ω^* and a polynomial with a root at $s = j\omega^*$. The case $\omega^* = 0$ is ruled out since this would contradict the requirement that $K_{\max}^e(0)$ and $K_{\min}^e(0)$ are of the same sign. Thus it is only necessary to check that the rectangle $\mathcal{I}(j\omega^*)$ excludes the origin of the complex plane for every $\omega^* > 0$. Suppose that the Kharitonov polynomials are stable. By the monotonic phase property of Hurwitz polynomials it follows that the corners $K^1(j\omega)$, $K^2(j\omega)$, $K^3(j\omega)$, $K^4(j\omega)$ of $\mathcal{I}(j\omega)$ start on the positive real axis (say), turn strictly counterclockwise around the origin and do not pass through it as ω runs from 0 to ∞. Now suppose by contradiction that $0 \in \mathcal{I}(j\omega^*)$ for some $\omega^* > 0$. Since $\mathcal{I}(j\omega)$ moves continuously with respect to ω and the origin lies outside of $\mathcal{I}(0)$ it follows that there exists $\omega_0 \leq \omega^*$ for which the origin just begins to enter the set $\mathcal{I}(j\omega_0)$. We now consider this limiting situation in which the origin lies on the boundary of $\mathcal{I}(j\omega_0)$ and is just about to enter this set as ω increases from ω_0. This is depicted in Figure 5.9. The origin can lie on one of the four sides of the image set rectangle, say AB. The reader can easily verify that in each of these cases

the entry of the origin implies that the phase angle (argument) of one of the corners, A or B on the side through which the entry takes place, *decreases* with increasing ω at $\omega = \omega_0$. Since the corners correspond to Kharitonov polynomials which are Hurwitz stable, we have a contradiction with the monotonic phase increase property of Hurwitz polynomials.

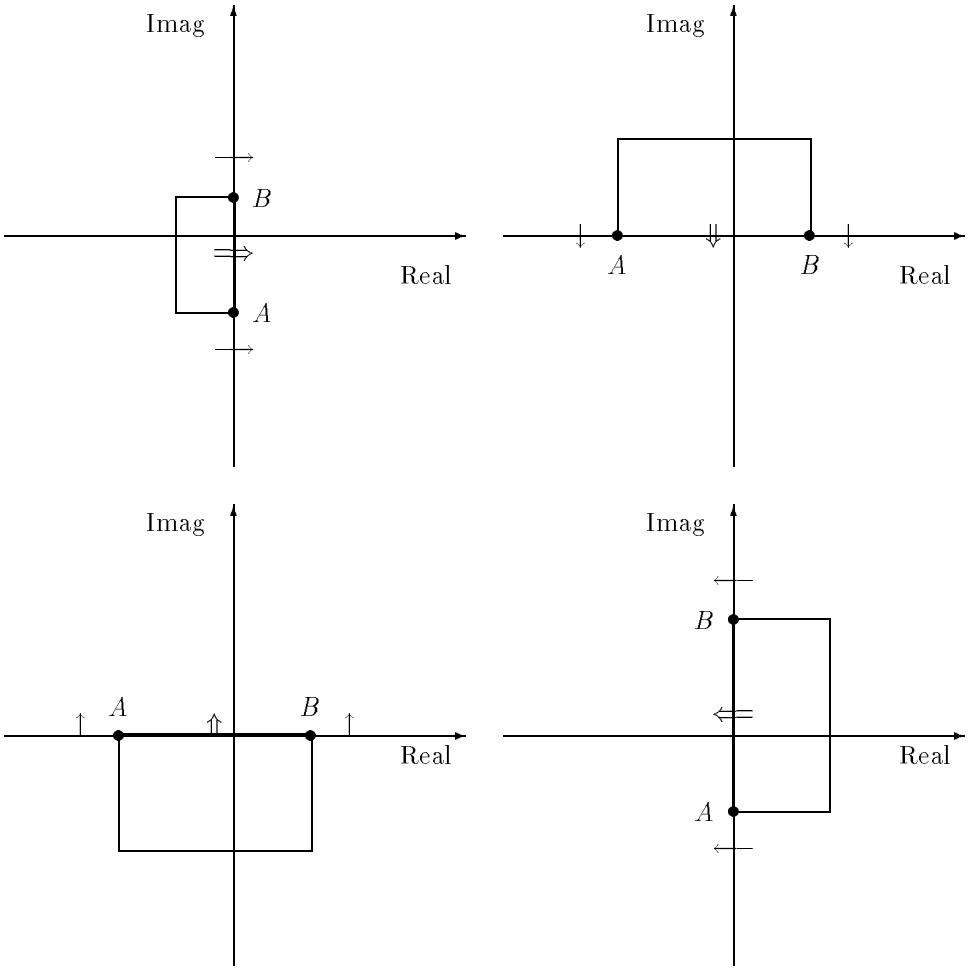

Figure 5.9. Alternative proof of Kharitonov's Theorem

5.4.3 Image Set Edge Generators and Exposed Edges

The interval family $\mathcal{I}(s)$, or equivalently, the coefficient set $\mathbf{\Delta}$, is a polytope and therefore, as discussed in Chapter 4, its stability is equivalent to that of its exposed edges. There are in general $(n+1)2^{n+1}$ such exposed edges. However from the image set arguments given above, it is clear that stability of the family $\mathcal{I}(s)$ is, in fact, also equivalent to that of the *four* polynomial segments $[K_1(s), K_2(s)]$, $[K_1(s), K_3(s)]$, $[K_2(s), K_4(s)]$ and $[K_3(s), K_4(s)]$. This follows from the previous continuity arguments and the fact that these polynomial segments generate the boundary of the image set $\mathcal{I}(j\omega)$ for *each* ω. We now observe that each of the differences $K_2(s) - K_1(s), K_3(s) - K_1(s), K_4(s) - K_2(s)$ and $K_4(s) - K_3(s)$ is either an *even* or an *odd* polynomial. It follows then from the Vertex Lemma of Chapter 2 that these segments are Hurwitz stable if and only if the endpoints $K_1(s), K_2(s), K_3(s)$ and $K_4(s)$ are. These arguments serve as yet another proof of Kharitonov's Theorem. They serve to highlight 1) the important fact that it is only necessary to check stability of that subset of polynomials which generate the boundary of the image set and 2) the role of the Vertex Lemma in reducing the stability tests to that of fixed polynomials.

5.5 EXTREMAL PROPERTIES OF THE KHARITONOV POLYNOMIALS

In this section we derive some useful extremal properties of the Kharitonov polynomials. Suppose that we have proved the stability of the family of polynomials

$$\delta(s) = \delta_0 + \delta_1 s + \delta_2 s^2 + \cdots + \delta_n s^n,$$

with coefficients in the box

$$\mathbf{\Delta} = [x_0, y_0] \times [x_1, y_1] \times \cdots \times [x_n, y_n].$$

Each polynomial in the family is stable. A natural question that arises now is the following: What point in $\mathbf{\Delta}$ is closest to instability? The stability margin of this point is in a sense the worst case stability margin of the interval system. It turns out that a precise answer to this question can be given in terms of the parametric stability margin as well as in terms of the gain margins of an associated interval system. We first deal with the extremal parametric stability margin problem.

5.5.1 Extremal Parametric Stability Margin Property

We consider a stable interval polynomial family. It is therefore possible to associate with each polynomial of the family the largest stability ball centered around it. Write

$$\underline{\delta} = [\delta_0, \delta_1, \cdots, \delta_n],$$

and regard $\underline{\delta}$ as a point in $\mathbb{R}^{n+1}$. Let $\|\underline{\delta}\|_p$ denote the p norm in $\mathbb{R}^{n+1}$ and let this be associated with $\delta(s)$. The set of polynomials which are unstable of degree n or

of degree less than n is denoted by $\mathcal{U}$. Then the radius of the stability ball centered at δ is

$$\rho(\delta) = \inf_{u \in \mathcal{U}} \|\underline{\delta} - \mathbf{u}\|_p.$$

We thus define a mapping from $\mathbf{\Delta}$ to the set of all positive real numbers:

$$\begin{aligned} \mathbf{\Delta} &\xrightarrow{\rho} \mathcal{R}^+ \backslash \{0\} \\ \delta(s) &\longrightarrow \rho(\delta). \end{aligned}$$

A natural question to ask is the following: Is there a point in $\mathbf{\Delta}$ which is the nearest to instability? Or stated in terms of functions: Has the function ρ a minimum and is there a precise point in $\mathbf{\Delta}$ where it is reached? The answer to that question is given in the following theorem. In the discussion to follow we drop the subscript p from the norm since the result holds for any norm chosen.

Theorem 5.4 (Extremal property of the Kharitonov polynomials) *The function*

$$\begin{aligned} \mathbf{\Delta} &\xrightarrow{\rho} \mathcal{R}^+ \backslash \{0\} \\ \delta(s) &\longrightarrow \rho(\delta) \end{aligned}$$

has a minimum which is reached at one of the four Kharitonov polynomials associated with $\mathbf{\Delta}$.

Proof. Let $K^i(s)$, $i = 1, 2, 3, 4$ denote the four Kharitonov polynomials . Consider the four radii associated with these four extreme polynomials, and let us assume for example that

$$\rho(K^1) = \min \left[\rho(K^1), \rho(K^2), \rho(K^3), \rho(K^4)\right]. \tag{5.23}$$

Let us now suppose, by way of contradiction, that some polynomial $\gamma(s)$ in the box is such that

$$\rho(\gamma) < \rho(K^1). \tag{5.24}$$

For convenience we will denote $\rho(\gamma)$ by ρ_γ, and $\rho(K^1)$ by ρ_1.

By definition, there is at least one polynomial situated on the hypersphere $S(\gamma(s), \rho_\gamma)$ which is unstable or of degree less than n. Let $\beta(s)$ be such a polynomial. Since $\beta(s)$ is on $S(\gamma(s), \rho_\gamma)$, there exists $\underline{\alpha} = [\alpha_0, \alpha_1, \cdots, \alpha_n]$ with $\|\underline{\alpha}\| = 1$ such that

$$\beta(s) = \gamma_0 + \alpha_0\rho_\gamma + (\gamma_1 + \alpha_1\rho_\gamma)s + \cdots + (\gamma_n + \alpha_n\rho_\gamma)s^n, \tag{5.25}$$

(α_0, α_1, $\cdots$, α_n can be positive or non positive here.)

But by (5.23), ρ_1 is the smallest of the four extreme radii and by (5.24) ρ_γ is less than ρ_1. As a consequence, the four new polynomials

$$\begin{aligned}
\delta_n^1(s) &= (x_0 - |\alpha_0|\rho_\gamma) + (x_1 - |\alpha_1|\rho_\gamma)s + (y_2 + |\alpha_2|\rho_\gamma)s^2 + (y_3 + |\alpha_3|\rho_\gamma)s^3 + \cdots \\
\delta_n^2(s) &= (x_0 - |\alpha_0|\rho_\gamma) + (y_1 + |\alpha_1|\rho_\gamma)s + (y_2 + |\alpha_2|\rho_\gamma)s^2 + (x_3 - |\alpha_3|\rho_\gamma)s^3 + \cdots \\
\delta_n^3(s) &= (y_0 + |\alpha_0|\rho_\gamma) + (x_1 - |\alpha_1|\rho_\gamma)s + (x_2 - |\alpha_2|\rho_\gamma)s^2 + (y_3 + |\alpha_3|\rho_\gamma)s^3 + \cdots \\
\delta_n^4(s) &= (y_0 + |\alpha_0|\rho_\gamma) + (y_1 + |\alpha_1|\rho_\gamma)s + (x_2 - |\alpha_2|\rho_\gamma)s^2 + (x_3 - |\alpha_3|\rho_\gamma)s^3 + \cdots
\end{aligned}$$

are all stable because

$$\|\delta_n^i - K^i\| = \rho_\gamma < \rho_i, \qquad i = 1, 2, 3, 4.$$

By applying Kharitonov's Theorem, we thus conclude that the new box

$$\mathbf{\Delta}_n = [x_0 - |\alpha_0|\rho_\gamma,\ y_0 + |\alpha_0|\rho_\gamma] \times \cdots \times [x_n - |\alpha_n|\rho_\gamma,\ y_n + |\alpha_n|\rho_\gamma] \tag{5.26}$$

contains only stable polynomials of degree n. The contradiction now clearly follows from the fact that $\beta(s)$ in (5.25) certainly belongs to $\mathbf{\Delta}_n$, and yet it is unstable or of degree less than n, and this proves the theorem. ♣

The above result tells us that, over the entire box, one is closest to instability at one of the Kharitonov corners, say $K^i(s)$. It is clear that if we take the box $\mathbf{\Delta}_n$, constructed in the above proof, (5.26) and replace ρ_γ by $\rho(K^i)$, the resulting box is larger than the original box $\mathbf{\Delta}$. This fact can be used to develop an algorithm that enlarges the stability box to its maximum limit. We leave the details to the reader but give an illustrative example.

Example 5.6. Consider the system given in Example 5.2:

$$G(s) = \frac{\delta_2 s^2 + \delta_1 s + \delta_0}{s^3(\delta_6 s^3 + \delta_5 s^2 + \delta_4 s + \delta_3)}$$

with the coefficients being bounded as follows:

$$\begin{array}{llll} \delta_0 \in [300, 400], & \delta_1 \in [600, 700], & \delta_2 \in [450, 500], & \\ \delta_3 \in [240, 300], & \delta_4 \in [70, 80], & \delta_5 \in [12, 14], & \delta_6 \in [1, 1]. \end{array}$$

We wish to verify if the system is robustly stable, and if it is we would like to calculate the smallest value of the stability radius in the space of $\delta = [\delta_0, \delta_1, \delta_2, \delta_3, \delta_4, \delta_5, \delta_6]$ as these coefficients range over the uncertainty box.

The characteristic polynomial of the closed loop system is

$$\delta(s) = \delta_6 s^6 + \delta_5 s^5 + \delta_4 s^4 + \delta_3 s^3 + \delta_2 s^2 + \delta_1 s + \delta_0.$$

Since all coefficients of the polynomial are perturbing independently, we can apply Kharitonov's Theorem. This gives us the following four polynomials to check:

$$\begin{aligned} K^1(s) &= 300 + 600s + 500s^2 + 300s^3 + 70s^4 + 12s^5 + s^6 \\ K^2(s) &= 300 + 700s + 500s^2 + 240s^3 + 70s^4 + 14s^5 + s^6 \\ K^3(s) &= 400 + 600s + 450s^2 + 300s^3 + 80s^4 + 12s^5 + s^6 \\ K^4(s) &= 400 + 700s + 450s^2 + 240s^3 + 80s^4 + 14s^5 + s^6. \end{aligned}$$

Since all four Kharitonov polynomials are Hurwitz, we proceed to calculate the worst case stability margin.

From the result established above,Theorem 5.4 we know that this occurs at one of the Kharitonov vertices and thus it suffices to determine the stability radius at these four vertices. The stability radius will be determined using a weighted ℓ_p norm. In other words we want to find the largest value of ρ_p such that the closed loop system remains stable for all δ satisfying

$$\left\{ [\delta_0, \cdots, \delta_6] : \left[\sum_{k=0}^{6} \left| \frac{\delta_k - \delta_k^0}{\alpha_k} \right|^p \right]^{\frac{1}{p}} \leq \rho_p(\delta) \right\}$$

where δ_k^0 represent the coefficients corresponding to the center (a Kharitonov vertex). It is assumed that $[\alpha_0, \alpha_1, \alpha_2, \alpha_3, \alpha_4, \alpha_5, \alpha_6] = [43,\ 33,\ 25,\ 15,\ 5,\ 1.5,\ 1]$. We can compute the stability radius by simply applying the techniques of Chapter 3 (Tsypkin-Polyak Locus, for example) to each of these fixed Kharitonov polynomials and taking the minimum value of the stability margin. We illustrate this calculation using two different norm measures, corresponding to $p = 2$ and $p = \infty$.

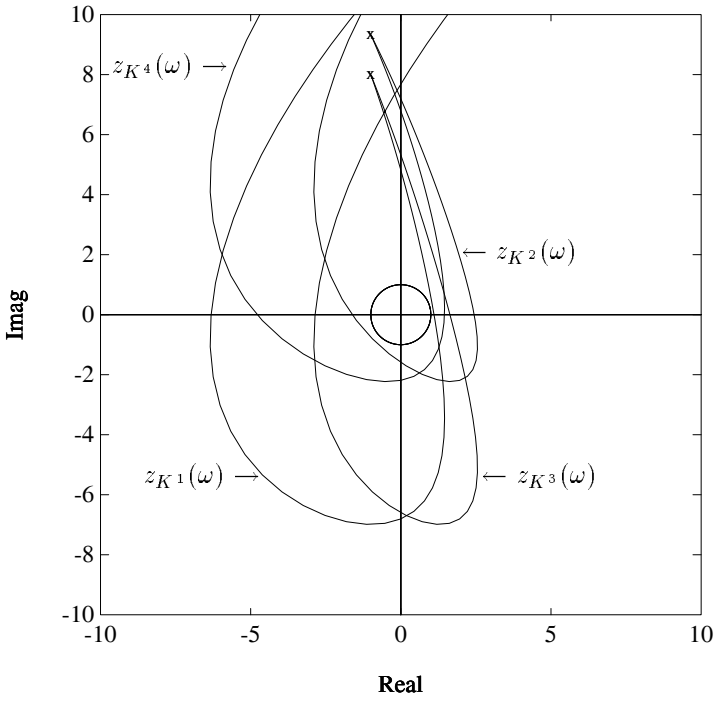

Figure 5.10. ℓ_2 stability margin (Example 5.6)

Figure 5.10 shows the four Tsypkin-Polyak loci corresponding to the four Kharitonov polynomials. The radius of the inscribed circle indicates the minimum weighted ℓ_2 stability margin in coefficient space. Figure 5.11 shows the extremal weighted ℓ_∞ stability margin. From these figures, we have

$$\rho_2(\delta) = 1 \quad \text{and} \quad \rho_\infty(\delta) = 0.4953.$$

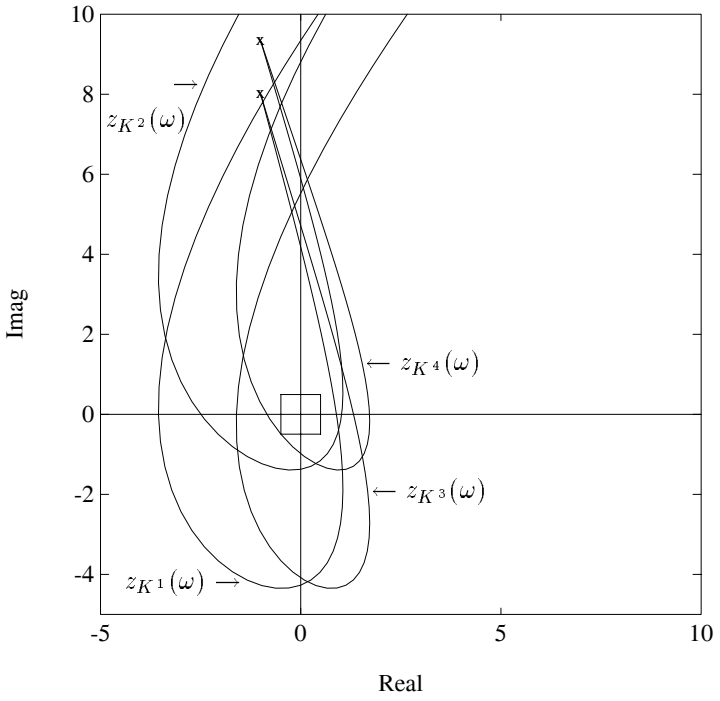

Figure 5.11. ℓ_∞ stability margin (Example 5.6)

5.5.2 Extremal Gain Margin for Interval Systems

Let us now consider the standard unity feedback control system shown below in Figure 5.12. We assume that the system represented by $G(s)$ contains parameter uncertainty. In particular let us assume that $G(s)$ is a proper transfer function which is a ratio of polynomials $n(s)$ and $d(s)$ the coefficients of which vary in independent intervals. Thus the polynomials $n(s)$ and $d(s)$ vary in respective independent interval polynomial families $\mathcal{N}(s)$ and $\mathcal{D}(s)$ respectively. We refer to such a family of

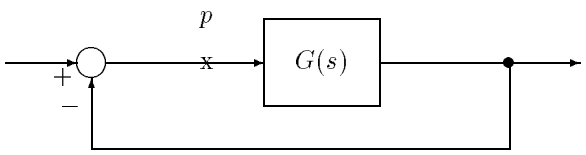

Figure 5.12. A feedback system

systems as an *interval system*. Let

$$\mathbf{G}(s) := \left\{ G(s) = \frac{n(s)}{d(s)} : n(s) \in \mathcal{N}(s), \quad d(s) \in \mathcal{D}(s) \right\}.$$

represent the interval family of systems in which the open loop transfer function lies.

We assume that the closed loop system containing the interval family $\mathbf{G}(s)$ is robustly stable. In other words we assume that the characteristic polynomial of the closed loop system given by

$$\Pi(s) = d(s) + n(s)$$

is of invariant degree n and is Hurwitz for all $(n(s),d(s)) \in (\mathcal{N}(s) \times \mathcal{D}(s))$. Let

$$\mathbf{\Pi}(s) = \{ \Pi(s) = n(s) + d(s) : n(s) \in \mathcal{N}(s), \quad d(s) \in \mathcal{D}(s) \}.$$

Then robust stability means that every polynomial in $\mathbf{\Pi}(s)$ is Hurwitz and of degree n. This can in fact be verified constructively. Let $K_N^i(s), i = 1,2,3,4$ and $K_D^j(s), j = 1,2,3,4$ denote the Kharitonov polynomials associated with $\mathcal{N}(s)$ and $\mathcal{D}(s)$ respectively. Now introduce the positive set of *Kharitonov systems* $\mathbf{G}_{\mathrm{K}}^{+}(s)$ associated with the interval family $\mathbf{G}(s)$ as follows:

$$\mathbf{G}_{\mathrm{K}}^{+}(s) := \left\{ \frac{K_N^i(s)}{K_D^i(s)} : i = 1,2,3,4 \right\}.$$

Theorem 5.5 *The closed loop system of Figure 5.12 containing the interval plant* $\mathbf{G}(s)$ *is robustly stable if and only if each of the positive Kharitonov systems in* $\mathbf{G}_K^+(s)$ *is stable.*

Proof. We need to verify that $\Pi(s)$ remains of degree n and Hurwitz for all $(n(s), d(s)) \in \mathcal{N}(s) \times \mathcal{D}(s)$. It follows from the assumption of independence of the families $\mathcal{N}(s)$ and $\mathcal{D}(s)$ that $\mathbf{\Pi}(s)$ is itself an interval polynomial family. It is easy to check that the Kharitonov polynomials of $\mathbf{\Pi}(s)$ are the four $K_N^i(s) + K_D^i(s), \quad i = 1,2,3,4$. Thus the family $\Pi(s)$ is stable if and only if the subset $K_N^i(s) + K_D^i(s), \quad i = 1,2,3,4$ are all stable and of degree n. The latter in turn is equivalent to the stability of the feedback systems obtained by replacing $G(s)$ by each element of $\mathbf{G}_{\mathrm{K}}^{+}(s)$. ♣

In classical control *gain margin* is commonly regarded as a useful measure of robust stability. Suppose the closed system is stable. The gain margin at the loop breaking point p is defined to be the largest value k^* of $k \geq 1$ for which closed loop stability is preserved with $G(s)$ replaced by $kG(s)$ for all $k \in [1, k^*)$. Suppose now that we have verified the robust stability of the interval family of systems $\mathbf{G}(s)$. The next question that is of interest is: What is the gain margin of the system at the loop breaking point p? To be more precise we need to ask: What is the *worst case* gain margin of the system at the point p as $G(s)$ ranges over $\mathbf{G}(s)$? An exact answer to this question can be given as follows.

Theorem 5.6 *The worst case gain margin of the system at the point p over the family $\mathbf{G}(s)$ is the minimum gain margin corresponding to the positive Kharitonov systems $\mathbf{G}_{\mathrm{K}}^{+}(s)$.*

Proof. Consider the characteristic polynomial $\Pi(s) = d(s) + kn(s)$ corresponding to the open loop system $kG(s)$. For each fixed value of k this is an interval family. For positive k the Kharitonov polynomials of this family are $K_D^i(s) + kK_N^i(s), i = 1, 2, 3, 4$. Therefore the minimum value of the gain margin over the set $\mathbf{G}(s)$ is in fact attained over the subset $\mathbf{G}_{\mathrm{K}}^{+}(s)$. ♣

Remark 5.6. A similar result can be stated for the case of a positive feedback system by introducing the set of negative Kharitonov systems (see Exercise 5.9).

5.6 ROBUST STATE-FEEDBACK STABILIZATION

In this section we give an application of Kharitonov's Theorem to robust stabilization. We consider the following problem: Suppose that you are given a set of n nominal parameters

$$\left\{a_0^0, a_1^0, \cdots, a_{n-1}^0\right\},$$

together with a set of prescribed uncertainty ranges: Δa_0, Δa_1, $\cdots$, Δa_{n-1}, and that you consider the family $\mathcal{I}_{\underline{0}}(s)$ of monic polynomials,

$$\delta(s) = \delta_0 + \delta_1 s + \delta_2 s^2 + \cdots + \delta_{n-1} s^{n-1} + s^n,$$

where

$$\delta_0 \in \left[a_0^0 - \frac{\Delta a_0}{2}, a_0^0 + \frac{\Delta a_0}{2}\right], \cdots, \delta_{n-1} \in \left[a_{n-1}^0 - \frac{\Delta a_{n-1}}{2}, a_{n-1}^0 + \frac{\Delta a_{n-1}}{2}\right].$$

To avoid trivial cases assume that the family $\mathcal{I}_{\underline{0}}(s)$ contains at least one unstable polynomial.

Suppose now that you can use a vector of n free parameters

$$\underline{k} = (k_0, k_1, \cdots, k_{n-1}),$$

to transform the family $\mathcal{I}_{\underline{0}}(s)$ into the family $\mathcal{I}_{\underline{k}}(s)$ described by:

$$\delta(s) = (\delta_0 + k_0) + (\delta_1 + k_1)s + (\delta_2 + k_2)s^2 + \cdots + (\delta_{n-1} + k_{n-1})s^{n-1} + s^n.$$

The problem of interest, then, is the following: Given Δa_0, Δa_1, $\cdots$, Δa_{n-1} the perturbation ranges fixed a priori, find, if possible, a vector $\underline{k}$ so that the new family of polynomials $\mathcal{I}_{\underline{k}}(s)$ is entirely Hurwitz stable. This problem arises, for example, when one applies a state-feedback control to a single input system where the matrices A, b are in controllable companion form and the coefficients of the characteristic polynomial of A are subject to bounded perturbations. The answer to this problem is always affirmative and is precisely given in Theorem 5.7. Before stating it, however, we need to prove the following lemma.

Lemma 5.3 *Let n be a positive integer and let $P(s)$ be a stable polynomial of degree $n-1$:*

$$P(s) = p_0 + p_1 s + \cdots + p_{n-1}s^{n-1}, \qquad \textit{with all } \; p_i > 0.$$

Then there exists $\alpha > 0$ such that:

$$Q(s) = P(s) + p_n s^n = p_0 + p_1 s + \cdots + p_{n-1}s^{n-1} + p_n s^n,$$

is stable if and only if: $\qquad p_n \in [0, \alpha)$.

Proof. To be absolutely rigorous there should be four different proofs depending on whether n is of the form $4r$ or $4r+1$ or $4r+2$ or $4r+3$. We will give the proof of this lemma when n is of the form $4r$ and one can check that only slight changes are needed if n is of the form $4r+j$, $\quad j = 1, 2, 3$.

If $n = 4r$, $r > 0$, we can write

$$P(s) = p_0 + p_1 s + \cdots + p_{4r-1}s^{4r-1},$$

and the even and odd parts of $P(s)$ are given by:

$$\begin{aligned} P_{\text{even}}(s) &= p_0 + p_2 s^2 + \cdots + p_{4r-2}s^{4r-2}, \\ P_{\text{odd}}(s) &= p_1 s + p_3 s^3 + \cdots + p_{4r-1}s^{4r-1}. \end{aligned}$$

Let us also define

$$\begin{aligned} P^e(\omega) &:= P_{\text{even}}(j\omega) = p_0 - p_2\omega^2 + p_4\omega^4 - \cdots - p_{4r-2}\omega^{4r-2}, \\ P^o(\omega) &:= \frac{P_{\text{odd}}(j\omega)}{j\omega} = p_1 - p_3\omega^2 + p_5\omega^4 - \cdots - p_{4r-1}\omega^{4r-2}. \end{aligned}$$

$P(s)$ being stable, we know by the Hermite-Biehler Theorem that $P^e(\omega)$ has precisely $2r-1$ positive roots $\omega_{e,1}$, $\omega_{e,2}$, $\cdots$, $\omega_{e,2r-1}$, that $P^o(\omega)$ has also $2r-1$ positive roots $\omega_{o,1}$, $\omega_{o,2}$, $\cdots$, $\omega_{o,2r-1}$, and that these roots interlace in the following manner:

$$0 < \omega_{e,1} < \omega_{o,1} < \omega_{e,2} < \omega_{o,2} < \cdots < \omega_{e,2r-1} < \omega_{o,2r-1}.$$

It can be also checked that,

$P^e(\omega_{o,j}) < 0$ if and only if j is odd, and $P^e(\omega_{o,j}) > 0$ if and only if j is even,

that is,

$$P^e(\omega_{o,1}) < 0,\ P^e(\omega_{o,2}) > 0,\ \cdots,\ P^e(\omega_{o,2r-2}) > 0,\ P^e(\omega_{o,2r-1}) < 0. \tag{5.27}$$

Let us denote

$$\alpha = \min_{j \text{ odd}} \left\{ \frac{-P^e(\omega_{o,j})}{(\omega_{o,j})^{4r}} \right\}. \tag{5.28}$$

By (5.27) we know that α is positive. We can now prove the following:

$$Q(s) = P(s) + p_{4r}s^{4r} \text{ is stable if and only if } \quad p_{4r} \in [0, \alpha).$$

$Q(s)$ is certainly stable when $p_{4r} = 0$. Let us now suppose that

$$0 < p_{4r} < \alpha. \tag{5.29}$$

$Q^o(\omega)$ and $Q^e(\omega)$ are given by

$$\begin{aligned} Q^o(\omega) &= P^o(\omega) = p_1 - p_3\omega^2 + p_5\omega^4 - \cdots - p_{4r-1}\omega^{4r-1}, \\ Q^e(\omega) &= P^e(\omega) + p_{4r}\omega^{4r} = p_0 - p_2\omega^2 + p_4\omega^4 - \cdots - p_{4r-2}\omega^{4r-2} + p_{4r}\omega^{4r}. \end{aligned}$$

We are going to show that $Q^e(\omega)$ and $Q^o(\omega)$ satisfy the Hermite-Biehler Theorem provided that p_{4r} remains within the bounds defined by (5.29).
First we know the roots of $Q^o(\omega) = P^o(\omega)$. Then we have that $Q^e(0) = p_0 > 0$, and also

$$Q^e(\omega_{o,1}) = P^e(\omega_{o,1}) + p_{4r}(\omega_{o,1})^{4r}.$$

But, by (5.28) and (5.29) we have

$$Q^e(\omega_{o,1}) < \underbrace{P^e(\omega_{o,1}) - \frac{P^e(\omega_{o,1})}{(\omega_{o,1})^{4r}}(\omega_{o,1})^{4r}}_{=0}.$$

Thus $Q^e(\omega_{o,1}) < 0$. Then we have

$$Q^e(\omega_{o,2}) = P^e(\omega_{o,2}) + p_{4r}(\omega_{o,2})^{4r}.$$

But by (5.27), we know that $P^e(\omega_{o,2}) > 0$, and therefore we also have

$$Q^e(\omega_{o,2}) > 0.$$

Pursuing the same reasoning we could prove in exactly the same way that the following inequalities hold

$$Q^e(0) > 0,\ Q^e(\omega_{o,1}) < 0,\ Q^e(\omega_{o,2}) > 0,\ \cdots, Q^e(\omega_{o,2r-2}) > 0,\ Q^e(\omega_{o,2r-1}) < 0. \tag{5.30}$$

From this we conclude that $Q^e(\omega)$ has precisely $2r-1$ roots in the open interval $(0,\ \omega_{o,2r-1})$, namely

$$\omega'_{e,1},\ \omega'_{e,2},\ \cdots,\ \omega'_{e,2r-1},$$

and that these roots interlace with the roots of $Q^o(\omega)$,

$$0 < \omega'_{e,1} < \omega_{o,1} < \omega'_{e,2} < \omega_{o,2} < \cdots < \omega'_{e,2r-1} < \omega_{o,2r-1}. \tag{5.31}$$

Moreover, we see in (5.30) that

$$Q^e(\omega_{o,2r-1}) < 0,$$

and since $p_{4r} > 0$, we also obviously have

$$Q^e(+\infty) > 0.$$

Therefore $Q^e(\omega)$ has a final positive root $\omega'_{e,2r}$ which satisfies

$$\omega_{o,2r-1} < \omega'_{e,2r}. \tag{5.32}$$

From (5.31) and (5.32) we conclude that $Q^o(\omega)$ and $Q^e(\omega)$ satisfy the Hermite-Biehler Theorem and therefore $Q(s)$ is stable.

To complete the proof of this lemma, notice that $Q(s)$ is obviously unstable if $p_{4r} < 0$ since we have assumed that all the p_i are positive. Moreover it can be shown that for $p_{4r} = \alpha$, the polynomial $P(s) + \alpha s^{4r}$ has a pure imaginary root and therefore is unstable. Now, it is impossible that $P(s) + p_{4r}s^{4r}$ be stable for some $p_{4r} > \alpha$, because otherwise we could use Kharitonov's Theorem and say,

$$P(s) + \frac{\alpha}{2}s^{4r} \text{ and } P(s) + p_{4r}s^{4r} \text{ both stable } \Longrightarrow P(s) + \alpha s^{4r} \text{ stable },$$

which would be a contradiction. This completes the proof of the theorem when $n = 4r$.

For the sake of completeness, let us just make precise that in general we have,

$$\begin{aligned}
\text{if } n = 4r, \quad & \alpha = \min_{j \text{ odd}} \left\{ \frac{-P^e(\omega_{o,j})}{(\omega_{o,j})^{4r}} \right\}, \\
\text{if } n = 4r+1, \quad & \alpha = \min_{j \text{ even}} \left\{ \frac{-P^o(\omega_{e,j})}{(\omega_{o,j})^{4r+1}} \right\}, \\
\text{if } n = 4r+2, \quad & \alpha = \min_{j \text{ even}} \left\{ \frac{P^e(\omega_{o,j})}{(\omega_{o,j})^{4r+2}} \right\}, \\
\text{if } n = 4r+3, \quad & \alpha = \min_{j \text{ odd}} \left\{ \frac{P^o(\omega_{e,j})}{(\omega_{o,j})^{4r+3}} \right\}.
\end{aligned}$$

The details of the proof for the other cases are omitted. ♣

We can now enunciate the following theorem to answer the question raised at the beginning of this section.

Theorem 5.7 *For any set of nominal parameters* $\{a_0, a_1, \cdots, a_{n-1}\}$, *and for any set of positive numbers* Δa_0, Δa_1, $\cdots$, Δa_{n-1}, *it is possible to find a vector* $\underline{k}$ *such that the entire family* $\mathcal{I}_{\underline{k}}(s)$ *is stable.*

Proof. The proof is constructive.

Step 1: Take any stable polynomial $R(s)$ of degree $n-1$. Let $\rho(R(\cdot))$ be the radius of the largest stability hypersphere around $R(s)$. It can be checked from the formulas of Chapter 3, that for any positive real number λ, we have

$$\rho(\lambda R(\cdot)) = \lambda \rho(R(\cdot)).$$

Thus it is possible to find a positive real λ such that if $P(s) = \lambda R(s)$,

$$\rho(P(\cdot)) > \sqrt{\frac{\Delta a_0{}^2}{4} + \frac{\Delta a_1{}^2}{4} + \cdots + \frac{\Delta a_{n-1}{}^2}{4}}. \tag{5.33}$$

Denote

$$P(s) = p_0 + p_1 s + p_2 s^2 + \cdots + p_{n-1} s^{n-1},$$

and consider the four following Kharitonov polynomials of degree $n-1$:

$$\begin{aligned}
P^1(s) &= \left(p_0 - \frac{\Delta a_0}{2}\right) + \left(p_1 - \frac{\Delta a_1}{2}\right) s + \left(p_2 + \frac{\Delta a_2}{2}\right) s^2 + \cdots, \\
P^2(s) &= \left(p_0 - \frac{\Delta a_0}{2}\right) + \left(p_1 + \frac{\Delta a_1}{2}\right) s + \left(p_2 + \frac{\Delta a_2}{2}\right) s^2 + \cdots, \\
P^3(s) &= \left(p_0 + \frac{\Delta a_0}{2}\right) + \left(p_1 - \frac{\Delta a_1}{2}\right) s + \left(p_2 - \frac{\Delta a_2}{2}\right) s^2 + \cdots, \\
P^4(s) &= \left(p_0 + \frac{\Delta a_0}{2}\right) + \left(p_1 + \frac{\Delta a_1}{2}\right) s + \left(p_2 - \frac{\Delta a_2}{2}\right) s^2 + \cdots.
\end{aligned} \tag{5.34}$$

We conclude that these four polynomials are stable since $\|P^i(s) - P(s)\| < \rho(P(s))$.

Step 2: Now, applying Lemma 5.3, we know that we can find four positive numbers α_1, α_2, α_3, α_4, such that

$$P^j(s) + p_n s^n \text{ is stable for } 0 \le p_n < \alpha_j, \quad j = 1, 2, 3, 4.$$

Let us select a single positive number α such that the polynomials,

$$P^j(s) + \alpha s^n \tag{5.35}$$

are all stable. If α can be chosen to be equal to 1 (that is if the four α_j are greater than 1) then we do choose $\alpha = 1$; otherwise we multiply everything by $\frac{1}{\alpha}$ which is greater than 1 and we know from (5.35) that the four polynomials

$$K^j(s) = \frac{1}{\alpha} P^j(s) + s^n,$$

are stable. But the four polynomials $K^j(s)$ are nothing but the four Kharitonov polynomials associated with the family of polynomials

$$\delta(s) = \delta_0 + \delta_1 s + \cdots + \delta_{n-1}s^{n-1} + s^n,$$

where

$$\delta_0 \in \left[\frac{1}{\alpha}p_0 - \frac{1}{\alpha}\frac{\Delta a_0}{2},\ \frac{1}{\alpha}p_0 + \frac{1}{\alpha}\frac{\Delta a_0}{2}\right], \cdots$$

$$\cdots, \delta_{n-1} \in \left[\frac{1}{\alpha}p_{n-1} - \frac{1}{\alpha}\frac{\Delta a_{n-1}}{2},\ \frac{1}{\alpha}p_{n-1} + \frac{1}{\alpha}\frac{\Delta a_{n-1}}{2}\right],$$

and therefore this family is entirely stable.

Step 3: It suffices now to chose the vector $\underline{k}$ such that

$$k_i + a_i^0 = \frac{1}{\alpha}p_i, \qquad \text{for } \ i = 1, \cdots, n-1.$$

♣

Remark 5.7. It is clear that in step 1 one can determine the largest box around $R(\cdot)$ with sides proportional to Δa_i. The dimensions of such a box are also enlarged by the factor λ when $R(\cdot)$ is replaced by $\lambda R(\cdot)$. This change does not affect the remaining steps of the proof.

Example 5.7. Suppose that our nominal polynomial is

$$s^6 - s^5 + 2s^4 - 3s^3 + 2s^2 + s + 1,$$

that is

$$(a_0^0, a_1^0, a_2^0, a_3^0, a_4^0, a_5^0) = (1, 1, 2, -3, 2, -1).$$

And suppose that we want to handle the following set of uncertainty ranges:

$$\Delta a_0 = 3, \quad \Delta a_1 = 5, \quad \Delta a_2 = 2, \quad \Delta a_3 = 1, \quad \Delta a_4 = 7, \quad \Delta a_5 = 5.$$

Step 1: Consider the following stable polynomial of degree 5

$$R(s) = (s+1)^5 = 1 + 5s + 10s^2 + 10s^3 + 5s^4 + s^5.$$

The calculation of $\rho(R(\cdot))$ gives: $\rho(R(\cdot)) = 1$. On the other hand we have

$$\sqrt{\frac{{\Delta a_0}^2}{4} + \frac{{\Delta a_1}^2}{4} + \cdots + \frac{{\Delta a_{n-1}}^2}{4}} = 5.31.$$

Taking therefore $\lambda = 6$, we have that

$$P(s) = 6 + 30s + 60s^2 + 60s^3 + 30s^4 + 6s^5,$$

has a radius $\rho(P(\cdot)) = 6$ that is greater than 5.31. The four polynomials $P^j(s)$ are given by

$$\begin{aligned}
P^1(s) &= 4.5 + 27.5s + 61s^2 + 60.5s^3 + 26.5s^4 + 3.5s^5, \\
P^2(s) &= 4.5 + 32.5s + 61s^2 + 59.5s^3 + 26.5s^4 + 8.5s^5, \\
P^3(s) &= 7.5 + 27.5s + 59s^2 + 60.5s^3 + 33.5s^4 + 3.5s^5, \\
P^4(s) &= 7.5 + 32.5s + 59s^2 + 59.5s^3 + 33.5s^4 + 8.5s^5.
\end{aligned}$$

Step 2: The application of Lemma 5.3 gives the following values

$$\alpha_1 \simeq 1.360, \quad \alpha_2 \simeq 2.667, \quad \alpha_3 \simeq 1.784, \quad \alpha_4 \simeq 3.821,$$

and therefore we can chose $\alpha = 1$, so that the four polynomials

$$\begin{aligned}
K^1(s) &= 4.5 + 27.5s + 61s^2 + 60.5s^3 + 26.5s^4 + 3.5s^5 + s^6, \\
K^2(s) &= 4.5 + 32.5s + 61s^2 + 59.5s^3 + 26.5s^4 + 8.5s^5 + s^6, \\
K^3(s) &= 7.5 + 27.5s + 59s^2 + 60.5s^3 + 33.5s^4 + 3.5s^5 + s^6, \\
K^4(s) &= 7.5 + 32.5s + 59s^2 + 59.5s^3 + 33.5s^4 + 8.5s^5 + s^6,
\end{aligned}$$

are stable.

Step 3: We just have to take

$$k_0 = p_0 - a_0 = 5, \quad k_1 = p_1 - a_1 = 29, \quad k_2 = p_2 - a_2 = 58,$$

$$k_3 = p_3 - a_3 = 63, \quad k_4 = p_4 - a_4 = 28, \quad k_5 = p_5 - a_5 = 7.$$

5.7 POLYNOMIAL FUNCTIONS OF INTERVAL POLYNOMIALS

In this section we extend the family of polynomials to which Kharitonov's Theorem applies. Consider the real interval polynomial

$$\mathcal{I}(s) = \left\{ a(s) : a_j \in [a_j^-, a_j^+], \quad j = 0, 1, 2, \cdots, n \right\}, \tag{5.36}$$

and a given polynomial

$$\varphi(z) = \alpha_0 + \alpha_1 z + \cdots + \alpha_m z^m. \tag{5.37}$$

We generate the polynomial family

$$\varphi(\mathcal{I}(s)) = \{\varphi(a(s)) : a(s) \in \mathcal{I}(s)\} \tag{5.38}$$

which consists of polynomials of the form

$$\alpha_0(s) + \alpha_1 a(s) + \alpha_2 a^2(s) + \cdots + \alpha_m a^m(s) \tag{5.39}$$

where $a(s) \in \mathcal{I}(s)$. In the following we answer the question: Under what conditions is the family $\varphi(\mathcal{I}(s))$ Hurwitz stable?

We note that the family $\varphi(\mathcal{I}(s))$ is in general neither interval nor polytopic. Moreover, even though the image set $\mathcal{I}(j\omega)$ is a rectangle the image set of $\varphi(\mathcal{I}(j\omega))$ is, in general a very complicated set. Therefore it is not expected that a vertex testing set or an edge testing will be available. However the result given below shows that once again it suffices to test the stability of four polynomials.

Let

$$K^1(s), K^2(s), K^3(s), K^4(s)$$

denote the Kharitonov polynomials associated with the family $\mathcal{I}(s)$. We begin with a preliminary observation.

Lemma 5.4 *Given the real interval polynomial $\mathcal{I}(s)$ and a complex number z the Hurwitz stability of the family*

$$\mathcal{I}(s) - z = \{a(s) - z : a(s) \in \mathcal{I}(s)\}$$

is equivalent to the Hurwitz stability of the polynomials $K^j(s) - z$, $j = 1, 2, 3, 4$.

The proof of this lemma follows easily from analysis of the image set at $s = j\omega$ of $\mathcal{I}(s) - z$ and is omitted.

Stability Domains

For a given domain Γ of the complex plane let us say that a polynomial is Γ-stable if all its roots lie in the domain Γ.

Consider a polynomial $a_k(s)$ of degree n. The plot $z = a_k(j\omega)$, $\omega \in (-\infty, +\infty)$, partitions the complex plane into a finite number of open disjoint domains. With each such domain Λ we associate the integer n_Λ, the number of the roots of the polynomial $a_k(s) - z$ in the left half plane, where z is taken from Λ. This number is independent of the particular choice of z in the domain and there is at most one domain Λ_k for which $n_\Lambda = n$. Let us associate this domain Λ_k with $a_k(s)$ and call it the *stability domain*. If it so happens that there is no domain for which $n_\Lambda = n$ we set $\Lambda_k = \emptyset$.

Define for each polynomial $K^j(s)$, the associated stability domain Λ_j, $j = 1, 2, 3, 4$ and let

$$\Lambda_0 := \cap_{k=1}^4 \Lambda_k.$$

Theorem 5.8 *Suppose that*

$$\Lambda_0 \neq \emptyset.$$

The polynomial family $\varphi(\mathcal{I}(s))$ is Hurwitz stable if and only if $\varphi(z)$ is Λ_0-stable, that is, all the roots of $\varphi(z)$ lie in the domain Λ_0.

Proof. Let $z_1, z_2, \cdots, z_m$ be the roots of (5.37). Then

$$\varphi(z) = \alpha_m(z - z_1)(z - z_2)\cdots(z - z_m)$$

and

$$\varphi(a(s)) = \alpha_m\,(a(s) - z_1)\,(a(s) - z_2)\cdots(a(s) - z_m)\,.$$

The Hurwitz stability of $\varphi(a(s))$ is equivalent to Hurwitz stability of the factors $a(s) - z_j$. This shows that Hurwitz stability of $\varphi(\mathcal{I}(s))$ is equivalent to Hurwitz stability of the interval polynomials $\mathcal{I}(s) - z_j$, $j = 1, 2, \cdots, m$. By Lemma 5.4 the family $\mathcal{I}(s) - z_j$ is Hurwitz stable if and only if $z_j \in \Lambda_0$. As a result the Hurwitz stability of $\varphi(\mathcal{I}(s))$ is equivalent to Λ_0-stability of $\varphi(z)$. ♣

This leads to the following useful result.

Theorem 5.9 *The polynomial family $\varphi(\mathcal{I}(s))$ is Hurwitz stable if and only if the four polynomials $\varphi\left(K^j(s)\right)$, $j = 1, 2, 3, 4$ are Hurwitz stable.*

Proof. Necessity is obvious because these four polynomials are members of $\varphi(\mathcal{I}(s))$. For sufficiency, we know that Hurwitz stability of $\varphi\left(K^j(s)\right)$ implies the Λ_j-stability of $\varphi(z)$. This means that $\varphi(z)$ is Λ_0-stable and hence, by the previous Theorem 5.8, $\varphi(\mathcal{I}(s))$ is Hurwitz stable. ♣

The above theorems describe two different methods of checking the stability of (5.38). In Theorem 5.8 one first has to construct the domains Λ_k and then check the Λ_0-stability of (5.37). In Theorem 5.9, on the other hand, one can directly check the Hurwitz stability of the four fixed polynomials $\varphi\left(K^j(s)\right)$.

Thus far we have considered the polynomial $\varphi(z)$ to be fixed. Suppose now that $\varphi(z)$ is an uncertain polynomial, and in particular belongs to a polytope

$$\Phi(z) = \{\varphi(z) : (\alpha_0, \alpha_1, \alpha_2, \cdots, \alpha_m) \in \mathbf{\Delta}\} \tag{5.40}$$

where $\mathbf{\Delta}$ is a convex polytope. We ask the question: Given an interval family (5.36) and a polytopic family (5.40) determine under what conditions is the polynomial family

$$\Phi(\mathcal{I}(s)) = \{\varphi(a(s)) : a(s) \in \mathcal{I}(s), \quad \varphi \in \Phi\} \tag{5.41}$$

Hurwitz stable?

We assume all polynomials in $\mathcal{I}$ have the same degree n and all polynomials in Φ have the same degree m.

Theorem 5.10 *Let $\Lambda_0 \neq \emptyset$. Then the family $\Phi(\mathcal{I}(s))$ is stable if and only if $\Phi(z)$ is Λ_0-stable.*

Proof. The family $\Phi(\mathcal{I}(s))$ is of the form

$$\Phi(\mathcal{I}(s)) = \{\varphi(\mathcal{I}(s)) : \varphi \in \Phi(z)\}\,.$$

By Theorem 5.8, the family $\varphi(\mathcal{I}(s))$ is Hurwitz stable if and only if $\varphi(z)$ is Λ_0-stable. ♣

From Theorem 5.9 applied to the above we have the following result.

Theorem 5.11 *The family $\Phi(\mathcal{I}(s))$ is Hurwitz stable if and only if the four families*

$$\Phi\left(K^j(s)\right) = \left\{\varphi\left(K^j(s)\right) : \varphi \in \Phi\right\}, \qquad j = 1, 2, 3, 4 \tag{5.42}$$

are Hurwitz stable.

Each of the families (5.42) has a polytopic structure and we can test for stability by testing the exposed edges. Let $\mathcal{E}_\Phi(z)$ denote the exposed edges of $\Phi(z)$. Each exposed edge is a one parameter family of the form

$$(1-\mu)\varphi_1(z) + \mu\varphi_2(z), \qquad \mu \in [0, 1]. \tag{5.43}$$

It generates the corresponding family

$$(1-\mu)\varphi_1\left(K^j(s)\right) + \mu\varphi_2\left(K^j(s)\right), \qquad \mu \in [0, 1] \tag{5.44}$$

which is an element of the exposed edge of $\Phi\left(K^j(s)\right)$. Collecting all such families (5.44) corresponding to the exposed edges of $\mathbf{\Delta}$, we have the following result.

Theorem 5.12 *The family $\Phi(\mathcal{I}(s))$ is stable if and only if the following four collections of one parameter families*

$$\mathcal{E}_{\Phi(K^j)} = \left\{\varphi\left(K^j(s)\right) : \varphi \in \mathcal{E}_\Phi\right\}, \qquad j = 1, 2, 3, 4$$

are stable.

This result is constructive as it reduces the test for robust stability to a set of one-parameter problems. We remark here that the uncertain parameters occurring in this problem appear both linearly (those from $\mathbf{\Delta}$) as well as *nonlinearly* (those from $\mathcal{I}(s)$).

5.8 SCHUR STABILITY OF INTERVAL POLYNOMIALS

We emphasize that Kharitonov's Theorem holds for Hurwitz stability, but in general does not apply to arbitrary regions. The following examples illustrates this fact for the case of Schur stability.

Example 5.8. The interval polynomial

$$\delta(z, p) = z^4 + pz^3 + \frac{3}{2}z^2 - \frac{1}{3}, \qquad p \in \left[-\frac{17}{8}, +\frac{17}{8}\right]$$

has the endpoints $\delta(z, -\frac{17}{8})$ and $\delta(z, \frac{17}{8})$ Schur stable but the midpoint $\delta(z, 0)$ is not Schur stable.

Example 5.9. Consider the interval polynomial

$$\delta(z) := z^4 + \delta_3 z^3 + \delta_2 z^2 + \delta_1 z - \frac{1}{2}$$

with

$$\delta_3 \in [-1, 0], \quad \delta_2 \in \left[\frac{109}{289}, \frac{109}{287}\right], \quad \delta_1 \in \left[\frac{49}{100}, \frac{51}{100}\right].$$

The four Kharitonov polynomials associated with $\delta(z)$

$$\begin{aligned}
K^1(z) &= -\frac{1}{2} + \frac{49}{100}z + \frac{109}{287}z^2 + z^4 \\
K^2(z) &= -\frac{1}{2} + \frac{51}{100}z + \frac{109}{287}z^2 - z^3 + z^4 \\
K^3(z) &= -\frac{1}{2} + \frac{49}{100}z + \frac{109}{289}z^2 + z^4 \\
K^4(z) &= -\frac{1}{2} + \frac{51}{100}z + \frac{109}{289}z^2 - z^3 + z^4
\end{aligned}$$

are all Schur stable. Furthermore, the rest of the vertex polynomials

$$\begin{aligned}
\hat{K}^1(z) &= -\frac{1}{2} + \frac{49}{100}z + \frac{109}{289}z^2 - z^3 + z^4 \\
\hat{K}^2(z) &= -\frac{1}{2} + \frac{49}{100}z + \frac{109}{287}z^2 - z^3 + z^4 \\
\hat{K}^3(z) &= -\frac{1}{2} + \frac{51}{100}z + \frac{109}{289}z^2 + z^4 \\
\hat{K}^4(z) &= -\frac{1}{2} + \frac{51}{100}z + \frac{109}{287}z^2 + z^4
\end{aligned}$$

are also all Schur stable. However, the polynomial

$$\hat{\delta}(z) = -\frac{1}{2} + \frac{1}{2}z + \frac{109}{288}z^2 - \frac{1}{4}z^3 + z^4$$

in the family has two roots at $0.25 \pm j0.9694$ which are not inside the unit circle. This shows that neither the stability of the Kharitonov polynomials nor even the stability of all the vertex polynomials guarantees the Schur stability of the entire family.

Schur stability of a polynomial is equivalent to the interlacing of the symmetric and antisymmetric parts of the polynomial evaluated along the unit circle. It is clear from the above example that interlacing of the vertex polynomials cannot guarantee the interlacing of the symmetric and antisymmetric parts of every member of the interval family. In the case of Hurwitz stability, the interlacing of the odd and even parts of the four Kharitonov polynomials in fact guarantees the interlacing along the $j\omega$ axis of every polynomial in the family.

In view of the above facts let us see what we *can* say about the Schur stability of an interval family of real polynomials. Let $\mathcal{I}(z)$ be the family of polynomials of the form

$$P(z) = a_n z^n + a_{n-1} z^{n-1} + \cdots + a_0$$

with coefficients belonging to a box $\mathbf{A}$:

$$\mathbf{A} := \{\underline{a} := (a_0, \cdots, a_n) \mid a_i \in [a_i^-, a_i^+], \quad i = 0, \cdots, n\}. \tag{5.45}$$

Introduce the vertices $\mathbf{V}$ and edges $\mathbf{E}$ of the box $\mathbf{A}$:

$$\mathbf{V} := \{(a_n, \cdots, a_0) : \ a_i = a_i^- \text{ or } a_i^+, \quad i = 0, \cdots, n\}. \tag{5.46}$$

and

$$\begin{aligned} \mathbf{E}_k := \{(a_n, \cdots, a_0) : \quad & a_i = a_i^- \text{ or } a_i^+, \quad i = 0, \cdots, n, \quad i \neq k \\ & a_k \in [a_k^-, a_k^+]\} \end{aligned} \tag{5.47}$$

and

$$\mathbf{E} = \cup_{k=0}^{n} \mathbf{E}_k. \tag{5.48}$$

The corresponding family of vertex and edge polynomials are defined by

$$\mathcal{I}_{\mathrm{V}}(z) := \{P(z) = a_n z^n + a_{n-1} z^{n-1} + \cdots + a_0 : (a_n, \cdots, a_0) \in \mathbf{V}\} \tag{5.49}$$

$$\mathcal{I}_{\mathrm{E}}(z) := \{P(z) = a_n z^n + a_{n-1} z^{n-1} + \cdots + a_0 : (a_n, \cdots, a_0) \in \mathbf{E}\}. \tag{5.50}$$

It is obvious that the interval family is a polytopic family and therefore stability of the family can be determined by that of the exposed edges. We state this preliminary result below.

Theorem 5.13 *Assume that the family of polynomials $\mathcal{I}(z)$ has constant degree. Then $\mathcal{I}(z)$ is Schur stable if and only if $\mathcal{I}_{\mathrm{E}}(z)$ is Schur stable.*

The proof is omitted as it follows from the image set arguments given in Chapter 4. The above result in fact holds for any stability region. It turns out that when we specifically deal with Schur stability, the number of edges to be tested for stability can be reduced and this is the result we present next.

In the rest of this section, *stable* will mean *Schur stable*. The first lemma given establishes a vertex result for an interval family with fixed upper order coefficients.

Lemma 5.5 *Let $n > 1$ and assume that in the family $\mathcal{I}(z)$ we have fixed upper order coefficients, namely that $a_i^- = a_i^+$ for $i = \dfrac{n}{2} + 1, \cdots, n$ if n is even, and $i = \dfrac{(n+1)}{2} + 1, \cdots, n$ if n is odd. Then the entire family $\mathcal{I}(z)$ is stable if and only if the family of vertex polynomials $\mathcal{I}_{\mathrm{V}}(z)$ is stable.*

Proof. If the entire family is stable it is obviously necessary that the vertex polynomials must be stable. Therefore we proceed to prove sufficiency of the condition. We know that the polynomial

$$P(z) = a_n z^n + a_{n-1} z^{n-1} + \cdots + a_0$$

is Schur stable if and only if the polynomial

$$F(s) := (s-1)^n P\left(\frac{s+1}{s-1}\right)$$

is Hurwitz stable. Now

$$\begin{aligned} F(s) := a_0(s-1)^n + a_1(s-1)^{n-1}(s+1) + a_2(s-1)^{n-2}(s+1)^2 \\ + \cdots + a_{\frac{n}{2}}(s-1)^{\frac{n}{2}}(s+1)^{\frac{n}{2}} + a_{\frac{n}{2}+1}(s-1)^{\frac{n}{2}-1}(s+1)^{\frac{n}{2}+1} \\ + \cdots + a_n(s+1)^n. \end{aligned} \tag{5.51}$$

Let $\mathcal{F}(s)$ be the family of polynomials of the form (5.51) with the parameter vector $\underline{a}$ ranging over $\mathbf{A}$:

$$\mathcal{F}(s) := \left\{ F(s) : a_i \in [a_i^-, a_i^+], \quad i \in (0, 1, \cdots, n) \right\}.$$

Since $\mathcal{F}(s)$ is a polytopic family, by the Edge Theorem, it is stable if and only if its exposed edges are. These edges correspond to the edges of $\mathbf{A}$, that is, to letting each a_i vary at a time. We give the detailed proof for the case in which n is even. Consider the set of *lower edges* obtained by letting a_k for some $k \in \left\{0, 1, \cdots, \frac{n}{2}\right\}$ vary in $[a_k^-, a_k^+]$ and fixing a_i, $i \in \{0, 1, \cdots, n\}$, $i \neq k$ at a vertex. With a view towards applying the Vertex Lemma (Chapter 2, Lemma 2.18) we determine the difference of the endpoints of these edge polynomials. These differences are of the form

$$\left[a_0^+ - a_0^-\right](s-1)^n, \left[a_1^+ - a_1^-\right](s-1)^{n-1}(s+1), \cdots, \left[a_{\frac{n}{2}}^+ - a_{\frac{n}{2}}^-\right](s-1)^{\frac{n}{2}}(s+1)^{\frac{n}{2}}.$$

From the Vertex Lemma we know that whenever these differences are of the form $A(s)s^t(as+b)Q(s)$ with $A(s)$ antiHurwitz and $Q(s)$ even or odd, edge (segment) stability is guaranteed by that of the vertices. We see that the difference polynomials above are precisely of this form. Therefore stability of the vertex polynomials suffices to establish the stability of the entire family. An identical proof works for the case n odd with the only difference being that the lower edges are defined with $k \in \left\{0, 1, \cdots, \frac{n}{2} + 1\right\}$. ♣

In the above result, we considered a special interval family where the upper order coefficients were fixed. Now let us consider an arbitrary interval family where all the coefficients are allowed to vary. For convenience let n_u be defined as follows:

$$\begin{aligned} \text{for n even} : n_u &= \left\{ \frac{n}{2} + 1, \frac{n}{2} + 2, \cdots, n \right\} \\ \text{for n odd} : n_u &= \left\{ \frac{n+1}{2} + 1, \frac{n+1}{2} + 2, \cdots, n \right\}. \end{aligned}$$

We refer to the coefficients a_k, $k \in n_u$ of the polynomial $P(z)$ as the upper coefficients. Also introduce a subset $\mathbf{E}^*$ of the edges $\mathbf{E}$ which we call *upper edges*. These edges are obtained by letting only one upper coefficient *at a time* vary within its interval bounds while all other coefficients are fixed at their upper or lower limits. The corresponding family of polynomials denoted $\mathcal{I}_{\mathrm{E}^*}(z)$ is

$$\mathcal{I}_{\mathrm{E}^*}(z) := \{P(z) = a_n z^n + a_{n-1} z^{n-1} + \cdots + a_0 : (a_n, \cdots, a_0) \in \mathbf{E}^*\} \tag{5.52}$$

A typical upper edge in $\mathcal{I}_{\mathrm{E}^*}(z)$ is defined by:

$$a_n z^n + \cdots + (\lambda a_k^- + (1-\lambda) a_k^+) z^k + \cdots + a_0 \tag{5.53}$$

$$k \in n_u, \quad a_i = a_i^- \text{ or } a_i^+, \quad i = 0, \cdots, n, \quad i \neq k.$$

There are

$$\left(\frac{n}{2}\right) 2^n, \ \ n \ even \tag{5.54}$$

$$\left(\frac{n+1}{2}\right) 2^n, \ \ n \ odd \tag{5.55}$$

such upper edges.

Example 5.10. Consider a second order polynomial

$$P(z) = a_2 z^2 + a_1 z + a_0$$

where

$$a_0 \in [a_0^-, a_0^+], \quad a_1 \in [a_1^-, a_1^+], \quad a_2 \in [a_2^-, a_2^+].$$

There are 4 upper edges given by:

$$\begin{aligned}
&(\lambda a_2^- + (1-\lambda) a_2^+) z^2 + a_1^- z + a_0^- \\
&(\lambda a_2^- + (1-\lambda) a_2^+) z^2 + a_1^- z + a_0^+ \\
&(\lambda a_2^- + (1-\lambda) a_2^+) z^2 + a_1^+ z + a_0^- \\
&(\lambda a_2^- + (1-\lambda) a_2^+) z^2 + a_1^+ z + a_0^+
\end{aligned}$$

In this case, the set of all exposed edges is 12.

We now have the following main result on the Schur stability of interval polynomials. As usual we assume that the degree of all polynomials in $\mathcal{I}(z)$ is n.

Theorem 5.14 *The family $\mathcal{I}(z)$ is stable if and only if the family of edge polynomials $\mathcal{I}_{\mathrm{E}^*}(z)$ is stable.*

Proof. By Lemma 5.5, the stability of the polytope $\mathcal{I}(z)$ is equivalent to that of the subsets obtained by fixing the lower coefficients at their vertices and letting the upper coefficients vary over intervals. The stability of each of these subpolytopes in turn can be obtained from their exposed edges. These edges precisely generate the family $\mathcal{I}_{\mathrm{E}^*}(z)$. This completes the proof. ♣

It is important to note here that even though this result is not Kharitonov like in the sense that the number of segments to be checked increases with the order of the polynomial, it still yields significant computational advantages over checking *all* the exposed edges. Indeed for an interval polynomial of degree n, we would have $(n+1)2^n$ exposed edges to check whereas the present result requires us to check (in the case n even) only $\binom{n}{2} 2^n$. As an example, for a second order interval polynomial there are 12 exposed edges, but only 4 upper edges. For a sixth order interval polynomial there are 448 exposed edges but only 192 upper edges.

Example 5.11. Consider the following second order polynomial

$$P(z) = a_2 z^2 + a_1 z + a_0$$

with coefficients varying in independent intervals

$$a_2 \in [2.5, 4], \qquad a_1 \in [-0.1, 0.25], \qquad a_0 \in [0.2, 0.8]$$

The corresponding exposed edges are obtained by letting one of the coefficients vary in an interval and fixing the other coefficients at a vertex. We obtain :

$$\begin{aligned}
E^1(\lambda, z) &= 2.5z^2 - 0.1z + 0.8 - 0.6\lambda \\
E^2(\lambda, z) &= 2.5z^2 + 0.25z + 0.8 - 0.6\lambda \\
E^3(\lambda, z) &= 4z^2 - 0.1z + 0.8 - 0.6\lambda \\
E^4(\lambda, z) &= 4z^2 + 0.25z + 0.8 - 0.6\lambda \\
E^5(\lambda, z) &= 2.5z^2 + (0.25 - 0.35\lambda)z + 0.2 \\
E^6(\lambda, z) &= 2.5z^2 + (0.25 - 0.35\lambda)z + 0.8 \\
E^7(\lambda, z) &= 4z^2 + (0.25 - 0.35\lambda)z + 0.2 \\
E^8(\lambda, z) &= 4z^2 + (0.25 - 0.35\lambda)z + 0.8 \\
E^9(\lambda, z) &= (4 - 1.5\lambda)z^2 - 0.1z + 0.2 \\
E^{10}(\lambda, z) &= (4 - 1.5\lambda)z^2 - 0.1z + 0.8 \\
E^{11}(\lambda, z) &= (4 - 1.5\lambda)z^2 + 0.25z + 0.2 \\
E^{12}(\lambda, z) &= (4 - 1.5\lambda)z^2 + 0.25z + 0.8
\end{aligned}$$

The upper edges associated with $P(z)$ are

$$\begin{aligned}
U^1(\lambda, z) &= (4 - 1.5\lambda)z^2 - 0.1z + 0.2 \\
U^2(\lambda, z) &= (4 - 1.5\lambda)z^2 - 0.1z + 0.8 \\
U^3(\lambda, z) &= (4 - 1.5\lambda)z^2 + 0.25z + 0.2 \\
U^4(\lambda, z) &= (4 - 1.5\lambda)z^2 + 0.25z + 0.8
\end{aligned}$$

One can see that the upper edges are a subset of the exposed edges. The evolution of the image set, evaluated along the unit circle, of the exposed edges and upper edges is shown in Figures 5.13 and 5.14 respectively.

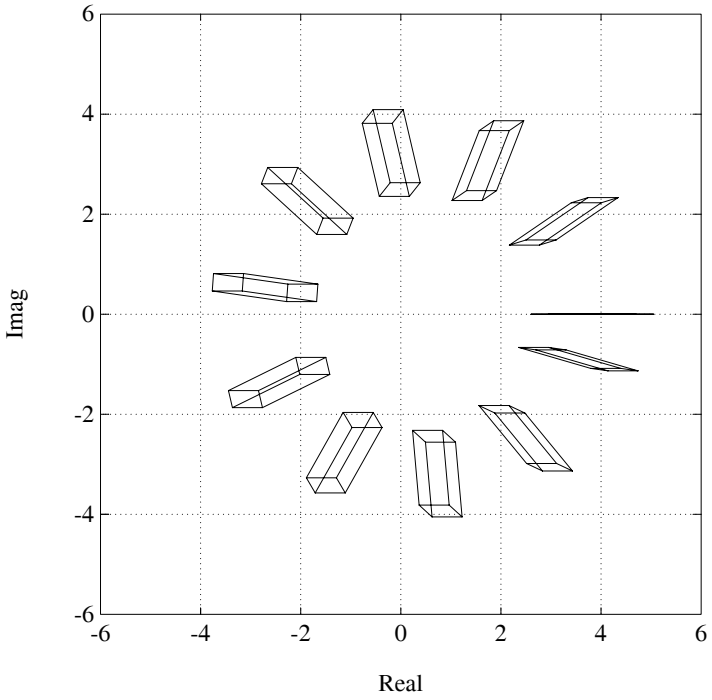

Figure 5.13. Evolution of the image set of the exposed edges (Example 5.11)

The image set excludes the origin, which shows that the entire family of polynomials is stable. One can note that the image set of the upper edges is a reduced subset of the image set of the exposed edges.

As a final note we again point out that robust Schur stability of an interval family can be ascertained by determining phase differences of the vertex polynomials. In the previous example this would have required the computation of the phases of eight vertex polynomials along with the stability check of a single polynomial in the family.

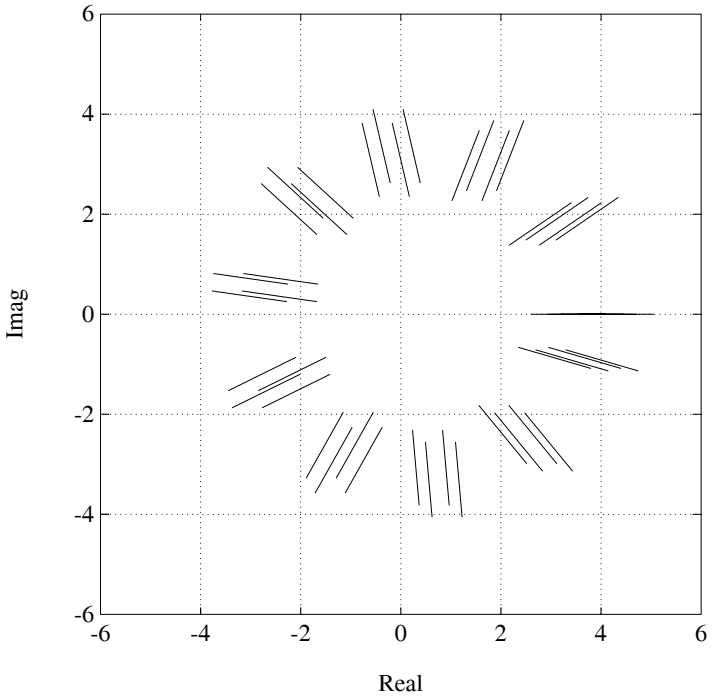

Figure 5.14. Evaluation of the image set of the upper edges (Example 5.11)

5.9 EXERCISES

5.1 Consider the control system shown in Figure 5.15. The parameters α_i, β_j vary

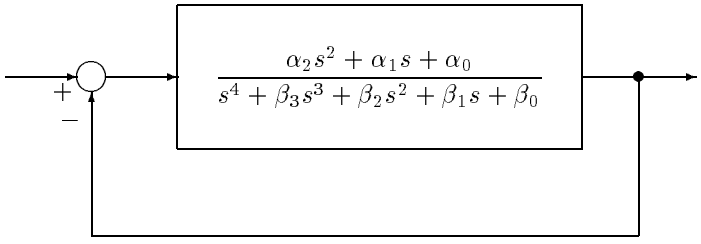

Figure 5.15. A feedback system (Exercise 5.1)

in the following ranges:

$$\alpha_0 \in [2, 6], \quad \alpha_1 \in [0, 2], \quad \alpha_2 \in [-1, 3],$$

and

$$\beta_0 \in [4,8], \quad \beta_1 \in [0.5,1.5], \quad \beta_2 \in [2,6], \quad \beta_3 \in [6,14].$$

Determine if the closed loop system is Hurwitz stable or not for this class of perturbations.

5.2 For the system in Exercise 5.1 determine the largest box with the same center and shape (i.e. the ratios of the lengths of the sides are prespecified) as prescribed in the problem, for which the closed loop remains stable.

5.3 Show by an example that Kharitonov's Theorem does not hold when the stability region is the shifted half plane $\mathrm{Re}[s] \leq -\alpha, \ \ \alpha > 0$.

5.4 Show that for interval polynomials of degree less than six it suffices to test fewer than four polynomials in applying Kharitonov's test. Determine for each degree the number of polynomials to be checked, in addition to the condition that the signs of the coefficients are the same.
Hint: Consider the interlacing tubes corresponding to the interval family for each degree.

5.5 Consider the Hurwitz stability of an interval family where the only coefficient subject to perturbation is δ_k, the coefficient of s^k for an arbitrary $k \in [0,1,2,..,n]$. Show that the δ_k axis is partitioned into at most one stable segment and one or two unstable segments.

5.6 Apply the result of Exercise 5.5 to the Hurwitz polynomial

$$\delta(s) = s^4 + \delta_3 s^3 + \delta_2 s^2 + \delta_1 s + \delta_0$$

with nominal parameters

$$\delta_3^0 = 4, \quad \delta_2^0 = 10, \quad \delta_1^0 = 12, \quad \delta_0^0 = 5.$$

Suppose that all coefficients except δ_3 remain fixed and δ_3 varies as follows:

$$\delta_3^- \leq \delta_3 \leq \delta_3^+.$$

Determine the largest interval (δ_3^-, δ_3^+) for which $\delta(s)$ remains Hurwitz. Repeat this for each of the coefficients δ_2, δ_1, and δ_0.

5.7 Consider the Hurwitz polynomial

$$\delta(s) = s^4 + \delta_3 s^3 + \delta_2 s^2 + \delta_1 s + \delta_0$$

with nominal parameters $\underline{\delta}^0 = [\delta_3^0, \delta_2^0, \delta_1^0, \delta_0^0]$ given by:

$$\delta_3^0 = 4, \quad \delta_2^0 = 10, \quad \delta_1^0 = 12, \quad \delta_0^0 = 5.$$

Suppose that the coefficients vary independently within a weighted l^∞ box of size ρ given by:

$$\mathbf{\Delta}_\rho := \left\{ \underline{\delta} : \delta_i^0 - \rho w_i \le \delta_i \le \delta_i^0 + \rho w_i, \quad i = 0, 1, 2, 3 \right\}$$

with weights $w_i \ge 0$. Find the maximal value of ρ for which stability is preserved assuming that $w_i = \delta_i^0$.

5.8 Consider an interval family and show that if the Kharitonov polynomials are completely unstable (i.e. their roots are all in the closed right half plane) then the entire family is completely unstable.

5.9 Consider the *positive feedback* control system shown in Figure 5.16 below:

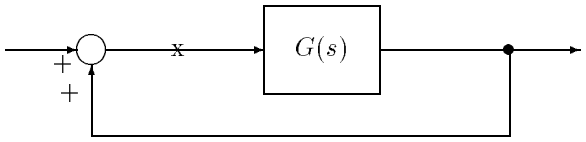

Figure 5.16. A feedback system (Exercise 5.9)

Let $G(s)$ belong to a family of interval systems $\mathbf{G}(s)$ as in Section 5.2. Show that the closed loop system is robustly stable (stable for all $G(s) \in \mathbf{G}(s)$) if and only if it is stable for each system in the set of negative Kharitonov systems

$$\mathbf{G}_{\mathrm{K}}^-(s) = \left\{ \frac{K_N^{5-i}(s)}{K_D^i(s)}, \quad i = 1, 2, 3, 4 \right\}$$

Prove that if the system is robustly stable, the minimum gain margin over the interval family $\mathbf{G}(s)$ is attained over the subset $\mathbf{G}_{\mathrm{K}}^-(s)$.

5.10 Let the state space representation of the system (A, b) be

$$A = \begin{bmatrix} 0 & 1 & 0 & 0 \\ 0 & 0 & 1 & 0 \\ 0 & 0 & 0 & 1 \\ a_0 & a_1 & a_2 & a_3 \end{bmatrix} \qquad B = \begin{bmatrix} 0 \\ 0 \\ 0 \\ 1 \end{bmatrix}$$

where

$$a_0 \in [0, 1.5], \quad a_1 \in [-1.5, 2], \quad a_2 \in [0, 1], \quad a_3 \in [1, 2].$$

Find the state feedback control law that robustly stabilizes the closed loop system.

5.11 Consider the Hurwitz stable interval polynomial family

$$\delta(s) = \delta_3 s^3 + \delta_2 s^2 + \delta_1 s + \delta_0$$

$$\delta_3 \in [1.5, 2.5], \quad \delta_2 \in [2, 6], \quad \delta_1 \in [4, 8], \quad \delta_0 \in [0.5, 1.5].$$

Determine the worst case parametric stability margin $\rho(\delta)$ over the parameter box in the ℓ_2 and ℓ_∞ norms.

5.12 For the interval polynomial

$$\delta(z) = \delta_3 z^3 + \delta_2 z^2 + \delta_1 z + \delta_0$$

$$\delta_3 \in [1-\epsilon, 1+\epsilon], \ \delta_2 \in \left[-\frac{1}{4}-\epsilon, -\frac{1}{4}+\epsilon\right],$$
$$\delta_1 \in \left[-\frac{3}{4}-\epsilon, -\frac{3}{4}+\epsilon\right], \ \delta_0 \in \left[\frac{3}{16}-\epsilon, \frac{3}{16}+\epsilon\right]$$

determine the maximal value of ϵ for which the family is Schur stable using Theorem 5.13.

5.13 Consider the interval family $\mathcal{I}(s)$ of real polynomials

$$\delta(s) = \delta_o + \delta_1 s + \delta_2 s^2 + \delta_3 s^3 + \delta_4 s^4 + \cdots + \delta_n s^n$$

where the coefficients lie within given ranges,

$$\delta_0 \in [x_0, y_0], \ \delta_1 \in [x_1, y_1], \ \cdots, \ \delta_n \in [x_n, y_n].$$

Suppose now that $x_n = 0$ and that $x_i > 0, \ \ i = 0, 1, 2, \cdots, n-1$. Show that the Hurwitz stability of the family can be determined by checking, in addition to the usual four Kharitonov polynomials

$$\hat{K}^1(s) = x_n s^n + y_{n-1}s^{n-1} + y_{n-2}s^{n-2} + x_{n-3}s^{n-3} + x_{n-4}s^{n-4} + \cdots,$$
$$\hat{K}^2(s) = x_n s^n + x_{n-1}s^{n-1} + y_{n-2}s^{n-2} + y_{n-3}s^{n-3} + x_{n-4}s^{n-4} + \cdots,$$
$$\hat{K}^3(s) = y_n s^n + x_{n-1}s^{n-1} + x_{n-2}s^{n-2} + y_{n-3}s^{n-3} + y_{n-4}s^{n-4} + \cdots,$$
$$\hat{K}^4(s) = y_n s^n + y_{n-1}s^{n-1} + x_{n-2}s^{n-2} + x_{n-3}s^{n-3} + y_{n-4}s^{n-4} + \cdots.$$

the following two additional polynomials

$$\hat{K}_5(s) = x_{n-1}s^{n-1} + x_{n-2}s^{n-2} + y_{n-3}s^{n-3} + y_{n-4}s^{n-4} + \cdots$$
$$\hat{K}_6(s) = y_{n-1}s^{n-1} + x_{n-2}s^{n-2} + x_{n-3}s^{n-3} + y_{n-4}s^{n-4} + \cdots$$

Hint: Note that $\hat{K}_5(s)$ and $\hat{K}_6(s)$ can be obtained from $\hat{K}_3(s)$ and $\hat{K}_4(s)$ respectively by setting $y_n = 0$. Now use the argument that for a given polynomial $q(s)$ of degree $n-1$, the family $s^n + \mu q(s)$, $\mu \in \left[\frac{1}{y_n}, \infty\right)$ is Hurwitz stable if and only if $q(s)$ and $y_n s^n + q(s)$ are Hurwitz stable.)

5.14 Prove Lemma 5.3 for the case $n = 4r + j, \quad j = 1, 2, 3.$

5.15 Let $\mathcal{I}_\rho(s)$ denote the interval polynomial family

$$a(s) = a_3 s^3 + a_2 s^2 + a_1 s + a_0$$

where

$$a_3 \in [1-\rho, 1+\rho], \quad a_2 \in [4-\rho, 4+\rho], \quad a_1 \in [6-\rho, 6+\rho], \quad a_0 \in [1-\rho, 1+\rho]$$

and let

$$\varphi(z) = \alpha_2 z^2 + \alpha_1 z + \alpha_0$$

with $\alpha_2 = 1$, $\alpha_1 = 3$, $\alpha_0 = 4$. Determine the maximum value of ρ for which the family $\varphi(\mathcal{I}_\rho(s))$ is Hurwitz stable.

5.16 In Exercise 5.15, suppose that the polynomial $\varphi(z)$ varies in a polytope

$$\Phi(z) = \{\varphi(z) = \alpha_2 z^2 + \alpha_1 z + \alpha_0 : \alpha_2 = 1, \alpha_1 \in [2,4], \alpha_0 \in [3,5]\}.$$

Determine the maximum value of ρ for which the family $\Phi(\mathcal{I}_\rho(s))$ is Hurwitz stable.

5.10 NOTES AND REFERENCES

The interval polynomial problem was originally posed by Faedo [92] who attempted to solve it using the Routh-Hurwitz conditions. Some necessary and some sufficient conditions were obtained by Faedo and the problem remained open until Kharitonov gave a complete solution. Kharitonov first published his theorem for real polynomials in 1978 [143], and then extended it to the complex case in [144]. The papers of Bialas [38] and Barmish [11] are credited with introducing this result to the Western literature. Several treatments of this theorem are available in the literature. Among them we can mention Bose [44], Yeung and Wang [240] and Minnichelli, Anagnost and Desoer [181] and Chapellat and Bhattacharyya [57]. A system-theoretic proof of Kharitonov's Theorem for the complex case was given by Bose and Shi [50] using complex reactance functions. That the set $\mathcal{I}(j\omega)$ is a rectangle was first pointed out by Dasgupta [75] and hence it came to be known as Dasgupta's rectangle. The proof in Minnichelli et. al. is based on the image set analysis given in Section 5.4. The proof in Chapellat and Bhattacharyya [57] is based on the Segment Lemma (Chapter 2). Mansour and Anderson [171] have proved Kharitonov's Theorem using the second method of Lyapunov. The computational approach to enlarging the ℓ_∞ box described in Exercise 5.7 was first reported in Barmish [11]. The extremal property of the Kharitonov polynomials, Theorem 5.4 was first proved by Chapellat and Bhattacharyya [56] and the robust stabilization result of Theorem 5.7 is adapted from Chapellat and Bhattacharyya [59]. Mansour, Kraus and Anderson [174] and Kraus, Anderson and Mansour [152] have given several results on robust Schur stability and strong Kharitonov theorems for Schur interval systems. Lemma 5.5 and

Theorem 5.14 were proved by Pérez, Abdallah and Docampo [188] and extend similar results due to Hollot and Bartlett [115], and Kraus, Mansour, and Jury [155]. In Kraus and Mansour [153] the minimal number of edges to be checked for Schur stability of an interval polynomial is derived. This number of course depends on n unlike the Hurwitz case where it is always 4. Rantzer [194] studied the problem of characterizing stability regions in the complex plane for which it is true that stability of *all* the vertices of an interval family guarantee that of the entire family. He showed that such regions $\mathcal{D}$, called Kharitonov regions, are characterized by the condition that $\mathcal{D}$ as well as $1/\mathcal{D}$ are both convex. Meressi, Chen and Paden [179] have applied Kharitonov's Theorem to mechanical systems. Mori and Kokame [183] dealt with the modifications required to extend Kharitonov's Theorem to the case where the degree can drop, i.e. $x_n = 0$ (see Exercise 5.12). Kharitonov's Theorem has been generalized by Chapellat and Bhattacharyya [58] for the control problem. This is described in Chapter 7. Various other generalizations of the Kharitonov's Theorem have been reported. In [45] Bose generalized Kharitonov's Theorem in another direction and showed that the scattering Hurwitz property of a set of bivariate interval polynomials could be established by checking only a finite number of extreme bivariate polynomials. Multidimensional interval polynomials were also studied by Basu [23]. Barmish [13] has reported a generalization of the so-called four polynomial concept of Kharitonov. The extension of Kharitonov's Theorem to polynomial functions of interval polynomials described in Section 5.7 are due to Kharitonov [146].

Chapter 6

THE EDGE THEOREM

This chapter deals with the robust stability of a polytopic family of polynomials with respect to an arbitrary stability region. Such problems arise in control systems whenever the characteristic polynomial coefficients are linear (including affine) functions of the uncertain parameters and these vary in intervals. The Edge Theorem shows that the root space of the entire family can be obtained from the root set of the exposed edges. Since the exposed edges are one-parameter sets of polynomials, this theorem effectively and constructively reduces the problem of determining the root space under multiple parameter uncertainty to a set of one-parameter root locus problems. The stability testing property of edges is also extended in this chapter to nested polytopic families.

6.1 INTRODUCTION

The Edge Theorem, due to Bartlett, Hollot and Lin appeared in 1988, and was largely motivated by a desire to extend Kharitonov's problem by taking dependencies between the coefficients of the polynomial into account and by dealing with general stability regions. As we have seen in Chapter 4 such dependencies arise in most practical situations and require the investigation of the robust stability of a polytopic family of polynomials. The interval family dealt with in Kharitonov's Theorem is a very special case of a polytopic family. The Edge Theorem gives a complete, exact and constructive characterization of the root set of a polytopic family. Such a characterization is of immense value in the analysis and design of control systems. This entire chapter is devoted to this elegant and useful theorem.

A polytopic family of polynomials can be thought of as the convex hull of a finite number of points (polynomials). Mathematically, this can be represented as the family

$$P(s) = \lambda_1 P_1(s) + \cdots + \lambda_n P_n(s)$$

where $P_i(s)$ are fixed real polynomials and the λ_i are real with $\lambda_i \geq 0$ and $\sum \lambda_i = 1$.

An alternative representation of a polytopic family, as used in Chapter 4, is of the form

$$P(s) = a_1 Q_1(s) + a_2 Q_2(s) + \cdots + a_m Q_m(s)$$

where each real parameter a_i varies independently in the interval $[\underline{a}_i, \bar{a}_i]$. In other words, the parameter vector $\mathbf{a} := [a_1, \cdots, a_m]$ varies in the hypercube

$$\mathbf{A} := \{\mathbf{a} \ : \ \underline{a}_i \leq a_i \leq \bar{a}_i, \quad i = 1, \cdots, m\}$$

In some problems, a polytopic family may arise because the system characteristic polynomial

$$\delta(s, \mathbf{p}) := \delta_0(\mathbf{p}) + \delta_1(\mathbf{p})s + \cdots + \delta_n(\mathbf{p})s^n$$

has coefficients $\delta_i(\mathbf{p})$ which are *linear functions* of the parameter vector $\mathbf{p}$. If $\mathbf{p}$ varies within a hypercube, it generates a polytopic family of characteristic polynomials. In control problems the elements of $\mathbf{p}$ could be physical parameters belonging to the plant or design parameters belonging to the controller.

The Edge Theorem gives an elegant solution to the problem of determining the root space of polytopic systems. As a byproduct we therefore can determine the robust stability of such systems also. It establishes the fundamental property that the root space boundary of a polytopic family of polynomials is contained in the root locus evaluated along the exposed edges. In the following section we give the proof of the Edge Theorem. This is followed by some illustrative examples. In the last section we derive an extension of the stability testing property of edges to nested polynomial families which are not polytopic and where the uncertain parameters appear nonlinearly.

6.2 THE EDGE THEOREM

Let us consider a family of n^{th} degree real polynomials whose typical element is given by

$$\delta(s) = \delta_0 + \delta_1 s + \cdots + \delta_{n-1}s^{n-1} + \delta_n s^n. \tag{6.1}$$

As usual, we identify $\mathcal{P}_n$ the vector space of all real polynomials of degree less than or equal to n with $\mathbb{R}^{n+1}$, and we will identify the polynomial in (6.1) with the vector

$$\underline{\delta} := [\delta_n, \delta_{n-1}, \cdots, \delta_1, \delta_0]^T. \tag{6.2}$$

Let $\Omega \subset \mathbb{R}^{n+1}$ be an m-dimensional *polytope*, that is, the convex hull of a finite number of points. As a polytope, Ω is a closed bounded set and therefore it is compact. We make the assumption that all polynomials in Ω have the same degree:

Assumption 6.1. The sign of δ_n is constant over Ω, either always positive or always negative.

Assuming for example that this sign is always positive, and using the fact that Ω is compact, it is always possible to find $\Delta > 0$ such that,

$$\delta_n > \Delta, \quad \text{for every} \quad \underline{\delta} \in \Omega. \tag{6.3}$$

A *supporting hyperplane* H is an affine set of dimension n such that $\Omega \cap H \neq \emptyset$, and such that every point of Ω lies on just one side of H. The *exposed sets* of Ω are

those (convex) sets $\Omega \cap H$ where H is a supporting hyperplane. The one dimensional exposed sets are called *exposed edges*, whereas the two-dimensional exposed sets are the *exposed faces*.

Before proceeding we need to introduce the notion of root space. Consider any $W \subset \Omega$. Then $R(W)$ is said to be the root space of W if,

$$R(W) = \{s : \delta(s) = 0, \quad \text{for some} \quad \underline{\delta} \in W\}. \tag{6.4}$$

Finally, recall that the boundary of an arbitrary set S of the complex plane is designated by ∂S. We can now enunciate and prove the Edge Theorem.

Theorem 6.1 (Edge Theorem)
Let $\Omega \subset \mathbb{R}^{n+1}$ be a polytope of polynomials which satisfies Assumption 6.1. Then the boundary of $R(\Omega)$ is contained in the root space of the exposed edges of Ω.

To prove the theorem we need two lemmas.

Lemma 6.1 *If a real s_r belongs to $R(\Omega)$, then there exists an exposed edge E of Ω such that $s_r \in R(E)$, and if a complex number s_c belongs to $R(\Omega)$, then there exists an exposed face F of Ω such that $s_c \in R(F)$.*

Proof. Consider an arbitrary $\underline{\delta}$ in Ω, and suppose that s_r is a real root of $\delta(s)$. We know that the set of all polynomials having s_r among their roots is a vector space $\mathcal{P}_{s_r}$ of dimension n. Let $aff(\Omega)$ denote the affine hull of Ω, that is, the smallest affine subspace containing Ω. Now, assume that $m = dim[aff(\Omega)] \geq 2$. Then we have that,

$$dim\,[\mathcal{P}_{s_r} \cap aff(\Omega)] \geq 1,$$

and this implies that this set $\mathcal{P}_{s_r} \cap aff(\Omega)$ must pierce the relative boundary of Ω. This relative boundary however, is the union of some $m-1$ dimensional polytopes which are all exposed sets of Ω. Therefore, at least one of these boundary polytopes Ω_{m-1} satisfies,

$$s_r \in R(\Omega_{m-1}).$$

If $dim[aff(\Omega_{m-1})] \geq 2$, we see that we can repeat the preceding argument and ultimately we will find a one-dimensional boundary polytope Ω_1 for which $s_r \in R(\Omega_1)$. But Ω_1 is just an exposed edge of Ω, so that s_r does indeed belong to the root space of the exposed edges of Ω. For the case of a complex root s_c, it suffices to know that the set of all real polynomials having s_c among their roots is a vector space $\mathcal{P}_{s_c}$ of dimension $n-1$. As a consequence the same reasoning as above holds, yielding eventually an exposed face Ω_2 of Ω for which $s_c \in R(\Omega_2)$. ♣

We illustrate this lemma in Figures 6.1, 6.2, and 6.3 with a three dimensional polytope Ω (see Figure 6.1). Here $\mathcal{P}_{s_r}$ is a subspace of dimension 2 and cuts the edges of Ω (see Figure 6.2). $\mathcal{P}_{s_c}$ is of dimension 1 and must penetrate a face of Ω (see Figure 6.3).

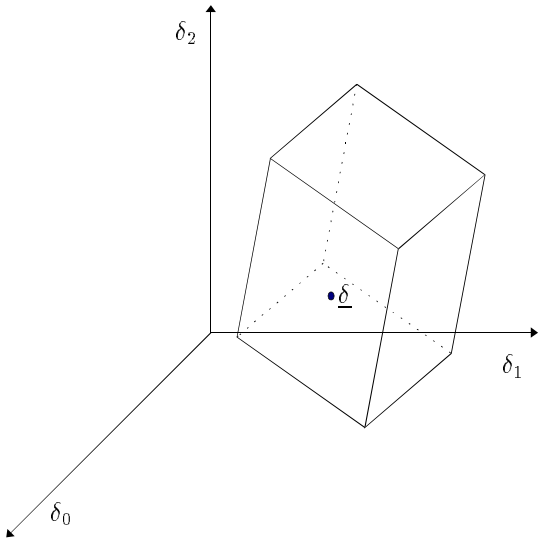

Figure 6.1. Polytope Ω

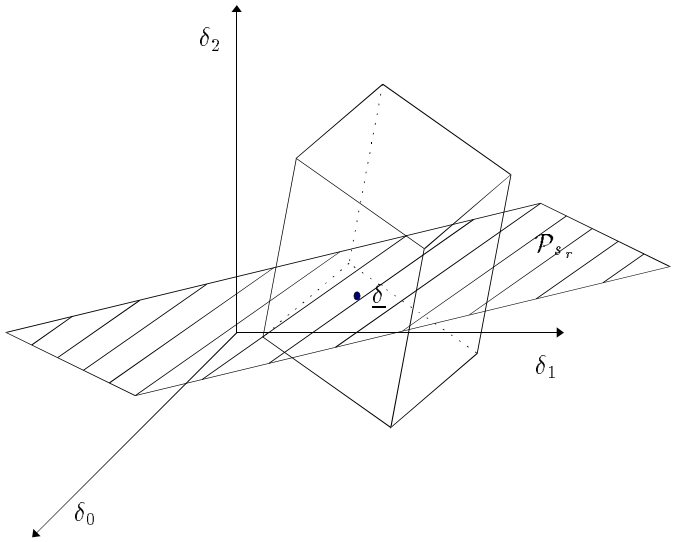

Figure 6.2. $\mathcal{P}_{s_r}$ cuts edges of Ω

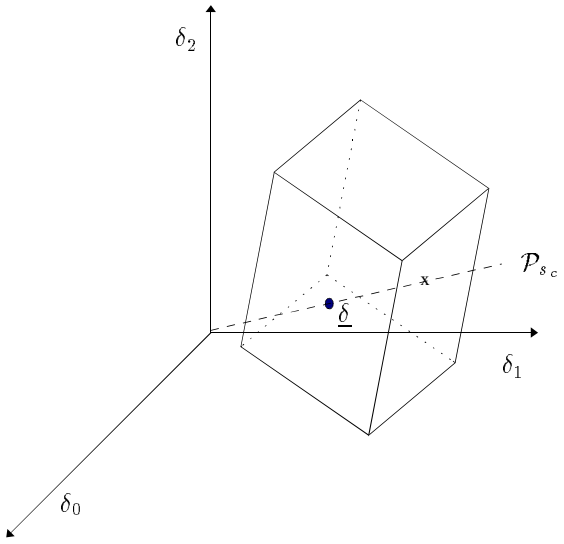

Figure 6.3. $\mathcal{P}_{s_c}$ penetrates a face of Ω

The conclusion of this first lemma is that if p_F is the number of exposed faces, then

$$R(\Omega) = \bigcup_{i=1}^{p_F} R(F_i). \tag{6.5}$$

The next lemma focuses now on an exposed face. Let F be an exposed face of Ω and let us denote by ∂F its relative boundary. Since F is a compact set and because of Assumption 6.1 on Ω, we know from Chapter 2 that $R(F)$ is itself a closed set. We have the following.

Lemma 6.2 *$\partial R(F) \subset R(\partial F)$.*

Proof. Let s^* be an arbitrary element of $\partial R(F)$, we want to show that s^* is also an element of $R(\partial F)$. Since ∂F is the union of exposed edges of Ω, it follows from Lemma 6.1 that if s^* is real then $s^* \in R(\partial F)$.

Now assume that s^* is complex. Since $R(F)$ is a closed set, $\partial R(F) \subset R(F)$, so that it is possible to find $\underline{\delta}^* \in F$ with $\delta^*(s^*) = 0$. We can write

$$\delta^*(s) = (s^2 + \alpha s + \beta)(d_{n-2}s^{n-2} + \cdots + d_1 s + d_0) \tag{6.6}$$

where $\alpha = -2\mathrm{Re}(s^*)$ and $\beta = |s^*|^2$. Let $aff(F)$ be the affine hull of F. Since F is two-dimensional it is possible to write $aff(F) = \{\underline{\delta}^* + V\lambda; \lambda \in \mathbb{R}^2\}$, where V is

some full rank $(n+1) \times 2$ matrix. On the other hand, an arbitrary element of the vector space of real polynomials with a root at s^* can be written as

$$P^*(s) = (s^2 + \alpha s + \beta)\left[((\mu_{n-2} + d_{n-2})s^{n-2} + \cdots + (\mu_1 + d_1)s + (\mu_0 + d_0)\right], \quad (6.7)$$

or more generally we can write,

$$\mathcal{P}_{s^*} = \{\underline{\delta}^* + W\mu : \mu = [\mu_{n-2}, \cdots, \mu_1, \mu_0]^T \in \mathbb{R}^{n-2}\}, \quad (6.8)$$

where W is the $(n+1) \times (n-1)$ matrix,

$$W = \begin{bmatrix} 1 & 0 & \cdots & 0 \\ \alpha & 1 & \cdots & 0 \\ \beta & \alpha & \cdots & 0 \\ 0 & \beta & \cdots & 0 \\ \vdots & \vdots & \ddots & \vdots \\ 0 & 0 & \cdots & 1 \\ 0 & 0 & \cdots & \alpha \\ 0 & 0 & \cdots & \beta \end{bmatrix}. \quad (6.9)$$

The intersection between $aff(F)$ and $\mathcal{P}_{s^*}$ contains all λ, μ satisfying,

$$\underline{\delta}^* + V\lambda = \underline{\delta}^* + W\mu, \text{ or equivalently, } [V, -W]\begin{bmatrix} \lambda \\ \mu \end{bmatrix} = 0. \quad (6.10)$$

Two possibilities have to be considered:

A. $[V, -W]$ does not have full rank

In this case, the space of solutions to (6.10) is either of dimension 1 or 2. If it is of dimension one, then the intersection $aff(F) \cap \mathcal{P}_{s^*}$ is a straight line which must intersect ∂F at a point $\hat{\underline{\delta}}$. Since $\hat{\underline{\delta}} \in \mathcal{P}_{s^*}$, $\hat{\delta}(s^*) = 0$, which implies that $s^* \in R(\partial F)$. If the dimension is two then $aff(F) \subset \mathcal{P}_{s^*}$ and for any $\hat{\underline{\delta}} \in \partial F$ we have $\hat{\delta}(s^*) = 0$ so that clearly $s^* \in R(\partial F)$.

B. $[V, -W]$ has full rank

In this case the intersection $aff(F) \cap \mathcal{P}_{s^*}$ is reduced to $\underline{\delta}^*$. We now prove that $\underline{\delta}^* \in \partial F$ and this is where the fact that $s^* \in \partial R(F)$ is utilized.
Indeed, $s^* \in \partial R(F)$ implies the existence of a sequence of complex numbers s_n such that $s_n \notin R(F)$ for all n and such that $s_n \longrightarrow s^*$ as $n \to +\infty$. In particular this implies that,

$$-2Re(s_n) \longrightarrow \alpha \quad \text{and} \quad |s_n|^2 \longrightarrow \beta \quad \text{as} \quad n \to +\infty. \quad (6.11)$$

As usual, let $\mathcal{P}_{s_n}$ be the vector space of all real polynomials with a root at s_n. An arbitrary element of $\mathcal{P}_{s_n}$ can be expressed as

$$P(s) = \delta^*(s) + \left((s^2 - 2\mathrm{Re}(s_n)s + |s_n|^2\right)(\mu_{n-2}s^{n_2} + \cdots + \mu_1 s + \mu_0) + \\ + \left(-(2\mathrm{Re}(s_n) + \alpha)s + (|s_n^2| - \beta)\right)\left(d_{n-2}s^{n-2} + \cdots + d_1 s + d_0\right),$$

or, similarly

$$\mathcal{P}_{s_n} = \{\underline{\delta}^* + W_n\mu + \nu_n : \mu = [\mu_{n-2}, \cdots, \mu_1, \mu_0] \in \mathbb{R}^{n-1}\}.$$

where,

$$W_n = \begin{bmatrix} 1 & 0 & \cdots & 0 \\ -2Re(s_n) & 1 & \cdots & 0 \\ |s_n|^2 & -2Re(s_n) & \cdots & 0 \\ 0 & |s_n|^2 & \cdots & 0 \\ \vdots & \vdots & \ddots & \vdots \\ 0 & 0 & \cdots & 1 \\ 0 & 0 & \cdots & -2Re(s_n) \\ 0 & 0 & \cdots & |s_n|^2 \end{bmatrix}. \tag{6.12}$$

and

$$\nu_n = \begin{bmatrix} d_{n-2} & 0 \\ d_{n-3} & d_{n-2} \\ d_{n-4} & d_{n-3} \\ \vdots & \vdots \\ d_0 & d_1 \\ 0 & d_0 \end{bmatrix} \begin{bmatrix} -\big(2Re(s_n) + \alpha\big) \\ |s_n|^2 - \beta \end{bmatrix}. \tag{6.13}$$

Clearly,

$$W_n \longrightarrow W \text{ and } \nu_n \longrightarrow 0 \text{ as } n \to +\infty. \tag{6.14}$$

Now, since $\det(\cdot)$ is a continuous function and since $\det[V\ , -W] \neq 0$, there must exist n_1 such that $\det[V\ -W_n] \neq 0$ for $n \geq n_1$. Also, for every n, the intersection between $\mathcal{P}_{s_n}$ and $aff(F)$ consists of all λ, μ that satisfy:

$$\underline{\delta}^* + W_n\mu + \nu_n = \underline{\delta}^* + V\lambda$$

or equivalently

$$[V\ , -W_n] \begin{bmatrix} \lambda \\ \mu \end{bmatrix} = \nu_n. \tag{6.15}$$

For $n \geq n_1$, the system (6.15) has a unique solution,

$$\begin{bmatrix} \lambda_n \\ \mu_n \end{bmatrix} = [V\ , -W_n]^{-1}\nu_n. \tag{6.16}$$

From (6.16) we deduce that $[\lambda_n^T, \mu_n^T] \longrightarrow 0$ when $n \to +\infty$.

We now show that $\underline{\delta}^*$ belongs to ∂F. Let us consider an arbitrary open neighborhood in $aff(F)$,

$$B_F(\underline{\delta}^*, \epsilon) = \{\underline{\delta} \in aff(F) : \|\underline{\delta} - \underline{\delta}^*\| < \epsilon\},$$

We must show that $B_F(\underline{\delta}^*, \epsilon)$ contains at least one vector not contained in F.

To do so, consider the intersection between $\mathcal{P}_{s_n}$ and $aff(F)$, that is the vector $\underline{\delta}_n = \underline{\delta}^* + V\lambda_n$. This vector belongs to $aff(F)$, and since λ_n goes to 0, it belongs to $B_F(\underline{\delta}^*, \epsilon)$ for n sufficiently large. Moreover, the polynomial corresponding to this vector has a root at s_n and we know that s_n does not belong to $R(F)$. Hence it must be the case that $\underline{\delta}_n$ does not belong to F, and this completes the proof of the lemma. ♣

Figures 6.4 and 6.5 illustrate this lemma. The sequence s_n converges to $s^* \in R(F)$ from outside of $R(F)$. The corresponding subspaces $\mathcal{P}_{s_n}$ converge to $\mathcal{P}_{s^*}$ from outside F. Thus $\mathcal{P}_{s^*}$ must touch an edge of F.

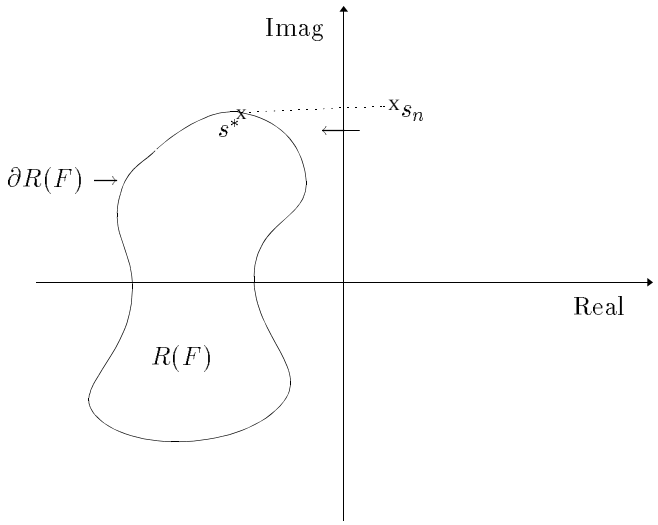

Figure 6.4. The sequence $s_n \notin R(F)$ converges to $s^* \in \partial R(F)$

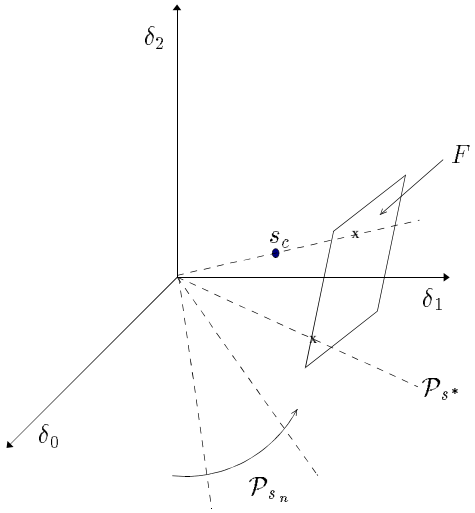

Figure 6.5. The sequence $\mathcal{P}_{s_n}(\mathcal{P}_{s_i} \cap F = \emptyset)$ converges to $\mathcal{P}_{s^*}$

Proof of the Edge Theorem (Theorem 6.1) From (6.5) and Lemma 6.2 we have

$$\partial R(\Omega) = \partial \bigcup_{i=1}^{p_F} R(F_i) = \bigcup_{i=1}^{p_F} \partial R(F_i) \subset \bigcup_{i=1}^{p_F} R(\partial F_i).$$

The ∂F_i are precisely the exposed edges of Ω and this proves the theorem. ♣

Let us now consider an arbitrary simply connected domain of the complex plane, that is, a subset of the complex plane in which every simple (i.e. without self-crossings) closed contour encloses only points of the set. We can state the following corollary:

Corollary 6.1 *If $\Gamma \subset C$ is a simply connected domain, then for any polytope satisfying Assumption 6.1, $R(\Omega)$ is contained in Γ if and only if the root space of all the exposed edges of Ω is contained in Γ.*

Exposed Edges

In general, a polytope is defined by its vertices and it is not immediately clear how to determine which are the exposed edges of Ω. However, it is clear that those exposed edges are part of all pairwise convex combinations of the vertices of Ω, and

therefore it is enough to check those. In the representation

$$\mathcal{P} := \{P(s) : P(s) = a_1 Q_1(s) + a_2 Q_2(s) + \cdots + a_m Q_m(s), \quad \mathbf{a} \in \mathbf{A}\}$$

where $\mathbf{a} = [a_1, a_2, \cdots, a_m]$ the exposed edges of the polytope $\mathcal{P}$ are obtained from the exposed edges of the hypercube $\mathbf{A}$ to which $\mathbf{a}$ belongs. This can be done by fixing all a_i except one, say a_k, at a vertex $\underline{a}_i$ or $\bar{a}_i$, and letting a_k vary in the interval $[\underline{a}_k, \bar{a}_k]$, and repeating this for $k = 1, \cdots, m$. In general, the number of line segments in the coefficient space generated by this exceeds the number of exposed edges of $\mathcal{P}$. Nevertheless, this procedure captures all the exposed edges.

We note that within the assumptions required by this result, stability verification amounts to checking the root-location of line segments of polynomials of the form

$$P_\lambda(s) = (1 - \lambda)P_1(s) + \lambda P_2(s), \qquad \lambda \in [0, 1]. \tag{6.17}$$

The root-locus technique can be used for this purpose. Alternatively the Segment Lemma given in Chapter 2 can also be used when the boundary of the domain Γ of interest can be parametrized easily. This theorem is the best result that one can expect at this level of generality, because as we have shown in Chapter 2 a line segment joining two stable polynomials is not necessarily stable. To reiterate, consider the following simple polytope consisting of the segment joining the two points

$$P_1(s) = 3s^4 + 3s^3 + 5s^2 + 2s + 1 \quad \text{and} \quad P_2(s) = s^4 + s^3 + 5s^2 + 2s + 5.$$

It can be checked that both $P_1(s)$ and $P_2(s)$ are Hurwitz stable and yet the polynomial

$$\frac{P_1(s) + P_2(s)}{2} \quad \text{has a root at} \quad s = j.$$

We illustrate the Edge Theorem with some examples.

6.3 EXAMPLES

Example 6.1. Consider the interval control system in Figure 6.6:

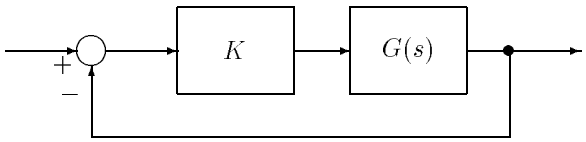

Figure 6.6. A gain feedback system (Example 6.1)

Let

$$G(s) = \frac{\delta_2 s^2 + \delta_0}{s(s^2 + \delta_1)}$$

and assume that $K = 1$. Then the characteristic polynomial of this family of systems is the interval polynomial

$$\delta(s) = s^3 + \delta_2 s^2 + \delta_1 s + \delta_0$$

where

$$\delta_2 \in [6, 8], \quad \delta_1 \in [14, 18], \quad \delta_0 \in [9.5, 10.5].$$

The three variable coefficients form a box with 12 edges in the coefficient space. By the Edge Theorem, the boundary of the root space of the interval polynomial family can be obtained by plotting the root loci along the exposed edges of the box. The root loci of the edges is shown in Figure 6.7. Since the entire root space of the set of characteristic polynomials is found to be in the LHP, the family of feedback systems is robustly stable.

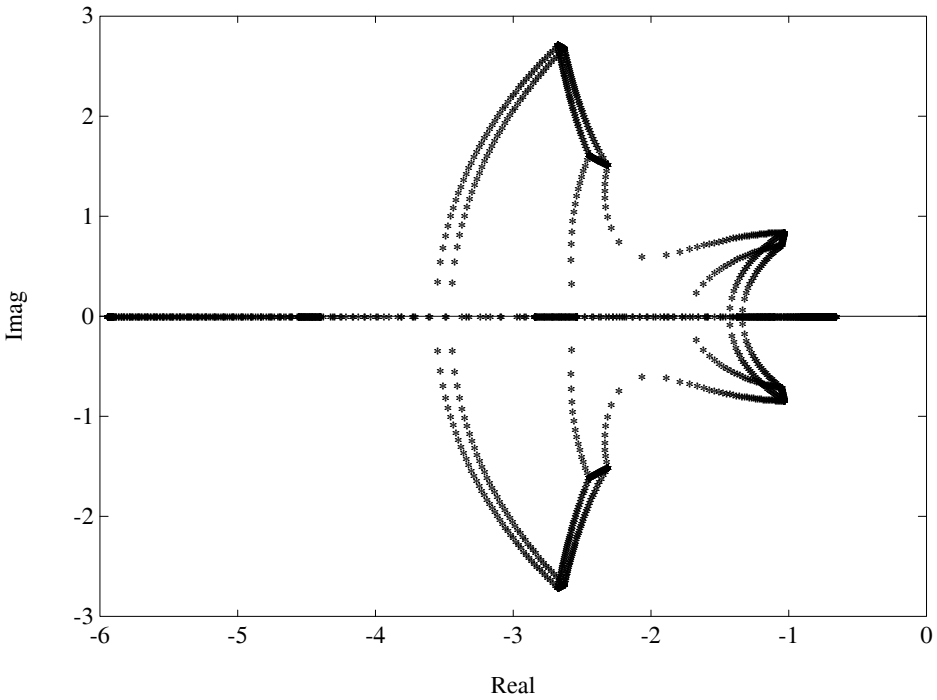

Figure 6.7. Root space for $K = 1$ (Example 6.1)

We remark that the robust stability of this system could have been checked by determining whether the Kharitonov polynomials are stable or not. However the Edge Theorem has given us considerably more information by generating the entire root set. From this set, depicted in Figure 6.7, we can evaluate the performance

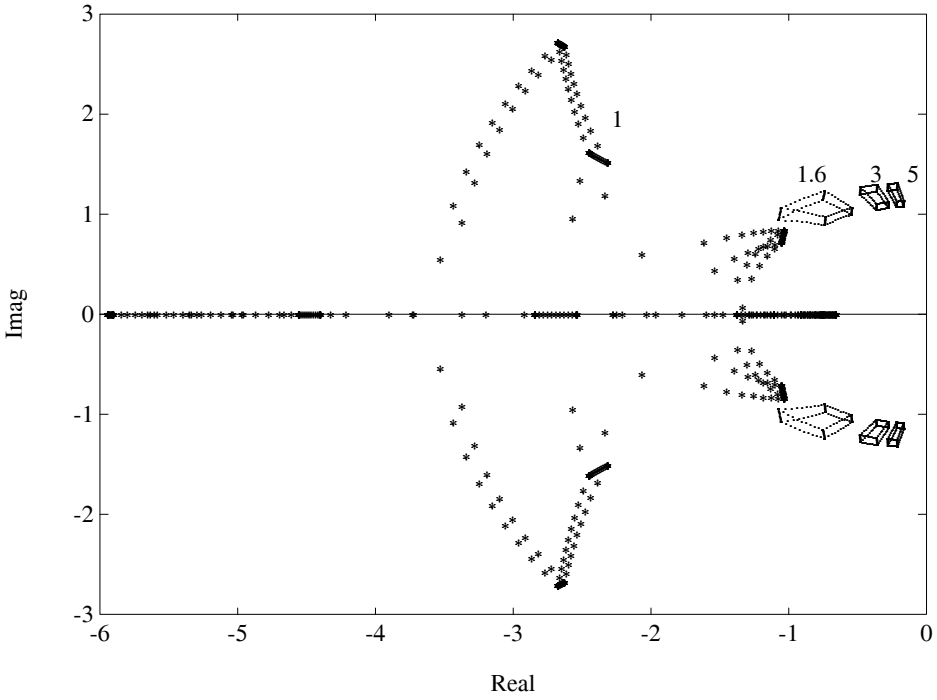

Figure 6.8. Root spaces for various K (Example 6.1)

of the system in terms of such useful quantities as the worst case damping ratio, stability degree (minimum distance of the root set to the imaginary axis), largest damped and undamped natural frequencies, etc.

The movement of the entire root space with respect to the gain K can be studied systematically by repeatedly applying the Edge Theorem for each K. Figure 6.8 shows the movement of the root space with respect to various gains K. It shows that the root space approaches the imaginary axis as the gain K approaches the value 5. The root sets of the Kharitonov polynomials are properly contained in the root space for small values of K. However as K approaches the value where the family is just about to become unstable, the roots of the Kharitonov polynomials move out to the right hand boundary of the root set. These roots are therefore the "first" set of roots of the system to cross the imaginary axis.

Example 6.2. Let us consider the unity feedback discrete time control system with forward transfer function:

$$G(z) = \frac{\delta_1 z + \delta_0}{z^2(z + \delta_2)}.$$

The characteristic polynomial is

$$\delta(z) = z^3 + \delta_2 z^2 + \delta_1 z + \delta_0.$$

Suppose that the coefficients vary in the intervals

$$\delta_2 \in [0.042, 0.158], \quad \delta_1 \in [-0.058, 0.058], \quad \delta_0 \in [-0.06, 0.056]$$

The boundary of the root space of the family can be generated by drawing the root loci along the 12 exposed edges of the box in coefficient space. The root space is inside the unit disc as shown in Figure 6.9. Hence the entire family is Schur stable.

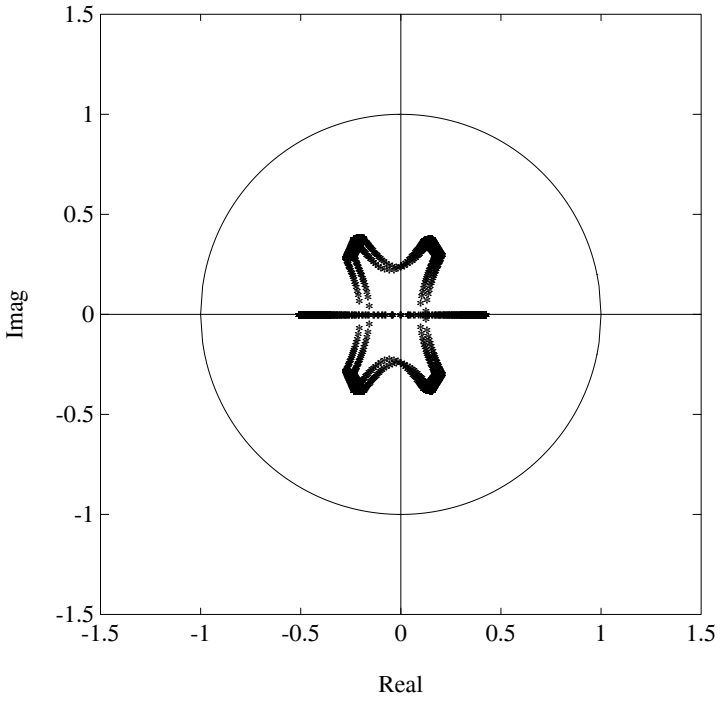

Figure 6.9. Root space of $\delta(z)$ (Example 6.2)

Example 6.3. Consider the interval plant

$$G(s) = \frac{s + a}{s^2 + bs + c}$$

where

$$a \in [1, 2], \quad b \in [9, 11], \quad c \in [15, 18].$$

The controller is

$$C(s) = \frac{3s+2}{s+5}.$$

The closed loop characteristic polynomial is

$$\begin{aligned}\delta(s) &= (s^2+bs+c)(s+5)+(s+a)(3s+2)\\ &= a(3s+2)+b(s^2+5s)+c(s+5)+(s^3+8s^2+2s).\end{aligned}$$

The boundary of the root space of $\delta(s)$ can be obtained by plotting the root loci along the 12 exposed edges. It can be seen from Figure 6.10 that the family $\delta(s)$ is stable since the root space is in the left half plane. Hence the given compensator robustly stabilizes the interval plant. From the root set generated we can evaluate the performance of the controller in terms of the worst case damping ratio, the minimum stability degree and the maximum frequency of oscillation.

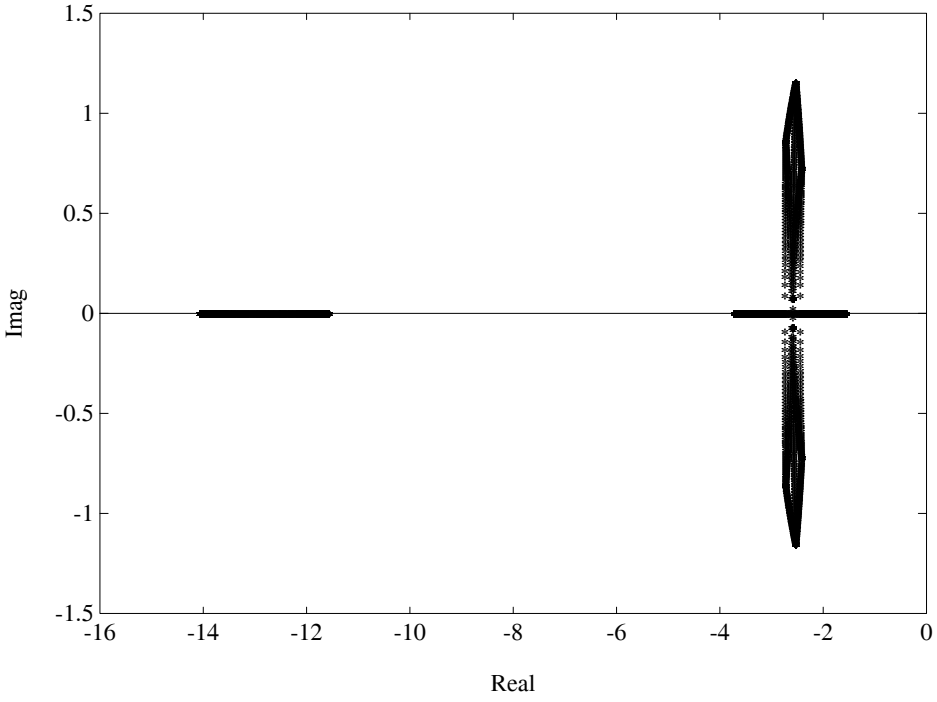

Figure 6.10. Root loci of the edges (Example 6.3)

The Edge Theorem has many useful applications. For instance, it can be effectively used to determine the coprimeness of two polytopic families of polynomials as shown in the following example.

Example 6.4. Consider the two polynomials

$$\delta_A(s) = p_0\delta_{A_0}(s) + p_1\delta_{A_1}(s) + p_2\delta_{A_2}(s)$$
$$\delta_B(s) = q_0\delta_{B_0}(s) + q_1\delta_{B_1}(s) + q_2\delta_{B_2}(s)$$

where

$$\delta_{A_0}(s) = 0.2s^4 + 2s^3 + 100s^2 + 600s + 5000$$
$$\delta_{A_1}(s) = 0.3s^4 + 8s^3 + 200s^2 + 1000s + 15000$$
$$\delta_{A_2}(s) = 0.5s^4 + 2s^3 + 115s^2 + 998s + 18194$$
$$\delta_{B_0}(s) = 0.1s^4 + 3s^3 + 50s^2 + 500s + 1000$$
$$\delta_{B_1}(s) = 0.3s^4 + 3s^3 + 50s^2 + 500s + 2000$$
$$\delta_{B_2}(s) = 0.6s^4 + 3s^3 + 88.5s^2 + 190.3s + 2229.1$$

and the nominal value of parameters $\mathbf{p}$ are

$$\mathbf{p}^0 = [p_0^0 \;\; p_1^0 \;\; p_2^0 \;\; q_0^0 \;\; q_1^0 \;\; q_2^0] = [1 \;\; 1 \;\; 1 \;\; 1 \;\; 1 \;\; 1].$$

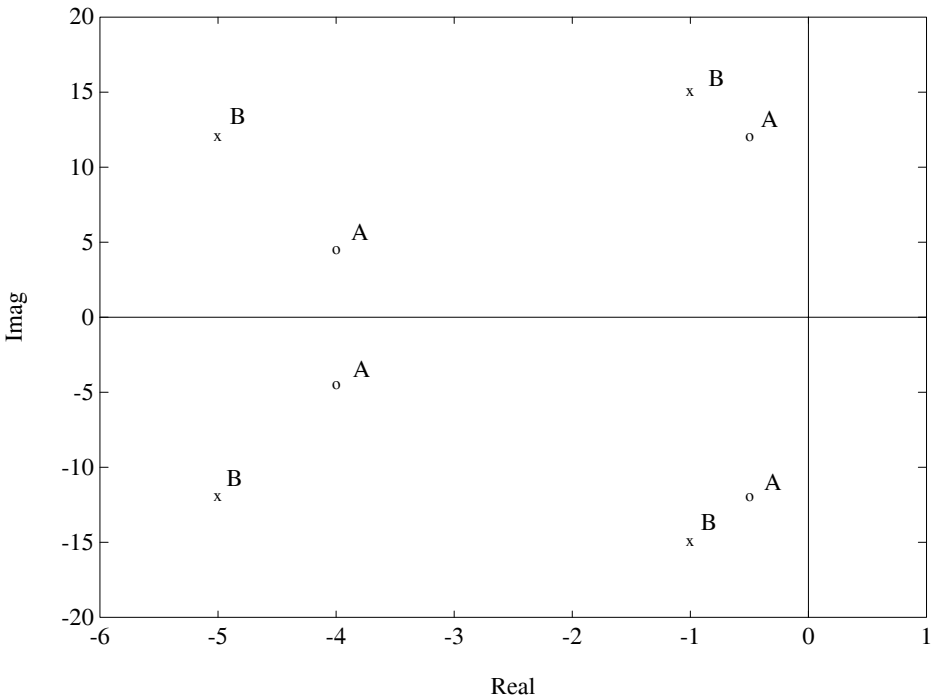

Figure 6.11. Roots of $\delta_A(s)$ and $\delta_B(s)$ (Example 6.4)

Figure 6.11 shows the roots of the two polynomials at the nominal parameter $\mathbf{p} = \mathbf{p}^0$. The roots of $\delta_A(s)$ and $\delta_B(s)$ are labeled in the figure as "A" and "B", respectively. Clearly, these two polynomials are coprime as the root sets are disjoint. Now suppose that the parameters $\mathbf{p}$ and $\mathbf{q}$ perturb in interval sets. We define perturbation boxes for the parameters $\mathbf{p}$ and $\mathbf{q}$ as follows:

$$\mathbf{\Pi}_p := \{[p_i - \omega_1\epsilon,\ p_i + \omega_1\epsilon], \quad i = 0, 1, 2\}$$
$$\mathbf{\Pi}_q := \{[q_i - \omega_2\epsilon, q_i + \omega_2\epsilon], \quad i = 0, 1, 2\}$$

where

$$[\omega_1 \ \ \omega_2] = [1 \ \ 5].$$

Suppose that we want to determine the maximum value of ϵ such that these two families of polynomials remain coprime. This can be accomplished by examining the root space for increment values of ϵ. We observe that the root spaces are touching each other at $\epsilon = 0.14$. As shown in Figure 6.12, certain polynomials in the $\delta_A(s)$ and $\delta_B(s)$ families share common roots at the "*" locations. Therefore, at this point the families cease to be coprime.

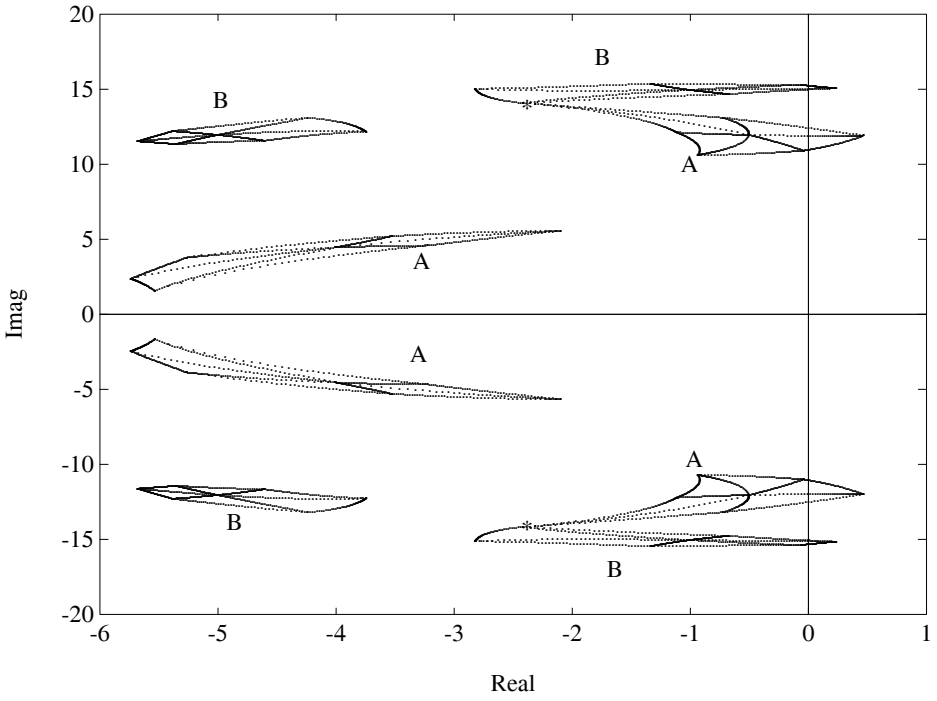

Figure 6.12. Root space of $\delta_A(s)$ and $\delta_B(s)$ for $\epsilon = 0.14$ (Example 6.4)

6.4 EXTENSIONS OF EDGE RESULTS

An important consequence of the Edge Theorem is that the stability of a polytopic family of polynomials can be ascertained from the stability of its exposed edges. This was exploited to develop robust stability tests for polytopic systems in Chapter 4. In this section we extend this stability testing property of the exposed edges to a larger family. This family consists of a polynomial function of a polytope. The results given here are analogous to the extensions of Kharitonov's Theorem to polynomial functions of interval polynomials, given in the last Chapter.

In the following we assume that an open subset $\mathcal{S}$ of the complex plane is given as the stability region, and stable will mean stability with respect to this region, unless specified otherwise. We shall also assume that all polynomial families under discussion are of constant degree.

Let

$$\mathcal{P}(s) = \left\{ a(s,\mathbf{p}) = \sum_{j=0}^{n} a_j(\mathbf{p}) s^j \ : \mathbf{p} \in \mathbf{P} \right\} \tag{6.18}$$

denote a real polytopic family of polynomials. Here $\mathbf{p} = [p_1, p_2, \cdots, p_l]$ is a real vector of uncertain parameters, $a_j(\mathbf{p})$ are linear functions of $\mathbf{p}$ and $\mathbf{P}$ is a convex polytope. We also suppose that

$$\varphi(z) = \alpha_0 + \alpha_1 z + \cdots + \alpha_m z^m, \tag{6.19}$$

is a given polynomial. We ask the question: Under what conditions is the family of polynomials

$$\varphi(\mathcal{P}(s)) = \{\varphi(a(s)) : a(s) \in \mathcal{P}(s)\} \tag{6.20}$$

stable?

Let $\mathcal{E}_{\mathcal{P}}(s)$ denote the subset of $\mathcal{P}(s)$ corresponding to the edges of $\mathcal{P}(s)$. We know that stability of the edge polynomials $\mathcal{E}_{\mathcal{P}}(s)$ implies stability of the polynomial family $\mathcal{P}(s)$. The next lemma follows from this.

Lemma 6.3 *Given the polytopic family (6.18) and a complex number z, the stability of the set of polynomials*

$$\mathcal{P}(s) - z = \{a(s) - z : a(s) \in \mathcal{P}(s)\}.$$

is implied by the stability of the family

$$\mathcal{E}_{\mathcal{P}}(s) - z = \{a(s) - z : a(s) \in \mathcal{E}_{\mathcal{P}}(s)\}.$$

Stability domains

Let us consider a one parameter family of polynomials

$$(1-\mu)a_k(s) + \mu a_j(s), \qquad \mu \in [0,1] \tag{6.21}$$

corresponding to an edge of $\mathbf{P}$. The image set of this segment at $s = j\omega$ is a complex plane line segment. As ω is swept from $-\infty$ to $+\infty$ this segment moves continuously on the complex plane and generates a "thick" curve which partitions the complex plane into a finite number of open disjoint domains. With each of these domains we associate an integer number defined as the number of roots of $a(s) - z$ in $\mathcal{S}$. This number is independent of the choice of $a(s)$ in the segment and z in the domain. There is at most one domain, Λ_{kj}, called the *stability domain* associated with $a_k(s)$ for which the integer number is equal to $n = \deg(a_k)$. With every element of $\mathcal{E}_{\mathcal{P}}(s)$ we associate such a stability domain Λ_{kj} of the complex plane and let Λ be the intersection of these domains:

$$\Lambda = \cap \Lambda_{kj}. \tag{6.22}$$

We will say that a polynomial is Λ-stable if all its roots lie in Λ. Then we have the following result.

Theorem 6.2 *Let $\Lambda \neq \emptyset$. Then the family (6.20) is stable if and only if $\varphi(z)$ is Λ-stable.*

Proof.
Sufficiency: The polynomial $\varphi(z)$ is Λ-stable, and so the roots $z_1, z_2, \cdots, z_m$ of $\varphi(z)$ lie in Λ. Now, stability of $\varphi(\mathcal{P}(s))$ is equivalent to stability of $\mathcal{P}(s) - z_j$, $j = 1, 2, \cdots, m$. By Lemma 6.3 stability of $\mathcal{P}(s) - z_j$ follows from the stability of the set $\mathcal{E}_{\mathcal{P}}(s) - z_j$. But the condition $z_j \in \Lambda$ guarantees stability of each of the sets $\mathcal{E}_{\mathcal{P}}(s) - z_j$, $j = 1, 2, \cdots, m$.
Necessity: Stability of $\varphi(\mathcal{P}(s))$ implies the stability of $\mathcal{P}(s) - z_j$, $j = 1, 2, \cdots, m$. By Lemma 6.3 the family $\mathcal{P}(s) - z_j$ is stable only if $\mathcal{E}_{\mathcal{P}}(s) - z_j$ is stable. This implies that $z_j \in \Lambda$, or $\varphi(z)$ is Λ-stable. ♣

This theorem can be given in the equivalent and more useful form.

Theorem 6.3 *The polynomial family $\varphi(\mathcal{P}(s))$ is stable if and only if the family*

$$\varphi\left(\mathcal{E}_{\mathcal{P}}(s)\right) = \{\varphi\left(a(s)\right) : a(s) \in \mathcal{E}_{\mathcal{P}}(s)\}$$

corresponding to the edges of $\mathcal{P}(s)$, is stable.

The proof of this result follows immediately from Theorem 6.2 and Lemma 6.3 and is left to the reader. The result is an extension of the stability testing property of exposed edges to a case where the uncertain parameters appear *nonlinearly* in the family.

We considered thus far that the polynomial $\varphi(z)$ is fixed. Now suppose that $\varphi(z)$ is an uncertain polynomial, and in particular belongs to a polytope. Let

$$\Phi(z) := \{\varphi(z) : (\alpha_0, \alpha_1, \alpha_2, \cdots, \alpha_m) \in \mathbf{\Delta}\} \tag{6.23}$$

where $\mathbf{\Delta}$ is a convex polytope. We are interested in determining conditions under which the polynomial family

$$\Phi(\mathcal{P}(s)) = \{\varphi(a(s)) : a(s) \in \mathcal{P}(s), \quad \varphi(z) \in \Phi(z)\} \tag{6.24}$$

is stable?

The uncertain parameters in the polynomial family (6.24) are the vector $\mathbf{p}$ which varies in $\mathbf{P}$ and enters the coefficients nonlinearly, and the parameters α_i which vary in $\mathbf{\Delta}$ and enter the coefficients linearly.

Theorem 6.4 *Let $\Lambda \neq \emptyset$. Then the family $\Phi(\mathcal{P}(s))$ is stable if and only if $\Phi(z)$ is Λ-stable.*

Proof. The result follows from Theorem 6.2 and the representation

$$\Phi(\mathcal{P}(s)) = \{\varphi(\mathcal{P}(s)) : \varphi(z) \in \Phi(z)\}.$$

♣

By applying Theorem 6.3 to the above result we immediately have the following.

Theorem 6.5 *The family $\Phi(\mathcal{P}(s))$ is stable if and only if $\Phi(\mathcal{E}_{\mathcal{P}}(z))$ is Λ-stable.*

For each fixed polynomial $a(s)$ in $\mathcal{E}_{\mathcal{P}}(s)$ $\Phi(a(s)$ is a polytopic family and therefore its stability can be found by testing its edges. This leads to the next result.

Theorem 6.6 *The family of polynomials $\Phi(\mathcal{P}(s))$ is stable if and only if each two parameter family of polynomials in $\mathcal{E}_{\Phi}(\mathcal{E}_{\mathcal{P}}(s))$ is stable.*

The set $\mathcal{E}_{\Phi}(\mathcal{E}_{\mathcal{P}}(s))$ consists of a finite number of two parameter families corresponding to pairs of edges of $\mathbf{P}$ and $\mathbf{\Delta}$. Let

$$(1-\mu)a_k(s) + \mu a_j(s), \qquad \mu \in [0.1] \tag{6.25}$$

correspond to an edge of $\mathbf{P}$ and let

$$(1-\nu)\varphi_u(z) + \nu\varphi_v(z), \qquad \nu \in [0.1] \tag{6.26}$$

correspond to an edge of $\mathbf{\Delta}$. Then the family

$$(1-\nu)\varphi_u\left((1-\mu)a_k(s) + \mu a_j(s)\right) + \nu\varphi_v\left((1-\mu)a_k(s) + \mu a_j(s)\right) \tag{6.27}$$

where $(\mu, \nu) \in [0,1] \times [0,1]$, is a typical element of $\mathcal{E}_{\Phi}(\mathcal{E}_{\mathcal{P}}(s))$.

Theorem 6.6 is a generalization of the stability testing property of edges to this new class of polynomial families, containing both linear and nonlinear dependency on uncertain parameters. It shows that the problem is effectively reduced to a set of two-parameter multilinear problems, or double-edge problems.

6.4.1 Maximizing the Uncertainty Set

The above results can be used to determine maximal nondestabilizing perturbations. We will consider the situation when $\mathcal{P}(s)$ or $\Phi(z)$ are polytopes of fixed shape but

variable size. We start with the case when Φ is a single polynomial $\varphi(z)$, but $\mathcal{P}$ is a polytope of variable size defined by

$$\mathbf{P}(r) = \left\{\mathbf{p} : \mathbf{p} - \mathbf{p}^0 \in r\mathcal{B}\right\}$$

where $\mathcal{B}$ is a convex polytope containing the origin. Let

$$\mathcal{P}_r(s) = \{a(s,\mathbf{p}) : \mathbf{p} \in \mathbf{P}(r)\}$$

and consider the Hurwitz stability of $\varphi\left(\mathcal{P}_r(s)\right)$. We let $a^0(s) := a(s,\mathbf{p}^0)$ and assume that $\varphi\left(a^0(s)\right)$ is stable. Our objective is to find the smallest positive r_0 such that $\varphi\left(\mathcal{P}_{r_0}(s)\right)$ is not stable. This r_0 determines the limit on how much we may enlarge the polytope $\mathbf{P}(r)$ without losing stability.

Theorem 6.3 can be applied to determine r_0. A typical edge of the family $\varphi\left(\mathcal{E}_{\mathcal{P}_r}(s)\right)$ is of the form

$$\varphi\left(a^0(s) + r(1-\mu)a^k(s) + r\mu a^j(s)\right), \qquad \mu \in [0,1]. \tag{6.28}$$

Denote by r_{kj} the smallest positive value of r such that the family (6.28) is not stable. For each such element of the set $\varphi\left(\mathcal{E}_{\mathcal{P}_r}(s)\right)$ we can find a corresponding r_{kj}. Let

$$r_0 = \min\left\{r_{kj}\right\}$$

where the minimum is taken over all elements of $\varphi\left(\mathcal{E}_{\mathcal{P}_r}(s)\right)$.

Theorem 6.7 *Let the polynomial $\varphi\left(a^0(s)\right)$ be stable. Then $\varphi\left(\mathcal{P}_r(s)\right)$ is stable if and only if $r < r_0$.*

This idea can also be applied to the case when $\varphi(z)$ is not fixed but lies in $\Phi(z)$. The problem is now to determine the smallest r such that the family $\Phi(\mathcal{P}_r(s))$ is unstable. We assume that the family $\Phi\left(a^0(s)\right)$ is stable. From Theorem 6.6 we see that we have to check the stability of elements of the set $\mathcal{E}_\Phi\left(\mathcal{E}_{\mathcal{P}_r}(s)\right)$ which consists of polynomials of the type

$$\begin{aligned}(1-\nu)\varphi_l\left(a^0(s) + r(1-\nu)a^k(s) + r\mu a^j(s)\right)\\ +\nu\varphi_m\left(a^0(s) + r(1-\mu)a^k(s) + r\mu a^j(s)\right)\end{aligned} \tag{6.29}$$

where $(\mu,\nu) \in [0,1]\times[0,1]$. Denote by r_{kj}^{lm} the smallest value of r such that (6.29) is not stable. This may be defined for every element of $\mathcal{E}_\Phi\left(\mathcal{E}_{\mathcal{P}_r}(s)\right)$.

Theorem 6.8 *Let the family $\Phi\left(a^0(s)\right)$ be stable. Then $\Phi(\mathcal{P}_r(s))$ is stable if and only if*

$$r < \min\left\{r_{kj}^{lm}\right\}$$

where the minimum is taken over all families from $\mathcal{E}_\Phi\left(\mathcal{E}_{\mathcal{P}_r}(s)\right)$.

For each value of r the two uncertain parameters (μ,ν) in (6.29) appear multilinearly. Such two-parameter multilinear problems can be solved analytically and are also effectively dealt with using the Mapping Theorem in Chapter 11.

6.5 EXERCISES

6.1 Using the Edge Theorem, check the robust Hurwitz stability of the following family of polynomials. Also show the root cluster of the family.

$$\delta(s) := s^3 + (a+3b)s^2 + cs + d$$

where $a \in [1,2]$, $b \in [0,3]$, $c \in [10,15]$ and $d \in [9,14]$.

6.2 Consider the plant $G(s)$ and the controller $C(s)$

$$G(s) := \frac{s+1}{s^2 - s - 1} \qquad C(s) := \frac{as+b}{s+c}.$$

First, choose the controller parameter $\{a^0, b^0, c^0\}$ so that the closed loop system has its characteristic roots at

$$-1 \pm j1 \quad \text{and} \quad -10.$$

Now for

$$a \in \left[a^0 - \frac{\epsilon}{2}, a^0 + \frac{\epsilon}{2}\right], \quad b \in \left[b^0 - \frac{\epsilon}{2}, b^0 + \frac{\epsilon}{2}\right], \quad c \in \left[c^0 - \frac{\epsilon}{2}, c^0 + \frac{\epsilon}{2}\right]$$

find the maximum value $\epsilon_{\max}$ of ϵ that robustly maintains closed loop stability. Find the root set of the system when the parameters range over a box with sides $\frac{\epsilon_{\max}}{2}$.

6.3 Repeat Exercise 6.2 with the additional requirement that the dominant pair of roots remain inside circles of radii 0.5 centered at $-1 \pm j1$.

6.4 Consider the discrete time plant $G(z)$ and the controller $C(z)$

$$G(z) := \frac{z-1}{z^2 + 2z + 3}, \qquad C(z) := \frac{az+b}{z+c}$$

Choose the controller parameter $\{a^0, b^0, c^0\}$ so that deadbeat control is achieved, namely all the closed loop poles are placed at $z = 0$. Use the Edge Theorem, find the maximum range of the controller parameters so that the closed loop poles remain inside the circle of radius 0.5 centered at the origin. Assume that the controller parameters are bounded by the same amount, i.e.,

$$a \in [a^0 - \epsilon, a^0 + \epsilon], \qquad b \in [b^0 - \epsilon, b^0 + \epsilon], \qquad c \in [c^0 - \epsilon, c^0 + \epsilon].$$

Find the root set of the system for the parameters $\{a, b, c\}$ varying in a box

$$a \in \left[a^0 - \frac{\epsilon}{2}, a^0 + \frac{\epsilon}{2}\right], \qquad b \in \left[b^0 - \frac{\epsilon}{2}, b^0 + \frac{\epsilon}{2}\right], \qquad c \in \left[c^0 - \frac{\epsilon}{2}, c^0 + \frac{\epsilon}{2}\right].$$

6.5 Consider the polynomials

$$s^2 + a_1 s + a_0 \qquad \text{and} \qquad s^2 + b_1 s + b_0$$

where

$$\left[a_1^0, a_0^0\right] = [2, 2], \quad \left[b_1^0, b_0^0\right] = [4, 8].$$

Now find the maximum value $\epsilon_{\max}$ of ϵ so that the families remain coprime as $[a_1, a_0]$ varies over the box $[a_1^0 - \epsilon, a_1^0 + \epsilon] \times [a_0^0 - \epsilon, a_0^0 + \epsilon]$ and b varies independently over the box $[b_1^0 - \epsilon, b_1^0 + \epsilon] \times [b_0^0 - \epsilon, b_0^0 + \epsilon]$.

6.6 Repeat Exercise 6.5, this time verifying coprimeness over the right half plane.

6.7 Consider a unity feedback system with the plant $G(s)$ and $C(s)$ given as

$$G(s) = \frac{s + b_0}{s^2 + a_1 s + a_0} \quad \text{and} \quad C(s) = \frac{s+1}{s+2}.$$

Assume that the plant parameters vary independently as:

$$a_0 \in [2, 4], \quad a_1 \in [2, 4], \quad b_0 \in [1, 3].$$

Determine the root space of the family of closed loop polynomials using the Edge Theorem.

6.8 Consider the two polynomials

$$A(s) = a_2 s^2 + a_1 s + a_0$$
$$B(s) = b_3 s^3 + b_2 s^2 + b_1 s + b_0$$

where the nominal values of the parameters are

$$a_0^0 = 2, \quad a_1 = 2, \quad a_2 = 1, \quad b_0 = 2.5, \quad b_1 = 7, \quad b_2 = 4.5, \quad b_3 = 1.$$

Suppose the parameter perturbations are:

$$a_i \in [a_i^0 - \epsilon, a_i^0 + \epsilon], \qquad i = 0, 1, 2$$
$$b_j \in [b_j^0 - \epsilon, b_j^0 + \epsilon], \qquad j = 0, 1, 2, 3.$$

Find the maximum value of ϵ for which the two polynomial sets remain coprime.
Answer: $\epsilon_{\max} = 0.25$

6.9 Let

$$A(s) = a_3 s_3^3 + a_2 s^2 + a_1 s + a_0$$
$$B(s) = b_3 s^3 + b_2 s^2 + b_1 s + b_0$$

and

$$\left[a_0^0, a_1^0, a_2^0, a_3^0, b_0^0, b_1^0, b_2^0, b_3^0\right] = [100, 100, 10, 3, 1, 3, 3, 3].$$

Assume that all the coefficients of the above two polynomials are allowed to perturb independently. Find the maximum value of ϵ so that the two polynomial families remain coprime when

$$\begin{aligned} a_i &\in \left[a_i^0 - \epsilon, a_i^0 + \epsilon\right], \qquad i = 0, 1, 2, 3 \\ b_j &\in \left[b_j^0 - \epsilon, b_j^0 + \epsilon\right], \qquad j = 0, 1, 2, 3. \end{aligned}$$

Answer: $\epsilon_{\max} = 0.525$

6.10 Repeat Exercise 6.9 with the requirement that the families remain coprime over the right half of the complex plane.

6.11 Consider the polytopic family $\mathcal{P}(s)$ consisting of polynomials $a(s)$:

$$a(s) = s^2 + (p_1 + p_2)s + p_1 : \quad p_1 \in [2, 4], p_2 \in [3, 7].$$

Let

$$\varphi(z) = z^2 + \alpha_1 z + \alpha_0$$

with $\alpha_1 = 3$, $\alpha_0 = 4$. Determine the Hurwitz stability of the family $\varphi(\mathcal{P}(s))$.

6.12 In Exercise 6.11 suppose that $\varphi(z)$ belongs to the family $\Phi(z)$ defined as

$$\Phi(z) = \left\{\varphi(z) = z^2 + \alpha_1 z + \alpha_0 : \alpha_1 \in [2, 4], \alpha_0 \in [3, 5]\right\}.$$

Determine the Hurwitz stability of the family $\Phi(\mathcal{P}(s))$.

6.13 Consider the polynomial $s^2 + a_1 s + a_0$ and let the coefficients (a_1, a_0) vary in the convex hull of the points

$$(0, 0), \quad (0, R), \quad (R^2, 0), \quad (R^2, 2R).$$

Show that the root space of this set is the intersection with the left half plane of the circle of radius R centered at the origin. Describe also the root space of the convex hull of the points

$$(0, 0), \quad (0, 2R), \quad (R^2, 0), \quad (R^2, 2R).$$

6.6 NOTES AND REFERENCES

The Edge Theorem is due to Bartlett, Hollot and Lin [21]. We note that the weaker and more obvious result in Corollary 6.1, that is, the stability detecting property of the exposed edges, is often referred to, loosely, in the literature as

the Edge Theorem. In fact as we have seen in Chapter 4, Corollary 6.1 applies to complex polytopic polynomial and quasipolynomial families. However, the root space boundary generating property does not necessarily hold in these more general situations. The extensions of the stability testing property of edges to polynomial functions of polytopes, reported in Section 6.4 are due to Kharitonov [146].

Chapter 7

THE GENERALIZED KHARITONOV THEOREM

In this chapter we study the Hurwitz stability of a family of polynomials which consists of a linear combination, with fixed polynomial coefficients, of interval polynomials. The Generalized Kharitonov Theorem given here provides a constructive solution to this problem by reducing it to the Hurwitz stability of a prescribed set of extremal line segments. The number of line segments in this test set is independent of the dimension of the parameter space. Under special conditions on the fixed polynomials this test set reduces to a set of vertex polynomials. This test set has many important extremal properties that are useful in control systems. These are developed in the subsequent chapters.

7.1 INTRODUCTION

In attempting to apply Kharitonov's Theorem directly to control systems we encounter a certain degree of conservatism. This is mainly due to the fact that the characteristic polynomial coefficients perturb interdependently, whereas a crucial assumption in Kharitonov's Theorem is that the coefficients of the characteristic polynomial vary *independently*. For example, in a typical situation, the closed loop characteristic polynomial coefficients may vary only through the perturbation of the plant parameters while the controller parameters remain fixed. We show by an example the precise nature of the conservativeness of Kharitonov's Theorem when faced by this problem.

Example 7.1. Consider the plant:

$$G(s) = \frac{n^p(s)}{d^p(s)} = \frac{s}{1 - s + \alpha s^2 + s^3}, \text{ where } \alpha \in [3.4, 5],$$

and has a nominal value

$$\alpha^0 = 4.$$

It is easy to check that the controller $C(s) = \dfrac{3}{s+1}$ stabilizes the nominal plant, yielding the nominal closed-loop characteristic polynomial,

$$\delta_4(s) = 1 + 3s + 3s^2 + 5s^3 + s^4.$$

To determine whether $C(s)$ also stabilizes the family of perturbed plants we observe that the characteristic polynomial of the system is

$$\delta_\alpha(s) = 1 + 3s + (\alpha - 1)s^2 + (\alpha + 1)s^3 + s^4.$$

In the space $(\delta_2,\ \delta_3)$, the coefficients of s^2 and s^3 describe the segment $[R_1, R_2]$ shown in Figure 7.1.

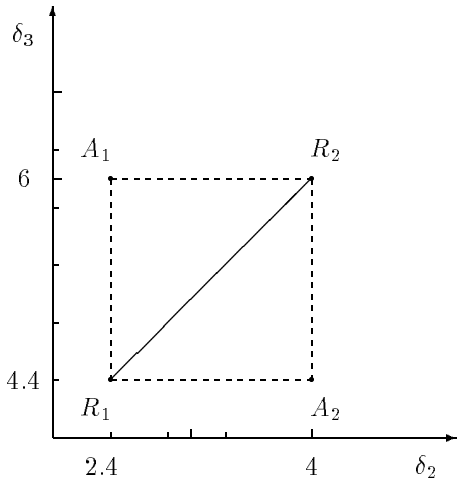

Figure 7.1. A box in parameter space is transformed into a segment in coefficient space (Example 7.1)

The only way to apply Kharitonov's theorem here is to enclose this segment in the box $\mathcal{B}$ defined by the two 'real' points R_1 and R_2 and two 'artificial' points A_1 and A_2 and to check the stability of the Kharitonov polynomials which correspond to the characteristic polynomial evaluated at the four corners of $\mathcal{B}$. But

$$\delta_{A_1}(s) = 1 + 3s + 2.4s^2 + 6s^3 + s^4,$$

is unstable because its third Hurwitz determinant H_3 is

$$H_3 = \begin{vmatrix} 6 & 3 & 0 \\ 1 & 2.4 & 1 \\ 0 & 6 & 3 \end{vmatrix} = -1.8 < 0.$$

Therefore, using Kharitonov's theorem here does not allow us to conclude the stability of the entire family of closed-loop systems. And yet, if one checks the values of the Hurwitz determinants along the segment $[R_1,\ R_2]$ one finds

$$H = \begin{vmatrix} 1+\alpha & 3 & 0 & 0 \\ 1 & \alpha-1 & 1 & 0 \\ 0 & 1+\alpha & 3 & 0 \\ 0 & 1 & \alpha-1 & 1 \end{vmatrix}$$

and

$$\begin{cases} H_1 &= 1+\alpha \\ H_2 &= \alpha^2-4 \\ H_3 &= 2\alpha^2-2\alpha-13 \\ H_4 &= H_3 \end{cases} \quad \text{all positive for } \alpha \in [3.4, 5].$$

This example demonstrates that Kharitonov's theorem provides only sufficient conditions which may sometimes be too conservative for control problems.

An alternative that we have in this type of situation is to apply the Edge Theorem of Chapter 6, since the parameters of the plant are within a box, which is, of course, a particular case of a polytope. However, we shall see that the solution given by the Edge Theorem, in general, requires us to carry out many redundant checks. Moreover, the Edge Theorem is not a generalization of Kharitonov's Theorem. An appropriate generalization of Kharitonov's Theorem would be expected to produce a test set that would enjoy the economy and optimality of the Kharitonov polynomials, without any unnecessary conservatism.

Motivated by these considerations, we formulate the problem of generalizing Kharitonov's Theorem in the next section. Before proceeding to the main results, we introduce some notation and notational conventions with a view towards streamlining the presentation.

7.2 PROBLEM FORMULATION AND NOTATION

We will be dealing with polynomials of the form

$$\delta(s) = F_1(s)P_1(s) + F_2(s)P_2(s) + \cdots + F_m(s)P_m(s). \tag{7.1}$$

Write

$$\underline{F}(s) := (F_1(s), F_2(s), \cdots, F_m(s)) \tag{7.2}$$

$$\underline{P}(s) := (P_1(s), P_2(s), \cdots, P_m(s)) \tag{7.3}$$

and introduce the notation

$$< \underline{F}(s), \underline{P}(s) >:= F_1(s)P_1(s) + F_2(s)P_2(s) + \cdots + F_m(s)P_m(s). \tag{7.4}$$

We will say that $\underline{F}(s)$ *stabilizes* $\underline{P}(s)$ if $\delta(s) =< \underline{F}(s), \underline{P}(s) >$ is *Hurwitz stable*. Note that throughout this chapter, stable will mean Hurwitz stable, unless otherwise stated.

The polynomials $F_i(s)$ are assumed to be fixed real polynomials whereas $P_i(s)$ are real polynomials with coefficients varying independently in prescribed intervals. An extension of the results to the case where $F_i(s)$ are complex polynomials or quasipolynomials will also be given in a later section.

Let $d^o(P_i)$ be the degree of $P_i(s)$

$$P_i(s) := p_{i,0} + p_{i,1}s + \cdots + p_{i,d^o(P_i)}s^{d^o(P_i)}. \tag{7.5}$$

and

$$\mathbf{p}_i := [p_{i,0}, p_{i,1}, \cdots, p_{i,d^o(P_i)}]. \tag{7.6}$$

Let $\underline{n} = [1, 2, \cdots, n]$. Each $P_i(s)$ belongs to an interval family $\mathbf{P}_i(s)$ specified by the intervals

$$p_{i,j} \in [\alpha_{i,j}, \beta_{i,j}] \quad i \in \underline{m} \quad j = 0, \cdots, d^o(P_i). \tag{7.7}$$

The corresponding parameter box is

$$\mathbf{\Pi}_i := \{\mathbf{p}_i : \alpha_{i,j} \leq p_{i,j} \leq \beta_{i,j}, \quad j = 0, 1, \cdots, d^o(P_i)\}. \tag{7.8}$$

Write $\underline{P}(s) := [P_1(s), \cdots P_m(s)]$ and introduce the family of m-tuples

$$\mathbf{P}(s) := \mathbf{P}_1(s) \times \mathbf{P}_2(s) \times \cdots \times \mathbf{P}_m(s). \tag{7.9}$$

Let

$$\mathbf{p} := [\mathbf{p}_1, \mathbf{p}_2, \cdots, \mathbf{p}_m] \tag{7.10}$$

denote the global parameter vector and let

$$\mathbf{\Pi} := \mathbf{\Pi}_1 \times \mathbf{\Pi}_2 \times \cdots \times \mathbf{\Pi}_m \tag{7.11}$$

denote the global parameter uncertainty set. Now let us consider the polynomial (7.1) and rewrite it as $\delta(s, \mathbf{p})$ or $\delta(s, \underline{P}(s))$ to emphasize its dependence on the parameter vector $\mathbf{p}$ or the m-tuple $\underline{P}(s)$. We are interested in determining the Hurwitz stability of the set of polynomials

$$\begin{aligned} \mathbf{\Delta}(s) &:= \{\delta(s, \mathbf{p}) : \mathbf{p} \in \mathbf{\Pi}\} \\ &= \{< \underline{F}(s), \underline{P}(s) >: \underline{P}(s) \in \mathbf{P}(s)\}. \end{aligned} \tag{7.12}$$

We call this a *linear interval polynomial* and adopt the convention

$$\mathbf{\Delta}(s) = F_1(s)\mathbf{P}_1(s) + F_2(s)\mathbf{P}_2(s) + \cdots + F_m(s)\mathbf{P}_m(s). \tag{7.13}$$

We shall make the following standing assumptions about this family.

Assumption 7.1.

a1) Elements of $\mathbf{p}$ perturb independently of each other. Equivalently, $\mathbf{\Pi}$ is an axis parallel rectangular box.

a2) Every polynomial in $\mathbf{\Delta}(s)$ is of the same degree.

The above assumptions will allow us to use the usual results such as the Boundary Crossing Theorem (Chapter 1) and the Edge Theorem (Chapter 6) to develop the solution. It is also justified from a control system viewpoint where loss of the degree of the characteristic polynomial also implies loss of bounded-input bounded-output stability. Henceforth we will say that $\mathbf{\Delta}(s)$ *is stable if every polynomial in* $\mathbf{\Delta}(s)$ *is Hurwitz stable.* An equivalent statement is that $\underline{F}(s)$ *stabilizes every* $\underline{P}(s) \in \mathbf{P}(s)$.

The solution developed below constructs an extremal set of line segments $\mathbf{\Delta}_{\mathrm{E}}(s) \subset \mathbf{\Delta}(s)$ with the property that the stability of $\mathbf{\Delta}_{\mathrm{E}}(s)$ implies stability of $\mathbf{\Delta}(s)$. This solution is constructive because the stability of $\mathbf{\Delta}_{\mathrm{E}}(s)$ can be checked, for instance by a set of root locus problems. The solution will be efficient since the number of elements of $\mathbf{\Delta}_{\mathrm{E}}(s)$ will be independent of the dimension of the parameter space $\mathbf{\Pi}$. The extremal subset $\mathbf{\Delta}_{\mathrm{E}}(s)$ will be generated by first constructing an extremal subset $\mathbf{P}_{\mathrm{E}}(s)$ of the m-tuple family $\mathbf{P}(s)$. The extremal subset $\mathbf{P}_{\mathrm{E}}(s)$ is constructed from the Kharitonov polynomials of $\mathbf{P}_i(s)$. We describe the construction of $\mathbf{\Delta}_{\mathrm{E}}(s)$ next.

Construction of the Extremal Subset

The Kharitonov polynomials corresponding to each $\mathbf{P}_i(s)$ are

$$\begin{aligned}
K_i^1(s) &= \alpha_{i,0} + \alpha_{i,1}s + \beta_{i,2}s^2 + \beta_{i,3}s^3 + \cdots \\
K_i^2(s) &= \alpha_{i,0} + \beta_{i,1}s + \beta_{i,2}s^2 + \alpha_{i,3}s^3 + \cdots \\
K_i^3(s) &= \beta_{i,0} + \alpha_{i,1}s + \alpha_{i,2}s^2 + \beta_{i,3}s^3 + \cdots \\
K_i^4(s) &= \beta_{i,0} + \beta_{i,1}s + \alpha_{i,2}s^2 + \alpha_{i,3}s^3 + \cdots
\end{aligned}$$

and we denote them as:

$$\mathcal{K}_i(s) := \{K_i^1(s), K_i^2(s), K_i^3(s), K_i^4(s)\}. \tag{7.14}$$

For each $\mathbf{P}_i(s)$ we introduce 4 line segments joining pairs of Kharitonov polynomials as defined below:

$$\mathcal{S}_i(s) := \left\{[K_i^1(s), K_i^2(s)], [K_i^1(s), K_i^3(s)], [K_i^2(s), K_i^4(s)], [K_i^3(s), K_i^4(s)]\right\}. \tag{7.15}$$

These four segments are called *Kharitonov segments.* They are illustrated in Figure 7.2 for the case of a polynomial of degree 2.

For each $l \in \{1, \cdots, m\}$ let us define

$$\mathbf{P}_{\mathrm{E}}^l(s) := \mathcal{K}_1(s) \times \cdots \times \mathcal{K}_{l-1}(s) \times \mathcal{S}_l(s) \times \mathcal{K}_{l+1}(s) \times \cdots \times \mathcal{K}_m(s). \tag{7.16}$$

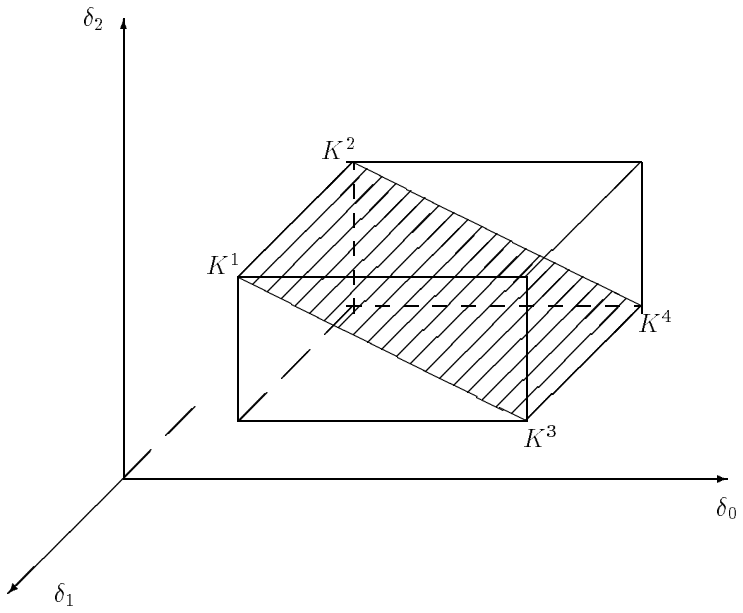

Figure 7.2. The four Kharitonov segments

A typical element of $\mathbf{P}_{\mathrm{E}}^{l}(s)$ is

$$\left(K_1^{j_1}(s), K_2^{j_2}(s), \cdots, K_{l-1}^{j_{l-1}}(s), (1-\lambda)K_l^1(s) + \lambda K_l^2(s), K_{l+1}^{j_{l+1}}(s), \cdots, K_m^{j_m}(s)\right) \tag{7.17}$$

with $\lambda \in [0,1]$. This can be rewritten as

$$\begin{aligned}(1-\lambda)&\left(K_1^{j_1}(s), K_2^{j_2}(s), \cdots, K_{l-1}^{j_{l-1}}(s), K_l^1(s), K_{l+1}^{j_{l+1}}(s), \cdots, K_m^{j_m}(s)\right)\\ &+\lambda\left(K_1^{j_1}(s), K_2^{j_2}(s), \cdots, K_{l-1}^{j_{l-1}}(s), K_l^2(s), K_{l+1}^{j_{l+1}}(s), \cdots, K_m^{j_m}(s)\right).\end{aligned} \tag{7.18}$$

Corresponding to the m-tuple $\mathbf{P}_{\mathrm{E}}^{l}(s)$, introduce the polynomial family

$$\mathbf{\Delta}_{\mathrm{E}}^{l}(s) := \{< \underline{F}(s), \underline{P}(s) >: \underline{P}(s) \in \mathbf{P}_{\mathrm{E}}^{l}(s)\}. \tag{7.19}$$

The set $\mathbf{\Delta}_{\mathrm{E}}^{l}(s)$ is also described as

$$\begin{aligned}\mathbf{\Delta}_{\mathrm{E}}^{l}(s) = F_1(s)\mathcal{K}_1(s) + \cdots + F_{l-1}(s)\mathcal{K}_{l-1}(s) + F_l(s)\mathcal{S}_l(s) + F_{l+1}(s)\mathcal{K}_{l+1}(s) +\\ \cdots + F_m(s)\mathcal{K}_m(s).\end{aligned} \tag{7.20}$$

A typical element of $\mathbf{\Delta}_{\mathrm{E}}^{l}(s)$ is the line segment of polynomials

$$F_1(s)K_1^{j_1}(s)+F_2(s)K_2^{j_2}(s)+\cdots+F_{l-1}(s)K_{l-1}^{j_{l-1}}(s)+F_l(s)\left[(1-\lambda)K_l^1(s)+\lambda K_l^2(s)\right]$$
$$+F_{l+1}(s)K_{l+1}^{j_{l+1}}(s)+\cdots+F_m(s)K_m^{j_m}(s) \tag{7.21}$$

with $\lambda \in [0,1]$.

The *extremal subset* of $\mathbf{P}(s)$ is defined by

$$\mathbf{P}_{\rm E}(s) := \cup_{l=1}^m \mathbf{P}_{\rm E}^l(s). \tag{7.22}$$

The corresponding *generalized Kharitonov segment* polynomials are

$$\begin{aligned}\mathbf{\Delta}_{\rm E}(s) &:= \cup_{l=1}^m \mathbf{\Delta}_{\rm E}^l(s)\\ &= \{< \underline{F}(s), \underline{P}(s) > :\ \underline{P}(s) \in \mathbf{P}_{\rm E}(s)\}.\end{aligned} \tag{7.23}$$

The set of m-tuples of Kharitonov polynomials are denoted $\mathbf{P}_{\rm K}(s)$ and referred to as the *Kharitonov vertices* of $\mathbf{P}(s)$:

$$\mathbf{P}_{\rm K}(s) := \mathcal{K}_1(s)\mathrm{x}\mathcal{K}_2(s)\mathrm{x}\cdots\mathrm{x}\mathcal{K}_m(s) \subset \mathbf{P}_{\rm E}(s). \tag{7.24}$$

The corresponding set of *Kharitonov vertex* polynomials is

$$\mathbf{\Delta}_{\rm K}(s) := \{< \underline{F}(s), \underline{P}(s) > :\ \underline{P}(s) \in \mathbf{P}_{\rm K}(s)\}. \tag{7.25}$$

A typical element of $\mathbf{\Delta}_{\rm K}(s)$ is

$$F_1(s)K_1^{j_1}(s)+F_2(s)K_2^{j_2}(s)+\cdots+F_m(s)K_m^{j_m}(s). \tag{7.26}$$

The set $\mathbf{P}_{\rm E}(s)$ is made up of one parameter families of polynomial vectors. It is easy to see that there are $m4^m$ such segments in the most general case where there are four distinct Kharitonov polynomials for each $\mathbf{P}_i(s)$. The parameter space subsets corresponding to $\mathbf{P}_{\rm E}^l(s)$ and $\mathbf{P}_{\rm E}(s)$ are denoted by $\mathbf{\Pi}_l$ and

$$\mathbf{\Pi}_{\rm E} := \cup_{l=1}^m \mathbf{\Pi}_l, \tag{7.27}$$

respectively. Similarly, let $\mathbf{\Pi}_{\rm K}$ denote the vertices of $\mathbf{\Pi}$ corresponding to the Kharitonov polynomials. Then, we also have

$$\mathbf{\Delta}_{\rm E}(s) := \{\delta(s,\mathbf{p}) : \mathbf{p} \in \mathbf{\Pi}_{\rm E}\} \tag{7.28}$$
$$\mathbf{\Delta}_{\rm K}(s) := \{\delta(s,\mathbf{p}) : \mathbf{p} \in \mathbf{\Pi}_{\rm K}\} \tag{7.29}$$

The set $\mathbf{P}_{\rm K}(s)$ in general has 4^m distinct elements when each $\mathbf{P}_i(s)$ has four distinct Kharitonov polynomials. Thus $\mathbf{\Delta}_{\rm K}(s)$ is a discrete set of polynomials, $\mathbf{\Delta}_{\rm E}(s)$ is a set of line segments of polynomials, $\mathbf{\Delta}(s)$ is a polytope of polynomials, and

$$\mathbf{\Delta}_{\rm K}(s) \subset \mathbf{\Delta}_{\rm E}(s) \subset \mathbf{\Delta}(s). \tag{7.30}$$

With these preliminaries, we are ready to state the Generalized Kharitonov Theorem (GKT).

7.3 THE GENERALIZED KHARITONOV THEOREM

Let us say that $\underline{F}(s)$ stabilizes a set of m-tuples if it stabilizes every element in the set. We can now enunciate the Generalized Kharitonov Theorem.

Theorem 7.1 (Generalized Kharitonov Theorem (GKT))
For a given m-tuple $\underline{F}(s) = (F_1(s), \cdots, F_m(s))$ of real polynomials:

I) $\underline{F}(s)$ stabilizes the entire family $\mathbf{P}(s)$ of m-tuples if and only if $\underline{F}$ stabilizes every m-tuple segment in $\mathbf{P}_{\mathrm{E}}(s)$. Equivalently, $\mathbf{\Delta}(s)$ is stable if and only if $\mathbf{\Delta}_{\mathrm{E}}(s)$ is stable.

II) Moreover, if the polynomials $F_i(s)$ are of the form

$$F_i(s) = s^{t_i}(a_i s + b_i)U_i(s)Q_i(s)$$

where $t_i \geq 0$ is an arbitrary integer, a_i and b_i are arbitrary real numbers, $U_i(s)$ is an anti-Hurwitz polynomial, and $Q_i(s)$ is an even or odd polynomial, then it is enough that $\underline{F}(s)$ stabilizes the finite set of m-tuples $\mathbf{P}_{\mathrm{K}}(s)$, or equivalently, that the set of Kharitonov vertex polynomials $\mathbf{\Delta}_{\mathrm{K}}(s)$ are stable.

III) Finally, stabilizing the finite set $\mathbf{P}_{\mathrm{K}}(s)$ is not sufficient to stabilize $\mathbf{P}(s)$ when the polynomials $F_i(s)$ do not satisfy the conditions in II). Equivalently, stability of $\mathbf{\Delta}_{\mathrm{K}}(s)$ does not imply stability of $\mathbf{\Delta}(s)$ when $F_i(s)$ do not satisfy the conditions in II).

The strategy of the proof is to construct an intermediate polytope $\mathbf{\Delta}_{\mathrm{I}}(s)$ of dimension $2m$ such that

$$\mathbf{\Delta}_{\mathrm{E}}(s) \subset \mathbf{\Delta}_{\mathrm{I}}(s) \subset \mathbf{\Delta}(s). \tag{7.31}$$

In the first lemma we shall show that the stability of $\mathbf{\Delta}_{\mathrm{E}}(s)$ implies the stability of $\mathbf{\Delta}_{\mathrm{I}}(s)$. The next two lemmas will be used recursively to show further that the stability of $\mathbf{\Delta}_{\mathrm{I}}(s)$ implies the stability of $\mathbf{\Delta}(s)$.

Recall that Kharitonov polynomials are built from even and odd parts as follows:

$$\begin{array}{ll} K_i^1(s) & = K_i^{\mathrm{even,min}}(s) + K_i^{\mathrm{odd,min}}(s) \\ K_i^2(s) & = K_i^{\mathrm{even,min}}(s) + K_i^{\mathrm{odd,max}}(s) \\ K_i^3(s) & = K_i^{\mathrm{even,max}}(s) + K_i^{\mathrm{odd,min}}(s) \\ K_i^4(s) & = K_i^{\mathrm{even,max}}(s) + K_i^{\mathrm{odd,max}}(s), \end{array} \tag{7.32}$$

where

$$\begin{array}{l} K_i^{\mathrm{even,min}}(s) = \alpha_{i,0} + \beta_{i,2}s^2 + \alpha_{i,4}s^4 + \cdots \\ K_i^{\mathrm{even,max}}(s) = \beta_{i,0} + \alpha_{i,2}s^2 + \beta_{i,4}s^4 + \cdots \\ K_i^{\mathrm{odd,min}}(s) = \alpha_{i,1}s + \beta_{i,3}s^3 + \alpha_{i,5}s^5 + \cdots \\ K_i^{\mathrm{odd,max}}(s) = \beta_{i,1}s + \alpha_{i,3}s^3 + \beta_{i,5}s^5 + \cdots. \end{array} \tag{7.33}$$

Now introduce the polytope $\mathbf{\Delta}_{\mathrm{I}}(s)$:

$$\mathbf{\Delta}_{\mathrm{I}}(s) := \left\{ \sum_{i=1}^{m} F_i(s) \Big((1-\lambda_i) K_i^{\mathrm{even,min}}(s) + \lambda_i K_i^{\mathrm{even,max}}(s) + (1-\mu_i) K_i^{\mathrm{odd,min}}(s) + \mu_i K_i^{\mathrm{odd,max}}(s) \Big) : (\lambda_1, \mu_1, \lambda_2, \mu_2, \cdots, \lambda_m, \mu_m), \quad \lambda_i \in [0,1], \mu_i \in [0,1] \right\}. \tag{7.34}$$

Lemma 7.1 *$\mathbf{\Delta}_{\mathrm{I}}(s)$ is stable if and only if $\mathbf{\Delta}_{\mathrm{E}}(s)$ is stable.*

Proof. It is clear that the stability of $\mathbf{\Delta}_{\mathrm{I}}(s)$ implies the stability of $\mathbf{\Delta}_{\mathrm{E}}(s)$ since $\mathbf{\Delta}_{\mathrm{E}}(s) \subset \mathbf{\Delta}_{\mathrm{I}}(s)$. To prove the converse, we note that the degree of all polynomials in $\mathbf{\Delta}_{\mathrm{I}}(s)$ is the same (see Assumption a2). Moreover, the exposed edges of $\mathbf{\Delta}_{\mathrm{I}}(s)$ are obtained by setting $2m-1$ coordinates of the set

$$(\lambda_1, \mu_1, \lambda_2, \mu_2, \cdots, \lambda_m, \mu_m)$$

to 0 or 1 and letting the remaining one range over $[0,1]$. It is easy to see that this family of line segments is nothing but $\mathbf{\Delta}_{\mathrm{E}}(s)$. Therefore, by the Edge Theorem it follows that the stability of $\mathbf{\Delta}_{\mathrm{E}}(s)$ implies the stability of $\mathbf{\Delta}_{\mathrm{I}}(s)$. ♣

We shall also need the following two symmetric lemmas.

Lemma 7.2 *Let $\mathcal{B}^e(s)$ be the family of real even polynomials*

$$B(s) = b_0 + b_2 s^2 + b_4 s^4 + \cdots + b_{2p} s^{2p},$$

$$\textit{where:} \qquad b_0 \in [x_0, y_0], b_2 \in [x_2, y_2], \cdots, b_{2p} \in [x_{2p}, y_{2p}],$$

and define,

$$K_1(s) = x_0 + y_2 s^2 + x_4 s^4 + \cdots$$
$$K_2(s) = y_0 + x_2 s^2 + y_4 s^4 + \cdots.$$

Let also $A(s)$ and $C(s)$ be two arbitrary but fixed real polynomials. Then,

A) $A(s) + C(s)B(s)$ is stable for every polynomial $B(s)$ in $\mathcal{B}^e(s)$ if and only if the segment $[A(s) + C(s)K_1(s), A(s) + C(s)K_2(s)]$ is stable.

B) Moreover if $C(s) = s^t(as+b)U(s)R(s)$ where $t \geq 0$, a and b are arbitrary real numbers, $U(s)$ is an anti-Hurwitz polynomial, and $R(s)$ is an even or odd polynomial, then $A(s)+C(s)B(s)$ is Hurwitz stable for every polynomial $B(s)$ in $\mathcal{B}^e(s)$ if and only if

$$A(s) + C(s)K_1(s), \quad \textit{and} \quad A(s) + C(s)K_2(s) \quad \textit{are Hurwitz stable.}$$

Proof. Let us assume that $A(s) + C(s)B(s)$ is stable for every polynomial $B(s)$ in $[K_1(s), K_2(s)]$, that is for every polynomial of the form,

$$B(s) = (1-\lambda)K_1(s) + \lambda K_2(s), \quad \lambda \in [0,1].$$

Let us now assume by way of contradiction, that $A(s) + C(s)P(s)$ was unstable for some polynomial $P(s)$ in $\mathcal{B}^e(s)$. Then we know that there must also exist a polynomial $Q(s)$ in $\mathcal{B}^e(s)$ such that

$$A(s) + C(s)Q(s)$$

has a root at the origin or a pure imaginary root. Let us at once discard the case of a polynomial $Q(s)$ in the box $\mathcal{B}^e(s)$, being such that

$$A(0) + C(0)Q(0) = 0. \tag{7.35}$$

Indeed, since $Q(0) = q_0$ belongs to $[x_0, y_0]$, it can be written

$$q_0 = (1-\lambda)x_0 + \lambda y_0, \qquad \text{for some } \lambda \text{ in } [0,1].$$

Then (7.35) would imply

$$\begin{aligned} A(0) + C(0)\left((1-\lambda)x_0 + \lambda y_0\right) &= A(0) + C(0)\left((1-\lambda)K_1(0) + \lambda K_2(0)\right) \\ &= 0, \end{aligned}$$

which would contradict our assumption that $A(s) + C(s)B(s)$ is stable. Suppose now that $A(s) + C(s)Q(s)$ has a pure imaginary root $j\omega$, for some $\omega > 0$. If this is true then we have

$$\begin{cases} A^e(\omega) + C^e(\omega)Q(\omega) = 0 \\ A^o(\omega) + C^o(\omega)Q(\omega) = 0. \end{cases} \tag{7.36}$$

Notice here that since $Q(s)$ is an even polynomial, we simply have

$$Q(j\omega) = Q^e(\omega) = Q_{even}(j\omega) := Q(\omega).$$

Now, (7.36) implies that for this particular value of ω we have

$$A^e(\omega)C^o(\omega) - A^o(\omega)C^e(\omega) = 0. \tag{7.37}$$

On the other hand, consider the two polynomials

$$B_1(s) = A(s) + C(s)K_1(s), \text{ and } B_2(s) = A(s) + C(s)K_2(s).$$

We can write for $i = 1, 2$

$$B_i^e(\omega) = (A + CK_i)^e(\omega) = A^e(\omega) + C^e(\omega)K_i(\omega)$$

and

$$B_i^o(\omega) = (A + CK_i)^o(\omega) = A^o(\omega) + C^o(\omega)K_i(\omega).$$

Thinking then of using the Segment Lemma (Chapter 2) we compute

$$B_1^e(\omega)B_2^o(\omega) - B_2^e(\omega)B_1^o(\omega) = \Big(A^e(\omega) + C^e(\omega)K_1(\omega)\Big)\Big(A^o(\omega) + C^o(\omega)K_2(\omega)\Big) - \Big(A^e(\omega) + C^e(\omega)K_2(\omega)\Big)\Big(A^o(\omega) + C^o(\omega)K_1(\omega)\Big),$$

which can be written as

$$B_1^e(\omega)B_2^o(\omega) - B_2^e(\omega)B_1^o(\omega) = (K_2(\omega) - K_1(\omega))(A^e(\omega)C^o(\omega) - A^o(\omega)C^e(\omega)),$$

and therefore because of (7.37),

$$B_1^e(\omega)B_2^o(\omega) - B_2^e(\omega)B_1^o(\omega) = 0. \tag{7.38}$$

Moreover, assume without loss of generality that

$$C^e(\omega) \geq 0, \text{ and } C^o(\omega) \leq 0, \tag{7.39}$$

and remember that due to the special form of $K_1(s)$ and $K_2(s)$ we have

$$K_1(\omega) \leq Q(\omega) \leq K_2(\omega), \qquad \text{for all } \omega \in [0, +\infty).$$

Then we conclude from (7.36) and (7.39) that

$$\begin{array}{l} B_1^e(\omega) = A^e(\omega) + C^e(\omega)K_1(\omega) \leq 0 \leq B_2^e(\omega) = A^e(\omega) + C^e(\omega)K_2(\omega), \\ B_2^o(\omega) = A^o(\omega) + C^o(\omega)K_2(\omega) \leq 0 \leq B_1^o(\omega) = A^o(\omega) + C^o(\omega)K_1(\omega). \end{array} \tag{7.40}$$

But if we put together equations (7.38) and (7.40) we see that

$$\begin{cases} B_1^e(\omega)B_2^o(\omega) - B_2^e(\omega)B_1^o(\omega) = 0 \\ B_1^e(\omega)B_2^e(\omega) \leq 0 \\ B_1^o(\omega)B_2^o(\omega) \leq 0. \end{cases}$$

We see therefore from the Segment Lemma (Chapter 2) that some polynomial on the segment $[B_1(s), B_2(s)]$ has the same $j\omega$ root, which here again is a contradiction of our original assumption that $A(s) + C(s)B(s)$ is stable. This concludes the proof of part A.

To prove part B, let us assume that $C(s)$ is of the form specified and that

$$B_1(s) = A(s) + C(s)K_1(s), \text{ and } B_2(s) = A(s) + C(s)K_2(s),$$

are both Hurwitz stable. Then

$$B_1(s) - B_2(s) = s^t(as + b)U(s)R(s)\left(K_1(s) - K_2(s)\right). \tag{7.41}$$

Since $K_1(s) - K_2(s)$ is even we conclude from the Vertex Lemma (Chapter 2) that the segment $[B_1(s), B_2(s)]$ is Hurwitz stable. This proves part B. ♣

The dual lemma is stated without proof.

Lemma 7.3 *Let $\mathcal{B}^o(s)$ be the family of real odd polynomials*

$$B(s) = b_1 s + b_3 s^3 + b_5 s^5 + \cdots + b_{2p+1} s^{2p+1},$$

$$\textit{where:} \qquad b_1 \in [x_1, y_1], \quad b_3 \in [x_3, y_3], \quad \cdots, \quad b_{2p+1} \in [x_{2p+1}, y_{2p+1}],$$

and define,

$$K_1(s) = x_1 s + y_3 s^3 + x_5 s^5 + \cdots$$
$$K_2(s) = y_1 s + x_3 s^3 + y_5 s^5 + \cdots .$$

Let also $D(s)$ and $E(s)$ be two arbitrary but fixed real polynomials. Then

a) $D(s) + E(s)B(s)$ is stable for every polynomial $B(s)$ in $\mathcal{B}^o(s)$ if and only if the segment $[D(s) + E(s)K_1(s), D(s) + E(s)K_2(s)]$ is Hurwitz stable.

b) Moreover if $E(s) = s^t(as + b)U(s)R(s)$ where $t \geq 0$, a and b are arbitrary real numbers, $U(s)$ is an anti-Hurwitz polynomial, and $R(s)$ is an even or odd polynomial, then $D(s)+E(s)B(s)$ is stable for every polynomial $B(s)$ in $\mathcal{B}^o(s)$ if and only if

$$D(s) + E(s)K_1(s), \ \textit{and} \ D(s) + E(s)K_2(s) \ \textit{are Hurwitz stable.}$$

Proof of GKT (Theorem 7.1) Since $\mathbf{\Delta}_{\mathrm{E}}(s) \subset \mathbf{\Delta}(s)$, it is only necessary to prove that the stability of $\mathbf{\Delta}_{\mathrm{E}}(s)$ implies that of $\mathbf{\Delta}(s)$. Therefore, let us assume that $\mathbf{\Delta}_{\mathrm{E}}(s)$ is stable, or equivalently that $\underline{F}(s)$ stabilizes $\mathbf{P}_{\mathrm{E}}(s)$. Now consider an arbitrary m-tuple of polynomials in $\mathbf{P}(s)$

$$\underline{P}(s) = (P_1(s), \cdots, P_m(s)) .$$

Our task is to prove that $\underline{F}(s)$ stabilizes this $\underline{P}(s)$. For the sake of convenience we divide the proof into four steps.

Step 1 Write as usual

$$P_i(s) = P_{i,\mathrm{even}}(s) + P_{i,\mathrm{odd}}(s), \quad i = 1, \cdots, m.$$

Since $\mathbf{\Delta}_{\mathrm{E}}(s)$ is stable, it follows from Lemma 7.1 that $\mathbf{\Delta}_{\mathrm{I}}(s)$ is stable. In other words,

$$\begin{aligned} \sum_{i=1}^{m} F_i(s) \Big(& (1-\lambda_i) K_i^{\mathrm{even,min}}(s) + \lambda_i K_i^{\mathrm{even,max}}(s) \\ & + (1-\mu_i) K_i^{\mathrm{odd,min}}(s) + \mu_i K_i^{\mathrm{odd,max}}(s) \Big) , \end{aligned} \tag{7.42}$$

is Hurwitz stable for all possible

$$(\lambda_1, \mu_1, \lambda_2, \mu_2, \cdots, \lambda_m, \mu_m) , \qquad \text{all in } [0, 1].$$

Step 2 In this step we show that stability of $\mathbf{\Delta}_{\mathrm{I}}(s)$ implies the stability of $\mathbf{\Delta}(s)$. In equation (7.42) set

$$D(s) = \sum_{i=1}^{m-1} F_i(s) \Big((1-\lambda_i) K_i^{\mathrm{even,min}}(s) + \lambda_i K_i^{\mathrm{even,max}}(s) + (1-\mu_i) K_i^{\mathrm{odd,min}}(s) + \mu_i K_i^{\mathrm{odd,max}}(s) \Big) + F_m(s) \left((1-\lambda_m) K_m^{\mathrm{even,min}}(s) + \lambda_m K_m^{\mathrm{even,max}}(s) \right),$$

and

$$E(s) = F_m(s).$$

We know from (7.42) that

$$D(s) + E(s) \left((1-\mu_m) K_m^{\mathrm{odd,min}}(s) + \mu_m K_m^{\mathrm{odd,max}}(s) \right)$$

is stable for all μ_m in $[0,1]$. But $K_m^{\mathrm{odd,min}}(s)$ and $K_m^{\mathrm{odd,max}}(s)$ play exactly the role of $K_1(s)$ and $K_2(s)$ in Lemma 7.3, and therefore we conclude that $D(s)+E(s)P_{m,\mathrm{odd}}(s)$ is stable. In other words

$$\begin{aligned} \sum_{i=1}^{m-1} F_i(s) \Big((1-\lambda_i) K_i^{\mathrm{even,min}}(s) + \lambda_i K_i^{\mathrm{even,max}}(s) + (1-\mu_i) K_i^{\mathrm{odd,min}}(s) \\ + \mu_i K_i^{\mathrm{odd,max}}(s) \Big) + F_m(s) \left((1-\lambda_m) K_m^{\mathrm{even,min}}(s) + \lambda_m K_m^{\mathrm{even,max}}(s) \right) \\ + F_m(s) P_{m,\mathrm{odd}}(s), \end{aligned} \tag{7.43}$$

is stable, and remains stable for all possible values

$$(\lambda_1, \mu_1, \lambda_2, \mu_2, \cdots, \lambda_m), \qquad \text{all in } [0,1],$$

since we fixed them arbitrarily. Proceeding, we can now set

$$A(s) = \sum_{i=1}^{m-1} F_i(s) \Big((1-\lambda_i) K_i^{\mathrm{even,min}}(s) + \lambda_i K_i^{\mathrm{even,max}}(s) + (1-\mu_i) K_i^{\mathrm{odd,min}}(s) + \mu_i K_i^{\mathrm{odd,max}}(s) \Big) + F_m(s) P_{m,\mathrm{odd}}(s)$$

and

$$C(s) = F_m(s).$$

Then we know by (7.43) that

$$A(s) + C(s) \left((1-\lambda_m) K_m^{\mathrm{even,min}}(s) + \lambda_m K_m^{\mathrm{even,max}}(s) \right)$$

is stable for all λ_m in $[0,1]$. But, here again, $K_m^{\mathrm{even,min}}(s)$ and $K_m^{\mathrm{even,max}}(s)$ play exactly the role of $K_1(s)$ and $K_2(s)$ in Lemma 7.2, and hence we conclude that $A(s) + C(s)P_{m,\mathrm{even}}(s)$ is stable. That is

$$\sum_{i=1}^{m-1} F_i(s) \Big((1-\lambda_i) K_i^{\mathrm{even,min}}(s) + \lambda_i K_i^{\mathrm{even,max}}(s) + (1-\mu_i) K_i^{\mathrm{odd,min}}(s) + \mu_i K_i^{\mathrm{odd,max}}(s) \Big) + F_m(s) P_{m,\mathrm{odd}}(s) + F_m(s) P_{m,\mathrm{even}}(s)$$

or finally

$$\sum_{i=1}^{m-1} F_i(s)\Big((1-\lambda_i)K_i^{\text{even,min}}(s)+\lambda_i K_i^{\text{even,max}}(s)+(1-\mu_i)K_i^{\text{odd,min}}(s) \\ +\mu_i K_i^{\text{odd,max}}(s)\Big)+F_m(s)P_m(s)$$

is stable, and this is true for all possible values

$$(\lambda_1,\mu_1,\lambda_2,\mu_2,\cdots,\lambda_{m-1},\mu_{m-1}), \quad \text{in } [0,1].$$

The same reasoning can be carried out by induction until one reaches the point where

$$F_1(s)P_1(s)+F_2(s)P_2(s)+\cdots+F_m(s)P_m(s),$$

is found to be stable. Since

$$\underline{P}(s)=(P_1(s),\cdots,P_m(s)),$$

was an arbitrary element of $\mathbf{P}(s)$, this proves that $\underline{F}(s)$ stabilizes $\mathbf{P}(s)$. Equivalently, $\mathbf{\Delta}(s)$ is stable. This concludes the proof of part I of the Theorem.

Step 3 To prove part II observe that a typical segment of $\mathbf{\Delta}_{\text{E}}(s)$ is

$$\delta_\lambda(s):=F_1(s)K_1^{j_1}(s)+\cdots+F_l(s)[\lambda K_l^{j_l}(s)+(1-\lambda)K_l^{i_l}(s)]+\cdots+F_m(s)K_m^{j_m}(s).$$

The endpoints of this segment are

$$\delta_1(s)=F_1(s)K_1^{j_1}(s)+\cdots+F_l(s)K_l^{j_l}(s)+\cdots+F_m(s)K_m^{j_m}(s)$$
$$\delta_2(s)=F_1(s)K_1^{j_1}(s)+\cdots+F_l(s)K_l^{i_l}(s)+\cdots+F_m(s)K_m^{j_m}(s).$$

The difference between the end points of this segment is

$$\begin{aligned}\delta_0(s)&:=\delta_1(s)-\delta_2(s)\\ &=F_l(s)[K_l^{j_l}(s)-K_l^{i_l}(s)].\end{aligned}$$

If $F_l(s)$ is of the form $s^t(as+b)U(s)R(s)$ where $t\geq 0$, a and b are arbitrary real numbers, $U(s)$ are anti-Hurwitz, and $R(s)$ is even or odd, then so is $\delta_0(s)$ since $K_l^{j_l}(s)-K_l^{i_l}(s)$ is either even or odd. Therefore, by the Vertex Lemma of Chapter 2, stability of the segment $[\delta_1(s),\delta_2(s)]$ for $\lambda\in[0,1]$ is implied by the stability of the vertices. We complete the proof of part II by applying this reasoning to every segment in $\mathbf{\Delta}_{\text{E}}(s)$.

Step 4 We prove part III by giving a counter example. Consider

$$\underline{P}(s)=(1.5-s-s^2,2+3s+\gamma s^2),\ \text{where } \gamma\in[2,16],$$

and

$$\underline{F}(s) = (1, 1 + s + s^2).$$

Then

$$\delta_\gamma(s) := F_1(s)P_1(s) + F_2(s)P_2(s) = 3.5 + 4s + (4+\gamma)s^2 + (3+\gamma)s^3 + \gamma s^4.$$

Here $\mathbf{P}_{\mathrm{K}}(s)$ consists of the two 2-tuples

$$P_1(s) = 1.5 - s - s^2, \quad P_2'(s) = 2 + 3s + 2s^2$$

and

$$P_1(s) = 1.5 - s - s^2, \quad P_2''(s) = 2 + 3s + 16s^2.$$

The corresponding polynomials of $\mathbf{\Delta}_{\mathrm{K}}(s)$ are

$$\delta_2(s) = 3.5 + 4s + 6s^2 + 5s^3 + 2s^4,$$
$$\delta_{16}(s) = 3.5 + 4s + 20s^2 + 19s^3 + 16s^4.$$

The Hurwitz matrix for δ_γ is

$$H = \begin{vmatrix} 3+\gamma & 4 & 0 & 0 \\ \gamma & 4+\gamma & 3.5 & 0 \\ 0 & 3+\gamma & 4 & 0 \\ 0 & \gamma & 4+\gamma & 3.5 \end{vmatrix}$$

and the Hurwitz determinants are

$$\begin{cases} H_1 = 3 + \gamma \\ H_2 = \gamma^2 + 3\gamma + 12 \\ H_3 = 0.5\gamma^2 - 9\gamma + 16.5 \\ H_4 = 3.5H_3. \end{cases}$$

Now one can see that H_1, H_2 are positive for all values of γ in $[2, 16]$. However H_3 and H_4 are positive for $\gamma = 2$, or $\gamma = 16$, but negative when, for example, $\gamma = 10$. Therefore it is not enough to check the stability of the extreme polynomials $\delta_\gamma(s)$ corresponding to the couples of polynomials in $\mathbf{P}_{\mathrm{K}}$ and one must check the stability of the entire segment

$$\left(P_1(s), (\lambda P_2'(s) + (1-\lambda)P_2''(s))\right), \quad \lambda \in [0, 1],$$

which is the only element in $\mathbf{P}_{\mathrm{E}}$ for this particular example. This completes the proof. ♣

An alternative way to prove step 2 is to show that if $\mathbf{\Delta}(s)$ contains an unstable polynomial then the polytope $\mathbf{\Delta}_{\mathrm{I}}(s)$ contains a polynomial with a $j\omega$ root. This contradicts the conclusion reached in step 1. This approach to the proof is sketched below.

Alternative Proof of Step 2 of GKT (Theorem 7.1)

If $\underline{F}(s)$ stabilizes every m-tuple segment in $\mathbf{P}_{\mathrm{E}}(s)$, we conclude from Step 1 that every polynomial of the form

$$\beta(s) = \sum_{i=1}^{m} F_i(s) \Big((1-\lambda_i) K_i^{\mathrm{even,min}}(s) + \lambda_i K_i^{\mathrm{even,max}}(s) + (1-\mu_i) K_i^{\mathrm{odd,min}}(s) + \mu_i K_i^{\mathrm{odd,max}}(s) \Big) \tag{7.44}$$

is stable for all possible

$$(\lambda_1, \mu_1, \lambda_2, \mu_2, \cdots, \lambda_m, \mu_m), \qquad \lambda_i \in [0,1], \quad \mu_i \in [0,1].$$

To complete the proof of part I we have to prove that the stability of these polynomials implies the stability of every polynomial in $\mathbf{\Delta}(s)$.

If every polynomial in (7.44) is stable, $\underline{F}(s)$ will not stabilize the entire family $\mathbf{P}(s)$ if and only if for at least one m-tuple

$$\underline{R}(s) := (R_1(s), R_2(s), \cdots, R_m(s))$$

in $\mathbf{P}(s)$ the corresponding polynomial

$$\delta(s) = F_1(s)R_1(s) + F_2(s)R_2(s) + \cdots + F_m(s)R_m(s)$$

has a root at $j\omega^*$ for some $\omega^* \geq 0$. This last statement is a consequence of the Boundary Crossing Theorem (Chapter 2). In other words, for this ω^* we would have

$$\delta(j\omega^*) = F_1(j\omega^*)R_1(j\omega^*) + F_2(j\omega^*)R_2(j\omega^*) + \cdots + F_m(j\omega^*)R_m(j\omega^*) = 0. \tag{7.45}$$

Consider now one of the polynomials $R_i(s)$. We can decompose $R_i(s)$ into its odd and even part

$$R_i(s) = R_i^{\mathrm{even}}(s) + R_i^{\mathrm{odd}}(s)$$

and we know that on the imaginary axis, $R_i^{\mathrm{even}}(j\omega)$ and $\frac{1}{j}R_i^{\mathrm{odd}}(j\omega)$, are, respectively, the real and imaginary parts of $R_i(j\omega)$. Then the associated extremal polynomials

$$K_i^{\mathrm{even,min}}(s), \quad K_i^{\mathrm{even,max}}(s), \quad K_i^{\mathrm{odd,min}}(s), \quad K_i^{\mathrm{odd,max}}(s)$$

satisfy the inequalities

$$K_i^{\mathrm{even,min}}(j\omega) \leq R_i^{\mathrm{even}}(j\omega) \leq K_i^{\mathrm{even,max}}(j\omega), \qquad \text{for all } \omega \in [0,\infty)$$

and

$$\frac{1}{j}K_i^{\mathrm{odd,min}}(j\omega) \leq \frac{1}{j}R_i^{\mathrm{odd}}(j\omega) \leq \frac{1}{j}K_i^{\mathrm{odd,max}}(j\omega), \qquad \text{for all } \omega \in [0,\infty). \tag{7.46}$$

Using (7.46) we conclude that we can find $\lambda_i \in [0,1]$ and $\mu_i \in [0,1]$ such that

$$\begin{aligned} R_i^{\text{even}}(j\omega^*) &= (1-\lambda_i)K_i^{\text{even,min}}(j\omega^*) + \lambda_i K_i^{\text{even,max}}(j\omega^*) \\ \frac{1}{j}R_i^{\text{odd}}(j\omega^*) &= (1-\mu_i)\frac{1}{j}K_i^{\text{odd,min}}(j\omega^*) + \mu\frac{1}{j}K_i^{\text{odd,max}}(j\omega^*). \end{aligned} \tag{7.47}$$

From (7.47) we deduce that we can write

$$\begin{aligned} R_i(j\omega^*) = (1-\lambda_i)K_i^{\text{even,min}}(j\omega^*) + \lambda_i K_i^{\text{even,max}}(j\omega^*) \\ +(1-\mu_i)K_i^{\text{odd,min}}(j\omega^*) + \mu_i K_i^{\text{odd,max}}(j\omega^*). \end{aligned} \tag{7.48}$$

However, substituting (7.48) for every $i = 1, \cdots, m$ into (7.45), we eventually get

$$\begin{aligned} \sum_{i=1}^{m} F_i(j\omega^*) \Big(&(1-\lambda_i)K_i^{\text{even,min}}(j\omega^*) + \lambda_i K_i^{\text{even,max}}(j\omega^*) \\ &+(1-\mu_i)K_i^{\text{odd,min}}(j\omega^*) + \mu_i K_i^{\text{odd,max}}(j\omega^*) \Big) = 0 \end{aligned}$$

but this is a contradiction with the fact that every polynomial $\beta(s)$ in (7.44) is stable as proved in Step 1.

Remark 7.1. One can immediately see that in the particular case $m = 1$ and $F_1(s) = 1$, the GKT (Theorem 7.1) reduces to Kharitonov's Theorem because $F_1(s) = 1$ is even and thus part II of the theorem applies.

Comparison with the Edge Theorem

The problem addressed in the Generalized Kharitonov Theorem (GKT) deals with a polytope and therefore it can also be solved by using the Edge Theorem. This would require us to check the stability of the exposed edges of the polytope of polynomials $\boldsymbol{\Delta}(s)$. GKT on the other hand requires us to check the stability of the segments $\boldsymbol{\Delta}_{\text{E}}(s)$. In general these two sets are quite different. Consider the simplest case of an interval polynomial containing three variable parameters. The 12 exposed edges and 4 extremal segments are shown in Figure 7.2. While two of the extremal segments are also exposed edges, the other two extremal segments lie on the exposed faces and are not edges at all. More importantly, the number of exposed edges depends exponentially on the number of the uncertain parameters (dimension of $\mathbf{p} \in \boldsymbol{\Pi}$). The number of extremal segments, on the other hand, depends only on m (the number of uncertain polynomials). To compare these numbers, consider for instance that each uncertain polynomial $P_i(s)$ has q uncertain parameters. Table 7.1 shows the number of exposed edges and number of segments $\mathbf{P}_{\text{E}}(s)$ for various values of m and q. We can see that the number of exposed edges grows exponentially with the number of parameters whereas the number of extremal segments remains constant for a fixed m.

Table 7.1. Number of exposed edges vs. number of extremal segments

m	q	Exposed Edges	Extremal Segments
2	2	32	32
2	3	80	32
2	4	192	32
.	.		
.	.		
3	4	24,576	192
.	.		
.	.		

Remark 7.2. In some situations, not all the coefficients of the polynomials are necessarily going to vary. In such cases, the number of extremal segments to be checked would be smaller than the maximum theoretical number, $m4^m$. With regard to the vertex result given in part II, it can happen that *some* $F_i(s)$ satisfy the conditions given in part II whereas other $F_i(s)$ do not. Suppose $F_l(s)$ satisfies the vertex conditions in part II. Then we can replace the stability check of the segments corresponding to $\mathbf{P}_{\mathrm{E}}^l(s)$ by the stability check of the corresponding vertices.

7.4 EXAMPLES

Example 7.2. Consider the plant

$$G(s) = \frac{P_1(s)}{P_2(s)} = \frac{s^3 + \alpha s^2 - 2s + \beta}{s^4 + 2s^3 - s^2 + \gamma s + 1}$$

where

$$\alpha \in [-1, -2], \quad \beta \in [0.5, 1], \quad \gamma \in [0, 1].$$

Let

$$C(s) = \frac{F_1(s)}{F_2(s)}$$

denote the compensator. To determine if $C(s)$ robustly stabilizes the set of plants given we must verify the Hurwitz stability of the family of characteristic polynomials $\boldsymbol{\Delta}(s)$ defined as

$$F_1(s)(s^3 + \alpha s^2 - 2s + \beta) + F_2(s)(s^4 + 2s^3 - s^2 + \gamma s + 1)$$

with $\alpha \in [-1, -2]$, $\beta \in [0.5, 1]$, $\gamma \in [0, 1]$. To construct the generalized Kharitonov segments, we start with the Kharitonov polynomials. There are two Kharitonov

polynomials associated with $P_1(s)$

$$K_1^1(s) = K_1^2(s) = 0.5 - 2s - s^2 + s^3$$
$$K_1^3(s) = K_1^4(s) = 1 - 2s - 2s^2 + s^3$$

and also two Kharitonov polynomials associated with $P_2(s)$

$$K_2^1(s) = K_2^3(s) = 1 - s^2 + 2s^3 + s^4$$
$$K_2^2(s) = K_2^4(s) = 1 + s - s^2 + 2s^3 + s^4.$$

The set $\mathbf{P}_{\mathrm{E}}^1(s)$ therefore consists of the 2 plant segments

$$\frac{\lambda_1 K_1^1(s) + (1-\lambda_1)K_1^3(s)}{K_2^1(s)} : \lambda_1 \in [0,1]$$
$$\frac{\lambda_2 K_1^1(s) + (1-\lambda_2)K_1^3(s)}{K_2^2(s)} : \lambda_2 \in [0,1].$$

The set $\mathbf{P}_{\mathrm{E}}^2(s)$ consists of the 2 plant segments

$$\frac{K_1^1(s)}{\lambda_3 K_2^1(s) + (1-\lambda_3)K_2^2(s)} : \lambda_3 \in [0,1]$$
$$\frac{K_1^3(s)}{\lambda_4 K_2^1(s) + (1-\lambda_4)K_2^2(s)} : \lambda_4 \in [0,1].$$

Thus, the extremal set $\mathbf{P}_{\mathrm{E}}(s)$ consists of the following four plant segments.

$$\frac{0.5(1+\lambda_1) - 2s - (1+\lambda_1)s^2 + s^3}{1 - s^2 + 2s^3 + s^4} : \lambda_1 \in [0,1]$$
$$\frac{0.5(1+\lambda_2) - 2s - (1+\lambda_2)s^2 + s^3}{1 + s - s^2 + 2s^3 + s^4} : \lambda_2 \in [0,1]$$

$$\frac{0.5 - 2s - s^2 + s^3}{1 + \lambda_3 s - s^2 + 2s^3 + s^4} : \lambda_3 \in [0,1], \qquad \frac{1 - 2s - 2s^2 + s^3}{1 + \lambda_4 s - s^2 + 2s^3 + s^4} : \lambda_4 \in [0,1].$$

Therefore, we can verify robust stability by checking the Hurwitz stability of the set $\mathbf{\Delta}_{\mathrm{E}}(s)$ which consists of the following four polynomial segments.

$$F_1(s)\left(0.5(1+\lambda_1) - 2s - (1+\lambda_1)s^2 + s^3\right) + F_2(s)\left(1 - s^2 + 2s^3 + s^4\right)$$
$$F_1(s)\left(0.5(1+\lambda_2) - 2s - (1+\lambda_2)s^2 + s^3\right) + F_2(s)\left(1 + s - s^2 + 2s^3 + s^4\right)$$
$$F_1(s)\left(0.5 - 2s - s^2 + s^3\right) + F_2(s)\left(1 + \lambda_3 s - s^2 + 2s^3 + s^4\right)$$
$$F_1(s)\left(1 - 2s - 2s^2 + s^3\right) + F_2(s)\left(1 + \lambda_4 s - s^2 + 2s^3 + s^4\right)$$
$$\lambda_i \in [0,1] : i = 1,2,3,4.$$

In other words, any compensator that stabilizes the family of plants $\mathbf{P}(s)$ must stabilize the 4 one-parameter family of extremal plants $\mathbf{P}_{\mathrm{E}}(s)$. If we had used the

Edge Theorem it would have been necessary to check the 12 line segments of plants corresponding to the exposed edges of $\mathbf{\Delta}(s)$.

If the compensator polynomials $F_i(s)$ satisfy the "vertex conditions" in part II of GKT, it is enough to check that they stabilize the plants corresponding to the four Kharitonov vertices. This corresponds to checking the Hurwitz stability of the four *fixed* polynomials

$$\begin{aligned}
&F_1(s)\left(1-2s-2s^2+s^3\right)+F_2(s)\left(1-s^2+2s^3+s^4\right)\\
&F_1(s)\left(1-2s-2s^2+s^3\right)+F_2(s)\left(1+s-s^2+2s^3+s^4\right)\\
&F_1(s)\left(0.5-2s-s^2+s^3\right)+F_2(s)\left(1+s-s^2+2s^3+s^4\right)\\
&F_1(s)\left(0.5-2s-s^2+s^3\right)+F_2(s)\left(1-s^2+2s^3+s^4\right)
\end{aligned}$$

Example 7.3. (Stable Example) Consider the interval plant and controller pair

$$G(s)=\frac{P_1(s)}{P_2(s)}=\frac{a_1s+a_0}{b_2s^2+b_1s+b_0} \quad \text{and} \quad C(s)=\frac{F_1(s)}{F_2(s)}=\frac{s^2+2s+1}{s^4+2s^3+2s^2+s}$$

where the plant parameters vary as follows:

$$a_1\in[0.1,0.2],\quad a_0\in[0.9,1],\quad b_2\in[0.9,1.0],\quad b_1\in[1.8,2.0],\quad b_0\in[1.9,2.1].$$

The characteristic polynomial of the closed loop system is

$$\delta(s)=F_1(s)P_1(s)+F_2(s)P_2(s).$$

From GKT, the robust stability of the closed loop system is equivalent to that of the set of 32 generalized Kharitonov segments. To construct these segments, we begin with the Kharitonov polynomials of the interval polynomials $P_1(s)$ and $P_2(s)$, respectively:

$$K_1^1(s)=0.9+0.1s,\quad K_1^2(s)=0.9+0.2s,\quad K_1^3(s)=1+0.1s,\quad K_1^4(s)=1+0.2s$$

and

$$\begin{aligned}
K_2^1(s)&=1.9+1.8s+s^2, & K_2^2(s)&=1.9+2s+s^2,\\
K_2^3(s)&=2.1+1.8s+0.9s^2, & K_2^4(s)&=2.1+2s+0.9s^2.
\end{aligned}$$

Then the corresponding generalized Kharitonov segments are

$$F_1(s)K_1^i(s)+F_2(s)\left(\lambda K_2^j(s)+(1-\lambda)K_2^k(s)\right)$$

and

$$F_1(s)\left(\lambda K_1^i(s)+(1-\lambda)K_1^j(s)\right)+F_2(s)K_2^k(s)$$

where $i, j, k \in \underline{4} \times \underline{4} \times \underline{4}$. For example, two such segments are

$$F_1(s)K_1^1(s) + F_2(s)\left(\lambda K_2^1(s) + (1-\lambda)K_2^2(s)\right) = (s^2+2s+1)(0.9+0.1s)$$
$$+(s^4+2s^3+2s^2+s)\left(\lambda(1.9+1.8s+s^2) + (1-\lambda)(1.9+2s+s^2)\right)$$

and

$$F_1(s)\left(\lambda K_1^1(s) + (1-\lambda)K_1^2(s)\right) + F_2(s)K_2^1 = (s^2+2s+1)$$
$$(\lambda(0.9+0.1s) + (1-\lambda)(0.9+0.2s)) + (s^4+2s^3+2s^2+s)(1.9+1.8s+s^2)$$

for $\lambda \in [0,1]$. The stability of these 32 segments can be checked in a number of ways such as the Segment Lemma (Chapter 2), Bounded Phase Conditions (Chapter 4) or the Zero Exclusion Theorem (Chapter 1). In Figure 7.3 we show the evolution of the image sets with frequency.

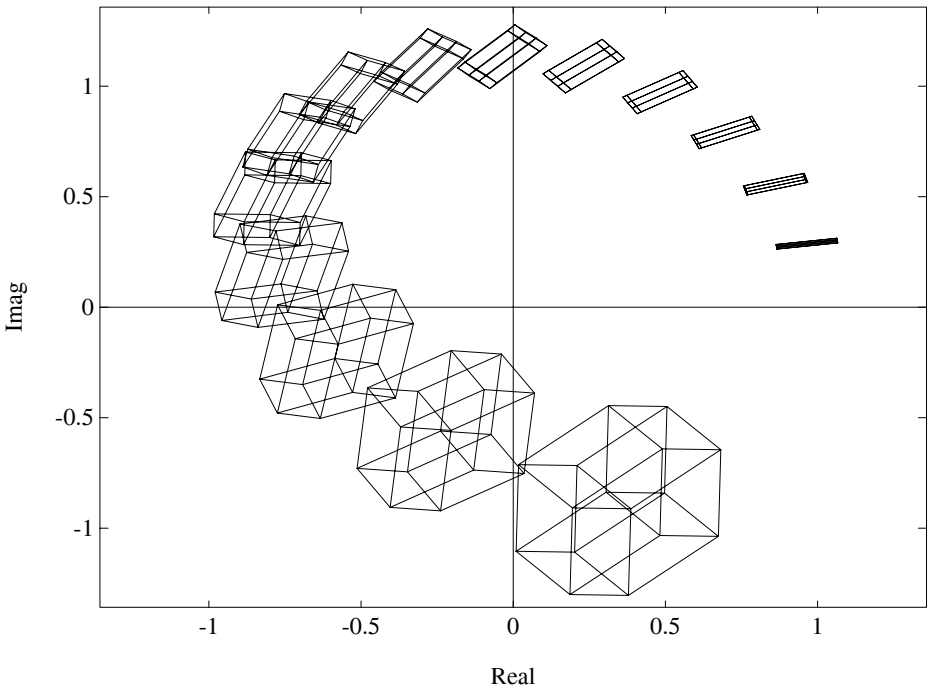

Figure 7.3. Image set of generalized Kharitonov segments (Example 7.3)

We see that the origin is excluded from the image sets for all frequency. In addition, since at least one element (a vertex polynomial) in the family is Hurwitz, the entire family is Hurwitz. Thus, we conclude that the controller $C(s)$ robustly stabilizes the interval plant.

Example 7.4. (Unstable Example) Consider the interval plant and controller pair

$$G(s) = \frac{P_1(s)}{P_2(s)} = \frac{a_1 s + a_0}{b_2 s^2 + b_1 s + b_0} \quad \text{and} \quad C(s) = \frac{F_1(s)}{F_2(s)} = \frac{s^2 + 2s + 1}{s^4 + 2s^3 + 2s^2 + s}$$

where the plant parameters vary in intervals as follows:

$$a_1 \in [0.1, 0.2], \quad a_0 \in [0.9, 1.5], \quad b_2 \in [0.9, 1.0], \quad b_1 \in [1.8, 2.0], \quad b_0 \in [1.9, 2.1].$$

The characteristic polynomial of the closed loop system is

$$\delta(s) = F_1(s)P_1(s) + F_2(s)P_2(s).$$

From GKT, the robust stability of the closed loop system is equivalent to that of the set of 32 generalized Kharitonov segments. We construct this set as in the previous example. The image set of these segments are displayed as a function of frequency in Figure 7.4.

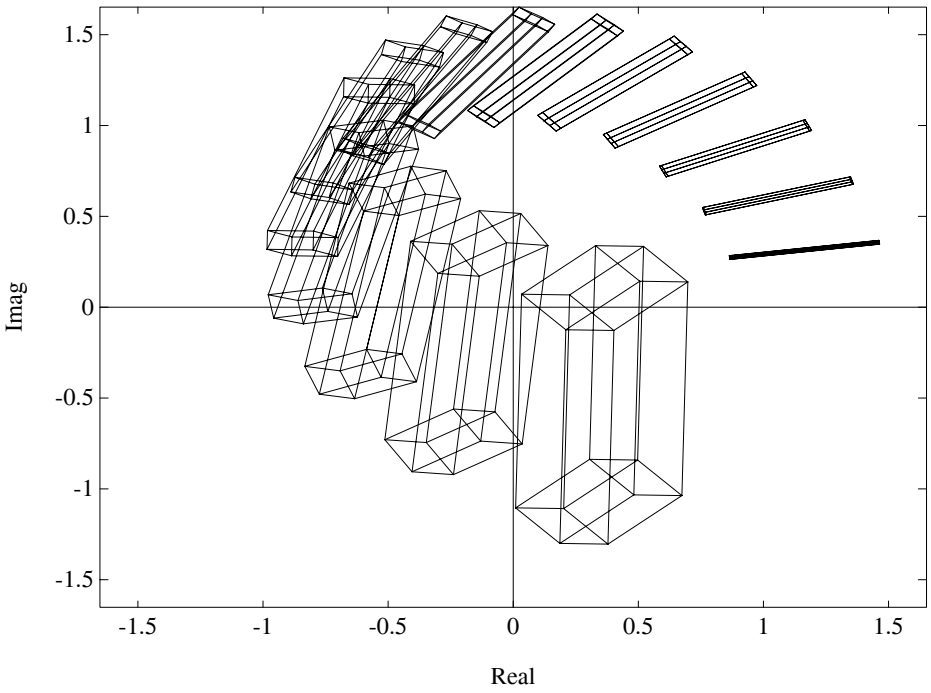

Figure 7.4. Image set of generalized Kharitonov segments (Example 7.4)

From this figure, we see that the origin is *included* in the image set at some frequencies. Thus we conclude that the controller $C(s)$ does not robustly stabilize the given family of plants $G(s)$.

Example 7.5. (Vertex Example) Let us consider the plant and controller

$$G(s) = \frac{P_1(s)}{P_2(s)} = \frac{a_2 s^2 + a_1 s + a_0}{b_2 s^2 + b_1 s + b_0} \quad \text{and} \quad C(s) = \frac{F_1(s)}{F_2(s)} = \frac{(3s+5)(s^2+1)}{s^2(s-5)}$$

where the plant parameters vary as $a_2 = -67$ and

$$a_1 \in [248, 250], \quad a_0 \in [623, 626], \quad b_2 \in [202, 203], \quad b_1 \in [624, 626], \quad b_0 \in [457, 458].$$

Then the characteristic polynomial of the closed loop system is

$$\delta(s) = F_1(s)P_1(s) + F_2(s)P_2(s).$$

In this particular problem, we observe that

$$F_1(s) : (\text{1st order})(\text{even}) \quad \text{and} \quad F_2(s) : s^t(\text{anti} - \text{Hurwitz}).$$

This satisfies the vertex condition of GKT. Thus, the stability of the 16 vertex

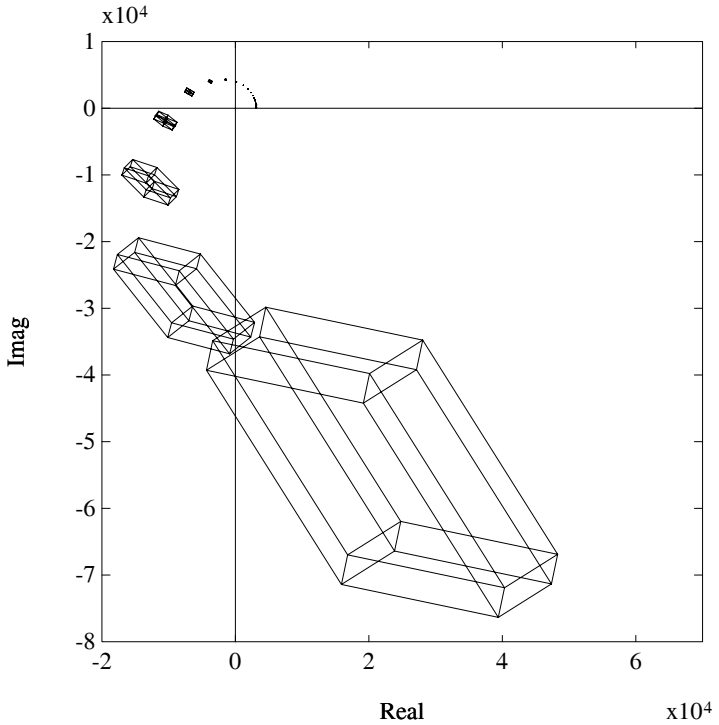

Figure 7.5. Image set of generalized Kharitonov segments (Example 7.5)

polynomials is equivalent to that of the closed loop system. Since all the roots of the 16 vertex polynomials

$$F_1(s)K_1^i(s) + F_2(s)K_2^j(s), \quad i = 1, 2, 3, 4; \quad j = 1, 2, 3, 4$$

lie in the left half of the complex plane, we conclude that the closed loop system is robustly stable. Figure 7.5 confirms this fact.

7.5 IMAGE SET INTERPRETATION

The Generalized Kharitonov Theorem has an appealing geometric interpretation in terms of the image set $\mathbf{\Delta}(j\omega)$ of $\mathbf{\Delta}(s)$. Recall that in Step 1 of the proof, the stability of $\mathbf{\Delta}(s)$ was reduced to that of the $2m$ parameter polytope $\mathbf{\Delta}_I(s)$. It is easy to see that even though $\mathbf{\Delta}_I(s)$ is in general a proper subset of $\mathbf{\Delta}(s)$, the image sets are in fact equal:

$$\mathbf{\Delta}(j\omega) = \mathbf{\Delta}_I(j\omega).$$

This follows from the fact, established is Chapter 5, that each of the m interval polynomials $\mathbf{P}_i(s)$ in $\mathbf{\Delta}(s)$ can be replaced by a 2-parameter family as far as its $j\omega$ evaluation is concerned. This proves that regardless of the dimension of the parameter space $\mathbf{\Pi}$, a linear interval problem with m terms can always be replaced by a $2m$ parameter problem. Of course in the rest of the Theorem we show that this $2m$ parameter problem can be further reduced to a set of one-parameter problems.

In fact, $\mathbf{\Delta}(j\omega)$ is a convex polygon in the complex plane and it may be described in terms of its vertices or exposed edges. Let $\partial\mathbf{\Delta}(j\omega)$ denote the exposed edges of $\mathbf{\Delta}(j\omega)$ and $\mathbf{\Delta}_{\mathrm{V}}(j\omega)$ denote its vertices. Then it is easy to establish the following.

Lemma 7.4

$$1)\ \ \partial\mathbf{\Delta}(j\omega) \subset \mathbf{\Delta}_{\mathrm{E}}(j\omega) \qquad\qquad 2)\ \ \mathbf{\Delta}_{\mathrm{V}}(j\omega) \subset \mathbf{\Delta}_{\mathrm{K}}(j\omega)$$

Proof. Observe that $\mathbf{\Delta}(j\omega)$ is the sum of complex plane sets as follows:

$$\mathbf{\Delta}(j\omega) = F_1(j\omega)\mathbf{P}_1(j\omega) + F_2(j\omega)\mathbf{P}_2(j\omega) + \cdots + F_m(j\omega)\mathbf{P}_m(j\omega).$$

Each polygon $F_i(j\omega)\mathbf{P}_i(j\omega)$ is a rectangle with vertex set $F_i(j\omega)\mathcal{K}_i(j\omega)$ and edge set $F_i(j\omega)\mathcal{S}_i(j\omega)$. Since the vertices of $\mathbf{\Delta}(j\omega)$ can only be generated by the vertices of $F_i(j\omega)\mathbf{P}_i(j\omega)$, we immediately have 2). To establish 1) we note that the boundary of the sum of two complex plane polygons can be generated by summing over all vertex-edge pairs with the vertices belonging to one and the edges belonging to the other. This fact used recursively to add m polygons shows that one has to sum vertices from $m-1$ of the sets to edges of the remaining set and repeat this over all possibilities. This leads to 1). ♣

The vertex property in 2) allows us to check robust stability of the family $\mathbf{\Delta}(s)$ by using the phase conditions for a polytopic family described in Chapter 4. More precisely, define

$$\phi_\delta(\lambda) := \arg\left(\frac{\delta(\lambda)}{\delta_0(\lambda)}\right). \tag{7.49}$$

and with $\delta_0(j\omega) \in \mathbf{\Delta}(j\omega)$,

$$\phi^+(j\omega) := \sup_{\delta_i(j\omega)\in\mathbf{\Delta}_K(j\omega)} \phi_{\delta_i}(j\omega), \quad 0 \le \phi^+ \le \pi$$
$$\phi^-(j\omega) := \inf_{\delta_i(j\omega)\in\mathbf{\Delta}_K(j\omega)} \phi_{\delta_i}(j\omega), \quad -\pi < \phi^- \le 0$$

and

$$\Phi_{\mathbf{\Delta}_K}(j\omega) := \phi^+(j\omega) - \phi^-(j\omega). \tag{7.50}$$

Theorem 7.2 *Assume that $\mathbf{\Delta}(s)$ has at least one polynomial which is stable, then the entire family is stable if and only if $\Phi_{\mathbf{\Delta}_K}(j\omega) < \pi$ for all ω.*

Example 7.6. Consider the plant controller pair of Example 7.3. We first check the stability of an arbitrary point in the family, say, one of the Kharitonov vertices. Next for each ω, we evaluate the maximum phase difference over the following 16 Kharitonov vertices

$$F_1(s)K_1^i(s) + F_2(s)K_2^j(s), \quad i = 1,2,3,4; \quad j = 1,2,3,4$$

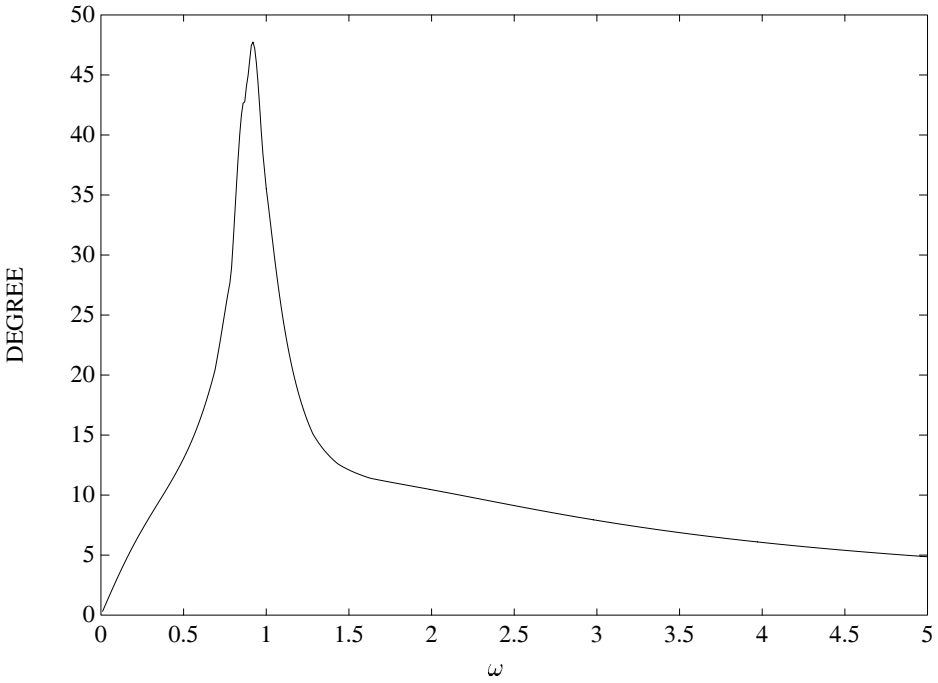

Figure 7.6. Maximum phase difference of Kharitonov vertices (Example 7.6)

The result is plotted in Figure 7.6. It shows that the maximum phase difference over these vertices never reaches 180° at any frequency. Thus we conclude that the system is robustly stable which agrees with the conclusion reached using the image set plot shown in Figure 7.3.

Example 7.7. For the plant controller pair of Example 7.4, we evaluate the maximum phase difference over the Kharitonov vertices at each frequency. The plot is shown in Figure 7.7.

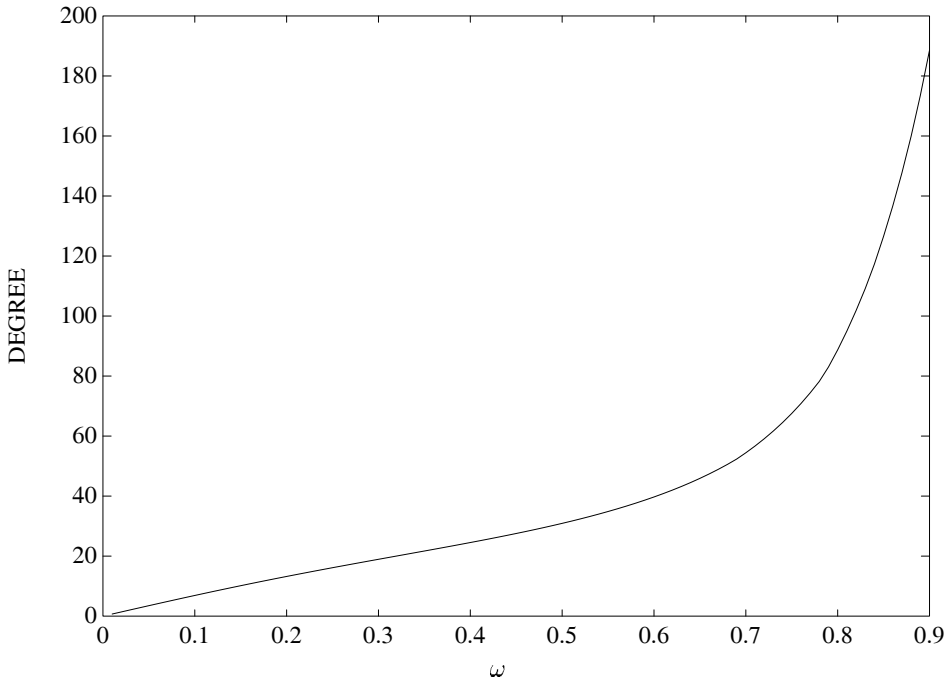

Figure 7.7. Maximum phase difference of Kharitonov vertices (Example 7.7)

This graph shows that the maximal phase difference reaches 180° showing that the family is *not* stable. This again agrees with the analysis using the image sets given in Figure 7.4.

7.6 EXTENSION TO COMPLEX QUASIPOLYNOMIALS

The main statement, namely part I, of the Generalized Kharitonov Theorem also holds when the $F_i(s)$ are complex polynomials and also when $F_i(s)$ are quasipolynomials. We state these results formally below but omit the detailed proof which,

in general, follows from the fact that the image set of the family $\mathbf{\Delta}(j\omega)$ is still generated by the same extremal segments even in these cases. Thus all that is needed is to ensure that the Boundary Crossing Theorem can be applied.

Consider the family of quasipolynomials

$$\mathbf{\Delta}(s) = F_1(s)\mathbf{P}_1(s) + F_2(s)\mathbf{P}_2(s) + \cdots + F_m(s)\mathbf{P}_m(s). \tag{7.51}$$

where $\mathbf{P}_i(s)$ are real independent interval polynomials as before, but now

$$\underline{F}(s) = (F_1(s), \cdots, F_m(s)),$$

is a fixed m-tuple of complex quasipolynomials, of the form

$$F_i(s) = F_i^0(s) + e^{-sT_i^1}F_i^1(s) + e^{-sT_i^2}F_i^2(s) + \cdots$$

with the $F_i^j(s)$ being complex polynomials satisfying the condition

$$\text{degree}\left[F_i^0(s)\right] > \text{degree}\left[F_i^j(s)\right], \quad j \neq 0. \tag{7.52}$$

We assume that every polynomial in the family

$$\mathbf{\Delta}^0(s) := F_1^0(s)\mathbf{P}_1(s) + F_2^0(s)\mathbf{P}_2(s) + \cdots + F_m^0(s)\mathbf{P}_m(s) \tag{7.53}$$

is of the same degree. Let $\mathbf{P}_{\mathrm{E}}(s)$ and $\mathbf{\Delta}_{\mathrm{E}}(s)$ be as defined in Section 2. The above degree conditions guarantee that the Boundary Crossing Theorem can be applied to the family $\mathbf{\Delta}(s)$. We therefore have the following extension of GKT to the case of complex quasipolynomials.

Theorem 7.3 (Generalized Kharitonov Theorem: Complex Polynomials and Quasipolynomials)
Let $\underline{F} = (F_1(s), \cdots, F_m(s))$, be a given m-tuple of complex quasipolynomials satisfying the conditions (7.52) above, and $\mathbf{P}_i(s), 1 = 1, 2...m$ be independent real interval polynomials satisfying the invariant degree assumption for the family (7.53). Then $\underline{F}$ stabilizes the entire family $\mathbf{P}(s)$ of m-tuples if and only if $\underline{F}$ stabilizes every m-tuple segment in $\mathbf{P}_{\mathrm{E}}(s)$. Equivalently, $\mathbf{\Delta}(s)$ is stable if and only if $\mathbf{\Delta}_{\mathrm{E}}(s)$ is stable.

The complex *polynomial* case is a special case of the above result obtained by setting $F_i^j(s) = 0$, $i = 1, 2, \cdots, m$; $j \neq 0$. We note that the vertex result, part II of GKT, that holds in the real case does not, in general, carry over to this complex quasipolynomial case. However in the case of complex polynomials the following vertex result holds.

Corollary 7.1 (Theorem 7.3)
Under the conditions of Theorem 7.3, suppose that

$$\underline{F}(s) = (F_1(s), \cdots, F_m(s)),$$

is an m-tuple of complex polynomials such that

$$\frac{d}{d\omega}\arg F_i(j\omega) \leq 0, \qquad i = 1, 2, \cdots, m.$$

Then $\underline{F}$ *stabilizes the entire family* $\mathbf{P}(s)$ *of m-tuples if and only if* $\underline{F}$ *stabilizes every m-tuple in* $\mathbf{P}_{\mathrm{K}}(s)$. *Equivalently,* $\mathbf{\Delta}(s)$ *is stable if and only if the Kharitonov vertex set* $\mathbf{\Delta}_{\mathrm{K}}(s)$ *is stable.*

Proof. The proof follows from the fact that the difference of the endpoints of a typical segment in $\mathbf{\Delta}_E(s)$ is of the form

$$\delta_0(s) = F_l(s)[K_l^{j_l}(s) - K_l^{i_l}(s)].$$

Since $[K_l^{j_l}(s) - K_l^{i_l}(s)]$ is real and odd or even, it follows that

$$\frac{d}{d\omega}\arg \delta_0(j\omega) = \frac{d}{d\omega}\arg F_i(j\omega) \leq 0, \quad i = 1, 2, \cdots, m.$$

Therefore, by the Convex Direction Lemma for the complex case (Lemma 2.15, Chapter 2), such segments are stable if and only if the endpoints are. These endpoints constitute the set $\mathbf{\Delta}_{\mathrm{K}}(s)$ and this completes the proof. ♣

The above results can be used to determine the robust stability of systems containing time delay. The theorem can be further extended to the case where $P_i(s)$ are complex interval polynomials by using Kharitonov's Theorem for the complex case given in Chapter 5. The detailed development of these ideas is left to the reader.

Example 7.8. (Time Delay Example) Let us consider the plant and controller

$$\begin{aligned} G(s) &= \frac{P_1(s)}{P_2(s)} \\ &= \frac{a_1 s + a_0}{b_2 s^2 + b_1 s + b_0} \end{aligned}$$

and

$$\begin{aligned} C(s) &= \frac{F_1(s)}{F_2(s)} \\ &= \frac{s^2 + 2s + 1}{s^4 + 2s^3 + 2s^2 + s} \end{aligned}$$

with a time delay of 0.1 sec where the plant parameters vary as

$$\begin{aligned} &a_1 \in [0.1, 0.2], \quad a_0 \in [0.9, 1], \\ &b_2 \in [0.9, 1.0], \quad b_1 \in [1.8, 2.0], \quad b_0 \in [1.9, 2.1]. \end{aligned}$$

Then the characteristic equation of the closed loop system is

$$\delta(s) = F_2(s)P_2(s) + e^{-sT}F_1(s)P_1(s)$$

where $T = 0.1$.

The robust stability of this time delay system can also be tested by GKT. Figure 7.8 shows that the image set excludes the origin. Therefore, the closed loop system is robustly stable. This fact is also verified by the Bounded Phase Conditions as shown in Figure 7.9.

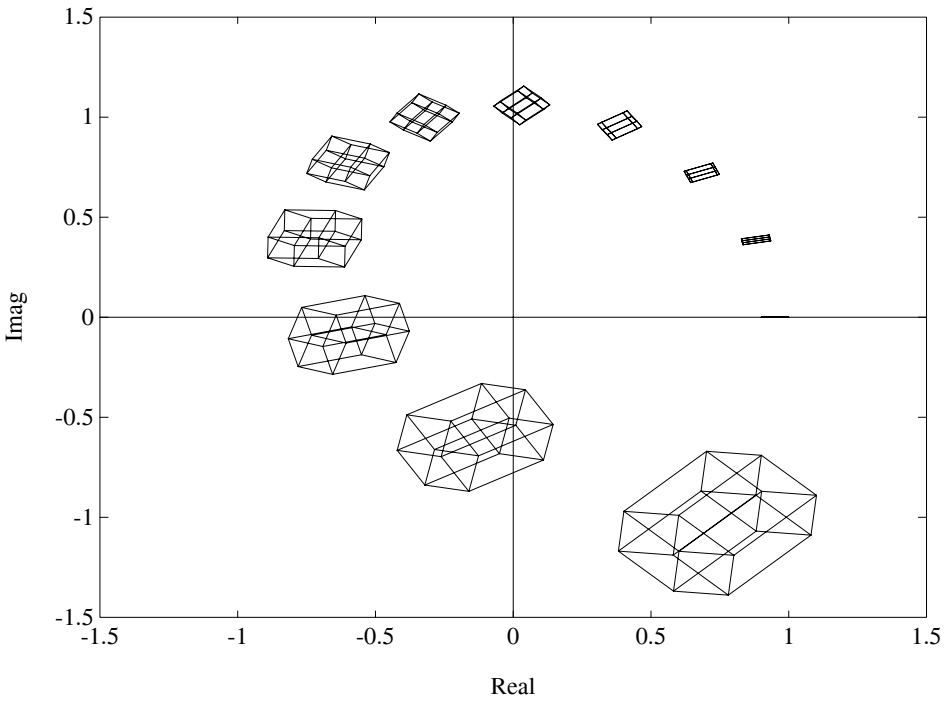

Figure 7.8. Image set of generalized Kharitonov segments (Example 7.8)

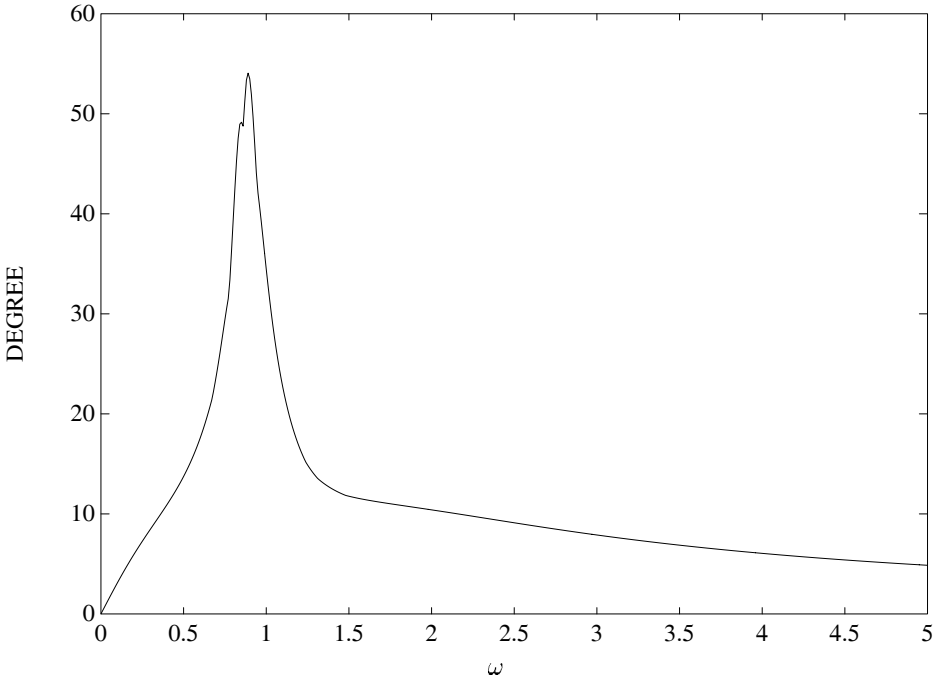

Figure 7.9. Maximum phase difference of Kharitonov vertices (Example 7.8)

We conclude this chapter by giving an application of the GKT to interval polynomials.

7.7 σ AND θ HURWITZ STABILITY OF INTERVAL POLYNOMIALS

Let

$$h(s) = h_0 + h_1 s + h_2 s^2 + \cdots + h_n s^n,$$

and consider the real interval polynomial family of degree n:

$$\mathcal{I}(s) := \left\{ h(s) : h_i^- \leq h_i \leq h_i^+, \quad i = 0, 1, \cdots, n \right\}$$

with the assumption $0 \notin [h_n^-, h_n^+]$. We consider the stability of the family $\mathcal{I}(s)$ with respect to two special stability regions.

First consider the *shifted Hurwitz* stability region (see Figure 7.10) defined for for a fixed real number $\sigma > 0$ by

$$\mathcal{S}_\sigma := \left\{ s : s \in \mathbb{C}^-, \quad \mathrm{Re}[s] < -\sigma \right\}.$$

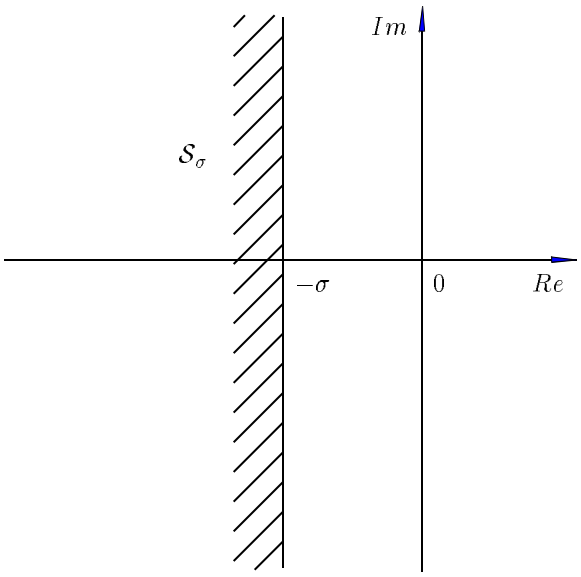

Figure 7.10. Shifted Hurwitz stability region

We shall say that $\mathcal{I}(s)$ is σ-*Hurwitz stable* if each polynomial in $\mathcal{I}(s)$ has all its roots in $\mathcal{S}_\sigma$. Introduce the set of *vertex polynomials* of $\mathcal{I}(s)$:

$$\mathbf{V}_I(s) := \left\{h(s) : h_i = h_i^+ \text{ or } h_i = h_i^-,\ i = 0, 1, 2, \cdots, n\right\}.$$

We have the following result.

Theorem 7.4 *The family $\mathcal{I}(s)$ is σ-Hurwitz stable if and only if the vertex polynomials $\mathbf{V}_I(s)$ are σ-Hurwitz stable.*

Proof. We set $s = -\sigma + p$ and write

$$h(s) = g(p) = h_0 + h_1(p-\sigma) + h_2(p-\sigma)^2 + \cdots + h_n(p-\sigma)^n.$$

The σ-Hurwitz stability of the family $\mathcal{I}(s)$ is equivalent to the Hurwitz stability of the *real linear interval family*

$$\mathcal{G}(p) := \left\{g(p) = h_0 + h_1(p-\sigma) + h_2(p-\sigma)^2 + \cdots + h_n(p-\sigma)^n : \right.$$
$$\left. h_i \in [h_i^-, h_i^+],\quad i = 0, 1, 2, \cdots, n\right\}$$

Let $\mathbf{V}_G(p)$ denote the vertex set associated with the family $\mathcal{G}(p)$. We now apply GKT to this family $\mathcal{G}(p)$ with

$$F_i = (p-\sigma)^{i-1} \text{ and } P_i = h_{i-1},\quad i = 0, 1, 2, \cdots, n+1$$

Since $F_0 = 1$ is even and $F_1, \ldots . F_{n+1}$ are anti-Hurwitz it follows from part II of GKT that it suffices to check the Hurwitz stability of the vertex set $\mathbf{V}_G(p)$. This is equivalent to checking the σ-Hurwitz stability of the $\mathbf{V}_I(s)$. ♣

Remark 7.3. The above lemma can also be used to find the largest value of σ for which the interval family $\mathcal{I}(s)$ is σ-Hurwitz stable. This value is sometimes called the *stability degree* of the family and indicates the distance of the root set of the family from the imaginary axis.

Using the above result we can derive a useful vertex result on σ-Hurwitz stability for the family of polynomials

$$\mathbf{\Delta}(s) := F_1(s)\mathbf{P}_1(s) + F_2(s)\mathbf{P}_2(s) + \cdots + F_m(s)\mathbf{P}_m(s). \tag{7.54}$$

Corollary 7.2 *The family $\mathbf{\Delta}(s)$, with $F_i(s)$ satisfying*

$$F_i(s) = s^{t_i} A_i(s)(a_i s + b_i), \qquad i = 1, \cdots, m$$

with $A_i(s)$ antiHurwitz is σ-Hurwitz stable for $\sigma \geq 0$ if and only if the Kharitonov vertex set of polynomials $\mathbf{\Delta}_{\mathrm{K}}(s)$ is σ-Hurwitz stable.

The proof of this result follows from Part II of GKT and is omitted.

Next let us consider a rotation of the complex plane obtained by setting $s = s' e^{j\theta}$. We define the *rotated Hurwitz* region (see Figure 7.11) by

$$\mathcal{S}_\theta := \left\{ s : \ s \in \mathbb{C}, \quad \mathrm{Re}\left[s e^{-j\theta} \right] < 0 \right\}.$$

We say that the family $\mathcal{I}(s)$ is *θ-Hurwitz stable* if each polynomial in $\mathcal{I}(s)$ has all its roots in $\mathcal{S}_\theta$. Note that if the family is Hurwitz stable and is also θ-Hurwitz stable then its root set lies in the shaded region shown in Figure 7.11. The following lemma establishes that $\mathcal{S}_\theta$ stability of $\mathcal{I}(s)$ can also be determined from the vertex set.

Theorem 7.5 *The family $\mathcal{I}(s)$ is θ-Hurwitz stable if and only if the vertex polynomials $\mathbf{V}_I(s)$ are θ-Hurwitz stable.*

Proof. The result can be readily derived by first substituting $s' = s e^{-j\theta}$ in $h(s)$ and then applying GKT to test the Hurwitz stability of the resulting *complex* linear interval family

$$1 \cdot h_0 + e^{j\theta} h_1 s' + e^{j2\theta} h_2 (s')^2 + \cdots + e^{jn\theta} h_n (s')^n, \quad h_i \in [h_i^-, h_i^+], \quad i = 0, 1, \cdots, n.$$

To apply GKT we set

$$F_i(s') = (e^{j\theta})^{i-1}, \quad P_i(s') = h_i (s')^i, \quad i = 1, 2, \cdots, n+1.$$

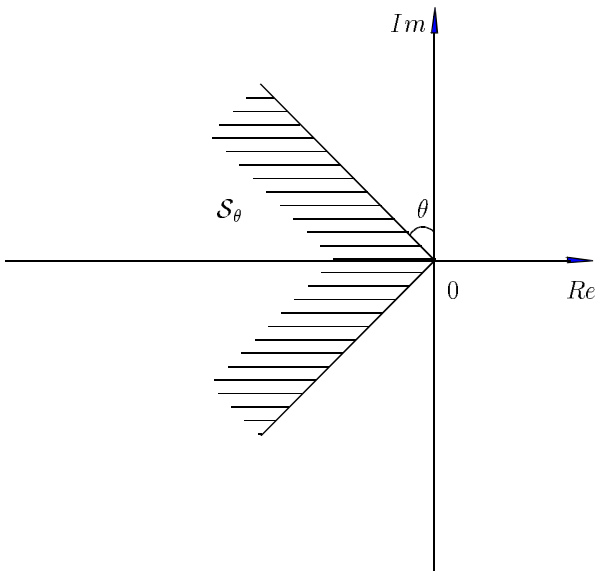

Figure 7.11. Rotated Hurwitz stability region

and test the Hurwitz stability of the family in the s' plane. This shows that the set is Hurwitz stable if and only if the corresponding segments with *only one* coefficient h_i varying at a time, with the rest of the $h_j, j \neq i$ set to the vertices, are Hurwitz stable in the s' plane. Consider a typical such complex segment. The difference between the endpoints of such a segment is a polynomial of the form

$$\delta_0(s') = (h_i^+ - h_i^-)(s')^i (e^{j\theta})^i.$$

Now by applying the Convex Direction Lemma for the complex case (Chapter 2, Lemma 2.15) we can see that

$$\frac{d}{d\omega} \arg \delta_0(j\omega) = 0.$$

Therefore such complex segments are stable if and only if the endpoints are. But this is equivalent to the θ-Hurwitz stability of the vertex set $\mathbf{V}_I(s)$. ♣

The maximum value θ^* of θ for which θ-Hurwitz stability is preserved for the family can be found using this result. The above two results can then be used to estimate the root space boundary of an interval polynomial family without using the excessive computations associated with the Edge Theorem.

7.8 EXERCISES

7.1 In a unity feedback system the plant transfer function is:

$$G(s) = \frac{\alpha_2 s^2 + \alpha_1 s + \alpha_0}{s^3 + \beta_2 s^2 + \beta_1 s + \beta_0}.$$

The nominal values of the plant parameters are

$$\begin{array}{lll} \alpha_2^0 = 1, & \alpha_1^0 = 5, & \alpha_0^0 = -2 \\ \beta_2^0 = -3, & \beta_1^0 = -4, & \beta_0^0 = 6. \end{array}$$

Determine a feedback controller of second order that places the 5 closed loop poles at -1, -2, -3, $-2+2j$, $-2-2j$. Suppose that the parameters of $G(s)$ are subject to perturbation as follows:

$$\alpha_1 \in [3,7], \quad \alpha_0 \in [-3,-1], \quad \beta_1 \in [-6,-2], \quad \beta_0 \in [5,7].$$

Determine if the closed loop is robustly stable with the controller designed as above for the nominal system.

7.2 Consider the two masses connected together by a spring and a damper as shown in Figure 7.12:

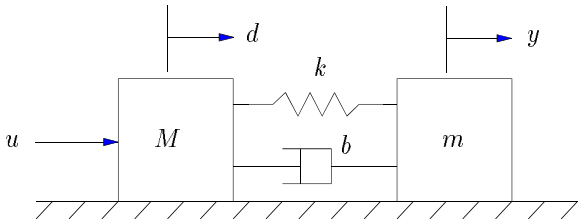

Figure 7.12. Mass-spring-damper system

Assuming that there is no friction between the masses and the ground, then we have the following dynamic equations:

$$\begin{aligned} M\ddot{d} + b(\dot{d} - \dot{y}) + k(d - y) &= u \\ m\ddot{y} + b(\dot{y} - \dot{d}) + k(y - d) &= 0. \end{aligned}$$

The transfer functions of the system are as follows:

$$\frac{y(s)}{u(s)} = \frac{\left(\frac{b}{m}s + \frac{k}{m}\right)}{Ms^2\left[s^2 + \left(1 + \frac{m}{M}\right)\left(\frac{b}{m}s + \frac{k}{m}\right)\right]}$$

$$\frac{d(s)}{u(s)} = \frac{\left(s^2 + \frac{b}{m}s + \frac{k}{m}\right)}{Ms^2\left[s^2 + \left(1 + \frac{m}{M}\right)\left(\frac{b}{m}s + \frac{k}{m}\right)\right]}.$$

The feedback controller

$$C(s) = \frac{n_{c_1}(s)}{d_c(s)}y(s) + \frac{n_{c_2}(s)}{d_c(s)}d(s)$$

with $d_c(s) = s^2 + \beta_1 s + \beta_0$, $n_{c_1}(s) = \delta_1 s + \delta_0$, $n_{c_2}(s) = \gamma_1 s + \gamma_0$, is to be designed so that the closed loop is stabilized. With nominal parameters $m = 1$, $M = 2$, $b = 2$, $k = 3$ determine the controller parameters so that the closed loop poles for the nominal system are all at -1. Determine if the closed loop remains stable when the parameters b and k suffer perturbations in their magnitudes of 50%. Determine the largest l^∞ box centered at the above nominal parameter in the b, k parameter space for which closed loop stability is preserved with the controller designed. Also, use the Boundary Crossing Theorem of Chapter 1 to plot the entire stability region in this parameter space.

7.3 In a unity feedback system

$$G(s) = \frac{s - z_0}{3s^3 - p_2 s^2 + s + p_0} \quad \text{and} \quad C(s) = \frac{\alpha_0 + \alpha_1 s + \alpha_2 s^2}{s^2 + \beta_1 s + \beta_0}$$

represent the transfer functions of the plant and controller respectively. The nominal values of the parameters $[z_0, p_0, p_2]$ are given by $[z_0^0, p_0^0, p_2^0] = [1, 1, 2]$. Find the controller parameters so that the closed loop poles are placed at $[-1, -2, -3, -2 - j, -2 + j]$. Determine if the closed loop system that results remains stable if the parameters $[z_0, p_0, p_2]$ are subject to a 50% variation in their numerical values centered about the nominal, i.e. $z_0 \in [0.5, 1.5]$, $p_0 \in [0.5, 1.5]$, $p_2 \in [1, 3]$.

7.4 In the previous problem let the plant parameters have their nominal values and assume that the nominal controller has been designed to place the closed loop poles as specified in the problem. Determine the largest l^∞ ball in the controller parameter space $x = [\alpha_0, \alpha_1, \alpha_2, \beta_0, \beta_1]$, centered at the nominal value calculated above, for which the closed loop system with the nominal plant remains stable.

7.5 In a unity feedback system with

$$G(s) = \frac{s + z_0}{s^2 + p_1 s + p_0} \quad \text{and} \quad C(s) = \frac{\alpha_2 s^2 + \alpha_1 s + \alpha_0}{s(s + \beta)}.$$

Assume that the nominal values of the plant parameters are

$$(z_0^0, p_0^0, p_1^0) := (1, 1, 1).$$

Choose the controller parameters $(\alpha_0, \alpha_1, \alpha_2, \beta)$ so that the closed loop system is stabilized at the nominal plant parameters. Check if your controller robustly stabilizes the family of the closed loop systems under plant parameter perturbations of 20%.

7.6 Consider the interval polynomial $s^3 + a_2 s^2 + a_1 s + a_0$ with

$$a_2 \in [15 - \epsilon, 15 + \epsilon], \qquad a_1 \in [10 - \epsilon, 10 + \epsilon], \qquad a_0 \in [7 - \epsilon, 7 + \epsilon].$$

For each value of $\epsilon = 1, 2, 3, 4, 5,$ and 6 determine the maximum value $\sigma^*(\epsilon)$ for which the family is σ^* Hurwitz stable. Plot a graph of ϵ vs. $\sigma^*(\epsilon)$ to display the result.

7.7 Repeat Exercise 7.6 this time computing the maximal value $\theta^*(\epsilon)$ for which the family is θ^*-Hurwitz stable.

7.8 Consider the unity feedback configuration with the plant and controller being

$$C(s) = \frac{s + 1}{s + 2} \quad \text{and} \quad G(s) = \frac{s + b_0}{s^2 + a_1 s + a_0}$$

where

$$a_0 \in [2, 4], \quad a_1 \in [2, 4], \quad b_0 \in [1, 3].$$

Is this closed loop system robustly stable?

7.9 Consider the unity feedback system shown in Figure 7.13 where

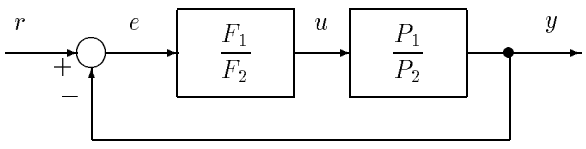

Figure 7.13. Feedback control system

$$\frac{F_1(s)}{F_2(s)} = \frac{2s^2 + 4s + 3}{s^2 + 3s + 4} \quad \text{and} \quad \frac{P_1(s)}{P_2(s)} = \frac{s^2 + a_1 s + a_0}{s(s^2 + b_1 s + b_0)}$$

with

$$a_1^0 = -2, \quad a_0^0 = 1, \quad b_0^0 = 2, \quad b_1^0 = 1.$$

Now let

$$a_0 \in [1-\epsilon, 1+\epsilon], \quad b_0 \in [2-\epsilon, 2+\epsilon]$$
$$a_1 \in [-2-\epsilon, -2+\epsilon], \quad b_1 \in [1-\epsilon, 1+\epsilon]$$

Find $\epsilon_{\max}$ for which the system is robustly stable.
Answer: $\epsilon_{\max} = 0.175$

7.10 Referring to the system given in Figure 7.13 with

$$\frac{F_1(s)}{F_2(s)} = \frac{2s^2+4s+3}{s^2+3s+4} \quad \text{and} \quad \frac{P_1(s)}{P_2(s)} = \frac{s^2+a_1s+a_0}{s(s^2+b_1s+b_0)}.$$

Let the nominal system be

$$\frac{P_1^0(s)}{P_2^0(s)} = \frac{s^2-2s+7}{s(s^2+8s-0.25)}.$$

Suppose that the parameters vary within intervals:

$$a_1 \in [-2-\epsilon, -2+\epsilon], \qquad a_0 \in [7-\epsilon, 7+\epsilon]$$
$$b_1 \in [8-\epsilon, 8+\epsilon], \qquad b_0 \in [-0.25-\epsilon, -0.25+\epsilon].$$

Find the maximum value of ϵ for robust stability of the family using GKT.
Answer: $\epsilon_{\max} = 0.23$

7.11 For the same configuration in Figure 7.13 with

$$\frac{F_1(s)}{F_2(s)} = \frac{26+27s}{-17+2s} \quad \text{and} \quad \frac{P_1(s)}{P_2(s)} = \frac{s+a_0}{s^2+b_1s+b_0}$$

with

$$a_0 \in [-1.5, -0.5], \quad b_1 \in [-2.5, -1.5], \quad b_0 \in [-1.5, -0.5]$$

Show that the family of closed loop systems is unstable using GKT.

7.9 NOTES AND REFERENCES

The Generalized Kharitonov Theorem was proved by Chapellat and Bhattacharyya in [58], where it was called the Box Theorem. The vertex condition that was given in [58] dealt only with the case where the $F_i(s)$ were even or odd. The more general vertex condition given here in part II of Theorem 7.1 is based on the Vertex Lemma (Chapter 2). In Bhattacharyya [30] and Bhattacharyya and Keel [33] a comprehensive survey of the applications of this theorem were given. In the latter papers this

result was referred to as the CB Theorem. A special case of the vertex results of part II of GKT is reported by Barmish, Hollot, Kraus, and Tempo [15]. A discrete time counterpart of GKT was developed by Katbab and Jury [130] but in this case the stability test set that results consists of manifolds rather than line segments. The results on σ and θ-Hurwitz stability are due to Datta and Bhattacharyya [78] and Theorem 7.4 was applied in Datta and Bhattacharyya [77] for quantitative estimates of robustness in Adaptive Control. Kharitonov and Zhabko [147] have used GKT to develop robust stability results for time-delay systems.

Chapter 8

FREQUENCY DOMAIN PROPERTIES OF LINEAR INTERVAL SYSTEMS

In this chapter we develop some useful frequency domain properties of systems containing uncertain parameters. The Generalized Kharitonov Theorem of the last chapter introduced a set of one parameter extremal plants which completely characterize the frequency domain behaviour of linear interval systems. We show here that this extremal set can be used to exactly calculate the uncertainty template at each frequency as well as the Bode, Nyquist and Nichols envelopes of the system. We also prove that the worst case gain, phase, and parametric stability margins of control systems containing such a plant occur over this extremal set. The utility of these tools in robust classical control design is illustrated by examples.

8.1 INTRODUCTION

Frequency response methods play a fundamental role in the fields of control, communications and signal processing. Classical control focuses on the frequency domain properties of control systems and has developed design methods based on simple but powerful graphical tools such as the Nyquist plot, Bode plots, and Nichols Chart. These techniques are well known and are popular with practicing engineers. However, they were developed for a fixed nominal system and in general are inapplicable when several uncertain parameters are present. In these situations it is necessary to evaluate the frequency domain behaviour of the *entire family* of systems in order to effectively carry out analysis and design.

A brute force approach to this problem (grid the uncertainty set) can be avoided by assuming a certain amount of structure for the perturbations even if such an assumption introduces some conservatism. In this chapter we shall consider the class of linear interval systems where the uncertain parameters lie in intervals and appear linearly in the numerator and denominator coefficients of the transfer functions. For

example, the family of transfer functions

$$\mathbf{G}(s) = \frac{4s^3 + \alpha_2 s^2 + \alpha_1 s + 5}{s^4 + 10\beta_3 s^3 + \beta_2 s^2 + (\beta_1 + 2\gamma_1)s}$$

where $\alpha_2, \alpha_1, \beta_3, \beta_2, \beta_1, \gamma_1$ vary in independent intervals is a linear interval system containing six interval parameters. In this example, the uncertainty template $\mathbf{G}(j\omega)$ at each frequency ω is a complex plane set generated by the parameter vector ranging over the six dimensional parameter box. With the results to be developed in this chapter we will be able to replace $\mathbf{G}(s)$ by a subset of systems $\mathbf{G}_{\mathrm{E}}(s)$. This extremal subset will allow us to constructively generate the *exact* boundary of the uncertainty template by means of a set of *one parameter* problems. These extremal systems will allow us to exactly calculate the boundaries of the Bode, Nyquist and Nichols plots of all transfer functions in the control system. They also can be used to calculate the worst case gain, phase, and parametric stability margins over the uncertain set of parameters. The utility of these concepts in control system design is illustrated by giving examples which robustify classical design techniques by incorporating parametric uncertainty.

We begin by considering an interval plant connected to a fixed feedback controller and develop the appropriate mathematical machinery for this system. The generalized Kharitonov segments introduced in Chapter 7 serve to define the extremal systems. Using these systems, we calculate the boundaries of the image sets of various system transfer functions evaluated at $s = j\omega$. These include the characteristic polynomial, open and closed loop transfer functions, sensitivity and complementary sensitivity and disturbance transfer functions. We also evaluate the worst case stability margins using these extremal systems. These results depend on some simple geometric facts regarding the sum and quotients of complex plane sets. We then generalize these results to the larger class of linear interval systems using essentially the same geometric ideas.

8.2 INTERVAL CONTROL SYSTEMS

Consider the feedback system shown in Figure 8.1 with

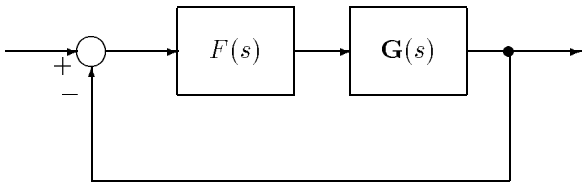

Figure 8.1. A unity feedback interval control system

$$F(s) := \frac{F_1(s)}{F_2(s)}, \qquad G(s) := \frac{N(s)}{D(s)}. \tag{8.1}$$

We suppose that $F(s)$ is fixed but $G(s)$ contains uncertain real parameters which appear as the coefficients of $N(s)$ and $D(s)$. Write

$$\begin{aligned} D(s) &:= a_0 + a_1 s + a_2 s^2 + a_3 s^3 + \cdots + a_{n-1} s^{n-1} + a_n s^n \\ N(s) &:= b_0 + b_1 s + b_2 s^2 + b_3 s^3 + \cdots + b_{m-1} s^{m-1} + b_m s^m \end{aligned} \tag{8.2}$$

where $a_k \in [a_k^-, \bar{a}_k^+]$, for $k \in \underline{n} := \{1, \cdots, n\}$ and $b_k \in [b_k^-, \bar{b}_k^+]$, for $k \in \underline{m}$. Let us define the interval polynomial sets

$$\begin{aligned} \mathbf{D}(s) &:= \{D(s) \ : \ a_0 + a_1 s + a_2 s^2 + \cdots + a_n s^n, \ a_k \in [a_k^-, a_k^+], \text{ for } \ k \in \underline{n}\} \\ \mathbf{N}(s) &:= \{N(s) \ : \ b_0 + b_1 s + b_2 s^2 + \cdots + b_m s^m, \ b_k \in [b_k^-, b_k^+], \text{ for } \ k \in \underline{m}\} \end{aligned}$$

and the corresponding set of *interval systems*:

$$\mathbf{G}(s) := \left\{ \ \frac{N(s)}{D(s)} \ : \ (N(s), D(s)) \in (\mathbf{N}(s) \mathrm{x} \mathbf{D}(s)) \ \right\}. \tag{8.3}$$

We refer to the unity feedback system in Figure 8.1 as an *interval control system.* For simplicity, we will use the notational convention

$$\mathbf{G}(s) = \frac{\mathbf{N}(s)}{\mathbf{D}(s)} \tag{8.4}$$

to denote the family (8.3). The characteristic polynomial of the system is

$$\delta(s) := F_1(s) N(s) + F_2(s) D(s) \tag{8.5}$$

and the set of system characteristic polynomials can be written as

$$\mathbf{\Delta}(s) := F_1(s) \mathbf{N}(s) + F_2(s) \mathbf{D}(s). \tag{8.6}$$

The control system is robustly stable if each polynomial in $\mathbf{\Delta}(s)$ is of the same degree and is Hurwitz. This is precisely the type of robust stability problem dealt with in the Generalized Kharitonov Theorem (GKT) of the last chapter, where we showed that Hurwitz stability of the control system over the set $\mathbf{G}(s)$ could be reduced to testing over the much smaller extremal set of systems $\mathbf{G}_{\mathrm{E}}(s)$.

Following the notation of the last chapter, let $\mathcal{K}_N(s)$ and $\mathcal{K}_D(s)$ denote Kharitonov polynomials associated with $\mathbf{N}(s)$ and $\mathbf{D}(s)$, and let $\mathcal{S}_N(s)$ and $\mathcal{S}_D(s)$ denote the corresponding sets of Kharitonov segments. Recall that these segments are pairwise convex combinations of Kharitonov polynomials sharing a common even or odd part. Define the *extremal subsets*, using the above notational convention:

$$\mathbf{G}_{\mathrm{E}}(s) := \frac{\mathcal{K}_N(s)}{\mathcal{S}_D(s)} \cup \frac{\mathcal{S}_N(s)}{\mathcal{K}_D(s)} \qquad \text{(extremal systems)} \tag{8.7}$$

$$\mathbf{G}_{\mathrm{K}}(s) := \frac{\mathcal{K}_N(s)}{\mathcal{K}_D(s)} \qquad \text{(Kharitonov systems).} \tag{8.8}$$

We shall say that $F(s)$ satisfies the *vertex condition* if the polynomials $F_i(s)$ are of the form

$$F_i(s) := s^{t_i}(a_i s + b_i)U_i(s)R_i(s), \quad i = 1, 2 \tag{8.9}$$

where t_i are nonnegative integers, a_i, b_i are arbitrary real numbers, $U_i(s)$ is an anti-Hurwitz polynomial, and $R_i(s)$ is an even or odd polynomial. We recall the result given by GKT.

Theorem 8.1 *The control system of Figure 8.1 is robustly stable that is stable for all $G(s) \in \mathbf{G}(s)$ if and only if it is stable for all $G(s) \in \mathbf{G}_{\mathrm{E}}(s)$. If in addition $F(s)$ satisfies the vertex condition, robust stability holds if the system is stable for each $G(s) \in \mathbf{G}_{\mathrm{K}}(s)$.*

The GKT thus reduces the problem of verifying robust stability over the multiparameter set $\mathbf{G}(s)$ to a set of one parameter stability problems over $\mathbf{G}_E(s)$ in general, and under the special conditions on $F(s)$ stated, to the vertex set $\mathbf{G}_K(s)$. In the rest of this chapter we shall show that the systems $\mathbf{G}_{\mathrm{E}}(s)$ and $\mathbf{G}_{\mathrm{K}}(s)$ enjoy many other useful boundary and extremal properties. They can be constructively used to carry out frequency response calculations in control system analysis and design. In fact, it will turn out that most of the important system properties such as worst case stability and performance margins over the set of uncertain parameters can be determined by replacing $G(s) \in \mathbf{G}(s)$ by the elements of $G(s) \in \mathbf{G}_{\mathrm{E}}(s)$. In some special cases one may even replace $G(s)$ by the elements of $\mathbf{G}_{\mathrm{K}}(s)$. The results are first developed for interval plants for the sake of simplicity. They hold for the more general class of linear interval systems as indicated in section 8.6.

8.3 FREQUENCY DOMAIN PROPERTIES

In order to carry out frequency response analysis and design incorporating robustness with respect to parameter uncertainty we need to be able to determine the complex plane images of various parametrized sets. In this section we will develop some computationally efficient procedures to generate such sets. We shall first consider the complex plane images of $\mathbf{\Delta}(s)$ and $\mathbf{G}(s)$ at $s = j\omega$. These sets, called uncertainty templates, are denoted $\mathbf{\Delta}(j\omega)$ and $\mathbf{G}(j\omega)$. Since $\mathbf{N}(s)$ and $\mathbf{D}(s)$ are interval families, $\mathbf{N}(j\omega)$ and $\mathbf{D}(j\omega)$ are axis parallel rectangles in the complex plane. $F_1(j\omega)\mathbf{N}(j\omega)$ and $F_2(j\omega)\mathbf{D}(j\omega)$ are likewise rotated rectangles in the complex plane. Thus $\mathbf{\Delta}(j\omega)$ is the complex plane sum of two rectangles whereas $\mathbf{G}(j\omega)$ is the quotient of two rectangles. We assume here that $0 \notin \mathbf{D}(j\omega)$. If this assumption fails to hold we can always "indent" the $j\omega$ axis to exclude those values of ω which violate the assumption. Therefore, throughout this chapter we will make the standing assumption that the denominator of any quotients exclude zero.

The next lemma will show us how to evaluate the sum and quotient of two complex plane polygons Q_1 and Q_2 with vertex sets V_1 and V_2, and edge sets E_1 and E_2, respectively. Let $\partial(\cdot)$ denote the boundary of the complex plane set $(\cdot)$.

Lemma 8.1

$$(a) \qquad \partial(Q_1 + Q_2) \subset (V_1 + E_2) \cup (E_1 + V_2)$$
$$(b) \qquad \partial\left(\frac{Q_1}{Q_2}\right) \subset \frac{E_1}{V_2} \cup \frac{V_1}{E_2}.$$

Proof. (a) From simple complex plane geometry the complex sum of two straight lines is generated by adding vertex-segment pairs. Thus the result is true for this case. For the general case it is known that $\partial(Q_1 + Q_2) \subset \partial Q_1 + \partial Q_2$. Then without loss of generality we let ∂Q_1 be an edge and ∂Q_2 be another edge and use the previous argument. This proves part (a) of the lemma.

(b) First, we establish that $z \in \partial\left(\frac{Q_1}{Q_2}\right)$ if and only if $0 \in \partial\left(Q_1 - zQ_2\right)$. Indeed if $z_0 \in \partial\left(\frac{Q_1}{Q_2}\right)$, then for every $\epsilon > 0$ the open disc $|z - z_0| < \epsilon$ contains points z such that $z \notin \frac{Q_1}{Q_2}$. Thus, $0 \notin Q_1 - zQ_2$. However, $0 \in Q_1 - z_0 Q_2$ since $z_0 \in \frac{Q_1}{Q_2}$. By continuity of $Q_1 - zQ_2$ with respect to z at z_0, it follows that $0 \in \partial(Q_1 - z_0 Q_2)$. Now suppose conversely that $0 \in \partial(Q_1 - z_0 Q_2)$. Then for every $\epsilon > 0$ the disc of radius ϵ centered at the origin contains points q such that $q \notin Q_1 - z_0 Q_2$. By continuity of the mapping $\frac{Q_1}{Q_2} \longrightarrow Q_1 - zQ_2$ with respect to z the inverse image z of the point q is close to z_0. But this point $z \notin \frac{Q_1}{Q_2}$ since $0 \notin Q_1 - zQ_2$. However, z can be chosen to be arbitrarily close to z_0. Since $z_0 \in \frac{Q_1}{Q_2}$, it follows that $z_0 \in \partial\left(\frac{Q_1}{Q_2}\right)$.

Now,

$$z \in \partial\left(\frac{Q_1}{Q_2}\right) \Longleftrightarrow 0 \in \partial(Q_1 - zQ_2) \Longleftrightarrow 0 \in (V_1 - zE_2) \cup (E_1 - zV_2)$$
$$\Longleftrightarrow z \in \frac{V_1}{E_2} \cup \frac{E_1}{V_2}. \tag{8.10}$$

♣

This lemma shows us the interesting fact that the boundaries of sums and quotients of two polygons can be determined by sums and quotients of the corresponding vertex-edge pairs. Figure 8.2 illustrates that the boundaries of the sum of two four sided polygons are obtained by generating the sum of all segment-edge pairs. Similarly, Figure 8.3 shows the sum of two general polygons.

It can be shown that the inverse image of a line segment which excludes the origin, is an arc of a circle passing through the origin (Exercise 8.4). This is shown in Figure 8.4. Therefore the inverse image of a polygon is bounded by such arcs as shown in Figure 8.5.

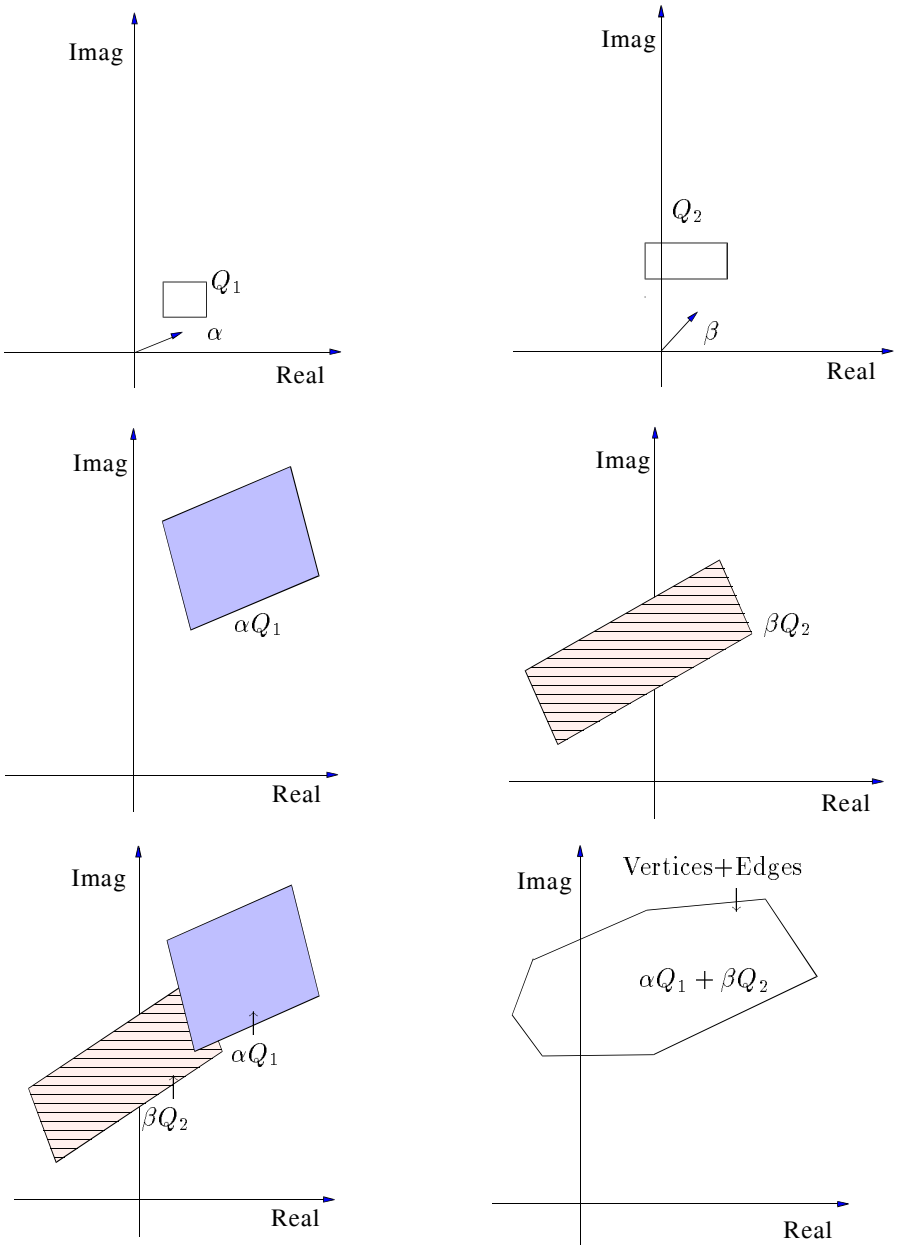

Figure 8.2. Illustration of sum of two polygons

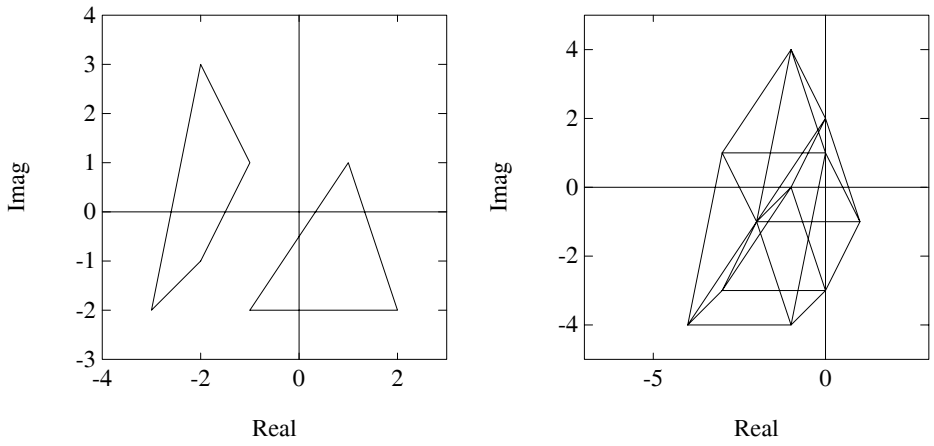

Figure 8.3. Sum of two polygons

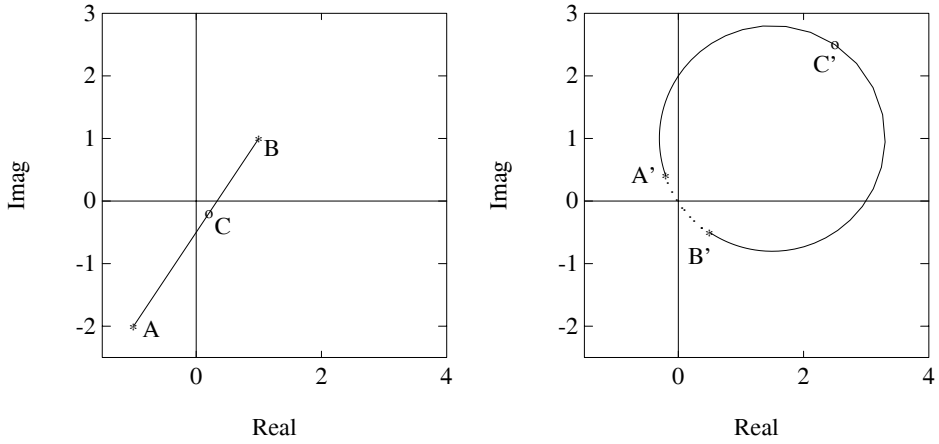

Figure 8.4. Line and inverse of line

To determine $\mathbf{\Delta}(j\omega)$ and $\mathbf{G}(j\omega)$ we note that the vertices of $\mathbf{N}(j\omega)$ and $\mathbf{D}(j\omega)$ correspond to the Kharitonov polynomials whereas the edges correspond to the Kharitonov segments. The set of points $\mathcal{K}_N(j\omega)$ are therefore the vertices of $\mathbf{N}(j\omega)$ and the four lines $\mathcal{S}_N(j\omega)$ are the edges of $\mathbf{N}(j\omega)$. $F_1(j\omega)\mathbf{N}(j\omega)$ is also a polygon with vertices $F_1(j\omega)\mathcal{K}_N(j\omega)$ and edges $F_1(j\omega)\mathcal{S}_N(j\omega)$. Similarly, $F_2(j\omega)\mathcal{K}_D(j\omega)$ and $F_2(j\omega)\mathcal{S}_D(j\omega)$ are the vertices and edges of the polygon $F_2(j\omega)\mathbf{D}(j\omega)$. The $j\omega$ image of the extremal systems $\mathbf{G}_{\mathrm{E}}(s)$ defined earlier exactly coincides with these

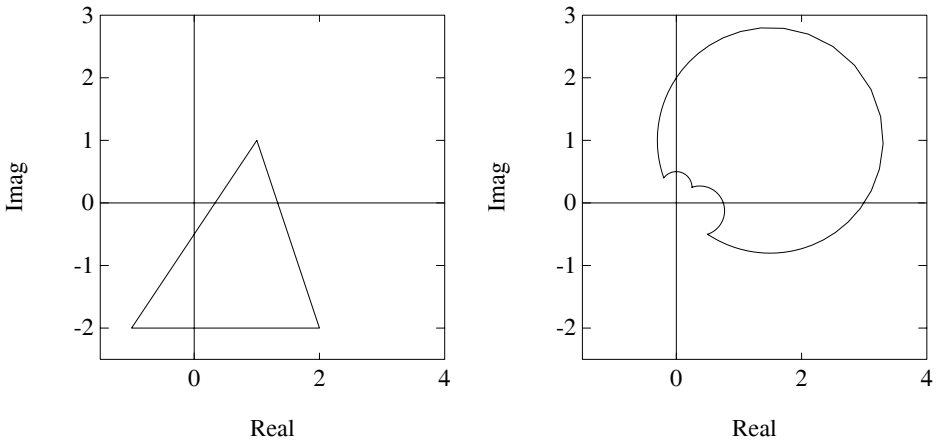

Figure 8.5. Polygon and the inverse of polygon

vertex-edge pairs. Let

$$(\mathbf{N}(s)\mathrm{x}\mathbf{D}(s))_{\mathrm{E}} := (\mathcal{K}_N(s)\mathrm{x}\mathcal{S}_D(s)) \cup (\mathcal{S}_N(s)\mathrm{x}\mathcal{K}_D(s)). \tag{8.11}$$

Recall that the *extremal systems* are

$$\mathbf{G}_{\mathrm{E}}(s) := \left\{ \frac{N(s)}{D(s)} \ : \ (N(s), D(s)) \in (\mathbf{N}(s)\mathrm{x}\mathbf{D}(s))_{\mathrm{E}} \right\} := \frac{\mathcal{K}_N(s)}{\mathcal{S}_D(s)} \cup \frac{\mathcal{S}_N(s)}{\mathcal{K}_D(s)} \tag{8.12}$$

and define

$$\mathbf{\Delta}_{\mathrm{E}}(s) := \{F_1(s)N(s) + F_2(s)D(s) \ : \ (N(s), D(s)) \in (\mathbf{N}(s)\mathrm{x}\mathbf{D}(s))_{\mathrm{E}}\}. \tag{8.13}$$

We can now state an important result regarding the boundary of image sets.

Theorem 8.2 (Boundary Generating Property)

$$\begin{aligned} a) \quad & \partial\mathbf{\Delta}(j\omega) \subset \mathbf{\Delta}_{\mathrm{E}}(j\omega) \\ b) \quad & \partial\mathbf{G}(j\omega) \subset \mathbf{G}_{\mathrm{E}}(j\omega) \end{aligned}$$

Proof. The proof of this theorem follows immediately from Lemma 8.1 and the observation regarding the vertices and edges of $\mathbf{N}(j\omega)$ and $\mathbf{D}(j\omega)$.

a) From Lemma 8.1,

$$\begin{aligned} \partial\mathbf{\Delta}(j\omega) \subset & (F_1(j\omega)\mathcal{K}_N(j\omega) + F_2(j\omega)\mathcal{S}_D(j\omega)) \\ & \cup (F_1(j\omega)\mathcal{S}_N(j\omega) + F_2(j\omega)\mathcal{K}_D(j\omega)) \\ = & \ \mathbf{\Delta}_{\mathrm{E}}(j\omega) \quad (see (8.11) \text{ and } (8.13)). \end{aligned}$$

b)

$$\begin{aligned}\partial\mathbf{G}(j\omega) &\subset \left[\frac{\mathcal{K}_N(j\omega)}{\mathcal{S}_D(j\omega)} \cup \frac{\mathcal{S}_N(j\omega)}{\mathcal{K}_D(j\omega)}\right] \\ &= \mathbf{G}_{\mathrm{E}}(j\omega) \quad (\text{see } (8.12)).\end{aligned}$$

♣

Example 8.1. Consider the problem of determining the frequency template of the interval plant

$$G(s) = \frac{n(s)}{d(s)} = \frac{b_1 s + b_0}{a_2 s^2 + a_1 s + a_0}$$

where the parameters vary as follows:

$$a_0 \in [1,2], \quad a_1 \in [2,3], \quad a_2 \in [2,3], \quad b_0 \in [1,2], \quad b_1 \in [2,3].$$

The Kharitonov polynomials of $d(s)$ and $n(s)$ are:

$$\begin{aligned}K_d^1(s) &= 3s^2 + 2s + 1 \\ K_d^2(s) &= 3s^2 + 3s + 1 \\ K_d^3(s) &= 2s^2 + 2s + 2 \\ K_d^4(s) &= 2s^2 + 3s + 2\end{aligned}$$

and

$$\begin{aligned}K_n^1(s) &= 2s + 1 \\ K_n^2(s) &= 3s + 1 \\ K_n^3(s) &= 2s + 2 \\ K_n^4(s) &= 3s + 2.\end{aligned}$$

Thus, the boundary of the entire frequency domain template is obtained by the frequency evaluation of the following 32 systems:

$$\frac{K_n^i(s)}{\lambda K_d^j(s) + (1-\lambda) K_d^k(s)}, \quad \text{and} \quad \frac{\lambda K_n^j(s) + (1-\lambda) K_n^k(s)}{K_d^i(s)},$$

for

$$i = 1,2,3,4; \quad (j,k) \in \{(1,2),(1,3),(2,3),(3,4)\}.$$

Figure 8.6 shows the template $\mathbf{G}(j\omega)$ at $\omega = 1$.

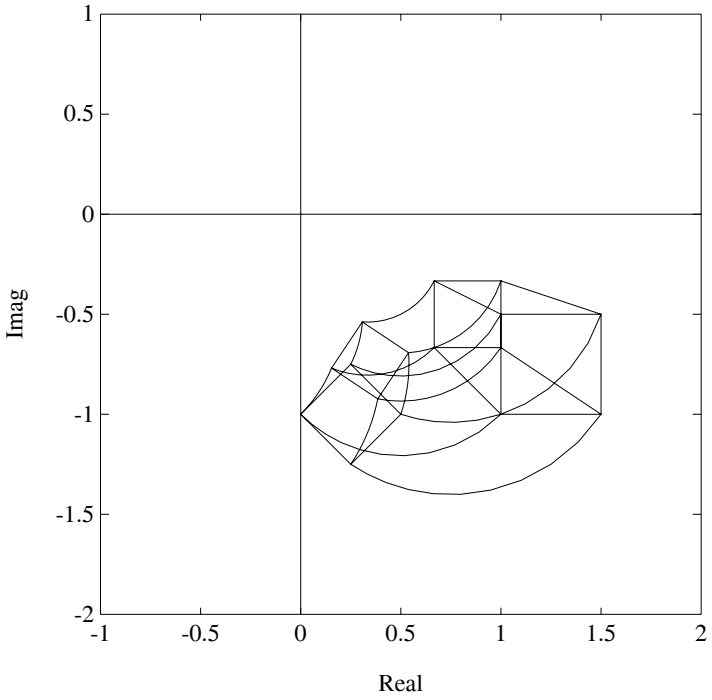

Figure 8.6. Frequency domain template $\mathbf{G}(j\omega)$ (Example 8.1)

Closed Loop Transfer Functions

Referring now to the control system in Figure 8.1, we consider the following transfer functions of interest in analysis and design problems:

$$\frac{y(s)}{u(s)} = G(s), \qquad \frac{u(s)}{e(s)} = F(s) \tag{8.14}$$

$$T^o(s) := \frac{y(s)}{e(s)} = F(s)G(s) \tag{8.15}$$

$$T^e(s) := \frac{e(s)}{r(s)} = \frac{1}{1 + F(s)G(s)} \tag{8.16}$$

$$T^u(s) := \frac{u(s)}{r(s)} = \frac{F(s)}{1 + F(s)G(s)} \tag{8.17}$$

$$T^y(s) := \frac{y(s)}{r(s)} = \frac{F(s)G(s)}{1 + F(s)G(s)}. \tag{8.18}$$

As $G(s)$ ranges over the uncertainty set $\mathbf{G}(s)$ the transfer functions $T^o(s)$, $T^y(s)$, $T^u(s)$, $T^e(s)$ range over corresponding uncertainty sets $\mathbf{T}^o(s)$, $\mathbf{T}^y(s)$, $\mathbf{T}^u(s)$, and $\mathbf{T}^e(s)$, respectively. In other words,

$$\mathbf{T}^o(s) := \{F(s)G(s) \ : \ G(s) \in \mathbf{G}(s)\} \tag{8.19}$$

$$\mathbf{T}^e(s) := \left\{ \frac{1}{1+F(s)G(s)} \ : \ G(s) \in \mathbf{G}(s) \right\} \tag{8.20}$$

$$\mathbf{T}^u(s) := \left\{ \frac{F(s)}{1+F(s)G(s)} \ : \ G(s) \in \mathbf{G}(s) \right\} \tag{8.21}$$

$$\mathbf{T}^y(s) := \left\{ \frac{F(s)G(s)}{1+F(s)G(s)} \ : \ G(s) \in \mathbf{G}(s) \right\}. \tag{8.22}$$

We will now show that the boundary generating property of the extremal subsets shown in Theorem 8.2 carries over to each of the system transfer functions listed above. In fact, we will show that the boundary of the image set at $s = j\omega$, the Nyquist plot and Bode plot boundaries of each of the above sets are all generated by the subset $\mathbf{G}_{\rm E}(s)$. Introduce the subsets of (8.19) - (8.22) obtained by replacing $\mathbf{G}(s)$ by $\mathbf{G}_{\rm E}(s)$:

$$\mathbf{T}^o_{\rm E}(s) := \{F(s)G(s) \ : \ G(s) \in \mathbf{G}_{\rm E}(s)\} \tag{8.23}$$

$$\mathbf{T}^e_{\rm E}(s) := \left\{ \frac{1}{1+F(s)G(s)} \ : \ G(s) \in \mathbf{G}_{\rm E}(s) \right\} \tag{8.24}$$

$$\mathbf{T}^u_{\rm E}(s) := \left\{ \frac{F(s)}{1+F(s)G(s)} \ : \ G(s) \in \mathbf{G}_{\rm E}(s) \right\} \tag{8.25}$$

$$\mathbf{T}^y_{\rm E}(s) := \left\{ \frac{F(s)G(s)}{1+F(s)G(s)} \ : \ G(s) \in \mathbf{G}_{\rm E}(s) \right\}. \tag{8.26}$$

The main result can now be stated.

Theorem 8.3 *For every $\omega \geq 0$,*

$$\begin{array}{ll} (a) & \partial \mathbf{T}^o(j\omega) \subset \mathbf{T}^o_{\rm E}(j\omega) \\ (b) & \partial \mathbf{T}^e(j\omega) \subset \mathbf{T}^e_{\rm E}(j\omega) \\ (c) & \partial \mathbf{T}^u(j\omega) \subset \mathbf{T}^u_{\rm E}(j\omega) \\ (d) & \partial \mathbf{T}^y(j\omega) \subset \mathbf{T}^y_{\rm E}(j\omega) \end{array}$$

The proof will require the following technical lemma.

Lemma 8.2 *Let $\mathcal{D}$ be a closed set in the complex plane with $0 \notin \mathcal{D}$. Then*

$$\partial\left(\frac{1}{\mathcal{D}}\right) = \frac{1}{\partial\mathcal{D}}. \tag{8.27}$$

Proof. Let $\frac{1}{d_0} \in \partial(\frac{1}{\mathcal{D}})$, then there exists an open disc such that $\left|\frac{1}{d} - \frac{1}{d_0}\right| < \epsilon$ for some d such that $\frac{1}{d} \notin \frac{1}{\mathcal{D}}$. This implies that $d \notin \mathcal{D}$ but $d_0 \in \mathcal{D}$. By the continuity of

the mapping with respect to d at d_0, it follows that $\frac{1}{d_0} \in \frac{1}{\partial \mathcal{D}}$. Conversely, suppose that $d_0 \in \partial \mathcal{D}$, equivalently $\frac{1}{d_0} \in \frac{1}{\partial \mathcal{D}}$. Then there exists an open disc such that $|d - d_0| < \epsilon$ for some $d \notin \mathcal{D}$. This implies that $\frac{1}{d} \notin \frac{1}{\mathcal{D}}$ while $\frac{1}{d_0} \in \frac{1}{\mathcal{D}}$. Again, by the continuity of the mapping with respect to d at d_0, we have $\frac{1}{d_0} \in \partial(\frac{1}{\mathcal{D}})$. ♣

Proof of Theorem 8.3

(a)

$$\begin{aligned}\partial \mathbf{T}^o(j\omega) &= \partial(\mathbf{G}(j\omega)F(j\omega)) = F(j\omega)\partial\mathbf{G}(j\omega) \\ &\subset F(j\omega)\mathbf{G}_{\mathrm{E}}(j\omega) = \mathbf{T}_{\mathrm{E}}(j\omega).\end{aligned}$$

(b) From Lemma 8.2,

$$\begin{aligned}\partial \mathbf{T}^e(j\omega) &= \partial\left(\frac{1}{1+\mathbf{G}(j\omega)F(j\omega)}\right) = \frac{1}{\partial(1+\mathbf{G}(j\omega)F(j\omega))} \\ &= \frac{1}{1+\partial(\mathbf{G}(j\omega)F(j\omega))}.\end{aligned}$$

Since $\partial(\mathbf{G}(j\omega)F(j\omega)) \subset \mathbf{G}_{\mathrm{E}}(j\omega)F(j\omega)$, we have $\partial \mathbf{T}^e(j\omega) \subset \mathbf{T}^e_{\mathrm{E}}(j\omega)$.

(c) Since $\mathbf{T}^u(j\omega) = F(j\omega)\mathbf{T}^e(j\omega)$ with a fixed $F(j\omega)$ for a fixed ω, the property shown in (c) carries over directly. Thus, $\partial \mathbf{T}^u(j\omega) \subset \mathbf{T}^u_{\mathrm{E}}(j\omega)$.

(d)

$$\begin{aligned}\partial \mathbf{T}^y(j\omega) &= \partial\left(\frac{1}{1+\frac{1}{F(j\omega)\mathbf{G}(j\omega)}}\right) = \frac{1}{\partial\left(1+\frac{1}{F(j\omega)\mathbf{G}(j\omega)}\right)} \\ &= \frac{1}{1+\frac{1}{F(j\omega)\partial\mathbf{G}(j\omega)}} \\ &\subset \frac{1}{1+\frac{1}{F(j\omega)\mathbf{G}_{\mathrm{E}}(j\omega)}} \\ &= \mathbf{T}^y_{\mathrm{E}}(j\omega)\end{aligned}$$

♣

Remark 8.1. This result shows that at every $\omega \geq 0$, the boundary of the image set of each transfer function in (8.19) - (8.22) is contained in the corresponding image set of the extremal systems. We point out that in the definition of the

interval plant $\mathbf{G}(s)$ we assumed that the numerator and denominator parameters were independent. This assumption obviously does not hold any longer when we deal with say, $\mathbf{T}^y(s)$ where the numerator and denominator depend on some common parameters. It is therefore useful to know that the boundary generating property of the set $\mathbf{G}_{\mathrm{E}}(s)$ carries over nevertheless. In a later section we will show that the boundary generating property of the set $\mathbf{G}_{\mathrm{E}}(s)$ will hold much more generally.

Example 8.2. Consider the system given in Example 8.1. Let us assume that $F(s) = 1$ and that we wish to calculate $\mathbf{T}^y(j\omega)$.

$$\mathbf{T}^y(s) = \left\{ \frac{G(s)}{1+G(s)} : G(s) \in \mathbf{G}(s) \right\}.$$

For this example, we have

$$T^y(s) = \frac{b_1 s + b_0}{a_2 s^2 + (a_1 + b_1)s + (a_0 + b_0)}$$

where

$$a_0 \in [1,2], \quad a_1 \in [2,3], \quad a_2 \in [2,3], \quad b_0 \in [1,2], \quad b_1 \in [2,3].$$

The denominator and numerator polynomials are dependent on some of the same perturbing parameters. However, Theorem 8.3 handles this dependency. Since $\partial \mathbf{T}^y(j\omega) \subset \mathbf{T}^y_{\mathrm{E}}(j\omega)$, it is enough to construct the following template:

$$\mathbf{T}^y_{\mathrm{E}}(j\omega) = \left\{ \frac{G(j\omega)}{1+G(j\omega)} : G(j\omega) \in \mathbf{G}_{\mathrm{E}}(j\omega) \right\}.$$

In other words, we simply replace $\mathbf{G}(s)$ by $\mathbf{G}_E(s)$ in $\mathbf{T}^y$. Thus we need to construct the image of the following transfer functions for $\lambda \in [0,1]$:

$$\frac{K_n^i(j\omega)}{\lambda K_d^k(j\omega) + (1-\lambda)K_d^l(j\omega) + K_n^i(j\omega)}$$

and

$$\frac{\lambda K_n^k(j\omega) + (1-\lambda)K_n^l(j\omega)}{\lambda K_n^k(j\omega) + (1-\lambda)K_n^l(j\omega) + K_d^i(j\omega)}$$

for $i = 1,2,3,4$ and $(k,l) \in \{(1,2),(1,3),(2,3),(3,4)\}$. The sets of Kharitonov polynomials corresponding to the denominator and numerator polynomials are defined in Example 8.1. The frequency domain template at $\omega = 1$ is shown in Figure 8.7.

8.4 NYQUIST, BODE, AND NICHOLS ENVELOPES

In the previous section we established that at a fixed frequency the image set template of various transfer function set can be constructed from the corresponding extremal transfer function set $\mathbf{G}_{\mathrm{E}}(s)$. In control system design it is important to

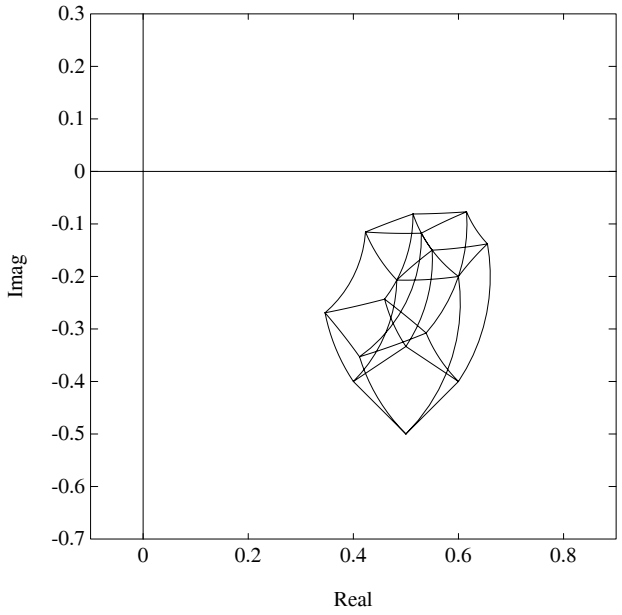

Figure 8.7. Frequency domain template $\mathbf{T}^y(j\omega)$ (Example 8.2)

see the behaviour of these transfer function families for all frequency. Denote the Nyquist plot of the family $\mathbf{G}(s)$ as

$$\mathbf{G} = \cup_{0 \leq \omega < \infty} \mathbf{G}(j\omega). \tag{8.28}$$

The boundary of $\mathbf{G}$ is the Nyquist envelope of $\mathbf{G}$. Similarly, the Nyquist plots of $\mathbf{T}^o(s)$, $\mathbf{T}^e(s)$, $\mathbf{T}^u(s)$, and $\mathbf{T}^y(s)$ are denoted respectively by $\mathbf{T}^o$, $\mathbf{T}^e$, $\mathbf{T}^u$, and $\mathbf{T}^y$. From the boundary property of Theorem 8.3, it follows that the envelopes of these Nyquist plots are generated by the extremal systems.

Theorem 8.4 (Nyquist Envelope)
The Nyquist plots of each of the transfer function sets $\mathbf{T}^o(s)$, $\mathbf{T}^y(s)$, $\mathbf{T}^u(s)$, *and* $\mathbf{T}^e(s)$ *are bounded by their corresponding extremal subsets:*

$$\begin{aligned}
&(a) \quad \partial\mathbf{G} \subset \mathbf{G}_{\mathrm{E}} \\
&(b) \quad \partial\mathbf{T}^o \subset \mathbf{T}^o_{\mathrm{E}} \\
&(c) \quad \partial\mathbf{T}^y \subset \mathbf{T}^y_{\mathrm{E}} \\
&(d) \quad \partial\mathbf{T}^u \subset \mathbf{T}^u_{\mathrm{E}} \\
&(e) \quad \partial\mathbf{T}^e \subset \mathbf{T}^e_{\mathrm{E}}.
\end{aligned} \tag{8.29}$$

The Bode envelopes of each of the system transfer functions $\mathbf{G}(s)$, $\mathbf{T}^o(s)$, $\mathbf{T}^e(s)$, $\mathbf{T}^u(s)$, and $\mathbf{T}^y(s)$ can also be constructed if we can determine the maximum and minimum values of the magnitude and phase of the family of systems at each frequency. From the boundary relations given in Theorem 8.3, it again follows that these maximum and minimum values occur over the subset $\mathbf{G}_{\mathrm{E}}(s)$. This leads us to the following result.

Theorem 8.5 (Bode Envelope)
The Bode magnitude and phase envelopes of each of the transfer function sets $\mathbf{G}(s)$, $\mathbf{T}^o(s)$, $\mathbf{T}^e(s)$, $\mathbf{T}^u(s)$, $\mathbf{T}^y(s)$ *are generated respectively by the extremal subsets,* $\mathbf{G}_{\mathrm{E}}(s)$, $\mathbf{T}^o_{\mathrm{E}}(s)$, $\mathbf{T}^e_{\mathrm{E}}(s)$, $\mathbf{T}^u_{\mathrm{E}}(s)$, $\mathbf{T}^y_{\mathrm{E}}(s)$.

It is instructive to interpret this result from the geometric point of view. Consider the Bode plot of the interval family $\mathbf{G}(s)$. For a fixed ω^*, the image of the interval transfer function is the quotient of two convex polygons in the complex plane where the polygons represent the images of the numerator and denominator polynomial families. This is depicted in Figure 8.8.

From Figure 8.8(a) and (b), we can see that the maximum and minimum magnitudes of $\mathbf{G}(j\omega^*)$ occur on one of the vertex-segment combinations of these polygons. Since the parameters in the numerator and denominator are independent we have:

$$\text{(a)} \qquad \max \left| \frac{\mathbf{N}(j\omega^*)}{\mathbf{D}(j\omega^*)} \right| = \frac{\max |\mathbf{N}(j\omega^*)|}{\min |\mathbf{D}(j\omega^*)|}$$

$$\text{(b)} \qquad \min \left| \frac{\mathbf{N}(j\omega^*)}{\mathbf{D}(j\omega^*)} \right| = \frac{\min |\mathbf{N}(j\omega^*)|}{\max |\mathbf{D}(j\omega^*)|}.$$

While the maximum magnitude always occurs at a vertex the minimum can occur on an edge. The maximum and minimum points will generate the extreme points of the Bode magnitude envelope at the frequency ω^*. On the other hand, as shown in Figure 8.8(c) and (d), the extreme points on the phase envelope are always generated by vertex-vertex pairs:

$$\text{(c)} \qquad \max \arg \frac{\mathbf{N}(j\omega^*)}{\mathbf{D}(j\omega^*)} = \max \arg \mathbf{N}(j\omega^*) - \min \arg \mathbf{D}(j\omega^*)$$

$$\text{(d)} \qquad \min \arg \frac{\mathbf{N}(j\omega^*)}{\mathbf{D}(j\omega^*)} = \min \arg \mathbf{N}(j\omega^*) - \max \arg \mathbf{D}(j\omega^*).$$

The relations given in the Theorem above are useful in constructing the Bode magnitude and phase envelopes as well as Nyquist envelopes. In classical control design techniques, the Nichols Chart is also a popular computational tool. For a fixed transfer function, the Nichols Chart is a plot of the magnitude versus the phase with frequency as a running parameter. When a family of parametrized systems is involved, we get at each frequency a *magnitude-phase template.* When this template is swept over all frequencies, we get the Nichols Envelope of the family. By using

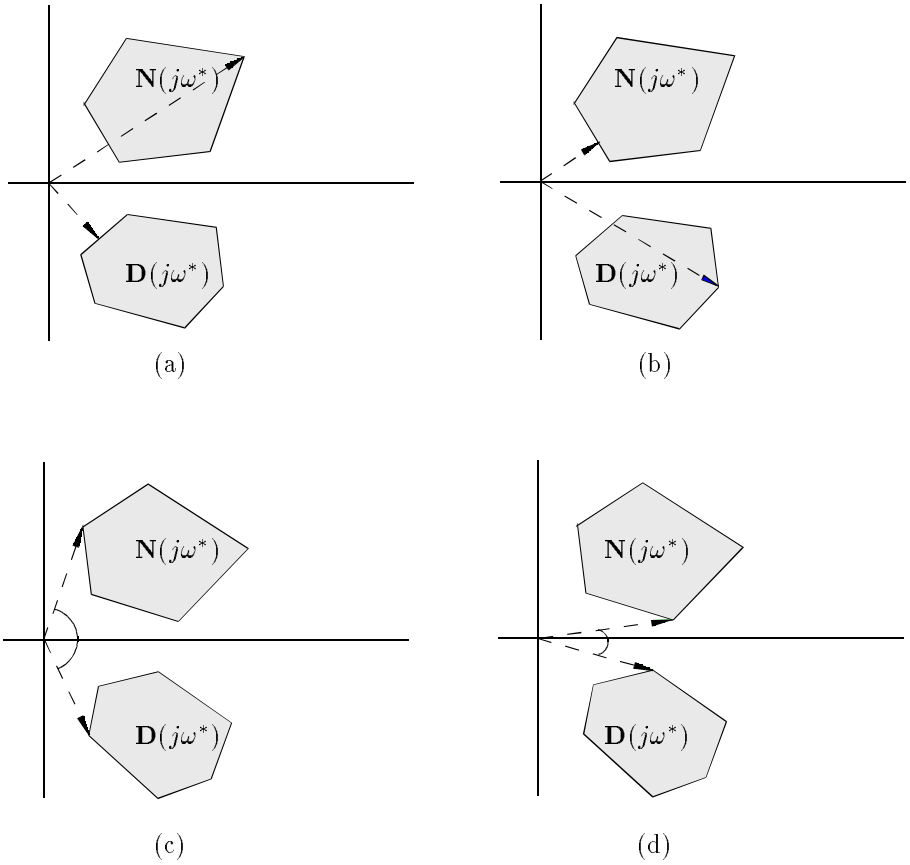

Figure 8.8. Extremal magnitude and phase of $\mathbf{N}(j\omega^*)$ and $\mathbf{D}(j\omega^*)$

the boundary property of Theorem 8.3 it can be seen that the Nichols Envelope is also generated by the extremal systems.

Theorem 8.6 (Nichols Envelope)
The Nichols Envelope of each of the transfer function sets $\mathbf{G}(s)$, $\mathbf{T}^o(s)$, $\mathbf{T}^e(s)$, $\mathbf{T}^u(s)$, $\mathbf{T}^y(s)$ *are generated respectively by the extremal subsets,* $\mathbf{G}_{\mathrm{E}}(s)$, $\mathbf{T}^o_{\mathrm{E}}(s)$, $\mathbf{T}^e_{\mathrm{E}}(s)$, $\mathbf{T}^u_{\mathrm{E}}(s)$, $\mathbf{T}^y_{\mathrm{E}}(s)$.

The Nichols template is obtained by mapping the points of the Nyquist plane (see Figure 8.9) into the Nichols plane (see Figure 8.10). This gives the exact Nichols template. The Nichols envelope can also be generated approximately from the Bode magnitude and phase envelopes of the family. At each frequency we draw

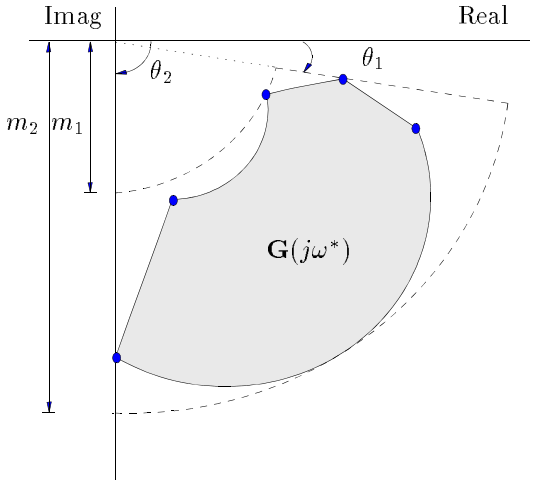

Figure 8.9. A Nyquist template

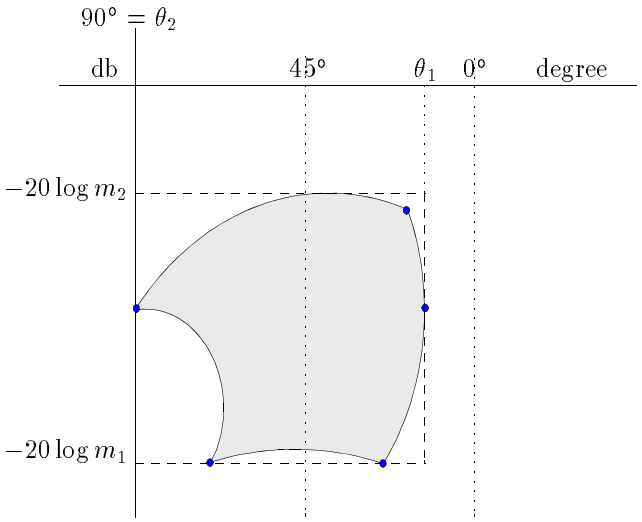

Figure 8.10. A Nichols template

a rectangle in the magnitude-phase plane (Nichols plane). The dashed rectangle shown in Figure 8.10 corresponds to the magnitude and phase ranges obtained from the Bode envelopes. When these overbounded images of $\mathbf{G}(j\omega)$ templates are swept over frequency, we obtain the approximate Nichols envelope which contains the actual envelope. We illustrate these computations with an example.

Example 8.3. Consider the plant and controller

$$G(s) = \frac{b_1 s + b_0}{a_2 s^2 + a_1 s + a_0} \qquad C(s) = \frac{s^2 + 2s + 1}{s^4 + 2s^3 + 2s^2 + s}$$

where the plant parameters vary as

$$b_1 \in [0.1, 0.2], \quad b_0 \in [0.9, 1.1]$$
$$a_2 \in [0.9, 1.0], \quad a_1 \in [1.8, 2.0], \quad a_0 \in [1.9, 2.1].$$

Figures 8.11, 8.12, and 8.13 show the frequency domain plots for this example.

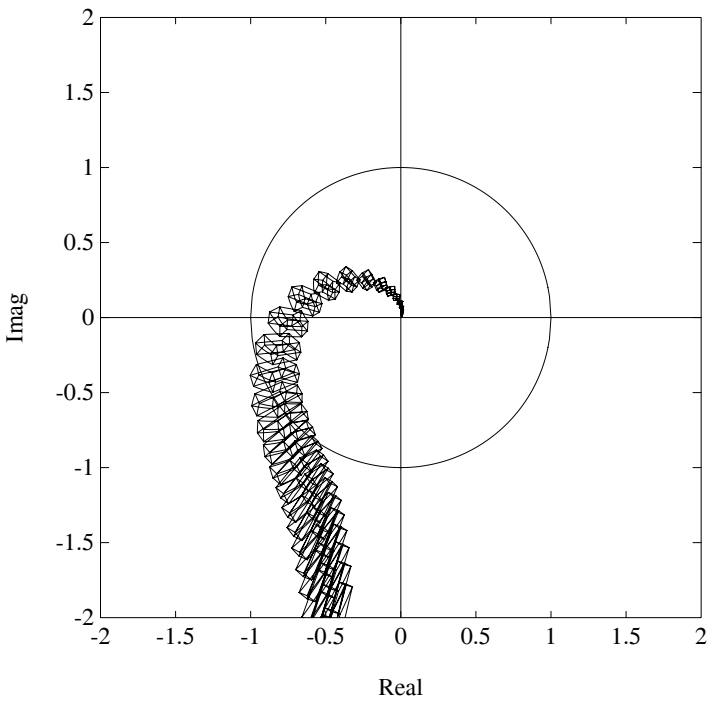

Figure 8.11. Nyquist templates (Example 8.3)

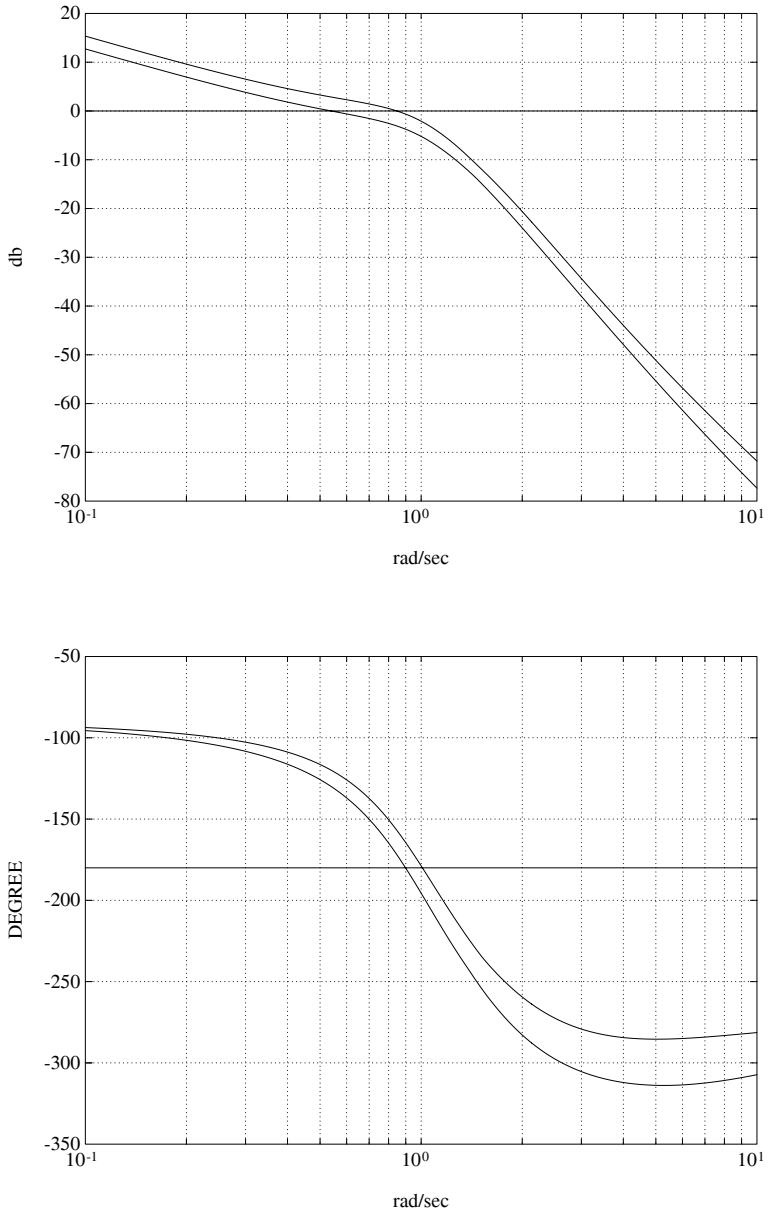

Figure 8.12. Bode envelopes (Example 8.3)

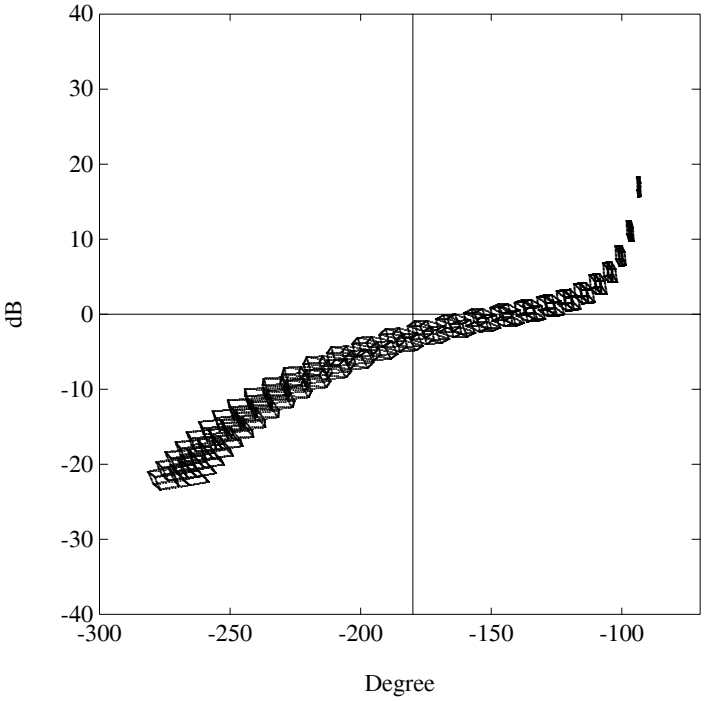

Figure 8.13. Nichols envelope (Example 8.3)

Conservatism of the Envelopes

For a fixed system, all of the above three frequency plots provide the same information on the system. However, for the case of a parametrized family of systems, the situation is quite different. The Nyquist and Nichols plots of a fixed system can be regarded as a string in the Nyquist or Nichols plane. For a parametrized family of systems, the Nyquist or Nichols plots therefore consists of a family of strings. However, the envelope of the plot is, in general, not a string that belongs to the family. In other words, there is no system in the family which generates the entire boundary of the envelope itself. On the other hand, every point on the boundary of the envelope has a string passing through it as shown in Figures 8.14 and 8.15.

The Bode envelopes in fact correspond to an overbound of the image of the complex plane set $\mathbf{G}(j\omega)$ at each frequency ω. Considering Figure 8.16, we also see that each point on the boundaries of the envelopes came from a true member system of the family. From the Bode envelopes, we notice that the smallest gain margin of the family is K. However, the member system passing through the "•" point in the magnitude plot does not correspond to the phase crossover point "•"

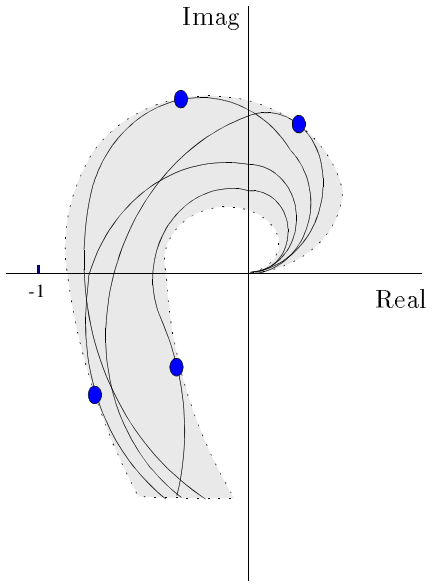

Figure 8.14. Nyquist envelope and Nyquist plots of individual member systems

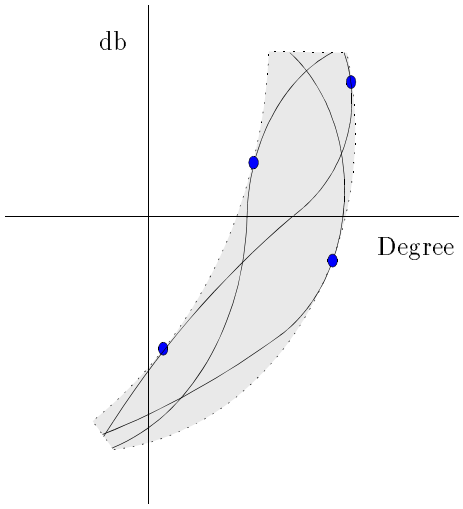

Figure 8.15. Nichols envelope and Nichols plots of individual member systems

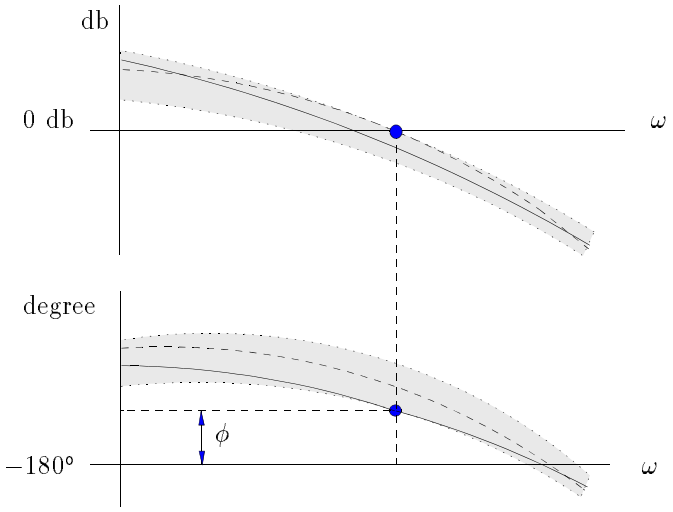

Figure 8.16. Bode envelopes and guaranteed phase margin

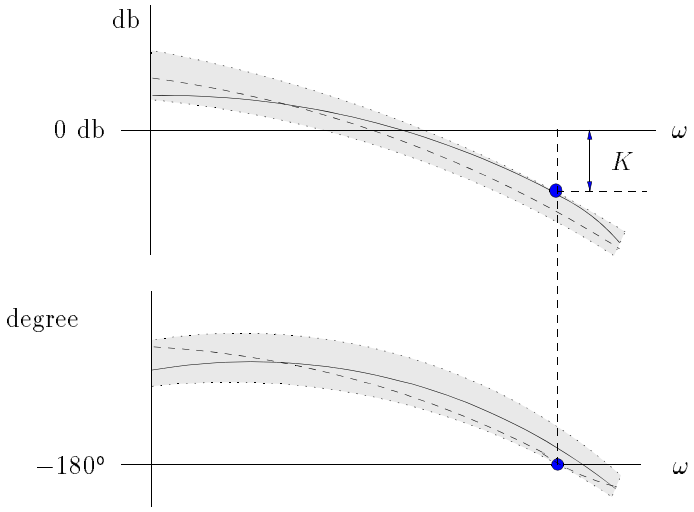

Figure 8.17. Bode envelopes and guaranteed gain margin

in the phase plot. Due to this phenomena, the true smallest gain margin might be bigger than K. A similar argument can be made for the case of the smallest phase margin (see Figure 8.17). This is because of the *independent* evaluation of the magnitude and phase envelopes of the family. In other words, despite the fact that each point on the boundaries of the Bode magnitude and phase envelopes, comes from some parameter in the family, the latter envelopes taken jointly, represent only the approximate set which corresponds to the dashed box in Figure 8.10 and equivalently, the dashed portion of the disc in Figure 8.9. Therefore, the smallest gain and phase margins read from the Bode envelopes would be conservative, with the degree of conservatism depending upon how big the actual image inside the dashed box is (see Figure 8.10).

Remark 8.2. The above boundary results remain valid if $F_i(s)$ are complex functions rather than real polynomials. This is useful in applications. For example, in systems containing time-delay $F_i(s)$ could contain terms such as e^{-Ts}. Also many robust performance problems reduce to verifying robust stability under real parameter perturbations using complex compensators.

8.5 EXTREMAL STABILITY MARGINS

In this section, we deal with the calculation of guaranteed stability margins. We will first consider the gain and phase margins at the loop breaking point "m" shown in Figure 8.18. When $G(s)$ contains parameter uncertainty the worst case values of

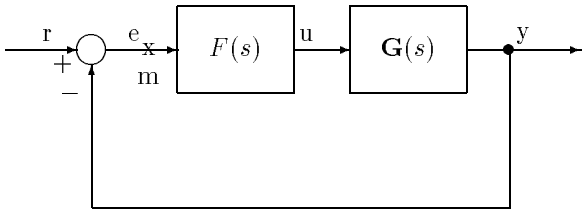

Figure 8.18. A unity feedback system

gain and phase margins over the parameter uncertainty set are important measures of robust performance. We show that these worst case margins in fact occur over the subset of extremal plants $\mathbf{G}_{\mathrm{E}}(s)$.

8.5.1 Guaranteed Gain and Phase Margins

Suppose that $F(s)$ robustly stabilizes the family $\mathbf{G}(s)$. The gain margin of the system for a fixed $G(s) \in \mathbf{G}(s)$ is defined to be the smallest value K_G for which

$$(1+K)F_1(s)N(s) + F_2(s)D(s)$$

remains stable for all $K \in [0, K_G)$. Similarly, the phase margin of the system for a fixed $G(s) \in \mathbf{G}(s)$ is defined to be the smallest value θ_G for which

$$e^{j\theta}F_1(s)N(s) + F_2(s)D(s)$$

remains stable for all $\theta \in [0, \theta_G)$. The worst case gain and phase margins are:

$$K^* := \inf_{G(s)\in\mathbf{G}(s)} K_G \qquad \theta^* := \inf_{G(s)\in\mathbf{G}(s)} \theta_G. \tag{8.30}$$

Theorem 8.7 (Extremal Gain and Phase Margin)

I)

$$K^* = \inf_{G(s)\in\mathbf{G}_{\mathrm{E}}(s)} K_G, \qquad \theta^* = \inf_{G(s)\in\mathbf{G}_{\mathrm{E}}(s)} \theta_G.$$

II) If $F_i(s)$ are real and satisfy the vertex conditions specified in part II of GKT, then we have

$$K^* = \inf_{G(s)\in\mathbf{G}_{\mathrm{K}}(s)} K_G$$

The proof of this theorem readily follows from the fact that $\mathbf{\Delta}(j\omega)$ and $\mathbf{\Delta}_{\mathrm{E}}(j\omega)$ share identical boundaries. Moreover, when $F_i(s)$ satisfy the vertex conditions the proof follows from the fact that $\mathbf{\Delta}(s)$ is stable if and only if $\mathbf{\Delta}_{\mathrm{K}}(s)$ is stable.

8.5.2 Worst Case Parametric Stability Margin

We now consider the worst case parametric stability margin. We assume as before that $F(s)$ robustly stabilizes $\mathbf{G}(s)$. The parameter $\mathbf{p}$ of dimension t consists of the coefficients of $\mathbf{N}(s)$ and $\mathbf{D}(s)$ and varies in the hypercube $\mathbf{\Pi}$. We will rewrite $\delta(s)$ in (8.5) as $\delta(s, \mathbf{p})$ to emphasize its dependence on the parameter $\mathbf{p}$. Let $\mathbf{\Pi}_{\mathrm{E}}$ denote the parameter subset of $\mathbf{\Pi}$ corresponding to the extremal systems $\mathbf{G}_{\mathrm{E}}(s)$. Let $\mathbf{\Pi}_{\mathrm{K}}$ denote the parameter subset of $\mathbf{\Pi}$ corresponding to the extremal systems $\mathbf{G}_{\mathrm{K}}(s)$.

Let $\|\cdot\|$ denote any norm in $\mathbb{R}^t$ and let $\mathcal{P}_u$ denote the set of points $\mathbf{u}$ in $\mathbb{R}^t$ for which $\delta(s, \mathbf{u})$ is unstable or loses degree (relative to its generic degree over $\mathbf{\Pi}$). Let

$$\rho(\mathbf{p}) = \inf_{\mathbf{u}\in\mathcal{P}_u} \|\mathbf{p} - \mathbf{u}\|_p$$

denote the radius of the stability ball (measured in the norm $\|\cdot\|$) and centered at the point $\mathbf{p}$. This number serves as the stability margin associated with the point $\mathbf{p}$ and indicates its distance from instability. If the box $\mathbf{\Pi}$ is stable we can associate

a stability margin, denoted $\rho(\mathbf{p})$, with each point in $\mathbf{\Pi}$. A natural question to ask then is: What is the worst case value of the parametric stability margin over $\mathbf{\Pi}$ and what is the point where it occurs? An answer to this question gives an indication of how close one can get to instability over the box $\mathbf{\Pi}$.

Define a mapping from $\mathbf{\Pi}$ to the set of all positive real numbers:

$$\begin{aligned} \mathbf{\Pi} &\xrightarrow{\rho} \mathcal{R}^+\backslash\{0\} \\ \mathbf{p} &\longrightarrow \rho(\mathbf{p}) \end{aligned}$$

Our question stated in terms of functions is: Has the function $\rho(\mathbf{p})$ a minimum and is there a precise point in $\mathbf{\Pi}$ where it is reached? The answer is provided by the following theorem:

Theorem 8.8 (Extremal Parametric Stability Margin)

I) The minimum value over $\mathbf{\Pi}$ *of* $\rho(\mathbf{p})$ *is reached at a point on the extremal set* $\mathbf{\Pi}_{\rm E}$.

II) If $F_i(s)$ *satisfy the vertex conditions, the minimum value of* $\rho(\mathbf{p})$ *is reached at a point on the extremal set* $\mathbf{\Pi}_{\rm K}$.

Proof. The theorem amounts to proving that

$$\inf_{\mathbf{p}\in\mathbf{\Pi}} \rho(\mathbf{p}) = \inf_{\mathbf{p}\in\mathbf{\Pi}_{\rm E}} \rho(\mathbf{p}).$$

Since $\mathbf{\Delta}(j\omega)$ and $\mathbf{\Delta}_E(j\omega)$ have the same boundary,

$$\begin{aligned} \inf_{\mathbf{p}\in\mathbf{\Pi}} \rho(\mathbf{p}) &= \inf_{\mathbf{p}\in\mathbf{\Pi}} \inf_{\mathbf{u}\in\mathcal{P}_u} \|\mathbf{p}-\mathbf{u}\|_p \\ &= \inf\{\|\mathbf{a}\| \ : \ \delta(j\omega, \mathbf{p}+\mathbf{a}) = 0, \mathbf{p}\in\mathbf{\Pi}, \omega\in[-\infty,+\infty]\} \\ &= \inf\{\|\mathbf{a}\| \ : \ \delta(j\omega, \mathbf{p}+\mathbf{a}) = 0, \mathbf{p}\in\mathbf{\Pi}_{\rm E}, \omega\in[-\infty,+\infty]\} \\ &= \inf_{\mathbf{p}\in\mathbf{\Pi}_{\rm E}} \inf_{\mathbf{u}\in\mathcal{P}_u} \|\mathbf{p}-\mathbf{u}\|_p \\ &= \inf_{\mathbf{p}\in\mathbf{\Pi}_{\rm E}} \rho(\mathbf{p}). \end{aligned} \tag{8.31}$$

The proof of part II is identical. ♣

Example 8.4. Consider the unity feedback control system with

$$G(s) = \frac{a_1 s + a_0}{b_2 s^2 + b_1 s + b_0}$$

and

$$F(s) = \frac{s^2 + 2s + 1}{s^4 + 2s^3 + 2s^2 + s}$$

where

$$a_1 \in [0.15-\epsilon, 0.15+\epsilon], \quad a_0 \in [1-\epsilon, 1+\epsilon],$$
$$b_2 \in [0.95-\epsilon, 0.95+\epsilon], \quad b_1 \in [1.9-\epsilon, 1.9+\epsilon], \quad b_0 \in [2-\epsilon, 2+\epsilon].$$

We wish to find the largest excursion of parameters allowed or equivalently the maximum value of ϵ for which closed loop stability is preserved. The image set plot at $\epsilon = 0.128$, shown in Figure 8.19, reveals that the phase difference reaches 180° at $\epsilon \approx 0.128$ (Figure 8.20). It is clear that any value of ϵ smaller than 0.128 results in smaller image sets than the ones shown in Figure 8.19. Moreover, if we sweep the frequency the connected image sets will form an envelope which does not contain the origin for $\epsilon = 0.128$. Therefore, an envelope corresponding to any value of ϵ smaller than 0.128 cannot contain the origin. Thus, we conclude that the feedback system remains stable under the perturbations bounded by this maximum value of ϵ.

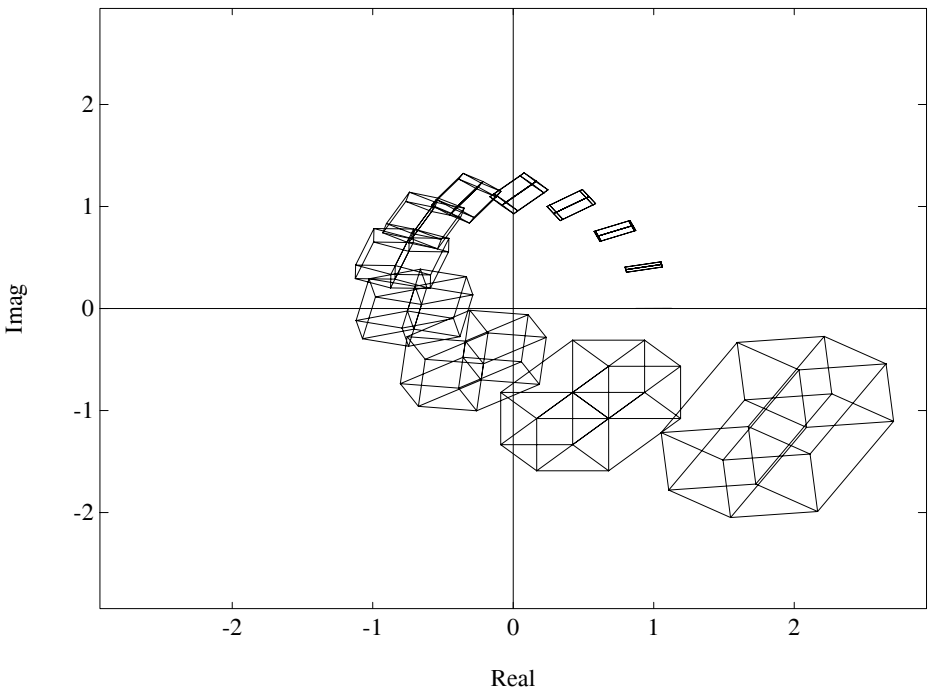

Figure 8.19. Image set plot at $\epsilon = 0.128$ (Example 8.4)

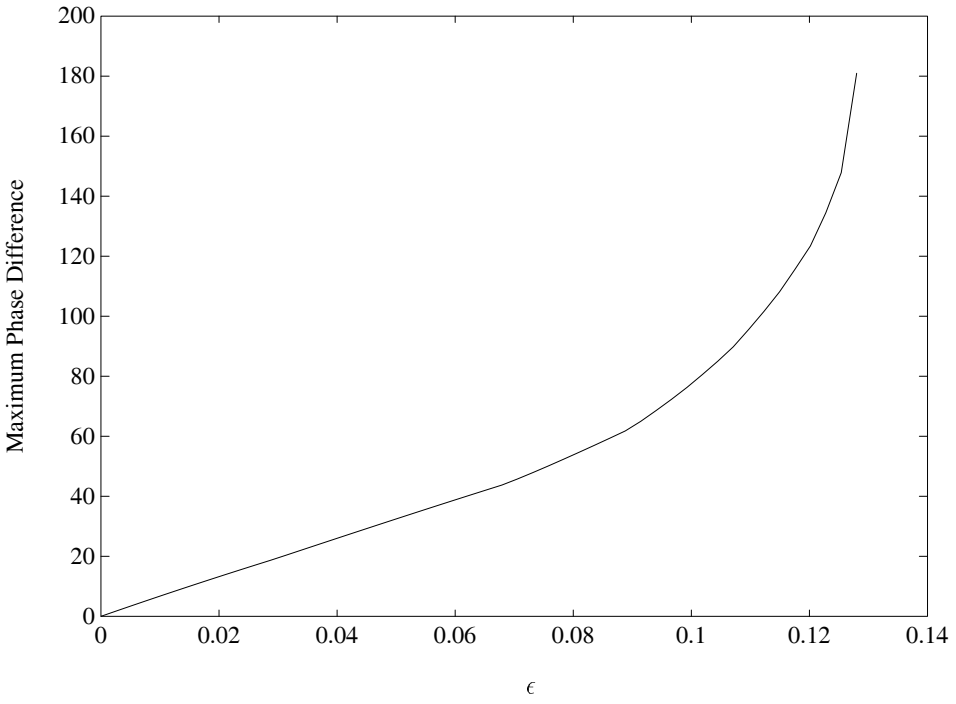

Figure 8.20. Phase plot (Example 8.4)

8.6 LINEAR INTERVAL CONTROL SYSTEMS

The results given so far in this chapter assume that $\mathbf{G}(s)$ is an interval plant, namely the ratio of interval polynomials. Each of the results given shows that a particular calculation involving $\mathbf{G}(\cdot)$ can be replaced by the corresponding calculation over the one parameter subsets $\mathbf{G}_{\mathrm{E}}(\cdot)$. This sort of simplification actually carries over to the more general class of *linear interval systems* $\mathbf{G}(s)$ defined below. Instead of repeating all the previous results, we show in this section how to construct the extremal subsets $\mathbf{G}_{\mathrm{E}}(s)$ and leave the details of the proofs to the reader.

We still consider the unity feedback system shown in Figure 8.1 with

$$F(s) := \frac{F_1(s)}{F_2(s)}, \qquad G(s) := \frac{N(s)}{D(s)}. \tag{8.32}$$

We suppose that $F(s)$ is fixed, $G(s)$ is subject to parametric uncertainty and is now

of the form

$$\begin{aligned} N(s) &:= L_1(s)A_1(s) + L_2(s)A_2(s) + \cdots + L_u(s)A_u(s) \\ D(s) &:= M_1(s)B_1(s) + M_2(s)B_2(s) + \cdots + M_v(s)B_v(s) \end{aligned} \tag{8.33}$$

with $A_i(s)$ and $B_j(s)$ being *independent* interval polynomials. Write

$$\begin{aligned} A_i(s) &:= a_0^i + a_1^i s + a_2^i s^2 + a_3^i s^3 + \cdots + a_{n_i-1}^i s^{n_i-1} + a_{n_i} s^{n_i} \\ B_j(s) &:= b_0^j + b_1^j s + b_2^j s^2 + b_3^j s^3 + \cdots + b_{d_j-1}^j s^{d_j-1} + b_{d_j}^j s^{d_j} \end{aligned} \tag{8.34}$$

where $a_k^i \in [a_k^{i-}, a_k^{i+}]$, for $k \in \underline{n_i}$ and $b_k^j \in [b_k^{j-}, b_k^{j+}]$, for $k \in \underline{d_j}$, and $L_i(s)$ and $M_j(s)$ are fixed polynomials in s. Let

$$\underline{A}(s) := [A_1(s), A_2(s), \cdots, A_u(s)], \quad \underline{B}(s) := [B_1(s), B_2(s), \cdots, B_v(s)]. \tag{8.35}$$

Let us define the sets

$$\begin{aligned} \mathbf{A}_i(s) &:= \{A_i(s) \ : \ a_0^i + a_1^i s + a_2^i s^2 + \cdots + a_{n_i}^i s^{n_i}, \ a_k^i \in [a_k^{i-}, a_k^{i+}], \text{ for } k \in \underline{n_i}\} \\ \mathbf{B}_j(s) &:= \{B_j(s) \ : \ b_0^j + b_1^j s + b_2^j s^2 + \cdots + b_{d_j}^j s^{d_j}, \ b_k^j \in [b_k^{j-}, b_k^{j+}], \text{ for } k \in \underline{d_j}\} \end{aligned}$$

$$\mathbf{N}(s) := \left\{ \sum_{i=1}^{u} L_i(s)A_i(s) \ : \ (A_1(s), \cdots, A_u(s)) \in \mathbf{A}_1(s) \times \cdots \times \mathbf{A}_u(s) \right\}$$

$$\mathbf{D}(s) := \left\{ \sum_{i=1}^{v} M_i(s)B_i(s) \ : \ (B_1(s), \cdots, B_v(s)) \in \mathbf{B}_1(s) \times \cdots \times \mathbf{B}_v(s) \right\}$$

and the corresponding set of uncertain systems

$$\mathbf{G}(s) := \left\{ \frac{N(s)}{D(s)} \ : \ (N(s), D(s)) \in (\mathbf{N}(s) \mathrm{x} \mathbf{D}(s)) \right\} := \frac{\mathbf{N}(s)}{\mathbf{D}(s)} \tag{8.36}$$

is called a *linear interval system*. The Kharitonov polynomials and segments associated with $\mathbf{A}_i(s)$ are denoted $\mathcal{K}_{A_i}(s)$ and $\mathcal{S}_{A_i}(s)$, respectively. $\mathcal{K}_{B_k}(s)$ and $\mathcal{S}_{B_k}(s)$ are defined similarly. Now let us define

$$\mathbf{A}_{\mathrm{K}}(s) := \mathcal{K}_{A_1}(s) \times \cdots \times \mathcal{K}_{A_u}(s), \qquad \mathbf{B}_{\mathrm{K}}(s) := \mathcal{K}_{B_1}(s) \times \cdots \times \mathcal{K}_{B_v}(s) \tag{8.37}$$

and

$$\begin{aligned} \mathbf{A}_{\mathrm{E}}^k(s) &:= \mathcal{K}_{A_1}(s) \times \cdots \times \mathcal{K}_{A_{k-1}}(s) \times \mathcal{S}_{A_k}(s) \times \mathcal{K}_{A_{k+1}}(s) \cdots \times \mathcal{K}_{A_u}(s), \\ \mathbf{B}_{\mathrm{E}}^j(s) &:= \mathcal{K}_{B_1}(s) \times \cdots \times \mathcal{K}_{B_{j-1}}(s) \times \mathcal{S}_{B_j}(s) \times \mathcal{K}_{B_{j+1}}(s) \cdots \times \mathcal{K}_{B_v}(s) \end{aligned} \tag{8.38}$$

for $k \in \underline{u}$ and $j \in \underline{v}$. Let

$$\mathbf{A}_{\mathrm{E}}(s) := \cup_{i=1}^{u} \mathbf{A}_{\mathrm{E}}^i(s), \qquad \mathbf{B}_{\mathrm{E}}(s) := \cup_{i=1}^{v} \mathbf{B}_{\mathrm{E}}^i(s). \tag{8.39}$$

Now introduce

$$\mathbf{N}_{\mathrm{K}}(s) := \left\{ N(s) \ : \ N(s) = \sum L_i(s)A_i(s), (A_1(s), \cdots, A_u(s)) \in \mathbf{A}_{\mathrm{K}}(s) \right\}$$
$$\mathbf{N}_{\mathrm{E}}(s) := \left\{ N(s) \ : \ N(s) = \sum L_i(s)A_i(s), (A_1(s), \cdots, A_u(s)) \in \mathbf{A}_{\mathrm{E}}(s) \right\} \quad (8.40)$$

Similar definitions hold for $\mathbf{D}_{\mathrm{K}}(s)$ and $\mathbf{D}_{\mathrm{E}}(s)$, and the extremal subsets are:

$$(\mathbf{N}(s)\mathrm{x}\mathbf{D}(s))_{\mathrm{E}} := (\mathbf{N}_{\mathrm{K}}(s)\mathrm{x}\mathbf{D}_{\mathrm{E}}(s)) \cup (\mathbf{N}_{\mathrm{E}}(s)\mathrm{x}\mathbf{D}_{\mathrm{K}}(s)). \quad (8.41)$$

The extremal subset of the family $\mathbf{G}(s)$ is:

$$\mathbf{G}_{\mathrm{E}}(s) := \left\{ \frac{N(s)}{D(s)} \ : \ (N(s), D(s)) \in (\mathbf{N}(s)\mathrm{x}\mathbf{D}(s))_{\mathrm{E}} \right\} := \frac{\mathbf{N}_{\mathrm{K}}(s)}{\mathbf{D}_{\mathrm{E}}(s)} \cup \frac{\mathbf{N}_{\mathrm{E}}(s)}{\mathbf{D}_{\mathrm{K}}(s)}. \quad (8.42)$$

In words the extremal set is obtained by fixing all the A_i, B_j at Kharitonov vertices except one and letting this one range over the Kharitonov segments. We remark here that in the more general case where some of the A_i and B_j happen to be identical the same procedure for constructing the extremal subset will work except that this constraint must be imposed on $\mathbf{G}_{\mathrm{E}}(s)$.

With the above definitions we can verify that $\mathbf{N}(j\omega)$ and $\mathbf{D}(j\omega)$ are polygons. The vertices of $\mathbf{N}(j\omega)$ are contained in the set $\mathbf{N}_{\mathrm{K}}(j\omega)$ and the edges of $\mathbf{N}(j\omega)$ are contained in $\mathbf{N}_{\mathrm{E}}(j\omega)$. Similar relations hold for $\mathbf{D}(j\omega)$. From this, it follows easily that for the class of linear interval systems $\mathbf{G}(s)$ defined in (8.33) - (8.36) each of the statements given in Theorems 8.1 - 8.8 remains valid with $\mathbf{G}_{\mathrm{E}}(s)$ defined as in (8.42). The conditions are constructive because here again $\mathbf{G}_{\mathrm{E}}(s)$ is a set of one parameter families. We illustrate the above calculations in the example below.

Example 8.5. Consider the linear interval system

$$G(s) = \frac{L_1(s)A_1(s)}{M_1(s)B_1(s) + M_2(s)B_2(s)} = \frac{5(\gamma_1 s + \gamma_0)}{s(\alpha_3 s^3 + \alpha_2 s^2) + (\beta_2 s^2 + \beta_1 s)}$$

where

$$\gamma_1 \in [0.40, 1.60], \quad \gamma_0 \in [19.40, 20.60], \quad \alpha_3 \in [0.40, 1.60],$$
$$\alpha_2 \in [7.40, 8.60], \quad \beta_2 \in [31.4, 32.6], \quad \beta_1 \in [74.45, 75.65].$$

Here, we illustrate the construction of Bode, Nyquist, and Nichols templates. First we write the Kharitonov polynomials of $A_1(s)$, $B_1(s)$, and $B_2(s)$:

$$K^1_{A_1}(s) = 1.6s^3 + 8.6s^2 \qquad K^2_{A_1}(s) = 0.4s^3 + 8.6s^2$$
$$K^3_{A_1}(s) = 1.6s^3 + 7.4s^2 \qquad K^4_{A_1}(s) = 0.4s^3 + 7.4s^2$$
$$K^1_{B_1}(s) = 32.6s^2 + 74.45s \qquad K^2_{B_1}(s) = 32.6s^2 + 75.65s$$
$$K^3_{B_1}(s) = 31.4s^2 + 74.45s \qquad K^4_{B_1}(s) = 31.4s^2 + 75.65s$$
$$K^1_{B_2}(s) = 0.4s + 19.4s \qquad K^2_{B_2}(s) = 1.6s^2 + 19.4s$$
$$K^3_{B_2}(s) = 0.4s^2 + 20.6s \qquad K^4_{B_1}(s) = 1.6s^2 + 20.6s$$

Then the extremal systems we will deal with are

$$\frac{L_1(s)\left(\lambda K^i_{A_1}(s)+(1-\lambda)K^k_{A_1}(s)\right)}{M_1(s)K^l_{B_1}(s)+M_2(s)K^j_{B_2}(s)},$$

$$\frac{L_1(s)K^i_{A_1}(s)}{M_1(s)\left(\lambda K^k_{B_1}(s)+(1-\lambda)K^l_{B_1}(s)\right)+M_2(s)K^j_{B_2}(s)},$$

$$\frac{L_1(s)K^i_{A_1}(s)}{M_1(s)K^j_{B_1}(s)+M_2(s)\left(\lambda K^k_{B_2}(s)+(1-\lambda)K^l_{B_2}(s)\right)},$$

for

$$i,j=1,2,3,4;\quad (k,l)\in\{(1,2),(1,3),(2,4),(3,4)\}.$$

Figures 8.21, 8.22 and 8.23 show the Nyquist, Bode and Nichols envelopes of the system respectively.

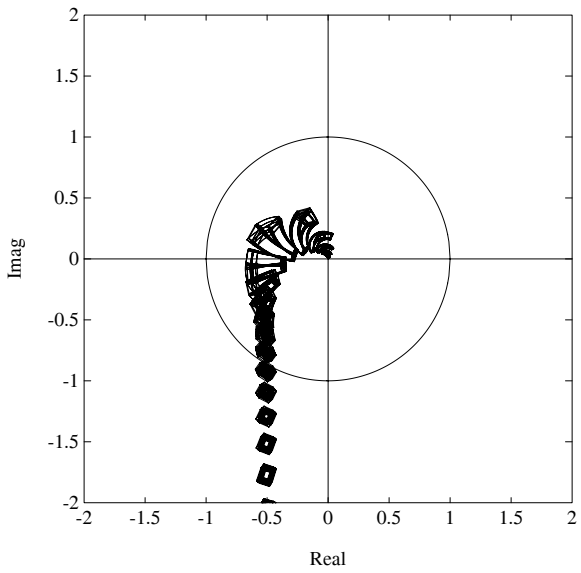

Figure 8.21. Nyquist templates of linear interval system (Example 8.5)

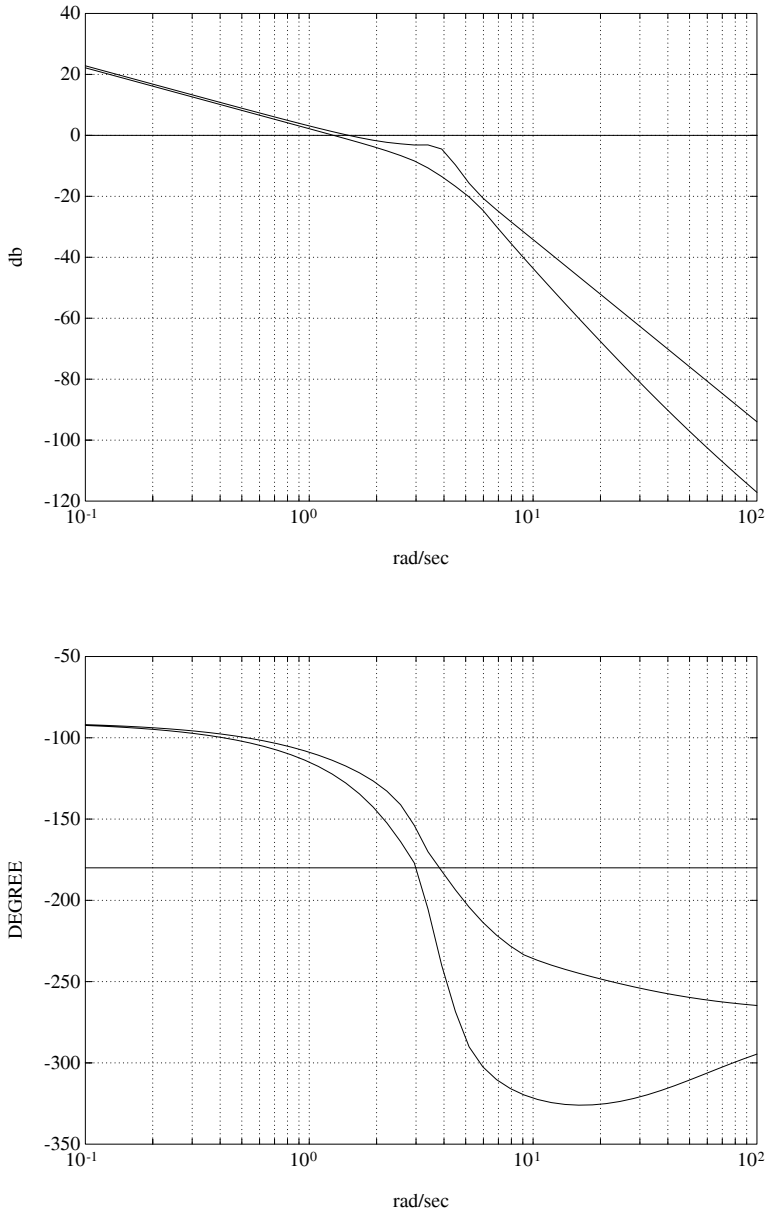

Figure 8.22. Bode envelopes of linear interval system (Example 8.5)

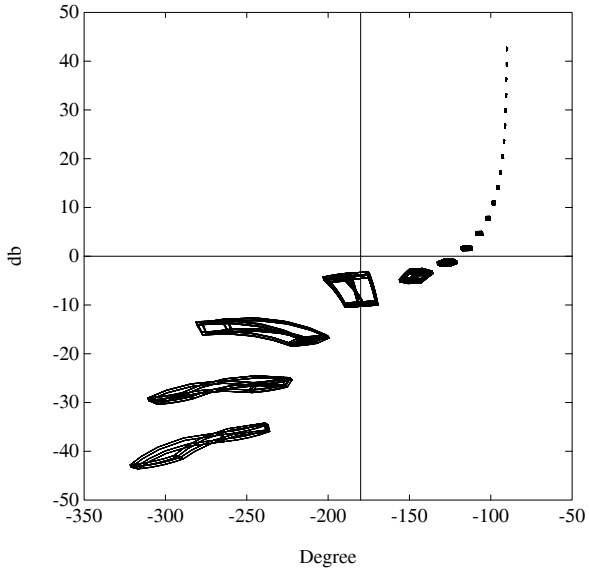

Figure 8.23. Nichols templates of linear interval system (Example 8.5)

8.7 POLYTOPIC SYSTEMS

In many models containing parametric uncertainty the only convenient representation is one where each independent parameter is explicitly displayed. In this case, we write

$$G(s) := \frac{a_1 L_1(s) + a_2 L_2(s) + \cdots + a_u L_u(s)}{b_1 M_1(s) + b_2 M_2(s) + \cdots + b_v M_v(s)} \tag{8.43}$$

and let

$$\mathbf{G}(s) := \left\{ G(s) \ : \ a_i^- \le a_i \le a_i^+, \quad b_j^- \le b_j \le b_j^+, \quad i \in \underline{u}, \quad j \in \underline{v} \right\} \tag{8.44}$$

denote the family of uncertain systems. Let

$$\mathbf{p} := [a_1, a_2, \cdots, a_u, b_1, b_2, \cdots, b_v] \tag{8.45}$$

denote the parameter vector and

$$\mathbf{\Pi} := \left\{ \mathbf{p} \ : \ a_i^- \le a_i \le a_i^+, \quad b_j^- \le b_j \le b_j^+, \quad i \in \underline{u}, \quad j \in \underline{v} \right\} \tag{8.46}$$

the uncertainty polytope. Write (8.43) as $G(s, \mathbf{p})$ to emphasize its dependence on $\mathbf{p}$. For convenience we refer to the family of systems $G(s, \mathbf{p}) : \mathbf{p} \in \mathbf{\Pi}$ represented in the form (8.43) as a *polytopic system*. Of course a polytopic system is just a special case of a linear interval system with the uncertain polynomials being of degree zero.

Let $\mathbf{\Pi}_{\mathrm{E}}$ denote the exposed edges of $\mathbf{\Pi}$ and introduce the extremal systems

$$\mathbf{G}_{\mathrm{E}}(s) := \{G(s,\mathbf{p}) \ : \ \mathbf{p} \in \mathbf{\Pi}_{\mathrm{E}}\}. \tag{8.47}$$

Now suppose that s^* is an arbitrary point in the complex plane, where the image set $\mathbf{G}(s^*)$ needs to be found. In the Hurwitz case we might have $s^* = j\omega$ and in a discrete time control system, for example, s^* could be a point on the unit circle. We have the following result.

Theorem 8.9

$$\partial\mathbf{G}(s^*) \subset \mathbf{G}_{\mathrm{E}}(s^*).$$

Proof. The proof follows from Lemma 8.1 applied to the polygons

$$Q_1 = \left\{a_1 L_1(s^*) + \cdots + a_u L_u(s^*) \ : \ a_i^- \le a_i \le a_i^+, \quad i \in \underline{u}\right\}$$
$$Q_2 = \left\{b_1 M_1(s^*) + \cdots + b_v M_v(s^*) \ : \ b_j^- \le b_j \le b_j^+, \quad j \in \underline{v}\right\}.$$

♣

All the results of Theorems 8.1 to 8.8 carry over to this general case with the extremal set $\mathbf{G}_{\mathrm{E}}(s)$ being defined by (8.47). The more general case where some $a_i,\ b_j$ are identical can be handled by imposing the same constraint on $\mathbf{G}_{\mathrm{E}}(s)$.

8.8 LINEAR FRACTIONAL TRANSFORMATIONS OF INTERVAL SYSTEMS

We have thus far assumed that our uncertain system is described by an interval system, a linear interval system, or a polytopic system model. In each of these cases we developed extremal and boundary results under the assumption that the numerator and denominator parameter sets are *disjoint* or that they perturb *independently*. On the other hand, we saw that these extremal and boundary results carry over to all the feedback system transfer functions even though, in some of these, the numerator and denominator do contain *common* uncertain parameters. A natural question to ask therefore is: What is a useful general model with interval parametric uncertainty, incorporating dependencies between numerator and denominator parameters, for which boundary or extremal results can be obtained? It turns out that a very broad class of systems of this type can be encompassed under the class of *linear fractional transformations* of an linear interval system.

Therefore, let us suppose that $\mathbf{G}(s)$ is a linear interval system (see (8.36)) with independent uncertain interval polynomials $A_i(s), B_j(s)$ and let $\mathbf{G}_{\mathrm{E}}(s)$ denote the extremal subset as defined in Section 8.6. Let $P(s), Q(s), R(s), S(s)$ be four arbitrary fixed functions and consider the transformation

$$H(s) = \frac{P(s)G(s) + Q(s)}{R(s)G(s) + S(s)}.$$

We suppose that the transformation is well defined ($R(s)G(s)+S(s)\neq 0$) and refer to such a transformation as a *linear fractional transformation*. Obviously $H(s)$ contains, in general, common interval parameters in the numerator and denominator even though $G(s)$ has only independent parameters in the numerator and denominator. As before let

$$\mathbf{H}(s) := \left\{ \frac{P(s)G(s)+Q(s)}{R(s)G(s)+S(s)} : G(s)\in \mathbf{G}(s) \right\}$$

and let

$$\mathbf{H}_{\mathrm{E}}(s) := \left\{ \frac{P(s)G(s)+Q(s)}{R(s)G(s)+S(s)} : G(s)\in \mathbf{G}_{\mathrm{E}}(s) \right\}.$$

We show below that under mild conditions on the set $P(s), Q(s), R(s), S(s)$ the boundary of the set $\mathbf{H}(j\omega)$ is generated by the extremal set $\mathbf{G}_{\mathrm{E}}(j\omega)$.

Theorem 8.10 *If*

$$P(j\omega)S(j\omega)-Q(j\omega)R(j\omega)\neq 0$$

we have

$$\partial\mathbf{H}(j\omega)\subset \mathbf{H}_{\mathrm{E}}(j\omega).$$

Proof. We know that the boundary of $\mathbf{G}(j\omega)$ is contained in $\mathbf{G}_{\mathrm{E}}(j\omega)$. Therefore all we need to show is that the transformation $G(s)\longrightarrow H(s)$ is a boundary preserving mapping. Write

$$P(j\omega)=p,\quad Q(j\omega)=q,\quad R(j\omega)=r,\quad S(j\omega)=s,\quad G(j\omega)=g,\quad H(j\omega)=h.$$

We see that under the assumption stated ($ps-qr\neq 0$), we can write

$$h=\left[\frac{qr-ps}{r}\right]\left[\frac{1}{rg+s}\right]+\frac{p}{r}=\frac{pg+q}{rg+s}.$$

Thus h is obtained from g by a sequence of operations consisting of multiplication by a complex number, addition of a complex number and inversion of a complex number. Each of these are boundary preserving operations (see Lemma 8.1) and so the result follows. ♣

Remark 8.3. With this result in hand it is easy to see that all the extremal and boundary results stated in this chapter carry over to linear fractional transformations of linear interval systems. The practical implication of this result is that by adjusting the set $P(s), Q(s), R(s), S(s)$ we can account for a large class of interdependencies between the perturbations. It is easy to show that all the transfer functions that occur in a closed loop system can be shown to be linear fractional transformations of $G(s)$ which satisfy the restriction stated in the theorem above. Thus it is not surprising that the extremal results stated in Theorem 8.3 hold. Finally, we point out that the boundary generating property of $\mathbf{G}_{\mathrm{E}}(s)$ continues to hold for any further linear fractional transformations applied to $H(s)$.

Example 8.6. Let us consider the block diagram shown in Figure 8.24. The closed

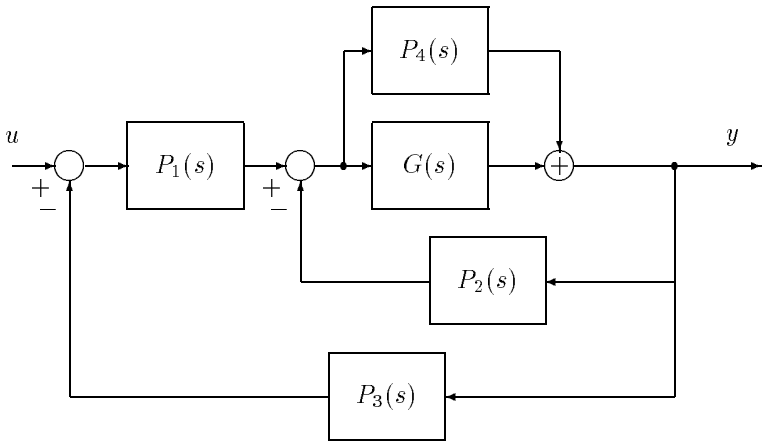

Figure 8.24. A feedback system

loop transfer function of the system is

$$\begin{aligned}\frac{y(s)}{u(s)} &= \frac{P_1(s)P_4(s) + P_1(s)G(s)}{1 + [P_1(s)P_3(s) + P_2(s)]\,P_4(s) + [P_1(s)P_3(s) + P_2(s)]\,G(s)} \\ &= H(s).\end{aligned}$$

If $G(s)$ belongs to an interval transfer function family $\mathbf{G}(s)$, then the family of output transfer functions is

$$\mathbf{H}(s)$$

$$= \left\{ \frac{P_1(s)P_4(s) + P_1(s)G(s)}{1 + [P_1(s)P_3(s) + P_2(s)]\,P_4(s) + [P_1(s)P_3(s) + P_2(s)]\,G(s)} : G(s) \in \mathbf{G}(s) \right\}$$

$$= \left\{ \frac{\overbrace{P_1(s)}^{P(s)}\,G(s) + \overbrace{P_1(s)P_4(s)}^{Q(s)}}{\underbrace{[P_1(s)P_3(s) + P_2(s)]}_{R(s)}\,G(s) + \underbrace{1 + [P_1(s)P_3(s) + P_2(s)]\,P_4(s)}_{S(s)}} : G(s) \in \mathbf{G}(s) \right\}.$$

Thus, if

$$P(j\omega)S(j\omega) - Q(j\omega)R(j\omega) \neq 0,$$

we have

$$\partial\mathbf{H}(j\omega) \subset \mathbf{H}_{\mathrm{E}}(j\omega).$$

The point is, that even though $\mathbf{H}(s)$ is *not* an interval transfer function, the boundary of $\mathbf{H}(j\omega)$ is captured by replacing $\mathbf{G}(s)$ by the elements of the extremal set

$\mathbf{G}_E(s)$ which is a considerable saving. Similar results hold for the Nyquist and Bode envelopes, and in fact all extremal properties of $\mathbf{H}(s)$ will occur on the subset $\mathbf{H}_E(s)$.

8.9 ROBUST PARAMETRIC CLASSICAL DESIGN

We illustrate the utility of the above tools in extending the design techniques of classical control to systems containing parameter uncertainty. The requirement of robust design is that the design specifications must be satisfied over the entire parameter set. Thus the worst case values must be acceptable. Since these worst case values occur over the extremal set $\mathbf{G}_{\mathrm{E}}(s)$, it suffices to verify that the specifications are met over this set.

8.9.1 Guaranteed Classical Design

Example 8.7. Consider the interval plant

$$\mathbf{G}(s) = \frac{n_0}{d_3 s^3 + d_2 s^2 + d_1 s + d_0}$$

with $n_0 \in [10, 20]$, $d_3 \in [0.06, 0.09]$, $d_2 \in [0.2, 0.8]$, $d_1 \in [0.5, 1.5]$, $d_0 = 0$. The objective is to design a controller so that the closed loop system

a) is robustly stable under all parameter perturbations,

b) possesses a guaranteed phase margin of at least 45°. In other words the worst case phase margin over the set of uncertain parameters must be better than 45°, and

c) possesses a bandwidth greater than or equal to 0.1 [rad/sec] with a reasonable value of resonant peak M_p.

We simply follow the standard classical control design techniques with the new tools developed here. First we construct the Bode envelopes of the open loop interval plant $\mathbf{G}(s)$. From the magnitude and phase envelopes, we observe that the worst case phase margin of 50° is achieved if the gain crossover frequency ω_c' is at 0.5 [rad/sec]. In order to bring the magnitude envelope down to 0 [dB] at the new crossover frequency ω_c', the phase lag compensator of the form

$$C(s) = \frac{1 + aTs}{1 + Ts}, \qquad a < 1$$

must provide the amount of attenuation equal to the minimum value of the magnitude envelope at ω_c':

$$\max_{G(j\omega_c') \in \mathbf{G}(j\omega_c')} |G(j\omega_c')| = -20 \log_{10} a[dB].$$

Thus, we have $a = 0.01$. Now we choose the corner frequency $\frac{1}{aT}$ to be one decade below ω_c':

$$\frac{1}{aT} = \left.\frac{\omega_c'}{10}\right|_{\omega_c'=0.5}$$

and we have $T = 2000$. Finally, the resulting phase lag compensator becomes

$$C(s) = \frac{1+20s}{1+2000s}.$$

Here we give some analysis to check whether the controller $C(s)$ satisfies the given design requirements. The robust stability of the closed loop system with the controller $C(s)$ may be easily determined by applying Theorem 8.1. Moreover by GKT since we use a first order controller it is only necessary to check the stability of the following vertex polynomials:

$$(1+2000s)K_d^i(s) + (1+20s)K_n^j(s), \qquad i = 1,2,3,4; j = 1,2$$

where

$$\begin{aligned} K_n^1(s) &:= 10 & K_n^2(s) &:= 20 \\ K_d^1(s) &:= 0.5s + 0.8s^2 + 0.09s^3 & K_d^2(s) &:= 1.5s + 0.8s^2 + 0.06s^3 \\ K_d^3(s) &:= 0.5s + 0.2s^2 + 0.09s^3 & K_d^4(s) &:= 1.5s + 0.2s^2 + 0.06s^3. \end{aligned}$$

The eight polynomials above are stable and this shows that the closed loop system remains stable under all parameter perturbations within the given ranges. Figure 8.25 shows the frequency response (Bode envelopes) of $\mathbf{G}(s)$ (uncompensated system) and $C(s)\mathbf{G}(s)$ (compensated system). Clearly, the guaranteed phase margin requirement of 45° is satisfied. The guaranteed gain margin of the system is 12 db. The closed loop response $|\mathbf{M}(j\omega)|$ called $\mathbf{T}^y(j\omega)$ in (8.22) is shown in Figure 8.26 where

$$\mathbf{M}(j\omega) := \mathbf{M}(s)|_{s=j\omega} := \left\{ M(s) \ : \ \frac{C(s)G(s)}{1+C(s)G(s)}, \ \ G(s) \in \mathbf{G}(s) \right\}. \tag{8.48}$$

Note that the $|\mathbf{M}(j\omega)|$ envelope shown in this figure is calculated from the result of Theorem 8.4. Figure 8.26 shows that the M_p of every system in the family lies between 1.08 and 1.3886. This also shows that the bandwidth of every system in the family lies in between 0.12 and 0.67 [rad/sec]. Thus, the design objective is achieved. Figure 8.27 shows the Nyquist plot of $C(s)\mathbf{G}(s)$. The center of the M-circle in Figure 8.27 is

$$\begin{aligned} \left(\frac{M_p^2}{1-M_p^2}, 0\right) &= \left(\frac{1.3886^2}{1-1.3886^2}, 0\right) \\ &= (-2.0772, 0) \end{aligned}$$

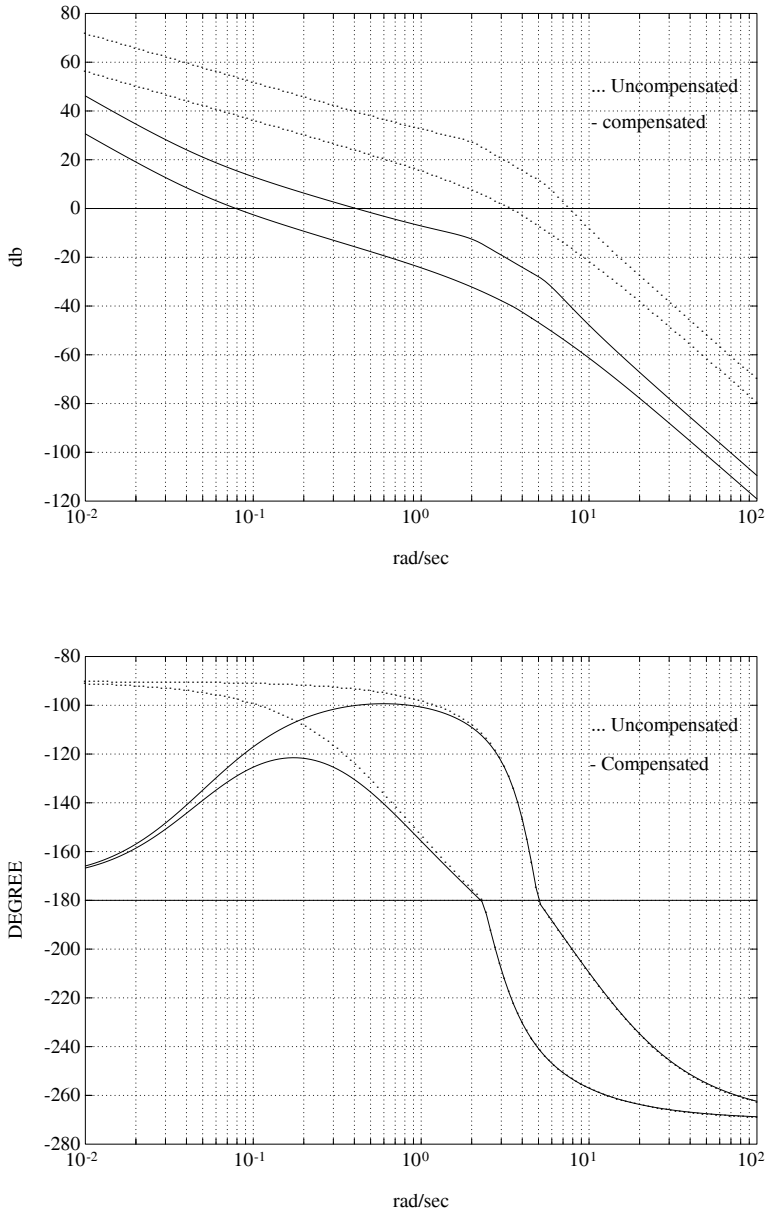

Figure 8.25. Bode envelopes of $\mathbf{G}(s)$ and $C(s)\mathbf{G}(s)$ (Example 8.7)

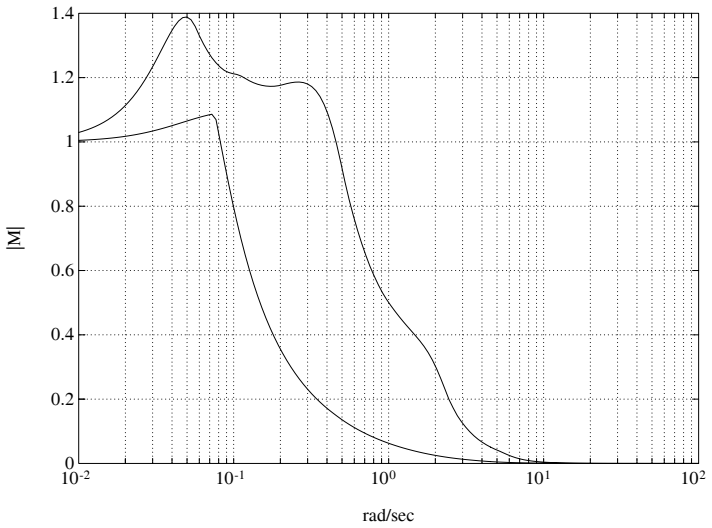

Figure 8.26. Closed-loop frequency response (Example 8.7)

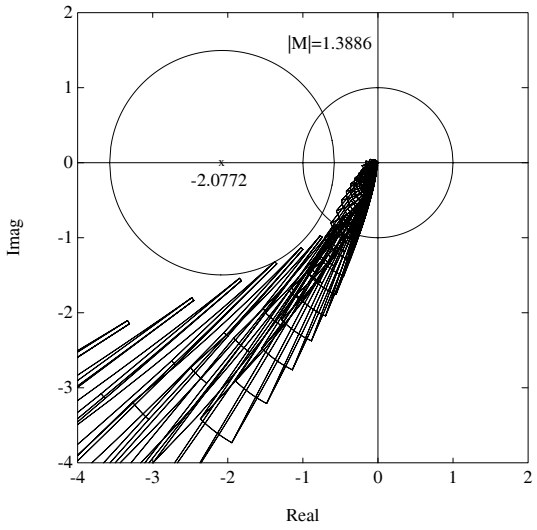

Figure 8.27. Nyquist envelope of $C(s)\mathbf{G}(s)$ with M-circle (Example 8.7)

and the radius of the circle is

$$r = \left| \frac{M_p}{1 - M_p^2} \right| = 1.496.$$

Example 8.8. (Lead-lag Compensation) We give an example of lead-lag compensation design utilizing the developments described above. Let us consider the interval plant

$$G(s) = \frac{a_0}{b_3 s^3 + b_2 s^2 + b_1 s + b_0}$$

with coefficients bounded as follows:

$$a_0 \in [5, 7], \quad b_3 \in [.09, .11], \quad b_2 \in [.9, 1.2], \quad b_1 \in [.8, 1.5], \quad b_0 \in [.1, .3]$$

The objective of the design is to guarantee that the entire family of systems has a phase margin of at least 60° and a gain margin of at least 30dB. From Figure 8.29, we observe that the phase margin 70° which is equal to the desired phase margin of 60° plus some safety factor can be obtained if the new gain-crossover frequency ω_c' is at 0.35 [rad/sec]. This means that the phase-lag compensator must reduce the maximum magnitude of $\mathbf{G}(j\omega_c')$ over the interval family to 0 [db]. Thus, we solve

$$-20 \log_{10} a = \max_{G(j\omega_c') \in \mathbf{G}(j\omega_c')} |G(j\omega_c')| = 28[\text{db}]$$

and we have

$$a = 0.0398.$$

In order that the phase lag of the compensator does not affect the phase at the new gain-crossover frequency ω_c', we choose the value of $1/aT$ to be at one decade below ω_c'. Thus,

$$T = \frac{10}{a\omega_c'} = \frac{10}{(0.0398)(0.35)} = 717.875.$$

Therefore, the lag compensator obtained is

$$C_1(s) = \frac{1 + aTs}{1 + Ts} = \frac{28.5714s + 1}{717.875s + 1}.$$

We have now achieved approximately 70° of guaranteed phase margin and 25dB of guaranteed gain margin.

To achieve the desired gain margin, we now wish to move the phase-crossover frequency ω_c'' to 4.7 [rad/sec]. If the magnitude plot does not move, we can achieve the gain margin of 35db at this frequency. Thus, we solve

$$-10 \log_{10} a = -(35 - 25) = -10[\text{db}]$$

and we have

$$a = 10.$$

Then,

$$\frac{1}{T} = \sqrt{a}\omega_c'' = \sqrt{10}(4.7) = 14.86$$

and $T = 0.0673$. Therefore, the cascaded lead compensator is

$$\begin{aligned} C_2(s) &= \frac{1}{a}\frac{1+aTs}{1+Ts} \\ &= \frac{1}{10}\frac{(10)(0.0673)s+1}{0.0673s+1} = \frac{s+1.485}{s+14.859}. \end{aligned}$$

From Figure 8.29, we verify that the compensated system provides approximately 105° of guaranteed phase margin and 50dB of guaranteed gain margin. Therefore, the controller

$$C(s) = C_2(s)C_1(s) = \frac{s+1.5}{s+15}\frac{28.5714s+1}{717.682s+1}$$

attains the design specifications robustly. Figures 8.28, 8.29 and 8.30 show the Nyquist, Bode and Nichols envelopes of the uncompensated and compensated systems.

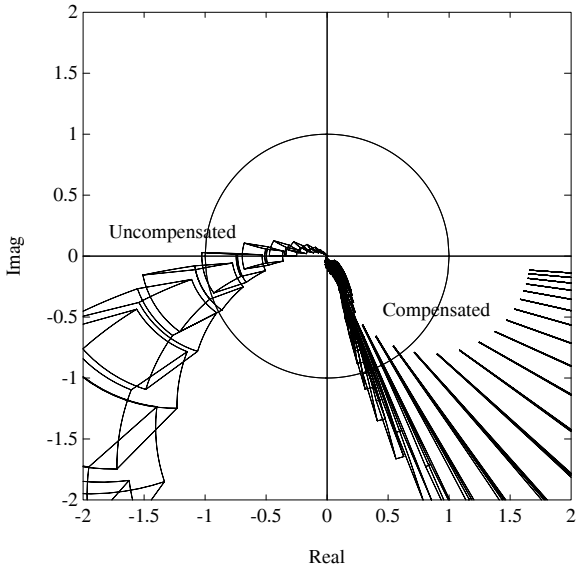

Figure 8.28. Nyquist envelope (Example 8.8)

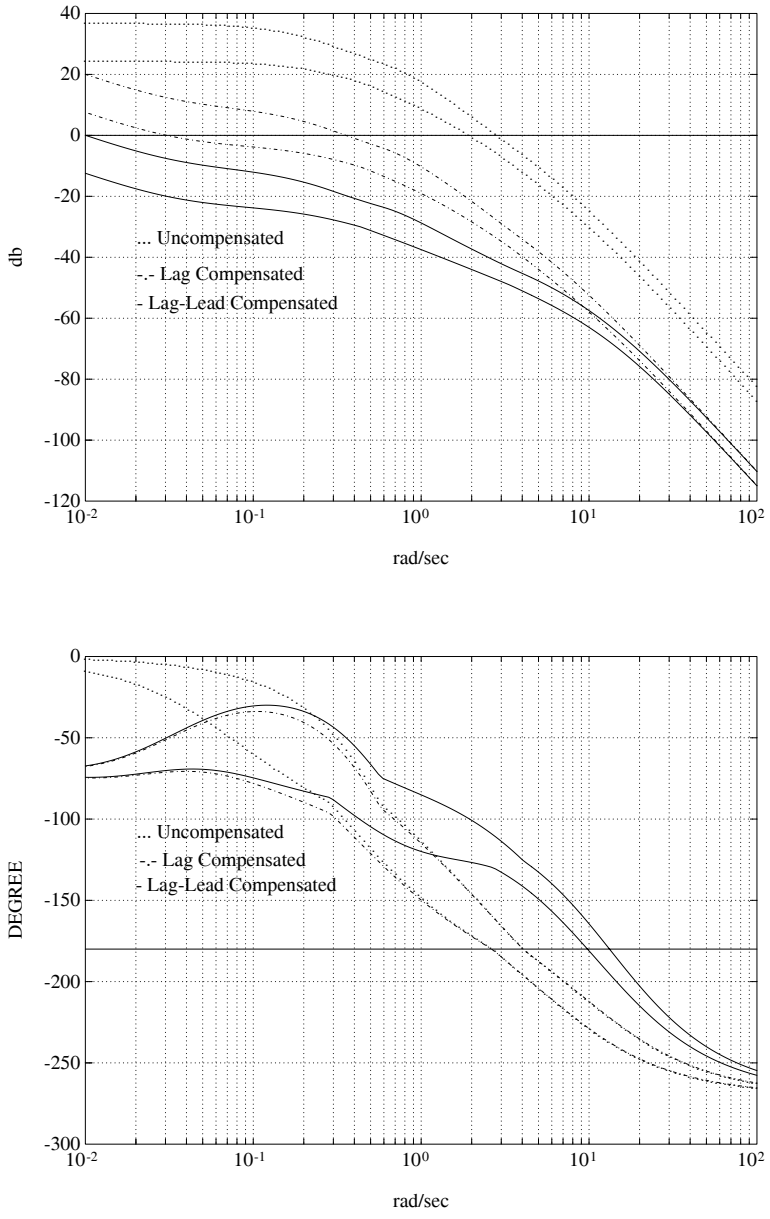

Figure 8.29. Bode envelopes (Example 8.8)

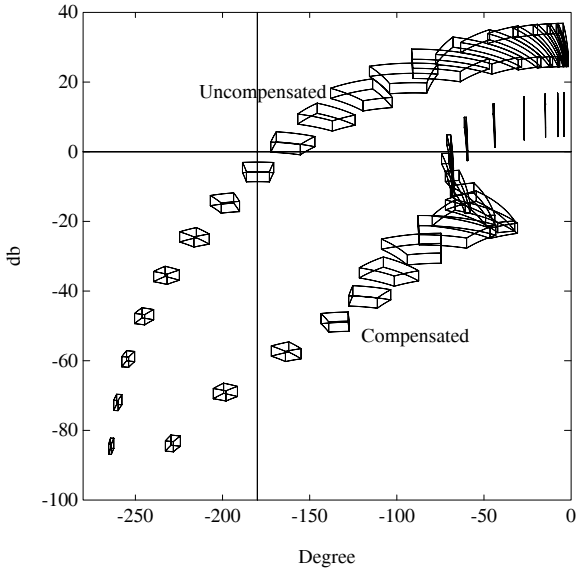

Figure 8.30. Nichols templates (Example 8.8)

Example 8.9. (PI Compensation) Consider the plant

$$G(s) = \frac{n_1 s + 1}{.02s^4 + d_3 s^3 + d_2 s^2 + .04s}$$

with its coefficients bounded by given intervals as follows:

$$n_1 \in [.35, .45], \quad d_3 \in [.25, .35], \quad b_2 \in [.9, 1.1]$$

The objective of the design is to guarantee that the entire family of closed loop systems has a phase margin of at least 45°.

Here we design a PI compensator of the form

$$C(s) = K_P + \frac{K_I}{s}.$$

From Figure 8.32 we see that the new gain-crossover frequency ω_c' should be moved to 0.034 [rad/sec]. Since the maximum magnitude at ω_c' is 55 [db], we let

$$G_p(j\omega_c') := \max_{G(j\omega_c') \in \mathbf{G}(j\omega_c')} |G(j\omega_c')| = -20 \log_{10} K_p = 54.89[\text{db}]$$

from which

$$K_P = 10^{-|G_p(j\omega_c')|[\text{db}]/20} = 10^{-54.89/20} = 0.0018.$$

In order that the phase lag of the PI compensator not effect the phase of the compensated system at ω_c', we choose the corner frequency K_I/K_P to be one decade below ω_c'. Thus,

$$K_I = \frac{\omega_c'}{10} K_P = \frac{0.034}{10}(0.0018) = 6.12 \times 10^{-6}.$$

Therefore, the PI compensator obtained is

$$C(s) = \frac{6.12 \times 10^{-6} + .0018s}{s}.$$

Figure 8.31 shows the Nyquist envelope while Figures 8.32 and 8.33 show the Bode and Nichols envelopes of the uncompensated and compensated systems. We can see that the phase margin specifications are robustly achieved.

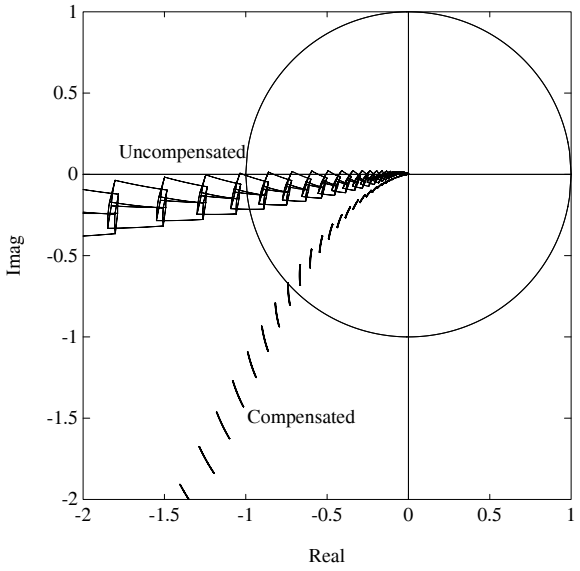

Figure 8.31. Nyquist envelope (Example 8.9)

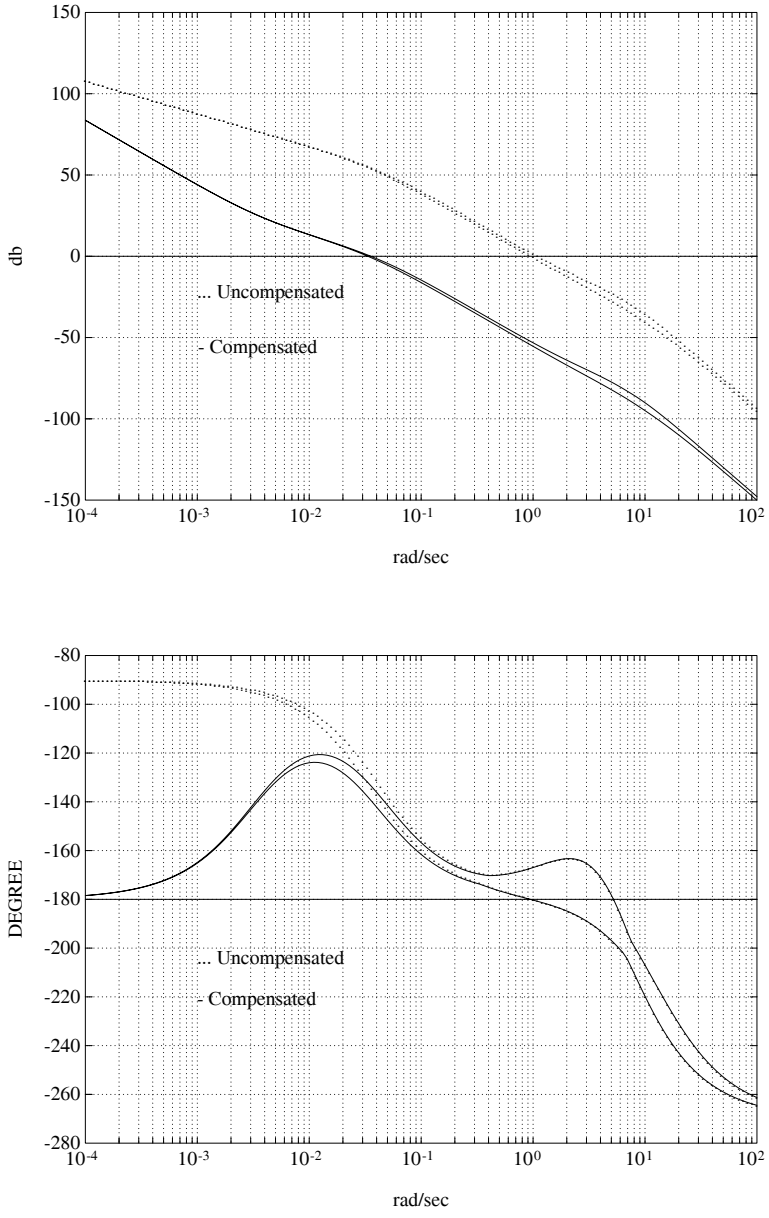

Figure 8.32. Bode envelopes (Example 8.9)

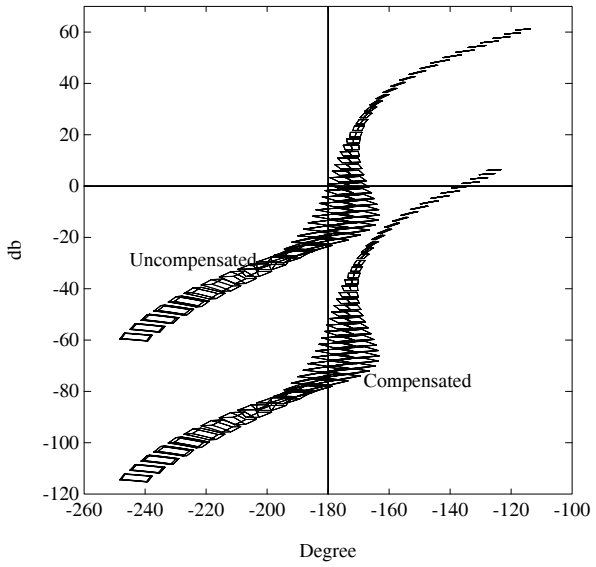

Figure 8.33. Nichols templates (Example 8.9)

8.9.2 Optimal Controller Parameter Selection

In the design problem, we interchange the role of plant and controller, and consider a family of controllers stabilizing a fixed plant $G(s)$. The design problem here is to select from the controller family the *best* parameter value according to some criterion. This type of problem is common in practice. Let us consider for example that this parameter selection is to be made to maximize gain margin or phase margin. The set of controller parameters may be given in terms of bounded values. In other words, we have a interval family of controllers stabilizing a fixed plant. To maximize the gain margin (or phase margin) over this set, we explore the boundary results given earlier.

In Section 8.4 we showed that the minimum gain margin (or phase margin) occurs over the extremal set. In practice, the maximum gain margin (or phase margin) will also frequently occur over the same set. To see this, we argue as follows. The Nyquist boundary of the system cuts the real axis over the range A to B (see Figure 8.34 and Figure 8.35). The point A corresponds to the minimum gain margin of the family. The point B is a potential candidate for the maximum gain margin (gain margin $= 1/OB$). Corresponding to the point B, there exists a set C_B of admissible (parameters lie within the given intervals) controllers whose Nyquist plots pass through the point B. Suppose that one of these controllers is such that the Nyquist plot does *not* cut the real axis at any other point (see Figure

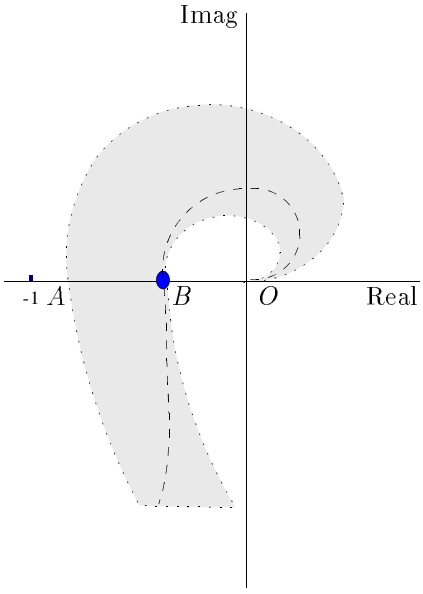

Figure 8.34. A system that delivers the maximum gain margin

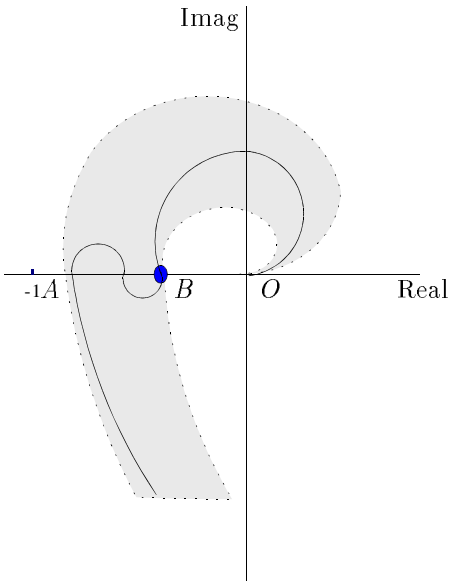

Figure 8.35. A system that does not deliver the maximum gain margin

8.34). It is clear that this controller delivers the maximum gain margin ($1/OB$) and is the optimally robust gain margin controller in the family. We can see that the maximum gain margin will be unrealizable only if each and every controller in C_B happens to cut the real axis at another point also (see Figure 8.35). Based on the above arguments, we suggest the following design procedure. First, check whether the given family of interval controllers stabilizes the plant $G(s)$ by using the GKT (Chapter 7). If so, we use this set of controllers. Otherwise, we determine the parametric stability margin around the nominal values of controller parameters and create the largest interval stabilizing controller family around this nominal. From this controller set we can find the controller parameters that provide the maximum gain or phase margin. This can be done by generating the Nyquist envelope of the family using the development discussed earlier. If the margin obtained is not satisfactory, we reset the controller parameters to the new nominal corresponding to the point B and create a new interval stabilizing family. We repeat this procedure until a satisfactory margin is achieved or the improvement of the margin is negligibly small. The set of stabilizing interval controllers can be determined by many different methods; for example the locus introduced by Tsypkin and Polyak (Chapter 4) may be used. Of course, there is no guarantee that a globally optimum design will be achieved by this method. However, a satisfactory robust design will often result.

Example 8.10. Consider the feedback system with the plant transfer function

$$G(s) := \frac{250}{.025s^2 + 1.75s + 30}$$

and controller transfer function

$$C(s) := \frac{\alpha s + 1}{s^2 + \beta s + \gamma}.$$

The nominal values of controller parameters are

$$\alpha_0 = 5, \quad \beta_0 = 2, \quad \gamma_0 = 1.$$

The phase margin of the given system with the nominal values of controller parameters is 19.55°. The objective is to tune the three controller parameters so that the resulting system has a phase margin of approximately 45°. We first find the ℓ_2 parametric stability margin r_1 around the nominal values of parameters $(\alpha_0, \beta_0, \gamma_0)$ by using the method proposed by Tsypkin and Polyak (Chapter 4). From this value of r_1, which was obtained as $r_1 = 1$, we create the family of stabilizing controllers in the form of an interval transfer function $\mathbf{C}_1(s)$. Using this interval controller family, we create the corresponding Nyquist envelope which shows the maximum obtainable phase margin of 29.85°. Using the formulas developed previously, we select the parameter values $(\alpha_1, \beta_1, \gamma_1)$, and consequently the controller $C(s, \alpha_1, \beta_1, \gamma_1) \in \mathbf{C}_1(s)$ that produces the maximum phase margin of 29.85°. Since the resulting controller $C(s, \alpha_1, \beta_1, \gamma_1)$ does not satisfy the given requirement, we proceed with a second

iteration. The parametric stability margin around $(\alpha_1, \beta_1, \gamma_1)$ we found is again 1. We now create a new interval family $\mathbf{C}_2(s)$ of stabilizing controllers. Using the same procedure as before, we find the controller $C_2(s, \alpha_2, \beta_2, \gamma_2) \in \mathbf{C}_2(s)$. This produces the maximum phase margin of 43.76°. In the table below we present the successive designs through several iterations and Figure 8.36 shows the Nyquist plot of the optimal system for each iteration.

iteration i	parameter ranges (α, β, γ)	parameter selected $(\alpha_i, \beta_i, \gamma_i)$	phase margin
0	–	$(5, 2, 1)$	19.55°
1	$([4, 6], [1, 3], [0, 2])$	$(4, 3, 2)$	29.85°
2	$([3, 5], [2, 4], [1, 3])$	$(3, 4, 1)$	43.76°

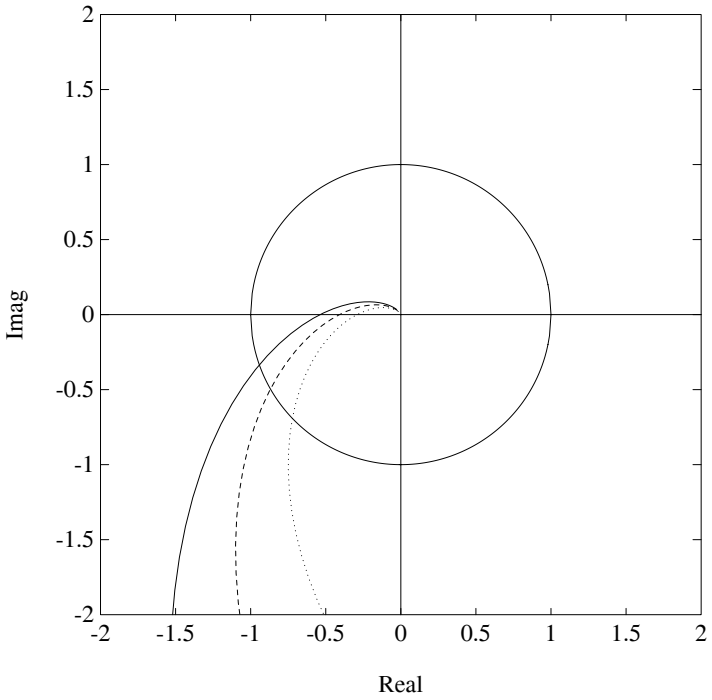

Figure 8.36. Nyquist plots of optimal systems (Example 8.10)

8.9.3 Discrete Time Control Systems

The frequency templates of discrete interval control systems can also be constructed similarly. We still use the basic geometric facts regarding the addition, multipli-

cation and division of complex plane image sets discussed here; however, the main simplifying tool used in the case of continuous systems, the GKT, is no longer applicable here. We illustrate this by an example.

Example 8.11. Consider the discrete-time feedback system shown in Figure 8.37. Let the interval plant $\mathbf{G}(z)$ and the controller $C(z)$ be

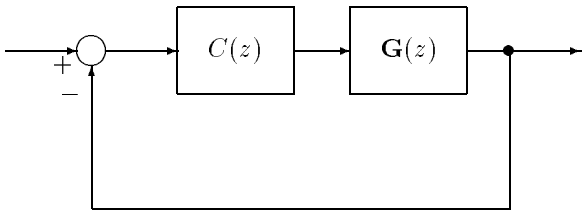

Figure 8.37. A discrete time feedback system (Example 8.11)

$$\mathbf{G}(z) = \frac{z+\alpha}{z^2+\beta z+\gamma} \quad \text{and} \quad C(z) = \frac{-0.2z-0.35}{z+3}$$

where

$$\alpha \in [0.8, 1.2] := [\alpha^-, \alpha^+],\ \beta \in [1.8, 2.2] := [\beta^-, \beta^+],\ \gamma \in [2.8, 3.2] := [\gamma^-, \gamma^+].$$

Then we have the extremal subset $\mathbf{G}_{\mathrm{E}}(z)$ consisting of the following 12 systems:

$$G_{\mathrm{E}_1}(z) = \frac{z+(\lambda\alpha^- + (1-\lambda)\alpha^+)}{z^2+\beta^- z+\gamma^-}, \qquad G_{\mathrm{E}_2}(z) = \frac{z+(\lambda\alpha^- + (1-\lambda)\alpha^+)}{z^2+\beta^+ z+\gamma^-}$$

$$G_{\mathrm{E}_3}(z) = \frac{z+(\lambda\alpha^- + (1-\lambda)\alpha^+)}{z^2+\beta^- z+\gamma^+}, \qquad G_{\mathrm{E}_4}(z) = \frac{z+(\lambda\alpha^- + (1-\lambda)\alpha^+)}{z^2+\beta^+ z+\gamma^+}$$

$$G_{\mathrm{E}_5}(z) = \frac{z+\alpha^-}{z^2+(\lambda\beta^- + (1-\lambda)\beta^+)z+\gamma^-}$$

$$G_{\mathrm{E}_6}(z) = \frac{z+\alpha^-}{z^2+(\lambda\beta^- + (1-\lambda)\beta^+)z+\gamma^+}$$

$$G_{\mathrm{E}_7}(z) = \frac{z+\alpha^+}{z^2+(\lambda\beta^- + (1-\lambda)\beta^+)z+\gamma^-}$$

$$G_{\mathrm{E}_8}(z) = \frac{z+\alpha^+}{z^2+(\lambda\beta^- + (1-\lambda)\beta^+)z+\gamma^+}$$

$$G_{\mathrm{E}_9}(z) = \frac{z + \alpha^-}{z^2 + \beta^- z + (\lambda\gamma^- + (1-\lambda)\gamma^+)}$$
$$G_{\mathrm{E}_{10}}(z) = \frac{z + \alpha^-}{z^2 + \beta^+ z + (\lambda\gamma^- + (1-\lambda)\gamma^+)}$$
$$G_{\mathrm{E}_{11}}(z) = \frac{z + \alpha^+}{z^2 + \beta^- z + (\lambda\gamma^- + (1-\lambda)\gamma^+)}$$
$$G_{\mathrm{E}_{12}}(z) = \frac{z + \alpha^+}{z^2 + \beta^+ z + (\lambda\gamma^- + (1-\lambda)\gamma^+)}$$

where in each case λ ranges over $[0, 1]$.

By searching over the family $\mathbf{G}_{\mathrm{E}}(z)$ with $z = e^{j\omega T}$ for $\omega \in [0, \infty)$ and a fixed T, we can obtain the frequency templates of the system. For illustration, the Bode envelopes of the above discrete time feedback system are given in Figure 8.38 for $T = 1$. The Nyquist and Nichols envelopes can also be generated similarly.

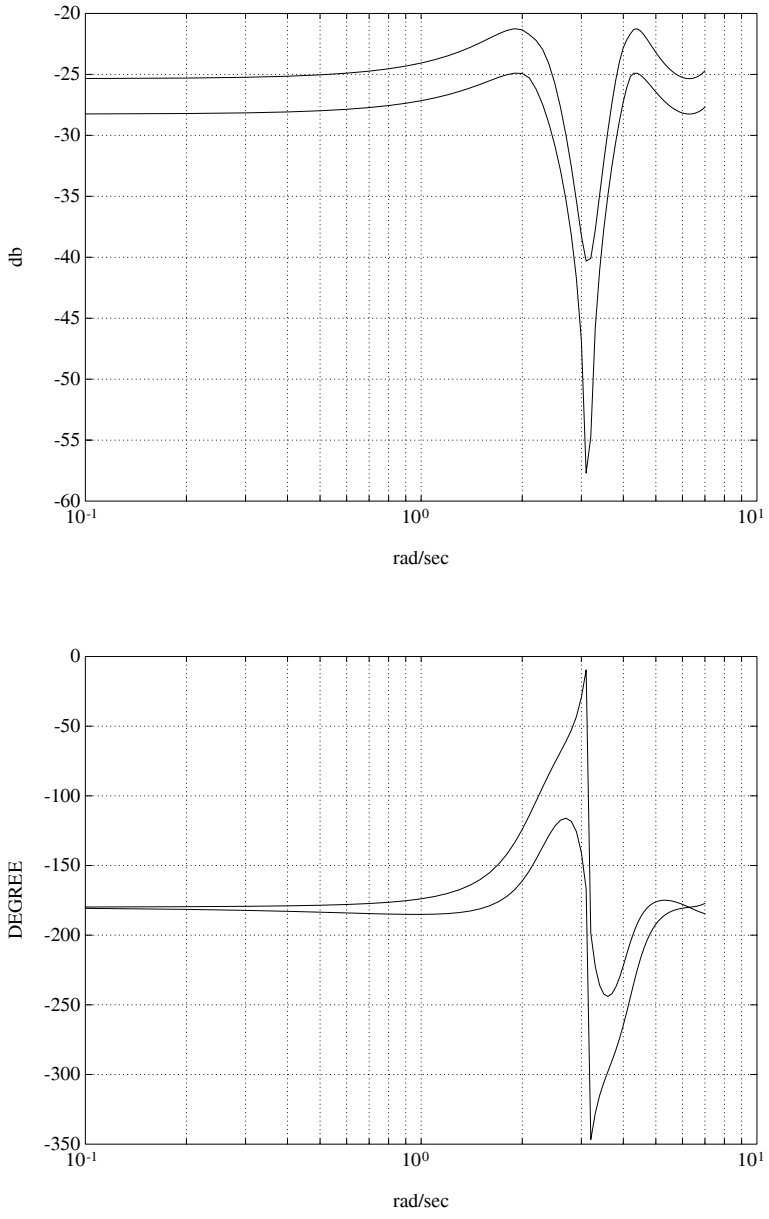

Figure 8.38. Bode envelopes (Example 8.11)

8.10 EXERCISES

8.1 Consider the family of transfer functions

$$\mathbf{G}(s) = \frac{4s^3 + \alpha_2 s^2 + \alpha_1 s + 5}{s^4 + 10\beta_3 s^3 + \beta_2 s^2 + (\beta_1 + 2\gamma_1)s}$$

where $\alpha_2, \in [1, 2], \alpha_1 \in [-2, 3]$, $\beta_3 \in [-1, 1]$, $\beta_2 \in [0.5, 1.5]$, $\beta_1 \in [-0.5, 1]$, $\gamma_1 \in [-4, -1]$. Determine a) the frequency template $\mathbf{G}(j\omega)$ at $\omega = 1, 10, 100$, b) the Nyquist, Bode and Nichols templates of $\mathbf{G}(s)$.

8.2 Consider the interval system

$$\mathbf{G}(s) = \frac{\mathbf{N}(s)}{\mathbf{D}(s)}$$

where $\mathbf{N}(s)$ and $\mathbf{D}(s)$ are interval polynomials. Let

$$\underline{\mu}_{\mathbf{G}}(j\omega) := \inf_{G \in \mathbf{G}} |G(j\omega)| \quad \text{and} \quad \bar{\mu}_{\mathbf{G}}(j\omega) := \sup_{G \in \mathbf{G}} |G(j\omega)|$$

with similar definitions holding with $\mathbf{G}(s)$ replaced by $\mathbf{G}_E(s)$. Prove the following formulas for computing the extremal Bode magnitude values for interval systems:

$$\underline{\mu}_{\mathbf{G}}(j\omega) = \underline{\mu}_{\underline{\mathbf{G}}_{\mathrm{E}}}(j\omega) \qquad \bar{\mu}_{\mathbf{G}}(j\omega) = \bar{\mu}_{\bar{\mathbf{G}}_{\mathrm{E}}}(j\omega)$$

where

$$\underline{\mathbf{G}}_{\mathrm{E}}(s) := \frac{\mathcal{S}_N(j\omega)}{\mathcal{K}_D(j\omega)} \qquad \bar{\mathbf{G}}_{\mathrm{E}}(s) := \frac{\mathcal{K}_N(j\omega)}{\mathcal{S}_D(j\omega)}$$

8.3 In the interval system considered above in Exercise 8.2, prove the further simplification for computing extremal Bode angle values:

$$\underline{\phi}_{\mathbf{G}}(j\omega) = \underline{\phi}_{\mathbf{G}_{\mathrm{K}}}(j\omega) \qquad \bar{\phi}_{\mathbf{G}}(j\omega) = \bar{\phi}_{\mathbf{G}_{\mathrm{K}}}(j\omega)$$

8.4 Prove that

$$\frac{1}{\lambda d_0 + (1-\lambda)d_1}, \quad \lambda \in [0, 1]$$

where d_0 and d_1 are arbitrary complex numbers, is an arc of a circle. The circle passes through the points $\frac{1}{d_0}$, $\frac{1}{d_1}$ and 0, the origin in the complex plane.

8.5 In the control system given in Figure 8.39

$$C(s) = \frac{2s^2 + 4s + 3}{s^2 + 3s + 4} \quad \text{and} \quad G(s) = \frac{s^2 + a_1 s + a_0}{s(s^2 + b_1 s + b_0)}$$

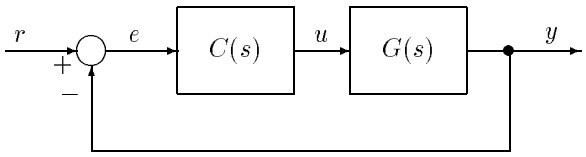

Figure 8.39. Feedback control system

with the nominal values of parameters being

$$a_1^0 = -2, \quad a_0^0 = 1, \quad b_0^0 = 2, \quad b_1^0 = 1.$$

Now let

$$a_0 \in [1-\epsilon, 1+\epsilon], \quad b_0 \in [2-\epsilon, 2+\epsilon]$$
$$a_1 \in [-2-\epsilon, -2+\epsilon], \quad b_1 \in [1-\epsilon, 1+\epsilon].$$

Assuming that $\epsilon = 0.0875$, determine

a) Bode envelopes of the open loop transfer function $C(s)G(s)$

b) From the Bode envelopes determine the worst case gain and phase margins of the system over the interval parameters

Answer: Gain margin=1.8014

c) Determine the worst case value over the parameter set, of M_p the peak value of the output transfer function evaluated over $j\omega$, for $\omega \in [0, \infty)$.

Answer: $M_p = 5.7075$

8.6 In the feedback system shown in Figure 8.39

$$a_1 \in (-2.115, -1.885), \qquad a_0 \in (6.885, 7.115)$$
$$b_1 \in (7.885, 8.115), \qquad b_0 \in (-0.365, -0.135)$$

Find the worst case gain and phase margin of the system.
Answer: $K^* = 5.6703$

8.7 Consider the block diagram given in Figure 8.39 with

$$a_1 \in [0.9, 1.1], \quad a_0 \in [-1.1, -0.9], \quad b_1 \in [-1.1, -0.9], \quad b_0 \in [1.9, 2.1].$$

Find the worst case gain and phase margins for the family by drawing the Bode magnitude and phase envelopes.

Answer: Gain margin=0.8358 = 1.55db. Phase margin=38.4381°)

8.8 In the control system shown in Figure 8.39

$$C(s) = \frac{20 + 30s + 12s^2}{-4 - 6s + s^2} \quad \text{and} \quad G(s) = \frac{a_0 + a_1 s + a_2 s^2}{s(b_0 + b_1 s + s^2)}$$

and the nominal plant transfer function

$$G^0(s) = \frac{1 + s + s^2}{s(1 + 2s + s^2)}.$$

Let

$$a_i \in [a_i^0 - \epsilon, a_i^0 + \epsilon], \qquad b_j \in [b_j^0 - \epsilon, b_j^0 + \epsilon], \qquad i, j = 0, 1, 2.$$

For $\epsilon = 0.2275$

a) Sketch the Bode magnitude and phase envelopes of the closed loop transfer function.

b) Find the worst case value of M_p.

c) Find the worst case gain and phase margins of the system.

8.9 For the system in Exercise 8.8, determine the worst case maximum steady state error over the parameter set when the reference input $r(t)$ is unit step.

8.10 Consider the stable interval transfer function $\mathbf{G}(s)$. Show that the steady state response with respect to step inputs for an interval transfer function is bounded by the steady state responses of its extremal systems $\mathbf{G}_{\mathrm{K}}(s)$.

8.11 NOTES AND REFERENCES

The boundary result of Theorem 8.2 is due to Tesi and Vicino [221]. The boundary result of Theorem 8.3 was reported by Keel and Bhattacharyya [132] and Keel, Shaw and Bhattacharyya [142]. The proofs of the frequency domain results of Theorems 8.4, 8.5, and 8.6 are given in Keel and Bhattacharyya [137]. In Bartlett [19] and Fu [98], the generation of frequency domain envelopes using the Edge Theorem is treated. The generation of Bode envelopes for interval plants are also dealt with by Bartlett, Tesi and Vicino [22]. Bartlett [20] showed that the extremal values of the steady state response of an interval plant for the case of multiaffine parameter dependencies are obtained from its vertex systems. Hollot and Tempo [117] showed that the Nyquist envelope of an interval family is *not* contained in the envelope of Nyquist plots of the Kharitonov plants. Applications of these frequency domain tools to classical control design, as described in Section 8.9, were reported in Keel and Bhattacharyya [135], Ahmad and Keel [5], and Ahmad, Keel and Bhattacharyya [6, 7].

Chapter 9

ROBUST STABILITY AND PERFORMANCE UNDER MIXED PERTURBATIONS

In this chapter we consider control systems containing parameter as well as unstructured uncertainty. Parametric uncertainty is modelled as usual by interval systems or linear interval systems. Two types of unstructured feedback perturbations are considered. First, we deal with unstructured uncertainty modelled as H_∞ norm bounded perturbations. A robust version of the Small Gain Theorem is developed for interval systems. An exact calculation of both the worst case parametric and the unstructured stability margins are given and the maximum values of various H_∞ norms over the parameter set are determined. It is shown that these occur on the same extremal subset which appear in the Generalized Kharitonov Theorem of Chapter 7. This solves the important problem of determining robust performance when it is specified in terms of H_∞ norms. Next, we deal with unstructured perturbations consisting of a family of nonlinear sector bounded feedback gains perturbing interval or linear interval systems. Extremal results for this robust version of the classical Absolute Stability problem are given. The constructive solution to this problem is also based on the extremal systems introduced in the Generalized Kharitonov Theorem (Chapter 7).

9.1 INTRODUCTION

Robustness of stability in the presence of unstructured uncertainty is an important and well developed subject in control system analysis. In the 1950's an important robustness problem called the *absolute stability problem* was formulated and studied. In this problem, also known as the Lur'e or Popov problem, a fixed linear system is subjected to perturbations consisting of all possible nonlinear feedback gains lying in a sector. In the 1980's a similar problem was studied by modelling the perturbations as H_∞ norm bounded perturbations of a fixed linear system.

In most practical systems it is important to consider at least two broad classes of uncertainties, namely *structured* and *unstructured* uncertainties. Unstructured uncertainties represent the effects of high frequency unmodeled dynamics, nonlinearities and the errors due to linearization, truncation errors, etc., and are usually modelled as a ball of norm-bounded operators. In the control literature it has been shown that certain types of robust performance problems, specified in terms of norms, can be posed as robust stability problems under unstructured perturbations. By structured uncertainty we mean parametric uncertainty representing lack of precise knowledge of the actual system parameters. Our goal in this chapter is to analyze the stability and performance of systems with uncertainties of mixed type with the objective of quantifying, as nonconservatively as possible, the amounts of the different kinds of perturbation that can be tolerated by the closed-loop system. We attempt to do this by considering unstructured perturbations of the above two types acting around an interval or linear interval system. We show that the extremal subsets introduced in the last two chapters again play a key role. These reduced sets in the plant parameter space are exactly where the worst case stability margins occur. Since these sets are one-parameter families of systems, the solution is constructive and computationally efficient. We begin in the next section with the case of H_∞ norm-bounded uncertainty.

9.2 SMALL GAIN THEOREM

In the approach to robust control using norms, uncertainty is usually modelled as norm bounded perturbations of the nominal transfer function in an appropriate normed algebra. The main tool for the analysis of stability of the closed-loop perturbed system under unstructured uncertainty is the Small Gain Theorem. In general, the Small Gain Theorem can be posed in any normed algebra, and it gives conditions under which a system of interconnected components is stable. In the algebra of stable transfer functions (H_∞), the Small Gain Theorem can be used to supply necessary and sufficient conditions for robust stability under stable (H_∞) perturbations.

In the following we will use the standard notation:

$$\mathbf{C}_+ := \{s \in C : \mathrm{Re}[s] > 0\},$$

and $H_\infty(\mathbf{C}_+)$ will represent the space of functions $f(s)$ that are bounded and analytic in $\mathbf{C}_+$ with the standard H_∞ norm,

$$\|f\|_\infty = \sup_{\omega \in \mathbf{R}} |\tilde{f}(j\omega)|,$$

where $\tilde{f}(j\omega)$ is the boundary function associated with $f(s)$.

We consider one version of the Small Gain Theorem. In this problem, a stable, linear time-invariant system is perturbed via feedback by a stable transfer function ΔP with bounded H_∞ norm, as illustrated by Figure 9.1. The question which

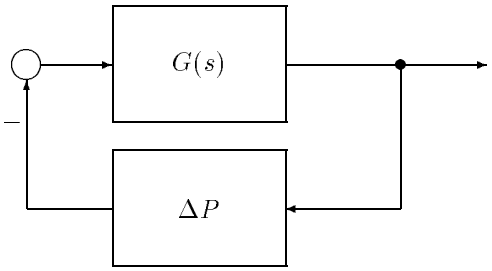

Figure 9.1. Stable system with H_∞ norm bounded feedback perturbation

is usually addressed in the robust stability literature is that of stability of the closed-loop system for all stable ΔP contained in an H_∞ ball of prescribed radius. Referring to Figure 9.1, we state the following well known result.

Theorem 9.1 (Small Gain Theorem)
If $G(s)$ is a stable transfer function, then the closed loop system remains stable for all perturbations ΔP satisfying $\|\Delta P\|_\infty < \alpha$, if and only if

$$\|G\|_\infty \leq \frac{1}{\alpha}. \tag{9.1}$$

Notice that in this result ΔP can be any H_∞ function. However, it has been shown that if (9.1) is violated then it is always possible to find a destabilizing ΔP which is a real rational function. We remark that an identical result also holds for a matrix transfer function $G(s)$. This result provides a way to account for unstructured perturbations of the fixed linear system G. In the next section we extend this result to the case where $G(s)$ is subject to parameter perturbations as well.

9.3 SMALL GAIN THEOREM FOR INTERVAL SYSTEMS

We now turn our attention to the case where in addition to the unstructured feedback perturbations, the linear part of the configuration in Figure 9.1 is subject to parametric perturbations also. As in the previous two chapters we will model parametric uncertainty by considering interval or linear interval systems. We present the results first for the case of an interval system. Let

$$G(s) = \frac{N(s)}{D(s)}$$

where $N(s)$ belongs to a family of real interval polynomials $\mathbf{N}(s)$ and $D(s)$ belongs to a family of real interval polynomials $\mathbf{D}(s)$. The interval family $\mathbf{G}(s)$ is written,

following the notational convention of the last two chapters, as

$$\mathbf{G}(s) := \frac{\mathbf{N}(s)}{\mathbf{D}(s)}. \tag{9.2}$$

Let $K_N^i(s)$ and $K_D^i(s)$, $i = 1, 2, 3, 4$ denote the Kharitonov polynomials associated with $\mathbf{N}(s)$ and $\mathbf{D}(s)$, respectively. Introduce the Kharitonov systems

$$\mathbf{G}_{\mathrm{K}}(s) = \left\{ \frac{K_N^i(s)}{K_D^j(s)} \ : \ i, j \in \{1, 2, 3, 4\} \right\}. \tag{9.3}$$

The robust version of the Small Gain Theorem for interval systems can be stated as follows.

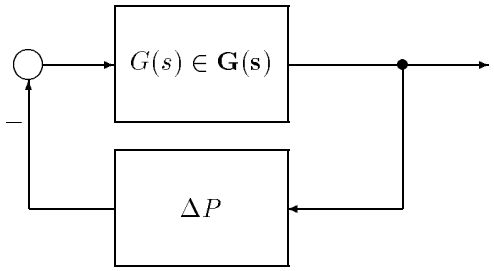

Figure 9.2. Closed loop system with H_∞ norm bounded function

Theorem 9.2 (Small Gain Theorem for Interval Systems)
Given the interval family $\mathbf{G}(s)$ of stable proper systems, the closed-loop in Figure 9.2 remains stable for all stable perturbations ΔP such that $\|\Delta P\|_\infty < \alpha$ if and only if

$$\alpha \leq \frac{1}{\max_{G \in \mathbf{G}_{\mathrm{K}}} \|G\|_\infty}. \tag{9.4}$$

The proof of this result follows from Theorem 9.1 (Small Gain Theorem) and the following lemma.

Lemma 9.1 *$\|G\|_\infty < 1$ for all $G(s)$ in $\mathbf{G}(s)$ if and only if $\|G\|_\infty < 1$ for the 16 elements of $\mathbf{G}_{\mathrm{K}}(s)$.*

The proof of this lemma is based on the following preliminary result, proved in Chapter 3, which characterizes proper rational functions $G(s)$ which are in $H_\infty(\mathbf{C}_+)$ and which satisfy $\|G\|_\infty < 1$.

Lemma 9.2 *Let*

$$G(s) = \frac{N(s)}{D(s)}$$

be a proper (real or complex) rational function in $H_\infty(\mathbf{C}_+)$, *with* degree$[D(s)] = q$ *and* n_q *and* d_q *denoting the leading coefficients of* $N(s)$ *and* $D(s)$, *respectively. Then* $\|G\|_\infty < 1$ *if and only if*

a1) $|n_q| < |d_q|$

b1) $D(s) + e^{j\theta}N(s)$ *is Hurwitz for all* θ *in* $[0, 2\pi)$.

The proof of this lemma is given in Chapter 3 (Lemma 3.1).

We can now prove Lemma 9.1.

Proof of Lemma 9.1 Necessity is obvious. For sufficiency we use the result of Lemma 9.2. First note that condition a1) of Lemma 9.2 is clearly true for all $G(s) \in \mathbf{G}(s)$ if it is true for the 16 Kharitonov systems.

Thus we prove that condition a2) is satisfied by any plant in $\mathbf{G}(s)$ if it is satisfied by the 16 plants of $\mathbf{G}_{\mathrm{K}}(s)$. We know from the bounding properties of Kharitonov polynomials that for an arbitrary element

$$G(s) = \frac{N(s)}{D(s)}$$

in $\mathbf{G}(s)$ and for any fixed $\omega \in \mathbb{R}$, there exists $i \in \{1, 2, 3, 4\}$ such that,

$$\left|\frac{N(j\omega)}{D(j\omega)}\right| \leq \left|\frac{K_N^i(j\omega)}{D(j\omega)}\right|.$$

Therefore, $\|G(s)\|_\infty < 1$, for all $G(s) \in \mathbf{G}(s)$, if and only if

$$\left\|\frac{K_N^i(s)}{D(s)}\right\|_\infty < 1, \qquad \text{for all } \; i \in \{1, 2, 3, 4\} \; \text{ and for all } \; D(s) \in \mathbf{D}(s).$$

Now for a fixed i, we have to check that, $D(s) + e^{j\theta}K_N^i(s)$ is Hurwitz, for all $D(s) \in \mathbf{D}(s)$, and for all $\theta \in [0, 2\pi)$. However, for a fixed $\theta \in [0, 2\pi)$, and a fixed $i \in \{1, 2, 3, 4\}$, the family of polynomials

$$\left\{ D(s) + e^{j\theta}K_N^i(s) \;:\; D(s) \in \mathbf{D}(s) \right\}$$

is an interval family of complex polynomials (with constant imaginary part) and therefore by Kharitonov's theorem for complex polynomials (see Chapter 5) this family is Hurwitz if and only if

$$K_D^l(s) + e^{j\theta}K_N^i(s)$$

is Hurwitz for all $l \in \{1, 2, 3, 4\}$. The proof of the Lemma is now completed by using again Lemma 9.2. ♣

The proof of Theorem 9.2 is an immediate consequence of the Small Gain Theorem and Lemma 9.2. We remark that at a *particular* frequency ω the maximum magnitude of $\|G(j\omega)\|$ does *not* necessarily occur at a Kharitonov vertex and therefore the result established in Theorem 9.2 is quite nontrivial.

Before proceeding we present a generalization of Lemma 9.2 to the multivariable case. Even though we will not use it, we believe that this generalization is of interest in its own right. Let $H_\infty^{m\times p}(\mathbf{C}_+)$ be the space of matrix-valued functions $F(s)$ that are bounded and analytic in $\mathbf{C}_+$ with the norm,

$$\|F\|_\infty = \sup_{\omega\in\mathbf{R}} \sigma_{\max}(\tilde{F}(j\omega))$$

where $\sigma_{\max}(\cdot)$ denotes the largest singular value of $(\cdot)$. For a constant complex matrix, $\|A\|$ will denote the following induced norm,

$$\|A\| = \sup_{\|v\|_2\le 1} \|Av\|_2 = \sigma_{\max}(A) \ .$$

Lemma 9.3 *Let $G(s)$ be a proper rational transfer function matrix in $H_\infty^{m\times p}(\mathbf{C}_+)$. Assume without loss of generality that $p \ge m$, and let $G(s) = N(s)D^{-1}(s)$ be a right coprime description of $G(s)$ over the ring of polynomial matrices, with $D(s)$ column-reduced, then $\|G\|_\infty < 1$ if and only if*

a2) $\|G(\infty)\| < 1$,

b2) $\det\left(D(s) + U\begin{bmatrix} I \\ 0 \end{bmatrix} N(s)\right)$ *is Hurwitz for all unitary matrices U in $C^{p\times p}$.*

Proof. *Sufficiency*: By contradiction if $\|G\|_\infty \ge 1$, then a2) implies that there exists $\omega_o \in \mathbb{R}$ such that $\|G^*(j\omega_o)G(j\omega_o)\| = 1$. But it is well known that $\|G(j\omega_o)\|^2 = \|G^*(j\omega_o)G(j\omega_o)\|$, and therefore for that same ω_o we have $\|G(j\omega_o)\| = 1$. Thus there exists $v \in C^p$ such that,

$$\|G(j\omega_o)v\|_2 = \|v\|_2 \ .$$

This implies that,

$$\left\| \begin{bmatrix} I \\ 0 \end{bmatrix} N(j\omega_o)D^{-1}(j\omega_o)v \right\|_2 = \|v\|_2 \ ,$$

and therefore there exists a unitary matrix U such that,

$$U\begin{bmatrix} I \\ 0 \end{bmatrix} N(j\omega_o)D^{-1}(j\omega_o)v = v \ .$$

As a result,

$$\det\left(D(j\omega_o) - U\begin{bmatrix} I \\ 0 \end{bmatrix} N(j\omega_o)\right) = 0 \ ,$$

and this is a contradiction.

Necessity: It is clear that condition a2) is necessary and therefore we assume that it holds in the following. In order to establish b2), the first step is to prove that,

$$\det\left(D(s)+\lambda\begin{bmatrix} I \\ 0 \end{bmatrix}N(s)\right)$$

is Hurwitz for all $\lambda \in [0,1]$. Consider the family of polynomials

$$\left\{P_\lambda(s)=\det\left(D(s)+\lambda\begin{bmatrix} I \\ 0 \end{bmatrix}N(s)\right):\lambda\in[0,1]\right\}.$$

Let us first show the following: a2) implies that this family has a constant degree. Indeed we can write,

$$D(s)=D_{hc}H_c(s)+D_{lc}(s),\ \ N(s)=N_{hc}H_c(s)+N_{lc}(s), \tag{9.5}$$

where $H_c(s)=\mathrm{diag}(s^{k_i}, i=1\cdots,p)$, k_i being the column-degree of the i^{th} column of $D(s)$, and $D_{lc}(s)$, $N_{lc}(s)$ contain the lower-degree terms.

It is easy to see that $G(\infty)=N_{hc}D_{hc}^{-1}$. Using (9.5) we also get

$$D(s)+\lambda\begin{bmatrix} I \\ 0 \end{bmatrix}N(s)=\left(D_{hc}+\lambda\begin{bmatrix} I \\ 0 \end{bmatrix}N_{hc}\right)H_c(s)+D_{lc}(s)+\lambda\begin{bmatrix} I \\ 0 \end{bmatrix}N_{lc}(s).$$

Now the fact that $D(s)$ is column-reduced implies that $\det(D_{hc})$ is nonzero. To prove our claim it is enough to show that

$$\det\left(D_{hc}+\lambda\begin{bmatrix} I \\ 0 \end{bmatrix}N_{hc}\right)\neq 0,\ \text{for all } \lambda\in(0,1].$$

Suppose by contradiction that for some $\lambda_o\in(0,1]$,

$$\det\left(D_{hc}+\lambda_o\begin{bmatrix} I \\ 0 \end{bmatrix}N_{hc}\right)=0.$$

This implies immediately that

$$\det\left(I+\lambda_o\begin{bmatrix} I \\ 0 \end{bmatrix}N_{hc}D_{hc}^{-1}\right)=\det\left(I+\lambda_o\begin{bmatrix} I & c \\ 0 \end{bmatrix}G(\infty)\right)=0.$$

Thus there would exist a vector $v\in C^p$ such that

$$\begin{bmatrix} I \\ 0 \end{bmatrix}G(\infty)v=\frac{1}{\lambda_o}v,$$

and therefore

$$\left\|\begin{bmatrix} I \\ 0 \end{bmatrix}G(\infty)v\right\|_2=\|G(\infty)v\|_2=\frac{1}{\lambda_o}\|v\|_2\geq\|v\|_2,$$

so that $\|G^*(\infty)G(\infty)\| = \|G(\infty)\|^2 \geq 1$, which is a contradiction.

With this claim we know that the family of polynomials $P_\lambda(s)$ contains one stable element, namely $P_0(s)$, and has a fixed degree. Using now the continuity of the roots of a polynomial with respect to its coefficients, we see that this family contains an unstable polynomial if and only if it also contains a polynomial with a root on the imaginary axis. However, if $P_{\lambda_o}(j\omega_o) = 0$ for some $\lambda_o \in (0, 1]$ and some $\omega_o \in \mathbb{R}$, then

$$\det\left(D(j\omega_o) + \lambda_o \begin{bmatrix} I \\ 0 \end{bmatrix} N(j\omega_o)\right) = 0,$$

and the same argument as above leads to the contradiction that

$$\|G^*(j\omega_o)G(j\omega_o)\| = \|G(j\omega_o)\|^2 \geq 1.$$

To complete the proof we need only apply the exact same reasoning as in the first step of the proof to the family of polynomials

$$\left\{P_U(s) = \det\left(D(s) + U \begin{bmatrix} I \\ 0 \end{bmatrix} N(s)\right) : U \text{ unitary matrix in } C^{p\times p}\right\}.$$

It can be proved first that this family has a constant degree, and the first part of the proof shows that it contains one stable polynomial (corresponding to $U = I$). Now note that the set of unitary matrices is pathwise connected. This is due to the fact that any unitary matrix U can be expressed as $U = e^{jF}$, where F is some Hermitian matrix, and therefore it is the image of a convex set under a continuous mapping. This implies in turn that the family of polynomials $P_U(s)$ is pathwise connected and thus allows us to use the continuity property of the roots of a polynomial with respect to its coefficients. ♣

9.3.1 Worst Case H_∞ Stability Margin

Theorem 9.2 states that in order to compute α the radius of the maximum allowable unstructured perturbation ball that does not destroy closed loop stability, it is sufficient to compute the maximum H_∞ norm of the Kharitonov systems. This is a tremendous reduction in computation since it replaces testing norms of an infinite family of functions to that of a finite set. In this context it is important to note that the boundary results of Chapter 8 already tell us that since $\partial\mathbf{G}(j\omega) \subset \partial\mathbf{G}_{\mathrm{E}}(j\omega)$, the maximum H_∞ norm over the parameter set occurs over the subset $\mathbf{G}_{\mathrm{E}}(s)$. The following example illustrates the use of these results.

Example 9.1. Consider the stable family $\mathbf{G}(s)$ of interval systems whose generic element is given by

$$G(s) = \frac{n_0 + n_1 s + n_2 s^2 + n_3 s^3}{d_0 + d_1 s + d_2 s^2 + d_3 s^3}$$

where

$$n_0 \in [1, 2], \quad n_1 \in [-3, 1], \quad n_2 \in [2, 4], \quad n_3 \in [1, 3],$$
$$d_0 \in [1, 3], \quad d_1 \in [2, 4], \quad d_2 \in [6, 7], \quad d_3 \in [1, 2].$$

$\mathbf{G}_{\mathrm{K}}(s)$ consists of the following 16 rational functions

$$G_1(s) = \frac{1-3s+4s^2+3s^3}{1+2s+7s^2+2s^3}, \quad G_2(s) = \frac{1-3s+4s^2+3s^3}{1+4s+7s^2+s^3}$$
$$G_3(s) = \frac{1-3s+4s^2+3s^3}{3+2s+6s^2+2s^3}, \quad G_4(s) = \frac{1-3s+4s^2+3s^3}{3+4s+6s^2+s^3},$$
$$G_5(s) = \frac{1+s+4s^2+s^3}{1+2s+7s^2+2s^3}, \quad G_6(s) = \frac{1+s+4s^2+s^3}{1+4s+7s^2+s^3},$$
$$G_7(s) = \frac{1+s+4s^2+s^3}{3+2s+6s^2+2s^3}, \quad G_8(s) = \frac{1+s+4s^2+s^3}{3+4s+6s^2+s^3},$$
$$G_9(s) = \frac{2-3s+2s^2+3s^3}{1+2s+7s^2+2s^3}, \quad G_{10}(s) = \frac{2-3s+2s^2+3s^3}{1+4s+7s^2+s^3},$$
$$G_{11}(s) = \frac{2-3s+2s^2+3s^3}{3+2s+6s^2+2s^3}, \quad G_{12}(s) = \frac{2-3s+2s^2+3s^3}{3+4s+6s^2+s^3},$$
$$G_{13}(s) = \frac{2+s+2s^2+s^3}{1+2s+7s^2+2s^3}, \quad G_{14}(s) = \frac{2+s+2s^2+s^3}{1+4s+7s^2+s^3},$$
$$G_{15}(s) = \frac{2+s+2s^2+s^3}{3+2s+6s^2+2s^3}, \quad G_{16}(s) = \frac{2+s+2s^2+s^3}{3+4s+6s^2+s^3}.$$

The 16 corresponding H_∞ norms are given by,

$$\begin{array}{llll} \|G_1\|_\infty = 2.112, & \|G_2\|_\infty = 3.0, & \|G_3\|_\infty = 5.002, & \|G_4\|_\infty = 3.0, \\ \|G_5\|_\infty = 1.074, & \|G_6\|_\infty = 1.0, & \|G_7\|_\infty = 1.710, & \|G_8\|_\infty = 1.0, \\ \|G_9\|_\infty = 3.356, & \|G_{10}\|_\infty = 3.0, & \|G_{11}\|_\infty = 4.908, & \|G_{12}\|_\infty = 3.0, \\ \|G_{13}\|_\infty = 2.848, & \|G_{14}\|_\infty = 2.0, & \|G_{15}\|_\infty = 1.509, & \|G_{16}\|_\infty = 1.0\ . \end{array}$$

Therefore, the entire family of systems remains stable under any unstructured feedback perturbations of H_∞ norm less than

$$\alpha = \frac{1}{5.002} = 0.19992\ .$$

To compute the worst case H_∞ stability margin of this system, without using the result of Lemma 9.2, we would need to plot the frequency template $\mathbf{G}(j\omega)$. From the boundary properties developed in Chapter 8 it follows that the maximum H_∞ norm occurs on the subset $\mathbf{G}_{\mathrm{E}}(j\omega)$. Figure 9.3 shows this template from which we find the worst case H_∞ stability margin to be 0.2002. This compares favorably with the previous computation of the H_∞ norm at the Kharitonov vertices, which was based on Lemma 9.2.

9.3.2 Worst Case Parametric Stability Margin

The converse problem, where a bound is fixed on the level α (size of the ball) of unstructured H_∞ perturbations that are to be tolerated and the largest parametric

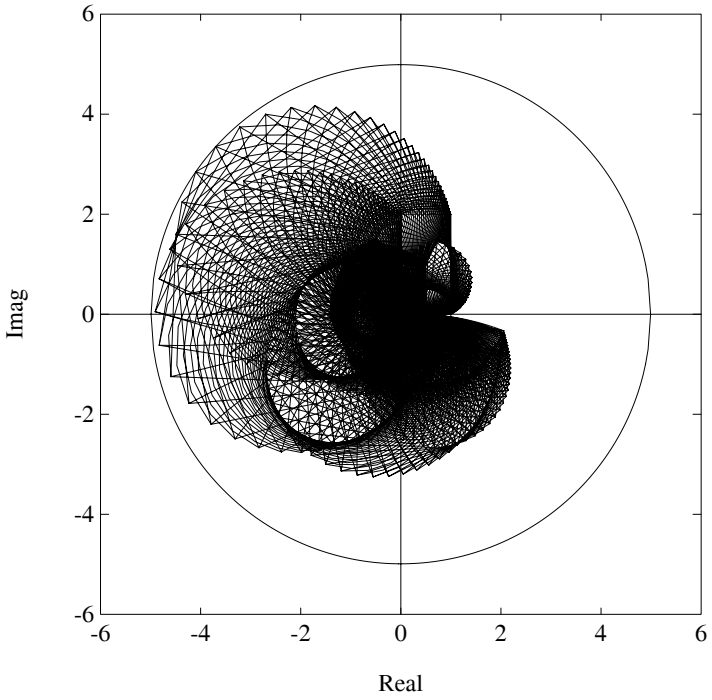

Figure 9.3. Frequency template of $\mathbf{G}_{\mathrm{E}}$ and H_∞ stability margin (Example 9.1)

stability ball is sought, is also important and will be considered in this subsection. In this case we start with a nominal stable system

$$G^o(s) = \frac{n_0^o + n_1^o s + \cdots + n_p^o s^p}{d_0^o + d_1^o s + \cdots + d_q^o s^q}$$

which satisfies $\|G^o\|_\infty = \alpha$. A bound $\frac{1}{\beta} < \frac{1}{\alpha}$ is then fixed on the desired level of unstructured perturbations. It is then possible to fix the structure of the parametric perturbations and to maximize a weighted l_∞ ball around the parameters of $G^o(s)$. More precisely, one can allow the parameters n_i, d_j of the plant to vary in intervals of the form

$$n_i \in [n_i^o - \epsilon\nu_i, n_i^o + \epsilon\nu_i], \quad d_j \in [d_j^o - \epsilon\mu_j, d_j^o + \epsilon\mu_j],$$

where the weights ν_i, μ_j are fixed and nonnegative. For each ϵ we get a family of interval systems $\mathbf{G}(s,\epsilon)$ and its associated set of Kharitonov systems $\mathbf{G}_{\mathrm{K}}(s,\epsilon)$. The structured stability margin is then given by the largest ϵ, say $\epsilon_{\max}$, for which every system $G(s)$ in the corresponding interval family $\mathbf{G}(s,\epsilon_{\max})$ satisfies $\|G\|_\infty \leq \beta$.

An upper bound ϵ_1 for $\epsilon_{\max}$ is easily found by letting ϵ_1 be the smallest number such that the interval family,

$$\left\{D(s) = d_0 + \cdots + d_q s^q : \ d_j \in [d_j^o - \epsilon_1 \mu_j, d_j^o + \epsilon_1 \mu_j]\right\}$$

contains an unstable polynomial. This upper bound is easily calculated using Kharitonov's Theorem. One way to compute $\epsilon_{\max}$ is then to use a bisection algorithm:

1. set LBOUND=0, UBOUND=ϵ_1.
2. Let $\epsilon = \dfrac{\text{UBOUND} + \text{LBOUND}}{2}$.
3. Update $\mathbf{G}_{\mathrm{K}}(s, \epsilon)$.
4. If the 16 systems in $\mathbf{G}_{\mathrm{K}}(s, \epsilon)$ have H_∞ norm $\leq \beta$ then set LBOUND $= \epsilon$, otherwise set UBOUND $= \epsilon$.
5. if |UBOUND $-$ LBOUND| is small enough then EXIT, otherwise GOTO 2.

This procedure requires, at each step, that we check the H_∞ norm of the 16 current Kharitonov systems. We illustrate the computation of the l_∞ structured margin in the following example.

Example 9.2. Let the nominal system be given by

$$G(s) = \frac{1 - s}{1 + 3s + s^2}.$$

The H_∞ norm of $G(s)$ is equal to 1. Let us fix the bound on the unstructured margin to be equal to $\frac{1}{2}$. To simplify the notation we assume that the perturbed system is of the form

$$G_{a,b,c,d}(s) = \frac{1 + a - (1 + b)s}{1 + c + (3 + d)s + s^2}$$

where

$$|a| \leq \epsilon, \ |b| \leq \epsilon, \ |c| \leq \epsilon, \ |d| \leq \epsilon \ . \tag{9.6}$$

We seek the largest ϵ such that for all (a, b, c, d) satisfying (9.6)

$$\|G_{a,b,c,d}\|_\infty \leq 2.$$

For this simple example, $\epsilon_{\max}$ can be computed analytically and is readily found to be equal to 1/3. The extremal systems are,

$$\frac{\frac{4}{3} - \frac{2}{3}s}{\frac{2}{3} + \frac{10}{3}s + s^2}, \quad \frac{\frac{4}{3} - \frac{4}{3}s}{\frac{2}{3} + \frac{10}{3}s + s^2}, \quad \frac{\frac{4}{3} - \frac{2}{3}s}{\frac{2}{3} + \frac{8}{3}s + s^2}, \quad \frac{\frac{4}{3} - \frac{4}{3}s}{\frac{2}{3} + \frac{8}{3}s + s^2} \ .$$

In the next section we extend the results of this section to the case where a feedback controller is present and $\mathbf{G}(s)$ is a set of linear interval systems.

9.4 ROBUST SMALL GAIN THEOREM

We now extend the results of the last section to the case in which a fixed feedback controller is connected to a class of linear interval systems. As we have seen before, this case occurs when the parameters of interest enter affine linearly into the transfer function coefficients. Let

$$\mathbf{G}(s) := \frac{\mathbf{N}(s)}{\mathbf{D}(s)} \tag{9.7}$$

be a family of *strictly proper* linear interval systems. We refer the reader to Chapter 8 (Section 8.6, p. 358) for precise definition of this family of systems as well as the definition of the extremal subset $\mathbf{G}_{\mathrm{E}}(s)$.

Assume that we have found a stabilizing controller $C(s)$ for the entire family. We therefore have a family of stable closed-loop systems and we consider unstructured additive perturbations as shown in Figure 9.4. The family of perturbed plants under

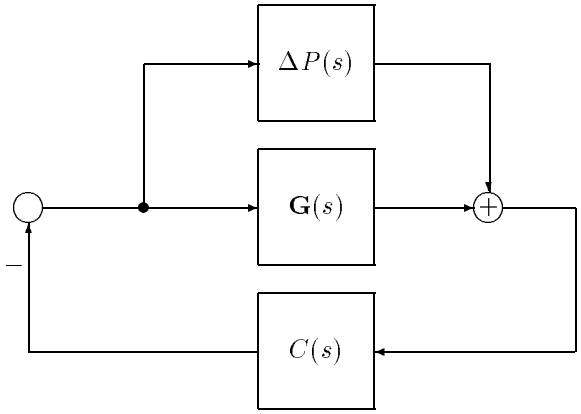

Figure 9.4. Closed loop system with additive norm bounded perturbations

consideration can be represented as

$$\{(G(s) + \Delta P) : G(s) \in \mathbf{G}(s), \quad \|\Delta P\|_\infty < \alpha\}.$$

In order to determine the amount of unstructured perturbations that can be tolerated by this family of additively perturbed interval systems we have to find the maximum of the H_∞ norm of the closed-loop transfer function

$$C(s)\left(1 + G(s)C(s)\right)^{-1}$$

over all elements $G(s) \in \mathbf{G}(s)$.

In the case of multiplicative perturbations we consider the family of perturbed plants to be:

$$\{(I + \Delta P)G(s) : G(s) \in \mathbf{G}(s), \quad \|\Delta P\|_\infty < \alpha\}.$$

Here, the level of unstructured perturbations α that can be tolerated by the closed loop system without becoming unstable is determined by the maximum value of the H_∞ norm

$$\left\| G(s)C(s)\left(1+G(s)C(s)\right)^{-1} \right\|_\infty$$

as $G(s)$ ranges over $\mathbf{G}(s)$.

The following theorem shows us that the exact level of unstructured perturbations that can be tolerated by the *family* of closed-loop systems, can be computed, in both the additive and multiplicative cases, by replacing $\mathbf{G}(s)$ by the subset $\mathbf{G}_{\mathrm{E}}(s)$ in the corresponding block diagram.

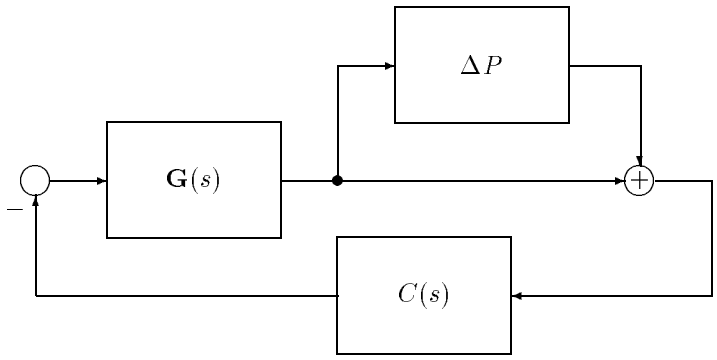

Figure 9.5. Closed loop system with multiplicative norm bounded perturbations

Theorem 9.3 (Robust Small Gain Theorem)
Given an interval family $\mathbf{G}(s)$ of strictly proper plants and a stabilizing controller $C(s)$ for $\mathbf{G}(s)$, the closed-loop in a) Figure 9.4 or b) Figure 9.5 remains stable for all stable perturbations ΔP such that $\|\Delta P\|_\infty < \alpha$ if and only if,

a) $\alpha \leq \frac{1}{\sup_{G\in\mathbf{G}_{\mathrm{E}}} \left\| C(s)(1+G(s)C(s))^{-1} \right\|_\infty}$

b) $\alpha \leq \frac{1}{\sup_{G\in\mathbf{G}_{\mathrm{E}}} \left\| G(s)C(s)(1+G(s)C(s))^{-1} \right\|_\infty}$.

Proof. For a) consider the family of transfer functions

$$\left\{ C(s)\left(1+G(s)C(s)\right)^{-1} \ : \ G(s)\in\mathbf{G}(s) \right\}$$

which we denote as

$$C(s)\left(1+\mathbf{G}(s)C(s)\right)^{-1}.$$

Recall from Theorem 8.4 (Chapter 8) that the boundary of the image of the above set at $s = j\omega$ is identical to the boundary of the image of the set

$$C(s)\left(1 + \mathbf{G}_{\mathrm{E}}(s)C(s)\right)^{-1}.$$

In other words,

$$\partial\left(C(j\omega)\left(1 + \mathbf{G}(j\omega)C(j\omega)\right)^{-1}\right) \subset C(j\omega)\left(1 + \mathbf{G}_{\mathrm{E}}(j\omega)C(j\omega)\right)^{-1}$$

From this it follows that

$$\sup_{G\in\mathbf{G}} \left|C(j\omega)\left(1 + G(j\omega)C(j\omega)\right)^{-1}\right| = \sup_{G\in\mathbf{G}_{\mathrm{E}}} \left|C(j\omega)\left(1 + G(j\omega)C(j\omega)\right)^{-1}\right|$$

for each $\omega \geq 0$. Therefore,

$$\sup_{G\in\mathbf{G}} \left\|C(s)\left(1 + G(s)C(s)\right)^{-1}\right\|_\infty = \sup_{G\in\mathbf{G}_{\mathrm{E}}} \left\|C(s)\left(1 + G(s)C(s)\right)^{-1}\right\|_\infty .$$

This completes the proof of a). The proof of b) is similar. ♣

Remark 9.1. The theorems given above are stated for an interval plant $\mathbf{G}(s)$. From the boundary results Theorem 8.3 established in Chapter 8 we know that identical results hold for linear interval systems (p. 358) and also for linear fractional transformations of linear interval systems (p. 363).

Theorem 9.3 allows for the computation of the unstructured stability margin for a prescribed level of structured perturbations. This stability margin can also serve as a measure of the performance of the system. The computation of

$$\sup_{G\in\mathbf{G}_{\mathrm{E}}} \left\|C(s)\left(1 + G(s)C(s)\right)^{-1}\right\|_\infty$$

is not very complicated as can be seen from the following example.

Example 9.3. (Computation of unstructured stability margin) Consider the interval plants,

$$\begin{aligned}\mathbf{G}(s) &= \frac{\mathbf{N}(s)}{\mathbf{D}(s)} \\ &= \frac{\beta s}{1 - s + \gamma s^2 + s^3} \quad : \quad \beta \in [1, 2],\ \gamma \in [3.4, 5].\end{aligned}$$

Using the results of GKT (Chapter 7) one can easily check that the controller

$$C(s) = \frac{3}{s + 1}$$

stabilizes the entire family. The transfer function family of interest is given by

$$C(s)\left(1+G_{\beta,\gamma}(s)C(s)\right)^{-1}=\frac{3(1-s+\gamma s^2+s^3)}{1+3\beta s+(\gamma-1)s^2+(\gamma+1)s^3+s^4}.$$

According to Theorem 9.3, to compute the H_∞ stability margin α, we have to find the maximum H_∞ norm of four one-parameter families of rational functions, namely

$$r_\lambda(s)=\frac{3(1-s+\lambda s^2+s^3)}{1+3s+(\lambda-1)s^2+(\lambda+1)s^3+s^4},\quad \lambda\in[3.4,5],$$

$$r_\mu(s)=\frac{3(1-s+\mu s^2+s^3)}{1+6s+(\mu-1)s^2+(\mu+1)s^3+s^4},\quad \mu\in[3.4,5],$$

$$r_\nu(s)=\frac{3(1-s+3.4s^2+s^3)}{1+3\nu s+2.4s^2+4.4s^3+s^4},\quad \nu\in[1,2],$$

$$r_\xi(s)=\frac{3(1-s+5s^2+s^3)}{1+3\xi s+4s^2+6s^3+s^4},\quad \xi\in[1,2].$$

Consider for example the case of $r_\lambda(s)$. We have

$$|r_\lambda(j\omega)|^2=\frac{9\left((1-\lambda\omega^2)^2+\omega^2(1+\omega^2)^2\right)}{\left(1-(\lambda-1)\omega^2+\omega^4\right)^2+\omega^2\left(3-(\lambda+1)\omega^2\right)^2}.$$

Letting $t=\omega^2$ we have to find

$$\sup_{t\geq 0,\lambda\in[3.4,5]} f(t,\lambda)=\sup_{t\geq 0,\lambda\in[3.4,5]}\frac{9\left((1-\lambda t)^2+t(1+t)^2\right)}{\left(1-(\lambda-1)t+t^2\right)^2+t\left(3-(1+\lambda)t\right)^2}.$$

Differentiating with respect to λ we get a supremum at,

$$\lambda_1(t)=\frac{-2t+3+\sqrt{4t^3+12t^2+1}}{2t}$$

or

$$\lambda_2(t)=\frac{-2t+3-\sqrt{4t^3+12t^2+1}}{2t}.$$

It is then easy to see that $\lambda_1(t)\in[3.4,5]$ if and only if $t\in[t_1,t_2]\cup[t_3,t_4]$ where,

$$t_1\simeq 0.39796,\quad t_2\simeq 0.64139,\quad t_3\simeq 15.51766,\quad t_4\simeq 32.44715\ ,$$

whereas, $\lambda_2(t)\in[3.4,5]$ if and only if $t\in[t_5,t_6]$ where,

$$t_5\simeq 0.15488,\quad t_6\simeq 0.20095\ .$$

As a result, the maximum H_∞ norm for $r_\lambda(s)$ is given by,

$$\max\left(\|r_{3.4}\|_\infty,\|r_5\|_\infty,\sqrt{\sup_{t\in[t_1,t_2]\cup[t_3,t_4]}f(t,\lambda_1(t))},\sqrt{\sup_{t\in[t_5,t_6]}f(t,\lambda_2(t))}\right)$$

where one can at once verify that,

$$f(t,\lambda_1(t)) = \frac{9\left(2t-1-\sqrt{4t^3+12t^2+1}\right)}{2t^2+7t-1-(t+1)\sqrt{4t^3+12t^2+1}}$$

and,

$$f(t,\lambda_2(t)) = \frac{9\left(2t-1+\sqrt{4t^3+12t^2+1}\right)}{2t^2+7t-1+(t+1)\sqrt{4t^3+12t^2+1}}.$$

This maximum is then easily found to be equal to,

$$\max(34.14944, 7.55235, 27.68284, 1.7028) = 34.14944\ .$$

Proceeding in the same way for $r_\mu(s)$, $r_\nu(s)$, and $r_\xi(s)$, we finally get

$$\max_{\beta\in[1,2],\gamma\in[3.4,5]} \left\| C(s)\left(1+G_{\beta,\gamma}(s)C(s)\right)^{-1}\right\|_\infty = 34.14944$$

where the maximum is in fact achieved for $\beta = 1$, $\gamma = 3.4$.

9.5 ROBUST PERFORMANCE

The result established in the last section that for the controller to tolerate a certain amount of unstructured uncertainty over the entire parametrized family $\mathbf{G}(s)$ it is necessary and sufficient that it achieves the same level of tolerance over the subset $\mathbf{G}_{\mathrm{E}}(s)$. In the H_∞ approach to robust control problems, system performance is measured by the size of the H_∞ norm of error, output and other transfer functions. When parameter uncertainty is present, it is appropriate to determine *robust performance* by determining the worst case performance over the parameter uncertainty set. This amounts to determining the maximum values of the H_∞ norm of various system transfer functions over the uncertainty set. For instance, in the control system shown in Figure 9.6 it may be desirable to minimize the H_∞ norm of the error transfer function

$$T^e(s) = \left(1+C(s)G(s)\right)^{-1} \tag{9.8}$$

in order to minimize the worst case tracking error. The H_∞ norm of the output transfer function

$$T^y(s) = C(s)G(s)\left(1+C(s)G(s)\right)^{-1} \tag{9.9}$$

known as M - *peak* in classical control is usually required to be small. To keep the control signal small the H_∞ norm of

$$T^u(s) = C(s)\left(1+C(s)G(s)\right)^{-1} \tag{9.10}$$

should be small.

The following theorem shows us that the worst case performance measured in any of the above norms over the set of systems $\mathbf{G}(s)$ can in fact be determined by replacing $G(s)$ in the control system by elements of the one-parameter family of systems $\mathbf{G}_{\mathrm{E}}(s)$.

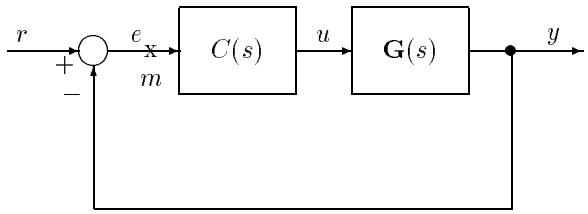

Figure 9.6. A standard unity feedback systems

Theorem 9.4 (Robust Performance)
The maximum value of the H_∞ norms of $T^e(s)$, $T^y(s)$ and $T^u(s)$ over $\mathbf{G}(s)$ is attained over $\mathbf{G}_{\mathrm{E}}(s)$:

$$\sup_{G\in\mathbf{G}} \left\| (1+C(s)G(s))^{-1} \right\|_\infty = \sup_{G\in\mathbf{G}_{\mathrm{E}}} \left\| (1+C(s)G(s))^{-1} \right\|_\infty$$

$$\sup_{G\in\mathbf{G}} \left\| C(s)G(s)\,(1+C(s)G(s))^{-1} \right\|_\infty = \sup_{G\in\mathbf{G}_{\mathrm{E}}} \left\| C(s)G(s)\,(1+C(s)G(s))^{-1} \right\|_\infty .$$

$$\sup_{G\in\mathbf{G}} \left\| C(s)\,(1+C(s)G(s))^{-1} \right\|_\infty = \sup_{G\in\mathbf{G}_{\mathrm{E}}} \left\| C(s)\,(1+C(s)G(s))^{-1} \right\|_\infty .$$

The proof of this theorem is identical to that of Theorem 9.3 and also follows from the boundary properties given in Chapter 8. Analogous results hold for systems where disturbances are present and also where the transfer functions under consideration are suitably weighted. These results precisely determine the role of the controller in robust stability and performance analysis and in the design of control systems containing parameter uncertainty.

Example 9.4. **(H_∞ Performance Example)** Let the plant and the stabilizing controller be

$$G(s) = \frac{\beta s}{s^3 + \alpha s^2 - s + 1}$$

and

$$C(s) = \frac{3}{s+1}$$

where

$$\alpha \in [3.4, 5], \quad \beta \in [1, 2].$$

A closed loop system transfer function is

$$T^u(s) = C(s)\left[1 + \mathbf{G}(s)C(s)\right]^{-1}.$$

To compute the worst case H_∞ stability margin of this closed loop system under additive perturbations, we only need to plot the frequency template

$$\mathbf{T}^u(j\omega) = C(j\omega)\left[1 + \mathbf{G}_{\mathrm{E}}(j\omega)C(j\omega)\right]^{-1}.$$

Figure 9.7 shows this template. From this we find that the worst case H_∞ stability margin is 0.0293.

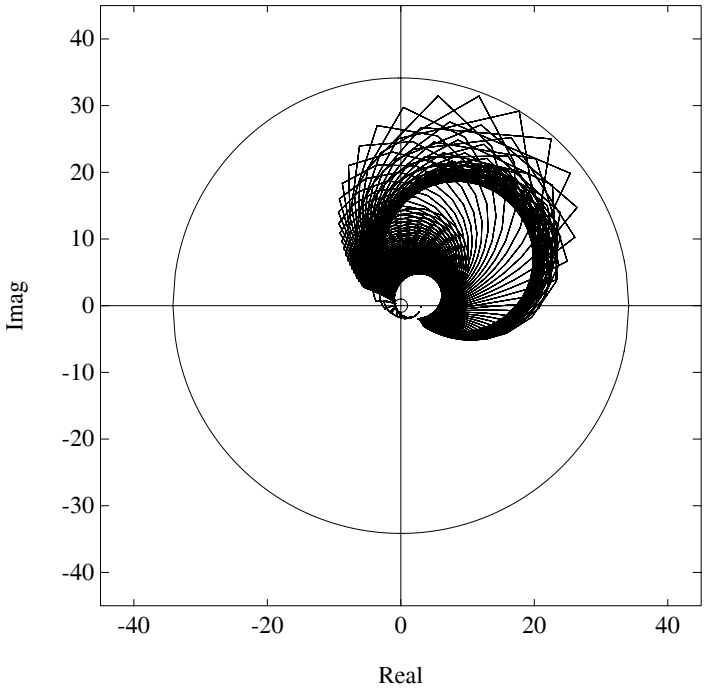

Figure 9.7. Frequency template of $\mathbf{T}^u(j\omega)$ and H_∞ stability margin (Example 9.4)

9.6 VERTEX RESULTS FOR EXTREMAL H_∞ NORMS

In this subsection we give some useful vertex results for the computation of the extremal H_∞ norm. We start by considering a control system containing an interval plant with multiplicative unstructured perturbations, connected to a feedback controller with a special structure.

Theorem 9.5 *Let a controller $C(s)$ be of the form*

$$C(s) = \frac{N_c(s)}{D_c(s)} = \frac{A_1(s)E_1(s)}{s^t A_2(s)E_2(s)} \tag{9.11}$$

where t is a positive integer, $A_i(s)$ are anti-Hurwitz and $E_i(s)$ are even polynomials. $C(s)$ stabilizes the feedback system in Figure 9.5 for all ΔP such that $\|\Delta P\|_\infty < \alpha$ if and only if it stabilizes $\mathbf{G}_{\mathrm{K}}(s)$ and

$$\alpha \leq \frac{1}{\sup_{G \in \mathbf{G}_{\mathrm{K}}} \left\| G(s)C(s)\left(1+G(s)C(s)\right)^{-1} \right\|_\infty}.$$

Proof. From Theorem 9.4 we already know that the extremal value of the H_∞ norm of $G(s)C(s)(1+G(s)C(s))^{-1}$ over the family $\mathbf{G}(s)$ occurs over the subset $\mathbf{G}_{\mathrm{E}}(s)$. Thus, we need only show that the maximum H_∞ norm of the closed loop transfer function $G(s)C(s)(1+G(s)C(s))^{-1}$ along an arbitrary segment of $\mathbf{G}_{\mathrm{E}}(s)$ is attained at one of the two vertex plants corresponding to its endpoints.

Now consider a specific extremal segment in $\mathbf{G}_{\mathrm{E}}(s)$ say,

$$G(s,\lambda) := \frac{K_N^1(s)}{K_D^3(s) + \lambda\left[K_D^2(s) - K_D^3(s)\right]}, \quad \lambda \in [0,1].$$

Denote the associated vertex systems by

$$V_1(s) = \left(C(s)\frac{K_N^1(s)}{K_D^3(s)}\left(1 + \frac{K_N^1(s)}{K_D^3(s)}C(s)\right)^{-1}\right)$$
$$V_2(s) = \left(C(s)\frac{K_N^1(s)}{K_D^2(s)}\left(1 + \frac{K_N^1(s)}{K_D^2(s)}C(s)\right)^{-1}\right).$$

We need to establish the implication

$$\max\left(\|V_1(s)\|_\infty, \|V_2(s)\|_\infty\right) < \frac{1}{\alpha} \tag{9.12}$$

$$\Downarrow$$

$$\left\| G(s,\lambda)C(s)\left(1+G(s,\lambda)C(s)\right)^{-1} \right\|_\infty < \frac{1}{\alpha}, \quad \text{for all} \;\; \lambda \in [0,1]. \tag{9.13}$$

By the hypotheses in (9.12) and Lemma 9.2, the following two polynomials are Hurwitz for any fixed real $\theta \in [0, 2\pi]$:

$$P_0(s) = K_N^1(s)N_c(s)(1-\alpha e^{j\theta}) + D_c(s)K_D^3(s)$$
$$P_1(s) = K_N^1(s)N_c(s)(1-\alpha e^{j\theta}) + D_c(s)K_D^2(s).$$

Consider now the complex segment of polynomials

$$P_\lambda(s) = P_0(s) + \lambda\left[P_1(s) - P_0(s)\right], \quad \lambda \in [0,1].$$

We have

$$\delta_0(s) := P_1(s) - P_0(s) = D_c(s)[K_D^3(s) - K_D^2(s)] = s^t A_2(s)E_2(s)[K_D^3(s) - K_D^2(s)].$$

It is easy to see that under the assumptions made on $C(s)$

$$\frac{d}{d\omega} \arg \delta_0(j\omega) \leq 0$$

since the anti-Hurwitz factor has nonpositive rate of change of phase while each of the other factors has a zero rate of change of phase. Thus $\delta_0(s)$ is a convex direction by Lemma 2.15 (Chapter 2) and therefore $P_\lambda(s)$ is Hurwitz for all $\lambda \in [0,1]$. This implies that

$$\begin{aligned} P_\lambda(j\omega) = K_N^1(j\omega)N_c(j\omega)(1-\alpha e^{j\theta}) + D_c(j\omega)K_D^3(j\omega) \\ +\lambda D_c(j\omega)\left[K_D^2(j\omega) - K_D^3(j\omega)\right] \neq 0, \\ \text{for all } \omega, \quad \text{for all } \lambda \in [0,1]. \end{aligned} \tag{9.14}$$

Since (9.14) holds for any $\theta \in [0, 2\pi]$, the conditions in Lemma 9.2 are satisfied for the transfer function

$$\alpha G(s,\lambda)C(s)\left(1+G(s,\lambda)C(s)\right)^{-1}, \quad \text{for all } \lambda \in [0,1].$$

Thus, it follows that (9.13) holds. This type of argument can be applied to each segment in $\mathbf{G}_E(s)$ to complete the proof. ♣

The extremal H_∞ norm calculation of the sensitivity and complementary sensitivity functions of a unity feedback system containing an interval plant $\mathbf{G}(s)$ also enjoy the vertex property. The sensitivity function is

$$S(s) = \frac{1}{1+G(s)} \tag{9.15}$$

and the complementary sensitivity function is

$$T(s) = 1 - S(s). \tag{9.16}$$

Lemma 9.4

$$\begin{aligned} \sup_{G\in\mathbf{G}} \|S(s)\|_\infty &= \sup_{G\in\mathbf{G}_K} \|S(s)\|_\infty \\ \sup_{G\in\mathbf{G}} \|T(s)\|_\infty &= \sup_{G\in\mathbf{G}_K} \|T(s)\|_\infty . \end{aligned}$$

We leave the proof to the reader as it is identical to the proof of the previous result, and based on Lemma 9.2 and the Complex Convex Direction Lemma (Lemma 2.15, Chapter 2).

To conclude this section we present without proof two special vertex results that do not follow from the Convex Direction Lemma. The first result holds for interval plants multiplied by a special type of weighting factor. As usual, let $\mathbf{G}(s)$ denote an interval transfer function family.

Lemma 9.5 *Let $p(s)$ be an arbitrary polynomial and β a positive real number such that $\dfrac{p(s)}{s+\beta}G(s)$ is proper and stable for every $G(s) \in \mathbf{G}(s)$. Then*

$$\sup_{G\in\mathbf{G}} \left\| \frac{p(s)}{s+\beta}G(s) \right\|_\infty = \sup_{G\in\mathbf{G}_{\mathrm{K}}} \left\| \frac{p(s)}{s+\beta}G(s) \right\|_\infty$$

The next vertex result holds for a limited class of weighted sensitivity and complementary sensitivity functions.

Lemma 9.6 *Let α and β be positive numbers with $\alpha \neq \beta$, $K_S > 1$ and $K_T < \dfrac{\beta}{\alpha}$. If the transfer functions*

$$\frac{s+\alpha}{s+\beta}S(s) \quad \text{and} \quad \frac{s+\alpha}{s+\beta}T(s)$$

are proper and stable for all $G(s) \in \mathbf{G}(s)$, then

$$\sup_{G\in\mathbf{G}} \left\| K_S\frac{s+\alpha}{s+\beta}S(s) \right\|_\infty = \sup_{G\in\mathbf{G}_{\mathrm{K}}} \left\| K_S\frac{s+\alpha}{s+\beta}S(s) \right\|_\infty$$
$$\sup_{G\in\mathbf{G}} \left\| K_T\frac{s+\alpha}{s+\beta}T(s) \right\|_\infty = \sup_{G\in\mathbf{G}_{\mathrm{K}}} \left\| K_T\frac{s+\alpha}{s+\beta}T(s) \right\|_\infty .$$

In the following section we turn to another model of unstructured perturbation, namely nonlinear feedback gains lying in a sector.

9.7 THE ABSOLUTE STABILITY PROBLEM

The classical Lur'e or Popov problem considers the stability of a fixed linear time invariant dynamic system perturbed by a family of nonlinear feedback gains. This problem is also known as the *absolute stability* problem. This framework is a device to account for unstructured perturbations of the fixed linear system. Consider the configuration in Figure 9.8 where a stable, linear time-invariant system is connected by feedback to a memoryless, time-varying nonlinearity.

The Absolute Stability problem is the following: Under what conditions is the closed-loop system in the configuration above globally, uniformly asymptotically stable for all nonlinearities in a prescribed class? We first consider the allowable nonlinearities to be time-varying and described by sector bounded functions. Specifically, the nonlinearity $\phi(t,\sigma)$ is assumed to be single-valued and satisfying (see Figure 9.9)

$$\phi(t,0) = 0, \quad \text{for all } t \geq 0,$$
$$0 \leq \sigma\phi(t,\sigma) \leq k\sigma^2. \tag{9.17}$$

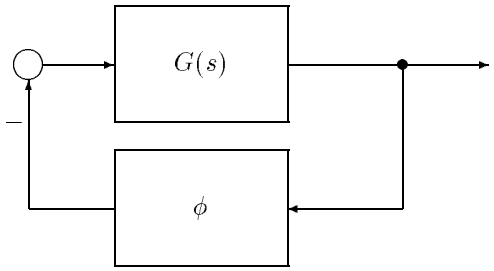

Figure 9.8. Absolute stability problem

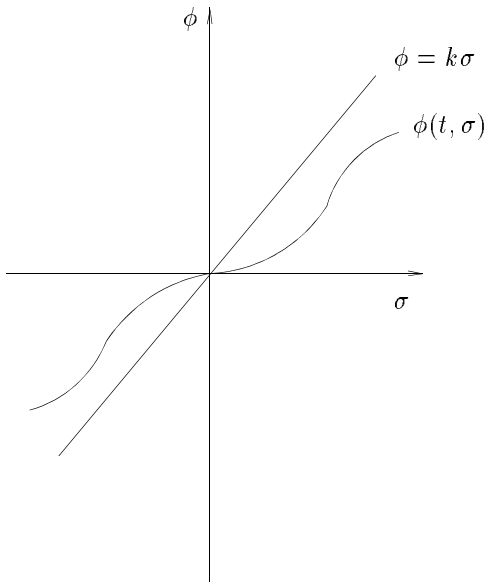

Figure 9.9. Sector bounded nonlinear function

Assumption (9.17) implies that $\phi(t,\sigma)$ is bounded by the lines $\phi = 0$ and $\phi = k\sigma$. Such nonlinearities are said to belong to a sector $[0, k]$.

An important condition that arises in the solution of this absolute stability problem is the property of strict positive realness (SPR) of a transfer function. This property is closely related to passivity and robustness of the system. The SPR property is defined as follows:

Definition 9.1. A proper transfer function $G(s)$ is said to be strictly positive real (SPR) if

1) $G(s)$ has no poles in the closed right half plane, and

2) $\mathrm{Re}[G(j\omega)] > 0, \quad \omega \in (-\infty, +\infty)$.

Referring to Figure 9.8, we first state a well-known result on absolute stability.

Theorem 9.6 (Lur'e Criterion)
If $G(s)$ is a stable transfer function, and ϕ belongs to the sector $[0, k_L]$, then a sufficient condition for absolute stability is that

$$\frac{1}{k_L} + \mathrm{Re}\,[G(j\omega)] > 0, \qquad \textit{for all } \omega \in \mathbb{R}. \tag{9.18}$$

We illustrate this with an example.

Example 9.5. Let us consider the following stable transfer function

$$G(s) = \frac{3.1s + 3.2}{s^4 + 1.1s^3 + 24.5s^2 + 2.5s + 3.5}$$

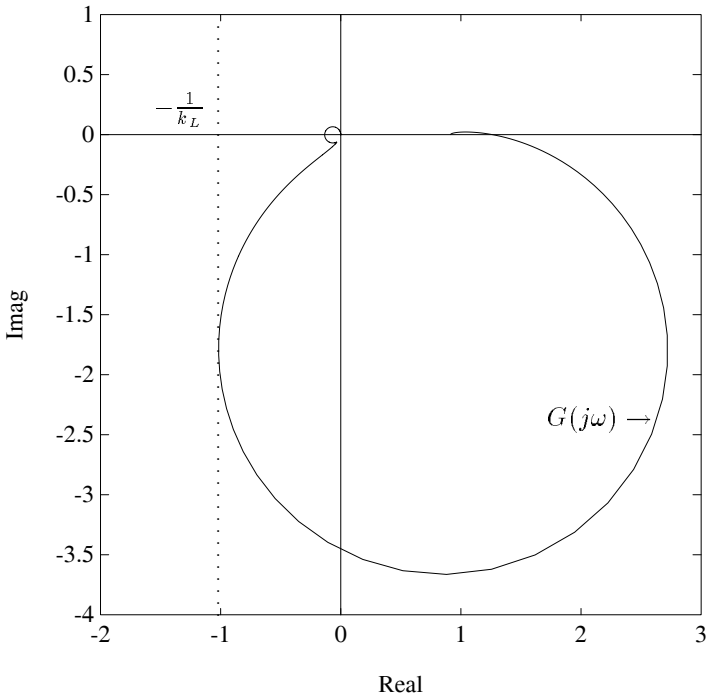

Figure 9.10. $G(j\omega)$: Lur'e problem (Example 9.5)

Figure 9.10 shows that the Lur'e gain k_L is obtained from the minimum real value of $G(j\omega)$. From Figure 9.10 we obtain $k_L = 0.98396$. Using the Lur'e gain, Figure 9.11 shows that

$$\frac{1}{k_L} + \mathrm{Re}\,[G(s)]$$

is SPR.

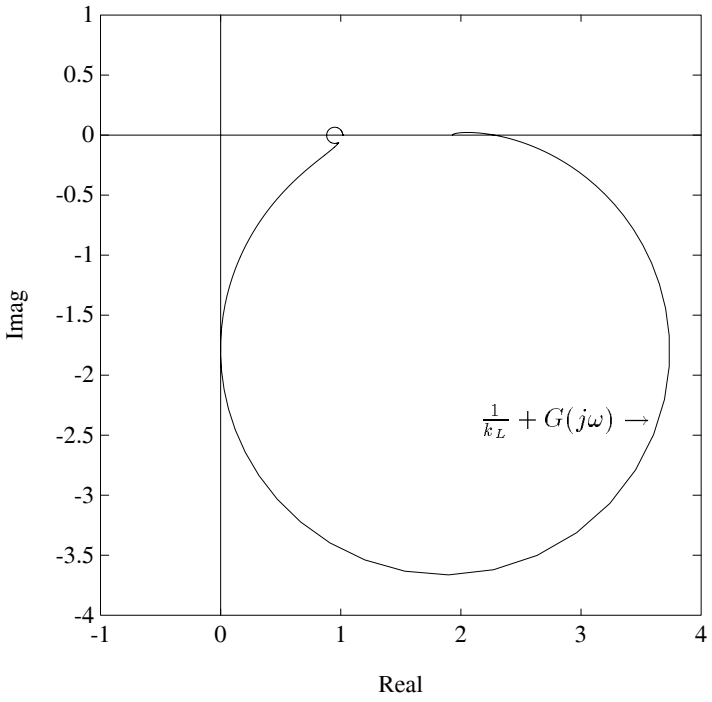

Figure 9.11. SPR property of $\frac{1}{k_L} + G(s)$ (Example 9.5)

We now impose the further restriction that the nonlinearity ϕ is time-invariant and enunciate the Popov criterion.

Theorem 9.7 (Popov Criterion)
If $G(s)$ is a stable transfer function, and ϕ is a time-invariant nonlinearity which belongs to the sector $[0, k_P]$, then a sufficient condition for absolute stability is that there exist a real number q such that

$$\frac{1}{k_P} + \mathrm{Re}\,[(1 + qj\omega)G(j\omega)] > 0, \qquad \textit{for all } \omega \in \mathbb{R}. \tag{9.19}$$

This theorem has a graphical interpretation which is illustrated in the next example.

Example 9.6. Consider the transfer function used in Example 9.5. To illustrate the Popov criterion, we need the *Popov plot*

$$\tilde{G}(j\omega) = \mathrm{Re}\,[G(j\omega)] + j\omega \mathrm{Im}\,[G(j\omega)]\,.$$

As shown in Figure 9.12, the limiting value of the Popov gain k_P is obtained by selecting a straight line in the Popov plane such that the Popov plot of $\tilde{G}(j\omega)$ lies below this line. From Figure 9.12 we obtain $k_P = 2.5$ We remark that the Lur'e gain corresponds to the case $q = 0$ in the Popov plot.

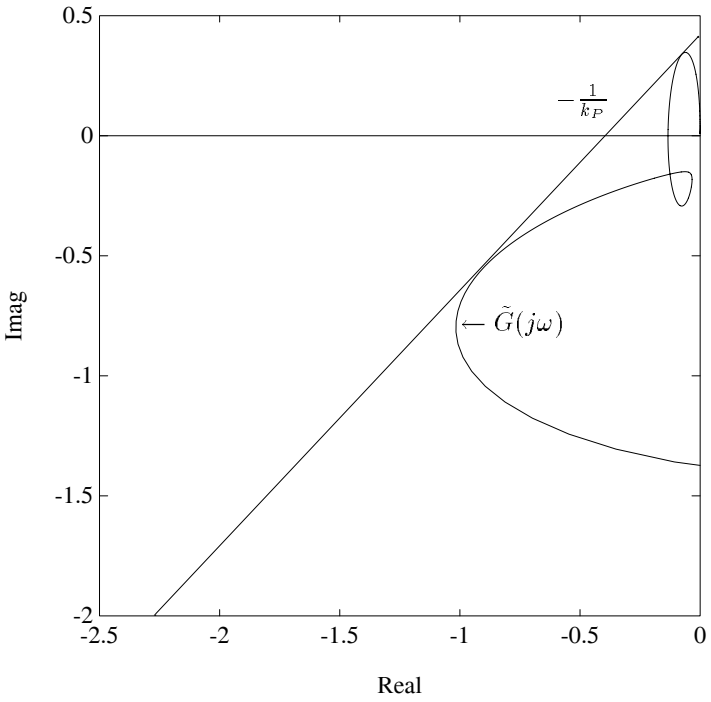

Figure 9.12. Popov criterion (Example 9.6)

In addition to the Lur'e and Popov criteria, there is another useful result in robust stability of nonlinear systems known as the *Circle Criterion*. It is assumed that the nonlinearity is time-invariant and lies in the sector $[k_1, k_2]$:

$$0 \leq k_1 \leq \phi(\sigma) \leq k_2. \tag{9.20}$$

Introduce the complex plane circle $\mathcal{C}$ centered on the negative real axis and cutting it at the points $-\dfrac{1}{k_1}$ and $-\dfrac{1}{k_2}$.

Theorem 9.8 (Circle Criterion)
If $G(s)$ is a stable transfer function and ϕ is a time-invariant nonlinearity which belongs to the sector $[k_1, k_2]$, then a sufficient condition for absolute stability is that the Nyquist plot $G(j\omega)$ stays out of the circle $\mathcal{C}$.

We illustrate this theorem with an example.

Example 9.7. Consider again the transfer function $G(s)$ used in Example 9.5. Figure 9.13 shows the plot of $G(j\omega)$ for $0 \leq \omega < \infty$. From Figure 9.13 we see that the smallest circle centered at -1 touches the $G(j\omega)$ locus and cuts the negative real axis at $-\dfrac{1}{k_2} = -0.3$ and $-\dfrac{1}{k_1} = -1.7$. This gives the absolute stability sector $[0.59, 3.33]$.

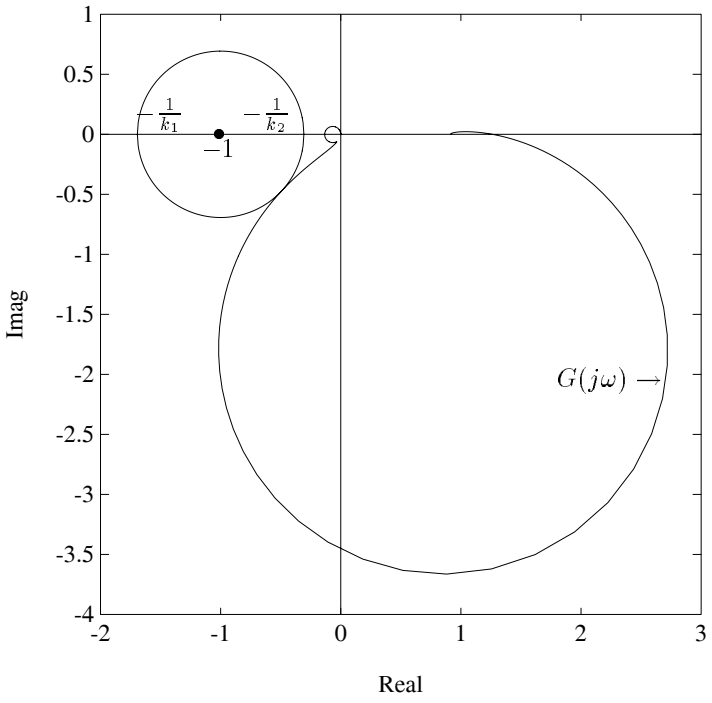

Figure 9.13. Circle criterion (Example 9.7)

In a later section we will consider the robust version of the absolute stability problem by letting the transfer function $G(s)$ vary over a family $\mathbf{G}(s)$. In this case it will be necessary to determine the infimum value of the stability sectors as $G(s)$

ranges over the family $\mathbf{G}(s)$. We will see that in each case these stability sectors can be found from the extremal systems $\mathbf{G}_{\mathrm{E}}(s)$ in a constructive manner. We develop some preliminary results on the SPR property that will aid in this calculation.

9.8 CHARACTERIZATION OF THE SPR PROPERTY

The importance of the SPR property in robustness can be seen from the fact that a unity feedback system containing a forward transfer function which is SPR has infinite gain margin and at least 90° phase margin. Our first result is a stability characterization of proper stable real transfer functions satisfying the SPR property. More precisely, let

$$G(s) = \frac{N(s)}{D(s)} \tag{9.21}$$

be a real proper transfer function with no poles in the closed right-half plane.

Theorem 9.9 *$G(s)$ is SPR if and only if the following three conditions are satisfied:*

a) $\mathrm{Re}[G(0)] > 0$,

b) $N(s)$ is Hurwitz stable,

c) $D(s) + j\alpha N(s)$ is Hurwitz stable for all α in $\mathbb{R}$.

Proof. Let us first assume that $G(s)$ is SPR and let us show that conditions b) and c) are satisfied since condition a) is clearly true in that case. Consider the family of polynomials:

$$\mathcal{P} := \{P_\alpha(s) = D(s) + j\alpha N(s) : \ \alpha \in \mathbb{R}\}.$$

Every polynomial in this family has the same degree as that of $D(s)$. Since this family contains a stable element, namely $P_0(s) = D(s)$, it follows from the continuity of the roots of a polynomial (Boundary Crossing Theorem of Chapter 1) that $\mathcal{P}$ will contain an unstable polynomial if and only if it also contains an element with a root at $j\omega$ for some $\omega \in \mathbb{R}$. Assume that for some α_o and ω in $\mathbb{R}$ we had that:

$$P_{\alpha_o}(j\omega) = D(j\omega) + j\alpha_o D(j\omega) = 0.$$

We write

$$D(j\omega) = D^e(\omega) + j\omega D^o(\omega) \tag{9.22}$$

with similar notation for $N(j\omega)$. Separating the real and imaginary parts of $P_{\alpha_o}(j\omega)$, we deduce that

$$D^e(\omega) - \alpha_o \omega N^o(\omega) = 0 \quad \text{and} \quad \omega D^o(\omega) + \alpha_o N^e(\omega) = 0.$$

But this implies necessarily that

$$N^e(\omega)D^e(\omega) + \omega^2 N^o(\omega)D^o(\omega) = 0$$

that is

$$\mathrm{Re}\,[G(j\omega)] = 0$$

and this contradicts the fact that $G(s)$ is SPR. Thus c) is also true.
Since c) is true it now implies that,

$$N(s) + j\beta D(s) \quad \text{is Hurwitz stable for all} \quad \beta \neq 0.$$

Therefore, letting β tend to 0 we see that $N(s)$ is a limit of Hurwitz polynomials of bounded degree. Rouché's theorem immediately implies that the unstable roots of $N(s)$, if any, can only be on the $j\omega-$axis. However, if $N(s)$ has a root on the $j\omega-$axis then $\mathrm{Re}\,[G(j\omega)] = 0$ at this root and again this contradicts the fact that $G(s)$ is SPR.

To prove the converse, we use the fact that a) and b) hold and reason by contradiction. Since a) holds it follows by continuity that $G(s)$ is not SPR if and only if for some $\omega \in \mathbb{R}$, $0 \neq \omega$, we have that $\mathrm{Re}\,[G(j\omega)] = 0$, or equivalently

$$N^e(\omega)D^e(\omega) + \omega^2 N^o(\omega)D^o(\omega) = 0. \tag{9.23}$$

Now, assume that at this particular ω, $N(s)$ satisfies

$$N^e(\omega) \neq 0, \quad \text{and} \quad N^o(\omega) \neq 0.$$

From (9.23) we then conclude that

$$\frac{D^e(\omega)}{\omega N^o(\omega)} = \frac{-\omega D^o(\omega)}{N^e(\omega)} = \alpha_o \tag{9.24}$$

and therefore

$$D^e(\omega) - \alpha_o \omega N^o(\omega) = 0, \quad \text{and} \quad \omega D^o(\omega) + \alpha_o N^e(\omega) = 0 \tag{9.25}$$

so that

$$[D + j\alpha_o N]\,(j\omega) = 0,$$

contradicting c).

On the other hand assume for example that $N^e(\omega) = 0$. Since $N(s)$ is stable, we deduce that $N^o(\omega) \neq 0$, and from (9.23) we also have that $D^o(\omega) = 0$. Therefore (9.24) is still true with

$$\alpha_o = \frac{D^e(\omega)}{\omega N^o(\omega)}.$$

♣

9.8.1 SPR Conditions for Interval Systems

Now consider the following family $\mathbf{G}(s)$ of transfer functions

$$G(s) = \frac{A(s)}{B(s)},$$

where $A(s)$ belongs to a family of real interval polynomials $\mathbf{A}(s)$, and $B(s)$ belongs to a family of real interval polynomials $\mathbf{B}(s)$, defined as follows:

$$\mathbf{A}(s) = \{A(s) \ : \ A(s) = a_0 + a_1 s + \cdots + a_p s^p, \text{ and } a_i \in [\alpha_i, \beta_i], \text{ for all } \ i = 0, \cdots, p\}$$
$$\mathbf{B}(s) = \{B(s) \ : \ B(s) = b_0 + b_1 s + \cdots + b_n s^n, \text{ and } b_j \in [\gamma_j, \delta_j], \text{ for all } \ j = 0, \cdots, n\}.$$

Let $K_A^i(s)$, $i = 1, 2, 3, 4$ and $K_B^i(s)$, $i = 1, 2, 3, 4$ denote the Kharitonov polynomials associated with $\mathbf{A}(s)$ and $\mathbf{B}(s)$ respectively. We call $\mathbf{G}(s)$ a family of interval plants and the *Kharitonov systems* associated with $\mathbf{G}(s)$ are naturally defined to be the 16 plants of the following set,

$$\mathbf{G}_{\mathrm{K}}(s) := \left\{ \frac{K_A^i(s)}{K_B^j(s)} \ : \ i, j \in \{1, 2, 3, 4\} \right\}.$$

We assume that the interval family $\mathbf{G}(s)$ is stable. Let γ be any given real number. We want to find necessary and sufficient conditions under which it is true that for all $G(s)$ in $\mathbf{G}(s)$:

$$\mathrm{Re}\,[G(j\omega)] + \gamma > 0, \quad \text{for all } \ \omega \in \mathbb{R}. \tag{9.26}$$

In other words we ask the question: Under what conditions is $G(s) + \gamma$ SPR for all $G(s)$ in $\mathbf{G}(s)$? The answer to this question is given in the following lemma.

Lemma 9.7 *Equation (9.26) is satisfied by every element in* $\mathbf{G}(s)$ *if and only if it is satisfied for the 16 Kharitonov systems in* $\mathbf{G}_{\mathrm{K}}(s)$.

Proof. For an arbitrary $A(s)$ in $\mathbf{A}(s)$ and an arbitrary $B(s)$ in $\mathbf{B}(s)$ we can write:

$$\mathrm{Re}\left[\frac{A(j\omega)}{B(j\omega)}\right] + \gamma > 0$$

$$\iff (A^e(\omega) + \gamma B^e(\omega))\, B^e(\omega) + \omega^2 \left(A^o(\omega) + \gamma B^o(\omega)\right) B^o(\omega) > 0. \tag{9.27}$$

The right hand side of this last inequality is linear in $A^e(\omega)$ and $A^o(\omega)$ and thus from the facts (see Chapter 5)

$$K_A^{\mathrm{e,min}}(\omega) := K_A^{\mathrm{even,min}}(j\omega) \le A^e(\omega) \le K_A^{\mathrm{e,max}}(\omega) := K_A^{\mathrm{even,max}}(j\omega)$$

$$K_A^{\mathrm{o,min}}(\omega) := \frac{K_A^{\mathrm{odd,min}}(j\omega)}{j\omega} \le A^o(\omega) \le K_A^{\mathrm{o,max}}(\omega) := \frac{K_A^{\mathrm{odd,max}}(j\omega)}{j\omega},$$

it is clear that it is enough to check (9.27) when $A(s)$ is fixed and equal to one of the 4 Kharitonov polynomials associated with $\mathbf{A}(s)$. To further explain this point, let $A(s)$ and $B(s)$ be arbitrary polynomials in $\mathbf{A}(s)$ and $\mathbf{B}(s)$ respectively and suppose arbitrarily that at a given ω we have $B^e(\omega) > 0$ and $B^o(\omega) > 0$. Then the expression in (9.27) is obviously bounded below by

$$\left(K_A^{e,\min}(\omega) + \gamma B^e(\omega)\right) B^e(\omega) + \omega^2 \left(K_A^{o,\min}(\omega) + \gamma B^o(\omega)\right) B^o(\omega),$$

which corresponds to $A(s) = K_A^1(s)$.

Now, since $A(s)$ is a fixed polynomial, we deduce from Theorem 9.9 that the following is true:

$$\text{Re}\left[\frac{A(j\omega)}{B(j\omega)}\right] + \gamma > 0, \quad \text{for all } \omega \in \mathbb{R}, \text{ and for all } B(s) \in \mathbf{B}(s),$$

if and only if the following three conditions are satisfied

1) $\text{Re}\left[\dfrac{A(0)}{B(0)}\right] + \gamma > 0$, for all $B(s) \in \mathbf{B}(s)$,

2) $A(s) + \gamma B(s)$ is Hurwitz stable for all $B(s) \in \mathbf{B}(s)$,

3) $B(s) + \dfrac{j\alpha}{1 + j\alpha\gamma} A(s)$ is Hurwitz stable for all $\alpha \in \mathbb{R}$ and all $B(s) \in \mathbf{B}(s)$.

Note that in condition 3) above we have used the fact that

$$\text{Re}\left[\frac{A(j\omega)}{B(j\omega)}\right] + \gamma > 0 \Longleftrightarrow \text{Re}\left[\frac{A(j\omega) + \gamma B(j\omega)}{B(j\omega)}\right] > 0,$$

and therefore condition c) of Theorem 9.9 can be written as

$$B(s) + j\alpha \left(A(s) + \gamma B(s)\right) \text{ stable for all } \alpha \in \mathbb{R}$$

which is of course equivalent to

$$B(s) + \frac{j\alpha}{1 + j\alpha\gamma} A(s) \quad \text{is Hurwitz stable for all } \alpha \in \mathbb{R}.$$

The family of polynomials defined by condition 2) is a real interval family so that by using Kharitonov's theorem for real polynomials, we deduce that condition 2) is equivalent to:

2′)

$$\begin{array}{ll} A(s) + \gamma K_B^1(s), & A(s) + \gamma K_B^2(s), \\ A(s) + \gamma K_B^3(s), & A(s) + \gamma K_B^4(s) \end{array}$$

stable.

The polynomials defined in 3) is a *complex interval family* for every α and thus Kharitonov's theorem for complex polynomials applies and 3) is equivalent to:

3′)

$$K_B^1(s) + \frac{j\alpha}{1+j\alpha\gamma}A(s), \qquad K_B^2(s) + \frac{j\alpha}{1+j\alpha\gamma}A(s),$$
$$K_B^3(s) + \frac{j\alpha}{1+j\alpha\gamma}A(s), \qquad K_B^4(s) + \frac{j\alpha}{1+j\alpha\gamma}A(s)$$

stable for all $\alpha \in \mathbb{R}$. Also 1) is equivalent to

1′)

$$\text{Re}\left[\frac{A(0)}{K_B^1(0)}\right] + \gamma > 0 \text{ and } \text{Re}\left[\frac{A(0)}{K_B^3(0)}\right] + \gamma > 0.$$

Thus by using Theorem 9.9 in the other direction, we conclude that when $A(s)$ is fixed,

$$\text{Re}\left[\frac{A(j\omega)}{B(j\omega)}\right] + \gamma > 0, \text{ for all } \omega \in \mathbb{R}, \text{ and for all } B(s) \in \mathbf{B}(s)$$

if and only if

$$\text{Re}\left[\frac{A(j\omega)}{K_B^k(j\omega)}\right] + \gamma > 0, \text{ for all } \omega \in \mathbb{R}, \text{ and for all } k \in \{1,2,3,4\},$$

and this concludes the proof of the lemma. ♣

As a consequence of Lemma 9.7 we have the following result.

Theorem 9.10 *Given a proper stable family* $\mathbf{G}(s)$ *of interval plants, the minimum of* $\text{Re}(G(j\omega))$ *over all* ω *and over all* $G(s)$ *in* $\mathbf{G}(s)$ *is achieved at one of the 16 Kharitonov systems in* $\mathbf{G}_{\text{K}}(s)$

Proof. First, since $\mathbf{G}(s)$ is proper it is clear that this overall minimum is finite. Assume for the sake of argument that the minimum of $\text{Re}\,[G(j\omega)]$ over all ω and over the 16 Kharitonov systems is γ_0, but that some plant $G^*(s)$ in $\mathbf{G}(s)$ satisfies

$$\inf_{\omega\in\mathbf{R}} \text{Re}\,[G^*(j\omega)] = \gamma_1 < \gamma_0. \tag{9.28}$$

Take any γ satisfying $\gamma_1 < \gamma < \gamma_0$. By assumption we have that

$$\inf_{\omega\in\mathbf{R}} \text{Re}\,[G(j\omega)] - \gamma > 0, \tag{9.29}$$

whenever $G(s)$ is one of the 16 Kharitonov systems. By Lemma 9.7 this implies that (9.29) is true for all $G(s)$ in $\mathbf{G}(s)$, and this obviously contradicts (9.28). ♣

We now look more carefully at the situation where one only needs to check that every plant $G(s)$ in $\mathbf{G}(s)$ has the SPR property. In other words, we are interested in the special case in which $\gamma = 0$. A line of reasoning similar to that of Theorem 9.10 would show that here again it is enough to check the 16 Kharitonov systems. However a more careful analysis shows that it is enough to check only 8 systems and we have the following result.

Theorem 9.11 *Every plant $G(s)$ in $\mathbf{G}(s)$ is SPR if and only if it is the case for the 8 following plants:*

$$G_1(s) = \frac{K_A^2(s)}{K_B^1(s)}, \quad G_2(s) = \frac{K_A^3(s)}{K_B^1(s)}, \quad G_3(s) = \frac{K_A^1(s)}{K_B^2(s)}, \quad G_4(s) = \frac{K_A^4(s)}{K_B^2(s)},$$

$$G_5(s) = \frac{K_A^1(s)}{K_B^3(s)}, \quad G_6(s) = \frac{K_A^4(s)}{K_B^3(s)}, \quad G_7(s) = \frac{K_A^2(s)}{K_B^4(s)}, \quad G_8(s) = \frac{K_A^3(s)}{K_B^4(s)}.$$

Proof. Using Definition 9.1 and Theorem 9.9, it is easy to see that every transfer function

$$G(s) = \frac{A(s)}{B(s)}$$

in the family is SPR if and only if the following three conditions are satisfied:

1) $A(0)B(0) > 0$ for all $A(s) \in \mathbf{A}(s)$ and all $B(s) \in \mathbf{B}(s)$,

2) $A(s)$ is Hurwitz stable for all $A(s) \in \mathbf{A}(s)$,

3) $B(s) + j\alpha A(s)$ is stable for all $A(s) \in \mathbf{A}(s)$, all $B(s) \in \mathbf{B}(s)$, and all $\alpha \in \mathbb{R}$.

By Kharitonov's theorem for real polynomials, it is clear that condition 2) is equivalent to:

2′) $K_A^1(s)$, $K_A^2(s)$, $K_A^3(s)$, $K_A^4(s)$ are Hurwitz stable.

Now, the simplification over Theorem 9.10 stems from the fact that here in condition 3), even if $A(s)$ is not a fixed polynomial, we still have to deal with a *complex interval family* since $\gamma = 0$. Hence, using Kharitonov's theorem for complex polynomials (see Chapter 5), we conclude that 3) is satisfied if and only if:

3′)

$$\begin{array}{ll} K_B^1(s) + j\alpha K_A^2(s), & K_B^1(s) + j\alpha K_A^3(s), \\ K_B^2(s) + j\alpha K_A^1(s), & K_B^2(s) + j\alpha K_A^4(s), \\ K_B^3(s) + j\alpha K_A^1(s), & K_B^3(s) + j\alpha K_A^4(s), \\ K_B^4(s) + j\alpha K_A^2(s), & K_B^4(s) + j\alpha K_A^3(s) \end{array}$$

are Hurwitz stable for all α in $\mathbb{R}$.

Note that you only have to check these eight polynomials whether α is positive or negative. As for condition 1) it is clear that it is equivalent to:

$1')$ $K_A^2(0)K_B^1(0) > 0$, $K_A^3(0)K_B^1(0) > 0$, $K_A^1(0)K_B^3(0) > 0$, $K_A^4(0)K_B^3(0) > 0$.

Once again using Theorem 9.9 in the other direction we can see that conditions $1')$, $2')$ and $3')$ are precisely equivalent to the fact that the eight transfer functions specified in Theorem 9.11 satisfy the SPR property. ♣

As a final remark on the SPR property we see that when the entire family is SPR as in Theorem 9.11, there are two cases. On one hand, if the family is strictly proper then the overall minimum is 0. On the other hand, when the family is proper but not strictly proper, then the overall minimum is achieved at one of the 16 Kharitonov systems even though one only has to check eight plants to verify the SPR property for the entire family. In fact, the minimum need not be achieved at one of these eight plants as the following example shows.

Example 9.8. Consider the following stable family $\mathbf{G}(s)$ of interval systems whose generic element is given by

$$G(s) = \frac{1 + \alpha s + \beta s^2 + s^3}{\gamma + \delta s + \epsilon s^2 + s^3}$$

where

$$\alpha \in [1, 2],\ \beta \in [3, 4],\ \gamma \in [1, 2],\ \delta \in [5, 6],\ \epsilon \in [3, 4].$$

$\mathbf{G}_{\mathrm{K}}(s)$ consists of the following 16 rational functions,

$$r_1(s) = \frac{1 + s + 3s^2 + s^3}{1 + 5s + 4s^2 + s^3}, \qquad r_2(s) = \frac{1 + s + 3s^2 + s^3}{1 + 6s + 4s^2 + s^3},$$
$$r_3(s) = \frac{1 + s + 3s^2 + s^3}{2 + 5s + 3s^2 + s^3}, \qquad r_4(s) = \frac{1 + s + 3s^2 + s^3}{2 + 6s + 3s^2 + s^3},$$
$$r_5(s) = \frac{1 + s + 4s^2 + s^3}{1 + 5s + 4s^2 + s^3}, \qquad r_6(s) = \frac{1 + s + 4s^2 + s^3}{1 + 6s + 4s^2 + s^3},$$
$$r_7(s) = \frac{1 + s + 4s^2 + s^3}{2 + 5s + 3s^2 + s^3}, \qquad r_8(s) = \frac{1 + s + 4s^2 + s^3}{2 + 6s + 3s^2 + s^3},$$
$$r_9(s) = \frac{1 + 2s + 3s^2 + s^3}{1 + 5s + 4s^2 + s^3}, \qquad r_{10}(s) = \frac{1 + 2s + 3s^2 + s^3}{1 + 6s + 4s^2 + s^3},$$
$$r_{11}(s) = \frac{1 + 2s + 3s^2 + s^3}{2 + 5s + 3s^2 + s^3}, \qquad r_{12}(s) = \frac{1 + 2s + 3s^2 + s^3}{2 + 6s + 3s^2 + s^3},$$
$$r_{13}(s) = \frac{1 + 2s + 4s^2 + s^3}{1 + 5s + 4s^2 + s^3}, \qquad r_{14}(s) = \frac{1 + 2s + 4s^2 + s^3}{1 + 6s + 4s^2 + s^3},$$
$$r_{15}(s) = \frac{1 + 2s + 4s^2 + s^3}{2 + 5s + 3s^2 + s^3}, \qquad r_{16}(s) = \frac{1 + 2s + 4s^2 + s^3}{2 + 6s + 3s^2 + s^3}.$$

The corresponding minima of their respective real parts along the imaginary axis are given by,

$$\begin{aligned}
&\inf_{\omega\in\mathbb{R}} \mathrm{Re}\,[r_1(j\omega)] = 0.1385416, && \inf_{\omega\in\mathbb{R}} \mathrm{Re}\,[r_2(j\omega)] = 0.1134093,\\
&\inf_{\omega\in\mathbb{R}} \mathrm{Re}\,[r_3(j\omega)] = 0.0764526, && \inf_{\omega\in\mathbb{R}} \mathrm{Re}\,[r_4(j\omega)] = 0.0621581,\\
&\inf_{\omega\in\mathbb{R}} \mathrm{Re}\,[r_5(j\omega)] = 0.1540306, && \inf_{\omega\in\mathbb{R}} \mathrm{Re}\,[r_6(j\omega)] = 0.1262789,\\
&\inf_{\omega\in\mathbb{R}} \mathrm{Re}\,[r_7(j\omega)] = 0.0602399, && \inf_{\omega\in\mathbb{R}} \mathrm{Re}\,[r_8(j\omega)] = 0.0563546,\\
&\inf_{\omega\in\mathbb{R}} \mathrm{Re}\,[r_9(j\omega)] = 0.3467740, && \inf_{\omega\in\mathbb{R}} \mathrm{Re}\,[r_{10}(j\omega)] = 0.2862616,\\
&\inf_{\omega\in\mathbb{R}} \mathrm{Re}\,[r_{11}(j\omega)] = 0.3011472, && \inf_{\omega\in\mathbb{R}} \mathrm{Re}\,[r_{12}(j\omega)] = 0.2495148,\\
&\inf_{\omega\in\mathbb{R}} \mathrm{Re}\,[r_{13}(j\omega)] = 0.3655230, && \inf_{\omega\in\mathbb{R}} \mathrm{Re}\,[r_{14}(j\omega)] = 0.3010231,\\
&\inf_{\omega\in\mathbb{R}} \mathrm{Re}\,[r_{15}(j\omega)] = 0.2706398, && \inf_{\omega\in\mathbb{R}} \mathrm{Re}\,[r_{16}(j\omega)] = 0.2345989\ .
\end{aligned}$$

Therefore the entire family is SPR and the minimum is achieved at $r_8(s)$. However $r_8(s)$ corresponds to

$$\frac{K_A^1(s)}{K_B^4(s)}$$

which is not among the eight rational functions of Theorem 9.11.

Complex Rational Functions

It is possible to extend the above results to the case of complex rational functions. In the following we give the corresponding results and sketch the small differences in the proofs. The SPR property for a complex rational function is again given by Definition 9.1. Thus a proper complex rational function

$$G(s) = \frac{N(s)}{D(s)}$$

is SPR if

1) $G(s)$ has no poles in the closed right half plane,

2) $\mathrm{Re}\,[G(j\omega)] > 0$ for all $\omega \in \mathbb{R}$, or equivalently,

$$\mathrm{Re}\,[N(j\omega)]\ \mathrm{Re}\,[D(j\omega)] + \mathrm{Im}\,[N(j\omega)]\ \mathrm{Im}\,[D(j\omega)] > 0,\ \text{for all } \omega \in \mathbb{R}$$

As with real rational functions, the characterization given by Theorem 9.9 is true and we state this below.

Theorem 9.12 *The complex rational function $G(s)$ is SPR if and only if the conditions a),b) and c) of Theorem 9.9 hold.*

Proof. The proof is similar to that for Theorem 9.9. However there is a slight difference in proving that the SPR property implies part c) which is,

$$D(s) + j\alpha N(s) \quad \text{is Hurwitz for all} \quad \alpha \in \mathbb{R}. \tag{9.30}$$

To do so in the real case, we consider the family of polynomials:

$$\mathcal{P} := \{P_\alpha(s) = D(s) + j\alpha N(s) \ : \ \alpha \in \mathbb{R}\}$$

and we start by arguing that this family of polynomials has constant degree. This may not be true in the complex case when the rational function is proper but not strictly proper. To prove that (9.30) is nevertheless correct we first observe that the same proof carries over in the strictly proper case. Let us suppose now that $N(s)$ and $D(s)$ have the same degree p and their leading coefficients are

$$n_p = n_p^r + jn_p^i, \qquad d_p = d_p^r + jd_p^i.$$

Then it is easy to see that the family $\mathcal{P}$ does not have constant degree if and only if

$$d_p^r n_p^r + d_p^i n_p^i = 0. \tag{9.31}$$

Thus if $G(s)$ is SPR and (9.31) is not satisfied then again the same proof works and (9.30) is true.

Now, let us assume that $G(s)$ is SPR, proper but not strictly proper, and that

$$G_\gamma(s) = G(s) + \gamma = \frac{N'(s)}{D(s)}, \quad \text{where } N'(s) = N(s) + \gamma D(s).$$

It is clear that $G_\gamma(s)$ is still SPR, and it can be checked that it is always proper and not strictly proper. Moreover, (9.31) cannot hold for $N'(s)$ and $D(s)$ since in that case,

$$d_p^r n'^r_p + d_p^i n'^i_p = d_p^r(n_p^r + \gamma d_p^r) + d_p^i(n_p^i + \gamma d_p^i) = \gamma((d_p^r)^2 + (d_p^i)^2) > 0.$$

Thus we conclude that for all $\alpha \in \mathbb{R}$,

$$D(s) + j\alpha(N(s) + \gamma D(s)) \quad \text{is Hurwitz stable.} \tag{9.32}$$

Now letting γ go to 0, we see that $D(s) + j\alpha N(s)$ is a limit of Hurwitz polynomials of bounded degree and therefore Rouché's theorem implies that the unstable roots of $D(s) + j\alpha N(s)$, if any, can only be on the $j\omega-$axis. However since $G(s)$ is SPR this cannot happen since,

$$d(j\omega) + j\alpha n(j\omega) = 0 \implies \begin{cases} \mathrm{Re}\,[D(j\omega)] - \alpha \mathrm{Im}\,[N(j\omega)] = 0 \\ \mathrm{Im}\,[D(j\omega)] + \alpha \mathrm{Re}\,[N(j\omega)] = 0, \end{cases}$$

and these two equations in turn imply that

$$\mathrm{Re}\,[N(j\omega)]\ \mathrm{Re}\,[D(j\omega)] + \mathrm{Im}\,[N(j\omega)]\ \mathrm{Im}\,[D(j\omega)] = 0,$$

a contradiction. ♣

Now consider a family $\mathbf{G}(s)$ of proper complex interval rational functions

$$G(s) = \frac{A(s)}{B(s)}$$

where $A(s)$ belongs to a family of complex interval polynomials $\mathbf{A}(s)$, and $B(s)$ belongs to a family of complex interval polynomials $\mathbf{B}(s)$. The Kharitonov polynomials for such a family are 8 extreme polynomials. We refer the reader to Chapter 5 for the definition of these polynomials. The Kharitonov systems associated with $\mathbf{G}(s)$ are the 64 rational functions in the set

$$\mathbf{G}_{\mathrm{K}}(s) = \left\{ \frac{K_A^i(s)}{K_B^j(s)} \ : \ i,j \in \{1,2,3,4,5,6,7,8\} \right\}.$$

Similar to the real case we have the following theorem.

Theorem 9.13 *Given a proper stable family $\mathbf{G}(s)$ of complex interval rational functions, the minimum of $\mathrm{Re}\,[G(j\omega)]$ over all ω and over all $G(s)$ in $\mathbf{G}(s)$ is achieved at one of the 64 Kharitonov systems.*

The proof is identical to that for the real case and is omitted.

One may also consider the problem of only checking that the entire family is SPR, and here again a stronger result holds in that case.

Theorem 9.14 *Every rational function $G(s)$ in $\mathbf{G}(s)$ is SPR if and only if it is the case for the 16 following rational functions:*

$$G_1(s) = \frac{K_A^2(s)}{K_B^1(s)}, \quad G_2(s) = \frac{K_A^3(s)}{K_B^1(s)}, \quad G_3(s) = \frac{K_A^1(s)}{K_B^2(s)}, \quad G_4(s) = \frac{K_A^4(s)}{K_B^2(s)},$$

$$G_5(s) = \frac{K_A^1(s)}{K_B^3(s)}, \quad G_6(s) = \frac{K_A^4(s)}{K_B^3(s)}, \quad G_7(s) = \frac{K_A^2(s)}{K_B^4(s)}, \quad G_8(s) = \frac{K_A^3(s)}{K_B^4(s)}.$$

$$G_9(s) = \frac{K_A^6(s)}{K_B^5(s)}, \quad G_{10}(s) = \frac{K_A^7(s)}{K_B^5(s)}, \quad G_{11}(s) = \frac{K_A^5(s)}{K_B^6(s)}, \quad G_{12}(s) = \frac{K_A^8(s)}{K_B^6(s)},$$

$$G_{13}(s) = \frac{K_A^5(s)}{K_B^7(s)}, \quad G_{14}(s) = \frac{K_A^8(s)}{K_B^7(s)}, \quad G_{15}(s) = \frac{K_A^6(s)}{K_B^8(s)}, \quad G_{16}(s) = \frac{K_A^7(s)}{K_B^8(s)}.$$

The proof is the same as for Theorem 9.11 and is omitted.

9.9 THE ROBUST ABSOLUTE STABILITY PROBLEM

We now extend the classical absolute stability problem by allowing the linear system $G(s)$ to lie in a family of systems $\mathbf{G}(s)$ containing parametric uncertainty. Thus, we are dealing with a robustness problem where parametric uncertainty as well as sector bounded nonlinear feedback gains are simultaneously present. For a given

class of nonlinearities lying in a prescribed sector the closed loop system will be said to be *robustly absolutely stable* if it is absolutely stable for every $G(s) \in \mathbf{G}(s)$. In this section we will give a constructive procedure to calculate the size of the stability sector using the Lur'e, Popov or Circle Criterion when $\mathbf{G}(s)$ is an interval system or a linear interval system. In each case we shall see that an appropriate sector can be determined by replacing the family $\mathbf{G}(s)$ by the extremal set $\mathbf{G}_{\mathrm{E}}(s)$. Specifically we deal with the Lur'e problem. However, it will be obvious from the boundary generating properties of the set $\mathbf{G}_{\mathrm{E}}(j\omega)$ that identical results will hold for the Popov sector and the Circle Criterion with time-invariant nonlinearities.

First consider the Robust Lur'e problem where the forward loop element $G(s)$ shown in Figure 9.14 lies in an interval family $\mathbf{G}(s)$ and the feedback loop contains as before a time-varying sector bounded nonlinearity ϕ lying in the sector $[0, k]$. As usual let $\mathbf{G}_{\mathrm{K}}(s)$ denote the transfer functions of the Kharitonov systems associated with the family $\mathbf{G}(s)$.

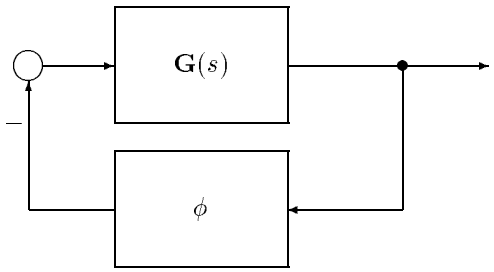

Figure 9.14. Robust absolute stability problem

Theorem 9.15 (Absolute Stability for Interval Systems)
The feedback system in Figure 9.14 is absolutely stable for every $G(s)$ in the the interval family $\mathbf{G}(s)$ of stable proper systems, if the time-varying nonlinearity ϕ belongs to the sector $[0, k]$ where

$$k = \infty, \ \textit{if} \inf_{\mathbf{G}_{\mathrm{K}}} \inf_{\omega \in \mathbf{R}} \mathrm{Re}\,[G(j\omega)] \geq 0,$$

otherwise

$$k < -\frac{1}{\inf_{\mathbf{G}_{\mathrm{K}}} \inf_{\omega \in \mathbf{R}} \mathrm{Re}\,[G(j\omega)]},$$

where $\mathbf{G}_{\mathrm{K}}(s)$ is the set of sixteen Kharitonov systems corresponding to $\mathbf{G}(s)$.

Proof. Let $G(s)$ be any member of the interval family. The following inequality holds because of Lemma 9.7.

$$\mathrm{Re}\left[\frac{1}{k} + G(j\omega)\right] \geq \inf_{G \in \mathbf{G}} \inf_{\omega} \mathrm{Re}\left[\frac{1}{k} + G(j\omega)\right]$$

$$= \inf_{G \in \mathbf{G}_{\mathrm{K}}} \inf_{\omega} \mathrm{Re}\left[\frac{1}{k} + G(j\omega)\right] > 0$$

By Theorem 9.6, the *absolute stability* of the closed loop system follows. ♣

We can extend this absolute stability result to feedback systems. Consider a feedback system in which a fixed controller $C(s)$ stabilizes each plant $G(s)$ belonging to a family of linear interval systems $\mathbf{G}(s)$. Let $\mathbf{G}_{\mathrm{E}}(s)$ denote the extremal set for this family $\mathbf{G}(s)$. Now suppose that the closed loop system is subject to nonlinear sector bounded feedback perturbations. Refer to Figure 9.15. Our task is to determine the size of the sector for which absolute stability is preserved for each $G(s) \in \mathbf{G}(s)$. The solution to this problem is given below.

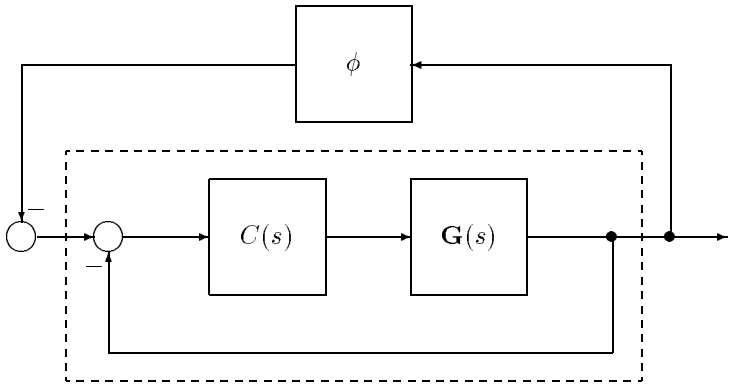

Figure 9.15. Closed loop system with nonlinear feedback perturbations

Theorem 9.16 (Absolute Stability of Interval Control Systems)
Given the feedback system in Figure 9.15 where $G(s)$ belongs to a linear interval family $\mathbf{G}(s)$, the corresponding nonlinear system is absolutely stable if the nonlinearity ϕ belongs to the sector $[0, k]$, where $k > 0$ must satisfy:

$$k = \infty, \ \textit{if} \inf_{\mathbf{G}_{\mathrm{E}}} \inf_{\omega \in \mathbf{R}} \mathrm{Re}\left[C(j\omega)G(j\omega)\left(1 + C(j\omega)G(j\omega)\right)^{-1}\right] \geq 0,$$

otherwise,

$$k < -\frac{1}{\inf_{\mathbf{G}_{\mathrm{E}}} \inf_{\omega \in \mathbf{R}} \mathrm{Re}\left[C(j\omega)G(j\omega)\left(1 + C(j\omega)G(j\omega)\right)^{-1}\right]}.$$

Proof. The stability of the system in Figure 9.15 is equivalent, to that of the system in Figure 9.16. The proof now follows from the fact that the boundary of

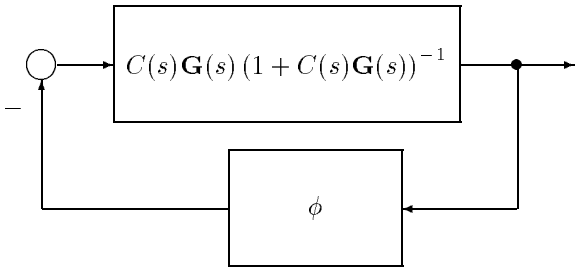

Figure 9.16. Transformed system

the set

$$\left\{C(j\omega)G(j\omega)\,(1+C(j\omega)G(j\omega))^{-1}\ :\ G(s)\in\mathbf{G}(s)\right\}$$

is identical with that of

$$\left\{C(j\omega)G(j\omega)\,(1+C(j\omega)G(j\omega))^{-1}\ :\ G(s)\in\mathbf{G}_{\mathrm{E}}(s)\right\}.$$

This boundary result was proved in Chapter 8. ♣

Remark 9.2. The result given above is stated in terms of an interval plant $\mathbf{G}(s)$. However it is straightforward to show, from the extremal and boundary results developed in Chapter 8, that identical results hold for linear interval systems and for linear fractional transformations of interval systems. This allows us to handle a much more general class of parametrized models.

We illustrate these results with some examples.

Example 9.9. (Robust Lur'e Problem) Consider the feedback configuration in Figure 9.15 and let the plant be given as

$$G(s)=\frac{\alpha_1 s+\alpha_0}{\beta_2 s^2+\beta_1 s+\beta_0}$$

where

$$\begin{aligned}&\alpha_0\in[0.9,1.1],\quad \alpha_1\in[0.1,0.2]\\ &\beta_0\in[1.9,2.1],\quad \beta_1\in[1.8,2],\quad \beta_2\in[0.9,1].\end{aligned}$$

A stabilizing controller is

$$C(s)=\frac{s^2+2s+1}{s^4+2s^3+2s^2+s}.$$

We suppose that the closed loop system is perturbed by sector bounded time-varying nonlinear gains. Then the closed loop transfer function family of interest is

$$\left\{ C(s)G(s)\left[1 + C(s)G(s)\right]^{-1} \ : \ G(s) \in \mathbf{G}(s) \right\}.$$

To compute an appropriate robust Lur'e stability sector for this closed loop system, we only need to plot the frequency template

$$\mathbf{T}(j\omega) = \{C(j\omega)G(j\omega)\left[1 + C(j\omega)G(j\omega)\right]^{-1} : \ G \ \in \ \mathbf{G}_{\mathrm{E}}\}$$

for each frequency. Figure 9.17 shows this set of templates.

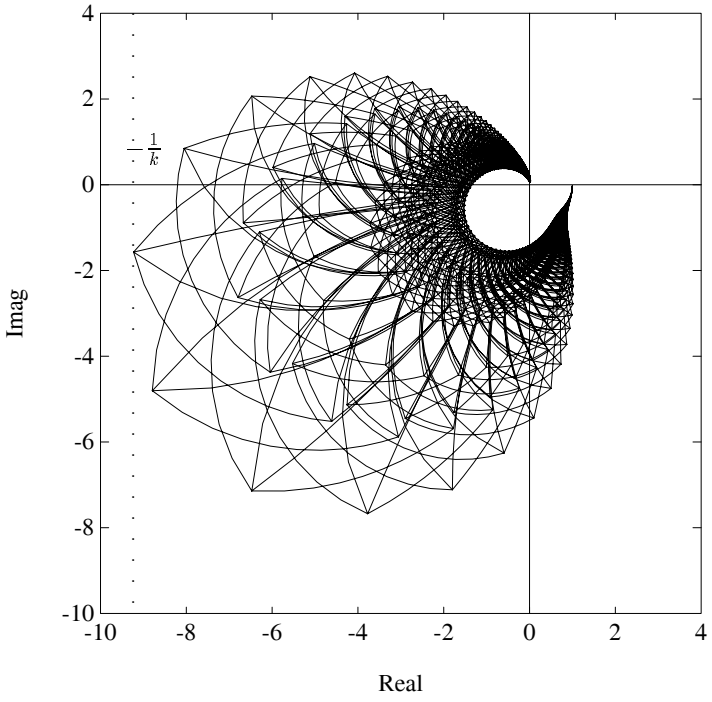

Figure 9.17. Frequency template of closed loop system $\mathbf{T}(j\omega)$ (Example 9.9)

We find the robust Lur'e gain from this as the largest value of k for which $\frac{1}{k} + \mathbf{T}(j\omega)$ becomes SPR. We get

$$\frac{1}{k} = 9.2294$$

and Figure 9.18 shows that adding this gain makes the entire family SPR.

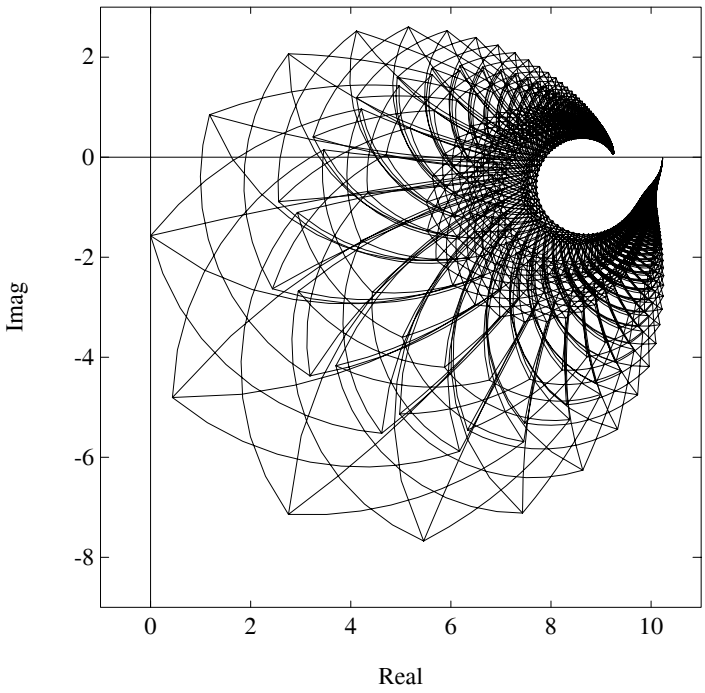

Figure 9.18. Frequency template of SPR system $\frac{1}{k} + \mathbf{T}(j\omega)$(Example 9.9)

Example 9.10. (Robust Popov Criterion) Consider the stable interval plant

$$G(s) = \frac{\alpha_1 s + \alpha_0}{s^4 + \beta_3 s^3 + \beta_2 s^2 + \beta_1 s + \beta_0}$$

where

$$\alpha_0 \in [3, 3.3], \quad \alpha_1 \in [3, 3.2]$$
$$\beta_0 \in [3, 4], \quad \beta_1 \in [2, 3], \quad \beta_2 \in [24, 25], \quad \beta_3 \in [1, 1.2].$$

To obtain the robust Popov gain we need to plot

$$\mathrm{Re}[G(j\omega)] + j\omega \mathrm{Im}[G(j\omega)] : G(j\omega) \in \mathbf{G}_(j\omega) \qquad \text{for } 0 \leq \omega < \infty$$

We can instead generate the boundary of the robust Popov plot by determining:

$$\mathrm{Re}[G(j\omega)] + j\omega \mathrm{Im}[G(j\omega)] : G(j\omega) \in \mathbf{G}_{\mathrm{E}}(j\omega). \qquad \text{for } 0 \leq \omega < \infty$$

This plot is shown in Figure 9.19. The Popov line is also shown in this figure from which we find the limiting value of the robust Popov gain to be

$$k_P \approx 0.4.$$

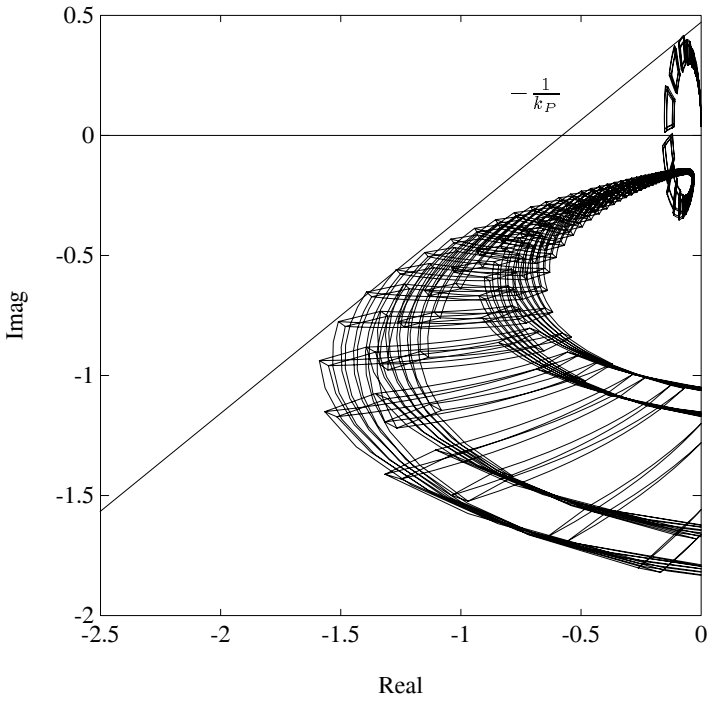

Figure 9.19. Popov criterion (Example 9.10)

Example 9.11. (Robust Circle Criterion) For the system in the previous example we can also use the Circle Criterion to determine a robust absolute stability sector for the family from the Nyquist envelope of $\mathbf{G}_{\mathrm{E}}(j\omega)$ for $0 \leq \omega < \infty$. Figure 9.20 shows that the radius of the smallest real axis centered circle (centered at -1) that touches the envelope is found to be $k_C = 0.6138$. From this the values of the robust absolute stability sector $[k_1, k_2]$ can be found as shown in Figure 9.20.

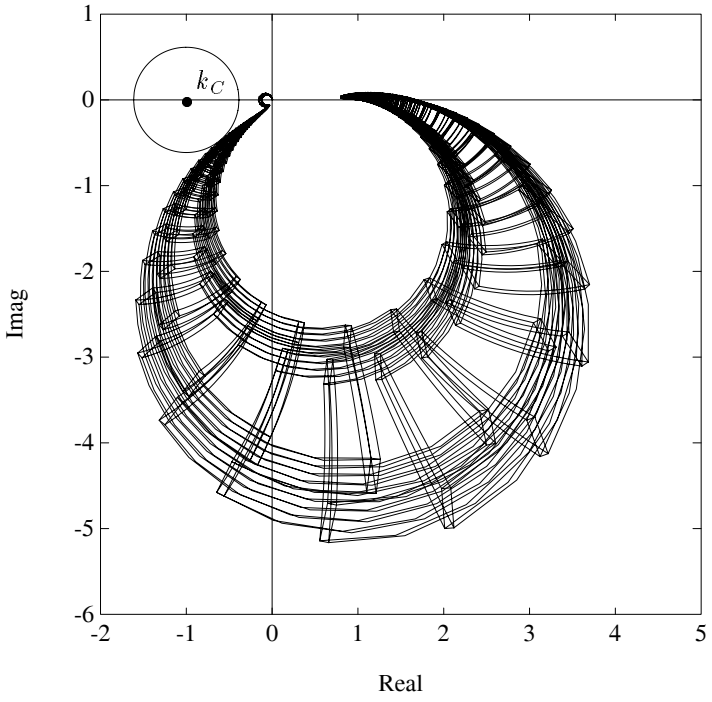

Figure 9.20. Circle criterion (Example 9.11)

9.10 EXERCISES

9.1 Consider the interval system

$$G(s) = \frac{b_1 s + b_0}{s^3 + a_2 s^2 + a_1 s + a_0},$$

where

$$a_0 \in [1, 2], \quad a_1 \in [2, 3], \quad b_0 \in [1, 2], \quad b_1 \in [2, 3].$$

Determine the H_∞ stability margin of this system using the Robust Small Gain Theorem.

9.2 For the interval system of Exercise 9.1 determine the size of a Popov and a Lur'e sector for which Robust Absolute Stability can be guaranteed.

9.3 Consider the feedback system consisting of the interval system given in Exercise 9.1 with a controller $C(s) = 5$. Assuming that the plant is perturbed by unstruc-

tured additive perturbations, determine the H_∞ stability margin of the closed loop system.

9.4 Repeat Exercise 9.3 for the case of multiplicative uncertainty.

9.5 For the interval plant of Exercise 9.1 and the controller $C(s) = 5$ determine the size of a sector such that the closed loop system is absolutely robustly stable for all feedback gains perturbing the plant and lying in the prescribed sector.

9.6 In Exercises 9.3 - 9.5 let $C(s) = \alpha$ a variable gain lying in the range $\alpha \in [1, 100]$. Determine in each case the optimum value of α to maximize

a) the additive H_∞ stability margin

b) the multiplicative H_∞ margin

c) the size of the feedback sector guaranteeing robust absolute stability.

9.7 Consider the feedback system shown in Figure 9.21.

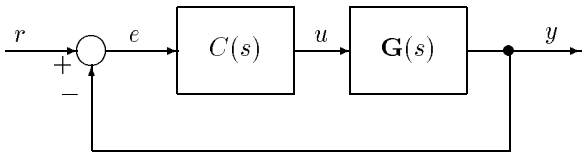

Figure 9.21. Feedback control system

Let

$$C(s) = \frac{2s^2 + 4s + 3}{s^2 + 3s + 4} \quad \text{and} \quad G(s) = \frac{s^2 + a_1 s + a_0}{s(s^2 + b_1 s + b_0)}$$

with the nominal values of the parameters being

$$a_1^0 = -2, \quad a_0^0 = 1, \quad b_0^0 = 2, \quad b_1^0 = 1.$$

Suppose that each parameter perturbs within the range ± 0.0875 Determine the worst case H_∞ stability margin assuming additive uncertainty around the interval plant $\mathbf{G}(s)$.
Answer: 0.3168

9.8 Consider again the interval transfer function $\mathbf{G}(s)$ and the control system in Exercise 9.7. Determine the worst case performance over the parameter set of the system measured in the H_∞ norm of

a) the sensitivity function.

b) the complementary sensitivity function.

9.9 In the block diagram shown in Figure 9.21

$$C(s) = \frac{20 + 30s + 12s^2}{-4 - 6s + s^2} \quad \text{and} \quad G(s) = \frac{a_0 + a_1 s + a2s^2}{s(b_0 + b_1 s + s^2)}$$

and the nominal plant transfer function is

$$G^0(s) = \frac{1 + s + s^2}{s(1 + 2s + s^2)}.$$

Assume that the parameters in $G(s)$ vary as

$$\begin{aligned} a_i &\in [a_i^0 - \epsilon, a_i^0 + \epsilon], \qquad i = 0, 1, 2 \\ b_j &\in [b_j^0 - \epsilon, b_j^0 + \epsilon], \qquad j = 0, 1, 2 \end{aligned}$$

where $\epsilon = 0.2275$. Sketch the Bode magnitude and phase envelopes of the closed loop transfer function. Find the worst case H_∞ norm of this transfer function.
Answer: Worst case (maximum) H_∞ norm = 4.807.

9.10 Consider the block diagram in Figure 9.21 and let

$$C(s) = \frac{s + 3}{4s + 7} \quad \text{and} \quad G(s) = \frac{s^2 + a_1 s + a_0}{s(s^2 + b_1 s + b_0)}$$

with the nominal values of the parameters being

$$a_1^0 = 5, \quad a_0^0 = 8, \quad b_1^0 = 6, \quad b_0^0 = 15.$$

If the parameters vary ± 2.8737 centered around their respective nominal values,

a) Determine the Bode magnitude and phase envelopes of the transfer function $\dfrac{y(s)}{r(s)}$. Find the maximum H_∞ norm of the transfer function over the parameters, i.e. the worst case M_p.

Answer: $M_p = 2.1212$

b) Find the worst case H_∞ additive stability margin (i.e. the unstructured block is an additive perturbation around $\mathbf{G}(s)$).

Answer: 2.1330

9.11 Suppose that the closed loop system given in Exercise 9.10 is perturbed by the nonlinear gain ϕ as shown in Figure 9.15.

a) Find the sector $[0, k]$ such that the corresponding nonlinear system is absolutely stable for all $G(s) \in \mathbf{G}(s)$ by plotting the Nyquist plot of an appropriate transfer function family.

b) Verify that the obtained sector guarantees the robust absolute stability of the system.

9.11 NOTES AND REFERENCES

The Small Gain Theorem (Theorem 9.1) is credited to Zames [244] and can be found in the book of Vidyasagar [232]. The Robust Small Gain Theorem for interval systems (Theorem 9.2), the worst case stability margin computations, and the Robust Small Gain Theorem for interval control systems (Theorem 9.3) were developed by Chapellat, Dahleh, and Bhattacharyya [63]. Theorem 9.2 was given by Mori and Barnett [182]. The vertex results given in Lemmas 9.4, 9.5 and 9.6 are due to Hollot and Tempo [116] who also showed by examples that the vertex results given in Lemma 9.6 do not hold if the weights are more complex than 1st order. The vertex result in Theorem 9.5 is due to Dahleh, Vicino and Tesi [72].

The SPR problem for interval transfer function families was first treated in Dasgupta [74], Dasgupta and Bhagwat [76] and Bose and Delansky [48]. The SPR problem for continuous and discrete time polytopic families has been considered by Šiljak [213]. The vertex results for the SPR problem for interval systems were first obtained in Chapellat, Dahleh, and Bhattacharyya [64].

The absolute stability problem was formulated in the 1950's by the Russian school of control theorists and has been studied as a practical and effective approach to the Robust Control problem for systems containing nonlinearities. For an account of this theory, see the books of Lur'e [165] and Aizerman and Gantmacher [9]. The Robust Absolute Stability problem was formulated and solved for interval systems in Chapellat, Dahleh, and Bhattacharyya [64] where the Lur'e problem was treated. These results were extended by Tesi and Vicino [222, 223] to the case where a controller is present. Marquez and Diduch [176] have shown that the SPR property for such systems can be verified by checking fewer segments than that specified by GKT. In Dahleh, Tesi and Vicino [71] the Popov version of the problem was considered. The crucial facts that make each of these results possible are the boundary results on transfer functions based on the GKT and established in Chapter 8. The Robust Lur'e problem with multiple nonlinearities has been studied by Grujič and Petkovski [104]. In [227] Tsypkin and Polyak treated the absolute stability problem in the presence of H_∞ uncertainty.

Chapter 10

MULTILINEAR INTERVAL SYSTEMS: THE MAPPING THEOREM

In this chapter we deal with robust stability problems where the uncertain interval parameters appear *multilinearly* in the characteristic polynomial coefficients. We introduce the Mapping Theorem which reveals a fundamental property of the image set of such systems. This property allows us to effectively approximate the image set evaluated at an arbitrary point in the complex plane by overbounding it with a union of convex polygons; moreover the accuracy of this approximation can be increased as much as desired. A computationally efficient solution to the robust stability problem can then be obtained by replacing the multilinear interval family with a test set consisting of a polytopic family. We also show how various worst case stability and performance margins over the interval parameter set can be estimated from this polytopic test set. These include gain and phase margins, H_∞ norms, absolute stability under sector bounded nonlinear feedback, and guaranteed time-delay tolerance.

10.1 INTRODUCTION

We begin by giving some examples of system models where parameters appear naturally in a multilinear form. A function $f(x_1, x_2, \cdots, x_n)$ is *multilinear* (*multiaffine*) if for each $i \in [1, 2, \cdots, n]$, f is a linear (affine) function of x_i when the $x_j, j \neq i$ are held constant. We shall use the term multilinear loosely to include the multiaffine case.

Multiloop Systems

Consider the signal flow graph of a multiloop system as shown in Figure 10.1.

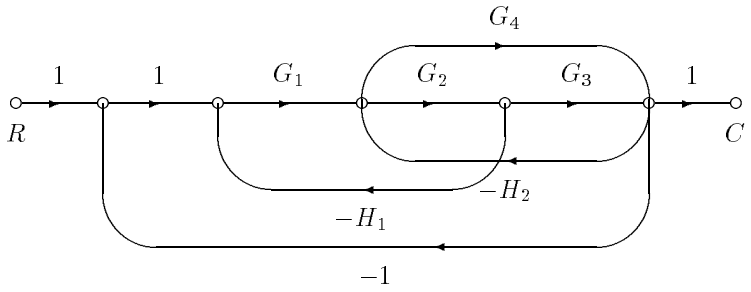

Figure 10.1. Signal flow graph

The closed loop transfer function is

$$\frac{C(s)}{R(s)} = \frac{G_1G_2G_3 + G_1G_4}{1 + G_1G_2H_1 + G_2G_3H_2 + G_1G_2G_3 + G_4H_2 + G_1G_4}.$$

We see that the numerator and denominator of the transfer function is a multilinear function of the gains G_i and H_j of the branches. If these transfer functions contain a vector of parameters appearing linearly in their coefficients then the closed loop transfer function coefficients will be multilinear functions of these parameters. This situation is, of course, not peculiar to this example and it is true that multilinear dependence holds generically in signal flow graphs.

State Space Models

Consider the state space equations of a system

$$\dot{x} = Ax + Bu.$$

The characteristic polynomial of the system, which determines whether it is stable or not is

$$\delta(s) = \det\left[sI - A\right].$$

It can be easily seen that the coefficients of the characteristic polynomial are multilinear functions of the entries a_{ij} of the matrix A. State space equations are frequently written with the states denoting physical variables such as currents, voltages, positions and velocities. It will therefore often be the case that distinct elements of the matrix A represent independent physical parameters. More generally, if uncertain parameters appear in multiple locations in the matrix A but have a "rank-one" structure the characteristic polynomial will once again be a multilinear function of these parameters.

Matrix Fraction Description with Interval Elements

Suppose that $G(s) = N(s)D^{-1}(s)$ and $C(s) = D_c^{-1}(s)N_c(s)$ represent matrix fraction descriptions of a plant and controller connected in a feedback loop. The characteristic polynomial of the closed loop system is

$$\delta(s) = \det\left[D_c(s)D(s) + N_c(s)N(s)\right]$$

If $C(s)$ is fixed and $G(s)$ contains parameter uncertainty it may be reasonable to model this by allowing the elements of $D(s)$ and $N(s)$ to be independent interval uncertain polynomials. It is now straightforward to verify that $\delta(s)$ is a multilinear function of the polynomials in $D(s)$ and $N(s)$ and consequently a multilinear function of the interval coefficients.

The point of the above examples is to show that multilinear parameter dependencies occur in a wide variety of system models. This is fortunate for us. Even though robustness issues in the general nonlinear dependency case are quite difficult to handle, efficient techniques are available for multilinear systems. A key result is the Mapping Theorem which will allow us to determine robust stability in a computationally effective manner. It will also allow us to determine various worst case stability margins and performance measures (robust performance) in the presence of parameter uncertainty.

10.2 THE MAPPING THEOREM

The Mapping Theorem deals with a family of polynomials which depend multilinearly on a set of interval parameters. We refer to such a family as a Multilinear Interval Polynomial. The Mapping Theorem shows us that the image set of such a family is *contained* in the convex hull of the image of the vertices. We state and prove this below.

Let $\mathbf{p} = [p_1, p_2, \cdots, p_l]$ denote a vector of real parameters. Consider the polynomial

$$\delta(s, \mathbf{p}) := \delta_0(\mathbf{p}) + \delta_1(\mathbf{p})s + \delta_2(\mathbf{p})s^2 + \cdots + \delta_n(\mathbf{p})s^n \tag{10.1}$$

where the coefficients $\delta_i(\mathbf{p})$ are *multilinear* functions of $\mathbf{p}$, $i = 0, 1, \cdots n$. The vector $\mathbf{p}$ lies in an uncertainty set

$$\mathbf{\Pi} := \left\{\mathbf{p} \ : \ p_i^- \le p_i \le p_i^+, \quad i = 1, 2, \cdots, l\right\}. \tag{10.2}$$

The corresponding set of *multilinear interval polynomials* is denoted by

$$\mathbf{\Delta}(s) := \{\delta(s, \mathbf{p}) \ : \ \mathbf{p} \in \mathbf{\Pi}\}. \tag{10.3}$$

Let $\mathbf{V}$ denote the vertices of $\mathbf{\Pi}$, i.e.,

$$\mathbf{V} := \left\{\mathbf{p} \ : \ p_i = p_i^+ \ \text{ or } \ p_i = p_i^-, \quad i = 1, 2, \cdots, l\right\} \tag{10.4}$$

and

$$\mathbf{\Delta}_{\mathrm{V}}(s) := \{\delta(s, \mathbf{p}) \ : \ \mathbf{p} \in \mathbf{V}\} := \{v_1(s), v_2(s), \cdots v_k(s)\}. \tag{10.5}$$

denote the set of *vertex polynomials*. Let $\bar{\mathbf{\Delta}}(s)$ denote the *convex hull* of the vertex polynomials $\{v_1(s), v_2(s), \cdots v_k(s)\}$:

$$\bar{\mathbf{\Delta}}(s) := \left\{ \sum_{i=1}^{i=k} \lambda_i v_i(s) : 0 \leq \lambda_i \leq 1, i = 1, 2 \cdots k \right\}.$$

The intersection of the sets $\mathbf{\Delta}(s)$ and $\bar{\mathbf{\Delta}}(s)$ contain the vertex polynomials $\mathbf{\Delta}_{\mathrm{V}}(s)$.

The Mapping Theorem deals with the image of $\mathbf{\Delta}(s)$ at $s = s^*$. Let $\mathbf{T}(s^*)$ denote the complex plane image of the set $\mathbf{T}(s)$ evaluated at $s = s^*$ and let *co* $\mathcal{P}$ denote the convex hull of a set of points $\mathcal{P}$ in the complex plane.

Theorem 10.1 (Mapping Theorem)
Under the assumption that $\delta_i(\mathbf{p})$ *are multilinear functions of* $\mathbf{p}$

$$\mathbf{\Delta}(s^*) \in co\ \mathbf{\Delta}_{\mathrm{V}}(s^*) = \bar{\mathbf{\Delta}}(s^*) \tag{10.6}$$

for each $s^* \in \mathbb{C}$.

Proof. For convenience we suppose that there are two uncertain parameters $\mathbf{p} := [p_1, p_2]$ and the uncertainty set $\mathbf{\Pi}$ is the rectangle $ABCD$ shown in Figure 10.2(a). Fixing $s = s^*$, we obtain $\delta(s^*, \mathbf{p})$ which maps $\mathbf{\Pi}$ to the complex plane. Let A', B', C', D' denote respectively the complex plane images of the vertices A, B, C, D under this mapping. Figures 10.2(b,c,d,e) show various configurations that can arise under this mapping. Now consider an arbitrary point I in $\mathbf{\Pi}$ and its complex plane image I'. The theorem is proved if we establish that I' is a convex combination of the complex numbers A', B', C', D'. We note that starting at an arbitrary vertex, say A, of $\mathbf{\Pi}$ we can reach I by moving along straight lines which are either edges of $\mathbf{\Pi}$ or are parallel to an edge of $\mathbf{\Pi}$. Thus, as shown in Figure 10.2(a), we move from A to E along the edge AB, and then from E to I along EF which is parallel to the edge AD. Because $\delta(s^*, \mathbf{p})$ is multilinear in the p_i it follows that the complex plane images of AB, EF, and CD, which are parallel to edges of $\mathbf{\Pi}$, are straight lines, respectively $A'B'$, $E'F'$, $C'D'$. Moreover, E' lies on the straight line $A'B'$, F' lies on the straight line $C'D'$, and I' lies on the straight line $E'F'$. Therefore, I' lies in the convex hull of $A'B'C'D'$.

The same reasoning works in higher dimensions. Any point in $\mathbf{\Pi}$ can be reached from a vertex by moving one coordinate at a time. In the image set this corresponds, because of multilinearity, to moving along straight lines joining vertices or convex combinations of vertices. By such movements we can never escape the convex hull of the vertices. The second equality holds by definition. ♣

We point out that the Mapping Theorem does not hold if $\mathbf{\Pi}$ is not an axis-parallel box since the image of the edge of an arbitrary polytope under a multilinear mapping is in general not a straight line. The Mapping Theorem will also not hold when the dependency on the parameters is polynomial rather than multilinear, because of the same reason.

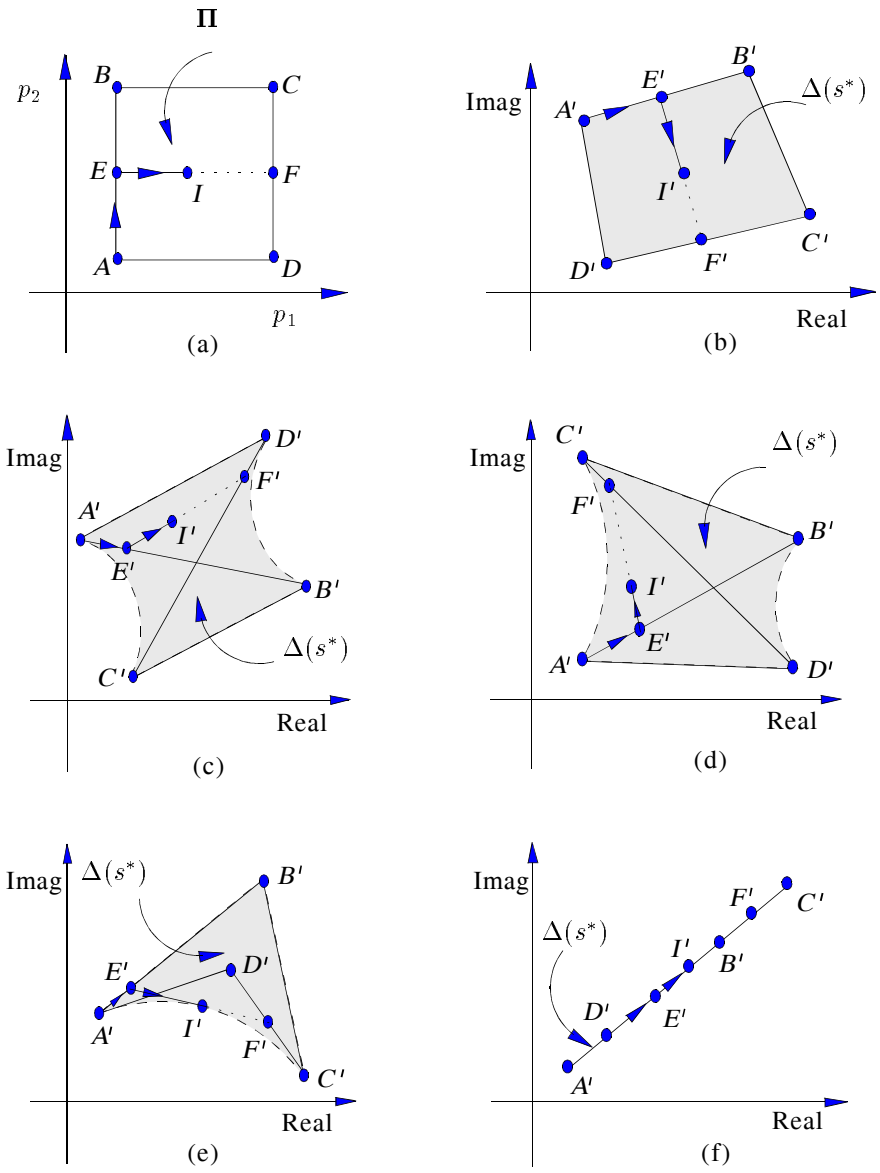

Figure 10.2. Proof of the Mapping Theorem

Example 10.1. Consider the multilinear interval polynomial

$$\delta(s, \mathbf{p}) = p_1 Q_1(s) + p_2 Q_2(s) + p_1 p_2 Q_3(s) + Q_4(s)$$

with

$$Q_1(s) = -6s + 2, \quad Q_2(s) = -5s - 1, \quad Q_3(s) = 10s + 3, \quad Q_4(s) = 7s + 5.$$

The parameter set $\mathbf{p}$ varies inside box $\mathbf{\Pi}$ depicted in Figure 10.3(a). The image set $\mathbf{\Delta}(s^*, \mathbf{p})$ of the family at $s^* = j1$ is shown in Figure 10.3(b). The convex hull of the image set $\mathbf{\Delta}(s^*)$ is also shown. This shows that

$$\mathbf{\Delta}(s^*, \mathbf{p}) \in co\ \mathbf{\Delta}_V(s^*, \mathbf{p}) = \bar{\mathbf{\Delta}}(s^*).$$

The four corners of the polygon in Figure 10.3(b) are the vertices of the image.

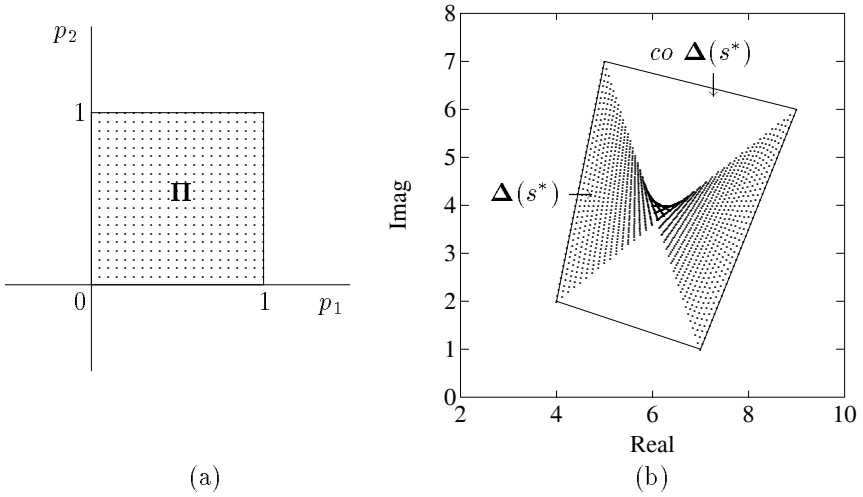

Figure 10.3. Parameter space, image set, and convex hull (Example 10.1)

This theorem shows us that the image set of the multilinear family $\mathbf{\Delta}(s)$ can always be approximated by overbounding it with the image of the polytopic family $\bar{\mathbf{\Delta}}(s)$. This approximation is extremely useful. In the next section we show how it allows us to determine robust stability and stability margins quantitatively.

10.3 ROBUST STABILITY VIA THE MAPPING THEOREM

As we have seen in earlier chapters, the robust stability of a parametrized family of polynomials can be determined by verifying that the image set evaluated at each point of the stability boundary excludes the origin. The Mapping Theorem shows us that the image set of a multilinear interval polynomial family is contained in the convex hull of the vertices. Obviously a sufficient condition for the entire image set to exclude zero is that the convex hull exclude zero. Since the image set $\mathbf{\Delta}(s^*)$ is overbounded by the convex hull of $\mathbf{\Delta}_{\mathrm{V}}(s^*)$, this suggests that the stability of the *multilinear* set $\mathbf{\Delta}(s)$ can be guaranteed by solving the easier problem of verifying the stability of the *polytopic* set $\bar{\mathbf{\Delta}}(s)$. We develop this idea in this section.

As usual, let $\mathcal{S}$, an open set in the complex plane, be the stability region. Introduce the set of edges $\mathbf{E}(s)$ of the polytope $\bar{\mathbf{\Delta}}(s)$:

$$\mathbf{E}(s) := \{\lambda v_i(s) + (1-\lambda)v_j(s) \ : \ v_i(s), v_j(s) \in \mathbf{\Delta}_{\mathrm{V}}(s)\}\,. \tag{10.7}$$

To proceed, we make some standing assumptions about the families $\mathbf{\Delta}(s)$ and $\bar{\mathbf{\Delta}}(s)$.

Assumption 10.1.

1) Every polynomial in $\mathbf{\Delta}(s)$ and $\bar{\mathbf{\Delta}}(s)$ is of the same degree.

2) $0 \notin \bar{\mathbf{\Delta}}(s_0)$ for some $s_0 \in \partial\mathcal{S}$.

3) At least one polynomial in $\mathbf{\Delta}(s)$ is stable.

Theorem 10.2 *Under the above assumptions, $\mathbf{\Delta}(s)$ is stable with respect to $\mathcal{S}$ if $\bar{\mathbf{\Delta}}(s)$ and equivalently $\mathbf{E}(s)$ is stable with respect to $\mathcal{S}$.*

Proof. Since the degree remains invariant, we may apply the Boundary Crossing Theorem (Chapter 1). Thus, $\mathbf{\Delta}(s)$ can be unstable if and only if $0 \in \mathbf{\Delta}(s^*)$ for some $s^* \in \partial\mathcal{S}$. By assumption, there exist $s_0 \in \partial\mathcal{S}$ such that

$$0 \notin \bar{\mathbf{\Delta}}(s_0) = co\ \mathbf{E}(s_0).$$

By the Mapping Theorem

$$\mathbf{\Delta}(s^*) \subset \bar{\mathbf{\Delta}}(s^*) = co\ \mathbf{E}(s^*).$$

Therefore, by continuity of the image set on s, $0 \in \mathbf{\Delta}(s^*)$ must imply the existence of $\bar{s} \in \partial\mathcal{S}$ such that $0 \in \mathbf{E}(\bar{s})$. This contradicts the stability of $\bar{\mathbf{\Delta}}(s)$ and of $\mathbf{E}(s)$. ♣

This theorem is just a statement of the fact that the origin can enter the image set $\mathbf{\Delta}(s^*)$ only by piercing one of the edges $\mathbf{E}(\bar{s})$. Nevertheless the result is rather remarkable in view of the fact that the set $\bar{\mathbf{\Delta}}(s)$ does not necessarily contain, nor is it contained in, the set $\mathbf{\Delta}(s)$. In fact the inverse image of $\mathbf{E}(s)$ in the parameter space will in general include points outside $\mathbf{\Pi}$. The theorem works because the *image set*

$\boldsymbol{\Delta}(s^*)$ *is overbounded* by $\bar{\boldsymbol{\Delta}}(s)$ at every point $s^* \in \partial\mathcal{S}$. This in turn happens because the Mapping Theorem guarantees that $\boldsymbol{\Delta}(s^*)$ is "concave" or bulges inward.

The test set $\bar{\boldsymbol{\Delta}}(s)$ or its edges $\mathbf{E}(s)$ are linearly parametrized families of polynomials. Thus, the above theorem allows us to test a multilinear interval family using all the techniques available in the linear case.

Example 10.2. Consider the multilinear interval polynomial

$$\delta(s, \mathbf{p}) = p_1 Q_1(s) + p_2 Q_2(s) + p_1 p_2 Q_3(s)$$

where

$$p_1 \in [1, 2], \quad p_2 \in [3, 4]$$

and

$$\begin{aligned} Q_1(s) &= s^4 + 4.3s^3 + 6.2s^2 + 3.5s + 0.6, \\ Q_2(s) &= s^4 + s^3 + 0.32s^2 + 0.038s + 0.0015, \\ Q_3(s) &= s^4 + 3.5s^3 + 3.56s^2 + 1.18s + 0.12. \end{aligned}$$

The edges of this system are,

$$\mathbf{E}(s) = \{E_i(s), \quad i = 1, 2, 3, 4\}$$

with

$$\begin{aligned} E_1(s) &= \left[\lambda p_1^- + (1-\lambda)p_1^+\right] Q_1(s) + p_2^- Q_2(s) + \left[\lambda p_1^- + (1-\lambda)p_1^+\right] p_2^- Q_3(s) \\ &= \lambda \left[p_1^- Q_1(s) + p_2^- Q_2(s) + p_1^- p_2^- Q_3(s)\right] \\ &\qquad +(1-\lambda)\left[p_1^+ Q_1(s) + p_2^- Q_2(s) + p_1^+ p_2^- Q_3(s)\right] \\ E_2(s) &= \left[\lambda p_1^- + (1-\lambda)p_1^+\right] Q_1(s) + p_2^+ Q_2(s) + \left[\lambda p_1^- + (1-\lambda)p_1^+\right] p_2^+ Q_3(s) \\ &= \lambda \left[p_1^- Q_1(s) + p_2^+ Q_2(s) + p_1^- p_2^+ Q_3(s)\right] \\ &\qquad +(1-\lambda)\left[p_1^+ Q_1(s) + p_2^+ Q_2(s) + p_1^+ p_2^+ Q_3(s)\right] \\ E_3(s) &= p_1^- Q_1(s) + \left[\lambda p_2^- + (1-\lambda)p_2^+\right] Q_2(s) + \left[\lambda p_2^- + (1-\lambda)p_2^+\right] p_1^- Q_3(s) \\ &= \lambda \left[p_1^- Q_1(s) + p_2^- Q_2(s) + p_1^- p_2^- Q_3(s)\right] \\ &\qquad +(1-\lambda)\left[p_1^- Q_1(s) + p_2^+ Q_2(s) + p_1^- p_2^+ Q_3(s)\right] \\ E_4(s) &= p_1^+ Q_1(s) + \left[\lambda p_2^- + (1-\lambda)p_2^+\right] Q_2(s) + \left[\lambda p_2^- + (1-\lambda)p_2^+\right] p_1^+ Q_3(s) \\ &= \lambda \left[p_1^+ Q_1(s) + p_2^- Q_2(s) + p_1^+ p_2^- Q_3(s)\right] \\ &\qquad +(1-\lambda)\left[p_1^+ Q_1(s) + p_2^+ Q_2(s) + p_1^+ p_2^+ Q_3(s)\right]. \end{aligned}$$

The stability of $\mathbf{E}(s)$ can be tested simply by applying the Segment Lemma (Chapter 2). Here, all edges in $\mathbf{E}(s)$ are found to be stable.

Bounded Phase Condition

An alternative way of stating Theorem 10.2 is to use the Bounded Phase Condition. Let $\Phi_{\mathbf{\Delta}_V}(s^*)$ equal the angle subtended at the origin by the points $\mathbf{\Delta}_V(s^*)$. Obviously, the stability of $\mathbf{E}(s)$ is equivalent, under the Assumptions 10.1, to the origin being excluded from $\bar{\mathbf{\Delta}}(s^*)$ for all $s^* \in \partial\mathcal{S}$, and this in turn is equivalent to the condition that the phase spread be less than π radians. Accordingly we have the following theorem.

Theorem 10.3 *Under the assumptions 10.1, $\mathbf{\Delta}(s)$ is stable with respect to $\mathcal{S}$ if*

$$\Phi_{\bar{\mathbf{\Delta}}_V}(s^*) < \pi, \qquad \text{for all } s^* \in \partial\mathcal{S}. \tag{10.8}$$

Example 10.3. Let us return to Example 10.2 and determine the robust stability of this multilinear interval polynomial by applying the Bounded Phase Condition. We first construct the set of vertex polynomials corresponding to the vertices of the parameter space box $\mathbf{\Pi} = [p_1,\ p_2]$.

$$\begin{aligned}
v_1(s) &= 7s^4 + 17.8s^3 + 17.84s^2 + 7.154s + 0.9645\\
v_2(s) &= 11s^4 + 32.6s^3 + 34.72s^2 + 14.194s + 1.9245\\
v_3(s) &= 9s^4 + 22.3s^3 + 21.72s^2 + 8.372s + 1.086\\
v_4(s) &= 14s^4 + 40.6s^3 + 42.16s^2 + 16.592s + 2.166.
\end{aligned}$$

The maximum phase difference over the vertex set at each frequency ω is computed as follows:

$$\Phi_{\bar{\mathbf{\Delta}}_V} = \sup_{i=2,3,4} \arg \frac{v_i(j\omega)}{v_1(j\omega)} - \inf_{i=2,3,4} \arg \frac{v_i(j\omega)}{v_1(j\omega)}.$$

The plot of the above phase function for all ω is shown in Figure 10.4. We find that the maximum phase difference over the vertex set does not reach 180° for any ω. Thus we conclude that the given multilinear polynomial family is Hurwitz stable.

10.3.1 Refinement of the Convex Hull Approximation

Since the stability of the set $\bar{\mathbf{\Delta}}(s)$ or $\mathbf{E}(s)$ is only a sufficient condition for the stability of $\mathbf{\Delta}(s)$, it can happen that $\mathbf{E}(s)$ is unstable but $\mathbf{\Delta}(s)$ is stable. In this case the sufficient condition given by the theorem can be tightened by introducing additional vertices. We illustrate this in the accompanying figures. Consider the multilinear polynomial

$$Q_0(s) + p_1Q_1(s) + p_2Q_2(s) + p_1p_2Q_3(s)$$

where

$$\begin{aligned}
Q_0(s) &= s^4 + s^3 + 2s^2 + s + 2,\\
Q_1(s) &= 2s^4 + 3s^3 + 4s^2 + s + 1,\\
Q_2(s) &= 1.5s^4 + 1.5s^3 + 3s^2 + s + 0.5,\\
Q_3(s) &= 3s^4 + 0.5s^3 + 1.5s^2 + 2s + 2
\end{aligned}$$

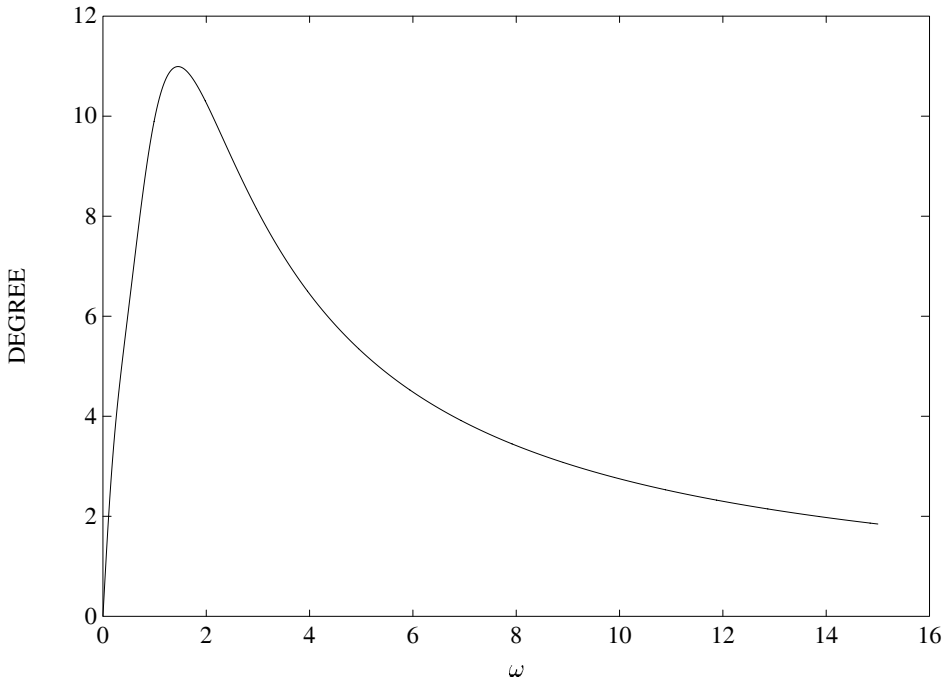

Figure 10.4. Maximum phase difference (Example 10.3)

and the parameter $\mathbf{p}$ varies within the box shown in Figure 10.5.

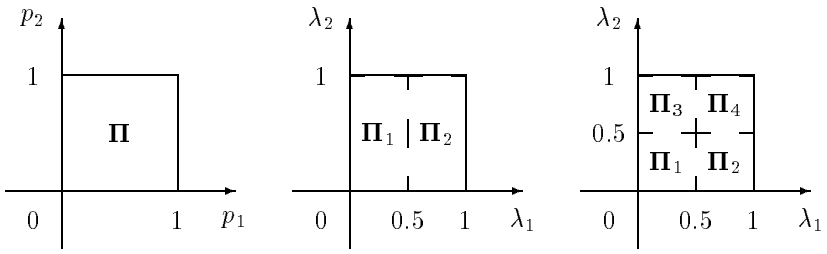

Figure 10.5. Additional vertices in parameter space

As shown in Figure 10.5 one may introduce additional vertices in the parameter

space. The corresponding image sets at $\omega = 0.85$ are shown in Figures 10.6, 10.7, and 10.8. We see that this amounts to decomposing the parameter box as a union of smaller boxes:

$$\mathbf{\Pi} = \bigcup_{i=1}^{t} \mathbf{\Pi}_i. \tag{10.9}$$

If $\mathbf{V}_i$ and $\mathbf{E}_i(z)$ denote the corresponding vertices and edges, we have

$$co\ \mathbf{\Delta}(z^*) \subset \bigcup_{i=1}^{t} \bar{\mathbf{\Delta}}_{\mathbf{V}_i}(z^*) = \bigcup_{i=1}^{t} co\ \mathbf{E}_i(z^*) \tag{10.10}$$

and therefore the stability of the set of line segments $\bigcup_{i=1}^{m} \mathbf{E}_i(z)$ would imply that of $\mathbf{\Delta}(z)$. We can see from Figures 10.7 and 10.8 that the nonconvex set $\bigcup_{i=1}^{m} \mathbf{E}_i(z^*)$ approximates $\mathbf{\Delta}(z^*)$ more closely as the number t of polytopes $\mathbf{\Pi}_i$ increases. It is clear therefore that the sufficient condition given here can be improved to any desired level of accuracy by checking the stability of smaller convex hulls.

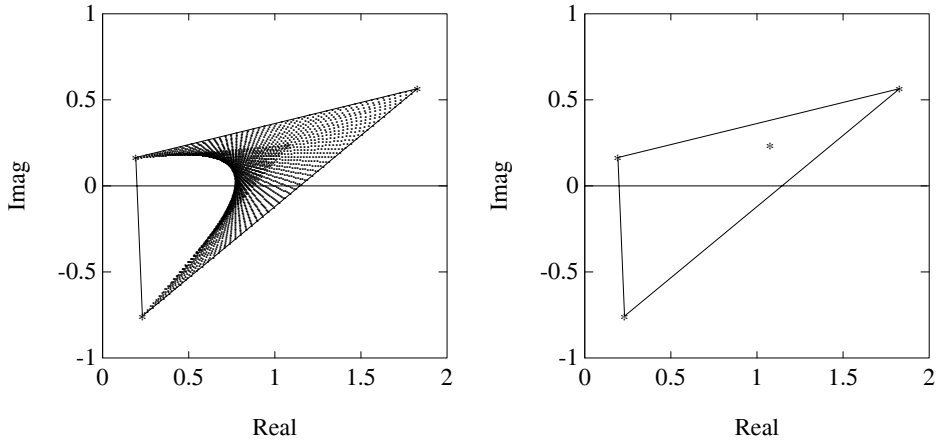

Figure 10.6. Image set and convex hull ($\omega = 0.85$)

10.4 MULTILINEAR INTERVAL SYSTEMS

In this section we consider system transfer functions which are ratios of multilinear interval polynomials. We call such systems *multilinear interval systems*. Our objective is to analyze feedback control systems containing such multilinear interval plants. In addition to determining robust stability, we are interested in calculating various types of stability and performance margins for such systems. Let $M(s)$

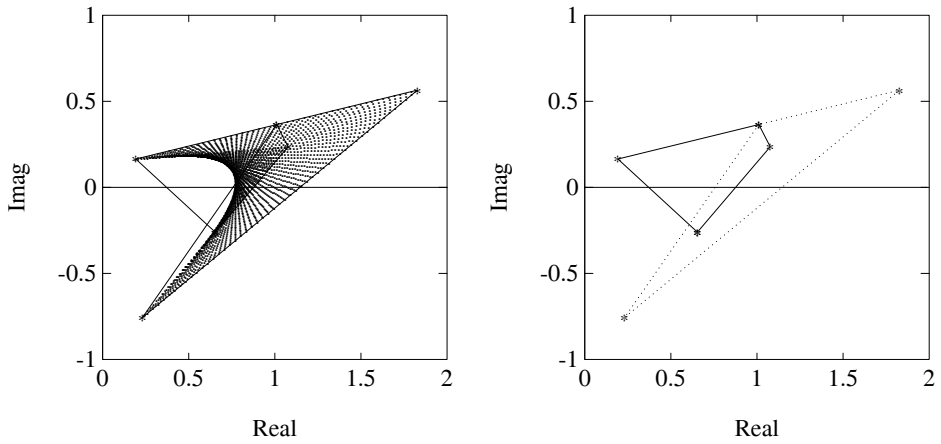

Figure 10.7. Image set and convex hull (2 partitions) ($\omega = 0.85$)

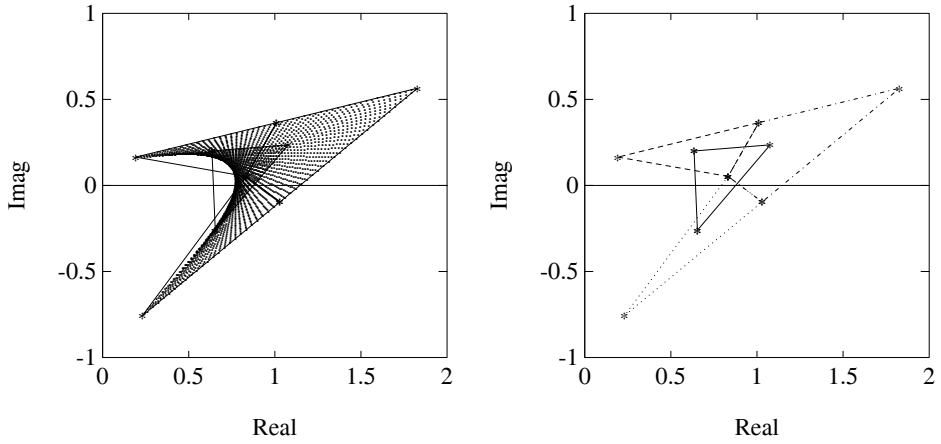

Figure 10.8. Image set and convex hull (4 partitions) ($\omega = 0.85$)

denote a transfer function which depends on the uncertain, interval, independent parameters $\mathbf{q}$ and $\mathbf{r}$:

$$M(s) = M(s, \mathbf{q}, \mathbf{r}) = \frac{N(s, \mathbf{q})}{D(s, \mathbf{r})}. \tag{10.11}$$

We assume that $N(s,\mathbf{q})$ and $D(s,\mathbf{r})$ are multilinear interval polynomials and $\mathbf{q}$ and $\mathbf{r}$ lie in axis parallel boxes $\mathbf{Q}$ and $\mathbf{R}$ respectively. Let

$$\mathbf{N}(s) := \{N(s,\mathbf{q}) : \mathbf{q} \in \mathbf{Q}\}$$

$$\mathbf{D}(s) := \{D(s,\mathbf{r}) : \mathbf{r} \in \mathbf{R}\}$$

and write

$$\mathbf{M}(s) := \left\{ \frac{N(s,\mathbf{q})}{D(s,\mathbf{r})} : \mathbf{q} \in \mathbf{Q}, \mathbf{r} \in \mathbf{R} \right\} := \frac{\mathbf{N}(s)}{\mathbf{D}(s)}.$$

Now, suppose that the multilinear interval plant we have described is part of a control system. For robustness studies, it is important that we obtain an assessment of the worst case stability margins and performance measures of the system over the uncertainty set $\mathbf{\Pi} := \mathbf{Q} \times \mathbf{R}$. We shall show here that by using the Mapping Theorem we can replace the family $\mathbf{M}(s)$ by a polytopic family $\bar{\mathbf{M}}(s)$ which has the property that any worst case stability or performance margin that is calculated for the family $\bar{\mathbf{M}}(s)$ serves as a corresponding *guaranteed* margin for the family $\mathbf{M}(s)$. The advantage that we gain is that worst case stability and performance margins can be evaluated *easily and exactly* for the family $\bar{\mathbf{M}}(s)$ since it is polytopic.

Construction of $\bar{\mathbf{M}}(s)$

Let $\mathbf{V}_Q$ denote the vertex set of $\mathbf{Q}$, $\mathbf{N}_{\mathrm{V}}(s)$ the corresponding vertex polynomials

$$\mathbf{N}_{\mathrm{V}}(s) := \{N(s,\mathbf{q}) : \mathbf{q} \in \mathbf{V}_Q\}$$

and $\bar{\mathbf{N}}(s)$ the convex hull of $\mathbf{N}_{\mathrm{V}}(s)$:

$$\bar{\mathbf{N}}(s) := \{\lambda N_i(s) + (1-\lambda)N_j(s) : N_i(s), N_j(s) \in \mathbf{N}_{\mathrm{V}}(s), \quad \lambda \in [0,1]\}.$$

In an identical manner we can define the sets $\mathbf{V}_R, \mathbf{D}_{\mathrm{V}}(s)$ and $\bar{\mathbf{D}}(s)$. Now we can introduce the transfer function sets

$$\mathbf{M}_{\mathrm{V}}(s) := \frac{\mathbf{N}_{\mathrm{V}}(s)}{\mathbf{D}_{\mathrm{V}}(s)}$$

and

$$\bar{\mathbf{M}}(s) := \frac{\bar{\mathbf{N}}(s)}{\bar{\mathbf{D}}(s)}.$$

From the Mapping Theorem we know that at every point $s^* \in \mathbb{C}$ the image sets of $\mathbf{N}(s)$ and $\mathbf{D}(s)$ contain the image of the vertices and are overbounded respectively by the images of the polytopic families $\bar{\mathbf{N}}(s)$ and $\bar{\mathbf{D}}(s)$ respectively:

$$\mathbf{N}_{\mathrm{V}}(s^*) \subset \mathbf{N}(s^*) \subset \bar{\mathbf{N}}(s^*)$$

$$\mathbf{D}_{\mathrm{V}}(s^*) \subset \mathbf{D}(s^*) \subset \bar{\mathbf{D}}(s^*).$$

As usual we assume that $0 \notin \bar{\mathbf{D}}(s^*)$ so that the above sets are well-defined. From the above it follows that the image set of $\mathbf{M}(s)$ contains the image of the vertices $\mathbf{M}_V(s)$ and is also overbounded by the image of $\bar{\mathbf{M}}(s)$.

Lemma 10.1

$$\mathbf{M}_{\mathrm{V}}(s^*) \subset \mathbf{M}(s^*) \subset \bar{\mathbf{M}}(s^*).$$

This result suggests that by substituting the multilinear interval family $\mathbf{M}(s)$ by the polytopic family $\bar{\mathbf{M}}(s)$ in a control system we can calculate a lower bound on the worst case stability margin or performance margin of the system. To state this more precisely suppose that $M(s) \in \mathbf{M}(s)$ is part of a feedback control system. We will assume that the order of the closed loop system, i.e. the degree of the characteristic polynomial, remains invariant over $M(s) \in \mathbf{M}(s)$ and also over $M(s) \in \bar{\mathbf{M}}(s)$. As usual let $\mathcal{S}$ denote a stability region that is relevant to the system under consideration.

Theorem 10.4 *Under the assumption of invariant order, robust stability of the control system holds with $M(s) \in \mathbf{M}(s)$ if it holds with $M(s) \in \bar{\mathbf{M}}(s)$.*

The proof of this result follows immediately from the image set bounding property of the set $\bar{\mathbf{M}}(s)$ evaluated at points s^* on the stability boundary $\partial\mathcal{S}$, which is stated in the Lemma above. The result holds for arbitrary stability regions with Hurwitz and Schur stability being particular cases.

Suppose now that we are dealing with a continuous time control system and that we have verified the robust Hurwitz stability of the system with $M(s) \in \bar{\mathbf{M}}(s)$. The next important issue is to determine the performance of the system in some suitably defined meaningful way. The usual measures of performance are gain margin, phase margin, time-delay tolerance, H_∞ stability or performance margins, parametric stability radius in the parameter $\mathbf{p}$ and nonlinear sector bounded stability margins as in the Lur'e or Popov problems treated in Chapter 8. Let μ refer to one of these performance measures and let us assume that increasing values of μ reflect better performance. Let μ^* denote the worst case value of μ over the set $M(s) \in \mathbf{M}(s)$, $\underline{\mu}$ denote the worst case value of μ over $M(s) \in \bar{\mathbf{M}}(s)$ and $\bar{\mu}$ denote the worst case value of μ over the vertex set $M(s) \in \mathbf{M}_{\mathrm{V}}(s)$. Then it is obviously true that

$$\underline{\mu} \leq \mu^* \leq \bar{\mu}.$$

Since $\bar{\mathbf{M}}(s)$ is a polytopic set, we can calculate $\underline{\mu}$ exactly. As in the Mapping Theorem, this lower bound can be increased by subdividing the box $\mathbf{\Pi}$ into smaller boxes. On the other hand, $\bar{\mu}$ can be calculated very easily because it is the minimum of μ evaluated over the vertex points. By subdividing the box $\mathbf{\Pi}$, this upper bound can be decreased and the gap between the upper and lower bounds can be reduced to arbitrarily small values by introducing additional vertices to refine the convex hull approximation. Thus the worst case performance over the parameter set $\mathbf{\Pi}$, also known as robust performance, can be accurately determined. In the following section we illustrate this procedure for estimating worst case performance in greater detail with numerical examples.

10.5 EXAMPLES

We illustrate the procedure for calculating robust stability and performance margins by examples.

10.5.1 Parametric Stability Margin

For a given uncertainty set $\mathbf{\Pi}$, we can verify robust stability using the Mapping Theorem. In applications, it is of interest to know how large $\mathbf{\Pi}$ can be without losing stability. This problem can also be solved using the convex hull approximation. We illustrate this with an example.

Example 10.4. Consider the discrete time feedback system as shown Figure 10.9.

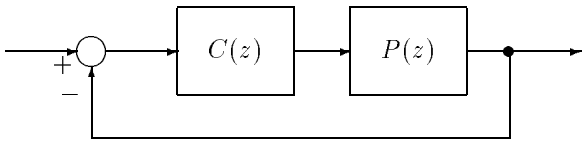

Figure 10.9. Discrete-time feedback systems (Example 10.4)

$$P(z) := \frac{P_1(z)}{P_2(z)} = \frac{z - z_0}{(z - p_1)(z - p_2)} \quad \text{and} \quad C(z) := \frac{C_1(z)}{C_2(z)} = \frac{z + 1.29}{z - 0.5}$$

and let the set of system parameters $\mathbf{p} = [z_0, p_1, p_2]$ vary in a box whose size varies with a dilation parameter ϵ as follows:

$$\begin{aligned} z_0 &\in [z_0^-, z_0^+] = [0.5 - \epsilon, 0.5 + \epsilon] \\ p_1 &\in [p_1^-, p_1^+] = [1.0 - \epsilon, 1.0 + \epsilon] \\ p_2 &\in [p_2^-, p_2^+] = [-1.0 - \epsilon, -1.0 + \epsilon]. \end{aligned}$$

The characteristic polynomial of the system is

$$\begin{aligned} \delta(z, \mathbf{p}) = z^3 + (0.5 - p_1 - p_2)z^2 + (1.29 + 0.5p_1 + 0.5p_2 + p_1p_2 - z_0)z \\ -0.5p_1p_2 - 1.29z_0. \end{aligned}$$

We see that the coefficients are multilinear functions of $\mathbf{p}$. Therefore Theorem 10.4 may be applied. We verify that the following member of the family is Schur stable:

$$\delta(z, \mathbf{p} = [0.5, 1, -1]) = z^3 + 0.5z^2 - 0.21z - 0.145.$$

We would like to determine the largest sized box for which we have closed loop stability. This can be regarded as the worst case parametric stability margin ϵ^* of

the family. Using a simple bisection algorithm, we find that a lower bound $\underline{\epsilon}$ on the the parametric stability margin ϵ^* is 0.125 as shown in Figure 10.10.

On the other hand we can get an upper bound $\bar{\epsilon}$ from the vertices. This gives $\bar{\epsilon} = 0.125$, which is the same as the lower bound, and thus the true value in this case.

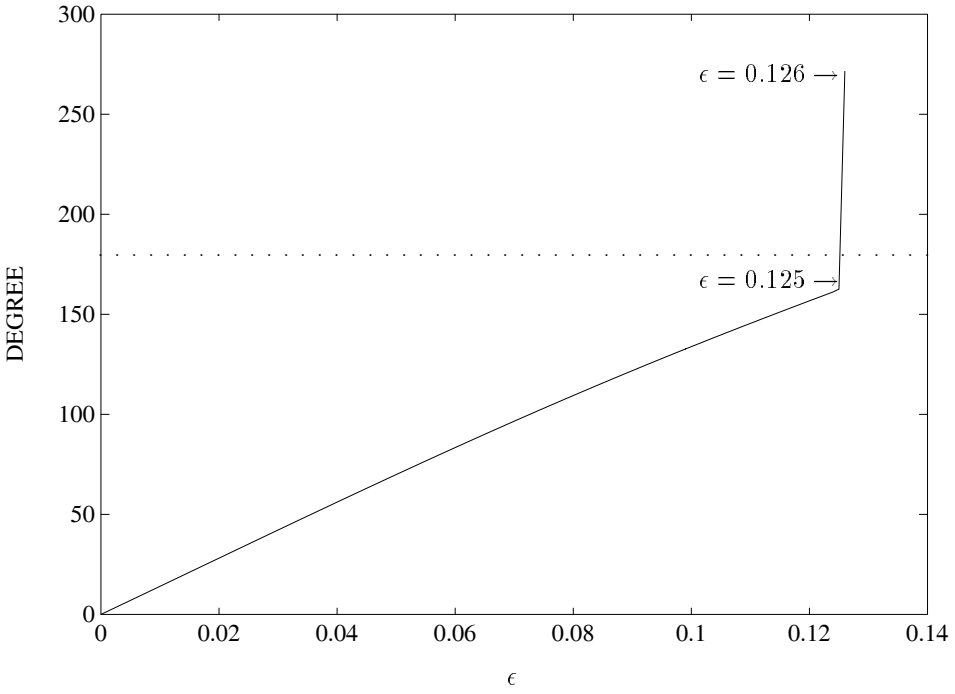

Figure 10.10. Maximum phase difference (Example 10.4)

10.5.2 Robust Gain, Phase, Time-delay and H_∞ Stability Margins

In this section we focus on a control system example and show how robust performance measured in each of the above ways, over a multilinear parameter set, can be estimated from the polytopic overbounding method discussed earlier.

Example 10.5. Consider the control system block diagram shown in Figure 10.11.

Let

$$F(s) := \frac{F_1(s)}{F_2(s)} = \frac{s+1}{s+2} \quad \text{and} \quad P(s) := \frac{P_1(s)}{P_2(s)} = \frac{s+p_1}{s^2+p_2 s+4}$$

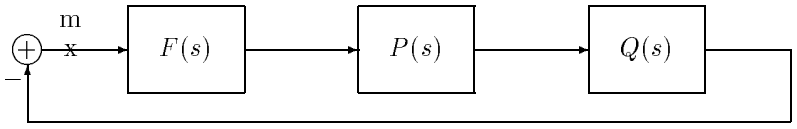

Figure 10.11. A multilinear interval control system (Example 10.5)

$$Q(s) := \frac{Q_1(s)}{Q_2(s)} = \frac{s + p_3}{s^3 + 3s^2 + p_4 s + 0.1}$$

where

$$p_1 \in [2.9, 3.1] =: [p_1^-, p_1^+] \qquad p_2 \in [1.9, 2.1] =: [p_2^-, p_2^+]$$
$$p_3 \in [4.9, 5.1] =: [p_3^-, p_3^+] \qquad p_4 \in [1.9, 2.1] =: [p_4^-, p_4^+].$$

The family of characteristic polynomials is

$$\mathbf{\Delta}(s, \mathbf{p}) = \{F_2(s)P_2(s)Q_2(s) + F_1(s)P_1(s)Q_1(s) \ : \ \mathbf{p} \in \mathbf{\Pi}\}$$

where the parameter space box is given as

$$\mathbf{\Pi} := \left\{\mathbf{p} : p_i \in [p_i^-, p_i^+] \ \ i = 1, 2, 3, 4\right\}.$$

Now we construct the 16 vertex polynomials corresponding to the vertex set $\mathbf{V}$ of $\mathbf{\Pi}$:

$$\mathbf{\Delta}_{\mathrm{V}}(s) = \{v(s, \mathbf{p}) \ : \ \mathbf{p} \in \mathbf{V}\} = \{v_i(s) = v_i(s, \mathbf{p}), \quad i = 1, 2, \cdots, 16\}.$$

The vertex polynomials $v_i(s)$ can be written down by setting $\mathbf{p}$ to a vertex value. For example:

$$\begin{aligned} v_1(s) &= v(s, p_1^+, p_2^+, p_3^+, p_4^+) \\ &= \underbrace{(s+2)(s^2 + p_2^+ s + 4)(s^3 + 3s^2 + p_4^+ s + 0.1)}_{V_1^D(s)} + \underbrace{(s+1)(s+p_1^+)(s+p_3^+)}_{V_1^N(s)}. \end{aligned}$$

Similarly, we can write $v_2(s)$, $\cdots$, v_{16}.

(a) To determine the worst case upper gain margin L^* over the parameter set, we replace the vertex polynomials as follows:

$$V_i(s, L) = V_i^D(s) + (1 + L)V_i^N(s), \quad i = 1, 2, \cdots, 16.$$

Now find the maximum phase difference over the entire set of vertex polynomials $\mathbf{\Delta}_{\mathrm{V}}(j\omega)$ for a fixed ω with a fixed L:

$$\Phi_{\mathbf{\Delta}_{\mathrm{V}}}(\omega, L) = \sup_{i, i \neq k} \arg \frac{V_i(j\omega, L)}{V_k(j\omega, L)} - \inf_{i, i \neq k} \arg \frac{V_i(j\omega, L)}{V_k(j\omega, L)}$$

where k is an arbitrary integer, $1 \leq k \leq 16$, and $i = 1, 2, \cdots, 16$. Then a lower bound $\underline{L}$ on the worst case gain margin is obtained by determining the largest real positive value of L such that all the edges connecting the vertices in $\mathbf{\Delta}_{\mathrm{V}}(s)$ remain Hurwitz. Equivalently, by the Bounded Phase Condition we have

$$\underline{L} = \inf_{L \geq 0} \left\{ L \ : \ \sup_{\omega} \Phi_{\mathbf{\Delta}_{\mathrm{V}}}(\omega, L) = 180^{\circ} \right\}.$$

Figure 10.12 shows that the maximum phase differences over the vertex set for each frequency ω for $L = 0$.

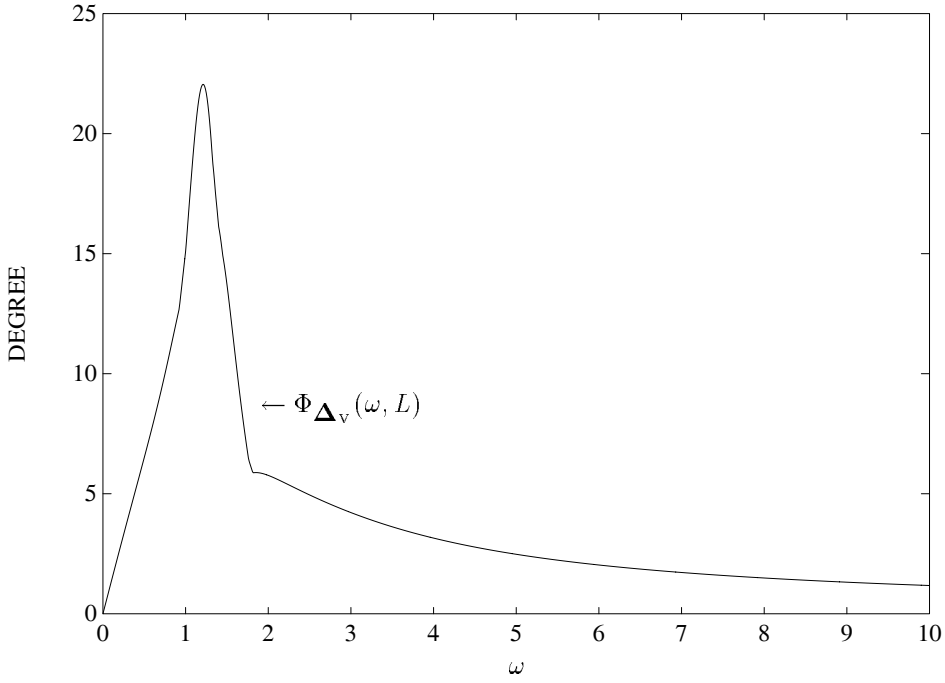

Figure 10.12. $\Phi_{\mathbf{\Delta}_{\mathrm{V}}}(\omega, L)$ vs. ω $(L = 0)$ (Example 10.5(a))

The figure shows that the maximum phase difference over vertices $\Phi_{\mathbf{\Delta}_{\mathrm{V}}}(\omega, L)$ does not reach 180° for any ω. This means that a larger value L is allowed. Figure 10.13 shows the plot of the maximum phase difference over the vertices and over all frequency in terms of L. From this we find that for $\underline{L} = 0.658$ there exists a frequency ω that results in $\Phi_{\mathbf{\Delta}_{\mathrm{V}}}(\omega, L) = 180^{\circ}$. Therefore,

$$\underline{L} \approx 0.658$$

On the other hand, we can determine an upper bound on L^* by finding the smallest gain margin over the vertex set. This turns out to be $\bar{L} = 0.658$ which is the same as $\underline{L}$, and therefore the exact margin in this case.

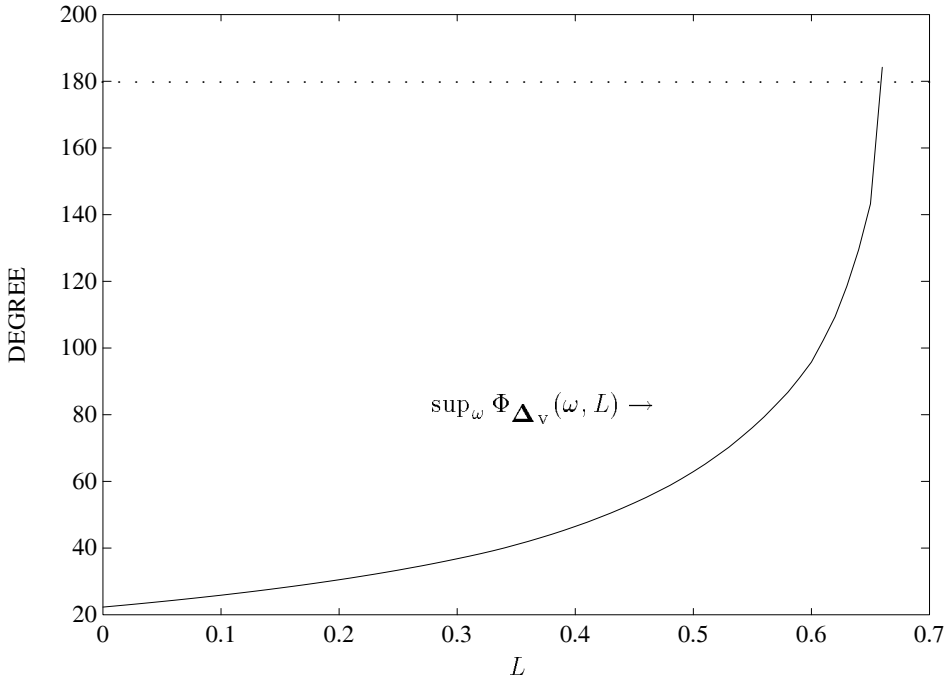

Figure 10.13. $\sup_\omega \Phi_{\mathbf{\Delta}_V}(\omega, L)$ vs. L (Example 10.5(a))

(b) To determine the worst case phase margin θ^* we modify each vertex polynomial as follows:

$$V_i(s, \theta) = V_i^D(s) + e^{j\theta} V_i^N(s), \quad i = 1, 2, \cdots, 16.$$

Then a lower bound $\underline{\theta}$ on θ^* can be obtained by finding the largest value of θ such that the Bounded Phase Condition is satisfied. Equivalently,

$$\underline{\theta} = \inf_{\theta \geq 0} \left\{ \theta \ : \ \sup_\omega \Phi_{\mathbf{\Delta}_V}(\omega, \theta) = 180^\circ \right\}.$$

Figure 10.14 shows the plot of the maximum phase difference over the vertices and over all ω in terms of θ. From this, we find that for $\underline{\theta} = 31.6273^\circ$ there exists ω that results in $\Phi_{\mathbf{\Delta}_V}(\omega, \theta) = 180^\circ$. Thus,

$$\underline{\theta} \approx 31.6273^\circ.$$

On the other hand, from the vertex systems we also get an upper bound $\bar{\theta} \approx 31.6273°$, which is the same as for $\underline{\theta}$, and hence $31.6273°$ is the true margin in this case.

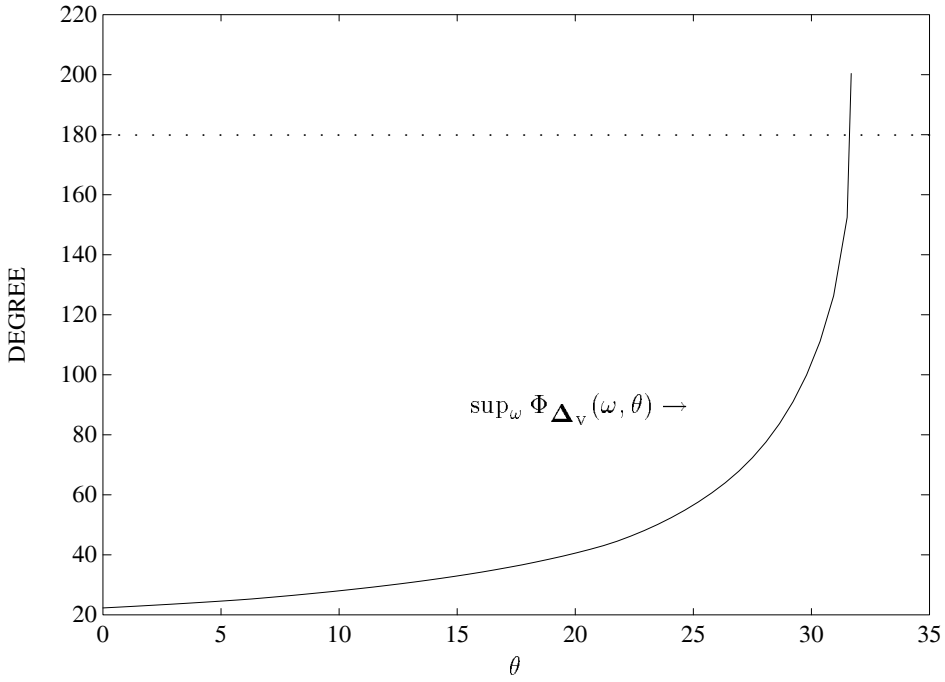

Figure 10.14. $\sup_\omega \Phi_{\mathbf{\Delta}_{\rm v}}(\omega, \theta)$ vs. θ (Example 10.5(b))

(c) To determine the worst case time delay margin T^*, we replace each vertex polynomial as follows:

$$V_i(s, T) = V_i^D(s) + e^{-j\omega T} V_i^N(s), \quad i = 1, 2, \cdots, 16.$$

A lower bound $\underline{T}$ on T^* is obtained by selecting the largest value of T such that the Bounded Phase Condition is satisfied. Equivalently,

$$\underline{T} = \inf_{T \geq 0} \left\{ T \ : \ \sup_{\omega} \Phi_{\mathbf{\Delta}_{\rm v}}(\omega, T) = 180° \right\}.$$

Figure 10.15 shows that at $T = 0.56$ there exists ω that results in $\Phi_{\mathbf{\Delta}_{\rm v}}(\omega, T) = 180°$. Thus we have

$$\underline{T} = 0.56 \ \text{ sec.}$$

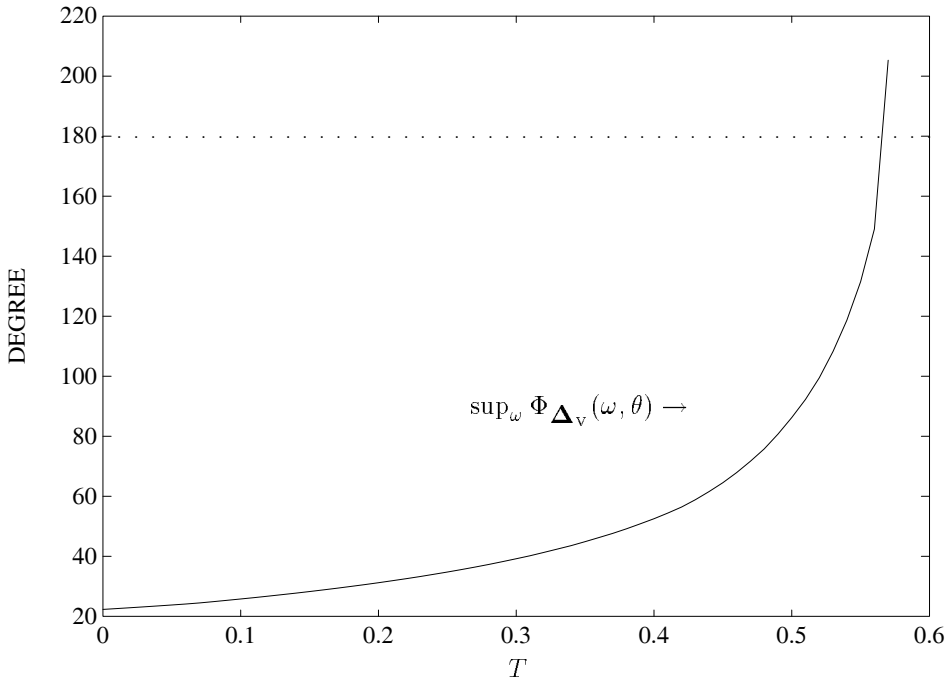

Figure 10.15. $\sup_\omega \Phi_{\mathbf{\Delta}_v}(\omega, \theta)$ vs. T (Example 10.5(c))

(d) To determine the worst case H_∞ stability margin, let us consider the case of additive perturbation where the H_∞ uncertainty block is connected around the two cascaded interval plants as shown in Figure 10.16.

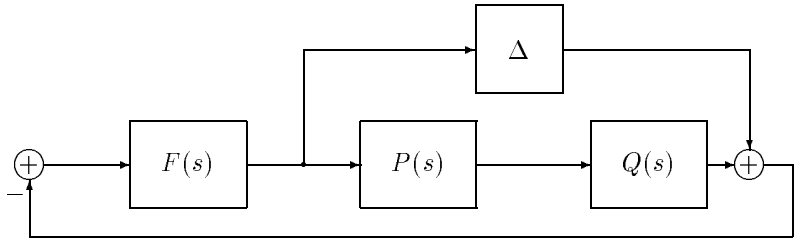

Figure 10.16. A multilinear interval system with H_∞ uncertainty (Example 10.5(d))

Then from

$$\left\| F(s)\left(1+F(s)P(s)Q(s)\right)^{-1}\right\|_{\infty} < \frac{1}{\beta},$$

we have the condition that

$$F_2(s)P_2(s)Q_2(s) + F_1(s)P_1(s)Q_1(s) + \beta e^{j\theta}F_1(s)P_2(s)Q_2(s)$$

$$= F_1(s)P_1(s)Q_1(s) + \left[1+\beta e^{j\theta}\frac{F_1(s)}{F_2(s)}\right]F_2(s)P_2(s)Q_2(s)$$

is Hurwitz for all $\theta \in [0, 2\pi)$ and $\mathbf{p} \in \mathbf{\Pi}$. Thus, the vertex polynomials can be written down as:

$$V_i(s,\beta,\theta) = V_i^N(s) + \left[1+\beta e^{j\theta}F(s)\right]V_i^D(s), \quad i = 1, 2, \cdots, 16.$$

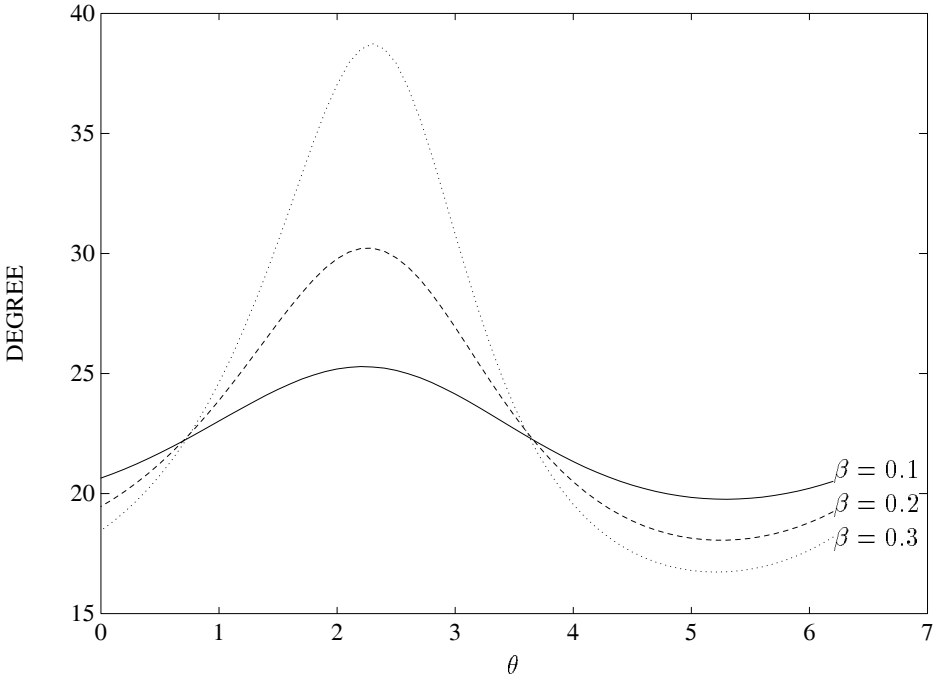

Figure 10.17. $\sup_\omega \Phi_{\mathbf{\Delta}_V}(\omega,\beta,\theta)$ vs. θ for $\beta = 0.1, 0.2, 0.3$. (Example 10.5(d))

A lower bound $\underline{\beta}$ on the worst case H_∞ stability margin β^* is obtained by selecting the largest positive value of β such that the Bounded Phase Condition

is satisfied for all $\theta \in [0, 2\pi)$. Equivalently,

$$\underline{\beta} = \inf_{\beta \geq 0} \left\{ \beta \ : \ \sup_{\theta} \sup_{\omega} \Phi_{\mathbf{\Delta}_{\mathrm{v}}}(\omega, \beta, \theta) = 180^{\circ} \right\}.$$

Figure 10.17 shows the maximum phase difference over the vertices and over all frequency for every fixed β. From Figure 10.18 we find that for any $\beta < 0.49$,

$$F_1(s)P_1(s)Q_1(s) + \left[1 + \beta e^{j\theta} \frac{F_1(s)}{F_2(s)}\right] F_2(s)P_2(s)Q_2(s)$$

is Hurwitz for all $\theta \in [0, 2\pi)$.

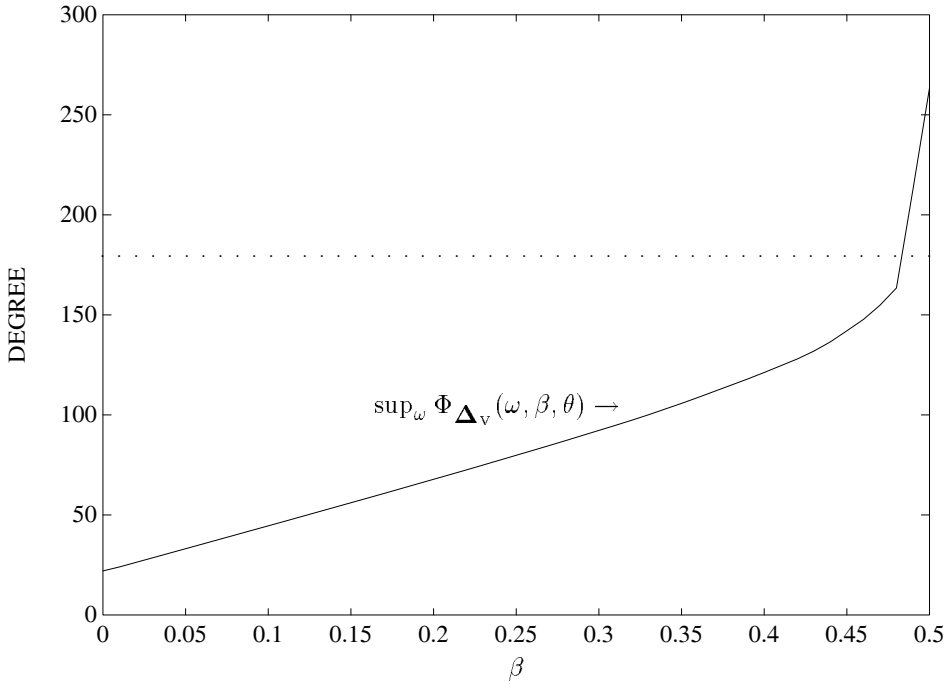

Figure 10.18. $\sup_{\omega} \Phi_{\mathbf{\Delta}_{\mathrm{v}}}(\omega, \beta, \theta)$ vs. β.(Example 10.5(d))

Thus, the lower bound on the worst case H_∞ stability margin is

$$\underline{\beta} \approx 0.49.$$

Now we can find an upper bound $\bar{\beta}$ by determining the H_∞ stability margins of the vertices and it turns out to be $\bar{\beta} \approx 0.49$. From these bounds we see that

$$\beta^* \approx 0.49.$$

Remark 10.1. Similar calculations can be used to estimate the size of the sector containing nonlinear gains for which a multilinear interval system remains absolutely stable. In other words, once we replace the multilinear family by the polytopic family $\bar{\mathbf{M}}(s)$, we may use the Lur'e, Popov or Circle Criterion to determine lower bounds on the size of the Robust Absolute Stability Sector. From the vertex systems we can find an upper bound on this sector. Exercise 10.1 deals with this type of problem.

Remark 10.2. Our definition of the multilinear interval system $\mathbf{M}(s)$ assumes that the numerator and denominator parameters $\mathbf{q}$ and $\mathbf{r}$ are independent. This restriction can be relaxed by replacing $M(s)$ by a linear fractional transformation $F(M(s))$ for all $M(s) \in \mathbf{M}(s)$. We simply construct the polytopic family $\bar{\mathbf{M}}(s)$ and replace the set $F(\mathbf{M}(s))$ by the set $F(\bar{\mathbf{M}}(s))$. From the image set bounding property of $\bar{\mathbf{M}}(s)$ and the fact that linear fractional transformations preserve boundaries it follows that at every point $s^* \in \mathbb{C}$:

$$F(\mathbf{M}(s^*)) \subset F(\bar{\mathbf{M}}(s^*)).$$

It is easy to see from the above that all the results and calculations derived in this chapter carry over to the set $F(\mathbf{M}(s))$. Since linear fractional transformations are a large class of transformations, this allows us to handle all sorts of dependencies in a convenient way. This is explored in Exercise 10.2.

10.6 EXERCISES

10.1 For the system given in Example 10.5, estimate the size of the sector containing nonlinear gains for which the entire multilinear family of closed loop systems remains robustly absolutely stable. Estimate the sectors using respectively the

a) Lur'e criterion

b) Popov criterion

c) Circle criterion.

10.2 In the feedback system shown below in Figure 10.19.
Let

$$G(s) = \frac{s+\alpha}{s+\beta}, \qquad C_1(s) = \frac{s+2}{s+3}, \qquad C_3(s) = \frac{2}{s+4}$$

with the nominal values $\alpha^0 = 1$, $\beta^0 = -5$.

a) Find a controller $C_2(s)$ that stabilizes the nominal closed loop system.

b) With the controller obtained in a), let $\alpha \in [1-\epsilon, 1+\epsilon]$ and $\beta \in [-5-\epsilon. -5+\epsilon]$. Find the maximum value of ϵ for which the closed loop system remains robustly stable.

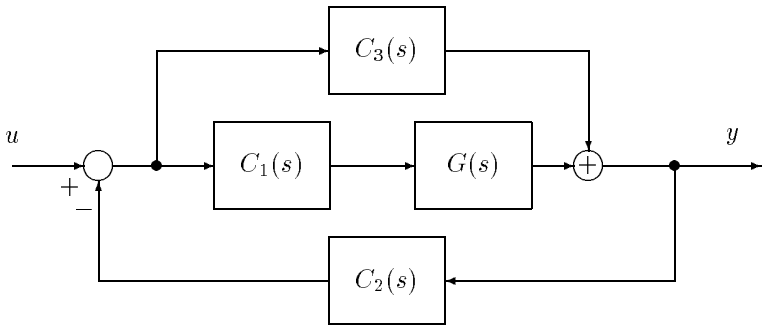

Figure 10.19. Feedback system (Exercise 10.2)

10.3 Consider the feedback system shown in Figure 10.20.

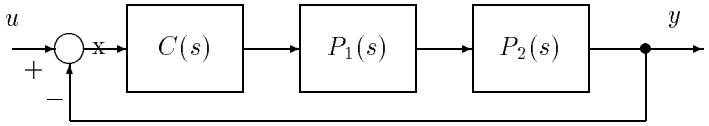

Figure 10.20. Feedback system (Exercise 10.3)

Let

$$C(s) = \frac{1}{s+1}, \quad P_1(s) = \frac{p_0}{s+q_0}, \quad P_2(s) = \frac{p_1}{s+q_1}$$

and let the parameters range over

$$q_0 \in [0.5, 1.5], \quad p_0 \in [0.5, 1.5], \quad q_1 \in [1.5, 2.5], \quad p_1 \in [0.5, 1.5].$$

a) Verify that the closed loop system is robustly stable.

b) Construct the polytopic system $\bar{\mathbf{M}}(s)$.

c) Using the polytopic system $\bar{\mathbf{M}}(s)$, estimate the maximum guaranteed gain margin measured at the loop breaking point "x".

d) Likewise estimate the maximum guaranteed phase margin at "x".

10.4 In the the feedback system of Exercise 10.3, suppose we want to expand the range of allowable parameter variations by letting the parameters vary as

$$q_0 \in [0.5 - \epsilon, 1.5 + \epsilon], \quad p_0 \in [0.5 - \epsilon, 1.5 + \epsilon],$$

$$q_1 \in [1.5 - \epsilon, 2.5 + \epsilon], \quad p_1 \in [0.5 - \epsilon, 1.5 + \epsilon].$$

What is the maximum value of ϵ for which the polytopic system $\bar{\mathbf{M}}(s)$ does not lose robust stability?

10.5 Suppose that unstructured additive uncertainty is introduced into the system in Exercise 10.3 as shown in Figure 10.21:

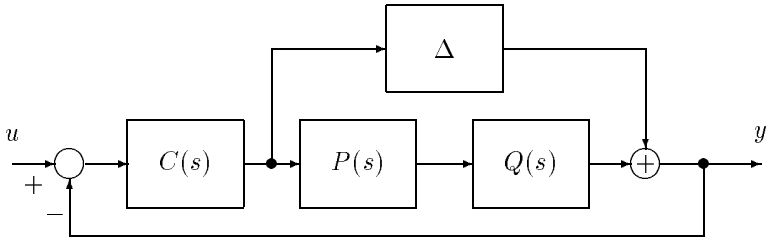

Figure 10.21. Feedback system with additive H_∞ uncertainty (Exercise 10.5)

Estimate the maximum additive H_∞ uncertainty that the closed loop system can tolerate, by using the polytopic system $\bar{\mathbf{M}}(s)$.

10.6 Suppose that unstructured perturbation is applied to the system in Exercise 10.3 in a multiplicative form as shown below in Figure 10.22.

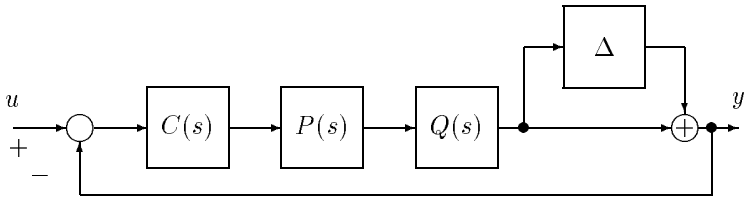

Figure 10.22. Feedback system with multiplicative H_∞ uncertainty (Exercise 10.6)

Find the maximum multiplicative H_∞ stability margin possessed by the closed loop system.

10.7 Suppose that a time-delay block, e^{-sT} is inserted at "x" in the feedback system of Exercise 10.3 (see Figure 10.20). Find a lower bound in the the time-delay that can be robustly tolerated by the closed loop system, using the polytopic system $\bar{\mathbf{M}}(s)$.

10.8 Consider the feedback system shown below in Figure 10.23.

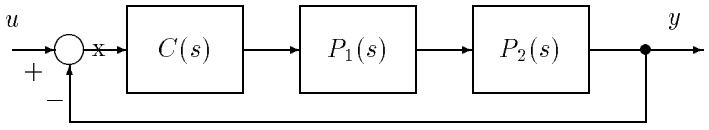

Figure 10.23. Feedback system (Exercise 10.8)

Let

$$C(s) = \frac{1}{s+1}, \qquad P_1(s) = \frac{s+\beta_0}{\alpha_1 s + \alpha_0}, \qquad P_2(s) = \frac{s+\delta_0}{\gamma_1 s + \gamma_0}.$$

and

$$\begin{aligned} &\alpha_1 \in [1,2], \quad \beta_0 \in [1,2], \quad \gamma_1 \in [1,5] \\ &\alpha_0 \in [1,2], \quad \delta_0 \in [1,3], \quad \gamma_0 \in [6,10]. \end{aligned}$$

a) Verify that the closed loop system is robustly stable.

b) Construct the polytopic system $\bar{\mathbf{M}}(s)$.

c) Using the polytopic system $\bar{\mathbf{M}}(s)$, find the maximum guaranteed gain margin measured at the loop breaking point "x".

d) Similarly estimate the maximum guaranteed phase margin measured at the point "x".

10.9 In the the feedback system of Exercise 10.8, suppose we want to expand the range of allowable parameter variations by letting the parameters vary as

$$\alpha_1 \in [1-\epsilon, 2+\epsilon], \quad \beta_0 \in [1-\epsilon, 2+\epsilon], \quad \gamma_1 \in [1-\epsilon, 5+\epsilon],$$

$$\alpha_0 \in [1-\epsilon, 2+\epsilon], \quad \delta_0 \in [1-\epsilon, 3+\epsilon], \quad \gamma_0 \in [6-\epsilon, 10+\epsilon].$$

Calculate the maximum value of ϵ for which the polytopic system $\bar{\mathbf{M}}(s)$ remains robustly stable?

10.10 Consider the feedback system shown below (Figure 10.24):
Let

$$C(s) = 2, \qquad P_1(s) = \frac{s+\beta_0}{s^2 + \alpha_1 s + \alpha_0}, \qquad P_2(s) = -\frac{s+\delta_0}{s+\gamma_0}$$

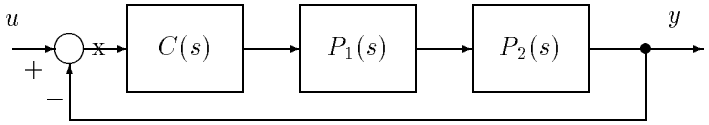

Figure 10.24. Feedback system (Exercise 10.10)

with

$$\alpha_1 \in [3,6], \quad \alpha_0 \in [1,2], \quad \delta_0 \in [1,2]$$
$$\gamma_0 \in [4,6], \quad \beta_0 \in [3,5].$$

a) Check whether the closed loop system is robustly stable.

b) Construct the polytopic system $\bar{\mathbf{M}}(s)$.

c) Using the polytopic system $\bar{\mathbf{M}}(s)$, estimate the maximum guaranteed gain margin at the loop breaking point "x".

d) Estimate the maximum guaranteed phase margin at "x".

10.11 In the the feedback system of Exercise 10.10, suppose we want to expand the range of allowable parameter variations by letting the parameters vary as

$$\alpha_1 \in [3-\epsilon, 6+\epsilon], \quad \alpha_0 \in [1-\epsilon, 2+\epsilon], \quad \delta_0 \in [1-\epsilon, 2+\epsilon],$$
$$\gamma_0 \in [4-\epsilon, 6+\epsilon], \quad \beta_0 \in [3-\epsilon, 5+\epsilon].$$

Evaluate the maximum value of ϵ for which the polytopic system $\bar{\mathbf{M}}(s)$ remains robustly stable?

10.7 NOTES AND REFERENCES

The Mapping Theorem was stated and proved in the 1963 book of Zadeh and Desoer [243]. It was effectively used in parametric stability margin calculations by deGaston and Safonov [80] and Sideris and Sanchez-Pena [210]. The mixed uncertainty stability margin calculations given in Section 10.3 were developed by Keel and Bhattacharyya [133, 134].

Vicino, Tesi and Milanese [230] gave an algorithm for calculating parametric stability margins in the case of nonlinearly correlated parameter dependence. In Hollot and Xu [118], Polyak [190] and Anderson, Kraus, Mansour and Dasgupta [10] conditions under which the image set of a multilinear interval polynomial reduces to a polygon are investigated.

Chapter 11

FREQUENCY DOMAIN PROPERTIES OF MULTILINEAR INTERVAL SYSTEMS

In this chapter we continue our development of the theory of robustness under multilinear interval uncertainty. We consider the robust Hurwitz stability and performance of control systems which contain transfer functions that are ratios of multilinear interval polynomials. The characteristic polynomial of such a system is a multilinear interval polynomial. We extend the Generalized Kharitonov Theorem (Chapter 7) to this case. This extension provides a set of extremal manifolds which serve as a reduced test set for robust stability. These manifolds are the multilinear counterpart of the extremal segments derived for the linear case and possess the same optimality and boundary generating properties. In particular, they can be used, in conjunction with the polytopic approximation based on the Mapping Theorem derived in Chapter 10, to generate frequency domain templates, Bode and Nyquist envelopes, to calculate worst case stability margins and to determine the robust performance of control systems under mixed parametric/unstructured uncertainty in a computationally efficient manner.

11.1 INTRODUCTION

Consider the feedback configuration shown in Figure 11.1. $F(s)$ is a fixed controller and $G_1(s)$ and $G_2(s)$ are independent subsystems containing parameter uncertainty. Let

$$F(s) := \frac{F_1(s)}{F_2(s)}, \quad G_1(s) := \frac{P_{11}(s)}{P_{21}(s)}, \quad G_2(s) := \frac{P_{12}(s)}{P_{22}(s)}. \tag{11.1}$$

If the subsystems $G_1(s)$ and $G_2(s)$ contain independent parameters it is reasonable to model them as *interval* or *linear interval* systems $\mathbf{G}_i(s)$, $i = 1, 2$. The

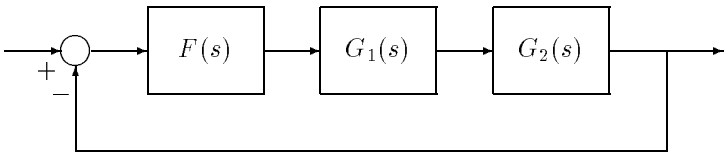

Figure 11.1. Interconnected Feedback System

characteristic polynomial of this feedback system is:

$$\delta(s) := F_1(s)P_{11}(s)P_{12}(s) + F_2(s)P_{21}(s)P_{22}(s). \tag{11.2}$$

The open loop transfer function

$$T^o(s) = F(s)G_1(s)G_2(s) = \frac{F_1(s)P_{11}(s)P_{12}(s)}{F_2(s)P_{21}(s)P_{22}(s)}$$

and the closed loop transfer function

$$\begin{aligned} T^c(s) &= \frac{F(s)G_1(s)G_2(s)}{1 + F(s)G_1(s)G_2(s)} \\ &= \frac{F_1(s)P_{11}(s)P_{12}(s)}{F_1(s)P_{11}(s)P_{12}(s) + F_2(s)P_{21}(s)P_{22}(s)}. \end{aligned}$$

These transfer functions have numerator and denominator polynomials that are multilinear functions of interval polynomials. In addition, the numerator and denominator in $T^o(s)$ have independent interval polynomials (parameters), but in $T^c(s)$ the numerator and denominator contain *common* interval polynomials.

For this class of systems we are interested in the following types of questions:

1) Does $F(s)$ robustly stabilize the system or not?

2) If $F(s)$ does robustly stabilize the system, what are the worst case gain margin, phase margin, parametric stability margin, H_∞ stability margin and performance measured in terms of H_∞ norms, as the parameters range over the uncertainty set?

3) How can one construct the Bode magnitude and phase, and Nyquist plots of various transfer function sets such as $T^o(s)$ and $T^c(s)$ generated by the uncertain parameters?

These questions were addressed in the previous chapter for an arbitrary stability region using the Mapping Theorem as a computational tool. In this chapter, we focus on the case of Hurwitz stability and show how the Generalized Kharitonov Theorem (GKT) derived in Chapter 7 can be extended to this multilinear case to

provide a great deal of simplification and computational efficiency. We first derive a multilinear version of GKT. This generalization provides us with an extremal test set for multilinear interval systems, with drastically reduced dimension of the parameter space, from which all the above questions can be answered. It will tell us, essentially that as long as the dependencies are multilinear, worst case stability margins and performance can be calculated for an arbitrary control system containing interval subsystems by replacing each interval subsystem $\mathbf{G}^i(s)$ by the corresponding extremal set of systems $\mathbf{G}^i_{\mathrm{E}}(s)$. The polytopic approximation derived in the last chapter can then be used on this extremal set to give a highly efficient computational solution to the design and analysis questions posed above. In the next section we describe the extension of GKT to the multilinear case.

11.2 MULTILINEAR INTERVAL POLYNOMIALS

To avoid notational complexity, we first consider the simplest multilinear polynomial form motivated by (11.2). We consider the Hurwitz stability of the characteristic polynomial family of the form

$$\delta(s) := F_1(s)P_{11}(s)P_{12}(s) + F_2(s)P_{21}(s)P_{22}(s) \tag{11.3}$$

where $F_i(s)$ are fixed real polynomials and $P_{ij}(s)$ are real interval polynomials with *independently* varying parameters. Let $\mathbf{p}$ denote the ordered set of coefficients of the polynomials $\{P_{11}(s), P_{12}(s)P_{21},(s)P_{22}(s)\}$. We assume that each coefficient varies in an independent interval, or equivalently that $\mathbf{p}$ varies in an axis-parallel box $\mathbf{\Pi}$. The dimension of the parameter space here is equal to the number of independently varying parameters contained in these polynomials. Referring to the notation used in Chapter 7 we let $\mathbf{P}_{ij}(s)$ denote the interval polynomial family and $\mathcal{K}_{ij}(s)$ and $\mathcal{S}_{ij}(s)$ denote the respective Kharitonov polynomials and Kharitonov segments (refer to Chapter 7 for the definition of these segments). The family of uncertain polynomials is represented, using the notation of Chapter 7, as

$$\mathbf{\Delta}(s) := F_1(s)\mathbf{P}_{11}(s)\mathbf{P}_{12}(s) + F_1(s)\mathbf{P}_{21}(s)\mathbf{P}_{22}(s). \tag{11.4}$$

Define

$$\mathbf{\Delta}^1_{\mathrm{E}}(s) := F_1(s)\mathcal{S}_{11}(s)\mathcal{S}_{12}(s) + F_2(s)\mathcal{K}_{21}(s)\mathcal{K}_{22}(s)$$
$$\mathbf{\Delta}^2_{\mathrm{E}}(s) := F_1(s)\mathcal{K}_{11}(s)\mathcal{K}_{12}(s) + F_2(s)\mathcal{S}_{21}(s)\mathcal{S}_{22}(s)$$

and introduce the extremal manifolds

$$\mathbf{\Delta}_{\mathrm{E}}(s) := \mathbf{\Delta}^1_{\mathrm{E}}(s) \cup \mathbf{\Delta}^2_{\mathrm{E}}(s). \tag{11.5}$$

Lemma 11.1 *Under the assumption that every polynomial in $\mathbf{\Delta}(s)$ is of the same degree and the parameters (coefficients) in the interval polynomials $\mathbf{P}_{11}(s)$, $\mathbf{P}_{12}(s)$, $\mathbf{P}_{21}(s)$, $\mathbf{P}_{22}(s)$ are independent, $\mathbf{\Delta}(s)$ is Hurwitz stable if and only if $\mathbf{\Delta}_{\mathrm{E}}(s)$ is Hurwitz stable.*

Proof. The proof consists of recursive application of the Generalized Kharitonov Theorem (GKT) in Chapter 7. From GKT, $\mathbf{\Delta}(s)$ is stable if and only if the following families:

$$F_1(s)\mathcal{S}_{11}(s)P_{12}(s) + F_2(s)\mathcal{K}_{21}(s)P_{22}(s) \tag{11.6}$$

and

$$F_1(s)\mathcal{K}_{11}(s)P_{12}(s) + F_2(s)\mathcal{S}_{21}(s)P_{22}(s) \tag{11.7}$$

are stable for each polynomial $P_{12}(s) \in \mathbf{P}_{12}(s)$ and $P_{22}(s) \in \mathbf{P}_{22}(s)$. Since each expression in (11.6) and (11.7) is linear in $P_{12}(s)$ and $P_{22}(s)$, we can apply GKT again to each such family and conclude that the stability of the family (11.6) is equivalent to the stability of the families of polynomials

$$F_1(s)\mathcal{S}_{11}(s)\mathcal{S}_{12}(s) + F_2(s)\mathcal{K}_{21}(s)\mathcal{K}_{22}(s) \tag{11.8}$$

$$F_1(s)\mathcal{S}_{11}(s)\mathcal{K}_{12}(s) + F_2(s)\mathcal{K}_{21}(s)\mathcal{S}_{22}(s) \tag{11.9}$$

and the stability of the family (11.7) is equivalent to the stability of the families

$$F_1(s)\mathcal{K}_{11}(s)\mathcal{K}_{12}(s) + F_2(s)\mathcal{S}_{21}(s)\mathcal{S}_{22}(s) \tag{11.10}$$

$$F_1(s)\mathcal{K}_{11}(s)\mathcal{S}_{12}(s) + F_2(s)\mathcal{S}_{21}(s)\mathcal{K}_{22}(s). \tag{11.11}$$

We note that each element of the families of polynomials in (11.9) and (11.11) is a polytope of polynomials. Therefore, by the Edge Theorem in Chapter 6, the stability of each such polytope is equivalent to the stability of its exposed edges. Since the segment polynomials are convex combinations of Kharitonov polynomials, we see that these exposed edges are contained in the families (11.8) and (11.10). Therefore, the theorem holds. ♣

For the general case, we have the *multilinear interval polynomial*

$$\mathbf{\Delta}(s) = F_1(s)\mathbf{P}_{11}(s)\cdots\mathbf{P}_{1r_1}(s) + \cdots + F_m(s)\mathbf{P}_{m1}(s)\cdots\mathbf{P}_{mr_m}(s) \tag{11.12}$$

where $F_i(s)$ are fixed and $P_{ij}(s)$ are interval polynomial families. The arguments used in the earlier case carry over to this case and the result will be presented without repeating the proof. We define

$$\begin{aligned}\mathbf{\Delta}^l_{\mathrm{E}}(s) := {} & F_1(s)\mathcal{K}_{11}(s)\cdots\mathcal{K}_{1r_1}(s) + \cdots + F_{l-1}(s)\mathcal{K}_{l-1,1}(s)\cdots\mathcal{K}_{l-1,r_{l-1}}(s) \\ & + F_l(s)\mathcal{S}_{l,1}(s)\cdots\mathcal{S}_{l,r_l}(s) + F_{l+1}\mathcal{K}_{l+1,1}(s)\cdots\mathcal{K}_{l+1,r_{l+1}} \\ & + \cdots + F_m(s)\mathcal{K}_{m,1}(s)\cdots\mathcal{K}_{m,r_m}(s)\end{aligned} \tag{11.13}$$

and introduce the *extremal manifolds*

$$\mathbf{\Delta}_{\mathrm{E}}(s) := \cup_{l=1}^{m}\mathbf{\Delta}^l_{\mathrm{E}}(s). \tag{11.14}$$

Theorem 11.1 *Under the assumption that every polynomial in $\mathbf{\Delta}(s)$ is of the same degree and the parameters (coefficients) in the interval polynomials $\mathbf{P}_{ij}(s)$ are independent, $\mathbf{\Delta}(s)$ is Hurwitz stable if and only if $\mathbf{\Delta}_{\mathrm{E}}(s)$ is Hurwitz stable.*

Remark 11.1. The theorem is also valid when some of the polynomials $F_i(s)$ are complex or quasipolynomials This follows from the corresponding fact that GKT (Chapter 7) holds when some of the fixed polynomials $F_i(s)$ are replaced by complex polynomials or quasipolynomials.

The next example illustrates the construction of the set of manifolds.

Example 11.1. (Extremal Manifolds for Multilinear Systems) Consider the characteristic polynomial

$$\delta(s) = F_1(s)P_{11}(s)P_{12}(s) + F_2(s)P_{21}(s)P_{22}(s)$$

where the fixed polynomials $F_1(s)$ are

$$F_1(s) = s + f_1, \qquad F_2(s) = s + f_2$$

and the interval polynomials are

$$\begin{aligned} P_{11}(s) &= a_2 s^2 + a_1 s + a_0, & P_{12}(s) &= b_2 s^2 + b_1 s + b_0, \\ P_{21}(s) &= c_2 s^2 + c_1 s + c_0, & P_{22}(s) &= d_2 s^2 + d_1 s + d_0, \end{aligned}$$

with all coefficients varying independently. The Kharitonov polynomials corresponding to $P_{11}(s)$, $P_{12}(s)$, $P_{21}(s)$ and $P_{22}(s)$ are:

$$\begin{aligned} K^1_{P_{11}}(s) &= a_2^+ s^2 + a_1^- s + a_0^-, & K^2_{P_{11}}(s) &= a_2^+ s^2 + a_1^+ s + a_0^-, \\ K^3_{P_{11}}(s) &= a_2^- s^2 + a_1^- s + a_0^+, & K^4_{P_{11}}(s) &= a_2^- s^2 + a_1^+ s + a_0^+, \\ K^1_{P_{12}}(s) &= b_2^+ s^2 + b_1^- s + b_0^-, & K^2_{P_{12}}(s) &= b_2^+ s^2 + b_1^+ s + b_0^-, \\ K^3_{P_{12}}(s) &= b_2^- s^2 + b_1^- s + b_0^+, & K^4_{P_{12}}(s) &= b_2^- s^2 + b_1^+ s + b_0^+, \\ K^1_{P_{21}}(s) &= c_2^+ s^2 + c_1^- s + c_0^-, & K^2_{P_{21}}(s) &= c_2^+ s^2 + c_1^+ s + c_0^-, \\ K^3_{P_{21}}(s) &= c_2^- s^2 + c_1^- s + a_0^+, & K^4_{P_{21}}(s) &= c_2^- s^2 + c_1^+ s + c_0^+, \\ K^1_{P_{22}}(s) &= d_2^+ s^2 + d_1^- s + d_0^-, & K^2_{P_{22}}(s) &= d_2^+ s^2 + d_1^+ s + d_0^-, \\ K^3_{P_{22}}(s) &= d_2^- s^2 + d_1^- s + d_0^+, & K^4_{P_{22}}(s) &= d_2^- s^2 + d_1^+ s + d_0^+. \end{aligned}$$

The sets of segments joining appropriate pairs of Kharitonov polynomials can also be obtained. Here we give only the segments corresponding to the interval polynomial $P_{11}(s)$; others can be similarly obtained.

$$\begin{aligned} S^1_{P_{11}}(s) &= \lambda K^1_{P_{11}}(s) + (1-\lambda) K^2_{P_{11}}(s) \\ S^2_{P_{11}}(s) &= \lambda K^1_{P_{11}}(s) + (1-\lambda) K^3_{P_{11}}(s) \\ S^3_{P_{11}}(s) &= \lambda K^2_{P_{11}}(s) + (1-\lambda) K^4_{P_{11}}(s) \\ S^4_{P_{11}}(s) &= \lambda K^3_{P_{11}}(s) + (1-\lambda) K^4_{P_{11}}(s). \end{aligned}$$

From the above, we now can write the manifolds:

$$\mathbf{\Delta}_1(s) = \left\{ F_1(s)K^i_{P_{11}}(s)K^j_{P_{12}}(s) + F_2(s)S^k_{P_{21}}(s)S^l_{P_{22}}(s) : (i,j,k,l) \in \underline{4} \times \underline{4} \times \underline{4} \times \underline{4} \right\}$$
$$\mathbf{\Delta}_2(s) = \left\{ F_1(s)S^i_{P_{11}}(s)S^j_{P_{12}}(s) + F_2(s)K^k_{P_{21}}(s)K^l_{P_{22}}(s) : (i,j,k,l) \in \underline{4} \times \underline{4} \times \underline{4} \times \underline{4} \right\}$$

and

$$\mathbf{\Delta}_{\mathrm{E}}(s) = \mathbf{\Delta}_1 \cup \mathbf{\Delta}_2.$$

As we can see, the total parameter space is of dimension 12. However, our problem is now reduced to checking the stability of 512 two-dimensional manifolds. Notice that each manifold remains of dimension two, even though the dimension of the parameter space can be increased arbitrarily. The dimension of the manifolds is increased only if the number of interval polynomials in a product term is increased.

11.2.1 Dependencies Between the Perturbations

The theorem is stated assuming that the polynomials $P_{ij}(s)$ perturb independently. In an interconnected multiloop control system, it will in general happen that some of the polynomials $P_{ij}(s)$ are in fact identical (see, for example, Exercise 11.1). Such dependencies can be easily handled. To avoid introducing cumbersome notation we illustrate the procedure with an example.

Consider the following multilinear interval polynomial family with dependencies between the perturbations:

$$\delta(s,\mathbf{p}) := F_1(s)P_{11}(s)P_{12}(s) + F_2(s)P_{21}(s)P_{22}(s) + F_3(s)P_{31}(s)P_{32}(s)$$

where $P_{11}(s) = P_{21}(s)$ and $P_{22}(s) = P_{32}(s)$ and each polynomial $P_{ij}(s)$ is interval. If we rewrite embedding the above constraints, we have

$$\delta(s,\mathbf{p}) = F_1(s)P_{11}(s)P_{12}(s) + F_2(s)P_{11}(s)P_{22}(s) + F_3(s)P_{31}(s)P_{22}(s). \tag{11.15}$$

Let us first fix $P_{11}(s)$ and $P_{31}(s)$ and apply GKT. This tells us that the Hurwitz stability of the set $\mathbf{\Delta}(s)$ is equivalent to stability of the sets

$$\mathbf{I}_1(s) = \{F_1(s)P_{11}(s)\mathcal{S}_{12}(s) + (F_2(s)P_{11}(s) + F_3(s)P_{31}(s))\mathcal{K}_{22}(s)\}$$
$$\mathbf{I}_2(s) = \{F_1(s)P_{11}(s)\mathcal{K}_{12}(s) + (F_2(s)P_{11}(s) + F_3(s)P_{31}(s))\mathcal{S}_{22}(s)\}$$

for each $(P_{11}(s), P_{31}(s)) \in \mathbf{P}_{11}(s) \times \mathbf{P}_{31}(s)$. We now apply GKT again to each of the sets $\mathbf{I}_1(s)$ and $\mathbf{I}_2(s)$ letting $P_{11}(s)$ and $P_{31}(s)$ now vary. This leads to the condition that the robust stability of $\mathbf{\Delta}(s)$ is equivalent to robust stability of the manifolds:

$$\mathbf{\Delta}_1(s) = \{\delta(s,\mathbf{p}) : P_{11} \in \mathcal{S}_{11},\ P_{12} \in \mathcal{S}_{12},\ P_{22} \in \mathcal{K}_{22},\ P_{31} \in \mathcal{K}_{31}\}$$
$$\mathbf{\Delta}_2(s) = \{\delta(s,\mathbf{p}) : P_{11} \in \mathcal{S}_{11},\ P_{12} \in \mathcal{K}_{12},\ P_{22} \in \mathcal{S}_{22},\ P_{31} \in \mathcal{K}_{31}\}$$
$$\mathbf{\Delta}_3(s) = \{\delta(s,\mathbf{p}) : P_{11} \in \mathcal{K}_{11},\ P_{12} \in \mathcal{S}_{12},\ P_{22} \in \mathcal{K}_{22},\ P_{31} \in \mathcal{S}_{31}\}$$
$$\mathbf{\Delta}_4(s) = \{\delta(s,\mathbf{p}) : P_{11} \in \mathcal{K}_{11},\ P_{12} \in \mathcal{K}_{12},\ P_{22} \in \mathcal{S}_{22},\ P_{31} \in \mathcal{S}_{31}\}.$$

Since $\mathbf{\Delta}_3(s)$ is a polytope, we now can apply the Edge Theorem (Chapter 6) to conclude that this is stable if and only if its exposed edges are. These exposed edges are

$$\{\delta(s,\mathbf{p}) : P_{11} \in \mathcal{K}_{11},\ P_{12} \in \mathcal{S}_{12},\ P_{22} \in \mathcal{K}_{22},\ P_{31} \in \mathcal{K}_{31}\} \tag{11.16}$$

$$\{\delta(s,\mathbf{p}) : P_{11} \in \mathcal{K}_{11},\ P_{12} \in \mathcal{K}_{12},\ P_{22} \in \mathcal{K}_{22},\ P_{31} \in \mathcal{S}_{31}\}. \tag{11.17}$$

It is easy to see that the manifolds (11.16) and (11.17) are contained in $\mathbf{\Delta}_1(s)$ and $\mathbf{\Delta}_4(s)$ respectively. Therefore the set of manifolds that finally need to be checked is

$$\mathbf{\Delta}_{\mathrm{E}}(s) := \mathbf{\Delta}_1(s) \cup \mathbf{\Delta}_2(s) \cup \mathbf{\Delta}_4(s). \tag{11.18}$$

Interval Polynomial Matrix

An important special case of dependent perturbations is that of interval polynomial matrices. Let $M(s)$ be an $n \times n$ polynomial matrix whose ij^{th} entry is the polynomial $P_{ij}(s)$. The characteristic polynomial associated with this matrix is $\det[M(s)]$. We assume that each $P_{ij}(s)$ belongs to an interval family $\mathbf{P}_{ij}(s)$ and the parameters of each $P_{ij}(s)$ are independent of all others. Let $\mathbf{M}(s)$ denote the corresponding set of matrices. We will say that the set is stable if $\det[M(s)]$ is Hurwitz stable for every $M(s) \in \mathbf{M}(s)$. To test Hurwitz stability of the family of characteristic polynomials so obtained we have the following result. Let $\mathbf{T}$ be the set of $n \times n$ permutation matrices obtained from the identity matrix. Corresponding to each $T \in \mathbf{T}$, introduce the set of polynomial matrices $M_T(s)$ where $P_{ij}(s)$ ranges over $\mathcal{K}_{ij}(s)$ if the ij^{th} entry of T is 0 and $P_{ij}(s)$ ranges over $\mathcal{S}_{ij}(s)$ if the ij^{th} entry of T is 1. Let $\mathbf{M}^*(s)$ denote the collection of matrices $M_T(s)$ obtained by letting T range over all permutation matrices $\mathbf{T}$.

Theorem 11.2 *$\mathbf{M}(s)$ is Hurwitz stable if and only if $\mathbf{M}^*(s)$ is Hurwitz stable.*

Proof. Consider the case $n = 3$.

$$M(s) := \begin{bmatrix} P_{11}(s) & P_{12}(s) & P_{13}(s) \\ P_{21}(s) & P_{22}(s) & P_{23}(s) \\ P_{31}(s) & P_{32}(s) & P_{33}(s) \end{bmatrix}.$$

Then

$$\begin{aligned} \det[M(s)] \ :=\ & P_{11}(s)P_{22}(s)P_{33}(s) + P_{12}(s)P_{23}(s)P_{31}(s) + P_{21}(s)P_{32}(s)P_{13}(s) \\ & - P_{13}(s)P_{22}(s)P_{31}(s) - P_{12}(s)P_{21}(s)P_{33}(s) - P_{11}(s)P_{23}(s)P_{32}(s). \end{aligned}$$

We see that we have a multilinear interval polynomial with dependencies. We can apply GKT recursively as we did in the previous example. We omit the detailed derivation. The final result is that the following six sets of manifolds need to be checked in order to determine the stability of the set:

$$\mathbf{\Delta}_1(s) := \{\det[M(s)] : P_{11} \in \mathcal{S}_{11},\ P_{22} \in \mathcal{S}_{22},\ P_{33} \in \mathcal{S}_{33},\ P_{12} \in \mathcal{K}_{12},$$

$$
\begin{aligned}
&P_{23} \in \mathcal{K}_{23},\ P_{31} \in \mathcal{K}_{31},\ P_{21} \in \mathcal{K}_{21},\ P_{32} \in \mathcal{K}_{32},\ P_{13} \in \mathcal{K}_{13}\} \\
\mathbf{\Delta}_2(s) := \{\det[M(s)] : &P_{11} \in \mathcal{S}_{11},\ P_{22} \in \mathcal{K}_{22},\ P_{33} \in \mathcal{K}_{33},\ P_{12} \in \mathcal{K}_{12}, \\
&P_{23} \in \mathcal{S}_{23},\ P_{31} \in \mathcal{K}_{31},\ P_{21} \in \mathcal{K}_{21},\ P_{32} \in \mathcal{S}_{32},\ P_{13} \in \mathcal{K}_{13}\} \\
\mathbf{\Delta}_3(s) := \{\det[M(s)] : &P_{11} \in \mathcal{K}_{11},\ P_{22} \in \mathcal{K}_{22},\ P_{33} \in \mathcal{S}_{33},\ P_{12} \in \mathcal{S}_{12}, \\
&P_{23} \in \mathcal{K}_{23},\ P_{31} \in \mathcal{K}_{31},\ P_{21} \in \mathcal{S}_{21},\ P_{32} \in \mathcal{K}_{32},\ P_{13} \in \mathcal{K}_{13}\} \\
\mathbf{\Delta}_4(s) := \{\det[M(s)] : &P_{11} \in \mathcal{K}_{11},\ P_{22} \in \mathcal{S}_{22},\ P_{33} \in \mathcal{K}_{33},\ P_{12} \in \mathcal{K}_{12}, \\
&P_{23} \in \mathcal{K}_{23},\ P_{31} \in \mathcal{S}_{31},\ P_{21} \in \mathcal{K}_{21}, P_{32} \in \mathcal{K}_{32},\ P_{13} \in \mathcal{S}_{13}\} \\
\mathbf{\Delta}_5(s) := \{\det[M(s)] : &P_{11} \in \mathcal{K}_{11},\ P_{22} \in \mathcal{K}_{22},\ P_{33} \in \mathcal{K}_{33},\ P_{12} \in \mathcal{K}_{12}, \\
&P_{23} \in \mathcal{K}_{23},\ P_{31} \in \mathcal{K}_{31},\ P_{21} \in \mathcal{S}_{21},\ P_{32} \in \mathcal{S}_{32},\ P_{13} \in \mathcal{S}_{13}\} \\
\mathbf{\Delta}_6(s) := \{\det[M(s)] : &P_{11} \in \mathcal{K}_{11},\ P_{22} \in \mathcal{K}_{22},\ P_{33} \in \mathcal{K}_{33},\ P_{12} \in \mathcal{S}_{12}, \\
&P_{23} \in \mathcal{S}_{23},\ P_{31} \in \mathcal{S}_{31},\ P_{21} \in \mathcal{K}_{21},\ P_{32} \in \mathcal{K}_{32},\ P_{13} \in \mathcal{K}_{13}\}\,.
\end{aligned}
$$

The reader can verify that the above expressions for the characteristic polynomials correspond to the family $\mathbf{M}^*(s)$ in this case. The result for arbitrary n is proved similarly. ♣

Boundary Generating Property of the Extremal Manifolds

We have established that Hurwitz stability of the family $\mathbf{\Delta}(s)$ is equivalent to the stability of the manifolds $\mathbf{\Delta}_{\mathrm{E}}(s)$. This equivalence also follows from the following boundary result relating the image sets $\mathbf{\Delta}(j\omega)$ and $\mathbf{\Delta}_{\mathrm{E}}(j\omega)$.

Theorem 11.3

$$
\partial\mathbf{\Delta}(j\omega) \subset \mathbf{\Delta}_{\mathrm{E}}(j\omega) \tag{11.19}
$$

Proof. The set $\mathbf{\Delta}(s)$ is a multilinear function of interval polynomials $\mathbf{P}_{ij}(s)$. The boundaries of the sum and product of two complex plane sets $\mathcal{Z}_i$ and $\mathcal{Z}_j$ $(i \neq j)$ satisfy the following properties:

$$
\begin{aligned}
\partial(\mathcal{Z}_i + \mathcal{Z}_j) &\subseteq \partial\mathcal{Z}_i + \partial\mathcal{Z}_j \\
\partial(\mathcal{Z}_i \cdot \mathcal{Z}_j) &\subseteq \partial\mathcal{Z}_i \cdot \partial\mathcal{Z}_j\,.
\end{aligned}
$$

Therefore, the boundary of $\mathbf{\Delta}(j\omega)$ is obtained by replacing each set $\mathbf{P}_{ij}(j\omega)$ with its boundary. However $\mathbf{P}_{ij}(j\omega)$ is an axis parallel rectangle whose vertices are the $j\omega$ images of the Kharitonov polynomials and whose edges are the $j\omega$ images of the Kharitonov segments. Equation (11.19) follows from this. ♣

The boundary result established above implies that the problem of checking robust stability is now reduced to verifying that the origin is excluded from the set $\mathbf{\Delta}_{\mathrm{E}}(j\omega)$ for each ω in $[0, \infty)$. This is a great deal simpler than the original problem because of the greatly reduced dimensionality of the set $\mathbf{\Delta}_{\mathrm{E}}(s)$ relative to the original set $\mathbf{\Delta}(s)$. However, this verification is still not easy because the set $\mathbf{\Delta}_{\mathrm{E}}(s)$ is multilinear in the parameters λ_i. At this point, the Mapping Theorem can be brought in and

used to approximate $\mathbf{\Delta}_{\mathrm{E}}(j\omega)$. Indeed, since $\mathbf{\Delta}_{\mathrm{E}}(s)$ depends multilinearly on the parameters λ_{ij} associated with the Kharitonov segments, the vertex set of $\mathbf{\Delta}(s)$ can be generated by setting the $P_{ij}(s)$ to the corresponding Kharitonov polynomials. Let

$$\mathbf{\Delta}_{\mathrm{K}}(s) = \{\delta(s,\mathbf{p}) \ : \ P_{ij}(s) = K_{ij}^{i_{ij}}(s), \quad i_{ij} \in \underline{4}, \quad i \in \underline{m}, \quad j \in \underline{r_m}\}. \tag{11.20}$$

We can also introduce the polytopic set consisting of convex combinations of the vertex polynomials:

$$\bar{\mathbf{\Delta}}(s) = \{\lambda v_i(s) + (1-\lambda)v_j(s) \ : \ v_i(s), v_j(s) \in \mathbf{\Delta}_{\mathrm{K}}(s), \quad \lambda \in [0,1]\}. \tag{11.21}$$

It follows from the Mapping Theorem now, that

$$co\ \mathbf{\Delta}_{\mathrm{E}}(j\omega) = co\ \mathbf{\Delta}_{\mathrm{K}}(j\omega) = \bar{\mathbf{\Delta}}_{\mathrm{K}}(j\omega).$$

Therefore, the condition that $\mathbf{\Delta}_{\mathrm{E}}(j\omega)$ excludes the origin can be replaced by the sufficient condition that $\bar{\mathbf{\Delta}}_{\mathrm{K}}(j\omega)$ exclude the origin. Since this latter set is a polytope, this condition can be verified by checking that the angle subtended by the set $\mathbf{\Delta}_{\mathrm{K}}(j\omega)$ at the origin, $\Phi_{\mathbf{\Delta}_{\mathrm{K}}}(j\omega)$ is less than π radians. Therefore we have proved the following result.

Theorem 11.4 *The family $\mathbf{\Delta}(s)$ is Hurwitz stable if it contains at least one stable polynomial and satisfies*

1) $0 \notin co\ \mathbf{\Delta}(j\omega)$ *for some* ω

2) $\Phi_{\mathbf{\Delta}_{\mathrm{K}}}(j\omega) < \pi, \qquad$ for all $\omega \in [0,\infty)$.

This result states that the Hurwitz stability of $\mathbf{\Delta}(s)$ can be determined by checking the phase difference of the vertex polynomials corresponding to the Kharitonov polynomials along the $j\omega$ axis. This is useful in view of the fact that the number of Kharitonov vertices is fixed whereas the vertices of $\mathbf{\Pi}$ increase exponentially with the dimension of the parameter space. We illustrate these results with examples.

Example 11.2. Consider the interconnected feedback system shown in Figure 11.2.

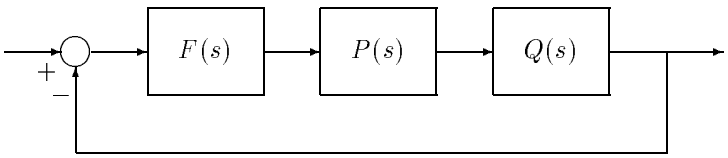

Figure 11.2. Interconnected Feedback System (Example 11.2)

Let

$$F(s) := \frac{F_1(s)}{F_2(s)} = \frac{s+2}{s+1},$$
$$P(s) := \frac{P_1(s)}{P_2(s)} = \frac{s^2+s+1}{s^3+a_2s^2+4s+a_0},$$
$$Q(s) := \frac{Q_1(s)}{Q_2(s)} = \frac{6.6s^3+13.5s^2+15.5s+20.4}{s^3+b_2s^2+3.5s+2.4}$$

and let the set of parameters $\mathbf{p} = [a_2, a_0, b_2]$ vary as follows:

$$a_2 \in [a_2^-, a_2^+] = [-3.625, -2.375],$$
$$a_0 \in [a_0^-, a_0^+] = [1.375, 2.625]$$
$$b_2 \in [b_2^-, b_2^+] = [2.875, 4.125].$$

The characteristic polynomial of the system is:

$$\begin{aligned}\delta(s,\mathbf{p}) = s^7 &+ (7.6+a_2+b_2)s^6\\ &+(40.8+a_2+b_2+a_2b_2)s^5\\ &+(85.7+a_0+3.5a_2+4b_2+a_2b_2)s^4\\ &+(137+a_0+5.9a_2+4b_2+a_0b_2)s^3\\ &+(158.3+3.5a_0+2.4a_2+a_0b_2)s^2\\ &+(101.8+5.9a_0)s+(40.8+2.4a_0).\end{aligned}$$

We verify that the following polynomial in the family is Hurwitz:

$$\begin{aligned}\delta(s,\mathbf{p}=[-3,2,3.5]) = s^7 &+ 8.1s^6+30.8s^5+80.7s^4+142.3s^3\\ &+165.1s^2+113.6s+45.6\end{aligned}$$

The parameter sets corresponding to the Kharitonov polynomials are

$$\left\{(a_2^+, a_0^-, b_2^+), (a_2^-, a_0^+, b_2^+), (a_2^+, a_0^-, b_2^-), (a_2^-, a_0^+, b_2^-)\right\}.$$

The set of Kharitonov vertex polynomials is

$$\mathbf{\Delta}_{\mathrm{K}}(s) = \{\delta_{K_1}(s), \delta_{K_2}(s), \delta_{K_3}(s), \delta_{K_4}(s)\}$$

where

$$\begin{aligned}\delta_{K_1}(s) &= s^7+9.35s^6+32.7531s^5+85.4656s^4+146.5344s^3+163.0844s^2\\ &\quad +109.9125s+44.1\\ \delta_{K_2}(s) &= s^7+8.10s^6+34.4719s^5+83.4344s^4+139.8156s^3+161.3656s^2\\ &\quad +109.9125s+44.1\\ \delta_{K_3}(s) &= s^7+8.10s^6+26.3469s^5+77.1844s^4+145.5656s^3+169.6156s^2\\ &\quad +117.2875s+47.1\\ \delta_{K_4}(s) &= s^7+6.85s^6+29.6281s^5+76.7156s^4+137.2844s^3+166.3344s^2\\ &\quad +117.2875s+47.1\end{aligned}$$

One approach is to check the Hurwitz stability of all convex combinations of these polynomials. This in turn can be done by using the Segment Lemma (Chapter 2). Alternatively, we may check the phase differences of these vertex polynomials. If the maximum phase difference is less than 180° (π radians) for all ω, the origin is excluded from convex hull of $\mathbf{\Delta}_{\mathrm{E}}(j\omega)$ for all ω. We show the convex hulls of image sets in Figure 11.3 for illustration.

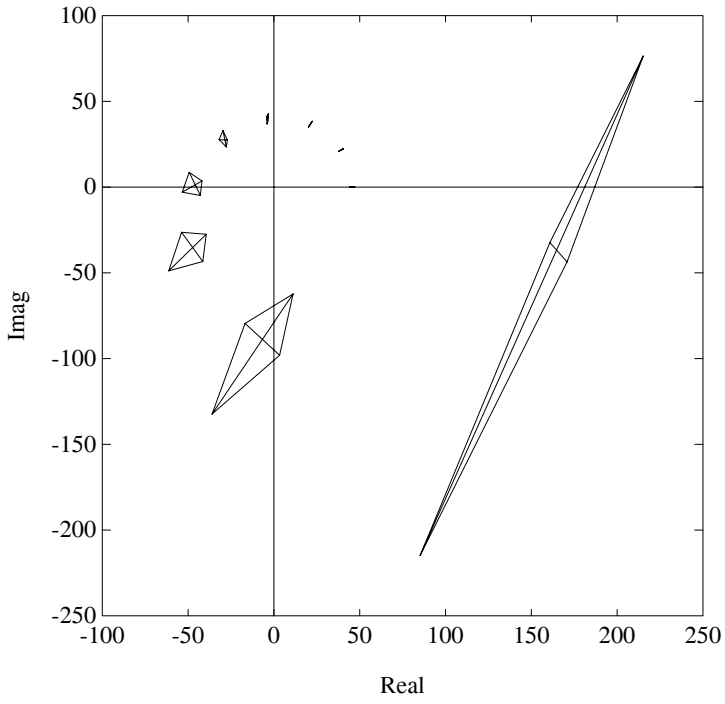

Figure 11.3. Convex hulls of image sets (Example 11.2)

We confirm robust stability by verifying (see Figure 11.4) the maximum phase difference never reaches 180° for all ω. We also note that if we had applied the Mapping Theorem directly to the three dimensional parameter space $\mathbf{p}$, we would have had to check 8 vertices as opposed to the 4 vertices checked here. This reduction is due to the application of the multilinear version of the Generalized Kharitonov Theorem.

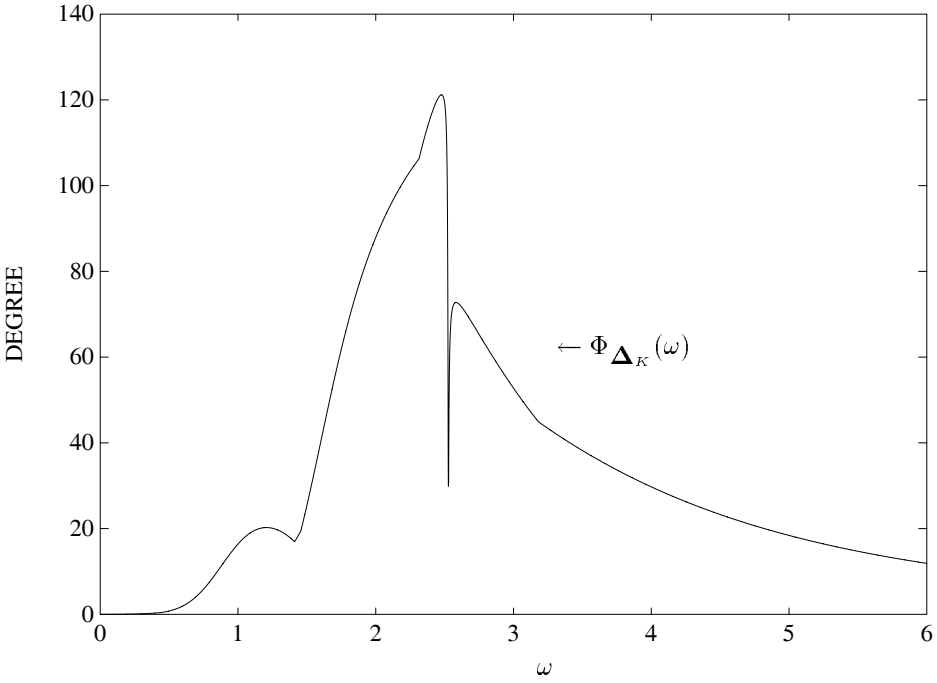

Figure 11.4. $\Phi_{\mathbf{\Delta}_K}(\omega)$ vs. ω (Example 11.2)

11.3 PARAMETRIC STABILITY MARGIN

Consider again the family of polynomials

$$\mathbf{\Delta}(s) = F_1(s)\mathbf{P}_{11}(s)\cdots\mathbf{P}_{1r_1}(s) + \cdots + F_m(s)\mathbf{P}_{m1}(s)\cdots\mathbf{P}_{mr_m}(s). \tag{11.22}$$

Let $\mathbf{p}_{ij}$ denote the vector of coefficients of the polynomials $P_{ij}(s)$. Each such coefficient belongs to a given interval and the corresponding box of parameters is denoted by $\mathbf{\Pi}_{ij}$. Then the box of uncertain parameters is

$$\mathbf{\Pi} := \mathbf{\Pi}_{11} \times \mathbf{\Pi}_{12} \times \cdots \times \mathbf{\Pi}_{mr_m}. \tag{11.23}$$

The extremal manifolds $\mathbf{\Delta}_{\mathrm{E}}(s)$ are defined as follows:

$$\begin{aligned}\mathbf{\Delta}^l_{\mathrm{E}}(s) := {} & F_1(s)\mathcal{K}_{11}(s)\cdots\mathcal{K}_{1r_1}(s) + \cdots + F_{l-1}(s)\mathcal{K}_{l-1,1}(s)\cdots\mathcal{K}_{l-1,r_{l-1}}(s) \\ & + F_l(s)\mathcal{S}_{l,1}(s)\cdots\mathcal{S}_{l,r_l}(s) + F_{l+1}\mathcal{K}_{l+1,1}(s)\cdots\mathcal{K}_{l+1,r_{l+1}} \\ & + \cdots + F_m(s)\mathcal{K}_{m,1}(s)\cdots\mathcal{K}_{m,r_m}(s)\end{aligned} \tag{11.24}$$

$$\mathbf{\Delta}_{\mathrm{E}}(s) := \cup_{l=1}^{m}\mathbf{\Delta}^l_{\mathrm{E}}(s). \tag{11.25}$$

The parameter space subsets corresponding to $\mathbf{\Delta}_{\mathrm{E}}^{l}(s)$ and $\mathbf{\Delta}_{\mathrm{E}}(s)$ are denoted by $\mathbf{\Pi}_l$ and

$$\mathbf{\Pi}_{\mathrm{E}} := \bigcup_{l=1}^{m} \mathbf{\Pi}_l. \tag{11.26}$$

Let $\mathbf{\Pi}_{\mathrm{K}}$ denote the parameter vector set corresponding to the case where each polynomial $P_{ij}(s)$ set to a corresponding Kharitonov polynomial. We write

$$\begin{aligned}
\mathbf{\Delta}(s) &= \{\delta(s,\mathbf{p}) \ : \ \mathbf{p} \in \mathbf{\Pi}\} \\
\mathbf{\Delta}_{\mathrm{E}}(s) &= \{\delta(s,\mathbf{p}) \ : \ \mathbf{p} \in \mathbf{\Pi}_{\mathrm{E}}\} \\
\mathbf{\Delta}_{\mathrm{K}}(s) &= \{\delta(s,\mathbf{p}) \ : \ \mathbf{p} \in \mathbf{\Pi}_{\mathrm{K}}\}.
\end{aligned}$$

In this section, we show that for the family $\mathbf{\Delta}(s)$ in (11.22) the worst case parametric stability margin over the uncertainty box $\mathbf{\Pi}$ occurs, in fact, on the set $\mathbf{\Pi}_{\mathrm{E}}$.

Let $\|\cdots\|$ denote any norm in $\mathbb{R}^n$ and let $\mathcal{P}_u$ denote the set of points $\mathbf{u}$ in $\mathbb{R}^n$ for which $\delta(s,\mathbf{u})$ is unstable or loses degree (relative to its degree over $\mathbf{\Pi}$). Let

$$\rho(\mathbf{p}) = \inf_{\mathbf{u}\in\mathcal{P}_u} \|\mathbf{p}-\mathbf{u}\|_p$$

denote the radius of the stability ball (measured in the norm $\|\cdot\|$) and centered at the point $\mathbf{p}$. This number serves as the stability margin associated with the point $\mathbf{p}$. If the box $\mathbf{\Pi}$ is stable we can associate a stability margin with each point in $\mathbf{\Pi}$. A natural question to ask is: What is the worst case stability margin in the norm $\|\cdot\|$ as $\mathbf{p}$ ranges over $\mathbf{\Pi}$? The answer to that question is provided in the following theorem.

Theorem 11.5 (Extremal Parametric Stability Margin)

$$\inf_{\mathbf{p}\in\mathbf{\Pi}} \rho(\mathbf{p}) = \inf_{\mathbf{p}\in\mathbf{\Pi}_{\mathrm{E}}} \rho(\mathbf{p}). \tag{11.27}$$

Proof. Since $\mathbf{\Delta}(j\omega)$ and $\mathbf{\Delta}_E(j\omega)$ have the same boundary,

$$\begin{aligned}
\inf_{\mathbf{p}\in\mathbf{\Pi}} \rho(\mathbf{p}) &= \inf_{\mathbf{p}\in\mathbf{\Pi}} \inf_{\mathbf{u}\in\mathcal{P}_u} \|\mathbf{p}-\mathbf{u}\|_p \\
&= \inf\{\|\mathbf{a}\| : \delta(j\omega,\mathbf{p}+\mathbf{a}) = 0, \quad \mathbf{p}\in\mathbf{\Pi}, \quad \omega\in[-\infty,+\infty]\} \\
&= \inf\{\|\mathbf{a}\| : \delta(j\omega,\mathbf{p}+\mathbf{a}) = 0, \quad \mathbf{p}\in\mathbf{\Pi}_{\mathrm{E}}, \quad \omega\in[-\infty,+\infty]\} \\
&= \inf_{\mathbf{p}\in\mathbf{\Pi}_{\mathrm{E}}} \inf_{\mathbf{u}\in\mathcal{P}_u} \|\mathbf{p}-\mathbf{u}\|_p = \inf_{\mathbf{p}\in\mathbf{\Pi}_{\mathrm{E}}} \rho(\mathbf{p}).
\end{aligned} \tag{11.28}$$

♣

Example 11.3. Consider the system in Example 11.2 with nominal values

$$a_2^0 = -3, \quad a_0^0 = 2, \quad b_2^0 = 3.5.$$

We compute the maximum parametric stability margin ϵ^* around the nominal values as follows:

$$a_2 \in [a_2^0 - \epsilon, a_2^0 + \epsilon], \quad a_0 \in [a_0^0 - \epsilon, a_0^0 + \epsilon], \quad b_2 \in [b_2^0 - \epsilon, b_2^0 + \epsilon].$$

From the four vertices given in Example 11.2, we have six segments bounding the convex hull of the images. To check the stability of these segments, we apply the Segment Lemma (Chapter 2) with incremental steps of ϵ. This gives $\epsilon^* = 0.63$. The image set of the characteristic polynomial with ϵ^* is shown in Figure 11.5. The figure shows that the image set is almost touching the origin and thus $\epsilon^* = 0.63$ is the parametric stability margin.

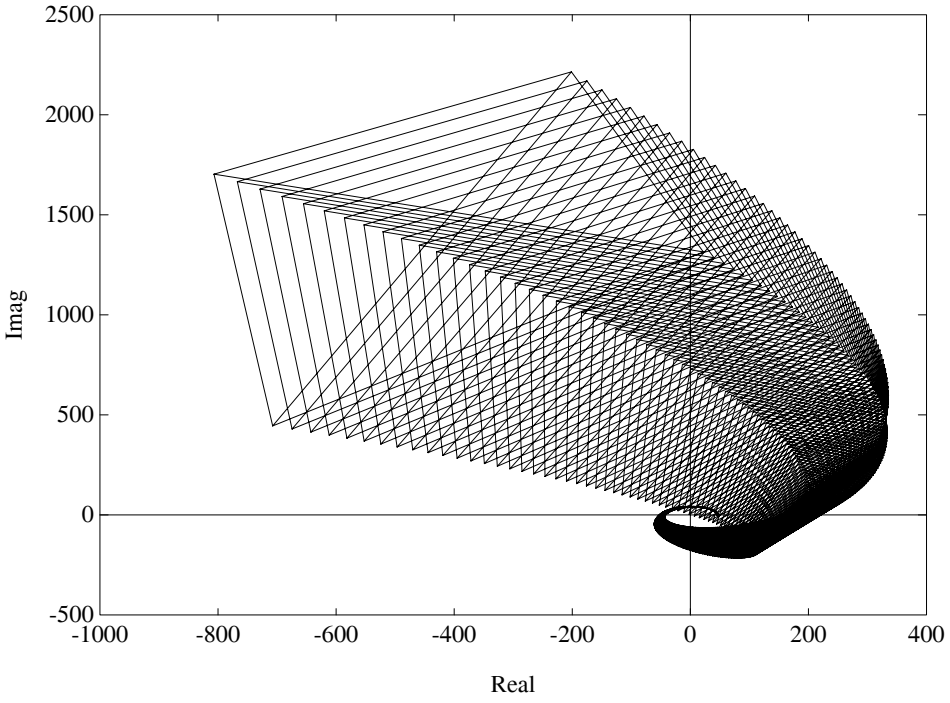

Figure 11.5. Image set for $\epsilon = 0.63$ (Example 11.3)

11.4 MULTILINEAR INTERVAL SYSTEMS

In the rest of this chapter, we will be dealing with transfer functions containing interval parameters with multilinear dependency. The transfer function in question could be embedded in a feedback control system and we will be interested in determining robust stability as well as worst case stability margins and performance

measures of such systems. We begin by first focussing on a *multilinear interval system*, namely one whose transfer function is a ratio of multilinear polynomials with independent parameters. To be specific we will consider single-input, single-output, proper, stable systems with transfer function of the form

$$G(s) = \frac{\gamma(s)}{\delta(s)}.$$

Here

$$\gamma(s) = H_1(s)L_{11}(s)L_{12}(s)\cdots L_{1r_1}(s) + \cdots\cdots + H_m(s)L_{m1}(s)L_{m2}(s)\cdots L_{mr_m}(s)$$

where the polynomials $H_i(s)$ are fixed and the polynomials $L_{ij}(s) \in \mathbf{L}_{ij}(s)$ are independent real interval polynomials. Let $\mathbf{l}$ denote the ordered set of coefficients of the interval polynomials; $\mathbf{l}$ varies in a prescribed axis parallel box $\mathbf{\Lambda}$; the corresponding family of polynomials $\gamma(s)$ is denoted by $\mathbf{\Gamma}(s)$. Similarly we suppose that

$$\delta(s) = F_1(s)P_{11}(s)P_{12}(s)\cdots P_{1r_1}(s) + \cdots\cdots + F_m(s)P_{m1}(s)P_{m2}(s)\cdots P_{mr_m}(s)$$

where the polynomials $F_i(s)$ are fixed, the polynomials $P_{ij}(s)$ are real interval polynomials with the vector of coefficients denoted by $\mathbf{p}$ varying in the prescribed box $\mathbf{\Pi}$. The resulting family of polynomials $\delta(s)$ is denoted $\mathbf{\Delta}(s)$. We also denote explicitly the dependence of $\delta(s)$ on $\mathbf{p}$ and of $\nu(s)$ on $\mathbf{l}$ by writing $\delta(s,\mathbf{p})$ and $\nu(s,\mathbf{l})$ whenever necessary. We make the standing assumption.

Assumption 11.1.

A1) Parameters $\mathbf{p}$ and $\mathbf{l}$ are independent.

A2) $\gamma(s,\mathbf{l})$ and $\delta(s,\mathbf{p})$ are coprime over $(\mathbf{p},\mathbf{l}) \in \mathbf{\Pi} \times \mathbf{\Lambda}$.

A3) $\delta(j\omega,\mathbf{p}) \neq 0$ for all $\mathbf{p} \in \mathbf{\Pi}$ and each $\omega > 0$.

Later in this section we show how to deal with the situations when assumption A1 does not hold. To display the dependence of a typical element $G(s)$ of $\mathbf{G}$ on $\mathbf{l}$ and $\mathbf{p}$ we write it as $G(s,\mathbf{p},\mathbf{l})$:

$$G(s,\mathbf{p},\mathbf{l}) = \frac{\gamma(s,\mathbf{l})}{\delta(s,\mathbf{p})} \tag{11.29}$$

We form the parametrized family of transfer functions

$$\mathbf{G}(s) = \{G(s,\mathbf{p},\mathbf{l}) \ : \ (\mathbf{p},\mathbf{l}) \in (\mathbf{\Pi} \times \mathbf{\Lambda})\} = \frac{\mathbf{\Gamma}(s)}{\mathbf{\Delta}(s)}. \tag{11.30}$$

In order to apply frequency domain methods of analysis and design to the family of systems $\mathbf{G}(s)$ it is necessary to obtain the image set $\mathbf{G}(j\omega)$. We first show how the boundary of this set can be evaluated. We proceed as in the linear case by determining an extremal multilinear interval family of systems $\mathbf{G}_{\mathrm{E}}(s)$. Introduce

the Kharitonov polynomials and segments associated with the $P_{ij}(s)$ and $L_{ij}(s)$ respectively, and construct the extremal polynomial manifolds $\mathbf{\Delta}_{\mathrm{E}}(s)$ and $\mathbf{\Gamma}_{\mathrm{E}}(s)$ and the vertex sets $\mathbf{\Delta}_{\mathrm{K}}(s)$ and $\mathbf{\Gamma}_{\mathrm{K}}(s)$ as in Section 11.2. Let $\mathbf{\Pi}_{\mathrm{E}}$, $\mathbf{\Lambda}_{\mathrm{E}}$ and $\mathbf{\Pi}_{\mathrm{K}}$, $\mathbf{\Lambda}_{\mathrm{K}}$ denote the corresponding manifolds and vertices in $\mathbf{\Pi}$ and $\mathbf{\Lambda}$ respectively:

$$\mathbf{\Gamma}_{\mathrm{E}}(s) = \{\gamma(s,\mathbf{l}) : \mathbf{l} \in \mathbf{\Lambda}_{\mathrm{E}}\}, \qquad \mathbf{\Gamma}_{\mathrm{K}}(s) = \{\gamma(s,\mathbf{l}) : \mathbf{l} \in \mathbf{\Lambda}_{\mathrm{K}}\}$$

$$\mathbf{\Delta}_{\mathrm{E}}(s) = \{\delta(s,\mathbf{p}) : \mathbf{p} \in \mathbf{\Pi}_{\mathrm{E}}\}, \qquad \mathbf{\Delta}_{\mathrm{K}}(s) = \{\delta(s,\mathbf{p}) : \mathbf{p} \in \mathbf{\Pi}_{\mathrm{K}}\}.$$

The *extremal set* $\mathbf{G}_{\mathrm{E}}(s)$ is then defined as

$$\mathbf{G}_{\mathrm{E}}(s) := \left\{ \frac{\gamma(s,\mathbf{l})}{\delta(s,\mathbf{p})} : (\mathbf{l} \in \mathbf{\Lambda}_{\mathrm{K}},\ \mathbf{p} \in \mathbf{\Pi}_{\mathrm{E}}) \text{ or } (\mathbf{l} \in \mathbf{\Lambda}_{\mathrm{E}},\ \mathbf{p} \in \mathbf{\Pi}_{\mathrm{K}}) \right\}. \tag{11.31}$$

Using our compact notational convention we can write

$$\mathbf{G}_{\mathrm{E}}(s) = \left(\frac{\mathbf{\Gamma}_{\mathrm{K}}(s)}{\mathbf{\Delta}_{\mathrm{E}}(s)}\right) \cup \left(\frac{\mathbf{\Gamma}_{\mathrm{E}}(s)}{\mathbf{\Delta}_{\mathrm{K}}(s)}\right).$$

Theorem 11.6 *Under the Assumption 11.1,*

$$\partial\mathbf{G}(j\omega) \subset \mathbf{G}_{\mathrm{E}}(j\omega)$$

for all $\omega \in [0,\infty)$.

Proof. The Assumption A3 guarantees that the set $\mathbf{G}(j\omega)$ is well defined. The proof of the theorem now follows from the boundary properties of the sets $\mathbf{\Delta}_{\mathrm{E}}(j\omega)$ and $\mathbf{\Gamma}_{\mathrm{E}}(j\omega)$, and the independence of the parameter $\mathbf{p}$ and $\mathbf{l}$. We know that

$$\begin{aligned} z \in \partial\mathbf{G}(j\omega) &= \partial\left(\frac{\mathbf{\Gamma}(j\omega)}{\mathbf{\Delta}(j\omega)}\right) \\ &\Leftrightarrow 0 \in \partial\left(\mathbf{\Gamma}(j\omega) - z\mathbf{\Delta}(j\omega)\right) \\ &\Leftrightarrow 0 \in \left(\mathbf{\Gamma}_{\mathrm{K}}(j\omega) - z\mathbf{\Delta}_{\mathrm{E}}(j\omega)\right) \cup \left(\mathbf{\Gamma}_{\mathrm{E}}(j\omega) - z\mathbf{\Delta}_{\mathrm{K}}(j\omega)\right) \\ &\Leftrightarrow z \in \left(\frac{\mathbf{\Gamma}_{\mathrm{K}}(j\omega)}{\mathbf{\Delta}_{\mathrm{E}}(j\omega)}\right) \cup \left(\frac{\mathbf{\Gamma}_{\mathrm{E}}(j\omega)}{\mathbf{\Delta}_{\mathrm{K}}(j\omega)}\right) = \mathbf{G}_{\mathrm{E}}(j\omega). \end{aligned}$$

♣

The proof given above and the formula for the boundary parallels the linear case treated in Chapter 8.

Now suppose that $G(s)$ is part of the control system shown in Figure 11.6.

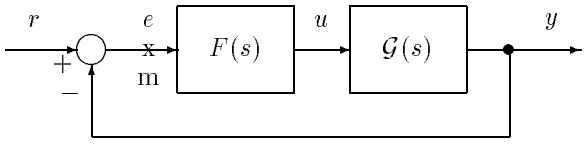

Figure 11.6. A unity feedback system

Define transfer functions:

$$\frac{y(s)}{u(s)} = G(s), \qquad \frac{u(s)}{e(s)} = F(s), \tag{11.32}$$

$$T^o(s) := \frac{y(s)}{e(s)} = F(s)G(s), \qquad T^e(s) := \frac{e(s)}{r(s)} = \frac{1}{1+F(s)G(s)}, \tag{11.33}$$

$$T^u(s) := \frac{u(s)}{r(s)} = \frac{F(s)}{1+F(s)G(s)}, \qquad T^y(s) := \frac{y(s)}{r(s)} = \frac{F(s)G(s)}{1+F(s)G(s)}. \tag{11.34}$$

As $G(s)$ ranges over the uncertainty set $\mathbf{G}(s)$, these transfer functions vary in corresponding sets.

$$\begin{aligned}
\mathbf{T}^o(s) &:= \{F(s)G(s) \ : \ G(s) \in \mathbf{G}(s)\} \\
\mathbf{T}^e(s) &:= \left\{ \frac{1}{1+F(s)G(s)} \ : \ G(s) \in \mathbf{G}(s) \right\} \\
\mathbf{T}^u(s) &:= \left\{ \frac{F(s)}{1+F(s)G(s)} \ : \ G(s) \in \mathbf{G}(s) \right\} \\
\mathbf{T}^y(s) &:= \left\{ \frac{F(s)G(s)}{1+F(s)G(s)} \ : \ G(s) \in \mathbf{G}(s) \right\}.
\end{aligned} \tag{11.35}$$

It turns out that the boundary of the image set, at $s = j\omega$, of each of the above sets is generated by the extremal set $\mathbf{G}_{\rm E}(s)$. Introduce the *extremal subsets*:

$$\mathbf{T}^o_{\rm E}(s) := \{F(s)G(s) \ : \ G(s) \in \mathbf{G}_{\rm E}(s)\} \tag{11.36}$$

$$\mathbf{T}^e_{\rm E}(s) := \left\{ \frac{1}{1+F(s)G(s)} \ : \ G(s) \in \mathbf{G}_{\rm E}(s) \right\} \tag{11.37}$$

$$\mathbf{T}^u_{\rm E}(s) := \left\{ \frac{F(s)}{1+F(s)G(s)} \ : \ G(s) \in \mathbf{G}_{\rm E}(s) \right\} \tag{11.38}$$

$$\mathbf{T}^y_{\rm E}(s) := \left\{ \frac{F(s)G(s)}{1+F(s)G(s)} \ : \ G(s) \in \mathbf{G}_{\rm E}(s) \right\}. \tag{11.39}$$

Theorem 11.7 *For every* $\omega \geq 0$,

$$\begin{array}{ll} (a) & \partial \mathbf{T}^o(j\omega) \subset \mathbf{T}^o_{\mathrm{E}}(j\omega) \\ (b) & \partial \mathbf{T}^e(j\omega) \subset \mathbf{T}^e_{\mathrm{E}}(j\omega) \\ (c) & \partial \mathbf{T}^u(j\omega) \subset \mathbf{T}^u_{\mathrm{E}}(j\omega) \\ (d) & \partial \mathbf{T}^y(j\omega) \subset \mathbf{T}^y_{\mathrm{E}}(j\omega) \end{array}$$

The proof of the above relations can be carried out in a manner identical to the proof of Theorem 8.3 in the linear case (Chapter 8) and is therefore omitted. In fact, all the boundary results related to the Nyquist and Bode envelopes proved in Chapter 8 carry over to the multilinear case with the corresponding extremal set $\mathbf{G}_{\mathrm{E}}(s)$. In the following subsection we show that these boundary results hold for a much larger class of functions of $\mathbf{G}(s)$.

11.4.1 Extensions of Boundary Results

In defining our multilinear interval system we had assumed that the numerator and denominator parameters of $G(s)$ are independent. However for closed loop transfer functions this assumption of independence does not hold. Nevertheless the boundary generating property of the set $\mathbf{G}_{\mathrm{E}}(s)$ still holds for these closed loop transfer functions. It is natural to attempt to generalize this boundary generating property to a large class of functions where dependencies between numerator and denominator parameters occur. Such dependencies invariably occur in the transfer functions associated with multiloop control systems. We begin with a multilinear function $Q(s)$ of several transfer functions $G^i(s), i = 1, 2 \cdots, q$. Let us assume that each $G^i(s)$ itself lies in a multilinear interval family of systems $\mathbf{G}^i(s)$ defined as in this section, with independent parameters in the numerator and denominator. We also assume that the parameters in $G^i(s)$ are independent of those in $G^j(s)$, $i \neq j$. Note that if we regard $Q(s)$ as a rational function its numerator and denominator polynomials contain common interval parameters. Let

$$\mathbf{Q}(s) := \{Q(s) : G^i(s) \in \mathbf{G}^i(s), \quad i = 1, 2 \cdots q\}.$$

We wish to determine the complex plane image set of the family $\mathbf{Q}(s)$ evaluated at $s = j\omega$:

$$\mathbf{Q}(j\omega) := \{Q(j\omega) : G^i(s) \in \mathbf{G}^i(s), \quad i = 1, 2 \cdots q\}.$$

Let $\mathbf{G}^i_{\mathrm{E}}(s)$ denote the extremal subset of $\mathbf{G}^i(s)$ and introduce

$$\mathbf{Q}_{\mathrm{E}}(j\omega) := \{Q(j\omega) : G^i(s) \in \mathbf{G}^i_{\mathrm{E}}(s), \quad i = 1, 2 \cdots q\}.$$

Then we can state the following boundary result.

Theorem 11.8

$$\partial \mathbf{Q}(j\omega) \subset \mathbf{Q}_{\mathrm{E}}(j\omega). \tag{11.40}$$

Proof. Let us introduce the complex numbers $s_i = G^i(j\omega)$ and the corresponding sets

$$\mathcal{Z}_i := \{G^i(j\omega) : G^i(s) \in \mathbf{G}^i(s), \quad i = 1, 2 \cdots q\}.$$

Since sums and products of complex plane sets satisfy the following boundary properties

$$\begin{aligned} \partial(\mathcal{Z}_i + \mathcal{Z}_j) &\subseteq \partial\mathcal{Z}_i + \partial\mathcal{Z}_j, \qquad (i \neq j) \\ \partial(\mathcal{Z}_i \cdot \mathcal{Z}_j) &\subseteq \partial\mathcal{Z}_i \cdot \partial\mathcal{Z}_j, \qquad (i \neq j). \end{aligned}$$

and

$$\partial\mathcal{Z}_i \subset \mathbf{G}^i_{\mathrm{E}}(j\omega), \qquad i = 1, 2 \cdots, q.$$

the multilinearity of the function $Q(s)$ gives us the conclusion stated. ♣

We can generalize the above property even further. Let $Q(s)$ be as above and consider a linear fractional transformation (LFT) $T(Q(s))$ defined by arbitrary functions $A(s), B(s), C(s)$ and $D(s)$

$$T(Q(s)) := Q_1(s) := \frac{A(s)Q(s) + B(s)}{C(s)Q(s) + D(s)}.$$

Introduce the set

$$T(\mathbf{Q}(s)) := \left\{ \frac{A(s)Q(s) + B(s)}{C(s)Q(s) + D(s)} : Q(s) \in \mathbf{Q}(s) \right\}.$$

Let us now impose the restriction

$$A(j\omega)D(j\omega) - B(j\omega)C(j\omega) \neq 0. \tag{11.41}$$

Under the above restriction $T(Q(j\omega))$ is a LFT of $Q(j\omega)$ and thus carries boundaries onto boundaries. Thus we know that the boundary of $\mathbf{Q}_1(j\omega)$ is also generated by the extremal systems $\mathbf{G}^i_{\mathrm{E}}(s)$.

Theorem 11.9 *Let $\mathbf{Q}(s)$ be as defined above and let $T(Q(s))$ be an LFT. Then, assuming (11.41) holds*

$$\partial T(\mathbf{Q}(j\omega)) \subset T(\mathbf{Q}_{\mathrm{E}}(j\omega)).$$

Remark 11.2. We remark that any LFT of $Q_1(s)$ as well as sums and products of LFT's continue to enjoy the boundary generating property of the extremal systems. In this way a large class of transfer functions occurring in closed loop systems can be handled.

Computation of $\mathbf{G}_{\mathrm{E}}(j\omega)$

As we have seen, the determination of the set $\mathbf{G}(j\omega)$ reduces to evaluating $\mathbf{G}_{\mathrm{E}}(j\omega)$, a set of smaller dimension. Nevertheless, $\mathbf{G}_{\mathrm{E}}(j\omega)$ is still a multilinear function of the uncertain segment parameters. The only way to exactly evaluate this set is by gridding over the uncertainty box. In general this procedure is computationally expensive or even infeasible. Fortunately, as we have seen earlier, the "concave" property of the image set of multilinear interval polynomials given by the Mapping Theorem allows us to overbound $\mathbf{G}_{\mathrm{E}}(j\omega)$ by a ratio of unions of convex polygons. Recall that

$$\mathbf{G}_{\mathrm{E}}(j\omega) = \left(\frac{\mathbf{\Gamma}_{\mathrm{K}}(j\omega)}{\mathbf{\Delta}_{\mathrm{E}}(j\omega)}\right) \cup \left(\frac{\mathbf{\Gamma}_{\mathrm{E}}(j\omega)}{\mathbf{\Delta}_{\mathrm{K}}(j\omega)}\right). \tag{11.42}$$

From the Mapping Theorem we have

$$\begin{aligned} \mathbf{\Gamma}_{\mathrm{E}}(j\omega) &\subset co\ \mathbf{\Gamma}_{\mathrm{K}}(j\omega) \\ \mathbf{\Delta}_{\mathrm{E}}(j\omega) &\subset co\ \mathbf{\Delta}_{\mathrm{K}}(j\omega). \end{aligned}$$

Now consider $\bar{\mathbf{G}}_{\mathrm{E}}(j\omega)$ defined by replacing $\mathbf{\Gamma}_{\mathrm{E}}(j\omega)$ and $\mathbf{\Delta}_{\mathrm{E}}(j\omega)$ by $co\ \mathbf{\Gamma}_{\mathrm{K}}(j\omega)$ and $co\ \mathbf{\Delta}_{\mathrm{K}}(j\omega)$ respectively. In other words,

$$\bar{\mathbf{G}}_{\mathrm{E}}(j\omega) = \left(\frac{\mathbf{\Gamma}_{\mathrm{K}}(j\omega)}{co\ \mathbf{\Delta}_{\mathrm{K}}(j\omega)}\right) \cup \left(\frac{co\ \mathbf{\Gamma}_{\mathrm{K}}(j\omega)}{\mathbf{\Delta}_{\mathrm{K}}(j\omega)}\right). \tag{11.43}$$

It is clear that $\bar{\mathbf{G}}_{\mathrm{E}}(j\omega)$ overbounds $\mathbf{G}_{\mathrm{E}}(j\omega)$:

$$\mathbf{G}_{\mathrm{E}}(j\omega) \subset \bar{\mathbf{G}}_{\mathrm{E}}(j\omega). \tag{11.44}$$

The evaluation of $\bar{\mathbf{G}}_{\mathrm{E}}(j\omega)$ is relatively easy because it consists of a union of one-parameter families of transfer functions of the types

$$\frac{\lambda U_1(j\omega) + (1-\lambda)U_2(j\omega)}{V(j\omega)} \quad \text{or} \quad \frac{U(j\omega)}{\lambda V_1(j\omega) + (1-\lambda)V_2(j\omega)}.$$

The union of these one-parameter families gives rise to $\bar{\mathbf{G}}_{\mathrm{E}}(j\omega)$ which overbounds the boundary of $\mathbf{G}(j\omega)$. The tightness of the approximation can be improved as we have seen before, by introducing additional vertices in the parameter set $\mathbf{\Pi} \times \mathbf{\Lambda}$. The guaranteed gain and phase margins of a control system containing parameter uncertainty may be obtained from these overbounded sets as shown in Figure 11.7. The image at $s = j\omega$ of each of the transfer function sets associated with the feedback system considered in Figure 11.6 can be overbounded by replacing $\mathbf{G}(j\omega)$ by $\bar{\mathbf{G}}_{\mathrm{E}}(j\omega)$, and in fact we can do the same for any linear fractional transformation of $G(s)$. An example of this calculation follows.

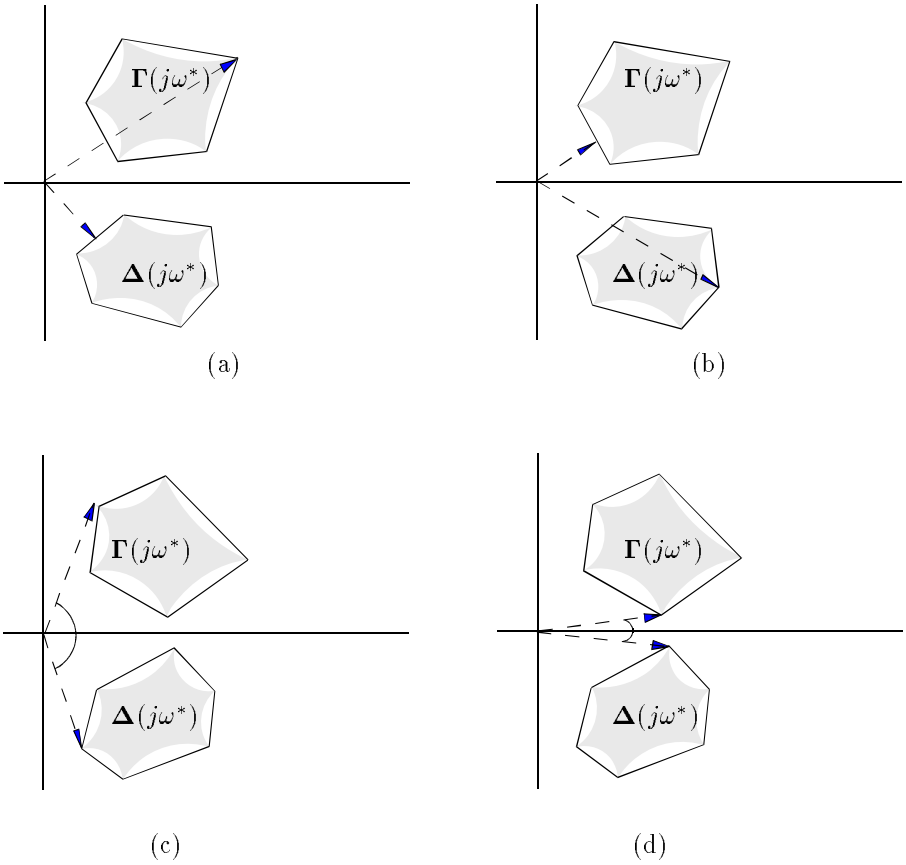

Figure 11.7. Guaranteed gain and phase margin using overbounded sets

Example 11.4. (Nyquist, Bode and Nichols Envelopes of Multilinear Systems) The purpose of this example to show how to construct the frequency domain envelopes (Nyquist, Bode and Nichols envelopes) of the multilinear interval family. Let us recall the system given in Example 11.1:

$$F(s)\underbrace{P(s)Q(s)}_{G(s)} = \frac{(s+2)(s^2+s+1)(6.6s^3+13.5s^2+15.5s+20.4)}{(s+1)(s^3+a_2s^2+4s+a_0)(s^3+b_2s^2+3.5s+2.4)}$$

where

$$a_2 \in [a_2^-, a_2^+] = [-3.625, -2.375], \qquad a_0 \in [a_0^-, a_0^+] = [1.375, 2.625]$$

$$b_2 \in [b_2^-, b_2^+] = [2.875, 4.125].$$

From Theorem 11.6, it is enough to consider $\mathbf{G}_{\mathrm{E}}(j\omega)$. Since this particular example has parameters only in the denominator, we have

$$\begin{aligned}\partial\left(F(j\omega)\mathbf{G}(j\omega)\right) &\subset F(j\omega)\mathbf{G}_{\mathrm{E}}(j\omega) \\ &= \frac{(s+2)(s^2+s+1)(6.6s^3+13.5s^2+15.5s+20.4)|_{s=j\omega}}{\boldsymbol{\Delta}_{\mathrm{E}}(j\omega)}\end{aligned}$$

where $\boldsymbol{\Delta}_{\mathrm{E}}(j\omega)$ consists of the six line segments joining the following four vertices:

$$\begin{aligned}&(s+1)(s^3+a_2^+s^2+4s+a_0^-)(s^3+b_2^+s^2+3.5s+2.4)|_{s=j\omega} \\ &(s+1)(s^3+a_2^+s^2+4s+a_0^-)(s^3+b_2^-s^2+3.5s+2.4)|_{s=j\omega} \\ &(s+1)(s^3+a_2^-s^2+4s+a_0^+)(s^3+b_2^+s^2+3.5s+2.4)|_{s=j\omega} \\ &(s+1)(s^3+a_2^-s^2+4s+a_0^+)(s^3+b_2^-s^2+3.5s+2.4)|_{s=j\omega}.\end{aligned}$$

Figures 11.8, 11.9, and 11.10 are obtained accordingly.

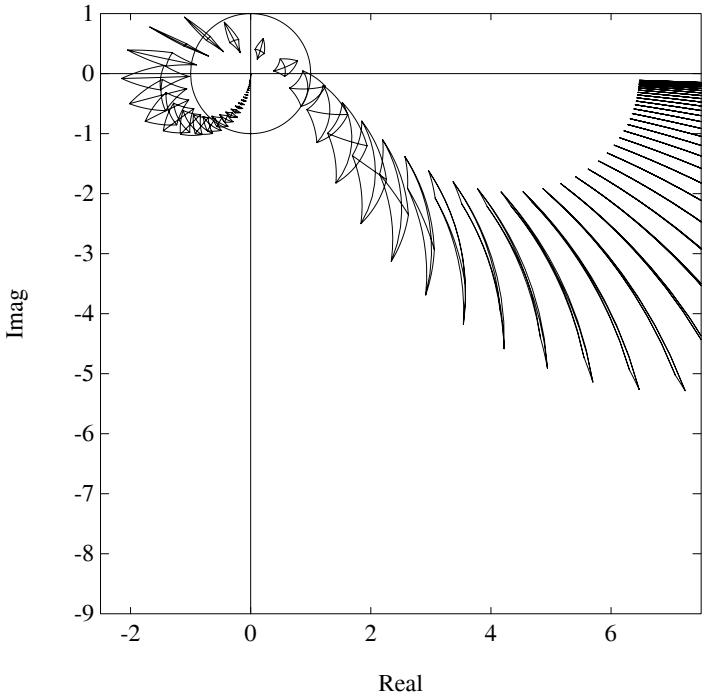

Figure 11.8. Nyquist envelope (Example 11.4)

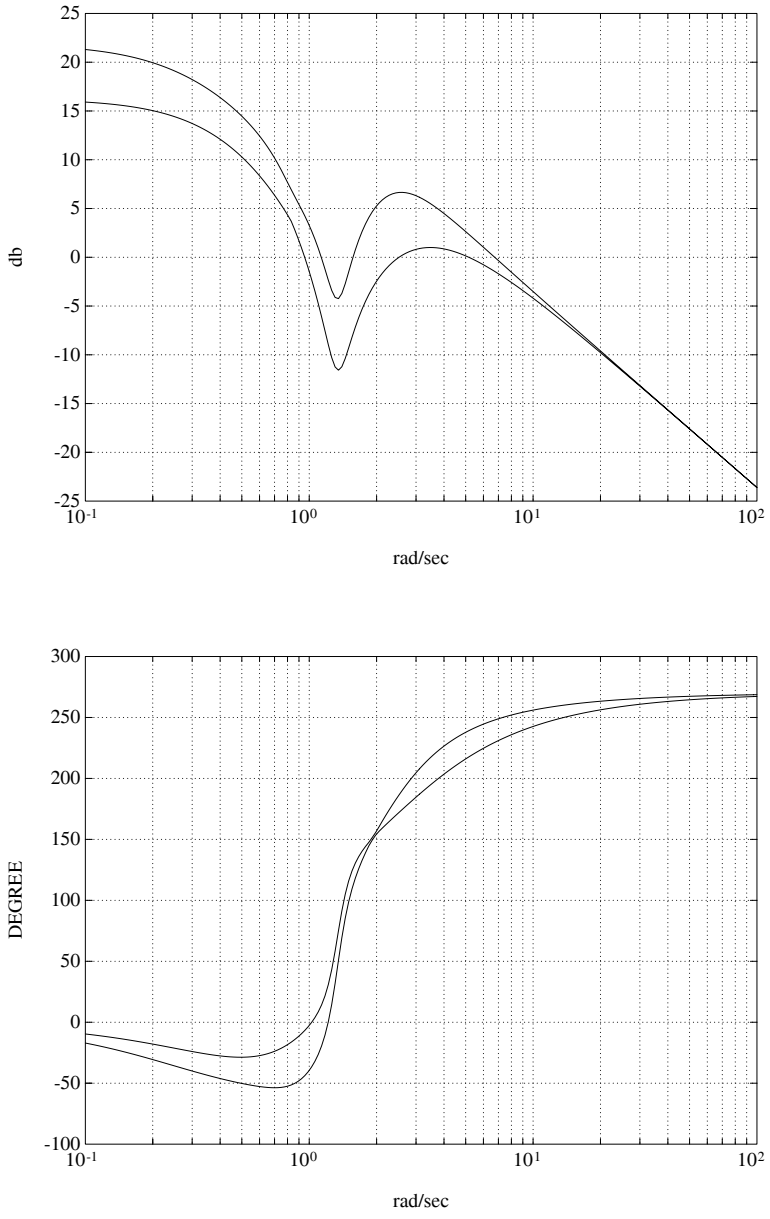

Figure 11.9. Bode magnitude and phase envelopes (Example 11.4)

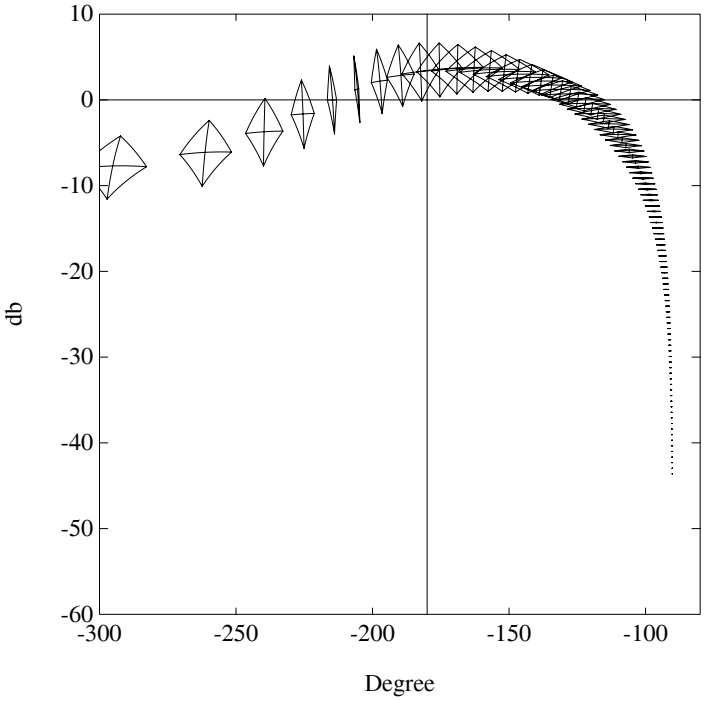

Figure 11.10. Nichols envelope (Example 11.4)

11.5 H_∞ STABILITY MARGIN

In this section we use the boundary results derived above to efficiently deal with many frequency domain measures of performance and, in particular, to determine worst case performance over the parameter set associated with a multilinear interval systems. As in Chapter 8 we will use the standard notation: $\mathbf{C}_+ := \{s \in C : \ \mathrm{Re}(s) \geq 0\}$, and $H_\infty(\mathbf{C}_+)$ will represent the space of functions $f(s)$ that are bounded and analytic in $\mathbf{C}_+$ with the standard H_∞ norm,

$$\|f\|_\infty = \sup_{\omega \in \mathbf{R}} |f(j\omega)|.$$

Let us consider the multilinear interval family of systems $\mathbf{G}(s)$ defined earlier (see (11.30)) and let us assume that the entire family is stable. To determine the unstructured stability margin of control systems containing the family $\mathbf{G}(s)$ we need to determine the supremum of the H_∞ norm of certain transfer functions over $\mathbf{G}(s)$. Since the H_∞ norm-bounded perturbations provide uniform perturbations at all frequencies, it is desirable to shape this perturbation by introducing a weight. Let

the weight $W(s)$ be a scalar stable proper transfer function

$$W(s) = \frac{n_w(s)}{d_w(s)}.$$

To start with, let us look at two specific robust stability problems involving mixed parametric-unstructured uncertainty:

Problem I: Consider the configuration in Figure 11.11, where $W(s)$ is a stable proper weight, $\mathbf{G}(s)$ is a stable multilinear interval family of systems, and ΔP is any H_∞ perturbation that satisfies $\|\Delta P\| < \alpha$. Find necessary and sufficient conditions for stability of the family of closed loop systems.

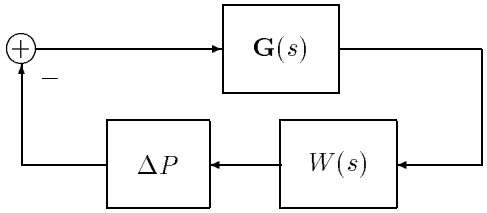

Figure 11.11.

Problem II: Consider the feedback configuration in Figure 11.12, where $W(s)$ is a stable proper weight, ΔP is any H_∞ perturbation that satisfies $\|\Delta P\| < \alpha$, and $C(s)$ is a controller that simultaneously stabilizes every element in the set $\mathbf{G}(s)$. Find necessary and sufficient conditions for stability of the family of closed loop systems.

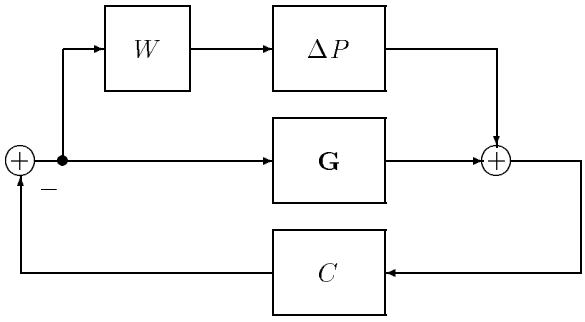

Figure 11.12.

The above problems are generalized versions of standard H_∞ robust stability problems where a fixed plant is considered. Here, the worst case solution is sought over the parameter set $\mathbf{\Pi} \times \mathbf{\Lambda}$. As in the case treated in Chapter 9 (linear case), we solve this problem by using the Small Gain Theorem and determining the worst case over the uncertainty set. The solution is accomplished by showing that the H_∞ norms in question attain their supremum value over the extremal set of transfer functions $\mathbf{G}_{\mathrm{E}}(s) \subset \mathbf{G}(s)$ defined in (11.31). We can now state the main result of this section.

Theorem 11.10 (Unstructured Stability Margins)

1) The configuration of (Figure 11.11) will be stable if and only if α satisfies

$$\alpha \leq \frac{1}{\sup_{g \in \mathbf{G}_{\mathrm{E}}} \|Wg\|_\infty} := \alpha_o^*.$$

2) The configuration of Problem II (Figure 11.12) will be stable if and only if α satisfies

$$\alpha \leq \frac{1}{\sup_{g \in \mathbf{G}_{\mathrm{E}}} \|WC(1+gC)^{-1}\|_\infty} := \alpha_c^*.$$

The proof of this theorem follows from the boundary properties proved in the last section. To state this in more detail, we use the following lemma.

Lemma 11.2 (Extremal H_∞ Properties)

$$\textit{Problem I}: \quad \sup_{g \in \mathbf{G}} \|Wg\|_\infty = \sup_{g \in \mathbf{G}_{\mathrm{E}}} \|Wg\|_\infty,$$

$$\textit{Problem II}: \quad \sup_{g \in \mathbf{G}} \|WC(1+gC)^{-1}\|_\infty = \sup_{g \in \mathbf{G}_{\mathrm{E}}} \|WC(1+gC)^{-1}\|_\infty.$$

Proof. We first consider the following:

$$\begin{aligned}
\sup_{g \in \mathbf{G}_{\mathrm{E}}} \|g\|_\infty &= \sup \{|c| : 0 = c\delta(j\omega, \mathbf{p}) + \gamma(j\omega, \mathbf{l}),\ \mathbf{p} \in \mathbf{\Pi},\ \mathbf{l} \in \mathbf{\Lambda},\ \omega \in [-\infty, +\infty]\} \\
&= \sup \{|c| : 0 = c\delta(j\omega, \mathbf{p}) + \gamma(j\omega, \mathbf{l}) \ , \\
&\qquad (\mathbf{p}, \mathbf{l}) \in (\mathbf{\Pi}_{\mathrm{E}} \times \mathbf{K}(\mathbf{\Lambda})) \cup (\mathbf{K}(\mathbf{\Pi}) \times \mathbf{\Lambda}_{\mathrm{E}}),\ \ \omega \in [-\infty, +\infty]\} \\
&= \sup_{g \in \mathbf{G}_{\mathrm{E}}} \|g\|_\infty.
\end{aligned}$$

Using arguments identical to the above, we conclude that

$$\sup_{g \in \mathbf{G}} \|Wg\|_\infty = \sup_{g \in \mathbf{G}_{\mathrm{E}}} \|Wg\|_\infty,$$

$$\sup_{g \in \mathbf{G}} \|WC(1+gC)^{-1}\|_\infty = \sup_{g \in \mathbf{G}_{\mathrm{E}}} \|WC(1+gC)^{-1}\|_\infty.$$

♣

Proof of Theorem 11.10 Consider the configuration of Figure 11.11. From the Small Gain Theorem the perturbed system is stable if and only if

$$\alpha \leq \frac{1}{\sup_{g \in \mathbf{G}} \|Wg\|_\infty} := \alpha_o^*.$$

From the Lemma 11.2, it follows that $\mathbf{G}$ can be replaced by $\mathbf{G}_{\mathrm{E}}$. A similar argument works for the configuration of Figure 11.12. ♣

Remark 11.3. The quantities α_o^* and α_c^* serve as unstructured H_∞ stability margins for the respective open and closed loop parametrized systems treated in Problems I and II.

Remark 11.4. In practice we can further replace $\mathbf{G}_{\mathrm{E}}(s)$ by the image set overbounding polytopic family $\bar{\mathbf{G}}_{\mathrm{E}}(s)$, and obtain lower bounds on these margins from $\bar{\mathbf{G}}_{\mathrm{E}}(s)$. We can also obtain upper bounds on these margins from the set of Kharitonov vertex systems of the family. Furthermore, the extremal results stated above also hold for any LFT of $\mathbf{G}(s)$.

11.6 NONLINEAR SECTOR BOUNDED STABILITY MARGIN

We now consider the effect of nonlinear perturbations on the multilinear interval family $\mathbf{G}(s)$ defined in the last section (see (11.30)). The nonlinear perturbations will consist of all possible nonlinear gains lying in a sector $[0, k]$. In other words, we consider the configurations in Figures 11.13 and 11.14.

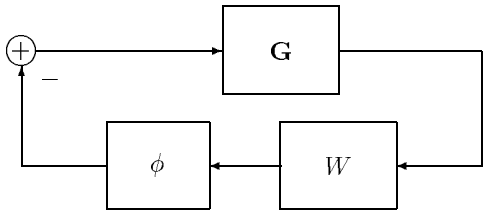

Figure 11.13.

The gain block ϕ consists of all nonlinear time-varying gains $\phi(t, \sigma)$ satisfying

$$\phi(t, 0) = 0 \quad \text{for all } t \geq 0 \qquad \text{and} \qquad 0 \leq \sigma\phi(t, \sigma) \leq k\sigma^2.$$

This implies that $\phi(t, \sigma)$ is bounded by the lines $\phi = 0$ and $\phi = k\sigma$. Such nonlinearities are said to belong to a sector $[0, k]$. $G(s)$ will be assumed to lie in the multilinear interval family $\mathbf{G}(s)$. The problem is to determine the largest size of the sector k for which robust stability is guaranteed. This is the multilinear version

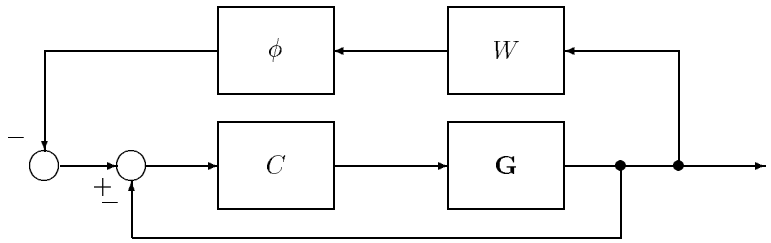

Figure 11.14.

of the robust Lur'e problem treated in Chapter 9. As before, the solution depends on the *strict positive realness* (SPR) properties of the family in question. First we have the following.

Lemma 11.3 (Extremal SPR Properties)

1) Let $\mathbf{G}(s)$ *be the multilinear interval family defined in (11.30) and assume that* $\mathbf{G}(s)$ *is stable. Then*

$$\inf_{G\in\mathbf{G}}\inf_{\omega\in\mathbf{R}}\mathrm{Re}(W(j\omega)G(j\omega)) = \inf_{G\in\mathbf{G}_{\mathrm{E}}}\inf_{\omega\in\mathbf{R}}\mathrm{Re}(W(j\omega)G(j\omega)).$$

2) If $C(s)$ *is a controller that stabilizes the entire family* $\mathbf{G}(s)$*, then*

$$\inf_{G\in\mathbf{G}}\inf_{\omega\in\mathbf{R}}\mathrm{Re}\left(W(j\omega)C(j\omega)G(j\omega)(1+C(j\omega)G(j\omega))^{-1}\right) = \inf_{G\in\mathbf{G}_{\mathrm{E}}}\inf_{\omega\in\mathbf{R}}\mathrm{Re}\left(W(j\omega)C(j\omega)G(j\omega)(1+C(j\omega)G(j\omega))^{-1}\right).$$

The proof of this lemma immediately follows from the boundary property given in Theorem 11.7.

Theorem 11.11 (Nonlinear Stability margin)

1) Let $k^* \geq 0$ *be defined by:*

$$\sup\left\{k \;:\; \frac{1}{k} + \inf_{G\in\mathbf{G}_{\mathrm{E}}}\inf_{\omega\in\mathbf{R}}\mathrm{Re}(W(j\omega)G(j\omega)) > 0\right\}$$

then the closed loop system in Figure 11.13 is absolutely stable for all nonlinear gains ϕ *lying in the sector* $[0, k^*]$*.*

2) Let $k^* \geq 0$ *be defined by:*

$$\sup\left\{k \;:\; \frac{1}{k} + \inf_{G\in\mathbf{G}_{\mathrm{E}}}\inf_{\omega\in\mathbf{R}}\mathrm{Re}\left(W(j\omega)C(j\omega)G(j\omega)(1+C(j\omega)G(j\omega))^{-1}\right) > 0\right\}$$

for the controller C, then the closed loop system in Figure 11.14 is absolutely stable for all nonlinear gains ϕ lying in the sector $[0, k^*]$.

Proof. From standard results on the Lur'e problem, stability is preserved for all k satisfying

$$\frac{1}{k} + \inf_{G \in \mathbf{G}} \inf_{\omega \in \mathbf{R}} \mathrm{Re}(W(j\omega)G(j\omega)) > 0.$$

By Lemma 11.3 we may replace $\mathbf{G}(j\omega)$ by $\mathbf{G}_{\mathrm{E}}(j\omega)$ in the above inequality. This proves 1). The proof of 2) is similar. ♣

Example 11.5. (Stability Sector for Multilinear Interval Systems) Consider the system used in Example 11.1. We plot the frequency domain image of the closed loop system transfer function

$$\mathbf{M}(s) := \left\{ \frac{F(s)G(s)}{1 + F(s)G(s)} : G(s) \in \mathbf{G}_{\mathrm{E}}(s) \right\}.$$

Figure 11.15 shows that the nonlinear sector is given by $\frac{1}{k} = 20.5012$.

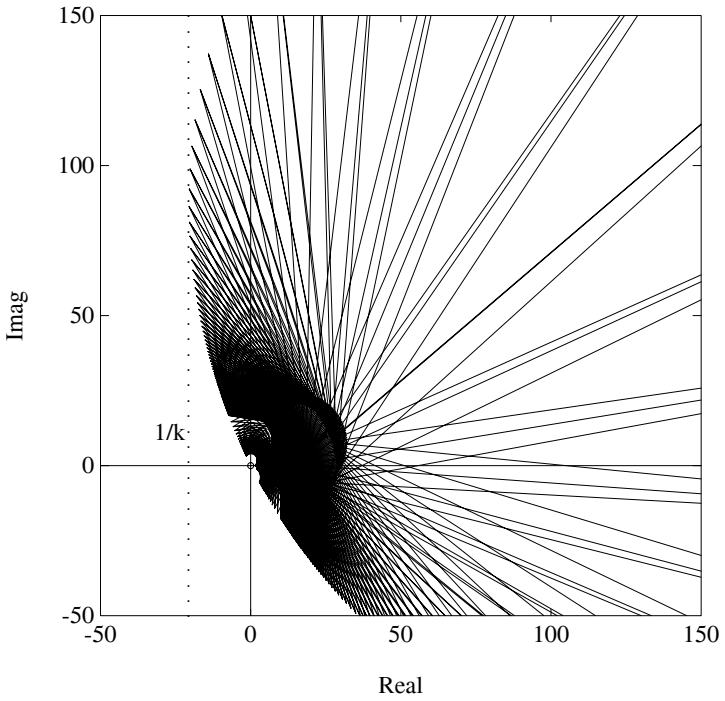

Figure 11.15. Frequency domain image of $\mathbf{M}(j\omega)$ (Example 11.5)

11.7 INTERVAL PLANTS AND DIAGONAL REPRESENTATION OF PERTURBATIONS

In the robust control literature it has become customary to represent system perturbations in a signal flow diagram where the perturbations are "pulled" out and displayed in a feedback matrix $\mathbf{\Delta}$ with independent diagonal or block-diagonal entries Δ_i as shown below in Figure 11.16.

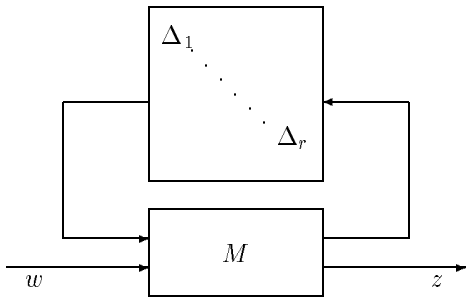

Figure 11.16. System with uncertainties represented in feedback form

$M(s)$ is a suitably defined interconnection transfer function matrix of appropriate size and Δ is a block diagonal matrix containing all the perturbations affecting the system dynamics. In general this would include real parametric uncertainty as well as norm-bounded uncertainty blocks with the latter representing either actual unmodelled dynamics or fictitious performance blocks. The popularity of this representation is due to the fact that almost all types of uncertainties including parametric and unstructured uncertainties can be accurately and explicitly represented in this framework. Moreover, the feedback representation allows us to use the Small Gain formulation and thus convert robust performance problems into robust stability problems.

Although this formulation does not add anything to the the rich structure of interval systems already developed, it is nevertheless instructive to interpret the solution given by the Generalized Kharitonov Theorem in the linear and multilinear cases in this framework. We begin in the next subsection with the diagonal representation of a single interval system. This is subsequently extended to the case of multiple interval systems and multiple norm-bounded perturbation blocks. This type of mixed perturbation problem arises in systems with several performance specifications. We show how the boundary properties of the extremal systems $\mathbf{G}_{\mathrm{E}}(s)$ established in the GKT play a role in the solution of these problems.

11.7.1 Diagonal Feedback Representation of an Interval System

Let $\mathbf{G}(s)$ be a interval plant

$$\mathbf{G}(s) = \left\{ \frac{N(s)}{D(s)} \ : \ (N(s) \times D(s) \in (\mathbf{N}(s) \times \mathbf{D}(s)) \right\} \tag{11.45}$$

where $\mathbf{N}(s)$ and $\mathbf{D}(s)$ are interval polynomial families. Referring to the notation defined in Chapter 5, the four Kharitonov polynomials associated with the interval polynomial $\mathbf{D}(s)$ can be written as follows:

$$\begin{aligned} K_D^1(s) &= D_{\min}^{\text{even}}(s) + D_{\min}^{\text{odd}}(s) \\ K_D^2(s) &= D_{\min}^{\text{even}}(s) + D_{\max}^{\text{odd}}(s) \\ K_D^3(s) &= D_{\max}^{\text{even}}(s) + D_{\min}^{\text{odd}}(s) \\ K_D^4(s) &= D_{\max}^{\text{even}}(s) + D_{\max}^{\text{odd}}(s). \end{aligned} \tag{11.46}$$

We know that, as far as frequency domain properties at $s = j\omega$ are concerned, the interval polynomial $\mathbf{D}(s)$ can be replaced by the following reduced 2-parameter family:

$$\mathbf{D}_R(s) = \left\{ D(s) \ : \ D^0(s) + \lambda_1 D_e(s) + \lambda_2 D_o(s) \ \ \lambda_i \in [-1, 1] \right\} \tag{11.47}$$

where

$$\begin{aligned} D_e(s) &= \frac{1}{2} \left(D_{\max}^{\text{even}}(s) - D_{\min}^{\text{even}}(s) \right) \\ D_o(s) &= \frac{1}{2} \left(D_{\max}^{\text{odd}}(s) - D_{\min}^{\text{odd}}(s) \right) \end{aligned}$$

and

$$D^0(s) = \frac{1}{2} \left[D_{\max}^{\text{even}}(s) + D_{\min}^{\text{even}}(s) + D_{\max}^{\text{odd}}(s) + D_{\min}^{\text{odd}}(s) \right]$$

is the *nominal* polynomial. Similarly $\mathbf{N}(s)$ can be replaced by:

$$\mathbf{N}_R(s) = \left\{ N(s) \ : \ N^0(s) + \lambda_3 N_e(s) + \lambda_4 N_o(s), \quad \lambda_i \in [-1, 1] \right\}. \tag{11.48}$$

It is clear from the above that an interval plant is completely characterized in the frequency domain by the 4-parameter family $\mathbf{G}_{\mathrm{R}}(s)$:

$$\mathbf{G}_{\mathrm{R}}(s) = \left\{ \frac{N(s)}{D(s)} \ : \ (N(s) \times D(s)) \in (\mathbf{N}_{\mathrm{R}}(s) \times \mathbf{D}_{\mathrm{R}}(s)) \right\}. \tag{11.49}$$

This is essentially what we proved in the first step of the proof of GKT given in Chapter 7. In the second step we proved further that it suffices to test stability of the extremal set $\mathbf{G}_{\mathrm{E}}(s)$. The polynomial set $\mathbf{G}_{\mathrm{K}}(s)$ corresponds to the vertices of the 4-dimensional box representing $\mathbf{G}_{\mathrm{R}}(s)$ while the 32 segments $\mathbf{G}_{\mathrm{E}}(s)$, correspond to the exposed edges of the same box.

Now write $y(s) = G(s)u(s)$,

$$y(s) = \frac{N^0(s) + \lambda_3 N_e(s) + \lambda_4 N_o(s)}{D^0(s) + \lambda_1 D_e(s) + \lambda_2 D_o(s)} u(s).$$

This may be rewritten as follows:

$$\begin{aligned} y(s) = \left[D^0(s)\right]^{-1} \big\{ &\left(N^0(s) + \lambda_3 N_e(s) + \lambda_4 N_o(s)\right) u(s) \\ &- \left(\lambda_1 D_e(s) + \lambda_2 D_o(s)\right) y(s) \big\} \end{aligned} \tag{11.50}$$

or, suppressing s, as

$$\begin{aligned} y = \left[(D^0)^{-1} N^0 + \lambda_3 (D^0)^{-1} N_e + \lambda_4 (D^0)^{-1} N_o\right] u \\ - \left[\lambda_1 (D^0)^{-1} D_e + \lambda_2 (D^0)^{-1} D_o\right] y. \end{aligned} \tag{11.51}$$

Corresponding to (11.51), we have the block diagram shown in Figure 11.17.

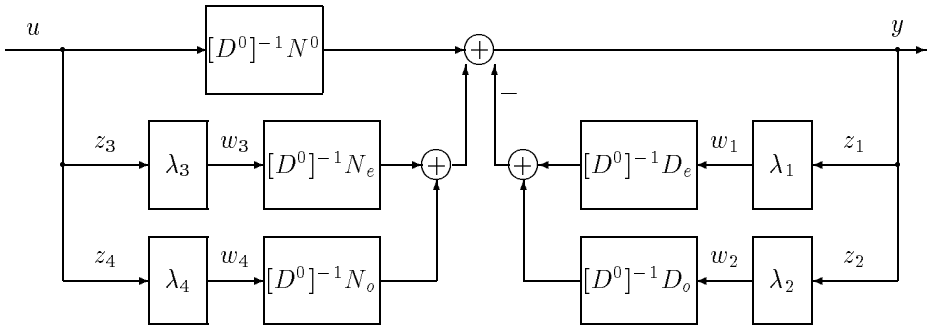

Figure 11.17. Four parameter structure

This input-output relation may be written as follows:

$$\begin{bmatrix} z_1 \\ z_2 \\ z_3 \\ z_4 \\ y \end{bmatrix} = (D^0)^{-1} \begin{bmatrix} -D_e & -D_o & N_e & N_o & N^0 \\ -D_e & -D_o & N_e & N_o & N^0 \\ 0 & 0 & 0 & 0 & D^0 \\ 0 & 0 & 0 & 0 & D^0 \\ -D_e & -D_o & N_e & N_o & N^0 \end{bmatrix} \begin{bmatrix} w_1 \\ w_2 \\ w_3 \\ w_4 \\ u \end{bmatrix} \tag{11.52}$$

with

$$w_i = \lambda_i z_i, \quad i = 1, 2, 3, 4. \tag{11.53}$$

Let $z := [z_1, z_2, z_3, z_4]^T$ and $w := [w_1, w_2, w_3, w_4]^T$. The above equations can then be rewritten as

$$z(s) = M_{11}(s)w(s) + M_{12}(s)u(s)$$

$$y(s) = M_{21}(s)w(s) + M_{22}(s)u(s)$$
$$w(s) = \Delta z(s).$$

where

$$M(s) = \begin{bmatrix} M_{11}(s) \vdots M_{12}(s) \\ \cdots \quad \cdots \\ M_{21}(s) \vdots M_{22}(s) \end{bmatrix}$$

$$= \begin{bmatrix} -[D^0]^{-1}D_e & -[D^0]^{-1}D_o & [D^0]^{-1}N_e & [D^0]^{-1}N_o & \vdots & [D^0]^{-1}N^0 \\ -[D^0]^{-1}D_e & -[D^0]^{-1}D_o & [D^0]^{-1}N_e & [D^0]^{-1}N_o & \vdots & [D^0]^{-1}N^0 \\ 0 & 0 & 0 & 0 & \vdots & 1 \\ 0 & 0 & 0 & 0 & \vdots & 1 \\ \cdots\cdots & \cdots\cdots & \cdots\cdots & \cdots\cdots & & \cdots\cdots \\ -[D^0]^{-1}D_e & -[D^0]^{-1}D_o & [D^0]^{-1}N_e & [D^0]^{-1}N_o & \vdots & [D^0]^{-1}N^0 \end{bmatrix} \quad (11.54)$$

and

$$\Delta = \Delta^R := \begin{bmatrix} \lambda_1 & & & \\ & \lambda_2 & & \\ & & \lambda_3 & \\ & & & \lambda_4 \end{bmatrix}.$$

Consequently, we have the configuration shown in Figure 11.18.

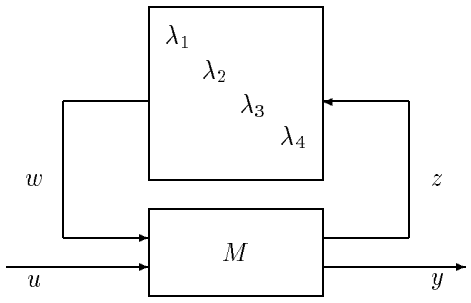

Figure 11.18. 4-parameter feedback representation of an interval system

The result established in Step 2 of the proof of GKT given in Chapter 7 tells us that robust stability of the four parameter feedback structure given in Figure 11.18 is further equivalent to that of a reduced set of one-parameter extremal feedback structures in which each structure contains a single perturbation block. In Figure 11.19 we display a typical such extremal system structure where λ_1 is the only perturbation block and the remaining λ's are set to the vertex values $+1$ or -1.

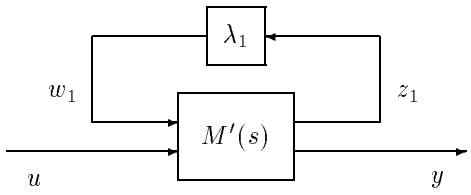

Figure 11.19. A typical element of the extremal set $\mathbf{G}_{\mathrm{E}}(s)$

This is denoted in the equations by writing $\lambda_2 = \lambda_2^*$, $\lambda_3 = \lambda_3^*$ and $\lambda_4 = \lambda_4^*$. The system equations assume the form

$$\begin{bmatrix} z_1 \\ y \end{bmatrix} = \underbrace{\begin{bmatrix} M'_{11}(s) & M'_{12}(s) \\ M'_{21}(s) & M'_{22}(s) \end{bmatrix}}_{M'(s)} \begin{bmatrix} w_1 \\ u \end{bmatrix} \tag{11.55}$$

with

$$w_1 = \lambda_1 z_1$$

where

$$M'_{11}(s) = M'_{21}(s) = (1 + \lambda_2^*[D^0]^{-1}D_o)^{-1}[D^0]^{-1}D_e$$
$$M'_{21}(s) = M'_{22}(s) = (1 + \lambda_2^*[D^0]^{-1}D_o)^{-1}[D^0]^{-1}N^0 + \lambda_3^*[D^0]^{-1}N_e + \lambda_4^*[D^0]^{-1}N_o.$$

The interval plant $\mathbf{G}(s)$ can *always* be replaced by the above set of one-parameter structures $\mathbf{G}_{\mathrm{E}}(s)$ regardless of the rest of the feedback system. If the intervals in which the parameters vary are not fixed *apriori* one can also determine their maximum permissible excursion using the same framework. The only difference in this case is that the Kharitonov polynomials, and therefore the system M' defined from them, have parameters which depend on the dilation parameter ϵ as shown below in Figure 11.20.

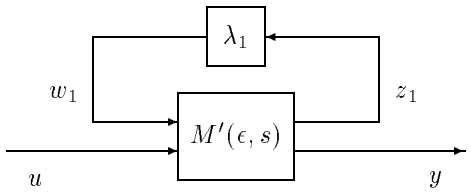

Figure 11.20. An element of $\mathbf{G}_{\mathrm{E}}(\epsilon, s)$

The limiting value ϵ^* of ϵ is determined as the smallest value of ϵ for which the control system containing one of the one parameter structures representing $\mathbf{G}_{\mathrm{E}}(\epsilon, s)$ acquires a pole on the imaginary axis. Thus ϵ^* can be found using several methods which include the Segment Lemma and the Bounded Phase Conditions of Chapter 2. Of course, by restricting attention to the class of controllers which satisfy the vertex conditions given in GKT we get further simplification in that *all* the λ's can be frozen at vertices, and ϵ^* can be found from the vertex systems.

The above discussion may be summarized by stating that if $\mathbf{G}(s)$ is an interval plant contained within a control system structure, we can always replace it with the set of one-parameter extremal systems $\mathbf{G}_{\mathrm{E}}(s)$ for the purposes of determining worst case performance and stability margins and for carrying out worst case frequency response analysis. This observation holds also for linear interval systems and polytopic systems as defined in Chapter 8. In the case of multilinear interval systems we can again replace the plant set $\mathbf{G}(s)$ by the corresponding set of extremal systems $\mathbf{G}_{\mathrm{E}}(s)$ which now consist of a set reduced dimensional multilinear systems in terms of the interval parameters λ_i. This can in turn be replaced by a polytopic family using the Mapping Theorem. Finally, an extremal one-parameter family can be constructed for this polytopic system as shown in this chapter.

11.7.2 Interval Plant with H_∞ Norm-Bounded Uncertainty

Now let us consider the mixed uncertainty system in Figure 11.21.

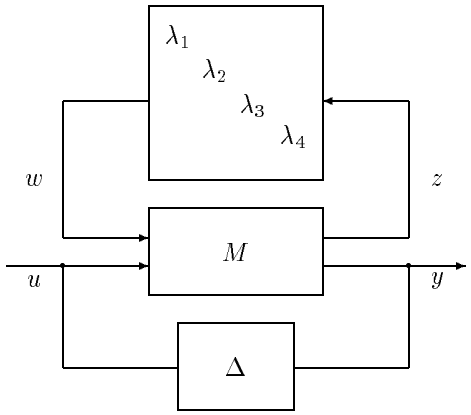

Figure 11.21. 4-parameter representation of interval system with unstructured uncertainty

It consists of an interval plant with an unstructured perturbation block Δ lying in a H_∞ ball of specified radius. As before, the interval plant can be represented in terms of four feedback parameters around a suitable interconnection transfer matrix $M(s)$. We can now represent all the perturbations, parametric as well as unstructured, in feedback form around a suitably defined system $P(s)$. Thus, we have the structure shown in Figure 11.22 with an appropriate $P(s)$.

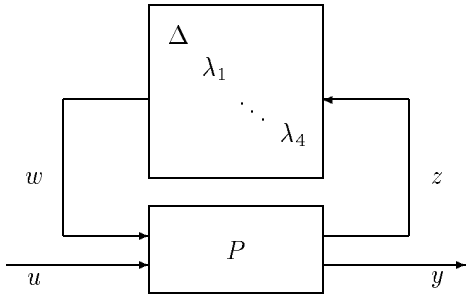

Figure 11.22. Feedback representation of mixed uncertainties

Moreover, by using the result of Chapter 9 on extremal values of H_∞ norms, this four-parameter system can be reduced to the extremal set of single parameter uncertainty problems. A typical element of this extremal set is shown in Figure 11.23 with an appropriate $P'(s)$.

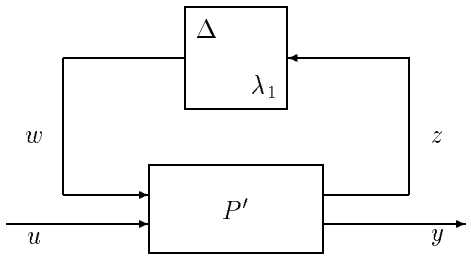

Figure 11.23. A typical element of the extremal set of systems

By eliminating the feedback loop associated with λ this can also be represented as the structure shown in Figure 11.24.

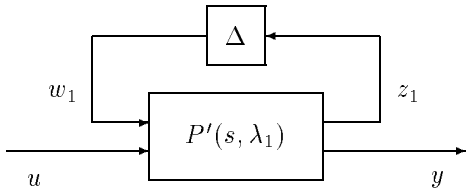

Figure 11.24. Equivalent representation of an extremal system

11.7.3 Multiple Interval Systems and Unstructured Blocks

Let us now consider the general configuration given in Figure 11.25.

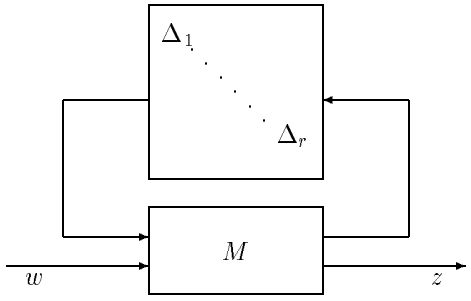

Figure 11.25. System with uncertainties represented in feedback form

$M(s)$ is an interconnection transfer function matrix of suitable dimensions and $\Delta^U(s)$ is a diagonal matrix containing all the unstructured system perturbations. The unstructured perturbations can be considered by introducing the class of perturbations $\mathbf{D}^u(r)$ defined as

$$\mathbf{D}^u(r) = \left\{ \Delta^U = \begin{bmatrix} \Delta_1 & & \\ & \ddots & \\ & & \Delta_r \end{bmatrix} \; : \; \Delta_i \in \mathbf{\Delta}_1 \right\} \tag{11.56}$$

where $\mathbf{\Delta}_1$ is a ball in the space of H_∞ real rational functions, denoted by RH_∞, with radius 1

$$\mathbf{\Delta}_1 = \{\Delta \; : \; \Delta \in RH_\infty, \;\; \|\Delta\|_\infty \leq 1\}\,.$$

Parametric perturbations or uncertainty can be modeled by letting interval transfer functions represent each physically distinct subsystem. These individual systems can then be "pulled out" and represented in feedback form as described earlier. The

result of doing this is the general representation of the system shown in Figure 11.26.

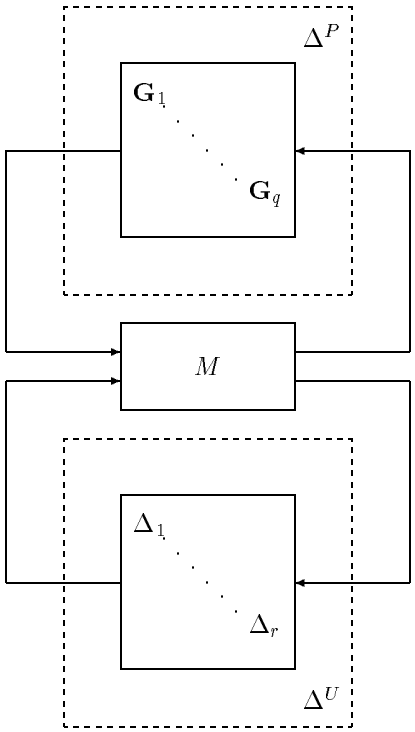

Figure 11.26. Feedback representation of multiple interval plants and unstructured uncertainties

In this representation, the Δ^U block represents multiple norm-bounded uncertainties, and the Δ^P block accounts for parameter perturbations modeled as the set of independent interval systems $\mathbf{G}^i(s)$ arranged in diagonal form:

$$\mathbf{D}^G(q) = \left\{ \begin{bmatrix} G_1 & & \\ & \ddots & \\ & & G_q \end{bmatrix} \; : \; G_i \in \mathbf{G}^i \right\}. \tag{11.57}$$

From the discussion of the last subsection we can immediately replace each interval system by a four-parameter set. Further we can also replace each interval system

$\mathbf{G}^i(s)$ by the corresponding extremal set $\mathbf{G}^i_{\mathrm{E}}$:

$$\mathbf{D}^G_{\mathrm{E}}(q) = \left\{ \begin{bmatrix} G_1 & & \\ & \ddots & \\ & & G_q \end{bmatrix} \; : \; G_i \in \mathbf{G}^i_{\mathrm{E}} \right\}. \tag{11.58}$$

For carrying out frequency domain analysis, the system in Figure 11.26 can therefore be replaced by Figure 11.27 where Δ^{UP} belongs to the mixed complex-real perturbation class $\mathbf{D}^{UP}$ defined as

$$\mathbf{D}^{UP}(r;4q) = \left\{ \begin{bmatrix} \Delta^U & & & \\ & \lambda_1 & & \\ & & \ddots & \\ & & & \lambda_{4q} \end{bmatrix} \right\}. \tag{11.59}$$

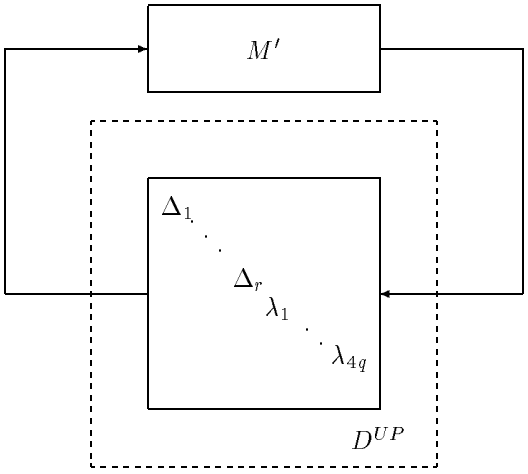

Figure 11.27. Feedback representation of mixed complex-real block diagonal uncertainties

This representation can be used to formulate a variety of robust stability and performance problems. We illustrate this by considering two specific examples.

Example 11.6. Consider the control system shown in Figure 11.28. In this system there are two independent subsystems containing parametric uncertainty which are modelled by the interval systems $G_1(s) \in \mathbf{G}^1(s)$ and $G_2(s) \in \mathbf{G}^2(s)$. Unstructured perturbations are represented by the block Δ_1, and appropriate scalings have been introduced to allow Δ_1 to belong to $\mathbf{\Delta}_1$, the H_∞ ball of radius unity. The specifications on the system performance are stated as the following requirements:

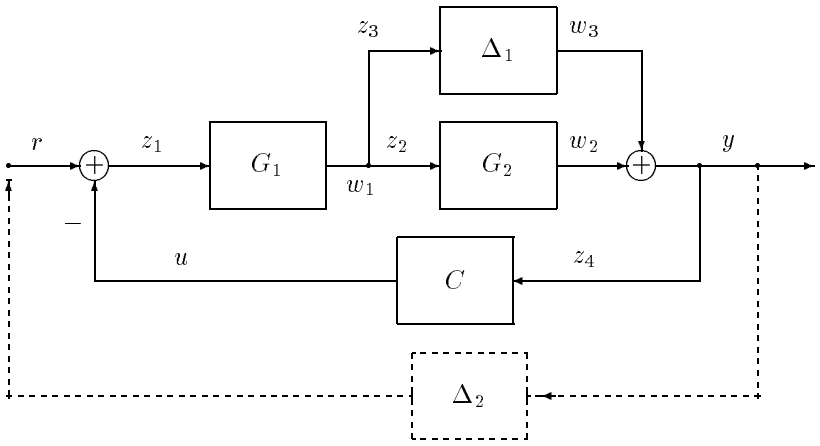

Figure 11.28. Robust performance problem (Example 11.6)

1) *Robust Stability* The system must be stable for all $G_1(s) \in \mathbf{G}^1(s)$, $G_2(s) \in \mathbf{G}^2(s)$, $\Delta_1 \in \mathbf{\Delta}_1$ and

2) *Robust Performance* The worst case H_∞ norm of the closed loop transfer function be bounded by unity:

$$\sup_{\mathbf{G}^1, \mathbf{G}^2, \mathbf{\Delta}_1} \|T_{ry}(G_1, G_2, \Delta_1)\|_\infty < 1,$$

where T_{ry} is the transfer function from r to y.

This problem can be cast in the framework developed above, and treated as a robust stability problem by introducing a fictitious performance block $\Delta_2 \in \mathbf{\Delta}_1$ connected between r and y as shown in Figure 11.28. The equations describing the system in Figure 11.28 are

$$\begin{bmatrix} z_1 \\ z_2 \\ z_3 \\ z_4 \\ y \end{bmatrix} = \begin{bmatrix} 0 & 0 & 0 & 1 & -1 \\ 1 & 0 & 0 & 0 & 0 \\ 1 & 0 & 0 & 0 & 0 \\ 0 & 1 & 1 & 0 & 0 \\ 0 & 1 & 1 & 0 & 0 \end{bmatrix} \begin{bmatrix} w_1 \\ w_2 \\ w_3 \\ r \\ u \end{bmatrix}$$

$$\begin{bmatrix} w_1 \\ w_2 \\ w_3 \\ r \\ u \end{bmatrix} = \begin{bmatrix} G_1 & 0 & 0 & 0 & 0 \\ 0 & G_2 & 0 & 0 & 0 \\ 0 & 0 & \Delta_1 & 0 & 0 \\ 0 & 0 & & \Delta_2 & 0 \\ 0 & 0 & 0 & 0 & C \end{bmatrix} \begin{bmatrix} z_1 \\ z_2 \\ z_3 \\ z_4 \\ y \end{bmatrix}.$$

The "feedback" perturbations belong to the class

$$\mathbf{D}^G(2) = \left\{ \begin{bmatrix} G_1 & \\ & G_2 \end{bmatrix} \ : \ G_1 \in \mathbf{G}^1, G_2 \in \mathbf{G}^2 \right\}$$

$$\mathbf{D}^U(2) = \left\{ \begin{bmatrix} \Delta_1 & \\ & \Delta_2 \end{bmatrix} \ : \ \Delta_1, \Delta_2 \in \mathbf{\Delta}_1 \right\}$$

and the interconnection matrix is

$$M = \begin{bmatrix} 0 & 0 & 0 & 1 & -1 \\ 1 & 0 & 0 & 0 & 0 \\ 1 & 0 & 0 & 0 & 0 \\ 0 & 1 & 1 & 0 & 0 \\ 0 & 1 & 1 & 0 & 0 \end{bmatrix}.$$

Example 11.7. We consider the system in Figure 11.29.

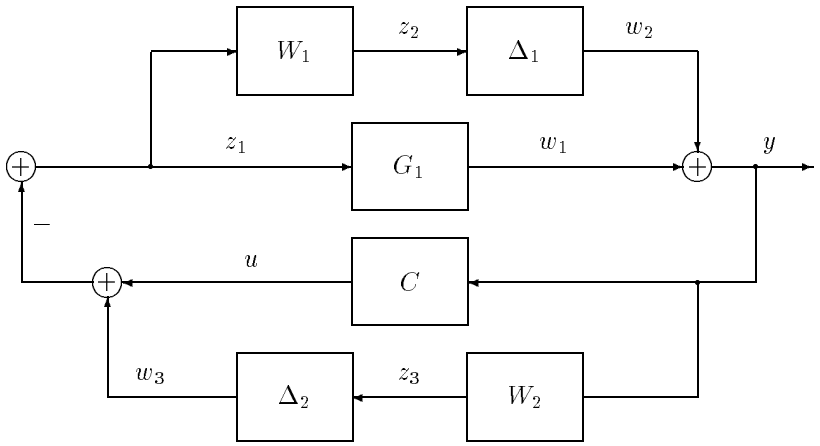

Figure 11.29. Robust stability problem (Example 11.7)

Parameter uncertainty is represented by the interval system $G_1(s) \in \mathbf{G}^1(s)$ and unstructured uncertainty consists of two independent blocks $\Delta_1, \Delta_2 \in \mathbf{\Delta}_1$. $W_1(s)$ and $W_2(s)$ represent frequency weightings and consist of fixed stable, proper minimum phase transfer functions. The system equations are

$$\begin{bmatrix} z_1 \\ z_2 \\ z_3 \\ y \end{bmatrix} = \begin{bmatrix} 0 & 0 & -1 & -1 \\ 0 & 0 & -W_1 & -W_1 \\ W_2 & W_2 & 0 & 0 \\ 1 & 1 & 0 & 0 \end{bmatrix} \begin{bmatrix} w_1 \\ w_2 \\ w_3 \\ u \end{bmatrix}$$

$$\begin{bmatrix} w_1 \\ w_2 \\ w_3 \\ u \end{bmatrix} = \begin{bmatrix} G_1 & 0 & 0 & 0 \\ 0 & \Delta_1 & 0 & 0 \\ 0 & 0 & \Delta_2 & 0 \\ 0 & 0 & 0 & C \end{bmatrix} \begin{bmatrix} z_1 \\ z_2 \\ z_3 \\ y \end{bmatrix}.$$

This configuration fits the general structure developed above with the "feedback" perturbation classes being

$$\mathbf{D}^G(1) = \left\{ G_1 \ : \ G_1 \in \mathbf{G}^1 \right\}$$

and

$$\mathbf{D}^U(2) = \left\{ \begin{bmatrix} \Delta_1 & \\ & \Delta_2 \end{bmatrix} \ : \ \Delta_1, \Delta_2 \in \mathbf{\Delta}_1 \right\}$$

and the interconnection matrix

$$M = \begin{bmatrix} 0 & 0 & -1 & -1 \\ 0 & 0 & -W_1 & -W_1 \\ W_2 & W_2 & 0 & 0 \\ 1 & 1 & 0 & 0 \end{bmatrix}.$$

11.7.4 Extremal Properties

We have shown that parameter uncertainty can be modelled by interval systems and that both parametric and norm-bounded uncertainty can be represented in feedback form. Moreover, each interval system can be replaced, as far as worst case frequency domain analysis is concerned, by the corresponding reduced 4-parameter family.

Let us now consider the system in Figure 11.26. Suppose that a stabilizing controller for the nominal system has been connected between y and u. The controller is stabilizing when the feedback perturbation is zero. Let $M(s)$ denote the interconnection matrix with the controller attached. We now wish to determine if the control system is robustly stable under the feedback perturbations given. This is a real-complex mixed perturbation robust stability problem with the diagonal "feedback" perturbation matrix (see Figure 11.27)

$$\mathbf{D}^{UP} = \left\{ D^{UP} = \begin{bmatrix} \Delta_1 & & & & & \\ & \ddots & & & & \\ & & \Delta_r & & & \\ & & & \lambda_1 & & \\ & & & & \ddots & \\ & & & & & \lambda_{4m} \end{bmatrix} \ : \ \Delta_1 \in \mathbf{\Delta}_1, \ |\lambda_i| \leq 1 \right\}.$$

We make the standing assumption that the McMillan degree of the system remains invariant under the perturbations. The first observation we can make is obvious.

Theorem 11.12 *The system in Figure 11.26 is Hurwitz stable for all* $D^P \in \mathbf{D}^G(m)$ *and all* $D^u \in \mathbf{D}^U(r)$ *if and only if the system in Figure 11.27 is Hurwitz stable for all* $D^{UP} \in \mathbf{D}^{UP}$.

The above theorem actually applies more generally. For instance a more general formulation could allow for repeated interval system blocks.

As a further simplification in the above result, we can replace each interval system $\mathbf{G}^i(s)$ by the corresponding set of extremal systems $\mathbf{G}^i_{\mathrm{E}}(s)$. This corresponds to replacing each set of 4 λ_i's in Figure 11.27 by their exposed edges.

Theorem 11.13 *The system in Figure 11.26 is Hurwitz stable for all* $D^P \in \mathbf{D}^G(m)$ *and all* $D^u \in \mathbf{D}^U(r)$ *if and only if the system in Figure 11.27 is Hurwitz stable for all* $D_P \in \mathbf{D}^G_{\mathrm{E}}(m)$ *and all* $D^u \in \mathbf{D}^U(r)$.

Proof. The proof of this result follows immediately from the fact that the characteristic equation of the system in Figure 11.27 is a multilinear function of the interval systems $\mathbf{G}^i_{\mathrm{E}}(s)$. Therefore, by the result derived in Theorem 11.8, we can replace each interval system $\mathbf{G}^i(s)$ by the corresponding extremal set $\mathbf{G}^i_{\mathrm{E}}(s)$. ♣

Remark 11.5. The result stated above can be interpreted in terms of the worst case norm-bounded stability margin of the system over the interval parameter uncertainty set. For a prescribed D^P, this stability margin is usually measured as a norm of the smallest destabilizing diagonal perturbation matrix Δ. The norm customarily used is the maximum singular value. The worst case value of this stability margin as D^P ranges over the interval systems can be found by restricting D^P to range over the extremal systems only. This is obviously a tremendous saving in computational effort.

11.8 EXERCISES

11.1 Consider the feedback system with a parallel structure in the forward path as shown in Figure 11.30.

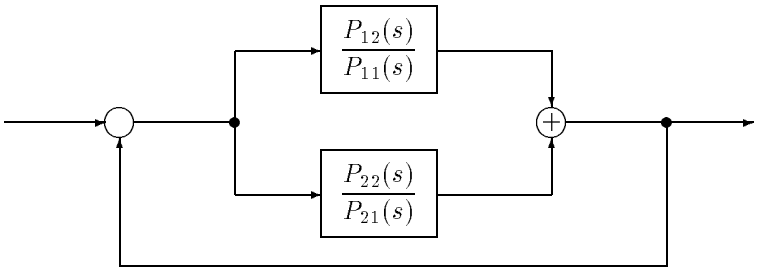

Figure 11.30. Feedback system with parallel structure (Exercise 11.1)

Suppose that

$$P_1(s) = \frac{P_{12}(s)}{P_{11}(s)} = \frac{\alpha_2 s^2 + \alpha_1 s + \alpha_0}{s^2 + \alpha_4 s + \alpha_3}$$
$$P_2(s) = \frac{P_{22}(s)}{P_{21}(s)} = \frac{\beta_2 s^2 + \beta_1 s + \beta_0}{s^2 + \beta_4 s + \beta_3}$$

where the parameters vary as follows:

$$\alpha_i \in [\alpha_i^-, \alpha_i^+], \quad \text{and} \quad \beta_i \in [\beta_i^-, \beta_i^+], \qquad i = 0, 1, 2, 3, 4.$$

a) Use the multilinear GKT (Theorem 11.1) to write down all the manifolds which are necessary to verify the robust Hurwitz stability of the closed loop system.

b) Write down all the manifolds which are necessary to verify the robust stability of the closed loop system with respect to the stability region which is a circle centered at $-\gamma$ with radius r where $\gamma > r > 0$.

c) One may observe that a significant reduction, in terms of the number of manifolds to be checked, is achieved for the case a) over b). Explain the reason.

11.2 Consider the feedback system shown in Figure 11.31.
Let

$$C(s) = \frac{1}{s+1}, \quad P_1(s) = \frac{p_0}{s+q_0}, \quad P_2(s) = \frac{p_1}{s+q_1}$$

with

$$q_0 \in [0.5, 1.5], \quad p_0 \in [0.5, 1.5], \quad q_1 \in [1.5, 2.5], \quad p_1 \in [0.5, 1.5].$$

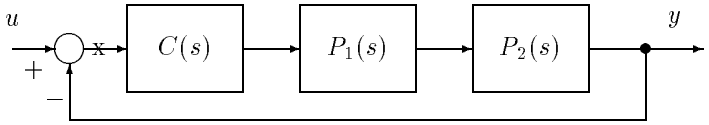

Figure 11.31. Feedback system (Exercise 11.2)

Using the polytopic approximation, plot the Bode magnitude and phase envelopes of the open loop system and estimate from this the guaranteed gain and phase margin of the family.

11.3 For the feedback system given in Exercise 11.2,

a) plot the Nyquist envelope of the closed loop transfer function by using the polytopic approximation,

b) from the plot in a) determine the exact guaranteed gain and phase margin of the system and compare with the estimates obtained in the previous exercise,

c) suppose that a nonlinear feedback gain is connected as shown in Figure 11.32.

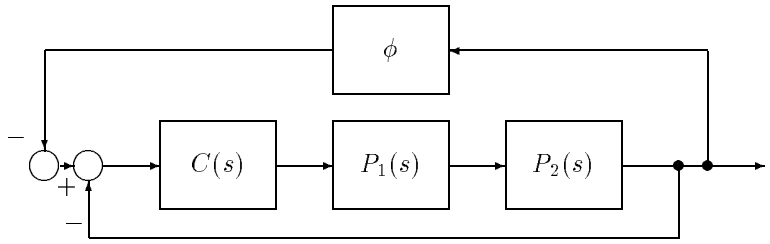

Figure 11.32. Feedback system with nonlinear gain (Exercise 11.3)

Determine the Lur'e sector for which the the closed loop system is robustly absolutely stable.

11.4 Referring to the system given in Exercise 11.2, find the maximum value of M-peak of the closed loop system. What can you say about the minimum value of M-peak?
Hint: The maximum value of M-peak is obtained by selecting the peak value of the upper curve of the magnitude envelope of the closed loop system. However, the peak value of the lower curve does not necessarily serve as the minimum value

of M-peak as it may not correspond to M-peak for some bona fide set of system parameters. It can only be a lower bound on the minimum M-peak.

11.5 Referring to the system in Exercise 11.2, plot the magnitude envelope of the error transfer function and determine the worst case amplitude of the error, with respect to unit amplitude sinusoidal inputs, over the parameter set given.

11.6 Consider the feedback system shown below in Figure 11.33.

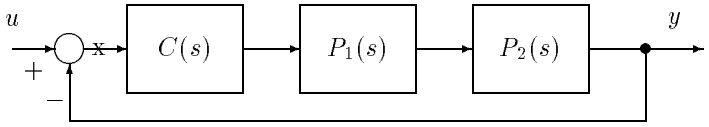

Figure 11.33. Feedback system (Exercise 11.6)

Let

$$C(s) = 2, \quad P_1(s) = \frac{s+\beta_0}{s^2+\beta_1 s+\beta_2}, \quad P_2(s) = -\frac{s+\alpha_0}{s+\alpha_1}$$

with the nominal values of the parameters being

$$\alpha_0^0 = 1.5, \quad \alpha_1^0 = 5, \quad \beta_0^0 = 4, \quad \beta_1^0 = 4.5, \quad \beta_2^0 = 1.5.$$

Determine the maximum parametric stability margin ϵ around these nominal values, i.e.the largest value of ϵ for which the system remains robustly stable for the parameter excursions

$$\alpha_i \in [\alpha_i^0 - \epsilon, \alpha_i^0 + \epsilon], \quad i = 0, 1 \quad \text{and} \quad \beta_j \in [\beta_j^0 - \epsilon, \beta_j^0 + \epsilon], \quad j = 0, 1, 2.$$

11.7 Referring to the system in Exercise 11.6 with ϵ being set to be the stability margin obtained in Exercise 11.6,

a) plot the Nyquist envelope of the open loop multilinear interval system as well as the Nyquist plot of the open loop nominal system,

b) plot the Bode magnitude and phase envelopes of the open loop family of systems as well as the Bode plots of the nominal system.

11.8 In the system of Exercise 11.6, suppose that unstructured uncertainty Δ is introduced as shown in Figure 11.34.
Find the maximum unstructured H_∞ uncertainty that can be tolerated by the system.

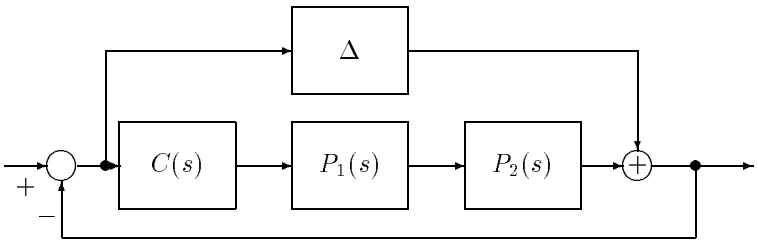

Figure 11.34. Feedback system with unstructured uncertainty (Exercise 11.8)

11.9 Let $C(s)$ be a fixed controller that robustly stabilizes an interval plant $\mathbf{G}(s)$ with extremal set $\mathbf{G}_{\mathrm{E}}(s)$. Define

$$M(s) := \begin{bmatrix} (1+G(s)C(s))^{-1} & (1+G(s)C(s))^{-1} \\ -G(s)C(s)\,(1+G(s)C(s))^{-1} & -G(s)C(s)\,(1+G(s)C(s))^{-1} \end{bmatrix}$$

and let

$$\mathbf{M}(s) := \{M(s) : G(s) \in \mathbf{G}(s)\},$$

and

$$\mathbf{M}_{\mathrm{E}}(s) := \{M(s) : G(s) \in \mathbf{G}_{\mathrm{E}}(s)\}.$$

Consider the perturbation structure $\mathbf{D}(2)$ of all diagonal perturbations of the form $D = \mathrm{diag}\,\{\Delta_1, \Delta_2\}$ where $\|\Delta_i\|_\infty < 1$. Let $M(s)$ be any element in $\mathbf{M}(s)$, and denote by $M(j\omega)$ its evaluation at the $j\omega$-axis. Let $\bar{\sigma}(M)$ denote the maximum singular value of M. We can define $\mu_{\mathbf{D}(2)}(M(j\omega)$ as follows:

$$\frac{1}{\mu_{\mathbf{D}(2)}(M(j\omega))} := \min\{\bar{\sigma}(D) : D \in \mathbf{D}(2), \quad \det(I + M(j\omega)D) = 0\}.$$

Show that

$$\sup_{M\in\mathbf{M}} \sup_{\omega} \mu_{\mathbf{D}(2)}(M(j\omega)) = \sup_{M\in\mathbf{M}_{\mathrm{E}}} \sup_{\omega} \mu_{\mathbf{D}(2)}(M(j\omega)).$$

Hint: Replace Δ_i in $\det(I + M(j\omega)D) = 0$ by complex numbers δ_i and apply the complex version of GKT (Chapter 7).

11.9 NOTES AND REFERENCES

The multilinear version of the Generalized Kharitonov Theorem given here is contained in the papers by Chapellat, Keel, and Bhattacharyya [66] and Chapellat, Dahleh, and Bhattacharyya [65]. The extremal properties with respect to various

margins given in this chapter are described in the paper by Chapellat, Keel, and Bhattacharyya [67]. The result on Hurwitz stability of interval polynomial matrices (Theorem 11.2) is due to Kokame and Mori [150]. The method of constructing the frequency template of a multilinear interval control systems given in Section 11.4.1 is described in Ahmad, Keel and Bhattacharyya [8]. Saeki [199] also obtained a sufficient condition for robust stability of such classes of systems by applying the Mapping Theorem to the Nyquist stability criterion. In Barmish and Shi [17] the case $m = 2$, $\mathbf{\Delta}(s) = P_{11}(s)P_{12}(s)+P_{21}(s)P_{22}$, was treated and alternative necessary and sufficient conditions for robust stability were derived. Kraus, Mansour and Anderson [154] showed that testing for real unstable roots of a multilinear polynomial could be achieved by examining the stability of a finite number of vertex polynomials while checking for unstable complex roots in general involved examining the real solutions of a set of simultaneous polynomial equations. In Zeheb [246] explicit necessary and sufficient conditions are derived for the case of two parameters. The representation given in Section 11.7 including Examples 11.6 and 11.7 are due to Dahleh, Tesi and Vicino [72] and the result described in Exercise 11.9 is due to Dahleh, Tesi and Vicino [70].

Chapter 12

STATE SPACE PARAMETER PERTURBATIONS

In this chapter we describe some robust parametric results formulated specifically for state space models. We first deal with the robust stability problem for interval matrices. When the parameters appear in the matrices in a unity rank perturbation structure, the characteristic polynomial of the matrix is a multilinear function of the parameters. This allows us to use the Mapping Theorem described in Chapter 11 to develop a computational algorithm based on calculating the phase difference over the vertices of the parameter set. Next we introduce some Lyapunov based methods for parameter perturbations in state space systems. A stability region in parameter space can be calculated using this technique and a numerical procedure for enlarging this region by adjusting the controller parameters is described. We illustrate this algorithm with an example. The last part of the chapter describes some results on matrix stability radius for the real and complex cases and for some special classes of matrices.

12.1 INTRODUCTION

Most of the results given in this book deal with polynomials containing parameter uncertainty. These results can be directly used when the system model is described by a transfer function whose coefficients contain the uncertain parameters. When the system model is described in the state space framework, the parameters appear as entries of the state space matrices. The polynomial theory can then be applied by first calculating the characteristic polynomial of the matrix as a function of its parameters. In this chapter, the aim is to provide some computational procedures which can determine robust stability and compute stability margins for the case in which parameters appear linearly in the state space matrices. Under the technical assumption that the perturbation structure is of unity rank the characteristic polynomial coefficients depend on the parameters in multilinear form. This allows us to use the Mapping Theorem of Chapter 11 to develop an effective computational technique to determine robust stability. This is illustrated with numerical examples.

Next, we describe a Lyapunov based technique to handle perturbations of state space matrices. A stability region in parameter space is determined by this method. While this method does not require us to compute the characteristic polynomial, the stability region obtained from this method is conservative. However, the method gives a direct way to handle perturbations of state space matrices. Furthermore, with these formulas, the stability margin can be increased through optimization over the controller parameter space. This procedure is referred to as robustification. The results are compared with the previously described method, which used the Mapping Theorem, via examples.

In the last part of the chapter we describe some formulas for the matrix stability margin for the real and complex cases and for some special classes of matrices.

12.2 STATE SPACE PERTURBATIONS

Consider the state space description of a linear system:

$$\begin{aligned} \dot{x} &= Ax + Bu \\ y &= Cx \end{aligned} \tag{12.1}$$

with the output feedback control

$$u = Ky. \tag{12.2}$$

The stability of the closed loop system is determined by the stability of the matrix $M := A + BKC$. We suppose that the matrices A, B, K, and C are subject to parameter perturbations. Let

$$\mathbf{p} := [p_1, p_2, \cdots, p_l] \tag{12.3}$$

denote the parameters subject to uncertainty and set

$$\mathbf{p} = \mathbf{p}^0 + \Delta\mathbf{p} \tag{12.4}$$

where $\mathbf{p}^0$ is the nominal parameter and $\Delta\mathbf{p}$ denotes a perturbation. Write

$$\begin{aligned} M(\mathbf{p}) &= M(\mathbf{p}^0 + \Delta\mathbf{p}) \\ &= M(\mathbf{p}^0) + \Delta M(\mathbf{p}^0, \Delta\mathbf{p}). \end{aligned} \tag{12.5}$$

Assuming that the entries of $\Delta M(\mathbf{p}^0, \Delta\mathbf{p})$ are linear functions of $\Delta\mathbf{p}$, we can write

$$\Delta M(\mathbf{p}^0, \Delta\mathbf{p}) = \Delta p_1 E_1 + \Delta p_2 E_2 + \cdots + \Delta p_l E_l. \tag{12.6}$$

We shall say that the perturbation structure is of *unity rank* when each matrix E_i has unity rank. The special attraction of unity rank perturbation structures is the fact that in this case the coefficients of the characteristic polynomial of M are multilinear functions of $\Delta\mathbf{p}$ as shown below. When the Δp_i vary in intervals,

this multilinear structure allows us to use the Mapping Theorem of Chapter 11 to develop an effective computational procedure to determine robust stability and stability margins in the parameter space $\mathbf{p}$. The stability margin will be measured as the smallest ℓ_∞ norm of the vector $\Delta\mathbf{p}$ required to make $M(\mathbf{p}^0, \Delta\mathbf{p})$ just unstable.

In the robust stability literature, state space perturbations are often treated by supposing that

$$\Delta M = DUE \tag{12.7}$$

where the matrix U is regarded as a perturbation. In this formulation, one can calculate the smallest induced norm of U for which $M + \Delta M$ just becomes unstable. We remark that the parametric stability margin, defined as the vector norm of the smallest destabilizing vector $\Delta\mathbf{p}$, has a physical significance in terms of the allowable perturbations of the parameter $\mathbf{p}$. Such a direct significance cannot be attached to the matrix norm. Nevertheless, it has become customary to consider matrix valued perturbations and we accordingly define the *matrix stability radius* as the norm of the smallest destabilizing matrix. We give some formulas for the calculation of the matrix stability radius in the real and complex cases.

12.3 ROBUST STABILITY OF INTERVAL MATRICES

We first establish that the unity rank perturbation structure leads to multilinear dependence of the characteristic polynomial coefficients on the parameter $\mathbf{p}$.

12.3.1 Unity Rank Perturbation Structure

Let us suppose that

$$M(\mathbf{p}) := \underbrace{M(\mathbf{p}^0)}_{M_0} + \Delta p_1 E_1 + \Delta p_2 E_2 + \cdots + \Delta p_l E_l. \tag{12.8}$$

Lemma 12.1 *Under the assumption that* $\operatorname{rank}(E_i) = 1$ *for each* i*, the coefficients of the characteristic polynomial of* $M(\mathbf{p})$ *are multilinear functions of* $\mathbf{p}$*.*

Proof. Write

$$\delta(s, \mathbf{p}) = \det\left[sI - M(\mathbf{p})\right].$$

In $\delta(s, \mathbf{p})$, fix all parameters p_j, $j \neq i$ and denote the resulting one parameter function as $\delta(s, p_i)$. To prove the lemma, it is enough to show that $\delta(s, p_i)$ is a linear function of p_i for fixed $s = s^*$. Now since E_i is of unity rank, we write $E_i = b_i c_i^T$ where b_i and c_i are appropriate column vectors. Then

$$\delta(s^*, p_i) = \det\left(s^* I - \underbrace{M_0 - \sum_{j \neq i} p_j E_j}_{\bar{A}} - p_i b_i c_i^T\right)$$

$$
\begin{aligned}
&= \det\left(s^*I - \bar{A} - p_i b_i c_i^T\right) \\
&= \det\left\{(s^*I - \bar{A})\left[I - p_i \underbrace{(s^*I - \bar{A})^{-1}}_{\hat{A}(s^*)} b_i c_i^T\right]\right\} \\
&= \det(s^*I - \bar{A}) \det\left(I - p_i \hat{A}(s^*) b_i c_i^T\right) \\
&= \det(s^*I - \bar{A}) p_i^n \det\left(p_i^{-1} I - \hat{A}(s^*) b_i c_i^T\right).
\end{aligned}
$$

Notice that $\hat{A}(s^*)b_i c_i^T$ is of unity rank. Let λ denote the only nonzero eigenvalue of this matrix. We have

$$
\begin{aligned}
\delta(s^*, p_i) &= p_i^n \left[p_i^{-n+1}\left(p_i^{-1} - \lambda\right)\right] \det\left(s^*I - \bar{A}\right) \\
&= p_i^n \left[p_i^{-n} - \lambda p_i^{-n+1}\right] \det\left(s^*I - \bar{A}\right) \\
&= (1 - \lambda p_i) \det\left(s^*I - \bar{A}\right).
\end{aligned}
$$

Thus we have proved that $\delta(s, p_i)$ is a linear function of p_i. ♣

12.3.2 Interval Matrix Stability via the Mapping Theorem

The objectives are to solve the following problems:

Problem 1 Determine if each matrix $M(\mathbf{p})$ remains stable as the parameter $\mathbf{p}$ ranges over given perturbation bounds $p_i^- \le p_i \le p_i^+, \quad i = 1, \cdots, l$.

Problem 2 With a stable $M(\mathbf{p}^0)$, determine the maximum value of ϵ so that the matrix $M(\mathbf{p})$ remains stable under all parameter perturbations ranging over $p_i^0 - w_i\epsilon \le p_i \le p_i^0 + w_i\epsilon$ for predetermined weights $w_i > 0$.

These problems may be effectively solved by using the fact that the characteristic polynomial of the matrix is a multilinear function of the parameters. This will allow us to use the algorithm developed in Chapter 11 for testing the robust stability of such families.

The problem 1 can be solved by the following algorithm:

Step 1: Determine the eigenvalues of the matrix $M(\mathbf{p})$ with $\mathbf{p}$ fixed at each vertex of $\mathbf{\Pi}$. With this generate the characteristic polynomials corresponding to the vertices of $\mathbf{\Pi}$.

Step 2: Verify the stability of the line segments connecting the vertex characteristic polynomials. This may be done by checking the Bounded Phase Condition or the Segment Lemma.

We remark that the procedure outlined above does not require the determination of the characteristic polynomial as a *function* of the parameter $\mathbf{p}$. It is enough to

know that the function is multilinear. To determine the maximum value of ϵ which solves the second problem, we may simply repeat the previous steps for incremental values of ϵ. In fact, an upper bound $\bar{\epsilon}$ can be found as that value of ϵ for which one of the *vertices* becomes just unstable. A lower bound $\underline{\epsilon}$ can be determined as the value of ϵ for which a *segment* joining the vertices becomes unstable as follows:

Step 1: Set $\underline{\epsilon} = \bar{\epsilon}/2$

Step 2: Check the maximal phase differences of the vertex polynomials over the parameter box corresponding to $\underline{\epsilon}$.

Step 3: If the maximal phase difference is less than π radians, then increase $\underline{\epsilon}$ to $\underline{\epsilon} + (\bar{\epsilon} - \underline{\epsilon})/2$ for example, and repeat Step 2.

Step 4: If the maximal phase difference is π radians or greater, then decrease $\underline{\epsilon}$ to $\underline{\epsilon} - (\bar{\epsilon} - \underline{\epsilon})/2$ and repeat Step 2.

Step 5: This iteration stops when the incremental step or decremental step becomes small enough. This gives a lower bound $\underline{\epsilon}$ and an upper bound $\bar{\epsilon}$.

If $\underline{\epsilon}$ and $\bar{\epsilon}$ are not close enough, we can refine the iteration by partitioning the interval uncertainty set into smaller boxes as in Chapter 10.

The following examples illustrate this algorithm.

12.3.3 Numerical Examples

Example 12.1. Consider the interval matrix:

$$A(\mathbf{p}) = \begin{bmatrix} p_1 & p_2 \\ p_3 & 0 \end{bmatrix}$$

where

$$\mathbf{p}^0 = [p_1^0, p_2^0, p_3^0] = [-3, -2, 1]$$

and

$$p_1 \in [p_1^-, p_1^+] = [-3 - \epsilon, -3 + \epsilon], \quad p_2 \in [p_2^-, p_2^+] = [-2 - \epsilon, -2 + \epsilon],$$

$$p_3 \in [p_3^-, p_3^+] = [1 - \epsilon, 1 + \epsilon].$$

The problem is to find the maximum value ϵ^* so that the matrix $A(\mathbf{p})$ remains stable for all $\epsilon \in [0, \epsilon^*]$. Although the solution to this simple problem can be worked out analytically we work through the steps in some detail to illustrate the calculations involved.

The characteristic polynomial of the matrix is:

$$\delta(s, \mathbf{p}) = s(s - p_1) - p_2 p_3.$$

In general this functional form is not required since only the vertex characteristic polynomials are needed and they can be found from the eigenvalues of the corresponding vertex matrices. Let us now compute the upper bound for ϵ. We have eight vertex polynomials parametrized by ϵ:

$$\mathbf{\Delta}_{\mathrm{V}}(s) := \{\delta_i(s,\mathbf{p}) : \mathbf{p} \in \mathbf{V}\}$$

where

$$\begin{aligned}\mathbf{V} := \{&(p_1^-, p_2^+, p_3^+), (p_1^-, p_2^-, p_3^+), (p_1^-, p_2^+, p_3^-), (p_1^-, p_2^-, p_3^-), (p_1^+, p_2^+, p_3^+),\\ &(p_1^+, p_2^-, p_3^+), (p_1^+, p_2^+, p_3^-), (p_1^+, p_2^-, p_3^-)\}\end{aligned}$$

We found that the vertex polynomial $\delta_3(s)$ has a $j\omega$ root at $\epsilon = 1$. Thus we set $\bar{\epsilon} = 1$. Using the multilinear version of GKT (Theorem 11.1), $\mathbf{\Delta}(s)$ is robustly Hurwitz stable if and only if the following sets are Hurwitz stable:

$$\begin{aligned}
\mathbf{L}_1 &= \left\{s\left[\lambda(s-p_1^-)+(1-\lambda)(s-p_1^+)\right] - p_2^+p_3^+ : \lambda \in [0,1]\right\}\\
\mathbf{L}_2 &= \left\{s\left[\lambda(s-p_1^-)+(1-\lambda)(s-p_1^+)\right] - p_2^-p_3^+ : \lambda \in [0,1]\right\}\\
\mathbf{L}_3 &= \left\{s\left[\lambda(s-p_1^-)+(1-\lambda)(s-p_1^+)\right] - p_2^+p_3^- : \lambda \in [0,1]\right\}\\
\mathbf{L}_4 &= \left\{s\left[\lambda(s-p_1^-)+(1-\lambda)(s-p_1^+)\right] - p_2^-p_3^- : \lambda \in [0,1]\right\}\\
\mathbf{M}_5 &= \left\{s(s-p_1^-) - \left[\lambda_1 p_2^- + (1-\lambda_1)p_2^+\right]\left[\lambda_2 p_3^- + (1-\lambda_2)p_3^+\right] :\right.\\
&\qquad \left.(\lambda_1,\lambda_2) \in [0,1]\times[0,1]\right\}\\
\mathbf{M}_6 &= \left\{s(s-p_1^+) - \left[\lambda_1 p_2^- + (1-\lambda_1)p_2^+\right]\left[\lambda_2 p_3^- + (1-\lambda_2)p_3^+\right] :\right.\\
&\qquad \left.(\lambda_1,\lambda_2) \in [0,1]\times[0,1]\right\}.
\end{aligned}$$

The $\mathbf{L}_i$, $i = 1,2,3,4$ are line segments of polynomials, so we rewrite them as follows:

$$\begin{aligned}
L_1 &= \lambda(s - p_1^- - p_2^+p_3^+) + (1-\lambda)(s - p_1^+ - p_2^+p_3^+)\\
L_2 &= \lambda(s - p_1^- - p_2^-p_3^+) + (1-\lambda)(s - p_1^+ - p_2^-p_3^+)\\
L_3 &= \lambda(s - p_1^- - p_2^+p_3^-) + (1-\lambda)(s - p_1^+ - p_2^+p_3^-)\\
L_4 &= \lambda(s - p_1^- - p_2^-p_3^-) + (1-\lambda)(s - p_1^+ - p_2^-p_3^-)
\end{aligned}$$

Now we need to generate the set of line segments that constructs the convex hull of the image sets of $\mathbf{M}_5$ and $\mathbf{M}_6$. This can be done by connecting every pair of vertex polynomials. The vertex set corresponding to $\mathbf{M}_5$ is:

$$\mathbf{M}_{5\mathrm{V}}(s) := \{M_5 : (\lambda_1,\lambda_2) \in \{(0,0),(0,1),(1,0),(1,1)\}\}.$$

If we connect every pair of these vertex polynomials, we have the line segments:

$$\begin{aligned}
L_5 &= s(s-p_1^-) - \left[\lambda p_2^+p_3^+ + (1-\lambda)p_2^+p_3^-\right]\\
&= \lambda(s^2 - p_1^-s - p_2^+p_3^+) + (1-\lambda)(s^2 - p_1^-s - p_2^+p_3^-)\\
L_6 &= s(s-p_1^-) - \left[\lambda p_2^+p_3^+ + (1-\lambda)p_2^-p_3^+\right]
\end{aligned}$$

$$
\begin{aligned}
&= \lambda(s^2 - p_1^- s - p_2^+ p_3^+) + (1-\lambda)(s^2 - p_1^- s - p_2^- p_3^+) \\
L_7 &= s(s - p_1^-) - \left[\lambda p_2^- p_3^+ + (1-\lambda) p_2^- p_3^-\right] \\
&= \lambda(s^2 - p_1^- s - p_2^- p_3^+) + (1-\lambda)(s^2 - p_1^- s - p_2^- p_3^-) \\
L_8 &= s(s - p_1^-) - \left[\lambda p_2^+ p_3^- + (1-\lambda) p_2^- p_3^-\right] \\
&= \lambda(s^2 - p_1^- s - p_2^+ p_3^-) + (1-\lambda)(s^2 - p_1^- s - p_2^- p_3^-) \\
L_9 &= s(s - p_1^-) - \left[\lambda p_2^+ p_3^- + (1-\lambda) p_2^- p_3^+\right] \\
&= \lambda(s^2 - p_1^- s - p_2^+ p_3^-) + (1-\lambda)(s^2 - p_1^- s - p_2^- p_3^+) \\
L_{10} &= s(s - p_1^-) - \left[\lambda p_2^+ p_3^+ + (1-\lambda) p_2^- p_3^-\right] \\
&= \lambda(s^2 - p_1^- s - p_2^+ p_3^+) + (1-\lambda)(s^2 - p_1^- s - p_2^- p_3^-).
\end{aligned}
$$

Similarly, for $\mathbf{M}_6$ we have the line segments:

$$
\begin{aligned}
L_{11} &= s(s - p_1^+) - \left[\lambda p_2^+ p_3^+ + (1-\lambda) p_2^+ p_3^-\right] \\
&= \lambda(s^2 - p_1^+ s - p_2^+ p_3^+) + (1-\lambda)(s^2 - p_1^+ s - p_2^+ p_3^-) \\
L_{12} &= s(s - p_1^+) - \left[\lambda p_2^+ p_3^+ + (1-\lambda) p_2^- p_3^+\right] \\
&= \lambda(s^2 - p_1^+ s - p_2^+ p_3^+) + (1-\lambda)(s^2 - p_1^+ s - p_2^- p_3^+) \\
L_{13} &= s(s - p_1^+) - \left[\lambda p_2^- p_3^+ + (1-\lambda) p_2^- p_3^-\right] \\
&= \lambda(s^2 - p_1^+ s - p_2^- p_3^+) + (1-\lambda)(s^2 - p_1^+ s - p_2^- p_3^-) \\
L_{14} &= s(s - p_1^+) - \left[\lambda p_2^+ p_3^- + (1-\lambda) p_2^- p_3^-\right] \\
&= \lambda(s^2 - p_1^+ s - p_2^+ p_3^-) + (1-\lambda)(s^2 - p_1^+ s - p_2^- p_3^-) \\
L_{15} &= s(s - p_1^+) - \left[\lambda p_2^+ p_3^- + (1-\lambda) p_2^- p_3^+\right] \\
&= \lambda(s^2 - p_1^+ s - p_2^+ p_3^-) + (1-\lambda)(s^2 - p_1^+ s - p_2^- p_3^+) \\
L_{16} &= s(s - p_1^+) - \left[\lambda p_2^+ p_3^+ + (1-\lambda) p_2^- p_3^-\right] \\
&= \lambda(s^2 - p_1^+ s - p_2^+ p_3^+) + (1-\lambda)(s^2 - p_1^+ s - p_2^- p_3^-).
\end{aligned}
$$

The total number of line segments joining vertex pairs in the parameter space is 28. However the actual number of segments we checked is 16. This saving is due to the multilinear version of GKT (Theorem 11.1), which reduces the set to be checked. By testing these segments we find that they are all stable for $\epsilon < 1$. Since $\epsilon = 1$ corresponds to the instability of the vertex polynomial $\delta_3(s)$ we conclude that the exact value of the stability margin is $\epsilon = 1$. The stability check of the segments can be carried out using the Segment Lemma of Chapter 2.

We can also solve this problem by using the Bounded Phase Condition. The set of vertices is

$$\mathbf{\Delta}_{\mathrm{V}}(s) = \{V_i, i = 1, 2, \cdots, 8\}$$

where

$$
\begin{aligned}
V_1(s) &= s^2 - p_1^+ s - p_2^+ p_3^+ = s^2 - 2s + 2 \\
V_2(s) &= s^2 - p_1^+ s - p_2^- p_3^+ = s^2 - 2s + 6
\end{aligned}
$$

$$
\begin{aligned}
V_3(s) &= s^2 - p_1^+ s - p_2^+ p_3^- = s^2 - 2s \\
V_4(s) &= s^2 - p_1^+ s - p_2^- p_3^- = s^2 - 2s \\
V_5(s) &= s^2 - p_1^- s - p_2^+ p_3^+ = s^2 - 4s + 2 \\
V_6(s) &= s^2 - p_1^- s - p_2^- p_3^+ = s^2 - 4s + 6 \\
V_7(s) &= s^2 - p_1^- s - p_2^+ p_3^- = s^2 - 4s \\
V_8(s) &= s^2 - p_1^- s - p_2^- p_3^- = s^2 - 4s.
\end{aligned}
$$

From the vertex set we see that the difference polynomials $V_i(s) - V_j(s)$ are either constant, first order, antiHurwitz or of the form cs and each of these forms satisfy the conditions of the Vertex Lemma in Chapter 2. Thus the stability of the vertices implies that of the edges. Thus the first encounter with instability can only occur on a vertex. This implies that the smallest value already found of $\epsilon = 1$ for which a vertex becomes unstable is the correct value of the margin.

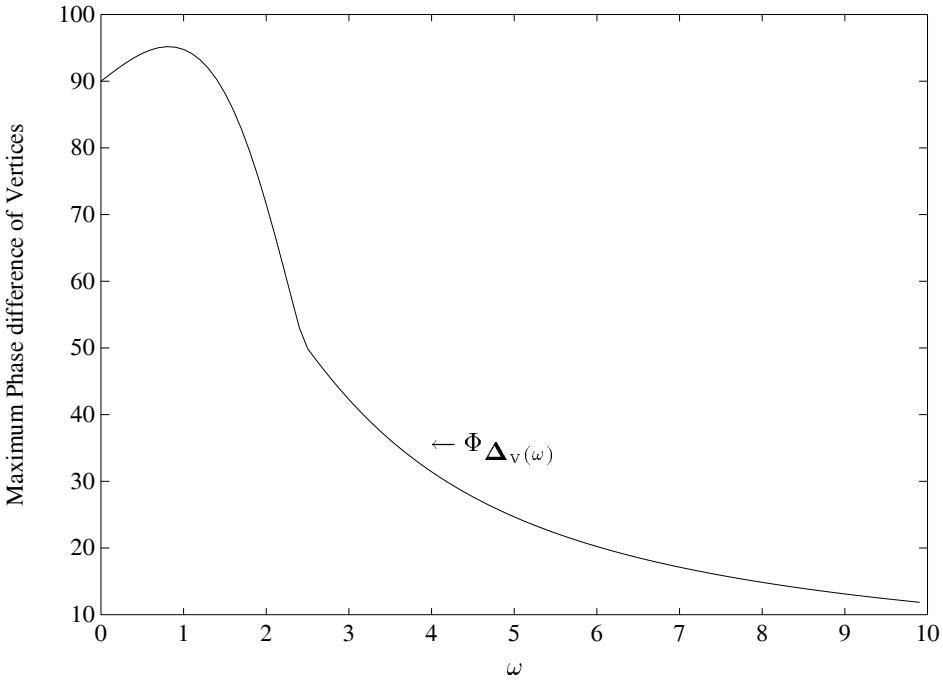

Figure 12.1. Maximum Phase Differences $\Phi_{\mathbf{\Delta}_{\mathrm{V}}(\omega)}$ (in degrees) of Vertex Polynomials (Example 12.1)

This conclusion can also be verified by checking the phases of the vertices. Since there are duplicated vertices, we simply plot phase differences of six distinct vertices of $\mathbf{\Delta}(j\omega)$ with $\epsilon = 1$. Figure 12.1 shows that the maximum phase difference plot as a function of frequency. This plot shows that the maximal phase difference never reaches 180 degrees confirming once again that $\epsilon = 1$ is indeed the true margin.

Remark 12.1. The phase of a vertex which touches the origin cannot be determined and only the phase difference over the vertex set is meaningful. The phase condition can therefore only be used to determine whether the line segment excluding endpoints, intersects the origin. Thus, the stability of all the vertices must be verified independently.

Example 12.2. Let

$$\begin{aligned}\frac{dx}{dt} &= (A + BKC)x \\ &= \left(\begin{bmatrix} -1 & 0 & 0 \\ 0 & -2 & 0 \\ 0 & 0 & -3 \end{bmatrix} + \begin{bmatrix} 1 & 0 \\ 0 & 1 \\ 1 & 1 \end{bmatrix} \begin{bmatrix} -1+k_1 & 0 \\ 0 & -1+k_2 \end{bmatrix} \begin{bmatrix} 1 & 0 & 1 \\ 0 & 1 & 0 \end{bmatrix} \right) x\end{aligned}$$

where

$$k_1 \in [k_1^-, k_1^+] = [-\epsilon, \epsilon] \qquad k_2 \in [k_2^-, k_2^+] = [-\epsilon, \epsilon].$$

We first find all the vertex polynomials.

$$\mathbf{\Delta}_{\mathrm{V}}(s) := \{\delta_i(s, \mathbf{k}_i) : \mathbf{k}_i \in \mathbf{V}, \quad i = 1, 2, 3, 4\}$$

where

$$\mathbf{V} := \left\{(k_1, k_2) : (k_1^+, k_2^+), (k_1^-, k_2^-), (k_1^-, k_2^+), (k_1^+, k_2^-)\right\}.$$

We found that the minimum value of ϵ such that a vertex polynomial just becomes unstable is 1.75. Thus, $\bar{\epsilon} = 1.75$. Then we proceed by checking either the phase condition or the Segment Lemma. If the Segment Lemma is applied, one must verify the stability of six segments joining the four vertices in $\mathbf{\Delta}_{\mathbf{V}}(s)$. If the phase condition is applied, one must evaluate the phases of the four vertex polynomials and find the maximum phase difference at each frequency to observe whether it reaches 180°. Again, the calculation shows that the smallest value of ϵ that results in a segment becoming unstable is 1.75. Thus $\underline{\epsilon} = 1.75$. This shows that the value obtained $\epsilon = 1.75$ is the true margin.

The algorithm can also be applied to the robust stability problem for nonHurwitz regions. The following example illustrates the discrete time case.

Example 12.3. Consider the discrete time system:

$$\underline{x}(k+1) = \begin{bmatrix} -0.5 & 0 & k_2 \\ 1 & 0.50 & -1 \\ k_1 & k_1 & 0.3 \end{bmatrix} \underline{x}(k)$$

For the nominal values of $k_1^0 = k_2^0 = 0$, the system is Schur stable. We want to determine the maximum value of ϵ^* so that for all parameters lying in the range

$$k_1 \in (-\epsilon^*, \epsilon^*) \qquad k_2 \in (-\epsilon^*, \epsilon^*)$$

the system remains Schur stable. Using the procedure, we find the upper bound $\bar{\epsilon} = 0.2745$ which is the minimum value of ϵ which results in a vertex polynomial just becoming unstable. Figure 12.2 shows that the maximum phase difference over all vertices at each $\theta \in [0, 2\pi)$ with $\epsilon = \bar{\epsilon}$ is less than $180°$. Thus we conclude from the Mapping Theorem that the exact parametric stability margin of this system is 0.2745.

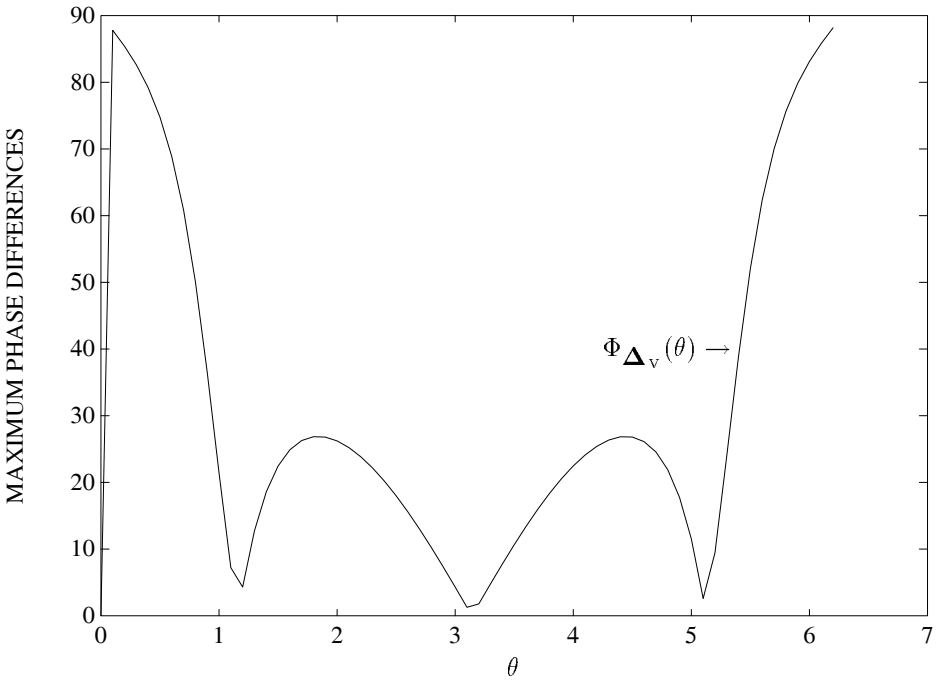

Figure 12.2. $\Phi_{\mathbf{\Delta}_v}(\theta)$ vs θ (Example 12.3)

In the next section we describe a Lyapunov function based approach to parameter perturbations in state space systems which avoids calculation of the characteristic polynomial.

12.4 ROBUSTNESS USING A LYAPUNOV APPROACH

Suppose that the plant equations in the state space form are

$$\begin{aligned} \dot{x} &= Ax + Bu \\ y &= Cx. \end{aligned} \tag{12.9}$$

The controller, of order t, is described by

$$\begin{aligned} \dot{x_c} &= A_c x_c + B_c y \\ u &= C_c x_c + D_c y. \end{aligned} \tag{12.10}$$

The closed-loop system equation is

$$\begin{bmatrix} \dot{x} \\ \dot{x_c} \end{bmatrix} = \begin{bmatrix} A + BD_cC & BC_c \\ B_cC & A_c \end{bmatrix} \begin{bmatrix} x \\ x_c \end{bmatrix}$$

$$= \left(\underbrace{\begin{bmatrix} A & 0 \\ 0 & 0_t \end{bmatrix}}_{A_t} + \underbrace{\begin{bmatrix} B & 0 \\ 0 & I_t \end{bmatrix}}_{B_t} \underbrace{\begin{bmatrix} D_c & C_c \\ B_c & A_c \end{bmatrix}}_{K_t} \underbrace{\begin{bmatrix} C & 0 \\ 0 & I_t \end{bmatrix}}_{C_t} \right) \begin{bmatrix} x \\ x_c \end{bmatrix}. \tag{12.11}$$

Now (12.10) is a stabilizing controller if and only if $A_t + B_t K_t C_t$ is stable. We consider the compensator order to be fixed at each stage of the design process and therefore drop the subscript t. Consider then the problem of robustification of $A + BKC$ by choice of K when the plant matrices are subject to parametric uncertainty.

Let $\mathbf{p} = [p_1, p_2, \cdots, p_r]$ denote a parameter vector consisting of physical parameters that enter the state-space description *linearly*. This situation occurs frequently since the state equations are often written based on physical considerations. In any case combination of primary parameters can always be defined so that the resulting dependence of A, B, C on $\mathbf{p}$ is linear. We also assume that the nominal model (12.9) has been determined with the nominal value $\mathbf{p}^0$ of $\mathbf{p}$. This allows us to treat $\mathbf{p}$ purely as a perturbation with nominal value $\mathbf{p}^0 = 0$. Finally, since the perturbation enters at different locations, we consider that $A + BKC$ perturbs to

$$A + BKC + \sum_{i=1}^{r} p_i E_i$$

for given matrices E_i which prescribe the structure of the perturbation.

We now state a result that calculates the radius of a spherical stability region in the parameter space $\mathbf{p} \in \mathbb{R}^r$. Let the nominal asymptotically stable system be

$$\dot{x}(t) = Mx(t) = (A + BKC)x(t) \tag{12.12}$$

and the perturbed equation be

$$\dot{x}(t) = \left(M + \sum_{i=1}^{r} p_i E_i \right) x(t) \tag{12.13}$$

where the p_i, $i = 1, \cdots, r$ are perturbations of parameters of interest and the E_i, $i = 1, \cdots, r$ are matrices determined by the structure of the parameter perturbations. Let $Q > 0$ be a positive definite symmetric matrix and let P denote the unique positive definite symmetric solution of

$$M^T P + PM + Q = 0. \tag{12.14}$$

Theorem 12.1 *The system (12.13) is stable for all p_i satisfying*

$$\sum_{i=1}^{r} |p_i|^2 < \frac{\sigma_{\min}^2(Q)}{\sum_{i=1}^{r} \mu_i^2} \tag{12.15}$$

where $\mu_i := \|E_i^T P + PE_i\|_2$.

Proof. Under the assumption that M is asymptotically stable with the stabilizing controller K, choose as a Lyapunov function

$$V(x) = x^T P x \tag{12.16}$$

where P is the symmetric positive definite solution of (12.14). Since M is an asymptotically stable matrix, the existence of such a P is guaranteed by Lyapunov's Theorem. Note that $V(x) > 0$ for all $x \neq 0$ and $V(x) \to \infty$ as $\|x\| \to \infty$. We require $\dot{V}(x) \leq 0$ for all trajectories of the system, to ensure the stability of (12.13). Differentiating (12.16) with respect to x along solutions of (12.14) yields

$$\begin{aligned} \dot{V}(x) &= \dot{x}^T P x + x^T P \dot{x} \\ &= x^T (M^T P + PM) x + x^T \left(\sum_{i=1}^{n} p_i E_i^T P + \sum p_i P E_i \right) x. \end{aligned} \tag{12.17}$$

Substituting (12.14) into (12.17) we have

$$\dot{V}(x) = -x^T Q x + x^T \left(\sum_{i=1}^{r} p_i E_i^T P + \sum_{i=1}^{r} p_i P E_i \right) x. \tag{12.18}$$

The stability requirement $\dot{V}(x) \leq 0$ is equivalent to

$$x^T \left(\sum_{i=1}^{r} p_i E_i^T P + \sum_{i=1}^{r} p_i P E_i \right) x \leq x^T Q x. \tag{12.19}$$

Using the so-called Rayleigh principle,

$$\sigma_{\min}(Q) \leq \frac{x^T Q x}{x^T x} \leq \sigma_{\max}(Q), \quad \text{for all} \;\; x \neq 0 \tag{12.20}$$

and we have

$$\sigma_{\min}(Q) x^T x \leq x^T Q x. \tag{12.21}$$

Thus, (12.19) is satisfied if

$$x^T \left(\sum_{i=1}^{r} p_i E_i^T P + \sum_{i=1}^{r} p_i P E_i \right) x \leq \sigma_{\min}(Q) x^T x. \tag{12.22}$$

Since

$$\begin{aligned} \left| x^T \left(\sum_{i=1}^{r} p_i E_i^T P + \sum_{i=1}^{r} p_i P E_i \right) x \right| &\leq \|x^T\|_2 \left\| \left(\sum_{i=1}^{r} p_i E_i^T P + \sum_{i=1}^{r} p_i P E_i \right) \right\|_2 \|x\|_2 \\ &\leq \|x\|_2^2 \left(\sum_{i=1}^{r} |p_i| \, \|E_i^T P + P E_i\|_2 \right), \end{aligned} \tag{12.23}$$

(12.22) is satisfied if

$$\sum_{i=1}^{r} \left(|p_i| \, \|E_i^T P + P E_i\|_2 \right) \leq \sigma_{\min}(Q). \tag{12.24}$$

Let

$$\mu_i := \|E_i^T P + P E_i\|_2 = \sigma_{\max}(E_i^T P + P E_i).$$

Then (12.24) can be rewritten as

$$\begin{aligned} &\sum_{i=1}^{r} \left(|p_i| \, \|E_i^T P + P E_i\|_2 \right) \\ &= \underbrace{(|p_1| \; |p_2| \; \cdots \; \cdots \; |p_r|)}_{\underline{\mathbf{p}}} \underbrace{\begin{pmatrix} \mu_1 \\ \mu_2 \\ \vdots \\ \vdots \\ \mu_r \end{pmatrix}}_{\underline{\mu}} \leq \sigma_{\min}(Q) \end{aligned} \tag{12.25}$$

which is satisfied if

$$\|\underline{\mathbf{p}}\underline{\mu}\|_2^2 \leq \|\underline{\mathbf{p}}\|_2^2 \, \|\underline{\mu}\|_2^2 \leq \sigma_{\min}^2(Q). \tag{12.26}$$

Using the fact that

$$\|\underline{\mathbf{p}}\|_2^2 = \sum_{i=1}^{r} |p_i|^2$$
$$\|\underline{\mu}\|_2^2 = \sum_{i=1}^{r} |\mu_i|^2$$

we obtain

$$\sum_{i=1}^{r} |p_i|^2 \leq \frac{\sigma_{\min}^2(Q)}{\sum_{i=1}^{r} \mu_i^2}. \tag{12.27}$$

♣

This theorem determines for the given stabilizing controller K, the quantity

$$\rho(K,Q) := \frac{\sigma_{\min}^2(Q)}{\sum_{i=1}^{r} \mu_i^2} = \frac{\sigma_{\min}^2(Q)}{\sum_{i=1}^{r} \|E_i^T P + P E_i\|_2^2} \tag{12.28}$$

which determines the range of perturbations for which stability is guaranteed and this is therefore the radius of a stability hypersphere in parameter space.

12.4.1 Robustification Procedure

Using the index obtained in (12.28) we now give an iterative design procedure to obtain the optimal controller K^* so that (12.28) is as large as possible. For a given K, the largest stability hypersphere we can obtain is

$$\max_Q \rho^2(K,Q) = \max_Q \frac{\sigma_{\min}^2(Q)}{\sum_{i=1}^{r} \mu_i^2} \tag{12.29}$$

and the problem of designing a robust controller with respect to structured parameter perturbations can be formulated as follows:

Find K to maximize (12.29), i.e.

$$\max_K \left\{ \max_Q \rho^2(K,Q) \right\} = \max_K \left\{ \max_Q \frac{\sigma_{\min}^2(Q)}{\sum_{i=1}^{r} \mu_i^2} \right\} \tag{12.30}$$

subject to all the eigenvalues of $A + BKC$ lying in the left half plane, i.e.

$$\lambda(A + BKC) \subset \mathbb{C}^-.$$

Equivalently

$$\max_{K,Q} \rho^2(K,Q) = \max_{K,Q} \frac{\sigma_{\min}^2(Q)}{\sum_{i=1}^{r} \mu_i^2} \tag{12.31}$$

subject to

$$\lambda(A + BKC) \subset \mathbb{C}^-.$$

Thus the following constrained optimization problem is formulated: For the given $(A,\ B,\ C)$ with the nominal stabilizing controller K define

$$(A+BKC)^T P + P(A+BKC) = -Q := -L^T L, \tag{12.32}$$

and the optimization problem

$$\min_{K,L} J := \min_{K,L} \frac{\sum_{i=1}^{r} \|E_i^T P + PE_i\|_2^2}{\sigma_{\min}^2(L^T L)} \tag{12.33}$$

subject to

$$J_c := \max_{\lambda(A+BKC)} \mathrm{Re}[\lambda] < 0.$$

Note that the positive definite matrix Q has been replaced without loss of generality by $L^T L$. For any square full rank matrix L, $L^T L$ is positive definite symmetric. This replacement also reduces computational complexity.

A gradient based descent procedure to optimize the design parameters K and L can be devised. The gradient of J with respect to K and L is given below. Before we state this result, we consider a slightly more general class of perturbations by letting

$$A = A_0 + \sum_{i=1}^{r} p_i A_i, \qquad B = B_0 + \sum_{i=1}^{r} p_i B_i. \tag{12.34}$$

Then we get

$$M = A_0 + B_0 KC \quad \text{and} \quad E_i = A_i + B_i KC. \tag{12.35}$$

Theorem 12.2 *Let J be defined as in (12.33) and let (12.34) and (12.35) hold. Then*

a)

$$\frac{\partial J}{\partial L} = \frac{2}{\sigma_{\min}^3(L^T L)} L$$

$$\left\{ \sigma_{\min}(L^T L) V^T - \sum_{i=1}^{r} \sigma_{\max}^2 \left(E_i^T P + PE_i\right) \left(u_m v_m^T + v_m u_m^T\right) \right\} \tag{12.36}$$

where V satisfies

$$(A_0 + B_0 KC)V + V(A_0 + B_0 KC)^T =$$

$$-\sum_{i=1}^{r} \sigma_{\max} \left(E_i^T P + PE_i\right) \left[E_i(u_{ai} v_{ai}^T + v_{ai} u_{ia}^T) + (u_{ai} v_{ai}^T + v_{ai} u_{ai}^T) E_i^T\right] \tag{12.37}$$

v_{ai} and u_{ai} are left and right singular vectors corresponding to $\sigma_{\max}(E_i^T P + PE_i)$, respectively, and v_m and u_m are left and right singular vectors corresponding to $\sigma_{\min}(L^T L)$.

b)

$$\frac{\partial J}{\partial K} = \frac{2}{\sigma_{\min}^2(L^T L)}$$

$$\left\{ \sum_{i=1}^{r} \sigma_{\max} \left(E_i^T P + P E_i \right) B_i^T P \left(v_{ai} u_{ai}^T + u_{ai} v_{ai}^T \right) + B^T P^T V^T \right\} C^T \quad (12.38)$$

c)

$$\frac{\partial J_c}{\partial K_{ij}} = \mathrm{Re} \left\{ \frac{v^T B_0 \left(\frac{\partial K}{\partial K_{ij}} \right) C w}{v^T w} \right\} \quad (12.39)$$

where v and w are the corresponding left and right eigenvectors of $(A_0 + B_0 K C)$ corresponding to $\lambda_{\max}$ the eigenvector with $\max\{\mathrm{Re}\,(\lambda)\}$.

The proof of this theorem is omitted. The gradient can be computed by solving the two equations (12.37) and (12.38). A gradient based algorithm for enlarging the radius of the stability hypersphere $\rho(K, Q)$ by iteration on (K, Q) can be devised using these gradients. This procedure is somewhat ad hoc but nevertheless it can be useful.

Example 12.4. A VTOL helicopter is described as the linearized dynamic equation:

$$\frac{d}{dt} \begin{bmatrix} x_1 \\ x_2 \\ x_3 \\ x_4 \end{bmatrix} = \begin{bmatrix} -0.0366 & 0.0271 & 0.0188 & -0.4555 \\ 0.0482 & -1.0100 & 0.0024 & -4.0208 \\ 0.1002 & p_1 & -0.7070 & p_2 \\ 0 & 0 & 1 & 0 \end{bmatrix} \begin{bmatrix} x_1 \\ x_2 \\ x_3 \\ x_4 \end{bmatrix} + \begin{bmatrix} 0.4422 & 0.1761 \\ p_3 & -7.5922 \\ -5.5200 & 4.4900 \\ 0 & 0 \end{bmatrix} \begin{bmatrix} u_1 \\ u_2 \end{bmatrix}$$

$$y = \begin{bmatrix} 0 & 1 & 0 & 0 \end{bmatrix} \begin{bmatrix} x_1 \\ x_2 \\ x_3 \\ x_4 \end{bmatrix}.$$

where

x_1	horizontal velocity, knots
x_2	vertical velocity, knots
x_3	pitch rate, degrees/sec
x_4	pitch angle, degrees
u_1	collective pitch control
u_2	longitudinal cyclic pitch control

The given dynamic equation is computed for typical loading and flight conditions of the VTOL helicopter at the airspeed of 135 knots. As the airspeed changes all the elements of the first three rows of both matrices also change. The most significant changes take place in the elements p_1, p_2, and p_3. Therefore, in the following all the other elements are assumed to be constants. The following bounds on the parameters are given:

$$\begin{aligned} p_1 &= 0.3681 + \Delta p_1, \qquad |\Delta p_1| \leq 0.05 \\ p_2 &= 1.4200 + \Delta p_2, \qquad |\Delta p_2| \leq 0.01 \\ p_3 &= 3.5446 + \Delta p_3, \qquad |\Delta p_3| \leq 0.04. \end{aligned}$$

Let

$$\Delta \mathbf{p} = [\Delta p_1, \Delta p_2, \Delta p_3]$$

and compute

$$\max \|\Delta \mathbf{p}\|_2 = 0.0648. \tag{12.40}$$

The eigenvalues of the open-loop plant are

$$\lambda(A) = \begin{pmatrix} 0.27579 \pm j0.25758 \\ -0.2325 \\ -2.072667 \end{pmatrix}.$$

The nominal stabilizing controller is given by

$$K_0 = \begin{bmatrix} -1.63522 \\ 1.58236 \end{bmatrix}.$$

Starting with this nominal stabilizing controller, we performed the robustification procedure. For this step the initial value is chosen as

$$L_0 = \begin{bmatrix} 1.0 & 0.0 & -0.50 & 0.06 \\ 0.5 & 1.0 & -0.03 & 0.00 \\ -0.1 & 0.4 & 1.00 & 0.14 \\ 0.2 & 0.6 & -0.13 & 1.50 \end{bmatrix}$$

The nominal values gave the stability margin

$$\rho_0 = 0.02712 < 0.0648 = \|\Delta \mathbf{p}\|_2$$

which does not satisfy the requirement (12.40). After 26 iterations we have

$$\rho^* = 0.12947 > 0.0648 = \|\Delta \mathbf{p}\|_2$$

which does satisfy the requirement. The robust stabilizing 0^{th} order controller computed is

$$K^* = \begin{bmatrix} -0.996339890 \\ 1.801833665 \end{bmatrix}$$

and the corresponding optimal L^*, P^* and the closed-loop eigenvalues are

$$L^* = \begin{bmatrix} 0.51243 & 0.02871 & -0.13260 & 0.05889 \\ -0.00040 & 0.39582 & -0.07210 & -0.35040 \\ 0.12938 & 0.08042 & 0.51089 & -0.01450 \\ -0.07150 & 0.34789 & -0.02530 & 0.39751 \end{bmatrix}$$

$$P^* = \begin{bmatrix} 2.00394 & -0.38940 & -0.50010 & -0.49220 \\ -0.38940 & 0.36491 & 0.46352 & 0.19652 \\ -0.50010 & 0.46352 & 0.61151 & 0.29841 \\ -0.49220 & 0.19652 & 0.29841 & 0.98734 \end{bmatrix}$$

$$\lambda(A + BK^*C) = \begin{pmatrix} -18.396295 \\ -0.247592 \pm j1.2501375 \\ -0.0736273 \end{pmatrix}.$$

This example can also be solved by the Mapping Theorem technique previously described. With the controller K^* obtained by the robustification procedure given above we obtained a stability margin of $\epsilon^* = 1.257568$ which is much greater than the value obtained by the Lyapunov stability based method. In fact, the Lyapunov stability based method gives $\rho^* = 0.12947$ which is equivalent to $\epsilon = 0.07475$. This comparison shows that the Mapping Theorem based technique gives a much better approximation of the stability margin than the Lyapunov based technique.

12.5 THE MATRIX STABILITY RADIUS PROBLEM

In this section, we suppose that the perturbations of the system model can be represented in the feedback form shown in Figure 12.3.

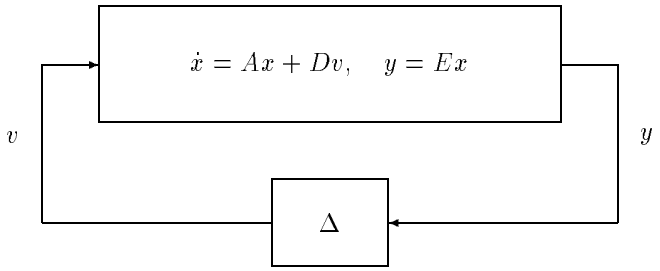

Figure 12.3. Feedback Interpretation of the Perturbed System

Thus we have

$$\begin{aligned} \dot{x} &= Ax + Dv \\ y &= Ex \\ v &= \Delta y. \end{aligned} \tag{12.41}$$

In the perturbed system, we therefore have

$$\dot{x} = (A + D\Delta E)x. \tag{12.42}$$

We regard the nominal system matrix to be A. Under perturbations it becomes $A + D\Delta E$ where E and D are given matrices defining the structure of the perturbations and Δ is an unstructured uncertainty block. In the following Δ will be allowed to be complex or real. In each case the size of the "smallest" destabilizing matrix Δ will be of interest. This problem is therefore a generalization of the gain and phase margin problems. In general, the signals v and y are artificially introduced and do not have any significance as inputs or outputs.

In the literature, it has become customary to measure the size of the perturbation using the operator norm of the matrix Δ. Let $\mathbb{K}$ denote a field. We will consider the two cases $\mathbb{K} = \mathbb{R}$ or $\mathbb{K} = \mathbb{C}$. Let $y \in \mathbb{K}^q$, $v \in \mathbb{K}^l$, and $\|\cdot\|_{\mathbb{K}^q}$ and $\|\cdot\|_{\mathbb{K}^l}$ denote given norms in $\mathbb{K}^q$ and $\mathbb{K}^l$, respectively. We measure the size of Δ by the corresponding operator norm

$$\|\Delta\| = \sup\left\{\|\Delta y\|_{\mathbb{K}^l} : y \in \mathbb{K}^q, \|y\|_{\mathbb{K}^q} \leq 1\right\}. \tag{12.43}$$

Let $\mathcal{S}$ denote the stability region in the complex plane as usual. Let $\Lambda(\cdot)$ denote the eigenvalues of the matrix $(\cdot)$. We will suppose that the nominal matrix A is stable. This means that $\Lambda(A) \subset \mathcal{S}$.

Definition 12.1. The stability radius, in the field $\mathbb{K}$, of A with respect to the perturbation structure (D, E) is defined as:

$$\mu = \inf\left\{\|\Delta\| : \Delta \in \mathbb{K}^{l\times q}, \Lambda(A + D\Delta E) \cap \mathcal{U} \neq \emptyset\right\}. \tag{12.44}$$

The operator norm of Δ is most often measured by its maximum singular value, denoted $\bar{\sigma}(\Delta)$:

$$\|\Delta\| = \bar{\sigma}(\Delta).$$

In this case it can easily be established by continuity of the eigenvalues of $A + D\Delta E$ on Δ, and the stability of A, that

$$\begin{aligned}
\mu &= \inf\left\{\bar{\sigma}(\Delta) : \Delta \in \mathbb{K}^{l\times q} \quad \text{and} \quad \Lambda(A + D\Delta E) \cap \mathcal{U} \neq \emptyset\right\} \\
&= \inf\left\{\bar{\sigma}(\Delta) : \Delta \in \mathbb{K}^{l\times q} \quad \text{and} \quad \Lambda(A + D\Delta E) \cap \partial\mathcal{S} \neq \emptyset\right\} \\
&= \inf_{s\in\partial\mathcal{S}} \inf\left\{\bar{\sigma}(\Delta) : \Delta \in \mathbb{K}^{l\times q} \quad \text{and} \quad \det(sI - A - D\Delta E) = 0\right\} \\
&= \inf_{s\in\partial\mathcal{S}} \inf\left\{\bar{\sigma}(\Delta) : \Delta \in \mathbb{K}^{l\times q} \quad \text{and} \quad \det\left[(I - \Delta \underbrace{E(sI - A)^{-1}D}_{G(s)}\right] = 0\right\} \\
&= \inf_{s\in\partial\mathcal{S}} \inf\left\{\bar{\sigma}(\Delta) : \Delta \in \mathbb{K}^{l\times q} \quad \text{and} \quad \det\left[I - \Delta G(s)\right] = 0\right\}.
\end{aligned} \tag{12.45}$$

For a fixed $s \in \partial\mathcal{S}$, write $G(s) = M$. Then the calculation above reduces to solving the optimization problem:

$$\inf\left\{\bar{\sigma}(\Delta) : \Delta \in \mathbb{K}^{l\times q} \quad \text{and} \quad \det\left[I - \Delta M\right] = 0\right\}. \tag{12.46}$$

When Δ is allowed to be a complex matrix, it can be shown easily that the solution to this optimization problem is given by

$$\bar{\sigma}(\Delta) = [\bar{\sigma}(M)]^{-1}. \tag{12.47}$$

When Δ is constrained to be a real matrix the solution is much more complicated due to the fact that M is a complex matrix. In the following subsections, we give the calculation of μ for the complex and real cases. These are called the *complex matrix stability radius* and *real matrix stability radius* respectively.

12.5.1 The Complex Matrix Stability Radius

Consider the case where (A, D, E) are regarded as complex matrices, $\mathbb{K} = \mathbb{C}$, and Δ is a complex matrix. In this case, we denote μ as μ_C and call it the complex matrix stability radius.

The theorem given below shows how μ_C can be determined. The proof is an immediate consequence of equations (12.45)-(12.47) above. As before, let the transfer matrix associated with the triple (A, D, E) be

$$G(s) = E(sI - A)^{-1}D. \tag{12.48}$$

Theorem 12.3 *If A is stable with respect to $\mathcal{S}$, then*

$$\mu_C = \frac{1}{\sup_{s\in\partial\mathcal{S}} \|G(s)\|} \tag{12.49}$$

where $\|G(s)\|$ denotes the operator norm of $G(s)$ and, by definition, $0^{-1} = \infty$.

When $\|\Delta\| = \bar{\sigma}(\Delta)$, the complex matrix stability radius is given by

$$\mu_C = \frac{1}{\sup_{s\in\partial\mathcal{S}} \bar{\sigma}(G(s))}. \tag{12.50}$$

The special case of this formula corresponding to the case where D and E are square, and $D = E = I$, is referred to as the unstructured matrix stability radius. In this case,

$$\mu_C = \frac{1}{\sup_{s\in\partial\mathcal{S}} \|(sI - A)^{-1}\|}. \tag{12.51}$$

In the case of Hurwitz stability, (12.49) becomes

$$\mu_C = \frac{1}{\|G(s)\|_\infty}. \tag{12.52}$$

12.5.2 The Real Matrix Stability Radius

In this section we give the results on the matrix stability radius problem when A, D, E are real matrices and Δ is constrained to be a real matrix. The main result shows that the real matrix stability radius can be computed by means of a two-parameter optimization problem. Let $\sigma_2(\cdot)$ denote the second largest singular value of the matrix $(\cdot)$, and $\mathrm{Re}[G(s)]$ and $\mathrm{Im}[G(s)]$ denote the real and imaginary parts of the matrix $G(s)$.

Theorem 12.4 *The real matrix stability radius is given by*

$$\mu_R = \inf_{s \in \partial \mathcal{S}} \inf_{\gamma \in (0,1]} \sigma_2 \left(\begin{bmatrix} \mathrm{Re}[G(s)] & -\gamma\ \mathrm{Im}[G(s)] \\ \gamma^{-1}\ \mathrm{Im}[G(s)] & \mathrm{Re}[G(s)] \end{bmatrix} \right) \tag{12.53}$$

The proof of this formula is rather lengthy and is omitted. An important feature of this formula is the fact that the function

$$\sigma_2 \left(\begin{bmatrix} \mathrm{Re}[G(s)] & -\gamma\ \mathrm{Im}[G(s)] \\ \gamma^{-1}\ \mathrm{Im}[G(s)] & \mathrm{Re}[G(s)] \end{bmatrix} \right) \tag{12.54}$$

is unimodal over $\gamma \in (0, 1]$.

We conclude this section with a simple example which emphasizes the fundamental difference between the complex and real stability radii.

12.5.3 Example

Example 12.5. Let

$$A = \begin{bmatrix} 0 & 1 \\ -1 & -B \end{bmatrix}, \qquad D = \begin{bmatrix} 0 \\ -B \end{bmatrix}, \qquad E = \begin{bmatrix} 1 & 0 \end{bmatrix}.$$

This triple could describe a linear oscillator with small damping coefficient $B > 0$ and perturbed restoring force 1. The associated transfer function

$$G(s) = E(j\omega I - A)^{-1} D = \frac{-B}{1 - \omega^2 + jB\omega}.$$

The real stability radius is easily seen to be,

$$\mu_R = \frac{1}{B}.$$

To compute the complex stability radius we determine

$$|G(j\omega)|^2 = \frac{B^2}{(1-\omega^2)^2 + B^2\omega^2}.$$

If $B < \sqrt{2}$, a simple calculation shows that $|G(j\omega)|^2$ is maximized when $\omega^2 = 1 - \frac{B^2}{2}$ so that

$$\mu_C^2 = \frac{\frac{B^4}{4} + B^2\left(1 - \frac{B^2}{2}\right)}{B^2} = 1 - \frac{B^2}{4}.$$

Now regarding B as a parameter we can see that μ_C is always bounded by 1 whereas μ_R can be made *arbitrarily large* by choosing small values of B. This suggests that complexifying real parameters could lead to highly conservative results. On the other hand it is also necessary to keep in mind that as B tends to 0 and μ_R tends to ∞, the poles of $G(s)$ approach the imaginary axis, indicating heightened sensitivity to unstructured perturbations.

12.6 TWO SPECIAL CLASSES OF INTERVAL MATRICES

In this section, we consider two special classes of interval matrices namely nonnegative matrices and the so-called Metzlerian matrices for which stronger results can be stated.

12.6.1 Robust Schur Stability of Nonnegative Matrices

Definition 12.2. A *nonnegative matrix* is a real matrix whose entries are nonnegative. Similarly, the matrix is said to be a *nonnegative interval matrix* if every element is nonnegative throughout their respective intervals:

$$\mathbf{A} := \left\{ A \in \mathbb{R}^{n\times n} : 0 \leq a_{ij}^- \leq a_{ij} \leq a_{ij}^+, \quad \text{for all } i,j \right\}. \tag{12.55}$$

Using the lower and upper bound matrices

$$A^- := \begin{bmatrix} a_{11}^- & \cdots & a_{1n}^- \\ \vdots & & \vdots \\ a_{n1}^- & \cdots & a_{nn}^- \end{bmatrix} \qquad A^+ := \begin{bmatrix} a_{11}^+ & \cdots & a_{1n}^+ \\ \vdots & & \vdots \\ a_{n1}^+ & \cdots & a_{nn}^+ \end{bmatrix},$$

we can represent a typical element of $\mathbf{A}$ by the notation:

$$0 \leq A^- \leq A \leq A^+. \tag{12.56}$$

The following definition and properties will play an important role throughout the section.

Definition 12.3. A real square matrix P is called a nonsingular *M-Matrix* if the following two conditions are satisfied:

a) $p_{ii} > 0$ for all i and $p_{ij} \leq 0$ for all $i \neq j$.

b) $P^{-1} \geq 0$ (P^{-1} is nonnegative).

Property 12.1.

A) Let $Q \in \mathbb{R}^{n\times n}$ with $Q \geq 0$. The matrix $\lambda I - Q$ is a nonsingular M-matrix if and only if $\rho(Q) < \lambda$ where $\rho(\cdot)$ is the spectral radius of the matrix $(\cdot)$.

B) The matrix P with $p_{ii} > 0$ for all i and $p_{ij} \leq 0$ for all $i \neq j$ is a nonsingular M-matrix if and only if all the leading principal minors of P are positive.

C) The characteristic polynomial of an M-matrix is antiHurwitz. Equivalently, all the eigenvalues of an M-matrix have positive real parts.

D) For $X, Y \in \mathbb{R}^{n\times n}$, if $0 \leq X \leq Y$, then $\rho(X) \leq \rho(Y)$.

The proofs of these properties may be found in the matrix theory literature referred to in the notes and references section of this chapter.

Let $A(\alpha)$ denote the α dimensional leading principal submatrix of A which consists of the first α rows and columns of A.

Theorem 12.5 *A nonnegative matrix $A \in \mathbb{R}^{n\times n}$ is Schur stable for all $A \in [A^-, A^+]$ if and only if $\rho(A^+) < 1$. Equivalently, all leading principal minors of $I - A^+$, $\det[I - A^+(\alpha)]$, are positive for $\alpha = 1, \cdots, n$.*

Proof. Necessity follows trivially since $A^+ \in [A^-, A^+]$ and Schur stability of A is equivalent to $\rho(A) < 1$. To prove sufficiency, we use Property 12.1. Since $A^- \leq A \leq A^+$, we know that $\rho(A) \leq \rho(A^+)$ from Property 12.1.D. Therefore, the nonnegative matrix A is Schur stable for all $A \in [A^-, A^+]$ if and only if $\rho(A^+) < 1$. Moreover, from Property 12.1.A we also know that $I - A^+$ is a nonsingular M-matrix since $\rho(A^+) < 1$. From Property 12.1.B, this is also equivalent to all the leading principal minors of $I - A^+$, $\det[I - A^+(\alpha)]$, being positive. ♣

12.6.2 Robust Hurwitz Stability of Metzlerian Matrices

An extremal result also holds for the case of Hurwitz stability of Metzlerian matrices defined below:

Definition 12.4. A matrix A is called a *Metzlerian matrix* if $a_{ii} < 0$ for all i and $a_{ij} \geq 0$ for all $i \neq j$. Similarly, an interval matrix $\mathbf{A}$ is said to be a *Metzlerian interval matrix* if every matrix $A \in \mathbf{A}$ is a Metzlerian matrix.

We have the following theorem.

Theorem 12.6 *A Metzlerian matrix $A \in \mathbb{R}^{n\times n}$ is Hurwitz stable for all $A \in [A^-, A^+]$ if and only if A^+ is Hurwitz stable. An equivalent condition is that all leading principal minors of $-A^+$ are positive, i.e. $\det[-A^+(\alpha)] > 0$ for $\alpha = 1, \cdots, n$.*

Proof. All we have to prove is that $A \in [A^-, A^+]$ is Hurwitz stable if and only if $-A^+$ is an M-matrix. The necessity of this condition is obvious because the stability of $A \in [A^-, A^+]$ implies that of A^+. Therefore $-A^+$ is antiHurwitz and consequently, $-A^+$ is an M-matrix. From Property 12.1.B, all the leading principal minors of $-A^+$ must be positive.

To prove sufficiency assume that $-A^+$ is an M-matrix. From the structure of the matrix $-A$, one can always find $\lambda > 0$ such that $\lambda I - (-A) \geq 0$ for all $A \in [A^-, A^+]$. We have

$$\lambda I - \big(\lambda I - (-A^+)\big) = -A^+$$

and since $-A^+$ is a nonsingular M-matrix it follows from Property 12.1.A that

$$\rho(\lambda I + A^+) < \lambda.$$

We also know from Property 12.1.D that

$$0 \leq \lambda I + A \leq \lambda I + A^+$$

implies that

$$\rho(\lambda I + A) \leq \rho(\lambda I + A^+)$$

Thus

$$\rho(\lambda I + A) < \lambda$$

and therefore from Property 12.1.A we conclude that $-A$ is an M-matrix. Therefore by Property 12.1.C A is Hurwitz stable. ♣

In the next subsection, we show that a much simpler solution can be obtained for the real stability radius problem if the interval matrix falls into one of these two classes.

12.6.3 Real Stability Radius

From the previous subsection, we know that the real stability radius of a matrix is obtained by first solving a minimization problem involving one variable and next performing a frequency sweep. However, for the case of both nonnegative and Metzlerian matrices, a direct formula can be given for their respective real stability radii.

Consider the real nonnegative system matrix A with $A \geq 0$ and with $\rho(A) < 1$ and subject to structured perturbations. The real matrix stability radius with respect to the unit circle is defined by

$$\mu_R = \inf \{\|\Delta\| : \Lambda(A + D\Delta E) \cap \mathcal{U} \neq \emptyset, \quad A + D\Delta E \geq 0\} \tag{12.57}$$

where the condition $A + D\Delta E \geq 0$ is imposed in order to ensure nonnegativity of the entire set. The calculation will depend on the well known Perron-Frobenius Theorem of matrix theory.

Theorem 12.7 (Perron-Frobenuis Theorem)
If the matrix $A \in \mathbb{R}^{n \times n}$ is nonnegative, then

a) A has a positive eigenvalue, r, equal to the spectral radius of A

b) There is a positive (right) eigenvector associated with the eigenvalue r;

c) The eigenvalue r has algebraic multiplicity 1.

The eigenvalue r will be called the Perron-Frobenius eigenvalue.

Theorem 12.8 *Let A be Schur stable. Then the real stability radius of the nonnegative system is given by*

$$\mu_R = \frac{1}{\bar{\sigma}\left(E(I-A)^{-1}D\right)}$$

Proof. $A + D\Delta E$ becomes unstable if and only if $\rho(A + D\Delta E) \geq 1$. Hence from the definition of the real stability radius, we have

$$\begin{aligned}\mu_R &= \inf\{\|\Delta\| : \rho(A + D\Delta E) \geq 1, \quad A + D\Delta E \geq 0\} \\ &= \inf\{\|\Delta\| : \rho(A + D\Delta E) = 1, \quad A + D\Delta E \geq 0\}.\end{aligned}$$

From Theorem 12.7 it follows that $A + D\Delta E \geq 0$ is unstable if and only if its Perron-Frobenius eigenvalue (spectral radius) $r \geq 1$. Therefore we have

$$\begin{aligned}\mu_R &= \inf\{\bar{\sigma}(\Delta) : \lambda_i(A + D\Delta E) = 1 \text{ for some } i\} \\ &= \inf\{\bar{\sigma}(\Delta) : \det[I - A - D\Delta C] = 0\} \\ &= \inf\left\{\bar{\sigma}(\Delta) : \det\left[I - \Delta E(I-A)^{-1}D\right] = 0\right\} \\ &= \frac{1}{\bar{\sigma}\left(E(I-A)^{-1}D\right)}.\end{aligned}$$

♣

A similar result holds for Hurwitz stability (see Exercise 12.1).

12.6.4 Robust Stabilization

Using the results obtained for nonnegative and Metzlerian matrices above, here we consider the problem of designing a robust state feedback controller for an interval state space system.

Let us first consider the discrete time system

$$\begin{aligned}x(k+1) &= Ax(k) + Bu(k) \\ y(k) &= Cx(k)\end{aligned} \tag{12.58}$$

where $A \in [A^-, A^+]$ while the matrices B,C are fixed. Note that in this problem neither A^- nor A^+ is necessarily nonnegative.

Let

$$u(k) = v + Kx(k) \tag{12.59}$$

so that the closed loop system is given by

$$x(k+1) = \underbrace{(A + BK)}_{A_{cl}}x(k) + Bv(k). \tag{12.60}$$

The following theorem provides a solution to this problem.

Theorem 12.9 *The feedback control law (12.59) robustly stabilizes the system (12.60) and A_{cl} remains nonnegative for all $A \in [A^-, A^+]$ if and only if*

$$A^- + BK \geq 0 \quad \text{and} \quad A^+ + BK \geq 0$$

and $A^+ + BK$ is Schur stable. Equivalently all the leading principal minors of the matrix $I - (A^+ + BK)$ are positive.

The proof of this theorem is a direct consequence of Theorem 12.5 and is omitted here.

Example 12.6. Consider the unstable interval discrete system

$$x(k+1) = \begin{bmatrix} [0.5, 0.6] & 0 & 0.5 \\ 1 & 0.5 & 1 \\ 0.5 & 0 & [-0.2, -0.1] \end{bmatrix} x(k) + \begin{bmatrix} 0 \\ 0 \\ 1 \end{bmatrix} u(k).$$

Suppose that we want to robustly stabilize the system by state feedback

$$u(k) = v(k) + Kx(k)$$

where $K = [k_1 \ k_2 \ k_3]$. Then the requirements $A^- + BK \geq 0$ and $A^+ + BK \geq 0$ lead to

$$\begin{aligned} 0.5 + k_1 &\geq 0 \\ k_2 &\geq 0 \\ -0.2 + k_3 &\geq 0 \end{aligned}$$

and the requirement that all the leading principal minors of $I - (A^+ + BK)$ be positive leads to

$$-0.25k_1 - 0.9k_2 - 0.2k_3 + 0.095 > 0.$$

Therefore, we select

$$K = [0 \ 0 \ 0.3].$$

A result similar to the previous theorem can be stated for the Hurwitz case and is given without proof:

Theorem 12.10 *The feedback control law $u(t) = Fx(t)$ robustly stabilizes the system*

$$\dot{x}(t) = Ax(t) + Bu(t)$$

and the closed loop matrix $A + BF$ is a Metzlerian matrix for all $A \in [A^-, A^+]$ if and only if

$$A^- + BF \quad \text{and} \quad A^+ + BF$$

are Metzlerian and $A^+ + BF$ is Hurwitz. Equivalently all the leading principal minors of $-(A^+ + BF)$ are positive.

12.7 EXERCISES

12.1 Using the result in Theorem 12.8, derive the real stability radius formula for Metzlerian matrices with respect to the Hurwitz stability region.
Answer: The term $(I - A)$ in Theorem 12.8 is replaced by $-A$.

12.2 Consider the matrix

$$A(\mathbf{p}) = \begin{bmatrix} -2 + p_1 & -3 + p_2 \\ 2 + p_3 & 0 \end{bmatrix}.$$

Estimate the stability radius in the space of the parameters p_i by using the result in Theorem 12.1. Assume that the nominal values of the parameters p_i are zero. (You may choose $Q = I$ for a first estimate then optimize over Q as in Section 12.4.1.)

12.3

$$A = \begin{bmatrix} 0.5 & 1 + p_1 & 0 \\ 0 & 0.5 & p_2 \\ p_3 & 0 & 0.25 \end{bmatrix}$$

Let p_i vary in the interval $[0, \epsilon]$. Find the maximum value of ϵ such that the interval matrix A remains Schur stable.

12.4

$$A = \begin{bmatrix} -1 & 1 + p_1 & p_4 \\ 0 & -2 & p_5 \\ p_2 & p_3 & -3 \end{bmatrix}$$

Find the maximum value of ϵ such that the interval matrix A remains Hurwitz stable for all $p_i \in [0, \epsilon]$.

12.5 With

$$A_0 = \begin{bmatrix} -1 & 1 & 0 \\ 0 & -2 & 0 \\ 1 & 1 & -3 \end{bmatrix}$$

and

$$D = \begin{bmatrix} 1 & 0 \\ 0 & 1 \\ 0 & 0 \end{bmatrix} \qquad E = \begin{bmatrix} 1 & 0 & 0 \\ 0 & 1 & 0 \end{bmatrix}$$

let

$$A := A_0 + D\Delta E.$$

1) Find the real matrix stability radius.

2) Find the complex matrix stability radius.

12.6 Consider Exercise 12.5, find the real stability radius subject to the restriction that the matrix A remains Metzlerian.

12.7 Consider the discrete time system:

$$x(k+1) = \begin{bmatrix} 0 & 1 & 0 \\ 0 & 0 & 1 \\ p_1 & p_2 & p_3 \end{bmatrix} x(k) + \begin{bmatrix} 0 \\ 0 \\ 1 \end{bmatrix} u(k)$$

where

$$p_1 \in [-2, 2], \quad p_2 \in [1, 3], \quad p_3 \in [-3, -1].$$

Design a state feedback control law that robustly stabilizes the system.
Hint: Constrain the closed loop matrix to remain nonnegative.

12.8 Consider the following transfer function matrix:

$$G(s) = \begin{bmatrix} \dfrac{1}{s+1} & \dfrac{1}{s+2} \\ \dfrac{1}{s+3} & \dfrac{1}{s+4} \end{bmatrix}$$

Suppose that this plant is perturbed by feedback perturbations as shown in Figure 12.4:

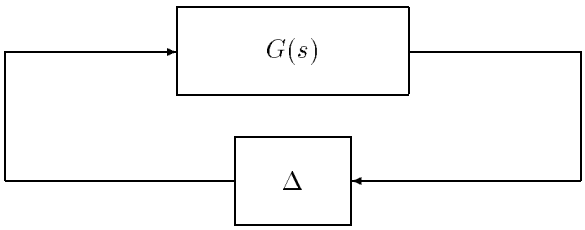

Figure 12.4. Feedback system

Compute the complex matrix stability radius with respect to Δ.

12.9 In Exercise 12.8, suppose that all the entries of Δ perturb within the interval $[-\epsilon, +\epsilon]$. Compute the real matrix stability radius $\epsilon_{\max}$ such that the closed loop system remains stable.
Hint: The characteristic equation of the closed loop system is multilinear in the parameters. One can apply the Mapping Theoerm based technique to this characteristic polynomial.

12.10 Consider the following discrete time system:

$$x(k+1) = \begin{bmatrix} 1 & 0 & p_1 \\ p_2 & -1 & 1 \\ 1 & p_3 & 1 \end{bmatrix} x(k) + \begin{bmatrix} 1 \\ 2 \\ -1 \end{bmatrix}$$

where the parameters vary as

$$p_1 \in [1-\epsilon, 1+\epsilon], \quad p_2 \in [2-\epsilon, 2+\epsilon], \quad p_3 \in [1-\epsilon, 1+\epsilon].$$

1) Find the state feedback control law such that the closed loop system poles are assigned at 0.7 and $-0.5 \pm j0.3$.

2) With this control compute the maximum value $\epsilon_{\max}$ such that the closed loop system remains Schur stable.

12.8 NOTES AND REFERENCES

In 1980, Patel and Toda [185] gave a sufficient condition for the robust stability of interval matrices using unstructured perturbations. Numerous results have followed since then. Most of these follow-up results treated the case of structured perturbations because of its practical importance over the unstructured perturbation case. Some of these works are found in Yedavalli [238], Yedavalli and Liang [239], Martin [177], Zhou and Khargonekar [247], Keel, Bhattacharyya and Howze [139], Sezer and Šiljak [204], Leal and Gibson [159], Foo and Soh, [95], and Tesi and Vicino [219]. Theorem 12.1 and the formula for the gradients given in Section 12.4.1 are proved in Keel, Bhattacharyya and Howze [139]. Most of the cited works employed either the Lyapunov equation or norm inequalities and provided sufficient conditions with various degrees of inherent conservatism. Using robust eigenstructure assignment techniques, Keel, Lim and Juang [141] developed a method to robustify a controller such that the closed loop eigenvalues remain inside circular regions centered at the nominal eigenvalues while it allows the maximum parameter perturbation. The alforithm for determining the stability of an interval matrix is reported in Keel and Bhattacharyya [138]. Hinrichsen and Pritchard [113] have given a good survey of the matrix stability radius problem. The formula for the real matrix stability radius is due to Qiu, Bernhardsson, Rantzer, Davison, Young, and Doyle [193] to which we refer the reader for the proof. The results given in Section 12.5 are taken from Hinrichsen and Pritchard [114] and [193]. The example in Section 12.5.3 is taken from [113].

Some of the difficulties of dealing with general forms of interval matrices along with various results are discussed in Mansour [168]. Theorem 12.5 is due to Shafai, Perev, Cowley and Chehab [208]. A different class of matrices called Morishima matrices is treated in Sezer and Šiljak [205]. The proofs of Property 12.1 may be found in the book by Berman and Plemmons [27] and [208]. The proof of Theorem 12.7 (Perron-Frobenius Theorem) is found in the book of Lancaster and

Tismenetsky [158, 27]. The real stability radius problem for nonnegative and Metzlerian matrices is credited to Shafai, Kothandaraman and Chen [207]. The robust stabilization problem described in Section 12.6.4 is due to Shafai and Hollot [206].

Chapter 13

ROBUST PARAMETRIC STABILIZATION

This chapter discusses the problem of robust stabilization of plants subject to parametric uncertainty. First, we consider a family of minimum phase plant transfer functions of denominator degree n and numerator degree m. We show that a single feedback compensator of order $n-m-1$ which is stable and minimum phase can always be designed to robustly (simultaneously) stabilize this family under *arbitrarily* large perturbations in the numerator and denominator coefficients. Next we show that it is sometimes possible to use standard synthesis techniques of H_∞ optimal control to design a robustly stabilizing compensator. The obvious technique is to overbound the frequency domain image sets induced by the parametric uncertainty with H_∞ norm bounded uncertainty. This is made possible in the case of linear interval plants by exploiting the extremal property of the generalized Kharitonov segments.We show this by simple numerical examples for single-input single-output interval plants. If the sizes of the intervals are not fixed *apriori*, this technique can always be used to find an appropriate size of interval perturbations for which robust stabilization is possible. The issue of robust performance is not explicitly dealt with but can be handled in the same manner, when it is measured in the H_∞ norm.

13.1 INTRODUCTION

The techniques described thus far are mostly directed towards *analyzing* the robust stability of control systems under various types of uncertainty. The underlying assumption in this type of analysis, is that a controller has already been designed by some means. The purpose of calculating worst case stability and performance margins is therefore to *evaluate* the proposed controller against a competing design. In practice, this analysis tool can itself serve as the basis of controller *design* as shown in various examples.

A different approach to robust controller design is to prespecify a desired level of performance or stability margin and attempt to find a controller from the entire set of stabilizing controllers that attains this objective. This is usually referred to

as *synthesis*.

In *optimal* synthesis, one searches for the best controller that optimizes a single criterion of performance. The optimization problem must be formulated so that it is both physically meaningful as well as mathematically tractable. An important optimal synthesis problem closely related to robust control is the H_∞ control problem. Here, one attempts to minimize the H_∞ norm of a "disturbance" transfer function over the set of all stabilizing controllers. An elegant theory of H_∞ based synthesis has been developed. It can be used to design for robust stability and performance by minimizing the norms of suitable transfer functions. The underlying theory is based on the Small Gain Theorem which provides for robust stability under norm bounded perturbations.

At the present time there does not exist a comprehensive and nonconservative theory of synthesis for systems subject to real parameter uncertainty. However partial results are available and design techniques can be developed based on what has been learnt so far. The purpose of this chapter is to explore these ideas in an elementary way.

In the next section we describe a procedure to synthesize a fixed order controller that is guaranteed to robustly stabilize a prescribed family of single-input, single-output minimum phase plants. The parametric perturbations affecting the plant are otherwise essentially *arbitrary*. Moreover, it is shown that the controller itself can always be stable and minimum phase and the order of the controller need be no higher than $n - m - 1$, where the plant has n poles and m zeroes.

Then we describe how H_∞ theory might be exploited to design controllers that provide robustness against parameter uncertainty. The essential link with the parametric theory is that we are able to "tightly" fit the level of unstructured disc-like uncertainty required to cover the actual parametric uncertainty. Once this is done, the H_∞ machinery can take over to produce an answer. We describe the approach using Nevanlinna-Pick interpolation as well as the state space formulation of H_∞ theory with illustrative numerical examples of robust parametric stabilization.

13.2 SIMULTANEOUS STRONG STABILIZATION

In this section stability will mean Hurwitz stability. We show how an infinite family of single input single output (SISO) plants can be simultaneously stabilized by a single stable, minimum phase controller, provided that each member in the family represents a minimum phase plant. Consider the standard unity feedback system of Figure 13.1, where the plant is a single input single output system described by the transfer function

$$G(s) = \frac{n(s)}{d(s)} = \frac{n_0 + n_1 s + \ldots + n_r s^r}{d_0 + d_1 s + \ldots + d_q s^q}.$$

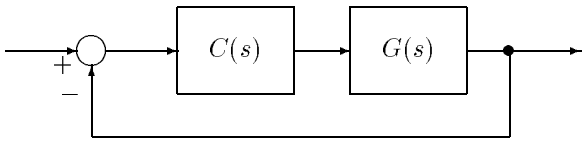

Figure 13.1. Unity feedback system

Let $\mathcal{F}_n$ be a compact set of polynomials $n(s)$ satisfying the following three properties.

Property 13.1.

A1) for all $n(\cdot) \in \mathcal{F}_n$, $n(\cdot)$ is stable.

A2) for all $n(\cdot) \in \mathcal{F}_n$, $n(\cdot)$ is of degree r (fixed degree).

A3) The sign of the highest coefficient of any polynomial $n(\cdot)$ in $\mathcal{F}_n$ is always the same, either always positive or always negative.

Let also $\mathcal{F}_d$ be a family of polynomials satisfying the following three properties:

Property 13.2.

B1) for all $d(\cdot) \in \mathcal{F}_d$, $d(\cdot)$ is of degree q (fixed degree).

B2) $\mathcal{F}_d$ is bounded, that is there exists a constant B such that:

$$\text{for all } d(\cdot) \in \mathcal{F}_d, \quad \text{for all } j \in [0, q], \quad |d_j| \leq B.$$

B3) The coefficient of order q of any polynomial $d(\cdot)$ in $\mathcal{F}_d$ is always of the same sign and bounded from below (or from above). That is,

$$\exists\ b > 0 \text{ such that for all } d(\cdot) \in \mathcal{F}_d, \quad d_q > b > 0,$$

or

$$\exists\ b < 0 \text{ such that for all } d(\cdot) \in \mathcal{F}_d, \quad d_q < b < 0.$$

Now, assuming that $r \leq q$, consider the family $\mathcal{P}$ of proper SISO plants described by their transfer functions

$$\mathcal{P} := \left\{ G(s) = \frac{n(s)}{d(s)},\ \text{where } n(s) \in \mathcal{F}_n,\ d(s) \in \mathcal{F}_d \right\}.$$

Then we have the following result.

Theorem 13.1 (Simultaneous Strong Stabilization)

i) $q = r$*: There exists a constant compensator that stabilizes the entire family of plants* $\mathcal{P}$*.*

ii) $q > r$*: There exists a proper, stable and minimum phase compensator* $C(s)$ *of order* $q - r - 1$ *that stabilizes the entire family of plants* $\mathcal{P}$*.*

First, we can assume without loss of generality that we have,

$$\text{for all } \; n(\cdot) \in \mathcal{F}_n, \quad n_r > 0, \tag{13.1}$$

and

$$\text{for all } \; d(\cdot) \in \mathcal{F}_d, \quad d_q > 0.$$

Then we can also assume, still without loss of generality, that the family $\mathcal{F}_d$ is itself compact, otherwise it would be enough to replace $\mathcal{F}_d$ by the family of interval polynomials $\mathcal{F}'_d$ defined by:

$$d_0 \in [-B, B], \; d_1 \in [-B, B], \; \cdots, \; d_{q-1} \in [-B, B], \; d_q \in [b, B].$$

Given this, the proof of this result now depends on some general properties of such compact stable families as $\mathcal{F}_n$, and of such compact families as $\mathcal{F}_d$.

Property 13.3. Since the family $\mathcal{F}_n$ contains only stable polynomials, and since they all satisfy Property A3 and (13.1), then any coefficient of any polynomial $n(\cdot)$ in $\mathcal{F}_n$ is positive. Moreover, since the set $\mathcal{F}_n$ is compact it is always possible to find two constants a and A such that,

$$\text{for all } \; n(\cdot) \in \mathcal{F}_n, \; \text{for all } \; j \in [0, r], \quad 0 < a \leq n_j \leq A. \tag{13.2}$$

Now, $\mathcal{F}_n$ being compact, it is always possible to find a closed bounded curve $\mathcal{C}$ included in the left-half plane that strictly contains all zeroes of any element in $\mathcal{F}_n$. For example it is well known that in view of (13.2), any zero z_n of an element $n(\cdot)$ of $\mathcal{F}_n$ satisfies:

$$|z_n| \leq 1 + \frac{A}{a}.$$

Hence, it is always possible to choose $\mathcal{C}$ as in Figure 13.2.

Once again by a compacity argument we can write:

$$\inf_{n(\cdot) \in \mathcal{F}_n} \left[\inf_{s \in \mathcal{C}} |n(s)| \right] = \alpha_n > 0.$$

Proof. We proceed by contradiction. If $\alpha_n = 0$, then it is possible to find a sequence of polynomials $n_k(s)$ in $\mathcal{F}_n$, such that for each $k > 0$,

$$\exists \; z_k \in \mathcal{C} \text{ such that } |n_k(z_k)| \leq \frac{1}{k}. \tag{13.3}$$

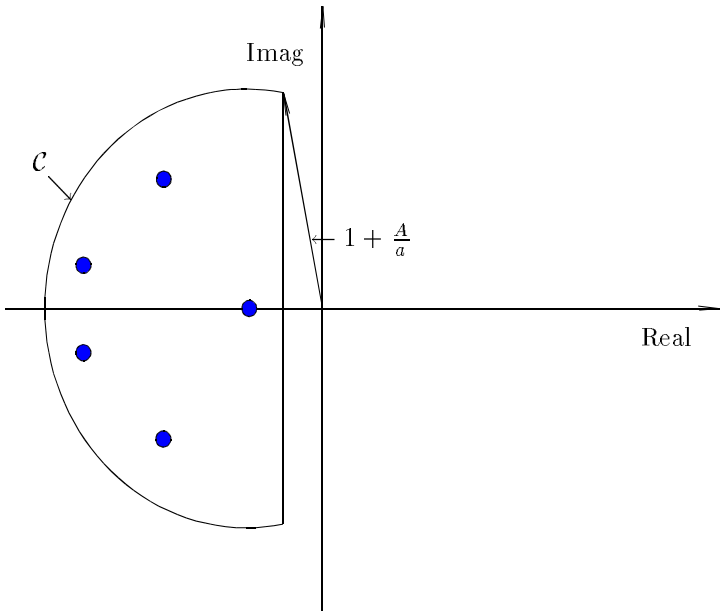

Figure 13.2. A possible choice for $\mathcal{C}$

But, $\mathcal{C}$ being compact in the complex plane, it is possible to find a subsequence $z_{\phi(k)}$ that converges to $z_0 \in \mathcal{C}$. Moreover, $n_{\phi(k)}(\cdot)$ is now a sequence of elements of the compact set $\mathcal{F}_n$, and therefore it is possible to find a subsequence $n_{\phi(\psi(k))}(\cdot)$ that converges to $n_0(\cdot) \in \mathcal{F}_n$. Then we have by (13.3),

$$|n_{\phi(\psi(k))}(z_{\phi(\psi(k))})| \leq \frac{1}{\phi(\psi(k))}. \tag{13.4}$$

Passing to the limit as k goes to infinity in (13.4), one gets:

$$n_0(z_0) = 0.$$

But this is a contradiction because $\mathcal{C}$ is supposed to strictly enclose all the zeroes of any polynomial in $\mathcal{F}_n$. ♣

Property 13.4. Since the family $\mathcal{F}_d$ is bounded we have that for any $d(\cdot)$ in $\mathcal{F}_d$,

$$\text{for all } \ s, \ |d(s)| \leq B\big(1 + |s| + \cdots + |s|^q\big) = \phi(s).$$

Let

$$\beta_d = \sup_{s \in \mathcal{C}} \phi(s).$$

Then β_d is finite (because $\mathcal{C}$ is compact and $\phi(\cdot)$ is continuous) and we have that

$$\sup_{d(\cdot)\in\mathcal{F}_d}\left[\sup_{s\in\mathcal{C}}|d(s)|\right]\leq\beta_d. \tag{13.5}$$

We can now proceed and prove i) and ii) of Theorem 13.1.

Proof of Theorem 13.1.i) Let $\mathcal{C}$ be a closed bounded curve enclosing every zero of each element in $\mathcal{F}_n$, and let α_n and β_d be defined as in (13.3) and (13.5). Then, if we choose ϵ such that $0<|\epsilon|<\frac{\alpha_n}{\beta_d}$,

$$\text{for all}\ \ n(\cdot)\in\mathcal{F}_n,\quad\text{and}\quad\text{for all}\ \ d(\cdot)\in\mathcal{F}_d$$

we have that

$$\text{for all}\ \ s\in\mathcal{C},\ \ |\epsilon d(s)|\leq|\epsilon|\beta_d<\alpha_n\leq|n(s)|. \tag{13.6}$$

Hence, by Rouché's Theorem, we conclude from (13.6) that, for this choice of ϵ, $n(s)+\epsilon d(s)$ has the same number of zeroes as $n(s)$ in $\mathcal{C}$, namely r. But since $n(s)+\epsilon d(s)$ is itself of degree r it is stable. ♣

Remark 13.1. In this case one can notice that the Property B3 of the family $\mathcal{F}_d$ is not needed.

Proof of Theorem 13.1.ii) Let us first suppose that $q=r+1$. Again let $\mathcal{C}$ be a closed bounded curve enclosing every zero of each element in $\mathcal{F}_n$, and let α_n and β_d be defined as in (13.3) and (13.5).
If we start by choosing ϵ_1 such that $0<\epsilon_1<\frac{\alpha_n}{\beta_d}$, and any μ such that $0<\mu<\epsilon_1$, then

$$\text{for all}\ \ n(\cdot)\in\mathcal{F}_n,\ \text{and for all}\ \ d(\cdot)\in\mathcal{F}_d$$

we have

$$\text{for all}\ \ s\in\mathcal{C},\quad|\mu d(s)|\leq\mu\beta_d<\alpha_n\leq|n(s)|.$$

Again we conclude by Rouché's Theorem that for any such μ, $n(s)+\mu d(s)$ has already r zeroes inside $\mathcal{C}$. Moreover it is also possible to find ϵ_2 such that for any μ satisfying $0<\mu<\epsilon_2$, we have that every coefficient of $n(s)+\mu d(s)$ is positive.
If we now choose any ϵ such that

$$0<\epsilon<\min(\epsilon_1,\epsilon_2),$$

we have that $n(s)+\epsilon d(s)$ is of degree less than or equal to $r+1$, has r stable roots, and all its coefficients are positive. But this implies that $n(s)+\epsilon d(s)$ is necessarily stable.

We now proceed by induction on $n=q-r$. Suppose that part ii) of the theorem is true when $q=r+p$, $p\geq1$. Let $\mathcal{F}_n$ and $\mathcal{F}_d$ be two families of polynomials satisfying Properties A1, A2, A3, and B1, B2, B3, respectively, and let us suppose that $q=r+p+1$.

Now consider the new family $\mathcal{F}'_n$ of polynomials $n'(s)$ of the form,

$$n'(s) = (s+1)n(s), \text{ where } n(s) \in \mathcal{F}_n.$$

Obviously $\mathcal{F}'_n$ is also a compact set and each element of $\mathcal{F}'_n$ satisfies Properties A1, A2, A3, but now with $r' = r+1$. Hence by the induction hypothesis it is possible to find a stable polynomial $n'_c(s)$ of degree less than or equal to $p-1$, and a stable polynomial $d'_c(s)$ of degree $p-1$ such that,

$$\text{for all } \; n(\cdot) \in \mathcal{F}_n, \text{ and for all } \; d(\cdot) \in \mathcal{F}_d$$

we have that

$$n(s)(s+1)n'_c(s) + d(s)d'_c(s) \text{ is stable .} \tag{13.7}$$

Now, let $n_c(s) = (s+1)n'_c(s)$, and consider the new family of polynomials $\mathcal{F}'_n$ described by (13.7). That is $\mathcal{F}'_n$ consists of all polynomials $n'(\cdot)$ of the form

$$n'(s) = n(s)n_c(s) + d(s)d'_c(s)$$

where $n(s)$ is an arbitrary element in $\mathcal{F}_n$ and $d(s)$ is an arbitrary element in $\mathcal{F}_d$. The new family of polynomials $\mathcal{F}'_d$ consists of all polynomials $d'(\cdot)$ of the form

$$d'(s) = sd'_c(s)d(s),$$

where $d(s)$ is an element of $\mathcal{F}_d$. Clearly the family $\mathcal{F}'_n$ is compact and satisfies Properties A1, A2, A3 with $r' = r+2p$, and $\mathcal{F}'_d$ is also a compact family of polynomials satisfying Properties B1, B2, B3 with $q' = r+2p+1$. Hence, by applying our result when $n = 1$, we can find an $\epsilon > 0$ such that

$$\text{for all } \; n'(\cdot) \in \mathcal{F}'_n, \quad \text{and} \quad \text{for all } \; d'(\cdot) \in \mathcal{F}'_d,$$

$$n'(s) + \epsilon d'(s) \text{ is stable.}$$

But, in particular, this implies that,

$$\text{for all } \; n(\cdot) \in \mathcal{F}_n, \quad \text{and} \quad \text{for all } \; d(\cdot) \in \mathcal{F}_d,$$

$$n(s)n_c(s) + d'_c(s)d(s) + \epsilon s d'_c(s)d(s) = n(s)n_c(s) + (\epsilon s+1)d'_c(s)d(s) \text{ is stable.}$$

Therefore, the controller defined by

$$C(s) = \frac{n_c(s)}{d_c(s)} = \frac{n_c(s)}{(\epsilon s+1)d'_c(s)},$$

is an answer to our problem and this ends the proof of Theorem 13.1. ♣

In the following sections we discuss first the problem of robust stabilization against unstructured perturbations, the related interpolation problems, and the use of this theory to solve robust stabilization problems under parameter uncertainty. We begin with a description of the Q parametrization.

13.3 INTERNAL STABILITY AND THE Q PARAMETERIZATION

In this section we derive some conditions for the internal stability of a feedback system in terms of the so-called Q parameter. This convenient parametrization allows stabilizing controllers to be determined for the nominal system, and also for perturbed systems.

Consider the standard single loop feedback configuration shown in Figure 13.3.

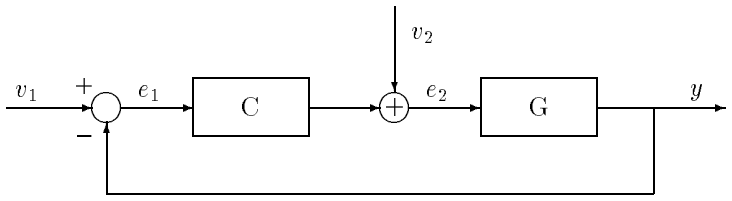

Figure 13.3. General closed-loop system

We assume that the controller and plant are both single-input single-output systems and are represented by the proper, real, rational transfer functions $C(s)$ and $G(s)$ respectively. We first discuss the problem of stabilizing a fixed plant $G(s) = G_0(s)$ with some $C(s)$. Throughout this chapter stability refers to Hurwitz stability unless specified otherwise. As usual we assume that there are no hidden pole-zero cancellations in the closed right half plane (RHP) in $G_0(s)$ as well as in $C(s)$. Let H denote the 2×2 transfer matrix between the *virtual input* $v = [v_1, v_2]'$ and $e = [e_1, e_2]'$. We have

$$H = \begin{bmatrix} H_{e_1,v_1} & H_{e_1,v_2} \\ H_{e_2,v_1} & H_{e_2,v_2} \end{bmatrix} = \begin{bmatrix} (1+G_0C)^{-1} & -G_0(1+CG_0)^{-1} \\ C(1+G_0C)^{-1} & (1+CG_0)^{-1} \end{bmatrix} \tag{13.8}$$

The closed loop system in Figure 13.3 is *internally stable* if and only if all the elements of H are stable and proper, or equivalently, H_∞ functions. This condition for stability is completely equivalent to that of stability of the characteristic polynomial. It guarantees that all signals in the loop remain bounded as long as the external virtual inputs at v_1 or v_2 are bounded.

The controller appears nonlinearly in H. A "linear" parametrization of the feedback loop can be obtained by introducing the *parameter*

$$Q(s) := \frac{C(s)}{1 + G_0(s)C(s)}. \tag{13.9}$$

The controller

$$C(s) = \frac{Q(s)}{1 - G_0(s)Q(s)} \tag{13.10}$$

and it can be seen that $C(s)$ is proper if and only if $Q(s)$ is proper. In terms of the parameter $Q(s)$

$$H = \begin{bmatrix} 1 - G_0Q & -G_0(1 - G_0Q) \\ Q & 1 - G_0Q \end{bmatrix} \tag{13.11}$$

and therefore the necessary and sufficient conditions for internal stability of the feedback system are the following:

Stability Conditions

1) $Q(s) \in H_\infty$;

2) $G_0(s)Q(s) \in H_\infty$;

3) $G_0(s)(1 - G_0(s)Q(s)) \in H_\infty$.

To proceed, we make the simplifying standing assumptions:

i) $G_0(s)$ has no poles on the $j\omega$ axis;

ii) The RHP poles $\alpha_i,\ i = 1, ...l$ of $G_0(s)$ are nonrepeated.

The stability conditions 1)-3) can then be translated into the equivalent conditions:

1′) $Q(s) \in H_\infty$;

2′) $Q(\alpha_i) = 0, \quad i = 1, \cdots, l$;

3′) $G_0(\alpha_i)Q(\alpha_i) = 1, \quad i = 1, \cdots, l$.

The search for a proper, rational stabilizing compensator $C(s)$ is thus reduced to the *equivalent* problem of finding a real, rational, proper function $Q(s)$ which satisfies the above conditions. Once a suitable $Q(s)$ is found, the compensator can be recovered from the inverse relation (13.10) above. Therefore we can parametrize all stabilizing compensators for $G_0(s)$ by parametrizing all functions $Q(s)$ which satisfy the above conditions. This is what we do next.

Let $\bar{\alpha}$ denote the conjugate of α and introduce the *Blaschke product*

$$B(s) = \Pi \left[\frac{\alpha_i - s}{\bar{\alpha}_i + s} \right] \tag{13.12}$$

and let

$$Q(s) := B(s)\tilde{Q}(s). \tag{13.13}$$

With this choice of $Q(s)$ condition 2′) is automatically satisfied for every stable $\tilde{Q}(s)$. Now let

$$\tilde{G}_0(s) := B(s)G_0(s) \tag{13.14}$$

so that

$$G_0(s)Q(s) = \frac{\tilde{G}_0(s)}{B(s)}B(s)\tilde{Q}(s) = \tilde{G}_0(s)\tilde{Q}(s). \tag{13.15}$$

We note that $B(s) \in H_\infty$ and $\tilde{G_0}(s) \in H_\infty$ so that conditions 1) and 2) for internal stability are satisfied if and only if $\tilde{Q}(s) \in H_\infty$. The remaining stability condition 3′) now becomes

$$\tilde{Q}(\alpha_i) = \frac{1}{\tilde{G_0}(\alpha_i)} := \tilde{\beta}_i. \tag{13.16}$$

If $G_0(s)$ is given, so are α_i and $\tilde{\beta}_i$ and therefore the problem of stabilizing the nominal system by some $C(s)$ is reduced to the *interpolation problem*:

Find a function $\tilde{Q}(s) \in H_\infty$ satisfying

$$\tilde{Q}(\alpha_i) = \tilde{\beta}_i, \quad i = 1, \cdots, l. \tag{13.17}$$

Once a $\tilde{Q}(s) \in H_\infty$ satisfying (13.17) is found, $Q(s) = B(s)\tilde{Q}(s)$ satisfies the stability conditions 1), 2) and 3), and hence the corresponding $C(s)$, which can be determined uniquely from (13.10), is guaranteed to be proper and stabilizing. It is straightforward to find a stable proper $Q(s)$ that satisfies the interpolation conditions (13.17). We also remark that the assumptions regarding the poles of $G_0(s)$ can be relaxed by placing some more interpolation conditions on $\tilde{Q}(s)$.

We shall see in the next section that in the problem of *robust stabilization*, additional restrictions in the form of a norm bound will have to be imposed on $\tilde{Q}(s)$.

13.4 ROBUST STABILIZATION: UNSTRUCTURED PERTURBATIONS

We continue with the problem setup and notation established in the last section, but suppose now that the plant transfer function is subject to unstructured norm bounded perturbations which belong to an additive or multiplicative class.

Additive and Multiplicative Perturbations

Write $G(s) = G_0(s) + \Delta G(s)$ with $\Delta G(s)$ specified by a frequency dependent magnitude constraint as follows. Let $r(s)$ be a given, real, rational, minimum phase (no zeroes in the closed RHP), H_∞ function. We introduce the definitions:

Definition 13.1. (Additive Perturbations) A transfer function $G(s)$ is said to be in the class $A(G_0(s), r(s))$ if

i) $G(s)$ has the same number of poles as $G_0(s)$;
ii) $|G(j\omega) - G_0(j\omega)| \leq |r(j\omega)|, \ |r(j\omega)| > 0, \ \text{for all} \quad \omega \in \mathbb{R}.$

Similarly we can also consider multiplicative perturbations. Here we have $G(s) = (1 + \Delta G(s))G_0(s)$ and a frequency dependent magnitude constraint is placed on $\Delta G(j\omega)$ using a suitable real, rational, minimum phase H_∞ function $r(s)$.

Definition 13.2. (Multiplicative Perturbations) A transfer function $G(s)$ is said to be in the class $M(G_0(s), r(s))$ if:

1) $G(s)$ has the same number of unstable poles as $G_0(s)$;
2) $G(s) = (1 + M(s))G_0(s)$ with $|M(j\omega)| < |r(j\omega)|$, for all $\omega \in \mathbb{R}$.

Suppose now that a compensator $C(s)$ which stabilizes $G_0(s)$ is given. We first establish the conditions for $C(s)$ to be a robust stabilizer for all plants in the class $A(G_0(s), r(s))$.

If $C(s)$ stabilizes $G_0(s)$ we have

$$G_0(j\omega)C(j\omega) + 1 \neq 0, \quad \text{for all} \quad \omega \in \mathbb{R} \tag{13.18}$$

and we also know that the Nyquist plot of $G_0(s)C(s)$ has the correct number of encirclements of the -1 point.

Now let us consider what happens to the stability of the closed loop system when $G_0(s)$ is replaced by its perturbed version $G(s) = G_0(s) + \Delta G(s)$. Since $G_0(s)$ and $G(s)$ have the same number of unstable poles, the only way that the closed loop can become unstable is by a change in the number of encirclements of the $-1 + j0$ point by the Nyquist plot of $G(s)C(s)$. In terms of frequency domain plots, this means that the plots of $G_0(j\omega)C(j\omega)$ and $G(j\omega)C(j\omega)$ lie on opposite sides of -1. Thus, stability of the perturbed system can be ensured if the perturbation $\Delta G(s)$ is of small enough size that the plot of $G(j\omega)C(j\omega)$ does not pass through the -1 point. This can be stated as the condition

$$1 + G(j\omega)C(j\omega) \neq 0, \qquad \text{for all} \quad \omega \in \mathbb{R} \tag{13.19}$$

or, equivalently as

$$(1 + G_0(j\omega)C(j\omega))(1 + (1 + G_0(j\omega)C(j\omega))^{-1}C(j\omega)\Delta G(j\omega)) \neq 0, \quad \text{for all} \quad \omega \in \mathbb{R}.$$

The above condition will hold as long as

$$\sup_{\omega} |(1 + G_0(j\omega)C(j\omega))^{-1}C(j\omega)\Delta G(j\omega)| < 1 \tag{13.20}$$

It follows from this analysis that a sufficient condition for robust stability with respect to the class $A(G_0(s), r(s))$ is given by

$$\|(1 + G_0(s)C(s))^{-1}C(s)r(s)\|_\infty < 1 \tag{13.21}$$

If the above condition is violated, a real rational admissible perturbation $\Delta G(s)$ can be constructed for which the closed loop system with $G(s) = G_0(s) + \Delta G(s)$ is unstable. Thus, the condition (13.21) is also necessary for robust stability.

Analogous results hold for multiplicative unstructured uncertainty. By arguing exactly as in the additive case we can show that a compensator $C(s)$ which stabilizes $G_0(s)$, stabilizes all plants $G(s)$ in the class $M(p_0(s), r(s))$ if

$$\|G_0(s)C(s)(1 + G_0(s)C(s))^{-1}r(s)\|_\infty < 1. \tag{13.22}$$

Henceforth we focus on the additive case since similar results hold for the multiplicative case. We see that the robustness condition (13.21) is equivalent to

$$\|Q(s)r(s)\|_\infty < 1. \tag{13.23}$$

Using the fact that $\|B(s)\|_\infty = 1$ we can write (13.23) as

$$\|\tilde{Q}(s)r(s)\|_\infty < 1. \tag{13.24}$$

Now introduce the function

$$u(s) := \tilde{Q}(s)r(s). \tag{13.25}$$

The robust stability condition can now be written as

$$\|u(s)\|_\infty < 1. \tag{13.26}$$

The interpolation conditions (13.17) on $\tilde{Q}(s)$ translate to corresponding ones on $u(s)$:

$$u(\alpha_i) = \tilde{Q}(\alpha_i)r(\alpha_i) = \frac{r(\alpha_i)}{\tilde{G}_0(\alpha_i)} = \beta_i, \quad i = 1, ...l. \tag{13.27}$$

In these terms, the robust stabilization problem is reduced to the following:

Interpolation Problem

Given complex numbers $\alpha_i, \beta_i,\ i = 1, \cdots, l$ find, if possible, a real rational function $u(s)$ which satisfies the conditions

a) $\|u(s)\|_\infty < 1$
b) $u(\alpha_i) = \beta_i,\ i = 1, \cdots, l.$

The solution of the above problem is described in the next section (Nevanlinna-Pick Interpolation).

In summary the robustly stabilizing controller $C(s)$ is determined from the steps:

Step 1 Determine the RHP poles α_i of $G_0(s)$, $B(s)$ and $\tilde{G}_0(s)$;

Step 2 Determine

$$\beta_i = \frac{r_(\alpha_i)}{\tilde{G}_0(\alpha_i)}, \quad i = 1, \cdots, l;$$

Step 3 Calculate a real rational H_∞ function $u(s)$ with $\|u(s)\|_\infty < 1$ solving the Interpolation Problem

$$u(\alpha_i) = \beta_i, \quad i = 1, \cdots, l$$

by using the Nevanlinna-Pick theory, described in the next section;

Step 4 Calculate $Q(s)$ from

$$Q(s) = \frac{B(s)u(s)}{r(s)};$$

Step 5 Determine $C(s)$ from

$$C(s) = \frac{Q(s)}{1 - G_0(s)Q(s)}.$$

In Step 3, $Q(s)$ must be an H_∞ function and this requires, since $B(s) \in H_\infty$, that

$$\frac{u(s)}{r(s)} \in H_\infty. \tag{13.28}$$

Since $u(s) \in H_\infty$ it follows that $Q(s) \in H_\infty$ if $\frac{1}{r(s)} \in H_\infty$. We have already assumed that $r(s)$ has no finite RHP zeros. The condition $\frac{1}{r(s)} \in H_\infty$ means that $r(s)$ should have relative degree zero, equivalently no zeros at infinity. If it is necessary to let $r(s)$ have relative degree 1, say, we need then to let $u(s)$ also have relative degree 1, so that we have $\frac{u(s)}{r(s)} \in H_\infty$. This translates to an additional interpolation condition

$$u(\infty) = 0.$$

on $u(s)$.

In the next section we describe the solution of the Interpolation Problem formulated above.

13.5 NEVANLINNA-PICK INTERPOLATION

In the previous section we established that robust stabilization against additive unstructured perturbations can be achieved provided we find a real rational function $u(s)$ with H_∞ norm $\|u\|_\infty < 1$ which satisfies the interpolation condition

$$u(\alpha_i) = \beta_i, \quad i = 1, \ldots, l; \quad \mathrm{Re}[\alpha_i] > 0, \ |\beta_i| < 1. \tag{13.29}$$

Once $u(s)$ is obtained, we can find the robustly stabilizing controller $C(s)$ using the Steps outlined in the previous section.

A real, rational, function $u(s)$ with $\|u\|_\infty < 1$ is also called a *strictly bounded real* (SBR) function. To get a proper controller, $u(s)$ needs to have relative degree at least as large as $r(s)$. Thus $u(s)$ needs to be proper if $r(s)$ has relative degree 0 and strictly proper ($u(\infty) = 0$) when the relative degree of $r(s)$ is 1.

A complex, stable, proper, rational function $u(s)$ with $\|u(s)\|_\infty < 1$ is called a Schur function. The problem of finding a Schur function $u(s)$ satisfying the interpolation conditions given above is known as the *Nevanlinna-Pick problem* (NP problem) and is outlined below without proofs. Once a Schur function $u(s)$ is found, an SBR function satisfying the same interpolation conditions can easily be found. First, we have the condition for the existence of a solution.

Theorem 13.2 *The Nevanlinna-Pick problem admits a solution if and only if the Pick matrix P, whose elements p_{ij} are given by*

$$p_{ij} = \frac{1 - \beta_i \overline{\beta}_j}{\alpha_i + \overline{\alpha}_j} \tag{13.30}$$

is positive definite.

If the Pick matrix is positive definite a solution exists. The solution is generated by successively reducing an interpolation problem with k interpolation points to one with $k-1$ points. The problem with one point has an obvious solution. This is the *Nevanlinna algorithm* and is described next.

Consider the linear fractional transformation mapping $u_i(s)$ to $u_{i-1}(s)$

$$u_{i-1}(s) = \frac{\rho_{i-1} + u_i(s)\left(\dfrac{s-\alpha_{i-1}}{s+\overline{\alpha}_{i-1}}\right)}{1 + \overline{\rho}_{i-1}\left(\dfrac{s-\alpha_{i-1}}{s+\overline{\alpha}_{i-1}}\right) u_i(s)}. \tag{13.31}$$

The inverse transformation is

$$u_i(s) = \frac{u_{i-1}(s) - \rho_{i-1}}{1 - \overline{\rho}_{i-1} u_{i-1}(s)} \left(\frac{s+\overline{\alpha}_{i-1}}{s-\overline{\alpha}_{i-1}}\right). \tag{13.32}$$

Let us denote these transformations compactly as

$$u_i(s) = T_{\rho_{i-1}} u_{i-1}(s); \quad u_{i-1}(s) = T^{-1}_{\rho_{i-1}} u_i(s). \tag{13.33}$$

It can be seen that

$$u_{i-1}(\alpha_{i-1}) = \rho_{i-1}, \quad \text{for all } \; u_i(s). \tag{13.34}$$

Moreover, it can be shown that $u_{i-1}(s)$ is Schur if $u_i(s)$ is Schur and conversely that $u_{i-1}(s)$ Schur and $u_{i-1}(\alpha_{i-1}) = \rho_{i-1}$ imply that $u_i(s)$ is Schur.

Now suppose that $i = 2$, $u_1(s) = u(s)$, $\rho_1 = \beta_1$ in (13.31). We see that $u(\alpha_1) = \beta_1$ regardless of $u_2(s)$ and the remaining $l-1$ interpolation conditions on $u_1(s)$ are transferred to $u_2(s)$:

$$\begin{aligned}
u_2(\alpha_2) &= T_{\rho_1}(u_1(\alpha_2)) = T_{\rho_1}(\beta_2) := \rho_2 \\
u_2(\alpha_3) &= T_{\rho_1}(u_1(\alpha_3)) = T_{\rho_1}(\beta_3) := \rho_{2,3} \\
&\vdots \\
u_2(\alpha_l) &= T_{\rho_1}(u_1(\alpha_l)) = T_{\rho_1}(\beta_l) := \rho_{2,l}.
\end{aligned}$$

Thus, the original problem of interpolating l with a Schur function $u_1(s)$ is reduced to the problem of interpolating $l-1$ points with a Schur function $u_2(s)$. In this way, a family of solutions $u(s)$, parametrized in terms of an arbitrary initial Schur function $u_{l+1}(s)$, can be obtained.

The above calculations can be organized by forming the *Fenyves array* as shown in Table 13.1.

Table 13.1. Fenyves array

α_1	α_2	α_3	$\cdots$	α_l	
ρ_1	$\rho_{1,2}$	$\rho_{1,3}$	$\cdots$	$\rho_{1,l}$	$u_1(s)$
	ρ_2	$\rho_{2,3}$	$\cdots$	$\rho_{2,l}$	$u_2(s)$
		$\cdots$	$\cdots$	$\cdots$	$\cdots$
				ρ_l	$u_l(s)$

where $u_1(s) = u(s)$, $\rho_1 = \beta_1$ and $\rho_{1,j} = \beta_j$

$$\rho_i = \frac{\rho_{i-1,i} - \rho_{i-1}}{1 - \overline{\rho}_{i-1}\rho_{i-1,i}} \quad \frac{\alpha_i + \overline{\alpha}_{i-1}}{\alpha_i - \alpha_{i-1}}; \quad 1 < i \leq l \tag{13.35}$$

and

$$\rho_{i,j} = \frac{\rho_{i-1,j} - \rho_{i-1}}{1 - \overline{\rho}_{i-1}\rho_{i-1,j}} \quad \frac{\alpha_j + \overline{\alpha}_{i-1}}{\alpha_j - \alpha_{i-1}}; \quad 1 < i < j \leq l \tag{13.36}$$

An existence condition equivalent to that of the positive definiteness of the Pick matrix is the following.

Theorem 13.3 *The Nevanlinna-Pick problem admits a solution if and only if the modulus of all the elements of the Fenyves array is less than one:* $|\rho_i| < 1$, $|\rho_{i,j}| < 1$.

The algorithm given generates a Schur function $u(s) = u_R(s) + ju_I(s)$ which satisfies the interpolation conditions. It can be shown that if the complex elements in the set α_i appear along with their conjugates and the corresponding β_i are also conjugated, then $u_R(s)$ is a real H_∞ function with $\|u_R(s)\|_\infty < 1$ which also satisfies the interpolation conditions. The above algorithm can also be suitably modified to handle the case when the nominal model has a pole at the origin. We show this in the examples.

In the next section we discuss how robust stabilization against parametric uncertainty might be attempted using the theory for unstructured perturbations.

13.6 OVERBOUNDING PARAMETRIC UNCERTAINTY BY UNSTRUCTURED UNCERTAINTY

In this section our objective is to show how the frequency domain uncertainty induced by parametric uncertainty can be "covered" by overbounding with a suitable bounding function $r(s)$. Once this is accomplished, the preceding theory of robust synthesis under norm bounded perturbations (Section 13.4) can be applied to the problem. If the procedure is successful the resulting controller robustly stabilizes the system under the given parametric uncertainty set.

Consider the feedback system shown in Figure 13.4.

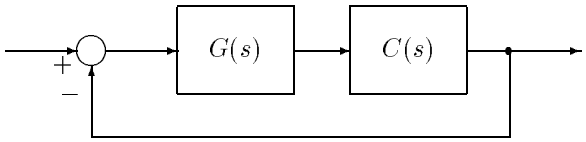

Figure 13.4. A unity feedback system

Suppose the system consists of a plant $G(s, \mathbf{p})$ containing a parameter $\mathbf{p}$ which varies in an uncertainty set $\Omega(\epsilon)$ about a nominal value $\mathbf{p}^0$. The parametric uncertainty set $\Omega(\epsilon)$ is defined by:

$$\Omega(\epsilon) := \left\{ \mathbf{p} : \|\mathbf{p} - \mathbf{p}^0\| \leq \epsilon \right\}.$$

Thus, the size of the uncertainty set Ω is parametrized by ϵ, and we shall loosely refer to $\Omega(\epsilon)$ as a set of plants. Ideally one would like to find the largest such set in the parameter space of the plant that can be robustly stabilized. This means that the free parameter ϵ needs to be increased and the set Ω enlarged until the maximum ϵ, $\epsilon_{\max}$ is reached for which the entire family of plants is stabilizable. It is also necessary to find at least one compensator $C(s)$ that will robustly stabilize the family of plants for any $\epsilon \leq \epsilon_{\max}$. This problem of finding $\epsilon_{\max}$ is as *yet unsolved.* However, we shall show that by using the extremal properties of the generalized Kharitonov segments and the techniques from H_∞ synthesis, we can determine an $\epsilon^* \leq \epsilon_{\max}$ such that a robustly stabilizing controller $C^*(s)$ can be found for the family of plants $\Omega(\epsilon^*)$.

Norm-bounded Uncertainty and Parametric Uncertainty

Our objective is to determine a bounding function $r(s)$ which bounds the frequency domain uncertainty induced by parametric uncertainty. To be specific, let us consider the parametric uncertainty to be modelled by an interval plant denoted by $\mathbf{G}^\epsilon(s)$:

$$\mathbf{G}^\epsilon(s) := \left\{ G(s) \ : \ G(s) = \frac{n(s,\epsilon)}{d(s,\epsilon)} = \frac{n_q(\epsilon)s^q + \cdots + n_0(\epsilon)}{d_q(\epsilon)s^q + \cdots + d_0(\epsilon)} \right\}, \tag{13.37}$$

where

$$n_i(\epsilon) \in [n_i^0 - w_i\epsilon, n_i^0 + w_i\epsilon], \qquad d_i(\epsilon) \in [d_j^0 - w_j\epsilon, d_j^0 + w_j\epsilon].$$

Here q is the plant order and $i, j = 0, \ldots, q$. The size of the plant coefficient perturbations are parametrized by the free parameter ϵ and the weighting factors w_i and w_j which are chosen to reflect scaling factors and the relative importance of the perturbations. The perturbation set $\Omega(\epsilon)$ is a box in the coefficient space of the

plant, each side of which has a length of $2w_i\epsilon$. The center of this box corresponds to the nominal coefficient values, $n_i^{p_0}$ and $d_i^{p_0}$.

The Bode uncertainty magnitude band induced by parametric uncertainty is

$$|G^\epsilon(j\omega) - G_0(j\omega)| = |\Delta G^\epsilon(j\omega)|. \tag{13.38}$$

We seek a stable, proper, real rational, minimum phase function $r(s)$ for which

$$|\Delta G^\epsilon(j\omega)| < |r(j\omega)|, \quad \text{for all} \ \ \omega \in \mathbb{R} \tag{13.39}$$

We know from Chapter 8 that at each frequency, the maximum magnitude in the complex plane template $\mathbf{G}^\epsilon(j\omega)$ will correspond to a point on one of the extremal segments of $\mathbf{G}^\epsilon(s)$ which we denote as $\mathbf{G}^\epsilon_{\rm E}(s)$. We can therefore search over the extremal segments $\mathbf{G}^\epsilon_{\rm E}(s)$ at all frequencies and calculate exactly the maximum perturbation $\delta(\epsilon,\omega)$ induced at the frequency ω. In other words

$$\delta(\epsilon,\omega) = \max_{G\in\mathbf{G}^\epsilon} |\Delta G^\epsilon(j\omega)|.$$

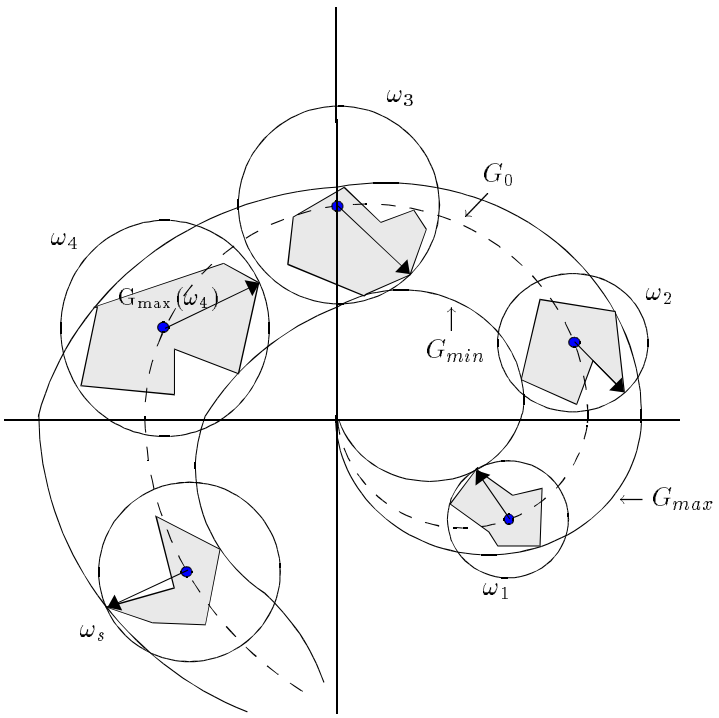

Figure 13.5. Parametric uncertainty converted to H_∞ uncertainty for an interval plant $G(s)$

Figure 13.5, which shows the polar plot for an arbitrary $G(s)$, is drawn to illustrate this overbounding for a prescribed value of ϵ.

In Figure 13.5 the uncertainty image set is induced by the variation of parameters within the ϵ-sized box in parameter space. These image sets are enclosed within a band which represents the minimum and maximum magnitudes at each frequency. The curves $G_{\min}$ and $G_{\max}$ are formed by the minimum and maximum magnitude points of $\mathbf{G}(s)$ at each frequency. The curve G_0 denotes the plot for the nominal plant. At each frequency, the largest distance between the nominal point and a point on the boundary of the uncertainty set is the maximum additive unstructured perturbation magnitude, $\delta(\omega)$ at that frequency. A circle drawn with its center at the nominal point and of radius $\delta(\omega)$ represents "the H_∞ uncertainty at that frequency and ϵ." The figure shows such sets for five frequencies. At frequency ω_4, for example, the center of the circle is named $G_0(\omega_4)$ and its radius is $\delta(\omega_4)$ which is equal to $\Delta G_{\max}(\omega_4)$. The conservativeness introduced by replacing the parametric uncertainty by the H_∞ uncertainty circles is obvious from Figure 13.5. Figure 13.6 shows the bigger and more conservative uncertainty band. It covers the uncertainty circles with radius $\delta(\omega)$ at each frequency.

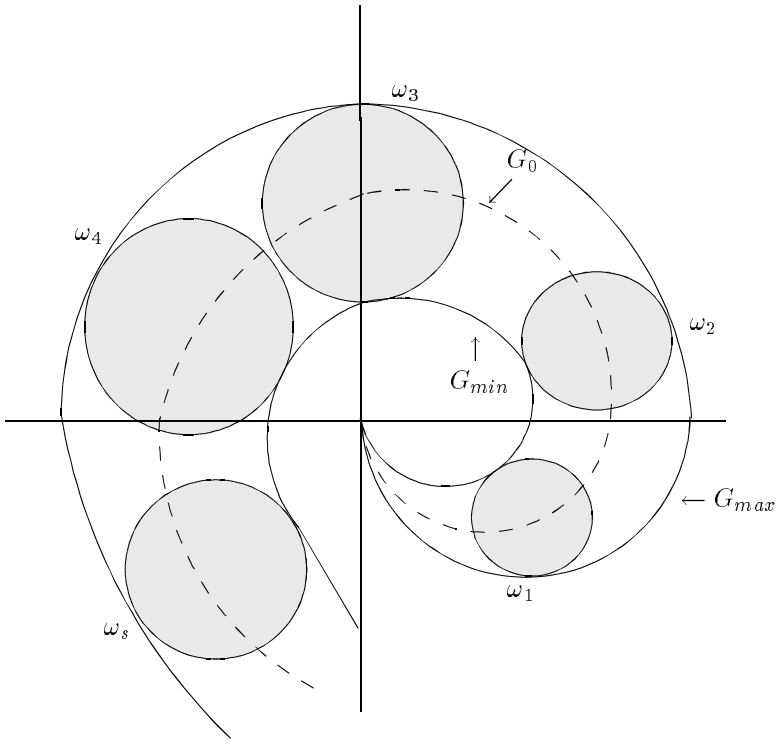

Figure 13.6. H_∞ uncertainty circles of radius $\delta(\omega)$

With this computation in hand we can proceed to the choice of a bounding function $r(s)$. The simplest choice of $r(s)$ is a constant

$$r(s) = r = \delta(\epsilon) = \max_{\omega \in \mathbf{R}} \delta(\epsilon, \omega) \tag{13.40}$$

which equals the radius of the largest such uncertainty circle over all frequencies. Figure 13.7 shows the uncertainty band for the above choice of $r(s)$.

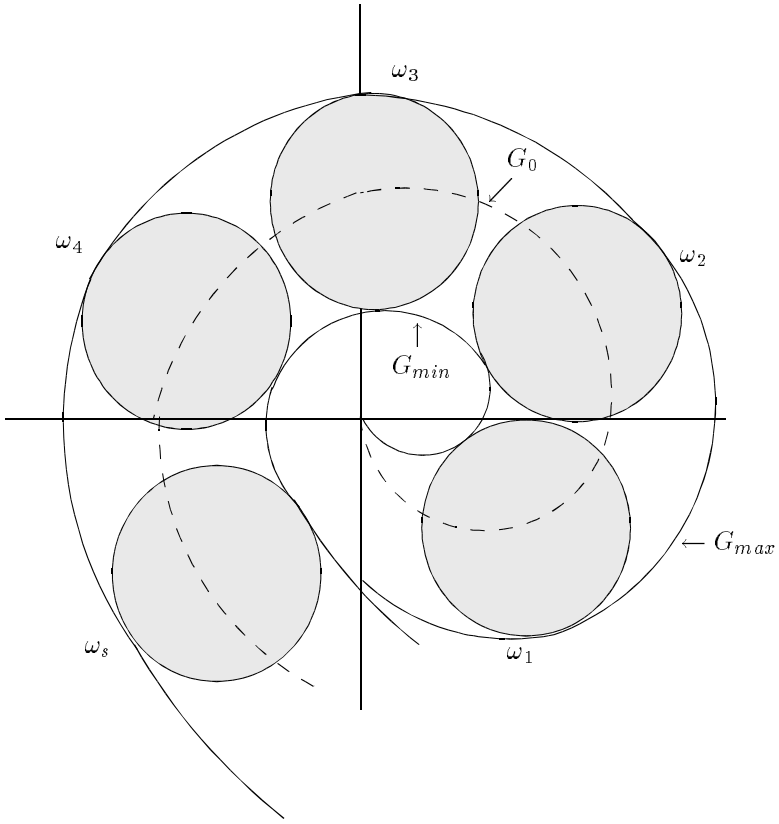

Figure 13.7. Uncertainty band when $r = \delta(\epsilon)$

Here, the circles of different sizes at different frequencies are all replaced by the biggest circle. In Figure 13.7 this is the circle at frequency ω_4. The choice of constant $r(s)$, although simple, gives a more conservative bounding of $\Delta G(s)$, which eventually means a lower value of $\epsilon_{\max}$. This conservativeness can often be minimized by introducing poles and zeros in $r(s)$ and shaping it such that $|r(j\omega)|$ approximates $\delta(\epsilon, \omega)$ at each ω as closely as possible from above:

$$|r(j\omega)| > \delta(\epsilon, \omega), \quad \text{for all } \omega \in \mathbb{R}.$$

We describe by examples how the H_∞ synthesis methods may be applied to interval plants. Let us start with an example for a stable nominal plant.

Example 13.1. Let the nominal plant be

$$G_0(s) = \frac{s+1}{s^3+8s^2+22s+20}$$

with poles at $-2, -3 \pm j$, all in the LHP. The perturbed plant is written as

$$G(s) = \frac{s+a}{s^3+bs^2+cs+d},$$

and the perturbation of the coefficients about the nominal is given by

$$a \in [1-\epsilon, 1+\epsilon], \quad b \in [8-\epsilon, 8+\epsilon], \quad c \in [22-\epsilon, 22+\epsilon], \quad d \in [20-\epsilon, 20+\epsilon].$$

Since it is assumed that the number of unstable poles of the plant should remain unchanged, it is required that ϵ be less than some ϵ_1 which is such that the entire family of plants is stable. This initial bound, ϵ_1 on ϵ can be found by checking the Hurwitz stability of the denominator Kharitonov polynomials:

$$\begin{aligned}
K_{d1}(s) &= s^3 + (8+\epsilon)s^2 + (22-\epsilon)s + (20-\epsilon) \\
K_{d2}(s) &= s^3 + (8+\epsilon)s^2 + (22+\epsilon)s + (20-\epsilon) \\
K_{d3}(s) &= s^3 + (8-\epsilon)s^2 + (22-\epsilon)s + (20+\epsilon) \\
K_{d4}(s) &= s^3 + (8-\epsilon)s^2 + (22+\epsilon)s + (20+\epsilon).
\end{aligned}$$

From the Routh-Hurwitz table for $K_{d1}(s), K_{d2}(s), K_{d3}(s), K_{d4}(s)$, it can be shown that $\epsilon_1 = 6.321$, i.e., the entire family of plants will be stable as long as $\epsilon < 6.321$.

Now, for each ϵ, all the extremal segments will have to be searched at each ω to get $\delta(\epsilon, \omega) = \max_{G \in \mathbf{G}^\epsilon} |\Delta G^\epsilon(j\omega)|$. Then

$$\delta(\epsilon) := \max_{\omega \in \mathbf{R}} \delta(\epsilon, \omega).$$

The next task is to find a suitable bounding function $r(s)$. Once an $r(s)$ is obtained, a robustly stabilizing compensator can be synthesized for the interval plant with parameter perturbations in that $\epsilon-$box. This can be done for any $\epsilon < 6.321$.

For a constant $r(s)$ we must have

$$r(s) = r = \delta(\epsilon).$$

To proceed let us set $\epsilon = 6$. For this choice of ϵ the numerator and denominator Kharitonov polynomials are:

$$\begin{aligned}
K_{n1}(s) = K_{n2}(s) &= s-5, & K_{n3}(s) = K_{n4}(s) &= s+7 \\
K_{d1}(s) &= s^3+14s^2+16s+14, & K_{d2}(s) &= s^3+14s^2+28s+14 \\
K_{d3}(s) &= s^3+2s^2+16s+26, & K_{d4}(s) &= s^3+2s^2+28s+26.
\end{aligned}$$

The numerator and denominator Kharitonov segments are

$$
\begin{aligned}
S_n(s,\lambda) &= (1-\lambda)K_{n1}(s) + \lambda K_{n3}(s) = s + (12\lambda - 5) \\
S_{d1}(s,\lambda) &= (1-\lambda)K_{d1}(s) + \lambda K_{d2}(s) = s^3 + 14s^2 + (12\lambda + 16)s + 14 \\
S_{d2}(s,\lambda) &= (1-\lambda)K_{d1}(s) + \lambda K_{d3}(s) = s^3 + (14 - 12\lambda)s^2 + 16s + (14 + 12\lambda) \\
S_{d3}(s,\lambda) &= (1-\lambda)K_{d2}(s) + \lambda K_{d4}(s) = s^3 + (14 - 12\lambda)s^2 + 28s + (14 + 12\lambda) \\
S_{d4}(s,\lambda) &= (1-\lambda)K_{d3}(s) + \lambda K_{d4}(s) = s^3 + 2s^2 + (16 + 12\lambda)s + 26,
\end{aligned}
$$

where $\lambda \in [0,1]$. The extremal plants are

$$
\begin{aligned}
G_1(s,\lambda) &= \frac{K_{n1}(s)}{S_{d1}(s,\lambda)}, \qquad G_2(s,\lambda) = \frac{K_{n1}(s)}{S_{d2}(s,\lambda)}, \qquad G_3(s,\lambda) = \frac{K_{n1}(s)}{S_{d3}(s,\lambda)}, \\
G_4(s,\lambda) &= \frac{K_{n1}(s)}{S_{d4}(s,\lambda)}, \qquad G_5(s,\lambda) = \frac{K_{n3}(s)}{S_{d1}(s,\lambda)}, \qquad G_6(s,\lambda) = \frac{K_{n3}(s)}{S_{d2}(s,\lambda)}, \\
G_7(s,\lambda) &= \frac{K_{n3}(s)}{S_{d3}(s,\lambda)}, \qquad G_8(s,\lambda) = \frac{K_{n3}(s)}{S_{d4}(s,\lambda)}, \qquad G_9(s,\lambda) = \frac{S_n(s,\lambda)}{K_{d1}(s)}, \\
G_{10}(s,\lambda) &= \frac{S_n(s,\lambda)}{K_{d2}(s)}, \qquad G_{11}(s,\lambda) = \frac{S_n(s,\lambda)}{K_{d3}(s)}, \qquad G_{12}(s,\lambda) = \frac{S_n(s,\lambda)}{K_{d4}(s)}.
\end{aligned}
$$

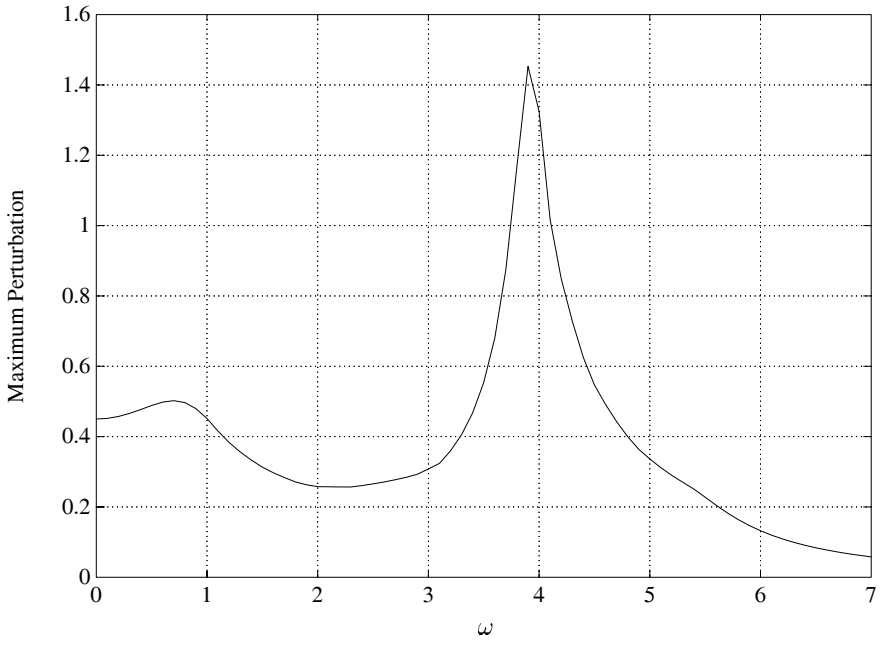

Figure 13.8. Maximum perturbation $\delta(\epsilon,\omega)$ vs ω for $\epsilon = 6$ (Example 13.1)

By searching through these extremal segment plants we get the plot of the maximum perturbation $\delta(\epsilon, \omega)$ at each ω as shown in Figure 13.8. The maximum value $\delta(6)$ of $\delta(6, \omega)$ is found to be 1.453. Therefore we choose $r = 1.453$ to proceed with our synthesis. Since there are no unstable poles in $G_0(s)$ there are no interpolation constraints. So, for the stable plant case, the controller can be parametrized in terms of an arbitrary Schur function $u(s)$. Let us pick $u(s) = u = 0.3 < 1$. Then

$$Q = \frac{u}{r} = \frac{0.3}{1.453} = 0.207$$

and

$$\begin{aligned} C(s) &= \frac{Q}{1 - G_0 Q} = \frac{u(s)}{r(s) - G_0(s)u(s)} \\ &= \frac{0.207(s^3 + 8s^2 + 22s + 20)}{s^3 + 8s^2 + 21.793s + 19.793}. \end{aligned}$$

This $C(s)$ stabilizes the interval plant $G(s)$ with coefficients varying in the intervals

$$a \in [-5, 7], \quad b \in [2, 14], \quad c \in [16, 28], \quad d \in [14, 26].$$

The above example shows that for an interval plant which is built around a *stable* nominal plant it is *always* possible to come up with a robustly stabilizing compensator so long as the coefficient perturbation, ϵ, is less than ϵ_1.

Next we consider an example of a nominal plant with a single unstable pole.

Example 13.2. Let the nominal plant be

$$G_0(s) = \frac{5s + 4}{(s - 3)(s + 5)} = \frac{5s + 4}{s^2 + 2s - 15},$$

and the interval plant be

$$G(s) = \frac{5s + a}{s^2 + bs + c},$$

where

$$a \in [4 - \epsilon, 4 + \epsilon], \quad b \in [2 - \epsilon, 2 + \epsilon], \quad c \in [-15 - \epsilon, -15 + \epsilon].$$

Using the Routh-Hurwitz criterion on the denominator Kharitonov polynomials, it can be shown that the number of unstable zeros of $K_{di}(s),\ i = 1, 2, 3, 4$ (and hence the number of unstable poles of the family of plants) does not change for any $\epsilon < 15$. The Blaschke product is

$$B(s) = \frac{3 - s}{3 + s}.$$

$$\tilde{G}_0(s) = B(s)P_0(s) = -\frac{5s + 4}{(s + 3)(s + 5)}$$

$$\tilde{G}_0(3) = -\frac{5(3) + 4}{(3 + 3)(3 + 5)} = -0.396$$

We have to find a Schur function $u(s)$ such that

$$u(3) = \frac{r(3)}{\tilde{G}_0(3)} = \frac{-r(3)}{0.396},$$

and it is necessary that

$$|u(3)| < 1.$$

Here, if the design is to be done with a constant r, it is necessary that $r < 0.396$ for a robust stabilizer to exist. Therefore $\delta(\epsilon) = 0.396$.

As before we now generate the $\delta - \epsilon$ graph relating unstructured perturbations to structured perturbations. This involves generating the extremal set and searching over it at each frequency for the largest perturbation $\delta(\epsilon, \omega)$ for each value of ϵ. The details of this calculation are left as an exercise (Exercise 13.3). By further maximizing this perturbation over ω, we obtain $\delta(\epsilon)$. The plot $\delta(\epsilon)$ vs ϵ is shown in Figure 13.9.

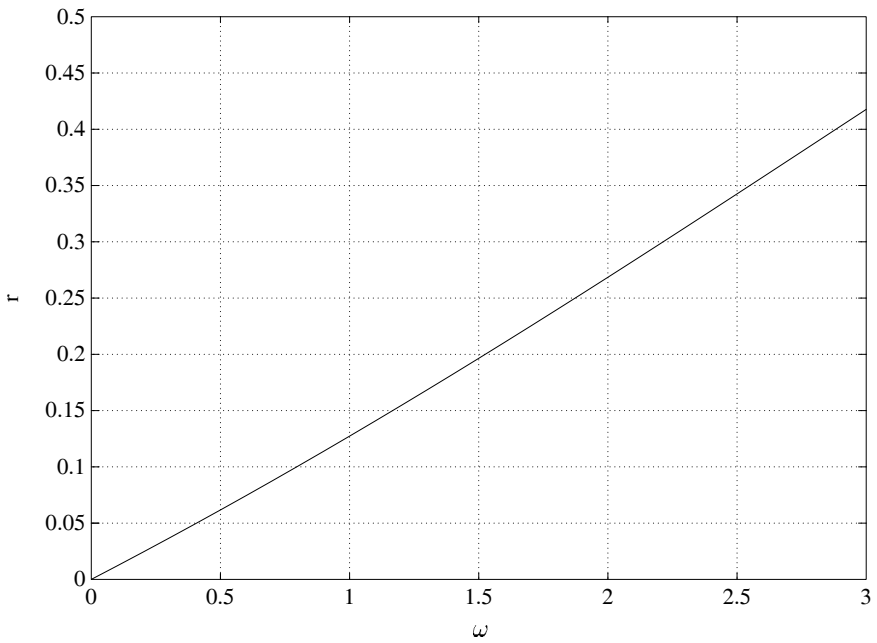

Figure 13.9. $\delta(\epsilon)$ vs ϵ (Example 13.2)

The value of ϵ corresponding to $\delta(\epsilon) = 0.396$ comes out to be equal to 2.83. Hence the maximum ϵ for which the plant can be robustly stabilized, with a constant r is 2.83.

To proceed let us choose the constant function $r(s) = r = \delta(2.83) = 0.396$. Hence $u(3) \approx 1 = u(s)$. Now

$$\tilde{Q} = \frac{u}{r} = -\frac{1}{0.396} = -2.532$$

$$Q(s) = B(s)\tilde{q}(s) = \frac{2.532(s-3)}{(s+3)}$$

and therefore,

$$C(s) = \frac{q(s)}{1 - G_0(s)Q(s)} = \frac{2.532(s+5)}{(s-1.584)}.$$

This $C(s)$ stabilizes $G(s)$ with

$$a \in [1.2, 6.8], \quad b \in [-0.8, 4.8], \quad c \in [-17.8, -12.2].$$

This can be verified by checking if $C(s)$ stabilizes the extremal segments of $\mathbf{G}(s)$.

Now suppose that we wish to tolerate a larger amount of parametric uncertainty, corresponding to, say $\epsilon = 4$. For this value of ϵ we verify that the maximum perturbation over all frequencies is $\delta = 0.578$. If a constant $r(s) = r$ were attempted we immediately fail to design a robust controller because of the required constraint $r \leq 0.396$.

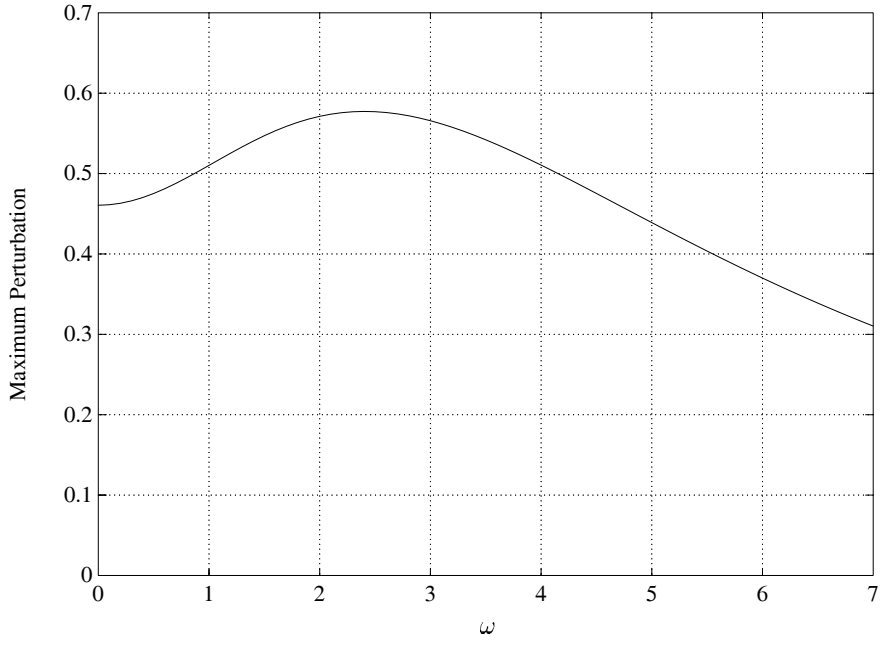

Figure 13.10. Maximum perturbation vs frequency for $\epsilon = 4$ (Example 13.2)

In this case it is obviously advisable to take the frequency information into account and attempt to design a rational function $r(s)$ that is loop-shaped to approximate $\delta(\epsilon, \omega)$ from above. This can be done from the plot of $\delta(4, \omega)$, as in Figure 13.10. One such $r(s)$ is:

$$r(s) = \frac{2.52(s + 0.6)}{(s + 1.3)(s + 2.4)}.$$

Figure 13.11 shows the plot of both $|r(j\omega)|$ and $\delta(4, \omega)$ and $|r(j\omega)|$ is seen to approximate $\delta(4, \omega)$ from above.

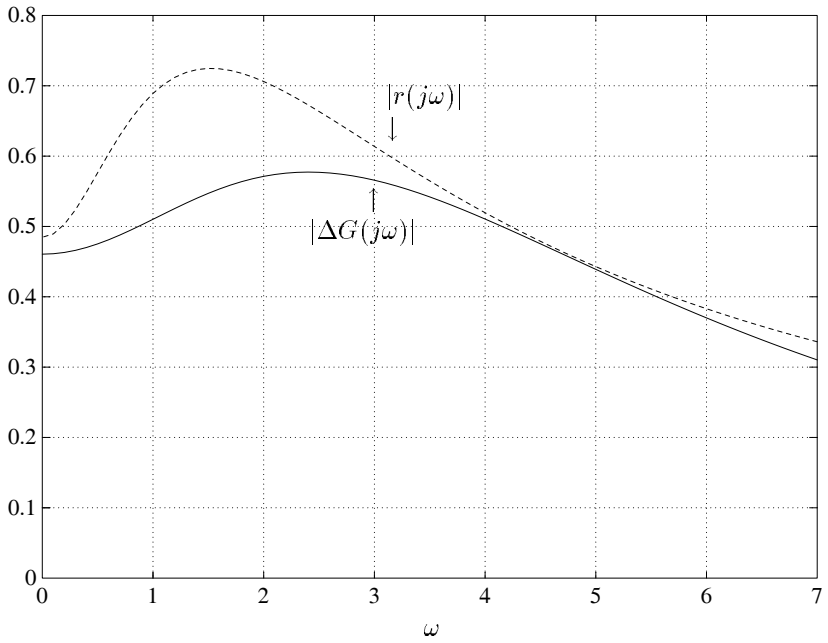

Figure 13.11. Maximum perturbation and $r(s)$ vs frequency for $\epsilon = 4$ (Example 13.2)

Then

$$u(3) = \frac{r(3)}{\tilde{G}_0(3)} = \frac{-2.52 \times 3.6}{4.3 \times 5.4 \times 0.395} = -0.987.$$

Since $r(s)$ is of relative degree 1, another interpolation condition on $u(s)$ is $u(\infty) = 0$ so that a proper controller is obtained.
Now, the second row of the Fenyves array will be

$$u_2(\infty) = \frac{u(\infty) + 0.987}{1 + 0.987u(\infty)} \left[\frac{s + 3}{s - 3}\right]_{s \to \infty} = 0.987.$$

Hence the Fenyves array is as shown in Table 13.2.

Table 13.2. Fenyves array

3	∞	
-0.987	0	$u(s)$
	0.987	$u_2(s)$

Since the elements of the Fenyves array are of modulus less than 1, hence an SBR function $u(s)$ exists which interpolates to

$$u(3) = -0.987, \quad u(\infty) = 0.$$

This can also be verified by checking for the non-negative definiteness of the Pick matrix. Here

$$\alpha_1 = 3, \quad \alpha_2 = \infty, \quad \text{and}$$
$$\beta_1 = -0.987, \quad \beta_2 = 0$$

so that the Pick matrix is

$$P = \begin{bmatrix} \dfrac{1 - 0.987^2}{6} & 0 \\ 0 & 0 \end{bmatrix} = \begin{bmatrix} 4.305 \times 10^{-3} & 0 \\ 0 & 0 \end{bmatrix}.$$

Since P is symmetric and has non-negative eigenvalues, it is non-negative definite. This also confirms the existence of $u(s)$.

Now, $u_2(s)$ can be parametrized in terms of an arbitrary Schur function $u_3(s)$, i.e.,

$$u_2(s) = \frac{0.987 + u_3(s)\left(\frac{s-\infty}{s+\infty}\right)}{1 + 0.987\left(\frac{s-\infty}{s+\infty}\right)u_3(s)} = \frac{0.987 - u_3(s)}{1 - 0.987u_3(s)}.$$

Choosing $u_3(s) = 0$, we get $u_2(s) = 0.987$. Then the next interpolation condition is $u(3) = -0.987$. This is satisfied by taking $u(s)$ as given below

$$u(s) = \frac{-0.987 + 0.987\left(\frac{s-3}{s+3}\right)}{1 - 0.987\left(\frac{s-3}{s+3}\right)u_2(s)} = \frac{-229.535}{s + 229.574}.$$

Then

$$\tilde{q}(s) = \frac{u(s)}{r(s)} = \frac{-91.0853(s+1.3)(s+2.4)}{(s+0.6)(s+229.574)},$$
$$q(s) = B(s)\tilde{q}(s) = \frac{91.0853(s+1.3)(s+2.4)(s-3)}{(s+0.6)(s+3)(s+229.574)}.$$

Therefore, the robust stabilizer is

$$C(s) = \frac{Q(s)}{1 - G_0(s)Q(s)} = \frac{91.0853(s+1.3)(s+2.4)(s+5)}{(s-217.47)(s+2.687)(s+0.53)}$$

for the interval plant

$$G(s) = \frac{5s+a}{s^2+bs+c}; \quad a \in [0,8], \quad b \in [-2,6], \quad c \in [-19,-11].$$

In general larger values of ϵ can be obtained by increasing ϵ in steps, and for each ϵ, an attempt can be made to find a $u(s)$ which is Schur and satisfies the interpolation constraints. Then a robust stabilizer can be obtained from this $u(s)$.

Example 13.3. (Robust Stabilization of Two-Phase Servomotor) A two-phase servomotor is very rugged and reliable and is commonly used for instrument servomechanisms. Its transfer function, with the control voltage E_c as the input and the displacement of the motor shaft Θ as the output, is given by

$$\frac{\Theta(s)}{E_c(s)} = \frac{K_c}{Js^2 + (f+K_n)s} \tag{13.41}$$

where

J is the equivalent moment of inertia of the motor shaft,

f is the equivalent viscous-friction coefficient of the motor shaft,

K_c and K_n are positive constants.

K_n is the negative of the slope of the torque-speed curve and K_c gives the variation of the torque with respect to E_c for a given speed. In the low-speed region, the variation of torque with respect to speed and control voltage, is linear. However, at higher speeds this linearity is not maintained. The above transfer function of the servomotor is derived for low-speed operating regions. The following example shows the robust stabilization of a servomotor whose parameters K_c and K_n vary due to the nonlinearity.

$$G(s) = \frac{\Theta(s)}{E(s)} = \frac{K_c}{s[Js + (f+K_n)]}$$

is the transfer function of the servomotor. Let the nominal values of the parameters be

$$\begin{aligned} K_c &= 0.0435 \text{ [oz} - \text{in./V]}, \\ K_n &= 0.0119 \text{ [oz} - \text{in./rad/sec]}, \\ J &= 7.77 \times 10^{-4} \text{ [oz} - \text{in.} - \text{sec}^2\text{]}, \text{ and} \\ f &= 0.005 \text{ [oz} - \text{in./rad/sec]}. \end{aligned}$$

These values are scaled up by 10^3, so that the nominal transfer function is

$$G_0(s) = \frac{43.5}{s(0.777s + 16.9)}.$$

Now let K_c and K_n vary in the intervals

$$K_c \in [43.5 - \epsilon, 43.5 + \epsilon],$$
$$K_n \in [11.9 - 0.7\epsilon, 11.9 + 0.7\epsilon].$$

If $K = f + K_n$, then

$$K \in [16.9 - 0.7\epsilon, 16.9 + 0.7\epsilon],$$

and

$$G(s) = \frac{K_c}{s(Js + K)}.$$

The block diagram in Figure 13.12 shows the closed-loop system with the interval plant $G(s)$ being the servomotor, $C(s)$ the stabilizing controller to be designed, and a position sensor of gain K_p in the feedback loop. Let us choose $K_p = 1$ so that we have a unity feedback system.

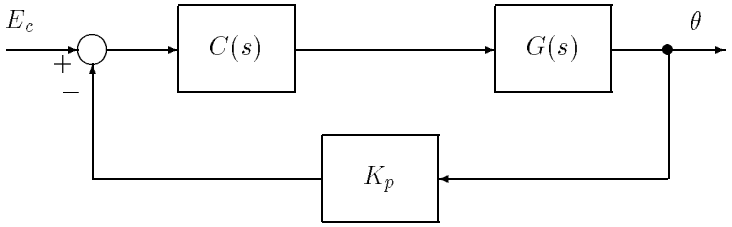

Figure 13.12. A feedback system (Example 13.3)

Since $G_0(s)$ does not have a pole in the RHP, it is necessary that $16.9 - 0.7\epsilon > 0$. This implies $\epsilon < 24.143$ in order to guarantee that no plant in the family has a pole in the RHP. The pole at the origin is assumed to be preserved under perturbations. Hence the uncertainty bound $r(s)$ must also have a pole at $s = 0$. So, we can write

$$r(s) = \frac{r'(s)}{s};$$

where $r'(s)$ is a minimum phase H_∞ function. Here $B(s) = 1$. Let

$$\tilde{G}_0(s) = sG_0(s) = \frac{43.5}{0.777s + 16.9}; \text{ and}$$
$$\tilde{q}(s) = \frac{q(s)}{s}.$$

Now an SBR function $u(s)$ needs to be found such that $u(s)$ interpolates to

$$u(0) = \frac{r'(0)}{\tilde{G}_0(0)} = \frac{r'(0)}{2.574},$$
$$u(\infty) = 0,$$

and it is necessary that $|u(0)| < 1$ which implies $|r'(0)| < 2.574$. For a constant r' we will have $r' = 2.574$. From the plot of δ vs ϵ as shown in Figure 13.13, we have $\epsilon_{\max} = 9.4$.

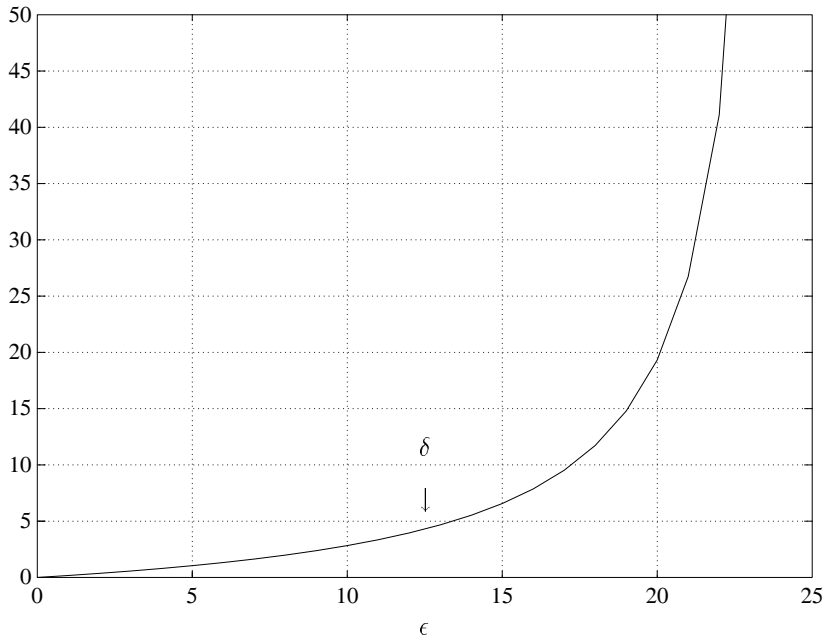

Figure 13.13. δ vs ϵ (Example 13.3)

Therefore, choosing $r' = 2.574$, we have $u(0) = 1$. A $u(s)$ which will interpolate to these two points can be chosen as

$$u(s) = \frac{1}{s+1}.$$

So

$$\tilde{q}(s) = \frac{u(s)}{r'} = \frac{1}{2.574(s+1)}, \text{ and}$$
$$Q(s) = s\tilde{Q}(s) = \frac{s}{2.574(s+1)}.$$

Therefore

$$C(s) = \frac{q(s)}{1 - G_0(s)Q(s)} = \frac{0.777s + 16.9}{2s + 45.5},$$

which should stabilize $G(s)$ for $\epsilon = 9.4$, i.e.,

$$K_c \in [34.1, 52.9], \qquad \text{and} \qquad K_n \in [5.32, 18.48].$$

A controller for perturbations greater than $\epsilon = 9.4$ can be obtained by choosing poles and zeros in $r'(s)$ that is, loop-shaping $r'(s)$ appropriately and redoing the interpolation.

The controller that results on applying the techniques described above depends on the procedure and is not guaranteed to succeed if the level of parametric uncertainty ϵ is specified apriori. However, it always produces a controller which robustly stabilizes the system against parametric uncertainty for small enough ϵ. The technique can be extended, in an obvious way to linear interval systems as well as multilinear interval systems using the extremal image set generating properties of the generalized Kharitonov segments, established in Chapters 8 and 11. We leave the details of this to the reader.

13.7 ROBUST STABILIZATION: STATE SPACE SOLUTION

In this section, we describe, without proof, the state-space approach to solving a standard H_∞ problem, which is to find an output feedback controller so that the H_∞ norm of the closed-loop transfer function is (strictly) less than a prescribed positive number γ. The existence of the controller depends upon the unique stabilizing solutions to two algebraic Riccati equations being positive definite and the spectral radius of their product being less than γ^2.

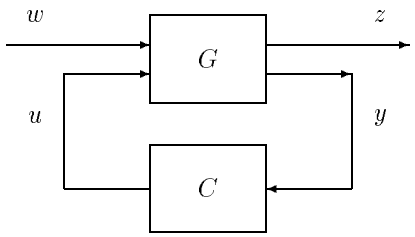

Figure 13.14. A feedback system

The feedback configuration is shown in Figure 13.14 where G is a linear system described by the state space equation:

$$\dot{x} = Ax + B_1 w + B_2 u$$

$$z = C_1 x + D_{11} w + D_{12} u$$
$$y = C_2 x + D_{21} w + D_{22} u$$

The following assumptions are made:

Assumption 13.1.

1) (A, B_1) is stabilizable and (C_1, A) is detectable.

2) (A, B_2) is stabilizable and (C_2, A) is detectable.

3) $D_{12}^T [C_1 \ D_{12}] = [0 \ I]$.

4) $\begin{bmatrix} B_1 \\ D_{21} \end{bmatrix} D_{21}^T = \begin{bmatrix} 0 \\ I \end{bmatrix}$.

Assumptions 1 and 2 together simplify the theorem statement and proof and also imply that internal stability is essentially equivalent to input-output stability ($T_{zw} \in \mathcal{RH}_\infty$). Assumptions 3 and 4 simplify the controller formula. It is also assumed that $D_{11} = D_{22} = 0$. This assumption is also made to simplify the formulas substantially.

Considering the Riccati equation

$$A^T X + XA + XRX - Q = 0, \tag{13.42}$$

where R and Q are real symmetric matrices and $X = Ric(H)$ denotes the solution of the Riccati equation associated with the Hamiltonian matrix:

$$H = \begin{bmatrix} A & R \\ Q & -A^T \end{bmatrix}. \tag{13.43}$$

The solution to the H_∞ optimal control problem is given by the following theorem.

Theorem 13.4 *There exists a compensator $C(s)$ such that*

$$\|T_{zw}(s)\|_\infty < \gamma$$

if and only if

1) $X_\infty = Ric(H_\infty) \geq 0$; *2)* $Y_\infty = Ric(J_\infty) \geq 0$; *3)* $\rho(X_\infty Y_\infty) < \gamma^2$;

where

$$H_\infty = \begin{bmatrix} A & \dfrac{B_1 B_1^T}{\gamma^2} - B_2 B_2^T \\ -C_1^T C_1 & -A^T \end{bmatrix}; \tag{13.44}$$

$$J_\infty = \begin{bmatrix} A^T & \dfrac{C_1 C_1^T}{\gamma^2} - C_2 C_2^T \\ -B_1 B_1^T & -A \end{bmatrix}; \tag{13.45}$$

and $\rho(\cdot)$ denotes the spectral radius of a matrix.

When the above condition holds, a controller is given by

$$C(s) := \begin{bmatrix} \hat{A}_\infty & -Z_\infty L_\infty \\ F_\infty & 0 \end{bmatrix} \tag{13.46}$$

where

$$\begin{aligned} \hat{A}_\infty &= A + \frac{B_1 B_1^T X_\infty}{\gamma^2} + B_2 F_\infty + Z_\infty L_\infty C_2; \\ L_\infty &= -Y_\infty C_2^T; \\ F_\infty &= -B_2^T X_\infty; \\ Z_\infty &= \left(I - \frac{Y_\infty X_\infty}{\gamma^2} \right)^{-1}. \end{aligned}$$

The following example uses the above method to synthesize a robust controller.

Example 13.4. Given the augmented plant

$$G(s) := \begin{bmatrix} A & B_1 & B_2 \\ C_1 & D_{11} & D_{12} \\ C_2 & D_{21} & D_{22} \end{bmatrix} = \begin{bmatrix} 1 & 0 & -1 \\ 0 & 0 & 0.2 \\ -1 & 1 & 0 \end{bmatrix}.$$

Let γ be chosen as 1. In the MATLAB Robust Control ToolBox, the function *hinfkgjd*, uses the above method to check stabilizability and generate the compensator. Using this function,

$$H = \begin{bmatrix} 1 & 25 \\ 0 & -1 \end{bmatrix},$$
$$J = \begin{bmatrix} 1 & 1 \\ 0 & -1 \end{bmatrix},$$

and their eigenvalues,

$$X = 0.08 \geq 0, \quad Y = 2 \geq 0,$$

and the spectral radius of their product,

$$\rho(XY) = 0.16 < \gamma^2 = 1.$$

Hence, the given system is stabilizable and the MATLAB function *hinfkgjd* gives the following compensator

$$C(s) := \begin{bmatrix} A_c & B_c \\ C_c & D_c \end{bmatrix} = \begin{bmatrix} -3.381 & -2 \\ 2.381 & 0 \end{bmatrix},$$

or equivalently

$$C(s) = \frac{-4.762}{s + 3.381}.$$

It is found that

$$T_{zw} = \frac{0.952(1 - s)}{s^2 + 2.381s + 1.381},$$

and

$$\|T_{zw}\|_\infty = 0.69 < 1.$$

We know that the closed loop system configuration shown in Figure 13.4 is a special case of the general feedback configuration shown in Figure 13.14. Figure 13.15 shows the same closed loop system, but with the plant block being broken into the nominal plant G_0 block and the perturbation block ΔG. The notation for signals used in Figure 13.15 is the same as in Figure 13.14. Here, x is the state vector of the nominal plant; u is the controlled input; z is the error signal and y is the measured variable vector which is contaminated by the disturbance w.

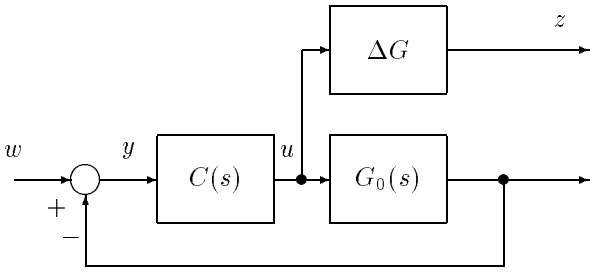

Figure 13.15. Closed-loop system configuration

Although Figure 13.15 shows the nominal plant and the perturbation as separate blocks, the perturbation is basically inherent to the plant and the error signal z is due to the plant perturbation. It is assumed that the compensator $C(s)$ stabilizes the nominal system. In order to minimize the effect of external disturbances, $C(s)$ should be such that the error signal z should not respond excessively to the external disturbance w. This translates to $\|T_{zw}(s)\|_\infty < \gamma$, where γ is some given number.

The transfer function $T_{zw}(s)$ is given by

$$T_{zw}(s) = \frac{C(s)(\Delta G)}{1 + C(s)G_0(s)}. \tag{13.47}$$

For this configuration, the block ΔG is uncontrollable and it makes sense to minimize the H_∞ norm of the transfer function from w to u:

$$T_{uw}(s) = \frac{C(s)}{1 + C(s)P_0(s)}. \tag{13.48}$$

Then, assuming a strictly proper plant, the state space equations will be

$$\dot{x} = Ax + B_2 u \tag{13.49}$$

$$y = C_2 x + w, \tag{13.50}$$

Here we have B_1 and C_1 as zero vectors, $D_{12} = 1$ and D_{21} as unit vectors so assumptions 2, 3 and 4 hold here.

We already know that $\|\Delta G(s)\|_\infty \leq r$. From the Small Gain Theorem, a necessary and sufficient condition for robust stability of our system is

$$\|(1 + G_0(s)C(s))^{-1}C(s)r\|_\infty < 1 \tag{13.51}$$

$$\Longrightarrow \|T_{uw}(s)\|_\infty < \frac{1}{r} = \gamma. \tag{13.52}$$

Now, with the help of Theorem 13.4, we can find $\gamma_{\min}$, the minimum value of γ that corresponds to the maximum value of r, $r_{\max}$, for which the system is robustly stabilizable. Once $r_{\max}$ is found, the corresponding $\epsilon_{\max}$ can be found from the r vs. ϵ plot of the plant. The controller $C^*(s)$ obtained for $r_{\max}$ is one that stabilizes the family of plants $\mathbf{G}_{\epsilon_{\max}}$.

Example 13.5. Let the interval plant be

$$G(s) = \frac{20(s^2 + as - 9)}{s^3 + bs^2 + s + c},$$

where

$$a \in [8 - \epsilon, 8 + \epsilon], \quad b \in [-4 - \epsilon, -4 + \epsilon], \quad c \in [6 - \epsilon, 6 + \epsilon],$$

and the nominal plant

$$G_0(s) = \frac{20(s^2 + 8s - 9)}{s^3 - 4s^2 + s + 6}.$$

Checking the Kharitonov polynomials of the denominator of $G(s)$, it is found that the number of unstable poles remains unchanged as long as $\epsilon < \epsilon_1 = 4$.

The state-space matrices for G_0 are

$$A = \begin{bmatrix} 4 & -1 & -6 \\ 1 & 0 & 0 \\ 0 & 1 & 0 \end{bmatrix};$$

$$B_1 = \begin{bmatrix} 0 \\ 0 \\ 0 \end{bmatrix}; \quad B_2 = \begin{bmatrix} 1 \\ 0 \\ 0 \end{bmatrix};$$

$$C_1 = [0\ 0\ 0]; \quad C_2 = [-20\ \ -160\ 180];$$

$$D_{11} = 0; \quad D_{12} = 1; \quad D_{21} = 1; \quad D_{22} = 0.$$

Now, an initial value of γ is chosen arbitrarily and γ is decreased in steps with the stabilizability condition being checked at each step, until a $\gamma = \gamma_{\min}$ is reached after

which one of the conditions of Theorem 13.4 fail. Here $\gamma_{\min}$ is found to be 0.333 so that $r_{\max}$ is 3. It was found that the spectral radius ρ for $\gamma = 0.333$ was

$$\rho = 0.105 < \gamma^2 = 0.111.$$

The compensator corresponding to $\gamma = 0.333$ is

$$C^*(s) = \frac{2.794s^2 + 19.269s + 16.475}{s^3 + 24.531s^2 + 202.794s + 544.101}.$$

Now $\epsilon_{\max}$ needs to be found from the r vs. ϵ plot. Again, the extremal segments of $G(s)$ are searched to obtain r for each ϵ. From the plot of r vs. ϵ in Figure 13.16, we have $\epsilon_{\max} = 0.4$.

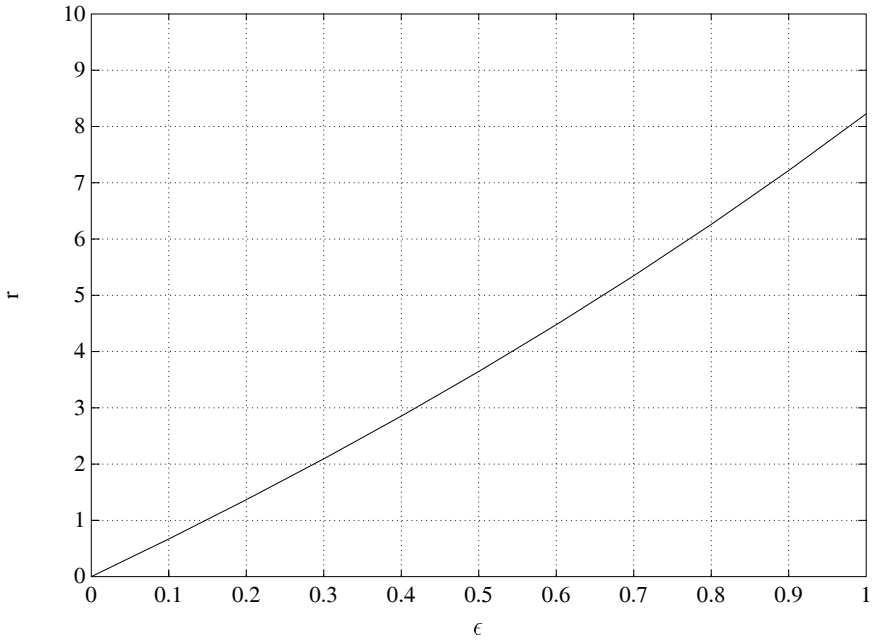

Figure 13.16. r vs ϵ (Example 13.5)

Therefore, $C^*(s)$ stabilizes the entire family $G(s)$ where

$$a \in [7.6, 8.4], \quad b \in [-4.4, -3.6], \quad c \in [5.6, 6.4].$$

The following example repeats Example 13.2 using the 2-Riccati equation.

Example 13.6.

$$G_0(s) = \frac{5s+4}{(s-3)(s+5)} = \frac{5s+4}{s^2+2s-15}.$$

The interval plant is

$$G(s) = \frac{5s+a}{s^2+bs+c}$$

with the intervals being

$$a \in [4-\epsilon, 4+\epsilon], \quad b \in [2-\epsilon, 2+\epsilon], \quad c \in [-15-\epsilon, -15+\epsilon].$$

Here the system and input-output matrices are:

$$A = \begin{bmatrix} -2 & 15 \\ 1 & 0 \end{bmatrix};$$
$$B_1 = \begin{bmatrix} 0 \\ 0 \end{bmatrix}; \quad B_2 = \begin{bmatrix} 1 \\ 0 \end{bmatrix};$$
$$C_1 = [0 \quad 0]; \quad C_2 = [-5 \quad -4];$$
$$D_{11} = 0; \quad D_{12} = 1; \quad D_{21} = 1; \quad D_{22} = 0.$$

Since we already know from Example 13.2 that $r_{\max} = 0.395$, we put $\gamma_{\min} = 1/0.395 = 2.532$ and check if the conditions of the Theorem are satisfied. The conditions were found to be satisfied with the spectral radius $\rho(X_\infty Y_\infty) = 6.382 < \gamma^2 = 6.386$. Since we require that

$$\rho(X_\infty Y_\infty) < \gamma^2,$$

and the value $\frac{\rho}{\gamma}$ is close to 1 we may conclude that $r_{\max} = 0.395$. The controller obtained is

$$C^*(s) = 28000\ \frac{s+5}{s^2+11090s-18070}.$$

$C^*(s)$ was found to stabilize all the extremal segments for the family of plants corresponding to $\epsilon = \epsilon_{\max} = 2.83$.

13.8 A ROBUST STABILITY BOUND FOR INTERVAL SYSTEMS

In this section we derive a bound on the parameter excursions allowed in an interval plant for which closed loop stability is preserved, with a given fixed controller. The result described here does not require the restriction that the number of unstable poles of the open loop system remain invariant under perturbations. The derivation is tailored to exploit an H_∞ technique which can be used to maximize this bound over the set of all stabilizing controllers.

Consider the feedback configuration of Figure 13.17.

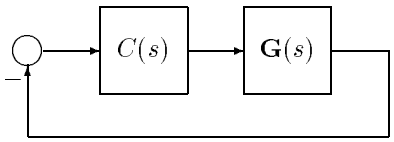

Figure 13.17. Interval Control System

Let $L(s) = C(s)G(s)$ denote the *loop gain*, $G_0(s)$ the nominal plant and $C(s)$ the fixed controller stabilizing $G_0(s)$. Let

$$C(s) = \frac{N_c(s)}{D_c(s)}, \qquad G_0(s) = \frac{N_p^0(s)}{D_p^0(s)} \qquad G(s) = \frac{N_p(s)}{D_p(s)} \tag{13.53}$$

$$N(s) = N_c(s)N_p(s), \qquad N_0(s) = N_c(s)N_p^0(s) \tag{13.54}$$

and

$$D(s) = D_c(s)D_p(s), \qquad D_0(s) = D_c(s)D_p^0(s). \tag{13.55}$$

We investigate the stability of the feedback system when the loop gain is perturbed from its nominal value L_0. Writing

$$L(s) = \frac{N(s)}{D(s)}, \qquad L_0(s) = \frac{N_0(s)}{D_0(s)}. \tag{13.56}$$

We make the following standing assumption:

Assumption 13.2. The polynomials $D(s)$ and $N(s)$ have the same degrees as the nominal polynomials $D_0(s)$ and $N_0(s)$, and $L_0(s)$ is proper.

Let

$$S_0(s) = \frac{D_0(s)}{D_0(s) + N_0(s)} \quad \text{and} \quad T_0(s) = \frac{N_0(s)}{D_0(s) + N_0(s)} \tag{13.57}$$

denote the sensitivity and complementary sensitivity functions respectively.

Theorem 13.5 (Robust Stability Criterion)
The closed loop system remains stable under all perturbations satisfying

$$\left| \frac{(D(j\omega) - D_0(j\omega))/D_0(j\omega)}{W_1(j\omega)} \right|^2 + \left| \frac{(N(j\omega) - N_0(j\omega))/N_0(j\omega)}{W_2(j\omega)} \right|^2 < \frac{1}{\delta} \tag{13.58}$$

for all $\omega \in [-\infty, \infty]$ *if*

$$|W_1(j\omega)S_0(j\omega)|^2 + |W_2(j\omega)T_0(j\omega)|^2 \leq \delta, \qquad \textit{for all } \omega \in [-\infty, \infty]$$

where $W_1(s)$ *and* $W_2(s)$ *are given stable proper rational functions.*

Proof. The perturbed and nominal closed loop characteristic polynomials are respectively,

$$D(s) + N(s) \quad \text{and} \quad D_0(s) + N_0(s).$$

Applying the Principle of the Argument to the proper rational function

$$\sigma(s) := \frac{D(s) + N(s)}{D_0(s) + N_0(s)}$$

leads to the conclusion that the perturbed closed loop system is stable if and only if the image of $\sigma(s)$ does not encircle the origin as s traverses the imaginary axis $j\omega$. Now let us rewrite $\sigma(s)$ in the form

$$\begin{aligned}
\sigma(s) &= \frac{D(s) + N(s)}{D_0(s) + N_0(s)} \\
&= \frac{D(s)}{D_0(s)} \underbrace{\frac{D_0(s)}{D_0(s) + N_0(s)}}_{S_0(s)} + \frac{N(s)}{N_0(s)} \underbrace{\frac{N_0(s)}{D_0(s) + N_0(s)}}_{T_0(s)} \\
&= 1 + \left[\frac{D(s)}{D_0(s)} - 1\right] S_0(s) + \left[\frac{N(s)}{N_0(s)} - 1\right] T_0(s).
\end{aligned}$$

Obviously a sufficient condition for the image of this function to not encircle the origin is that

$$\left| \left[\frac{D(j\omega)}{D_0(j\omega)} - 1\right] S_0(j\omega) + \left[\frac{N(j\omega)}{N_0(j\omega)} - 1\right] T_o(j\omega) \right| < 1$$

for $\omega \in [-\infty, \infty]$ or equivalently

$$\begin{aligned}
&\left| \frac{(D(j\omega) - D_0(j\omega))/D_0(j\omega)}{W_1(j\omega)} W_1(j\omega) S_0(j\omega) + \right. \\
&\qquad \left. \frac{(N(j\omega) - N_0(j\omega))/N_0(j\omega)}{W_2(j\omega)} W_2(j\omega) T_0(j\omega) \right| < 1
\end{aligned} \tag{13.59}$$

From the Cauchy-Schwarz inequality we have

$$\begin{aligned}
&\left| \frac{(D(j\omega) - D_0(j\omega))/D_0(j\omega)}{W_1(j\omega)} W_1(j\omega) S_0(j\omega) + \right. \\
&\qquad \left. \frac{(N(j\omega) - N_0(j\omega))/N_0(j\omega)}{W_2(j\omega)} W_2(j\omega) T_0(j\omega) \right|^2 \\
&\leq \left(\left| \frac{(D(j\omega) - D_0(j\omega))/D_0(j\omega)}{W_1(j\omega)} \right|^2 + \left| \frac{(N(j\omega) - N_0(j\omega))/N_0(j\omega)}{W_2(j\omega)} \right|^2 \right) \\
&\qquad \cdot \left(|W_1(j\omega) S_0(j\omega)|^2 + |W_2(j\omega) T_0(j\omega)|^2 \right).
\end{aligned}$$

Thus the conditions given in the theorem guarantee that (13.59) holds. This prevents any encirclements of the origin by the Nyquist locus of $\sigma(s)$ which proves that stability is preserved. ♣

Suppose now that a controller stabilizing the nominal plant is given and that

$$\sup_{\omega \in \mathbf{R}} \left(|W_1(j\omega) S_0(j\omega)|^2 + |W_2(\omega) T_0(j\omega)|^2 \right) = \delta. \tag{13.60}$$

The theorem derived above shows that the smaller δ is, the more robust the feedback system is. An interpretation of this is that robust stability is obtained if a weighted sum of the input and output signals (y_1 and y_2) as in Figure 13.18 can be tightly bounded.

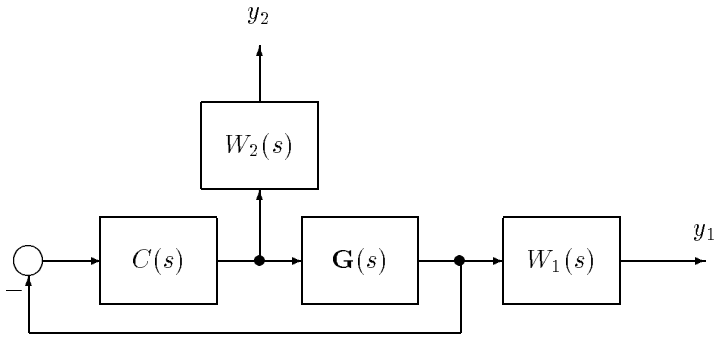

Figure 13.18. Interpretation of robust stability

We shall now relate δ to the allowable parameter excursions in the plant family $\mathbf{G}(s)$, assuming specifically that $\mathbf{G}(s)$ is an interval plant.

We first introduce an obvious but useful property of interval polynomials from which our result will follow. Let

$$p(s) = p_0 + p_1 s + p_2 s^2 + \cdots + p_q s^q$$

denote a real polynomial, $\mathbf{p}$ the vector of coefficients and $\mathbf{\Pi}$ be the box in the coefficient space defined as

$$p_i \in [p_i^0 - w_i \epsilon, p_i^0 + w_i \epsilon], \quad i = 0, 1, 2, \cdots, q$$

where p_i^0 and w_i are the nominal value and a weight, respectively. Then interval family of polynomials is defined as

$$\mathbf{p}(s, \epsilon) = \left\{ p(s, \epsilon) = p_0 + p_1 s + p_2 s^2 + \cdots + p_q s^q : \mathbf{p} \in \mathbf{\Pi} \right\} \tag{13.61}$$

Let $p^0(s)$ be the nominal polynomial with coefficients p_i^0 for $i = 0, 1, 2, \cdots, q$ and let $K_p^k(s, \epsilon)$, $i = 1, 2, 3, 4$ denote the Kharitonov polynomials associated with the interval family $\mathbf{p}(s, \epsilon)$.

Lemma 13.1 *For each ω,*

$$\begin{aligned}\sup_{\mathbf{p}\in\mathbf{\Pi}} \left|p(j\omega,\epsilon)-p^0(j\omega)\right| &= \max_{k=1,2,3,4} \left|K_p^k(j\omega,\epsilon)-p^0(j\omega)\right| \\ &= \left|K_p^i(j\omega,\epsilon)-p^0(j\omega)\right| \quad \text{for any } i=1,2,3,4 \\ &= \epsilon\left|K_p^i(j\omega,1)-p^0(j\omega)\right| \end{aligned} \tag{13.62}$$

Proof. The proof of this lemma follows from the fact that the image set $\mathbf{p}(j\omega,\epsilon)$, at each ω is a rectangle with corners equal to the images of the Kharitonov polynomials and moreover the distance from the center to each corner is equal. ♣

In fact it is easy to see that

$$\sup_{\mathbf{p}\in\mathbf{\Pi}} \left|p(j\omega,\epsilon)-p^0(j\omega)\right| = \epsilon\left|w_0+w_2\omega^2+w_4\omega^4\cdots+j\omega(w_1+w_3\omega^2+w_5\omega^4\cdots\right|$$

Now let us bring in the interval plant parametrized by μ:

$$\begin{aligned}\mathbf{G}(s) &= \frac{\mathbf{N}_{\mathrm{p}}(s)}{\mathbf{D}_{\mathrm{p}}(s)} \\ &= \left\{ G(s)=\frac{n_0+n_1s+\cdots+n_qs^q}{d_0+d_1s+\cdots+d_qs^q}: \right. \\ &\qquad \left. n_i\in[n_i^-,n_i^+], d_i\in[d_i^-,d_i^+],\ i=0,1,2,\cdots,q\right\}\end{aligned}$$

where

$$n_i\in[n_i^0-w_n^i\mu, n_i^0+w_n^i\mu], \quad \text{and} \quad d_i\in[d_i^0-w_d^i\mu, d_i^0+w_d^i\mu]$$

and d_i^0, n_i^0 are nominal values. For convenience, we let $K_{D_p}(s,\mu)$ and $K_{N_p}(s,\mu)$ denote any of the Kharitonov polynomials of $\mathbf{D}_p(s)$ and $\mathbf{N}_p(s)$, respectively. Our problem is to determine how large μ can be without losing stability.

Suppose that the weighting functions $W_1(s)$ and $W_2(s)$ are selected to satisfy

$$\left|\frac{K_{D_p}(j\omega,1)-D_p^0(j\omega)}{D_p^0(j\omega)}\right| < |W_1(j\omega)| \tag{13.63}$$

$$\left|\frac{K_{N_p}(j\omega,1)-N_p^0(j\omega)}{N_p^0(j\omega)}\right| < |W_2(j\omega)|\,. \tag{13.64}$$

Theorem 13.6 *Let weighting functions $W_1(s)$ and $W_2(s)$ be selected satisfying (13.63) and (13.64), and let $C(s)$ be a stabilizing compensator for the nominal plant $G_0(s)$. If*

$$\left\| \ |W_1(s)S_0(s)|^2+|W_2(s)T_0(s)|^2 \ \right\|_\infty = \delta \tag{13.65}$$

then $C(s)$ robustly stabilizes the interval plant $\mathbf{G}(s)$ for all $\mu < \mu_{\max}$ where

$$\mu_{\max} = \frac{1}{\sqrt{2\delta}}. \tag{13.66}$$

Proof. Recall that

$$C(s) = \frac{N_c(s)}{D_c(s)}, \qquad G_0(s) = \frac{N_p^0(s)}{D_p^0(s)} \qquad G(s) = \frac{N_p(s)}{D_p(s)} \tag{13.67}$$

and

$$N(s) = N_c(s)N_p(s), \qquad N_0(s) = N_c(s)N_p^0(s), \tag{13.68}$$

$$D(s) = D_c(s)D_p(s), \qquad D_0(s) = D_c(s)D_p^0(s). \tag{13.69}$$

From Lemma 13.1 we know that for a fixed ω

$$\left|\frac{D(j\omega,\mu) - D_0(j\omega)}{D_0(j\omega)}\right| \leq \mu \left|\frac{\left[K_{D_p}(j\omega,1) - D_p^0(j\omega)\right]}{D_p^0(j\omega)}\right|$$

$$\left|\frac{N(j\omega,\mu) - N_0(j\omega)}{N_0(j\omega)}\right| \leq \mu \left|\frac{\left[K_{N_p}(j\omega,1) - N_p^0(j\omega)\right]}{N_p^0(j\omega)}\right|.$$

for $D_p(s) \in \mathbf{D}_p(s)$ and $N_p(s) \in \mathbf{N}_p(s)$. Now

$$\sup_{D_p(s)\in\mathbf{D}_{p(s)}} \left|\frac{D(j\omega) - D_0(j\omega)}{D_0(j\omega)}\right| = \mu \left|\frac{K_{D_p}(j\omega,1) - D_p^0(j\omega)}{D_p^0(j\omega)}\right| < \mu \left|W_1(j\omega)\right|$$

$$\sup_{N_p(s)\in\mathbf{N}_{p(s)}} \left|\frac{N(j\omega) - N_0(j\omega)}{N_0(j\omega)}\right| = \mu \left|\frac{K_{N_p}(j\omega,1) - N_p^0(j\omega)}{N_p^0(j\omega)}\right| < \mu \left|W_2(j\omega)\right|.$$

Therefore the condition (13.58) for robust stability given in Theorem 13.5 is satisfied if

$$\mu^2 + \mu^2 < \frac{1}{\delta}. \tag{13.70}$$

It follows that

$$\mu_{\max} = \frac{1}{\sqrt{2\delta}}.$$

♣

Remark 13.2. It is clear that $\mu_{\max}$ can be increased (and therefore larger parameter excursions allowed) by choosing $C(s)$ to make δ small. There are techniques available in the H_∞ control literature for designing the controller $C(s)$ to minimize δ over the set of all stabilizing controllers for $G_0(s)$. The details of this procedure are omitted and we refer the reader to the literature.

Summary

In this chapter we have presented two synthesis results concerning the robust stability problem. These results are but two steps towards the solution to the general robust synthesis problem, but so little is known about this solution that every step is of interest. We have shown here that a minimum phase interval plant can always be stabilized by a stable controller of order $n - m - 1$ regardless of the magnitude of the perturbations. Many problems are still to be solved in this domain. For example, it would be interesting to extend the robust state feedback stabilization of Chapter 5 to the case when (A, B) are not in controllable companion form. Another open problem of particular interest is the following. In view of the generalization of Kharitonov's theorem given in Chapter 7, consider a Single-Input Single-Output interval plant and find the necessary and sufficient conditions for the existence of a stabilizing controller. Moreover, if stabilization is possible, give a constructive method for finding the controller. If the four Kharitonov polynomials associated with the numerator of the interval plant are stable, then every plant in the family is minimum phase, and the problem is reduced to that of Section 13.2 of this chapter and it is always possible to find a solution. On the other hand, if these Kharitonov polynomials are not all stable, there will not always be a solution and the solution if it exists certainly need not be a 'high-gain' controller as in Section 13.2.

The multivariable versions of the problems of robust stabilization under additive and multiplicative unstructured uncertainty described in this chapter are fully developed and well documented in the literature. This theory is based on the YJBK parametrization of all stabilizing controllers, inner outer factorization of transfer matrices and on minimal H_∞ norm solutions to matrix interpolation problems. These results are thoroughly treated in textbooks on H_∞ control theory. Moreover they relate only indirectly to robustness under parametric uncertainty and since our purpose is only to demonstrate by examples the use of H_∞ techniques in robust parametric problems we omit their treatment here. We have also omitted various other techniques such as robustness under coprime factor perturbations as developed in the H_∞ literature, which can certainly be profitably used in parametric uncertainty problems. In the specific case of coprime factor perturbations, we could relax the assumption of constant number of RHP poles in the family of uncertain plants, and the absence of $j\omega$ axis poles in the nominal plant $G_0(s)$. Establishing connections between parametric and nonparametric uncertainty, and extending robust parametric results to multivariable systems, is an area of ongoing research. The simple examples given here may be the beginnings of a much more sophisticated framework.

13.9 EXERCISES

13.1 Find a robust stabilizing controller that stabilizes the following interval plant.

$$G(s) = \frac{n(s)}{d(s)} = \frac{\alpha_2 s^2 + \alpha_1 s + \alpha_0}{\beta_3 s^3 + \beta_2 s^2 + \beta_1 s + \beta_0}$$

where the parameters vary as follows:

$$\begin{array}{llll} \alpha_2 \in [1,2], & \alpha_1 \in [2,4], & \alpha_0 \in [1,3], & \\ \beta_3 \in [1,2], & \beta_2 \in [-1,2], & \beta_1 \in [0.5,1], & \beta_0 \in [-1.5,1]. \end{array}$$

13.2 Repeat Exercise 13.1 with the following interval plant.

$$G(s) = \frac{\alpha_2 s^2 + \alpha_1 s + \alpha_0}{\beta_4 s^4 + \beta_3 s^3 + \beta_2 s^2 + \beta_1 s + \beta_0}$$

where

$$\begin{array}{lll} \alpha_2 \in [1,3], & \alpha_1 \in [0.5,1.5], & \alpha_0 \in [2.5,3.5], \\ \beta_4 \in [-3,-1], & \beta_3 \in [-2,2], & \beta_2 \in [-1.5,1.5], \\ \beta_1 \in [0.5,-0.5], & \beta_0 \in [-1.5,-0.5]. & \end{array}$$

13.3 Consider the plant

$$G(s) = \frac{5s + a}{s^2 + bs + c}$$

and suppose that the parameters vary within the intervals

$$a \in [4-\epsilon, 4+\epsilon], \quad b \in [2-\epsilon, 2+\epsilon], \quad c \in [-15-\epsilon, -15+\epsilon].$$

Plot the relationship between parametric uncertainty ϵ and maximal unstructured uncertainty $\delta(\epsilon, \omega)$. What is the constant $\delta(\epsilon)$ which corresponds to the parametric uncertainty $\epsilon = 2$.
Answer: For $\epsilon = 2$, $\delta = 0.27$.

13.4 Example 13.1 used a constant r to represent the unstructured perturbation $\|\Delta G(j\omega)\|$. Repeat this example with a rational function $r(s)$ that loopshapes the uncertainty function $\delta(\epsilon, \omega)$.

13.5 Using the same nominal plant and controller transfer functions as in Example 13.1, solve the following problem:

1) Compute the maximum allowable perturbation $\epsilon_{\max}$ by using the method described in Section 13.8. Choose the weight functions $W_1(s)$ and $W_2(s)$ to be both 1.

2) Using GKT (Chapter 7), compute $\epsilon_{\max}$.

3) Compare these two results and discuss the difference.

13.6 Repeat Example 13.1 by using the 2 Riccati equation method described in Section 13.7.

Hint: MATLAB function *hinfkgjd* is needed to solve this problem. The function is a part of MATLAB Robust Control ToolBox.

13.7 In Example 13.1 the constant r was used to bound the structured uncertainty.

1) Rework this problem with a rational function $r(s)$ that is loopshaped to bound the uncertainty function $\delta(\omega)$.

2) Let us call the controller obtained from Example 13.1 $C_1(s)$ and the solution of 1) $C_2(s)$. With these respective controllers, compute the true maximum structured uncertainty bound $\epsilon_{\max}$.

Hint: Once the controller is given, the true $\epsilon_{\max}$ can be found by applying GKT.

13.8 Let the nominal plant be

$$G_0(s) = \frac{30s + 10}{(s+2)(s-3)(s-2)} = \frac{30s + 10}{s^3 - 3s^2 - 4s + 12}$$

and the interval plant

$$G(s) = \frac{30s + a}{s^3 + bs^2 + cs + d}$$

with the intervals being

$$a \in [10 - \epsilon, 10 + \epsilon], \quad b \in [-3 - \epsilon, -3 + \epsilon], \quad c \in [-4 - \epsilon, -4 + \epsilon], \quad d \in [12 - \epsilon, 12 + \epsilon].$$

Find a robust stabilizing controller and the corresponding value of ϵ.

13.10 NOTES AND REFERENCES

The results on simultaneous strong stabilization given in this chapter are based on Chapellat and Bhattacharyya [60]. The problem treated in Section 13.2 has also been treated by Barmish and Wei [18]. The problem of simultaneous stabilization of a discrete set of plants has been considered by Vidyasagar and Viswanadham [235] Saeks and Murray [200] and Blondel [41]. Property 13.3 may be found in the book of Marden [175]. Rantzer and Megretski have given a convex parametrization of robust parametric stabilizers [196]. The section on Nevanlinna-Pick interpolation is adapted from Dorato, Fortuna and Muscato [85]. A proof of the Nevanlinna algorithm for the matrix case, as well as multivariable versions of the unstructured, additive, multiplicative and coprime factor perturbation problems are thoroughly treated in Vidyasagar [231]. The application of H_∞ techniques for robust parametric synthesis is adapted from S. Bhattacharya, L.H. Keel and S.P. Bhattacharyya [28]. The state space solution of the H_∞ optimal control problem via Riccati equations, Theorem 13.4, is due to Doyle, Glover, Khargonekar and Francis [91]. The proof of Theorem 13.2 can be found in Walsh [236]. Theorem 13.5 is due to Kwakernaak [157] and the result of Theorem 13.6 is due to Patel and Datta [186].

Chapter 14

INTERVAL MODELLING, IDENTIFICATION AND CONTROL

As we have seen in earlier chapters, sharp and nonconservative estimates of robust stability margin and performance can be obtained for interval system models. Motivated by this, it is natural to attempt to model a family of uncertain systems using the interval framework. This chapter presents a such a technique. It consists of taking the frequency domain input and output data obtained from experimental test signals, and fitting an "interval transfer function" that contains the complete frequency domain behavior with respect to the test signals. Identification with such an interval model allows one to predict the worst case performance and stability margins using the results on interval systems given in the previous chapters. The algorithm is illustrated by applying it to experimental data obtained from an 18 bay Mini-Mast truss structure and a T-shape truss structure which are used in research on space structures.

14.1 INTRODUCTION

Obtaining a very accurate mathematical description of a system is usually impossible and very costly. It also often increases the complexity of the corresponding control mechanism. A recent trend in the area of system identification is to try to model the system uncertainties to fit the available analysis and design tools of robust control.

The interval transfer function described throughout this book is interpreted as a family of transfer functions whose coefficients are bounded by some known intervals and centered at the nominal values. In many cases this is unnatural in the sense that physical parameter perturbations do not correspond to transfer function coefficients. In order to relax this limitation, approaches to deal with linearly or multilinearly correlated perturbations have also been developed. On the other hand, if we observe

the developments in the interval system area we see that the *nominal system* has very little significance. These results in fact emphasize the *boundary properties* of the family of systems under consideration. In fact, virtually all the important results in this field are based on the boundary generating extreme points, edges, and segments of the interval family of systems.

With this background in mind, suppose that the behavior of the plant is described by some known test input and its corresponding measurement output. Due to noise, nonlinearities and inaccurate measurements, a fixed linear time-invariant identified model will never exactly represent the data obtained from the plant. Our aim, in this chapter, is to present an algorithm to obtain a reasonable interval transfer function model around, but not necessarily centered in, a nominally identified transfer function so that the entire frequency domain behavior of the physical plant is completely contained in that of the model.

This is applied to two experimental test structures. First, the algorithm is demonstrated by using the Mini-Mast truss structure. In this example, we show how to construct an interval transfer function model from the experimental data set. The frequency response of the resulting interval transfer function contains that of the experimental structure. For the second example, an interval transfer function is constructed to capture sets of experimental data that represent structural changes due to various added masses. Once the corresponding interval transfer functions are obtained, they are verified via the frequency domain analysis techniques described in Chapter 8 as well as their performance based on root locations described in Chapter 6.

In the next section, a simple technique is described. This technique deals with a single set of experimental data and constructs an interval transfer function which represents a reasonably small family containing the experimental data set.

14.2 INTERVAL MODELING WITH A SINGLE DATA SET

Consider the configuration shown in Figure 14.1.

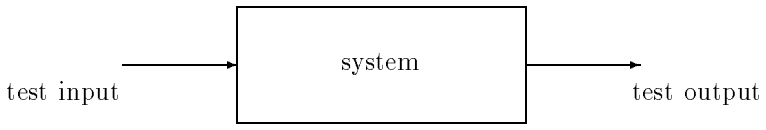

Figure 14.1. Experimental structure

In system identification, one applies test inputs and measures the system response in order to identify the parameters of an appropriate proposed mathematical model. It is also common that these test signals are represented in the form of frequency domain data. In fact, there are numerous techniques available to determine

a best possible linear time-invariant model that closely fits this frequency domain data set. Suppose that the test frequencies are $\omega_1,\omega_2,\cdots,\omega_N$ and the complex numbers $u(j\omega_i),y(j\omega_i)$ denote in phasor notation the input-output pair at the frequency ω_i. Let

$$y(j\omega_i) := D(j\omega_i)u(j\omega_i), \quad i = 1,2,\cdots,N \tag{14.1}$$

denote the test data generated from an identification experiment. Suppose that $G^I(s)$ is the transfer function of a linear time-invariant system which is such that $G^I(j\omega)$ is closest to $D(j\omega)$ in some norm sense. In general it is not possible to find a single rational function $G^I(s)$ for which $G^I(j\omega_i) = D(j\omega_i)$ and the more realistic identification problem is to in fact identify an entire family $\mathbf{G}(s)$ of transfer functions which is capable of "explaining" or "validating" the data in the sense that for each data point $D(j\omega_i)$ there exists some transfer function $G_i(s) \in \mathbf{G}(s)$ with the property that $G_i(j\omega_i) = D(j\omega_i)$. The family $\mathbf{G}(s)$ can be parametrized in many alternative ways. For instance, an unstructured approach to describing $\mathbf{G}(s)$ using a normed algebra is to let each element $G(s)$ of $\mathbf{G}(s)$ be described as $G(s) = G^I(s) + \Delta G(s)$ where the norm $|\Delta G(s)| < \rho$. In such a case, the family $\mathbf{G}(s)$ is identified once $G^I(s)$ and ρ are determined. In general, the identification algorithm should also be efficient in the sense that the family $\mathbf{G}(s)$ that it produces should be ideally minimal among the set of all such families that explain the data. In the unstructured case described above, this translates to choosing a small value of ρ.

The objective here is to develop an identification algorithm in a framework where the family of linear time-invariant systems $\mathbf{G}(s)$ is obtained by letting the transfer function coefficients lie in intervals around those of the nominal $G^I(s)$. The identification requirement is that

$$D(j\omega_i) \in \mathbf{G}(j\omega_i) \qquad \text{for all} \quad \omega_i. \tag{14.2}$$

Let

$$G^I(s) := \frac{n_0 + n_1 s + n_2 s^2 + n_3 s^3 + \cdots + n_n s^n}{d_0 + d_1 s + d_2 s^2 + d_3 s^3 + \cdots + d_n s^n}. \tag{14.3}$$

We define

$$G(s) := \frac{\hat{n}_0 + \hat{n}_1 s + \hat{n}_2 s^2 + \hat{n}_3 s^3 + \cdots + \hat{n}_n s^n}{\hat{d}_0 + \hat{d}_1 s + \hat{d}_2 s^2 + \hat{d}_3 s^3 + \cdots + \hat{d}_n s^n} \tag{14.4}$$

and

$$\begin{aligned} \mathbf{G}(s) := \{G(s) : \hat{n}_i \in [n_i - \mathrm{w}_{n_i}\epsilon^-_{n_i}, n + \mathrm{w}_{n_i}\epsilon^+_{n_i}], \\ \hat{d}_i \in [d_i - \mathrm{w}_{d_i}\epsilon^-_{d_i}, d + \mathrm{w}_{d_i}\epsilon^+_{d_i}], \qquad \text{for all} \quad i\} \end{aligned} \tag{14.5}$$

where

$$\begin{aligned} \underline{\mathrm{w}} &:= \left[\mathrm{w}_{d_0} \cdots \mathrm{w}_{d_n}\ \mathrm{w}_{n_0} \cdots \mathrm{w}_{n_n}\right] \\ \underline{\epsilon}^+ &:= \left[\epsilon^+_{d_0} \cdots \epsilon^+_{d_n}\ \epsilon^+_{n_0} \cdots \epsilon^+_{n_n}\right] \\ \underline{\epsilon}^- &:= \left[\epsilon^-_{d_0} \cdots \epsilon^-_{d_n}\ \epsilon^-_{n_0} \cdots \epsilon^-_{n_n}\right]. \end{aligned} \tag{14.6}$$

The components of w are to be regarded as weights chosen *apriori* whereas the ϵ's are to be regarded as dilation parameters to be determined by the identification algorithm and the data $D(j\omega_i)$

Remark 14.1. Note that in the expression in (14.5) we use vectors $\epsilon_{n_i}^{\pm}$ and $\epsilon_{d_i}^{\pm}$ instead of a single ϵ. This setting allows n_i and d_i to not necessarily be the center point of the intervals in which $\hat{n}_i$ and $\hat{d}_i$, lie respectively. This flexibility is important to achieve the minimum possible size of the family $\mathbf{G}(s)$.

The requirements on the identified interval model $\mathbf{G}(s)$ become:

1) *Membership Requirement:* $D(j\omega_i) \in \mathbf{G}(j\omega_i)$, for all i.

2) *Size Requirement:* $\|\underline{\epsilon}^{\pm}\|$ as small as possible.

3) *Frequency Response Requirement:* the weights $\underline{\mathrm{w}}$ must be chosen so that the frequency response of $\mathbf{G}(j\omega)$ is bounded as tightly as possible for every frequency.

Both size and frequency response requirements are crucial because uniformly smaller intervals do not necessarily map to smaller image sets or a smaller family. For example, slightly bigger intervals in higher order coefficients may result in much bigger image sets than those due to significantly larger intervals in lower order coefficients.

14.2.1 Interval System Modeling

As described above, the procedure is divided into two parts. First, we identify a linear time-invariant model $G^I(s)$ which represents the test data $D(j\omega)$ as closely as possible. A variety of algorithms are available in the system identification literature and any algorithm can be taken for this step. Here, a simple least squares based algorithm is described. Once the nominal model is obtained, then the tightest intervals around each coefficient of the nominal transfer function $G^I(s)$ should be created while satisfying the membership and frequency response requirements.

14.2.2 Nominal System Identification

First, a brief description of a standard least squares method to identify a nominal transfer function whose frequency response fits the given test data $D(j\omega_i)$ as closely as possible is given. An appropriate order of model may be determined by checking the singular values of the Hankel matrix generated from the impulse response data. Under the assumption that the data is noise free, the number of nonzero singular values determines the order of the system. The details are omitted here. Interested readers may refer to the references [3] and [122]. After determining the appropriate order, n, of the system, we let the nominal transfer function be

$$G^I(s) := \frac{n(s)}{d(s)}. \tag{14.7}$$

The nominal transfer function coefficients must be selected to minimize the following index:

$$\sum_{i=1}^{N} \left\{ W^I(j\omega_i) \{ \mathrm{Re}[D(j\omega_i)d(j\omega_i) - n(j\omega_i)] \}^2 + \{ \mathrm{Im}[D(j\omega_i)d(j\omega_i) - n(j\omega_i)] \}^2 \right\}. \tag{14.8}$$

This least square problem generates $2N$ linear equations for $2n$ unknown coefficients of the transfer function. The weight W^I may be selected by finding the minimum variance estimator of unknowns. Since the relative error in the valley parts of the frequency response is more significant than the one in the peak parts, it is in general necessary to assign high weights for the frequency ranges in the valley parts of the frequency response.

14.2.3 Weight Selection

As shown in (14.5), the size of the interval of variation for each coefficient of the family $\mathbf{G}(s)$ depends on w and ϵ. In this subsection we consider the problem of finding an appropriate set of weights $\underline{\mathrm{w}}$. The weight selection procedure is extremely important because inappropriate selection of weights may result in an unnecessarily large family. This results in a large image set in the complex plane at some frequencies, even though the intervals themselves may be small.

It is natural to think that a weight represents the average sensitivity of a coefficient of the nominal model with respect to the variation of data points. Thus, we establish the following reasonable algorithm for selecting weights.

Suppose the test data consists of N data points obtained at corresponding frequencies,

$$D(j\omega) := \{ D(j\omega_i) = \alpha_i + j\beta_i, \quad i = 1, 2, \cdots, N \}. \tag{14.9}$$

Let us define the l^{th} model set as follows:

$$G_l(j\omega) = \begin{cases} D(j\omega_i), & i = l \\ G^I(j\omega_i), & i = 1, 2, \cdots, l-1, l+1, \cdots, N \end{cases}$$

In other words, the model $G_l(j\omega)$ is identical to the nominal identified model $G^I(j\omega)$ with the l^{th} data point replaced by the l^{th} component of the test data $D(j\omega)$. Now we construct the l^{th} identified model, which we call $G_l^I(s)$, which is identified from the l^{th} data set $G_l(j\omega)$. Let

$$G_l^I(s) := \frac{n_0^l + n_1^l s + n_2^l s^2 + n_3^l s^3 + \cdots + n_n^l s^n}{d_0^l + d_1^l s + d_2^l s^2 + d_3^l s^3 + \cdots + d_n^l s^n} \tag{14.10}$$

and

$$\mathbf{p} := \begin{bmatrix} n_0 & n_1 & \cdots & n_n & d_0 & d_1 & \cdots & d_n \end{bmatrix}. \tag{14.11}$$

If we assume that $|G_l(j\omega) - G_l^I(j\omega)|$ is small, the sensitivity of the coefficients of

the nominal model with respect to variations in the l^{th} data point is described as

$$\frac{\partial \mathbf{p}}{\partial G^I(j\omega_l)} := \begin{bmatrix} |n_0 - n_0^l| \\ \vdots \\ |n_n - n_n^l| \\ |d_0 - d_0^l| \\ \vdots \\ |d_n - d_n^l| \end{bmatrix}. \tag{14.12}$$

Collecting the sensitivity of the coefficients of the nominal model with respect to the variation of all the data points, $l = 1, 2, \cdots, N$, we have

$$\frac{\partial \mathbf{p}}{\partial G^I(j\omega)} :=$$

$$\begin{bmatrix} \dfrac{\partial \mathbf{p}}{\partial G^I(j\omega_1)} \\ \dfrac{\partial \mathbf{p}}{\partial G^I(j\omega_2)} \\ \vdots \\ \dfrac{\partial \mathbf{p}}{\partial G^I(\omega_N)} \end{bmatrix} = \begin{bmatrix} |n_0 - n_0^1| & \cdots & |d_0 - d_0^1| & \cdots & |d_n - d_n^1| \\ |n_0 - n_0^2| & \cdots & |d_0 - d_0^2| & \cdots & |d_n - d_n^2| \\ \vdots & & & & \\ |n_0 - n_0^N| & \cdots & |d_0 - d_0^N| & \cdots & |d_n - d_n^N| \end{bmatrix}.$$

The weights are then defined as the average of these for each coefficient:

$$\begin{aligned} \underline{\mathrm{w}} &:= \frac{1}{N}\left[\textstyle\sum_{l=1}^N |n_0 - n_0^l|, \cdots, \sum_{l=1}^N |d_n - d_n^l|\right] \\ &:= \left[\mathrm{w}_{n_0}, \cdots, \mathrm{w}_{n_n}, \mathrm{w}_{d_0}, \cdots, \mathrm{w}_{d_n}\right]. \end{aligned} \tag{14.13}$$

Using this selected weight, we proceed to determine the intervals of the transfer function coefficients.

14.2.4 Interval System Identification

After determining an appropriate weight vector w, we need to find $\underline{\epsilon}^{\pm}$ to satisfy the given requirements. We now first consider the membership requirement. Recall the nominal system given in (14.3) and substitute $s = j\omega$, then we have

$$\begin{aligned} G^I(j\omega) &:= \frac{n(j\omega)}{d(j\omega)} \\ &= \frac{(n_0 - \omega^2 n_2 + \cdots) + j(\omega n_1 - \omega^3 n_3 + \cdots)}{(d_0 - \omega^2 d_2 + \cdots) + j(\omega d_1 - \omega^3 d_3 + \cdots)} \\ &:= \frac{n^{\text{even}}(\omega) + j n^{\text{odd}}(\omega)}{d^{\text{even}}(\omega) + j d^{\text{odd}}(\omega)}. \end{aligned} \tag{14.14}$$

Since the nominal model transfer function $G^I(s)$ cannot perfectly represent the data set $D(j\omega)$, we have the following relationships for a particular frequency w_i.

$$\begin{aligned} D(j\omega_i) &= \alpha_i + j\beta_i \approx G^I(j\omega_i) \\ &= \frac{n^{\text{even}}(\omega_i) + jn^{\text{odd}}(\omega_i)}{d^{\text{even}}(\omega_i) + jd^{\text{odd}}(\omega_i)}. \end{aligned} \tag{14.15}$$

The difference may be added to the coefficients of the nominal model as follows:

$$\begin{aligned} D(j\omega_i) &= \alpha_i + j\beta_i \\ &= \frac{(\hat{n}_0 - \omega_i^2\hat{n}_2 + \cdots) + j(w_i\hat{n}_1 - \omega_i^3 n_3 + \cdots)}{(\hat{d}_0 - \omega_i^2\hat{d}_2 + \cdots) + j(w_i\hat{d}_1 - \omega_i^3 d_3 + \cdots)} \end{aligned}$$

where $\hat{n}_i := n_i + \mathrm{w}_{n_i}\epsilon_{n_i}$ and $\hat{d}_i := d_i + \mathrm{w}_{d_i}\epsilon_{d_i}$ for all i. If we rewrite this in terms of a linear matrix equation, we have

$$A(\omega_i, \alpha_i, \beta_i)W\underline{\epsilon}^i = B(\omega_i, \alpha_i, \beta_i) \tag{14.16}$$

where

$$A(\omega_i, \alpha_i, \beta_i) :=$$

$$\begin{bmatrix} \alpha_i & -\beta_i\omega_i & -\alpha_i\omega_i^2 & \beta_i\omega_i^3 & \cdots & -1 & 0 & \omega_i^2 & 0 & -\omega_i^4 & 0 & \cdots \\ \beta_i & \alpha_i\omega_i & -\beta_i\omega_i^2 & -\alpha_i\omega_i^3 & \cdots & 0 & \omega_i & 0 & -\omega_i^3 & 0 & \omega_i^5 & \cdots \end{bmatrix} \tag{14.17}$$

$$W := \begin{bmatrix} \mathrm{w}_{d_0} & & & & \\ & \cdots & & & \\ & & \mathrm{w}_{n_0} & & \\ & & & \cdots & \end{bmatrix}$$

$$\underline{\epsilon}^i := \begin{bmatrix} \epsilon^i_{d_0} & \cdots & \epsilon^i_{d_n} & \epsilon^i_{n_0} & \cdots & \epsilon^i_{n_n} \end{bmatrix}$$

and

$$B(\omega_i, \alpha_i, \beta_i) :=$$

$$\begin{bmatrix} -\alpha_i(d_0 - \omega_i^2 d_2 + \omega_i^4 d_4 - \cdots) + \beta_i(\omega_i d_1 - \omega_i^3 d_3 + \omega_i^5 d_5 - \cdots) \\ +(n_0 - \omega_i^2 n_2 + \omega_i^4 n_4 - \cdots) \\ -\beta_i(d_0 - \omega_i^2 d_2 + \omega_i^4 d_4 - \cdots) - \alpha_i(\omega_i d_1 - \omega_i^3 d_3 + \omega_i^5 d_5 - \cdots) \\ +(\omega_i n_1 - \omega_i^3 n_3 + \omega_i^5 n_5 - \cdots) \end{bmatrix}.$$

Here we assume without loss of generality that $A(\omega_i, \alpha_i, \beta_i)$ has full row rank. Then the minimum norm solution $\underline{\epsilon}_i$ can be computed as

$$\underline{\epsilon}_i = A(\cdot)^T \left[A(\cdot)A(\cdot)^T\right]^{-1} B(\cdot). \tag{14.18}$$

After finding $\underline{\epsilon}_i$ for all $i = 1, 2, \cdot, N$, the intervals of the transfer function coefficients are determined as follows:

$$\epsilon^-_{n_k} := \min_i\{0, \epsilon^i_{n_k}\} \qquad \epsilon^+_{n_k} := \max_i\{0, \epsilon^i_{n_k}\} \tag{14.19}$$

$$\epsilon^-_{d_k} := \min_i\{0, \epsilon^i_{d_k}\} \qquad \epsilon^+_{d_k} := \max_i\{0, \epsilon^i_{d_k}\} \tag{14.20}$$

for all k. Clearly, the procedure guarantees the satisfaction of the three requirements given earlier. Once the interval model is obtained, various extremal properties of this model can used in assessing the performance of any proposed controllers. These would exploit the results on interval systems developed in earlier chapters.

In the next section, the technique is illustrated by applying it to a large space structure experimental facility developed at NASA's Langley Research Center.

14.3 APPLICATION TO A MINI-MAST SYSTEM

14.3.1 Model Description

The Mini-Mast system shown in Figure 14.2 is a 20.16 meter-long deployable truss located in the Structural Dynamics Research Laboratory at NASA Langley Research Center. It is used as a ground test article for research in the areas of structural analysis, system identification, and control of large space structures. The Mini-Mast was constructed from graphite-epoxy tubes and titanium joints by using precision fabrication techniques. The 102 measurements shown in Figure 14.2 were derived using 51 noncontacting displacement sensors distributed from Bay 2 through Bay 18. Three shakers are located circumferentially around the truss at Bay 9 and their locations are selected primarily to excite the low frequency modes below 10 Hz. There are two bending modes and one torsion mode in this low frequency range. These three modes are designed to be separated from the other frequency modes. The experimental data used in this example is obtained by using one displacement sensor output at Bay 9 from one input. In this example, we use the experimental data within the 45 [rad/sec] low frequency range with 180 frequency data points. This low frequency range covers the three low frequency modes described earlier. Figure 14.3 shows the frequency response test data.

14.3.2 Interval Model Identification

Using the weighted least squares method described earlier, we select $W^I(j\omega)$ shown in Figure 14.4 (Top). The identified model obtained is

$$G^I(s) = \frac{n_0 + n_1 s + n_2 s^2 + n_3 s^3 + n_4 s^4 + n_5 s^5}{d_0 + d_1 s + d_2 s^2 + d_3 s^3 + d_4 s^4 + d_5 s^5 + s^6}$$

where

$$\begin{array}{ll} n_0 = -5.78 \times 10^4 & d_0 = 2.96 \times 10^7 \\ n_1 = \ 5.88 \times 10^2 & d_1 = 2.15 \times 10^5 \\ n_2 = -8.74 \times 10^2 & d_2 = 1.10 \times 10^6 \\ n_3 = \ 0.073 & d_3 = 2.75 \times 10^3 \\ n_4 = -0.967 & d_4 = 2.21 \times 10^3 \\ n_5 = \ 3.48 \times 10^{-5} & d_5 = 2.58 \end{array}$$

The eigenvalues of the identified model transfer function are as follows:

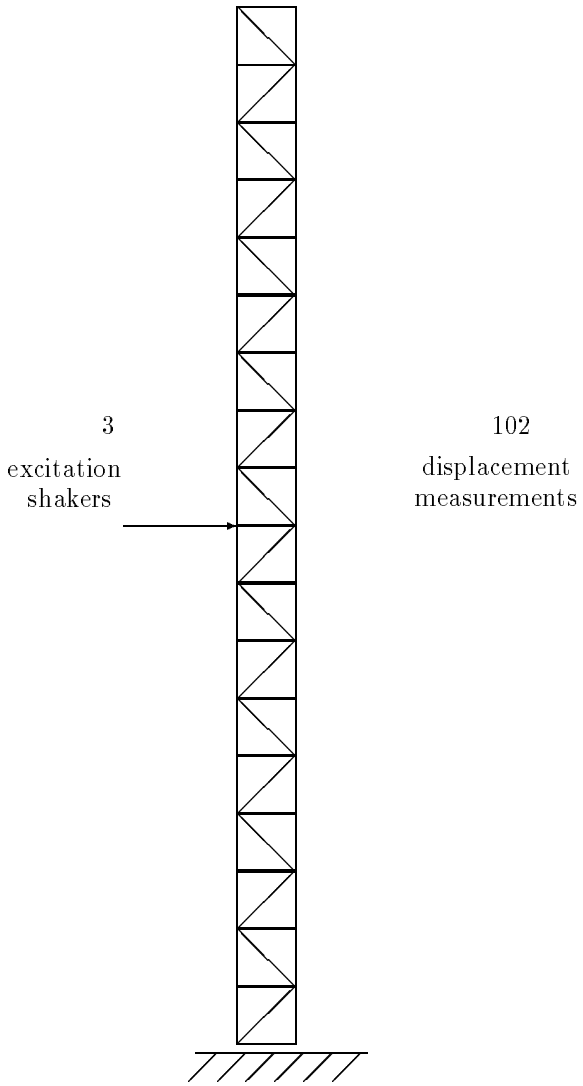

Figure 14.2. Mini-Mast structure

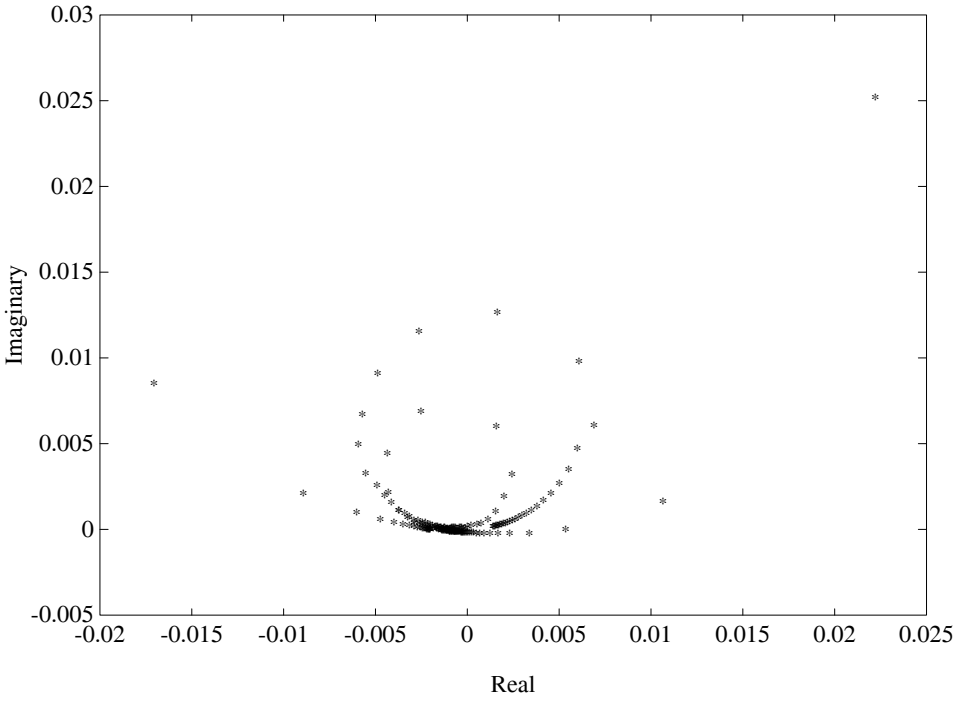

Figure 14.3. Experimental data set

	Eigenvalues	Mode
1	$-7.11 \times 10^{-2} \pm j5.3560$	1st bending mode
2	$-4.22 \times 10^{-1} \pm j26.302$	1st torsion mode
3	$-7.99 \times 10^{-1} \pm j38.616$	2nd bending mode

The magnitude and phase comparisons of the test data and the identified model are given in Figure 14.4 (Middle and Bottom). The dashed lines denote the frequency response of $D(j\omega)$ and the solid lines denote the frequency response of $G^I(j\omega)$. The dotted lines in Figure 14.4 (Middle) indicates the error in magnitude (i.e. $|D(j\omega) - G^I(j\omega)|$) for illustration.

We now create intervals around this nominal identified model. The weight selection method described in Section 14.2.3 gives the following weights for each coefficient:

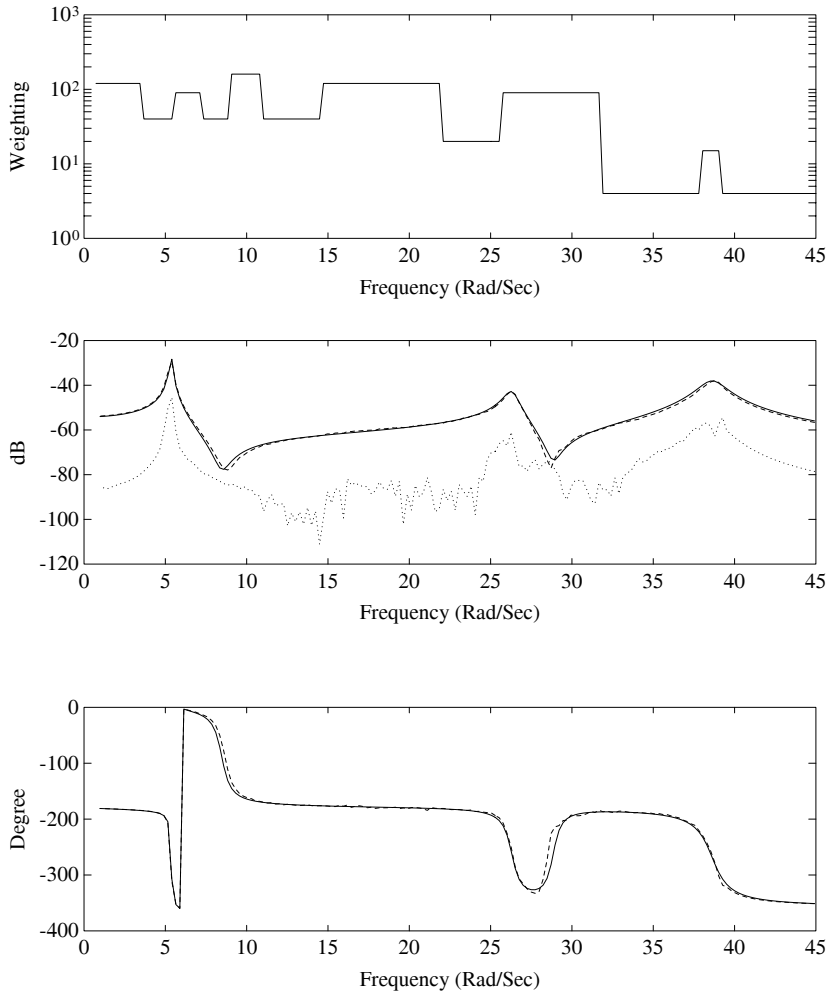

Figure 14.4. Least square weights (Top), Magnitude plots of identified model, experimental data, model error(Middle), Phase plots of identified model and experimental data (Bottom)

$$
\begin{aligned}
w_{n_0} &= 2.7053 \times 10 & w_{d_0} &= 3.9152 \times 10^{3} \\
w_{n_1} &= 1.2041 & w_{d_1} &= 2.2715 \times 10^{2} \\
w_{n_2} &= 2.3214 \times 10^{-1} & w_{d_2} &= 5.8095 \times 10 \\
w_{n_3} &= 4.0113 \times 10^{-3} & w_{d_3} &= 1.5250 \\
w_{n_4} &= 2.4768 \times 10^{-4} & w_{d_4} &= 5.9161 \times 10^{-2} \\
w_{n_5} &= 2.9620 \times 10^{-6} & w_{d_5} &= 1.2520 \times 10^{-3}
\end{aligned}
$$

This set of weights produced the following interval system:

$$\mathbf{G}(s) := \frac{\hat{n}_0 + \hat{n}_1 s + \hat{n}_2 s^2 + \hat{n}_3 s^3 + \hat{n}_4 + \hat{n}_5 s^5}{\hat{d}_0 + \hat{d}_1 s + \hat{d}_2 s^2 + \hat{d}_3 s^3 + \hat{d}_4 + \hat{d}_5 s^5 + s^6}$$

where

$$\begin{aligned}
\hat{n}_0 &\in [-6.006, -5.666]\times 10^4 & \hat{d}_0 &\in [2.936, 2.979]\times 10^7 \\
\hat{n}_1 &\in [\ 4.769,\ 7.840]\times 10^2 & \hat{d}_1 &\in [2.0663, 2.2335]\times 10^5 \\
\hat{n}_2 &\in [-8.959, -8.609]\times 10^2 & \hat{d}_2 &\in [1.092, 1.099]\times 10^6 \\
\hat{n}_3 &\in [-4.9791,\ 5.6904]\times 10^{-1} & \hat{d}_3 &\in [2.672, 2.841]\times 10^3 \\
\hat{n}_4 &\in [-9.749, -9.373]\times 10^{-1} & \hat{d}_4 &\in [2.209, 2.219]\times 10^3 \\
\hat{n}_5 &\in [-0.8570,\ 1.1648]\times 10^{-4} & \hat{d}_5 &\in [2.526, 2.619]\times 10^0
\end{aligned}$$

14.3.3 Model Validation

Figure 14.3 shows the polar plot of the test data for each frequency at which measurements were taken. Each mode of the polar plot has been separated in Figures 14.5(a), (b), (c) for illustration. The frequency envelope of the Interval Model is generated from the extremal segment set $\mathbf{G}_{\mathrm{E}}(s)$. These figures show that every data point of the test data is bounded by the image set generated by the interval model at the corresponding frequency. Figure 14.5(d) was drawn for the entire frequency range. These figures show that the uncertainty model obtained here is a valid interval model for the given test data set. Similarly, Figure 14.6 shows the magnitude and phase plots of the test data and the interval model. Clearly, both magnitude and phase plots of the test data are contained in the tightly bounded tubes representing the boundary of the frequency responses of the interval system.

In the next section another application is discussed. In this example, multiple data sets are used to identify the corresponding interval transfer function. Each data set represents the experimental structure with a specific set of added masses.

14.4 VIBRATION SUPPRESSION CONTROL OF A FLEXIBLE STRUCTURE

The objective of this example is to apply theoretical developments on interval systems to a laboratory experiment and to achieve meaningful robust control design and analysis of the vibration control problem of a flexible structure. Specifically, a controller is designed to damp structural vibrations such that changes in structural parameters can be tolerated. Therefore, it can be guaranteed that the level of damping will be bounded inside a predicted range.

The test structure is a scaled version of a typical flexible truss-like space structure and the parametric uncertainty is represented by mass added to various locations on the structure. This type of structural change is common in many space-bound dynamic systems. For example, appendage articulation or decreasing fuel weight over the life of a satellite are all possible system variations. While inertial changes were

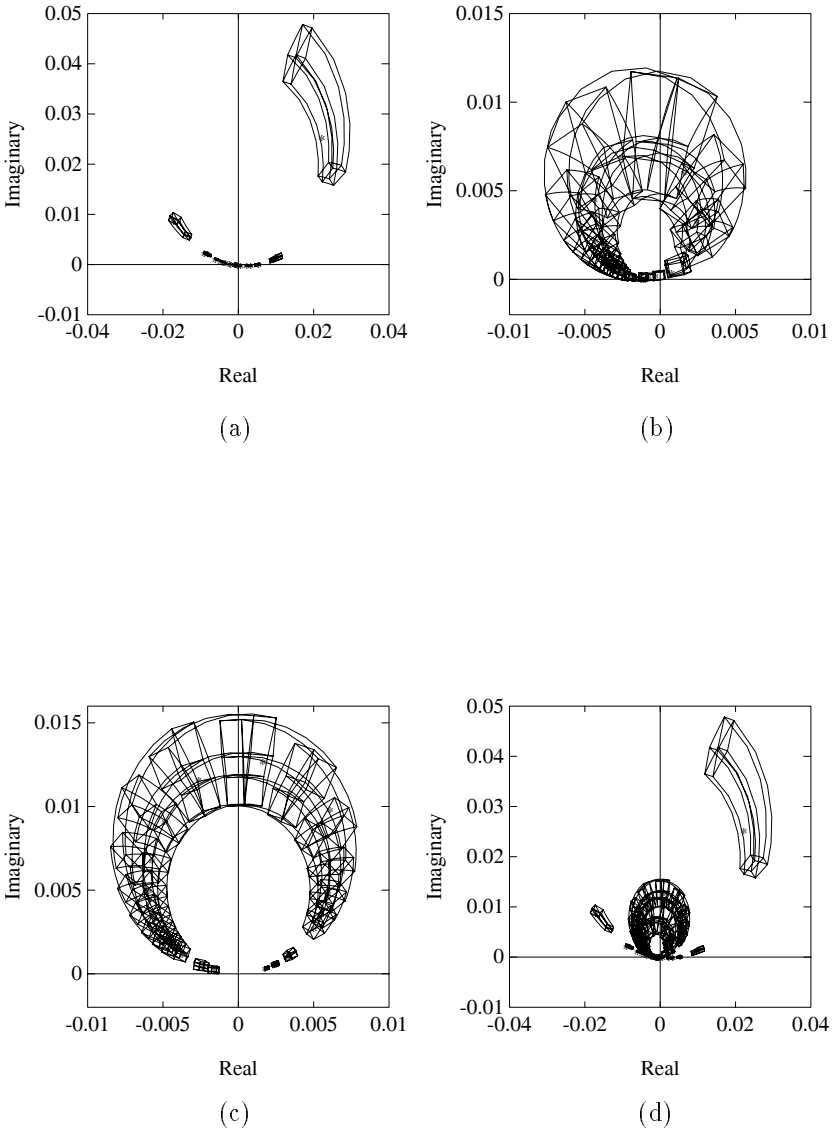

Figure 14.5. Nyquist images of interval model and experimental data (a) first mode, (b) second mode, (c) third mode, (d) image set of the system

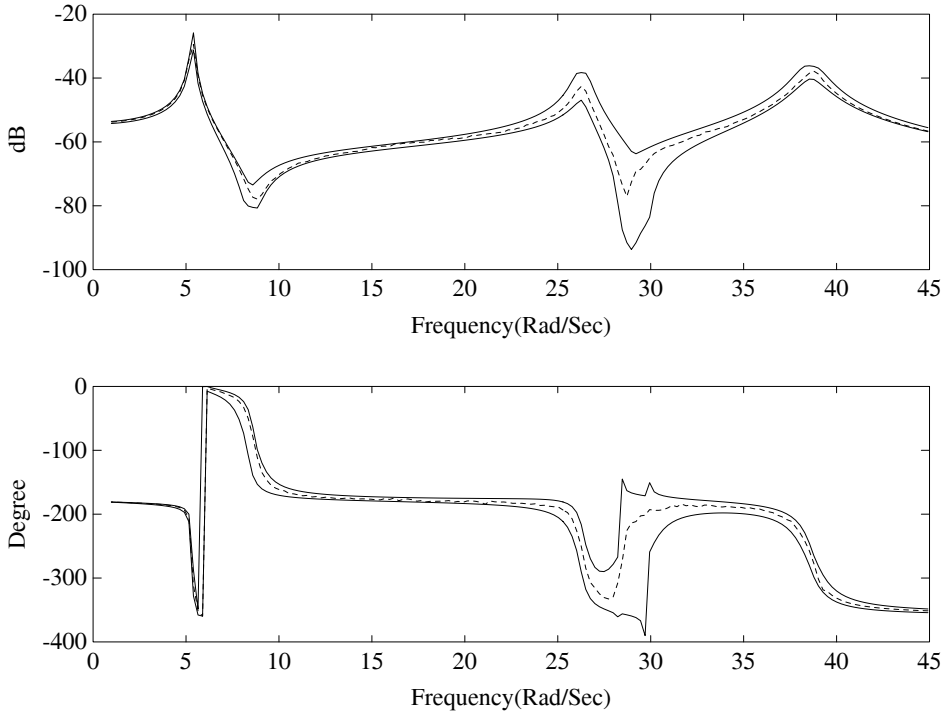

Figure 14.6. Bode plots of interval model and experimental data

chosen for this investigation, this by no means limits the methodology presented herein. Indeed, the effects of changes of any plant parameter, such as structural damping or moduli, could be accounted for in these interval system techniques. We start by describing the structural dynamics of the system.

Structural Dynamics

A 10-bay aluminum truss structure that was built for this experiment is shown in Figure 14.7. Each bay of the structure is a 0.5 meter cube made of hollow aluminum tubing joined at spherical nodes with threaded fasteners. The last three bays of the structure form a T-section. This is done so that the torsional modes of vibration will be more pronounced. The final structure has a mass of $31.5kg$ and is cantilevered horizontally from a massive monolithic base.

Figure 14.7. Ten Bay MeroForm Truss with T-section

A Finite Element Model (FEM) of the structure is shown in Figure 14.8. A modal analysis is performed on the model giving information about the structure's modal frequencies and mode shapes. The solution results in 7 modes of vibration in the 100Hz bandwidth. In order to establish the credibility of the model as well as embed

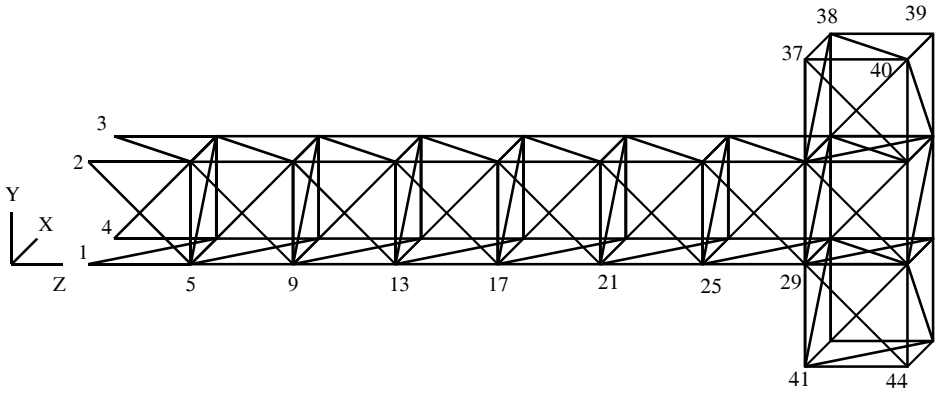

Figure 14.8. Finite element model of 10 bay truss including node number

natural structural damping data, experimental frequency domain data is collected from the structure using a Tektronix 2642A Fourier Analyzer. The input applied to the structure consists of an impulse applied to Node 40 (see Figure 14.8) of the structure, and the output is from an accelerometer mounted at Node 40 as well. The natural frequencies and damping ratios are extracted from the experimental data using the Eigensystem Realization Algorithm (ERA) method which we will not describe here. Interested readers may refer to reference [101]. Table 14.1 shows the resulting values for the first seven modes from the FEM model as well as the experimental data. From the FEM model we also extract a reduced-order mass matrix M and stiffness matrix K for the structure. The equation of motion for a multi-degree of freedom system is transformed into the standard modal form so that the modal damping matrix can easily be included. Transforming this back into physical coordinates yields the mass, stiffness, and damping matrices. Hence the following second-order lumped-mass parameter model of the structure was used to represent the structural dynamics.

$$M\ddot{x} + D\dot{x} + Kx = Bu \tag{14.21}$$

The vector x represents the physical coordinates of the structure, the vector u represents the force input into the structures, the triple (M, D, K) represents the

Table 14.1. Results of FEM model and ERA identified model

	Mode	FEM model	ERA model	
		Frequency(Hz)	Frequency(Hz)	Damping(ξ)
1	Vertical Bending	9.22	9.45	.0120
2	Horizontal Bending	9.31	9.70	.0140
3	Torsional	18.13	19.69	.0080
4	Vertical Bending	47.43	49.01	.0020
5	Horizontal Bending	55.12	60.30	.0010
6	Torsional	84.73	92.84	.0006
7	Mixed Motion	87.48	98.70	.0003

dynamics of the structure and the matrix B represents the input matrix. The damping matrix was developed from ERA identified modal parameters,

$$D = (S_m^T)^{-1} \Lambda_D S_m^{-1} \tag{14.22}$$

where

$$\Lambda_D = \text{diag}\,[2\xi_1 w_1, \ldots, 2\xi_n w_n]$$

and S_m is a mass normalized modal matrix for the reduced order model. The model represents a baseline model of the structure used in control design.

Actuator Dynamics

A reaction mass actuator (RMA) shown in Figure 14.9 is used to input force into the structure. This actuator uses a mass-magnet and electrical coil assembly to accelerate a proof-mass. An amplified signal applied to the stationary electrical coil creates a magnetic field. The constant field of the magnet inside the moving mass reacts against the new magnetic field causing force and hence movement of the mass. The mass rides on shafts which are limited to linear motion. The mass has a total usable travel length of about 2.5 cm. Any acceleration of the mass caused by force imparted from the coil results in an equal but opposite reaction force on the actuator's housing. When the actuator is mounted on the structure, the force is imparted on the structure. Hence, the actuator is space-realizable because it

requires no inertial reference frame such as the earth.

Figure 14.9. Reaction Mass Actuator assembly used for motion control

The actuator contains an internal non-contacting displacement sensor to aid in keeping the mass centered with respect to its housing. The block diagram of Figure 14.10 shows the local control scheme used for keeping the mass centered. The PD type controller contains a proportional feedback loop which acts as a spring and a derivative feedback loop which adds an equivalent viscous damping to the motion of the mass. The resulting system acts like a simple single degree of freedom mass-spring-damper system. Notice that a first-order filter is included to reduce the effects of high frequency noise in the damping loop. Realizing that the force output of the actuator is actually the inertial acceleration of the mass, the output force of the actuator has the following dynamics.

$$\frac{F(s)}{V_{\text{in}}(s)} = \frac{m\tau s^3 + ms^2}{m\tau s^3 + ms^2 + (c + k\tau)s + k} \tag{14.23}$$

where m is the reaction mass, k is the equivalent stiffness, c is the equivalent viscous damping constant, and τ is the time constant of the noise filter. This transfer

function represents the force output $F(s)$ with respect to the voltage input $V_{\text{in}}(s)$ applied to the RMA's coil, the output of the PD controller. As shown in Figure 14.7,

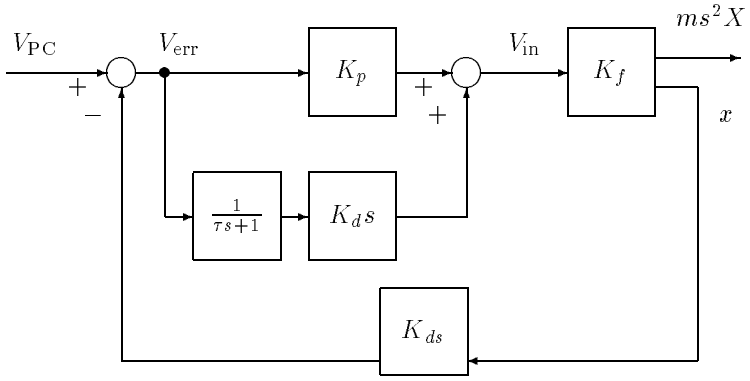

Figure 14.10. Block diagram of the local centering control system of RMA

the actuator is mounted between Node 39 and Node 40 of the structure. This location on the end of the structure is chosen because the modal participation factors of the first few modes of the structure are large at this location. A second-order model of the actuator and structure is created by combining the mass, stiffness, and damping coefficients of the actuator's local feedback system with the mass, stiffness, and damping matrices of the structure. This can be done when the constant τ is small enough that it doesn't have an effect in the frequency range of interest.

It should be noted that several design considerations were made when building an actuator and setting the local feedback gains. First, the actuator is designed so that its mass is small compared to the structure. The reaction mass is approximately 1.67 kg and the parasitic mass is $1.6kg$ so that the actuator is just over 10% of the structure's mass. Note also that the efficiency ratio of the actuator itself is 51%. The damping ratio of the actuator affects the damping in the structure both passively (without active control) and with the active control designed. These considerations were taken into account when choosing the internal damping in the actuator.

Parametric Uncertainty

The uncertainty of the structure considered here is due to masses added to Nodes 44 and 17. We want to examine the structural changes that occur when each added mass varies from 0kg to 2.5kg. In order to observe the frequency domain behaviour of the system with respect to the changes of these added masses, we take the following six samples of various weights of added masses as shown in Table 14.2. As

Table 14.2. 2 Masses Added to Structure

Case	1	2	3	4	5	6
Node 17	$0Kg$	$0.5Kg$	$1.0Kg$	$1.5Kg$	$2.0Kg$	$2.5Kg$
Node 44	$0Kg$	$0.5Kg$	$1.0Kg$	$1.5Kg$	$2.0Kg$	$2.5Kg$

a result, the modal frequencies are shifted as the masses are varied. Our particular interest is the model uncertainty for the first horizontal mode and the first torsional mode with the natural frequencies ranging 4 to 24Hz. The output measurement is from an accelerometer located at node 40 in the horizontal direction and the input is generated by applying the random signal to the RMA actuator. Figure 14.11 illustrates the change in the frequency peaks of the experimental data when these inertial parameters change.

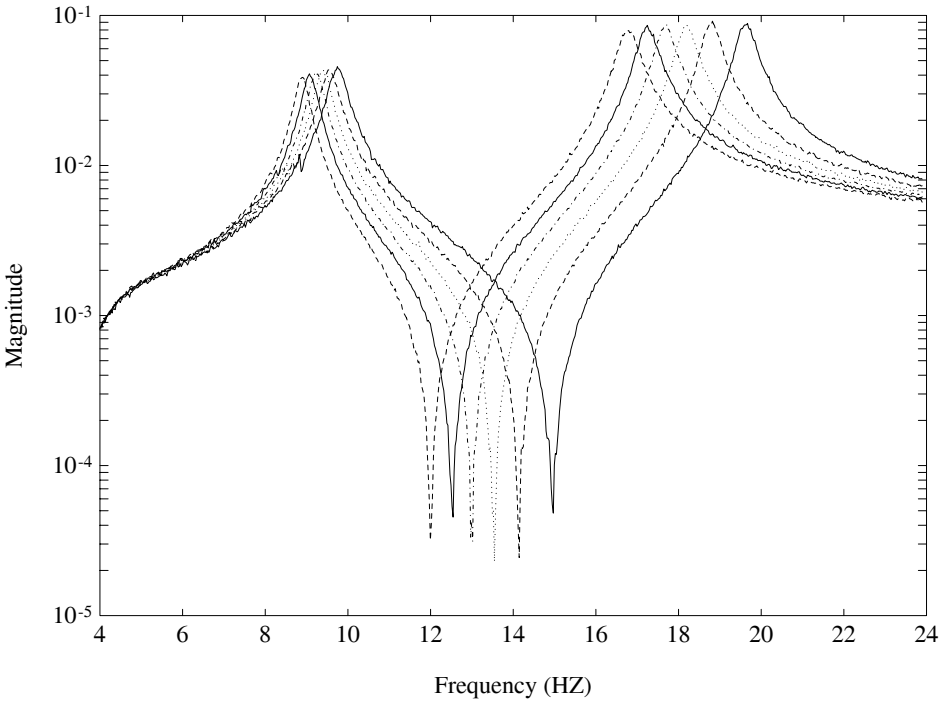

Figure 14.11. Experimental frequency response function with different added masses: From Right to Left $0Kg$, $1Kg$, $2Kg$, $3Kg$, $4Kg$, $5\ Kg$.

Therefore, it is reasonable to assume that for any value of added mass ranging 0 to 2.5 kg the frequency response of the corresponding structure remains inside the thinnest envelope covering the frequency response of these six sampled structures. By combining (14.21) and (14.23), we arrive at a transfer function expression of the actuator-structure composite system

$$G(s,p) = \frac{s^2 X(s,p)}{V_{\text{in}}(s)} \tag{14.24}$$

where $V_{\text{in}}(s)$ is the voltage across the actuator coils and $s^2X(s,p)$ is the response of an accelerometer. The unknown parameter, p, represents the uncertainty in the structural dynamics. Although we are using inertia to generate a family of perturbed systems, this by no means limits the techniques presented here to inertial perturbations only.

Vibration Suppression Control Law

The controller is designed using classical root locus techniques. Later it is cast in terms of interval control systems to observe the robustness of the closed loop system. Vibration damping is accomplished using a local velocity feedback (LVF) control scheme. Velocity feedback is fed into a single actuator from an accelerometer located at Node 40 horizontal direction, such that,

$$u = -K_v \dot{x}. \tag{14.25}$$

The control design is based on the model as in (14.21). Here we consider the model of the first horizontal bending mode and the first torsional mode. Feeding back the velocity term through feedback gain, K_v, the closed loop pole locations of the system are predicted. After varying the gain, a root locus plot is created. The resulting plot shows a trend of increased damping in all of the modes as the actuator gain increases. As expected, the actuator's damping is predicted to decrease and thus the pole of the actuator dominated mode moves toward the left half plane.

To implement the controller, a negative velocity signal is fed to the actuator to "cancel out" the motion of the structure, or reduce its velocity. An accelerometer is mounted on the housing of the actuator, and is thus connected to the structure. In order to get a velocity signal, the acceleration signal from the sensor must be integrated. However, integration of electrical signals results in exponential growth of any DC noise or DC offsets anywhere in the system. Therefore, we use a "velocity estimator" and the estimator is formulated as

$$\frac{\hat{V}(s)}{a(s)} = \frac{s}{s^2 + w_c s + w_c^2} \tag{14.26}$$

where w_c is the break frequency of the filter, $\hat{V}(s)$ is an estimated velocity signal and $a(s)$ is the accelerometer input. The value used here is $0.5Hz$, and since the

estimator acts like an ideal integrator at frequencies above $6w_c$, the feedback signal should be proportional to the velocity of the structure.

Initially, the controllers are implemented for the structural system with no added mass. Figure 14.12 shows the significantly increased damping in the first two modes(horizontal bending and torsional). The control is successful in increasing the system damping, but the question of robustness still remains unanswered. How much will slight changes in the system affect the closed loop control of the structure? The interval control model answers this question.

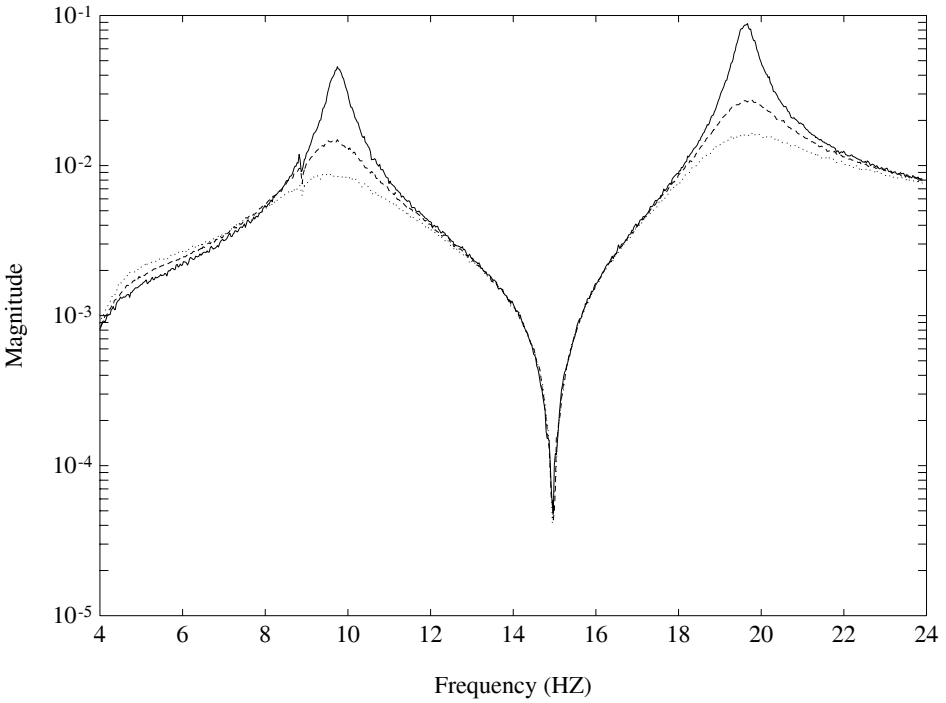

Figure 14.12. Experimental frequency response function of the open-loop and closed-loop systems with zero added masses: — Open-Loop; - - Closed-Loop $K_v = 30$; ... Closed-Loop $K_v = 60$.

14.4.1 Model Identification

Model Structure

The objective of this section is to construct a family of models such that its frequency response contains the six samples of experimental data shown in Figure 14.11. Each data set consists of 900 data points over the frequency ranging 4 to $24Hz$. We first

select the transfer function of the nominal model with an appropriate order:

$$\begin{aligned} g_0(s) &= \frac{n_0(s)}{d_0(s)} \\ &= \frac{n_m^0 s^m + n_{m-1}^0 s^{m-1} + \cdots + n_1^0 s + n_0^0}{s^m + d_{m-1}^0 s^{m-1} + \cdots + d_1^0 s + d_0^0} \end{aligned} \tag{14.27}$$

Here, we choose the structure of the family of transfer functions as follows:

$$\mathbf{G}(s) = \left\{ g(s) \;:\; \frac{n_0(s) + \sum_{i=1}^{m+1} \alpha_i r_i(s)}{d_0(s) + \sum_{j=1}^{m} \beta_j q_j(s)} \right\} \tag{14.28}$$

where $r_i(s)$ and $q_i(s)$ are base polynomials of degree m and $m-1$, respectively. The parameters α_i and β_i are the interval parameters which will be determined by their limiting values:

$$\alpha_i \in [\alpha_i^-, \alpha_i^+], \qquad \beta_i \in [\beta_i^-, \beta_i^+], \qquad \text{for all } \; i$$

Upon the determination of the interval family $\mathbf{G}(s)$, we expect that the frequency response of every structure corresponding to each and every value of added mass ranging over 0 to 2.5kg remains inside that of the family $\mathbf{G}(s)$.

In the next subsection we show how to determine the desired family of transfer functions $\mathbf{G}(s)$, equivalently determining a nominal model $g_0(s)$, a set of base polynomials $(r_i(s), q_i(s))$, and the limiting values of interval parameters α_i and β_i. We will call this type of model an *interval model*.

Interval Model Identification

The algorithm to generate an interval model starts with identifying a model for each sample set of data. Any standard identification technique can be used for this purpose and here we again use a least squares based system identification technique. We first determine the order of the transfer function:

$$\begin{aligned} g_i(s) &= \frac{n_i(s)}{d_i(s)} \\ &= \frac{n_m^i s^m + n_{m-1}^i s^{m-1} + \ldots + n_0^i}{s^m + d_{m-1}^i s^{m-1} + \ldots + d_0^i}, \qquad i = 1, \cdots, 6. \end{aligned} \tag{14.29}$$

Once a judicious choice of the order of the transfer function is made, determination of the coefficients of each transfer function may be found by solving a least square problem. Let $D_i(\omega)$ be the i^{th} sample data set consisting of 900 data points and $W(\omega)$ is a positive weighting function, then the least square solution generates the coefficient set of the transfer function $g_i(s)$, which minimizes the index:

$$J_i = \sum_{k=1}^{900} W(w_k) \left[R(\omega_k)^2 + I(\omega_k)^2 \right] \tag{14.30}$$

where

$$R(\omega_k) := \text{Real}\,[D_i(\omega_k)d_i(j\omega) - n_i(j\omega)]$$
$$I(\omega_k) := \text{Imag}\,[D_i(\omega_k)d_i(j\omega) - n_i(j\omega)]\,.$$

We repeat this procedure for all six test data sets to obtain the transfer functions $g_i(s)$, $i = 1, \ldots, 6$. A typical choice for the nominal model $g_0(s)$ is the average of these:

$$n_i^0 = \frac{1}{6}\sum_{k=1}^{6} n_i^k \qquad \text{and} \qquad d_i^0 = \frac{1}{6}\sum_{k=1}^{6} d_i^k. \tag{14.31}$$

The parameter perturbation vectors of the i^{th} identified model are defined as

$$\Delta n_i = n_i - n_0, \qquad \Delta d_i = d_i - d_0 \tag{14.32}$$

In order to determine the set of base polynomials $r_i(s)$ and $q_i(s)$ in (14.28), we employ a Singular Value Decomposition. To illustrate this SVD technique, we first form a matrix for the uncertainty of the denominator as

$$\Delta D = [\Delta \mathbf{d}_1 \;\; \Delta \mathbf{d}_2 \;\; \ldots \;\; \Delta \mathbf{d}_6]\,. \tag{14.33}$$

The SVD factors the matrix ΔD as

$$\Delta D = USV^T, \tag{14.34}$$

where U and V are orthonormal matrices and S is a rectangular matrix

$$S = [S_m \;\; 0] \tag{14.35}$$

with $S_m = \text{diag}[s_1,\ s_2,\ \ldots,\ s_m]$ and monotonically nonincreasing s_i, $i = 1, 2, \cdots, m$

$$s_1 \geq s_2 \geq \cdots \geq s_m \geq 0. \tag{14.36}$$

The number of non-zero singular values s_i is the rank of the matrix ΔD.

Suppose that the size of the perturbation matrix ΔD is $m \times n$ with $n \geq m$ and the number of the non-zero singular values is m_k. Then the corresponding coordinate vector of the perturbation $\Delta \mathbf{d}_i$ relative to this basis is

$$\Delta \mathbf{q}_i = U^T \Delta \mathbf{d}_i. \tag{14.37}$$

Thus, we have

$$\begin{aligned}[\Delta \mathbf{q}_1 \;\; \ldots \;\; \Delta \mathbf{q}_n] &= U^T\,[\Delta \mathbf{d}_1 \;\; \ldots \;\; \Delta \mathbf{d}_n] \\ &= U^T \Delta D.\end{aligned}$$

Here the singular value matrix is expressed as

$$S = \begin{bmatrix} S_{m_k} & 0 \\ 0 & 0 \end{bmatrix} = \begin{bmatrix} S^0_{m_k} \\ 0 \end{bmatrix} \tag{14.38}$$

with $S_{m_k} = \text{diag}\,[s_1,\ s_2,\ \ldots,\ s_{m_k}]$. Thus,

$$\begin{aligned}[\Delta\mathbf{q}_1\ \Delta\mathbf{q}_2\ \ldots\ \Delta\mathbf{q}_n] &= [\Delta\mathbf{d}_1\ \ldots\ \Delta\mathbf{d}_n] \\ &= U^T\Delta D \\ &= U^T U S V^T \\ &= U^T U \begin{bmatrix} S^0_{m_k} V^T \\ 0 \end{bmatrix} \\ &= I_m \begin{bmatrix} S^0_{m_k} V^T \\ 0 \end{bmatrix} \\ &= \begin{bmatrix} S^0_{m_k} V^T \\ 0 \end{bmatrix}\end{aligned}$$

where $S^0_{m_k} V^T$ is an $m_k \times n$ matrix. The last $m - m_k$ elements of any $\Delta\mathbf{q}_i$ are zero. From this, it is clear that all the uncertainty vectors $\Delta\mathbf{d}_i$ are inside the space spanned by the first m_k orthonormal vectors of U.

Furthermore, since $S^0_{m_k} V^T$ is of full rank, the dimension of the uncertainty matrix ΔD is m_k. Notice that the i^{th} $(i \le m_k)$ row vector of the matrix $[\Delta\mathbf{q}_1\ \ldots\ \Delta\mathbf{q}_n]$ is $s_i V_i^T$ with norm s_i. The j^{th} element of vector $s_i V_i$ represents the perturbation $\Delta\mathbf{d}_j$ in the direction of $\mathbf{u}_i$. Each singular value s_i indicates the magnitude of the perturbations in the direction of $\mathbf{u}_i$.

For structures with low damping, the scalar value d_0^0, which is the multiplicative product of the squares of all the natural frequencies, may be many orders larger than the scalar d^0_{m-1}, which is the sum of $2\xi_i w_i$ where ξ_i and w_i are the damping ratio and the natural frequency of the i^{th} mode, respectively. For example, we will show that d_0^0 of the first two modes in the model of the ten-bay structure is 10^7 times larger than d_3^0 of this model. Thus we need to compute the perturbation matrix with proper weights and we denote this weighted perturbation matrix as ΔD^W:

$$\Delta D^W = W_d^{-1}\Delta D \tag{14.39}$$

where $W_d = \text{diag}[w_d^1\ w_d^2\ \ldots\ w_d^m]$ and w_d^i is the standard deviation of the i^{th} row vector of ΔD. To find the distribution of the weighted uncertainty, we again use SVD to factor the matrix

$$\Delta D^W = U^W S^W (V^W)^T, \quad \text{where } U^W = [\mathbf{u}_1^W\ \ldots\ \mathbf{u}_m^W]. \tag{14.40}$$

Here the singular value s_i indicates the weighted perturbations distributed in the direction of $\mathbf{u}_i^W$. The corresponding coordinate vector of the uncertainty $\Delta\mathbf{d}_i^W$ relative to the basis $\{\mathbf{u}_1^W, \ldots, \mathbf{u}_m^W\}$ is

$$\Delta\mathbf{q}_i^W = (U^W)^T\Delta\mathbf{d}_i^W \tag{14.41}$$

Since the basis $\{\mathbf{u}_1^W, \ldots, \mathbf{u}_m^W\}$ corresponds to the weighted perturbation matrix ΔD^W, we want to find a basis corresponding to the nonweighted perturbation

matrix ΔD. From (14.39) and (14.40), the matrix ΔD can be written as

$$\Delta D = W_d U^W S (V^W)^T. \tag{14.42}$$

The basis for the nonweighted perturbation matrix ΔD is computed as

$$U_d = W_d U^W, \quad \text{where } U_d = [\mathbf{u}_{d1}\ \mathbf{u}_{d2}\ \ldots\ \mathbf{u}_{dm}] \tag{14.43}$$

The basis $\{\mathbf{u}_{d1}, \ldots, \mathbf{u}_{dm}\}$ for the nonweighted perturbation matrix ΔD is equivalent to the basis $\{\mathbf{u}_1^W, \ldots, \mathbf{u}_m^W\}$ for the weighted perturbation matrix ΔD^W. The corresponding coordinate vector of the uncertainty $\Delta \mathbf{d}_i$ relative to the basis $\{\mathbf{u}_{d1}, \ldots, \mathbf{u}_{dm}\}$ is

$$\begin{aligned} \Delta \mathbf{q}_i &= U_d^{-1} \Delta \mathbf{d}_i \\ &= (U^W)^{-1} (W_d)^{-1} (W_d) \Delta \mathbf{d}_i^W \\ &= (U^W)^T \Delta \mathbf{d}_i^W = \Delta \mathbf{q}_i^W. \end{aligned} \tag{14.44}$$

Notice that the nonweighted perturbation coordinate vector $\Delta \mathbf{q}_i$ is the same as the weighted coordinate vector $\Delta \mathbf{q}_i^W$. Both perturbation matrices therefore share the same singular values. The fixed polynomials $\mathbf{q}_i(s)$ of the interval model in (14.28) are now composed of the basis vectors of U_d,

$$\mathbf{q}_i(s) = \sum_{j=1}^{m} \mathbf{u}_{di}(j) s^{m-j} \tag{14.45}$$

where $\mathbf{u}_{di}(j)$ is the j^{th} element of vector $\mathbf{u}_{di}$. Finally, we determine the bounds for the corresponding polynomial $\mathbf{q}_j(s)$ as

$$\beta_j^+ = \max_{1 \le i \le 6} (\Delta \mathbf{q}_i(j)), \quad j = 1, \ldots, m \tag{14.46}$$

$$\beta_j^- = \min_{1 \le i \le 6} (\Delta \mathbf{q}_i(j)), \quad j = 1, \ldots, m \tag{14.47}$$

where $\Delta \mathbf{q}_i(j)$ is the j^{th} element of vector $\Delta \mathbf{q}_i$. This interval model represents an optimal linear box of the determined polynomials to cover the perturbation. Similarly, we also apply the SVD technique to the numerator perturbation matrix to obtain $r_i(s)$, α_i^-, and α_i^+.

The above procedure insures that each transfer function $g_i(s)$, $i = 1, 2, \cdots, 6$ that represents the system with different added masses is contained in the interval transfer function $\mathbf{G}(s)$. Consequently, we will be justified in carrying out design and analysis on this interval model.

14.4.2 Experimental Results

We utilize the techniques developed in Chapters 6 and 8 to analyze the vibration suppression control of the ten-bay truss structure with added mass uncertainty. A

reaction mass actuator(RMA) located between nodes 39 and 40 is used to excite and control the structure's motion. An accelerometer located at node 40 is used to measure the acceleration in the x direction at this position. Here we consider the model for the modes within the $4-24$ Hz frequency range. There are two modes, one bending mode and one torsional mode, in this bandwidth. The experimental frequency domain data were collected using a Tektronix 2642A Fourier Analyzer. The controller consists of a proportional-derivative (PD) system connected to the actuator. The transfer function of the actuator is denoted as $g_a(s)$, and we denote the transfer function of the actuator-structure composite system as $g_i(s)$. The 900 point frequency response functions of the experimental system with actuator dynamics (actuator-structure composite system) are expressed as

$$g_i(j\omega_k) = g_a(j\omega_k)g_i^0(j\omega_k), \quad k = 1, 2, \cdots, 900 \tag{14.48}$$

where g_i is the i^{th} set of experimental data and g_i^0 represents the system dynamics excluding actuator dynamics. The transfer function of the actuator is given by

$$\begin{aligned} g_a(s) &= \frac{n_a(s)}{d_a(s)} \\ &= \frac{2.3853 \times 10^{-3}s^3 + 1.6745s^2}{2.3853 \times 10^{-3}s^3 + 1.6745s^2 + 25.781s + 1251.3}. \end{aligned} \tag{14.49}$$

This includes the second order dynamics of the RMA, plus a first order filter used in conjunction with a PD controller which keeps the center of its mass positive at stroke. Following the modeling procedure described, we first apply the least squares technique to each set of data g_i^0 to obtain the identified model for each case of incremented added masses given in Table 14.2. Figure 14.13 compares the experimental data and the identified models including actuator dynamics. The figure shows that each identified model closely fits the corresponding experimental data set. The two peaks of each set of experimental data represent two structural modes and the natural frequency of each mode decreases when the added weight increases. Also the magnitude of each mode changes slightly for all the cases. Table 14.3 shows the structural eigenvalues of these six identified models. After we obtained the identified structural models excluding actuator dynamics, we computed the nominal model as the average of these six models and we have

$$\begin{aligned} g_0(s) &= \frac{n_0(s)}{d_0(s)} \\ &= \frac{-3.463 \times 10^{-3}s^4 - 1.173 \times 10^{-3}s^3 - 24.68s^2}{s^4 + 5.241s^3 + 16255s^2 + 40225s + 4.412 \times 10^7}. \end{aligned} \tag{14.50}$$

Recall the model structure in (14.28). If we determine the coefficients of the base polynomials $r_i(s)$ and $q_i(s)$, and intervals of the parameters α_i and β_i, the interval model will be completely determined. By applying the interval modelling procedure described in Section 14.4.1, the coefficients of these polynomials and intervals of the

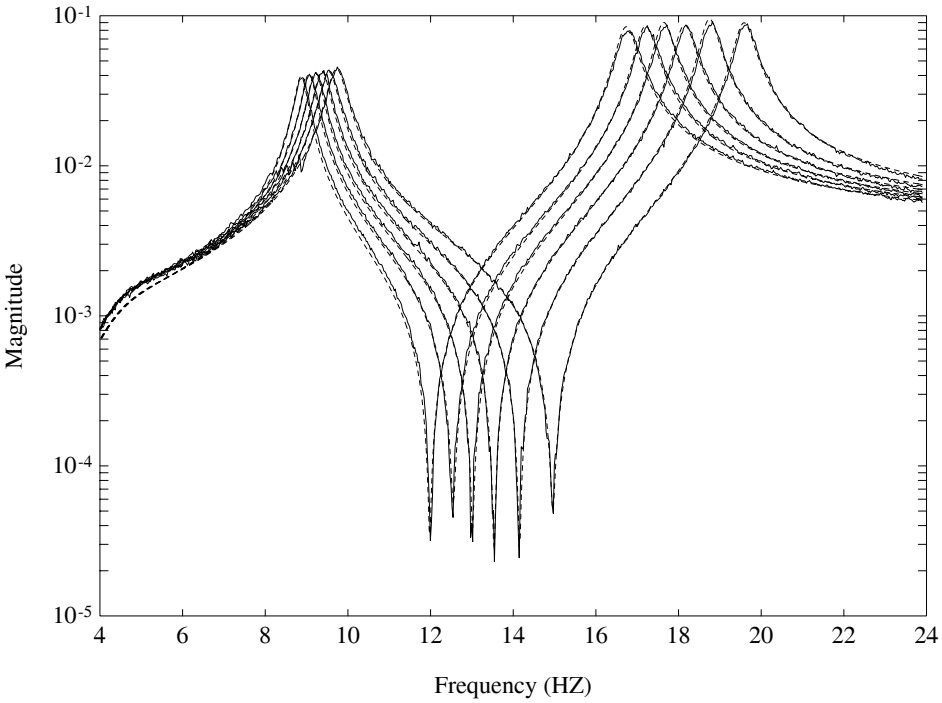

Figure 14.13. Experimental frequency response function (—) and Identified Models (- -): From Right to Left $0Kg$, $1Kg$, $2Kg$, $3Kg$, $4Kg$, $5\ Kg$.

Table 14.3. Eigenvalues of the identified models

Model No.	First mode	Second mode
1	-1.3864±j61.094	-1.4733±j123.00
2	-1.3065±j59.930	-1.3677±j117.76
3	-1.1854±j58.892	-1.4871±j113.96
4	-1.1081±j57.902	-1.4167±j110.79
5	-1.0424±j56.929	-1.4873±j108.03
6	-0.9581±j55.724	-1.5050±j105.10

parameters are obtained as shown in Tables 14.4 and 14.5. Table 14.4 shows that the coefficients of the denominator depicting the model uncertainty are dominated by the uncertainty in the direction of the first singular vector. The perturbation distributed in the direction of the fourth singular vector is around 1000 times smaller

Table 14.4. Coefficients of $q_i(s)$ and intervals of β_i

	$q_1(s)$	$q_2(s)$	$q_3(s)$	$q_4(s)$
s^3	1.4326×10^{-1}	-2.5118×10^{-1}	-1.8767×10^{-2}	-1.0399×10^{-3}
s^2	8.6678×10^{2}	5.5011×10^{2}	-8.0878×10^{2}	1.1301×10^{3}
s^1	4.1568×10^{3}	1.8545×10^{3}	6.8649×10^{3}	8.2205×10^{2}
s^0	4.0831×10^{6}	2.5353×10^{6}	-2.4265×10^{6}	-6.1023×10^{6}
β^+	3.1117×10^{0}	2.8036×10^{-1}	2.5123×10^{-2}	2.5140×10^{-3}
β^-	-2.3396×10^{0}	-2.1055×10^{-1}	-3.3913×10^{-2}	-2.5161×10^{-3}

Table 14.5. Coefficients of $r_i(s)$ and intervals of α_i

	$r_1(s)$	$r_2(s)$	$r_3(s)$	$r_4(s)$	$r_5(s)$
s^4	-8.7360×10^{-4}	-3.2529×10^{-5}	9.2234×10^{-5}	0	0
s^3	-1.3370×10^{-4}	3.8897×10^{-4}	1.0547×10^{-5}	0	0
s^2	-3.3372×10^{0}	-1.0513×10^{0}	-3.5316×10^{0}	0	0
s^1	0	0	0	1	0
s^0	0	0	0	0	1
α^+	2.4339×10^{0}	1.0485×10^{0}	6.3217×10^{-2}	0	0
α^-	-1.8816×10^{0}	-1.3450×10^{0}	-3.5834×10^{-2}	0	0

than that of the first singular vector. Table 14.5 shows that the model uncertainty of the numerator part is dominated by the uncertainty in the directions of the first two singular vectors. The Edge Theorem (Chapter 6) is now applied to the interval model obtained. Figure 14.14 shows the root clusters for two structural modes of interest. Experimentally identified eigenvalues are also included for comparison. From the interval model of the structure we obtained, we now can write the interval model of the system which includes the actuator dynamics (actuator-structure composite system), as follows:

$$G(s) = \frac{n_a(s)\left[n_0(s) + \sum_{i=1}^{m+1} \alpha_i r_i(s)\right]}{d_a(s)\left[d_0(s) + \sum_{i=1}^{m} \beta_i q_i(s)\right]}$$

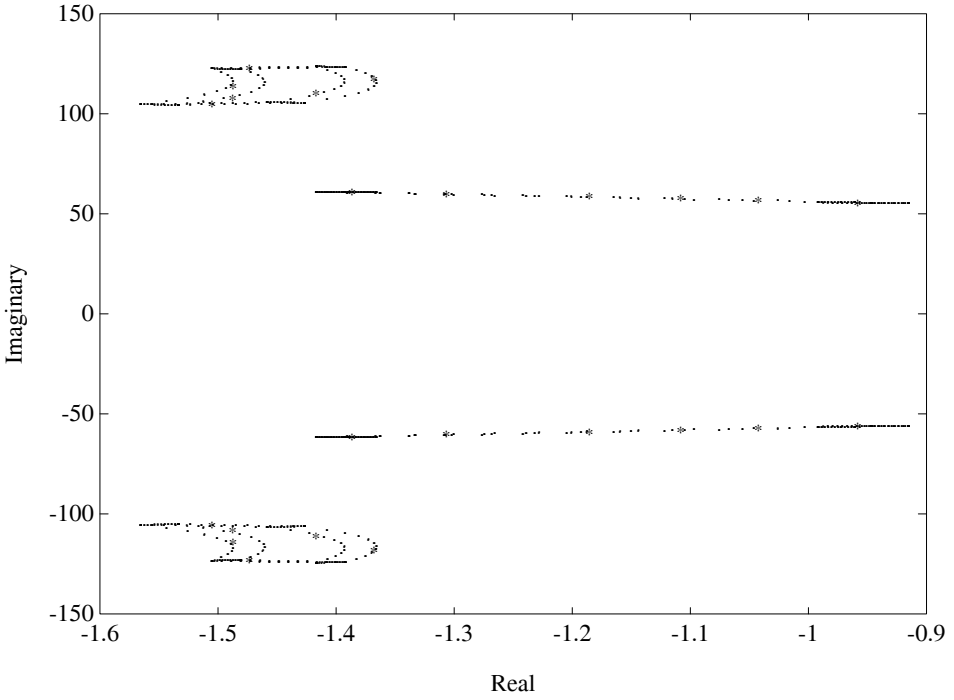

Figure 14.14. Root cluster (.) of closed-loop interval model and eigenvalues (*) of open-loop experimental structure for various added masses.

$$= \frac{n_a(s)n_0(s) + \sum_{i=1}^{m+1} \alpha_i n_a(s) r_i(s)}{d_a(s)d_0(s) + \sum_{i=1}^{m} \beta_i d_a(s) q_i(s)}. \tag{14.51}$$

Next, we apply the techniques described in Chapter 8 to obtain the magnitude envelopes of the interval model given in (14.51). Figure 14.15 shows the magnitude envelopes and the magnitude plots of the experimental transfer functions $g_i(\omega)$ for $i = 1, 2, \cdots, 6$. It is seen that the magnitude envelopes cover all the experimental data sets. It should be noted that these six experimental transfer functions represent a sample of all parametric changes which correspond to added masses at nodes 17 and 44. The interval model on the other hand accounts for the dynamics of the system for continuous changing masses at these two nodes up to $2.5Kg$. To verify the identified interval system by using the closed-loop experiment, we first design a local velocity feedback controller based on the root loci techniques for the vibration suppression of the structure. The transfer function of the controller is

$$K(s) = \frac{n_k(s)}{d_k(s)} = \frac{-110K_v s}{s^2 + \pi s + \pi^2}$$

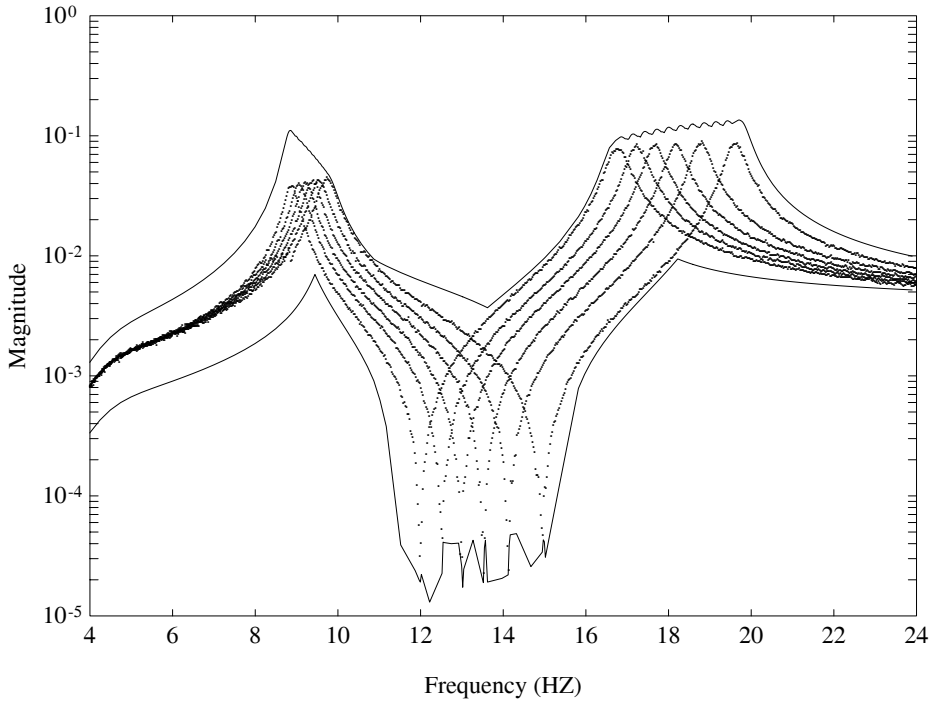

Figure 14.15. Magnitude envelope (—) of interval model and experimental data (..) for the open-loop system frequency response functions.

where K_v is the velocity feedback gain. The controller is designed for the structure without added masses. With $K_v = 30$, the damping ratio of the first mode is increased from 2.2% to 6.6% and the damping ratio of the second mode from 1.2% to 3.9%. The closed-loop interval system transfer function with the controller $K(s)$ can be computed as

$$T(s) = \frac{d_k(s)\left[n_a(s)n_0(s) + \sum_{i=1}^{m+1}\alpha_i(n_a(s)r_i(s))\right]}{d_k(s)\left[d_a(s)d_0(s) + \sum_{i=1}^{m}\beta_i(d_a(s)q_i(s))\right] + n_k(s)\left[n_a(s)n_0(s) + \sum_{i=1}^{m+1}\alpha_i(n_a(s)r_i(s))\right]}.$$

This interval system representation may be separated into the fixed and perturbation terms

$$T(s) = \frac{\alpha(s) + \sum_{i=1}^{m+1}\alpha_i\alpha_{1i}(s)}{\beta(s) + \sum_{i=1}^{m}\beta_i\beta_{1i}(s) + \sum_{i=1}^{m+1}\alpha_i\beta_{2i}(s)} \tag{14.52}$$

where the fixed part of the polynomials are

$$\alpha(s) = d_k(s)n_a(s)n_0(s),$$

$$\beta(s) = d_k(s)d_a(s)d_0(s) + n_k(s)n_a(s)n_0(s)$$

and the perturbation part polynomials are

$$\begin{aligned}\alpha_{1i}(s) &= d_k(s)n_a(s)r_i(s)\\ \beta_{1i}(s) &= d_k(s)d_a(s)q_i(s)\\ \beta_{2i}(s) &= n_k(s)n_a(s)r_i(s).\end{aligned}$$

Figure 14.16 depicts the magnitude envelope of the closed-loop interval system which shows that the envelope bounds the magnitude of the experimental transfer functions.

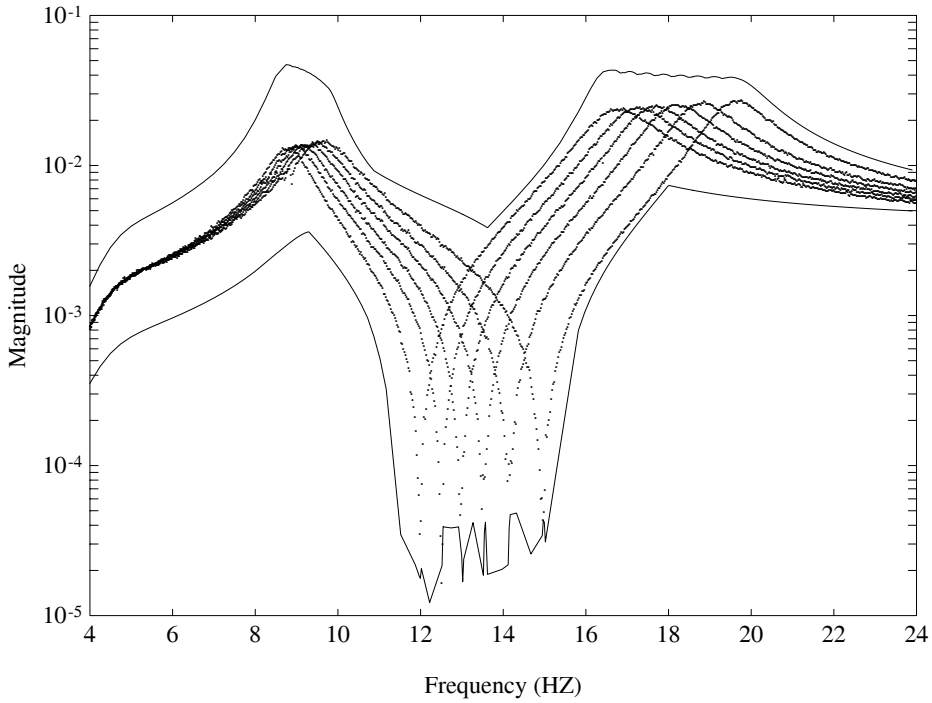

Figure 14.16. Magnitude envelope (—) of interval model and experimental data (..) for the closed-loop system frequency response functions.

The root clusters of the closed-loop interval system are also plotted by applying the Edge Theorem (Chapter 6) and it is given in Figure 14.17. The damping for each mode of the closed-loop family of systems is increased and this is verified by comparing the boundaries of the root clusters in Figures 14.14 and 14.17. Thus, from this root cluster plot, one can predict the worst case damping of the closed loop system while the added mass varies anywhere in between 0 to $2.5Kg$. In

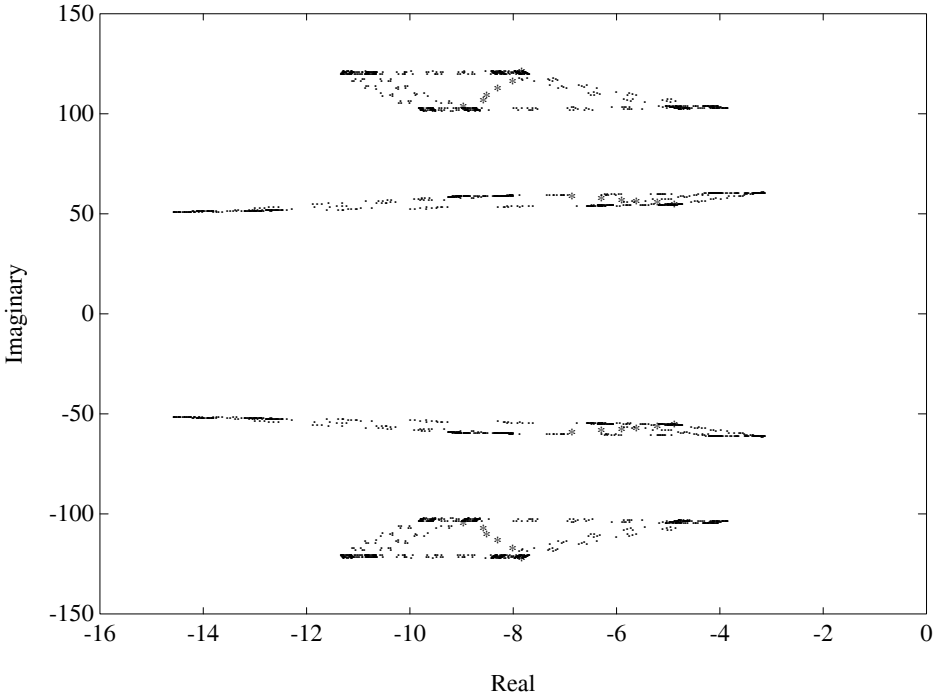

Figure 14.17. Root cluster (.) of closed-loop interval model and eigenvalues (*) of closed-loop experiment for $K_v = 60$.

other words, as long as the varied system remains inside the Bode envelope given in Figure 14.15, the poles of the closed loop system will remain inside the cluster regions shown in Figure 14.17.

14.5 NOTES AND REFERENCES

In this chapter we have freely employed a variety of terms used to explain system identification and the control structure experiment. We intentionally did not explain these terms in detail because our emphasis lies in interval system identification. However, the interested reader may refer to the following references for further details. An excellent collection of papers dealing with the issue of system identification and robust control is to be found in Kosut, Goodwin and Polis [151], [1], and references therein. These are mainly focused on the H_∞, ℓ_1 and μ problems. The least square approach used in Section 14.2.2 to determine a nominal linear time-invariant transfer function is described in detail by Adcock [3] and also by Juang and Pappa [122]. The method of selecting the normalized least square weight $W^I(j\omega)$ and its effect on the identified model are discussed in Bayard, Hadaegh,

Yam, Scheid, Mettler, and Milman [24]. They also discussed the problem of selecting an appropriate order of the transfer function in detail. The MATLAB ToolBox for Eigensystem Realization Algorithm (ERA) which was used to extract the natural frequencies and damping ratios from the experimental data for the second example was developed by Juang, Phan and Horta [123]. The details of the Reaction Mass Actuator (RMA) can be found in the work of Garcia, Webb and Duke [102]. The details of a Local Velocity Feedback (LVF) scheme which was used to accomplish vibration damping can be found in Zimmerman, Horner and Inman [248]. A velocity estimator is also described in Hallauer and Lamberson [107]. The first experiment was developed by Keel, Lew and Bhattacharyya [140]. The experiment was also modified to reflect mixed H_∞ and parametric uncertainty, and various results are reported in Lew, Keel and Juang [161, 162]. The second experiment was performed by Lew, Link, Garcia and Keel [163] and the related results are reported in Link, Lew, Garcia and Keel [164]. Different approaches of interval system modeling are also reported by Sotirov and Shafai [209] and [217].

References

[1] Special issue on system identification for robust control design. *IEEE Transactions on Automatic Control*, vol. 37, no. 7 (July 1992).

[2] Ackermann, J. *Robust Control: Systems with Uncertain Physical Parameters*. Springer-Verlag, New York, NY, 1993.

[3] Adcock, J. L. Curve fitter for pole - zero analysis. *Hewlett - Packard Journal* (January 1987).

[4] Aguirre, G., Chapellat, H., and Bhattacharyya, S. P. Stability margins for discrete-time uncertain systems. In *Proceedings of the 1989 IEEE Conference on Decision and Control* (Tampa, FL, December 1989).

[5] Ahmad, S. S. and Keel, L. H. Robust lead-lag compensation for uncertain linear systems. In *Proceedings of the 1992 IEEE Symposium on Circuits and Systems* (San Diego, CA, 1992), pp. 2716 – 2719.

[6] Ahmad, S. S., Keel, L. H., and Bhattacharyya, S. P. Computer aided robust control design for interval control system. In *Proceedings of the IEEE Symposium on Computer Aided Control System Design* (Napa, CA, 1992), pp. 82 – 89.

[7] Ahmad, S. S., Keel, L. H., and Bhattacharyya, S. P. Robust PID control and lead-lag compensator for linear interval systems. In *Robustness of Dynamic Systems with Parameter Uncertainties*, M. Mansour, S. Balemi, and W. Truöl, Eds. Birkhäuser, Berlin, 1992, pp. 251 – 260.

[8] Ahmad, S. S., Keel, L. H., and Bhattacharyya, S. P. Frequency domain templates for design of multilinear interval control systems. Tech. Rep., Tennessee State University, January 1994. ISE Report No. ACS-94-1.

[9] Aizerman, M. A. and Gantmacher, F. R. *Absolute stability of regulator systems*. Holden-Day Publishing Co., San Francisco, CA, 1964. Russian Edition, 1963.

[10] Anderson, B. D. O., Kraus, F., Mansour, M., and Dasgupta, S. Easily testable sufficient conditions for the robust stability of systems with multiaffine parameter dependence. In *Robustness of Dynamic Systems with Parameter Uncertainties*, M. Mansour, S. Balemi, and W. Truöl, Eds. Birkhäuser, Berlin, 1992, pp. 81 – 92.

[11] Barmish, B. R. Invariance of strict Hurwitz property of polynomials with perturbed coefficients. *IEEE Transactions on Automatic Control*, vol. AC-29, no. 10 (October 1984), pp. 935 – 936.

[12] Barmish, B. R. New tools for robustness analysis. In *Proceedings of the 27th IEEE Conference on Decision and Control* (Austin, TX, December 1988), pp. 1 – 6.

[13] Barmish, B. R. A generalization of Kharitonov's four polynomial concept for robust stability problems with linearly dependent coefficient perturbations. *IEEE Transactions on Automatic Control*, vol. 34, no. 2 (February 1989), pp. 157 – 165.

[14] Barmish, B. R. *New Tools for Robustness of Linear Systems.* Macmillan Publishing Co., New York, NY, 1994.

[15] Barmish, B. R., Hollot, C. V., Kraus, F. J., and Tempo, R. Extreme point results for robust stabilization of interval plants with first order compensators. *IEEE Transactions on Automatic Control*, vol. 37, no. 6 (June 1992), pp. 707 – 714.

[16] Barmish, B. R., Khargonekar, P. P., Shi, Z., and Tempo, R. Robustness margin need not be a continuous function of the problem data. *Systems & Control Letters*, vol. 15 (1989), pp. 371 – 381.

[17] Barmish, B. R. and Shi, Z. Robust stability of a class of polynomials with coefficients depending multilinearly on perturbations. *IEEE Transactions on Automatic Control*, vol. AC-35, no. 9 (September 1990), pp. 1040 – 1043.

[18] Barmish, B. R. and Wei, K. H. Simultaneous stabilization of single input single output systems. In *Proceedings of the International Symposium on Mathematical Theory of Networks and Systems* (Stockholm, Sweden, 1985).

[19] Bartlett, A. C. Nyquist, Bode, and Nichols plots of uncertain systems. In *Proceedings of the 1990 American Control Conference* (San Diego, CA, 1990), pp. 2033 – 2036.

[20] Bartlett, A. C. Vertex results for the steady state analysis of uncertain systems. *IEEE Transactions on Automatic Control*, vol. 37, no. 11 (November 1992), pp. 1758 – 1762.

[21] Bartlett, A. C., Hollot, C. V., and Lin, H. Root location of an entire polytope of polynomials: it suffices to check the edges. *Mathematics of Controls, Signals and Systems*, vol. 1 (1988), pp. 61 – 71.

[22] Bartlett, A. C., Tesi, A., and Vicino, A. Frequency response of uncertain systems with interval plants. *IEEE Transactions on Automatic Control*, vol. 38, no. 6 (June 1993), pp. 929 – 933.

[23] Basu, S. On boundary implications of stability and positivity properties of multidimensional systems. *IEEE Proceedings*, vol. 78, no. 4 (April, 1990), pp. 614 – 626.

[24] Bayard, D. S., Hadaegh, F. Y., Yam, Y., Scheid, R. E., Mettler, E., and Milman, M. H. Automated on-orbit frequency domain identification for large space structures. *Automatica*, vol. 27, no. 6 (November 1991), pp. 931 – 946.

[25] Bellman, R. E. The theory of dynamic programming. *Proceedings of National Academy of Science, USA*, vol. 38 (1954), pp. 716 – 719.

[26] Bellman, R. E. *Introduction to the Mathematical Theory of Control Processes, Vol. 1.* Academic Press, New York, NY, 1967.

[27] Berman, A. and Plemmons, R. J. *Nonnegative Matrices in the Mathematical Science.* Academic Press, New York, NY, 1979.

[28] Bhattacharya, S., Keel, L. H., and Bhattacharyya, S. P. Robust stabilizer synthesis for interval plants using H_∞ methods. In *Proceedings of the 1993 IEEE Conference on Decision and Control* (San Antonio, Texas, December 1993), pp. 3003 – 3008.

[29] Bhattacharyya, S. P. *Robust stabilization against structured perturbations.* Lecture Notes in Control and Information Sciences, vol. 99, Springer-Verlag, New York, NY, 1987.

[30] Bhattacharyya, S. P. Robust parametric stability: The role of the CB segments. In *Control of Uncertain Dynamic Systems*, S. P. Bhattacharyya and L. H. Keel, Eds. CRC Press, Littleton, MA, 1991, pp. 381 – 402.

[31] Bhattacharyya, S. P. Vertex results in robust stability. Tech. Rep., TCSP Report, Texas A&M University, April 1991.

[32] Bhattacharyya, S. P. and Keel, L. H., Eds. *Control of Uncertain Dynamic Systems.* CRC Press, Littleton, MA, 1991.

[33] Bhattacharyya, S. P. and Keel, L. H. Robust stability and control of linear and multilinear interval systems. In *Control and Dynamic Systems*, C. T. Leondes, Ed., vol. 51. Academic Press, New York, NY, 1992, pp. 31 – 78.

[34] Bhattacharyya, S. P., Keel, L. H., and Howze, J. W. Stabilization of linear systems with fixed order controllers. *Linear Algebra and its Applications*, vol. 98 (1988), pp. 57 – 76.

[35] Bhattacharyya, S. P. and Pearson, J. B. On the linear servomechanism problem. *International Journal of Control*, vol. 12, no. 5 (1970), pp. 795 – 806.

[36] Bhattacharyya, S. P. and Pearson, J. B. On error systems and the servomechanism problem. *International Journal of Control*, vol. 15, no. 6 (1972), pp. 1041 – 1062.

[37] Bhattacharyya, S. P., Pearson, J. B., and Wonham, W. M. On zeroing the output of a linear system. *Information and Control*, vol. 2 (1972), pp. 135 – 142.

[38] Bialas, S. A necessary and sufficient condition for stability of interval matrices. *International Journal of Control*, vol. 37 (1983), pp. 717 – 722.

[39] Bialas, S. A necessary and sufficient condition for the stability of convex combinations of stable polynomials and matrices. *Bulletin of Polish Academy of Science*, vol. 33 (1985), pp. 473 – 480.

[40] Biernacki, R. M., Hwang, H., and Bhattacharyya, S. P. Robust stabilization of plants subject to structured real parameter perturbations. *IEEE Transactions on Automatic Control*, vol. AC-32, no. 6 (June 1987), pp. 495 – 506.

[41] Blondel, V. *Simultaneous Stabilization of Linear Systems.* Lecture Notes in Control and Information Sciences, Springer-Verlag, New York, NY, 1994.

[42] Bode, H. W. *Network Analysis and Feedback Amplifier Design.* D. Van Nostrand Publishing Co., New York, NY, 1945.

[43] Bose, N. K. *Digital Filters.* Elsevier-Science North-Holland, Krieger Publishing Co., New York, NY, 1993.

[44] Bose, N. K. A system-theoretic approach to stability of sets of polynomials. *Contemporary Mathematics*, vol. 47 (1985), pp. 25 – 34.

[45] Bose, N. K. Robust multivariable scattering Hurwitz interval polynomials. *Linear Algebra and its Application*, vol. 98 (1988), pp. 123 – 136.

[46] Bose, N. K. Test of Hurwitz and Schur properties of convex combination of complex polynomials. *IEEE Transactions on Automatic Control*, vol. 36, no. 9 (September 1989), pp. 1245 – 1247.

[47] Bose, N. K. Argument conditions for Hurwitz and Schur polynomials from network theory. *IEEE Transactions on Automatic Control*, vol. 39, no. 2 (February 1994), pp. 345 – 346.

[48] Bose, N. K. and Delansky, J. F. Boundary implications for interval positive rational functions. *IEEE Transactions on Circuits and Systems*, vol. CAS-36 (1989), pp. 454 – 458.

[49] Bose, N. K. and Shi, Y. Q. Network realizability theory approach to stability of complex polynomials. *IEEE Transactions on Automatic Control*, vol. 34, no. 2 (February 1987), pp. 216 – 218.

[50] Bose, N. K. and Shi, Y. Q. A simple general proof of Kharitonov's general stability criterion. *IEEE Transactions on Circuits and Systems*, vol. CAS-34 (1987), pp. 1233 – 1237.

[51] Boyd, S. P. and Barratt, C. H. *Linear Controller Design: Limits of Performance*. Prentice-Hall Publishing Co., Englewood Cliffs, NJ, 1990.

[52] Brasch, F. M. and Pearson, J. B. Pole placement using dynamic compensator. *IEEE Transactions on Automatic Control*, vol. AC-15, no. 1 (February 1970), pp. 34 – 43.

[53] Chang, B. C. and Pearson, J. B. Optimal disturbance reduction in linear multivariable systems. *IEEE Transactions on Automatic Control*, vol. AC-29, no. 10 (October 1984), pp. 880 – 887.

[54] Chapellat, H. Geometric conditions for robust stability. Master's thesis, Department of Electrical Engineering, Texas A&M University, College Station, Texas, U.S.A., 1987.

[55] Chapellat, H. *Robust stability and control under structured and unstructured perturbations*. PhD thesis, Department of Electrical Engineering, Texas A&M University, College Station, Texas, U.S.A., 1990.

[56] Chapellat, H. and Bhattacharyya, S. P. Calculation of maximal stability domains using an optimal property of Kharitonov polynomials. In *Analysis and Optimization of Systems*. Lecture Notes in Control and Information Sciences, vol. 62, Springer-Verlag, 1988, pp. 22 – 31.

[57] Chapellat, H. and Bhattacharyya, S. P. An alternative proof of Kharitonov's theorem. *IEEE Transactions on Automatic Control*, vol. AC-34, no. 4 (April 1989), pp. 448 – 450.

[58] Chapellat, H. and Bhattacharyya, S. P. A generalization of Kharitonov's theorem: robust stability of interval plants. *IEEE Transactions on Automatic Control*, vol. AC-34, no. 3 (March 1989), pp. 306 – 311.

[59] Chapellat, H. and Bhattacharyya, S. P. Robust stability and stabilization of interval plants. In *Robustness in Identification and Control*, M. Milanese, R. Tempo, and A. Vicino, Eds. Plenum Press, New York, NY, 1989, pp. 207 – 229.

[60] Chapellat, H. and Bhattacharyya, S. P. Simultaneous strong stabilization. Tech. Rep., EE Department Report, Texas A&M University, 1989.

[61] Chapellat, H., Bhattacharyya, S. P., and Dahleh, M. Robust stability of a family of disc polynomials. *International Journal of Control*, vol. 51 (1990), pp. 1353 – 1362.

[62] Chapellat, H., Bhattacharyya, S. P., and Keel, L. H. Stability margin for Hurwitz polynomials. In *Proceedings of the 27th IEEE Conference on Decision and Control* (Austin, TX, December 1988), pp. 1392 – 1398.

[63] Chapellat, H., Dahleh, M., and Bhattacharyya, S. P. Robust stability under structured and unstructured perturbations. *IEEE Transactions on Automatic Control*, vol. AC-35, no. 10 (October 1990), pp. 1100 – 1108.

[64] Chapellat, H., Dahleh, M., and Bhattacharyya, S. P. On robust nonlinear stability of interval control systems. *IEEE Transactions on Automatic Control*, vol. AC-36, no. 1 (January 1991), pp. 59 – 67.

[65] Chapellat, H., Dahleh, M., and Bhattacharyya, S. P. Robust stability manifolds for multilinear interval systems. *IEEE Transactions on Automatic Control*, vol. 38, no. 2 (February 1993), pp. 314 – 318.

[66] Chapellat, H., Keel, L. H., and Bhattacharyya, S. P. Stability margins for multilinear interval control systems. In *Proceedings of the 30th IEEE Conference on Decision and Control* (Brighton, UK, December 1991), pp. 894 – 899.

[67] Chapellat, H., Keel, L. H., and Bhattacharyya, S. P. Extremal robustness properties of multilinear interval systems. *Automatica*, vol. 30, no. 6 (June 1994), pp. 1037 – 1042.

[68] Chapellat, H., Mansour, M., and Bhattacharyya, S. P. Elementary proofs of some classical stability criteria. *IEEE Transactions on Education*, vol. 33, no. 3 (March 1990), pp. 232 – 239.

[69] Cohn, A. Uber die anzahl der wurzein einer algebraischen gleichung in einem kreise. *Math. Zeit.*, vol. 14 (1922), pp. 110 – 148.

[70] Dahleh, M., Tesi, A., and Vicino, A. Robust stability and performance of interval plants. *Systems & Control Letters*, vol. 19 (1992), pp. 353 – 363.

[71] Dahleh, M., Tesi, A., and Vicino, A. On the robust Popov criterion for interval Lur'e system. *IEEE Transactions on Automatic Control*, vol. 38, no. 9 (September 1993), pp. 1400 – 1405.

[72] Dahleh, M., Tesi, A., and Vicino, A. An overview of extremal properties for robust control of interval plants. *Automatica*, vol. 29, no. 3 (May 1993), pp. 707 – 722.

[73] Dahleh, M. A. and Pearson, J. B. ℓ^1 optimal feedback controllers for MIMO discrete-time systems. *IEEE Transactions on Automatic Control*, vol. AC-32, no. 4 (April 1987), pp. 314 – 322.

[74] Dasgupta, S. A Kharitonov like theorem for systems under nonlinear passive feedback. In *Proceedings of the 26th IEEE Conference on Decision and Control* (Los Angeles, CA, December 1987), pp. 2062 – 2063.

[75] Dasgupta, S. Kharitonov's theorem revisited. *Systems & Control Letters*, vol. 11 (1988), pp. 381 – 384.

[76] Dasgupta, S. and Bhagwat, A. S. Conditions for designing strictly positive real transfer functions for adaptive output error identification. *IEEE Transactions on Circuits and Systems*, vol. CAS-34 (1987), pp. 731 – 736.

[77] Datta, A. and Bhattacharyya, S. P. On a quantitative theory of robust adaptive control: an interval plant approach. In *Proceedings of the 1994 American Control Conference* (June 1994), pp. 58 – 62.

[78] Datta, A. and Bhattacharyya, S. P. On determining the δ and θ-Hurwitz stability of interval polynomials. In *Proceedings of the 1995 American Control Conference* (June 1995), To appear.

[79] Davison, E. J. The robust control of a servomechanism problem for linear time-invariant systems. *IEEE Transactions on Automatic Control*, vol. AC-21, no. 1 (January 1976), pp. 25 – 34.

[80] deGaston, R. R. E. and Safonov, M. G. Exact calculation of the multiloop stability margin. *IEEE Transactions on Automatic Control*, vol. AC-33, no. 2 (February 1988), pp. 156 – 171.

[81] Desoer, C. A., Liu, R. W., Murray, J., and Saeks, R. Feedback system design: The fractional representation approach to analysis and synthesis. *IEEE Transactions on Automatic Control*, vol. AC-25 (June 1980), pp. 399 – 412.

[82] Dieudonné, J. *Eléments d'analyse, Tome 1: Fondements de l'analyse moderne*. Gauthier-Villars, Editeur, Paris, 1969.

[83] Dorato, P., Ed. *Robust Control*. IEEE Press, New York, NY, 1987.

[84] Dorato, P., Abdallah, C., and Cerone, V. *Linear Quadratic Control: An Introduction.* Macmillan Publishing Co., New York, NY, 1994.

[85] Dorato, P., Fortuna, L., and Muscato, G. *Robust Control for Unstructured Perturbations: An Introduction.* Lecture Notes in Control and Information Sciences, vol. 168, Springer-Verlag, New York, NY, 1992.

[86] Dorato, P. and Yedavalli, R. K., Eds. *Recent Advances in Robust Control.* IEEE Press, New York, NY, 1989.

[87] Doyle, J. C. Guaranteed margins for LQG regulators. *IEEE Transactions on Automatic Control*, vol. AC-23, (August 1978), pp. 756 – 757.

[88] Doyle, J. C. Analysis of feedback systems with structured uncertainties. *Proceeding of IEE - D*, vol. 129, no. 6 (1982), pp. 242 – 250.

[89] Doyle, J. C. Synthesis of robust controllers and filters. In *Proceedings of the* 22^{nd} *IEEE Conference on Decision and Control* (December 1983), pp. 109 – 114.

[90] Doyle, J. C. Structured uncertainty in control system design. In *Proceedings of the 24th IEEE Conference on Decision and Control* (Ft. Lauderdale, FL, December 1985), pp. 260 – 265.

[91] Doyle, J. C., Glover, K., Khargonekar, P. P., and Francis, B. A. State space solution to standard H_2 and H_∞ control problems. *IEEE Transactions on Automatic Control*, vol. AC-34, no. 8 (August 1989), pp. 831 – 847.

[92] Faedo, S. A new stability problem for polynomials with real coefficients. *Ann. Scuola Norm. Sup. Pisa Sci. Fis. Mat. Ser.* 3 - 7 (1953), pp. 53 – 63.

[93] Ferreira, P. M. G. The servomechanism problem and the method of the state space in the frequency domain. *International Journal of Control 23*, vol. 2 (1976), pp. 245 – 255.

[94] Ferreira, P. M. G. and Bhattacharyya, S. P. On blocking zeros. *IEEE Transactions on Automatic Control*, vol. AC-22, no. 2 (1977), pp. 258 – 259.

[95] Foo, Y. K. and Soh, Y. C. Stability analysis of a family of matrices. *IEEE Transactions on Automatic Control*, vol. 35, no. 11 (November 1990), pp. 1257 – 1259.

[96] Francis, B. A. and Wonham, W. M. The internal model principle for linear multivariable regulators. *Applied Mathematics and Optimization*, vol. 2, no. 2 (1975), pp. 170 – 194.

[97] FRANCIS, B. A. AND ZAMES, G. On H_∞-optimal sensitivity theory for SISO feedback systems. *IEEE Transactions on Automatic Control*, vol. AC-29, no. 1 (January 1984), pp. 9 – 16.

[98] FU, M. Computing the frequency response of linear systems with parametric perturbation. *Systems & Control Letters*, vol. 15 (1990), pp. 45 – 52.

[99] FU, M. AND BARMISH, B. R. Polytopes and polynomials with zeros in a prescribed set. *IEEE Transactions on Automatic Control*, vol. 34, no. 5 (May 1989), pp. 544 – 546.

[100] FU, M., OLBROT, A. W., AND POLIS, M. P. Robust stability for time-delay systems: The Edge theorem and graphical tests. *IEEE Transactions on Automatic Control*, vol. 34, no. 8 (August 1989), pp. 813 – 820.

[101] GANTMACHER, F. R. *The Theory of Matrices, Vol. 2.* Chelsea Publishing Company, New York, NY, 1959.

[102] GARCIA, E., WEBB, S., AND DUKE, J. Passive and active control of complex flexible structure using reaction mass actuators. *ASME Journal of Vibrations and Acoustics*, vol. 117, no. 1 (January 1995), To appear.

[103] GLOVER, K. Robust stabilization of linear multivariable systems: relations to approximation. *International Journal Control*, vol. 43 (March 1986), pp. 741 – 766.

[104] GRUJIČ, L. T. AND PETKOVSKI, D. On robustness of Lur'e systems with multiple nonlinearities. *Automatica*, vol. 23 (1987), pp. 327 – 334.

[105] GUILLEMIN, E. A. *The Mathematics of Circuit Analysis.* John Wiley & Sons, Inc., New York, NY, 1949.

[106] HALE, J. K. *Functional Differential Equations.* Applied Mathematical Sciences, vol. 3, Springer-Verlag, New York, 1971.

[107] HALLAUER, W. AND LAMBERSON, S. Experimental active vibration damping of a plane truss using hybrid actuation. In *Proceedings of the 30th AIAA/ASME/ASCE/AHX/ASC Structures, Structural Dynamics and Materials Conference* (Mobile, AL, 1989), pp. 80 – 89.

[108] HAYKIN, S. *Adaptive Filter Theory.* Prentice-Hall publishing Co., Englewood Cliffs, NJ, 1986.

[109] HERMITE, C. Sur le nombre de racines d'une équation algebrique comprise entre des limites données. *J. Reine Angew. Math.*, vol. 52 (1856), pp. 39 – 51.

[110] HINRICHSEN, D. AND MÅRTENSSON, B., Eds. *Control of Uncertain Systems.* Birkhäuser, Berlin, 1990.

[111] HINRICHSEN, D. AND PRITCHARD, A. J. New robustness results for linear systems under real perturbations. In *Proceedings of the 27th IEEE Conference on Decision and Control* (1988), pp. 1375 - 1379.

[112] HINRICHSEN, D. AND PRITCHARD, A. J. An application of state space methods to obtain explicit formulae for robustness measures of polynomials. In *Robustness in Identification and Control*, M. Milanese, R. Tempo, and A. Vicino, Eds. Plenum Publishing Co., New York, 1989, pp. 183 – 206.

[113] HINRICHSEN, D. AND PRITCHARD, A. J. Real and complex stability radii: a survey. In *Control of Uncertain Systems*, D. Hinrichsen and B. Mårtensson, Eds. Birkhäuser, 1990, pp. 119 – 162.

[114] HINRICHSEN, D. AND PRITCHARD, A. J. A robustness measure for linear systems under structured real parameter perturbations. Tech. rep., Institut fur Dynamische Systeme, Bremen, Germany, 1991. Report No. 184.

[115] HOLLOT, C. V. AND BARTLETT, A. C. Some discrete-time counterparts to Kharitonov's stability criterion for uncertain systems. *IEEE Transactions on Automatic Control*, vol. AC-31, no. 4 (April 1986), pp. 355 – 356.

[116] HOLLOT, C. V. AND TEMPO, R. H_∞ performance of weighted interval plants: complete characterization of vertex results. In *Proceedings of the 1993 American Control Conference* (San Francisco, CA, 1993), pp. 617 - 619.

[117] HOLLOT, C. V. AND TEMPO, R. On the Nyquist envelope of an interval plant family. *IEEE Transactions on Automatic Control*, vol. 39, no. 2 (February 1994), pp. 391 – 396.

[118] HOLLOT, C. V. AND XU, Z. L. When is the image of a multilinear function a polytope? a conjecture. In *Proceedings of the 28th IEEE Conference on Decision and Control* (Tampa, FL, 1989), pp. 1890 – 1891.

[119] HOLLOT, C. V. AND YANG, F. Robust stabilization of interval plants using lead or lag compensators. *Systems & Control Letters*, vol. 14 (1990), 9 – 12.

[120] HOROWITZ, I. *Synthesis of Feedback Control Systems*. Academic Press, New York, NY, 1963.

[121] HURWITZ, A. Uber die bedingungen, unter welchen eine gleichung nur wurzeln mit negativen reellen teilen besitzt. *Math. Ann.*, vol. 46 (1895), pp. 273 – 284.

[122] JUANG, J.-N. AND PAPPA, R. S. An eigensystem realization algorithm for modal parameter identification and model reduction. *AIAA Journal of Guidance, Control, and Dynamics*, vol. 8, no. 5 (September-October 1985), pp. 620 – 627.

[123] Juang, J.-N., Phan, M., and Horta, L. G. User's Guide for System/Observer/Controller Identification Toolbox. Tech. Rep., NASA Technical Memorandum 107566, 1992.

[124] Jury, E. I. *Sampled-data Control Systems.* John Wiley & Sons, Inc., New York, NY, 1958.

[125] Kalman, R. E. Contribution to the theory of optimal control. *Bol. Soc. Matem. Mexicana* (1960), pp. 102 – 119.

[126] Kalman, R. E. On the general theory of control systems. In *Proceedings of the 1st IFAC Congress* (Moscow, USSR, 1960), vol. 1, Butterworth, London, 1961, pp. 481 – 492.

[127] Kalman, R. E. When is a linear control system optimal? *ASME Transactions Series D (Journal of Basic Engineering)* (1964), pp. 51 – 60.

[128] Kalman, R. E. and Bucy, R. S. New results in linear filtering and prediction theory. *ASME Transactions (Journal of Basic Engineering)*, vol. 83 (1961), pp. 95 – 107.

[129] Kang, H. I. *Extreme point results for robustness of control systems.* PhD thesis, Department of Electrical and Computer Engineering, University of Wisconsin, Madison, Wisconsin, U.S.A., 1992.

[130] Katbab, A. and Jury, E. I. Robust Schur-stability of control systems with interval plants. *International Journal of Control*, vol. 51, no. 6 (1990), pp. 1343 – 1352.

[131] Keel, L. H. *Computer Aided Control System Design for Linear Time-invariant Systems.* PhD thesis, Department of Electrical Engineering, Texas A&M University, College Station, Texas, U.S.A., 1986.

[132] Keel, L. H. and Bhattacharyya, S. P. Frequency domain design of interval controllers. In *Control of Uncertain Dynamic Systems*, S. P. Bhattacharyya and L. H. Keel, Eds. CRC Press, Littleton, MA, 1991, pp. 423 – 438.

[133] Keel, L. H. and Bhattacharyya, S. P. Parametric stability margin for multilinear interval control systems. In *Proceedings of the 1993 American Control Conference* (San Francisco, CA, 1993), pp. 262 – 266.

[134] Keel, L. H. and Bhattacharyya, S. P. Stability margin for multilinear interval systems via phase conditions: A unified approach. In *Proceedings of the 1993 American Control Conference* (San Francisco, CA, 1993), pp. 3112 – 3116.

[135] KEEL, L. H. AND BHATTACHARYYA, S. P. Control system design for parametric uncertainty. *International Journal of Robust and Nonlinear Control*, vol. 4, no. 1 (January-February 1994), pp. 87 – 100.

[136] KEEL, L. H. AND BHATTACHARYYA, S. P. Phase properties of Hurwitz polynomials and segments. Tech. Rep., Tennessee State University, November 1994. ISE Report No. ACS-94-2.

[137] KEEL, L. H. AND BHATTACHARYYA, S. P. Robust parametric classical control design. *IEEE Transactions on Automatic Control*, vol. 39, no. 7 (July 1994), pp. 1524 – 1530.

[138] KEEL, L. H. AND BHATTACHARYYA, S. P. Robust stability of interval matrices: a computational approach. *International Journal of Control* (1995), To appear.

[139] KEEL, L. H., BHATTACHARYYA, S. P., AND HOWZE, J. W. Robust control with structured perturbations. *IEEE Transactions on Automatic Control*, vol. 33, no. 1 (January 1988), pp. 68 – 78.

[140] KEEL, L. H., LEW, J.-S., AND BHATTACHARYYA, S. P. System identification using interval dynamic models. In *Proceedings of the 1994 American Control Conference* (Baltimore, MD, June 1994), pp. 1537 – 1542.

[141] KEEL, L. H., LIM, K. B., AND JUANG, J.-N. Robust eigenvalue assignment with maximum tolerance to system uncertainties. *AIAA Journal of Guidance, Control, and Dynamics*, vol. 14, no. 3 (May-June 1991), pp. 615 – 620.

[142] KEEL, L. H., SHAW, J., AND BHATTACHARYYA, S. P. Robust control of interval systems. In *Robust Control*. Lecture Notes in Control and Information Sciences, vol. 183, Springer-Verlag, Tokyo, Japan, 1992, pp. 24 – 31.

[143] KHARITONOV, V. L. Asymptotic stability of an equilibrium position of a family of systems of linear differential equations. *Differential Uravnen*, vol. 14 (1978), pp. 2086 – 2088. Translation in *Differential Equations*, vol. 14, pp. 1483 - 1485, 1979.

[144] KHARITONOV, V. L. The Routh-Hurwitz problem for families of polynomials and quasipolynomials. *Izvetiy Akademii Nauk Kazakhskoi SSR, Seria fizikomatematicheskaia*, vol. 26 (1979), pp. 69 – 79.

[145] KHARITONOV, V. L. Interval stability of quasipolynomials. In *Control of Uncertain Dynamic Systems*, S. P. Bhattacharyya and L. H. Keel, Eds. CRC Press, Littleton, MA, 1991, pp. 439 – 446.

[146] KHARITONOV, V. L. Robust stability of nested polynomial families. Tech. rep., institut für Dynamische Systeme, Universität Bremen, Germany, May 1994. Report No. 306.

[147] KHARITONOV, V. L. AND ZHABKO, A. P. Robust stability of time delay systems. *IEEE Transactions on Automatic Control*, vol. 39, no. 12 (December 1994), pp.2388 – 2397.

[148] KIMURA, H. Robust stabilizability for a class of transfer functions. *IEEE Transactions on Automatic Control*, vol. AC-29, no. 9 (September 1984), pp. 788 – 793.

[149] KOGAN, J. *Robust Stability and Convexity*. Springer-Verlag, New York, NY, 1994.

[150] KOKAME, H. AND MORI, T. A Kharitonov-like theorem for interval polynomial matrices. *Systems & Control Letters*, vol. 16 (1991), pp. 107 – 116.

[151] KOSUT, R. L., GOODWIN, G. C., AND POLIS, M. P. Introduction: Special issue on system identification for control design. *IEEE Transactions on Automatic Control*, vol. 37, no. 7 (July 1992), pp. 899 – 899.

[152] KRAUS, F. J., ANDERSON, B. D. O., AND MANSOUR, M. Robust Schur polynomial stability and Kharitonov's theorem. *International Journal of Control*, vol. 47 (1988), pp. 1213 – 1225.

[153] KRAUS, F. J. AND MANSOUR, M. On robust Schur stability of discrete systems. In *Proceedings of the 29th IEEE Conference on Decision and Control* (Honolulu, Hawaii, December 1990), pp. 421 – 422.

[154] KRAUS, F. J., MANSOUR, M., AND ANDERSON, B. D. O. Robust stability of polynomials with multilinear parameter dependence. *International Journal of Control*, vol. 50 (1989), pp. 1745 – 1762.

[155] KRAUS, F. J., MANSOUR, M., AND JURY, E. I. Robust Schur stability of interval polynomial. In *Proceedings of the IEEE Conference on Decision and Control* (Tampa, FL, 1989), pp. 1908 – 1910.

[156] KUCERA, V. *Discrete Linear Control: The Polynomial Equation Approach*. John Wiley & Sons, Inc., New York, NY, 1979.

[157] KWAKERNAAK, H. The polynomial approach to H_∞ optimal regulation. In *H_∞-Control Theory*, Lecture Notes in Mathematics, vol. 1496, Springer-Verlag, Berlin, 1991, pp. 141 – 221.

[158] LANCASTER, P. AND TISMENETSKY, M. *The Theory of Matrices with Applications*. Academic Press, San Diego, CA, 1985.

[159] LEAL, M. A. AND GIBSON, J. S. A first-order Lyapunov robustness method for linear systems with uncertain parameters. *IEEE Transactions on Automatic Control*, vol. 35, no. 9 (September 1990), pp. 1068 – 1070.

[160] LEVIN, B. J. *Distribution of zeros of entire functions*, vol. 5. American Mathematical Society, Providence, Rhode Island, 1980. Translation of Mathematical Monographs.

[161] LEW, J.-S., KEEL, L. H., AND JUANG, J.-N. Quantification of model error via an interval model with nonparametric error bound. In *Proceedings of the 1993 AIAA Guidance, Navigation, and Control Conference* (Montery, CA, August 1993), pp. 1254 – 1263.

[162] LEW, J.-S., KEEL, L. H., AND JUANG, J.-N. Quantification of parametric uncertainty via an interval model. *AIAA Journal of Guidance, Control, and Dynamics*, vol. 17, no. 6, (November-December 1994), pp. 1212 – 1218

[163] LEW, J.-S., LINK, T. L., GARCIA, E., AND KEEL, L. H. Interval model identification for flexible structures with uncertain parameters. In *Proceedings of the 1994 ASME Structures, Structural Dynamics, and Materials Conference* (Hilton Head, SC, April 1994), pp. 42 – 47.

[164] LINK, T. L., LEW, J.-S., GARCIA, E., AND KEEL, L. H. Robustness verification for flexible structures via interval control systems. In *Proceedings of the 1994 AIAA Guidance, Navigation, and Control Conference* (Scollsdale, AZ, August 1994), pp. 252 – 260.

[165] LURIE, A. I. *On some nonlinear problems in the theory of automatic control.* H. M. Stationary Office, London, 1957. Russian Edition, 1951.

[166] MAC FARLANE, A. G. J. AND POSTLETHWAITE, I. The generalized Nyquist stability criterion and multivariable root-loci. *International Journal of Control*, vol. 25 (January 1977), pp. 81 – 127.

[167] MACIEJOWSKI, J. M. *Multivariable Feedback Design.* Addison - Wesley, Reading, MA, 1988.

[168] MANSOUR, M. Robust stability of interval matrices. In *Proceedings of the 28th IEEE Conference on Decision and Control* (Tampa, FL, December 1989), pp. 46 – 51.

[169] MANSOUR, M. Robust stability in systems described by rational functions. In *Control and Dynamic Systems*, C. T. Leondes, Ed., vol. 51. Academic Press, New York, NY, 1992, pp. 79 – 128.

[170] MANSOUR, M. On robust stability of linear systems. *Systems & Control Letters*, vol. 22 (1994), pp. 131 – 143.

[171] MANSOUR, M. AND ANDERSON, B. D. O. Kharitonov's theorem and the second method of Lyapunov. In *Robustness of Dynamic Systems with Parameter Uncertainties*, M. Mansour, S. Balemi, and W. Truöl, Eds. Birkhäuser, Berlin, 1992, pp. 3 – 12.

[172] MANSOUR, M., BALEMI, S., AND TRUÖL, W., Eds. *Robustness of Dynamic Systems with Parameter Uncertainties*. Birkhäuser, Berlin, 1992.

[173] MANSOUR, M. AND KRAUS, F. J. Argument conditions for Hurwitz and Schur stable polynomials and the robust stability problem. Tech. rep., ETH, Zurich, Tech. Report, 1990.

[174] MANSOUR, M., KRAUS, F. J., AND ANDERSON, B. D. O. Strong Kharitonov theorem for discrete systems. In *Robustness in Identification and Control*, M. Milanese, R. Temp, and A. Vicino, Eds. Plenum Press, New York, NY, 1989.

[175] MARDEN, M. *Geometry of Polynomial*. American Mathematical Society, Providence, RI, 1966.

[176] MARQUEZ, H. J. AND DIDUCH, C. P. On strict positive realness of interval plants. *IEEE Transactions on Circuits and Systems*, vol. 40, no. 8 (August 1993), pp. 551 – 552.

[177] MARTIN, J. M. State-space measures for stability robustness. *IEEE Transactions on Automatic Control*, vol. AC-32, no. 6 (June 1987), pp. 509 – 512.

[178] MAXWELL, T. C. On governors. *Proceedings of the Royal Society*, vo. 16 (1868), pp. 270 – 283.

[179] MERESSI, T., CHEN, D., AND PADEN, B. Application of Kharitonov's theorem to mechanical systems. *IEEE Transactions on Automatic Control*. vo. 38, no. 3 (March 1993), pp. 488 – 491.

[180] MILANESE, M., TEMPO, R., AND VICINO, A., Eds. *Robustness in Identification and Control*. Prenum Press, New York, NY, 1989.

[181] MINNICHELLI, R. J., ANAGNOST, J. J., AND DESOER, C. A. An elementary proof of Kharitonov's stability theorem with extensions. *IEEE Transactions on Automatic Control*, vol. AC-34, no. 9 (September 1989), pp. 995 – 998.

[182] MORI, T. AND BARNETT, S. On stability tests for some classes of dynamical systems with perturbed coefficients. *IMA Journal of Mathematical Control and Information*, vol. 5 (1988), pp. 117 – 123.

[183] MORI, T. AND KOKAME, H. Stability of interval polynomials with vanishing extreme coefficients. In *Recent Advances in Mathematical Theory of Systems, Control, Networks, and Signal Processing I*. Mita Press, Tokyo, Japan, 1992, pp. 409 – 414.

[184] NYQUIST, H. Regeneration theory. *Bell System Technical Journal*, vol. 11 (1932), pp. 126 – 147.

[185] PATEL, R. V. AND TODA, M. Quantitative measures of robustness for multivariable systems. In *Proceedings of American Control Conference* (San Francisco, CA, May 1980).

[186] PATEL, V. V. AND DATTA, K. B. H_∞-based synthesis for a robust controller of interval plants. *Automatica*, Submitted for publication.

[187] PEARSON, J. B. Compensator design for dynamic optimization. *International Journal of Control*, vol. 9 (1968), pp. 473 – 473.

[188] PÉREZ, F., ABDALLAH, C., AND DOCAMPO, D. Extreme point stability tests for discrete-time polynomials. In *Proceedings of the 31th IEEE Conference on Decision and Control* (Tucson, AZ, December 1992), pp. 1552 – 1553.

[189] PETERSEN, I. R. A new extension to Kharitonov's theorem. In *Proceedings of IEEE Conference on Decision and Control* (Los Angeles, CA, December 1987), pp. 2070 – 2075.

[190] POLYAK, B. T. Robustness analysis for multilinear perturbations. In *Robustness of Dynamic Systems with Parameter Uncertainties*, M. Mansour, S. Balemi, and W. Truöl, Eds. Birkhäuser, Berlin, 1992, pp. 93 – 104.

[191] POLYAK, B. T. AND SHMULYIAN, S. B. Frequency domain criteria for robust stability of bivariate polynomials. *IEEE Transactions on Circuits and Systems*, vol. 41, no. 2 (February 1994), pp. 161 – 167.

[192] PONTRJAGIN, L. S. On the zeros of some elementary transcendental functions. *Akad. Nauk SSSR Ser. Mat.*, vol. 6 (1942), pp. 115 – 134. English translation, American Mathematical Society Translation, vol. 2 (1955), pp. 95 – 110.

[193] QIU, L., BERNHARDSSON, B., RANTZER, A., DAVISON, E. J., YOUNG, P. M., AND DOYLE, J. C. A formula for computation of the real stability radius. In *Proceedings of the 1993 IFAC World Congress* (Sidney, Australia, 1993).

[194] RANTZER, A. Kharitonov's weak theorem holds if and only if the stability region and its reciprocal are convex. *International Journal of Robust and Nonlinear Control* (1992).

[195] RANTZER, A. Stability conditions for polytopes of polynomials. *IEEE Transactions on Automatic Control*, vol. AC-37, no. 1 (January 1992), pp. 79–89.

[196] RANTZER, A. AND MEGRETSKI, A. A convex parameterization of robustly stabilizing controllers. *IEEE Transactions on Automatic Control*, vol. 39, no. 9 (September 1994), pp. 1802 – 1808.

[197] ROSENBROCK, H. H. *State Space and Multivariable Theory.* John Wiley & Sons, Inc., New York, NY, 1970.

[198] Routh, E. J. *A Treatise on the Stability of a Given State of Motion.* Macmillan Publishing Co., London, 1877.

[199] Saeki, M. A method of robust stability analysis with highly structured uncertainties. *IEEE Transactions Automatic Control*, vol. AC-31, no. 10 (October 1986), pp. 925 – 940.

[200] Saeks, R. and Murray, J. Fractional representation, algebraic geometry and the simultaneous stabilization problem. *IEEE Transactions on Automatic Control*, vol. AC-27, no. 8 (August 1982), pp. 895 – 903.

[201] Safonov, M. G. and Verma, M. S. ℓ_∞ optimization and Hankel approximation. *IEEE Transactions on Automatic Control*, vol. AC-30, no. 3 (March 1985), pp. 279 – 280.

[202] Schur, I. Uber potenzreichen, die in innern des einheitkreises beschrankt sind. *J. Reine Angew. Math.*, vol. 147 (1918), pp. 205 – 232.

[203] Schur, I. Uber potenzreichen, die in innern des einheitkreises beschrankt sind. *J. Reine Angew. Math.*, vol. 148 (1918), pp. 122 – 145.

[204] Sezer, M. E. and Šiljak, D. D. A note on robust stability bounds. *IEEE Transactions on Automatic Control*, vol. 34, no. 11 (November 1989), pp. 1212 – 1215.

[205] Sezer, M. E. and Šiljak, D. D. On stability of interval matrices. *IEEE Transactions on Automatic Control*, vol. 39, no. 2 (1994), pp. 368 – 371.

[206] Shafai, B. and Hollot, C. V. Nonnegative stabilization of interval discrete systems. In *Control of Uncertain Dynamic Systems*, S. P. Bhattacharyya and L. H. Keel, Eds. CRC Press, Littleton, MA, 1991, pp. 471 – 490.

[207] Shafai, B., Kothandaraman, M., and Chen, J. Real and complex stability radii for nonnegative and Metzlerian systems. In *Proceedings of the 1993 IEEE Conference on Decision and Control* (San Antonio, TX, 1993), pp. 3482 – 3484.

[208] Shafai, B., Perev, K., Cowley, D., and Chehab, Y. A necessary and sufficient condition for the stability of nonnegative interval discrete systems. *IEEE Transactions on Automatic Control*, vol. 36, no. 6 (1991), pp. 742 – 746.

[209] Shafai, B. and Sotirov, G. Interval identification and robust control design: A new perspective. In *Proceedings of the 1991 IFAC Symposium on Design Methods for Control Systems* (Zurich, Switzerland, September 1991), pp. 246 – 251.

[210] Sideris, A. and Sánches Peña, R. S. S. Fast computation of the multivariable stability margin for real interrelated uncertain parameters. *IEEE Transactions on Automatic Control*, vol. 34, no. 12 (December 1989), pp. 1272 – 1276.

[211] Šiljak, D. D. *Nonlinear Systems: Parametric Analysis and Design.* John Wiley & Sons, Inc., New York, NY, 1969.

[212] Šiljak, D. D. Parameter space methods for robust control design: a guided tour. *IEEE Transactions on Automatic Control*, vol. AC-34, no. 7 (July 1989), pp. 674 – 688.

[213] Šiljak, D. D. Polytopes of nonnegative polynomials. In *Proceedings of the 1989 American Control Conference* (Pittsburgh, PA, June 1989), pp. 193 – 199.

[214] Soh, C. B., Berger, C. S., and Dabke, K. P. On the stability properties of polynomials with perturbed coefficients. *IEEE Transactions on Automatic Control*, vol. AC-30, no. 10 (October 1985), pp. 1033 – 1036.

[215] Soh, Y. C. and Foo, Y. K. Generalized Edge Theorem. *Systems & Control Letters*, vol. 12 (1989), pp. 219 – 224.

[216] Soh, Y. C. and Foo, Y. K. A note on the Edge Theorem. *Systems & Control Letters*, vol. 15 (1990), pp. 41 – 43.

[217] Sotirov, G. and Shafai, B. Interval identification of linear systems with bounded errors in both input and output variables. In *Proceedings of the 1991 IEEE Conference on Decision and Control* (Brighton, U.K., December 1991), pp. 648 – 649.

[218] Tesi, A. and Vicino, A. A new fast algorithm for robust stability analysis of linear control systems with linearly correlated parametric uncertainty. *Systems & Control Letters*, vol. 13 (1989), pp. 321 – 329.

[219] Tesi, A. and Vicino, A. Robust stability of state-space models with structured uncertainties. *IEEE Transactions on Automatic Control*, vol. 35, no. 2 (February 1990), pp. 191 – 195.

[220] Tesi, A. and Vicino, A. Robustness analysis for linear dynamical systems with linearly correlated parameter uncertainties. *IEEE Transactions on Automatic Control*, vol. 35, no. 2 (February 1990), pp. 186 – 190.

[221] Tesi, A. and Vicino, A. Kharitonov segments suffice for frequency response analysis of interval plant-controller families. In *Control of Uncertain Dynamic Systems*, S. P. Bhattacharyya and L. H. Keel, Eds. CRC Press, Littleton, MA, 1991, pp. 403 – 415.

[222] TESI, A. AND VICINO, A. Robust absolute stability of Lur'e control systems in parameter space. *Automatica*, vol. 27, no. 2 (March 1991), pp. 147 – 151.

[223] TESI, A. AND VICINO, A. Robust strict positive realness: new results for interval plant plus controller families. In *Proceedings of the 30th IEEE Conference on Decision and Control* (Brighton, UK, December 1991), pp. 421 – 426.

[224] TIN, M. A. Discrete time robust control systems under structured perturbations: Stability manifolds and extremal properties. Master's thesis, Department of Electrical Engineering, Texas A&M University, College Station, Texas, U.S.A., 1992.

[225] TSYPKIN, Y. Z. AND POLYAK, B. T. Frequency domain criteria for ℓ_p-robust stability of continuous linear systems. *IEEE Transactions on Automatic Control*, vol. AC-36, no. 12 (December 1991), pp. 1464 – 1469.

[226] TSYPKIN, Y. Z. AND POLYAK, B. T. Frequency domain criterion for robust stability of polytope of polynomials. In *Control of Uncertain Dynamic Systems*, S. P. Bhattacharyya and L. H. Keel, Eds. CRC Press, Littleton, MA, 1991, pp. 491 – 499.

[227] TSYPKIN, Y. Z. AND POLYAK, B. T. Robust absolute stability of continuous systems. In *Robustness of Dynamic Systems with Parameter Uncertainties*, M. Mansour, S. Balemi, and W. Truöl, Eds. Birkhäuser, Berlin, 1992, pp. 113 – 124.

[228] VAIDYANATHAN, P. AND MITRA, S. K. A unified structural interpretation of some well-known stability test procedures for linear systems. *IEEE Proceedings*, vol. 75, no. 4 (April 1987), pp. 478 – 497.

[229] VICINO, A. AND TESI, A. Regularity condition for the stability margin problem with linear dependent perturbations. *SIAM Journal on Control and Optimization*, vol. 33, no. 5 (May 1995), To appear.

[230] VICINO, A., TESI, A., AND MILANESE, M. Computation of nonconservative stability perturbation bounds for systems with nonlinearly correlated uncertainties. *IEEE Transactions on Automatic Control*, vol. AC-35, no. 7 (July 1990), pp. 835 – 841.

[231] VIDYASAGAR, M. *Nonlinear Systems Analysis*. Prentice-Hall Publishing Co., Englewood Cliffs, NJ, 1978.

[232] VIDYASAGAR, M. *Control System Synthesis: A Factorization Approach*. MIT Press, Cambridge, MA, 1985.

[233] VIDYASAGAR, M. Optimal rejection of persistent bounded disturbances. *IEEE Transactions on Automatic Control*, vol. AC-31, no. 6 (June 1986), pp. 527 – 534.

[234] VIDYASAGAR, M. AND KIMURA, H. Robust controllers for uncertain linear multivariable systems. *Automatica*, vol. 22, no. 1 (January 1986), pp. 85 – 94.

[235] VIDYASAGAR, M. AND VISWANSADHAM, N. Algebraic design techniques for reliable stabilization. *IEEE Transactions on Automatic Control*, vol. AC-27, no. 5 (October 1988), pp. 1085 – 1095.

[236] WALSH, J. L. *Interpolation and Approximation by Rational Function in the Complex Domain.* American Mathematical Society, 1935.

[237] WONHAM, W. M. *Linear Multivariable Control: a Geometric Approach, 3rd Edition.* Springer-Verlag, New York, NY, 1985.

[238] YEDAVALLI, R. K. Improved measures of stability for linear state space model. *IEEE Transactions on Automatic Control*, vol. AC-30, no. 6 (June 1985), pp. 577 – 579.

[239] YEDAVALLI, R. K. AND LIANG, Z. Reduced conservatism in stability robustness bounds by state transformation. *IEEE Transactions on Automatic Control*, vol. AC-31, no. 9 (September 1986), pp. 863 – 865.

[240] YEUNG, K. S. AND WANG, S. S. A simple proof of Kharitonov's theorem. *IEEE Transactions on Automatic Control*, vol. 32, no. 4 (April 1987), pp. 822 – 823.

[241] YOULA, D. C., JABR, H. A., AND BONGIORNO, J. J. Modern Wiener - Hopf design of optimal controllers - Part I: The single input single output case. *IEEE Transactions on Automatic Control*, vol. AC-21, no. 1, (February 1976), pp. 3 – 13.

[242] YOULA, D. C., JABR, H. A., AND BONGIORNO, J. J. Modern Wiener - Hopf design of optimal controllers - Part II: The multivariable case. *IEEE Transactions on Automatic Control*, vol. AC-21 (June 1976), pp. 319 – 338.

[243] ZADEH, L. A. AND DESOER, C. A. *Linear Systems Theory.* McGraw Hill Book Co., New York, NY, 1963.

[244] ZAMES, G. Functional analysis applied to nonlinear feedback systems. *IEEE Transactions on Circuit Theory*, vol. CT-10, (September 1963), pp. 392 – 404.

[245] ZAMES, G. Feedback and optimal sensitivity: Model reference transformations, multiplicative seminorms, and approximate inverses. *IEEE Transactions on Automatic Control*, vol. AC-26, no. 2 (April 1981), pp. 301 – 320.

[246] ZEHEB, E. Necessary and sufficient condition for the robust stability of a continuous systems: the continuous dependency case illustrated by multilinear dependence. *IEEE Transactions on Circuits and Systems*, vol. 37, no. 1 (January 1990), pp. 47 – 53.

[247] ZHOU, K. AND KHARGONEKAR, P. P. Stability robustness bounds for linear state space models with structured uncertainty. *IEEE Transactions on Automatic Control*, vol. AC-32, no. 7 (July 1987), pp. 621 – 623.

[248] ZIMMERMAN, D. C., HORNER, G. C., AND INMAN, D. J. Microprocessor controlled force actuator. *AIAA Journal of Guidance, Navigation, and Control*, vol. 11, no. 3 (May-June 1988), pp. 230 – 236.

Author Index

V

W

X

Y

Z

Subject Index

D

E

F

G

L

M

N

O

P

Q

R

T

U

V

W

Y

Z